Advances in Pharmaceutical Product Development and Research Series

BIOMATERIALS AND BIONANOTECHNOLOGY

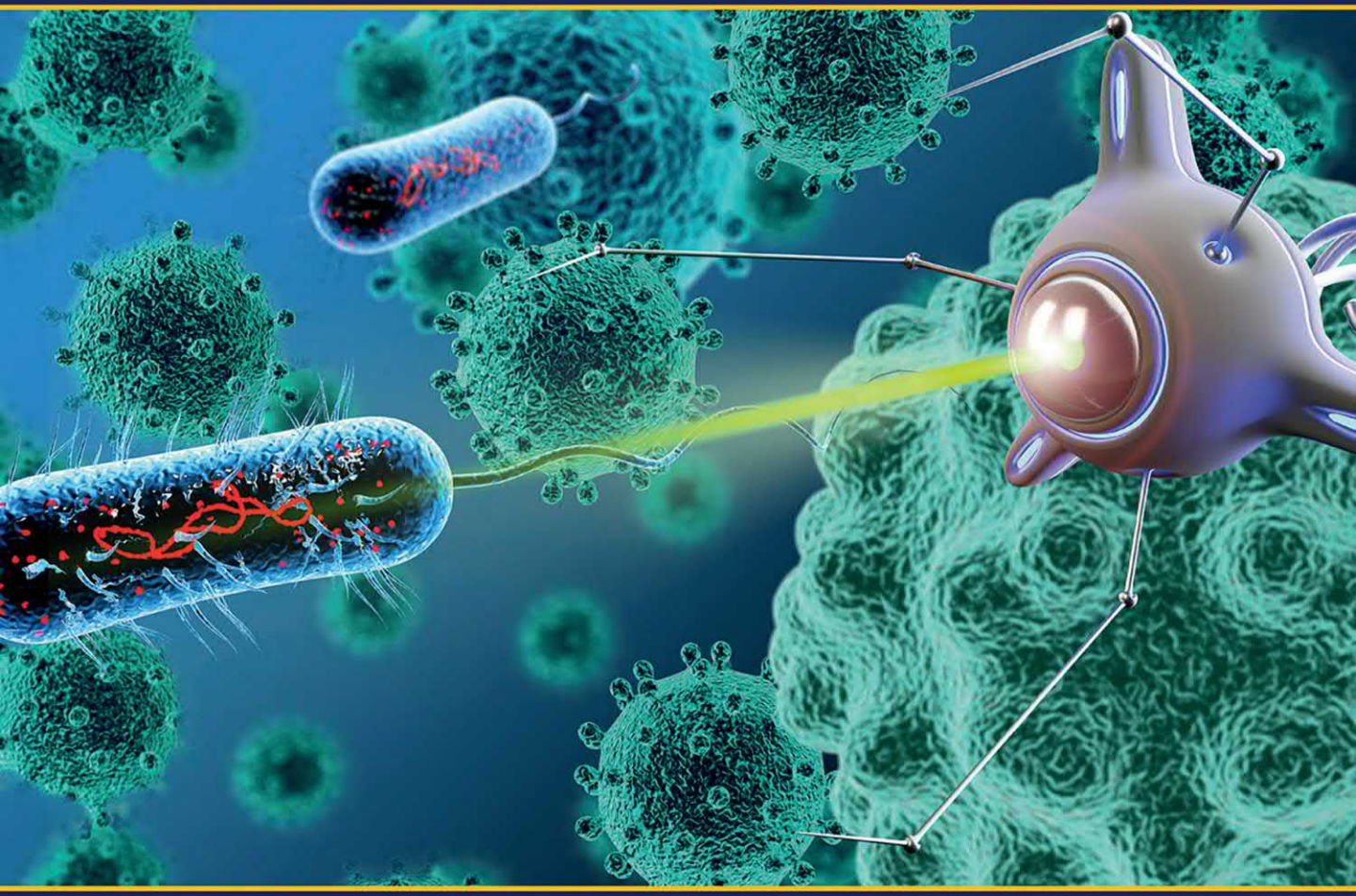

Edited by

Rakesh K. Tekade

BIOMATERIALS AND BIONANOTECHNOLOGY

ADVANCES IN PHARMACEUTICAL PRODUCT DEVELOPMENT AND RESEARCH SERIES

BIOMATERIALS AND BIONANOTECHNOLOGY

Edited by

RAKESH K. TEKADE

National Institute of Pharmaceutical Education and Research (NIPER)—Ahmedabad, Gandhinagar, India

ELSEVIER

ACADEMIC PRESS

An imprint of Elsevier

Academic Press is an imprint of Elsevier
125 London Wall, London EC2Y 5AS, United Kingdom
525 B Street, Suite 1650, San Diego, CA 92101, United States
50 Hampshire Street, 5th Floor, Cambridge, MA 02139, United States
The Boulevard, Langford Lane, Kidlington, Oxford OX5 1GB, United Kingdom

Copyright © 2019 Elsevier Inc. All rights reserved.

No part of this publication may be reproduced or transmitted in any form or by any means, electronic or mechanical, including photocopying, recording, or any information storage and retrieval system, without permission in writing from the publisher. Details on how to seek permission, further information about the Publisher's permissions policies and our arrangements with organizations such as the Copyright Clearance Center and the Copyright Licensing Agency, can be found at our website: www.elsevier.com/permissions.

This book and the individual contributions contained in it are protected under copyright by the Publisher (other than as may be noted herein).

Notices

Knowledge and best practice in this field are constantly changing. As new research and experience broaden our understanding, changes in research methods, professional practices, or medical treatment may become necessary.

Practitioners and researchers must always rely on their own experience and knowledge in evaluating and using any information, methods, compounds, or experiments described herein. In using such information or methods they should be mindful of their own safety and the safety of others, including parties for whom they have a professional responsibility.

To the fullest extent of the law, neither the Publisher nor the authors, contributors, or editors, assume any liability for any injury and/or damage to persons or property as a matter of products liability, negligence or otherwise, or from any use or operation of any methods, products, instructions, or ideas contained in the material herein.

British Library Cataloguing-in-Publication Data
A catalogue record for this book is available from the British Library

Library of Congress Cataloging-in-Publication Data
A catalog record for this book is available from the Library of Congress

ISBN: 978-0-12-814427-5

For Information on all Academic Press publications
visit our website at https://www.elsevier.com/books-and-journals

Publisher: Andre Gerhard Wolff
Acquisition Editor: Erin Hill-Parks
Editorial Project Manager: Jennifer Horigan
Production Project Manager: Kiruthika Govindaraju
Cover Designer: Mark Rogers

Typeset by MPS Limited, Chennai, India

Dedication

First of all, I thank almighty God for giving me this opportunity to serve the scientific fraternity through the book series *Advances in Pharmaceutical Product Development and Research*. This book is devoted to my father, Shri Ganpat Rao Tekade—I know you are always watching me and showering your blessings on me from heaven. My dedication goes to my loving mother (Smt. Godavari Tekade), whose prayers have always followed me and clung to me all my life. My dedication goes to my best friend, my support system, my wife Muktika Tekade, whose words of encouragement, deep faith in me and my ability, have always caused the flower of never-tiring efforts to blossom in my eyes. Your hope gives me the courageous determination to fight back, even when the things go off-track and uphill. My dedication to the twinkles of my eyes: my daughter ☺, my treasure Manyata and my son ☺, my superhero Atharva for being my rock stars and my number one fans. Kids, your hugs give me an intense reason to smile, even when worries abound. I hope one day you will comprehend why I spent tireless time on writing. I love you guys, forever! A special feeling of gratitude to my sisters and remembrance to my brother. I would also like to thank my friends for their motivation. My superior respect goes toward all my teachers and mentors (Prof. N.K. Jain, Prof. Xiankai Sun, Prof. Antony D' Emanuele, Prof. Mahavir Chougule) for being my role models.

List of Contributors

Ruwaida W. Abdo Faculty of Pharmacy, Philadelphia University, Amman, Jordan
Sarfaraz Ahmed Department of Pharmaceutical Chemistry, Global Institute of Pharmaceutical Education and Research, Kashipur, Uttarakhand, India
Raghuram Rao Akkinepalli National Institute of Pharmaceutical Education and Research, Mohali, India
Amal Al-Aboudi Department of Chemistry, Faculty of Science, The University of Jordan, Amman, Jordan
Noor Al-Attraqchi Department of Pharmacognosy, Mosul University, Mosul, Iraq
Omar Husham Ahmed Al-Attraqchi Faculty of Pharmacy, Philadelphia University, Amman, Jordan
Bilal Al-Jaidi Faculty of Pharmacy, Philadelphia University, Amman, Jordan
Shahd Z. Alkelany Faculty of Pharmacy, Philadelphia University, Amman, Jordan
Saket Asati Department of Pharmaceutical Sciences, Dr. Hari Singh Gour University, Sagar, India
Shantanu Bandopadhyay Faculty of Pharmacy, Naraina Vidyapeeth Group of Institutions, Kanpur, Uttar Pradesh, India
Nabamita Bandyopadhyay Molecular Biology Division, National Institute of Malaria Research (NIMR), Dwarka, Delhi, India
Renu Chadha University Institute of Pharmaceutical Sciences (UIPS), Panjab University, Chandigarh, India
Silki Chandel Department of Pharmaceutical Sciences, Dr. Hari Singh Gour University, Sagar, India
Rubhan Chandran Haematology Unit, Department of Pathology, Faculty of Medicine and Health Sciences, Universiti Putra Malaysia, Selangor, Malaysia
Sunita Chawla National Institute of Pharmaceutical Education and Research (NIPER)—Ahmedabad, Gandhinagar, India
Hira Choudhury Department of Pharmaceutical Technology, School of Pharmacy, The International Medical University, Kuala Lumpur, Malaysia
Yashu Chourasiya Department of Pharmacology, Shri Bherulal Pharmacy Institute, Indore, India
Pran Kishore Deb Faculty of Pharmacy, Philadelphia University, Amman, Jordan
Abdelbary Elhissi College of Pharmacy, Qatar University, Doha, Qatar
Piyush Ghode School of Pharmacy and Technology Management, NMIMS, Shirpur, India
Bapi Gorain Faculty of Health and Medical Science, School of Pharmacy, Taylor's University, Subang Jaya, Malaysia

Islam Hamad Department of Pharmacy, Faculty of Health Sciences, American University of Madaba, Madaba, Jordan

Gillian A. Hutcheon School of Pharmacy and Biomolecular Sciences, Liverpool John Moores University, Liverpool, United Kingdom

Abdulmutallab Yousef Jaber Faculty of Pharmacy, Philadelphia University, Amman, Jordan

Aviral Jain Ravi Shankar College of Pharmacy, Bhopal, India

Priyanka Jain Department of Pharmaceutical Sciences, Dr. Hari Singh Gour University, Sagar, India

Dnyaneshwar Kalyane National Institute of Pharmaceutical Education and Research (NIPER)—Ahmedabad, Gandhinagar, India

Devesh Kapoor National Institute of Pharmaceutical Education and Research (NIPER)—Ahmedabad, Gandhinagar, India; Department of Pharmacy, Dr. Dayaram Patel Pharmacy College, Bardoli, India

Kaushik Kuche National Institute of Pharmaceutical Education and Research (NIPER)—Ahmedabad, Gandhinagar, India

Umesh Kumar Atneriya School of Pharmacy, Devi Ahilya Vishwavidyalaya, Takshila Campus, Indore, India

Neha Maheshwari School of Pharmacy, Devi Ahilya Vishwavidyalaya, Takshila Campus, Indore, India

Rahul Maheshwari National Institute of Pharmaceutical Education and Research (NIPER)—Ahmedabad, Gandhinagar, India

Tuan Mazlelaa Tuan Mahmood Faculty of Pharmacy, The National University of Malaysia (UKM), Kuala Lumpur, Malaysia

Ankita Mane Acropolis Institute of Pharmaceutical Education and Research (AIPER), Manglia, Indore, India

Disha Mehtani Department of Pharmaceutics, Sri Aurobindo Institute of Pharmacy, Indore, India

Haifa'a Marouf Abdellatif Odetallah Faculty of Pharmacy, Philadelphia University, Amman, Jordan

Pramina Kumari Pandey National Institute of Pharmaceutical Education and Research (NIPER)—Ahmedabad, Gandhinagar, India

Vikas Pandey Department of Pharmaceutical Sciences, Dr. Hari Singh Gour University, Sagar, India

Divya Pandit University Institute of Pharmaceutical Sciences (UIPS), Panjab University, Chandigarh, India

Abhimanyu Patharkar National Institute of Pharmaceutical Education and Research (NIPER)—Ahmedabad, Gandhinagar, India

Lana Qadumii Faculty of Science, Philadelphia University, Amman, Jordan

Nidhi Raval National Institute of Pharmaceutical Education and Research (NIPER)—Ahmedabad, Gandhinagar, India

Ankit Seth Department of Pharmaceutical Engineering & Technology, Indian Institute of Technology, Banaras Hindu University, Varanasi, India

Mukesh Chandra Sharma School of Pharmacy, Devi Ahilya Vishwavidyalaya, Takshila Campus, Indore, India

Piyoosh Sharma Department of Pharmaceutical Engineering & Technology, Indian Institute of Technology, Banaras Hindu University, Varanasi, India

Abeer Jabra Shnoudeh Faculty of Pharmacy, Philadelphia University, Amman, Jordan

Sushant K. Shrivastava Department of Pharmaceutical Engineering & Technology, Indian Institute of Technology, Banaras Hindu University, Varanasi, India

Namrata Soni Faculty of Health Sciences, Sam Higginbottom Institute of Agriculture, Technology and Sciences (Deemed University), Allahabad, India

Vandana Soni Department of Pharmaceutical Sciences, Dr. Hari Singh Gour University, Sagar, India

Johnson Stanslas Pharmacotherapeutics Unit, Department of Medicine, Faculty of Medicine and Health Sciences, Universiti Putra Malaysia, Serdang, Selangor, Malaysia

Hiba Salim Surchi Faculty of Pharmacy, Philadelphia University, Amman, Jordan

Muktika Tekade School of Pharmacy, Devi Ahilya Vishwavidyalaya, Takshila Campus, Indore, India

Rakesh K. Tekade National Institute of Pharmaceutical Education and Research (NIPER)—Ahmedabad, Gandhinagar, India

Eusni Rahayu Mohd. Tohit Haematology Unit, Department of Pathology, Faculty of Medicine and Health Sciences, Universiti Putra Malaysia, Selangor, Malaysia

Vivek Yadav Department of Pharmacology, Institute of Pharmacy, Chhatrapati Shahu Ji Maharaj University, Kanpur, Uttar Pradesh, India

Susanne R. Youngren-Ortiz Research and Development, Akorn Pharmaceuticals, Inc., Vernon Hills, IL, United States

About the Editor

Rakesh K. Tekade—*Series Editor*

Dr. Rakesh K. Tekade, assistant professor of the Department of Pharmaceutics, is an academician, formulation scientist, and industry expert with years of experience in drug delivery and therapeutics development. He received his B.Pharm degree in Pharmacy from IPS Academy affiliated to R.G.P.V. University, Bhopal. He received his master's and doctoral degrees in Pharmaceutical Sciences from the Dr. H.S. Gour University, Sagar (India) with Prof. Jain's group. After his master's degree, he served as Research and Development Scientist at Ranbaxy Research Laboratories, Dewas (India). Dr. Tekade is a recipient of commonwealth fellowship (United Kingdom) to pursue research training at the University of Central Lancashire, United Kingdom with Prof. D'Emanuele's dendrimer group. He is a recipient of several internationally acclaimed fellowships and awards including a Commonwealth Fellowship (Preston, United Kingdom), IRISH Government Postdoctoral Fellowship (Ireland), National Doctoral Fellowship (AICTE, India), CSIR Senior Research Fellowship (CSIR, India), and AICTE Junior Research Fellowship (AICTE, India), and he has received many meritorious awards.

Dr. Tekade's lab investigates the design, development, and characterization of next-generation targeted nanotechnology-based translational nanomedicine for the site-specific delivery of therapeutic drugs, siRNA, microRNA, plasmids, proteins, and peptides for the treatment of cancer, diabetes, and neurodegenerative disorders. An overarching goal of his current research interests encompasses development of novel polymeric nanomaterial for effective cytosolic delivery of gene therapeutics. Development of laser-activatable nanoplatforms for the treatment of cancer as well as for the prevention of postsurgical relapse of resectable tumors is another thrust goal of his research focus. His research work involves the principles of polymer chemistry, nanotechnology, molecular biology, pharmacokinetics/pharmacodynamics, and imaging techniques. His research group also investigates the pharmacokinetics, pharmacodynamics, and molecular dynamics of several compounds and nanoformulations against cancer cell lines and tumorigenic mouse models. Dr. Tekade has over 100 publications, 4 patents applications, over 90 reference book chapters, and 5 editorial articles (>3800 citations; *H*-index of 33; cumulative impact factor: 395.10). He has delivered several invited research talks and presented research findings are more than 40 scientific conferences. He has authored three books and is a series editor for the widely recognized *Advances in Pharmaceutical Sciences and Research* book series. To date he has mentored 1 postdoctoral, 4 Ph.D., 30 MS/M.Pharm, and 10 B.Pharm/Biomedical Science students. As an editor, he has published five widely referenced books, namely *Dosage Form Design Parameters*, *Dosage Form Design Considerations*, *Fundamentals of Drug Delivery*, *Biomaterials and Bionanotechnology*, and *Drug Delivery*

Systems (https://www.elsevier.com/catalog/pharma/pharmaceutical-science/drug-delivery/advances-in-pharmaceutical-product-development-and-research). He also serves as an expert reviewer for more than 50 peer-reviewed international journals of repute.

Affiliations and Expertise

Assistant Professor, Department of Pharmaceutics, National Institute of Pharmaceutical Education and Research (NIPER) Ahmedabad, India

CHAPTER

1

Design of Materials and Product Specifications

Divya Pandit[1], *Pran Kishore Deb*[2] *and Renu Chadha*[1]

[1]University Institute of Pharmaceutical Sciences (UIPS), Panjab University, Chandigarh, India
[2]Faculty of Pharmacy, Philadelphia University, Amman, Jordan

OUTLINE

1.1 Introduction 2

1.2 Objectives and Scope of Design of Materials and Product Specifications 2

1.3 Pharmaceutical Product Specification 3
1.3.1 Concepts and the Need 3
1.3.2 The Rationale for Designing Specifications 3
1.3.3 Associated Terminologies 4
1.3.4 Types of Specifications 4

1.4 Designing of Specification 5
1.4.1 Guidelines for Designing Specification for Drug Substance/Drug Product 5
1.4.2 Guidelines for Designing Specification for Packaging Material 10

1.5 Handling of Out-of-Specification 11
1.5.1 Phase I Investigation 12
1.5.2 Phase II Investigation 12

1.6 Finished Pharmaceutical Product 12
1.6.1 Regulatory Requirements 12
1.6.2 Schematic Plan for Verification of Specification 14
1.6.3 Labeling 14
1.6.4 Shelf-Life and Storage 14

1.7 Importance of Specification on Pharmaceutical Quality System 15

1.8 Conclusion 15

Acknowledgment 16

Abbreviations 16

References 16

Further reading 17

Biomaterials and Bionanotechnology
DOI: https://doi.org/10.1016/B978-0-12-814427-5.00001-9

© 2019 Elsevier Inc. All rights reserved.

1.1 INTRODUCTION

It is the prerequisite responsibility of pharmaceutical companies to ensure that patients receive effective medicines of good quality. Manufacturers require assistance in the form of a comprehensive quality system model for implementation to meet their intended purpose and protect public health. This led to the establishment of various guidelines with a mandate to develop, establish and promote standards for the delivery of health care with respect to pharmaceuticals. However, these guidelines are a minimum requirement that is periodically reviewed and revised with the inception of new technological developments.

One of the control strategies for confirming the quality of the pharmaceutical product is to design raw material and finished product specification. During the International Conference of Drug Regulatory Authorities, officials from the United States, European Union (EU), and Japan felt a need to harmonize the requirements of pharmaceutical products, which led to the establishment of International Conference on Harmonization of Technical Requirements for the Registration of Pharmaceuticals for Human Use (ICH), with observers from WHO, Canada, and EFTA (Handoo et al., 2012). According to ICHQ6 (Quality guideline of International Conference on Harmonization of technical requirements for registration of pharmaceuticals for human use), specifications are the critical quality standard of tests in the form of numerical value or range to which a drug substance or drug product should conform (ICH, Q6A, 1999).

1.2 OBJECTIVES AND SCOPE OF DESIGN OF MATERIALS AND PRODUCT SPECIFICATIONS

A drug substance or its product needs to comply with the pharmacopoeial monograph. In case the monograph is not available then it should comply with the specifications mentioned in the NDA (new drug application). Regulatory authorities of some important pharmaceutical markets like the United States, EU, and Japan took an initiative to harmonize NDAs in the form of ICH guidelines to decrease the differences in technical requirements of various regulatory agencies for drug development. The ICH provided a platform for harmonization through feedback from both industry and regulatory representatives. ICHQ6A is one of the key ICH guidelines that is concerned with the specifications of new drug substances and drug products, while ICHQ6B deals with specification designing for biologicals (ICHQ6, 1999). The Food and Drug Administration (FDA) published a guidance pertaining to it with an objective to establish a single set of global specifications for new drug substances and their products (FDA, US, 2000).

The main objective of ICHQ6 is to identify the critical quality attributes that impact safety and efficacy of the drug substance or drug product and provide the reference to analytical procedures for their testing with acceptance criteria while maintaining the adequate accuracy and precision. Besides this, quality by design (QbD) approaches and clinical experience are the tools that are employed in establishing the specifications and nowadays this data is solicited by regulatory agencies like FDA. All the manufacturers need to propose and justify their acceptance criteria to regulatory authorities in the form of specifications for approval. This led to the thorough characterization of raw materials and final products by the

manufacturers to ensure that they don't put the patient at risk due to inadequate safety, quality, or efficacy of the pharmaceutical product. Hence, designing of specification became an indispensable step in pharmaceutical product development.

1.3 PHARMACEUTICAL PRODUCT SPECIFICATION

1.3.1 Concepts and the Need

The specification is a quality standard that determines the most appropriate means for reaching the stated objective of the manufacturer. Specifications cover general quality characteristics of the pharmaceuticals particularly related to pharmacotechnical aspects. Monographs or general chapters in pharmacopeia provide approved specifications. Some relevant information is also obtained by technical guidelines. For example, besides the ICHQ6 guideline, Q1, Q3, Q4, Q8, Q9, Q10 on stabilities, impurities, pharmacopeia, pharmaceutical development, quality risk management, and pharmaceutical quality system, respectively, are helpful in identifying the critical quality attributes and quantitative development of the acceptance criteria. An appropriate specification for each aspect of quality studied during the phase of development and during the validation of the manufacturing process should be determined as the applicant has to furnish appropriate analytical validation data in the marketing authorization application (MAA). The width of the upper and lower specification limits affect the shelf-life of the product. The tighter the specification limits, the higher are the chances of batch rejection, whereas the broader the specifications, the higher the incidences of acceptance of poor quality of the pharmaceutical product (Riley et al., 2013).

The regulatory authorities recognize that only a limited amount of data may be available at the time of filing. Therefore, the revised acceptance criteria can be proposed later when adequate data is available. Hence, the industry has an opportunity to loosen or tighten their specification based on the data with justification for each procedure and related acceptance criterion (FDA, US, 2000). The quality of drug substances and drug products is judged by the specifications applied to them throughout development, therefore, designing of specifications need to be done cautiously with appropriate justification.

1.3.2 The Rationale for Designing Specifications

Specifications are one of the essential components of quality assurance and are designed with a rationale to assist the manufacturers to select scientifically based test procedures for pharmaceutical development in a harmonized way with the adequate justification of acceptance criteria for the new pharmaceutical product. The acceptance criteria are set on the basis of experience and data furnished from the representative and registration batches. The justification for the acceptance criteria is based on the development data, stability data of scale-up/validation batches along with the primary stability batches at different conditions, test data for a drug product or drug substance that were used in toxicology and clinical studies, pharmacopeial standards, etc. Besides this, while designing the specifications, due emphasis should be given to analytical and manufacturing variability.

Adequate designing of specifications assures the quality of the pharmaceutical product at release and during shelf-life (FDA, US, 2000).

1.3.3 Associated Terminologies

There are some terminologies used in this chapter with which reader must be acquainted. Therefore, such terminologies are explained below for better clarity.

- *Drug substance*: It is the active ingredient that is responsible for physiological or pharmacological action but does not include any intermediates used in its synthesis.
- *Pharmaceutical product*: It is the product in a finished dosage form that contains drug substance, with or without other inactive ingredients (FDA, US, 2017).
- *Critical quality attribute*: These are the parameters that need to be controlled effectively as they have a huge impact on the safety and/or efficacy of the product (Riley et al., 2013).
- *Periodic or skip testing*: It is the testing performed on specific tests parameters on preselected batches at predetermined intervals, rather than performing it on a batch-to-batch basis as it is hypothesized that the batches that were not tested still comply to the specifications for that product. For example, microbiological testing or residual solvents for solid oral dosage forms. This concept is generally implemented postapproval and in case the results suggest to reinstate routine testing, then batch-by-batch release testing needs to be initiated.
- *Parametric release*: This employs the monitoring of operational alternatives that can be more accurately controlled and measured instead of routine testing. For example, monitoring of parameters like temperature, pressure, and time can be done for adequately validated terminal sterilization to have better sterility assurance than performing end-product sterility testing. However, parametric release requires revalidation of the process after some interval of time.
- *Alternative procedures*: These are the alternative methods that are comparable or superior to the official procedure and can be used to measure an attribute. For example, the spectrophotometric procedure can be used for release tablets that do not degrade during manufacturing instead of an official chromatographic method. However, chromatographic procedures need to be applied during the shelf-life analysis.
- *Reference standard/reference material*: It is a substance used as the standard in an identification, assay, or purity test (FDA, US, 2000).

1.3.4 Types of Specifications

There are three types of specifications as indicated in Fig. 1.1 that set acceptance criteria at different stages of product development.

Each of this type is defined as follows:

- *In-process specification*: It is the acceptance criteria for tests performed during the manufacture of a drug substance or drug product prior to their release (Chen et al., 2017). However, it should be validated to show that product performance characteristics do not change from the in-process stage to the release stage.

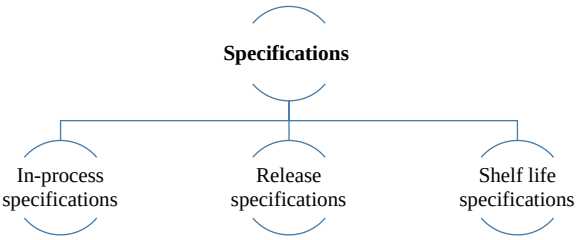

FIGURE 1.1 Types of specifications.

- *Release specification*: It is the regulatory acceptance criteria for the release of the pharmaceutical product. It is tighter than the shelf-life specification to establish restrictive criteria for the release of the product.
- *Shelf-life specification*: It is the regulatory acceptance criteria applicable throughout the shelf-life of the pharmaceutical product.

It is to be noted that the different acceptance criteria for release and shelf-life specifications apply in case of drug products only. It is done to establish more restrictive criteria for the release of a drug product than to the shelf-life so that the product remains within the regulatory acceptance criterion throughout its shelf-life. In the EU, different release and shelf-life specifications are admissible where applicable but in Japan and the United States, this concept is applicable to in-house criteria only and not to regulatory release criteria (ICH, Q6A, 1999).

1.4 DESIGNING OF SPECIFICATION

1.4.1 Guidelines for Designing Specification for Drug Substance/Drug Product

The experience gained through QbD approaches, lab batches stability data, and registration batches data provides insight into the process and analytical variability, which is a handful for designing of the specification. Various statistical tools like mean, median, mode, capability analysis, standard deviation, etc. are instrumental for the quantitative development of acceptance criteria. Regulatory requirements as mentioned in the ICH guideline Q6A and Q6B has a paramount impact in designing of the specification. These guidelines help in identification and assignment of appropriate range to critical quality attribute. However, approaches other than those set forth in this guideline are also acceptable. Besides this, the regulatory authorities' expectations also influence the design of specification. For example, FDA seeks clinical experience for establishing specifications. Therefore, the pharmaceutical industry has to fulfill all the regulatory requirements to furnish acceptance criteria for various critical quality attributes that provide the quality assurance of the product (Riley et al., 2013).

1.4.1.1 Justification for Specification

The pharmaceutical manufacturer has to provide a scientific rationale for the selection of the critical quality attributes and quantitative acceptance criteria. The justification should consider the key points depicted in Table 1.1.

TABLE 1.1 Key Points to Be Considered While Justifying Specifications

Key points while justifying specifications
• Specifications are linked to the manufacturing process and account for variability arising due to it • Specifications are linked to analytical procedures and account for variability arising due to them • Specification accounts for the stability, scale-up/validation batches • Specifications are linked to preclinical and clinical studies • Specifications are linked to development data and process validation data for proposing exclusion of tests where applicable

Justification of specification for each procedure and acceptance criterion needs to be prepared at the initial phase of specification setting. The relevant approaches are based on development data, pharmacopoeial standards, stability studies data, toxicology, and clinical studies data. Therefore, the initial specifications are based on the data of the tests of the parameters of the product, which are critical for controlling its quality and are supported by toxicology and early clinical studies. The applicant needs to justify an alternative approach. It is important to consider the manufacturing process data from the manufacturing sites for establishing initial tests and acceptance criteria. Stability and validation batches data plays a key role in the justification of specifications. The range of the specifications should be such that it can accommodate the reasonable analytical and manufacturing variability. However, the actual results obtained form the platform for the selection of the relevant approach. Graphical representation of the results is appreciated as it eases the process of justifying individual acceptance criteria clearly (ICH, Q6A, 1999).

1.4.1.2 Pharmacopoeial Test and Evolving Methodology

Different legal authorities exist for different regions for quality control of pharmaceuticals. These pharmacopeias contain monographs that contain information about specific tests for the drug substance or drug product. For example, USP (United States Pharmacopoeia) contains the monograph of the drug product, USP-NP (USP and National Formulary) contains the monograph of excipients, etc. "General requirements for dosage form" in international pharmacopeia also provide recommendations in this regard. However, in case the monograph does not exist for a particular pharmaceutical then the manufacturer has to follow the specification established in the regulatory filing. ICH guideline 4QB describes the evaluation and recommendation of pharmacopoeial texts with topic-specific annexes that provide information about these texts with their implementation.

There are general chapters in pharmacopeia designated as "< >" that contain descriptions of methods, unlike monographs, which are specific to drug substance or drug product (Riley et al., 2013). A pharmacopoeial harmonization policy was also approved by the Pharmacopoeial Discussion Group, which works to harmonize the monograph to the general chapter to reduce the manufacturer's burden by performing different analytical procedures in different ways with different acceptance criteria (USP Chapter ‹1196›, 2006).

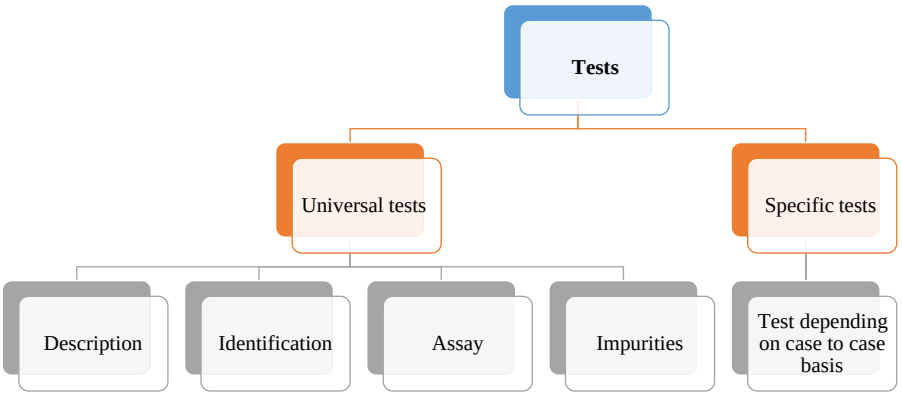

FIGURE 1.2 Types of tests of drug substances and drug product. *Source: Based on, EMEA, 3AQ11a, 1991. Guideline on Specifications and Control Tests on the Finished Product. Directive 75/318/EEC.*

The pharmacopoeial monograph usually provides the statements about the pharmaceutical like name, description, packaging, storage, identification, tests, procedures, acceptance criteria, and storage conditions (Chan et al., 2014). The tests for drug substances and drug products are universal and specific as described in Fig. 1.2 (EMEA, 3AQ11a, 1991).

Some of the universal tests/criteria are described in Table 1.2 for drug substances and drug products.

Similarly, Fig. 1.3 indicates the specific tests of drug substance whereas Fig. 1.4A–C indicate the specific tests for the oral solid drug product, oral liquid drug product, and parenteral drug product.

All the above-said parameters need to be analyzed by analytical procedures according to the approved validation protocol. Good analytical precision is required to avoid out-of-specification (OOS). In case a new source of error has been identified that had not occurred during method development or validation, then as a remedial step the modification of method needs to be done with method revalidation of appropriate parameters (Riley et al., 2013). Mostly the basic scheme of the validation procedures is similar but sometimes they differ in particular parameters. In this situation, ICH and FDA guidelines are helpful in the pharmaceutical and biomedical analysis, respectively (Mikus and Novotny, 2015).

Generally physical and physicochemical methods are used for the analysis of drug substances and their products. Physical methods involve methods for determination of physical properties like solubility, color, density or specific gravity, moisture content, transparency, melting, freezing, boiling points of a drug substance or its product. Physicochemical methods like optical, electrochemical, and chromatography are undertaken to study the resultant physical phenomena of chemical reactions. Titration methods are also extensively used in cases where sensitivity at milligram (mg) level is optimum with negligible interference. Chromatographic methods like gas chromatography (GC), high-performance liquid chromatography (HPLC), and ultra-performance liquid

TABLE 1.2 Universal Tests/Criteria for Drug Substance and Drug Product

Tests/ Criteria	Drug Substance	Drug Product
Description	A qualitative description of the physical state of the new drug substance, that is, solid/liquid, color	A qualitative description of the dosage form, that is, shape, size, color
Identification	It includes specific test for the new drug substance to establish its identity while discriminating it from the closely related structure that are likely to be present, that is, infrared spectroscopy, chromatographic procedures involving different principles, or combination of tests into a single procedure for separation (e.g., HPLC/UV diode array, HPLC/MS, or GC/MS). It also includes a procedure for a chiral assay for an optically active substance	It includes a specific test for the new drug substance to establish its identity while discriminating it from the closely related structures that are likely to be present, that is, infrared spectroscopy, chromatographic procedures involving different principles or combination of tests into a single procedure for separation (e.g., HPLC/UV diode array, HPLC/MS, or GC/MS)
Assay	A specific procedure to determine the content of the drug substance. It should be a stability-indicating procedure	A specific procedure to determine the content of the drug substance. It should be the stability-indicating procedure. It is also acceptable to use the same procedure for both assays of the new drug substance and quantitation of impurities
Impurities	It includes organic impurities, inorganic impurities, and residual solvents	It includes organic impurities, inorganic impurities, and residual solvents. It is to be noted that the process of impurities is normally controlled during drug substance testing, therefore, they are not included in the total impurities limit. However, if the synthesis impurity is also a degradation impurity then it should be monitored and included in the total degradation product limit

GC, Gas chromatography; *HPLC*, high-performance liquid chromatography; *MS*, mass spectrometry.
Based on, EMEA, 3AQ11a, 1991. Guideline on Specifications and Control Tests on the Finished Product. Directive 75/318/EEC.

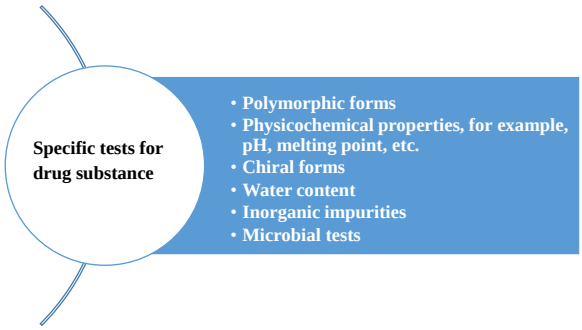
Specific tests for drug substance
• Polymorphic forms
• Physicochemical properties, for example, pH, melting point, etc.
• Chiral forms
• Water content
• Inorganic impurities
• Microbial tests

FIGURE 1.3 Specific tests of the drug substance.

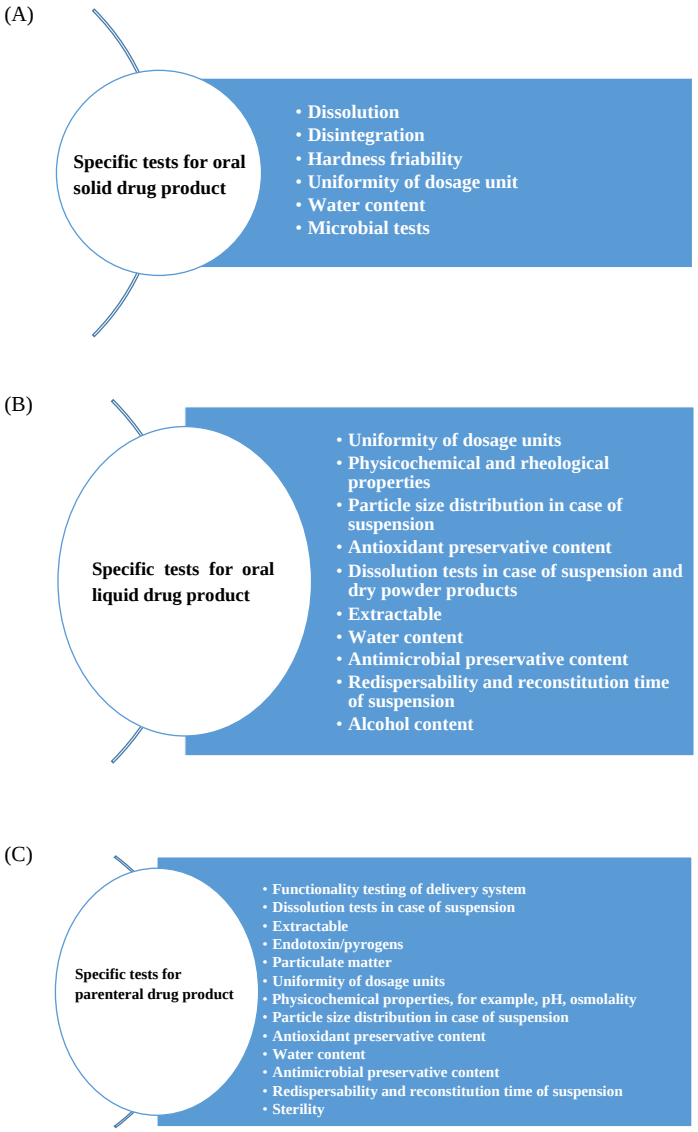
(A)
Specific tests for oral solid drug product
• Dissolution
• Disintegration
• Hardness friability
• Uniformity of dosage unit
• Water content
• Microbial tests
(B)
Specific tests for oral liquid drug product
• Uniformity of dosage units
• Physicochemical and rheological properties
• Particle size distribution in case of suspension
• Antioxidant preservative content
• Dissolution tests in case of suspension and dry powder products
• Extractable
• Water content
• Antimicrobial preservative content
• Redispersability and reconstitution time of suspension
• Alcohol content
(C)
Specific tests for parenteral drug product
• Functionality testing of delivery system
• Dissolution tests in case of suspension
• Extractable
• Endotoxin/pyrogens
• Particulate matter
• Uniformity of dosage units
• Physicochemical properties, for example, pH, osmolality
• Particle size distribution in case of suspension
• Antioxidant preservative content
• Water content
• Antimicrobial preservative content
• Redispersability and reconstitution time of suspension
• Sterility

FIGURE 1.4 (A) Specific tests of the oral solid drug product. (B) Specific tests of the oral liquid drug product. (C) Specific tests of the parenteral drug product.

chromatography are preferable. However, hyphenated techniques like GC−MS/MS or LC-NMR are considered to be powerful analytical tools with high sensitivity and accuracy using the very small amount of samples for analysis (Ravisankar et al., 2015). New analytical technologies or their modifications can be used if they are adequately justified and increase quality assurance (ICH, Q6A, 1999).

1.4.2 Guidelines for Designing Specification for Packaging Material

Packaging material has a huge impact on the identification, quality, and stability of a drug substance or its product, as it provides adequate degree of protection, presentation, identification, and information, and minimizes the loss of constituents without interacting with them so that it does not cause toxicity or hamper the quality to an extent beyond the limits specified in the individual monograph. The common packaging materials are container, closure, carton, and box. The containers may be of plastic, glass, metal (e.g., aluminum) and closure may be made of plastic, glass, cork, metal, or rubber. Since packaging material surrounds the pharmaceutical product throughout its shelf-life, there are some critical aspects of the packaging material that need to be considered for ensuring quality, integrity, and compatibility depending upon the material used. For example, containers made up of glass are tested by crushed glass test, chemical resistance test, etc. The closure materials are tested by self-seal ability test, transparency test, extractive test, etc.

Various regulatory agencies like FDA, WHO, and ICH guidelines have laid down the requirement for testing of packaging materials. Similarly, the US, European, and Japanese pharmacopeias also describe packaging materials requirement and acceptance criteria through a different way of classification and presentation. The International Organization for Standardization also issues the standards on packaging (WHO Technical Report 902, 2002).

1.4.2.1 Justification for Specification

The selected packaging material needs to conform to prescribed standards as laid down by various guidelines depending upon the product nature, use, and climatic variables. However, the recommendations of the international pharmacopeia are only advisory; hence the in-house quantitative standards need to be ascertained. The specification of the packaging material should be such designed so that it controls the quality of the product against interaction of the packaging material with the product itself through leaching, absorption, or chemical means. Similarly, it should control the interaction of the product with the packaging material, which can adversely affect its physical properties and deteriorate its protective function. Besides this, the specification should be informative and instrumental in the correct identification of the product. The justification for the specifications should support the acceptance criteria that assure the fulfillment of the above-stated objectives throughout the shelf-life. It explains the suitability of packaging material based on some of the critical factors as highlighted in Fig. 1.5.

1.4.2.2 Pharmacopoeial Tests and Evolving Methodology

It is imperative to control the quality and security of packaging material. 21 Code of Federal Regulations Part 211, Subpart G defines the material examination and usage criteria (Takahashi and Aldridge, 2015). General chapters of various pharmacopeia also provide the information about the testing procedures. For example, Indian Pharmacopeia (2007), Volume 1, 6.1, 6.2, 6.3 provide container and closure information for pharmaceutical and parenteral products. The suitability of the container closure system is generally judged on the basis of studies like extraction studies, interaction studies (sorption/migration), moisture permeability, light transmission, or any additional treatments like sterilization, etc. The general parameters to be tested for packaging material are briefly given in Fig. 1.6.

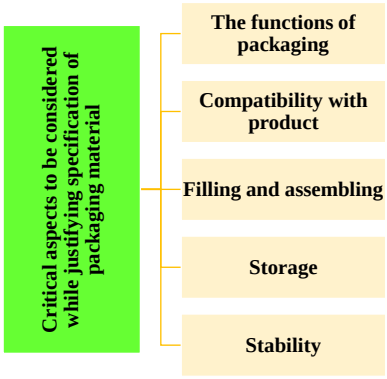

FIGURE 1.5 Critical aspects to be considered while justifying the specification of packaging material.

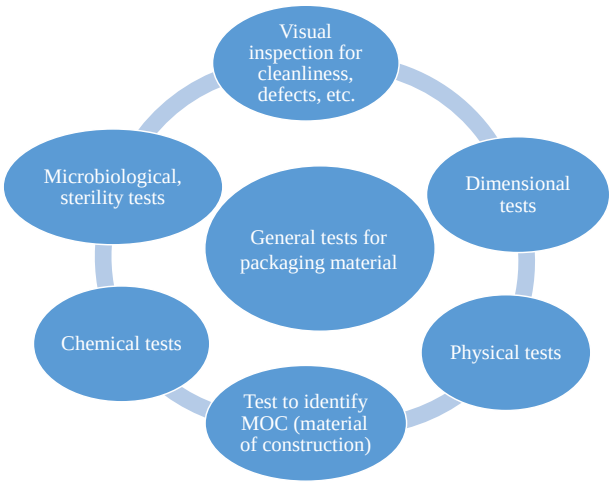

FIGURE 1.6 General tests for packaging material. *Source: Based on, EMEA, 3AQ11a, 1991. Guideline on Specifications and Control Tests on the Finished Product. Directive 75/318/EEC.*

The quality of a pharmaceutical product and its packaging material are interrelated therefore the quality assurance requirements for the packing materials are the same as subjected to the pharmaceutical product in line with GMP requirements.

1.5 HANDLING OF OUT-OF-SPECIFICATION

The OOS is the test results that fail to conform to the specifications established either by the manufacturer or in drug applications, official compendia, or drug master files. Since specifications ensure that raw material, containers, closures and finished drug products adhere to the established standards based on scientifically sound procedures, therefore, it is important to maintain the conformity of test results to established specifications. Therefore, in case of OOS, general CGMP regulations mandate well-documented, thorough, unbiased, timely, and scientifically sound investigation. These regulatory authorities provide some recommendations for finding the root cause of an

OOS. The investigation is generally carried out in two phases. Phase I investigation is carried out at the laboratory level, whereas phase II investigation is carried out in full-scale up to any level. A step-by-step summary of the general recommendations of handling OOS is described below.

1.5.1 Phase I Investigation

The first step is the identification and assessment of the accuracy of OOS results during laboratory investigation. Test preparations showing OOS should be retained, if stable, so that laboratory error or instrument malfunctions are tested using the same test preparation in question. It needs to be documented and analysts have to inform their supervisor of the situation. The supervisor evaluates potential problems that could happen w.r.t. the analyst and analytical tools. The analyst's knowledge of the process is tested and chromatograms are checked for the anomaly. Instrument and test procedure performance is checked along with verification of reference standards, solvents, etc. that are involved in the testing process. All the proceedings are documented with observation. In the case of the laboratory, the error is identified, the manufacturer needs to take corrective action to prevent recurrence of the identified error. However, if no analytical error is observed during this investigation then full-scale OOS investigation is conducted.

1.5.2 Phase II Investigation

This investigation usually consists of a review of the production process, sampling procedures, and/or additional laboratory work. It may include additional laboratory testing like retesting a portion of the original sample or resampling. It also involves evaluation of the impact of concerned OOS on already distributed batches. Such investigation comprises of a brief, clear, and informative statement of the cause for the investigation. Following it is the summary of all the aspects of the manufacturing process that may contribute to the problem. Root cause analysis is done using various tools like fishbone diagram, why−why analysis, etc. The results are compiled with the assignment of actual or probable cause. It is reviewed whether the same problem has occurred previously. Usually, the root cause identified at this stage involves lack of robustness in the product, inadequate raw material characterization or substantial variation introduced by one or more unit operations of the manufacturing process, or a combination of all these factors. Finally, the corrective actions are stated to prevent the reoccurrence of the same problem. If the OOS investigation successfully identifies the root cause at this stage then the investigation can be terminated after including comments and the signatures of concerned production and quality control personnel (FDA, US, 2006).

1.6 FINISHED PHARMACEUTICAL PRODUCT

1.6.1 Regulatory Requirements

The pharmaceutical industry is a highly regulated industry that aims to develop a product that suffices the diverse market requirements while protecting the well-being

of the customer. National governments of various countries have established regulatory authorities and formulated guidelines for drug regulations in their region. Some of the regulatory bodies are FDA, European Medicines Agency, Department of Health, Therapeutic Goods Administration, Pharmaceutical and Medical Devices Agency, Tanzania Food and Drugs Authority, Commonwealth Independent States, Medicines Control Council, Agência Nacional De Vigilância Sanitária (National Health Surveillance Agency), and the Gulf Co-Operation Council. Efforts to harmonize various elements of drug regulatory activities have been initiated by various interharmonized documents called Common Technical Documents that are used for NDA and MAA in ICH regions like the United States, EU, and Japan as well as in some non-ICH regions like Australia and Canada. It is the recommended format for NDA by FDA, and mandatory format in the EU and Japan (Handoo et al., 2012). It has five modules, which are as follows:

- Module 1: Regional administrative information
- Module 2: Quality overall review (not part of CTD)
- Module 3: Quality (nonclinical overview, clinical overview, nonclinical summary, clinical summary)
- Module 4: Nonclinical study report
- Module 5: Clinical study report (ICH, M4, 2016)

The quality guidelines of ICH lay down the framework for the CTD, and the pharmaceutical industry has to conform to CTD with respect to the general analytical requirement to assure the quality of the product. CTD can also be used for clinical trials application with some modification (Riley et al., 2013).

One should have knowledge of differences and commonness between the pharmaceutical legislation and regulatory requirements specific to regulated and emerging markets for worldwide regulatory dossier filing. For example, the general procedure during abbreviated new drug application (ANDA) approval in the United States is that once a complete application has been filed by the applicant in acceptable form, the OGD (Office of Generic Drugs)/CDER (Centre for Drug Evaluation or Research) review the chemistry, pharmacology, microbiology, clinical pharmacology and biopharmaceutics, medical and labeling review. If all these are accepted then after successful plant inspection the ANDA is approved (Handoo et al., 2012).

The monitoring of quality characteristics pertaining to the manufacturing process and its validation for developing finished products are required while applying for marketing authorization dossier. It helps in maintaining the consistency of the quality of the finished product produced through the identification of the key features of the process and the product and increases the scalability and batch reproducibility. Specifications help in quantitatively monitoring these parameters (EMEA, 3AQ11a, 1991). The major quality characteristics that need to be monitored through specifications are indicated in Table 1.3.

Since, ICH Q6A, Q6B, and Q2 help the pharmaceutical industry to understand the expectations of the regulatory authorities for the dossier, hence, the adherence to the guidelines is imperative during drug development.

TABLE 1.3 Major Quality Parameters of the Finished Product to Be Monitored Through Specification

- Pharmaceutical aspects determined by physical tests, that is, friability, hardness
- Identification and assay of active pharmaceutical ingredient
- Identification and assay of preservative or another excipient like antioxidant
- Purity test, that is, microbial, residual solvent
- Pharmaceutical test, that is, dissolution
- Safety test, that is, toxicity

API, Active pharmaceutical ingredient.
Based on, EMEA, 3AQ11a, 1991. Guideline on Specifications and Control Tests on the Finished Product. Directive 75/318/EEC.

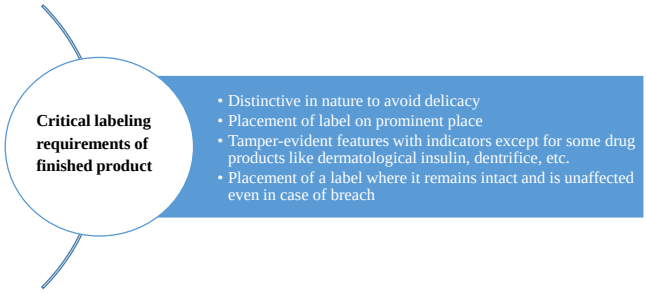
Critical labeling requirements of finished product
• Distinctive in nature to avoid delicacy
• Placement of label on prominent place
• Tamper-evident features with indicators except for some drug products like dermatological insulin, dentrifice, etc.
• Placement of a label where it remains intact and is unaffected even in case of breach

FIGURE 1.7 Critical labeling requirements of the finished product. *Source: Modified from, Takahashi, K., Aldridge A.A., 2015. Packaging & Labeling. Regulatory Education for Industry (REdI): Focus on CGMPs & FDA Inspections Sheraton. Silver Spring, MD.*

1.6.2 Schematic Plan for Verification of Specification

The pharmaceutical industry has to showcase in its marketing authorization dossier the schematic plan for verification of specification, that is, whether the tests are performed periodically or routinely. If the pharmaceutical/chemical/physical/biological/microbiological tests are done periodically then the periodicity of tests should also be indicated. The scheme should also indicate any modification based on experience during drug development and related adjustments made on the basis of results. However, the product should comply with the specifications regardless of the scheme employed (EMEA, 3AQ11a, 1991).

1.6.3 Labeling

The USP defines labeling as written, graphic, or printed matter applied on the container or enclosed in any package. Labels are applied to the container of the product throughout manufacturing. They help in identification of the product and prevent cross-contamination besides providing information regarding its strength, purity, packaging, storage, the name of the manufacturer or distributor, manufacturing and expiry date, quantity, and special instructions (Veronin, 2011). Critical labeling requirements are shown in Fig. 1.7.

1.6.4 Shelf-Life and Storage

Shelf-life is determined on the basis of storage conditions. The physical, chemical, biopharmaceutical, microbiological, and biological stability profile of the product is studied

in different stability conditions. Accelerated stability study helps in the extrapolation of real-time data beyond the recommended period using the Arrhenius equation, to establish tentative shelf-life. The proposed shelf-life is on the basis of the least stable stability profile of the product. The manufacturer has to continue the real-time stability study and establish the data for submission to the registration authority, however, the proposed shelf-life should not be more than the twice the period covered by the real-time studies (Matthews, 1999).

The general storage conditions as defined by WHO are a dry well-ventilated area having temperatures 15°C−25°C or as per climatic conditions, up to 30°C. It is to be noted that this definition excludes extraneous odors, intense light, and contamination. Since the normal storage conditions are not always applicable, therefore, the recommended storage conditions should be determined in the conditions prevailing within the country of use. The proposed storage condition of the finished product should be such that the API does not degrade easily and no significant changes are caused by the quality parameter. Precautionary statements, like "protect from light," etc. can be included based on characteristics of the product but should not be used to hide the stability problems (WHO, 1997).

1.7 IMPORTANCE OF SPECIFICATION ON PHARMACEUTICAL QUALITY SYSTEM

Specifications set the quality level of a drug substance or its product that is intended for marketing. Since the specifications are based on the data gathered from the batches analyzed, they pave the path for reaching the stated objective. Compliance with a drug substance/drug product to the specification establishes its efficacy, safety, and consistent pharmacotechnical properties. Moreover, the manufacturer can deduce the storage condition at which the behavior of the medicinal component is maintained in compliance with the specifications (EMEA, 3AQ11a, 1991). If specifications are not designed appropriately then it can lead to false OOS, which can cause recall of good batch. Moreover, it is also recommended to have alert limits based on stability data and batch history. It is helpful in avoiding OOS by chance where even though the mean of the result is well within the limit, any one value is outside the limit (Riley et al., 2013). Hence specifications are imperative as per pharmaceutical quality system perspective.

1.8 CONCLUSION

Designing of the specifications of drug substances and their products has gained importance in drug development, biopharmaceuticals, and analytical method due to regulatory requirements to get the product approved for marketing. It helps in producing a quality product with cost-effective procedures, which is ultimately helpful for the review process by regulatory bodies. It controls the physical, chemical, microbiological, or biological characteristics along with the analytical target profile of the product within the desired range to ensure its quality. It builds robustness, trustworthiness in the product while increasing the consistency to manufacture quality product every time. Identification and controlling

of the factors that affect the product quality on the basis of scientific knowledge form the platform of principle for designing of the specification. Hence, for companies to excel in global competition, the importance of specification in drug development cannot be ignored.

Acknowledgment

Authors would like to express sincere gratitude to CSIR, New Delhi, India for awarding the research grant (Project ID: 02(0279)/16/EMR-II) to support this work. We would also like to thank Sentiss Pharma Pvt. Ltd. for imparting training and experience on the given subject, which helped in the completion of the chapter.

ABBREVIATIONS

ANDA	abbreviated new drug application
API	active pharmaceutical ingredient
CDER	Centre for Drug Evaluation or Research
CTD	common technical document
EFTA	European Free Trade Association
EU	European Union
FDA	Food and Drug Administration
GC–MS	gas chromatography–mass spectrometry
GMP	good manufacturing practices
ICH	International Conference on Harmonization of Technical Requirements for the Registration of Pharmaceuticals for Human Use
LC-NMR	liquid chromatography-nuclear magnetic resonance
MAA	marketing authorization application
NDA	new drug application
OGD	office of generic drugs
OOS	out-of-specification
QbD	quality by design
USP	United States Pharmacopoeia
USP-NF	United States Pharmacopoeia and National Formulary
WHO	World Health Organization

References

Chan, C.C., Chow, K., Mckay, B., Fung, M., 2014. Specification setting and stability studies in the development of the therapeutic solution. Therapeutic Delivery Solutions. John Wiley & Sons, Inc, Hoboken, NJ.

Chen, W., Stithit, S., Zheng, J.Y., 2017. Specification setting and manufacturing process control for solid oral drug products. Pharm. Theory Pract. e2, 677–693.

EMEA, 3AQ11a, 1991. Guideline on Specifications and Control Tests on the Finished Product. Directive 75/318/EEC.

FDA, US, 2000. Q6A specifications: test procedures and acceptance criteria for new drug substances and new drug products: chemical substances. Published in the Federal Register. 65 (251), 83041–83063.

FDA, US, 2006. Guidance for Industry Investigating Out-of-Specification (OOS) Test Results for Pharmaceutical Production.

FDA, US, 2017. 21CFR314.3, Definitions. Vol 5.

Handoo, S., et al., 2012. A comprehensive study on regulatory requirements for development and filing of generic drugs globally. Int. J. Pharm. Invest. 2 (3), 99–105. https://www.fda.gov/downloads/Drugs/DevelopmentApprovalProcess/SmallBusinessAssistance/UCM456372.pdf (Accessed on 16/01/2018).
ICH, Q6A, 1999. Specifications: Test Procedures and Acceptance Criteria for New Drug Substances and New Drug Products: Chemical Substances.
ICH, M4, 2016. Organization of the Common Technical Document for the Registration of Pharmaceuticals for Human Use.
Indian Pharmacopoeia, 2007. The Government of Indian Ministry of Health and Family Welfare, The Indian Pharmacopeia Commission, Ghaziabad. Vol. 1, 6.1, 6.2, 6.3, 363–372.
Matthews, B.R., 1999. Regulatory aspects of stability testing in Europe. Drug Dev. Ind. Pharm. 25 (7), 831–856.
Mikus, P., Novotny, L., 2015. On the importance of pharmaceutical analysis. Res. Rev.: J. Pharm. Anal. 4 (3), 13–14.
Ravisankar, P., Navya, C.N., Pravallika, D., Sri, D.N., 2015. A review on step-by-step analytical method validation. IOSR J. Pharm. 5, 7–19.
Riley, C.M., Rosanske, T.W., Riley, S.R.R., 2013. Specification of Drug Substances and Products: Development and Validation of Analytical Methods. Elsevier, Oxford.
Takahashi, K., Aldridge A.A., 2015. Packaging & Labeling. Regulatory Education for Industry (REdI): Focus on CGMPs & FDA Inspections Sheraton. Silver Spring, MD.
USP Chapter ‹1196›, 2006. Pharmacopeial Harmonization. US Pharmacopeia (USP) 29–National Formulary (NF) 24 [US Pharmacopeial Convention (USP)]. Rockville, MD, pp. 3031–3035.
Veronin, M., 2011. Packaging and labeling of pharmaceutical products obtained from the internet. J. Med. Internet Res. 13 (1), e22, 1–13.
WHO, 1997. Quality Assurance of Pharmaceuticals—A Compendium of Guidelines and Related Materials. Geneva, Vol. 1.
WHO Technical Report 902, 2002. Guidelines on packaging for pharmaceutical products.

Further reading

FDA, US, 1998. Guidance for Industry Manufacturing, Processing, or Holding Active Pharmaceutical Ingredients. Published in the Federal Register, 53.
ICH, Q8 (R2), 2009. Pharmaceutical Development.

CHAPTER

2

Engineered Mesenchymal Stem Cells as Nanocarriers for Cancer Therapy and Diagnosis

Sunita Chawla[1], *Muktika Tekade*[2], *Rahul Maheshwari*[1], *Yashu Chourasiya*[3], *Gillian A. Hutcheon*[4] *and Rakesh K. Tekade*[1]

[1]National Institute of Pharmaceutical Education and Research (NIPER)—Ahmedabad, Gandhinagar, India [2]School of Pharmacy, Devi Ahilya Vishwavidyalaya, Takshila Campus, Indore, India [3]Department of Pharmacology, Shri Bherulal Pharmacy Institute, Indore, India [4]School of Pharmacy and Biomolecular Sciences, Liverpool John Moores University, Liverpool, United Kingdom

OUTLINE

2.1 Introduction 20
2.1.1 Nanotechnology as an Emerging Platform in Cancer Disease Management 20
2.1.2 Mesenchymal Stem Cells 23
2.1.3 Human Mesenchymal Stem Cells 25

2.2 Engineering Mesenchymal Stem Cells as a Novel Formulation Strategy in Cancer Treatment 27
2.2.1 Nanoparticles Engineered Mesenchymal Stem Cells in Breast Cancer Management 30
2.2.2 Lung Cancer 31
2.2.3 Brain Cancer 34
2.2.4 Bone Cancer 39
2.2.5 Ovarian Cancer 42
2.2.6 Other Mesenchymal Stem Cell Nanoparticles in Cancer Treatment 42

2.3 What Future Holds for Multifunctional Stem Cell Platform? 46

2.4 Conclusion and Future Prospects 48

Acknowledgment 49

Abbreviations 49

References 51

Biomaterials and Bionanotechnology
DOI: https://doi.org/10.1016/B978-0-12-814427-5.00002-0

© 2019 Elsevier Inc. All rights reserved.

2.1 INTRODUCTION

2.1.1 Nanotechnology as an Emerging Platform in Cancer Disease Management

Cancer is a prominent driving factor of mortality and morbidity across the world (Soni et al., 2017). Consequently, the growth of novel drug delivery systems, such as nanocarriers, is very important for future cancer therapy (Maheshwari et al., 2015a; Mody et al., 2014). The function of nanocarriers is to enhance the pharmacologic properties of traditional chemotherapy methods by varying the biodistribution and pharmacokinetics of the drug. Nanomedicine is defined as the utilization of nanotechnology for the design of therapy, diagnosis, control, regulation, and proper functioning of living systems (Tekade et al., 2017) and is being widely used in the medical field, especially in drug delivery (Al-Qattan et al., 2018).

In drug delivery applications, drugs can be delivered to specific cells using nanoparticles (NPs) (Maheshwari et al., 2015b; Soni et al., 2016). NPs are a colloidal delivery system with size from 1 to 1000 nm and can be either a matrix or vesicular type with each possessing different properties and release characteristics (Kreuter, 1994). Moreover, NPs have huge aspect ratio compared with other carriers and a good capability to absorb and carry additional compounds. When the agent of interest (e.g., chemotherapeutic, radionucleotide, or DNA) is dissolved, captured in, adsorbed, or attached to their surface, NPs are able to prevent their premature degradation and allow prolonged release (Muniswamy et al., 2019).

Prior studies have shown that the encapsulation of drugs in colloidal delivery systems allows a considerable decrease in the required drug dose and thus reduces toxic effects (Tekade, 2018). One of the problems with NPs is the imperfect biodistribution in the host and the difficulty in targeting a specific organ in the body. The nanotoxicity profile of NPs must also be accounted for in the design of new therapeutic devices. There are different types of NPs in targeted drug delivery systems such as liposomes, polymeric micelles, drug−polymer conjugates, dendrimers, etc. (Fig. 2.1). The source materials of engineered NPs are either from biological origin such as; phospholipids, lipids, lactic acid, dextran, dendrimer, and chitosan, or from nonbiological sources such as synthetic polymers, gold, carbon, silica, and metals (Tekade et al., 2014, 2015a; Dwivedi et al., 2013; Choudhury et al., 2017).

NPs are proficient in targeting tumors and can improve cancer therapy. NPs can also enhance the stability of drugs and protect them against degradation but are prone to form agglomerates that can potentially occlude capillaries (Choudhury et al., 2017; Ghanghoria et al., 2016). The well-known phenomenon of enhanced permeation and retention (EPR) effect can be utilized to passively accumulate NPs in tumors but this is likely to be limited to tumors that are well-perfused (Kobayashi et al., 2014); that being said, even inside extremely vascularized tumors, the presence of supraperfused and hypoxic areas have been recognized. Active targeting strategies for surface-functionalized NPs utilize specific ligands with a binding capacity to surface antigens or receptors that are overexpressed on tumor cells (Singh Dhakad et al., 2013). While a considerable improvement in delivery efficacy has been observed with targeted NPs, often these targeting approaches still rely on the early passive gathering at tumor sites with the help of the EPR effect

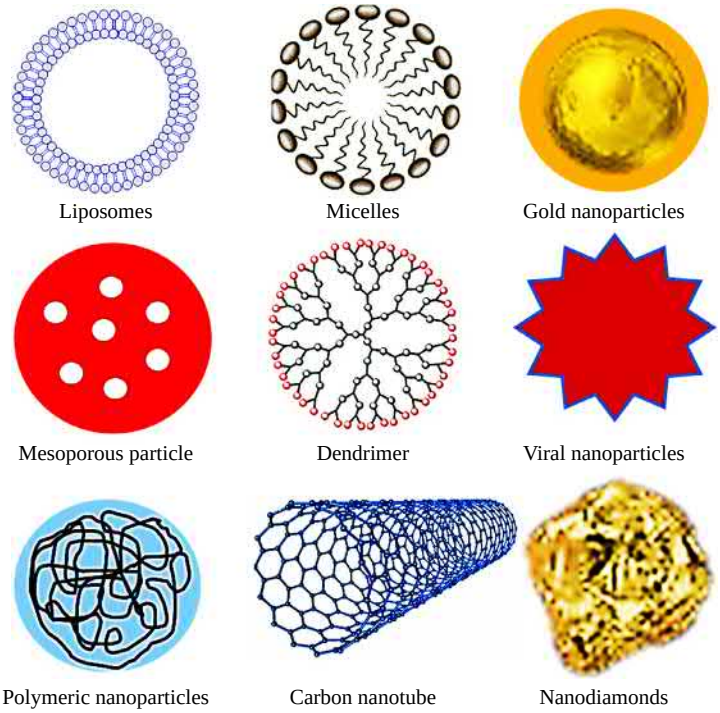

FIGURE 2.1 Schematic diagram of novel nanocarrier drug delivery systems (DDS) for cancer treatment. *DDS*, drug delivery systems.

(Bae and Park, 2011). In such instances, considering their tumor-tropism properties, mesenchymal stem cells (MSCs) could essentially be used as cellular vectors to chaperone NP delivery in vivo to significantly enhance the active transmigration across the endothelial barrier and the subsequent accumulation of payload in the target tissues to a greater extent (Tekade et al., 2015b). A field that is growing fast is nanopharmacology, which aims to improve drug delivery to an exact location with high efficacy and fewer unwanted effects.

Drug-loaded NPs are utilized to enhanced delivery and uptake of the drug to the target cells and thus decrease the unwanted effects of the free drug to nontarget cells, but to achieve this is a great challenge. Even with the assistance of the EPR effect (Dua et al., 2017) along with using conjugated targeting moieties (Loo et al., 2005; Farokhzad et al., 2006; Nasongkla et al., 2004), most of the NPs administered directly in the bloodstream are quickly cleared by the reticuloendothelial system (RES).

Often a small portion of NPs eventually gathers in a specific tumor site, which can be insufficient to exert the optimal therapeutic effect (Huang et al., 2010; Minchinton and Tannock, 2006). Other limitations hindering efficacy are the dense extracellular matrix, elevated intratumoral (IT) interstitial fluid pressure, strict vascular endothelial cell barriers, and the particularly solid tumor construction within hypoxic areas (Jain and Stylianopoulos, 2010; Primeau et al., 2005). There are presently few FDA permitted nanomedicines available on the market: brentuximab vedotin (targets protein CD30), Trastuzumab emtansine [targets the human epidermal growth factor receptor 2 (HER2)], Doxil (increases tumor accumulation by the EPR effect and kills cancer cells), DaunoXome, Marqibo, Abraxane (Dawidczyk et al., 2014).

Beyond drug delivery, other applications of NPs in nanomedicine include detection and diagnosis, gene delivery, biomolecular mapping, and molecular imaging. NPs are utilized as a contrast agent in therapeutic imaging tools such as magnetic resonance, optical imaging, computed tomography, ultrasound, and many more. In vivo biological mechanisms occur at the nanoscale, so the use of metal NPs (e.g., colloidal gold, nanodiamonds, quantum dots, iron oxide crystals, and semiconductor nanocrystals) to cross biological barriers and interact with biomolecules in the fluids, tissues, or cells within the body opens a new gateway for treatment and diagnostics (Saraf et al., 2018).

The early detection of malignancy can be achieved by improving the tissue permeation and target-specificity by utilizing an NP-based diagnostic probe (Prabhu and Patravale, 2012). The advantage of taking a theranostic approach to multifunctional medical products is the ability for actual stalking of the targeted delivery of therapeutics to the patient (Melancon et al., 2012). Another therapeutic use is thermotherapy, which uses NPs to generate heat to target and destroy cancer cells (Johannsen et al., 2007). A few of the nanomedicines available and their application in the market are shown in Table 2.1. A more comprehensive review of these nanomedicines has previously been provided (Wang et al., 2013).

TABLE 2.1 Approved Nanoformulation for Cancer Treatment

Product	Therapeutic Agent	Nanoplatform	Uses	Approval Year	Reference
Doxil	Doxorubicin hydrochloride	PEGylated liposome	Treatment of Kaposi's sarcoma patients with HIV, ovarian cancer	1995	
Myocet	Doxorubicin	Non-PEGylated liposomes	Metastatic breast cancer	2000	Leonard et al. (2009)
Eligard	Leuprolide acetate	PLGH	Prostate cancer	2002	Sartor (2003)
Oncaspar	Asparginase	PEG	Acute lymphoblastic leukemia	2006	Dinndorf et al. (2007)
Abraxane	Paclitaxel	Albumin nanoparticle	Lung, breast, pancreatic cancer	2005	Miele et al. (2009)
Marqibo	Vincristine	Liposome	Lymphoblastic leukemia	2012	Silverman and Deitcher (2013)
Onivyde	Irinotecan	Liposome	Pancreatic cancer	2015	Passero Jr et al. (2016)
LEP-ETU	Paclitaxel	Liposome	Ovarian cancer	2015	Sofias et al. (2017)
Vyxeos	Daunorubicin and cytarabine	Liposome	AML	2018	

AML, Acute myeloid leukemia; *PLGH*, poly (DL-lactide-*co*-glycolide).

2.1.2 Mesenchymal Stem Cells

In tumor disease management the poor biodistribution of chemotherapeutic agents, especially in inherent solid tumors, remains an important challenge. Thus, approaches that promote tumor-targeted drug delivery have the possible way to augment therapeutic efficacy. While painstaking endeavors are delivered to construct nanocarrier systems that can enhance drug delivery, new paradigms that exploit the utilization of cellular carriers with homing properties to allow extensive IT distribution could be a feasible alternative. Of the potential cellular candidates, MSCs are an interesting example. MSCs are multipotent progenitor cells that are spindle-shaped with the ability to distinguish into tissue-specific cell types (Jo et al., 2010). The Global Society for Cell Therapy characterizes MSCs as having CD73, CD90, and CD105 surface markers and lacking CD11b, CD14, CD19, CD34, CD45, CD79a, and HLA-DR surface markers, compared with other cells (Dominici et al., 2006).

MSCs were recognized in 1970 by Friedenstein and colleagues (Friedenstein et al., 1970) and since then much research has been performed the use of MSCs in health care. The effectiveness of MSCs has been demonstrated in the therapy of both immune and nonimmune diseases, such as control of development, wound healing, and replacement of cells that are damaged or missing due to pathological conditions (Wei et al., 2013). However, there is still a growing concern around the possibility of tumor formation by the MSCs themselves (Torsvik and Bjerkvig, 2013).

In addition to the capability to distinguish into tissue-specific cell types, other capabilities of MSCs include contributing to the vascularization process and increasing the effects of immunosuppression (Sordi, 2009). MSCs are capable of regulating apoptosis and fibrosis, promoting angiogenesis, stimulating mitosis, as well as moderating immune responses (Shah, 2012). These unique tumor-tropic properties have resulted in the increasing use of MSCs as tumor-targeting vehicles in various tumor models including melanoma (Studeny et al., 2002), breast cancer, glioblastoma, and colorectal cancer (Gutova et al., 2008). MSCs have surface markers such as SDF-1 (stromal-derived-factor-1), IFN-γ, CCL5/CCR5, and CCR2 that permit them to home to places of inflammation, such as diseased tissues, in vivo (Zhao et al., 2014; Sohni and Verfaillie, 2013) and accelerate the regeneration of injured tissues.

Various nanomaterials have undoubtedly provided a multipurpose stage in biomedical applications. However, NPs may provide deprived delivery and tissue penetration into tumors because of their unsuitable size, shape, or surface chemistry (Smith et al., 2012). As such, the search for a universal carrier that could improve diagnosis and therapeutic plans has brought MCSs back into attention. In the past, engineering of MSCs for imaging and therapeutic purposes has been typically achieved through the transduction of MSCs via transfection albeit an inherent risk of transformation (Hodgkinson et al., 2010; Hu et al., 2010). Aside from tumor tropism, the therapeutic potential of MSC has also been attributed to a comprehensive range of other biological events such as antiinflammatory, immunomodulatory, and tissue reparative events. Indeed, studies have shown that MSCs express genes that code for a multitude of arteriogenic cytokines to encourage in vitro and in vivo arteriogenesis mainly because of paracrine mechanisms (Yagi and Kitagawa, 2013).

Furthermore, MSCs have low immunogenicity and can be found and harvested from many different tissues followed by ex vivo expansion to reach a clinically related number (Mariani and Facchini, 2012, Gao et al., 2013). In nutshell, by harnessing the unique

TABLE 2.2 Mesenchymal Stem Cell (MSC) Engineered Nanoformulation in Various Cancer Treatment

Carrier	Therapeutic Agent	Objective	Outcome	References
An exosome derived from MSC	Paclitaxel	To form paclitaxel-loaded exosome (derived from MSC)	Used as a drug delivery carrier in breast cancer treatment	Kalimuthu et al. (2018)
MSC loaded NPs	Doxorubicin	Dual drug loading using MSC and doxorubicin conjugated polymer	For the treatment of metastatic lung cancer	Yao et al. (2017)
MSC containing silica NPs	Doxorubicin	Targeted drug delivery using antigen–antibody reaction in the cytoplasm	The drug intratumoral drug distribution increased compared with encapsulated doxorubicin in silica NPs	Li et al. (2011)
MSC with NPs	Paclitaxel	Prolonged release drug delivery	Treatment of lung cancer	Layek et al. (2018)
MSC	TRAIL	Drug delivery through TRAIL expressing MSC	To treat metastasis cancer of lung, squamous, cervical, breast	Loebinger et al. (2009a)
hMSC	Telomerase hTERT gene	For examination of the neoplastic potential of stem cell	The hMSC can be used in tissue engineering and drug delivery	Serakinci et al. (2004)
MIAMI	Coumarin-6	To estimate the efficiency of MIAMI cells to cross BBB	NP-loaded MIAMI cells capable to cross BBB can be used in drug delivery in brain cancer	Roger et al. (2010)

hMSCs, Human mesenchymal stem cells; *NP*, nanoparticle.

tropism of MSCs, it is possible to formulate multifunctional nanoplatforms that strategically integrate the strengths of stem cells and nanomedicine for better active-targeted delivery. Table 2.2 provides a brief summary of nanoengineered MSC as a drug delivery carrier in cancer treatment.

The disadvantages of MSCs are that the vectors and cytokines used are limited and the fate of MSCs in vivo is little understood. It has also been reported that in addition to the tumor-tropic belongings, MSCs might also promote tumor angiogenesis and growth of various tumors due to their angiogenic and proneoplastic properties (Zhu et al., 2006b; Yu et al., 2008). It is believed that MSCs promote tumor growth in several ways (Galderisi et al., 2010); promoting angiogenesis, promoting the metastasis, moderating the immune response in cancer cells, and making a place to support cancer stem cell existence. The mass movement of MSCs from bone marrow and other organs to tumors is the primary important stage in MSCs homing behavior.

The mesengenic process involves the proliferation, commitment, lineage progression, differentiation, and maturation of MSC from different organs such as bone, cartilages, muscle, muscle tissues, etc. (Fig. 2.2) (DiMarino et al., 2013). The migratory behavior and tumor-tropic characteristics of MSCs make them useful carriers for targeted delivery of anticancer agents and they are currently being developed for stem cell therapeutic approaches that seek to cure damaged tissues, relieve inflammation, and treat cancers.

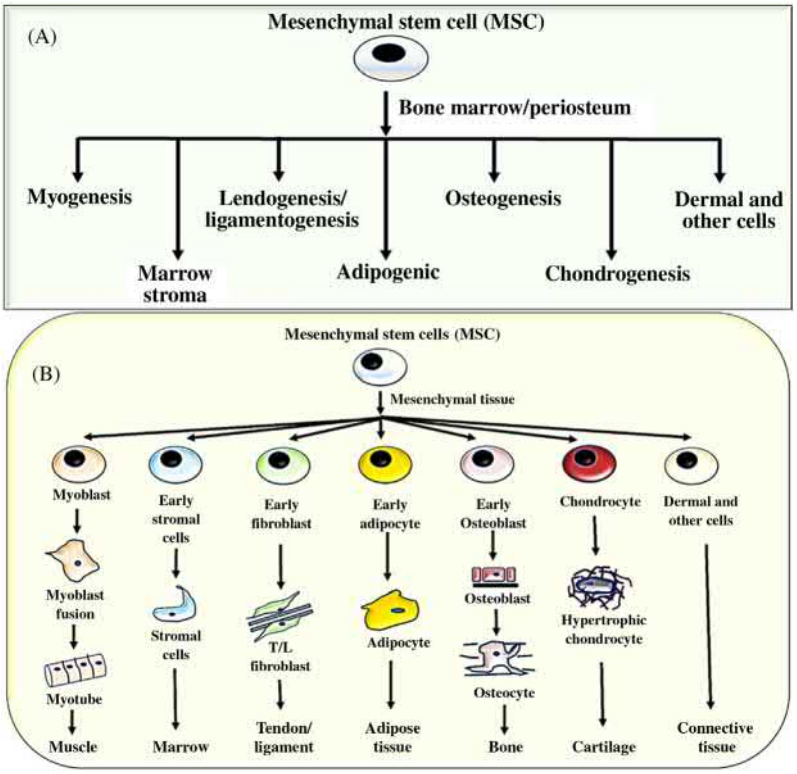

FIGURE 2.2 (A) Various mesangial process during the proliferation of MSCs in bone marrow or periosteum. (B) The mesangial process describing progression, differentiation, and maturation of MSCs. *MSC*, Mesenchymal stem cell.

However, the protumorigenicity properties might slightly reduce the interest in using MSCs as drug or gene therapy delivery carriers. Therefore, numerous plans need to be investigated to hinder the proneoplastic properties of MSCs while retaining their tumortropic properties. One such strategy is to selectively eliminate MSCs after the delivery procedure by activating their suicide gene (Gao et al., 2013).

2.1.3 Human Mesenchymal Stem Cells

The human mesenchymal stem cells (hMSCs) are gaining more importance toward their therapeutic uses in cancer treatment and research areas such as tissue engineering and regenerative medicine. hMSCs are nonhematopoietic cells resulting from bone marrow that express distinct surface markers from hematopoietic stem cells (HSCs). hMSCs can be characterized by the expression of CD105 (SH2), SH3, Stro-1, CD13, CD73, and CD90 but absence of HSCs indicators such as CD11b, CD14, CD19, CD34, CD45, CD79a, and HLA-DR on the cell surface (Lv et al., 2014; Dominici et al., 2006). hMSCs exhibit unique characteristics including the potential for self-renewal, the capability to distinguish into a variety of mesodermal lineage cells, and the lack of the MHC class II surface antigen required for activation of T lymphocytes (Fig. 2.3) (Javazon et al., 2004; Caplan, 2005, 2009).

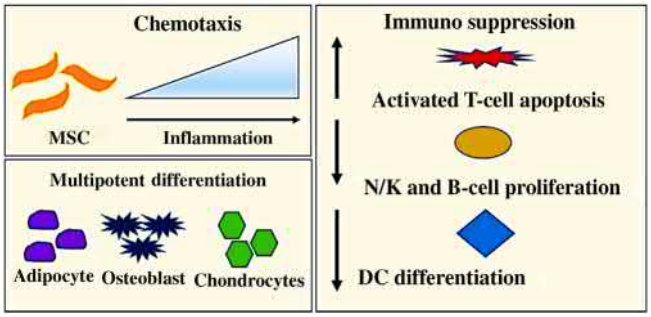

FIGURE 2.3 Image summarizing the features of MSCs: cell migration toward the site of inflammation, multipotent differentiative potential, and immunosuppression. *DC*, Dendritic cells; *MSC*, mesenchymal stem cell; *NK*, natural killers. *Source: From Corradetti, B., Ferrari, M., 2016. Nanotechnology for mesenchymal stem cell therapies. J. Control. Release 240, 242–250.*

hMSCs also have an immunomodulatory and antiinflammatory effect, through secretion of paracrine factors, to modulate the immune system and regulate inflammatory responses, thus helping hMSC to induce tolerance and increase survival after transplantation (Uccelli et al., 2008). Interestingly, hMSCs are able to travel specifically to locations of tissue injury or inflammation and accumulate within tumor stroma via chemotactic gradients, which makes them a potentially exciting drug delivery tool to track down and eradicate tumor cells (Loebinger and Janes, 2010). This tumor-tropic and migratory property of hMSCs is credited to (1) their inherent properties, and (2) stimuli produced by a tumor.

It has been reported that hMSCs express many types of receptors like cell–cell receptor, growth receptors, chemokine receptors, cytokine receptors, immunomodulating receptors, etc.:

- *Growth factor receptors*: Important for hMSCs self-renewal and differentiation (Stosich et al., 2007): EGFR, bFGFR, IGFR, PDGFR, TGFβRI, and RII. hMSCs also express hepatocyte growth receptor (HGFR, c-met) (Neuss et al., 2004, Son et al., 2006).
- *Chemokine receptors*: Important for homing, migration, and engraftment of hMSCs to places of injury and to locations of a tumor. CXC, CC, C, or CX3C chemokines are classified as G-protein-coupled receptors (Murphy et al., 2000). hMSCs are recognized to upregulate CCR1, CCR2, CCR4, CCR6, CCR7, CCR9, CCR10, CXCR1, CXCR2, CXCR4, CXCR5, CXCR6, and CX3CR1 receptors, and also have secretion of different chemokines (Ringe et al., 2007; Fox et al., 2007).
- *Cytokine receptors*: IL-1R, IL-3R, IL-4R, IL-6R, IL-7R, IFNϒR, and TNFI and IIR (Erices and Conget, 2001). These receptors have various signaling mechanism and structural organization. So that can be divided into TNF receptor families and type I and II cytokines (Boulay et al., 2003).
- *CD 44 receptor*: Involved in cell–matrix interactions (Drosse et al., 2008; Schieker et al., 2004). In authority for attaching to hyaluronic acid (HA) (Zhu et al., 2006a; Shah et al., 2018).
- *Cell–cell receptors*: Notch 1, 2, and 3 receptors and their ligand (Jagged-1, Jagged-2, DLL-1, DLL-3, and DLL-4). Surface molecules of the immunoglobulin superfamily (Majumdar et al., 2003): ICAM-1 and -2, VCAM-1, and ALCAM.
- *Immunomodulating receptors*: Toll-like receptors (TLRs) 1, 2, 3, 4, 5, 6 and 9 (Tomchuck et al., 2008). Recognize foreign pathogens and injured tissues. Determining the enrollment, relocation, and immunomodulating function of hMSCs at the site of injury.

Indoleamine 2,3-dioxygenase (IDO), IL-6, and IL-10 have been reported mediating the immunomodulating part of hMSCs (Noël et al., 2007). The absence of effect of costimulatory molecules (CD80, CD40, and CD86) and MHC class II protects hMSCs from NK (natural killer) cells lysis and T-cell activation (Rasmusson et al., 2003).

The performance of multiple functions for regeneration of tissue requires hMSCs to make contact with local stimuli like TLRs, chemoattractant inflammatory cytokines, which helps in stimulation of hMSCs (Crisostomo et al., 2008; Caplan and Dennis, 2006; Jing et al., 2011). The adhesion molecules, P-selectin and VCAM-1, are a key mediator in hMSCs rolling and attachment to vascular endothelial cells in the course of extravasations to the place of injury or tumor (Rüster et al., 2006).

Other than cell adhesion molecules and chemokines, several MMPs, for example, membrane type 1 MMP (MT1-MMP) and MMP-2, also play an important role in invasiveness of hMSCs through extracellular matrix barriers for migration (Ries et al., 2007; Ding et al., 2009). The discovery of hMSCs plays a vital role in designing of targeted delivery of the drug.

2.2 ENGINEERING MESENCHYMAL STEM CELLS AS A NOVEL FORMULATION STRATEGY IN CANCER TREATMENT

Over the years, with an increasing amount of data available, the discovery CSCs in a diversity of solid tumors was based upon the tumor-initiating capabilities of mice following xenotransplantation after isolation of primary tumors (Hanahan and Weinberg, 2011). This comprises a complex extracellular matrix where immune, inflammatory cells, fibroblasts, blood vessels, and fat cells exist. The activated fibroblast in tumor cells is carcinoma-associated fibroblasts (CAFs) or tumor-associated fibroblasts (TAFs).

A study has explained that CAFs/TAFs can be found in MSCs (Quante et al., 2011). Transforming growth factor b1 (TGFb1) stimulation can make MSCs go through myofibroblast differentiation. Stimulation of TGFb1 can produce hypomethylated MSCs, which show variation in gene expression profiles concerning myofibroblast signatures. It expresses indicators like tenascin-C, a-SMA (alpha-smooth muscle actin) and fibroblast surface protein (FSP), and also increases secretion and expression of growth stimulating factors like SDF-1 and chemokine (C−C motif) ligand 5 (CCL5)/RANTES (Wang et al., 2004).

Likewise, CAFs are more hypomethylated than usual stromal cells and it has been calculated that the smallest 20% of CAFs initiate from MSCs (Quante et al., 2011). MSCs in bone marrow contribute to the generation of a stem cell cancer (CSC) place, which can be moved to the tumor location by CXCR4 signaling and thus stimulate tumor growth. MSCs in the tumor place express IL-6, Wnt5a, BMP4, and Gremlin-1 (Quante et al., 2011). IL-6, expressed in both MSCs and tumor cells, can increase stimulation of domain creation and support tumor initiation by transcription activators (JAK/STAT) and activation of the Janus kinase/signal transducers pathway (Hsu et al., 2012). MSC still appear to retain a tendency to boost the tumorsphere development and tumor start rather than tumor activation. Fig. 2.4 represents a generation of tumor-associated MSCs.

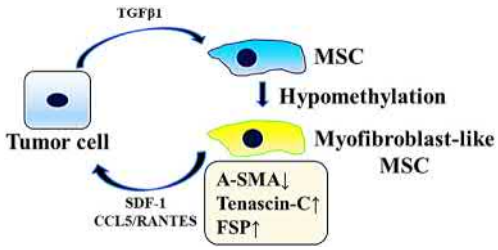

FIGURE 2.4 Generation of tumor-associated MSCs. *MSCs*, Mesenchymal stem cells.

Tumor cell–secreted TGFb1 induces hypomethylation and increases the myofibroblastic gene signature in MSCs, with upregulated expression of a-SMA, tenascin-C, and FSP. Tumor stimulation also induces increased secretion of MSC produced CCL5/RANTES and SDF-1, which act in a paracrine way to stimulate the growth of tumor and survival (Wang et al., 2004). Despite this, MSCs still tend to reduce tumor growth. MSCs can home into places of tumor stroma and inflammation for targeted delivery of drug moiety.

CSCs share similar properties as normal stem cells (Shen et al., 2016). This has brought CSCs into the limelight as it is believed that CSCs show a crucial part in tumor progression, drug resistance, metastasis of a tumor, and even reappearance (Shen et al., 2016; Chen et al., 2013). This CSC hypothesis has a focus for its discovery and development of CSC-related treatments and this is important when applying CSCs to nanomedicine applications. For instance, NPs can help to increase the bioavailability of CSC-specific agents.

Nanomedicine helps to overcome the drug resistance of CSCs. Tumors have phenotypically distinct cell populations with heterogeneous tissues and plasticity is often displayed in CSCs by transitioning among stem cell states and non–stem cell states in a reversible manner. While sustaining tumor growth, the remaining residual differentiated tumor cells can able to switch to CSCs, for that reason the depletion of CSCs is not sufficient to allow tumor regression (Gupta et al., 2009). So, it is important to develop a combinational therapy plan to attack both bulk non-CSCs as well as occasional CSCs populations (Verma et al., 2015).

The conventional approach to cancer treatment includes surgery, chemotherapy, and radiotherapy. However, conventional cancer therapies have their own limitations since these treatments lack specificity to target only specific cancer cells. Therefore, many tumors still have a poor prognosis after conventional treatment due to recurrence and metastasis following initial remission. The challenges of cancer treatment lie in the unproductive delivery of the anticancer agent to the site of action.

Stem cells used in conjunction with nanoformulations may enhance the therapeutic response by using different possible ways for delivering an actual effective amount of drug at the targeted site (Fig. 2.5). For example, for targeted delivery of payloads into the blood–brain barrier (BBB) with deeper tumor penetration may be facilitated by receptor-mediated transcytosis that can be demonstrated by NPs bearing a specific receptor targeting moiety (Kim et al., 2014a). Modifications can be made to the surface of NPs; for example, the incorporation of chlorotoxin onto functionalized iron oxide NPs resulted in a noteworthy enhancement in total uptake within the brain tumors of mice (Kim et al., 2014a).

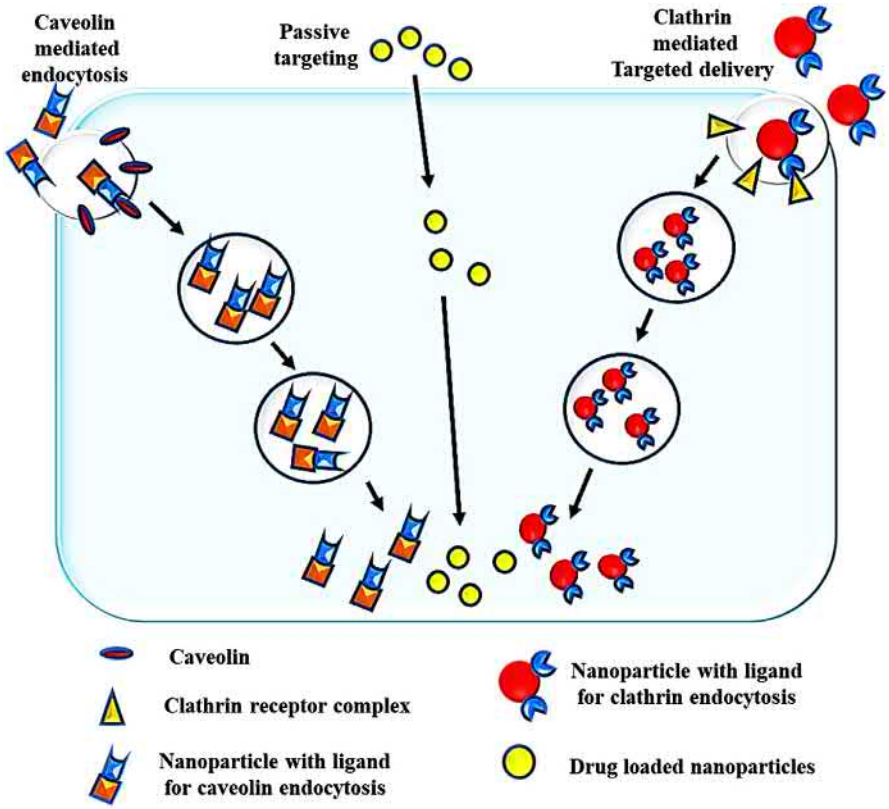

FIGURE 2.5 Nanoparticles may be incorporated into stem cell carriers through three different mechanisms depicted: (1) caveolin-mediated endocytosis, (2) clathrin-mediated endocytosis, and (3) passive transport. Following the endolysosomal escape, nanoparticles accumulate in the cytosol, which together with sustained drug release leads to cell membrane degradation and targeted drug release to tumor cells.

In bone marrow–derived MSCs, there are several additional subpopulations with potential uses as drug delivery agents, such as MAPCs (multipotent adult progenitor cells), MIAMI (marrow-isolated adult multilineage inducible) cells, and VSEL (very small embryonic-like) stem cells. Maintaining of MSCs' viability after incorporating it with drug-loaded NPs and to confirm that those drugs did not affect the MSCs before it reaches tumor site is very important. One option is transduction of MSCs with Multidrug-resistant 1 (MDR1) to make them resistant to chemotherapeutic agents. There are various administration routes for MSCs delivery to target tumor in vivo such as intravenous (IV), intraperitoneal, IT injection, or an intravascular delivery can be used. The extensive use of IT injection, although showing promising results in a few studies, is limited to special tumor microenvironments of a solid tumor. Intravascular injections are less invasive and allow multiple injections. Other novel target strategies include the use of magnet and combination treatment with local irradiation. For the evaluation of the safe use of nanoengineered MSCs a few strategies, such as the design of MSCs with the ability to kill both tumor cells

as well as MSCs themselves with the incorporation of some suicide gene inside them, are being investigated.

2.2.1 Nanoparticles Engineered Mesenchymal Stem Cells in Breast Cancer Management

Zhang et al. formulated PEG-*b*-PCL polymeric micelles of salinomycin (SAL) and octreotide conjugated paclitaxel (OCT-PTX) used in combination to treat breast cancer, which showed promising antitumor response in vivo and in vitro. A good antitumor response was observed due to the action of paclitaxel toward the bulk cancer cells plus the action of SAL activity against CSCs (Zhang et al., 2012).

The finding from the research work of Sun et al. is that all-*trans*-retinoic acid (ATRA) acts as a differentiation moiety for CSCs. So that can be used to treat breast cancer by encapsulating a chemotherapeutic agent such as doxorubicin. They prepared NPs-loaded siRNA using a double emulsion method. When this formulation was tested in vivo using systemic administration, it managed to augment the enhancement of the drugs in tumor tissues as well as in CSCs. The result from in vitro study inferred that the formulated NPs containing siRNA for targeting to PIK1 (polo-like kinase 1) (an oncogene) can treat breast CSCs derived from MDA-MB-231 breast cancer cells (Sun et al., 2015).

Currently, doxorubicin (DOX) is usually administered by IV injection with possible adverse events including asthenia, hand−foot syndrome, neutropenia, anemia, hypersensitivity, and cardiac toxicity (rare) (Iwamoto, 2013). In this regard, Paris et al. studied MSCs derived from placenta, as carriers of mesoporous silica NPs containing DOX, to target mammary tumors. These studies targeted cancer using chemistry to structurally modify NPs to carry drugs and biology where decidua-derived mesenchymal stem cells (DMSCs) from human placenta were exploited for their migratory and tumor homing properties to kill tumor cells (Paris et al., 2016). There was no increase of lactate dehydrogenase (LDH) with increasing NPs concentration, suggesting that NPs was not able to produce cell death in DMSCs after 24 hours and this was subsequently confirmed with the [3-(4,5-dimethylthiazol-2-yl)-5-(3-carboxymethoxyphenyl)-2-(4-sulfophenyl)-2H-tetrazolium) (MTS) assay as shown in Fig. 2.6.

The NP charge and exposure time can have an effect on the internalization process. Incubation DMSCs with + ve NPs at an amount of 200 μg/mL for 2 hours was optimal for internalization as indicated using fluorescence intensity with − ve NPs localized around the nucleus. − ve NPs internalized better than + ve NPs over a shorter duration of time (1-hour incubation). Since DMSCs require 3 days to reach the tumor site (Vegh et al., 2013) NPs should be internalized in the DMSCs for at least 3 days. All NPs remained internalized up to 5 days suggesting they would remain stable and will reach the tumor site. The migration properties of DMSCs were the same regardless whether they contained + ve NPs, − ve NPs, or control (without any NPs). Overall the researchers concluded that + ve NPs were most suitable based on cellular uptake, retention time, and, importantly, lysosomal escape capabilities. In vivo migration studies on NMU (*N*-nitroso-*N*-methyl urea) derived tumor rats showed that, after tail-vein injections, + ve NPs were localized inside the tumor indicating the tumor homing properties of DMSCs. In conclusion, MSCs can be a good approach to treat breast cancer by a delivery therapeutic agent at the targeted site with better efficacy.

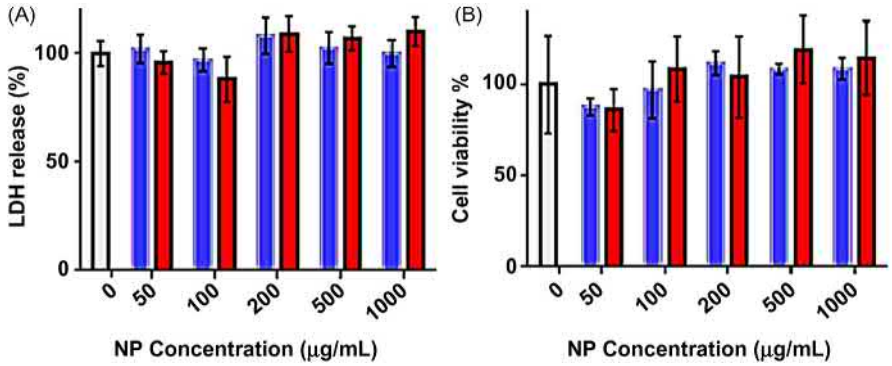

FIGURE 2.6 (A) LDH activity after 24-hour internalization and (B) MTS assay at 24 h after endocytosis. Blue (−ve-NPs) and red (+ve-NPs). Data showed mean ± SD ($n = 3$). *LDH*, Lactate dehydrogenase. *Source: From Paris, J.L., De La Torre, P., Manzano, M., Cabañas, M.V., Flores, A.I., Vallet-Regí, M., 2016. Decidua-derived mesenchymal stem cells as carriers of mesoporous silica nanoparticles. In vitro and in vivo evaluation on mammary tumors. Acta Biomater. 33, 275–282.*

2.2.2 Lung Cancer

Loebinger et al. have tested MSCs labeled with iron oxide NPs in a metastatic lung cancer model using MRI (magnetic resonance imaging). This study has demonstrated the homing capability of iron oxide labeled MSCs to identify and visualize it in real-time in vivo. Metastatic lung tumor models were injected with MSCs double layered with iron NPs resulting in migration of MSCs to lung metastasis area in vivo. The methods used in this study have suggested that tracking down MSC to cancer cells can help in early phase clinical studies before cancer therapy (Loebinger et al., 2009b). In another research, Sadhukha et al. studied the probable of using nanoengineered MSCs loaded with PLGA-NPs containing paclitaxel for targeting tumor tissue orthotropic lung model of mouse.

NPs uptake in MSCs reached a steady state at 4- and 6-hour (Fig. 2.7A) and demonstrated a time-dependent increased as shown by fluorescent staining (Fig. 2.7B). The nanoengineered MSCs' viability is not affected by cellular uptake mechanism as shown by a consistent low 7-amino actinomycin D (7-AAD) level that reflects the cellular viability marker (Fig. 2.7C–L). Paclitaxel release was sustainable with 2.1% released within 24 hours (Fig. 2.7M and N). The nanoengineered MSCs having overexpression of P-gp mediated efflux. Due to this, the internalization of drug loaded NPs into MSC is less. This can be shown by the low intracellular accumulation of calcein AM, compared with MSCs treated with the P-gp inhibitor, Zosuquidar. Long-term NPs uptake over 5 days did not affect the MSCs survival (Sadhukha et al., 2014).

The cytotoxic ability of nanoengineered MSCs on A549 and MA148 cells, studied using MTS analysis after 3 and 5 days posttreatment, showed that cell survival was dose-dependent (Fig. 2.8).

The in vivo biodistribution in an animal model of nanoengineered MSCs compared with NPs (Fig. 2.9) showed that nanoengineered MSCs were more concentrated in the lung. Infrared fluorescent profiles displayed a remarkable difference in NP distribution

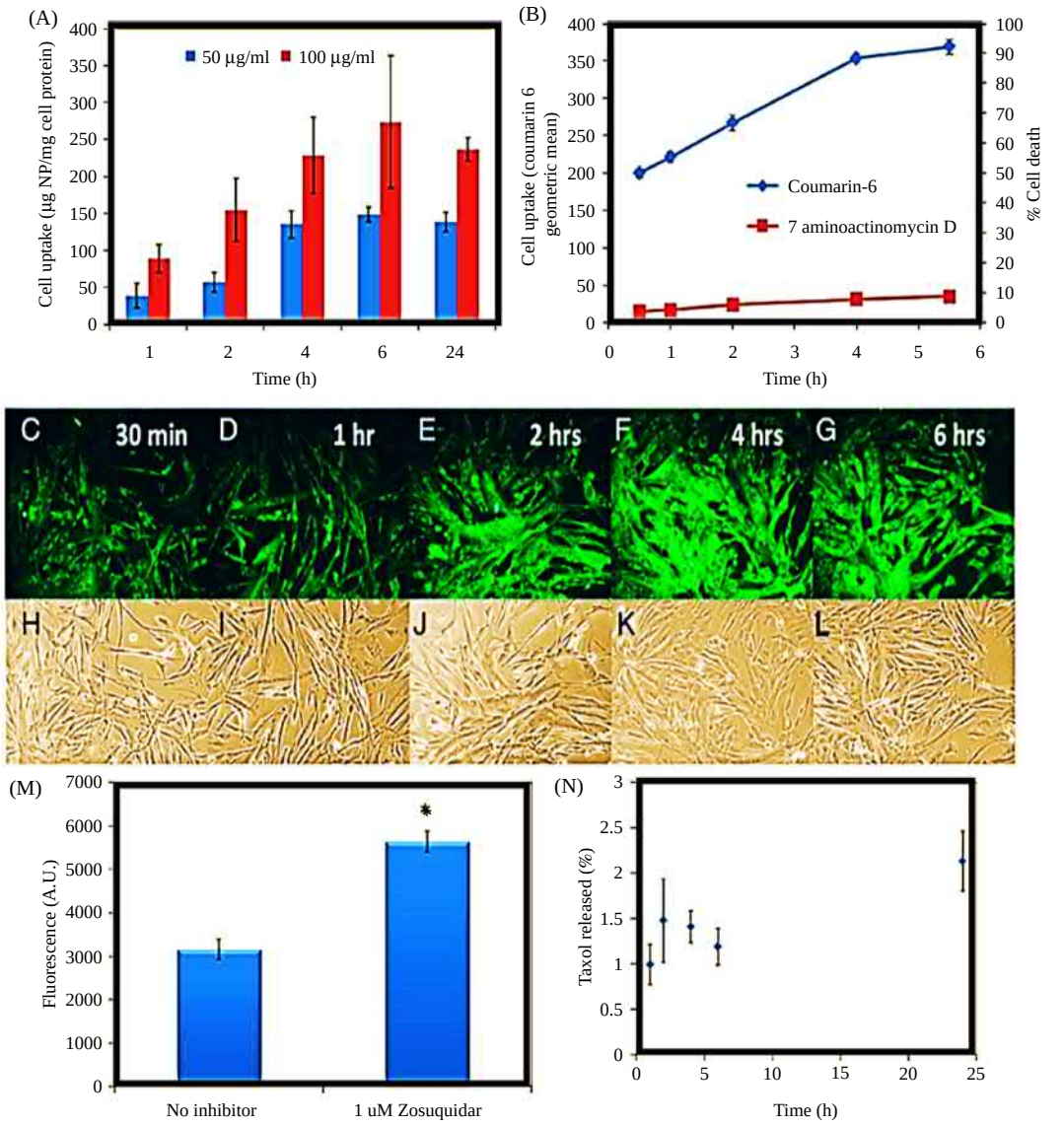

FIGURE 2.7 Cellular uptake of NPs. (A) Quantitative analysis of the cellular uptake of NPs. (B) Cellular uptake of NPs and cell viability assayed by flow cytometry. (C–L) Visual observation of NPs loaded MSCs under a fluorescent microscope (C–G) and phase-contrast microscope (H–L) at different time intervals after incubation with NPs. (M) Role of P-gp in drug efflux from MSCs in vitro. (N) In vitro drug release from nanoengineered MSCs. (A, N, and M): Data are shown as mean ± SD ($n = 3$). *MSCs*, Mesenchymal stem cells; *NPs*, nanoparticles. *Source: From Sadhukha, T., O'brien, T.D., Prabha, S., 2014. Nanoengineered mesenchymal stem cells as targeted therapeutic carriers. J. Control. Release 196, 243–251.*

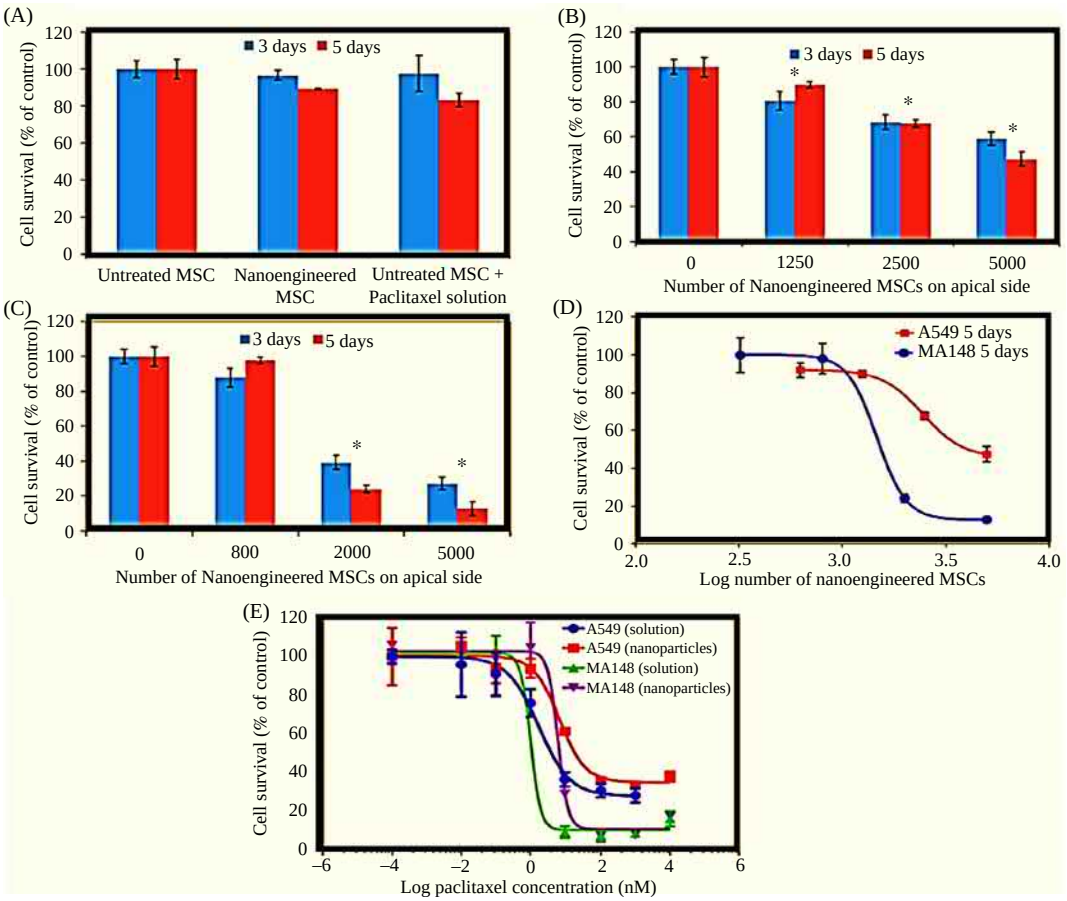

FIGURE 2.8 Cytotoxic potential of nanoengineered MSCs. (A) Long-term survival of MSCs after NP or solution added using MTS assay. (B) A549 cells. (C) MA148 cells. (D) IC50 values for A549 and MA148 cells after 5 days. (E) Dose–response curve for cytotoxicity in A549 and MA148 cells after 3 days of treatment with paclitaxel in solution or nanoparticles. *MSCs*, Mesenchymal stem cells; *NPs*, nanoparticles. *Source: From Sadhukha, T., O'brien, T.D., Prabha, S., 2014. Nanoengineered mesenchymal stem cells as targeted therapeutic carriers. J. Control. Release 196, 243–251.*

after 10 minutes, 1.5 hours, and 3 hours. Nanoengineered MSCs were engaged on the site of the tumor for up to 3 hours, which is sufficient for drug interaction. After 24 hours, fluorescence signals were visible in the lung, abdomen, and from the kidney to the bladder demonstrating that the nanoengineered MSCs did not accumulate in the host body and hence may not cause toxicity issues (Sadhukha et al., 2014).

The above findings showed that by using nanoengineered MSCs, the release of cancer-treating drugs, for example, paclitaxel, can be regulated and directed to a targeted area such as a tumor site. Interestingly, nanoengineered MSCs did not change MSCs characteristics such as the ability of differentiation, drugs efflux, cell viability, and migration

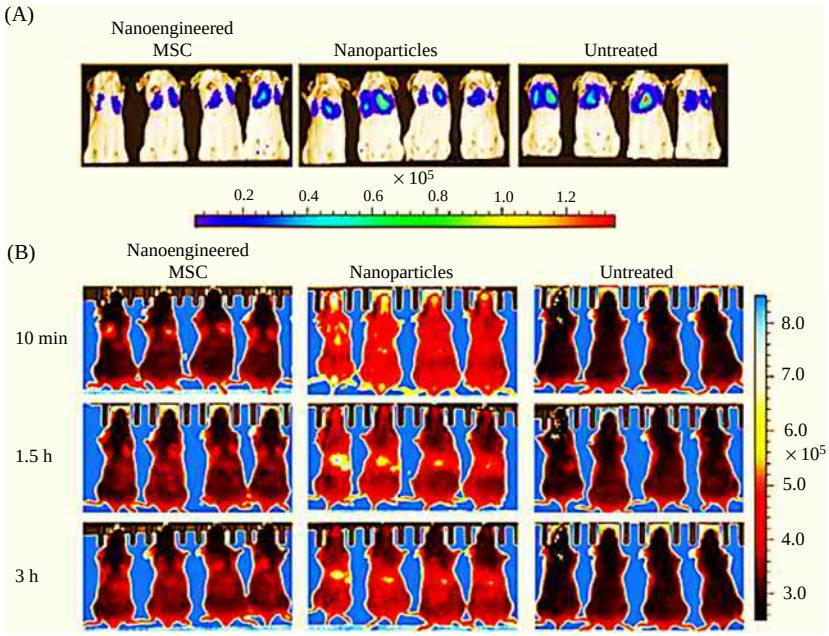

FIGURE 2.9 In vivo biodistribution of nanoengineered MSCs mice bearing orthotopic lung tumors were studied. (A) Bioluminescent imaging of tumor in mice lungs postinjection. (B) Fluorescent imaging of mice at different time interval posttreatment. *MSCs*, Mesenchymal stem cells. *Source: From Sadhukha, T., O'brien, T.D., Prabha, S., 2014. Nanoengineered mesenchymal stem cells as targeted therapeutic carriers. J. Control. Release 196, 243–251.*

behavior, probably due to the nanoscale size of the particles. MSCs show resistance to being killed, hence concerns regarding the effect of long-term exposure to MSCs have been raised and as MSCs were also found to undergo malignant transformation in vitro their use remains controversial (Momin et al., 2010).

MSCs have been shown to move to the bladder in mice orthotopic lung tumor models, suggesting nanoengineered MSCs were en route to be excreted and may not accumulate in the host. Since excretion is dependent on kidney function, patients with kidney disease may experience complications (Humphreys et al., 2005).

2.2.3 Brain Cancer

Brain cell targeting can be achieved using an exclusive subpopulation of hMSCs: MIAMI cells. In an investigation Rogers et al. aimed at evaluating the cellular uptake, retention, viability, and differentiation in vivo of poly-lactic acid (PLA) and lipid (LNC) NPs by MIAMI cells. PLA-NP and LNC loaded with coumarin-6 were prepared and their characteristic features were studied before incubation with MIAMI cells. MIAMI cells loaded with both NPs differentiate into osteoblast and adipocytes after day 7 similar to unloaded MIAMI cells showed no cytotoxicity. In vivo test results have suggested that MIAMI cells loaded with both NPs do travel and locate around brain tumor whereas

unloaded MIAMI cells don't. This finding suggests the potential of MIAMI cells loaded with NP is better in terms of targeting brain cancer than unloaded MIAMI cells (Roger et al., 2010).

In another interesting investigation, Huang et al. engineered MSCs having multifunctional mesoporous silica NPs for brain tumor targeting. The study involves an MSC platform that combined the tumor tropism of stem cells and multimodality imaging of HA coated mesoporous silica NPs (HA-MSNs) with near infra-red dye ZW800, FITC, ^{64}Cu, and Gd^{3+} imaging agents for MRI, PET, and optical imaging. The study suggests that the uptake mechanism of MSN was dependent on pinocytosis and phagocytosis and HA-MSNs depend on receptor-mediated endocytosis. HA-MSNs' cellular uptake amount at 30 minutes was equal to the uptake of MSNs at 2 hours, showing enhanced HA coating effects on NP cellular internalization rates. Intracellular changes in location were observed in HA-MSN and MSN, the particles were first found in the endosomes and then lysosomes, and after 3 days numerous particles were present in the cytoplasm.

MSC treated with MSN and HA-MSN revealed about 300-fold intensification in fluorescence signal after 2 hours of incubation when compared with unprocessed cells. The signal of HA-MSN was 1.6 ± 0.44-fold more than MSN at 1, 3, 5, and 7 days after NP therapy. There was less cytotoxicity of HA-MSNs on MSCs and no significant characteristic effect on MSCs. The in vivo validation of MSC platform has shown that MSCs can migrate by 9.2 ± 1.6 in terms of traveled cell number when accompanied with U87MG neural cells, indicating the tumor-tropic migration of MSCs. HA-MSN and MSN labeled MSCs still have the migratory capability to U87MG cells with 7.6 ± 2.3-fold and 8.7 ± 1.9-fold rise in cell migration, respectively. In vivo tumor delivery of MSC-platform tested with MRI, PET, and optical imaging were successful by targeting orthotropic glioblastoma across the BBB with a 5.2 ± 1.3-fold increase tumor cell internalization by MSC-HA-MSN-^{64}Cu within 24 hours after injection than HA-MSN-^{64}Cu alone (Fig. 2.10).

The unique combination of an MSC platform with NPs could offer a potential clinical application for diagnosis and therapies for brain cancer in the near future. These findings showed that the MSC-based targeted orthotropic glioblastoma across the BBB had actively advanced by 5.2 ± 1.3-fold compared with free NPs thereby confirming the theory of the transmigratory effect of cellular NPs across the endothelial barrier and accumulation in cell-attached cargo in tissues were two-log more than those systemically infused free particles. To modulate stem cell behavior for the efficient targeted delivery, small molecular agents Gd^{3+} were loaded to the MSC-platform in which the in vivo fate was tracked using MRI imaging with successful delivery found in U87MG glioblastoma-bearing mice model. This report confirmed the migratory effect of the multifunctional MSCs platform towards the targeted tumor side of the glioblastoma; however, there was no report shown on the residues of particles (Huang et al., 2013).

Proceeding to the study of Ferrociphenol, or 2-ferrocenyl-1,1-bis(4-hydroxyphenyl)-but-1-one, which is a chemical analog of 4-hydroxytamoxifen, an active metabolite of tamoxifen, which is known to produce an antiproliferative effect in malignant glioma. Clavreul et al. (2015) evaluated the targeting, distribution, and therapeutic efficacy of ferrociphenol (Fc-diOH) LNC-loaded MIAMI cells in an orthotopic U87MG glioblastoma model (Clavreul et al., 2015). MIAMI cells entrapped an optimal dose of about 20 pg Fc-diOH per cell. It suggests that MIAMI cells internalized Fc-diOH LNCs without inducing cell death,

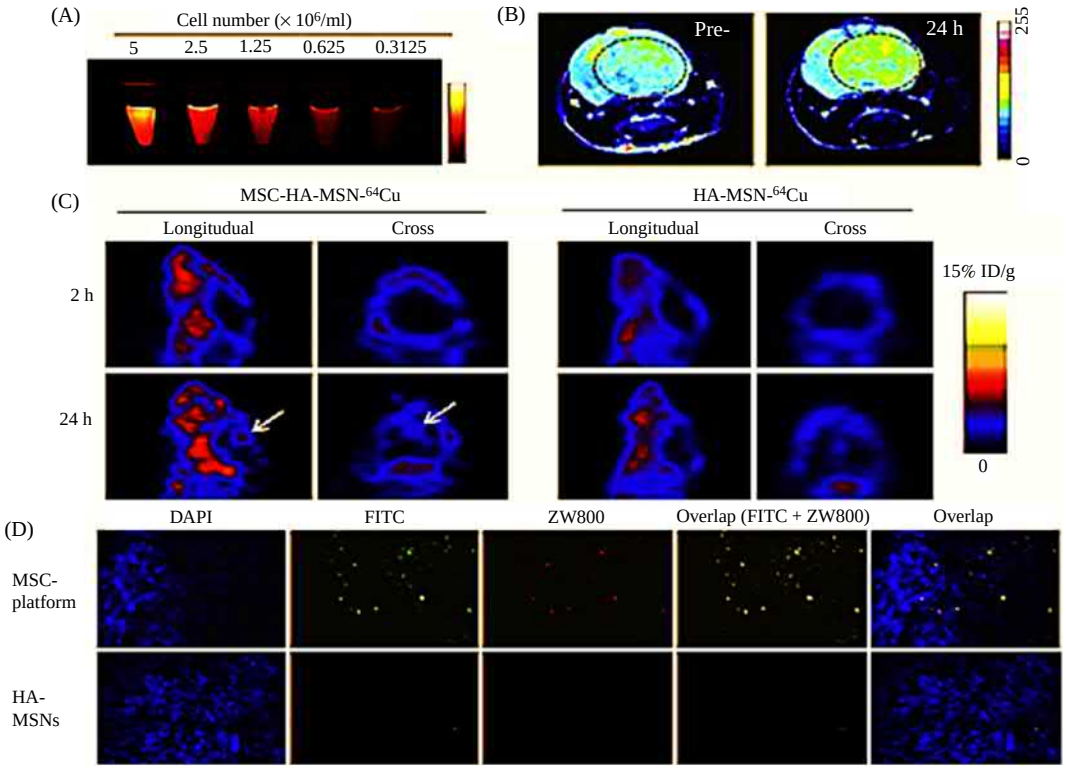

FIGURE 2.10 In vivo multimodal imaging of the tumor homing of the MSC-platform to orthotopic U87MG glioblastoma. (A) The near-infrared fluorescence signal of MSCs labeled (B) MR imaging demonstrated the increased signal at the tumor sites after MSC-platform administration for 24 h compared with preinjection. (C) PET imaging of the tumor targeting of the MSC-platform and HA-MSN-64Cu at the indicated time points. (D) Frozen tissue slices. *MR*, Magnetic resonance; *MSCs*, mesenchymal stem cells; *PET*, positron emission tomography. *Source: From Huang, X., Zhang, F., Wang, H., Niu, G., Choi, K.Y., Swierczewska, M., et al., 2013. Mesenchymal stem cell-based cell engineering with multifunctional mesoporous silica nanoparticles for tumor delivery. Biomaterials 34, 1772–1780.*

and MIAMI cells carrying Fc-diOH LNCs elicit a cytotoxic effect on U87MG glioma cells in an in vitro assay utilizing the CyQUANT cell proliferation kit. The assay confirmed the migration capacity of loaded and unloaded MIAMI cells toward U87MG in conditioned medium. The increased median survival of U87MG-bearing female athymic Swiss nude was observed following IT injection of Fc-diOH LNC-loaded MIAMI cells (3.6 μg/mouse) compared with injection of Fc-diOH LNCs alone, which may be attributed to peritumoral distribution and prolonged residence time of the drug present around and within the brain tumors.

In another study Altaner et al. (2014) assessed the therapeutic efficacy of human bone marrow and adipose tissue-derived MSCs expressing the suicide genes of yeast CD (cytosine deaminase)/UPRT (uracil phosphoribosyltransferase) to treat rats bearing C6 glioblastomas, by activation of prodrug, 5-fluorocytosine (5-FC), directly within the tumor mass.

5-FC is converted into 5-fluorouridine monophosphate by the CD/UPRT enzyme. The therapeutic approach can be targeted to tumor cells, disseminated tumor cells in the brain tissue, and glioblastoma stem-like cells (Altaner et al., 2014). The Kaplan–Meier survival curves indicated that surgical resection of the tumors improved survival times in resected animals, depending on the degree of surgical intervention.

The study concluded with the revelation of the complete tumor regression in 71.4% of animals. The research involves the histopathologic verification of the nonappearance of brain tumor cells at 158 days after C6 tumor injection. Subsequently, partial resection and repeated intracerebral injections resulted in permanent and comprehensive tumor regression in 50% of rats (Altaner et al., 2014).

Results from these investigations showed that this approach elicited whole tumor relapse in 33% of rats. Histopathological analysis after 237 days showed an absence of glioblastoma cells in brains of surviving rats. Hence, the fused CD/UPRT gene therapy may induce a strong inhibition of tumor growth leading to a remedial outcome. Phase I trial also aims to study the feasibility of repeated dosages of NSCs, each followed by a 7-day course of 5-FC and leucovorin. Hence, studies are going to find the relative efficacy of NSCs and MSCs as cellular vehicles; NSC may be difficult to harvest and isolate from intact brain tissue but its safety has been tested in many clinical trials as treatment for neurodegenerative disorders such as PD (Parkinson's disease), stroke, and ALS (amyotrophic lateral sclerosis).

MSCs are chosen as vectors for TRAIL (tumor necrosis factor apoptosis-inducing ligand) gene therapy as they are resistant to TRAIL-mediated apoptosis, and allow for prolonged expression and emission of the therapeutic agent in brain tumors. Kim et al. (2014a,b) examined the antitumor result of MSC-TRAIL treatment joined with temozolomide (TMZ) on U87MG, U373MG, and T98G human glioma cells, as a potential strategy to overcome TRAIL resistance (Kim et al., 2014b). An adenovirus vector containing the secretable trimeric form of the *TRAIL* gene was used to infect the MSCs. To assess the in vitro MSC-TRAIL-induced cytotoxicity and TMZ-mediated cell death, cell viability was noted with the help of the MTT assay and results showed that TMZ in combination with TRAIL significantly eradicated U87MG and T98G cells, but only a small cytotoxic outcome was observed in U373MG cells, which are extremely unaffected by TRAIL.

One of the main challenges to treat brain tumor is the problem of crossing the BBB, which bounds the way of molecules, including drugs, to the brain (Zhao et al., 2015). The BBB allows only specific molecules to enter into the CNS as explained in Fig. 2.11.

Roger et al. (2010) studied the capacity of MSCs as cellular vehicles for delivery of NPs to brain tumors using a subpopulation of MSCs (MIAMI cells) as a vehicle to carry 2 types of NPs: PLA and LNCs. In this study, as a model, coumarin-6 within PLA-NPs and LNCs was used to study the efficiency of MIAMI cells in overcoming the BBB and reach a tumor site. Cellular NP uptake studies explained that the viability of MIAMI cells loaded with PLA-NPs was not affected at concentrations of the drug up to 200 μg/mL and for LNCs, up to 2 mg/mL (Fig. 2.12) and the uptake of PLA-NPs was near completion within 30 minutes and at 100% completion at 2-hour incubation (Roger et al., 2010).

Intracellular retention of NPs showed that more than 95% of cells fluoresced after 3 days for PLA-NPs and for LNC, only 46% of cells still fluoresced after 3 days (Fig. 2.13A). This was confirmed by decreasing fluorescence signal as shown in Fig. 2.13B.

Overall, this study has shown that MSCs can be used as vehicles for NPs delivery in brain tumors. This is because they do not affect the cell viability and differentiation, and at

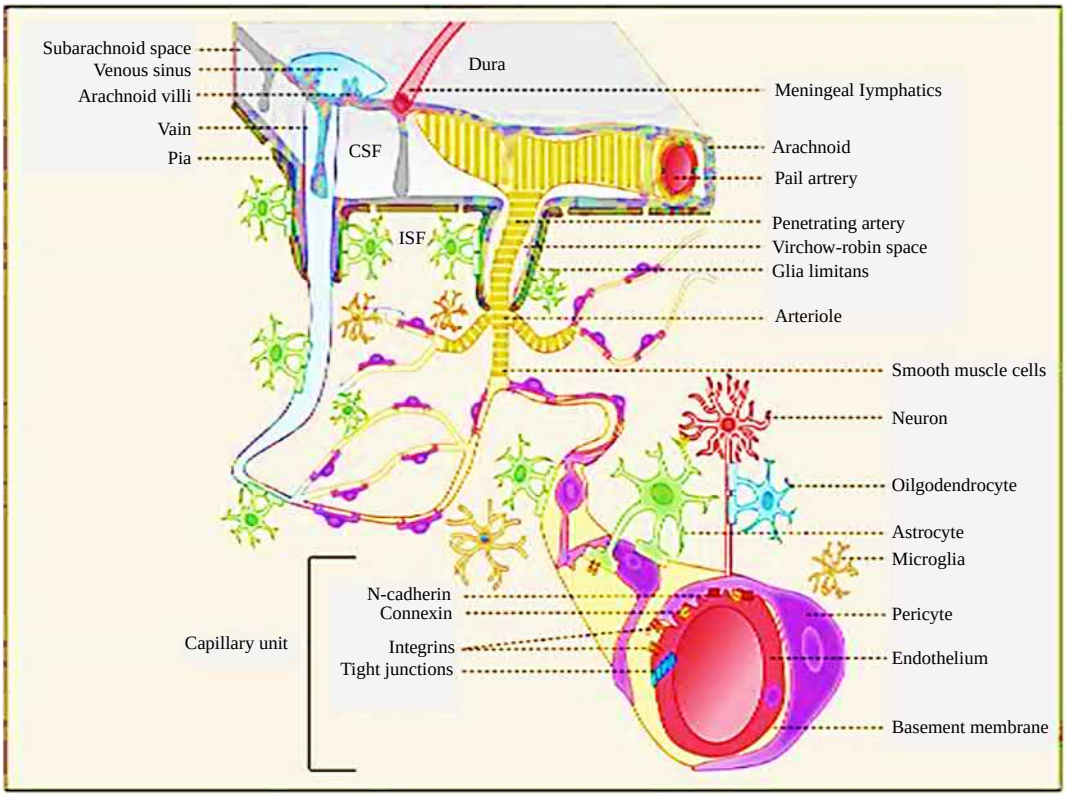

FIGURE 2.11 BBB only allowed certain molecules to cross over from blood vessel to the central nervous system. *BBB*, Blood–brain barrier. *Source: From Zhao, Z., Nelson, A.R., Betsholtz, C., Zlokovic, B.V., 2015. Establishment and dysfunction of the blood–brain barrier. Cell 163, 1064–1078.*

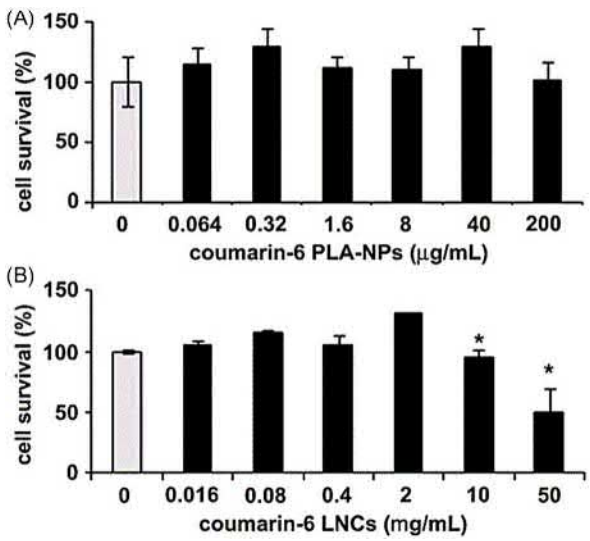

FIGURE 2.12 Cell viability evaluation of MIAMI cells post 1 h incubation with (A) PLA-NPs (0–200 μg/mL) and (B) LNCs (0–5 mg/mL). Incubation time was 1 h. Data are shown the mean ± standard error of the mean ($n = 4$, $^*P < .05$). *LNC*, Lipid; *MIAMI*, marrow-isolated adult multilineage inducible; *NPs*, nanoparticles; *PLA*, poly-lactic acid. *Source: From Roger, M., Clavreul, A., Venier-Julienne, M.-C., Passirani, C., Sindji, L., Schiller, P., et al., 2010. Mesenchymal stem cells as cellular vehicles for delivery of nanoparticles to brain tumors. Biomaterials 31, 8393–8401.*

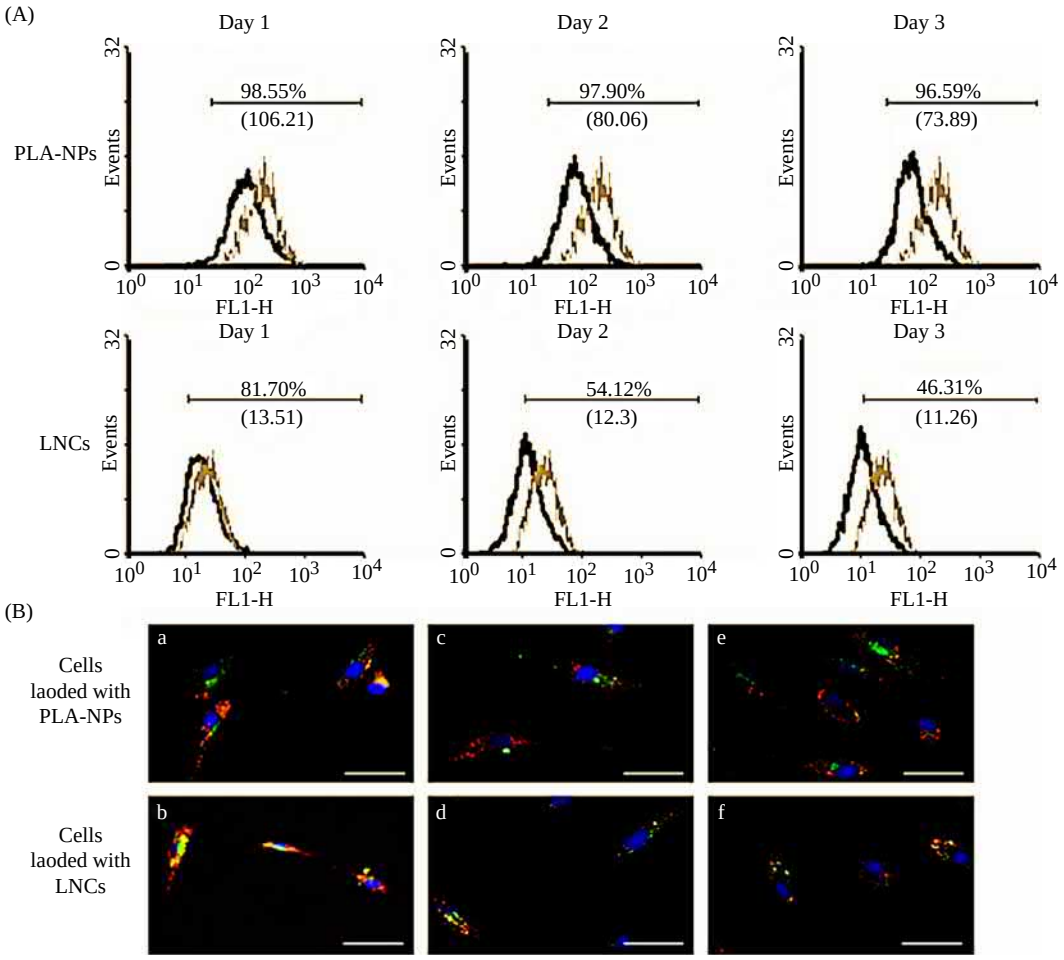

FIGURE 2.13 Cellular retention of NPs analyzed by flow cytometry (A) and fluorescent microscopy (B). (A) Incubation of 1 h at 37°C. PLA-NPs of 100 μg/mL and LNCs of 1 mg/mL. Gray histogram represent retention at 0 days. (B) Day 0 of incubation: (a) and (b), Day 3: (c) and (d), Day 7: (e) and (f). Staining: Dapi for nuclei (*blue*) and lysotracker for lysosomes (*red*). The green fluorescence represents Coumarin-6. *LNC*, Lipid. *Source: From Roger, M., Clavreul, A., Venier-Julienne, M.-C., Passirani, C., Sindji, L., Schiller, P., et al., 2010. Mesenchymal stem cells as cellular vehicles for delivery of nanoparticles to brain tumors. Biomaterials 31, 8393–8401.*

the same time, these NPs are efficiently internalized into MSCs (Roger et al., 2010). Moreover, in an experimental human glioma model, these NP-loaded cells were capable to travel to the brain tumor.

2.2.4 Bone Cancer

Duchi et al. (2013) studied the potential of using MSCs as the delivery carrier in vitro for porphyrin loaded NPs to kill osteosarcoma (OS) using a photoinduction method. Average

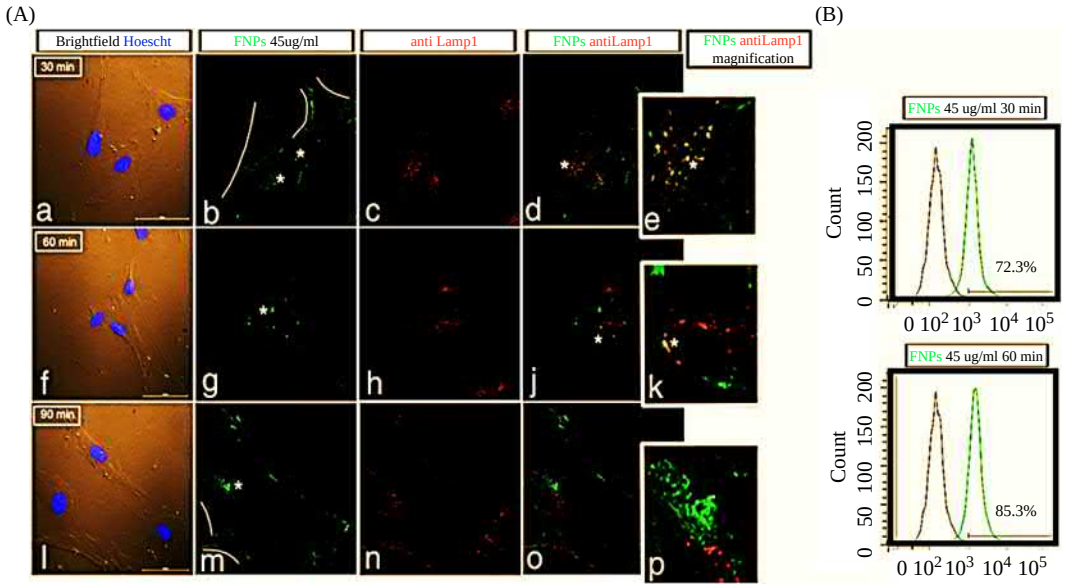

FIGURE 2.14 Intracellular uptake of FNPs loaded into MSC. (A) Immunostaining assay in MSC loaded with 45 μg/mL FNPs, imaged with a confocal laser microscope. (a–e) FNPs accumulated within 30 min within plasma membrane (*white lines* in b) and late endocytic compartments (* in b and e). (f–k) Within 60 min, FNPs more concentrated in cell cytoplasm (* in g) and less in organelles (* in k). (l–p) Within 90 min. FNPs accumulated onto plasma membrane (*white lines* in m) and strongly aggregated in the cytoplasm (* in m). Red: anti-Lamp1, Green: FNPs, Blue: cell nuclei. (B) MSC labeling efficiency assay by FACS analysis. Green: loaded NPs; black: unloaded NPs. *FNP*, Fluorescent core–shell PMMA nanoparticles; *MSC*, Mesenchymal stem cell. *Source: From Duchi, S., Sotgiu, G., Lucarelli, E., Ballestri, M., Dozza, B., Santi, S., et al., 2013. Mesenchymal stem cells as delivery vehicle of porphyrin loaded nanoparticles: effective photoinduced in vitro killing of osteosarcoma. J. Control. Release 168, 225–237.*

atomic force microscopy diameter was 14 ± 5 nm and average hydrodynamic diameter was 39 nm for FNPs (fluorescent core–shell PMMA NPs). TPPS [meso-tetrakis (4-sulfonatophenyl) porphyrin] from nanospheres is tightly bonded to the cationic shell and data showed no TPPS released during in vitro experiments. Authors observed that about one hour is required for intracellular incorporation of FNPs (with >85%). Further, it was noted that to attain this, the ideal concentration was about 45 μg/mL FNPs (Fig. 2.14A and B).

WST-1 and Methylene Blue assay found no noteworthy reduction in cell proliferation up to 6 days postloading FNPs and TPPS-FNPs at 45 μg/mL. The different cytotoxic effect was observed with the help of TPPS-FNPs at 90 μg/mL. The retention of FNPs in MSC was found to be 100% up to 24 hours. After 72 hours, retention was reduced to 50%, probably due to MSC doubling in the TPPS-FNPs loaded MSC and subsequently leading to cell death of OS cells (Duchi et al., 2013). The photoactivation released sufficient ROS to kill OS cells in a quick time frame at 1:5 ratio of TPPS-FNPs loaded MSCs to OS cells (Fig. 2.15). No cell death was reported on noncoated TPPS-FNPs. Nanoengineered MSCs carrying TPPS-FNPs were still efficient to be photostimulated to kill OS cells after 7 days' postloading treatment. The second photoactivation was found to completely eliminate tumor cells in the study (Duchi et al., 2013).

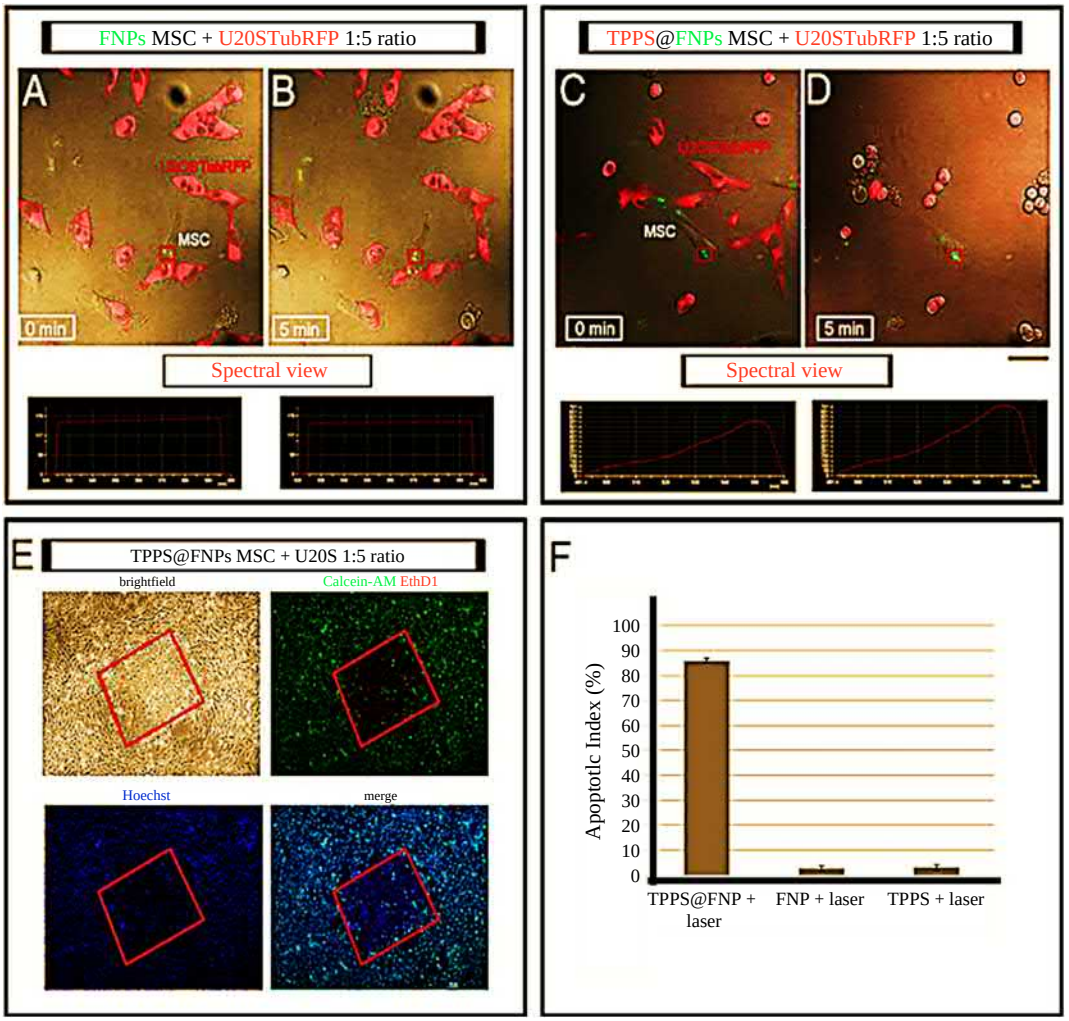

FIGURE 2.15 Photoactivation of TPPS-FNPs-MSCs leads to cell death of OS cells. Coculture assay at 1:5 ratio (MSC: tumor). (A and B) stimulated of FNPs-MSC show no cell death. (C and D) stimulated TPPS-NPs-MSC after 5 min induced cell death. (E) Live and dead apoptosis assay. Green: Calcein-AM, red: ethidium, blue: Hoechst, red: photostimulation with 405 nm laser. (F) Apoptosis measurement result. *MSC*, Mesenchymal stem cell; *FNP*, fluorescent core–shell PMMA nanoparticles; *TPPS*, meso-tetrakis (4-sulfonatophenyl) porphyrin. *Source: From Duchi, S., Sotgiu, G., Lucarelli, E., Ballestri, M., Dozza, B., Santi, S., et al., 2013. Mesenchymal stem cells as delivery vehicle of porphyrin loaded nanoparticles: effective photoinduced in vitro killing of osteosarcoma. J. Control. Release 168, 225–237.*

It was noticed that in this study, the researchers used a laser with a wavelength of 405 nm (blue light) on cell lines that could not penetrate tissue deeply to the tumor site in vivo. This limitation can be overcome by devices such as hollow needles that can be directed to tumor sites (Agostinis et al., 2011). In addition, the lights generated could exert localized action without affecting other normal tissues far from tumor sites. However, in

this study, the effect of engineering on the migration properties of MSCs towards tumor cells was not analyzed and verified by researchers. More details related to the question of how much TPPS-FNPs-MSC have affected healthy cells is still warranted in literature. Perhaps, more in vivo research is needed using a tumor-induced animal model.

2.2.5 Ovarian Cancer

The efficiency of anticancer drug delivery system has been investigated extensively by utilizing drug encapsulated colloidal system targeted directly to tumor cells. The study by Sadhukha et al. hypothesized that the speed and success of loading and retention of cytotoxic therapeutic agent in MSCs were enabled through incorporation in NP-encapsulated form. In this study, paclitaxel-containing NPs in MSCs were used to determine the migration ability in an in vivo mouse orthotopic lung tumor model, and in vitro using A549 lung carcinoma and MA148 ovarian cancer cells. The encapsulated NPs had an early burst release that occurred in the first 4 hours followed by a steady release of drug molecules over 9 days. This study also suggested that maximal uptake of NPs in MSCs occurred at 100 μg/mL of NPs for 4–6 hours without affecting the viability of MSCs. In both tumor cell lines, MA148 and A549, there was significant cell death in the presence of nanoengineered MSCs between 3 and 5 days indicating continuous drug release. The nanoengineered MSCs encapsulated with near-infrared dye showed significant fluorescent effect migrating directly to the lung of the animal model as the home site of inflammation. However, the source of NPs used to encapsulate chemotherapeutic drugs remains unclear (Sadhukha et al., 2014).

2.2.6 Other Mesenchymal Stem Cell Nanoparticles in Cancer Treatment

A study by Yang and Kopecek designed combination therapy against liver CSC using HPMA copolymer-cyclopamine conjugate (P-CYP) and HPMA copolymer-docetaxel (P-DTX) for removing tumor mass. P-CYP was shown to be toxic to CSCs (Yang and Kopeček, 2015). This combination was able to kill both CSCs and non-CSC fractions; thus, it is a potent combination for inhibiting tumor growth. The opportunity of incorporating manifold therapeutic mediators concurrently with more ability is one of the main properties that a nanocarrier should have.

In another study by Zuo et al. the focus was on inhibition of transforming growth factor β (TGF-β) signaling pathway by encouraging tumor penetration of NPs for CSC therapy (Chari and McDonnell, 2007). This study focused more on the presence of a secondary niche whereby CSCs exist with a more hypoxic microenvironment. This is because studies have been proposed that hypoxic cells are additionally resistant to conventional treatment and have the chances of tumor regression afterward fruitful treatment (Chari and McDonnell, 2007; Zuo et al., 2016). In the treatment of cancer, NP drug–based delivery systems provide advantages (Dimri et al., 2015). The obstacle to using NP drug–based delivery systems is the need for extravasation of drugs from tumor vessels and to diffuse deeper to be internalized by CSCs. This study used a combination of TβR-1 inhibitor and NPs to function as siRNA carrier as a rational and effective therapy against CSCs.

The easily obtained DMSCs constitute a homogeneous population with known inhibitory property in primary tumor growth and also new tumor development. In research, two different types of mesoporous silica NPs (−ve-NPs and +ve-NPs) were internalized into DMSCs, which was fluorescently labeled for tracking purposes by using fluorescence microscopy. The result showed that there was no significant growth in LDH release in the culture medium of DMSCs that were incubated with NPs after 24 hours in a concentration up to 1 mg/mL; hence inferring no toxicity of NPs towards DMSCs. The findings also showed that +ve-NPs internalized better than −ve-NPs onto DMSCs with a concentration and incubation time of 200 μg/mL and 2 h, respectively, which might be because of interaction with −ve-charged phospholipid of the cell membrane. Moreover, the NPs were found retained in the cells at day 5 confirming the survival of the NPs in the cells until they reach the target tumor tissue, which takes around 3 days. In vivo testing results obtained from tumor-induced rat model confirmed that DMSCs carried NPs showed retention capability in homing towards the tumor cells. Besides that, there was apoptosis/necrosis effect observed on cancer cells as NPs carried by DMSCs were preloaded with doxorubicin, an anticancer drug (Paris et al., 2016).

A notable research by Martinez-Quintanilla et al. (2013) explained the engineering of human and murine MSCs coexpressing an S-TRAIL (a secretable variant of tumor necrosis factor apoptosis-inducing ligand) and HSV-TK (herpes simplex virus thymidine kinase) in GBM (glioblastoma multiforme) model. Findings indicated that the MSCs induce tumor cell−specific killing mediated by caspase, MCSs can be checked by PET imaging employing an ^{18}F-FHBG radioactive substrate for HSV-TK, and MSCs may be selectively removed post−tumor treatment by administration of the prodrug ganciclovir. Hence, from these articles by Kim et al. (2014a,b) and Martinez-Quintanilla et al. (2013), TRAIL gene therapy for brain cancer treatment may be applied in combination with potential drugs, diagnostic agents, or suicide genes respectively to enable the translation into clinical practice. However, the use of viral vectors for therapeutic gene transductions has several drawbacks such as the risk of immunogenicity, insertional mutagenesis, toxicity, and more manufacturing costs (Roger et al., 2012).

Iron oxide NPs (IO-NPs) is one of the extensively used methods to track cells in preclinical models. Therefore, in this study, the uptake of IO-NPs (10 nm) loaded in biodegradable poly(lactide-*co*-glycolide) microparticles (IO:PLGA-MPs, 0.4−3 μm) in MSCs will be illustrated which enhances molar relaxivity parameters such as the R2 relaxivity (fivefold), R2 signal (twofold), and residence time inside the cells (threefold) related with IO-NPs alone. Moreover, by means of a sequence of in vitro and in vivo models, the effects of IO:PLGA-MPs on MSCs viability, migration, propagation, and cell homing capability have been evaluated (Xu et al., 2012).

Interestingly, it was published that there was no observable effect on cell viability for both kinds of magnetic particles as shown in Fig. 2.16A, compared with native cells 24 hours following internalization of particles. Therefore, MSCs were labeled with two types of magnetic particles to assess the potential effect on cell proliferation, then it was studied for 12 days (Fig. 2.16B), whereby typically at day 9, confluence was reached. Similar rates of proliferation were shown for MSCs labeled with both types of magnetic particles compared with the control. In 5 days, the number of MSCs tripled. Transwell assay was done to detect the migration of MSCs in vitro. MSCs modified with IO-NPs

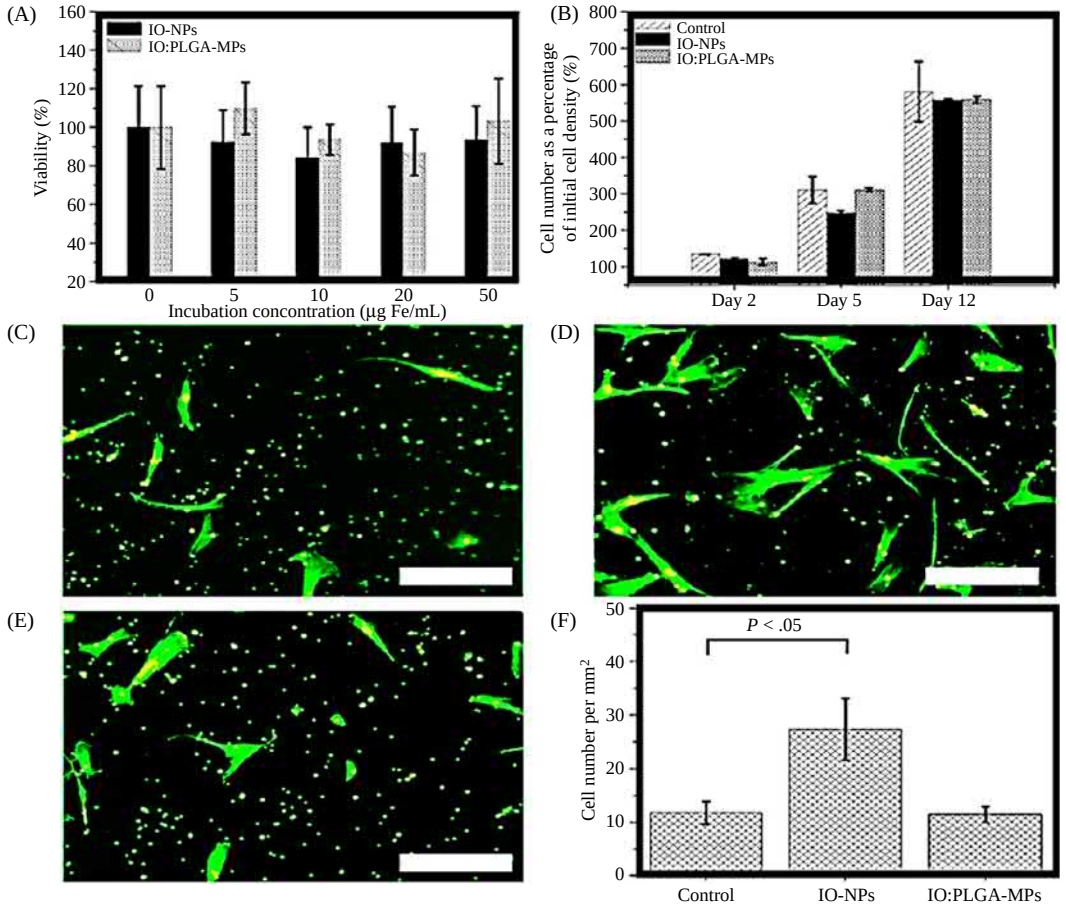

FIGURE 2.16 Impact of particle labeling on cell viability, migration, and proliferation. (A) The viability of iron-labeled MSCs as a function of iron concentration during the incubation. (B) The proliferation of MSCs labeled with magnetic particles. (C) Unmodified control MSCs (D) MSCs labeled with IO-NPs, (C) MSCs labeled with IO:PLGA-MPs. (F) Quantification of migrated MSCs. *IO-NP*, Iron oxide nanoparticle; *MSC*, mesenchymal stem cell. *Source: From Xu, C., Miranda-Nieves, D., Ankrum, J.A., Matthiesen, M.E., Phillips, J.A., Roes, I., et al., 2012. Tracking mesenchymal stem cells with iron oxide nanoparticle loaded poly (lactide-co-glycolide) microparticles. Nano Lett. 12, 4131–4139.*

showed a statistically significant result whereby it increased the level of migration rate (Fig. 2.16C, D, and F), which was similar to findings of the previous study. Comparable migration rate through the 8-μm membrane was shown by MSCs labeled with IO:PLGA-MPs as the unlabeled MSCs (Fig. 2.16C, E, and F).

MSC migration is not affected by the internalization of IO:PLGA-MPs. In this study, to know further about the homing ability of MSCs in vivo, a study will be performed in an inflamed ear of a mouse model. The results showed that unmodified MSCs prefer to migrate to inflamed areas. Likewise, a similar response was shown by IO:PLGA-MPs labeled MSCs. In the inflamed ear, nearly 20-fold additional cells per unit volume were observed compared with noninflamed (saline) ear. In MSCs labeled with IO-NPs and

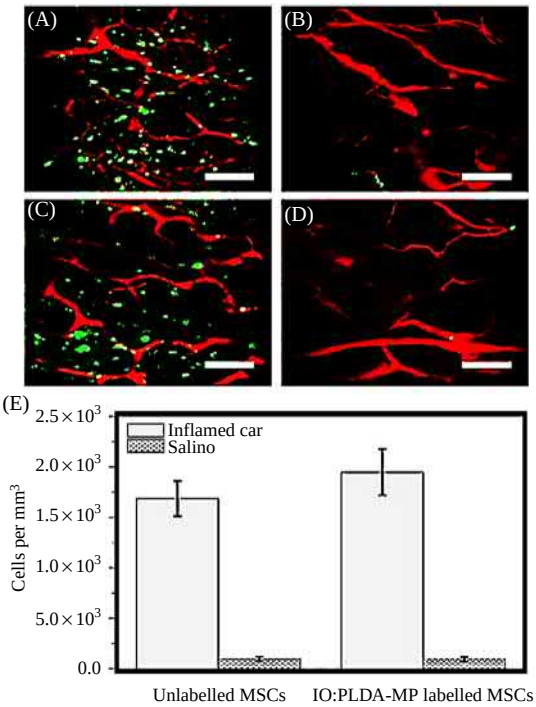

FIGURE 2.17 (A and B) Representative images of homed unlabeled MSCs and (C and D) MSCs prelabeled with PLGA-MPs in the (A and C) lipopolysaccharide (LPS) ears and (B and D) saline ears. A green signal indicates MSC and red signal is from the blood vessels perfused with FITC-Dextran. (E) Quantification of the MSCs in LPS and saline ears. *MSC*, Mesenchymal stem cell. *Source: From Xu, C., Miranda-Nieves, D., Ankrum, J.A., Matthiesen, M.E., Phillips, J.A., Roes, I., et al., 2012. Tracking mesenchymal stem cells with iron oxide nanoparticle loaded poly (lactide-co-glycolide) microparticles. Nano Lett. 12, 4131–4139.*

unmodified control MSCs, 1/3 MSCs have already migrated from the blood vessel into the ear tissue areas, displaying that labeling of the particle does not affect migration through transendothelial regions (Fig. 2.17) (Xu et al., 2012).

Interestingly, in the current study, using the in vitro and in vivo experiments, it is evident that the inherent cell properties such as proliferation, viability, migration, and the homing capability to inflamed regions were not affected by the internalization of MSCs with IO:PLGA-MPs.

Hence, labeling MSCs with IO:PLGA-MPs might serve us with great benefit for the purpose of longitudinal tracking of MSCs without affecting cell properties (Xu et al., 2012). In a study by Dai et al., engineered MSCs were used to serve as a possible carrier for paclitaxel (TAX)-loaded NPs. The efficacy of NPs uptake can be influenced by the size, starving time of MSCs, surface charge, incubating time, and concentration (Dai et al., 2013).

Synthesis of chitosan–DNA NPs was performed by complexation of DNA plasmid to the cationic polymer, hence the result has shown that by applying CTS (chitosan) in the study, level of gene transfection increased and it has led to a lengthening of the time period for MSCs expression. Other than that, the findings showed that modification of paclitaxel-loaded PLGA-NPs to CTS that have acid soluble properties might enhance the zeta potential of NPs. Transwell filter experiments were carried out to examine the migratory ability of MSCs and CTS-TAX-NP-MSCs. MSCs have shown efficient and active migratory action towards all three cell types in this study and there were important alterations between all three cell types, that is, HT-29 (human colon carcinoma cell), Skov-3

(human ovarian carcinoma cell), and LLC (Lewis lung carcinoma cells) ($P < .05$). Hence, tumor types should be selected properly prior to the development of NP-MSCs as a vehicle for targeted drug delivery systems.

Significant feature for the migratory activity of MSCs is dependent on passage. Among passages 3–5, passage 3 specifically has an advanced migratory activity. MSC at passage number 3 was chosen as the drug delivery carrier in consideration of the effect of passage on the uptake of NPs and migratory activities. From the previous data is has been concluded that MSCs are very sensitive to numerous kinds of anticancer therapeutic agents, specifically cytotoxic mediators like paclitaxel; therefore this is the main challenge on how to maintain the MSCs vitality after internalization of paclitaxel. Hence, this study showed that the time needed to improve the migratory activities for MSCs after internalization of CTS-TAX-NP and reverse back the multidrug resistance (MDR) is 6 days (Dai et al., 2013).

2.3 WHAT FUTURE HOLDS FOR MULTIFUNCTIONAL STEM CELL PLATFORM?

With these encouraging preliminary outcomes, it could be reasonable to hypothesize that the therapeutic combination of small molecule drugs, NP and MSCs would signify an extremely talented device for efficient targeted drug delivery. In principle, such a multifunctional system would circumvent the challenge of achieving selective NP biodistribution and uptake by taking advantage of the tumor tropism of MSCs while avoiding the occurrence of undesirable off-target effects related with systemic dispersion of toxic small molecules as well as a photosensitizer. While such idea of multifunctionalization (Fig. 2.18), that is, the incorporation of corresponding strong point from multiple imaging modalities and multiple therapeutic techniques to create the so-called "combo" nanomedicine is truly inspiring, the enduring hurdle lies in imparting multifunctionalization to these stem cell products since chemical alteration could be restricted by several chief features, such as stem cell sensitivity to atmosphere and dynamic fluids of cellular parts (Kemp et al., 2016).

Specifically, the achievement of stem cell–based multifunctional nanoplatforms needs the understanding of their in vivo behavior as well as controlled delivery. In fact, the in vivo fate of MSCs after IV injection has been earlier explained by Kidd et al. (2009) in a systematic research work showing that in healthy mice, following IV injection, MSCs preferentially traveled to the lung, liver, and finally the spleen, Interestingly, such migratory pattern varied in a wound model, where early dwelling in the lungs is followed by migration to the wound positions between 3 and 5 days.

Moreover, IV injection in mice with MDA-MB-231 metastatic tumors confirmed tropism for lung metastasis. Undoubtedly, the synergism of single multifunctionalized platform will only allow faster diagnostics and therapeutics with more precision. For that, MSCs as one of the components is certainly useful owing to its reported tumor-homing nature. With several types of multifunctionalized platforms described that are found to participate in numerous imaging and therapeutic activity (Yu et al., 2012), the combination of MSCs with multifunctional NPs will inevitably advance the future development of effective

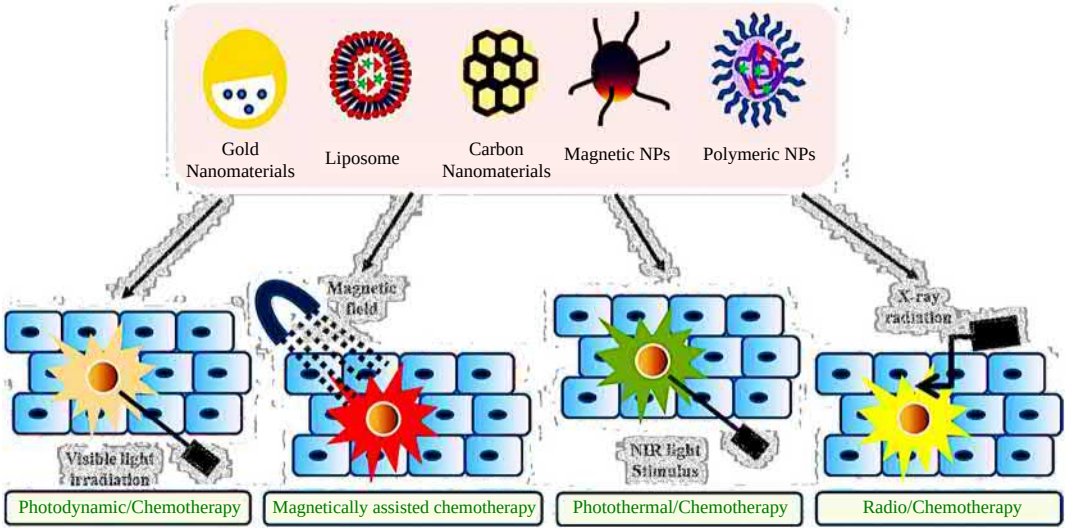

FIGURE 2.18 Nanocarriers combine chemotherapy with physically destructive modalities that induce tumor ablation (photothermal/magnetic).

theranostic for cancer management (Conte et al., 2013). To this regard, it is worth considering some implications of the growth of stem cell–based therapeutics. Regulatory standards require that for stem cell and tissue-based therapy to be measured harmless, only negligible operation, without alteration of biological properties, is allowed from their isolation to their transplant (Deasy et al., 2013).

The greatest progressive cellular therapies, including the practice of nanotechnologies, encounter the conditions for the more-than-negligibly manipulated category devices (Burger, 2003). In such circumstances, their safety will be dependent on the "primary mode of action" (Bagchi et al., 2012). Regulations governing cell therapies are depicted in Fig. 2.19 (Ridgway et al., 2015). Since a thorough consideration is obligatory for such mixture products, the route to translating these innovations into clinical practice may become less straightforward.

Photodynamic therapy (PDT) destroys cells via reactive oxygen species, which is an invasive process. Combination of photosensitizer, light, and oxygen produced singlet oxygen that causes significant cell death via apoptosis or necrosis. One of the challenges for a successful PDT in cancer therapy is the high dependence on the localization of the tumor site (Agostinis et al., 2011). This research showed that by using nanoengineered MSCs, it is possible to deliver sufficient photosensitizers to target tumor site with precision. Interestingly, it only required a low dose nanoengineered MSCs (loaded with photosensitizer). This could be due to the protective properties of NPs. Thus, it is expected that patients may have a lower risk of side effects compared with conventional cancer therapy such as chemotherapy, which required high doses agents. In this study, surprisingly, the characterization of MSCs isolated from patients (donors) was only based on the determination of surface markers.

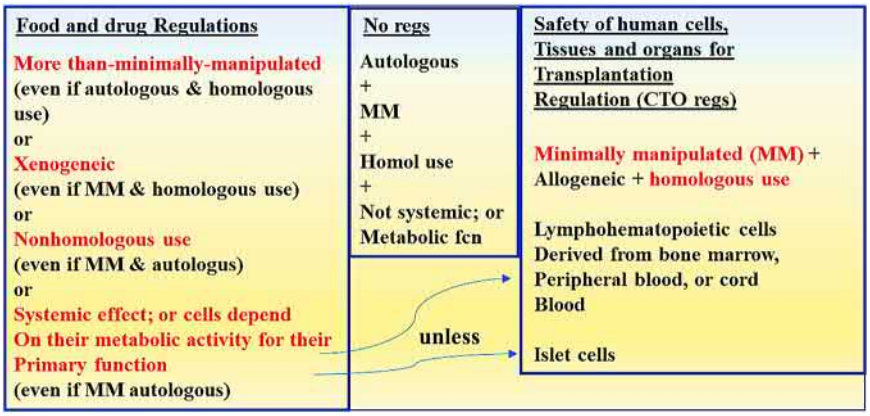

FIGURE 2.19 Regulations governing cell therapies. Two distinct sets of regulations are available and applied based on specific criteria. Cells for human treatment meet the definition of a drug but autologous cells that are minimally manipulated are not covered by regulations if they perform the same basic function, there is not a systemic effect, and the primary function is not dependent on metabolic activity. "MM" means cell processing does not alter the biological characteristics that are relevant to their claimed utility. "Homologous use" means the cells perform the same basic function after transplantation. *MM*, Minimally manipulated. *Source: From Ridgway, A., Agbanyo, F., Wang, J., Rosu-Myles, M., 2015. Regulatory oversight of cell and gene therapy products in Canada. In: Regulatory Aspects of Gene Therapy and Cell Therapy Products. Springer.*

2.4 CONCLUSION AND FUTURE PROSPECTS

The application of MSCs may improve the efficacy of diagnosis and therapy because of their homing capability towards tumors. MSCs have a potency to radically change cancer therapies using NPs as drug carriers as only a small amount of drug is required to deliver a therapeutic dose with reduced toxicity. Apart from the studies mentioned here, there are many more positive results incorporating stem cells and MSCs in cancer. Of course, all the research needs more depth in understanding of certain areas regarding combining NPs with MSCs and a successful human trial before it can actually be used in clinical settings.

MSCs have applications like targeted delivery of anticancer therapeutic agents that have improved both therapeutic indexes and minimized the toxic effects of the anticancer drug. Although MSCs were proven to be useful as a delivery agent, the fate of the cells in vivo is yet to be discovered as the regeneration property of MSCs could possibly initiate unnecessary tumor growth. Moreover, cell homing ability of MSCs could be enhanced through modification of cell surface receptors, which requires further investigation.

There are many benefits that follow the use of MSCs, such as (1) toxicological issues, (2) efficacy and safety, (3) migration efficiency towards neoplastic tissues, (4) maintenance of optimal drug stability and controlled release, and (5) translational issues concerning the use of animal models in preclinical studies of glioma (Auffinger et al., 2013).

Furthermore, the fate of MSCs inside a brain tumor(s) and tumor environment still needs careful evaluation due to the potential crosstalk among MSCs and malignant cancer cells.

Furthermore, the performance and features of stem cells may be changed by loaded NPs and such modifications may offer improvements in migration efficiency and ways to target malignant glioma. Combination therapies seem to be a promising avenue particularly for the synergistic treatment of cancers due to their heterogeneous and complex nature.

MSCs indeed proved to be potential vehicles to deliver drug-loaded NPs to many tumor sites including brain tumor, overcoming the BBB. The major concern when using stem-based therapies in cancer treatment such as MSCs is the safety of the stem cells. Thus before the transition from bench to bedside is possible, researchers need to show the fate of these MSCs after they released NPs to the tumor site. A few methods can be applied such as optimal imaging using bioluminescent luciferase. It would be desired to selectively eliminate these nanoengineered MSCs by incorporating activatable cellular suicide genes or turn off gene expression, preventing from transforming into malignant cancer.

As shown in reviews, it's clear that the benefit of using MSCs is the capacity for optimized dosage of the therapeutic agent with its high surface area and the protective properties on agents it carries from being targeted by the host before it reaches the tumor site. Importantly, the nanoengineered MSCs should migrate towards the malignant site and deposit the loaded NPs close to the tumor mass.

In conclusion, to enable translational application of nanoengineered MSCs to clinical practice, a few challenges need to be addressed such as selection of the best sources of MSCs for diverse types of cancer, best route of administration of MSCs for particular cancer, total number of MSCs and NPs needed, choices of therapeutic drugs and risk of contraindications in clinical use. One of the major concerns using MSCs as drug delivery vehicles is that there is very little understanding about the nature of these cells and tendency of these cells to initiate tumor growth. Also, some degree of tumor selectivity is needed to practice MSCs for cancer therapy, however, approaches to enhance the tumor homing ability of MSCs might enhance the chances for application of MSCs in future studies. However, in this context, more studies are needed before the clinical application of MSC therapy is proposed. Additionally, enhancement in the approaches for gene transduction to cells and advancement in molecular and cell biology areas are needed to develop optimal targeted cellular vectors.

Acknowledgment

The authors would like to acknowledge the Science and Engineering Research Board (Statutory Body Established Through an Act of Parliament: SERB Act 2008), Department of Science and Technology (DST), Government of India for the grant (#ECR/2016/001964) allocated to Dr. Tekade for research work on drug and gene delivery. The author also acknowledges DST-SERB for N-PDF funding (PDF/2016/003329) for work on targeted cancer therapy. Authors would also like to acknowledge Department of Pharmaceuticals, Ministry of Chemicals and Fertilizers, India, for supporting research on cancer and diabetes at NIPER–Ahmedabad.

ABBREVIATIONS

a-SMA alpha-smooth muscle actin
ATRA all-*trans*-retinoic acid
BBB blood–brain barrier

CAFs carcinoma-associated fibroblasts
CD cytosine deaminase
c-FLIP cellular FLICE-inhibitory protein
CNS central nervous system
CSCs cancer stem cells
DMSCs decidua-derived mesenchymal stem cells
DNA deoxyribonucleic acid
ECM extracellular matrix
EPR enhanced permeation and retention
ERK extracellular signal-regulated kinase
Fc-diOH Ferrociphenol
FISH fluorescence in situ hybridization
FITC fluorescein isothiocyanate
FNPs fluorescent core−shell PMMA nanoparticles
FSP fibroblast surface protein
GBM glioblastoma multiforme
HA hyaluronic acid
hMSCs human mesenchymal stem cells
IDO indoleamine 2,3-dioxygenase
IL interleukin
IO-NPs iron oxide nanoparticle
MAPCs multipotent adult progenitor cells
MAPK mitogen-activated protein kinase
MDR multidrug resistance
MIAMI marrow-isolated adult multilineage inducible
MRI magnetic resonance imaging
MSCs mesenchymal stem cells
MSNs mesoporous silica nanoparticles
MTT 3-(4,5-dimethylthiazol-2-yl)-2,5-diphenyltetrazolium bromide
NIR near infra-red
NPs nanoparticles
OS osteosarcoma
P-CYP copolymer-cyclopamine conjugate
PDT photodynamic therapy
P-DTX copolymer-docetaxel
PET positron emission tomography
PLA poly-lactic acid
PLGA poly DL-lactide-co-glycolide
PLK 1 polo-like kinase 1
PTX paclitaxel
ROS reactive oxygen species
SAL salinomycin
SDF-1 stromal-derived-factor-1
SEM scanning electron microscopy
siRNA small silencing ribonucleic acid TAFs
TEM transmission electron microscopy
TGF-β transforming growth factor β
TGFb1 transforming growth factor b1
TLRs Toll-like receptors
TMZ temozolomide
TPPS meso-tetrakis (4-sulfonatophenyl) porphyrin
TRAIL tumor necrosis factor apoptosis-inducing ligand
UPRT uracil phosphoribosyltransferase

VSEL very small embryonic-like
XIAP x-linked inhibitor of apoptosis
5-FC 5-fluorocytosine

References

Agostinis, P., Berg, K., Cengel, K.A., Foster, T.H., Girotti, A.W., Gollnick, S.O., et al., 2011. Photodynamic therapy of cancer: an update. CA: Cancer J. Clin. 61, 250–281.

Altaner, C., Altanerova, V., Cihova, M., Ondicova, K., Rychly, B., Baciak, L., et al., 2014. Complete regression of glioblastoma by mesenchymal stem cells mediated prodrug gene therapy simulating clinical therapeutic scenario. Int. J. Cancer 134, 1458–1465.

Al-Qattan, M.N., Deb, P.K., Tekade, R.K., 2018. Molecular dynamics simulation strategies for designing carbon-nanotube-based targeted drug delivery. Drug Discov. Today 23, 235–250.

Auffinger, B., Morshed, R., Tobias, A., Cheng, Y., Ahmed, A.U., Lesniak, M.S., 2013. Drug-loaded nanoparticle systems and adult stem cells: a potential marriage for the treatment of malignant glioma? Oncotarget 4, 378.

Bae, Y.H., Park, K., 2011. Targeted drug delivery to tumors: myths, reality and possibility. J. Control. Release 153, 198.

Bagchi, M., Moriyama, H., Shahidi, F., 2012. Bio-Nanotechnology: A Revolution in Food, Biomedical and Health Sciences. John Wiley & Sons.

Boulay, J.-L., O'shea, J.J., Paul, W.E., 2003. Molecular phylogeny within type I cytokines and their cognate receptors. Immunity 19, 159–163.

Burger, S., 2003. Current regulatory issues in cell and tissue therapy. Cytotherapy 5, 289–298.

Caplan, A.I., 2005. Mesenchymal stem cells: cell–based reconstructive therapy in orthopedics. Tissue Eng. 11, 1198–1211.

Caplan, A., 2009. Why are MSCs therapeutic? New data: new insight. J. Pathol. 217, 318–324.

Caplan, A.I., Dennis, J.E., 2006. Mesenchymal stem cells as trophic mediators. J. Cell. Biochem. 98, 1076–1084.

Chari, N.S., Mcdonnell, T.J., 2007. The sonic hedgehog signaling network in development and neoplasia. Adv. Anat. Pathol. 14, 344–352.

Chen, K., Huang, Y.-H., Chen, J.-L., 2013. Understanding and targeting cancer stem cells: therapeutic implications and challenges. Acta Pharmacol. Sin. 34, 732.

Choudhury, H., Gorain, B., Chatterjee, B., Mandal, U.K., Sengupta, P., Tekade, K.K., 2017. Pharmacokinetic and pharmacodynamic features of nanoemulsion following oral, intravenous, topical and nasal route. Curr. Pharm. Des. 23, 2504–2531.

Clavreul, A., Montagu, A., Lainé, A.-L., Tétaud, C., Lautram, N., Franconi, F., et al., 2015. Targeting and treatment of glioblastomas with human mesenchymal stem cells carrying ferrociphenol lipid nanocapsules. Int. J. Nanomed. 10, 1259.

Conte, C., Ungaro, F., Maglio, G., Tirino, P., Siracusano, G., Sciortino, M., et al., 2013. Biodegradable core-shell nanoassemblies for the delivery of docetaxel and Zn(II)-phthalocyanine inspired by combination therapy for cancer. J. Control. Release 167, 40–52.

Corradetti, B., Ferrari, M., 2016. Nanotechnology for mesenchymal stem cell therapies. J. Control. Release 240, 242–250.

Crisostomo, P.R., Wang, Y., Markel, T.A., Wang, M., Lahm, T., Meldrum, D.R., 2008. Human mesenchymal stem cells stimulated by TNF-α, LPS, or hypoxia produce growth factors by an NFκB-but not JNK-dependent mechanism. Am. J. Physiol.-Cell Physiol. 294, C675–C682.

Dai, T., Yang, E., Sun, Y., Zhang, L., Zhang, L., Shen, N., et al., 2013. Preparation and drug release mechanism of CTS-TAX-NP-MSCs drug delivery system. Int. J. Pharm. 456, 186–194.

Dawidczyk, C.M., Kim, C., Park, J.H., Russell, L.M., Lee, K.H., Pomper, M.G., et al., 2014. State-of-the-art in design rules for drug delivery platforms: lessons learned from FDA-approved nanomedicines. J. Control. Release 187, 133–144.

Deasy, B.M., Anderson, J.E., Zelina, S., 2013. Regulatory issues in the therapeutic use of stem cells. Reenerative Medicine and Tissue Engineering. InTech.

Dimarino, A.M., Caplan, A.I., Bonfield, T.L., 2013. Mesenchymal stem cells in tissue repair. Front. Immunol. 4, 201.

Dimri, M., Cho, J.-H., Kang, M., Dimri, G.P., 2015. PLK1 inhibition down-regulates polycomb group protein BMI1 via modulation of the miR-200c/141 cluster. J. Biol. Chem. 290, 3033–3044.

Ding, Y., Xu, D., Feng, G., Bushell, A., Muschel, R.J., Wood, K.J., 2009. Mesenchymal stem cells prevent the rejection of fully allogenic islet grafts by the immunosuppressive activity of matrix metalloproteinase-2 and -9. Diabetes 58, 1797–1806.

Dinndorf, P.A., Gootenberg, J., Cohen, M.H., Keegan, P., Pazdur, R., 2007. FDA drug approval summary: pegaspargase (oncaspar) for the first-line treatment of children with acute lymphoblastic leukemia (ALL). Oncologist 12, 991–998.

Dominici, M., LE Blanc, K., Mueller, I., Slaper-Cortenbach, I., Marini, F., Krause, D., et al. 2006. Minimal criteria for defining multipotent mesenchymal stromal cells. The International Society for Cellular Therapy position statement. Cytotherapy, 8, 315-317.

Drosse, I., Volkmer, E., Capanna, R., De Biase, P., Mutschler, W., Schieker, M., 2008. Tissue engineering for bone defect healing: an update on a multi-component approach. Injury 39, S9–S20.

Dua, K., Bebawy, M., Awasthi, R., Tekade, R.K., Tekade, M., Gupta, G., et al., 2017. Application of chitosan and its derivatives in nanocarrier based pulmonary drug delivery systems. Pharm. Nanotechnol. 5, 243–249.

Duchi, S., Sotgiu, G., Lucarelli, E., Ballestri, M., Dozza, B., Santi, S., et al., 2013. Mesenchymal stem cells as delivery vehicle of porphyrin loaded nanoparticles: effective photoinduced in vitro killing of osteosarcoma. J. Control. Release 168, 225–237.

Dwivedi, P., Kumar Tekade, R., Kumar Jain, N., 2013. Nanoparticulate carrier mediated intranasal delivery of insulin for the restoration of memory signaling in Alzheimer's disease. Curr. Nanosci. 9, 46–55.

Erices, A., Conget, P., 2001. Mesenchymal stem cells. Exp. Biol. Med. 226, 507–520.

Farokhzad, O.C., Cheng, J., Teply, B.A., Sherifi, I., Jon, S., Kantoff, P.W., et al., 2006. Targeted nanoparticle-aptamer bioconjugates for cancer chemotherapy in vivo. Proc. Natl. Acad. Sci. U.S.A. 103, 6315–6320.

Fox, J.M., Chamberlain, G., Ashton, B.A., Middleton, J., 2007. Recent advances into the understanding of mesenchymal stem cell trafficking. Br. J. Haematol. 137, 491–502.

Friedenstein, A., Chailakhjan, R., Lalykina, K., 1970. The development of fibroblast colonies in monolayer cultures of guinea-pig bone marrow and spleen cells. Cell Prolif. 3, 393–403.

Galderisi, U., Giordano, A., Paggi, M.G., 2010. The bad and the good of mesenchymal stem cells in cancer: Boosters of tumor growth and vehicles for targeted delivery of anticancer agents. World J. Stem Cells 2, 5.

Gao, Z., Zhang, L., Hu, J., Sun, Y., 2013. Mesenchymal stem cells: a potential targeted-delivery vehicle for anticancer drug loaded nanoparticles. Nanomed.: Nanotechnol. Biol. Med. 9, 174–184.

Ghanghoria, R., Tekade, R.K., Mishra, A.K., Chuttani, K., Jain, N.K., 2016. Luteinizing hormone-releasing hormone peptide tethered nanoparticulate system for enhanced antitumoral efficacy of paclitaxel. Nanomedicine 11, 797–816.

Gupta, P.B., Onder, T.T., Jiang, G., Tao, K., Kuperwasser, C., Weinberg, R.A., et al., 2009. Identification of selective inhibitors of cancer stem cells by high-throughput screening. Cell 138, 645–659.

Gutova, M., Najbauer, J., Frank, R.T., Kendall, S.E., Gevorgyan, A., Metz, M.Z., et al., 2008. Urokinase plasminogen activator and urokinase plasminogen activator receptor mediate human stem cell tropism to malignant solid tumors. Stem Cells 26, 1406–1413.

Hanahan, D., Weinberg, R.A., 2011. Hallmarks of cancer: the next generation. Cell 144, 646–674.

Hodgkinson, C.P., Gomez, J.A., Mirotsou, M., Dzau, V.J., 2010. Genetic engineering of mesenchymal stem cells and its application in human disease therapy. Hum. Gene Ther. 21, 1513–1526.

Hsu, H.-S., Lin, J.-H., Hsu, T.-W., Su, K., Wang, C.-W., Yang, K.-Y., et al., 2012. Mesenchymal stem cells enhance lung cancer initiation through activation of IL-6/JAK2/STAT3 pathway. Lung Cancer 75, 167–177.

Hu, Y.-L., Fu, Y.-H., Tabata, Y., Gao, J.-Q., 2010. Mesenchymal stem cells: a promising targeted-delivery vehicle in cancer gene therapy. J. Control. Release 147, 154–162.

Huang, R., Ke, W., Liu, Y., Wu, D., Feng, L., Jiang, C., et al., 2010. Gene therapy using lactoferrin-modified nanoparticles in a rotenone-induced chronic Parkinson model. J. Neurol. Sci. 290, 123–130.

Huang, X., Zhang, F., Wang, H., Niu, G., Choi, K.Y., Swierczewska, M., et al., 2013. Mesenchymal stem cell-based cell engineering with multifunctional mesoporous silica nanoparticles for tumor delivery. Biomaterials 34, 1772–1780.

Humphreys, B.D., Soiffer, R.J., Magee, C.C., 2005. Renal failure associated with cancer and its treatment: an update. J. Am. Soc. Nephrol. 16, 151–161.

Iwamoto, T., 2013. Clinical application of drug delivery systems in cancer chemotherapy: review of the efficacy and side effects of approved drugs. Biol. Pharm. Bull. 36, 715–718.
Jain, R.K., Stylianopoulos, T., 2010. Delivering nanomedicine to solid tumors. Nat. Rev. Clin. Oncol. 7, 653.
Javazon, E.H., Beggs, K.J., Flake, A.W., 2004. Mesenchymal stem cells: paradoxes of passaging. Exp. Hematol. 32, 414–425.
Jing, Y., Han, Z., Zhang, S., Liu, Y., Wei, L., 2011. Epithelial-mesenchymal transition in tumor microenvironment. Cell Biosci. 1, 29.
Jo, J.-I., Aoki, I., Tabata, Y., 2010. Design of iron oxide nanoparticles with different sizes and surface charges for simple and efficient labeling of mesenchymal stem cells. J. Control. Release 142, 465–473.
Johannsen, M., Gneveckow, U., Taymoorian, K., Thiesen, B., Waldöfner, N., Scholz, R., et al., 2007. Morbidity and quality of life during thermotherapy using magnetic nanoparticles in locally recurrent prostate cancer: results of a prospective phase I trial. Int. J. Hyperthermia 23, 315–323.
Kalimuthu, S., Gangadaran, P., Rajendran, R.L., Zhu, L., Oh, J.M., Lee, H.W., et al., 2018. A new approach for loading anticancer drugs into mesenchymal stem cell-derived exosome mimetics for cancer therapy. Front. Pharmacol. 9, 1116.
Kemp, J.A., Shim, M.S., Heo, C.Y., Kwon, Y.J., 2016. "Combo" nanomedicine: co-delivery of multi-modal therapeutics for efficient, targeted, and safe cancer therapy. Adv. Drug Deliv. Rev. 98, 3–18.
Kidd, S., Spaeth, E., Dembinski, J.L., Dietrich, M., Watson, K., Klopp, A., et al., 2009. Direct evidence of mesenchymal stem cell tropism for tumor and wounding microenvironments using in vivo bioluminescent imaging. Stem Cells 27, 2614–2623.
Kim, S.-S., Rait, A., Kim, E., Pirollo, K.F., Nishida, M., Farkas, N., et al., 2014a. A nanoparticle carrying the p53 gene targets tumors including cancer stem cells, sensitizes glioblastoma to chemotherapy and improves survival. ACS Nano 8, 5494–5514.
Kim, S.M., Woo, J.S., Jeong, C.H., Ryu, C.H., Jang, J.-D., Jeun, S.-S., 2014b. Potential application of temozolomide in mesenchymal stem cell-based TRAIL gene therapy against malignant glioma. Stem Cells Transl. Med. 3, 172–182.
Kobayashi, H., Watanabe, R., Choyke, P.L., 2014. Improving conventional enhanced permeability and retention (EPR) effects; what is the appropriate target? Theranostics 4, 81.
Kreuter, J. 1994. Nanoparticles. In: Colloidal Drug Delivery Systems, pp. 219–342, CRC press.
Layek, B., Sadhukha, T., Panyam, J., Prabha, S., 2018. Nanoengineered mesenchymal stem cells increase therapeutic efficacy of anticancer drug through true active tumor targeting. Mol. Cancer Ther. 17, 1196–1206.
Leonard, R., Williams, S., Tulpule, A., Levine, A., Oliveros, S., 2009. Improving the therapeutic index of anthracycline chemotherapy: focus on liposomal doxorubicin (Myocet). Breast 18, 218–224.
Li, L., Guan, Y., Liu, H., Hao, N., Liu, T., Meng, X., et al., 2011. Silica nanorattle–doxorubicin-anchored mesenchymal stem cells for tumor-tropic therapy. ACS Nano 5, 7462–7470.
Loebinger, M.R., Janes, S.M., 2010. Stem cells as vectors for antitumour therapy. Thorax 65, 362–369.
Loebinger, M.R., Eddaoudi, A., Davies, D., Janes, S.M., 2009a. Mesenchymal stem cell delivery of TRAIL can eliminate metastatic cancer. Cancer Res. 69, 4134–4142.
Loebinger, M.R., Kyrtatos, P.G., Turmaine, M., Price, A.N., Pankhurst, Q., Lythgoe, M.F., et al., 2009b. Magnetic resonance imaging of mesenchymal stem cells homing to pulmonary metastases using biocompatible magnetic nanoparticles. Cancer Res. 0008-5472. CAN-09-1912.
Loo, C., Lowery, A., Halas, N., West, J., Drezek, R., 2005. Immunotargeted nanoshells for integrated cancer imaging and therapy. Nano Lett. 5, 709–711.
Lv, F.-J., Tuan, R.S., Cheung, K.M., Leung, V.Y., 2014. Concise review: the surface markers and identity of human mesenchymal stem cells. Stem Cells 32, 1408–1419.
Maheshwari, R., Tekade, M., A Sharma, P., Kumar Tekade, R., 2015a. Nanocarriers assisted siRNA gene therapy for the management of cardiovascular disorders. Curr. Pharm. Des. 21, 4427–4440.
Maheshwari, R.G., Thakur, S., Singhal, S., Patel, R.P., Tekade, M., Tekade, R.K., 2015b. Chitosan encrusted nonionic surfactant based vesicular formulation for topical administration of ofloxacin. Sci. Adv. Mater. 7, 1163–1176.
Majumdar, M.K., Keane-Moore, M., Buyaner, D., Hardy, W.B., Moorman, M.A., Mcintosh, K.R., et al., 2003. Characterization and functionality of cell surface molecules on human mesenchymal stem cells. J. Biomed. Sci. 10, 228–241.

Mariani, E., Facchini, A., 2012. Clinical applications and biosafety of human adult mesenchymal stem cells. Curr. Pharm. Des. 18, 1821–1845.
Martinez-Quintanilla, J., Bhere, D., Heidari, P., He, D., Mahmood, U., Shah, K., 2013. Therapeutic efficacy and fate of bimodal engineered stem cells in malignant brain tumors. Stem Cells 31, 1706–1714.
Melancon, M.P., Stafford, R.J., Li, C., 2012. Challenges to effective cancer nanotheranostics. J. Control. Release 164, 177–182.
Miele, E., Spinelli, G.P., Miele, E., Tomao, F., Tomao, S., 2009. Albumin-bound formulation of paclitaxel (Abraxane ABI-007) in the treatment of breast cancer. Int. J. Nanomed. 4, 99.
Minchinton, A.I., Tannock, I.F., 2006. Drug penetration in solid tumours. Nat. Rev. Cancer 6, 583.
Mody, N., Tekade, R.K., Mehra, N.K., Chopdey, P., Jain, N.K., 2014. Dendrimer, liposomes, carbon nanotubes and PLGA nanoparticles: one platform assessment of drug delivery potential. AAPS PharmSciTech 15, 388–399.
Momin, N.E., Vela, G., Zaidi, H.A., Quiñones-Hinojosa, A., 2010. The oncogenic potential of mesenchymal stem cells in the treatment of cancer: directions for future research. Curr. Immunol. Rev. 6, 137–148.
Muniswamy, V.J., Raval, N., Gondaliya, P., Tambe, V., Kalia, K., Tekade, R.K., 2019. 'Dendrimer-Cationized-Albumin' encrusted polymeric nanoparticle improves BBB penetration and anticancer activity of doxorubicin. Int. J. Pharm. 555, 77–99.
Murphy, P., Baggiolini, M. Charo, I., Hebert, C.A., Horuk, R., Matsushima, K., et al., 2000. International union of pharmacology. XXII. Nomenclature for chemokine receptors. Pharmacol. Rev. 52, 145–176.
Nasongkla, N., Shuai, X., Ai, H., Weinberg, B.D., Pink, J., Boothman, D.A., et al., 2004. cRGD-functionalized polymer micelles for targeted doxorubicin delivery. Angew. Chem. Int. Ed. 43, 6323–6327.
Neuss, S., Becher, E., Wöltje, M., Tietze, L., Jahnen-Dechent, W., 2004. Functional expression of HGF and HGF receptor/c-met in adult human mesenchymal stem cells suggests a role in cell mobilization, tissue repair, and wound healing. Stem Cells 22, 405–414.
Noël, D., Djouad, F., Bouffi, C., Mrugala, D., Jorgensen, C., 2007. Multipotent mesenchymal stromal cells and immune tolerance. Leuk. Lymphoma 48, 1283–1289.
Paris, J.L., De La Torre, P., Manzano, M., Cabañas, M.V., Flores, A.I., Vallet-Regí, M., 2016. Decidua-derived mesenchymal stem cells as carriers of mesoporous silica nanoparticles. In vitro and in vivo evaluation on mammary tumors. Acta Biomater. 33, 275–282.
Passero JR, F.C., Grapsa, D., Syrigos, K.N., Saif, M.W., 2016. The safety and efficacy of Onivyde (irinotecan liposome injection) for the treatment of metastatic pancreatic cancer following gemcitabine-based therapy. Expert Rev. Anticancer Ther. 16, 697–703.
Prabhu, P., Patravale, V., 2012. The upcoming field of theranostic nanomedicine: an overview. J. Biomed. Nanotechnol. 8, 859–882.
Primeau, A.J., Rendon, A., Hedley, D., Lilge, L., Tannock, I.F., 2005. The distribution of the anticancer drug Doxorubicin in relation to blood vessels in solid tumors. Clin. Cancer Res. 11, 8782–8788.
Quante, M., Tu, S.P., Tomita, H., Gonda, T., Wang, S.S., Takashi, S., et al., 2011. Bone marrow-derived myofibroblasts contribute to the mesenchymal stem cell niche and promote tumor growth. Cancer Cell 19, 257–272.
Rasmusson, I., Ringdén, O., Sundberg, B., Le Blanc, K., 2003. Mesenchymal stem cells inhibit the formation of cytotoxic T lymphocytes, but not activated cytotoxic T lymphocytes or natural killer cells. Transplantation 76, 1208–1213.
Ridgway, A., Agbanyo, F., Wang, J., Rosu-Myles, M., 2015. Regulatory oversight of cell and gene therapy products in Canada. Regulatory Aspects of Gene Therapy and Cell Therapy Products. Springer.
Ries, C., Egea, V., Karow, M., Kolb, H., Jochum, M., Neth, P., 2007. MMP-2, MT1-MMP, and TIMP-2 are essential for the invasive capacity of human mesenchymal stem cells: differential regulation by inflammatory cytokines. Blood 109, 4055–4063.
Ringe, J., Strassburg, S., Neumann, K., Endres, M., Notter, M., Burmester, G.R., et al., 2007. Towards in situ tissue repair: human mesenchymal stem cells express chemokine receptors CXCR1, CXCR2 and CCR2, and migrate upon stimulation with CXCL8 but not CCL2. J. Cell. Biochem. 101, 135–146.
Roger, M., Clavreul, A., Venier-Julienne, M.-C., Passirani, C., Sindji, L., Schiller, P., et al., 2010. Mesenchymal stem cells as cellular vehicles for delivery of nanoparticles to brain tumors. Biomaterials 31, 8393–8401.
Roger, M., Clavreul, A., Menei, P., 2012. Mesenchymal stem cells: role for delivering nanoparticles to brain tumors. In: Stem Cells and Cancer Stem Cells, vol. 3. Springer.

Rüster, B., Göttig, S., Ludwig, R.J., Bistrian, R., Müller, S., Seifried, E., et al., 2006. Mesenchymal stem cells display coordinated rolling and adhesion behavior on endothelial cells. Blood 108, 3938–3944.
Sadhukha, T., O'brien, T.D., Prabha, S., 2014. Nanoengineered mesenchymal stem cells as targeted therapeutic carriers. J. Control. Release 196, 243–251.
Saraf, J., Kalia, K., Bhattacharya, P., Tekade, R.K., 2018. Growing synergy of nanodiamonds in neurodegenerative interventions. Drug Discov. Today (in press).
Sartor, O., 2003. Eligard: leuprolide acetate in a novel sustained-release delivery system. Urology 61, 25–31.
Schieker, M., Pautke, C., Reitz, K., Hemraj, I., Neth, P., Mutschler, W., et al., 2004. The use of four-colour immunofluorescence techniques to identify mesenchymal stem cells. J. Anat. 204, 133–139.
Serakinci, N., Guldberg, P., Burns, J.S., Abdallah, B., Schrødder, H., Jensen, T., et al., 2004. Adult human mesenchymal stem cell as a target for neoplastic transformation. Oncogene 23, 5095.
Shah, K., 2012. Mesenchymal stem cells engineered for cancer therapy. Adv. Drug Deliv. Rev. 64, 739–748.
Shah, K., Chawla, S., Gadeval, A., Reddy, G., Maheshwari, R., Kalia, K., et al., 2018. Nanostructured hyaluronic acid-based materials for the delivery of siRNA. Curr. Pharm. Des. 24, 2678–2691.
Shen, S., Xia, J.-X., Wang, J., 2016. Nanomedicine-mediated cancer stem cell therapy. Biomaterials 74, 1–18.
Silverman, J.A., Deitcher, S.R., 2013. Marqibo® (vincristine sulfate liposome injection) improves the pharmacokinetics and pharmacodynamics of vincristine. Cancer Chemother. Pharmacol. 71, 555–564.
Singh Dhakad, R., Kumar Tekade, R., Kumar Jain, N., 2013. Cancer targeting potential of folate targeted nanocarrier under comparative influence of tretinoin and dexamethasone. Curr. Drug Deliv. 10, 477–491.
Smith, B.R., Kempen, P., Bouley, D., Xu, A., Liu, Z., Melosh, N., et al., 2012. Shape matters: intravital microscopy reveals surprising geometrical dependence for nanoparticles in tumor models of extravasation. Nano Lett. 12, 3369–3377.
Sofias, A.M., Dunne, M., Storm, G., Allen, C., 2017. The battle of "nano" paclitaxel. Adv. Drug Deliv. Rev. 122, 20–30.
Sohni, A., Verfaillie, C.M., 2013. Mesenchymal stem cells migration homing and tracking. Stem Cells Int. 2013, 130763.
Son, B.R., Marquez-Curtis, L.A., Kucia, M., Wysoczynski, M., Turner, A.R., Ratajczak, J., et al., 2006. Migration of bone marrow and cord blood mesenchymal stem cells in vitro is regulated by stromal-derived factor-1-CXCR4 and hepatocyte growth factor-c-met axes and involves matrix metalloproteinases. Stem Cells 24, 1254–1264.
Soni, N., Soni, N., Pandey, H., Maheshwari, R., Kesharwani, P., Tekade, R.K., 2016. Augmented delivery of gemcitabine in lung cancer cells exploring mannose anchored solid lipid nanoparticles. J. Colloid Interface Sci. 481, 107–116.
Soni, N., Tekade, M., Kesharwani, P., Bhattacharya, P., Maheshwari, R., Dua, K., et al., 2017. Recent advances in oncological submissions of dendrimer. Curr. Pharm. Des. 23, 3084–3098.
Sordi, V., 2009. Mesenchymal stem cell homing capacity. Transplantation 87, S42–S45.
Stosich, M.S., Bastian, B., Marion, N.W., Clark, P.A., Reilly, G., Mao, J.J., 2007. Vascularized adipose tissue grafts from human mesenchymal stem cells with bioactive cues and microchannel conduits. Tissue Eng. 13, 2881–2890.
Studeny, M., Marini, F.C., Champlin, R.E., Zompetta, C., Fidler, I.J., Andreeff, M., 2002. Bone marrow-derived mesenchymal stem cells as vehicles for interferon-β delivery into tumors. Cancer Res. 62, 3603–3608.
Sun, R., Liu, Y., Li, S.-Y., Shen, S., Du, X.-J., Xu, C.-F., et al., 2015. Co-delivery of all-trans-retinoic acid and doxorubicin for cancer therapy with synergistic inhibition of cancer stem cells. Biomaterials 37, 405–414.
Tekade, R.K., 2018. Basic Fundamentals of Drug Delivery. Academic Press.
Tekade, R.K., Youngren-Ortiz, S.R., Yang, H., Haware, R., Chougule, M.B., 2014. Designing hybrid onconase nanocarriers for mesothelioma therapy: a Taguchi orthogonal array and multivariate component driven analysis. Mol. Pharm. 11, 3671–3683.
Tekade, R.K., Tekade, M., Kumar, M., Chauhan, A.S., 2015a. Dendrimer-stabilized smart-nanoparticle (DSSN) platform for targeted delivery of hydrophobic antitumor therapeutics. Pharm. Res. 32, 910–928.
Tekade, R.K., Youngren-Ortiz, S.R., Yang, H., Haware, R., Chougule, M.B., 2015b. Albumin-Chitosan Hybrid Onconase Nanocarriers for Mesothelioma Therapy. AACR.
Tekade, R.K., Maheshwari, R., Soni, N., Tekade, M., Chougule, M.B., 2017. Chapter 1—Nanotechnology for the development of nanomedicine A2—Mishra, Vijay. In: Kesharwani, P., Amin, M.C.I.M., Iyer, A. (Eds.), Nanotechnology-Based Approaches for Targeting and Delivery of Drugs and Genes. Academic Press.

Tomchuck, S.L., Zwezdaryk, K.J., Coffelt, S.B., Waterman, R.S., Danka, E.S., Scandurro, A.B., 2008. Toll-like receptors on human mesenchymal stem cells drive their migration and immunomodulating responses. Stem Cells 26, 99–107.

Torsvik, A., Bjerkvig, R., 2013. Mesenchymal stem cell signaling in cancer progression. Cancer Treat. Rev. 39, 180–188.

Uccelli, A., Moretta, L., Pistoia, V., 2008. Mesenchymal stem cells in health and disease. Nat. Rev. Immunol. 8, 726.

Vegh, I., Grau, M., Gracia, M., Grande, J., De La Torre, P., Flores, A., 2013. Decidua mesenchymal stem cells migrated toward mammary tumors in vitro and in vivo affecting tumor growth and tumor development. Cancer Gene Ther. 20, 8.

Verma, R.K., Yu, W., Singh, S.P., Shankar, S., Srivastava, R.K., 2015. Anthothecol-encapsulated PLGA nanoparticles inhibit pancreatic cancer stem cell growth by modulating sonic hedgehog pathway. Nanomed.: Nanotechnol. Biol. Med. 11, 2061–2070.

Wang, D., Park, J.S., Chu, J.S., Krakowski, A., Luo, K., Chen, D.J., et al., 2004. Proteomic profiling of bone marrow mesenchymal stem cells upon transforming growth factor β1 stimulation. J. Biol. Chem. 279, 43725–43734.

Wang, R., Billone, P.S., Mullett, W.M., 2013. Nanomedicine in action: an overview of cancer nanomedicine on the market and in clinical trials. J. Nanomater. 2013, 1.

Wei, X., Yang, X., Han, Z.-P., Qu, F.-F., Shao, L., Shi, Y.-F., 2013. Mesenchymal stem cells: a new trend for cell therapy. Acta Pharmacol. Sin. 34, 747.

Xu, C., Miranda-Nieves, D., Ankrum, J.A., Matthiesen, M.E., Phillips, J.A., Roes, I., et al., 2012. Tracking mesenchymal stem cells with iron oxide nanoparticle loaded poly(lactide-*co*-glycolide) microparticles. Nano Lett. 12, 4131–4139.

Yagi, H., Kitagawa, Y., 2013. The role of mesenchymal stem cells in cancer development. Front. Genet. 4, 261.

Yang, J., Kopeček, J., 2015. Polymeric biomaterials and nanomedicines. J. Drug Deliv. Sci. Technol. 30, 318–330.

Yao, S., Li, X., Liu, J., Sun, Y., Wang, Z., Jiang, Y., 2017. Maximized nanodrug-loaded mesenchymal stem cells by a dual drug-loaded mode for the systemic treatment of metastatic lung cancer. Drug Deliv. 24, 1372–1383.

Yu, J.M., Jun, E.S., Bae, Y.C., Jung, J.S., 2008. Mesenchymal stem cells derived from human adipose tissues favor tumor cell growth in vivo. Stem Cells Dev. 17, 463–474.

Yu, M.K., Park, J., Jon, S., 2012. Targeting strategies for multifunctional nanoparticles in cancer imaging and therapy. Theranostics 2, 3.

Zhang, Y., Zhang, H., Wang, X., Wang, J., Zhang, X., Zhang, Q., 2012. The eradication of breast cancer and cancer stem cells using octreotide modified paclitaxel active targeting micelles and salinomycin passive targeting micelles. Biomaterials 33, 679–691.

Zhao, W., Phinney, D.G., Bonnet, D., Dominici, M., Krampera, M., 2014. Mesenchymal stem cell biodistribution, migration, and homing in vivo. Stem Cells Int. 2014.

Zhao, Z., Nelson, A.R., Betsholtz, C., Zlokovic, B.V., 2015. Establishment and dysfunction of the blood-brain barrier. Cell 163, 1064–1078.

Zhu, H., Mitsuhashi, N., Klein, A., Barsky, L.W., Weinberg, K., Barr, M.L., et al., 2006a. The role of the hyaluronan receptor CD44 in mesenchymal stem cell migration in the extracellular matrix. Stem Cells 24, 928–935.

Zhu, W., Xu, W., Jiang, R., Qian, H., Chen, M., Hu, J., et al., 2006b. Mesenchymal stem cells derived from bone marrow favor tumor cell growth in vivo. Exp. Mol. Pathol. 80, 267–274.

Zuo, Z.-Q., Chen, K.-G., Yu, X.-Y., Zhao, G., Shen, S., Cao, Z.-T., et al., 2016. Promoting tumor penetration of nanoparticles for cancer stem cell therapy by TGF-β signaling pathway inhibition. Biomaterials 82, 48–59.

CHAPTER

3

Guiding Factors and Surface Modification Strategies for Biomaterials in Pharmaceutical Product Development

Neha Maheshwari[1], *Umesh Kumar Atneriya*[1], *Muktika Tekade*[1], *Mukesh Chandra Sharma*[1], *Abdelbary Elhissi*[2] *and Rakesh K. Tekade*[3]

[1]School of Pharmacy, Devi Ahilya Vishwavidyalaya, Takshila Campus, Indore, India [2]College of Pharmacy, Qatar University, Doha, Qatar [3]National Institute of Pharmaceutical Education and Research (NIPER)—Ahmedabad, Gandhinagar, India

OUTLINE

3.1 Introduction to Biomaterials: Concept and Understanding 58

3.2 Surface Modification of Biomaterials: Role in Product Development 59

3.2.1 Enhancement of Drug Loading 60
3.2.2 Selective Targeting 60
3.2.3 Enhanced Drug Delivery to the Brain 61
3.2.4 Macrophage Targeting 61
3.2.5 Enhanced Transdermal Delivery 61
3.2.6 Enhancement of Drug Stability 62
3.2.7 Reduction of Blood Toxicity 62
3.2.8 Enhanced Uptake by Cancer and Inflamed Tissues 62
3.2.9 Enhancement of Bioadhesion 63
3.2.10 Increased Blood Plasma Half-Life 63
3.2.11 Site-Selective Drug Release Through the Enteric Coating 64
3.2.12 Multiple Drug Release via Layer-by-Layer Approach 64

3.3 Strategies Employed in the Surface Modification of Biomaterials 65

3.3.1 Plasma Polymerization 65

Biomaterials and Bionanotechnology
DOI: https://doi.org/10.1016/B978-0-12-814427-5.00003-2

© 2019 Elsevier Inc. All rights reserved.

3.3.2 *Heparinization to Improve Blood Compatibility* 67
3.3.3 *Peptide Functionalization* 69
3.3.4 *Calcium Phosphate Deposition* 72
3.3.5 *Thermal Spray Deposition* 73
3.3.6 *Ion Beam Assisted Deposition* 74
3.3.7 *Pulsed Laser Physical Vapor Deposition* 74
3.3.8 *Microarc Oxidation* 75
3.3.9 *Magnetron Sputtering Deposition* 76
3.3.10 *Electrophoretic Deposition* 77
3.3.11 *Electrochemical Deposition* 77
3.3.12 *Sol–Gel Methods* 78
3.3.13 *Hot Isostatic Pressing* 79
3.3.14 *Biomimetic Coatings* 80
3.4 Future Remarks and Conclusion 81
Acknowledgment 82
Abbreviations 82
References 82
Further Reading 87

3.1 INTRODUCTION TO BIOMATERIALS: CONCEPT AND UNDERSTANDING

The word *biomaterial* covers any material anticipated to interact with the biological system to supplant living material that has lost its function (Sharma et al., 2015). Biomaterials are helpful in a variety of applications including the stimulation of new tissue growth. As per the definition proposed by the American National Institute of Health, "biomaterial is any substance or combination of substances, other than drugs, synthetic or natural in origin, which can be used for any period of time, which augments or replaces partially or totally any tissue, organ or function, to maintain or improve the quality of life of the individual" (Sculean et al., 2015). Biomaterials can be broadly classified into natural and synthetic with distinct bioreactivity (Fig. 3.1).

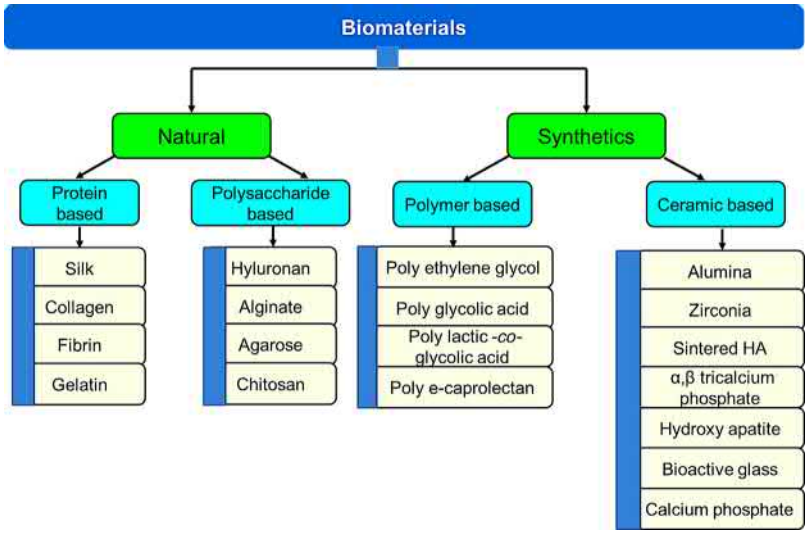

FIGURE 3.1 A diagrammatic view of various natural and synthetic material used as biomaterials for application in pharmaceutical product development.

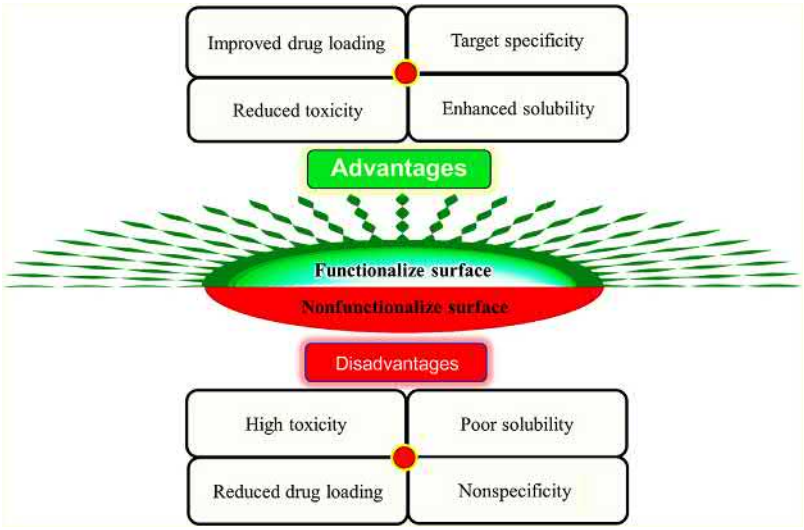

FIGURE 3.2 The depiction of the difference in properties of functionalized and nonfunctionalized surface for pharmaceutical product development.

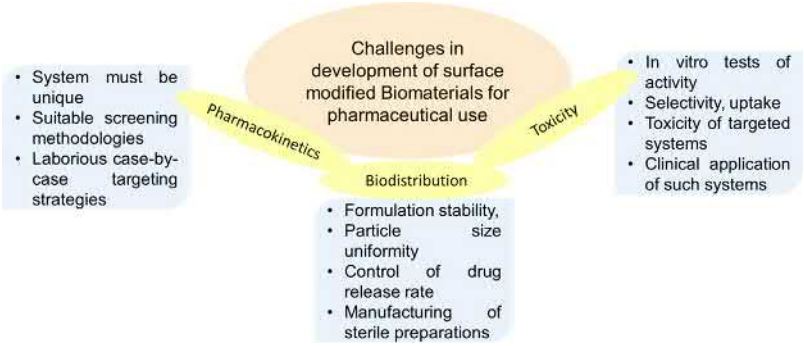
Challenges in development of surface modified Biomaterials for pharmaceutical use
Pharmacokinetics
Biodistribution
Toxicity
• System must be unique
• Suitable screening methodologies
• Laborious case-by-case targeting strategies
• Formulation stability,
• Particle size uniformity
• Control of drug release rate
• Manufacturing of sterile preparations
• In vitro tests of activity
• Selectivity, uptake
• Toxicity of targeted systems
• Clinical application of such systems

FIGURE 3.3 Challenges in the successful development of surface modified biomaterials. They may categorized into problems associated with pharmacokinetics, biodistribution, and toxicity.

The understanding of the biomaterial and their interactions with the biological surface is important and required for the successful execution of biomedical applications such as tissue regeneration (Fattahi et al., 2014). This understanding may also be important to find out the regenerative abilities of biomaterials aiding their design with better functionalities, for example, biological compatibility and bioactivity (Ramot et al., 2016). Advantages of surface functionalization of biomaterials over nonfunctionalized surface are represented in Fig. 3.2.

However, development of a fitting functionalized biomaterial for pharmaceutical application poses many challenges as shown in Fig. 3.3.

3.2 SURFACE MODIFICATION OF BIOMATERIALS: ROLE IN PRODUCT DEVELOPMENT

Over the past decade, the use of biomaterials has increased day by day. However, biomaterial instability is a limitation (Rashid et al., 2016). Therefore vast attention is being

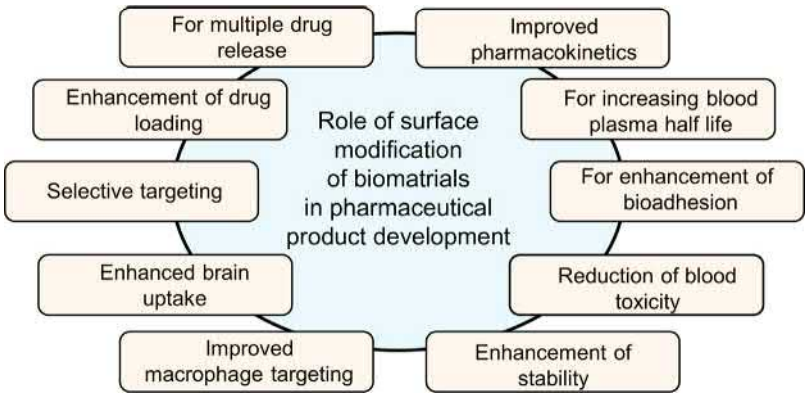
For multiple drug release
Improved pharmacokinetics
Enhancement of drug loading
For increasing blood plasma half life
Role of surface modification of biomatrials in pharmaceutical product development
Selective targeting
For enhancement of bioadhesion
Enhanced brain uptake
Reduction of blood toxicity
Improved macrophage targeting
Enhancement of stability

FIGURE 3.4 Role of surface modification of biomaterials in pharmaceutical product development.

paid by the researchers on the modification of biomaterials for successful application in pharmaceutical product development (Fig. 3.4).

3.2.1 Enhancement of Drug Loading

Drug loading can be increased by modifying the polymer surface. Usually, the number of binding sites of the polymer can be increased to enhance the drug binding capacity with the polymeric structure. Moreover, the three-dimensional (3D) structure of the polymers can be changed to get higher drug loading. This can be achieved by various means for instance by heating the polymer at different temperatures considering that its stability does not get altered (Dhakad et al., 2013; Gajbhiye et al., 2009a,b; Jain and Tekade, 2013). It can also be adjusted by altering the concentration of polymer, hybridizing the polymer, by using the polymers with high loading zones like dendrimers (Pelipenko et al., 2015; Prajapati et al., 2009; Tekade and Chougule, 2013; Tekade et al., 2008, 2009).

Polymer surface modification can also be done by treating the polymer with different chemicals. For example, investigators have performed in situ polymerizations of oral drug delivery systems (with ibuprofen as a model drug), resulting in enhanced drug loading. They used the annealing polymerization (using polyethylene) to modify the polymeric surface and to achieve higher drug loading. The results showed 76% drug loading efficiency, which was far greater than the normal oral formulation without polymeric surface modification (45%) (Liow et al., 2016).

3.2.2 Selective Targeting

Surface modification of biomaterials can also be done by adding moieties on the polymer surfaces to enable polymer interaction with the target receptor site. The receptor binding moieties very easily take the polymeric formulation toward the organ where the drug is targeted (Al-Qattan et al., 2018; Tekade et al., 2017a,b; Tekade and Sun, 2017; Zhang et al., 2015).

For example, human liver is mainly composed of hepatocytes. Nearly 80% of these hepatocytes have asialoglycoprotein receptors, which have strong binding affinities toward

the glucose moiety. Thus modifying the polymeric structure by attaching glucose onto the polymer surface may increase the polymer affinity toward the liver, resulting in improved targeting of the drug incorporated into the polymeric matrix. The chemical modification of the polymers can be performed by sugar containing reagents like polylactide (PLA)–polyaminoacid conjugates, lactosaminated human albumin, galactosylated phospholipid-polyaminoacid, and lactosaminated carboxymethyl chitosan (Jiang et al., 2015).

3.2.3 Enhanced Drug Delivery to the Brain

In vertebrates, the most complex organ is the brain. The cerebral cortex is the largest part containing about 15–33 billion neurons. Each neuron is connected by synapses to several thousand other neurons. Brain cells are mainly composed of glial cells and neurons. Among these components, neurons are considered as the most important cells of the brain. Due to high complexity and better protections in the brain (via the blood–brain barrier; BBB), it is very difficult to design appropriate brain targeting. Polymeric surface modification may help at enhancing penetration of the drug across the BBB, resulting in improved brain targeting (Kumar et al., 2018).

Zhang et al. attempted to prepare polymeric micelles for the drug Docetaxel by using *p*-hydroxybenzoic acid as targeting ligand to achieve better brain targeting. They found that the prepared micelles had a better spherical shape in the nanosize range (mean diameter around 18 ± 3 nm), with better encapsulation efficiency and higher drug loading. In vitro, cellular uptake experiments proved that there was 1.2 times higher uptake in the brain compared with the unmodified micelles. Here the polymeric surface was modified using the acidic strength that alters the pH of the polymer, making it suitable for targeting the brain and enhancing the drug uptake (Zhang et al., 2013).

3.2.4 Macrophage Targeting

Biomaterial surface modification also helps in enhancing macrophage targeting. Macrophages have the ability to fight against dreadful diseases such as cancers and atherosclerosis (Zhou et al., 2011).

Yu et al. have prepared polymeric micelles to achieve better macrophage targeting. In these micelles, the polymeric surface was modified by using mannose conjugation. CD206 was used as macrophage and dendritic cells act as a tumor-associated macrophage. The results showed that the mannosylated nanoparticles actively improved the silencing RNA delivery into primary macrophages. This increase was nearly fourfold as compared with the nontargeted formulation of the same carrier system (Yu et al., 2013).

3.2.5 Enhanced Transdermal Delivery

Surface modification of biomaterials may increase the transdermal penetration via increasing the accessibility of the developed systems inside the skin. Hence, the drug is always given in specific quantity as well as with another adjuvant to maintain the

therapeutic level at the desired site. Any increase in drug concentration may cause toxic effects whilst a decrease in concentration may produce no effects (Maheshwari et al., 2012).

Researchers are trying to maintain the dose within the therapeutic window. To achieve this, polymers are greatly helpful. In principle, polymers represent a group of monomers with 3D structures. The drug can be loaded or conjugated within the polymeric structure. The drug takes time to release within the blood as the drug needs to cross the various 3D layers of the polymeric matrix before reaching to the bloodstream. This can reduce the risk of blood toxicity (Tekade et al., 2017).

3.2.6 Enhancement of Drug Stability

Most drugs have various stability issues. Many drugs are liable to metabolic deactivation (i.e., they form inactive metabolites). Others may degrade during storage by various processes such as hydrolysis, oxidation, nitration, conjugation, photooxidation, pH change, etc. Such drugs, when they come directly into contact with light, oxygen, water, or other media, become highly susceptible to degradation. Polymerization may help in protecting the drug from the external environment. The polymers when modified by using specific chemical agents, entraps the drug within their 3D structure and hence protecting the drug from the detrimental external environment (Dua et al., 2017; Maheshwari et al., 2015; Soni et al., 2017; Tekade et al., 2015).

Cesium lead halide has low chemical and structural stability; these halide molecules have limited processability due to their instability. Meyns et al. have developed a new method to coat halide molecules, which resulted in increased chemical as well as optical stability and processability of the formulation. This method was based on the incorporation of polymer, that is, poly(maleic anhydride-alt-1-octadecene) into the synthesis process. The presence of this polymer in the ligand stabilizes the formulation by tightening the ligand bind (Meyns et al., 2016).

3.2.7 Reduction of Blood Toxicity

Excessive drug uptake by the body may elicit severe toxic effects. Hence, drugs are always given in limited doses as well as with adjuvant materials to maintain the level of the drug in the body within the therapeutic range. Any increase in level as compared with its therapeutic concentration may produce toxic effects and a decrease in level may produce no effect (Choudhury et al., 2017; Ghanghoria et al., 2016; Gorain et al., 2016; Moeendarbari et al., 2016; Tekade et al., 2018).

3.2.8 Enhanced Uptake by Cancer and Inflamed Tissues

The enhanced permeability and retention (EPR) effect is the mechanism by which high−molecular weight nontargeted drugs and prodrugs accumulate in tissues that offer increased vascular permeability, such as in sites of inflammation or cancer. Attributes of the EPR effect were first described in 1986 by Matsumura and Maeda Matsumura and

Maeda (Maeda and Matsumura, 2011). In their landmark study, the increased tumor uptake and retention of the proteinaceous anticancer drug styrene–maleic acid polymer-functionalized neocarzinostatin [molecular weight (MW), ~16 kDa] was explained by the binding of styrene–maleic acid polymer-functionalized neocarzinostatin to plasma albumin (MW, ~67 kDa). Compared with the native small-molecule neocarzinostatin, this albumin-bound macromolecular drug (MW, ~83 kDa) displayed increased accumulation of the tumor tissue, offering prolonged duration of action and increased therapeutic efficacy. The generality of the EPR effect and its dependence on molecular size was demonstrated further by the encapsulation of styrene–maleic acid polymer-functionalized neocarzinostatin in Lipiodol (ethiodized poppyseed oil) liposomes; a result that fueled research interest in liposomal formulations as drug delivery systems of anticancer drugs.

It is also a fact that for tumors with a dysplastic stroma (e.g., pancreatic cancer), the vasculature may be poorly perfused and even collapsed or obstructed by tumor-associated fibroblasts or pericytes that adhere tightly to the vascular wall. It is therefore of interest that in addition to structural or architectural vascular abnormalities, impairment of lymphatic drainage and permeability enhancing factors (e.g., nitric oxide, bradykinin, vascular endothelial growth factors, angiotensin II, prostaglandins, cytokines) contribute to the EPR effect. Surprisingly, there is insufficient highlight on the role of nutritional pathways that constitute the basis for increased blood flow to the tumor site, including vascular transport mechanisms that could potentially be exploited for uptake of macromolecules and nanoparticles (Chopdey et al., 2015; Mody et al., 2014; Tekade and Sun, 2017; Tekade et al., 2014; Youngren et al., 2013).

3.2.9 Enhancement of Bioadhesion

The adhesive properties of polymers make them highly beneficial for enhancing and prolonging the contact of the polymer-based formulation with the biological membranes. Hence, these polymers are widely used in the preparation of bioadhesive drug delivery systems. Most of the natural polymers such as sugars, proteins, carbohydrates, gelatin, starch, and hydroxyl propyl-methoxy cellulose have adhesive properties and are used for bio- and mucoadhesion. This property yields a strong commercial interest in these polymers as these polymers are biocompatible and hence can be used for biomedical applications like skin and various other body tissues (Mansuri et al., 2016a).

However, the extent of bioadhesion depends upon the nature of the polymer used. The power of polymer contact with the skin or other body organs can be modified or altered through surface modifications of the polymer, resulting in temporary or permanent adhesion to suit the needed application (Mansuri et al., 2016b).

3.2.10 Increased Blood Plasma Half-Life

PEGylation is one of the most widely used technologies to achieve longer blood plasma half-life and prolonged circulation time of the formulation. In this approach, the polymer is conjugated with polyethylene glycol (PEG). Owing to the nontoxic nature of PEG, it does not allow the polymer to be engulfed by the macrophages and

get degraded by enzymes. This results in a longer circulation time in the bloodstream (Gajbhiye et al., 2009a,b).

Since the formulation is not engulfed by the macrophages, the degradation rate of the drug-loaded into the polymeric formulation becomes much lower, and its release, while the formulation is circulated in the blood, becomes slower. This can increase drug stability, prolong blood plasma half-life, reduce drug toxicity, and lower the drug dose needed to achieve the desired therapeutic effect (Gajbhiye et al., 2007).

3.2.11 Site-Selective Drug Release Through the Enteric Coating

Drugs having high systemic toxicity, low aqueous solubility, poor cellular permeability, or low instability at physiological pH are ideal candidates for incorporation into polymeric delivery systems. Drug delivery for sustained release can also be achieved by preparing polymer formulations that depend upon the nature, type, and 3D geometry of the polymer. The chemical architecture of the polymer can influence the release pattern of the active drug loaded in the polymer (Maheshwari et al., 2017).

The controlled/sustained release of active ingredient can be achieved by using linkers between drugs and polymers that get degraded by a change in external environment like an acidic medium or presence of some specific enzymes. Some polymers show a change in their structure or nature such as pore size and permeability when the external stimulus is changed, which results in the release of active moiety. These polymers are also known as "smart polymers"; they release drug from the conjugate due to change in the polymer properties in presence of external stimuli (Mody et al., 2014).

For example, the pH of the stomach is different from that of the intestine. If we use a polymeric enteric coat that is soluble only in basic pH, then there will be no drug release in the stomach because the polymer is not affected by the acidic pH of the stomach. However, in the basic pH of the intestine, the polymer will be dissolved. In this way, an enteric coating can facilitate site-specific drug release. Some examples of pH-sensitive polymers include poly(methacrylic-*g*-ethylene glycol), poly(orthoesters), poly(acrylic acid), poly(methacrylic acid).

3.2.12 Multiple Drug Release via Layer-by-Layer Approach

With the surface modification of polymer, various physical and chemical properties of the polymers can be modified. The 3D structure of the polymers can be changed to obtain better drug release. This can be achieved by either heating the polymer at different temperatures considering that its stability is not affected by changing the pH of the environmental conditions. Modifications in polymers can also be done by radioactive substances (radiation may cause changes in the geometry of polymers, inducing changes in physical and chemical properties of the polymer). Polymer surface modification can also be done by treating the polymer with different chemicals (Li et al., 2014).

It is possible to design a formulation containing different layers of different polymers or different layers of the same polymer, and then control the release of the drug incorporated by using the above-mentioned methods. The drug can be loaded in between these layers.

The same drug or even different types of drug can be loaded in between the layers, giving the opportunity to design a polymeric formulation of more than one drug. By doing so, we can control and sustain the release of the same or multiple drugs, depending on the desired therapeutic application (Huang et al., 2017).

3.3 STRATEGIES EMPLOYED IN THE SURFACE MODIFICATION OF BIOMATERIALS

So far, various techniques have been employed to modify the surface of biomaterials. In this chapter, we tried to cover most of them. A representation of the most widely used techniques in this field is shown in Fig. 3.5.

3.3.1 Plasma Polymerization

Currently, an increased interest in the preparation of organic ultrathin films deposited by plasma has been seen. This technology is the method of choice for modifying the surfaces of materials for tissue engineering and biomedical applications where the bulk mechanical properties have dictated the choice of material; however, the surfaces of such materials continue to elicit an undesirable biological–biomaterial response (Inagaki, 2014).

This is an emerging technology that takes advantage of events that occur at the nanometer and/or micrometer scale length. For example, in devices utilizing microfluidic channels, the ratio of surface to bulk material is extremely high; hence the property of the surface in relation to the efficacy of the technology is dominant. Thus in microfluidics, surface functionalization of microchannels can be utilized to both reduce the unwanted surface events and promote others. One particular feature of the plasma deposition of

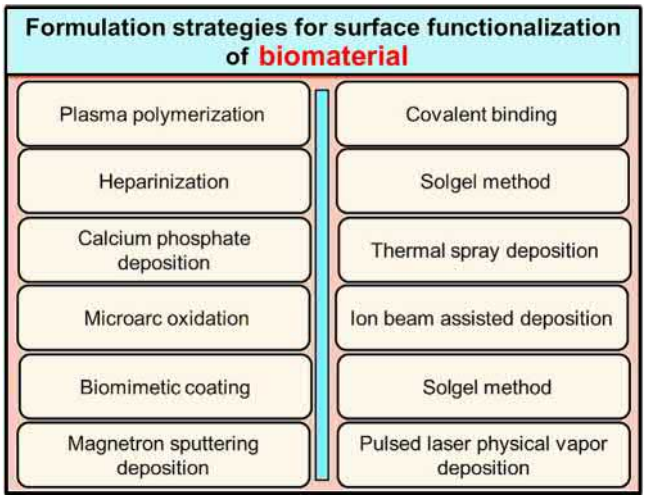

FIGURE 3.5 Various technologies/methodologies for the surface modification of biomaterials.

organic films often referred to as "plasma polymerization." This provides a significant advantage over other techniques where specific substrate chemistry is required, for example, gold for thiols or oxidized surfaces for silanes; however, considerable commercial development of this technique has not yet happened and poor understanding of plasma systems, their operation, the chemical processes responsible for plasma polymer film growth coupled with the blanket description of these surfaces as biocompatible, based mainly upon short-term in vitro studies, have restricted significant progress in this field (Hegemann et al., 2017).

Historically the scientific investigation of plasmas began in the late 19th century when Sir William Crookes described a DC discharge in an evacuated column as "the fourth state of matter"; yet, it was Irving Langmuir in 1929, who first defined an ionized gas using the term "plasma." However, in the 1950s the first industrial application of plasma processing occurred with the development of the modern integrated circuit (IC). Today anisotropic plasma etching allows patterning of ICs and the semiconductor industry, with its desire for ever smaller features on microchips, has proven to be one of the main driving forces behind the research in plasma processing.

This research, in turn, led to the almost ubiquitous implementation of plasma and plasma processing technology throughout the relevant industry. Low-temperature plasma surface modification is particularly applied to polymeric materials where there is opportunity to modify surface properties such as wettability, adhesion, permeability, and biocompatibility without causing thermal damages. Generation of low-temperature plasma is achieved by using DC or AC fields at reduced pressure and ionization can occur typically in the region of 1−100 seconds of mTorr (0.133−10 seconds Pascals). Methods of excitation include DC, radio frequency (RF at 13.56 MHz), and microwave (MW at 2.45 GHz) and this power source may be coupled directly, with the electrodes within the plasma chamber, indirectly with the electrodes external to the chamber, or by combination (Garcia-Torres et al., 2014).

For DC plasma the coupling is typically conductive between two electrodes and, depending on the application, a range of conducting materials can be used for electrode fabrication. With RF sources, the power, coupled to the electron current, can be capacitive or inductive. RF power coupling offers some significant advantages over DC and AC sources for industrial applications. RF plasma can process insulating materials without sputtering of the electrodes and so, can be used for deposition from organic monomers. Since the RF power is deposited in the plasma by displacement rather than particle currents, it is easier to couple through the chamber wall, resulting in less ion and electron bombardment of the electrodes. In general, RF-generated plasma is more stable with electrons with higher temperatures for the same densities than an equivalent DC or AC plasma. This can be beneficial where an increased number of free radicals, plasma chemical reactions or dissociation, and ionization reactions are needed (Hirsch et al., 2018).

The previous research has been performed with RF power, where the preparation of plasma polymer films was considered, typically 13.56 MHz, in glass reactor vessels with external coil configurations, or bands to couple the power, although many studies with internal electrodes have also been undertaken. Early designs were based on glass tubes that were either purposely made with ports for the vacuum, monomers, and any diagnostic equipment, or utilized lengths of glass tube supplied as high-pressure column

components. These glass vessels are costly to design, produce and necessitated the use of an external driven coil. Power from a generator is coupled to the system via an external driver electrode.

To match the impedance of the generator to that of the plasma, a matching network incorporating variable capacitors is required. In the coil configuration, the coil itself can be terminated at the ground or left as an open circuit. An important point to note is the excitation wire passes over and around the chamber such that for RF at 13.56 MHz oscillating plasma sheaths sustain the plasma.

This type of system is utilized by many researchers to place the nonconducting polymer substrate on the vessel floor such that any coupling of the RF through the vessel wall and substrate may induce large self-bias potentials on the substrate itself leading to energetic ions bombarding of the substrate. Substrates mounted on a platform in the center of the vessel can also experience this self-bias and energetic ion bombardment; however, these potentials are usually much smaller. The matching network, cables, and radiative losses of RF power result in poor power coupling efficiencies such that in a typical coil-wound system as little as 20%−50% of the power on the dial is actually transmitted to the plasma.

As the quantity of this power supply increases, the coupling efficiency decreases before reaching a maximum saturation level. The level at which this saturation occurs is dependent on many factors including the geometry and volume of the reaction chamber, the operating pressure, and the choice of gas and/or monomer(s). Since no two experimental systems are exactly the same, some small differences in design can lead to large changes in power coupling efficiency, and it is impossible to directly correlate processes and process parameters between two or more systems. To eliminate such variations various attempts have been made for the development of RF reference cell (Garcia-Torres et al., 2014).

However, comparative studies with these systems have highlighted the difficulty of equivalent system construction and diagnosis. Capacitively coupled systems fitted with internal electrodes are an alternative. For the modification of the plasma parameters such systems are efficient with regard to power coupling, and also adjusting the distance between the electrodes.

3.3.2 Heparinization to Improve Blood Compatibility

Surface modification by heparinization is a process of modification of polymeric biomaterial with heparin to obtain improved blood compatibility. The process is also termed heparin immobilization and heparinized surface. Based on the chemical nature of heparin, molecular designs of a heparinized surface can be achieved (Matsumoto et al., 2018).

The heparin molecule contains hydroxyl (−OH), carboxyl (−COOH), amino ($-NH_2$), and sulfate ($-SO_3$). The reactivity of heparin is based on the reaction and interaction between these functional groups and the functional groups at the surface of the material. A distinctive heparin surface immobilization procedure is divided into two steps:

Step 1: Study of the chemical structure of the substrate surface, cleaning the surface, modification of the surface to commence reactive groups.
Step 2: Reaction between heparin and the modified surface, or purification to obtain heparinized surfaces.

Surface heparinization can be achieved by using three different techniques, namely, ionic binding of heparin, covalent binding of heparin, and physical blending of heparin for controlled release, as discussed in the subsequent section (Matsumoto et al., 2018).

3.3.2.1 Ionic Binding of Heparin

As heparin has a strong anionic character, it can bind to cationic surfaces to form an ionic complex. Gott et al. (1968) first reported a process of coating a graphite layer onto a solid polymer surface, followed by adsorption of a quaternary ammonium salt, benzalkonium chloride, over the graphite layer. After the ionic complexation, a heparin modified surface, designated graphite benzalkonium-heparin, was obtained. The most commonly used method for ionic binding heparin involves a pretreatment of a polymer surface with a chemical solution, such as tridodecyl methyl ammonium chloride in a solvent of 1%–5% concentration.

However, these surface binding technologies cannot create a stable heparinized surface. Cellulose dialysis membranes treated with ethylene amine and subsequent treatment by heparin produced antithrombogenic materials. To create a stable heparinized surface, heparin was firstly bound to the polymer surface by ionic complexing, followed by crosslinking using glutaraldehyde as a crosslinking agent.

3.3.2.2 Covalent Binding of Heparin

To create a stable heparinized surface, heparin can covalently bind to the polymer surface. This generally involves an introduction of functional groups at the surface of heparin. For example, heparin can be covalently bound to polyurethane catheters via three steps:

Step 1: Hydrolysis of polyurethane in 3 M NaOH in the presence of isopropanol to introduce hydroxyl and amine groups.
Step 2: Reaction of free amine groups with phosgene and diaminoalkane spacers were coupled to the isocyanate groups.
Step 3: The terminal amine groups of the immobilized spacer were used for coupling with 1-ethyl-3-(3-dimethyl aminopropyl) carbodiimide (EDC) activated heparin and a heparinized surface thus was formed at the level of 2–4 g/cm^2.

Heparin can also be covalently bound to collagen using EDC according to the following steps:

Step 1: Heparin and EDC are dissolved in water.
Step 2: Collagen is added in the solid form, that is, film, powder, or fiber.
Step 3: The pH is changed to 4.8 to start the immobilization process, and further purification of the collagen with water is conducted to obtain a heparinized collagen surface.

Using a polyethylene oxide (PEO) spacer to immobilize heparin can enhance the bioactivity of the bound heparin. A typical method is shown as follows:

Step 1: Activation of polymer surfaces to introduce reactive groups.
Step 2: Coupling PEO-diamines (Jeffamine) or PEO–OH to the surface to introduce PEO spacer with reactive groups.

Step 3: Using EDC as a coupling agent to react with heparin or end-point method to bind heparin.

The heparin activity was measured on the basis of the prolongation of activated partial thromboplastin time. The flexible PEO spacer appeared to relieve the steric hindrance by the carrier to the formation of a heparin complex with cofactor AT III.

3.3.2.3 Physical Blending of Heparin for Controlled Release

Heparin releasing system was prepared by blending polyurethane with silk fibroin and heparin. The percentage and the release rate of the cumulative amount of the released heparin were controlled by the loading amount of heparin in the film, the thickness of the film and the composition ratio of silk fibroin to polyurethane. The more prolonged release of heparin can be achieved by increasing the film thickness, the loading amount of heparin, and the content of silk fibroin inside the film. Long lasting antithrombogenicity and high bioactivity of the raw heparin can be maintained for the blended film. Coagulation time tests showed that the composite film had good blood compatibility (Cheng et al., 2014).

3.3.3 Peptide Functionalization

In this, the functionality of the peptides can be introduced to a surface via chemical synthesis or by molecular self-assembly. The functionalization strategy to be followed is generally dictated by the chemical composition of the material rather than the scale of the surface. Peptide functionalization was carried out on glass, ceramics, metals (e.g., titanium or gold) and polymers (Lee et al., 2015). By introducing functionality chemical groups to these surfaces, peptides can be covalently attached through a variety of coupling reactions. Self-assembled monolayers (SAMs) of alkanethiols on gold produce two-dimensional (2D) surface materials that can be further functionalized with biomolecules. On the other hand, cysteine (with $-CH_2-SH$ side chains) containing peptides have been used to directly attach the peptides to the surfaces. Similarly, gold nanoparticles may be functionalized via attachment of thiol-containing peptides (Liang et al., 2015).

3.3.3.1 Covalent Approach

The general strategy of solid phase peptide synthesis (SPPS) on 2D/3D biomaterials surface. Where X is an N-terminal protecting group, Y is an amino acid side chain protecting group and R is an amino acid residue. As described above, peptide functionalization can be achieved either by step-wise synthesis or by using a one-step coupling process of a presynthesized peptide. The advantage of step-wise synthesis to functionalize a surface is that the desired peptide is rapidly synthesized directly on the surface, and any by-products and unreacted starting materials can be washed away, meaning further purification is not required. There are two approaches utilized for step-wise synthesis on surfaces photolithography and SPOT-synthesis. These methods can be easily programmed and consent for the production of large libraries of peptides in parallel, using small quantities of reagents in a rapid manner (Mäde et al., 2014).

Merrifield first described SPPS in 1963, where he demonstrated the synthesis of a tetrapeptide on a solid support. This Nobel Prize–winning advance in chemistry is now the

standard way of producing peptides and proteins in a synthetic manner. It has opened the door for the synthesis of natural proteins, which are difficult to express in bacteria, as well as the amalgamation of unnatural amino acids, and permits backbone modification and allows the synthesis of D-proteins and peptides (which contain D-amino acids). While usually performed on functionalized polymeric beads that have good swelling properties in organic solvents (such as polystyrene) researchers perform SPPS directly onto biomaterial surfaces that allocate for chemical functionalization and biochemical assay to be performed on the same platform (Stewart, 2007).

Examples of materials that have been used in this context are cellulose, poly(ethylene glycol acrylamide) copolymer (PEGA) in the form of beads or (micropatterned) surfaces, PEG-amine monolayers on the glass, aminosilanized silicon oxide and SAMs of alkanethiols on gold. In some cases, such as PEGA (peptide functionalized surfaces), which is biocompatible, the materials were directly used as a platform for liquid crystal based enzyme sensing and as switchable surfaces for enzymatically controlled cell attachment. Unlike the natural production of peptides and proteins, SPPS proceeds from C-terminal to N-terminal fashion. The general procedure relies on the step-wise synthesis of the repeated cycle of covalently coupling single protected amino acid to the amine functionalized solid support, followed by deprotection of the N-terminal, allowing the next amino acid to be coupled (Punetha et al., 2017).

Once synthesis is complete the amino acid side chains can be deprotected and the peptide then cleaved from the solid support (or used further on support as described above). The use of an insoluble but porous solid support means that the growing amino acid chain is covalently linked to the surface, whilst other reagents and by-products can be washed away via filtration. There are two main strategies used for SPPS: *t*-butoxy carbonyl (Boc) and Fluorenyl methoxycarbonyl (Fmoc). The Boc strategy was adopted by Merrifield and is still used when synthesizing nonnatural peptides that are base sensitive. The Fmoc strategy is more widely used now for routine synthesis as the final peptide product can be cleaved under milder basic conditions than Boc (Stewart, 2007).

The fluorogenic and chromogenic nature of the fluorenyl-group provides a convenient spectroscopic handle for monitoring reactions. A plethora of protecting groups are used for side chain and N- and C-terminal protection; such protecting group strategies can be selected to allow further functionalization of the growing amino acid chain. The removal of these groups from the peptide chain and subsequent cleavage from the solid support can become complex and cleavage mixtures should be chosen with some thought, for example, M, C, and Y residues are susceptible to alkylation by cations produced in the cleavage process, and adding scavengers to the cleavage mixture can largely suppress such side reactions. Typical protecting groups for SPPS are shown in Table 3.1.

The reader is encouraged to investigate the various synthesis strategies available for the production of the desired peptide chain. In particular, the selection of protecting groups can prove very important in preventing unwanted reactions when deprotecting side chain residues. Chemical suppliers often provide invaluable information for the design of SPPS strategies (Fields and Noble, 1990).

Various activating agents can be used to couple the amino acids to the amine residues on the solid support. The common mechanisms rely on the activation of the

TABLE 3.1 Typical Protecting Groups for Solid Phase Peptide Synthesis (SPPS)

Name	Conditions of Removal	Comments
t-Butoxy carbonyl	Acid labile	Amine protection
9-*H*-Fluorene-9-yl methoxycarbonyl (Fmoc)	Base labile	Amine protection
2,2,4,6,7-Pentamethyl dihydrobenzofuran-5-sulfonyl (Pbf)	Acid labile	Standard derivative for the introduction of "R" in Fmoc SPPS
2,2,5,7,8-Penta methylchroman-6-sulfonyl (Pem)	Acid labile	Derivative in the introduction of R in SPPS
Trityl (Trt)	Acid labile	Can be removed without unwanted alkylation of W. residues
Benzyl (Bzl)	Acid labile	Carboxylic acid protection
t-Butyl (*t*-Bu)	Acid labile	Carboxylic acid protection
O-3-Methyl-pent-3-yl (OMpe)	Acid labile	The bulky protecting group provides protection against by-product formulation compared with tBu
p-Methoxytrityl (Mmt)	Acid labile	Used in the synthesis of branched peptides

carboxyl group. Carbodiimides react with the carboxylic acid of the reagent to form the highly reactive *O*-acyl urea, which then reacts directly with the solid-supported amine to yield the desired amide and a urea by-product. The *O*-acyl urea can also lead to oxazolone formation, which leads to epimerization (racemization) whilst acetyl transfer to form the unreactive *N*-acyl urea is often observed. The addition of benzotriazole reagents to the reaction is typically used to overcome this problem. Recently, ethyl cyano(hydroxyamino) acetate has been developed as a nonexplosive alternative to hydroxybenzotriazole (HOBt). Currently, onium salts based upon the triazoles have been introduced for the efficient catalysis of amide bond formation (Subirós-Funosas et al., 2009).

3.3.3.2 *One-Step Functionalization*

The alternative method to step-wise synthesis relies on direct immobilization of a presynthesized peptide onto the (biomaterial) surface. Here, the peptide is first synthesized on a polystyrene solid support via step-wise synthesis and then cleaved and purified before attaching it to the required surface. With this approach, the amino acid side chain residues (e.g., $-NH_2$ of lysine or the $-SH$ of cysteine) are often used as a mode of attachment, but frequently specific functionality must be built into the molecule prior to immobilization. A variety of coupling reactions have been used for this purpose, using aqueous media or organic solvents. Some reacting agents are represented in Table 3.2.

TABLE 3.2 Common Activating Agents Used in One-Step Functionalization

Name and Acronym
Diisopropyl carbodiimide
Diisohexyl carbodiimide
1-Ethyl-3-(3-dimethylamino) carbodiimide HCl salt
1-Hydroxybenzotriazole
1-Hydroxy-7-azabenzotriazole
Ethyl cyano (hydroxyamino) acetate

3.3.4 Calcium Phosphate Deposition

Surface chemistry of biomaterials is modified to provide enhanced cell attachment, growth, and tissue formation, which can be easily achieved via various processes and in turn, are not detrimental to the mechanical properties of the bulk material. The most common involve the deposition of calcium phosphate on to the implant surface which is able to direct cells to an osteogenic phenotype. The typical techniques have recently been investigated for metallic and polymer materials. In this method, a chemical bond is formed between human bone and an implant material, which requires there to be either bone growth onto or into the prosthesis (He et al., 2014).

As far back as in the 1960s, it was known that calcium phosphate coatings would give much better fixation of load-bearing implants than using cement such as polymethylmethacrylate. Calcium phosphates such as hydroxyapatite (HA) are more suitable since they closely resemble the mineral phase in human bone, which is composed of inorganic apatite crystals and organic collagen. HA, when used in vivo, has shown it is noninflammatory and it does not cause a pathological reaction. Hence, it is suitable as a biological coating material on otherwise inert materials (Surmenev et al., 2014).

Once a calcium phosphate has been coated onto a substrate material, the coating properties are required to meet certain criteria set by the US Food and Drug Administration and International Standard Organization. It calls for the minimum crystallinity to be 62% and the purity of the coating to be 95% with the tensile strength and shear strength being less than 50.8 and 22 MPa, respectively. All commercially produced coatings meet these standards and currently investigated calcium phosphate (CaP) deposition techniques work toward attaining these values to provide improved bioactive fixation of implants, which would aid the long- and short-term success of implants. Typical calcium phosphate coating techniques include ion beam assisted deposition, plasma spray deposition, magnetron sputtering, and nonthermal biomimetic methods performed under normal atmospheric conditions. Plasma spraying techniques are the main route used commercially to coat metals such as titanium with HA. It is a high-temperature process that is more complex and expensive than other techniques such as biomimetics (Hadisi et al., 2015).

3.3.5 Thermal Spray Deposition

Plasma spraying was established as the most widely used commercial method of preparing CaP coatings in the 1980s. Since then, numerous research groups and companies have used this technique to coat biomaterials such as Ti and Co–Cr alloys because it is a reproducible and cost-effective technique. The spraying process involves injecting an HA powder into a plasma flame at high temperature. The powder is heated and forced at high pressure and velocity, toward the substrate material. A molten particle of HA can have an outside temperature of at least 1000°C. Owing to this very high temperature, the thin outer layer of each HA particle will inevitably undergo phase transitions. This surface should be sufficiently large to be compatible to plasticize the outer layer and allow a dense and strongly adhesive coating to be formed and also it should be small enough so that it would not affect the overall crystalline phase deposited on the substrate material (Fauchais et al., 2014).

The factors of deposition in plasma affecting the phase purity of the resultant coating have been noted to relate the type of gas that is used, and because of the rate, it accelerates the powder toward the substrate. The type of plasma spraying performed can be abbreviated according to the atmosphere surrounding the process. If air is used, it is denoted as APS (air plasma spraying). This helps in the passing of gases or gas mixtures through a flame. Because of an electric arc, the gas dissociates and form ions, which collide with atoms in the gas, which forms a plasma flame. As the CaP powder is passed into the plasma flame, in it gets melted and then accelerated toward the substrate. Among the specific atmospheres available for plasma spraying the most commonly used at present are VPS (vacuum plasma spraying) or low pressure plasma spraying, which are able to improve the quality of the coating; more crystalline form is produced by APS, and its adhesive strength is increased (Barrows et al., 2014).

However, it comes at a higher price since the technique is more costly compared with conventional techniques. The type of coating material and substrate used can also affect the outcome of the process and temperature of both materials. All these and other parameters, as mentioned below, need to be considered when performing plasma spraying of CaP. Performing VPS, that is, at lower pressures, allows to increase in the velocity of particles and for any undesirable reaction products to be minimized, such as amorphous CaP or calcium oxide. The main disadvantage of this technique is the increasing of substrate surface temperature, but this is counteracted by the resultant coating, which has good adhesion and high density (Chen et al., 2015).

Apart from that, high-velocity oxy-fuel spray deposition was first developed in the 1980s and involves the mixture of a gaseous or liquid fuel and oxygen; a combustion spray technique. The combustion process generates the heat and accelerates the particles at very high velocities toward the substrate surface and it ensures coating with good adhesive strength. The flame temperature is lower than that used in conventional plasma spraying, minimizing overheating or vaporization of the particles (Mauer et al., 2015).

Once the particles adhere to the substrate, their heat is quickly dissipated to the substrate, which allows the rapid solidification of the coating, helping to retain its crystallinity, and an improved bonding strength as compared with other techniques. However, the resultant coating has a lower density due to the insufficient melting of each particle

surface. The processing conditions, as for plasma spraying, have a significant effect on the structure of the resultant coating and its mechanical and in vitro properties (Richards and Wadley, 2014).

Using HA as a coating in composite form, with the addition of yttrium-stabilized zirconia and titania, improved the mechanical performance of the coatings, but the processing technique caused chemical reactions between the individual components, which had a detrimental effect on the performance of the coated material in vitro. Animal studies have shown that plasma sprayed HA-coated implants allow faster bone growth with a higher percentage of bone contact on the samples plasma sprayed with HA. As well as these in vivo results, there has been a much clinical success with HA plasma-sprayed metals. The most recent report mentioned earlier showed how well implants had been accepted in patients after 13 years of implantation (Monteiro et al., 2015).

However, it has also been documented that these uncemented prostheses are difficult to extract when revision surgery is required due to ongoing pain or infection. There have also been problems in a few implants with third-body wear due to coatings containing high amounts of amorphous CaP being worn away causing inflammatory problems and the need for revision surgery.

3.3.6 Ion Beam Assisted Deposition

This deposition method comprises an electron beam that vaporizes a HA target, while an argon ion beam is focused onto the substrate to assist deposition. It creates a deposition of HA, which has high adhesive strength; the strength increases as the current is increased and the increase in bonding strength, which is due to the atomic interaction at the interface between substrate and HA coating. Ion beam deposition easily allows densification of the coating and lower thermal stresses to exist, preventing delamination of the coating. The deposited layers formed by this technique are amorphous, regardless of the current use, which indicates that the coatings need to be heat treated to get sufficient stability to the coatings in vivo (Rigort and Plitzko, 2015).

The final level of crystallinity, and hence, the degree of bioactivity, is also vital and is dependent on the time, temperature, and amount of water vapor present during the deposition process. A graded crystallinity can be achieved by heating the substrate during the deposition process, which can be beneficial to the rate of bone growth and mechanical stability and strength of the coating. It has been proposed that the presence of an amorphous layer at the top of such a coating can allow for faster osteointegration once placed in vivo (Mahapatro, 2015).

3.3.7 Pulsed Laser Physical Vapor Deposition

Physical vapor deposition is a complex process that involves laser ablation of a target material and the deposition through nucleation and film growth of the ablated material onto a substrate. The individual steps are vital for the final film crystallinity and stability. Pulsed laser deposition can also be used to create multicomponent stoichiometric films from one target (Duta et al., 2018).

Pulsed laser can be used to synthesize metastable materials that would otherwise be difficult to fabricate with standard techniques. Nanocrystalline coatings can also be created as well as composite coatings. Numerous calcium phosphates have been used as coating materials including HA, octacalcium phosphate [$Ca_8H_2(PO_4)_6 \cdot 5H_2O$ (OCP)], and alpha and beta-tricalcium phosphates (beta-TCPs). Pulsed laser deposition was used by various groups to form thin HA coatings on polished substrates. The process involves the ablation of an HA target in a water vapor atmosphere and depositing the ablated HA material onto a heated substrate (400°C−800°C) (Yang et al., 2015).

Neale et al. grew thin films of HA onto Ti alloy substrates that had been precoated with a buffer layer of TiN. This buffer layer improved the adhesion of the HA film to the substrate. The benefits of this TiN layer were again forced when Ti alloys were not pretreated and allowed to form an oxide layer between the film and the substrate. The presence of this oxide layer was a point of weakness and was detrimental to both the strength and microhardness of the films. Analysis of the coating revealed they had a rough surface, which would be beneficial for osteoblast cell adhesion. As well as the effect of surface roughness, the beneficial effects of increased crystallinity and laser fluence were demonstrated when human osteoblast cells were cultured on thin HA films created by pulsed laser physical vapor deposition (Nelea et al., 2000).

Enhanced cell proliferation occurred on these films due in part to the improved HA coating crystallinity, which would result in reduced dissolution and release of calcium and phosphorus ions. Nanosized OCP deposited onto titanium has demonstrated good bioactivity and is more resorbable than HA. Both fibro- and osteoblast cells were able to differentiate and grow on these surfaces and adhered strongly to the OCP films formed by physical vapor deposition (Dorozhkin, 2010).

3.3.8 Microarc Oxidation

Microarc oxidation (MAO), also known as plasma electrolytic oxidation, anodic spark deposition, or microarc discharge oxidation, is an electrochemical surface treatment that results in the generation of oxide layers on metals. MAO can be performed at ambient temperature and can be used on substrates with complex geometries. MAO has been used to form various calcium phosphate coatings on metal alloys (Han et al., 2003).

Processing parameters are altered, which determines the morphology and composition of the calcium phosphate coating formed. Using the various applied voltages, for example by changing the cathode voltage during coating synthesis, will affect both the phase composition and morphology of the resultant film. However, an optimum needs to be found since voltages that are too high, above a few hundred, will destroy the coating, and voltages that are too low will lead to pore formation, which will be detrimental to the strength of the coatings. As well as varying equipment parameters, the concentration of the HA used in Ti-based coatings on titanium alloys can also be adjusted (Ma et al., 2014).

By increasing the HA content, the behavior of these coatings in simulated body fluid (SBF) will change from anatase (low crystallinity) and amorphous CaP to the presence of rutile. As the HA content is further increased, the crystallinity of the coatings is improved, elevating their bioactivity. Creating composite coatings with an HA filler has

demonstrated suitable bioactivity and the ability to control the calcium phosphate phase composition and mechanical properties of these coatings when produced by MAO. Ion-substituted HA coatings, for example, strontium-HA, made via MAO methods have also proven to offer promising results in vitro (Chen et al., 2006).

3.3.9 Magnetron Sputtering Deposition

Magnetron sputtering is a high-rate vacuum coating technique that allows the deposition of many types of materials, including metals and ceramics, onto as many types of substrate materials by the use of a specially formed magnetic field applied to a diode sputtering target. It allows a faster deposition rate at lower pressures compared with other techniques and is able to create strongly adhesive coatings on complex geometries including those made of heat-sensitive substrates such as polymers. Due to the desirable properties of this technique, many researchers have used this process to apply CaP films onto metallic and nonmetallic implants (Zhu et al., 2018).

It has been demonstrated to be a promising method for forming a biocompatible coating on metal, plastic, and ceramic substrates since a wide variety of materials can be used and the processing parameters and postprocedure heat treatments such as postdeposition or in situ annealing can be applied. Altering parameters such as the gas pressure (argon) can have a marked effect on the HA coating crystallinity, causing dehydroxylation and amorphous calcium phosphate formation when the gas pressures are too high (Zhang et al., 2017). In the mid-1990s, Wolke et al. were among the first to try radio frequency magnetron sputtering as an alternative method to deposit thin films of HA onto titanium substrates. A crystalline layer was formed on the titanium surface with a preferred crystallographic orientation and a uniform and dense structure (Wolke et al., 1994).

Developments in magnetron sputtering led to findings that this technique could be used to vary the coating thickness, which could subsequently be heat treated to form a crystalline structure. Such heat-treated coatings have high adhesive strength, but due to the annealing process, are prone to cracking when thicker coatings are applied ($>0.1\ \mu m$). Despite these drawbacks, magnetron-sputtered HA coatings allow for a strong bond to be formed with an adjacent bone when implanted via the growth of fibrillar collagen matrices and carbonate apatite crystals (Kawasaki et al., 2016).

The microstructure and bonding strength of HA coatings produced using magnetron sputtering on Ti substrates can be improved by the formation of a TiN buffer layer and by altering the substrate temperature during the sputtering process. Using the TiN buffer provides an improved bonding strength between the substrate and HA film and heating the substrate allows the coating to be transformed from an amorphous to a more crystalline HA structure.

As well as metals, polymers and ceramics can also be coated successfully using magnetron sputtering producing fully dense and strongly adherent calcium phosphate coatings. For such substrates, ion-substituted HAs and composite coatings of HA/TiO_2 can be applied. The use of substituted apatites such as silicon-substituted HA has been shown to encourage bone bonding much more than pure HA and has been used as a coating material for various load-bearing implant materials (Ivanova et al., 2016).

3.3.10 Electrophoretic Deposition

Electrophoretic deposition has been used to form CaP coatings on various substrate materials. This process involves an electric field that is employed to deposit charged particles (cathodic or anodic) in a liquid (not water) onto a conducting substrate of opposite charge. It is a highly versatile and low-cost procedure that allows any 3D object (including porous materials) to be uniformly coated, and has been used successfully to deposit bioactive coatings onto medical implants (Rad et al., 2014).

Varied thicknesses of calcium phosphate coating can be formed on metal substrates by changing the electric field and deposition time during electrophoresis. Resultant coatings are uniformly distributed and densified, but due to differences in thermal expansion coefficients of the metal substrate and ceramic coating can lead to cracking. By performing repeat depositions at room temperature and by varying the dispersant type (e.g., glycol for ethanol), the issue of coating cracking can be minimized (Xiong et al., 2014).

Another process applied to improve the adhesion between substrate and CaP coating is the use of an intermediate layer. Silica, calcium-silica, or titania can be deposited onto metals allowing the "second," HA coating to bind strongly and without the formation of any cracks. The use of nanoparticulate HA coatings alone and as this "second" layer has indicated a new trend in electrophoretic techniques for biometals, which also overcomes the issue of coating cracking. The intermediate layer acts as a diffusion barrier that prevents decomposition of the nanosized HA, which would otherwise occur due to ion migration from the metal substrate into the HA (Roudan et al., 2017).

The intermediate coatings are also an effective chemical barrier to the release of potentially inflammatory metal ions from the bulk implant material. Recently, composites have also gained interest as materials for coatings applied by electrophoresis. Coatings of silicon-substituted HA and polycaprolactone (PCL, a known biodegradable polymer) on titanium substrates have shown improved bonding strength compared with Si-HA alone due to the addition of PCL. This polymer can degrade over time and does not hinder the bioactivity of the HA. Substrates besides titanium and titanium alloys, such as stainless steel, have also been coated effectively with calcium phosphates and calcium phosphate composites using electrophoretic techniques (Pishbin et al., 2015). Composite HA–chitosan coatings on stainless steel demonstrated that a uniform and well-adhered coating could be produced with HA nanoparticle preferred orientation being increased with increasing chitosan content.

3.3.11 Electrochemical Deposition

The process of electrochemical deposition involves the decomposition of an aqueous electrolyte, which, for the formation of an appetite coating on biomaterials, must contain calcium and phosphorus ions. Bioactive coatings obtained by electrochemical deposition are composed of interlocking calcium phosphate crystal networks. These are formed via a nucleation and growth process that is affected by various factors such as electrolytic solution composition (additions of $NaNO_3$ or NaF) or concentration, electric current density, deposition time, and solution pH. These factors can be tailored to control the purity, crystallinity, stoichiometry, morphology, and mechanical strength of the resulting coatings (Asri et al., 2016).

Varying the current density has a direct effect on the local pH of the solution and can determine the morphology and crystalline structure of the resultant coatings. The electrolyte temperature can affect the amount of coating that is deposited on the surface of metals such that when the temperature is increased, more calcium and phosphate ions are absorbed. The degree of aqueous solution supersaturation used to form CaP coatings can also control the morphology and length of apatite crystals (Karimzadeh et al., 2017).

All these parameters can aid the bioactivity of the final coated metal, enhancing the rate at which early fixation occurs. Numerous modified electrochemical techniques have been used to improve the adhesive strength between apatite coatings and substrates. These have included the formation of a composite coating by the combination of HA with vinyl acetate and the anodic oxidation of TiO_2 nanotubes onto titanium substrate prior to HA deposition. Vinyl acetate alters the morphology of the HA crystals and causes a significant increase in the adhesive strength of the coating (Yan et al., 2015). The anodic pretreatment of the metal substrate leads to the formation of a TiO_2/dicalcium phosphate dihydrate coating, which can be converted to a more crystalline structure by immersion in an alkaline solution. SBF is a solution that can be used as the electrolyte source during electrochemical CaP deposition. SBF at different temperatures can affect the phase composition of the coating produced. With increasing temperatures, the structure of the CaP coating becomes more crystalline and carbonate-rich (Xu et al., 2015).

Using SBF during electrochemical deposition at body temperature and pH (around 37°C and pH 7.40) causes the calcium phosphate crystals to be thin and nanosized. Once these crystals are formed, spheres of water-rich amorphous CaP can grow on this layer, which, depending on the current density used, will be transformed into crystalline needles of HA. The higher the current density, the more crystalline the coating and, hence, the ability to control the solubility and adhesive strength of these coatings.

Electrochemically deposited CaP coatings can be formed with ionic substitutions in their structure, such as carbonate and fluoride. Carbonate-substituted apatite can be coated onto titanium plates using electrolytes containing calcium and phosphate ions (SBF levels) but without the use of a pH buffer. These can sustain osteoblast cell activity. The addition of fluoride ions to apatite can be applied to both orthopedic and dental percutaneous implants, retaining the bioactivity of the HA and passing on the beneficial antibacterial properties of fluorine (Bakin et al., 2016).

Along with these forms of substituted apatites, composites such as CaPs with chitosan and collagen, HA with poly(vinyl acetate) and polypyrrole are also proving to give excellent results, both biologically and mechanically, even on NiTi shape-memory orthopedic alloys. The addition of polypyrrole to apatite during the electrochemical deposition using SBF as the electrolyte promotes the incorporation of carbonate ions into the calcium phosphate coating. The carbonate-substituted HA enhancing the bioactivity of the coated material (Su et al., 2017).

3.3.12 Sol–Gel Methods

Sol–gel processing is a wet chemistry approach that results in ceramic coatings with an exact chemical and microstructural composition. The desired coating content is mixed at a

low temperature as a colloidal suspension of inorganic particles and then heat treated at high temperatures (up to 1000°C) to densify the coating on the substrate. Sol–gel processing allows for the production of thin films with excellent adhesion properties that can be applied to complex geometries and to nonmetallic such as polymers due to the low sintering temperatures, which can be used to heat treat the "green" coatings (Mohamed et al., 2017).

Significant amounts of research have reported the benefits of using this technique to deposit calcium phosphate onto metallic substrates. Following the sol–gel treatment, coated samples are heat treated, which affects the stability, purity, and crystallinity of the resultant calcium phosphates. Trace amounts of calcium oxide and beta-TCP have been noted when heat-treating HA, but these are undesirable phases due to beta-TCP being much more soluble than HA (reducing bioactivity and coating adhesive strength) and CaO lacking biocompatibility and dissolving in body fluids at a faster rate than TCP (Fu et al., 2015).

However, these phases can be avoided and monophasic HA produced by increasing the aging time to more than 24 hours. Variations in the processing parameters can also control the quality of the resulting coating material. For example, by increasing the calcining temperature and changing the pH of the sol solutions an HA coating with high purity and crystallinity can be produced, which in turn, will have better coating stability in vivo and induce optimum levels of bioactivity. As well as controlling the processing parameters, starting material compositions can also be tailored (Tielmann et al., 2014).

Substituted forms of HA such as fluoride- and silicon-HA are beneficial at increasing the bioactivity of the calcium phosphate coatings and increasing the crystallinity of the apatite film. Pretreating substrate surfaces with titanium oxide or calcium phosphate compounds using electrophoresis promote both the mechanical strength of the apatite coatings and their bioactivity. A similar favorable result in bonding strength is witnessed when magnetron sputtering and electrochemical deposition techniques employ TiO_2 precoating (Perumal et al., 2014).

3.3.13 Hot Isostatic Pressing

The aim of hot isostatic pressing (HIP) is to overcome the problems associated with plasma spraying of HA such as coating porosity and weak bonding to the substrate. Prior to HIP being performed, the HA powder is applied to the surface of the substrates by techniques such as mixing with water and then air-spraying onto Ti substrates. At temperatures above 800°C, the Ti-coated samples are cold pressed with a pressure of around 700 bar to produce optimum, well-adhered coatings. This ensures coatings with a greater density than with plasma spraying alone. In vivo testing illustrated that using higher pressures led to improved bone/implant bonding values compared with sand-blasted Ti implants or those cold pressed at lower pressures (Suresh et al., 2017).

Despite the success in vivo, it was found that this technique contaminated the coatings with metal and SiO_2 particles due to the glass tubing that was used during the HIP process. More recent work has involved plasma spraying Ti alloy substrates (the most successful commercial form of HA coating to date) and then performing HIP on the resultant materials. The HIP process allows for a reduction in the porosity of the coatings since

pores, especially those of 10–300 nm are detrimental to the mechanical strength of coatings (Cai et al., 2016).

The HIP process compresses the pores and dramatically increases the density of the coatings, hence enhancing the mechanical properties of the HA. Hydrothermal forms of the HIP process are also becoming a more prominent method of depositing dense layers of HA onto substrates. It is a double layer technique that allows for the hydrothermal treatment to be performed during the HIP, creating coatings on curved surfaces with good bonding strength (Wu et al., 2017).

3.3.14 Biomimetic Coatings

Calcium phosphate, which is found in natural hard tissues, can be produced spontaneously in physiological, supersaturated solutions at low temperatures. It can be used to grow bone-like apatite on potential implant materials and is particularly suitable for the coating of biodegradable polymeric materials and degradable tissue engineering scaffolds. The first group to grow calcium phosphate on a substrate using an in vitro biomimetic process was Hyakuna et al. (1990).

They demonstrated the ability of this solution, with ion concentrations close to those of human blood plasma, to induce apatite crystal formation on $CaO–SiO_2$–based glasses. The thickness of this calcium phosphate coating can be controlled with most bioactive samples forming an amorphous or amorphous crystalline structure on their surface. Since its development, SBF has become one of the simplest in vitro techniques for observing the potential in vivo bioactivity of a material.

When using SBF as the basic physiological solution for apatite formation, modifications in experimental conditions such as temperature, time, or ion concentration allow for the tailoring of the apatite formed and the creation of biomimetic coatings on otherwise inert materials. These bioactive coatings cause the formation of a direct chemical bond with a bone when placed in the body. Increasing the concentration of SBF to twice that of normal amounts leads to apatite layers forming on polymers such as polyethylene terephthalate (PET). This occurs due to an increased ionic activity but the formation of apatite with Ca/P ratios, which are lower and more bioresorbable. Bone-like apatite can be formed on polymers and metals by increasing the concentration of SBF (Hyakuna et al., 1990).

However, reducing the Mg^{2+} and HCO^3 ion content in this solution allows for faster apatite nucleation and growth due to the removal of the known inhibitory effect of these ions. As well as increasing the concentration of SBF and removing known inhibitory ions, the addition of nucleating agents to the solution can also induce apatite precipitation on the surface of materials. Chemical or physical modification of the substrate surface can also be beneficial to apatite formation. Certain negatively charged surface –OH groups are able to promote CaP formation, including Si–OH, Ti–OH, and Zr–OH, which along with being anionic, have a certain spatial arrangement favorable for apatite formation. When considering polymers, surface groups such as $-COOH$, $-CONH_2$, $-OH$, and $-NH_2$, have an apatite nucleating effect, whereas $-CH_3$ surface groups are unable to induce such an effect.

The influence of a moisture-insensitive, corrosion technique such as sodium hydroxide treatment followed by a heat treatment can allow the formation of an apatite layer on

metals such as Ti and its alloys. A sodium titanate mesh-like surface structure is formed, which allows a CaP layer to develop in vivo. Non–surface damaging processes, that is, without the need for corrosion or surface etching, can be performed, which are not detrimental to the mechanical properties of the substrate. Repeated dipping of substrates into a supersaturated calcium phosphate solution and removing and air-drying allows the growth of calcium phosphate crystals on substrate materials. The mechanism of apatite growth is thought to be via an evaporation-induced surface crystallization process (Mendes et al., 2016).

However, the mechanical stability and bioactivity of these types of coatings need to be analyzed. A similar dipping technique to form a nano-CaP-rich hydrogel composite coating on substrates has demonstrated good adhesive strength and promising results when tested in vitro in SBF and with human osteoblast-like cells. Inducing bioactivity in polymers such as PCL, PET, and polylactic acid (PLA) can be achieved by biomimetic processes that use bioactive glass particles to stimulate apatite nuclei formation on the substrates in SBF or by alkaline treatments, which partially hydrolyze the surface of polymers and generate oxygen-containing functional groups for calcium and phosphate ion interaction (Cools et al., 2018).

An apatite layer is able to form on these biodegradable polymers after only 24 hours in SBF. The apatite layer formed via the alkali treatment produces coatings with adhesive strengths that make them highly suitable for scaffold applications in bone tissue engineering, outperforming composites currently used clinically for bone replacement. Starch-based biodegradable polymers have gained much interest for use as bone replacement materials with bioactive coatings. Surface modification treatments such as UV radiation, the use of ethylene oxide, or the combination of these polymers with sodium silicate gels can allow for apatite nucleation sites to be formed, which is particularly beneficial for porous polymer scaffolds (Ferreira and Mousavi, 2018).

As well as the success of coating biodegradable polymers with apatite, composite scaffolds of degradable polymers and ceramics have recently been enhanced by the use of biomimetics to form a bioactive coating. Although ceramic-reinforced polymer scaffolds are an improvement on conventional ceramic substitutes, the osteoinductive ability of these scaffolds must be further enhanced to make them suitable for bone tissue engineering. Apatite-coated porous PLA/nano-HA is one such composite that has benefited from being biomimetically coated with apatite, resulting in significantly increased cell proliferation and growth rates compared with uncoated HA/PLA composites (Motamedian et al., 2015).

3.4 FUTURE REMARKS AND CONCLUSION

While bulk properties may initially determine material suitability for an application, the physical aspects of the material surface, as well as the chemistry, are paramount to the function of many biomedical devices. Physical modification results in a change in the topography or morphology of the surface with little to no change in the chemistry, such as etching, grit-blasting, and machining. Well-established chemical techniques include plasma and chemical vapor deposition, atomic layer deposition, and electrochemical deposition. Chemical treatment can result in oxidizing/nitriding/carbiding a surface,

surface functionalization, ion infusion, single layer coatings, or coatings comprising many layers of different compositions. The goal of modifying the surface of a biomaterial is to create a specific chemical and physical environment that offers a favorable cellular response in the hard or soft tissue. However, it is important to note that in some instances, textured surfaces are detrimental to the function of the device such as articulating surfaces or cardiovascular devices.

Further "smart" biomaterials and systems are being investigated to provide more tailored and effective responsive systems that possess finer control of disease states. The main aim for the pharmaceutical industry is to ensure that the characteristics of the dosage form material, triggering stimulus, and disease-specific environment are all considered and accounted for in the design and engineering stages. These parameters need to be focused and work in harmony with one another so as to achieve the most effective disease-specific, controlled drug release that allows the best targeted therapeutic effect.

Acknowledgment

The authors would like to acknowledge Science and Engineering Research Board (Statutory Body Established Through an Act of Parliament: SERB Act 2008), Department of Science and Technology (DST), Government of India for a grant (#ECR/2016/001964) allocated to Dr. Tekade for research work on drug and gene delivery. The author also acknowledges DST-SERB for N-PDF funding (PDF/2016/003329) to Dr. Rahul Maheshwari in Dr. Tekade's lab for work on targeted cancer therapy. Authors would also like to acknowledge the Department of Pharmaceuticals, Ministry of Chemicals and Fertilizers, India, for supporting research on cancer and diabetes at NIPER, Ahmedabad.

ABBREVIATIONS

BBB blood–brain barrier
EDC 1-ethyl-3-(3-dimethyl aminopropyl) carbodiimide
EPR enhanced permeability and retention
IC integrated circuits
MW molecular weight
PEG polyethylene glycol
PEO polyethylene oxide
PLA Polylactic acid

References

Al-Qattan, M.N., Deb, P.K., Tekade, R.K., 2018. Molecular dynamics simulation strategies for designing carbon-nanotube-based targeted drug delivery. Drug Discov. Today 23, 235–250.

Asri, R., Harun, W., Hassan, M.-A., Ghani, S., Buyong, Z., 2016. A review of hydroxyapatite-based coating techniques: sol–gel and electrochemical depositions on biocompatible metals. J. Mech. Behav. Biomed. Mater. 57, 95–108.

Bakin, B., Delice, T.K., Tiric, U., Birlik, I., Azem, F.A., 2016. Bioactivity and corrosion properties of magnesium-substituted CaP coatings produced via electrochemical deposition. Surf. Coat. Technol. 301, 29–35.

Barrows, A.T., Pearson, A.J., Kwak, C.K., Dunbar, A.D., Buckley, A.R., Lidzey, D.G., 2014. Efficient planar heterojunction mixed-halide perovskite solar cells deposited via spray-deposition. Energy Environ. Sci. 7 (9), 2944–2950.

Cai, C., Song, B., Xue, P., Wei, Q., Wu, J.-m, Li, W., et al., 2016. Effect of hot isostatic pressing procedure on performance of Ti6Al4V: surface qualities, microstructure and mechanical properties. J. Alloys Compd. 686, 55–63.

Chen, J.-z, Shi, Y.-l, Wang, L., Yan, F.-y, Zhang, F.-q, 2006. Preparation and properties of hydroxyapatite-containing titania coating by micro-arc oxidation. Mater. Lett. 60 (20), 2538–2543.

Chen, X., Gong, Y., Suo, X., Huang, J., Liu, Y., Li, H., 2015. Construction of mechanically durable superhydrophobic surfaces by thermal spray deposition and further surface modification. Appl. Surf. Sci. 356, 639–644.

Cheng, C., Sun, S., Zhao, C., 2014. Progress in heparin and heparin-like/mimicking polymer-functionalized biomedical membranes. J. Mater. Chem. B 2 (44), 7649–7672.

Chopdey, P.K., Tekade, R.K., Mehra, N.K., Mody, N., Jain, N.K., 2015. Glycyrrhizin conjugated dendrimer and multi-walled carbon nanotubes for liver specific delivery of doxorubicin. J. Nanosci. Nanotechnol. 15, 1088–1100.

Choudhury, H., Gorain, B., Tekade, R.K., Pandey, M., Karmakar, S., Pal, T.K., 2017. Safety against nephrotoxicity in paclitaxel treatment: oral nanocarrier as an effective tool in preclinical evaluation with marked in vivo antitumor activity. Regul. Toxicol. Pharmacol. 91, 179–189.

Cools, P., Asadian, M., Nicolaus, W., Declercq, H., Morent, R., De Geyter, N., 2018. Surface treatment of PEOT/PBT (55/45) with a dielectric barrier discharge in air, helium, argon and nitrogen at medium pressure. Materials 11 (3), 391.

Dhakad, R.S., Tekade, R.K., Jain, N.K., 2013. Cancer targeting potential of folate targeted nanocarrier under comparative influence of tretinoin and dexamethasone. Curr. Drug Deliv. 10, 477–491.

Dorozhkin, S.V., 2010. Nanosized and nanocrystalline calcium orthophosphates. Acta Biomater. 6 (3), 715–734.

Dua, K., Bebawy, M., Awasthi, R., Tekade, R.K., Tekade, M., Gupta, G., et al., 2017. Application of chitosan and its derivatives in nanocarrier based pulmonary drug delivery systems. Pharm. Nanotechnol. 5, 243–249.

Duta, L., Ristoscu, C., Stan, G., Husanu, M., Besleaga, C., Chifiriuc, M., et al., 2018. New bio-active, antimicrobial and adherent coatings of nanostructured carbon double-reinforced with silver and silicon by matrix-assisted pulsed laser evaporation for medical applications. Appl. Surf. Sci. 441, 871–883.

Fattahi, P., Yang, G., Kim, G., Abidian, M.R., 2014. A review of organic and inorganic biomaterials for neural interfaces. Adv. Mater. 26 (12), 1846–1885.

Fauchais, P.L., Heberlein, J.V., Boulos, M.I., 2014. Thermal Spray Fundamentals: From Powder to Part. Springer Science & Business Media.

Ferreira, M.S.V., Mousavi, S.H., 2018. Nanofiber technology in the ex vivo expansion of cord blood-derived hematopoietic stem cells. Nanomed. Nanotechnol. Biol. Med. 14, 1707–1718.

Fields, G.B., Noble, R.L., 1990. Solid phase peptide synthesis utilizing 9-fluorenylmethoxycarbonyl amino acids. Chem. Biol. Drug Des. 35 (3), 161–214.

Fu, C., Hu, X., Yang, Z., Shen, L., Zheng, Z., 2015. Preparation and properties of waterborne bio-based polyurethane/siloxane cross-linked films by an in situ sol–gel process. Prog. Org. Coat. 84, 18–27.

Gajbhiye, V., Vijayaraj Kumar, P., Kumar Tekade, R., Jain, N., 2007. Pharmaceutical and biomedical potential of PEGylated dendrimers. Curr. Pharm. Des. 13 (4), 415–429.

Gajbhiye, V., Kumar, P.V., Tekade, R.K., Jain, N., 2009a. PEGylated PPI dendritic architectures for sustained delivery of H_2 receptor antagonist. Eur. J. Med. Chem. 44 (3), 1155–1166.

Gajbhiye, V., Palanirajan, V.K., Tekade, R.K., Jain, N.K., 2009b. Dendrimers as therapeutic agents: a systematic review. J. Pharm. Pharmacol. 61, 989–1003.

Garcia-Torres, J., Sylla, D., Molina, L., Crespo, E., Mota, J., Bautista, L., 2014. Surface modification of cellulosic substrates via atmospheric pressure plasma polymerization of acrylic acid: structure and properties. Appl. Surf. Sci. 305, 292–300.

Ghanghoria, R., Tekade, R.K., Mishra, A.K., Chuttani, K., Jain, N.K., 2016. Luteinizing hormone-releasing hormone peptide tethered nanoparticulate system for enhanced antitumoral efficacy of paclitaxel. Nanomedicine 11, 797–816.

Gorain, B., Choudhury, H., Tekade, R.K., Karan, S., Jaisankar, P., Pal, T.K., 2016. Comparative biodistribution and safety profiling of olmesartan medoxomil oil-in-water oral nanoemulsion. Regul. Toxicol. Pharmacol. 82, 20–31.

Gott, V.L., Whiffen, J.D., Valiathan, S.M., 1968. Graphite-benzalkonium-heparin coatings on plastics and metals. Ann. N.Y. Acad. Sci. 146 (1), 21–29.

Hadisi, Z., Nourmohammadi, J., Mohammadi, J., 2015. Composite of porous starch-silk fibroin nanofiber-calcium phosphate for bone regeneration. Ceram. Int. 41 (9), 10745–10754.

Han, Y., Hong, S.-H., Xu, K., 2003. Structure and in vitro bioactivity of titania-based films by micro-arc oxidation. Surf. Coat. Technol. 168 (2-3), 249–258.
He, C., Jin, X., Ma, P.X., 2014. Calcium phosphate deposition rate, structure and osteoconductivity on electrospun poly(L-lactic acid) matrix using electrodeposition or simulated body fluid incubation. Acta Biomater. 10 (1), 419–427.
Hegemann, D., Nisol, B., Watson, S., Wertheimer, M.R., 2017. Energy conversion efficiency in low-and atmospheric-pressure plasma polymerization processes, Part II: HMDSO. Plasma Chem. Plasma Process. 37 (1), 257–271.
Hirsch, U., Ruehl, M., Teuscher, N., Heilmann, A., 2018. Antifouling coatings via plasma polymerization and atom transfer radical polymerization on thin film composite membranes for reverse osmosis. Appl. Surf. Sci. 436, 207–216.
Huang, G., Zhang, K.-L., Chen, S., Li, S.-H., Wang, L.-L., Wang, L.-P., et al., 2017. Manganese-iron layered double hydroxide: a theranostic nanoplatform with pH-responsive MRI contrast enhancement and drug release. J. Mater. Chem. B 5 (20), 3629–3633.
Hyakuna, K., Yamamuro, T., Kotoura, Y., Oka, M., Nakamura, T., Kitsugi, T., et al., 1990. Surface reactions of calcium phosphate ceramics to various solutions. J. Biomed. Mater. Res. A 24 (4), 471–488.
Inagaki, N., 2014. Plasma Surface Modification and Plasma Polymerization. CRC Press.
Ivanova, A.A., Surmeneva, M.A., Tyurin, A., Pirozhkova, T., Shuvarin, I., Prymak, O., et al., 2016. Fabrication and physico-mechanical properties of thin magnetron sputter deposited silver-containing hydroxyapatite films. Appl. Surf. Sci. 360, 929–935.
Jain, N.K., Tekade, R.K., 2013. Dendrimers for enhanced drug solubilization. Drug Delivery Strategies for Poorly Water-Soluble Drugs. John Wiley & Sons Ltd, pp. 373–409.
Jiang, T., Singh, B., Choi, Y.-J., Akaike, T., Cho, C.-S., 2015. Liver tissue engineering using functional marine biomaterials. Functional Marine Biomaterials. Elsevier.
Karimzadeh, I., Aghazadeh, M., Ganjali, M.R., Norouzi, P., Doroudi, T., Kolivand, P.H., 2017. Saccharide-coated superparamagnetic Fe_3O_4 nanoparticles (SPIONs) for biomedical applications: an efficient and scalable route for preparation and in situ surface coating through cathodic electrochemical deposition (CED). Mater. Lett. 189, 290–294.
Kawasaki, H., Suda, Y., Ohshima, T., Yagyu, Y., Ihara, T., 2016. Preparation of Er_2O_3 and TiO_2 multilayer films as optical filter using magnetron sputtering deposition. IEEE Trans. Plasma Sci. 44 (12), 3066–3070.
Kumar, M., Sharma, P., Maheshwari, R., Tekade, M., Shrivastava, S.K., Tekade, R.K., 2018. Beyond the blood–brain barrier: facing new challenges and prospects of nanotechnology-mediated targeted delivery to the brain. Nanotechnology-Based Targeted Drug Delivery Systems for Brain Tumors. Elsevier.
Lee, T.T., García, J.R., Paez, J.I., Singh, A., Phelps, E.A., Weis, S., et al., 2015. Light-triggered in vivo activation of adhesive peptides regulates cell adhesion, inflammation and vascularization of biomaterials. Nat. Mater. 14 (3), 352.
Li, Q.-L., Sun, Y., Sun, Y.-L., Wen, J., Zhou, Y., Bing, Q.-M., et al., 2014. Mesoporous silica nanoparticles coated by layer-by-layer self-assembly using cucurbit[7]uril for in vitro and in vivo anticancer drug release. Chem. Mater. 26 (22), 6418–6431.
Liang, D.-S., Su, H.-T., Liu, Y.-J., Wang, A.-T., Qi, X.-R., 2015. Tumor-specific penetrating peptides-functionalized hyaluronic acid-*d*-α-tocopheryl succinate based nanoparticles for multi-task delivery to invasive cancers. Biomaterials 71, 11–23.
Liow, S.S., Dou, Q., Kai, D., Karim, A.A., Zhang, K., Xu, F., et al., 2016. Thermogels: in situ gelling biomaterial. ACS Biomater. Sci. Eng. 2 (3), 295–316.
Ma, X., Zhu, S., Wang, L., Ji, C., Ren, C., Guan, S., 2014. Synthesis and properties of a bio-composite coating formed on magnesium alloy by one-step method of micro-arc oxidation. J. Alloys Compd. 590, 247–253.
Mäde, V., Els-Heindl, S., Beck-Sickinger, A.G., 2014. Automated solid-phase peptide synthesis to obtain therapeutic peptides. Beilstein J. Org. Chem. 10, 1197.
Maeda, H., Matsumura, Y., 2011. EPR Effect Based Drug Design and Clinical Outlook for Enhanced Cancer Chemotherapy. Elsevier.
Mahapatro, A., 2015. Bio-functional nano-coatings on metallic biomaterials. Mater. Sci. Eng., C 55, 227–251.
Maheshwari, R., Sharma, P., Tekade, M., Atneriya, U., Dua, K., Hansbro, P.M., et al., 2017. Microsponge embedded tablets for sustained delivery of nifedipine. Pharm. Nanotechnol. 5 (3), 192–202.
Maheshwari, R.G., Tekade, R.K., Sharma, P.A., Darwhekar, G., Tyagi, A., Patel, R.P., et al., 2012. Ethosomes and ultradeformable liposomes for transdermal delivery of clotrimazole: a comparative assessment. Saudi Pharm. J. 20 (2), 161–170.

Maheshwari, R.G., Thakur, S., Singhal, S., Patel, R.P., Tekade, M., Tekade, R.K., 2015. Chitosan encrusted nonionic surfactant based vesicular formulation for topical administration of ofloxacin. Sci. Adv. Mater. 7 (6), 1163–1176.
Mansuri, S., Kesharwani, P., Jain, K., Tekade, R.K., Jain, N., 2016a. Mucoadhesion: a promising approach in drug delivery system. React. Funct. Polym. 100, 151–172.
Mansuri, S., Kesharwani, P., Tekade, R.K., Jain, N.K., 2016b. Lyophilized mucoadhesive-dendrimer enclosed matrix tablet for extended oral delivery of albendazole. Eur. J. Pharmaceut. Biopharmaceut. 102, 202–213.
Matsumoto, Y., Fujita, T., Fukushima, S., Shimahara, Y., Kume, Y., Yamashita, K., et al., 2018. Early postoperative heparinization is crucial for prevention of cerebral vascular accident in patients with HeartMate II. J. Heart Lung Transplant. 37 (4), S369.
Mauer, G., Jarligo, M., Rezanka, S., Hospach, A., Vaßen, R., 2015. Novel opportunities for thermal spray by PS-PVD. Surf. Coat. Technol. 268, 52–57.
Mendes, M.W., Ágreda, C.G., Bressiani, A.H., Bressiani, J.C., 2016. A new titanium based alloy Ti–27Nb–13Zr produced by powder metallurgy with biomimetic coating for use as a biomaterial. Mater. Sci. Eng., C 63, 671–677.
Meyns, M., Perálvarez, M., Heuer-Jungemann, A., Hertog, W., Ibáñez, M., Nafria, R., et al., 2016. Polymer-enhanced stability of inorganic perovskite nanocrystals and their application in color conversion LEDs. ACS Appl. Mater. Interfaces 8 (30), 19579–19586.
Mody, N., Tekade, R.K., Mehra, N.K., Chopdey, P., Jain, N.K., 2014. Dendrimer, liposomes, carbon nanotubes and PLGA nanoparticles: one platform assessment of drug delivery potential. AAPS PharmSciTech 15 (2), 388–399.
Moeendarbari, S., Tekade, R., Mulgaonkar, A., Christensen, P., Ramezani, S., Hassan, G., et al., 2016. Theranostic nanoseeds for efficacious internal radiation therapy of unresectable solid tumors. Sci. Rep. 6, 20614.
Mohamed, M.A., Salleh, W.N.W., Jaafar, J., Rosmi, M.S., Hir, Z.A.M., Mutalib, M.A., et al., 2017. Carbon as amorphous shell and interstitial dopant in mesoporous rutile TiO_2: bio-template assisted sol–gel synthesis and photocatalytic activity. Appl. Surf. Sci. 393, 46–59.
Monteiro, I.P., Shukla, A., Marques, A.P., Reis, R.L., Hammond, P.T., 2015. Spray-assisted layer-by-layer assembly on hyaluronic acid scaffolds for skin tissue engineering. J. Biomed. Mater. Res. A 103 (1), 330–340.
Motamedian, S.R., Hosseinpour, S., Ahsaie, M.G., Khojasteh, A., 2015. Smart scaffolds in bone tissue engineering: a systematic review of literature. World J. Stem Cells 7 (3), 657.
Nelea, V., Ristoscu, C., Chiritescu, C., Ghica, C., Mihailescu, I., Pelletier, H., et al., 2000. Pulsed laser deposition of hydroxyapatite thin films on Ti-5Al-2.5Fe substrates with and without buffer layers. Appl. Surf. Sci. 168 (1-4), 127–131.
Pelipenko, J., Kocbek, P., Kristl, J., 2015. Critical attributes of nanofibers: preparation, drug loading, and tissue regeneration. Int. J. Pharm. 484 (1-2), 57–74.
Perumal, S., Kumar Ramadass, S., Madhan, B., 2014. Sol–gel processed mupirocin silica microspheres loaded collagen scaffold: a synergistic bio-composite for wound healing. Eur. J. Pharm. Sci. 52, 26–33.
Pishbin, F., Cordero-Arias, L., Cabanas-Polo, S., Boccaccini, A., 2015. Bioactive polymer–calcium phosphate composite coatings by electrophoretic deposition. Surface Coating and Modification of Metallic Biomaterials. Elsevier.
Prajapati, R.N., Tekade, R.K., Gupta, U., Gajbhiye, V., Jain, N.K., 2009. Dendimer-mediated solubilization, formulation development and in vitro-in vivo assessment of piroxicam. Mol. Pharmaceutics 6, 940–950.
Punetha, V.D., Rana, S., Yoo, H.J., Chaurasia, A., McLeskey Jr, J.T., et al., 2017. Functionalization of carbon nanomaterials for advanced polymer nanocomposites: a comparison study between CNT and graphene. Prog. Polym. Sci. 67, 1–47.
Rad, A.T., Solati-Hashjin, M., Osman, N.A.A., Faghihi, S., 2014. Improved bio-physical performance of hydroxyapatite coatings obtained by electrophoretic deposition at dynamic voltage. Ceram. Int. 40 (8), 12681–12691.
Ramot, Y., Haim-Zada, M., Domb, A.J., Nyska, A., 2016. Biocompatibility and safety of PLA and its copolymers. Adv. Drug Delivery Rev. 107, 153–162.
Rashid, J.I.A., Yusof, N.A., Abdullah, J., Hashim, U., Hajian, R., 2016. Surface modifications to boost sensitivities of electrochemical biosensors using gold nanoparticles/silicon nanowires and response surface methodology approach. J. Mater. Sci. 51 (2), 1083–1097.
Richards, B.T., Wadley, H.N., 2014. Plasma spray deposition of tri-layer environmental barrier coatings. J. Eur. Ceram. Soc. 34 (12), 3069–3083.
Rigort, A., Plitzko, J.M., 2015. Cryo-focused-ion-beam applications in structural biology. Arch. Biochem. Biophys. 581, 122–130.

Roudan, M., Ramesh, S., Wong, Y., Chandran, H., Krishnasamy, S., Teng, W., et al., 2017. Sintering behavior and characteristic of bio-based hydroxyapatite coating deposited on titanium. J. Ceram. Process. Res. 18 (9), 640–645.

Sculean, A., Nikolidakis, D., Nikou, G., Ivanovic, A., Chapple, I.L., Stavropoulos, A., 2015. Biomaterials for promoting periodontal regeneration in human intrabony defects: a systematic review. Periodontology 2000 68 (1), 182–216.

Sharma, P.A., Maheshwari, R., Tekade, M., Tekade, R.K., 2015. Nanomaterial based approaches for the diagnosis and therapy of cardiovascular diseases. Curr. Pharm. Des. 21 (30), 4465–4478.

Soni, N., Tekade, M., Kesharwani, P., Bhattacharya, P., Maheshwari, R., Dua, K., et al., 2017. Recent advances in oncological submissions of dendrimer. Curr. Pharm. Des. 23, 3084–3098.

Stewart, J.M., 2007. Bradykinin in solid-phase peptide synthesis. Int. J. Pept. Res. Ther. 13 (1-2), 3–5.

Su, Y., Zheng, Y., Tang, L., Qin, Y.-X., Zhu, D., 2017. Calcium phosphate coatings for metallic orthopedic biomaterials. Orthopedic Biomaterials. Springer.

Subirós-Funosas, R., Prohens, R., Barbas, R., El-Faham, A., Albericio, F., 2009. Oxyma: an efficient additive for peptide synthesis to replace the benzotriazole-based HOBt and HOAt with a lower risk of explosion. Chemistry 15 (37), 9394–9403.

Suresh, M.B., Biswas, P., Mahender, V., Johnson, R., 2017. Comparative evaluation of electrical conductivity of hydroxyapatite ceramics densified through ramp and hold, spark plasma and post sinter hot isostatic pressing routes. Mater. Sci. Eng., C 70, 364–370.

Surmenev, R.A., Surmeneva, M.A., Ivanova, A.A., 2014. Significance of calcium phosphate coatings for the enhancement of new bone osteogenesis—a review. Acta Biomater. 10 (2), 557–579.

Tekade, R.K., Chougule, M.B., 2013. Formulation development and evaluation of hybrid nanocarrier for cancer therapy: taguchi orthogonal array based design. Biomed. Res. Int. 2013, 712678.

Tekade, R.K., Sun, X., 2017a. The Warburg effect and glucose-derived cancer theranostics. Drug Discov. Today 22, 1637–1653.

Tekade, R.K., Dutta, T., Tyagi, A., Bharti, A.C., Das, B.C., Jain, N.K., 2008. Surface-engineered dendrimers for dual drug delivery: a receptor up-regulation and enhanced cancer targeting strategy. J. Drug Target. 16, 758–772.

Tekade, R.K., Kumar, P.V., Jain, N.K., 2009. Dendrimers in oncology: an expanding horizon. Chem. Rev. 109, 49–87.

Tekade, R.K., Youngren-Ortiz, S.R., Yang, H., Haware, R., Chougule, M.B., 2014. Designing hybrid onconase nanocarriers for mesothelioma therapy: a Taguchi orthogonal array and multivariate component driven analysis. Mol. Pharmaceutics 11, 3671–3683.

Tekade, R.K., Tekade, M., Kumar, M., Chauhan, A.S., 2015. Dendrimer-stabilized smart-nanoparticle (DSSN) platform for targeted delivery of hydrophobic antitumor therapeutics. Pharm. Res. 32, 910–928.

Tekade, R.K., Maheshwari, R., Tekade, M., 2017. 4 Biopolymer-based nanocomposites for transdermal drug delivery. Biopolymer-Based Composites. Woodhead Publishing.

Tekade, R.K., Maheshwari, R., Tekade, M., Chougule, M.B., 2017a. Chapter 8—Solid lipid nanoparticles for targeting and delivery of drugs and genes A2—Mishra, Vijay. In: Kesharwani, P., Amin, M.C.I.M., Iyer, A. (Eds.), Nanotechnology-Based Approaches for Targeting and Delivery of Drugs and Genes. Academic Press, pp. 256–286.

Tekade, R.K., Maheshwari, R., Tekade, M., Chougule, M.B., 2017b. Solid lipid nanoparticles for targeting and delivery of drugs and genes. Nanotechnology-Based Approaches for Targeting and Delivery of Drugs and Genes 256.

Tekade, R.K., Maheshwari, R., Jain, N.K., 2018. 9 Toxicity of nanostructured biomaterials A2—Narayan, Roger. Nanobiomaterials. Woodhead Publishing.

Tielmann, P., Kierkels, H., Zonta, A., Ilie, A., Reetz, M.T., 2014. Increasing the activity and enantioselectivity of lipases by sol–gel immobilization: further advancements of practical interest. Nanoscale 6 (12), 6220–6228.

Wolke, J., Van Dijk, K., Schaeken, H., De Groot, K., Jansen, J., 1994. Study of the surface characteristics of magnetron-sputter calcium phosphate coatings. J. Biomed. Mater. Res. A 28 (12), 1477–1484.

Wu, M.-W., Chen, J.-K., Lin, B.-H., Chiang, P.-H., 2017. Improved fatigue endurance ratio of additive manufactured Ti-6Al-4V lattice by hot isostatic pressing. Mater. Des. 134, 163–170.

Xiong, Y., Lu, C., Wang, C., Song, R., 2014. The *n*-MAO/EPD bio-ceramic composite coating fabricated on ZK60 magnesium alloy using combined micro-arc oxidation with electrophoretic deposition. Appl. Surf. Sci. 322, 230–235.

Xu, Y., Zhou, M., Wen, L., Wang, C., Zhao, H., Mi, Y., et al., 2015. Highly ordered three-dimensional Ni-TiO_2 nanoarrays as sodium ion battery anodes. Chem. Mater. 27 (12), 4274–4280.

Yan, Y., Zhang, X., Mao, H., Huang, Y., Ding, Q., Pang, X., 2015. Hydroxyapatite/gelatin functionalized graphene oxide composite coatings deposited on TiO_2 nanotube by electrochemical deposition for biomedical applications. Appl. Surf. Sci. 329, 76–82.

Yang, H.-M., Chan, Y.-C., Hsu, T.-H., Chen, H.-W., Lee, J.-W., Duh, J.-G., et al., 2015. Synthesis and characterization of nacre-inspired zirconia/polyimide multilayer coatings by a hybrid sputtering and pulsed laser deposition technique. Surf. Coat. Technol. 284, 118–128.

Youngren, S.R., Tekade, R.K., Gustilo, B., Hoffmann, P.R., Chougule, M.B., 2013. STAT6 siRNA matrix-loaded gelatin nanocarriers: formulation, characterization, and ex vivo proof of concept using adenocarcinoma cells. Biomed. Res. Int. 2013, 858946.

Yu, S.S., Lau, C.M., Barham, W.J., Onishko, H.M., Nelson, C.E., Li, H., et al., 2013. Macrophage-specific RNA interference targeting via "click", mannosylated polymeric micelles. Mol. Pharmaceutics 10 (3), 975–987.

Zhang, F., Li, C., Yan, M., He, J., Yang, Y., Yin, F., 2017. Microstructure and nanomechanical properties of co-deposited Ti-Cr films prepared by magnetron sputtering. Surf. Coat. Technol. 325, 636–642.

Zhang, J., Ma, X., Lin, D., Shi, H., Yuan, Y., Tang, W., et al., 2015. Magnesium modification of a calcium phosphate cement alters bone marrow stromal cell behavior via an integrin-mediated mechanism. Biomaterials 53, 251–264.

Zhang, Z., Wei, X., Zhang, X., Lu, W., 2013. *p*-Hydroxybenzoic acid (*p*-HA) modified polymeric micelles for brain-targeted docetaxel delivery. Chin. Sci. Bull. 58 (21), 2651–2656.

Zhou, J., Tsai, Y.-T., Weng, H., Baker, D.W., Tang, L., 2011. Real time monitoring of biomaterial-mediated inflammatory responses via macrophage-targeting NIR nanoprobes. Biomaterials 32 (35), 9383–9390.

Zhu, C., Zhou, J., Li, J., Yang, Y., Xu, W., Zhong, L., et al., 2018. Room temperature sputtering deposition of high-haze Ga-doped ZnO transparent conductive thin films on self-textured bio-based poly(ethylene 2,5-furandicarboxylate) substrates. Ceram. Int. 44 (1), 369–373.

Further Reading

Goddard, J.M., Hotchkiss, J., 2007. Polymer surface modification for the attachment of bioactive compounds. Prog. Polym. Sci. 32 (7), 698–725.

CHAPTER

4

Biomaterials for Sustained and Controlled Delivery of Small Drug Molecules

Disha Mehtani[1], *Ankit Seth*[2], *Piyoosh Sharma*[2], *Neha Maheshwari*[3], *Devesh Kapoor*[4], *Sushant K. Shrivastava*[2] *and Rakesh K. Tekade*[5]

[1]Department of Pharmaceutics, Sri Aurobindo Institute of Pharmacy, Indore, India [2]Department of Pharmaceutical Engineering & Technology, Indian Institute of Technology, Banaras Hindu University, Varanasi, India [3]School of Pharmacy, Devi Ahilya Vishwavidyalaya, Takshila Campus, Indore, India [4]Department of Pharmacy, Dr. Dayaram Patel Pharmacy College, Bardoli, India [5]National Institute of Pharmaceutical Education and Research (NIPER)—Ahmedabad, Gandhinagar, India

OUTLINE

4.1 Introduction 90

4.2 Biomaterial Science and Biomaterials 91
- *4.2.1 Purpose and Definition* 91
- *4.2.2 Requirements for Biomaterials* 92
- *4.2.3 Synthesis (Additive Manufacturing) and Properties of Biomaterials* 92
- *4.2.4 Types of Biomaterials* 94

4.3 Biomaterial Applications for Sustained and Controlled Release for Various Drug Delivery Systems 96
- *4.3.1 Oral Drug Delivery* 96
- *4.3.2 Ocular Drug Delivery* 97
- *4.3.3 Drug Delivery to Ear* 98
- *4.3.4 Pulmonary Drug Delivery* 99
- *4.3.5 Transdermal Drug Delivery* 100
- *4.3.6 Central Nervous System Drug Delivery (Brain and Spine)* 101

Biomaterials and Bionanotechnology
DOI: https://doi.org/10.1016/B978-0-12-814427-5.00004-4

© 2019 Elsevier Inc. All rights reserved.

4.3.7 Cardiovascular Drug Delivery 102
4.3.8 Orthopedic Drug Delivery 104
4.3.9 Injectable Drug Delivery 104
4.3.10 Implantable Drug Delivery 105
4.3.11 Drug Delivery for Wound Closure 106
4.3.12 Localized Drug Targeting (Cancer and Immunotherapy) 107
4.4 Advancements in Biomaterial Applications 107
4.4.1 Smart Components: Stimuli-Responsive Biomaterials 108
4.4.2 Intelligent Drug Delivery Systems 116
4.5 Challenges in Using Biomaterials for Drug Delivery 126
4.5.1 General Aspects 126
4.5.2 Biological Events Upon Host–Biomaterial Interaction and Solutions 128
4.5.3 Examples of Smart Biomaterial Challenges and Toxicities 131
4.5.4 Biological Assessment Tests 132
4.6 Regulatory and Patent Aspect of Biomaterials Employed for Sustained and Controlled Delivery of Small Drug Molecule 134
4.7 Future Prospects and Conclusion 135
Acknowledgments 136
References 136
Further reading 152

4.1 INTRODUCTION

The emergence of the technology for controlling the release of a drug from its formulation has a massive impact on dosage form design and development in the pharmaceutical sector (Tekade et al., 2017b). In the last few decades, there has been an obvious increase in the use of novel drug delivery systems (NDDS) as a patient-friendly substitute to conventional formulations (Tibbitt et al., 2016). These systems were extensively explored to enhance the therapeutic performance of the drug candidate by controlling its release kinetics. The inimitable potential of NDDS to afford physical stability sustained release, as well as targeted delivery of drugs, may conceivably create innovative vistas for safe, accurate, and quality treatment of numerous diseases (Rai et al., 2016). Also, the exclusive features lead to the maximum utilization of the drug and decreased fluctuations in plasma drug concentrations resulting in reduced adverse effects (van Dijk et al., 2017).

Controlled drug delivery systems typically comprise a drug candidate along with a biodegradable and biocompatible material like polymers (Holowka and Bhatia, 2016), lipids, dendrimers, etc. Delivery of the drug with predictable release kinetics for scheduled periods is one of the distinct features of controlled release systems. To upsurge the performance and accomplish site-specific targeting, controlled release systems are often functionalized by surface tailoring with bioactive molecules that can selectively interact with the target (Lai et al., 2015). Sustained release systems on the other hand usually comprise of polymers or other agents that influence the overall dissolution rate of the drug candidate to sustain the therapeutic response for extended periods (Holowka and Bhatia, 2014).

Discovery and utilization of biomaterials are one of the key breakthroughs in the design and development of NDDS. The wide array of these biomaterials coupled with technological advancements in synthetic chemistry unlocked a floodgate of innovative prospects in biocompatible and biodegradable systems for delivering therapeutics. Scientists have made promising developments in characterizing biomaterial owing to their enormous applications in NDDS for boosting substantial advancements in medicines as well as diagnostics. Enormous research efforts have been put toward examining the applications of novel biomaterials to fabricate medical implants that can treat, repair or replace any organ or tissue, without unfavorable side effects.

4.2 BIOMATERIAL SCIENCE AND BIOMATERIALS

4.2.1 Purpose and Definition

With the advancement of pharmaceutical industries and focus on better patient compliance, biomaterials for particular biomedical applications have rapidly expanded during the last 20 years. By definition, a biomaterial is a material that is in whole or in part composed of living matter, such as polymer scaffolding perfused with cells. These materials may be used as a medical device that augments or replaces natural tissue for therapeutic effect. The combination of synthetic and living material derived from stem cells could enable the repair of heart valves, bone, cartilage, and other tissues by replacing or patching the damaged parts with materials that are genetically identical to the patient, and therefore safe from immunological rejection (Park and Lakes, 2007).

Biomaterials are largely divided into polymeric materials, ceramics, and metals. Ceramics and metals are mainly used for the replacement of hard tissue (orthopedics), whereas polymeric materials are applied to both the (temporary) replacement of soft and hard tissues. There are different parts of biomaterial science, which includes chemistry, tissue engineering, biology, elements of medicine, and material science (Williams, 1976).

For cranial defects replacements, first gold and ivory were used as biomaterials. Romans and Egyptians were involved in this work. Since the 1900s placenta has been employed as biologic material. The first manufactured plastic employed for cranial defects was celluloid. After World War II the very first polymer employed was polymethyl methacrylate (PMMA). The field of biomaterials shifted towards inert material with the development of bioactive compounds to explicit precise biological response at the interface of the materials in the 1980s and 1990s (Harris et al., 2014).

A biomaterial is any substance natural or fabricated by humans. It is a part of the whole of a living structure biomedical device that exhibits, surges, and shifts a natural function. It can be employed for a heart valve. It can also be used for an interactive reason such as hip implants coated by hydroxyapatite (HA). Biomaterials can also be employed in day-to-day life for dental surgery and drug delivery. They can also be employed for bone plates, bone cement, artificial ligament and tendons, blood vessel prostheses, skin repair devices, cochlear replacements, and contact lenses (Biagini et al., 1991; MacNeil, 2008).

4.2.2 Requirements for Biomaterials

They are classified into three categories according to their reaction of the tissues. First is bioinert materials, the adjoining bone tissue having unswerving contact from these materials. Between implant and the tissue, no chemical reaction will take place. Second is biotolerant materials alienated from the bone tissue by a layer of fibrous tissue, and last are bioactive materials. These kinds of materials have the characteristics of developing chemical bonds with bone tissue, known as osseointegration (Zarb et al., 2008).

A biomaterial should be compatible with different excipients of the formulation. The biomaterial should not exhibit any kind of unfavorable reaction from the body and vice versa. It does not yield any carcinogenic effects on the body. It should be nontoxic. It should have sufficient mechanical and physical properties to provide as intensification or substitution of tissues of the body. For commercial utilization, it will be acquiescent so that can be transformed into dissimilar shapes. It should be cheap in price and readily available (Parida et al., 2012). It should have an exceptional confrontation to degradation such as corrosion confrontation for metals or confrontation to biological dilapidation in polymers. It should have high wear resistance to diminish wear debris production. It should have little modulus to diminish bone reabsorption. An ideal biomaterial should have the following characteristics, which are shown in Fig. 4.1.

4.2.3 Synthesis (Additive Manufacturing) and Properties of Biomaterials

For the accomplishment of certain applications of biomaterial, its physical, chemical, and mechanical properties should be taken into consideration. The vital property needed for a biomaterial is that it should not elicit an adverse reaction when placed into the system.

4.2.3.1 Physical Properties

Physical properties of biomaterials are fundamental to the response of cell adhesion. When cells adhere to the biomaterial surface physical/chemical reactions between cell and biomaterial occur. These reactions may be influenced by factors such as the nature of the cell, biomaterial surface characteristics, and environmental causes. The biomaterial surface properties comprise wettability, filler, roughness, softness, and chemical composition. Biological response of the biomaterial can be affected by wettability (hydrophobicity/hydrophilicity), which is an important parameter. It depicts the steadiness in between liquid and the intermolecular interactions of solid surface.

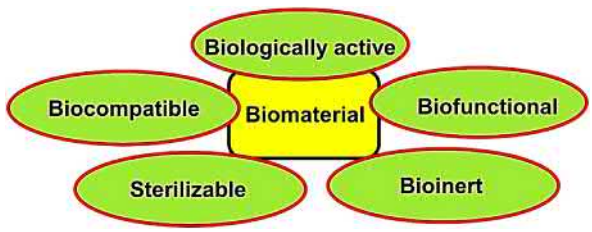

FIGURE 4.1 Characteristic properties of biomaterials.

In relation with a surface charge, investigators observed better biocompatibility, cellular affinity, and cellular differentiation on the periphery of biomaterials implanted utilizing positive ions and negative ions. For an instant, 2-hydroxyethyl methacrylate (HEMA) gels incorporated with positive charges promoted better adhesion and spreading of fibroblasts and osteoblasts when compared with negative or neutral charges (Chang and Wang, 2011).

4.2.3.2 *Chemical Properties*

These properties also manipulate the category of cell bond and figure out the chemical stability and reactivity of biomaterial. The corporeal environment is harsh and could be a reason for corrosion of these materials. Corrosion of biomaterials not only changes the stability of chemical but gives impact on the mechanical integrity, with the probable untimely collapse of the material as well. Functional groups of the surface can also manipulate the biomaterial response of biomaterial since the chemical functionality of surface affects adsorbed protein interactions. Recurrently used examples as relates to biomaterials are carboxyl (−COOH), hydroxyl (−OH), amino ($-NH_2$), and methyl ($-CH_3$) groups (Alatorre-Meda and Mano, 2016).

4.2.3.3 *Mechanical Properties*

For biomaterial used for specific mechanical application, some of the criteria that should be studied include fatigue, ductility, tensile strength, yield strength, Young's modulus, compression strength, and wear debris. We can determine biomaterial mechanical properties by studying tensile and shear properties, bending properties, and time-dependent properties (Basu, 2017b).

4.2.3.3.1 TENSILE AND SHEAR PROPERTIES

Different types of forces can be applied to a material such as tensile, compressive, shear, and torsion. For performing tensile testing, force is applied as tensile, compressive, or shear. Engineering stress (σ) and engineering strain (ε) are the parameters that are measured.

$\sigma = \frac{F}{A0}$:Force applied perpendicular to the cross-section of the sample

Compression testing is performed especially for biomaterials subjected to compressive forces during operation such as orthopedic implants. Forces are parallel to the top and bottom faces in shear testing.

Shear stress(τ) = $\frac{F}{A0}$

Shear strain (γ) = tan θ, θ = is the deformation angel.

Some other mechanical properties include viscoelastic flow in which performance is intermediate between solid and liquid. For fatigue, the fracture can happen after a number of cycles even if the stress is applied well below the yield stress. The ability of a material to plastically deform under a stress field at the tip of a crack is toughness. Surface characterization of biomaterials can be done by analyzing critical surface tension, contact angle measurement, electron spectroscopy for chemical analysis, X-ray photoelectron spectroscopy, secondary ion mass spectrometry, and scanning tunneling microscopy (Basu, 2017b).

TABLE 4.1 Examples of Metals With Their Diverse Applications

Material	Applications
Gold alloys	Dental restorations
Silver products	Antibacterial agents
Platinum and Pt−Ir	Electrodes
Ni−Ti	Bone plates, stents, orthodontic wires
316L stainless steel	Fracture fixation, stents, surgical instruments

4.2.4 Types of Biomaterials

4.2.4.1 Metals

Metals are the extensively employed for load-bearing implants. However, mostly frequent orthopedic operating procedures engage the use of metallic implants. They are available in various ranges from simple wires and screws to fracture fixation plates and total joint prostheses (artificial joints) for ankles, shoulders, knees, and hips. In addition to orthopedics, metallic implants are employed in cardiovascular surgery, maxillofacial surgery, and used as dental materials (Kraišnik et al., 2018). The most widely used metals are stainless steels, commercially pure titanium and titanium alloys, and cobalt-base alloys. The examples of metals are given below in Table 4.1.

4.2.4.2 Polymers

For packing of implanted devices biostable and biocompatible polymers is commonly used. The main criterion, which includes gas permeability and water permeability of the packaging of the polymer to guard the electronic circuit of the device from wetness and ions inside the human system (He and Benson, 2017).

Polyvinylidene fluoride is a widely used polymer because it is chemically inert, with a strong piezoelectric effect and high resistance to hydrolysis. This material also has good stiffness and strength. Polyethylene is porous high-density polyethylene and has superior biocompatibility, excellent elasticity, and strong antiinfective properties. It has fast drying characteristics with low melting temperature. It has superior chemical resistance along with excellent mechanical properties. Polypropylene is nontoxic and high melting point having first-class dielectric properties. PMMA is light in weight having poor thermal and electrical conductivity. It is mechanically strong and radiolucent. Silicone has good electrical insulation with high gas permeability. It is hydrophobic in nature and has low toxicity. Liquid crystal polymer is chemically inert, resistant to fire, and exhibits low moisture absorption. It has decent MRI (medical resonance imaging) capability. It is able to mold into thin layers (Basu, 2017a). Here below in Table 4.2 polymers and their diverse applications are mentioned.

4.2.4.3 Ceramics and Glasses

The ceramics that are used for repair and restoration of diseased or smashed parts of musculoskeletal systems are called bioceramics (Hench and Kokubo, 2016). Bioceramics

TABLE 4.2 Examples of Polymers With Their Diverse Applications

Materials	Applications
Polyethylene	Joint replacement
PVC	Tubing
PMMA	Dental restoration, Intraocular lenses
Silicones	Ophthalmology, soft tissue replacement
Polyesters	Drug delivery systems, vascular prostheses
Polyethylene	Joint replacement
PVC	Tubing
PMMA	Dental restoration, intraocular lenses
Silicones	Ophthalmology, soft tissue replacement
Polyesters	Drug delivery systems, vascular prostheses

PMMA, Polymethyl methacrylate.

TABLE 4.3 Examples of Ceramics and Glasses With Their Diverse Applications

Material	Applications
Carbons	Heart valves, dental implants, percutaneous devices
Porcelain	Dental restorations
Zirconia	Joint replacement
Calcium phosphate	Bone repair and augmentation
Bioactive glasses	Bone replacement

can be classified as bioinert high strength ceramics, bioactive ceramics, and bioresorbable ceramics. Bioceramics may be resorbable like tricalcium phosphate (TCP), alumina, zirconia, HA. Bioceramics have three attachment mechanisms: morphology fixation, biological fixation, and bioactive fixation. Bioglasses are a fascinating, multitalented class of materials and architecturally all silica-based glasses have the similar basic building block—SiO_4^{4-}. These bioglasses are entrenched in a biomaterial support to figure out prosthetics for hard tissues. Such prosthetics are biocompatible, show exceptional mechanical properties, and are helpful for orthopedic and dental prosthetics. The glass ceramic has higher mechanical properties, high-quality biocompatibility, bioactivity, and negative toxicity making it constructive as a biomaterial used for artificial bone and dental implants (Li et al., 2014b). The bioactive glass ceramic has two chief crystal phases: mica, and apatite. Different examples of ceramics and glasses are given in Table 4.3.

Various biomaterials along with the capacity of tissue bonding are given in Table 4.4.

TABLE 4.4 Biomaterials Along With the Capacity of Bonding With Tissues

	The Capacity for Bonding With Tissues	
Biomaterial	**Bone**	**Soft**
Bioglass	Exists	Exists
Cerabone	Exists	None
Ceravital	Exists	None
Hydroxyapatite ceramics	Exists	None
Corundum ceramics	None	None

TABLE 4.5 Examples of Composites With Their Diverse Applications

Material	Applications
PMMA-glass fillers	Dental restorations (dental cements)
BIS-GMA-quartz/silica filler	Dental restorations

PMMA, Polymethyl methacrylate.

4.2.4.4 Composites

Carbon nanotube (CNT) composites are widely used for its exclusive electrical, mechanical, and surface properties. CNT also shows superconductivity character alongside unambiguous axis when pooled with zeolite as a composite (Tekade et al., 2017a). They have been made of plastic, glass, carbon and different ceramic matrices with different types of fibers having SiC, stainless steel, phosphate glass. These composites can be coated on metals to offer outstanding porosity and packing density within the films itself, lowering the ionization of the metal encapsulated (Yokoi et al., 2017). Diverse examples of composites are given in Table 4.5.

4.3 BIOMATERIAL APPLICATIONS FOR SUSTAINED AND CONTROLLED RELEASE FOR VARIOUS DRUG DELIVERY SYSTEMS

4.3.1 Oral Drug Delivery

The oral route for drug delivery is always considered as a preferred route of drug administration owing to the ease of self-administration of medications by the patients (Dilnawaz, 2017). However, there remain several challenges in the oral delivery of drugs due to the presence of anatomical barriers, variable pH, proteolytic enzymes, and diverse microflora of the GI tract (Banerjee et al., 2016). Despite these shortcomings, biomaterial-based oral drug delivery systems have been proven to provide innovative solutions to circumvent these hurdles. Out of the several biomaterials for oral drug delivery, chitosan (CS) is a promising material that gained considerable attention owing to its nontoxic nature and distinctive biological properties (Leong and Sung, 2013).

CS retains mucoadhesive, biodegradable, biocompatible, and film forming characteristics that account for its popularity and widespread applications in the area of drug delivery (Huang et al., 2017). CS has been chemically modified by attaching several functional groups so as to enhance its performance for delivering therapeutics via the oral route (Ji et al., 2014). In an investigation, CS and *O*-carboxymethyl CS nanoparticles were developed for pH-dependent oral delivery of an anticancer drug (doxorubicin) with 42% absolute bioavailability and less toxicity (Feng et al., 2013). CS and its derivatives were successfully and safely utilized for the oral delivery of hydrophilic therapeutic macromolecules like cyclosporine A, exendin 4, salmon calcitonin, nucleic acid, insulin, and its derivatives (Chen et al., 2013).

To improve the therapeutic effectiveness, reduce the adverse effects, and reverse drug resistance, the strategy of nanoparticles-based oral delivery of chemotherapeutic agents is gaining remarkable impetus for effective cancer treatment (Biswas et al., 2014). Nanocrystals, polymeric nanoparticles, and lipid-based carriers based on biomaterials have been successfully utilized to effectively deliver anticancer therapeutics. The oral delivery systems have been modified to deliver sensitive therapeutic agents like insulin. For example poly(anhydride) microspheres and pH-dependent poly(methacrylic acid)-graft-poly(ethylene glycol) hydrogels have been designed to protect and deliver insulin (Tibbitt et al., 2016).

Mucoadhesive systems were effectively fabricated to extend the release of oral therapeutics as well as to target specific sites of the gut. These systems were also engineered to protect the bioactives from enzyme activity of the gastrointestinal tract (Netsomboon and Bernkop-Schnürch, 2016). Gastroretentive drug delivery systems were also designed to extend the mean residence time of the drug in the stomach (Lopes et al., 2016). Altogether the significant use of biomaterials paved a new path inefficient oral delivery of therapeutics and to overcome the associated challenges.

4.3.2 Ocular Drug Delivery

Cataracts, diabetic retinopathy, intraocular tumors, age-related macular degeneration, and glaucoma are the most prevalent ocular disorders that result in visual impairment. Complex physiology reflex blinking, lacrimal drainage, and tear dilution are the major constraints for conventional drug delivery to the eye especially in the posterior segment (Fangueiro et al., 2016).

Substantial developments in the field of polymer and nanoscience have led to several advancements in novel bioengineered biomaterials for ocular delivery of therapeutic agents. Several vesicular and particulate drug delivery systems like liposomes, cyclodextrins (CyDs), nanoparticles, niosomes, nanoemulsions, and nanospheres were investigated for ocular drug delivery with enhanced efficacy and lower side effects (Lalu et al., 2017). Several synthetic, natural, and bioadhesive polymers have emerged as potential carriers for delivering therapeutics to the eye (Tekade et al., 2017c).

Many hydrogels, like alginate, fibrin, CS, collagen, and gelatin were reported for good permeation and bioadhesive characteristics (Maheshwari et al., 2015b). Poly(D,L-lactide-*co*-glycolide) (PLGA), copolymer of polyethylene glycol (PEG) and PLGA,

polybeta(1−4)-D-glucosamine, poly(HEMA), poly(*N*-isopropylacrylamide) (NIPAAm) (PNIPAAMs), Poloxamer 407, Pluronic F127, and several other polymers were effectively utilized in several nanoformulations for extending drug release in the ocular globe (Kang-Mieler et al., 2017). Some of the polymers were reported for the development of polymeric micelles of several drugs like ciprofloxacin, diclofenac, cyclosporine, lornoxicam, etc., for ocular delivery (Mandal et al., 2017). Hydrogel-based soft contact lenses have also gained considerable attention in the field of ocular therapeutics for treating corneal wounds (Gupta and Aqil, 2012).

Use of dendrimer-based biomaterials with unique characteristics over conventional polymers was reported to increase the corneal retention time of topical formulations. Also, dendrimers were reported for sustaining and controlling the release of the drugs from the formulation (Kumar Tekade et al., 2015; Soni et al., 2017).

In a study, polyamidoamine dendrimers were used to develop rapid dissolving nanofibers as an alternative to eye drops, for the topical delivery of brimonidine tartrate in glaucoma with improved efficacy (Lancina et al., 2017). Use of these diverse biomaterials clearly justifies their immense usage in designing and developing a variety of NDDS for effective management of ocular disorders and enormous scope of clinical translation in the future.

4.3.3 Drug Delivery to Ear

Delivery of therapeutics to the inner part of the ear has been a challenging task over the past several years. The blood−labyrinth barrier, composed of the tight junctions endothelial cellular layer, is the main barrier that separates the inner ear from systemic circulation (Ishiyama et al., 2017). Therapeutic strategies involving delivery of drugs in a controlled manner is a requisite for the treatment of a plethora of inner ear disorders like presbycusis, Ménière's disease, trauma, genetic diseases, acute and chronic otitis, and autoimmune inner ear diseases (McCall et al., 2010).

Novel biomaterial-based nanomedicines are believed to overcome the drawbacks of conventional medicines (Soni et al., 2016; Tekade et al., 2017d). Several nanoformulations like polymeric nanoparticles, solid lipid nanoparticles, liposomes, and polymersomes provide efficient drug concentrations in the ear (Hoskison et al., 2013). In an investigation, it was revealed that poly(2-hydroxyethyl aspartamide) based polymersomes are a safe and effective carrier of the drug into the inner ear (Kim et al., 2015). Liposomes were also reported as an efficient carrier for drug delivery to the inner ear through the round window membrane (RWM) (Buckiová et al., 2012). In a recent study, it was revealed that coumarin-6 bearing PLGA nanoparticles were successfully transported to the inner ear via local application through the RWM (Zhang et al., 2018a). Lipid nanocapsules were also investigated as potential carriers to deliver the drugs efficiently to the cochlea through the RWM (Pritz et al., 2013). In another examination, rhodamine B-loaded bovine serum albumin nanoparticles were reported to exhibit a controlled release profile and considerable permeability across the RWM of guinea pigs (Yu et al., 2014).

Hydrogels were also explored for delivering drugs to the inner ear and reported for significant results. A biodegradable gelatin polymer Gelfoam was reported as a drug delivery carrier for the inner ear disorders. It was revealed that gentamycin loaded Gelfoam, placed

on RWM, successfully treated vertigo in 75% of patients and tinnitus in 48% of patients of Meniere's disease. Another hydrogel, hyaluronic acid−carboxymethyl cellulose polymer, was investigated to deliver dexamethasone to the RWM by intratympanic route.

It has been found that dexamethasone loaded hydrogel efficiently alleviated the hearing loss linked to the trauma of cochlear implantation. Several other hydrogels like Poloxamer 407, CS glycosylated derivative, thiol-modified hyaluronic acid, and CS glycerophosphate hydrogel were also explored for sustained/controlled release of the drug to the middle and inner ear (Liu et al., 2013). Delivery of therapeutics to the inner ear is complex and the available drug delivery systems are still in their infancy. Therefore there is an enormous scope to develop more efficient and safe drug delivery systems for clinical settings.

4.3.4 Pulmonary Drug Delivery

The pulmonary route has been extensively explored as a preferential route for delivering several therapeutic agents to the lungs for treating disorders like asthma and chronic obstructive pulmonary diseases and other pulmonary disorders. High blood perfusion and large surface area of the lungs provides a physiological advantage, making this route versatile for drug delivery (Ali, 2010). However, the mean residence time for the drug to remain at the mucosal surface represents a challenge for the formulation scientist. Therefore the use of bioadhesive polymer like CS gained considerable attention to increase the mucosal residence time of the drug and increase its absorption. CS-based aerosolized preparations were reported in the literature. Aerosolized powder inhalers containing beclometasone dipropionate, CS, and leucine have been reported in an investigation for pulmonary delivery. Another CS-based aerosolized preparation was reported to sustain the release of terbutaline sulfate. Both the formulations exhibit considerable dispersibility and aerodynamic properties (Harris et al., 2013).

The pulmonary route has also been explored to administer several antibiotics to treat the pulmonary infections caused by several Gram-negative and Gram-positive bacteria. Inhalational drug delivery involving biomaterial-based nanoformulations offers advantages of high antibiotic concentrations at the targeted site, rapid onset of action, and reduced side effects (Flume and VanDevanter, 2015).

Recently an inhalational formulation was approved by FDA to treat lung infection caused by *Pseudomonas aeruginosa* in cystic fibrosis patients (Moreno-Sastre et al., 2015). Initially, tobramycin loaded PLGA nanoparticles were developed for pulmonary delivery. The surface properties and size of the nanoparticles were optimized by using poly(vinyl alcohol) and CS whereas the entrapment efficiency and release characteristics were enhanced by using alginate. The optimized formulations exhibit significant in vitro antibacterial activity and considerable aerodynamic properties (Ungaro et al., 2012).

Furthermore, biomaterials (glycerol distearate and glyceryl behenate) based lipid nanoparticles loaded with tobramycin was reported and characterized for treating local lung infections in cystic fibrosis. The resulting nanoparticles sustained the drug release and exhibit high drug entrapment efficiency. The formulation was found to be active against *P. aeruginosa*. In vivo assay in mice revealed the significant distribution of nanoparticles in the lungs (Moreno-Sastre et al., 2016).

Biomaterials-based nanoformulation of many antitubercular drugs like isoniazid, rifampicin, and pyrazinamide were developed and evaluated for pulmonary delivery in guinea pigs (Ingle et al., 2016). Liposomes were also extensively explored for pulmonary delivery of therapeutics. Some liposomal formulations of antibiotics like amikacin (Arikace) and ciprofloxacin (Lipoquin and Pulmaquin) have already reached clinical trials (Waters and Ratjen, 2014; Cipolla et al., 2014; Ehsan et al., 2014).

Aerosolized liposomes mediated delivery of insulin was also meticulously explored in rodent models for pulmonary delivery (Sonia and Sharma, 2014). Altogether the use of biopolymers, lipids, and other biomaterials coupled with advanced nanotechnology, for delivering therapeutics via pulmonary route is of paramount importance and may provide a viable alternative for the development of novel strategies of controlled drug delivery and target (Maheshwari et al., 2012).

4.3.5 Transdermal Drug Delivery

Transdermal patches are formulated to deliver the active drugs across the skin into the systemic circulation in a sustained or controlled manner (Alkilani et al., 2015). Apart from improved patient convenience and compliance, the transdermal route offers other advantages of bypassing first-pass metabolism and avoidance of gastric/enzymatic drug degradation (Ita, 2014).

Steady-state concentrations of the drug in plasma can be accomplished with this route. About 20 drugs have been successfully formulated into transdermal patches that are approved by US-FDA and are commercially available (Pastore et al., 2015). Hydrogels made of several natural polymers (like cellulose, CS, gelatin, starch) and synthetic polymers [like polyvinyl alcohol, polyvinyl pyrrolidone, polycaprolactone (PCL)] have gained noteworthy attention in the development of transdermal drug delivery systems (Santos et al., 2018).

Owing to its film-forming and bioadhesive properties, CS, found its extensive application in the development of transdermal patches. In an investigation, a CS-based transdermal patch of Glibenclamide nanocrystals was developed. It was demonstrated that the patches show a significant flux of Glibenclamide across the skin of rat and reduce in vivo blood glucose level considerably in animal models (Ali and Hanafy, 2017).

In another study, rivastigmine loaded CS microparticles were formulated for transdermal delivery. The patch with microparticles exhibits significant permeation of rivastigmine as compared with control (Sadeghi et al., 2016). Alginate was also reported for the fabrication of transdermal patches, owing to its biocompatible and nontoxic nature. Sodium alginate and CS microneedle patches were successfully developed and exhibits significant permeation of bovine serum albumin across dermatomed human abdominal skin and rat skin respectively. The results suggested that the microneedle patches may function as potential devices for transdermal drug delivery (Chen et al., 2012c; Demir et al., 2013). Donepezil, formulated in sodium alginate patches shows substantial permeation rate across pig skin which account for its probable use in neurological disorders like Alzheimer's disease (Nguyen et al., 2017).

Cellulose and its derivatives have also been reported for their widespread acceptability in the fabrication of transdermal patches. An antiepileptic drug topiramate has been

formulated in a hydroxyl propyl methyl cellulose (HPMC) based transdermal patch along with other film forming polymers. Results of in vitro and ex vivo studies suggested that the patches containing Eudragit L 100 and polyvinyl pyrrolidone as film formers and oleic acid as penetration enhancer shows maximum permeation (Cherukuri et al., 2017).

HPMC and hydroxyl propyl cellulose were also investigated to fabricate microneedle patches loaded with donepezil hydrochloride. The findings suggested an immediate release of donepezil hydrochloride that may account for its application in Alzheimer's disease (Kim et al., 2016). The availability of starch and pectin in abundance encouraged their application in transdermal drug delivery. In an investigation, a reservoir type of transdermal patch of starch nanocrystals loaded with acyclovir was successfully fabricated, that showed considerable stability and adhesion (Bakrudeen et al., 2016).

In another investigation, dermal patches of pectin were developed with different concentrations of insulin. The patches efficiently deliver the appropriate amount of insulin into the bloodstream and reduce the blood glucose levels in rats (Hadebe et al., 2014). Most of the commercial patches were developed by using synthetic polymers. PCL has gained considerable attention amongst aliphatic polyesters owing to its rheological characteristics (Santos et al., 2018).

In a study, a microneedle patch was developed from PCL and PEG for transdermal delivery of hydrophilic molecules with higher drug loading capacity (Ko et al., 2015). Other synthetic polymers like polyvinyl alcohol (Chen et al., 2015a; Maji et al., 2013), polyvinyl pyrrolidone (Quinn et al., 2015), and acrylic and its derivatives (Zhang et al., 2016; Jung et al., 2015) were also reported for fabricating transdermal patches. To date several biomaterials have been explored to fabricate robust and sophisticated patches to deliver therapeutic agents into the bloodstream via skin, providing their controlled release and fewer side effects.

4.3.6 Central Nervous System Drug Delivery (Brain and Spine)

Neurological disorders are highly prevalent worldwide with an enormous social impact. The presence of highly selective barriers like a blood–brain barrier and blood–cerebrospinal fluid barrier along with the complex physiology of the brain restricts the entry of drugs to CNS (Khambhla et al., 2016). To circumvent these obstacles, several novel strategies involving biomaterials-based drug delivery systems have been fabricated for delivering therapeutic agents to the brain. Nanoparticles have been explored for delivering a variety of therapeutics to the brain. Nanoparticles engineered with specific ligands or surfactants have been proven to be promising for site-specific drug delivery to the brain (Elzoghby et al., 2016).

Owing to their biocompatibility, safety, and biodegradability, several polymers have been tested to develop potential nanocarriers and nanomaterials (Maheshwari et al., 2015a; Sharma et al., 2015). Polymers such as PLGA, PEG, PCL, *N*-(2-hydroxypropyl)-methacrylate copolymers (HPMAs), poly(lactic acid) (PLA), poly(glutamic acid) (PGA) poly(amino acids), and polyanhydrides have been investigated to develop polymeric nanoparticles (Masserini, 2013). In a study, quercetin loaded polymeric micelles with

considerable release characteristics, biodistribution, blood-brain barrier (BBB) permeability, intracellular uptake, and antitumor activity were reported (Wang et al., 2016a). In another recent research, galantamine loaded PLGA-PEG nanoparticles tailored with ascorbic acid have been developed. The surface modification of nanoparticles resulted in enhanced cellular uptake. The results also revealed considerable biodistribution of the drug in the brain as well as the significant therapeutic efficacy of the formulation in cognitive decline (Gajbhiye et al., 2017).

Importance of PEG coating of nanoparticles for increasing the penetration and reducing the clearance by the reticuloendothelial system was demonstrated by Zhang et al. in a recent study. Cisplatin loaded nanoparticles with PEG coating showed the controlled release of the drug and increased penetration into the tumor tissue along with low clearance rate (Zhang et al., 2017a).

Biomaterials like cholesterol, fatty acids, or phospholipids have also gained enormous attention in developing bilayered vesicles called liposomes for brain targeting. Liposomes are able to carry both hydrophilic and hydrophobic drugs. Owing to the unique advantages of liposomes along with the possibility of surface engineering, these versatile carriers bear enormous potential for delivering therapeutics to the brain (Tsou et al., 2017).

In a research, doxorubicin-loaded liposomes modified with stable *d*-peptide ligands (^{D}CDX/^{D}A7R-LS) for efficient internalization into the brain and glioma cells have been developed. The results revealed a promising antiglioma activity of the formulation (Ying et al., 2016). In another recent investigation levodopa and glutathione coloaded liposomal drug delivery system modified with maltodextrin has been reported for effective brain targeting (Gurturk et al., 2017). Dual-mediated doxorubicin-loaded liposomes tailored with transferrin and cell penetrating peptide was reported in a recent investigation. Surface modification was done to enhance receptor specificity and internalization as well as to reduce the lysosomal clearance (Liu et al., 2017a).

Biomaterials-based approaches were also exploited for delivering drugs to the injured spinal cord for regeneration and recovery in a controlled manner (Ziemba and Gilbert, 2017). Altogether, biomaterial is likely to play substantial roles in prospective strategies for delivering therapeutics to the nervous system.

4.3.7 Cardiovascular Drug Delivery

Drug delivery to the cardiovascular system is different from delivery to other systems because of the anatomy and physiology of the vascular system; it supplies blood and nutrients to all organs of the body. Drugs can be introduced into the vascular system for systemic effects or targeted to an organ via the regional blood supply. The use of biomaterials will surge with 15% compound annual growth rate. The estimated global market will be US$88.7 billion by the end of 2018. The Asian market will also see an attractive rise in compound annual growth rate by 22.4% (Kresse et al., 2000).

Cardiovascular biomaterial can be classified into three categories: metal biomaterial, polymers, and biological materials. Biomaterials, both natural and synthetic, exhibit great potential in cardiac repair and regeneration, either as a carrier for drug delivery or as an

TABLE 4.6 Biomaterial Characteristics Employed as Cardiovascular Biomaterials

Properties	Xenograft	Allograft
Corrosion resistance	Reasonable	Reasonable
Blood compatibility	Good	Very good
Bold flow dynamics	Good	Good
Durability and strength	Reasonable	Reasonable

TABLE 4.7 Polymer Properties Used as Cardiovascular Biomaterial

Properties	Polyamides	Polyolefin	Polyester	PTFE	Polyurethanes
Strength	++	++++	++++	+++++	++
Hardness	++	+++++	+++++	+++++	+++
Rigidity	++	+++++	+++++	+++++	+++
Blood compatibility	++++	+++	++	+	++++

High, +++++; Good, ++++; Better, +++; Moderate, ++; Low, +. *PTFE*, Polytetrafluoroethylene.

extracellular matrix (ECM) substitute scaffold. Liu et al. have shown that an injectable CS hydrogel enhanced stem cell engraftment and survival by improving oxidative stress in the ischemic heart through reactive oxygen species scavenging and chemokine recruitment. A CS–collagen hydrogel has also been used to deliver an angiopoietin-1 analog to enhance endothelial cell function and survival. Indeed, the angiopoietin-1 analog-bound hydrogel mitigated endothelial cell apoptosis and stimulated endothelial cell tube-like structure formation (Liu et al., 2012; Miklas et al., 2013).

The characteristics of the cardiovascular biomaterial as well as some properties of polymer used as a cardiovascular biomaterial are presented in Tables 4.6 and 4.7.

Martins et al. mixed conductive CNTs with CS to form a CS/carbon scaffold with similar elastic properties to the native myocardium. This conductive scaffold not only supported neonatal rat cardiomyocytes survival in vitro, but also increased the expression of myosin heavy chain, troponin T, and connexin-43, which are involved in muscle contraction and electrical coupling and are important for the organization of cell electrical signal transmission.

Zhou et al. also developed a carbon nanofiber/gelatin hydrogel scaffold that supported in vitro culture of neonatal rat cardiac cells and integrated with the host myocardium when implanted post–myocardial infarction (MI) in the rat heart. Heart function as assessed by fractional shortening and ejection fraction evaluated by echocardiography was improved after hydrogel injection while progression of pathological deterioration (e.g., ventricular dilation) was inhibited (Martins et al., 2014; Zhou et al., 2014). In Fig. 4.2, surface modification methods are given for cardiovascular biomaterials.

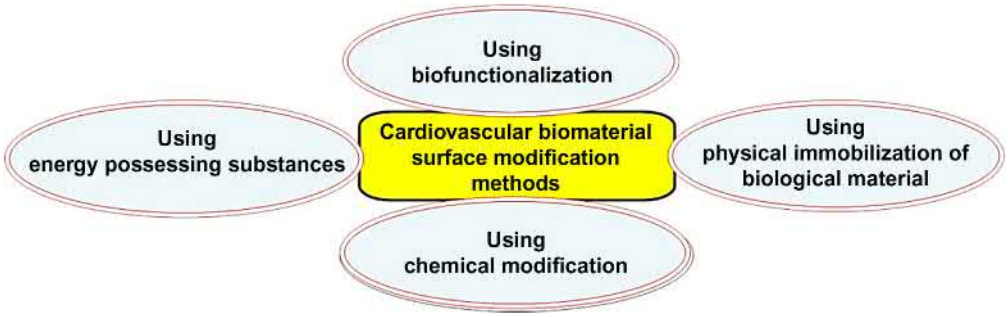

FIGURE 4.2 Surface modification methods of cardiovascular biomaterial.

4.3.8 Orthopedic Drug Delivery

Structural biomaterials including metals, plastics, and ceramics are frequently used in orthopedic surgery, for fixation of fractures, for reconstructive purposes in joint replacement, spinal diseases and deformities, and in numerous other orthopedic subspecialties. Orthopedic implants used as drug delivery systems have targeted infection. The combination of bone cement and antibiotics can then be considered as a precursor approach in drug delivery systems for orthopedic applications.

Orthopedic implants deliver a drug with three different options. In the first case, the drug can be coated on the implant. In the second case, the drug can be incorporated in a scaffold or cement. In the last case, the drug can be incorporated into beads.

Wasko and Kaminski (2015) performed a systematic review of current evidence of antibiotic cement nails (ACNs) in orthopedic trauma and provided an up-to-date analysis of the indications, operative technique, failure mechanisms, complications, outcomes, and outlooks for the ACNs use in long bone infection.

The review by Kavanaugh et al. summarizes emerging particle-based technologies for the detection and treatment of OA (osteoarthritis) that could lead to disease-modifying therapies for OA that are currently lacking in clinical practice. Polyurethane (PU) biomaterials have been extensively used because they have potential as compliant orthopedic bearing materials (Kavanaugh et al., 2016).

Porous biomaterials have been extensively used in an assortment of orthopedic applications. Porous scaffolds stimulate the cellular responses and accelerate osteogenesis. The porous structures of scaffolds, as well as their compositions, dictate cellular responses such as their adhesion, penetration, differentiation, nutrition diffusion, and bone ingrowth.

4.3.9 Injectable Drug Delivery

The parenteral administration route is the most effective and common form of delivery for active drug substances with metabolic bioavailabilities drugs, for which the bioavailability is limited by high first-pass metabolism effect of other physicochemical limitation and for drugs with a narrow therapeutic index. Biomaterial injection provides an

opportunity to concurrently introduce cellular components and depots of bioactive agents. Biologically derived, synthetic, and hybrid materials have been applied, as well as designed expressly for this purpose, although optimal design parameters, including degradation rate and profile, injectability, elastic modulus, and various possible bioactivities largely remain to be elucidated.

Biomaterial has shown good therapeutic potential in preclinical models for MI and peripheral artery disease. Drug delivery systems can be designed for carrying a drug, protecting it from unwanted metabolism, localizing the drug at the desired site of action, releasing the drug at a desired controlled rate, targeting drug release to specific tissues or cells, and minimizing unwanted side effects caused by high doses and systemic delivery. Injectable biomaterials can meet these requirements, offer improved compliance through ease of administration, and allow the prolonged duration of a single treatment (Langer, 1990).

Particulate systems can be injected either at the site of action or into the circulation. These systems are suspensions of small particles on the scale of nanometers to hundreds of microns, which entrap or protect the drug and then release it due to diffusion, degradation, dissociation, or metabolism. Injectable in situ forming gels typically release drugs at a rate limited either by diffusion of the drug through the material or degradation of the material itself. However, it is desirable for a variety of applications that the material be able to release the drug preferentially depending on its environment.

In situ forming drug delivery systems can be loaded with drug and injected through a needle, forming a solid or semisolid gel depot of the drug inside the body at the injection site (Packhaeuser et al., 2004).

Aqueous solubility change materials have a lower critical solution temperature (LCST), a temperature below which the material is soluble and above which the material is insoluble. Examples are NIPAAm-based systems, and temperature-responsive block copolymer systems (Zhang and Hoogenboom, 2015).

4.3.10 Implantable Drug Delivery

Implantable devices are called upon to serve a variety of functions, from vascular stents that preserve blood flow to electrostimulation devices that regulate heart rhythm or block spurious signals in the brain to orthopedic devices that mechanically reinforce the spine or restore range of motion of hips and knees. Implantable drug delivery devices offer several advantages over conventional oral or parenteral dosage forms. First, implantable devices allow site-specific drug administration where the drug is needed most. Biosensors work on the concept of biomicroelectron mechanical systems (MEMS) and are emerging as a potential noninvasive approach to detect and monitor biomarkers. Continuous glucose monitoring systems are boronic acid or diborononic acid-based sensors that can be implanted under the skin and fluorescence could be detected through the skin.

For the early diagnosis of cardiovascular diseases, cholesterol biosensors are used for the estimation of free and total cholesterol. Zirconia was used for dental prosthetic surgery with endosseous implants in the early 1990s. Cranin et al. published the first research work on zirconia in 1975. Ceramic implants were introduced for osseointegration, less plaque accumulation resulting in improvement of the soft tissue management, and esthetic

consideration as an alternative to titanium implants. Implants have been gaining popularity among patients and frequently are being considered as a first treatment option (Hoffmann et al., 2008; Özkurt and Kazazoğlu, 2011).

Titanium has a good record of being used successfully as an implant material and this success with titanium implants is credited to its excellent biocompatibility due to the formation of a stable oxide layer on its surface (Cranin, 1982).

Abdolrahimzadeh et al. evaluated the effectiveness of one or two intravitreal injections of a sustained release dexamethasone implant in patients with persistent macular edema following uncomplicated phacoemulsification. They observed a statistically significant improvement of mean central foveal thickness and best corrected visual acuity with one or two intravitreal dexamethasone implants over 12 months (Abdolrahimzadeh et al., 2016).

4.3.11 Drug Delivery for Wound Closure

An ideal regenerative or responsive biomaterial recruits precursor cells to form new viable tissue in vivo and stimulates wound healing (Mathur, 2009). Developing biomaterials with the intrinsic ability to autonomously repair the mechanical and chemical damage would be particularly important for implants that replace tissues that are also capable of self-repair. The porcine dermis is a biomaterial dressing available in the market with the brand name of EZ-DERM. Synthetic biomaterials offer many advantages over natural biomaterials as they can be synthesized and modified in a controlled manner according to the specific requirements needed to produce constant and homogeneous physical and chemical properties as well as stability (Zhong et al., 2010).

PUs are copolymers containing urethane groups. They are formed by conjugation of diol and diisocyanate groups. An example of nontoxic PUs used for the treatment of burns and wounds is Pellethane 2363-80A, which can accelerate epithelialization (Wright et al., 1998).

Teflon is synthesized from tetrafluoroethylene at high temperature and pressure. Teflon is noncarcinogenic, insoluble in polar and nonpolar solvents, and easily sterilized. Furthermore, its shape is easily modified using low pressure, resulting in a comfortable fit to the injured area (Raphael et al., 1999).

Silicone is nontoxic, nonallergenic, and highly biocompatible. Silicone is resistant to biodegradation and can be used in the fabrication of implant elastomers used in soft tissue repair and in the production of hypodermic needles and syringes. Moreover, it is often used as a wound support material in severe burns and wounds, for scar treatment, and as a nonadherent interface material in many dressings (Losi et al., 2004).

The emollient, demulcent, astringent, antimicrobial, antiinflammatory, and antioxidant properties of natural products may be beneficial for the wound healing progression. Natural polymers such as CS, collagen, elastin, and fibrinogen are biocompatible substrates that are similar to macromolecules recognized by the human body (Mogoşanu et al., 2012).

In the category of scaffolds, Eweida and Marei (2015) reviewed the online published literature for the studies that performed ECM revitalization believing that, in chronic and difficult-to-heal wounds, revitalizing the ECM scaffolds would be beneficial to overcome the defective host tissue interaction. Akagi et al. (2015) evaluated the utility of a HA and poly-DL-lactide scaffold compared with β-TCP, at a loading site as a new bioresorbable scaffold.

4.3.12 Localized Drug Targeting (Cancer and Immunotherapy)

Biomaterial properties, such as size, shape, charge, surface chemistry, morphology, and physiochemical properties can be easily tailored to tackle specific challenges in cancer and immune therapy. Thus, biomaterials enable useful, innovative approaches for improving the current technologies available for studying, detecting, and treating cancer. Biomaterials are also currently used in the detection and diagnosis of cancer; such diagnostics include the development of biomaterials-based immunoassays, which detect biomarkers and biomaterials to facilitate the delivery of contrast agents for imaging.

A wide spectrum of biomaterials is being applied for the targeted and sustained delivery of therapeutic agents. Due to the difficulties and high costs of developing new therapeutics and detection and diagnosis methods, the focus should be placed on applying biomaterials that optimize currently available approaches. Smart hydrogel-based carriers and drug reservoirs could overcome the weaknesses of conventional therapy methods and provide targeted, localized, and adjusted delivery systems for genes, drugs, and radioisotopes.

Hydrogels provide correlative and/or complementary combined therapies, such as chemotherapy and hyperthermia, chemotherapy and radiotherapy, and chemotherapy and gene therapy. Tumor imaging via a long-term modified nanomagnet-loaded hydrogel has demonstrated a reliable biodegradable imaging platform for tumor imaging and anticancer drug screening (Sinha et al., 2006).

Polyanhydride poly[bis(*p*-carboxy-phenoxy)propane-sebacic acid[copolymer [p(CPP:SA)] is a material that has been used widely for the delivery of cancer drugs in a form of an implantable device. The biocompatibility of this material has been widely tested and found to be nontoxic (Walter et al., 1994).

Xie et al. developed electrospun paclitaxel-loaded PLGA ultrafine-fiber implants for the treatment of brain gliomas. The drug and PLGA were dissolved in methylene chloride with or without the different amount of the organic salt tetrabutylammonium tetraphenylborate and electrospun to produce different meshes with a fiber diameter of around 30 nm to 10 μm (Xie and Wang, 2006).

Biomaterial-based implantable devices, the local delivery of cancer therapeutic agents, which can overcome obstacles faced by systemic delivery, may result in a more successful outcome. As a consequence, advancements in treatment by the application of local delivery devices may allow the repurposing of drugs that may have previously failed with a systemic treatment.

4.4 ADVANCEMENTS IN BIOMATERIAL APPLICATIONS

The success of biomaterial-based drug delivery systems is based on the integration of the smart components into intelligent drug delivery systems. The controlled release systems can be rate programmed (diffusion/dissolution based conventional systems), activation modulated (trigger mediated), or feedback regulated (self-regulated) (Alvarez-Lorenzo and Concheiro, 2014).

4.4.1 Smart Components: Stimuli-Responsive Biomaterials

Smart components are stimuli-responsive biomaterials that exhibit reversible molecular transitions/fundamental changes in biomaterial characteristics on exposure to various triggers (temperature, magnetic field, pH, etc.) ultimately altering the drug release abilities as depicted in Fig. 4.3 (Alvarez-Lorenzo and Concheiro, 2014; Hoffman, 2013).

Smart biomaterials offer various advantages over conventional drug release system (Potter, 2018). The most important being more precise drug control, increased drug uptake and targeting, less toxicity, convenient hydrophobic drug delivery (Hou et al., 2017), increased efficiency and patient compliance (Ashammakhi and Kaarela, 2017). The key concerns of this on/off release system are that the "on" trigger is possible at the site of use/action, smart biomaterials are prompt to respond to the trigger (at optimum intensities), and the trigger mediated transitions are reversible (in most cases).

Certain surface modification techniques are employed to render the biomaterial with stimuli responsiveness like self-assembled monolayers, thin polymeric network film, grafting, and layer by layer (Costa et al. 2013). Stimuli-responsive biomaterials can be engineered in various forms by virtue of noncovalent interactions (with or without trigger mediated) (Ye et al., 2015): (1) self-assembling structure/peptides (Guven et al., 2015), (2) host–guest complex systems, for example, recently fabricated cucurbit(*n*)until-type molecular containers (Isaacs, 2014), cryptand recognition based mechanically interlocked host–organic guest systems (Zhang et al., 2014a); (3) high affinity hydrogen bonding based supramolecules; and (4) metal ion–ligand coordination systems (Du et al., 2015; Bryksin et al., 2014; Webber, 2016).

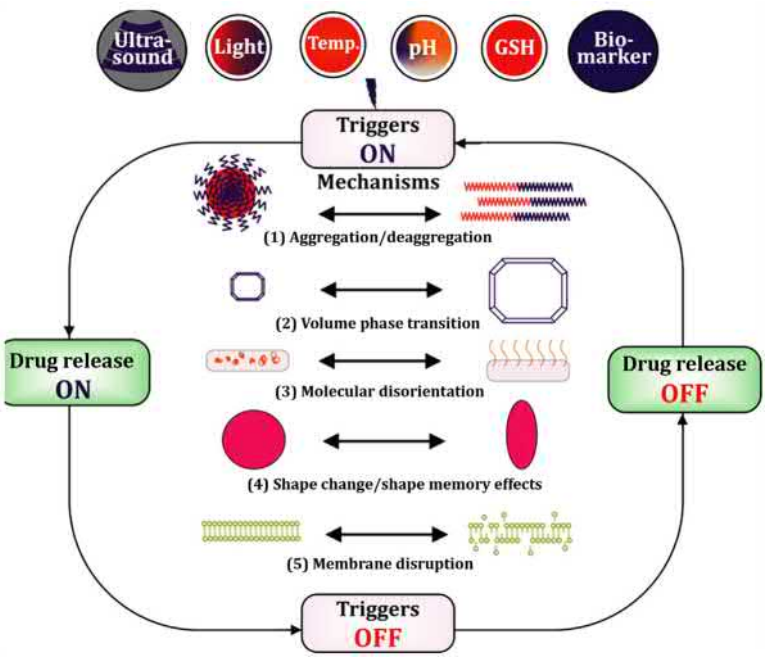

FIGURE 4.3 Schematic representation of molecular transitions in biomaterials occurring in response to various triggers/stimuli.

4.4.1.1 *Different Stimuli-Responsive Biomaterials*

4.4.1.1.1 PHYSICAL STIMULI-RESPONSIVE BIOMATERIALS

4.4.1.1.1.1 THERMORESPONSIVE BIOMATERIALS Temperature change leads to reversible changes in the polymer chains like altered intramolecular H-bonding, change in solubility, and conformational changes leading to shrinking or swelling mechanisms, thus exploiting it as a trigger to control drug release rates. Thermoresponsive polymers are either (1) LCST type, for example, PNIPAAM (LCST RANGE 30°C−35°C) (Hoffman, 2013), poly(2-oxazoline)s (POxs), etc., that undergo phase separation (soluble coils to insoluble globule state) above LCST; (2) upper critical solution temperature type, for example, polyacrylamide/polyacrylic acid (PAAc) interpenetrating networks (UCST—25°C) that undergo phase separation upon cooling; or (3) thermoinduced shape-memory polymers that undergo crystal to amorphous mobility at temperature above glass transition (Tg) or melting range (Tm) causing deformation and shape change that reverts to original upon cooling (Kim and Matsunaga, 2017).

Lendlein and coworkers developed PCL and PEG (shape-memory polymers) based thermoresponsive particles (spherical to ellipsoidal) into an implantable device that showed the prolonged release of enoxacin, nitrofurantoin in rats (Wischke et al., 2010).

Liu et al. (2017b) prepared thermoresponsive copolymer alginate-*g*-poly(*n*-isopropyl acrylamide) based injectable hydrogel that released doxorubicin-encapsulated micelles at a sustained rate and increased drug uptake in resistant AT3B-1 cells. Brush hydrogels were prepared by Lue et al. using thermoresponsive copolymer a NIPAAm and acrylic acid (AAc) grafted on polycarbonate porous surface. Above LCST, the increased release was observed through pores due to shrunk copolymer brush (Lue et al., 2011). Temperature sensitive liposomes have been widely investigated as nanocarriers for drug delivery. ''ThermoDox'' thermosensitive liposome (TSL) system is FDA approved (for phase III) for hepatocellular carcinoma and (for phase II) for breast cancer. Local temperature increase can be achieved by radiofrequency thermal ablation, microwave hyperthermia, and high intensity focused ultrasound (US) for activating TSL. Chen et al. (2012b) fabricated doxorubicin loaded TSL containing ammonium carbonate that released carbon dioxide upon decomposition when temperature increases to 40°C leading to liposomal membrane disruption and thus drug release.

In another research by Al-Ahmady et al. (2012), leucine peptide zipper was inserted into liposomes that opened when the temperature was increased to 43°C resulting in drug release. Ta et al. (2014) developed PNIPAAmco-PAAc based TSL for doxorubicin release in solid tumors. Further, Kono et al.'s (2010) reported ultra−temperature-sensitive liposomes prepared by poly [2-(2-ethoxy) methoxyethyl vinyl ether showing higher temperature sensitivity and thus better tumor selectivity and therapeutic efficacy.

"Smart nano bombs" were fabricated by Lee et al. (2009) comprising of superexpandable Pluronic/PEI nanogel (with/without drug) that showed tremendous swelling from 150 nm at 37°C to 1.4 mm (800 fold), when temperature was decreased to 20°C (cryotherapy), leading to increased hydrostatic pressure within the cells, intracellular component breakdown, and ultimately tumor necrotic cell death. Stimuli-responsive theragrippers for gastrointestinal cancer were prepared by Malachowski et al. containing the alternating rigid panels of bi poly(propylene fumarate) and flexible hinges of poly(*N*-isopropylacrylamide-*co*-AAc) that reversibly open and close (in opposite direction)

at around body temperature. These displayed excellent tissue gripping capabilities, resisting to be carried away by the GIT flow and chemomechanically controlled release of doxorubicin overcoming the basic limitation of the patch, that is, initial application force and contact time (Malachowski et al., 2014).

4.4.1.1.1.2 MAGNETIC-RESPONSIVE BIOMATERIALS Magnetically active biomaterials are mainly composed of a magnetic core of magnetite (Fe_3O_4) or maghemite (Fe_2O_3) nanoparticles having better colloidal stability, dispersion, and less/no dipolar attraction on applying oscillating or alternating magnetic fields than ferromagnetic particles (Chan et al., 2013; Mura et al., 2013). The magnetic responses of therapeutic interests are either magnetic guidance under a permanent magnetic field that can be explored for magnetic imaging and monitoring and magnetic heating mostly under the alternating magnetic field, owing to Brownian motion and Neel relaxation based rotational motion of the particles (Karimi et al., 2016). This is mainly explored for targeted hyperthermia for selective heat damage to tumor cells or controlling drug release by virtue of conformational changes due to temperature increase (Chan et al., 2013).

Hydrophobic drug-loaded Pluronic-F127 micelles containing superparamagnetic iron oxide (SPIO) nanoparticles and hydrophobic drug were encapsulated in ferrogels and showed drug release by micellar squeezing due to iron oxide nanoparticles approaching each other (Chan et al., 2013). Louguet et al. reported the increased release of doxorubicin by magnetic heating occurring in silica-coated MagNPs functionalized with thermosensitive block copolymer brushes under AC-magnetic field. Nanotherms are European Union Regulatory approved magnetic nanostructures containing an iron oxide core with an aminosaline coating for glioblastoma (Liu et al., 2016). Effective suppression of tumor growth was observed by PEGylated Mn−Zn ferrite nanocrystals under alternating magnetic field (Alvarez-Lorenzo and Concheiro, 2014).

4.4.1.1.1.3 ELECTRICAL-RESPONSIVE BIOMATERIALS Electroactive/conducting polymers (EAPs) like polypyrrole, polyaniline, polyazulene, etc., undergo varied activation mechanisms when the external electric field is applied, that is, (1) drug diffusion initiated by charged ions, (2) conformational changes due to redox switching of EAPs, (3) electroerosion, and (4) electroporation, that is, improving drug permeability by increasing cell membrane porosity (Pillay et al., 2014). These can be used to achieve sustained, pulsed, or programmed drug release. In a study done by Ying et al., increased release of antiepileptic drug phenytoin sodium was observed in electroresponsive hydrogel nanoparticles because of an increased degree of ionization under external electric field brought by polyelectrolyte poly(sodium 4-vinylbenzene sulfonate). Dexamethasone loaded nanocomposite film was formed by GO-conducting polymer [poly(pyrrole) (PPy)] and showed linear drug release with significant temporal control. The major limitations being restricted drug binding due to charge and molecular weight and the fatigue of conductive polymers with repeated electrical stimulation cycles causing irreversible oxidation, decreased conductivity, and functional and structural problems (Ying et al., 2014).

4.4.1.1.1.4 LIGHT-RESPONSIVE BIOMATERIALS Ultraviolet (10−400 nm), visible, or near-infrared (NIR) regions (650−900 nm) of the light spectrum are used as triggers for

inducing and controlling drug release (Karimi et al., 2016). Although UV is less frequently used because of potential tissue damage, photodestruction of actives, and inability to penetrate deeply. NIR, on the contrary, penetrates deeply about 10 cm into the body due to lower tissue absorption and scattering as well as causes less cell damage than visible light triggered (Mura et al., 2013).

Drug release is achieved by two sets of mechanisms: photochemical changes and photothermal changes. Photochemical changes include the following:

1. Dynamic photooxidation, for example, by octabutoxy phthalocyanine, etc., and production of reactive oxygen species causing membrane disruptions and prodrug activation.
2. Photoisomerization, for example, spiropyran−merocyanine isomerization, *trans−cis* isomerization of azobenzene. Nanoparticles for curcumin release for heart failure were designed on the basis of pore opening and closing occurring due to α-CyD azobenzene conjugation upon irradiation with 365 nm UV light.
3. Photoinduced rearrangements like diazocarbonyl to ketene intermediate followed by a (2 + 2) cycloaddition (Wolf rearrangement) (Karimi et al., 2016).
4. Photocross-linking.
5. Bond photolysis, for example, nitrobenzyl and coumarin derivatives.
6. Photopolymerization.
7. Photochemical hydrophobicity switch (Ruskowitz and DeForest, 2018). Photothermal changes are generated by local heating due to the absorption of incident photons onto the conductive or photothermal biomaterials. This induces phase transition and drug release.

Moreover, photoabsorption by gold nanostructures produces a heated electron gas, increases temperature followed by heat exchange with nanostructure lattice and surrounding cells (Zangabad et al., 2018; Timko and Kohane, 2014). These are frequently being used for local hyperthermia-based cancer treatment or tumor cell death. Apart from this two-photon excitation (TPE), or upconversion nanoparticles (UCNPs), have been proven to be promising platforms for cancer treatment (Yang et al., 2016).

In a recent study, NIR absorbing gold−silica nanoshells were coated by thermally responsive poly(*N*-isopropylacrylamide-*co*-acrylamide) hydrogel that showed swelling governed drug release at elevated temperature and markedly increased doxorubicin uptake (three times) by colon carcinoma cells upon NIR exposure (Strong and West, 2015).

Liu et al. (2015) synthesized doxorubicin loaded folate tagged nanoscaled drug delivery system, comprising of a gold nanorod-like core and mesoporous silica shell (GNR@MSNP) that showed target cell (KB cells) killing and drug release by localized photothermal ablation upon NIR irradiation. Injectable hollow microspheres were prepared by PLGA shell and a core made up of vancomycin and polypyrrole nanoparticles for treating subcutaneous abscesses by a dual mechanism of photothermally induced hyperthermia and antibiotic therapy for bacterial cytotoxicity when activated by NIR light (Chiang et al., 2015).

Kost et al. fabricated NIR activated implantable reservoir coated by nanocomposite membrane whose permeability varies upon NIR irradiation. Sustained release for 3 hours followed by reproducible pulsatile drug release was observed, for example, insulin

implant in the diabetic rat (Kost et al., 1987). Multifunctional mitochondria targeting, chemophotothermal mesoporous silica-encapsulated gold nanorods were prepared with a cytochrome *c*-specific binding aptamer attachment showing efficient mitochondrial accumulation in cancer cells upon NIR irradiation (Ju et al., 2014).

Wang et al. (2016b) synthesized nanobombs comprising a lipid and multiple polymers for cytosolic delivery of microRNAs breaking all intracellular and extracellular barriers and destroying tumor cells. Qiu et al. developed black phosphorus based hydrogel nanostructure for cancer therapy and made up of a low−melting point agarose and PEGylated black phosphorous nanostructures. Drug-loaded hydrogel underwent controllable softening or melting due to heat generated by photosensitizer black phosphorus upon NIR irradiation (Qiu et al., 2018).

You et al. prepared NIR and pH dual responsive cisplatin loaded nanocomposites comprising of core-crosslinked PEG with poly(ε-caprolactone) (PEG5k-PCL10k) block copolymer and lecithin as biodegradable polymer doped with polyaniline. Herceptin was tagged to target cisplatin to HER2 receptors in breast cancer cells. The system showed very efficient drug uptake and release under acidic conditions when exposed to a NIR laser (808 nm, 1.54 W) for 5 minutes (You et al., 2017).

Shi et al. developed multifunctional porous Zn1.1Ga1.8Ge0.1O4: Cr^{3+}, Eu^{3+} @SiO_2 nanoprobes made up of mesoporous silica nanospheres. The system showed excellent doxorubicin delivery upon a brighter NIR emission (696 nm), high tumor targeting due to folic acid conjugation and long-persistence luminescence for 15 days (to be used for tumor diagnosis and monitoring) (Shi et al., 2015a).

4.4.1.1.1.5 MECHANICAL-RESPONSIVE BIOMATERIALS Only a few types of research have been reported for mechanoresponsive biomaterials for drug delivery application. These materials undergo aggregation or disaggregation or molecular structure or phase volume changes upon application of pressure or high shear stress leading to drug release. For example, CyD alginate inclusion complexes showed destabilization by mechanical compression leading to the controlled release of loaded ondansetron. Lenticular liposomes became unstable and ruptured in the elevated shear stress of atherosclerosis. Microscale aggregates of nanoparticles broke up into nanocomponents under local high shear stress for treatment of thrombosis (Karimi et al., 2016).

4.4.1.1.1.6 ULTRASOUND-RESPONSIVE BIOMATERIALS US waves are acoustic waves with frequencies higher than 20 kHz can act as a trigger for drug therapeutics and imaging applications due to its good energy focus and significant effective depth. US waves (low/high intensity) when passing through the tissues cause mechanical or thermal stimulation. Mechanical stimulation includes cavitation, that is, oscillations accompanied by expansion and contraction, acoustic streaming, and sonoporation. Microbubble-based drug delivery comprises of the gas-filled core that can contain air, nitrogen, or perfluorocarbons and is surrounded by a layer/layers of lipids, proteins, or polymers (Zangabad et al., 2018).

In context, Rapoport et al. developed a microbubble system with a core made up of 1% PFP (perfluoropentane) and coated by PEG−PLLA poly(ethylene oxide)-*co*-poly(L-lactide) that showed paclitaxel delivery to A2780 ovarian carcinoma when cells exposed to unfocused 1 MHz US for 1 minute. Thermal stimulation on the other side may cause local

tissue heating by applying focused US beam. This may be explored for cancer cell destruction, for example, paclitaxel-loaded nanoparticles were prepared for pancreatic cancer upon activation with focused US. Spivak et al. (2013) reported increased uptake of gold nanoparticles containing calcium sensitizer (Simdax) for improving the contractile strength of the myocardium in a rat model of heart failure.

4.4.1.1.2 CHEMICAL STIMULI-RESPONSIVE BIOMATERIALS

4.4.1.1.2.1 PH-RESPONSIVE BIOMATERIALS The pH-responsive polymers such as anionic type, for example, PAAc, polyaspartic acid, etc., and cationic type, for example, poly(*b*-amino ester), poly(L-histidine) are either weakly acidic (carboxylic acid) or basic (ammonia) groups, that release protons or accept free protons respectively in response to the environmental pH (Chan et al., 2013). pH-responsive biomaterials (including pH sensitive lipids/peptides) undergo chemical changes in response to environmental pH change like protonation, charge reversal, and bond cleavage leading to conformational changes in the polymer chain resulting in swelling or collapse of the polymeric network facilitating the drug release process. For example, PAAc with p*K*a 4.25 releases protons at higher pH and gets ionized leading to polymeric chain swelling and ultimately drug release (Kanamala et al., 2016). It is evident that pH varies within the body lysosomes (4.5−5), Golgi apparatus (6.4), and cytosol (7.4) (Liu et al., 2016). Moreover, pH shows alteration with the healthy state or diseased state, for example, there is an acidic milieu in pathological conditions like bacterial infection, wound healing, and tumor cells (Mura et al., 2013).

The pH-responsive PLGA-*b*-polyhistidine-*b*-PEG triblock copolymer nanoparticle was prepared for systemic antibiotic therapy that showed charge switch at localized acidic sites of bacterial infections and increased nanoparticle uptake in bacteria. The tumor cells have more acidic environment than healthy cells because of an inadequate supply of O_2, causing lactic acid generation (glycolysis) by virtue of Warburg effect (Zangabad et al., 2018). This has motivated pH-responsive drug delivery for cancer therapy. Recently, Li et al. synthesized self-assembled nanosystems by integration of pillararene and UCNPs via the host−guest complexation showed efficient delivery of doxorubicin to human cervical cancer (HeLa) cells by nanosystems protonation and collapse under tumor acidic conditions (Li et al., 2018).

Acid-sensitive hydrazone-based nanosystems have also been explored for cancer therapies (e.g., for breast cancer targeting by Lale et al.). In a similar study, disulfiram encapsulated pH-sensitive polymeric micelles were prepared with poly(styrene-*co*-maleic anhydride) derivative, adipic dihydrazide and doxorubicin conjugated by hydrazone bond. The system was proved effective for multidrug resistance (MDR) cancer, with rapid release of disulfiram and hydrazone conjugated doxorubicin release by pH-dependent mechanisms (Karimi et al., 2016; Liu et al., 2016). Similarly, PMAA-Polysorbate 80 grafted starch (PMAA-PS80-*g*-St) nanoparticles showed pH-responsive delivery of doxorubicin due to reduced drug−polymer electrostatic interactions at pH = 6 and exhibited 20-fold increase in MDR cancer cell cytotoxicity. The pH-sensitive liposomes were made of 1,2-dipalmitoyl-sn-glycerol-3-phosphoethanolamine showing phase transition from lamellar to a fusogenic hexagonal at acidic pH for siRNA delivery. siRNA therapy is well known for the treatment of various gene mediated diseases (Maheshwari et al., 2017). Mesoporous

silica nanoparticles (MSNs) with pH-sensitive DNA end caps (molecular gated structures) were synthesized that showed molecular gate openings with pH change from 5 to 8 suggesting its potential for being controlled drug release carriers (Chan et al., 2013).

4.4.1.1.2.2 REDOX-RESPONSIVE BIOMATERIALS Redox-responsive drug delivery systems have been proved efficient for cancer and gene therapy. The major redox couple in human cells is GSH−glutathione disulfide that is governed by NADP + /NADPH and glutathione reductase. Others with redox potential for drug delivery are central thiol/disulfide redox couples, cysteine/cystine (CySH/CySSCy), Trx-1 and thioredoxin-2 (Trx-2). Reactive oxygen species like hydrogen peroxide, superoxide, or OH radicals also contribute to intra- and extracellular redox potential especially in correlation to pathological conditions like inflammation (oxidative environment), atherosclerosis, cancer, etc. (Karimi et al., 2016; Liu et al., 2016). GSH concentration varies intracellularly and extracellularly, in cell components including cytoplasm, mitochondria, nuclei (all have different redox environment), as well as healthy and diseased cells, for example, tumor cells have four times more GSH (Liu et al., 2016; Alvarez-Lorenzo and Concheiro, 2014).

The approaches for designing redox-responsive drug delivery system are through (1) developing micelles, mesoporous silica nanomaterials, liposomes, dendrimer−drug conjugates or nanogels with disulfide cross-linkages (reducible by GSH) or thiol-cleavable bonds or GSH-responsive crosslinking agents; or (2) redox micelle oxidation can rupture micelles into hydrophilic monomers and release the hydrophobic drug, for example, Wang et al. prepared redox-sensitive shell-detachable micelles for GSH responsive improved release of doxorubicin in MDR A549 cancer cells. GSH responsive MSN was prepared with immobilized RGD (arginine-glycine-aspartic acid) containing peptide conjugated through disulfide bond onto MSN and showing doxorubicin release GSH trigger disulfide bond cleavage. Camptothecin (hydrophobic drug) loaded crosslinked micelles were prepared to show drug release by redox-responsive disulfide bond cleavage (Karimi et al., 2016).

4.4.1.1.3 BIOLOGICAL STIMULI-RESPONSIVE BIOMATERIALS

4.4.1.1.3.1 DIFFERENT BIOMOLECULAR-RESPONSIVE BIOMATERIALS The variation in the concentration of biomolecules like glucose, adenosine triphosphate, deoxyribose nucleic acid, and reactive oxygen species in a healthy state and diseased (pathological) state of the living system creates the basis for developing biomolecule responsive smart drug delivery systems by virtue of molecular recognition based analyte responsiveness (Culver et al., 2017).

Glucose-responsive insulin delivery systems being a classic example have been designed with different approaches like glucose oxidase mediated conversion of glucose to gluconic acid, using glucose-binding proteins such as high affinity concanavalin A lectin contained in nanostructures, or self-regulated glucose-responsive system employing phenylboronic acid utilizing its glucose-binding tendency in its charged form (hydrophilic), leading to swelling and insulin release. The latter requires far higher glucose levels than normal to show this behavior.

ROS (like hydroxyl radicals (HO^-) and hydrogen peroxide (H_2O_2) responsive β-CD-based smart DDSs371 were developed based on the ROS-mediated solubility switch or degradation by integrating oxidation-sensitive boronic ester units into the structure. 2D

DNA-graphene hybrid nanocarrier was generated by conjugating ATP/ATP aptamer binding complex for site-specific doxorubicin controlled release in an ATP rich environment. DNA aptamer conjugated MSN were prepared for targeting the drug to cancer cells via aptamer-based recognition and vitamin H responsive antitumor drug release as vitamin H concentration is found higher in cancer cells than in normal cells (Alvarez-Lorenzo and Concheiro, 2014). Biomolecule sensitive tissue-type plasminogen activator delivery has been reported to treat localized thrombolysis (Karimi et al., 2016).

4.4.1.1.3.2 ENZYME-RESPONSIVE BIOMATERIALS Enzyme-responsive biomaterials undergo physicochemical changes upon enzyme catalysis. Enzymes in the living systems are not equally expressed in all the tissues, rather some enzymes get overexpressed in certain specific tissues and their levels may vary further in pathological conditions. This makes enzyme-responsive biomaterials efficient platforms for smart drug delivery because of their impeccable biorecognition capabilities, catalytic properties, and high selectivity (Mura et al., 2013).

Proteases are found overexpressed in cancer (e.g., matrix metalloprotease-2) and inflammation (Kessenbrock et al., 2015). Cheah et al. (2017) used this concept and designed controlled-release nanoparticles with a specific peptide sequence as a linker to attach DOX and aminoglutethimide (AGM) to *N*-(2-hydroxypropyl)-methacrylamide HPMA. Thamphiwatana et al. structured liposomes with lipid components responsive to phospholipase A2 (PLA2) (an enzyme secreted by *Helicobacter pylori*, the causative organism of peptic ulcers and other gastric abnormalities) (Thamphiwatana et al., 2014). PLA2 caused liposomal membrane disruption and subsequent drug release. *b*-D-Galactosidase/glycosidase responsive controlled and increased doxorubicin delivery to HeLa and LLC-PK1 cells was observed in hybrid MSN (Islam et al., 2017).

Some other such systems are elastase responsive systems for pulmonary diseases, oxidoreductases responsive systems in Alzheimer's and cancer, and azoreductase (an enzyme released by colonic microflora) responsive systems for targeted colonic delivery, for example, azobenzene and amphiphilic diblock copolymer formed by covalent coupling. Glucose-responsive hydrogels of polymethacrylic acid-based nanocarriers containing glucose oxidase were prepared where glucose oxidase converted glucose to gluconolactone in presence of optimum glucose amounts. This led to an H_2O_2 generation that oxidized sulfur-containing bonds and destabilized the nanocarriers for insulin release (Karimi et al., 2016).

4.4.1.2 Multiple Stimuli-Responsive Biomaterial Systems

Although single factor (like pH, temp, biomolecular, etc.) stimuli responsiveness can ensure drug delivery to the target (disease) site, these individual factors are not exclusively located to these sites leading to suboptimal selectivity; for example, extensive matrix metalloproteinase (MMP) activity has been used as cancer cells marker but it also prevails in healthy joints (Badeau et al., 2018). So, to increase the site specificity and versatility multiple responsive drug delivery systems can be designed keeping in consideration multiple cues and inherent constraints in utilizing various triggers (Perez et al., 2013).

Badeau et al. (2018) drafted a modular chemical framework for biocomputation of multiple biologically presented inputs simultaneously that are multiple triggers/environment cues, followed by a user-programmed Boolean logic-based algorithm (logic gates)

considering molecular framework and stimuli labile moieties crosslinking, and provided a functional output in terms of material degradation and therapeutic delivery. This makes the challenging part of evaluating the complex multiple responses simultaneously more workable.

4.4.1.2.1 Dual Stimuli-Responsive Biomaterial Systems

Recent developments for dual/multiple stimuli-responsive biomaterial systems are summarized below. A pH/redox dual sensitive doxorubicin-loaded PEGylated nanosized polymeric lipid vesicle based system was developed with increased doxorubicin release at pH 5 as well as with 10 mM of GSH for antitumor activity. A pH/temperature dual responsive polymeric system was developed by Shim et al. containing both pH-responsive component and poly(ε-caprolactone-*co*-lactide) (PCLA) in a triblock with PEG, PCLA−PEG−PCLA, as the thermosensitive moiety exhibiting sol to gel transitions from pH 8 to pH 7.4 and 37°C (Chan et al., 2013).

pH/enzyme dual stimuli-responsive liposomes were prepared by Zhang et al. for pH and esterase responsive delivery of camptothecin and siRNA (Zangabad et al., 2018). A pH/magnetic-responsive polymeric systems have been reported for improved drug release and monitoring the site and extent of ischemia.

4.4.1.2.2 Tri Stimuli-Responsive Biomaterial Systems

A unique microbubble-based US/magnetic/glucose tristimuli-responsive system was designed containing L-arginine and embedded SPIO Fe_3O_4 nanoparticles and glucose oxidase in the shell. After the system had reached the target cell, H_2O_2 was generated in presence of glucose by glucose oxidase. On applying a magnetic field, the porosity of polymer shell increased, causing exchange of arginine solution inside and H_2O_2 solution outside the microcontainers, leading to NO gas generation on applying US/acoustic field and further rupture of the polymeric shell by NO gas bubbles (Liu et al., 2016).

Jing et al. developed doxorubicin loaded PLA polymeric magnetic coated nanoparticle system (magnetic/temperature/pH tri stimuli-responsive) tagged with Mn−porphyrin for targeting to HeLa cells and imaging that showed higher cytotoxicity against prostate tumor cells at 40°C and pH of 6.4. Similarly, a triresponsive (magnetic/temperature/pH) microcarrier was developed by Liu et al. using polyvinyl alcohol conjugated with PAA. The high daunorubicin loading (98%) was reported along with good drug release under acidic conditions and due to magnetic hyperthermia (Jing et al., 2013).

Shi et al. reported the fabrication of pH, NIR light, and temperature tristimuli-responsive self-assembled hydrogel system composed of GO nanosheets crosslinked in a Pluronic solution. Photothermal gelation was observed upon NIR irradiation (Shi et al., 2015b).

4.4.2 Intelligent Drug Delivery Systems

Molecular imprinting. DNA origami, microfluidics, and many such advancements have led to the development of specialized biomaterial-based drug delivery systems at the nano- and microlevels.

4.4.2.1 *Affinity-Based Drug Delivery Systems*

These systems are based on the affinity of the device material for the target drug owing to the noncovalent interactions between them leading to alterable drug loading by tailoring the affinity (Alvarez-Lorenzo et al., 2013). Major such systems for controlled drug delivery applications include molecular imprinting based, heparin-based (heparin-drug binding affinity controls the drug release), and CyD-based (improving solubility mainly for small hydrophobic drugs) (Mohtaram et al., 2013).

4.4.2.1.1 RECOGNITION MOLECULAR SYSTEMS

Polymeric systems are engineered to be able to recognize the specific molecule with high affinity, that is, selectively binding to a specific guest molecule out of several competing species. These find applications in various areas of assays, catalysis, mass transport, separations, and drug delivery applications by target disease cell recognition, immune response reduction, and monitoring levels of specific compounds (Arifuzzaman and Zhao, 2016; Battista et al., 2018). Molecular imprinting is one of such techniques to develop recognition ability by creating guest complementary binding cavities within the polymeric structure so that the need for custom design for each individual guest is bypassed (Dhanashree et al., 2016).

Functionalized monomers, that is, monomers with target receptor mimicking complexing site and the template molecules (that may/may not be a drug) are copolymerized together using crosslinkers and/or initiators if necessary. This is followed by removing the template molecules by washing or bond cleavage leading to the development of chemically stereospecific sites (binding cavities/nano/microvacuoles) that are complementary to the template molecules. When the template molecule is a drug, the washing out process can be shortened. In the cases where the reaction achieves completion without any monomer release from the structure, then the washing out and drug reloading steps can be avoided (Alvarez-Lorenzo et al., 2013; Chen et al., 2015b; Suedee, 2013) (Fig. 4.4).

Recently, molecularly imprinted nanoparticles (MINPs) containing imprinted surfactant micelles having hydrophilic exterior and hydrophobic core with hydrogen bonding governed molecular recognition were developed for various nonsteroidal antiinflammatory drugs (Arifuzzaman and Zhao, 2016). Awino et al. prepared MINPs containing imprinted micelles with high binding affinity using Naproxen or Indomethacin as the template molecules. He termed the imprinted cavities as "synthetic antibodies" due to high specificity and suggested them to be better than the lengthy and massive process to generate natural antibodies for achieving recognition (Awino and Zhao, 2015).

The key features of molecular imprinting based drug delivery systems include recognition based improved drug loading and prolonged release because of "Tarzan Swing" mechanism (drug moving from one site to another) (Alvarez-Lorenzo et al., 2013), for example, the preparation of recognition polymeric hydrogel-based soft biomimetic contact lenses containing ketotifen fumarate and/or diclofenac sodium. They exhibited a remarkable increase in drug loading, sustained release, reduced ocular irritation/side effects, and increased bioavailability (Ali and Byrne, 2013).

As for recognition based rupture/drug delivery, when polymeric structures are dried after template removal, nanovacuoles/cavities undergo changes in physical characteristics

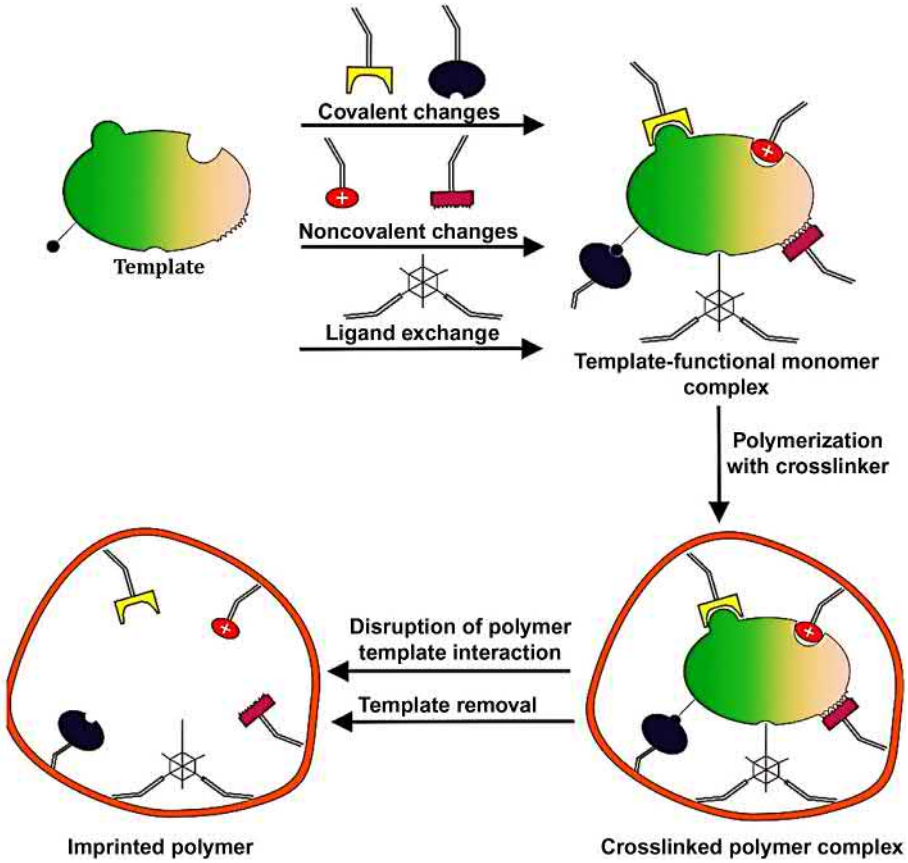

FIGURE 4.4 Schematic diagram showing the process of molecular imprinting.

(notably decreased size). Reintroduction of the template to the system generates mechanical stress at the template binding stereospecific site leading to rupturing and drug release, for example, epinephrine imprinted recognition hydrogel-based multilayered films have recently been reported containing fine particles encapsulating bactericides, essential oils and other OTC drugs for local skin treatment. The drug release from the polymeric film was sweat triggered, that is, by actives produced by human sweating (epinephrine). Peppas et al. (2014) also prepared molecular imprinted recognition polymer based multicoated layered tablets.

Different isomers or enantiomers of many chiral therapeutic compounds, for example, chlorpheniramine, morphine, promethazine, etc., are known to have different binding affinities to respective chiral receptors in vivo and thus exhibit varied potencies, for example, (*S*)-isomer of warfarin is more potent than (*R*)-warfarin as an anticoagulant. Molecularly imprinted polymers (MIPs) have been proved useful for chiral separation of enantiomeric therapeutic compounds owing to their predetermined selectivity, hence facilitating the release of the desirable enantiomer (Suedee, 2013). Suksuwan et al. developed

poloxamer-based composite nanoparticle comprising of thermoresponsive MIP. The system showed enantioselective delivery of *R*-thalidomide at a controlled rate to cancer cells because of protected chiral MIP and enantiomer recognition (Suksuwan et al., 2015).

In a study done by Tang et al., molecular crowding technique was employed in imprinted polymers by incorporating polystyrene as a macromolecular cosolute in prepolymerization mixture and aminoglutethimide as a model drug. Crowding assisted MIPs exhibited zero-order extended release for 18 hrs, increased imprinting surface area (10 times), increased imprinting factor (6 times), reduced diffusivity (two orders), and remarkably high relative bioavailability (266.3%) in comparison to MIP without crowding effect (Tang et al., 2015).

Various studies on stimuli-responsive MIPS have proved them to be excellent carriers to achieve programmed drug delivery. Tanaka et al. developed thermoresponsive imprinted polymeric gel containing PNIPAm as temperature sensitive moiety and methacrylamidopropyl trimethyl-ammonium chloride as functional monomers exhibiting high affinity towards target molecules pyranine-3 or pyranine-4 due to electrostatic interactions. Temperature-mediated reversible swelling/shrinking behavior causes variation in the affinity. Although affinity decreased in the swollen state it recovered upon shrinking.

Zhang et al. developed doxorubicin loaded pH-responsive molecularly imprinted hydrogel made up of HEMA and MBA displaying NMT 10% drug release at pH 7.2 (in contrast to 60% drug release at pH 5.0) ensuring the sustained delivery. Certain biomolecule responsive MIPs have also been developed. Glycoprotein imprinted gel conjugated with ligands for tumor marker glycoprotein (lectin and antibody molecules) showed specific recognition abilities for saccharide and peptide chains in α-fetoprotein AFP (target tumor marker glycoprotein) (Zhang et al., 2014c).

Configurational biomimetic imprinting polymers have been engineered to render the drug delivery systems more biocompatible and elicit reduced immune response upon contact. Biomaterials (natural/synthetic) may initiate receptor-mediated cellular interactions like immunogenicity or signaling activation upon cellular adhesion (Imanishi, 2018). The techniques used for downstreaming these interactions and signaling as well as generating the biomimetic surfaces are biomaterial functionalization with ECM macromolecules or synthetic binding motifs, nanopatterning of biomaterials so as to duplicate ECM structures, and using "natural like" biomaterials (Rahmany and Van Dyke, 2013).

Biomimetic nanofibers have been developed with their alignment in replication to the ECM for the specific tissue, for example, presence of interwoven collagen fibers in the cardiac ventricular myocardium, use of spiral-structured nanofibers for bone defect reconstructions. Because alignment of nanofibers can guide cell growth and extension, 3D biomimetic gelatin−sugar hydrogel-based scaffolds were formed with good thermal and mechanical properties for in vitro organ growth and related biomimetic applications (Masutani et al., 2016; Li et al., 2014a; He et al., 2014).

4.4.2.2 Reservoir-Based Drug Delivery Systems

Reservoir-based delivery systems are porous structures composed of the polymer matrix in which the drug is dissolved or suspended. In general, drug release is governed by diffusion, degradation, and erosion. Microspheres, microsponges, nanoparticles, hydrogels, etc., are known for controlled and sustained drug application (Mohtaram et al., 2013; Garg and Goyal, 2014).

4.4.2.2.1 MICROFABRICATION

The design of microstructural units has undergone numerous innovations including the specialized microparticulate systems and fabrication of functionalized 3D structured microdevices. Collaborating mechanical, structural, and electronic features renders the drug delivery more controlled, effective, and safe through various routes.

Multicompartment microparticles have been prepared by electrohydrodynamic atomization for chemotherapeutic use. Microneedle patches composed of numerous micron-sized solid needles have been used for more patient compliant and painless transdermal drug delivery (Prausnitz, 2017), for example, lidocaine for local anesthesia, 5-aminolevulinic acid for skin impairment, zolmitriptan for migraine (Balmayor et al., 2011), and recently hafnium oxide (HfO_2) coated microneedles (Zhang et al., 2018b). Microchannel systems of varying lengths, widths, straightness, and numbers were fabricated for controlled and pH-responsive drug delivery of gemcitabine base and doxorubicin HCl (Yang et al., 2017). Microfluidic channels built into neural recording probes (rigid silicone or flexible parylene) enabled controlled localized neural delivery (Yue et al., 2013; Hardy et al., 2015).

Venuta et al. developed multistage vector platforms codelivering siRNA-containing 1,2-dioleoyl-in phosphatidylcholine liposomes and docetaxel-containing poly(lactic-*co*-glycolic acid) (PLGA)/PEG nanoparticles. These contain multiple components to be released at intended compartments that are microparticles at the vascular level, nanoparticles at tissue interstitium followed by drug component addressing respective biological barriers (Venuta et al., 2017). Antensteiner et al. (2017) fabricated conducting polymer microcups as neural devices for in vitro release of dexamethasone.

A microfabricated microporous, PEG-grafted polydimethylsiloxane membrane placed at a small distance to glucose-responsive insulin implant was reported to act as barrier to inflammatory cell migration, reducing inflammatory response thereby improving biocompatibility and to prevent leukocyte-mediated degradation of the implant for at least 30 days, thereby improving the functional duration of the implant and efficacy by threefold (Li et al., 2015; Zorlutuna et al., 2012). Hydrogel microfabrication based on 3D bioprinting, photolithography, micromolding, and microcontact printed structures composed of biodegradable, biocompatible polyelectrolytes were also recently fabricated for engineered drug delivery (Yanagawa et al., 2016; Wang et al., 2015; Gauvin et al., 2012).

4.4.2.2.2 NANOBIOMATERIALS

For many decades, various nanostructures like nanoparticles, nanomicelles, nanocapsules, ceramic nanostructures (e.g., mesoporous silica nanostructures) (Argyo et al., 2013), metallic nanostructures (e.g., gold and silver based), peptide-based, nucleic acid−based, carbon nanostructures, etc., formed by self-assembly due to driving forces like electrostatic interactions, $\pi-\pi$ staking, hydrogen bond, hydrophobic effect, etc., have been successfully used for systemic and more importantly targeted or localized drug delivery (Lu et al., 2016).

The nanomaterials can be surface modified to either ligand derived active targeting and/or to add stimuli responsiveness to the surface, for example, ferrogel made up of iron oxide nanoparticles containing Pluronic-F127 micelles showed drug release in response to the applied magnetic field (Mura et al., 2013). Nanohybrids, for example, incorporation of

nanoclay like structures to delay drug diffusion (Mishra et al., 2014) or nanocomposite gels, that is, incorporating nanostructures into polymeric gels, have showed sustained levels of drug release.

A thermosensitive hydrogel containing paclitaxel nanocrystals exhibited more localized retention capacity and longer retention time in murine 4T1 tumor cells than just nanocrystals (Lin et al., 2014). Nanoliposomes have a good tendency towards both hydrophilic and lipophilic drug and flexible surface modifications. Zong et al. (2016) prepared 5-fluorouracil loaded pH-sensitive polydopamine−coated liposomes for controlled release. Chen et al. (2012a) developed thermo/pH-sensitive liposomal gel as a more efficient delivery of arctigenin to treat vaginal candidiasis.

4.4.2.2.2.1 CARBON NANOTUBES CNTs (single or multiwalled) improved therapeutic efficacy in diseases such as cancer, tuberculosis, AIDS, etc. (Kuche et al., 2018). CNTs and carbon nanofibers offer numerous advantages like high surface area, improved cellular uptake, nonimmunogenicity, and low toxicity (Mehra and Palakurthi, 2016; Stout, 2015). Moreover, these can be produced in various different shapes, sizes (Sciortino et al., 2017), and have superior mechanical, thermoelectrical, structural, and optical properties (Dineshkumar et al., 2015; Eatemadi et al., 2014). Recently, Wang et al. (2017) developed TiO_2 nanotubes with an electrochemical anodizing technique for localized sustained delivery with improved biocompatibility. In the study by Qin et al., a thermal/pH sensitive nanogel containing doxorubicin loaded CS/PNIPAAm@SWCNTs (single-walled carbon nanotubes) showed repetitive, rapid release and increased cytotoxicity in HeLa cells upon irradiation under NIR light. Doxorubicin release was found faster at 40°C, pH 5.0 than 25°C, pH 7.4 (Qin et al., 2015) (Fig. 4.5).

In spite of various advantages, CNTs have limitations in their drug delivery applications like the presence of impurities (amorphous carbon or catalyst bore, requiring purification methods like oxidative acid treatment), hydrophobic nature, insolubility, and aggregation tendencies (Saito et al., 2014). Surface engineering or functionalization of CNTs can help overcome the solubility issues and minimize toxicities (Tan et al., 2014). Gliotoxin loaded functionalized SWCNTs conjugated with chitooligosaccharide and targeting molecules like folic acid exhibited significant cytotoxicity against human cervical cancer (HeLa) cells (Bhatnagar et al., 2014).

Conjugation of targeting ligand to CNTs improves the cellular uptake, for example, linking angiopep-2 to functionalized- multi-walled carbon nanotubes (f-MWCNTs) (improved brain delivery in porcine brain endothelial cells) (Kafa et al., 2016), linking RGD to SWCNTs (increased the tumor uptake and penetration) (Smith et al., 2014), linking Endoglin/CD105 antibody to magnetic SWCNTs (enhanced theranostics evaluated in murine breast cancer model), etc. (Al Faraj et al., 2015). Bioactive molecules are chemically conjugated to the surface of CNTs through cleavable bonds (hydrolytic/disulfide) to achieve the controlled drug release (e.g., paclitaxel attached to poly citric acid via cleavable ester bonds to form MWCNT conjugates) and to improve biocompatibility (e.g., PEGylation) (Mehra and Palakurthi, 2016).

4.4.2.2.2.2 NANOFIBROUS SCAFFOLDS Nanofibers, referring to fibers with <1000 nm diameter, have exclusive advantages like structural similarity to ECM, tunable porosity,

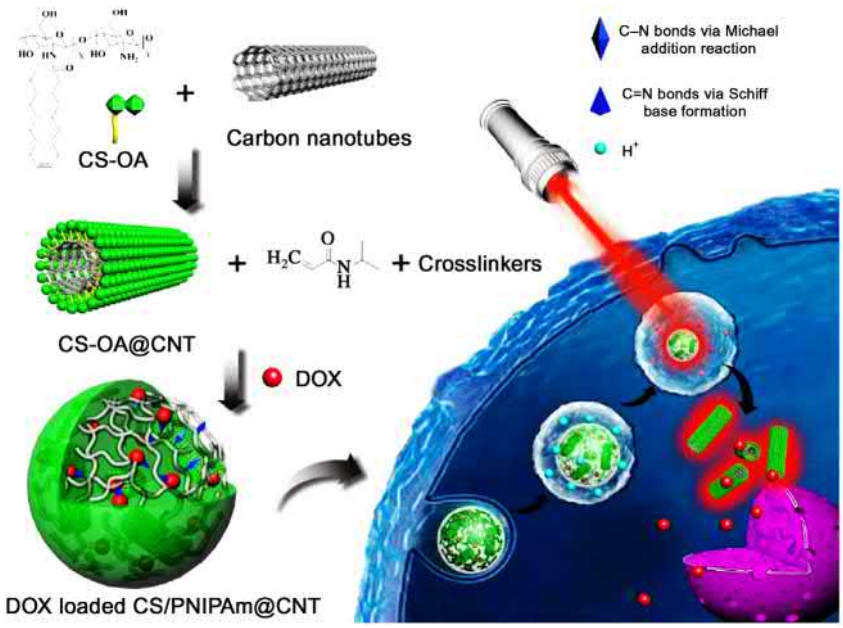

FIGURE 4.5 Schematic representation of NIR light induced drug release from DOX/CS/PNIPAAm@CNT nanoparticles. *CNT*, Carbon nanotube; *CS*, chitosan; *OA*, oleic acid; *NIR*, near-infrared. *Source: Adapted with permission from Qin, Y., Chen, J., Bi, Y., Xu, X., Zhou, H., Gao, J., et al. 2015. Near-infrared light remote-controlled intracellular anti-cancer drug delivery using thermo/pH sensitive nanovehicle. Acta Biomater. 17, 201–209.*

flexible surface functionalization, high-surface-area-to-volume ratio, ability to fabricate into various shapes, and decreased initial burst release (Morie et al., 2016; Son et al., 2014). They serve as unique platforms for drug delivery applications, for example, tacrolimus containing poly(L-lactide-*co*-glycolide) nanofibers for recurrent pulmonary venous obstruction and wound dressings/healing applications, for example, salicylic acid containing PEG-PLA nanofibers for helping wound healing by supporting cell attachment (Garg et al., 2015; Goins et al., 2017; Ahmed et al., 2014).

Nanofibers have shown enhanced drug loading and controlled drug release, for example, doxorubicin loaded polyethylene oxide/CS/graphene oxide (GO) electrospun nanofibrous scaffolds showed 98% drug loading owing to the porous structure and $\pi-\pi$ stacking interaction (Ardeshirzadeh et al., 2015). Further drug loading can be enhanced by using techniques like complexation, for example, electrospun poly(ϵ-caprolactone) (PCL) nanofibers containing inclusion complexes of naproxen and beta-CyD showed higher drug release due to solubility enhancement than those loaded with uncomplexed naproxen (Canbolat et al., 2014).

Numerous fabrication methods are well established to prepare nanofibers like fibermesh, fiber-bonding, mechanical drawing, template synthesis, self-assembly, melt-blown, phase separation, and electrospinning (He et al., 2014). Electrospinning, being the most simple, versatile, and cost-effective, is most frequently used among all these methods. In this method, a high electric field (10–20 kV) is applied to the polymer solution getting

ejected from the eluting nozzle, resulting into a fine fiber jet formation from the tip of the "Taylor cone," followed by solvent evaporation and solid polymeric fiber scaffolds/mesh accumulation at the ground collector. Further, patterning of nanofiber is achieved if needed (Li et al., 2014a; Eatemadi et al., 2016; Zamani et al., 2013). Fiber morphology is mainly governed by various parameters like polymer concentration, solution volatility, applied voltage, flow rate, etc. (Garg et al., 2015; Zamani et al., 2013).

Drug loading is mainly achieved by adsorption or dipping process (active/passive process). Various techniques are employed to incorporate drug into nanofibers depending on the form of drug−polymer before electrospinning like blending electrospinning (drug−polymer solution), coaxial process (drug at core and polymer at periphery), and emulsion electrospinning (dispersion of droplets containing drug in the polymer) (Pillay et al., 2013; Zhang et al., 2017b). Of which, the latter two generate core−shell nanofibrous structures that are observed to have prolonged drug release, for example, electrospun poly (ε-caprolactone diol)-based PU (PCL-Diol-*b*-PU) core/shell nanofibrous scaffolds prepared by coaxial electrospinning process showed sustained release of temozolomide against glioblastoma tumors 30 days and zero initial burst release (Irani et al., 2018). Moreover, drug-eluting fibers are reported to have extended drug release up to 90 days employing composite nanofibers prepared by dispersing drug-loaded nanoparticles into the polymer solution, for example, doxorubicin loaded PLA/PEG/MWCNT entrapped into electrospun nanofiber showed the extended release of doxorubicin (indirect drug loading) (Aboutalebi Anaraki et al., 2015).

A dual electrospinning nozzle system is exploited to generate layers of nanofiber sheets leading to reduced burst release and sustained drug delivery. Okuda et al. developed a tetralayered nanofibrous mesh of poly(L-lactide-*co*-*e*-caprolactone) using sequential electrospinning method comprising of first drug mesh, second drug mesh, and without drug nanofibrous meshes/sheets stacked layer by layer to achieve time-programmed dual drug delivery (Zhang et al., 2017b). Another example of advanced drug loading in electrospun nanofiber is fabricating a promising nanoimplant for postoperative cancer treatment in the form of PLA/natural pearl powder nanofibrous mat containing doxorubicin hydrochloride (DOX) (Dai et al., 2017). Poly(lactic-*co*-glycolic acid) electrospun nanofibrous mats have also been used for local antibiotic delivery of tetracycline hydrochloride (Maleki et al., 2014). Further, nanofibrous mats can be coated to achieve improved mechanical stability and cell adhesion, for example, PCL nanofibrous mats can be coated with polyelectrolyte multilayers containing poly(diallyldimethylammonium chloride) (PDADMAC) and poly (sodium 4-styrene sulfonate) (PSS).

Moreover, multilayered nano/microfibers can be fabricated for controlling the drug release pattern, for example, ketoprofen loaded ethyl cellulose-based trilayered nanofibers were formed by triaxial electrospinning process containing increasing levels of ketoprofen from outer to inner layer exhibiting a linear drug release pattern with zero initial burst release (Zhang et al., 2017b). Biomimetic electrospun nanofibers can be obtained by various ways like tuning the alignment of nanofibers structures (random, spiral, tubular, sheath) replicating the ECM for target tissues and treatment of nanofibers, for example, treatment with plasma improves cell adhesion and migration owing to more number of hydrophilic functional groups (amine and carboxyl) (Wang et al., 2013; He et al., 2014).

There are certain drawbacks in employing nanofibers for drug delivery, the major being drug aggregation along fiber surface, difficulty in achieving uniform fiber size distribution, and most importantly loss of bioactivity of the encapsulated drug upon exposure to the toxic solvents and the electric field in the electrospinning process. The latter can be resolved by forming nanofiber composites by encapsulating drug into nanocarriers like MSNs, halloysite, nano-HA (HAp), nanotubes, etc., and further immobilizing them on the nanofiber's surface or incorporating into the nanofibers via electrospinning, for example, PLLA nanofiber containing doxorubicin loaded MSNs capped with $CaCO_3$ exhibited both effective drug protection as well as sustained drug release (40 days). It was observed that in the acidic environment of tumor pH < 6.8, $CaCO_3$ got dissolved, opening the entrance pores of MSNs within nanofiber leading to drug release (Zhang et al., 2017b).

4.4.2.2.2.3 DNA-BASED NANOSTRUCTURES In the last decade, DNA-based nanostructures and mechanical nanodevices have served as a unique platform for safe and efficient drug delivery because of several advantages they serve like selective as well as multiple functionalization, flexible drug loading, and low immunogenicity. DNA origami is an approach of constructing 2D and 3D nanostructures like a tube, triangle, tetrahedrons, barrels, etc., by programmed self-assembly of bacteriophage DNA and hundreds of complementary staple DNA strands. Drug loading can be achieved either by intercalation within a structure or linking onto the fabricated DNA origami structure (Endo et al., 2013). Recently, doxorubicin-loaded DNA triangles and DNA nanotubes prepared by self-assembly of M13mp18 phage DNA and complementary DNA helper strands displayed prominent therapeutic efficacy without systemic toxicity examined for orthotopic breast tumors in mice (Zhang et al., 2014b). Folate functionalized nanohybrid particles consisting of polypropylene oxide hydrophobic core and DNA shell were prepared to deliver hydrophobic drug doxorubicin to the target cells (Endo et al., 2013).

4.4.2.2.3 HYDROGELS

Hydrogels are water-swollen and water-insoluble, homogenous or heterogeneous, 3D networks derived from physical or chemical cross-linking of natural and/or synthetic polymers (Metters and Lin, 2007). Hydrogels are widely used for wound healing/repair (e.g., hydrogel containing curcumin loaded polymeric micelles for cutaneous wound repair), tissue regeneration (hydroxyethyl methacrylatealginate–gelatin cryogel for lung muscle regeneration), and controlled drug delivery [crosslinked CS with PGA (*g*-PGA) hydrogels for colon-specific drug delivery] (Peppas and Van Blarcom, 2016). In addition to the polymer borne challenges, hydrogels have two major issues to be dealt with. These are decontamination/sterilization of hydrogels and improving the mechanical strength so as to enhance drug loading into hydrogel matrix, for example, mechanically tough Pluronic F127/Laponit was synthesized by Wu et al. (Vashist et al., 2014).

In recent years, studies have been done to explore various prospects of hydrogel-based drug delivery. Sacran based hydrogel (a recently extracted safe polysaccharide from cyanobacterium *Aphanothece sacrum*) showed sustained drug release patterns for acidic, basic, and neutral drugs, that is, 4-biphenyl acetic acid, chlorpheniramine maleate, and prednisolone respectively (Motoyama et al., 2014). Novel techniques are reported in the literature to tune the drug release patterns like molecularly imprinted hydrogels, MEMS based

hydrogels, enzyme/biomolecule immobilization based hydrogels, and micropatterned polymeric hydrogels. Varied functionality was obtained in temozolamide loaded Ag-Au bimetallic nanoparticles using PEG-based hydrogel system (Wu et al., 2010). Nanohybrids and nanocomposites are reported to provide sustained drug release, for example, agarose/zinc basic salt inorganic hybrid hydrogel prepared by Gwak et al. (2012) showed sustained release of ferulic acid. Liu et al. (2014c) prepared hydrogel containing erythromycin loaded pluronic F-127 micelles for extended release.

Copper-free click chemistry principles like azide-alkyne cycloaddition, oxime reaction, thiol-ene chemistry, tetrazole-alkene, and Diels Alder reaction have been recently reported to create versatile 3D hydrogel systems (biomimetic/micropatterned/microgels/nanogels) because of major advantages like avoiding the use of toxic catalysts or immunogenic enzymes and no interference with the encapsulated drug due to its unique bioorthogonal feature. Bowman et al. prepared 3D alkyne rich patterned PEG hydrogels from PEG-4-SH and PEG-dialkyne via thiol-yne reaction (Jiang et al., 2014).

Photocrosslinkable hyperbranched polyesters hydrogels can encapsulate hydrophobic drug molecules within the cavity due to the presence of a hydrophobic inner core (Zhang et al., 2013). Hydrogels with hydrophobic polymeric blocks like PLA, PLGA, PCL, poly(p-phenylene oxide), polyhydroxybutyrate etc., are promising carriers for extended release of hydrophobic drug, for example, photocrosslinked PLA−PEG−PLA triblock copolymer nanogel of camptothecin and PLGA−PEG−PLGA based OncoGel of paclitaxel for local delivery to solid tumors (McKenzie et al., 2015). Covalently crosslinked mucin hydrogels showed sustained release of both hydrophobic drugs (paclitaxel decreasing HeLa cells viability) and hydrophilic drug (polymyxin B inhibiting bacterial proliferation) (Duffy et al., 2015).

Intelligent stimuli-responsive hydrogels are designed to achieve signal triggered programmed drug release, for example, CS-PEG hydrogel containing glucose oxidase and catalase has been prepared for glucose-responsive insulin delivery where insulin is released because of hydrogel swelling at low pH created by glucose oxidase-catalyzed glucose conversion to gluconic acid (Farahani et al., 2016). Amphiphilic CS/silica hybrid hydrogel system has been developed for the electroresponsive release of ethosuximide (anticonvulsant).

DNA/aptamer-based hydrogels pave a unique engineering path for target responsive hydrogel that is biocompatible with selective binding ability. Aptamers are single-stranded DNA prepared by a process called the systematic evolution of ligands by exponential enrichment. The strategies to prepare DNA hydrogel include (1) crosslinking of nucleic acid structures (self-assembly/hybridization), but all DNA hydrogel may not be cost-effective; (2) crosslinking of nucleic acid structures attached as chain branches to the polymer chain; and (3) forming polymeric networks with nucleic acid structures entrapped within.

Further, DNA hydrogels showed switchable physical, structural, and chemical properties along with switchable transitions occurring in response to external trigger like temperature, pH, metal ions, G-quadruplex or i-motif, for example, integrating nucleic acid bridges/hairpin structure with thermoresponsive PNIPAAM chains showed reversible sol↔gel ↔solid transitions (Kahn et al., 2017).

Wang et al. developed acrylamide based DNA hydrogel networks containing aptamer/platelet-derived growth factor-BB (PDGF-BB) complex that demonstrated sustained release. Moreover, release rates were governed by the affinity of the complex that is clear

from release percentages of PDGF-BB in first 24 hours (70% native gel without aptamer, 40% low-affinity aptamer-based hydrogel, 10% of PDGF-BB high-affinity aptamer-based hydrogel). Aptamer-based hydrogels show impeccable molecular recognition. DNA hydrogel containing the ATP-binding aptamer sequence, the two acrydite-modified DNAs, and acrylamide monomers displayed very specific recognition and extraction of ATP (target) from the dual molecular pool (ATP and GTP). ATP (target) release occurs following polymer chain dissociation and dissolution when crosslinker DNA gets hybridized with the encountered complementary sequence. Aptamer sequences in nanogels direct the targeted specific delivery, for example, doxorubicin loaded DNA nanogel showed specific cytotoxicity against CCRF-CEM cells because of the incorporated sgc8 aptamer targets CCRFCEM cancer cells. Incorporation of therapeutic antisense DNA in hydrogels has been proven helpful in selectively killing drug-resistant cancer cells (Lu et al., 2015).

4.5 CHALLENGES IN USING BIOMATERIALS FOR DRUG DELIVERY

4.5.1 General Aspects

The biomaterial-based drug delivery can achieve success in clinics if the fate of biomaterial in the body is thoroughly studied along with the drug fate. By 2020, the global market sale of biomaterials and medical devices is expected to reach around $400 billion, thereby increasing the need to ascertain the biosafety potential of biomaterials (Yin and Luan, 2016).

Biomaterial systems that have smart functions can lessen the adverse effects, prevent degradation of drug, and augment the bioavailability as the site of action. To accomplish a broad translational promise, one has to rely on sound scientific and engineering practice and should be remarkably observant in formulating and evaluating the fabricated systems. Our biomaterials, once fabricated into functional devices, should do better than the accepted practice when it comes to efficacy, side effects, and costs; the expectation is to improve in all three aspects. Innovative fabrication technologies capable of handling multimodal biomaterials and other biological materials, such as regulatory molecules and cells, will be required to achieve this goal.

The physical, chemical, mechanical, and biological properties of biomaterial properties must be examined right from the developmental stage. Some natural polymers are found to be biocompatible and nontoxic but pose processability and reproducibility problems, for example, widely used CS is nonantigenic and nontoxic but processing takes a long duration (Liu et al., 2014b). Certain synthetic polymers generally have good mechanical properties but poor cell recognition/attachment and more cell reactions, for example, PCL shows long-term release, but systemic or local reactions (Sankar et al., 2014). The use of composite polymers to overcome the disadvantages of natural or synthetic polymers is reported in various studies, for example, poly(acrylonitrile) and ferric chloride showed excellent biocompatibility and nontoxic nature (Cai et al., 2010).

The biomaterial-based drug delivery has undoubtedly proved advantageous but has to overcome several hurdles in the way to reach clinics. The basic desirable attributes of biomaterial-based drug delivery are targetability, drug release control, entrapment capacity, porosity, stability (both drug and delivery system), sterility, applicability, processability, and cost-effectiveness (Liu et al., 2014a; Tahir et al., 2013; Braghirolli et al., 2014; Taha et al., 2014).

In addition to these, the biomaterials need to be scrutinized for several validated biological assessments like biocompatibility, hemocompatibility, biodegradability/bioclearance, bacterial infection, cytotoxicity, genotoxicity, mutagenicity, carcinogenicity, immunogenicity, material mediated pyrogenicity, reproductive/developmental toxicity, sensitization, intracutaneous reactions like irritation, inflammation, allergic responses, issues related to implantable biomaterials like fibrosis encapsulation, calcification, stent restenosis, etc., and other acute/chronic toxicity (Bertrand and Leroux, 2012; Grund et al., 2011; Tekade et al., 2018).

The barrier in the way is to examine all possible unintended interactions occurring between biomaterial and host cells that can complicate/interfere with the intended functions like target drug release or can prove deleterious to host cells, as depicted in Fig. 4.6.

The drug, delivery system (by virtue of both material and design of biomaterials), activation method employed (pH, temperature, magnetic, etc.), route of delivery, and host-related factors—any of these individually/together may contribute in the generation of these biological responses. For instance, positively charged nanoparticles induce higher cytotoxicity due to higher cell membrane penetration than negatively charged nanoparticles (Hühn et al., 2013). Diverse biomaterial challenges and advantages on the basis of the delivery system are given in Table 4.8.

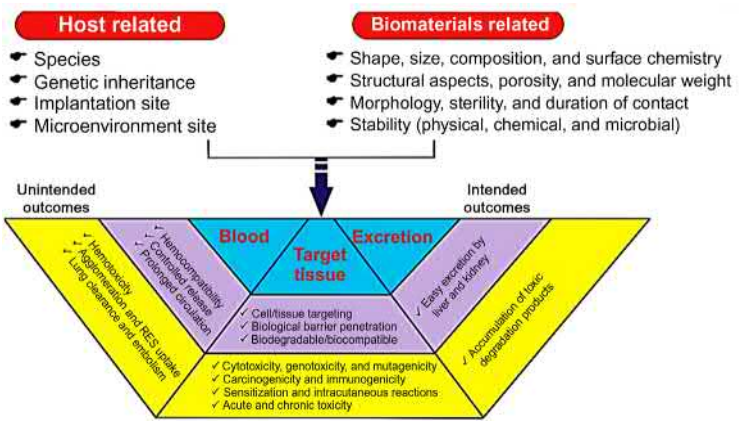

FIGURE 4.6 Biological outcomes due to host–biomaterial interactions.

TABLE 4.8 Challenges and Advantages of Diverse Biomaterial

Material Type	Advantage	Challenge
Fibers or conduits	Physical guidance clues	Requires invasive surgery
Hydrogel	Injectable or Space filling membrane sealing	No guidance cues burst release
Nanoparticle	Controlled or extended release Injectable within the hydrogel	No guidance cues

Further, there are some more challenges in the path of biomaterials-based implants/medical devices that include:

- Tissue regeneration, that is, survivability analysis of biomaterial implants like skeletal prostheses, coronary artery bypass graft, etc., to check for failure rate (McMahon et al., 2011).
- Tissue engineering of soft tissues, that is, ensuring the long-term stability postimplantation by maintaining blood supply in tissue engineered construct (Day, 2005; Verrier et al., 2004a).
- Stem cell engineering, that is, selecting the most appropriate stem cells to form the highly purified required phenotypic tissue (exhibiting the properties of self-renewal and potential to differentiate into required lineage) (Hubbell et al., 2009).

4.5.2 Biological Events Upon Host–Biomaterial Interaction and Solutions

4.5.2.1 Protein Adsorption

The supramolecular biomaterials initiate sequences of biological responses when they interact with living systems due to the recognition of nonself (biomaterial). The biomaterial–host interface thus needs to be studied. The biomaterials, when coming in contact with living tissues, encounter adsorption of surrounding biomolecules (lipids and mainly proteins like albumin, apolipoproteins, immunoglobulin G, fibrinogen, complement factors, etc.) on the surface forming a conditioning film also known as biomolecular/protein corona (Drießen, 2016; Tenzer et al., 2013; Chanana et al., 2013; Wan et al., 2015). This eventually affects the biomaterial functionality by altering drug release, uptake, distribution, localization, etc. These biological interactions can inhibit the intended task of the biomaterial (Rahman and Mahmoudi, 2015; Mirshafiee et al., 2013).

Different functional groups on the biomaterial surface render different cell, tissue, and protein responses, for example, amine ($-NH_2$) positive charge (hydrophilic) is reported to trigger acute inflammatory responses in vivo, carbonyl (−COOH) does the opposite, PEG provides biocompatibility, and phospholipid analogs provide bio/hemocompatibility (Tang et al., 2008). Several surface modification techniques are employed like physical methods (adsorption films, micro/nanopatterning), chemical methods (ozone treatment, silanization, fluorination, incorporation of functional group, etc.), biological methods (lipid/protein–enzyme immobilization, antibacterial activation, heparinization, hyaluronic acid coating), and radiation methods (corona discharge, laser, photoactivation) (Guney et al., 2013). For instance, the polymeric forming brushes onto various substrates by employing surface-initiated atomic transfer radical polymerization exhibited improved endothelial cell spreading, proliferation, and orientation in gelatin grafted plasma treated PCL nanofibers (Prabhakaran et al., 2008).

It is reported that protein adsorption onto hydrophilic surfaces is found weaker than that in the case of hydrophobic surfaces. The improvement of hydrophilicity of biomaterial surface, for example, by plasma treatment, introducing functional groups like hydroxyl, carbonyl, amino, sulfate, etc., coating with a hydrophilic polymer, photooxidation, etc., can control protein adsorption (Evans-Nguyen et al., 2006). Protein–surface interactions can be prevented by various techniques like adding hydrophilic groups like PEG (PEGylation)

that increase the circulation lifetime of biomaterial carrier (Williams, 2008; Liu et al., 2005), neutral groups (no H_2 bond donor), short amino acid sequences like RGD that promote cell adhesion due to specific integrin interactions/growth factors to the biomaterial surface. For instance, the fluorination of PU surfaces and PEG-modified PU surfaces showed decreased protein adsorption. Moreover, in case of smart biomaterial like temperature-sensitive PNIPAAm exhibited protein adsorption that was mostly influenced by temperature, grafting density, and graft thickness (Shamim et al., 2006; Nagase et al., 2008; Xue et al., 2011).

Various adverse effects on biomaterial functionality have been reported due to protein adsorption (Caracciolo et al., 2017), for example, reduced release of anticancer drug from MSNs (Paula et al., 2013) increased immune toxicity (Mahmoudi et al., 2012; De Paoli et al., 2014), and increased viability of A 549 cancer cells due to fetal bovine serum protein corona coating on the surface of graphene oxide nanosheet (Hajipour et al., 2015; Hu et al., 2011).

4.5.2.2 *Biocompatibility*

Biocompatibility is a broad term for appropriate biomaterial−host response ensuring biosafety, that is, absence of various local and systemic toxicities without compromising functionality, that is, ability to perform the intended task. Biocompatibility is not a new concept but with emerging novel biomaterials (natural/synthetic) with unknown toxicity variables, the need for the establishment of validated biosafety assessment methods for biomaterials has increased (Ratner et al., 2004; Arshady, 2003). Various techniques have been reported to improve biocompatibility:

1. Surface patterning as cellular behaviors are affected by microgrooves/ridges present on a biomaterial surface: (1) chemical patterning like microcontact printing, for example, imprinting hydrophobic ($-CH_3$) and hydrophilic ($-OH$) thiol compounds onto gold surface in desired pattern by Singhvi et al. (1994); (2) physical patterning, for example, micropillars/rectangular ridges of various width and height affected cell adhesion (Wilkerson et al., 2001; Zhang et al., 1999); or (3) employing a combination of both.
2. Immobilizing different peptides onto hydrophobic and/or hydrophilic blocks of the polymeric surface for improved biomaterial−cell interaction (surface properties) like cellular adhesion, for example, integrin selective peptide RGD (arginine-glycine-aspartic acid) (Desmet et al., 2009), RGDC (arginine-glycine-aspartic acid-cystine), etc. (Zhang et al., 2009).

4.5.2.3 *Hemocompatibility*

Hemocompatibility is a state of biocompatibility wherein blood−biomaterial interaction shows an absence of blood coagulation system activation, activation of platelet/leukocyte function, change in plasma protein, initiation of complement cascade (i.e., recognizing, opsonizing, and clearing foreign material within blood) (Hamad et al., 2008, 2010; Andersen et al., 2013; Salvador-Morales et al., 2006) and most important thrombogenicity (Klement et al., 2006). When biomaterial comes in contact with cardiovascular system protein adsorption (e.g., fibrinogen) is followed by irreversible platelet activation leading to thrombus formation (Vitte et al., 2004).

Surfaces can be rendered hemocompatible by implementing approaches like (1) controlling the surface properties of polymer (achieving minimum interfacial free energy); (2) incorporating antithrombogenic substances like heparin, urokinase and prostacyclin into the polymer, for example, heparin immobilized PU surfaces showed reduced protein adsorption and platelet adherence (Michanetzis et al., 2003; Aksoy et al., 2008); (3) making use of repairing and adsorption mechanisms of living tissue like pseudo-endothelialization; (4) other techniques like albumin coating on the polymer surface, PEGylation, for example, PEGMA PEG methacrylate and *N*-vinyl pyrrolidine as cografted monomer efficiently resist protein adsorption and reduce platelet adhesion (Kuo et al., 2012). Thromboelastography can be employed as in vitro assay to predict in vivo thrombogenicity potential (Wolf and Andwraon, 2012; Shankarraman et al., 2012).

4.5.2.4 Bacterial Infection

The protein corona/conditioning film formation is followed by long-range or short-range bacterial attachment that tends to grow, forming colonies and leading to biofilm formation, which poses the risk of chronic infection (Hall-Stoodley et al., 2004; Katsikogianni and Missirlis, 2004). Moreover, the bacterial adhesion gets affected by environmental, bacterial, as well as material surface characteristics (Contreras-García et al., 2010). The microbiological tests conducted on vancomycin loaded devices showed the small possibility of biofilm formation by methicillin-resistant *Staphylococcus aureus*. The controlled release of vancomycin can be achieved by prolonged suture-based grafting of PAAc networks (García-Vargas et al., 2014). The common microbes associated with medical devices are *Staphylococcus aureus*, *Staphylococcus epidermidis*, *Pseudomonas aeuroginosa*, and *Escherichia coli*; these restrict the lifetime of medical devices (Tuson and Weibel, 2013; Hall-Stoodley et al., 2004).

Certain approaches can be employed to render the surfaces antibacterial:

1. Surface coating with antibiotics (Hume et al., 2004), for example, coating of levofloxacin loaded liposomes over the contact lenses for both Gram-positive and Gram-negative antibacterial properties (Danion et al., 2007). This approach has a limitation of antibody resistance development that can be overcome by adding metabolites like fructose, mannitol, glucose, and pyruvate (Stewart and Costerton, 2001; Gottenbos et al., 2002).
2. Surface coating with silver (being toxic to microbes and least toxic to animal cells) (Fu et al., 2006; Vasilev et al., 2010), for example, silver nanocrystal/graphene nanosheet PAA grafted nanohybrid was proved effective against Gram-positive *S. aureus* and Gram-negative *E. coli* (Tai et al., 2012).
3. Surface modification with antibacterial agents, altering hydrophobicity, attaching functional groups with antibacterial activity, complexing with antiseptics like iodine (Luo et al., 2010), or coating with biomacromolecules with antibacterial properties, for example, 80% antibacterial efficiency was observed in PNIPAAm/PU hydrogel grafted nonwoven fabrics modified with CS (possessing antibacterial property) (Liu et al., 2009).

Recently, various approaches have been used to control infection caused by biomaterial implants or medical devices:

1. Layered polymer brushes with bacteria-repellent and/or bactericidal properties, for example, a surface-initiated photoiniferter-mediated polymerization approach used to

fabricate antibacterial surface containing PEG antifouling bottom layer for bacterial attachment suppression a quaternary ammonium compound bactericidal top layer (Banerjee et al., 2011).

2. Deoxyribonuclease coating onto the polymeric surface (e.g., polycarboxylate modified polymer) can prevent bacterial adhesion and biofilm formation by cleaving extracellular deoxyribonucleic acid without developing biocide resistance (Yuan et al., 2014).
3. An infection-resistant slippery surface is created by infusing fluorocarbon bound osmotically driven wrinkling surface with fluorocarbon liquid that repels various liquids resisting infection and thrombus formation (Yuan et al., 2015).

The challenges associated with decontamination/sterilization of biomaterials-based drug delivery systems need further attention (Kikuchi et al., 2017). The strict and complex sterilization techniques are required to minimize the risk of nosocomial infections and mortality/morbidity caused by inadequate sterilization of instruments and devices (Busscher et al., 2012). The most commonly used sterilization techniques for medical devices are steam, EO, and irradiation (Luan et al., 2011; Luan et al., 2010). Therefore radiation-resistant polymer-based biomaterials should be used, for example, incorporating antiirradiation agents into bulk polymers (Shi et al., 2010).

4.5.2.5 Biodegradation

Biodegradable biomaterials (e.g., PLGA, PLA, PCL, CS, gelatin, etc.) (Mahapatro and Singh, 2011) are preferred over nonbiodegradable ones (e.g., metal colloids, ceramics) due to nonrequirement of future removal (Salvador-Morales et al., 2006). Moreover, accumulation of nonbiodegradable nanoparticles in the mononuclear phagocytic cell such as liver and spleen leads to potentially toxic outcomes (Owens and Peppas, 2006). Many smart polymers like PNIPAAm and PPAAc having high molecular weights (supramolecules) effectively reach the cellular target but after delivery the drug, they are not biodegradable, not readily excreted by the kidney, and tend to accumulate. The biodegradation and bioclearance study of biomaterial becomes significant to assure nonaccumulation in the body.

PLGA microparticles are reported to show toxicity (peritoneal adhesion) while nanoparticles didn't because of bioclearance within a day (Kohane et al., 2006; Kohane, 2007). The degradation products may have different physical and compatibility characteristics. Moreover, biodegradation pathways and degradation product characteristics must be studied along with toxicity profile, for example, PU-coated breast implants had favorable chances of cleavage of the adipate ester bond releasing 2,4-toluenediamine, which is known to have carcinogenic potential. Although, blood and urine analysis showed very small amounts of free 2,4-toluenediamine (Castel et al., 2015).

4.5.3 Examples of Smart Biomaterial Challenges and Toxicities

Smart materials undergo molecular transitions exposing new surfaces to the immune system leading to complement activation in some cases. Biomaterials-based drug delivery are mainly intended for sustained release, which suggests its residence at a particular site for a long time. This can ultimately lead to local irritation, for example, local tissue toxicity caused by sustained release delivery of local anesthetics. Mostly applied triggers are

nonspecific, so their effects on living cells need to be studied in both cases, whether the trigger applied is focused or unfocused. Biomaterial toxicity evaluation is done, for example, the retention of neurotoxicity potential of AAm monomer in widely used thermosensitive polymer PNIPAAm is still questionable though polymer washing before drug incorporation possibly reduces the chances of presence of AAm monomer in PNIPAAm formulations (Hoffman, 2013).

Numerous biomaterial linked toxicities may arise due to varied reasons like thrombosis/carcinogenesis by leachable compounds from biomaterial, for example, MSNs have been extensively used because of their more stable and drug protectant nature leading to extended drug release. They are biocompatible in an appropriate dosage. But, the presence and/or leaching of residual chemicals (from synthesis) can lead to accumulation and below 10% mortality rate is reported (Tang et al., 2012; Tarn et al., 2013). Few types of research revealed intraperitoneal administration of CNTs (though unlikely) caused inflammation and carcinogenicity (Takagi et al., 2008). Although histological reactions to subcutaneously implanted MWCNTs were studied using carbon black tattoo ink as reference material These showed acute but mild inflammation that resolved early and no carcinogenicity potential (Hara et al., 2011). CNTs may induce oxidative stress leading to cytotoxicity due to retention of catalyst metals (Fe, Co, Ni, etc.) used in the production method (Cheng et al., 2009).

Plasticizer-free polymers should be designed for biomedical applications so as to prevent the contact of the leachable plasticizer with blood, drugs, and intravenous injection fluids in service, for example, plasticizer diethyl hexyl phthalate not chemically bound to polymer PVC. Styrene thermoplastic elastomers are utilized to overcome such issues (Simmchen et al., 2012; Luo et al., 2014).

Nanoparticles have been observed to exhibit both

1. Immunostimulation, for example, raised antibody response and vaccine efficacy was observed with lipid-coated polysaccharide nanoparticle-based rabies vaccine (Bengtsson et al., 2016); mostly inflammation due to cytokines secretion (more seen in cationic nanoparticles than anionic nanoparticles) (Hwang et al., 2015)
2. Immunosuppression, for example, suppressed arthritis induced inflammation was observed with type II collagen-containing PLGA nanoparticles (Asakawa et al., 2015).

FDA-friendly natural/synthetic biomaterials (approved biocompatible), for example, PEG, PLGA, dextran should be used in fabricating drug delivery systems (Hoffman, 2013). These smart and complex systems at times pose difficulty in achieving reproducibility and quality control as even small variations can lead to significant functionality changes. Regulatory authorities are thus working on establishing standards for preparation and evaluation of smart biomaterial systems. The standards for biocompatibility assessment of medical devices are documented in ISO 10993.

4.5.4 Biological Assessment Tests

Regulatory agencies have devised various aspects of biological evaluation under the name of biological hot buttons (including chronic inflammation, immune response, innate

immunity, and acquired immunity) and tissue response continuum (including acute/chronic inflammation, foreign body reaction, granulation tissue, fibrous encapsulation) (Reeve and Baldrick, 2017).

Certain criteria must be ascertained for biocompatibility evaluation. The evaluation method (selection of cytotoxicity cell line, etc.) must be in accordance with the intended application; quantitative and statistical analysis should be possible; multiple pathways to the response being evaluated should be considered; in vivo verification of in vitro result must be done; cost and ease of use must be considered; phenotypic interactions must be considered (McNally and Anderson, 2015); method should ensure detailed and complete analysis/interpretation of the response, for example, in an attempt to determine the release and presence of fibroblast growth factor (FBF); quantitation of both metalloproteinases (MMPs) and the tissue inhibitor for MMPs would provide more complete analysis; must provide sufficient information on molecular biological changes upon cell exposure to biomaterial (Jones et al., 2008).

Biocompatibility evaluations include (1) in vitro studies examining cell ability to survive in presence of biomaterial, for example, MTT assay (quantitate dye production by functioning of mitochondria) (Foldbjerg et al., 2011; Wang et al., 2010), dye-based cell membrane integrity test, measurement of DNA synthesis, cell proliferation (Chang et al., 2011; Alexandrescu et al., 2013), examination of cell death as tissue injury markers upon both direct and indirect exposure of biomaterials (Brauchle et al., 2014); (2) in vivo studies for more accurate and complete assessment of any unfavorable reaction upon biomaterial exposure as in some cases variations are observed in vitro and in vivo assessments, for example, UV cross-linkable CS showed mild suppression of cell viability in cell culture and vigorous peritoneal adhesions in vivo (Yeo et al., 2006), and bupivacaine killed 100% of muscle cell in culture and showed little/no injury when injected in vivo (Padera et al., 2008; Padera et al., 2006).

In vivo biocompatibility assay for injected /implanted biomaterial can be performed by various techniques like hematoxylin−eosin stained paraffin-embedded section as immunohistochemical study method for inflammation morphology, electron microscopy for detecting tissue injury signs, antibody-based assays for examining the release of proinflammatory molecules (Padera et al., 2008). Nyska et al. reported a histopathological assessment of the adverse reactions produced by biomaterials-based implants, for example, granulomatous reaction in case of hyaluronic acid used as a dermal filler. Various preliminary study techniques are reported for longitudinal imaging and quantification of inflammation in such cases like staining, electron microscopy, or using in vivo/ex vivo compact MRI (Nyska et al., 2014).

The results of in vitro biocompatibility tests should be relevantly predictive of in vivo results. Certain evaluation techniques are designed taking this into consideration, like bio-Raman spectroscopy and modular immune in vitro construct (MIMIC) (Pyrgiotakis et al., 2008; Schanen et al., 2009).

Bio-Raman spectroscopy is in situ testing of cells residing in a special environmental chamber provided with a microscope and a gas support system. The cell viability, cell cycle, metabolism, mitosis, differentiation, dedifferentiation, mineralization, and onset of the death of single cells and cell assemblages are monitored in real time without damage to the cells that further enhances in vivo result prediction.

Cell exposure to biomaterial may cause alterations of DNA, RNA, proteins, lipids, and carbohydrates within the cells causing changes in spectroscopic signatures of the cells in

the chamber that are examined in this method (Swain et al., 2008; Pyrgiotakis et al., 2008). The method can also be used to detect the varied the biological actions of cytotoxic agents (Triton X-100) and genotoxic agents (Etoposide, VP16) by determining cell death mechanism, that is, cell membrane disruption (cytotoxic) or DNA disruption/breakage (genotoxic) (Verrier et al., 2004b; Owen et al., 2006).

Human autologous MIMIC is used to study biomaterial interaction with the human immune system utilizing blood vein endothelial cells and monocyte-derived dendritic cells to examine the short-term and the long-term immune responses (T cell responses, inflammatory response, memory response). For instance, this method was used for assessing the immunogenicity of titanium dioxide nanoparticles and showed increased levels of proinflammatory cytokines, raised maturation and expression of costimulatory molecules on dendritic cells. In vitro assay results and in vivo inflammatory responses were found to be correlated (Schanen et al., 2009).

The carcinogenic potential of biomaterial needs to be examined. Medical devices are needed to undergo in vitro cytotoxicity evaluation commonly up to 7 days over a tumor-derived macrophage cell line either leukemias (human promyelocytic leukemia HL-60)/lymphomas (human acute monocytic lymphoma THP-1) observing neoplastic changes with respect to the reference (Correia et al., 2011).

Certain evaluation tests are reported to examine the mutagenic, genotoxic, and apoptotic potential of biomaterials, for example,

1. The Ames test (reverse mutation test) with *Salmonella typhimurium* and other test strains to quantify restoration ability of amino acid biosynthesis in bacteria that originally is lacking due to mutation (Di Sotto et al., 2009).
2. The comet assay to examine DNA damage in individual cells at various levels and repair kinetics (Cveticanin et al., 2009).
3. The micronucleus test to use cells with micronuclei as a marker of gene damage of interest in the animal cell (Lindberg et al., 2009; Muller et al., 2008).
4. Studying apoptotic and nonapoptotic cell death by examining the induction of apoptosis signals in macrophages and other cells (Vittorio et al., 2009).

Biomaterial induced cell signaling events can be examined by (1) microarray study, that is, examining the changes in cellular expression/cell signaling in different human cells on exposure to biomaterial, for example, MWCNTs impacts cellular signaling event by suppressing osteoclast differentiation due to inhibition of nuclear migration of the transcription factor NFATc1 (Narita et al., 2009) or (2) proteomics-based studies examining change in protein expression related to stress, redox, metabolism, apoptosis, etc., using keratinocytes, monoblastic leukemia cells, and hepatoma cells (Yuan et al., 2011).

4.6 REGULATORY AND PATENT ASPECT OF BIOMATERIALS EMPLOYED FOR SUSTAINED AND CONTROLLED DELIVERY OF SMALL DRUG MOLECULE

Medical devices are classified as class I, class II, and class III. The device classification explains the regulatory requirements for a general type device. Most of the class I devices

TABLE 4.9 Different Patents on Biomaterials

Patent No. and Date	Description of Patent
US 9,415,110 B1, 16/08/16	Method and composition for targeted drug delivery to the lower GI tract
WO 2012095346, 19/07/12	A composite comprising silica aerogel and hydrogel useful for drug or protein delivery, and for biomaterials
US 20120183985, 19/07/2012	Manufacture of microtissues for inducing growth of hair follicle, involving simultaneously seeding several dermal papilla cells and keratinocytes on a biomaterial substrate surface with a predetermined ratio and predetermined cell density
WO 2012094708, 19/07/2012	A biomaterial comprising a porous polymer, osteoinductive compound, and bone anticatabolic compound; useful for treating dental injury or defect, and bone injuries or defects, such as bone fracture and joint replacement
US 20120208722, 16/08/12	A method of preparing a SERS platform for the detection of a biomaterial, comprising contacting a portion of acid functional groups on the surface of a solid substrate with at least one cyclooctyne having a biomaterial attached to it, to form a triazole
JP 2012157578, 23/08/12	Biological implant material comprising calcium phosphate and titanium hydride; useful for stimulating growth and proliferation of osteoblasts, and used as medical biomaterials, for example, artificial bone
US 2012/0265001 A1, 18/10/12	Composite magnetic nanoparticle drug delivery system
US 7,226,615 B2, 5/06/07	Expandable foam-like biomaterials and methods

SERS, Surface-enhanced Raman spectroscopy.

exempt from premarket notification 510(k). These are a simple type of low-risk device. In this general controls include a prohibition against adulterated or misbranded devices, banned devices, good manufacturing practices, a listing of devices types, record keeping, repair, replacement, and refund. Class II devices needed premarket notification 510(k).

These have high risk and more complex type of devices needed special controls. Ten to 15% of clinical data is required and 90 days needed for the FDA to review these kinds of devices. For these devices, special controls consist of labeling, design controls, tracking, guidance, performance standards, postmarket surveillance, and most of class III require premarket application PMA. These are the most complex type of devices and have the highest risk. They may include postapproval study requirements, and they require 320 total FDA days to review. Such devices are life sustaining or life supporting and present an unreasonable risk of illness or injury. Descriptions of the different patents are given in Table 4.9 (Langer and Peppas, 1981).

4.7 FUTURE PROSPECTS AND CONCLUSION

The past few decades have witnessed huge progress in the field of biomaterial science. Biomaterials have a broad spectrum of applications including tissue engineering, wound

healing, and drug delivery. In drug delivery applications, biomaterials not only serve as efficient and precise drug carriers but also perform drug monitoring and diagnostics. Biomaterial-based drug delivery systems have been proved excellent to achieve sustained drug release, precise drug control, improved therapeutic efficiency, reduced side effects, and increased patient compliance. Moreover, their contribution in drug delivery covers an ample range from robust biomaterial-based bioartificial structures/mechanical devices to the sophisticated drug delivery systems like MIPs, etc. Biomaterial-based drug delivery has been successfully possible through various routes like oral, ocular, pulmonary, transdermal, neural, etc., to treat multiple diseases including cancer and many immunological disorders. Multidimensional advancements have been seen in the techniques employed like configurational biomimetic imprinting, aptamer/DNA-based hydrogels and nanostructures, microfluidics, tristimuli-responsive biomaterial systems, etc.

Most of the studies until now have been focused on biomaterial design and characterization; unfortunately, safety concerns have not been studied and established to the same extent. Biomaterials will certainly need more detailed scrutiny concerning biocompatibility (biosafety/biofunctionality), biodegradability (bioclearance), and toxicological issues (cytotoxicity, immunogenicity etc.). In spite of several types of research done on biomaterial-based drug delivery, very few have reached the clinical phases. Regulatory authorities are still working on setting up the standards for preparation and evaluation of novel smart biomaterial systems to achieve reproducible quality control for such dynamic systems. Any unknown variable (even a small variation) related to the macromolecular biomaterial may demand years of clinical evaluation. Moreover, the cost involved may be high due to uncertain risk–benefit ratio owing to insufficient information database of newly developed biomaterials. The innovations in biomaterial science will undoubtedly pave the way for the next generation of drug delivery systems provided all the physical, chemical, mechanical, and biological aspects regarding biomaterials are meticulously examined.

Acknowledgments

The authors would like to acknowledge the Science and Engineering Research Board (Statutory Body Established through an Act of Parliament: SERB Act 2008), Department of Science and Technology, Government of India for grant (grant no. ECR/2016/001964) allocated to Dr. Tekade for research work on gene delivery and N-PDF funding to Dr. Maheshwari (PDF/2016/003329) for work on targeted cancer therapy in Dr. Tekade's Laboratory. The authors also acknowledge the support by the Fundamental Research Grant (FRGS/1/2015/TK05/IMU/03/1) scheme of the Ministry of Higher Education, Malaysia to support research on gene delivery.

References

Abdolrahimzadeh, S., Plateroti, P., Scarinci, F., Plateroti, A.M., 2016. Accidental intralenticular dexamethasone intravitreal implant with the resolution of macular oedema in central retinal vein occlusion. Acta Ophthalmol. 94 (8), e810–e811.

Aboutalebi Anaraki, N., Roshanfekr Rad, L., Irani, M., Haririan, I., 2015. Fabrication of PLA/PEG/MWCNT electrospun nanofibrous scaffolds for anticancer drug delivery. J. Appl. Polym. Sci. 132 (3), 41286.

Ahmed, E.-S., Wei-ming, C., Xiu-mei, M., 2014. Preparation of antibacterial electrospun PVA/regenerated silk fibroin nanofibrous composite containing ciprofloxacin hydrochloride as a wound dressing. J. Donghua Univ. (Eng. Ed.) 31 (5), 566–571.

Akagi, H., Ochi, H., Soeta, S., Kanno, N., Yoshihara, M., Okazaki, K., et al., 2015. A comparison of the process of remodeling of hydroxyapatite/poly-D/L-lactide and beta-tricalcium phosphate in a loading site. BioMed Res. Int. 2015, 730105.

Aksoy, E.A., Hasirci, V., Hasirci, N., Motta, A., Fedel, M., Migliaresi, C., 2008. Plasma protein adsorption and platelet adhesion on heparin-immobilized polyurethane films. J. Bioact. Compat. Polym. 23 (6), 505–519.

Al Faraj, A., Shaik, A.P., Shaik, A.S., 2015. Magnetic single-walled carbon nanotubes as efficient drug delivery nanocarriers in breast cancer murine model: noninvasive monitoring using diffusion-weighted magnetic resonance imaging as sensitive imaging biomarker. Int. J. Nanomed. 10, 157.

Al-Ahmady, Z.S., Al-Jamal, W.T., Bossche, J.V., Bui, T.T., Drake, A.F., Mason, A.J., et al., 2012. Lipid–peptide vesicle nanoscale hybrids for triggered drug release by mild hyperthermia in vitro and in vivo. ACS Nano 6 (10), 9335–9346.

Alatorre-Meda, M., Mano, J.F., 2016. General characterization of chemical properties of natural-based biomaterials. Biomater. Nat. Adv. Devices Ther. 517–531.

Alexandrescu, L., Syverud, K., Gatti, A., Chinga-Carrasco, G., 2013. Cytotoxicity tests of cellulose nanofibril-based structures. Cellulose 20 (4), 1765–1775.

Ali, H.S., Hanafy, A.F., 2017. Glibenclamide nanocrystals in a biodegradable chitosan patch for transdermal delivery: engineering, formulation, and evaluation. J. Pharm. Sci. 106 (1), 402–410.

Ali, M., 2010. Pulmonary drug delivery. *Handbook of Noninvasive Drug Delivery Systems*. Elsevier.

Ali, M., Byrne, M.E., 2013. Controlled and Extended Delivery of Hyaluronic Acid and Comfort Molecules via a Contact Lens Platform. Google Patents.

Alkilani, A.Z., McCrudden, M.T., Donnelly, R.F., 2015. Transdermal drug delivery: innovative pharmaceutical developments based on disruption of the barrier properties of the stratum corneum. Pharmaceutics 7 (4), 438–470.

Alvarez-Lorenzo, C., Concheiro, A., 2014. Smart drug delivery systems: from fundamentals to the clinic. Chem. Commun. 50 (58), 7743–7765.

Alvarez-Lorenzo, C., Gonzalez-Chomon, C., Concheiro, A., 2013. Molecularly imprinted hydrogels for affinity-controlled and stimuli-responsive drug delivery. Smart Mater. Drug Deliv. 2, 313–348.

Andersen, A.J., Robinson, J.T., Dai, H., Hunter, A.C., Andresen, T.L., Moghimi, S.M., 2013. Single-walled carbon nanotube surface control of complement recognition and activation. ACS Nano 7 (2), 1108–1119.

Antensteiner, M., Khorrami, M., Fallahianbijan, F., Borhan, A., Abidian, M.R., 2017. Conducting polymer microcups for organic bioelectronics and drug delivery applications. Adv. Mater. 29 (39), 1702576.

Ardeshirzadeh, B., Anaraki, N.A., Irani, M., Rad, L.R., Shamshiri, S., 2015. Controlled release of doxorubicin from electrospun PEO/chitosan/graphene oxide nanocomposite nanofibrous scaffolds. Mater. Sci. Eng. C 48, 384–390.

Argyo, C., Weiss, V., Bräuchle, C., Bein, T., 2013. Multifunctional mesoporous silica nanoparticles as a universal platform for drug delivery. Chem. Mater. 26 (1), 435–451.

Arifuzzaman, M., Zhao, Y., 2016. Water-soluble molecularly imprinted nanoparticle receptors with hydrogen-bond-assisted hydrophobic binding. J. Org. Chem. 81 (17), 7518–7526.

Arshady, R., 2003. *Polymeric Biomaterials: Chemistry, Concepts, Criteria*. *Introduction to Polymeric Biomaterials: The Polymeric Biomaterials Series*. *Citus Books, London*, pp. 1–62.

Asakawa, M., Yoshida, H., Sakai, R., Saeki, K., Okada, M., Kanamori, M., et al., 2015. A novel JAK-STAT inhibitor, 2-[(3-carbamoyl-2-thienyl) amino]-2-oxoethyl (2,6-dichlorophenyl) acetate, suppresses helper T cell differentiation in vitro and collagen-induced arthritis in vivo. Biochem. Biophys. Res. Commun. 468 (4), 766–773.

Ashammakhi, N., Kaarela, O., 2017. Stimuli-responsive biomaterials: next wave. J. Craniofac. Surg. 28 (7), 1647–1648.

Awino, J.K., Zhao, Y., 2015. Polymeric nanoparticle receptors as synthetic antibodies for nonsteroidal antiinflammatory drugs (NSAIDs). ACS Biomater. Sci. Eng. 1 (6), 425–430.

Badeau, B.A., Comerford, M.P., Arakawa, C.K., Shadish, J.A., DeForest, C.A., 2018. Engineered modular biomaterial logic gates for environmentally triggered therapeutic delivery. Nat. Chem. 10, 251–258.

Bakrudeen, H.B., Sudarvizhi, C., Reddy, B., 2016. Starch nanocrystals based hydrogel: construction, characterizations and transdermal application. Mater. Sci. Eng. C 68, 880–889.

Balmayor, E.R., Azevedo, H.S., Reis, R.L., 2011. Controlled delivery systems: from pharmaceuticals to cells and genes. Pharm. Res. 28 (6), 1241–1258.

Banerjee, A., Qi, J., Gogoi, R., Wong, J., Mitragotri, S., 2016. Role of nanoparticle size, shape and surface chemistry in oral drug delivery. J. Control. Release 238, 176–185.
Banerjee, I., Pangule, R.C., Kane, R.S., 2011. Antifouling coatings: recent developments in the design of surfaces that prevent fouling by proteins, bacteria, and marine organisms. Adv. Mater. 23 (6), 690–718.
Basu, B., 2017a. Biomaterials Science and Tissue Engineering: Principles and Methods. Cambridge University Press.
Basu, B., 2017b. Mechanical properties of biomaterials. Biomaterials for Musculoskeletal Regeneration. Springer.
Battista, E., Scognamiglio, P.L., Di Luise, N., Raucci, U., Donati, G., Rega, N., et al., 2018. Turn-on fluorescence detection of protein by molecularly imprinted hydrogels based on supramolecular assembly of peptide multifunctional blocks. J. Mater. Chem. B 6 (8), 1207–1215.
Bengtsson, K.L., Song, H., Stertman, L., Liu, Y., Flyer, D.C., Massare, M.J., et al., 2016. Matrix-M adjuvant enhances antibody, cellular and protective immune responses of a Zaire Ebola/Makona virus glycoprotein (GP) nanoparticle vaccine in mice. Vaccine 34 (16), 1927–1935.
Bertrand, N., Leroux, J.-C., 2012. The journey of a drug-carrier in the body: an anatomo-physiological perspective. J. Control. Release 161 (2), 152–163.
Bhatnagar, I., Venkatesan, J., Kim, S.-K., 2014. Polymer functionalized single walled carbon nanotubes mediated drug delivery of gliotoxin in cancer cells. J. Biomed. Nanotechnol. 10 (1), 120–130.
Biagini, G., Bertani, A., Muzzarelli, R., Damadei, A., DiBenedetto, G., Belligolli, A., et al., 1991. Wound management with *N*-carboxybutyl chitosan. Biomaterials 12 (3), 281–286.
Biswas, A.K., Islam, M.R., Choudhury, Z.S., Mostafa, A., Kadir, M.F., 2014. Nanotechnology based approaches in cancer therapeutics. Adv. Nat. Sci.: Nanosci. Nanotechnol. 5 (4), 043001.
Braghirolli, D.I., Steffens, D., Quintiliano, K., Acasigua, G.A.X., Gamba, D., Fleck, R.A., et al., 2014. The effect of sterilization methods on electronspun poly(lactide-*co*-glycolide) and subsequent adhesion efficiency of mesenchymal stem cells. J. Biomed. Mater. Res., B: Appl. Biomater. 102 (4), 700–708.
Brauchle, E., Thude, S., Brucker, S.Y., Schenke-Layland, K., 2014. Cell death stages in single apoptotic and necrotic cells monitored by Raman microspectroscopy. Sci. Rep. 4, 4698.
Bryksin, A.V., Brown, A.C., Baksh, M.M., Finn, M., Barker, T.H., 2014. Learning from nature–novel synthetic biology approaches for biomaterial design. Acta Biomater. 10 (4), 1761–1769.
Buckiová, D., Ranjan, S., Newman, T.A., Johnston, A.H., Sood, R., Kinnunen, P.K., et al., 2012. Minimally invasive drug delivery to the cochlea through application of nanoparticles to the round window membrane. Nanomedicine 7 (9), 1339–1354.
Busscher, H.J., Van Der Mei, H.C., Subbiahdoss, G., Jutte, P.C., Van Den Dungen, J.J., Zaat, S.A., et al., 2012. Biomaterial-associated infection: locating the finish line in the race for the surface. Sci. Transl. Med. 4 (153), 153rv10.
Cai, Y., Wang, Q., Wei, Q., You, Q., Huang, F., Song, L., et al., 2010. Structure, thermal, and antibacterial properties of polyacrylonitrile/ferric chloride nanocomposite fibers by electrospinning. Int. J. Polym. Anal. Charact. 15 (2), 110–118.
Canbolat, M.F., Celebioglu, A., Uyar, T., 2014. Drug delivery system based on cyclodextrin-naproxen inclusion complex incorporated in electrospun polycaprolactone nanofibers. Colloids Surf., B: Biointerfaces 115, 15–21.
Caracciolo, G., Farokhzad, O.C., Mahmoudi, M., 2017. Biological identity of nanoparticles in vivo: clinical implications of the protein corona. Trends Biotechnol. 35 (3), 257–264.
Castel, N., Soon-Sutton, T., Deptula, P., Flaherty, A., Parsa, F.D., 2015. Polyurethane-coated breast implants revisited: a 30-year follow-up. Arch. Plast. Surg. 42 (2), 186.
Chan, A., Orme, R.P., Fricker, R.A., Roach, P., 2013. Remote and local control of stimuli responsive materials for therapeutic applications. Adv. Drug Deliv. Rev. 65 (4), 497–514.
Chanana, M., Rivera_Gil, P., Correa-Duarte, M.A., Liz-Marzán, L.M., Parak, W.J., 2013. Physicochemical properties of protein-coated gold nanoparticles in biological fluids and cells before and after proteolytic digestion. Angew. Chem. Int. Ed. 52 (15), 4179–4183.
Chang, H.-I., Wang, Y., 2011. Cell responses to surface and architecture of tissue engineering scaffolds. Regenerative Medicine and Tissue Engineering—Cells and Biomaterials. InTech.
Chang, Y., Yang, S.-T., Liu, J.-H., Dong, E., Wang, Y., Cao, A., et al., 2011. In vitro toxicity evaluation of graphene oxide on A549 cells. Toxicol. Lett. 200 (3), 201–210.

Cheah, H.Y., Šarenac, O., Arroyo, J.J., Vasić, M., Lozić, M., Glumac, S., et al., 2017. Hemodynamic effects of HPMA copolymer based doxorubicin conjugate: a randomized controlled and comparative spectral study in conscious rats. Nanotoxicology 11 (2), 210–222.
Chen, D., Sun, K., Mu, H., Tang, M., Liang, R., Wang, A., et al., 2012a. pH and temperature dual-sensitive liposome gel based on novel cleavable mPEG-Hz-CHEMS polymeric vaginal delivery system. Int. J. Nanomed. 7, 2621.
Chen, K.-J., Liang, H.-F., Chen, H.-L., Wang, Y., Cheng, P.-Y., Liu, H.-L., et al., 2012b. A thermoresponsive bubble-generating liposomal system for triggering localized extracellular drug delivery. ACS Nano 7 (1), 438–446.
Chen, M.-C., Ling, M.-H., Lai, K.-Y., Pramudityo, E., 2012c. Chitosan microneedle patches for sustained transdermal delivery of macromolecules. Biomacromolecules 13 (12), 4022–4031.
Chen, M.-C., Mi, F.-L., Liao, Z.-X., Hsiao, C.-W., Sonaje, K., Chung, M.-F., et al., 2013. Recent advances in chitosan-based nanoparticles for oral delivery of macromolecules. Adv. Drug Deliv. Rev. 65 (6), 865–879.
Chen, M.-C., Ling, M.-H., Kusuma, S.J., 2015a. Poly-γ-glutamic acid microneedles with a supporting structure design as a potential tool for transdermal delivery of insulin. Acta Biomater. 24, 106–116.
Chen, W., Ma, Y., Pan, J., Meng, Z., Pan, G., Sellergren, B., 2015b. Molecularly imprinted polymers with stimuli-responsive affinity: progress and perspectives. Polymers 7 (9), 1689–1715.
Cheng, C., Müller, K.H., Koziol, K.K., Skepper, J.N., Midgley, P.A., Welland, M.E., et al., 2009. Toxicity and imaging of multi-walled carbon nanotubes in human macrophage cells. Biomaterials 30 (25), 4152–4160.
Cherukuri, S., Batchu, U.R., Mandava, K., Cherukuri, V., Ganapuram, K.R., 2017. Formulation and evaluation of transdermal drug delivery of topiramate. Int. J. Pharm. Invest. 7 (1), 10.
Chiang, W.-L., Lin, T.-T., Sureshbabu, R., Chia, W.-T., Hsiao, H.-C., Liu, H.-Y., et al., 2015. A rapid drug release system with a NIR light-activated molecular switch for dual-modality photothermal/antibiotic treatments of subcutaneous abscesses. J. Control. Release 199, 53–62.
Cipolla, D., Shekunov, B., Blanchard, J., Hickey, A., 2014. Lipid-based carriers for pulmonary products: preclinical development and case studies in humans. Adv. Drug Deliv. Rev. 75, 53–80.
Contreras-García, A., Bucio, E., Concheiro, A., Alvarez-Lorenzo, C., 2010. Polypropylene grafted with NIPAAm and APMA for creating hemocompatible surfaces that load/elute nalidixic acid. React. Funct. Polym. 70 (10), 836–842.
Correia, D.V., Fogli, M., Hudspeth, K., da Silva, M.G., Mavilio, D., Silva-Santos, B., 2011. Differentiation of human peripheral blood Vδ1 + T cells expressing the natural cytotoxicity receptor NKp30 for recognition of lymphoid leukemia cells. Blood 118 (4), 992–1001.
Costa, R.R., Alves, N.M., Rodríguez-Cabello, J.C., Mano, J.F., 2013. Stimuli-responsive surfaces for biomedical applications. Biomater. Surf. Sci. Chapter 4, 63–87.
Cranin, N., 1982. The requirements and clinical performance of dental implants. Biocompatibility Dent. Mater 4, 92–102.
Culver, H.R., Clegg, J.R., Peppas, N.A., 2017. Analyte-responsive hydrogels: intelligent materials for biosensing and drug delivery. Acc. Chem. Res. 50 (2), 170–178.
Cveticanin, J., Joksic, G., Leskovac, A., Petrovic, S., Sobot, A.V., Neskovic, O., 2009. Using carbon nanotubes to induce micronuclei and double strand breaks of the DNA in human cells. Nanotechnology 21 (1), 015102.
Dai, J., Jin, J., Yang, S., Li, G., 2017. Doxorubicin-loaded PLA/pearl electrospun nanofibrous scaffold for drug delivery and tumor cell treatment. Mater. Res. Express 4 (7), 075403.
Danion, A., Arsenault, I., Vermette, P., 2007. Antibacterial activity of contact lenses bearing surface-immobilized layers of intact liposomes loaded with levofloxacin. J. Pharm. Sci. 96 (9), 2350–2363.
Day, R.M., 2005. Bioactive glass stimulates the secretion of angiogenic growth factors and angiogenesis in vitro. Tissue Eng. 11 (5-6), 768–777.
De Paoli, S.H., Diduch, L.L., Tegegn, T.Z., Orecna, M., Strader, M.B., Karnaukhova, E., et al., 2014. The effect of protein corona composition on the interaction of carbon nanotubes with human blood platelets. Biomaterials 35 (24), 6182–6194.
Demir, Y.K., Akan, Z., Kerimoglu, O., 2013. Sodium alginate microneedle arrays mediate the transdermal delivery of bovine serum albumin. PLoS One 8 (5), e63819.
Desmet, T., Morent, R., De Geyter, N., Leys, C., Schacht, E., Dubruel, P., 2009. Nonthermal plasma technology as a versatile strategy for polymeric biomaterials surface modification: a review. Biomacromolecules 10 (9), 2351–2378.

Dhanashree, S., Priyanka, M., Manisha, K., Vilasrao, K., 2016. Molecularly imprinted polymers: novel discovery for drug delivery. Curr. Drug Deliv. 13 (5), 632–645.
Di Sotto, A., Chiaretti, M., Carru, G.A., Bellucci, S., Mazzanti, G., 2009. Multi-walled carbon nanotubes: lack of mutagenic activity in the bacterial reverse mutation assay. Toxicol. Lett. 184 (3), 192–197.
Dilnawaz, F., 2017. Polymeric biomaterial and lipid based nanoparticles for oral drug delivery. Curr. Med. Chem. 24 (22), 2423–2438.
Dineshkumar, B., Krishnakumar, K., Bhatt, A., Paul, D., Cherian, J., John, A., et al., 2015. Single-walled and multi-walled carbon nanotubes based drug delivery system: cancer therapy: a review. Indian J. Cancer 52 (3), 262.
Drießen, M.D., 2016. Investigation of Nanoparticle Toxicity: Characterization of Protein Corona and Evaluation of Oxidative Stress by Protein Carbonylation. Freie Universität Berlin.
Du, X., Zhou, J., Shi, J., Xu, B., 2015. Supramolecular hydrogelators and hydrogels: from soft matter to molecular biomaterials. Chem. Rev. 115 (24), 13165–13307.
Duffy, C.V., David, L., Crouzier, T., 2015. Covalently-crosslinked mucin biopolymer hydrogels for sustained drug delivery. Acta Biomater. 20, 51–59.
Eatemadi, A., Daraee, H., Karimkhanloo, H., Kouhi, M., Zarghami, N., Akbarzadeh, A., et al., 2014. Carbon nanotubes: properties, synthesis, purification, and medical applications. Nanoscale Res. Lett. 9 (1), 393.
Eatemadi, A., Daraee, H., Zarghami, N., Melat Yar, H., Akbarzadeh, A., 2016. Nanofiber: synthesis and biomedical applications. Artif. Cells Nanomed. Biotechnol. 44 (1), 111–121.
Ehsan, Z., Wetzel, J.D., Clancy, J.P., 2014. Nebulized liposomal amikacin for the treatment of *Pseudomonas aeruginosa* infection in cystic fibrosis patients. Expert Opin. Invest. Drugs 23 (5), 743–749.
Elzoghby, A.O., Abd-Elwakil, M.M., Abd-Elsalam, K., Elsayed, T.M., Hashem, Y., Mohamed, O., 2016. Natural polymeric nanoparticles for brain-targeting: implications on drug and gene delivery. Curr. Pharm. Des. 22 (22), 3305–3323.
Endo, M., Yang, Y., Sugiyama, H., 2013. DNA origami technology for biomaterials applications. Biomater. Sci. 1 (4), 347–360.
Evans-Nguyen, K.M., Fuierer, R.R., Fitchett, B.D., Tolles, L.R., Conboy, J.C., Schoenfisch, M.H., 2006. Changes in adsorbed fibrinogen upon conversion to fibrin. Langmuir 22 (11), 5115–5121.
Eweida, A., Marei, M., 2015. Naturally occurring extracellular matrix scaffolds for dermal regeneration: do they really need cells? BioMed Res. Int. 839694.
Fangueiro, J.F., Veiga, F., Silva, A.M., Souto, E.B., 2016. Ocular drug delivery-new strategies for targeting anterior and posterior segments of the eye. Curr. Pharm. Des. 22 (9), 1135–1146.
Farahani, B.V., Ghasemzadeh, H., Afraz, S., 2016. Thermodynamic studies of insulin loading into a glucose responsive hydrogel based on chitosan-polyacrylamide-polyethylene glycol. J. Chin. Chem. Soc. 63 (5), 438–444.
Feng, C., Wang, Z., Jiang, C., Kong, M., Zhou, X., Li, Y., et al., 2013. Chitosan/o-carboxymethyl chitosan nanoparticles for efficient and safe oral anticancer drug delivery: in vitro and in vivo evaluation. Int. J. Pharm. 457 (1), 158–167.
Flume, P.A., VanDevanter, D.R., 2015. Clinical applications of pulmonary delivery of antibiotics. Adv. Drug Deliv. Rev. 85, 1–6.
Foldbjerg, R., Dang, D.A., Autrup, H., 2011. Cytotoxicity and genotoxicity of silver nanoparticles in the human lung cancer cell line, A549. Arch. Toxicol. 85 (7), 743–750.
Fu, J., Ji, J., Fan, D., Shen, J., 2006. Construction of antibacterial multilayer films containing nanosilver via layer-by-layer assembly of heparin and chitosan-silver ions complex. J. Biomed. Mater. Res., A 79 (3), 665–674.
Gajbhiye, K.R., Gajbhiye, V., Siddiqui, I.A., Pilla, S., Soni, V., 2017. Ascorbic acid tethered polymeric nanoparticles enable efficient brain delivery of galantamine: an in vitro-in vivo study. Sci. Rep. 7 (1), 11086.
García-Vargas, M., González-Chomón, C., Magariños, B., Concheiro, A., Alvarez-Lorenzo, C., Bucio, E., 2014. Acrylic polymer-grafted polypropylene sutures for covalent immobilization or reversible adsorption of vancomycin. Int. J. Pharm. 461 (1–2), 286–295.
Garg, T., Goyal, A.K., 2014. Biomaterial-based scaffolds–current status and future directions. Expert Opin. Drug Deliv. 11 (5), 767–789.
Garg, T., Rath, G., Goyal, A.K., 2015. Biomaterials-based nanofiber scaffold: targeted and controlled carrier for cell and drug delivery. J. Drug Target. 23 (3), 202–221.

Gauvin, R., Chen, Y.-C., Lee, J.W., Soman, P., Zorlutuna, P., Nichol, J.W., et al., 2012. Microfabrication of complex porous tissue engineering scaffolds using 3D projection stereolithography. Biomaterials 33 (15), 3824–3834.
Goins, A., Ramaswamy, V., Dirr, E., Dulany, K., Irby, S., Webb, A., et al., 2017. Development of poly(1,8 octanediol-*co*-citrate) and poly(acrylic acid) nanofibrous scaffolds for wound healing applications. Biomed. Mater. 13 (1), 015002.
Gottenbos, B., Busscher, H., Van Der Mei, H., Nieuwenhuis, P., 2002. Pathogenesis and prevention of biomaterial centered infections. J. Mater. Sci.: Mater. Med. 13 (8), 717–722.
Grund, S., Bauer, M., Fischer, D., 2011. Polymers in drug delivery—state of the art and future trends. Adv. Eng. Mater. 13 (3), B61–B87.
Guney, A., Kara, F., Ozgen, O., Aksoy, E.A., Hasirci, V., Hasirci, N., 2013. Surface modification of polymeric biomaterials. Biomater. Surf. Sci. Chapter 5, 89–158.
Gupta, H., Aqil, M., 2012. Contact lenses in ocular therapeutics. Drug Discov. Today 17 (9-10), 522–527.
Gurturk, Z., Tezcaner, A., Dalgic, A.D., Korkmaz, S., Keskin, D., 2017. Maltodextrin modified liposomes for drug delivery through the blood–brain barrier. MedChemComm 8 (6), 1337–1345.
Guven, S., Chen, P., Inci, F., Tasoglu, S., Erkmen, B., Demirci, U., 2015. Multiscale assembly for tissue engineering and regenerative medicine. Trends Biotechnol. 33 (5), 269–279.
Gwak, G.H., Paek, S.M., Oh, J.M., 2012. Electrophoretic preparation of an organic–inorganic hybrid of layered metal hydroxide and hydrogel for a potential drug-delivery system. Eur. J. Inorg. Chem. 2012 (32), 5269–5275.
Hadebe, S.I., Ngubane, P.S., Serumula, M.R., Musabayane, C.T., 2014. Transdermal delivery of insulin by amidated pectin hydrogel matrix patch in streptozotocin-induced diabetic rats: effects on some selected metabolic parameters. PLoS One 9 (7), e101461.
Hajipour, M.J., Raheb, J., Akhavan, O., Arjmand, S., Mashinchian, O., Rahman, M., et al., 2015. Personalized disease-specific protein corona influences the therapeutic impact of graphene oxide. Nanoscale 7 (19), 8978–8994.
Hall-Stoodley, L., Costerton, J.W., Stoodley, P., 2004. Bacterial biofilms: from the natural environment to infectious diseases. Nat. Rev. Microbiol. 2 (2), 95.
Hamad, I., Hunter, A.C., Rutt, K.J., Liu, Z., Dai, H., Moghimi, S.M., 2008. Complement activation by PEGylated single-walled carbon nanotubes is independent of C1q and alternative pathway turnover. Mol. Immunol. 45 (14), 3797–3803.
Hamad, I., Al-Hanbali, O., Hunter, A.C., Rutt, K.J., Andresen, T.L., Moghimi, S.M., 2010. Distinct polymer architecture mediates switching of complement activation pathways at the nanosphere–serum interface: Implications for stealth nanoparticle engineering. ACS Nano 4 (11), 6629–6638.
Hara, K., Aoki, K., Usui, Y., Shimizu, M., Narita, N., Ogihara, N., et al., 2011. Evaluation of CNT toxicity by comparison to tattoo ink. Mater. Today 14 (9), 434–440.
Hardy, J.G., Hernandez, D.S., Cummings, D.M., Edwards, F.A., Shear, J.B., Schmidt, C.E., 2015. Multiphoton microfabrication of conducting polymer-based biomaterials. J. Mater. Chem. B 3 (25), 5001–5004.
Harris, D.A., Fong, A.J., Buchanan, E.P., Monson, L., Khechoyan, D., Lam, S., 2014. History of synthetic materials in alloplastic cranioplasty. Neurosurg. Focus 36 (4), E20.
Harris, R., Acosta, N., Heras, A., 2013. Chitosan and inhalers: a bioadhesive polymer for pulmonary drug delivery. Inhaler Devices. Elsevier.
He, C., Nie, W., Feng, W., 2014. Engineering of biomimetic nanofibrous matrices for drug delivery and tissue engineering. J. Mater. Chem. B 2 (45), 7828–7848.
He, W., Benson, R., 2017. Polymeric biomaterials, Applied Plastics Engineering Handbook, *second ed*. Elsevier.
Hench, L., Kokubo, T., 2016. Properties of bioactive glasses and glass-ceramics. Handbook of Biomaterial Properties. Springer.
Hoffman, A.S., 2013. Stimuli-responsive polymers: biomedical applications and challenges for clinical translation. Adv. Drug Deliv. Rev. 65 (1), 10–16.
Hoffmann, O., Angelov, N., Gallez, F., Jung, R.E., Weber, F.E., 2008. The zirconia implant-bone interface: a preliminary histologic evaluation in rabbits. Int. J. Oral Maxillofac. Implants 23 (4), 691.
Holowka, E., Bhatia, S.K., 2016. Drug Delivery. Springer.
Holowka, E.P., Bhatia, S.K., 2014. Controlled-release systems. Drug Delivery. Springer.
Hoskison, E., Daniel, M., Al-Zahid, S., Shakesheff, K., Bayston, R., Birchall, J., 2013. Drug delivery to the ear. Ther. Deliv. 4 (1), 115–124.

Hou, X., Zhou, H., Wang, L., Tang, J., Chen, C., Jiang, G., et al., 2017. Multifunctional near-infrared dye-magnetic nanoparticles for bioimaging and cancer therapy. Cancer Lett. 390, 168–175.
Hu, W., Peng, C., Lv, M., Li, X., Zhang, Y., Chen, N., et al., 2011. Protein corona-mediated mitigation of cytotoxicity of graphene oxide. ACS Nano 5 (5), 3693–3700.
Huang, G., Liu, Y., Chen, L., 2017. Chitosan and its derivatives as vehicles for drug delivery. Drug Deliv. 24 (2), 108–113.
Hubbell, J.A., Thomas, S.N., Swartz, M.A., 2009. Materials engineering for immunomodulation. Nature 462 (7272), 449.
Hume, E., Baveja, J., Muir, B., Schubert, T., Kumar, N., Kjelleberg, S., et al., 2004. The control of *Staphylococcus epidermidis* biofilm formation and in vivo infection rates by covalently bound furanones. Biomaterials 25 (20), 5023–5030.
Hühn, D., Kantner, K., Geidel, C., Brandholt, S., De Cock, I., Soenen, S.J., et al., 2013. Polymer-coated nanoparticles interacting with proteins and cells: focusing on the sign of the net charge. ACS Nano 7 (4), 3253–3263.
Hwang, T.-L., Aljuffali, I.A., Lin, C.-F., Chang, Y.-T., Fang, J.-Y., 2015. Cationic additives in nanosystems activate cytotoxicity and inflammatory response of human neutrophils: lipid nanoparticles versus polymeric nanoparticles. Int. J. Nanomed. 10, 371.
Imanishi, Y., 2018. Synthesis of Biocomposite Materials: Chemical and Biological Modifications of Natural Polymers. CRC Press.
Ingle, A., Shende, S., Pandit, R., Paralikar, P., Tikar, S., Kon, K., et al., 2016. Nanotechnological applications for the control of pulmonary infections. The Microbiology of Respiratory System Infections. Elsevier.
Irani, M., Mir Mohamad Sadeghi, G., Haririan, I., 2018. Electrospun biocompatible poly(ε-caprolactonediol)-based polyurethane core/shell nanofibrous scaffold for controlled release of temozolomide. Int. J. Polym. Mater. Polym. Biomater. 67 (6), 361–366.
Isaacs, L., 2014. Stimuli responsive systems constructed using cucurbit [*n*] uril-type molecular containers. Acc. Chem. Res. 47 (7), 2052–2062.
Ishiyama, G., Lopez, I.A., Ishiyama, P., Vinters, H.V., Ishiyama, A., 2017. The blood labyrinthine barrier in the human normal and Meniere's disease macula utricle. Sci. Rep. 7 (1), 253.
Islam, M.S., Haque, P., Rashid, T.U., Khan, M.N., Mallik, A.K., Khan, M.N.I., et al., 2017. Core–shell drug carrier from folate conjugated chitosan obtained from prawn shell for targeted doxorubicin delivery. J. Mater. Sci.: Mater. Med. 28 (4), 55.
Ita, K., 2014. Transdermal drug delivery: progress and challenges. J. Drug Deliv. Sci. Technol. 24 (3), 245–250.
Ji, J., Wang, L., Yu, H., Chen, Y., Zhao, Y., Zhang, H., et al., 2014. Chemical modifications of chitosan and its applications. Polym. Plast. Technol. Eng. 53 (14), 1494–1505.
Jiang, Y., Chen, J., Deng, C., Suuronen, E.J., Zhong, Z., 2014. Click hydrogels, microgels and nanogels: emerging platforms for drug delivery and tissue engineering. Biomaterials 35 (18), 4969–4985.
Jing, L., Liang, X., Li, X., Yang, Y., Dai, Z., 2013. Covalent attachment of Mn-porphyrin onto doxorubicin-loaded poly(lactic acid) nanoparticles for potential magnetic resonance imaging and pH-sensitive drug delivery. Acta Biomater. 9 (12), 9434–9441.
Jones, J.A., McNally, A.K., Chang, D.T., Qin, L.A., Meyerson, H., Colton, E., et al., 2008. Matrix metalloproteinases and their inhibitors in the foreign body reaction on biomaterials. J. Biomed. Mater. Res., A 84 (1), 158–166.
Ju, E., Li, Z., Liu, Z., Ren, J., Qu, X., 2014. Near-infrared light-triggered drug-delivery vehicle for mitochondria-targeted chemo-photothermal therapy. ACS Appl. Mater. Interfaces 6 (6), 4364–4370.
Jung, E., Lee, E.Y., Choi, H.-K., Ban, S.-J., Choi, S.-H., Kim, J.S., et al., 2015. Development of drug-in-adhesive patch formulations for transdermal delivery of fluoxetine: in vitro and in vivo evaluations. Int. J. Pharm. 487 (1-2), 49–55.
Kafa, H., Wang, J.T.-W., Rubio, N., Klippstein, R., Costa, P.M., Hassan, H.A., et al., 2016. Translocation of LRP1 targeted carbon nanotubes of different diameters across the blood–brain barrier in vitro and in vivo. J. Control. Release 225, 217–229.
Kahn, J.S., Hu, Y., Willner, I., 2017. Stimuli-responsive DNA-based hydrogels: from basic principles to applications. Acc. Chem. Res. 50 (4), 680–690.
Kanamala, M., Wilson, W.R., Yang, M., Palmer, B.D., Wu, Z., 2016. Mechanisms and biomaterials in pH-responsive tumour targeted drug delivery: a review. Biomaterials 85, 152–167.

Kang-Mieler, J.J., Dosmar, E., Liu, W., Mieler, W.F., 2017. Extended ocular drug delivery systems for the anterior and posterior segments: biomaterial options and applications. Expert Opin. Drug Deliv. 14 (5), 611–620.
Karimi, M., Ghasemi, A., Zangabad, P.S., Rahighi, R., Basri, S.M.M., Mirshekari, H., et al., 2016. Smart micro/nanoparticles in stimulus-responsive drug/gene delivery systems. Chem. Soc. Rev. 45 (5), 1457–1501.
Katsikogianni, M., Missirlis, Y., 2004. Concise review of mechanisms of bacterial adhesion to biomaterials and of techniques used in estimating bacteria-material interactions. Eur. Cell Mater. 8 (3), 37–57.
Kavanaugh, T.E., Werfel, T.A., Cho, H., Hasty, K.A., Duvall, C.L., 2016. Particle-based technologies for osteoarthritis detection and therapy. Drug Deliv. Transl. Res. 6 (2), 132–147.
Kessenbrock, K., Wang, C.-Y., Werb, Z., 2015. Matrix metalloproteinases in stem cell regulation and cancer. Matrix Biol. 44, 184–190.
Khambhla, E., Shah, V., Baviskar, K., 2016. Drug delivery to CNS: challenges and opportunities with emphasis on biomaterials based drug delivery strategies. Curr. Pharm. Des. 22 (19), 2913–2922.
Kikuchi, I.S., Cardoso Galante, R.S., Dua, K., Malipeddi, V.R., Awasthi, R., Ghisleni, D.D., et al., 2017. Hydrogel based drug delivery systems: a review with special emphasis on challenges associated with decontamination of hydrogels and biomaterials. Curr. Drug Deliv. 14 (7), 917–925.
Kim, D.-K., Park, S.-N., Park, K.-H., Park, C.W., Yang, K.-J., Kim, J.-D., et al., 2015. Development of a drug delivery system for the inner ear using poly(amino acid)-based nanoparticles. Drug Deliv. 22 (3), 367–374.
Kim, J.-Y., Han, M.-R., Kim, Y.-H., Shin, S.-W., Nam, S.-Y., Park, J.-H., 2016. Tip-loaded dissolving microneedles for transdermal delivery of donepezil hydrochloride for treatment of Alzheimer's disease. Eur. J. Pharm. Biopharm. 105, 148–155.
Kim, Y.-J., Matsunaga, Y.T., 2017. Thermoresponsive polymers and their application as smart biomaterials. J. Mater. Chem. B 5 (23), 4307–4321.
Klement, P., Du, Y.J., Berry, L.R., Tressel, P., Chan, A.K., 2006. Chronic performance of polyurethane catheters covalently coated with ATH complex: a rabbit jugular vein model. Biomaterials 27 (29), 5107–5117.
Ko, P.-T., Lee, I.-C., Chen, M.-C., Tsai, S.-W., 2015. Polymer microneedles fabricated from PCL and PCL/PEG blends for transdermal delivery of hydrophilic compounds. J. Taiwan Inst. Chem. Eng. 51, 1–8.
Kohane, D.S., 2007. Microparticles and nanoparticles for drug delivery. Biotechnol. Bioeng. 96 (2), 203–209.
Kohane, D.S., Tse, J.Y., Yeo, Y., Padera, R., Shubina, M., Langer, R., 2006. Biodegradable polymeric microspheres and nanospheres for drug delivery in the peritoneum. J. Biomed. Mater. Res., A 77 (2), 351–361.
Kono, K., Ozawa, T., Yoshida, T., Ozaki, F., Ishizaka, Y., Maruyama, K., et al., 2010. Highly temperature-sensitive liposomes based on a thermosensitive block copolymer for tumor-specific chemotherapy. Biomaterials 31 (27), 7096–7105.
Kost, J., Wolfrum, J., Langer, R., 1987. Magnetically enhanced insulin release in diabetic rats. J. Biomed. Mater. Res., A 21 (12), 1367–1373.
Kraišnik, M., Đurić, A., Milutinović, M., 2018. Characterization of mechanical properties of metal biomaterials. Biomaterials in Clinical Practice. Springer.
Kresse, M., Pfefferer, D., Lawaczek, R., Wagner, S., Ebert, W., Elste, V., et al. 2000. Iron-Containing Nanoparticles with Double Coating and Their Use in Diagnosis and Therapy. Google Patents.
Kuche, K., Maheshwari, R., Tambe, V., Mak, K.-K., Jogi, H., Raval, N., et al., 2018. Carbon nanotubes (CNTs) based advanced dermal therapeutics: current trends and future potential. Nanoscale 10, 8911–8937.
Kumar Tekade, R., Maheshwari, R.G., Sharma, P.A., Tekade, M., Chauhan, A.S., 2015. siRNA therapy, challenges and underlying perspectives of dendrimer as delivery vector. Curr. Pharm. Des. 21 (31), 4614–4636.
Kuo, W.-H., Wang, M.-J., Chang, C.-W., Wei, T.-C., Lai, J.-Y., Tsai, W.-B., et al., 2012. Improvement of hemocompatibility on materials by photoimmobilization of poly(ethylene glycol). J. Mater. Chem. 22 (19), 9991–9999.
Lai, M.-H., Clay, N.E., Kim, D.H., Kong, H., 2015. Bacteria-mimicking nanoparticle surface functionalization with targeting motifs. Nanoscale 7 (15), 6737–6744.
Lalu, L., Tambe, V., Pradhan, D., Nayak, K., Bagchi, S., Maheshwari, R., et al., 2017. Novel nanosystems for the treatment of ocular inflammation: Current paradigms and future research directions. J. Control. Release 268, 19–39.
Lancina III, M.G., Singh, S., Kompella, U.B., Husain, S., Yang, H., 2017. Fast dissolving dendrimer nanofiber mats as alternative to eye drops for more efficient antiglaucoma drug delivery. ACS Biomater. Sci. Eng. 3 (8), 1861–1868.
Langer, R., 1990. New methods of drug delivery. Science 249 (4976), 1527–1533.

Langer, R., Peppas, N.A., 1981. Present and future applications of biomaterials in controlled drug delivery systems. Biomaterials 2 (4), 201–214.

Lee, Y., Park, S.Y., Kim, C., Park, T.G., 2009. Thermally triggered intracellular explosion of volume transition nanogels for necrotic cell death. J. Control. Release 135 (1), 89–95.

Leong, K.W., Sung, H.-W., 2013. Nanoparticle-and biomaterials-mediated oral delivery for drug, gene, and immunotherapy. Adv. Drug Deliv. Rev. 65 (6), 757–758.

Li, H., Xu, Y., Xu, H., Chang, J., 2014a. Electrospun membranes: control of the structure and structure related applications in tissue regeneration and drug delivery. J. Mater. Chem. B 2 (34), 5492–5510.

Li, H., Wei, R., Yan, G., Sun, J., Li, C., Wang, H., et al. 2018. Smart self-assembled nanosystem based on water-soluble pillararene and rare-earth-doped upconversion nanoparticles for pH-responsive drug delivery. ACS Appl. Mater. Interfaces 10, 4910–4920.

Li, J., Chu, M.K., Gordijo, C.R., Abbasi, A.Z., Chen, K., Adissu, H.A., et al., 2015. Microfabricated microporous membranes reduce the host immune response and prolong the functional lifetime of a closed-loop insulin delivery implant in a type 1 diabetic rat model. Biomaterials 47, 51–61.

Li, R.W.K., Chow, T.W., Matinlinna, J.P., 2014b. Ceramic dental biomaterials and CAD/CAM technology: state of the art. J. Prosthodont. Res. 58 (4), 208–216.

Lin, Z., Gao, W., Hu, H., Ma, K., He, B., Dai, W., et al., 2014. Novel thermosensitive hydrogel system with paclitaxel nanocrystals: High drug-loading, sustained drug release and extended local retention guaranteeing better efficacy and lower toxicity. J. Control. Release 174, 161–170.

Lindberg, H.K., Falck, G.C.-M., Suhonen, S., Vippola, M., Vanhala, E., Catalán, J., et al., 2009. Genotoxicity of nanomaterials: DNA damage and micronuclei induced by carbon nanotubes and graphite nanofibres in human bronchial epithelial cells in vitro. Toxicol. Lett. 186 (3), 166–173.

Liu, B., Hu, J., Meng, Q., 2009. Nonwoven supported temperature-sensitive poly(*N*-isopropylacrylamide)/polyurethane copolymer hydrogel with antibacterial activity. J. Biomed. Mater. Res., B: Appl. Biomater. 89 (1), 1–8.

Liu, C., Liu, X.-N., Wang, G.-L., Hei, Y., Meng, S., Yang, L.-F., et al., 2017a. A dual-mediated liposomal drug delivery system targeting the brain: rational construction, integrity evaluation across the blood–brain barrier, and the transporting mechanism to glioma cells. Int. J. Nanomed. 12, 2407.

Liu, D., Yang, F., Xiong, F., Gu, N., 2016. The smart drug delivery system and its clinical potential. Theranostics 6 (9), 1306.

Liu, H., Hao, J., Li, K.S., 2013. Current strategies for drug delivery to the inner ear. Acta Pharm. Sin. B 3 (2), 86–96.

Liu, J., Liu, J., Xu, H., Zhang, Y., Chu, L., Liu, Q., et al., 2014a. Novel tumor-targeting, self-assembling peptide nanofiber as a carrier for effective curcumin delivery. Int. J. Nanomed. 9, 197.

Liu, J., Detrembleur, C., Pauw-Gillet, D., Mornet, S., Jérôme, C., Duguet, E., 2015. Gold nanorods coated with mesoporous silica shell as drug delivery system for remote near infrared light-activated release and potential phototherapy. Small 11 (19), 2323–2332.

Liu, M., Song, X., Wen, Y., Zhu, J.-L., Li, J., 2017b. injectable thermoresponsive hydrogel formed by alginate-*g*-poly(*N*-isopropylacrylamide) that releases doxorubicin-encapsulated micelles as a smart drug delivery system. ACS Appl. Mater. Interfaces 9 (41), 35673–35682.

Liu, R., Xu, X., Zhuang, X., Cheng, B., 2014b. Solution blowing of chitosan/PVA hydrogel nanofiber mats. Carbohydr. Polym. 101, 1116–1121.

Liu, T., Wu, T., Liu, H., Ke, B., Huang, H., Jiang, Z., et al., 2014c. Ultraviolet-crosslinked hydrogel sustained-release hydrophobic antibiotics with long-term antibacterial activity and limited cytotoxicity. J. Appl. Polym. Sci. 131 (13), 40438.

Liu, Z., Wang, H., Wang, Y., Lin, Q., Yao, A., Cao, F., et al., 2012. The influence of chitosan hydrogel on stem cell engraftment, survival and homing in the ischemic myocardial microenvironment. Biomaterials 33 (11), 3093–3106.

Liu, Z.-M., Xu, Z.-K., Wan, L.-S., Wu, J., Ulbricht, M., 2005. Surface modification of polypropylene microfiltration membranes by the immobilization of poly(*N*-vinyl-2-pyrrolidone): a facile plasma approach. J. Membr. Sci. 249 (1-2), 21–31.

Lopes, C.M., Bettencourt, C., Rossi, A., Buttini, F., Barata, P., 2016. Overview on gastroretentive drug delivery systems for improving drug bioavailability. Int. J. Pharm. 510 (1), 144–158.

Losi, P., Lombardi, S., Briganti, E., Soldani, G., 2004. Luminal surface microgeometry affects platelet adhesion in small-diameter synthetic grafts. Biomaterials 25 (18), 4447–4455.
Lu, C.-H., Qi, X.-J., Li, J., Yang, H.-H., 2015. Aptamer-based hydrogels and their applications. Aptamers Selected by Cell-SELEX for Theranostics. Springer.
Lu, H., Wang, J., Wang, T., Zhong, J., Bao, Y., Hao, H., 2016. Recent progress on nanostructures for drug delivery applications. J. Nanomater. 2016, 20.
Luan, S., Shi, H., Yao, Z., Wang, J., Song, Y., Yin, J., 2010. Effect of electron beam irradiation sterilization on the biomedical poly(octene-*co*-ethylene)/polypropylene films. Nucl. Instrum. Methods Phys. Res., Sect. B 268 (9), 1474–1477.
Luan, S., Yang, H., Shi, H., Zhao, J., Wang, J., Yin, J., 2011. Stabilization of polypropylene, polypropylene blends with poly(styrene-*b*-(ethylene-*co*-butylene)-*b*-styrene) under irradiation: a comparative investigation. Nucl. Instrum. Methods Phys. Res., Sect. B 269 (2), 94–99.
Lue, S.J., Chen, C.-H., Shih, C.-M., Tsai, M.-C., Kuo, C.-Y., Lai, J.-Y., 2011. Grafting of poly(*N*-isopropylacrylamide-*co*-acrylic acid) on micro-porous polycarbonate films: regulating lower critical solution temperatures for drug controlled release. J. Membr. Sci. 379 (1-2), 330–340.
Luo, H., Sun, G., Shen, Y., Xu, K., 2014. Evaluation of the di (2-ethylhexyl) phthalate released from polyvinyl chloride medical devices that contact blood. SpringerPlus 3 (1), 58.
Luo, J., Deng, Y., Sun, Y., 2010. Antimicrobial activity and biocompatibility of polyurethane—iodine complexes. J. Bioact. Compat. Polym. 25 (2), 185–206.
MacNeil, S., 2008. Biomaterials for tissue engineering of skin. Mater. Today 11 (5), 26–35.
Mahapatro, A., Singh, D.K., 2011. Biodegradable nanoparticles are excellent vehicle for site directed in-vivo delivery of drugs and vaccines. J. Nanobiotechnol. 9 (1), 55.
Maheshwari, R., Tekade, M., Sharma, P.A., Tekade, R.K., 2015a. Nanocarriers assisted siRNA gene therapy for the management of cardiovascular disorders. Curr. Pharm. Des. 21 (30), 4427–4440.
Maheshwari, R., Tekade, M., Gondaliya, P., Kalia, K., D'Emanuele, A., Tekade, R.K., 2017. Recent advances in exosome-based nanovehicles as RNA interference therapeutic carriers. Nanomedicine (London) 12 (21), 2653–2675.
Maheshwari, R.G., Tekade, R.K., Sharma, P.A., Darwhekar, G., Tyagi, A., Patel, R.P., et al., 2012. Ethosomes and ultradeformable liposomes for transdermal delivery of clotrimazole: a comparative assessment. Saudi Pharm. J. 20 (2), 161–170.
Maheshwari, R.G., Thakur, S., Singhal, S., Patel, R.P., Tekade, M., Tekade, R.K., 2015b. Chitosan encrusted non-ionic surfactant based vesicular formulation for topical administration of ofloxacin. Sci. Adv. Mater. 7 (6), 1163–1176.
Mahmoudi, M., Saeedi-Eslami, S.N., Shokrgozar, M.A., Azadmanesh, K., Hassanlou, M., Kalhor, H.R., et al., 2012. Cell "vision": complementary factor of protein corona in nanotoxicology. Nanoscale 4 (17), 5461–5468.
Maji, P., Gandhi, A., Jana, S., Maji, N., 2013. Preparation and characterization of maleic anhydride cross-linked chitosan-polyvinyl alcohol hydrogel matrix transdermal patch. J. PharmaSciTech 2, 62–67.
Malachowski, K., Breger, J., Kwag, H.R., Wang, M.O., Fisher, J.P., Selaru, F.M., et al., 2014. Stimuli-responsive theragrippers for chemomechanical controlled release. Angew. Chem. 126 (31), 8183–8187.
Maleki, M., Amani-Tehran, M., Latifi, M., Mathur, S., 2014. A study on electrospun nanofibrous mats for local antibiotic delivery. Adv. Mater. Res. 829, 510–514. Trans Tech Publ.
Mandal, A., Bisht, R., Rupenthal, I.D., Mitra, A.K., 2017. Polymeric micelles for ocular drug delivery: from structural frameworks to recent preclinical studies. J. Control. Release 248, 96–116.
Martins, A.M., Eng, G., Caridade, S.G., Mano, J.O.F., Reis, R.L., Vunjak-Novakovic, G., 2014. Electrically conductive chitosan/carbon scaffolds for cardiac tissue engineering. Biomacromolecules 15 (2), 635–643.
Masserini, M., 2013. Nanoparticles for brain drug delivery. ISRN Biochem. 238428.
Masutani, E.M., Yoza, B.A., Tanaka, T.T., Russ, C.R., Ellison, A.K.D., Reiss, D.S., 2016. Apparatus for Building Complex 3D Biomimetic Scaffolds. Google Patents.
Mathur, A.B., 2009. Regenerative wound healing via biomaterials. Bioengineering Research of Chronic Wounds. Springer.
McCall, A.A., Swan, E.E.L., Borenstein, J.T., Sewell, W.F., Kujawa, S.G., McKenna, M.J., 2010. Drug delivery for treatment of inner ear disease: current state of knowledge. Ear Hear. 31 (2), 156.

McKenzie, M., Betts, D., Suh, A., Bui, K., Kim, L.D., Cho, H., 2015. Hydrogel-based drug delivery systems for poorly water-soluble drugs. Molecules 20 (11), 20397–20408.
McMahon, R.E., Qu, X., Jimenez-Vergara, A.C., Bashur, C.A., Guelcher, S.A., Goldstein, A.S., et al., 2011. Hydrogel–electrospun mesh composites for coronary artery bypass grafts. Tissue Eng., C: Methods 17 (4), 451–461.
McNally, A.K., Anderson, J.M., 2015. Phenotypic expression in human monocyte-derived interleukin-4-induced foreign body giant cells and macrophages in vitro: dependence on material surface properties. J. Biomed. Mater. Res., A 103 (4), 1380–1390.
Mehra, N.K., Palakurthi, S., 2016. Interactions between carbon nanotubes and bioactives: a drug delivery perspective. Drug Discov. Today 21 (4), 585–597.
Metters, A., Lin, C., 2007. Biodegradable Hydrogels: Tailoring Properties and Function Through Chemistry and Structure. CRC Press, Taylor and Francis Group, Boca Raton, FL.
Michanetzis, G., Katsala, N., Missirlis, Y., 2003. Comparison of haemocompatibility improvement of four polymeric biomaterials by two heparinization techniques. Biomaterials 24 (4), 677–688.
Miklas, J.W., Dallabrida, S.M., Reis, L.A., Ismail, N., Rupnick, M., Radisic, M., 2013. QHREDGS enhances tube formation, metabolism and survival of endothelial cells in collagen-chitosan hydrogels. PLoS One 8 (8), e72956.
Mirshafiee, V., Mahmoudi, M., Lou, K., Cheng, J., Kraft, M.L., 2013. Protein corona significantly reduces active targeting yield. Chem. Commun. 49 (25), 2557–2559.
Mishra, A., Singh, S.K., Dash, D., Aswal, V.K., Maiti, B., Misra, M., et al., 2014. Self-assembled aliphatic chain extended polyurethane nanobiohybrids: emerging hemocompatible biomaterials for sustained drug delivery. Acta Biomater. 10 (5), 2133–2146.
Mogoşanu, G., Popescu, F.C., Busuioc, C.J., Pârvănescu, H., Lascăr, I., 2012. Natural products locally modulators of the cellular response: therapeutic perspectives in skin burns. Rom. J. Morphol. Embryol. 53 (2), 249–262.
Mohtaram, N.K., Montgomery, A., Willerth, S.M., 2013. Biomaterial-based drug delivery systems for the controlled release of neurotrophic factors. Biomed. Mater. 8 (2), 022001.
Moreno-Sastre, M., Pastor, M., Salomon, C., Esquisabel, A., Pedraz, J., 2015. Pulmonary drug delivery: a review on nanocarriers for antibacterial chemotherapy. J. Antimicrob. Chemother. 70 (11), 2945–2955.
Moreno-Sastre, M., Pastor, M., Esquisabel, A., Sans, E., Viñas, M., Fleischer, A., et al., 2016. Pulmonary delivery of tobramycin-loaded nanostructured lipid carriers for *Pseudomonas aeruginosa* infections associated with cystic fibrosis. Int. J. Pharm. 498 (1-2), 263–273.
Morie, A., Garg, T., Goyal, A.K., Rath, G., 2016. Nanofibers as novel drug carrier–an overview. Artif. Cells Nanomed. Biotechnol. 44 (1), 135–143.
Motoyama, K., Tanida, Y., Hata, K., Hayashi, T., Higashi, T., Ishitsuka, Y., et al., 2014. Potential use of a megamolecular polysaccharide sacran as a hydrogel-based sustained release system. Chem. Pharm. Bull. 62 (7), 636–641.
Muller, J., Decordier, I., Hoet, P.H., Lombaert, N., Thomassen, L., Huaux, F., et al., 2008. Clastogenic and aneugenic effects of multi-wall carbon nanotubes in epithelial cells. Carcinogenesis 29 (2), 427–433.
Mura, S., Nicolas, J., Couvreur, P., 2013. Stimuli-responsive nanocarriers for drug delivery. Nat. Mater. 12 (11), 991.
Nagase, K., Kobayashi, J., Kikuchi, A., Akiyama, Y., Kanazawa, H., Okano, T., 2008. Effects of graft densities and chain lengths on separation of bioactive compounds by nanolayered thermoresponsive polymer brush surfaces. Langmuir 24 (2), 511–517.
Narita, N., Kobayashi, Y., Nakamura, H., Maeda, K., Ishihara, A., Mizoguchi, T., et al., 2009. Multiwalled carbon nanotubes specifically inhibit osteoclast differentiation and function. Nano Lett. 9 (4), 1406–1413.
Netsomboon, K., Bernkop-Schnürch, A., 2016. Mucoadhesive vs. mucopenetrating particulate drug delivery. Eur. J. Pharm. Biopharm. 98, 76–89.
Nguyen, T.T., Van Giau, V., Vo, T.K., 2017. Current advances in transdermal delivery of drugs for Alzheimer's disease. Indian J. Pharmacol. 49 (2), 145.
Nyska, A., Schiffenbauer, Y.S., Brami, C.T., Maronpot, R.R., Ramot, Y., 2014. Histopathology of biodegradable polymers: challenges in interpretation and the use of a novel compact MRI for biocompatibility evaluation. Polym. Adv. Technol. 25 (5), 461–467.
Owen, C.A., Selvakumaran, J., Notingher, I., Jell, G., Hench, L.L., Stevens, M.M., 2006. In vitro toxicology evaluation of pharmaceuticals using Raman micro-spectroscopy. J. Cell. Biochem. 99 (1), 178–186.

Owens III, D.E., Peppas, N.A., 2006. Opsonization, biodistribution, and pharmacokinetics of polymeric nanoparticles. Int. J. Pharm. 307 (1), 93–102.
Özkurt, Z., Kazazoğlu, E., 2011. Zirconia dental implants: a literature review. J. Oral Implantol. 37 (3), 367–376.
Packhaeuser, C., Schnieders, J., Oster, C., Kissel, T., 2004. In situ forming parenteral drug delivery systems: an overview. Eur. J. Pharm. Biopharm. 58 (2), 445–455.
Padera, R., Bellas, E., Julie, Y.T., Hao, D., Kohane, D.S., 2008. Local myotoxicity from sustained release of bupivacaine from microparticles. Anesthesiology 108 (5), 921–928.
Padera, R.F., Tse, J.Y., Bellas, E., Kohane, D.S., 2006. Tetrodotoxin for prolonged local anesthesia with minimal myotoxicity. Muscle Nerve 34 (6), 747–753.
Parida, P., Behera, A., Mishra, S.C., 2012. Classification of biomaterials used in medicine. Int. J. Adv. Appl. Sci. 1 (3), 125–129.
Park, J., Lakes, R.S., 2007. Biomaterials: An Introduction. Springer Science & Business Media.
Pastore, M.N., Kalia, Y.N., Horstmann, M., Roberts, M.S., 2015. Transdermal patches: history, development and pharmacology. Br. J. Pharmacol. 172 (9), 2179–2209.
Paula, A.J., Araujo Junior, R.T., Martinez, D.S.F.T., Paredes-Gamero, E.J., Nader, H.B., Durán, N., et al., 2013. Influence of protein corona on the transport of molecules into cells by mesoporous silica nanoparticles. ACS Appl. Mater. Interfaces 5 (17), 8387–8393.
Peppas, N.A., Van Blarcom, D.S., 2016. Hydrogel-based biosensors and sensing devices for drug delivery. J. Control. Release 240, 142–150.
Peppas, N.A., Ekerdt, B., Gomez-Burgaz, M., 2014. Method and Process for the Production of Multi-Coated Recognitive and Releasing Systems. Google Patents.
Perez, R.A., Won, J.-E., Knowles, J.C., Kim, H.-W., 2013. Naturally and synthetic smart composite biomaterials for tissue regeneration. Adv. Drug Deliv. Rev. 65 (4), 471–496.
Pillay, V., Dott, C., Choonara, Y.E., Tyagi, C., Tomar, L., Kumar, P., et al., 2013. A review of the effect of processing variables on the fabrication of electrospun nanofibers for drug delivery applications. J. Nanomater. 789289.
Pillay, V., Tsai, T.S., Choonara, Y.E., du Toit, L.C., Kumar, P., Modi, G., et al., 2014. A review of integrating electroactive polymers as responsive systems for specialized drug delivery applications. J. Biomed. Mater. Res., A 102 (6), 2039–2054.
Potter, F.F.E., 2018. Using "smart" biomaterials and systems for targeted drug delivery. Assessment 15, 43.
Prabhakaran, M.P., Venugopal, J., Chan, C.K., Ramakrishna, S., 2008. Surface modified electrospun nanofibrous scaffolds for nerve tissue engineering. Nanotechnology 19 (45), 455102.
Prausnitz, M.R., 2017. Engineering microneedle patches for vaccination and drug delivery to skin. Ann. Rev. Chem. Biomol. Eng. 8, 177–200.
Pritz, C.O., Dudás, J., Rask-Andersen, H., Schrott-Fischer, A., Glueckert, R., 2013. Nanomedicine strategies for drug delivery to the ear. Nanomedicine 8 (7), 1155–1172.
Pyrgiotakis, G., Bhowmick, T., Finton, K., Suresh, A., Kane, S., Bellare, J., et al., 2008. Cell (A549)–particle (Jasada bhasma) interactions using Raman spectroscopy. Biopolymers 89 (6), 555–564.
Qin, Y., Chen, J., Bi, Y., Xu, X., Zhou, H., Gao, J., et al., 2015. Near-infrared light remote-controlled intracellular anti-cancer drug delivery using thermo/pH sensitive nanovehicle. Acta Biomater. 17, 201–209.
Qiu, M., Wang, D., Liang, W., Liu, L., Zhang, Y., Chen, X., et al., 2018. Novel concept of the smart NIR-light-controlled drug release of black phosphorus nanostructure for cancer therapy. Proc. Natl. Acad. Sci. U.S.A. 115, 501–506.
Quinn, H.L., Bonham, L., Hughes, C.M., Donnelly, R.F., 2015. Design of a dissolving microneedle platform for transdermal delivery of a fixed-dose combination of cardiovascular drugs. J. Pharm. Sci. 104 (10), 3490–3500.
Rahman, M., Mahmoudi, M., 2015. Disease specific protein corona. In: Colloidal Nanoparticles for Biomedical Applications X. International Society for Optics and Photonics, 93380V.
Rahmany, M.B., Van Dyke, M., 2013. Biomimetic approaches to modulate cellular adhesion in biomaterials: a review. Acta Biomater. 9 (3), 5431–5437.
Rai, V.K., Mishra, N., Agrawal, A.K., Jain, S., Yadav, N.P., 2016. Novel drug delivery system: an immense hope for diabetics. Drug Deliv. 23 (7), 2371–2390.

Raphael, K.G., Marbach, J.J., Wolford, L.M., Keller, S.E., Bartlett, J.A., 1999. Self-reported systemic, immune-mediated disorders in patients with and without proplast-teflon implants of the temporomandibular joint. J. Oral Maxillofac. Surg. 57 (4), 364–370.
Ratner, B.D., Hoffman, A.S., Schoen, F.J., Lemons, J.E., 2004. Biomaterials Science: An Introduction to Materials in Medicine. Elsevier.
Reeve, L., Baldrick, P., 2017. Biocompatibility assessments for medical devices–evolving regulatory considerations. Expert Rev. Med. Devices 14 (2), 161–167.
Ruskowitz, E.R., DeForest, C.A., 2018. Photoresponsive biomaterials for targeted drug delivery and 4D cell culture. Nat. Rev. Mater. 3, 17087.
Sadeghi, M., Ganji, F., Taghizadeh, S.M., Daraei, B., 2016. Preparation and characterization of rivastigmine transdermal patch based on chitosan microparticles. Iran. J. Pharm. Res.: IJPR 15 (3), 283.
Saito, N., Haniu, H., Usui, Y., Aoki, K., Hara, K., Takanashi, S., et al., 2014. Safe clinical use of carbon nanotubes as innovative biomaterials. Chem. Rev. 114 (11), 6040–6079.
Salvador-Morales, C., Flahaut, E., Sim, E., Sloan, J., Green, M.L., Sim, R.B., 2006. Complement activation and protein adsorption by carbon nanotubes. Mol. Immunol. 43 (3), 193–201.
Sankar, D., Shalumon, K., Chennazhi, K., Menon, D., Jayakumar, R., 2014. Surface plasma treatment of poly (caprolactone) micro, nano, and multiscale fibrous scaffolds for enhanced osteoconductivity. Tissue Eng., A 20 (11-12), 1689–1702.
Santos, L.F., Correia, I.J., Silva, A.S., Mano, J.F., 2018. Biomaterials for drug delivery patches. Eur. J. Pharm. Sci. 118, 49–66.
Schanen, B.C., Karakoti, A.S., Seal, S., Drake III, D.R., Warren, W.L., Self, W.T., 2009. Exposure to titanium dioxide nanomaterials provokes inflammation of an in vitro human immune construct. ACS Nano 3 (9), 2523–2532.
Sciortino, N., Fedeli, S., Paoli, P., Brandi, A., Chiarugi, P., Severi, M., et al., 2017. Multiwalled carbon nanotubes for drug delivery: efficiency related to length and incubation time. Int. J. Pharm. 521 (1-2), 69–72.
Shamim, N., Hong, L., Hidajat, K., Uddin, M., 2006. Thermosensitive-polymer-coated magnetic nanoparticles: adsorption and desorption of bovine serum albumin. J. Colloid Interface Sci. 304 (1), 1–8.
Shankarraman, V., Davis-Gorman, G., Copeland, J.G., Caplan, M.R., McDonagh, P.F., 2012. Standardized methods to quantify thrombogenicity of blood-contacting materials via thromboelastography. J. Biomed. Mater. Res., B: Appl. Biomater. 100 (1), 230–238.
Sharma, P.A., Maheshwari, R., Tekade, M., Tekade, R.K., 2015. Nanomaterial based approaches for the diagnosis and therapy of cardiovascular diseases. Curr. Pharm. Des. 21 (30), 4465–4478.
Shi, H., Shi, D., Yin, L., Luan, S., Yin, J., Stagnaro, P., 2010. Preparation of PP-*g*-PEG by using partial preirradiated polypropylene as initiator and its properties. Polym. Bull. 65 (9), 929–940.
Shi, J., Sun, X., Li, J., Man, H., Shen, J., Yu, Y., et al., 2015a. Multifunctional near infrared-emitting long-persistence luminescent nanoprobes for drug delivery and targeted tumor imaging. Biomaterials 37, 260–270.
Shi, K., Liu, Z., Wei, Y.-Y., Wang, W., Ju, X.-J., Xie, R., et al., 2015b. Near-infrared light-responsive poly(*N*-isopropylacrylamide)/graphene oxide nanocomposite hydrogels with ultrahigh tensibility. ACS Appl. Mater. Interfaces 7 (49), 27289–27298.
Simmchen, J., Ventura, R., Segura, J., 2012. Progress in the removal of di-[2-ethylhexyl]-phthalate as plasticizer in blood bags. Transfus. Med. Rev. 26 (1), 27–37.
Singhvi, R., Kumar, A., Lopez, G.P., Stephanopoulos, G.N., Wang, D., Whitesides, G.M., et al., 1994. Engineering cell shape and function. Science 264 (5159), 696–698.
Sinha, R., Kim, G.J., Nie, S., Shin, D.M., 2006. Nanotechnology in cancer therapeutics: bioconjugated nanoparticles for drug delivery. Mol. Cancer Ther. 5 (8), 1909–1917.
Smith, B.R., Ghosn, E.E.B., Rallapalli, H., Prescher, J.A., Larson, T., Herzenberg, L.A., et al., 2014. Selective uptake of single-walled carbon nanotubes by circulating monocytes for enhanced tumour delivery. Nat. Nanotechnol. 9 (6), 481.
Son, Y.J., Kim, W.J., Yoo, H.S., 2014. Therapeutic applications of electrospun nanofibers for drug delivery systems. Arch. Pharm. Res. 37 (1), 69–78.
Soni, N., Soni, N., Pandey, H., Maheshwari, R., Kesharwani, P., Tekade, R.K., 2016. Augmented delivery of gemcitabine in lung cancer cells exploring mannose anchored solid lipid nanoparticles. J. Colloid Interface. Sci. 481, 107–116.

Soni, N., Tekade, M., Kesharwani, P., Bhattacharya, P., Maheshwari, R., Dua, K., et al., 2017. Recent advances in oncological submissions of dendrimer. Curr. Pharm. Des. 23 (21), 3084–3098.
Sonia, T.A., Sharma, C.P., 2014. Oral Delivery of Insulin. Elsevier.
Spivak, M.Y., Bubnov, R.V., Yemets, I.M., Lazarenko, L.M., Tymoshok, N.O., Ulberg, Z.R., 2013. Development and testing of gold nanoparticles for drug delivery and treatment of heart failure: a theranostic potential for PPP cardiology. EPMA J. 4 (1), 20.
Stewart, P.S., Costerton, J.W., 2001. Antibiotic resistance of bacteria in biofilms. Lancet 358 (9276), 135–138.
Stout, D.A., 2015. Recent advancements in carbon nanofiber and carbon nanotube applications in drug delivery and tissue engineering. Curr. Pharm. Des. 21 (15), 2037–2044.
Strong, L.E., West, J.L., 2015. Hydrogel-coated near infrared absorbing nanoshells as light-responsive drug delivery vehicles. ACS Biomater. Sci. Eng. 1 (8), 685–692.
Suedee, R., 2013. The use of molecularly imprinted polymers for dermal drug delivery. Pharm. Anal. Acta 4 (8), 1–23.
Suksuwan, A., Lomlim, L., Rungrotmongkol, T., Nakpheng, T., Dickert, F.L., Suedee, R., 2015. The composite nanomaterials containing (*R*)-thalidomide-molecularly imprinted polymers as a recognition system for enantioselective-controlled release and targeted drug delivery. J. Appl. Polym. Sci. 132 (18), 41930.
Swain, R.J., Jell, G., Stevens, M.M., 2008. Noninvasive analysis of cell cycle dynamics in single living cells with Raman micro-spectroscopy. J. Cell. Biochem. 104 (4), 1427–1438.
Ta, T., Bartolak-Suki, E., Park, E.-J., Karrobi, K., McDannold, N.J., Porter, T.M., 2014. Localized delivery of doxorubicin in vivo from polymer-modified thermosensitive liposomes with MR-guided focused ultrasound-mediated heating. J. Control. Release 194, 71–81.
Taha, A.A., Hriez, A.A., Wu, Y.-n, Wang, H., Li, F., 2014. Direct synthesis of novel vanadium oxide embedded porous carbon nanofiber decorated with iron nanoparticles as a low-cost and highly efficient visible-light-driven photocatalyst. J. Colloid Interface Sci. 417, 199–205.
Tahir, M., Cao, C., Mahmood, N., Butt, F.K., Mahmood, A., Idrees, F., et al., 2013. Multifunctional *g*-C_3N_4 nanofibers: a template-free fabrication and enhanced optical, electrochemical, and photocatalyst properties. ACS Appl. Mater. Interfaces 6 (2), 1258–1265.
Tai, Z., Ma, H., Liu, B., Yan, X., Xue, Q., 2012. Facile synthesis of Ag/GNS-*g*-PAA nanohybrids for antimicrobial applications. Colloids Surf., B: Biointerfaces 89, 147–151.
Takagi, A., Hirose, A., Nishimura, T., Fukumori, N., Ogata, A., Ohashi, N., et al., 2008. Induction of mesothelioma in p53 + / − mouse by intraperitoneal application of multi-wall carbon nanotube. J. Toxicol. Sci. 33 (1), 105–116.
Tan, J.M., Arulselvan, P., Fakurazi, S., Ithnin, H., Hussein, M.Z., 2014. A review on characterizations and biocompatibility of functionalized carbon nanotubes in drug delivery design. J. Nanomater. 2014, 111.
Tang, F., Li, L., Chen, D., 2012. Mesoporous silica nanoparticles: synthesis, biocompatibility and drug delivery. Adv. Mater. 24 (12), 1504–1534.
Tang, L., Thevenot, P., Hu, W., 2008. Surface chemistry influences implant biocompatibility. Curr. Top. Med. Chem. 8 (4), 270–280.
Tang, L., Zhao, C.-Y., Wang, X.-H., Li, R.-S., Yang, J.-R., Huang, Y.-P., et al., 2015. Macromolecular crowding of molecular imprinting: a facile pathway to produce drug delivery devices for zero-order sustained release. Int. J. Pharm. 496 (2), 822–833.
Tarn, D., Ashley, C.E., Xue, M., Carnes, E.C., Zink, J.I., Brinker, C.J., 2013. Mesoporous silica nanoparticle nanocarriers: biofunctionality and biocompatibility. Acc. Chem. Res. 46 (3), 792–801.
Tekade, R.K., Maheshwari, R., Soni, N., Tekade, M., 2017a. Carbon nanotubes in targeting and delivery of drugs. In: Kesharwani, P., Amin, M.C.I.M., Iyer, A. (Eds.), Nanotechnology-Based Approaches for Targeting and Delivery of Drugs and Genes. Academic Press.
Tekade, R.K., Maheshwari, R., Soni, N., Tekade, M., Chougule, M.B., 2017b. Nanotechnology for the Development of Nanomedicine. In: Kesharwani, P., Amin, M.C.I.M., Iyer, A. (Eds.), Nanotechnology-Based Approaches for Targeting and Delivery of Drugs and Genes. Academic Press.
Tekade, R.K., Maheshwari, R., Tekade, M., 2017c. Biopolymer-based nanocomposites for transdermal drug delivery. Biopolymer-Based Composites. Woodhead Publishing.
Tekade, R.K., Maheshwari, R., Tekade, M., Chougule, M.B., 2017d. Solid lipid nanoparticles for targeting and delivery of drugs and genes. In: Kesharwani, P., Amin, M.C.I.M., Iyer, A. (Eds.), Nanotechnology-Based Approaches for Targeting and Delivery of Drugs and Genes. Academic Press.

Tekade, R.K., Maheshwari, R., Jain, N.K., 2018. Toxicity of nanostructured biomaterials. Nanobiomaterials. Woodhead Publishing.
Tenzer, S., Docter, D., Kuharev, J., Musyanovych, A., Fetz, V., Hecht, R., et al., 2013. Rapid formation of plasma protein corona critically affects nanoparticle pathophysiology. Nat. Nanotechnol. 8 (10), 772.
Thamphiwatana, S., Gao, W., Pornpattananangkul, D., Zhang, Q., Fu, V., Li, J., et al., 2014. Phospholipase A2-responsive antibiotic delivery via nanoparticle-stabilized liposomes for the treatment of bacterial infection. J. Mater. Chem. B 2 (46), 8201–8207.
Tibbitt, M.W., Dahlman, J.E., Langer, R., 2016. Emerging frontiers in drug delivery. J. Am. Chem. Soc. 138 (3), 704–717.
Timko, B.P., Kohane, D.S., 2014. Prospects for Near-Infrared Technology in Remotely Triggered Drug Delivery. Taylor & Francis.
Tsou, Y.H., Zhang, X.Q., Zhu, H., Syed, S., Xu, X., 2017. Drug delivery to the brain across the blood–brain barrier using nanomaterials. Small 13 (43), 1701921.
Tuson, H.H., Weibel, D.B., 2013. Bacteria–surface interactions. Soft Matt. 9 (17), 4368–4380.
Ungaro, F., d'Angelo, I., Coletta, C., d'Emmanuele di Villa Bianca, R., Sorrentino, R., Perfetto, B., et al., 2012. Dry powders based on PLGA nanoparticles for pulmonary delivery of antibiotics: modulation of encapsulation efficiency, release rate and lung deposition pattern by hydrophilic polymers. J. Control. Release 157 (1), 149–159.
van Dijk, F., Teekamp, N., Beljaars, L., Post, E., Zuidema, J., Steendam, R., et al., 2017. Pharmacokinetics of a sustained release formulation of PDGFβ-receptor directed carrier proteins to target the fibrotic liver. J. Control. Release 269, 258–265.
Vashist, A., Vashist, A., Gupta, Y., Ahmad, S., 2014. Recent advances in hydrogel based drug delivery systems for the human body. J. Mater. Chem. B 2 (2), 147–166.
Vasilev, K., Sah, V.R., Goreham, R.V., Ndi, C., Short, R.D., Griesser, H.J., 2010. Antibacterial surfaces by adsorptive binding of polyvinyl-sulphonate-stabilized silver nanoparticles. Nanotechnology 21 (21), 215102.
Venuta, A., Wolfram, J., Shen, H., Ferrari, M., 2017. Post-nano strategies for drug delivery: multistage porous silicon microvectors. J. Mater. Chem. B 5 (2), 207–219.
Verrier, S., Blaker, J.J., Maquet, V., Hench, L.L., Boccaccini, A.R., 2004a. PDLLA/Bioglass composites for soft-tissue and hard-tissue engineering: an in vitro cell biology assessment. Biomaterials 25 (15), 3013–3021.
Verrier, S., Notingher, I., Polak, J., Hench, L., 2004b. In situ monitoring of cell death using Raman microspectroscopy. Biopolymers 74 (1-2), 157–162.
Vitte, J., Benoliel, A., Pierres, A., Bongrand, P., 2004. Is there a predictable relationship between surface physical-chemical properties and cell behaviour at the interface. Eur. Cell Mater. 7, 52–63.
Vittorio, O., Raffa, V., Cuschieri, A., 2009. Influence of purity and surface oxidation on cytotoxicity of multiwalled carbon nanotubes with human neuroblastoma cells. Nanomed.: Nanotechnol. Biol. Med. 5 (4), 424–431.
Walter, K.A., Cahan, M.A., Gur, A., Tyler, B., Hilton, J., Colvin, O.M., et al., 1994. Interstitial taxol delivered from a biodegradable polymer implant against experimental malignant glioma. Cancer Res. 54 (8), 2207–2212.
Wan, S., Kelly, P.M., Mahon, E., Stöckmann, H., Rudd, P.M., Caruso, F., et al., 2015. The "sweet" side of the protein corona: effects of glycosylation on nanoparticle–cell interactions. ACS Nano 9 (2), 2157-–22166.
Wang, G., Wang, J.-J., Chen, X.-L., Du, L., Li, F., 2016a. Quercetin-loaded freeze-dried nanomicelles: Improving absorption and antiglioma efficiency in vitro and in vivo. J. Control. Release 235, 276–290.
Wang, H., Agarwal, P., Zhao, S., Yu, J., Lu, X., He, X., 2016b. A near-infrared laser-activated "nanobomb" for breaking the barriers to microRNA delivery. Adv. Mater. 28 (2), 347–355.
Wang, P., Henning, S.M., Heber, D., 2010. Limitations of MTT and MTS-based assays for measurement of antiproliferative activity of green tea polyphenols. PLoS One 5 (4), e10202.
Wang, Q., Huang, J.-Y., Li, H.-Q., Zhao, A.Z.-J., Wang, Y., Zhang, K.-Q., et al., 2017. Recent advances on smart TiO_2 nanotube platforms for sustainable drug delivery applications. Int. J. Nanomed. 12, 151.
Wang, X., Ding, B., Li, B., 2013. Biomimetic electrospun nanofibrous structures for tissue engineering. Mater. Today 16 (6), 229–241.
Wang, Z., Xia, J., Yan, Y., Tsai, A.-C., Li, Y., Ma, T., et al., 2015. Facile functionalization and assembly of live cells with microcontact-printed polymeric biomaterials. Acta Biomater. 11, 80–87.
Wasko, M.K., Kaminski, R., 2015. Custom-made antibiotic cement nails in orthopaedic trauma: review of outcomes, new approaches, and perspectives. BioMed Res. Int. 2015, 387186.

Waters, V., Ratjen, F., 2014. Inhaled liposomal amikacin. Expert Rev. Respir. Med. 8 (4), 401–409.
Webber, M.J., 2016. Engineering responsive supramolecular biomaterials: toward smart therapeutics. Bioeng. Transl. Med. 1 (3), 252–266.
Wilkerson, W.R., Seegert, C.A., Feinberg, A.W., Zhao, L.C., Callow, M., Baney, R., et al., 2001. Bioadhesion studies on microtextured siloxane elastomers. Polym. Prepr. Am. 42 (1), 147–148.
Williams, D., 1976. Biomaterials and biocompatibility. Med. Prog. Technol. 4 (1–2), 31–42.
Williams, D.F., 2008. On the mechanisms of biocompatibility. Biomaterials 29 (20), 2941–2953.
Wischke, C., Neffe, A.T., Steuer, S., Lendlein, A., 2010. Comparing techniques for drug loading of shape-memory polymer networks–effect on their functionalities. Eur. J. Pharm. Sci. 41 (1), 136–147.
Wolf, M., Andwraon, J., 2012. Practical approach to blood compatibility assessments: general considerations and standards. Biocompatibility and Performance of Medical Devices. Elsevier.
Wright, K.A., Nadire, K.B., Busto, P., Tubo, R., McPherson, J.M., Wentworth, B.M., 1998. Alternative delivery of keratinocytes using a polyurethane membrane and the implications for its use in the treatment of full-thickness burn injury. Burns 24 (1), 7–17.
Wu, W., Shen, J., Banerjee, P., Zhou, S., 2010. Core–shell hybrid nanogels for integration of optical temperature-sensing, targeted tumor cell imaging, and combined chemo-photothermal treatment. Biomaterials 31 (29), 7555–7566.
Xie, J., Wang, C.-H., 2006. Electrospun micro-and nanofibers for sustained delivery of paclitaxel to treat C6 glioma in vitro. Pharm. Res. 23 (8), 1817.
Xue, C., Yonet-Tanyeri, N., Brouette, N., Sferrazza, M., Braun, P.V., Leckband, D.E., 2011. Protein adsorption on poly(*N*-isopropylacrylamide) brushes: dependence on grafting density and chain collapse. Langmuir 27 (14), 8810–8818.
Yanagawa, F., Sugiura, S., Kanamori, T., 2016. Hydrogel microfabrication technology toward three dimensional tissue engineering. Regenerative Ther. 3, 45–57.
Yang, D., Lee, J.S., Choi, C.-K., Lee, H.-P., Cho, S.-W., Ryu, W., 2017. Microchannel system for rate-controlled, sequential, and pH-responsive drug delivery. Acta Biomater. 68, 249–260.
Yang, G., Liu, J., Wu, Y., Feng, L., Liu, Z., 2016. Near-infrared-light responsive nanoscale drug delivery systems for cancer treatment. Coord. Chem. Rev. 320, 100–117.
Ye, E., Chee, P.L., Prasad, A., Fang, X., Owh, C., Yeo, V.J.J., et al., 2015. Supramolecular soft biomaterials for biomedical applications. In-Situ Gelling Polymers. Springer.
Yeo, Y., Burdick, J.A., Highley, C.B., Marini, R., Langer, R., Kohane, D.S., 2006. Peritoneal application of chitosan and UV-cross-linkable chitosan. J. Biomed. Mater. Res., A 78 (4), 668–675.
Yin, J., Luan, S., 2016. Opportunities and challenges for the development of polymer-based biomaterials and medical devices. Regenerative Biomater. 3 (2), 129–135.
Ying, M., Zhan, C., Wang, S., Yao, B., Hu, X., Song, X., et al., 2016. Liposome-based systemic glioma-targeted drug delivery enabled by all-d peptides. ACS Appl. Mater. Interfaces 8 (44), 29977–29985.
Ying, X., Wang, Y., Liang, J., Yue, J., Xu, C., Lu, L., et al., 2014. Angiopep-conjugated electro-responsive hydrogel nanoparticles: therapeutic potential for epilepsy. Angew. Chem. Int. Ed. 53 (46), 12436–12440.
Yokoi, T., Miyazaki, T., Kawashita, M., Ohtsuki, C., 2017. Bioactive glass-ceramics. Nanobioceramics for Healthcare Applications. World Scientific.
You, C., Wu, H., Wang, M., Zhang, Y., Wang, J., Luo, Y., et al., 2017. Near-infrared light and pH dual-responsive targeted drug carrier based on core-crosslinked polyaniline nanoparticles for intracellular delivery of cisplatin. Chem. Eur. J. 23 (22), 5352–5360.
Yu, Z., Yu, M., Zhang, Z., Hong, G., Xiong, Q., 2014. Bovine serum albumin nanoparticles as controlled release carrier for local drug delivery to the inner ear. Nanoscale Res. Lett. 9 (1), 343.
Yuan, J., Gao, H., Ching, C.B., 2011. Comparative protein profile of human hepatoma HepG2 cells treated with graphene and single-walled carbon nanotubes: an iTRAQ-coupled 2D LC–MS/MS proteome analysis. Toxicol. Lett. 207 (3), 213–221.
Yuan, S., Zhao, J., Luan, S., Yan, S., Zheng, W., Yin, J., 2014. Nuclease-functionalized poly(styrene-*b*-isobutylene-*b*-styrene) surface with antiinfection and tissue integration bifunctions. ACS Appl. Mater. Interfaces 6 (20), 18078–18086.
Yuan, S., Luan, S., Yan, S., Shi, H., Yin, J., 2015. Facile fabrication of lubricant-infused wrinkling surface for preventing thrombus formation and infection. ACS Appl. Mater. Interfaces 7 (34), 19466–19473.

Yue, Z., Moulton, S.E., Cook, M., O'leary, S., Wallace, G.G., 2013. Controlled delivery for neuro-bionic devices. Adv. Drug Delivery Rev. 65 (4), 559–569.
Zamani, M., Prabhakaran, M.P., Ramakrishna, S., 2013. Advances in drug delivery via electrospun and electrosprayed nanomaterials. Int. J. Nanomed. 8, 2997.
Zangabad, P.S., Mirkiani, S., Shahsavari, S., Masoudi, B., Masroor, M., Hamed, H., et al., 2018. Stimulus-responsive liposomes as smart nanoplatforms for drug delivery applications. Nanotechnol. Rev. 7 (1), 95–122.
Zarb, G.A., Albrektsson, T., Baker, G., Eckert, S., Stanford, C., Tarnow, D., et al., 2008. Osseointegration: on Continuing Synergies in Surgery, Prosthodontics, Biomaterials. Quintessence Publishing Company.
Zhang, C., Luo, H., Lin, G., Zhu, Z., Zhang, F., Zhang, J., et al., 2016. Transdermal patches for D-threo-methylphenidate (free base): formulation aspects and in vivo pharmacokinetics. J. Drug Deliv. Sci. Technol. 35, 50–57.
Zhang, C., Nance, E.A., Mastorakos, P., Chisholm, J., Berry, S., Eberhart, C., et al., 2017a. Convection enhanced delivery of cisplatin-loaded brain penetrating nanoparticles cures malignant glioma in rats. J. Control. Release 263, 112–119.
Zhang, H., Lin, C.-Y., Hollister, S.J., 2009. The interaction between bone marrow stromal cells and RGD-modified three-dimensional porous polycaprolactone scaffolds. Biomaterials 30 (25), 4063–4069.
Zhang, H., Patel, A., Gaharwar, A.K., Mihaila, S.M., Iviglia, G., Mukundan, S., et al., 2013. Hyperbranched polyester hydrogels with controlled drug release and cell adhesion properties. Biomacromolecules 14 (5), 1299–1310.
Zhang, L., Xu, Y., Cao, W., Xie, S., Wen, L., Chen, G., 2018a. Understanding the translocation mechanism of PLGA nanoparticles across round window membrane into the inner ear: a guideline for inner ear drug delivery based on nanomedicine. Int. J. Nanomed. 13, 479.
Zhang, M., Yan, X., Huang, F., Niu, Z., Gibson, H.W., 2014a. Stimuli-responsive host–guest systems based on the recognition of cryptands by organic guests. Acc. Chem. Res. 47 (7), 1995–2005.
Zhang, Q., Hoogenboom, R., 2015. Polymers with upper critical solution temperature behavior in alcohol/water solvent mixtures. Prog. Polym. Sci. 48, 122–142.
Zhang, Q., Jiang, Q., Li, N., Dai, L., Liu, Q., Song, L., et al., 2014b. DNA origami as an in vivo drug delivery vehicle for cancer therapy. ACS Nano 8 (7), 6633–6643.
Zhang, Q., Zhang, L., Wang, P., Du, S., 2014c. Coordinate bonding strategy for molecularly imprinted hydrogels: Toward pH-responsive doxorubicin delivery. J. Pharm. Sci. 103 (2), 643–651.
Zhang, Q., Li, Y., Lin, Z.Y.W., Wong, K.K., Lin, M., Yildirimer, L., et al., 2017b. Electrospun polymeric micro/nanofibrous scaffolds for long-term drug release and their biomedical applications. Drug Discov. Today 22 (9), 1351–1366.
Zhang, S., Yan, L., Altman, M., Lässle, M., Nugent, H., Frankel, F., et al., 1999. Biological surface engineering: a simple system for cell pattern formation. Biomaterials 20 (13), 1213–1220.
Zhang, Y.-h, Campbell, S.A., Karthikeyan, S., 2018b. Finite element analysis of hollow out-of-plane HfO_2 microneedles for transdermal drug delivery applications. Biomed. Microdevices 20 (1), 19.
Zhong, S., Zhang, Y., Lim, C., 2010. Tissue scaffolds for skin wound healing and dermal reconstruction. Wiley Interdiscip. Rev. Nanomed. Nanobiotechnol. 2 (5), 510–525.
Zhou, J., Chen, J., Sun, H., Qiu, X., Mou, Y., Liu, Z., et al., 2014. Engineering the heart: evaluation of conductive nanomaterials for improving implant integration and cardiac function. Sci. Rep. 4, 3733.
Ziemba, A.M., Gilbert, R.J., 2017. Biomaterials for local, controlled drug delivery to the injured spinal cord. Front. Pharmacol. 8, 245.
Zong, W., Hu, Y., Su, Y., Luo, N., Zhang, X., Li, Q., et al., 2016. Polydopamine-coated liposomes as pH-sensitive anticancer drug carriers. J. Microencapsulation 33 (3), 257–262.
Zorlutuna, P., Annabi, N., Camci-Unal, G., Nikkhah, M., Cha, J.M., Nichol, J.W., et al., 2012. Microfabricated biomaterials for engineering 3D tissues. Adv. Mater. 24 (14), 1782–1804.

Further reading

Hayakawa, Y., Ishiwatari, K., Matsushita, J., Takahashi, R., Takehana, T., 2012. Recent patent applications in biomaterials. Nat. Biotechnol. 30 (10), 957.

CHAPTER

5

Biotechnology-Based Pharmaceutical Products

Pran Kishore Deb[1], *Omar Husham Ahmed Al-Attraqchi*[1], *Johnson Stanslas*[2], *Amal Al-Aboudi*[3], *Noor Al-Attraqchi*[4] *and Rakesh K. Tekade*[5]

[1]Faculty of Pharmacy, Philadelphia University, Amman, Jordan [2]Pharmacotherapeutics Unit, Department of Medicine, Faculty of Medicine and Health Sciences, Universiti Putra Malaysia, Serdang, Selangor, Malaysia [3]Department of Chemistry, Faculty of Science, The University of Jordan, Amman, Jordan [4]Department of Pharmacognosy, Mosul University, Mosul, Iraq [5]National Institute of Pharmaceutical Education and Research (NIPER)—Ahmedabad, Gandhinagar, India

OUTLINE

5.1 Introduction 154
5.1.1 Differences to be Considered for Biotechnology-Based Products in Comparison With Conventional Drugs 155

5.2 Production Process for Biotechnology-Based Products 155
5.2.1 Upstream Process 156
5.2.2 Downstream Process 161

5.3 Overview of Pharmacokinetics of Pharmaceutical Biotechnology-Based Products 164
5.3.1 Absorption 165
5.3.2 Distribution 165
5.3.3 Metabolism and Excretion 167
5.3.4 Approaches Used for Improving the Pharmacokinetic Profile of Biotechnology-Based Pharmaceutical Products 167

5.4 Problems Associated With Biotechnology-Based Pharmaceutical Products 168
5.4.1 Formulation Stability of Pharmaceutical Biotechnology-Based Products 169
5.4.2 Immunogenicity of Biotechnology-Based Pharmaceutical Products 171
5.4.3 Ethical and Regulatory Concerns of Biotechnology 171

Biomaterials and Bionanotechnology
DOI: https://doi.org/10.1016/B978-0-12-814427-5.00005-6

© 2019 Elsevier Inc. All rights reserved.

5.5 Biotechnology-Based Products: Processing, Production, and Application Perspectives 172
5.5.1 Antibiotics 172
5.5.2 Hormones 173
5.5.3 Enzymes 175
5.5.4 Blood Clotting Factors 175
5.5.5 Cytokines 176
5.5.6 Monoclonal Antibodies 177
5.5.7 Vaccines 178
5.6 A Summary of Commercially Available Leading Biotechnology-Based Products 179
5.7 Nanobiotechnology 180
5.8 Gene Therapy 181
5.9 Pharmacogenomics 182
5.10 Stem Cell Therapy 182
5.11 Conclusion 183
Abbreviations 184
References 184
Further reading 189

5.1 INTRODUCTION

Biotechnology-based pharmaceutical therapeutic products have become an essential portion of marketed clinical therapeutic agents. Driven by the advances in molecular biology, immunology, and recombinant deoxyribonucleic acid (DNA) technology, pharmaceutical biotechnology has greatly evolved and continues to evolve at a high rate with more products being approved (Lin, 2009). There are more than 200 approved biotechnology-based therapeutic products that are used for combating and preventing various diseases such as cancer, infectious diseases, diabetes, and growth disorders. The number of biotechnology-based therapeutic agents that are in clinical trials is also substantially high, and these agents are being developed for the treatment of different pathological conditions that are affecting a large portion of the population such as Alzheimer, cardiovascular conditions, and arthritis. Thus these products are of high importance in the pharmaceutical industry, however, although these products share many similarities with the conventional drugs, there are differences that need to be considered when dealing with biotechnology-based products (Kayser and Warzecha, 2012).

Biotechnology involves the use of living organisms or their products for beneficial human purposes such as for medical, industrial, or environmental purposes (Nehal et al., 2011). The advancement in recombinant DNA technology has made a great impact on the success of the development of these products. This technology allows for manipulation of DNA fragments from different sources, such as inserting a human gene into a bacterial plasmid. This ability to manipulate DNA fragments along with the ability to insert the recombinant DNA into different cells can be used for the production of therapeutic proteins and peptides such as insulin hormone and monoclonal antibodies (Nagaich, 2015).

There are other aspects of biotechnology that are promising and have the potential for greatly improving medicine. For example, gene therapy, which involves the correction of defects in the genes, is a promising approach that is being investigated for the ability to

treat various diseases related to genetic mutations such as hypertension, diabetes, and cancer (Therrien et al., 2010; Wong et al., 2010). Another promising area is pharmacogenomics, which deals with the use of information derived from the genomics of the patient to help the physicians in making better therapeutic decisions (Roy, 2013).

5.1.1 Differences to be Considered for Biotechnology-Based Products in Comparison With Conventional Drugs

There are essential differences between the conventional small drug molecules and the biotechnology-based drugs at different levels including synthesis, purification, formulation stability, and biopharmaceutical properties. The synthesis of conventional small molecules usually proceeds via in vitro chemical reactions with proper purification processes to obtain the desired compounds. On the other hand, biotechnology-based products are usually synthesized inside living cells, such as bacterial cells that are cultured and genetically modified to allow the production of the desired compounds. Purification of the compounds synthesized from the cells can be more complex and require different methods and multiple steps to be successful (Ho and Gibaldi, 2004).

Since most of the biotechnology-based products are biomolecules such as proteins, peptides, and nucleic acids, the formulation stability can be more challenging in comparison with the conventional drugs' formulation stability. This is because the biomolecules such as proteins usually have relatively large molecular size and are held in their correct three-dimensional (3D) structures via weak noncovalent interactions. Therefore they are highly susceptible to chemical and physical degradation. Indeed, formulation stability has been shown in many cases to be a challenging problem for proteins and nucleic acids–based pharmaceutical formulations (Florence and Attwood, 2011). There are also differences that need to be considered in the biological performance of the biotechnology-based products such as therapeutic proteins and peptides. Mainly, the pharmacokinetics of these products can be different because of the large molecular size as well as instability. For example, proteins are known to be highly unstable in the gastrointestinal tract (GIT) because of the harsh environmental factors such as extreme pH values and the presence of proteolytic enzymes that can readily hydrolyze protein and peptide molecules. Therefore oral delivery of most of the biotechnology-based products is not possible and requires the use of a specialized oral delivery system such as nanoparticle carriers or other systems (Lin, 2009).

5.2 PRODUCTION PROCESS FOR BIOTECHNOLOGY-BASED PRODUCTS

The production process of biotechnology-based products can be divided mainly into two stages: upstream and downstream processing. Upstream processing is the stage where the targeted compound such as a protein is synthesized and increased quantitatively by the host cells such as bacterial cells. The next stage is the downstream process, which is concerned with the isolation and purification of the targeted compound synthesized by

the host cells. In the following sections, the basic concepts of recombinant DNA technology, vectors, and host cells that are used in the production of pharmaceutical biotechnology-based products are discussed.

5.2.1 Upstream Process

The upstream process is the stage that is involved in the synthesis and production of the targeted compound inside the host cells. For the upstream process to be efficient, a suitable host cell should be selected that can synthesize the targeted compound in proper amounts. In cases where the targeted compound is a protein or peptide molecule, the gene of that compound should be isolated and cloned (Kayser and Warzecha, 2012). There is a variety of efficient technologies available for this purpose. The cloned gene is then inserted into a vector molecule, which is required to allow the gene to replicate in the host cell as well as to be expressed at an efficient rate. There are different types of vector molecules; in the case of bacterial cells, plasmids are the most common vectors. The vector that contains the gene of interest is inserted in the host cells, which will express the gene and produce the targeted molecule. After the targeted compound is produced at the desired amount, the upstream process is over and the culture of cells is then harvested for the downstream process (Nagaich, 2015; Doherty and Suh, 2000).

5.2.1.1 Gene Cloning

The term *gene cloning* refers to the process of isolation of a fragment of DNA and making copies of this DNA fragment without alteration in the sequence of nucleotides in the DNA fragment. The produced copies of the DNA fragments can be manipulated as required and inserted into a vector molecule for further insertion into cells such as bacterial cells. This ability to clone genes and manipulate them allowed for great progress in understanding the functions of the genes as well as in utilizing them for various purposes including the production of pharmaceutical biotechnology products. There are various technologies that can be used in gene cloning. The recombinant DNA technology is particularly important in the production of many pharmaceutical biotechnology products such as insulin. This technology depends on the use of enzymes and vectors to manipulate fragments of DNA as required and inserting them into different types of cells (Zhou et al., 2001; Doherty and Suh, 2000).

5.2.1.2 Recombinant Deoxyribonucleic Acid Technology

The fundamental concept of recombinant DNA technology involves the isolation, cloning of a gene, and inserting this gene by proper methods into a host cell that can express the gene as a part of its genome to produce the protein or peptide product of that gene. The gene must first be inserted into a proper vector prior to insertion into the host cell. The cloned genes can be manipulated as required by using various restriction and ligase enzymes, which are an essential part of the success of recombinant DNA technology (Nagaich, 2015; Doherty and Suh, 2000). The general concept of recombinant DNA technology is depicted in Fig. 5.1.

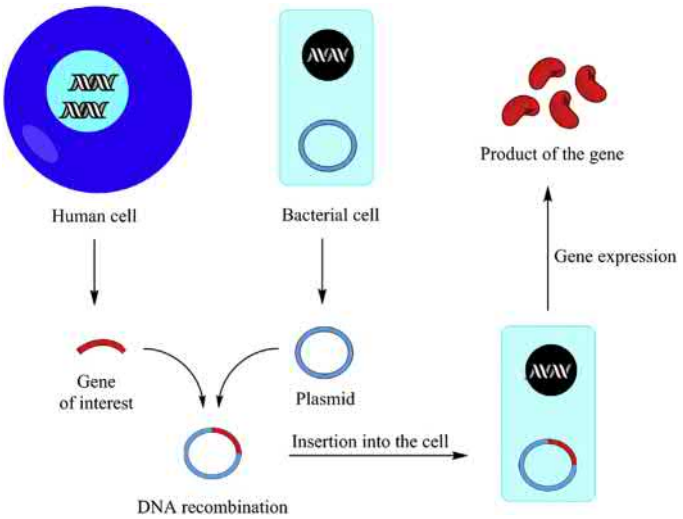

FIGURE 5.1 Recombinant DNA technology used for insertion of a human gene into a bacterial cell. *DNA*, Deoxyribonucleic acid.

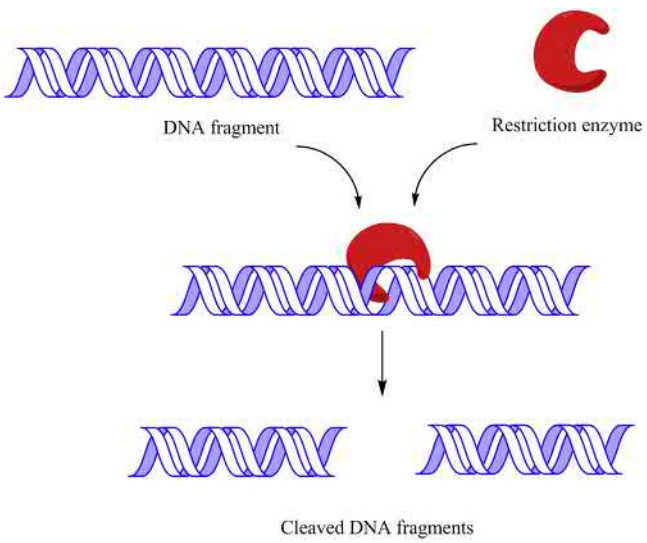

FIGURE 5.2 General action of restriction enzymes on a DNA fragment. *DNA*, Deoxyribonucleic acid.

Restriction enzymes can be defined as enzymes that have the ability to cleave the phosphodiester bond between nucleotides in the DNA molecule. The restriction enzymes recognize specific nucleotides sequences that are usually in the length of six to eight base pairs, which are also known as restriction sites. There have been a large number of restriction enzymes identified along with their restriction sites, which enables cleaving the DNA at the desired nucleotide sequence. The general action of restriction enzymes is shown in Fig. 5.2 (Pray, 2008; Loenen et al., 2013).

On the other hand, DNA ligases are enzymes that catalyze the formation of a phosphodiester bond between two adjacent nucleotides in a DNA molecule. Ligases require an

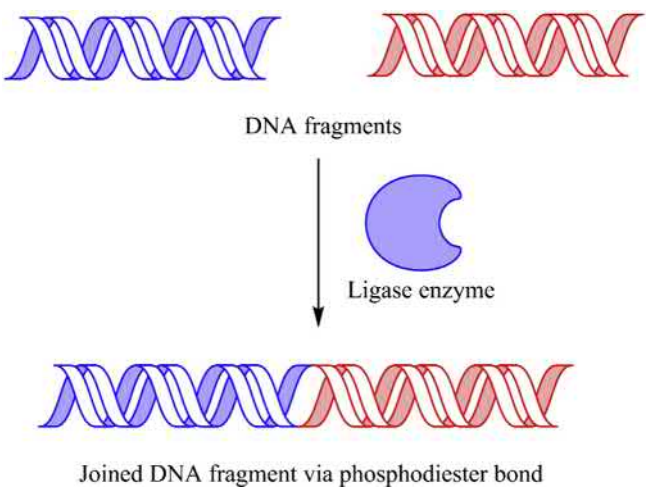

FIGURE 5.3 General action of a ligase enzyme on DNA fragments. *DNA*, Deoxyribonucleic acid.

energy source such as ATP to catalyze the reaction. The general action of ligase enzymes is shown in Fig. 5.3. Thus restriction enzymes and ligases can be thought of as tools used for cutting and linking different fragments of DNA molecules and rearranging them as required (Ellenberger and Tomkinson, 2008; Shuman, 2009).

5.2.1.2.1 VECTORS

To introduce the gene of interest into the host cells, the gene must first be inserted into a proper vector molecule. The bacterial plasmid is a commonly used vector for the insertion of a gene of interest into a bacterial cell. A plasmid is a small circular DNA molecule that exists and replicates independently from the chromosomal DNA in the bacterial cell. The vector must have several properties to allow for successful expression of the gene in the host cells (Lodish et al., 2008). The vector must be well characterized with known restriction sites that allow the use of restriction enzymes to cleave it and insert the gene of interest and rejoin it with proper ligase enzymes. Also, the vector must have an origin of replication for it to be able to replicate inside the host cells. A promoter sequence must also be present in the vector to ensure efficient transcription and hence synthesis of the desired compound. Another requirement is a method of selection to differentiate the cells that took up the vectors, because not all the cells in the culture can take up the vector, in fact, usually only a small proportion of the cells successfully take up the vector while the majority of the cells do not. The method of selection is usually an antibiotic resistance gene in the vector such as streptomycin resistance gene. By culturing the cells in a medium that contains the antibiotic, only cells that took up the vector containing the antibiotic resistance gene will survive in this medium while the cells that do not contain the vector will be killed by the antibiotic in the medium (Lodish et al., 2008).

The insertion of a plasmid vector molecule into host cells can be achieved by different methods. Electroporation is a common and efficient method for this purpose, which involves the use of electromagnetic energy on the bacterial cells to create pores in the cell

membranes. Subsequently, the plasmid vector can enter into the cells through these pores in the cell membrane (Sinko, 2011).

5.2.1.2.2 HOST CELLS

There are a variety of host cells that can be used for expressing the gene of interest to obtain the desired compound. The choice of the host cell depends on several factors, which include economic aspects, presence or absence of posttranslational modification, and other factors. Bacterial host cells such as *E*scherichia *coli* have the advantage of being well understood for this purpose as well as being relatively cheap to culture and grow. The limitations of using these cells as the expression system mainly include the inability to carry out posttranslational modification processes on the synthesized protein or peptide such as glycosylation. This can be problematic because many endogenous human proteins and peptides are glycosylated (Choi et al., 2006; Swartz, 2001). On the other hand, eukaryotic cells such as yeast, Chinese hamster ovary (CHO), and baby hamster kidney (BHK) cells can carry out posttranslational modifications that occur on human proteins to a relatively good extent (Jayapal et al., 2007; Bhopale and Nanda, 2005). Mammalian cells can also be used as host cells for the expression of the gene of interest. Although low yields are usually observed in this type of host cell, recent advances have substantially improved the yield of produced proteins. Mammalian cells have the advantages of proper posttranslational modifications as well as correct folding of the therapeutic proteins (Wurm, 2004).

5.2.1.3 Deoxyribonucleic Acid Libraries

A DNA library can be defined as a collection of DNA fragments that have been cloned and inserted into host cells for storage. Mainly there are two types of DNA libraries: genomic DNA libraries and the complementary DNA (cDNA) libraries (Ferrier, 2014).

5.2.1.3.1 GENOMIC DEOXYRIBONUCLEIC ACID LIBRARIES

Genomic DNA libraries are created from treating the entire DNA of an organism with restriction enzymes to cleave the DNA and generate smaller DNA fragments. The generated fragments are then inserted into vectors through the usage of ligase enzymes and the vectors are, in turn, inserted into host cells. Therefore the entire genome of an organism is represented by the created genomic DNA library. Since the gene of interest may contain more than one restriction site that the restriction enzyme can cleave, the gene of interest may be cleaved by the restriction enzymes at these sites and hence will not be kept intact as one fragment in a vector. To avoid this, usually, the action of the enzyme is controlled either by reducing the amount of enzyme used or by reducing the time the enzyme allowed to act on the DNA. This increases the probability of keeping the gene of interest intact (Lodish et al., 2008; Wu et al., 2006).

5.2.1.3.2 COMPLEMENTARY DEOXYRIBONUCLEIC ACID LIBRARIES

Unlike the genomic DNA libraries, which are constructed from the entire DNA of an organism or a cell, the cDNA libraries are constructed from the messenger ribonucleic acid (mRNA) molecules that are present in a tissue. The construction of a cDNA library is performed by collecting the mRNA present in a certain tissue then converting it into cDNA by the action of reverse transcriptase enzyme. This enzyme has the ability to catalyze the

formation of cDNA strand from an mRNA template. The resulting cDNA is double stranded with one strand being the mRNA and the other strand is a single DNA strand. The mRNA strand can be cleaved by using alkali conditions, and then by treating the cDNA with DNA polymerase, the mRNA strand will be removed and a double-stranded cDNA will be formed. The construction process of cDNA libraries is shown in Fig. 5.4 (Harbers, 2008; Ying, 2004). The resulted cDNA can be incorporated into vectors and subsequently into host cells. Amplification of the cDNA can be achieved usually by using the polymerase chain reaction, which is a commonly used method for amplification of DNA. Since the cDNA sequence is created directly from the corresponding mRNA, the introns regions are not present. On the other hand, in the case of genomic libraries, introns are present because the DNA of the genomic library is created directly from the DNA of the organism (Wu et al., 2006).

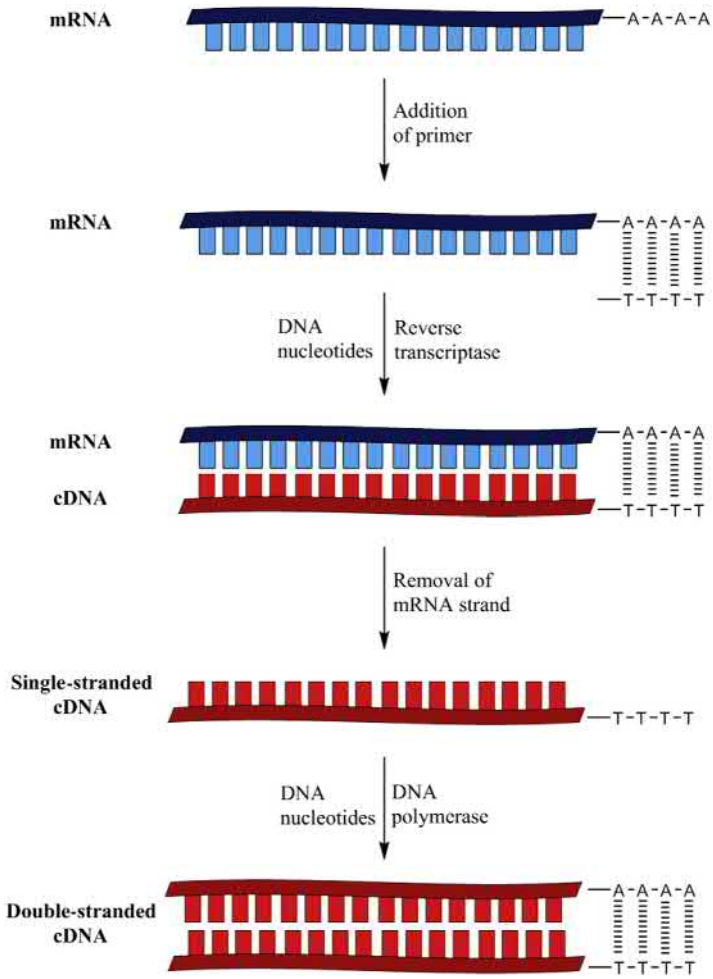

FIGURE 5.4 The construction process of a cDNA library. *cDNA*, Complementary deoxyribonucleic acid.

5.2.2 Downstream Process

Following the upstream process in which the host cells synthesize the compound of interest, the downstream process is conducted. The downstream process is concerned with the isolation and purification of the synthesized compounds from the host cells or the biological medium in which it is present. The downstream process can be complex and usually consists of many steps that involve the use of various separation methods. This is because the biological medium in which the protein of interest resides contains a large number of other molecules (contaminants) that belong to the cell or the culture medium. These contaminants can have various degrees of similarity with the protein of interest in terms of physicochemical properties. Naturally, the more similar the contaminants are with the protein of interest, the more difficult the separation of the protein of interest from these contaminants (Gottschalk, 2012; Straathof, 2011).

5.2.2.1 Isolation and Purification of Biotechnology-Based Products

Isolation and purification of the compound of interest that has been synthesized in the host cells begins with harvesting these cells from the culture medium, which is usually discarded. On the other hand, in the cases where the compound of interest is secreted by the cells into the culture medium instead of remaining inside the cells, then the cells are removed while the culture medium is kept. This initial step represents the bulk separation of the compound of interest, which is still present with various other contaminants. Following this step, different methods are employed for further purification (Gottschalk, 2012). Various chromatographic methods are used depending on the different physicochemical properties of the protein of interest as the bases for separation.

Size exclusion chromatography (also known as gel filtration) is a technique that can be used for the separation of proteins, DNA, or other molecules based on the molecular size. This method involves the use of porous beads that have suitable pore sizes as the stationary phase for separating the compound of interest (Sinko, 2011). The liquid mixture containing the compound of interest and other molecules is passed through the column that contains the stationary phase. Molecules with a size smaller than the pore size of the beads will enter through them and be hindered as they pass through the column. While the molecules with a size larger than the pore size of the beads will not enter through the beads and will be eluted at a faster rate than the smaller molecules. Therefore separation of the molecules will occur based on the size of the molecules, smaller molecules will take a longer time to pass through the column while larger molecules will take a shorter time. The porous size of the stationary phase can be adjusted as required and gels with various pore sizes are commercially available. Size exclusion chromatography can also be used for detection of the molecular weight of the compounds. The principle of size exclusion chromatography is shown in Fig. 5.5 (Patil et al., 2014).

Ion exchange chromatography is another method that is frequently used during the purification process of biomolecules such as proteins. This method depends on the charge of the present molecules in a mixture as the base for separation (Saraswat et al., 2013). The stationary phase consists of resins that are covalently linked with negatively

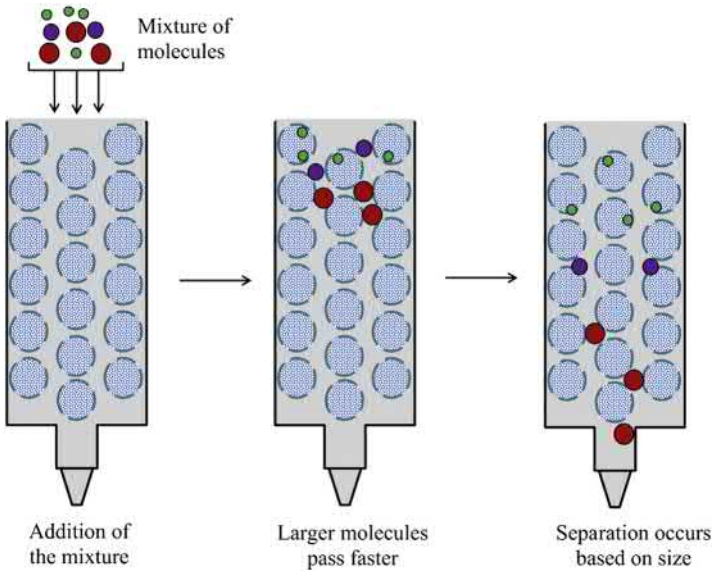

FIGURE 5.5 The principle of size exclusion chromatography.

or positively charged groups depending on the charge of the compound to be separated. In the case where the compound of interest in negatively charged, a positively charged resin is used and vice versa. The mixture of molecules is passed through the column containing the resins. The molecules with opposite charge of the charge of the resins will be attracted and hence are retained in the column, while molecules with the same charge of charge of the resins or with the neutral charge will not be retained and will be eluted from the column. The bound molecules can then be unbound from the resins by using a proper salt concentration that removes them from the resins. The principle of ion exchange chromatography is shown in Fig. 5.6 (Yigzaw et al., 2009; Saraswat et al., 2013).

Affinity chromatography involves the use of a known ligand that binds to the compound of interest such as a protein. The ligand is linked to a resin via covalent bonds and is used in a column as the stationary phase. The liquid mixture containing the protein of interest and the contaminants is passed through the column. The protein of interest will bind to the ligand and will be retained in the column while the contaminants will pass through and be eluted as they do not interact with the ligand (Sinko, 2011). Therefore the affinity chromatography makes use of the affinity of the protein of interest for a ligand for the separation from the contaminants. The protein of interest can be then unbound from the ligand by various methods. For example, by using competitive molecules for the ligand or changing of the conditions of the solution such as the pH value to disfavor the binding of the protein to the ligand. However, it is important to keep the structure of the protein intact during this process. A relatively high degree of purification can be achieved by using this method. The principle of affinity chromatography is demonstrated in Fig. 5.7 (Saraswat et al., 2013).

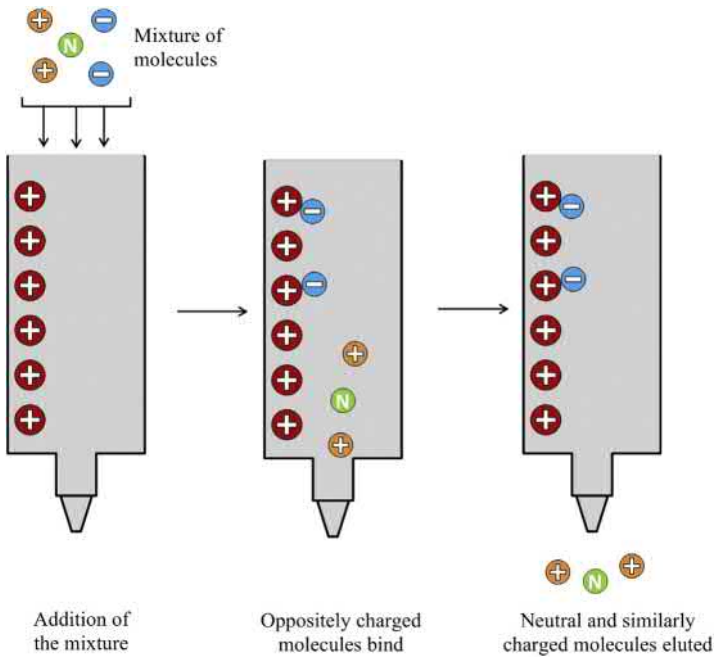
Mixture of molecules
Addition of the mixture
Oppositely charged molecules bind
Neutral and similarly charged molecules eluted

FIGURE 5.6 The principle of ion exchange chromatography.

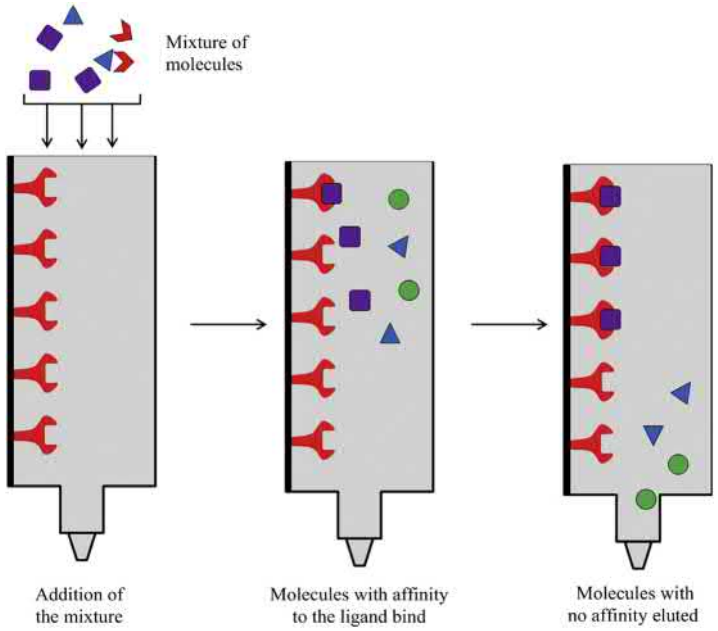
Mixture of molecules
Addition of the mixture
Molecules with affinity to the ligand bind
Molecules with no affinity eluted

FIGURE 5.7 Demonstration of the principle of affinity chromatography.

5.2.2.2 *Characterization of Biotechnology-Based Products*

Characterization of the produced protein or other therapeutic molecules is an essential step that is required to get the product approved. The characterization of biotechnology-based products requires extensive analysis that involves various methods to characterize the physicochemical as well as the biological properties of the produced compound. The structural stability of the product should be analyzed for possible changes under different conditions such as different temperature and pH values (Kaltashov et al., 2012; Muneeruddin et al., 2015).

There is a wide range of techniques that are employed for these purposes, for example, spectroscopic methods such as ultraviolet, Fourier transform infrared, and fluorescence spectroscopy. These methods can be used to monitor subtle changes of the protein structure as well as the presence of impurities through observing the differences in the spectra of the protein solution. Chromatographic methods can also be used for analytical purposes of the produced proteins such as size exclusion and ion exchange chromatography (Sinko, 2011).

Another method that is commonly used is gel electrophoresis, which is based on the migration of charged molecules in a gel matrix during the application of an electric current. In sodium dodecyl sulfate–polyacrylamide gel electrophoresis (SDS–PAGE) to ensure that all the molecules in the gel have the same charge, SDS is applied to give them a negative charge. Therefore the migration of the molecules will be based on the size of the molecules as they pass through the gel matrix. The gel serves to hinder large molecules to pass while allowing smaller molecules to pass at a faster rate (Roy and Kumar, 2014)

Biological assays are also required and are considered to be of prime importance to characterize the biological activities of the product. Biological assays cover a wide range of testing methods for the biological effects of the molecule that include ligand binding assays, cell-based assays, and whole animal assays. The ligand binding assays are used for testing the binding of the molecule such as a protein to the ligand, which is done in vitro. For example, the enzyme-linked immunosorbent assay method is commonly employed for testing the binding of a molecule to a ligand (Lequin, 2005).

5.3 OVERVIEW OF PHARMACOKINETICS OF PHARMACEUTICAL BIOTECHNOLOGY-BASED PRODUCTS

A good pharmacokinetic profile is an absolute requirement for any therapeutic substance that is intended for clinical applications, in addition to having proper pharmacodynamics property. It has been shown that many drug candidates fail to be marketed as drugs because of their poor pharmacokinetic profile even though they show good pharmacodynamics with regard to the binding to their target (Pran Kishore et al., 2018a,b; Shantanu et al., 2018; Arpna et al., 2018; Rahul et al., 2018). This principle also applies to biotechnology-based products, which mainly include proteins, peptides, and nucleic acids. Although many of these products are based on the endogenous molecules and hence possess optimal binding properties to their targets, exogenous administration of these molecules can result in significant difference in the biological activity (Tang et al., 2004; Balakumar et al., 2018; Pran Kishore et al., 2018a). Since most of the biotechnology-based

products are peptides and proteins such as insulin and cytokines, they have unfavorable pharmacokinetic properties (Pran Kishore et al., 2018b). These unfavorable pharmacokinetic properties are mainly because of the physicochemical properties of proteins and peptides (Tang et al., 2004). In the following sections, the absorption, distribution, metabolism, and excretion processes for biotechnology-based products are discussed.

5.3.1 Absorption

Generally, most of the biotechnology-based products such as proteins and peptides are not administrated by the oral route because they cannot be absorbed from the GIT. Proteins and peptides are inherently unstable in the environment of the GIT because they are highly susceptible to enzymatic hydrolysis by the proteolytic enzymes present in different parts of the GIT. The proteolytic enzymes are responsible for the degradation of proteins and peptides into smaller peptide fragments and individual amino acids that can be readily absorbed. The general action of proteolytic enzymes is shown in Fig. 5.8. The unfavorable pH values in different parts of the GIT such as the highly acidic pH in the stomach can also inactivate the administrated protein by denaturation (Lin, 2009; Yoshioka and Stella, 2002; Pal et al., 2018). Another property of proteins and peptides that is considered to be a major cause for the poor absorption is the relatively large molecular size that prevents them from being absorbed across the intestinal mucosa. In addition, many proteins and peptides do not possess proper lipophilicity for diffusion across cellular membranes. Thus oral administration of most therapeutic proteins and peptides is not possible unless a proper oral delivery system is employed (Woodley, 1994; Lin, 2009; Venkat Ratnam et al., 2018).

Since the oral route of administration is not suitable for most therapeutic proteins and peptides, many formulations are prepared for administration via other routes. For example, the parenteral route of administration offers many advantages for the administration of proteins and peptides in comparison with the oral route. The parenteral routes of administration commonly used for therapeutic proteins and peptides preparations include intravenous (IV) injection, intramuscular (IM) injection, and subcutaneous (SC) injection (Zhang and Meibohm, 2012). The IV injection has the advantage of complete delivery of the administrated therapeutic agent to the systemic circulation and bypasses many of the problems associated with other routes. For instance, the problems associated with the oral route such as presystemic elimination are avoided. IM and SC administrations are subject to variability in the systemic absorption because they are affected by factors such as blood flow in the site of administration as well as metabolism of the administrated substances. On the other hand, parenteral administration is considered to be an invasive and inconvenient method of administration for most patients (Florence and Attwood, 2011; Amarji et al., 2018)

5.3.2 Distribution

After the absorption of any therapeutic agent to the systemic circulation, it must be transferred to the site of action where it interacts with its target to exert its therapeutic

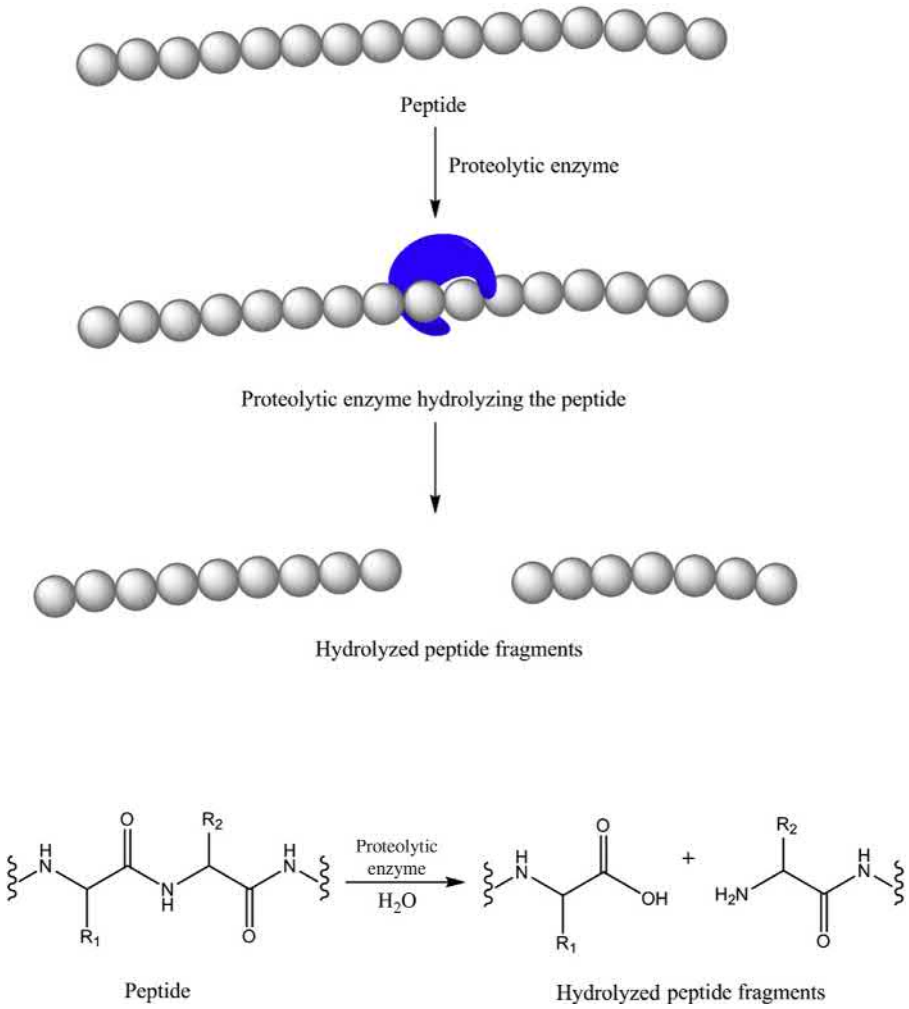

FIGURE 5.8 The general action of proteolytic enzymes on peptide fragments.

effect. The volume of distribution for an administrated substance is determined mainly by its physicochemical properties and the plasma protein binding (Pran Kishore et al., 2018a,b). Physicochemical properties such as lipophilicity and molecular weight can influence the volume of distribution of the substance. In the case of biomolecules such as proteins and nucleic acids, the relatively large molecular weight and the low lipophilicity result in a low volume of distribution indicating that they are mainly retained in the plasma or extracellular place. This reflects the inability to diffuse across the cellular membrane into other compartments (Shargel and Yu, 2016).

The plasma protein binding is another factor that influences the volume of distribution of the administrated substances. Generally, it is considered that therapeutic substances

that are bound to the plasma proteins are pharmacologically inactive and only the unbound (free) fraction can reach and interact with its target to produce the therapeutic effect. The major plasma proteins that are known to be involved with the binding to therapeutic substances include albumin, alpha1-acid glycoprotein, and lipoproteins. High levels of plasma proteins binding can cause the therapeutic proteins and peptides to be limited in the plasma space and hence have low volumes of distribution. The inability to distribute properly to the site of action can result in reduced biological activity. Thus the plasma protein binding of biotechnology products should be taken into consideration as it affects both the pharmacokinetics as well as the pharmacodynamics of the product (Pran Kishore et al., 2018b).

5.3.3 Metabolism and Excretion

Most biotechnology-based products such as proteins, peptides, and nucleic acids are susceptible to metabolism by various enzymes that are normally present for the degradation of endogenous protein and peptide molecules. Extensive metabolism of the administered therapeutic agents can result in significantly short circulation half-life, which is undesirable in most cases as it does not lead to the required therapeutic effects. Proteins and peptides are hydrolyzed by the proteolytic enzymes present in various parts of the body, although the main sites for their metabolism are the GIT, the liver, and the kidney (Zhang and Meibohm, 2012; Ashok et al., 2018). The most important factor that determines the rate of proteins and peptides metabolism appears to be the molecular weight of the molecule. It has been observed that the lower the molecular weight of the protein or peptide, the shorter is the circulation half-life. The proteins and peptides are hydrolyzed to smaller peptide fragments as well as individual amino acids that can be further metabolized in the body. The nucleic acids are also susceptible to degradation by various nuclease enzymes (Lin, 2009).

The renal excretion of a macromolecule such as proteins and peptides can participate in the elimination process of these molecules. The main factor that determines the extent to which the molecule is eliminated through glomerular filtration is the molecular size. Molecules that have large sizes that cannot be filtered across the glomeruli will not be eliminated by glomerular filtration. On the other hand, molecules that are small enough to pass through the glomeruli and are hydrophilic can be readily eliminated by glomerular filtration and are excreted in the urine (Lin, 2009; Zhang and Meibohm, 2012).

5.3.4 Approaches Used for Improving the Pharmacokinetic Profile of Biotechnology-Based Pharmaceutical Products

There are various approaches that can be employed to improve the pharmacokinetic profile of pharmaceutical biotechnology products including proteins and peptides (Jain et al., 2013). For example, chemical modification of the structure of the therapeutic molecule is one of the approaches for improving the oral bioavailability of a protein or a peptide. The chemical modifications are conducted to circumvent one or more of the

unfavorable properties of the protein or peptide such as susceptibility to enzymatic hydrolysis or inability to diffuse across cellular membranes (Gupta and Sharma, 2009). PEGylation is one of the most successful chemical modifications that has been shown to highly enhance the pharmacokinetic properties of proteins in many cases. PEGylation refers to the process of the attachment of a polyethylene glycol (PEG) polymer to the protein, peptides, or nucleic acids. The impact of PEGylation on the pharmacokinetics of the therapeutic molecule can be enormously beneficial. For example, the attached polymer can protect the protein or peptide from proteolytic enzymes hydrolysis by acting as a shield that prevents the enzyme from accessing the sites of hydrolysis in the protein or peptide structure. Also, PEGylation can improve the solubility of the protein or peptide, reduce the immunogenicity, increase the circulation half-life and reduce clearance (Pasut and Veronese, 2012; Gupta and Sharma, 2009). Nobex Corporation's HIM2 is an example of a product (insulin) that utilized the PEGylation approach, which allowed successful oral delivery and showed good biological activity (Hamman and Steenekamp, 2011).

Other approaches include the use of a carrier system such as liposomes, microspheres, and nanoparticles. Although these carriers have different properties, their main function is to protect the carrier molecule from the harsh environmental factors of the GIT such as extreme pH and enzymatic hydrolysis (Renukuntla et al., 2013). The use of absorption enhancers such as surfactants and chelating agents is another approach that can enhance the oral bioavailability of proteins and peptides. However, there are many safety issues associated with the clinical application of absorption enhancers, especially on long-term use (Choonara et al., 2014).

For more detailed explanations of the proteins and peptides drug delivery systems, the reader is referred to Chapter 16, Protein/Peptide Drug Delivery Systems: Practical Considerations in Pharmaceutical Product Development, which provides a more comprehensive picture of the topic (Pran Kishore et al., 2018c,d).

5.4 PROBLEMS ASSOCIATED WITH BIOTECHNOLOGY-BASED PHARMACEUTICAL PRODUCTS

There are various problems associated with biotechnology-based products that are encountered at different stages of the product development. Formulation stability can be a challenging problem for biotechnology-based products to a higher extent in comparison with conventional drugs formulations. Especially, the physical stability of the product is a major concern (Florence and Attwood, 2011). Another problem that is more likely to be encountered with large molecules such as proteins is the immunogenicity, which should be thoroughly considered and assessed. Since a major portion of biotechnology-based products is large molecules, there is a possibility of initiating an undesirable immune response in the administered patient (Pineda et al., 2016). Ethical and regulatory concerns are also present because biotechnology involves the manipulation of genes in living organisms; many ethical concerns have been raised including concerns regarding the possible misuse of these products (Resink, 2012).

5.4.1 Formulation Stability of Pharmaceutical Biotechnology-Based Products

Pharmaceutical biotechnology-based therapeutic formulations can suffer from various stability problems similar to those found in conventional drug formulations. While the main stability problems in conventional drug formulations are related to the chemical stability, macromolecules such as proteins and peptides can further suffer from physical stability problems related to their 3D structure. Distortion of the proteins 3D structure will lead to loss of their biological activity. Therefore both the chemical and physical stabilities of proteins and peptides need to be taken into consideration. The chemical degradation causes a change in the chemical structure of the molecule by forming and/or breaking covalent bonds in the molecule. On the other hand, physical degradation refers to the disruption of noncovalent forces that are required for keeping the secondary, tertiary, or quaternary structure of the molecule (Florence and Attwood, 2011; Pran Kishore et al., 2018a).

5.4.1.1 Chemical Degradation

Proteins and peptides are susceptible to chemical degradation via various pathways. For example, one common reaction observed in protein and peptide formulations is the deamidation reaction. In this reaction, the amide side of an asparagine or a glutamine residue is hydrolyzed to the corresponding carboxylic acid. For example, the adrenocorticotropic hormone, which is a peptide hormone, can suffer from chemical degradation pathway (Bhatt et al., 1990). Another type of chemical reaction that can occur readily in proteins and peptides formulations is the racemization reaction. All the 20 common amino acid residues except glycine have a chiral center at the alpha carbon and in the racemization reaction, inversion of this chiral center occurs. The structures of the 20 amino acids that are present in proteins are shown in Fig. 5.9. This reaction usually proceeds in alkaline media. Casein is an example of a protein that can exhibit racemization at various amino acids residues. Hydrolysis is another common degradation pathway for proteins and peptides in pharmaceutical formulations. For example, secretin can suffer from hydrolysis of aspartic acid in acidic media. Other frequently encountered chemical degradation pathways include beta-elimination, oxidation, and formation of disulfide bonds (Yoshioka and Stella, 2002).

5.4.1.2 Physical Degradation

Although the physical degradation is usually of less importance in small drug molecules, it is of high significance in case of macromolecules such as proteins and nucleic acids. This is because the native correctly folded structure is required for the molecule to exert its biological activity, where changes in the 3D structure can cause loss of activity. Physical degradation is caused mainly by factors related to the environment of the molecules including the pH of the medium, the heat, and the presence of other molecules that may interact and disrupt the native structure of the macromolecule (Florence and Attwood, 2011).

Protein molecules can suffer from denaturation, which involves unfolding of the protein and distortion of the secondary or tertiary structure leading to the loss of

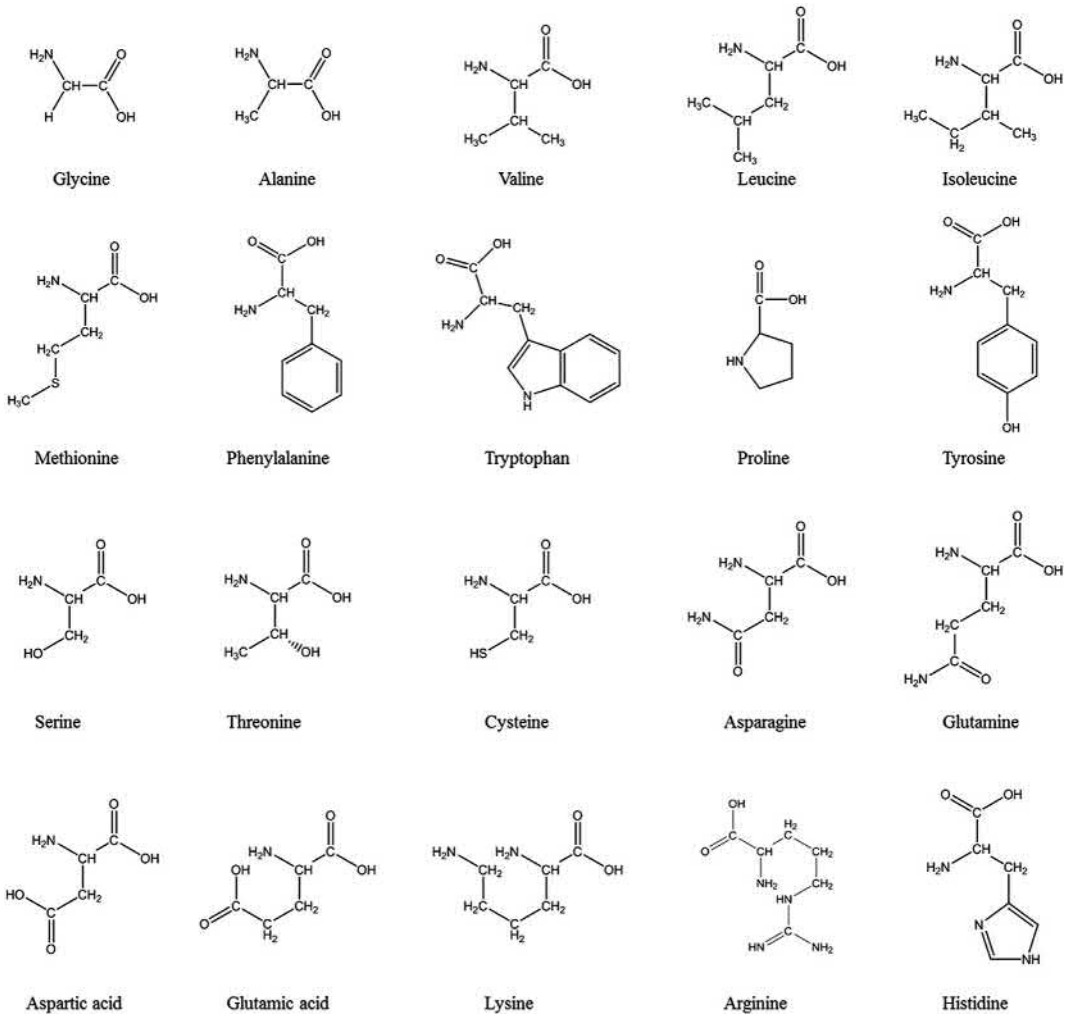

FIGURE 5.9 Structures of the 20 amino acids present in proteins.

activity. Denaturation can be caused by extreme pH values as well as changes in the optimum heat for the protein and can be reversible or irreversible. In the case of reversible denaturation, the protein's secondary or tertiary structure can be returned to its correct shape by removing the cause of the denaturation such as heat. While in the case of irreversible denaturation, the correct secondary or tertiary structure of the protein is not regained by removing the cause of denaturation. Denaturation of proteins can cause subsequent physical stability problems such as precipitation and aggregation of the denatured protein molecules. DNA molecules are also susceptible to

physical degradation, for example, DNA molecules with relatively high molecular weights can be broken in the solution as a result of stirring in the solution (Yoshioka and Stella, 2002).

5.4.2 Immunogenicity of Biotechnology-Based Pharmaceutical Products

Since most of the biotechnology-based therapeutic products are macromolecules such as proteins, they carry the risk of initiating immune responses upon administration by the patients. Although the initiated immune response can be clinically insignificant, in some cases it can be severe and lead to fatal consequences. Therefore assessment of immunogenicity for biotechnology-based therapeutic products is of prime importance to ensure the efficacy and safety of the product (Pineda et al., 2016).

In the case of exogenous proteins of nonhuman origins such as those extracted from microorganisms, plants, or other animals, the immune response (mediated by T cells) to such foreign proteins (which are considered as antigens) leads to the faster neutralization of antibodies. On the other hand, in the case of proteins that are of human origins, the immune response is mediated by the B cells and involves the production of binding antibodies. The immune response may also be initiated by the impurities present in the product or by aggregates of denatured proteins (Kessler et al., 2006).

The factors that influence the immunogenicity are related to both the product and the host. In the case of the product associated factors, the structural characteristics of the protein can be important such as the extent of glycosylation and the presence of epitopes. The host associated factors include mainly genetic factors related to the ability of antibodies production that bind to the protein. Other factors influencing immunogenicity include the dose of the administrated product as well as the route of administration (Schellekens, 2005).

5.4.3 Ethical and Regulatory Concerns of Biotechnology

There have been many ethical concerns raised regarding the use of biotechnology as it interferes and manipulates the genetic sequences of living organisms. For example, it has been questioned whether acts such as the insertion of genes from one organism into a different one are ethical and should be allowed. Another huge concern regarding biotechnology-based therapy is about gene therapy, which involves genetic engineering of humans. Although the main goal of gene therapy is to treat human diseases through genetic modifications, there is a possibility of misusing it to change or modulate other human traits (Polkinghorne, 2000; Powers, 2004). Patency in biotechnology research is considered as one of the major aspects of ethical concern. Patency of naturally occurring products is not allowed, there must be enough human intervention on the product to allow it to be patented. However, the extent of the required human intervention to allow the product to be patented is difficult to be clearly defined. For example, it is difficult to draw clear boundaries on whether things such as genetically modified organisms or DNA

sequences can be patented as human products (Resink, 2012). Thus the research in biotechnology is being continuously ethically questioned and various fears have been raised regarding the possible misuses of this field.

5.5 BIOTECHNOLOGY-BASED PRODUCTS: PROCESSING, PRODUCTION, AND APPLICATION PERSPECTIVES

As previously mentioned, there are various classes of biotechnology-based products that are produced for the treatment or prevention of different pathological conditions. In the following sections, various classes of biotechnology-based products are discussed along with their production process and therapeutic applications.

5.5.1 Antibiotics

Antibiotics are molecules that have the ability to inhibit the growth or killing of microorganisms. Various antibiotics have been discovered that can be used against a wide range of pathogenic microorganisms such as bacteria and fungi (Clardy et al., 2009). Therefore large-scale production of antibiotics is an important part of biotechnology-based products. An example of a class of antibiotics produced by the fermentation process is the beta-lactam antibiotics class, which includes the penicillins and the cephalosporins. The general structure of penicillin and cephalosporin is shown in Fig. 5.10. The beta-lactam antibiotics are one of the most clinically used antibiotics for the treatment of bacterial infections. Their mechanism of action involves the inhibition of a peptidoglycan transpeptidase enzyme that is required by the bacterial cell for completing the synthesis of the cell wall. Therefore inhibition of this enzyme by the beta-lactams prevents the completion of the cell wall synthesis and without an intact cell wall, the bacterial cell will not be able to survive (Silverman and Hollady, 2014; Purohit et al., 2007).

The biosynthesis of penicillins and cephalosporins has been well demonstrated metabolically and the precursors are the amino acids L-cysteine, L-valine, and L-aminoadipic acid.

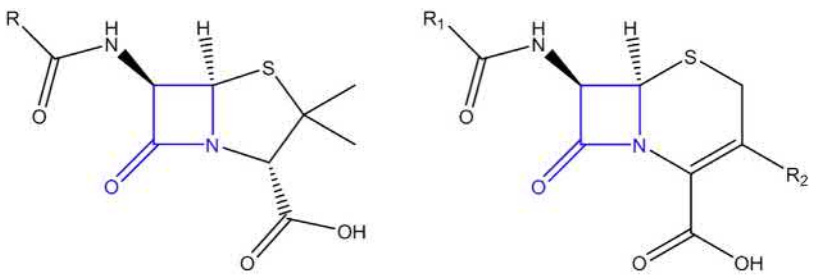

Penicillin Cephalosporin

FIGURE 5.10 General chemical structures of penicillins and cephalosporins with the beta-lactam ring shown in blue.

Penicillins G and V are produced by a fed-batch fermentation process that is conducted under aseptic conditions in tank reactors made of stainless steel. The different factors such as the pH, the temperature, and the gases are controlled using computers. The carbon source is usually carbohydrates such as glucose and most of the carbon is used for cellular maintenance and growth while only about 10% of the carbon is actually used for penicillin synthesis. Corn steep liquor, ammonium sulfate, and ammonia can be used as nitrogen sources in the medium (Elander, 2003).

The semisynthetic penicillins are molecules that have the 6-amino penicillanic acid (6-APA) scaffold. Production of 6-APA by the fermentation process is usually inefficient, therefore, it is more common to obtain 6-APA by removing the side chain of penicillin G or V. Removing the side chain of Penicillin G can be done by treating it with the enzyme penicillin G acylase, which catalyzes the conversion of Penicillin G to 6-APA. The resulting 6-APA is then treated with acid chlorides to obtain various semisynthetic penicillins (Arroyo et al., 2003).

5.5.2 Hormones

There are therapeutically important hormones that are proteins or peptides in nature, such as insulin and human growth hormone (hGH). Therefore these hormones can be produced by recombinant DNA technology. The insulin hormone, which is used for the treatment of diabetes (mainly type I) is a notable example of the success of biotechnology-based products (Voet and Voet, 2011).

5.5.2.1 Insulin Hormone

Human insulin is a 51-amino acid nonglycosylated peptide hormone that consists of two polypeptide chains, namely chains A and B. Insulin is synthesized in the beta cells of the pancreas, however, the initial form of insulin is a precursor molecule called preproinsulin that consists of 86 amino acids. This precursor molecule is converted to another insulin precursor called proinsulin via cleavage of the N-terminal signal peptide by proteolytic enzymes. The proinsulin is further cleaved internally to give the polypeptide chains A and B of insulin and the C peptide. Disulfide bonds between the polypeptide chains A and B are formed to give the final form of the insulin, which is stored in the beta cells of the pancreas for secretion (Luzhetskyy et al., 2012).

Human insulin hormone has various effects on different metabolic processes, as it has a significant role in the regulation of carbohydrates metabolism and hence blood glucose levels. Additionally, insulin also has various effects on the metabolism of proteins and lipids. The inability to produce sufficient insulin hormone gives rise to diabetes mellitus type 1, which is a metabolic disease in which the glucose levels are elevated in the blood as well as in the urine. Other metabolic abnormalities include high rates of ketogenesis, beta-oxidation of fatty acids, and gluconeogenesis (Voet and Voet, 2011). Diabetes is a prevalent condition that affects a wide range of population with the possible progression of the disease to different complications or even death. The causes of the insulin deficiency include the progressive destruction of the beta cells that synthesize and secrete insulin by autoimmune conditions or viral infections.

Treating diabetes type 1 can be achieved through the administration of a proper insulin formulation to compensate for the deficient endogenous insulin and lower the blood glucose levels (Walsh, 2014a).

In the past, the majority of the insulin preparations contained insulin extracted from the pancreas of animals such as pigs. However, this method suffered from several issues such as immunogenicity of the extracted insulin as well as the possible contaminants presents in the pancreatic extracts that could cause harmful effects on the patient. Recombinant DNA technology can be used to produce human insulin with better properties as well as in larger quantities. Insulin can be prepared by the expression of the nucleotide sequence that codes for the proinsulin polypeptide in a suitable host, usually *E. coli* cells. The synthesized proinsulin molecules are converted to insulin by the action of proteolytic enzymes. It is also possible to use separate systems for the production of the polypeptide chains A and B, then to isolate and purify them from the different systems. Finally, the two chains are joined by the disulfide bonds to give the final product (Luzhetskyy et al., 2012). To ensure the purity of insulin preparations from any impurities that can arise from the production process, various methods such as HPLC can be employed to remove these impurities and give high purity insulin preparations (Walsh, 2014b).

5.5.2.2 *Human Growth Hormone*

hGH, also known as somatotropin, is a 191-amino acid nonglycosylated peptide hormone with a molecular weight of 22,000 Da. This hormone is synthesized in the cells of the anterior pituitary; however, this initially synthesized form contains an additional peptide sequence that is cleaved later to give the hGH that circulate in the blood. This hormone is essential for proper human growth and development processes, and any deficiencies can result in growth abnormalities (Jamil, 2007; Simpson et al., 2002). The effects of the hGH include metabolic regulation of various pathways such as increasing the synthesis of proteins, decreasing glucose metabolism, and increasing lipolysis. The hGH products have been shown to be successful in treating various conditions such as hGH deficiency, Prader–Willi syndrome, and Turner syndrome. In addition to the effectiveness of the hGH in treating these conditions, it also has good safety profile as no serious side effects are present (Iglesias and Diez, 1999; Takeda et al., 2010).

There are several pharmaceutical companies that produce recombinant hGH using different methods in the production, isolation, and purification of the hormone. *E. coli* cells can be used as the host cells because the hGH is nonglycosylated. For example, Genotropin is produced into the host system as a fusion protein, where an attached signal sequence (enterotoxin II signal sequence) allows the protein to be secreted into the periplasmic space. Once the fusion protein is at the periplasmic space, a peptidase enzyme cleaves the fusion protein into the active form of hGH with all residues except the N-terminal methionine residue. After the hormone has been expressed in the cells, the cells are harvested and the content is released by freezing and thawing process. Several chromatographic methods are then required for the purification of the protein (Luzhetskyy et al., 2012). The available formulations of the recombinant hGH are usually supplied in a lyophilized form (Beale, 2011).

5.5.3 Enzymes

Enzymes are proteins that are used for the catalysis of chemical reactions in the cells and are responsible for the synthesis and degradation of various biological molecules. Therefore enzymes can also play roles in pathological conditions, as the deficiency of enzymes can cause various diseases depending on the function of the deficient enzyme. For example, if an enzyme that is responsible for the degradation of a certain compound is deficient, then the accumulation of that compound can lead to metabolic abnormalities and harmful effects (Silverman and Hollady, 2014). Deficiencies of enzymes mainly arise because of hereditary conditions. Because of these various roles of enzymes in pathological conditions, the production of enzymes as drugs for the treatment of different diseases is an attractive approach. Various biotechnology-based enzymes have been introduced into the market and have been shown to be successful for the treatment of the targeted diseases (Yari et al., 2017; Kunamneni et al., 2018).

For example, Gaucher's disease is caused by the deficiency of the enzyme beta-glucocerebrosidase, and is a hereditary condition. This enzyme is responsible for the catalysis of the hydrolysis of glucocerebroside to give the corresponding ceramide and glucose. A deficiency of a properly functioning beta-glucocerebrosidase in the cells will lead to the accumulation of the substrate glucocerebroside, which is a glycolipid. The glucocerebroside accumulates mainly in the macrophages, which are called Gaucher's cells in this case. These Gaucher's cells can accumulate in other body organs and cause further complications such as anemia. The spleen, liver, and bone marrow are the main sites of accumulation, although it is possible for the accumulation to occur in other organs such as the kidney (Smith et al., 2017; Beale, 2011). Recombinant beta-glucocerebrosidase produced by CHO cells can be provided as an enzyme therapy for the treatment of this Gaucher's disease by catalyzing the hydrolysis of the glucocerebroside and thus normalizing the metabolic pathway (Beale, 2011).

Another example of using enzyme therapy to treat pathological conditions is in chronic pancreatitis treatment. In this condition, different enzymes are used including lipase and amylases, which are pancreatic enzymes for the treatment of chronic pancreatitis (Inatomi et al., 2016).

5.5.4 Blood Clotting Factors

The blood clotting process involves a series of various plasma proteins that function with each other to properly carry out the clotting process. In cases where any of these factors is absent or deficient, the clotting process will not proceed properly leading to serious pathological conditions such as hemophilia A and B (Palta et al., 2014; Zimmerman and Valentino, 2013). Deficiencies of clotting factors can be caused by genetic disorders, although nongenetic blood clotting disorders can occur because of liver dysfunction or deficiency in vitamin K, which plays an important role in the coagulation process. Normally, treating the conditions related to blood clotting factors deficiency is achieved through administration of the deficient blood clotting factor. The sources of the blood clotting factors can be the blood of healthy human donors or by recombinant DNA technology–based production (Sutor et al., 1999; Zimmerman and Valentino, 2013).

Blood clotting factors from the blood of a healthy human donor are obtained by treating several purification steps as well as sterilization (Di Minno et al., 2016). Purification of

blood clotting factors can be done through fractionation techniques although chromatographic techniques can also be employed in purifying some clotting factors. Sterilization of the produced form is done by filtration. The final preparation is freeze-dried and usually, an anticoagulant agent is added to the preparation. The major drawback of using blood clotting factors obtained from donors is the possibility of the presence of viral contaminants or other pathogens, which will be transferred to the patient receiving the treatment and thus resulting in infectious diseases. Screening of blood donations, as well as the addition of antiviral agents to the final preparation, can help in preventing the possible viral transmission to the patients receiving the treatment (Franchini, 2013; Walsh, 2014c).

Another method for the production of blood clotting factors is by using recombinant DNA technology. In this case, the recombinant blood clotting factors preparation has the advantage of being devoid of the possible viral and pathogenic contaminants that are associated with obtaining the clotting factors from blood donors. Since the majority of blood clotting factors are glycosylated, in addition to having other posttranslational modifications, it is necessary to use a eukaryotic cell as the host. The used cells for production include CHO cells as well as BHK cells. The final form is purified using different chromatographic methods and the final product is usually supplied in a lyophilized form (Pipe, 2008; Lusher, 2000; Lee, 1999).

5.5.5 Cytokines

Cytokines are a group of protein molecules produced mainly by the leukocytes that regulate the immunological and inflammatory response in addition to carrying out various other functions such as controlling the growth and differentiation of cells. Cytokines act through activation of the receptors on the target's cell surface. Although cytokines are secreted mainly by the leukocytes, certain other cells in the body can also produce them (Vilček and Feldmann, 2004). There are different classes of cytokines, including interferons and interleukins, which are of a particular interest in the therapeutic applications of cytokines. Because of the diverse functions of cytokines, their use as therapeutic agents has great potential for treating various conditions such as cancer and viral infections (Tayaland Kalra, 2008).

5.5.5.1 Interferons

Interferons are a class of cytokines that have antiviral activity as well as potential anticancer effects. Interferons can be classified into two types, the type I consists of alpha-interferon and beta-interferons, while type II consists of gamma-interferon. Type I interferons are produced by different cells in response to various stimuli (Vilček and Feldmann, 2004). The cells include specialized dendritic cells and macrophages. The stimulus can be viruses or certain molecules such as double-stranded RNA. On the other hand, type II interferon is produced mainly by the natural killer cells as well as the T cells and secreted in response to different stimuli. All the interferons act by binding to different heterodimeric receptors on the targeted cell's surface and transduce the signal through the activation of the Janus-activated kinase as well as signal transducer and activator of

transcription. This leads to the expression of different genes to give the required biological response (Darnell et al., 1994; Vilček and Feldmann, 2004).

All the three mentioned interferons can be used clinically for treating various conditions that are related to viral infections as well as cancer. Available alpha-interferon preparations include recombinant interferon$_{2a}$ (Rofereon-A, Roche), which is produced as a nonglycosylated protein that consists of 165 amino acids. This product is indicated mainly for the treatment of hepatitis B and C as well as Kaposi's sarcoma (El-Baky and Redwan, 2015; Jones and Itri, 1986).

Interferon-beta$_{1b}$ (betaferon, Schering) is a human beta-interferon-based product produced for treating relapsing/remitting multiple sclerosis. The host cells used for expression are *E. coli* cells with identical amino acid sequence except for one cysteine residue that is replaced by a serine residue for improving the stability during the synthesis process inside the cells (Rojas et al., 2014; Zvonova et al., 2017).

Therapeutic preparations of gamma-interferon are also available; for example, gamma-interferon$_{1b}$ is a polypeptide chain that is composed of 140 amino acids. Although the gamma-interferon produced naturally in the cells is a glycosylated polypeptide, the commercial form is nonglycosylated as the host used is *E. coli* cells. Indications of this product include severe malignant osteoporosis as well as chronic granulomatous (Watson, 2011).

5.5.5.2 *Interleukins*

Interleukins are a class of cytokines that are secreted by different cells of the immune system and their main function is the regulation of immunity. Interleukins function by binding to specific receptors on the surface of the target cells as evident with all other cytokines (Vilček and Feldmann, 2004). The polypeptide chain of interleukins can be glycosylated or nonglycosylated. In many cases, it has been found that removing the carbohydrate portion of a glycosylated interleukin does not significantly affect the biological activity. Several interleukins have been introduced into the market as therapeutic products for treating various pathological conditions, mainly cancer (Walsh, 2014d).

For example, an interleukin-2-based product, Proleukin, is one of the interleukins that have been approved for the treatment of melanoma as well as renal cell carcinoma. Normally, this interleukin is glycosylated, however, since the host is *E. coli* cells, the produced form does not contain a carbohydrate moiety. In spite of the absence of the carbohydrate moiety, the activity of the produced interleukins is not affected in a significant manner (Klatzmann and Abbas, 2015; Sanchez-Garcia et al., 2016).

5.5.6 Monoclonal Antibodies

The monoclonal antibodies are promising biochemical agents that have a wide range of applications in biotechnology and biomedicine. They can be used as therapeutic agents for the treatment as well as vaccines in addition to various other applications (Ganguly and Wakchaure, 2016). Monoclonal antibodies possess many advantages over polyclonal antibodies including their high binding affinity, high selectivity for their antigens and the consistency of production. Because antibody-producing cells such as B lymphocytes cannot be cultured for extended periods of time, monoclonal antibodies cannot be obtained

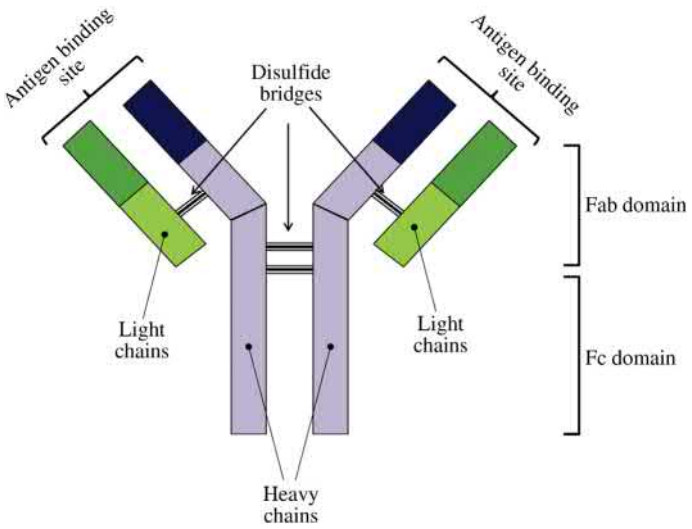

FIGURE 5.11 The general structure of an antibody.

by this method. However, it is possible to produce monoclonal antibodies in a more consistent manner by using the hybridoma technology and the DNA technology. The general structure of an antibody is shown in Fig. 5.11 (Walsh, 2014a).

The hybridoma technology involves the use of myeloma cells, which are immortal cells, to produce immortal cells that can generate the antibody of interest. This is achieved by fusing the myeloma cells and the antibody-secreting cells to produce hybridomas. These hybridomas have the ability to produce the antibody of interest in a similar manner to the antibody-secreting cells used in the fusion process. Also, the hybridomas are immortal cells as the myeloma cells used in the fusion are also immortal cells. Therefore the hybridomas are both immortal cells and can produce the antibody of interest and these cells can be further cultured to produce larger quantities. The general principle of hybridoma technology is demonstrated in Fig. 5.12 (Tomita and Tsumoto, 2011; Yagami et al., 2013).

An example of a monoclonal antibody drug used in treating cancer is trastuzumab (Herceptin), which is used for the treatment of breast cancer (Molina et al., 2001).

5.5.7 Vaccines

Vaccine preparations are administrated for the purpose of providing prevention against a particular disease. Vaccines act through stimulating the immune system to generate memory cells that allow for an enhanced immune system response against the pathogen upon exposure. Vaccines can be attenuated living pathogens that are unable to exert a harmful effect when administered. However, they still have their ability to stimulate the immune system for response and to produce immunity against them (Watson, 2011). Production of these attenuated living vaccines can be achieved by different methods such as genetic engineering techniques that remove genes responsible for pathogenicity. Vaccines can also be dead pathogens that still have their antigens present on their surfaces. The antigens will stimulate the immune response to produce immunity and because these

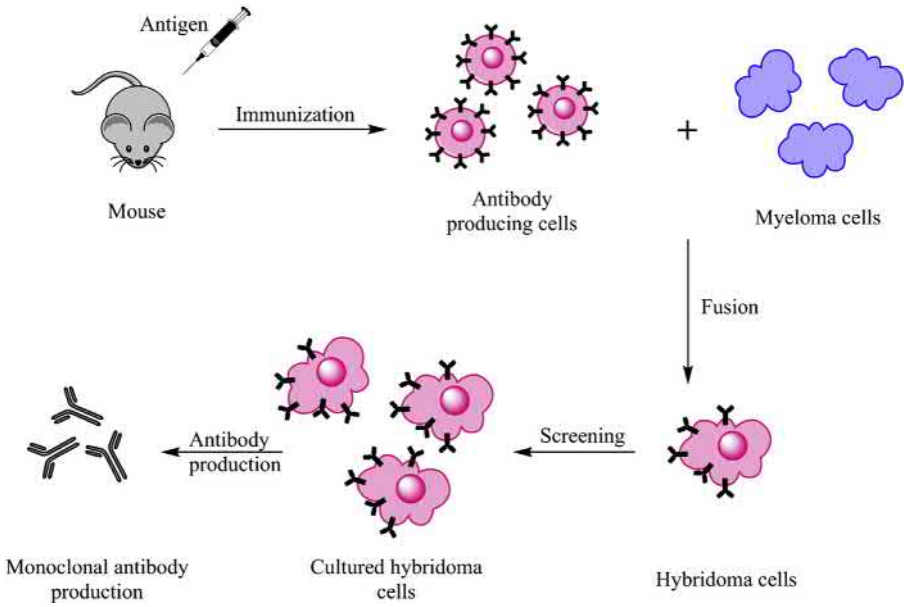

FIGURE 5.12 The general principle of hybridoma technology.

pathogens are inactivated, they carry no risk of pathogenicity. Inactivation of these pathogens can be achieved by treating them with chemical agents such as formaldehyde or by exposing them to heat (Delrue et al., 2012; Stauffer et al., 2006). Another type of vaccine involves the extraction of the antigens that are responsible for the immune response from the pathogens and inactivating them. These inactivated antigens are nonharmful upon administration, while the same types are still capable of stimulating an immune response. In this approach, biotechnology can be used for the production of these antigens, which are safe but can cause an immune response to obtaining immunity (Watson, 2011).

For example, the hepatitis B vaccine has been successfully produced through biotechnology-based methods for use in the prevention of hepatitis B viral infection. A glycoprotein on the surface of the virus serves as the antigen for immune response induction. The *E. coli* cells are not used as host cells because of the improper folding observed in the protein when these cells are used. The production can take place successfully in yeast cells. Both glycosylated and nonglycosylated proteins are produced, however, glycosylation of the antigen does not seem to have a significant role concerning the ability to stimulate the immune response (Scolnick et al., 1984; Petre et al., 1987).

5.6 A SUMMARY OF COMMERCIALLY AVAILABLE LEADING BIOTECHNOLOGY-BASED PRODUCTS

There are many biotechnology-based pharmaceutical products approved for medical applications in various parts of the world. Most of these products are protein-based

TABLE 5.1 A Summary of Important Biotechnology-Based Pharmaceutical Products That Are Approved for Medical Applications.

Product	Therapeutic Application	Year of Approval
Insuman	Diabetes mellitus	1997
Optisulin	Diabetes mellitus	2000
Nutropin AQ	Growth disorders	2001
Nutropin AQ	Diabetes mellitus	1997
Benefix	Hemophilia B	1997
Tenecteplase	Myocardial infarction	2001
Xigris	Sepsis	2002
Infergen	Chronic hepatitis C	1999
Avonex	Relapsing multiple sclerosis	1997
Rebif	Relapsing multiple sclerosis	1998
Humalog	Diabetes mellitus	1996
Beromun	Adjuvant therapy after removal of the tumor by surgery	1999
Enbrel	Rheumatoid arthritis	2000
Remicade	Crohn's disease	1999
Cerezyme	Gaucher's disease	1997

therapeutic agents that are indicated for the treatment of different diseases such as diabetes mellitus, growth disorders, hemophilia, and various others. Other medical applications include vaccination to introduced immunity against specific types of diseases such as hepatitis B. In addition, monoclonal antibodies-based products can be used for the diagnosis of specific pathological conditions such as ovarian adenocarcinoma. Table 5.1 provides a summary of important biotechnology-based pharmaceutical products that are approved for medical applications (Walsh, 2003; Ganguly and Wakchaure, 2016).

5.7 NANOBIOTECHNOLOGY

Nanobiotechnology has a wide range of applications in biomedicine including the treatment of pathological conditions, the design of drug delivery systems and in the diagnoses of various diseases. Nanobiotechnology also has applications in various stages of drug discovery and development such as in the target identification and validation, lead compound generation, and optimization. In addition, some nanomaterials have been investigated as drug candidates themselves such as dendrimers and carbon nanotubes (CNTs) (Jain, 2005).

An example of the application of nanobiotechnology is the development of cancer vaccines carriers. Cancer vaccines are used in tumor immunotherapy, which involves activation of the patient's immune system and allowing it to recognize the tumor cells and kill these cells, which are normally not recognized by the immune system. This method of treatment can be used as an alternative treatment to the other traditional methods of cancer treatment or adjuvant to them (Peek et al., 2008). The main advantages of tumor immunotherapy over other methods such as chemotherapy include the selectivity for the cancer cells, which means a highly reduced toxicity to the normal cells. This advantage can be significant since the majority of the drugs used in chemotherapy are known for their severe toxic effects on normal healthy cells. Another advantage of this treatment method is that the activation of the immune system to recognize tumor cells will allow for the long-term prevalence of the immunity against these cells even in cases of the reappearance of the tumor. A proper vaccine carrier is required for the success of tumor immunotherapy, and in this regard, different nanoparticle carriers have been investigated for this purpose. The nanocarrier should possess several important properties to ensure the suitability for application in tumor immunotherapy; these properties include having proper loading capacity, biocompatibility, good safety profile, and reasonable cost. The biodegradability of the carrier should also be taken into consideration as well as the products of the degradation should be nontoxic. Examples of nanocarriers that have been investigated for their use as vaccine carriers for treating cancer include liposomes, viruses, and acrosomes (Geary et al., 2012).

5.8 GENE THERAPY

Gene therapy represents a highly promising approach for treating various pathological conditions by correcting the genetic defects that are responsible for the disease. Since many diseases such as cancer, hemophilia, and diabetes are caused by genetic mutations in specific genes, it is believed that correcting these mutations and restoring them to normal can cure the disease. Therefore gene therapy not only offers treatment of the symptoms of the disease but also provides the potential to completely cure the disease. Correction of mutations can be done through the replacement of the defective gene by a normal cloned gene or by the insertion of the required gene as an additional gene that when expressed, the produced protein will have the desired therapeutic effects (Beale, 2011). In the case where the genetic medications are carried out on a somatic cell in the body, the induced changes will be maintained as long as the cell is alive. While in the case where the genetic modifications are carried out on germ cells, the induced changes will be passed on to the subsequent generations. The process of gene transfer can be conducted via two different methods, either in vivo or ex vivo. In the case of the in vivo gene transfer method, the gene transfer process takes place directly in the cells. On the other hand, in the ex vivo gene transfer method, the cells are removed from the body prior to the gene transfer, and after the process is complete the cells are reintroduced into the body (Ferrier, 2014).

An essential factor for the success of the gene transfer process is the use of the proper vector for the gene. The development of a good vector for transferring genes represents a challenge for the advancement and success of gene therapy; therefore various types of

vectors have been investigated for this purpose. Examples of vectors that have protein for use in gene therapy include viruses and CNTs. Other challenges that need to be overcome for the success of gene therapy include the circumvention of adverse effects such as immunological responses as well as achieving proper expression periods of the gene that allows for the treatment of the disease. In addition to having potential in the treatment of diseases, gene therapy can also have other important applications such as developing genetically modified animal models for studying human pathological conditions (Ferrier, 2014; Beale, 2011).

5.9 PHARMACOGENOMICS

Pharmacogenomics is concerned with the use of information obtained from the genome sequence of the patient to allow for better therapeutic decisions regarding the treatment and drug prescription. The basis of pharmacogenomics comes from the fact that the response of a patient to a drug can be affected by the degree of activity of certain genes. The therapeutic response, as well as the toxicity of the administrated drug, can be largely influenced by the genome of the patient. Therefore by obtaining information from the genetic sequence of the patient, the physician can make better therapeutic decisions by selecting drugs that are more effective as well as safer for the patient. In the case where an invading pathogen is present, genomic information of the pathogen can also be used to improve the treatment process. Other types of therapies such as gene therapy and antisense therapy, which are dependent on the genomics of the patient, are also improved by pharmacogenomics. The general concept of pharmacogenomics is depicted in Fig. 5.13 (Roy, 2013; Beale, 2011).

An example of a case where the genomics of the patient needs to be taken into consideration when prescribing drugs is the effect of drug transporters on the administrated drug. Drug transporters are proteins that are expressed in different locations with different levels and can influence the absorption and distribution of the drug in the body and hence the efficacy of the drug. The toxicity of the drug and the drug–drug interactions are also affected by the action of drug transporters on the administrated drug. The expression of the drug transporters is subject to genetic variations; therefore determination of these variations can help in predicting the effects of these transporters on a given drug. It should be noted that the expression of the drug transporters can also be affected by other factors such as environmental factors (Tsunoda, 2013).

5.10 STEM CELL THERAPY

Stem cells are the undifferentiated type of cells that have the potential to differentiate into different types of cells depending on the chemical agents they are treated with. The clinical potential of stem cells lies in the possibility of using these cells for damaged tissue and even complete organ replacement. Stem cells taken from embryos involved in genetic diseases such as cystic fibrosis can also be used for achieving a better understanding of the mechanisms underlying these pathological conditions. The possibility to isolate human

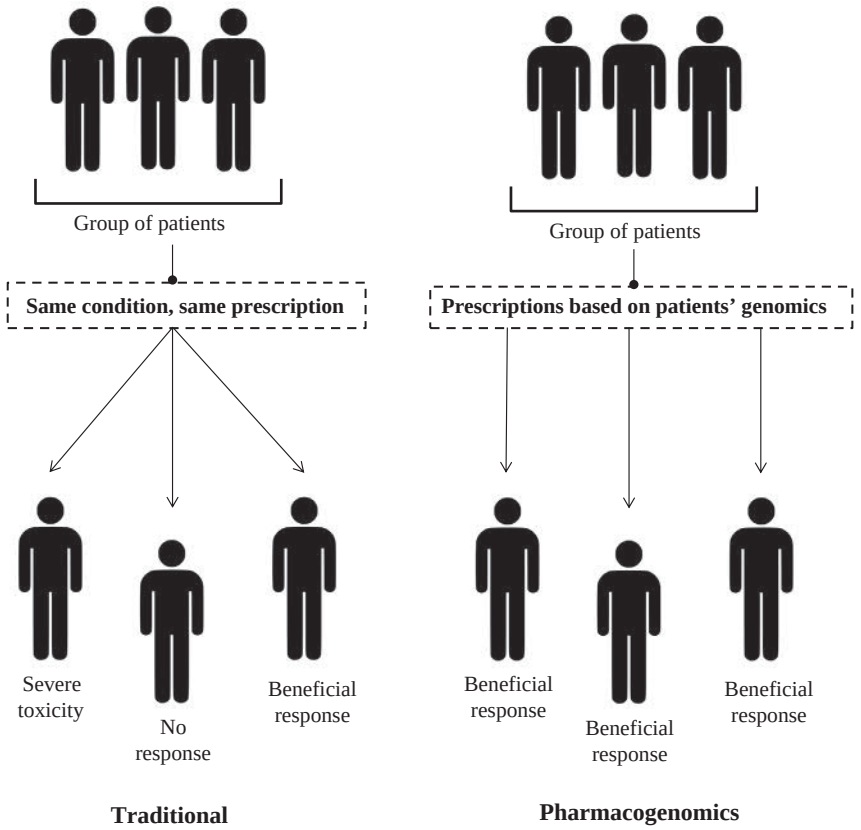

FIGURE 5.13 The general concept of pharmacogenomics.

embryonic stem cells is an important advancement in the stem cell therapy field, as these cells can be induced to differentiate into various types of cells. For example, it is possible to obtain in vitro neural cells, hematopoietic cells, hepatocytes, and other types of cells from human embryonic stem cells (Barh et al., 2012).

5.11 CONCLUSION

The biotechnology-based products have created a great impact on the pharmaceutical industry and continue to show great success in the development of therapeutic agents. The production process of biotechnology-based therapeutic products is composed mainly of two stages, namely the upstream processing and the downstream processing. In the upstream processing, the desired therapeutic molecule such as a protein is produced by a host cell, which should be properly selected to successfully express the gene for that therapeutic protein. Following the production of the desired molecule in the host cells in a sufficient amount, the downstream processing is conducted which involves the isolation and

purification of the targeted molecule from the host cells or the culture medium. Different methods and steps are usually required for the successful isolation and purification of the synthesized target molecule. Proper characterization of the produced therapeutic agents is also an absolute requirement in the production process of biotechnology-based products.

The pharmacokinetic properties of biotechnology-based products can be different from those of the conventional small drug molecules, although the general principles are similar. Usually, large biomolecules such as proteins have poor pharmacokinetic profile due to their instability inside the GIT as well as the plasma. Therefore the special oral delivery system is usually required for proteins or peptides that are intended for oral administration.

There are various other problems associated with biotechnology-based products, which include their unstable nature in pharmaceutical formulations as they are susceptible to both chemical and physical degradation. Immunogenicity of large molecules should also be considered since it may lead to fatal consequences. In addition, there have been many ethical and regulatory concerns raised on biotechnology-based products such as patents on living organisms.

Currently, various classes of therapeutic products are being produced through biotechnology such as antibiotics, enzymes, hormones, monoclonal antibodies, and vaccines. These products are used in treating and preventing different diseases that affect a large portion of the population.

There are many promising biotechnology-based approaches being developed for the improvement of medicine as well as for the treatment of various diseases. For example, gene therapy, pharmacogenomics, and stem cell therapy are biotechnology-based approaches that have the potential for highly improving the treatment process in different ways.

ABBREVIATIONS

6-APA	6-amino penicillanic acid
BHK	baby hamster kidney
cDNA	complementary deoxyribonucleic acid
CHO	Chinese hamster ovary
CNTs	carbon nanotubes
DNA	deoxyribonucleic acid
mRNA	messenger ribonucleic acid
PEG	polyethylene glycol
RNA	ribonucleic acid
SDS	sodium dodecyl sulfate
SDS–PAGE	sodium dodecyl sulfate–polyacrylamide gel electrophoresis

References

Amarji, B., Sara Nidal, A., Bairag, U., Pran Kishore, D., Al-Attraqchi, O., Choudhury, A.A., et al., 2018. Chapter-18: Four stages of pharmaceutical product development: preformulation, prototype development and scale-up, biological aspects, and commercialization. In: Tekade, R.K. (Ed.), Dosage Form Design Considerations: Advances in Pharmaceutical Product Development and Research Series, vol. I. Academic Press, pp. 637–668.

Arpna, I., Mahendra, P., Piyoosh, A.S., Sara Nidal, A., Abeer, S., Rahul, M., et al., 2018. Chapter-6: Influence of drug properties and routes of drug administration on the design of controlled release systems.

In: Tekade, R.K. (Ed.), Dosage Form Design Considerations: Advances in Pharmaceutical Product Development and Research Series, vol. I. Academic Press, pp. 179–223.
Arroyo, M., De la Mata, I., Acebal, C., Castillon, M.P., 2003. Biotechnological applications of penicillin acylases: state-of-the-art. Appl. Microbiol. Biotechnol. 60 (5), 507–514.
Ashok, K.S., Al-Najjar, B.M.O., Pran Kishore, D., Rakesh Kumar, T., 2018. Chapter-8: First pass metabolism considerations in pharmaceutical product development. In: Tekade, R.K. (Ed.), Dosage Form Design Considerations: Advances in Pharmaceutical Product Development and Research Series, vol. I. Academic Press, pp. 259–286.
Balakumar, C., Sarah Nedal, A., Al-Attraqchi, O., Kaushik, K., Rakesh, K.T., 2018. Chapter-21: Computer aided prediction of pharmacokinetic (ADMET) properties. In: Tekade, R.K. (Ed.), Dosage Form Design Parameters: Advances in Pharmaceutical Product Development and Research Series, vol. II. Academic Press, pp. 731–755.
Barh, D., Ahmed, S., Bhattacharjee, A., 2012. In silico and ultrahigh-throughput screening (uHTS) in drug discovery: an overview. In: Kayser, O., Warzecha, H. (Eds.), Pharmaceutical Biotechnology Drug Discovery and Clinical Applications. Wiley Blackwell, Germany, pp. 453–490.
Beale, J.M., 2011. Biotechnology and drug discovery. In: Beale, J.M., Block, J.H. (Eds.), Wilson and Gisvold's Textbook of Organic Medicinal and Pharmaceutical chemistry., twelfth ed. Lippincott Williams & Wilkins, China, pp. 119–155.
Bhatt, N.P., Patel, K., Borchardt, R.T., 1990. Chemical pathways of peptide degradation I. Deamidation of adrenocorticotropic hormone. Pharm. Res. 7, 539–599.
Bhopale, G.M., Nanda, R.K., 2005. Recombinant DNA expression products for human therapeutic use. Curr. Sci. 89 (4), 614–622.
Choi, J.H., Keum, K.C., Lee, S.Y., 2006. Production of recombinant proteins by high cell density culture of *Escherichia coli*. Chem. Eng. Sci. 61 (3), 876–885.
Choonara, B.F., Choonara, Y.E., Kumar, P., Bijukumar, D., du Toit, L.C., Pillay, V., 2014. A review of advanced oral drug delivery technologies facilitating the protection and absorption of protein and peptide molecules. Biotechnol. Adv. 32 (7), 1269–1282.
Clardy, J., Fischbach, M.A., Currie, C.R., 2009. The natural history of antibiotics. Curr. Biol. 19 (11), R437–R441.
Darnell, J.E., Kerr, I.M., Stark, G.R., 1994. JAK-STAT pathways and transcriptional activation in response to IFNs and other extracellular signaling proteins. Science 264 (5164), 1415–1421.
Delrue, I., Verzele, D., Madder, A., Nauwynck, H.J., 2012. Inactivated virus vaccines from chemistry to prophylaxis: merits, risks, and challenges. Expert Rev. Vaccines 11 (6), 695–719.
Di Minno, G., Perno, C.F., Tiede, A., Navarro, D., Canaro, M., Güertler, L., et al., 2016. Current concepts in the prevention of pathogen transmission via blood/plasma-derived products for bleeding disorders. Blood Rev. 30 (1), 35–48.
Doherty, A.J., Suh, S.W., 2000. Structural and mechanistic conservation in DNA ligases. Nucleic Acids Res. 28 (21), 4051–4058.
Elander, R.P., 2003. Industrial production of β-lactam antibiotics. Appl. Microbiol. Biotechnol. 61 (5–6), 385–392.
El-Baky, N.A., Redwan, E.M., 2015. Therapeutic alpha-interferons protein: structure, production, and biosimilar. Prep. Biochem. Biotechnol. 45 (2), 109–127.
Ellenberger, T., Tomkinson, A.E., 2008. Eukaryotic DNA ligases: structural and functional insights. Annu. Rev. Biochem. 77, 313–338.
Ferrier, D.R., 2014. Biotechnology and human diseases, Lippincott's Illustrated Reviews: Biochemistry, sixth ed. Lippincott Williams & Wilkins, China, pp. 465–488.
Florence, A.T., Attwood, D., 2011. Peptides, proteins and other biopharmaceuticals, Physicochemical Principal of Pharmacy., fifth ed. Pharmaceutical Press, UK, pp. 451–478.
Franchini, M., 2013. The modern treatment of hemophilia: a narrative review. Blood Transfus. 11 (2), 178–182.
Ganguly, S., Wakchaure, R., 2016. Hybridoma technology: a brief review on its diagnostic and clinical significance. Pharm. Biol. Eval. 3 (6), 554–555.
Geary, S.M., Lemke, C.D., Krishnamachari, Y., Salem, A.K., 2012. New nanobiotechnological strategies for the development of vectors for cancer vaccines. In: Kayser, O., Warzecha, H. (Eds.), Pharmaceutical Biotechnology Drug Discovery and Clinical Applications. Wiley Blackwell, Germany, pp. 391–422.
Gottschalk, U., 2012. Downstream processing. In: Kayser, O., Warzecha, H. (Eds.), Pharmaceutical Biotechnology Drug Discovery and Clinical Applications. Wiley Blackwell, Germany, pp. 179–200.

Gupta, H., Sharma, A., 2009. Recent trends in protein and peptide drug delivery systems. Asian J. Pharm. 3 (2), 69–75.
Hamman, J.H., Steenekamp, J.H., 2011. Oral peptide drug delivery: strategies to overcome challenges. In: Castanho, M., Santos, N.C. (Eds.), Peptide Drug Discovery and Development: Translational Research in Academia and Industry. Wiley, pp. 71–90.
Harbers, M., 2008. The current status of cDNA cloning. Genomics 91 (3), 232–242.
Ho, R.J., Gibaldi, M., 2004. Comparative drug development of proteins and genes versus small molecules. Biotechnology and Biopharmaceuticals: Transforming Proteins and Genes Into Drugs. Wiley, pp. 11–20.
Iglesias, P., Diez, J.J., 1999. Clinical applications of recombinant human growth hormone in adults. Expert Opin. Pharmacother. 1 (1), 97–107.
Inatomi, O., Fujimoto, T., Hasegawa, H., Osaki, R., Imaeda, H., Bamba, S., et al., 2016. Therapeutic efficacy of pancreatic enzyme supplement and clinical characteristics in early chronic pancreatitis. Pancreatology 16 (4), S106–S107.
Jain, K.K., 2005. The role of nanobiotechnology in drug discovery. Drug Discov. Today 10 (21), 1435–1442.
Jain, A., Jain, A., Gulbake, A., Shilpi, S., Hurkat, P., Jain, S.K., 2013. Peptide and protein delivery using new drug delivery systems. Crit. Rev. Ther. Drug Carrier Syst. 30 (4), 293–329.
Jamil, S.A., 2007. Structure-function relation of somatotropin with reference to molecular modeling. Curr. Prot. Pept. Sci. 8 (3), 283–292.
Jayapal, K.P., Wlaschin, K.F., Hu, W., Yap, M.G., 2007. Recombinant protein therapeutics from CHO cells-20 years and counting. Chem. Eng. Prog. 103 (10), 40.
Jones, G.J., Itri, L.M., 1986. Safety and tolerance of recombinant interferon alfa-2a (Roferon®-A) in cancer patients. Cancer 57 (S8), 1709–1715.
Kaltashov, I.A., Bobst, C.E., Abzalimov, R.R., Wang, G., Baykal, B., Wang, S., 2012. Advances and challenges in analytical characterization of biotechnology products: mass spectrometry-based approaches to study properties and behavior of protein therapeutics. Biotechnol. Adv. 30 (1), 210–222.
Kayser, O., Warzecha, H., 2012. Pharmaceutical biotechnology and industrial applications-learning lessons from molecular biology. In: Kayser, O., Warzecha, H. (Eds.), Pharmaceutical Biotechnology Drug Discovery and Clinical Applications. Wiley Blackwell, Germany, pp. 3–15.
Kessler, M., Goldsmith, D., Schellekens, H., 2006. Immunogenicity of biopharmaceuticals. Nephrol. Dial. Transplant. 21 (Suppl. 5), v9–v12.
Klatzmann, D., Abbas, A.K., 2015. The promise of low-dose interleukin-2 therapy for autoimmune and inflammatory diseases. Nat. Rev. Immunol. 15 (5), 283–294.
Kunamneni, A., Ogaugwu, C., Goli, D., 2018. Enzymes as therapeutic agents. In: Nunes, C., Kumar, V. (Eds.), Enzymes in Human and Animal Nutrition. *Elsevier*, pp. 301–312.
Lee, C., 1999. Recombinant clotting factors in the treatment of hemophilia. Thromb. Haemost. 82 (02), 516–524.
Lequin, R.M., 2005. Enzyme immunoassay (EIA)/enzyme-linked immunosorbent assay (ELISA). Clin. Chem. 51 (12), 2415–2418.
Lin, J.H., 2009. Pharmacokinetics of biotech drugs: peptides, proteins and monoclonal antibodies. Curr. Drug Metabol. 10 (7), 661–691.
Lodish, H., Berk, A., Kaiser, C.A., Krieger, M., Bretscher, A., Ploegh, H., et al., 2008. DNA cloning and characterization, Molecular Cell Biology., sixth ed. W. H. Freeman and Company, New York, pp. 176–191.
Loenen, W.A., Dryden, D.T., Raleigh, E.A., Wilson, G.G., Murray, N.E., 2013. Highlights of the DNA cutters: a short history of the restriction enzymes. Nucleic Acids Res. 42 (1), 3–19.
Lusher, J.M., 2000. Recombinant clotting factors. BioDrugs 13 (4), 289–298.
Luzhetskyy, A., Weitnaur, G., Bechthold, A., 2012. Prokaryotic cells in biotech production. In: Kayser, O., Warzecha, H. (Eds.), Pharmaceutical Biotechnology Drug Discovery and Clinical Applications. Wiley Blackwell, Germany, pp. 15–42.
Molina, M.A., Codony-Servat, J., Albanell, J., Rojo, F., Arribas, J., Baselga, J., 2001. Trastuzumab (herceptin), a humanized anti-Her2 receptor monoclonal antibody, inhibits basal and activated Her2 ectodomain cleavage in breast cancer cells. Cancer Res. 61 (12), 4744–4749.
Muneeruddin, K., Nazzaro, M., Kaltashov, I.A., 2015. Characterization of intact protein conjugates and biopharmaceuticals using ion-exchange chromatography with online detection by native electrospray ionization mass spectrometry and top-down tandem mass spectrometry. Anal. Chem. 87 (19), 10138–10145.

Nagaich, U., 2015. Recombinant DNA technology: a revolutionizing outlook. J. Adv. Pharm. Technol. Res. 6 (4), 147.
Nehal, M.M., Patel, P.M., Patel, N.M., 2011. A review on regulatory aspects of biotechnology derived product. Int. J. Res. Ayurveda Pharm. 2 (5), 1495–1500.
Pal, Y., Deb, P.K., Bandopadhyay, S., Nabamita, B., Rakesh, K.T., 2018. Chapter-3: Role of physicochemical parameters on drug absorption and their implications for pharmaceutical product development. In: Tekade, R.K. (Ed.), Dosage Form Design Considerations: Advances in Pharmaceutical Product Development and Research Series, vol. I. Academic Press, pp. 85–116.
Palta, S., Saroa, R., Palta, A., 2014. Overview of the coagulation system. Indian J. Anaesth. 58 (5), 515–523.
Pasut, G., Veronese, F.M., 2012. State of the art in PEGylation: the great versatility achieved after forty years of research. J. Control. Release 161 (2), 461–472.
Patil, S.V., Patil, R.Y., Barge, V.U., 2014. Size-exclusion chromatography in biotech industry. J. Microbiol. Biotechnol. 3 (4), 11–14.
Peek, L.J., Middaugh, C.R., Berkland, C., 2008. Nanotechnology in vaccine delivery. Adv. Drug Deliv. Rev. 60 (8), 915–928.
Petre, J., Van Wijnendaele, F., De Neys, B., Conrath, K., Van Opstal, O., Hauser, P., et al., 1987. Development of a hepatitis B vaccine from transformed yeast cells. Postgrad. Med. J. 63, 73–81.
Pineda, C., Hernández, G.C., Jacobs, I.A., Alvarez, D.F., Carini, C., 2016. Assessing the immunogenicity of biopharmaceuticals. BioDrugs 30 (3), 195–206.
Pipe, S.W., 2008. Recombinant clotting factors. Thromb. Haemost. 100 (5), 840–850.
Polkinghorne, J.C., 2000. Ethical issues in biotechnology. Trends Biotechnol. 18 (1), 8–10.
Powers, P.E., 2004. Ethical issues in biotechnology. Technol. Cult. 45 (1), 221–222.
Pran Kishore, D., Al-Attraqchi, O., Jaber, A.Y., Amarji, B., Tekade, R.K., 2018a. Chapter-2: Physicochemical aspects to be considered in pharmaceutical product development. In: Tekade, R.K. (Ed.), Dosage Form Design Considerations: Advances in Pharmaceutical Product Development and Research Series, vol. I. Academic Press, pp. 57–83.
Pran Kishore, D., Al-Attraqchi, O., Mailavaram, R., Tekade, R.K., 2018b. Chapter-11: Protein and tissue binding: implication on pharmacokinetic parameters. In: Tekade, R.K. (Ed.), Dosage Form Design Considerations: Advances in Pharmaceutical Product Development and Research Series, vol. I. Academic Press, pp. 371–399.
Pran Kishore, D., Al-Attraqchi, O., Balakumar, C., Anant, P., Tekade, R.K., 2018c. Chapter-16: Protein/peptide drug delivery systems: practical considerations in pharmaceutical product development. In: Tekade, R.K. (Ed.), Basic Fundamentals of Drug Delivery: Advances in Pharmaceutical Product Development and Research Series, vol. III. Academic Press, pp. 651–684.
Pran Kishore, D., Al-Attraqchi, O., Al-Qattan, M.N., Mailavaram, R., Tekade, R.K., 2018d. Chapter-19: Applications of computers in pharmaceutical product formulation. In: Tekade, R.K. (Ed.), Dosage Form Design Parameters: Advances in Pharmaceutical Product Development and Research Series, vol. II. Academic Press, pp. 665–703.
Pray, L., 2008. Restriction enzymes. Nat. Educ. 1 (1), 38.
Purohit, S.S., Kakrani, H.N., Saluja, A.K., 2007. Production of antibiotics. In: Pharmaceutical Biotechnology. Jodhpur, Student Edition, pp. 196–212.
Rahul, M., Pooja, T., Neetu, S., Nidhi, R., Pran Kishore, D., Basant, A., et al., 2018. Chapter-7: Stability and degradation studies for drug and drug product. In: Tekade, R.K. (Ed.), Dosage Form Design Considerations: Advances in Pharmaceutical Product Development and Research Series, vol. I. Academic Press, pp. 225–257.
Renukuntla, J., Vadlapudi, A.D., Patel, A., Boddu, S.H., Mitra, A.K., 2013. Approaches for enhancing oral bioavailability of peptides and proteins. Int. J. Pharm. 447 (1–2), 75–93.
Resink, D.B., 2012. Patents in the pharmaceutical biotechnology industry: legal and ethical issues. In: Kayser, O., Warzecha, H. (Eds.), Pharmaceutical Biotechnology Drug Discovery and Clinical Applications. Wiley Blackwell, Germany, pp. 269–284.
Rojas, J.J., Patrucco, L., Cristiano, E., 2014. Current and emerging treatments for relapsing multiple sclerosis in Argentinian patients: a review. Degen. Neurol. Neuromusc. Dis. 4, 103–109.
Roy, L.H., 2013. Developing perspectives on pharmacogenomics. In: Betino, J.S., DeVane, C.L., Fuhr, U., Kashuba, A.D., Ma, J.D. (Eds.), Pharmacogenomics and Introduction and Clinical Perspective. McGraw Hill, New York, pp. 1–8.

Roy, S., Kumar, V., 2014. A practical approach on SDS PAGE for separation of protein. Int. J. Sci. Res 3 (8), 955–960.
Sanchez-Garcia, L., Martín, L., Mangues, R., Ferrer-Miralles, N., Vázquez, E., Villaverde, A., 2016. Recombinant pharmaceuticals from microbial cells: a 2015 update. Microbial Cell Fact. 15 (1), 33–40.
Saraswat, M., Musante, L., Ravidá, A., Shortt, B., Byrne, B., Holthofer, H., 2013. Preparative purification of recombinant proteins: current status and future trends. BioMed Res. Int. 2013, 1–18.
Schellekens, H., 2005. Factors influencing the immunogenicity of therapeutic proteins. Nephrol. Dial. Transplant. 20 (Suppl. 6), vi3–vi9.
Scolnick, E.M., McLean, A.A., West, D.J., McAleer, W.J., Miller, W.J., Buynak, E.B., 1984. Clinical evaluation in healthy adults of a hepatitis B vaccine made by recombinant DNA. JAMA 251 (21), 2812–2815.
Shantanu, B., Nabamita, B., Pran Kishore, D., Chhater, S., Rakesh, K.T., 2018. Chapter-12: Pre-formulation studies of drug substances, protein and peptides: role in drug discovery and pharmaceutical product development. In: Tekade, R.K. (Ed.), Dosage Form Design Considerations: Advances in Pharmaceutical Product Development and Research Series, vol. I. Academic Press, pp. 401–433.
Shargel, L., Yu, A., 2016. Targeted drug delivery systems and biotechnological products, Applied Biopharmaceutics & Pharmacokinetics, seventh ed. McGraw Hill Education, pp. 615–634.
Shuman, S., 2009. DNA ligases: progress and prospects. J. Biol. Chem. 284 (26), 17365–17369.
Silverman, R., Hollady, M., 2014. Enzyme inhibition and inactivation, The Organic Chemistry of Drug Design and Drug Action, third ed. Elsevier, San Diego, CA, pp. 207–274.
Simpson, H., Savine, R., Sönksen, P., Bengtsson, B.Å., Carlsson, L., Christiansen, J.S., et al., 2002. Growth hormone replacement therapy for adults: into the new millennium. Growth Horm. IGF Res. 12 (1), 1–33.
Sinko, P.J., 2011. Pharmaceutical biotechnology, Martin's Physical Pharmacy and Pharmaceutical Sciences, sixth ed. Lippincott Williams & Wilkins, China, pp. 516–561.
Smith, L., Mullin, S., Schapira, A.H., 2017. Insights into the structural biology of Gaucher disease. Exp. Neurol. 298, 180–190.
Stauffer, F., El-Bacha, T., Da Poian, A.T., 2006. Advances in the development of inactivated virus vaccines. Recent Patents Anti-Infective Drug Discov. 1 (3), 291–296.
Straathof, A.J.J., 2011. The proportion of downstream costs in fermentative production processes. In: second ed. Murray, M. (Ed.), Comprehensive Biotechnology, vol. 2. Academic Press, Burlington, MA, pp. 811–814.
Sutor, A.H., von Kries, R., Cornelissen, M.E., McNinch, A.W., Andrew, M., 1999. Vitamin K deficiency bleeding (VKDB) in infancy. Thromb. Haemost. 81 (03), 456–461.
Swartz, J.R., 2001. Advances in *Escherichia coli* production of therapeutic proteins. Curr. Opin. Biotechnol. 12 (2), 195–201.
Takeda, A., Cooper, K., Bird, A., Baxter, L., Frampton, G.K., Gospodarevskaya, E., et al., 2010. Recombinant human growth hormone for the treatment of growth disorders in children: a systematic review and economic evaluation. Health Technol. Assess. (Winchester, England) 14 (42), 1–209.
Tang, L., Persky, A.M., Hochhaus, G., Meibohm, B., 2004. Pharmacokinetic aspects of biotechnology products. J. Pharm. Sci. 93 (9), 2184–2204.
Tayal, V., Kalra, B.S., 2008. Cytokines and anti-cytokines as therapeutics—an update. Eur. J. Pharmacol. 579 (1–3), 1–12.
Therrien, J.P., Kim, S.M., Terunuma, A., Qin, Y., Tock, C.L., Pfützner, W., et al., 2010. A gene therapy approach for long-term normalization of blood pressure in hypertensive mice by ANP-secreting human skin grafts. Proc. Natl. Acad. Sci. 107 (3), 1178–1183.
Tomita, M., Tsumoto, K., 2011. Hybridoma technologies for antibody production. Immunotherapy 3 (3), 371–380.
Tsunoda, S.M., 2013. Drug transporters. In: Betino, J.S., DeVane, C.L., Fuhr, U., Kashuba, A.D., Ma, J.D. (Eds.), Pharmacogenomics and Introduction and Clinical Perspective. McGraw Hill, New York, pp. 89–104.
Venkat Ratnam, D., Pran Kishore, D., Rahul, M., Piyoosh, S., Rakesh, K.T., 2018. Chapter-5: Physico-chemical, pharmaceutical and biological considerations in GIT absorption of drugs. In: Tekade, R.K. (Ed.), Dosage Form Design Considerations: Advances in Pharmaceutical Product Development and Research Series, vol. I. Academic Press, pp. 149–178.
Vilček, J., Feldmann, M., 2004. Historical review: cytokines as therapeutics and targets of therapeutics. Trends Pharmacol. Sci. 25 (4), 201–209.
Voet, D., Voet, J.G., 2011. Signal transduction, Biochemistry, fourth ed. Wiley, New York, pp. 671–743.

Walsh, G., 2003. Pharmaceutical biotechnology products approved within the European Union. Eur. J. Pharm. Biopharm. 55 (1), 3–10.
Walsh, G., 2014a. Hormones and growth factors used therapeutically, Proteins Biochemistry and Biotechnology., second ed. Wiley Blackwell, pp. 233–256.
Walsh, G., 2014b. Interferons, Interleukins and tumor necrosis factors, Proteins Biochemistry and Biotechnology., second ed. Wiley Blackwell, pp. 257–276.
Walsh, G., 2014c. Therapeutic antibodies, Proteins Biochemistry and Biotechnology., second ed. Wiley Blackwell, pp. 205–232.
Walsh, G., 2014d. Therapeutic proteins: blood products, vaccines and enzymes, Proteins Biochemistry and Biotechnology, second ed. Wiley Blackwell, pp. 177–204.
Watson, D.G., 2011. Biotechnology produced products. In: Watson, D.G. (Ed.), Pharmaceutical Chemistry. Elsevier, Edinburgh, pp. 553–580.
Wong, M.S., Hawthorne, W.J., Manolios, N., 2010. Gene therapy in diabetes. Self/nonself 1 (3), 165–175.
Woodley, J.F., 1994. Enzymatic barriers for GI peptide and protein delivery. Crit. Rev. Therap. Drug Carrier Syst. 11 (2–3), 61–95.
Wu, C., Xu, Z., Zhang, H.B., 2006. DNA libraries. Rev. Cell Biol. Mol. Med. 1, 385–425.
Wurm, F.M., 2004. Production of recombinant protein therapeutics in cultivated mammalian cells. Nat. Biotechnol. 22 (11), 1393–1398.
Yagami, H., Kato, H., Tsumoto, K., Tomita, M., 2013. Monoclonal antibodies based on hybridoma technology. Pharm. Patent Anal. 2 (2), 249–263.
Yari, M., Ghoshoon, B.M., Vakili, B., Ghasemi, Y., 2017. Therapeutic enzymes: applications and approaches to pharmacological improvement. Curr. Pharm. Biotechnol. 18 (7), 531–540.
Yigzaw, Y., Hinckley, P., Hewig, A., Vedantham, G., 2009. Ion exchange chromatography of proteins and clearance of aggregates. Curr. Pharm. Biotechnol. 10 (4), 421–426.
Ying, S.Y., 2004. Complementary DNA libraries. Mol. Biotechnol. 27 (3), 245–252.
Yoshioka, S., Stella, V.J., 2002. Stability of peptide and protein pharmaceuticals. Stability of Drugs and Dosage Forms. Kluwer Academic Publishers, New York, pp. 187–204.
Zhang, T., Meibohm, B., 2012. Pharmacokinetics and pharmacodynamics of therapeutic peptides and proteins. In: Kayser, O., Warzecha, H. (Eds.), Pharmaceutical Biotechnology Drug Discovery and Clinical Applications. Wiley Blackwell, Germany, pp. 337–368.
Zhou, G., Yang, G., Fu, T., 2001. Gene cloning techniques. J. Huazhong (Central China) Agric. Univ. 20 (6), 584–592.
Zimmerman, B., Valentino, L.A., 2013. Hemophilia: in review. Pediatr. Rev. 34 (7), 289–294.
Zvonova, E.A., Ershov, A.V., Ershova, O.A., Sudomoina, M.A., Degterev, M.B., Poroshin, G.N., et al., 2017. PASylation technology improves recombinant interferon-β1b solubility, stability, and biological activity. Appl. Microbiol. Biotechnol. 101 (5), 1975–1987.

Further reading

Furie, B., Furie, B.C., 1988. The molecular basis of blood coagulation. Cell 53 (4), 505–518.
Rathi, C., Meibohm, B., 2006. Pharmacokinetics of peptides and proteins. Rev. Cell Biol. Mol. Med. 1 (2), 300–326.

CHAPTER

6

Approaches to the Development of Implantable Therapeutic Systems

Ankita Mane[1], *Neha Maheshwari*[2], *Piyush Ghode*[3], *Mukesh Chandra Sharma*[2] *and Rakesh K. Tekade*[4]

[1]Acropolis Institute of Pharmaceutical Education and Research (AIPER), Manglia, Indore, India [2]School of Pharmacy, Devi Ahilya Vishwavidyalaya, Takshila Campus, Indore, India [3]School of Pharmacy and Technology Management, NMIMS, Shirpur, India [4]National Institute of Pharmaceutical Education and Research (NIPER)—Ahmedabad, Gandhinagar, India

OUTLINE

6.1 Introduction 192
- *6.1.1 Skin* 192
- *6.1.2 Implantable Drug Delivery System* 193

6.2 Biodegradable and Nonbiodegradable Implant Systems 194
- *6.2.1 Nonbiodegradable Systems* 194
- *6.2.2 Biodegradable Systems* 196

6.3 Mechanism of Drug Release From an Implantable Drug Delivery System 198
- *6.3.1 Diffusion-Controlled Release* 198
- *6.3.2 Chemically Controlled Release* 198
- *6.3.3 Swelling Controlled Release* 199
- *6.3.4 Osmotically Controlled Release* 200
- *6.3.5 Magnetic Controlled Release* 200

6.4 Implantable Pump System 201
- *6.4.1 Infusion Pumps* 201
- *6.4.2 Peristaltic Pumps* 202
- *6.4.3 Osmotic Pumps* 202
- *6.4.4 Positive Displacement Pumps* 203

6.5 Atypical Implantable Drug Delivery Systems 204
- *6.5.1 Micro/Nanofabricated Implantable Drug Delivery Systems* 204
- *6.5.2 Ceramic Drug Delivery Systems* 205

6.6 Modeling of an Implantable Drug Delivery System 205
- *6.6.1 Empirical Models* 206
- *6.6.2 Mathematical Models* 208

Biomaterials and Bionanotechnology
DOI: https://doi.org/10.1016/B978-0-12-814427-5.00006-8

© 2019 Elsevier Inc. All rights reserved.

6.7 Approaches for Development of Implantable Therapeutic Systems 210
6.7.1 Controlled Drug release by Diffusion 210
6.7.2 Controlled Drug Release by Activation 211
6.7.3 Lucentis in a New Vehicle 211
6.7.4 Biosilicon Technology 212
6.7.5 Replenish Mini Pump 213
6.7.6 Encapsulated Cell Technology 213
6.8 Manufacturing and Sterilization Protocols 214
6.8.1 Coacervation Phase Separation 215
6.8.2 Emulsion Phase Separation 215
6.8.3 Spray Drying 215
6.8.4 Air Suspension 216
6.8.5 Solvent Extraction 216
6.8.6 PRINT 217
6.9 Benefits of Controlled Drug Administration via Implantation 217
6.10 Commercially Available Advanced Implantable Devices 218
6.11 Future Scope and Conclusion 220
Acknowledgment 220
References 220

6.1 INTRODUCTION

The last several decades have witnessed the development of various controlled drug delivery systems due to the various advantages they provide. These advantages include controlled delivery of active agent at a programmed rate, maintaining an optimum and effective level of drug for long period, reduced untoward effects, reduced dosing frequency, increased patient compliance, drug delivery to intended site, and efficient utilization of active agent. Owing to these advantages over conventional dosage forms, controlled release systems have been technologically advanced in recent years and are categorized according to the mechanism through which the release of the therapeutic agent is controlled. The list includes reservoir systems, matrix systems, osmotic systems, swelling systems, monolithic systems, pendant systems, ion-exchange resin systems, magnetic systems, and chemical systems (Pundir et al., 2017).

Among the above-stated systems, implantable systems are gaining importance as they are found to be a versatile method suitable for long-term drug delivery with minimal risk of infection and minimal risk to patient's life. Before continuing discussion of implantable systems it is necessary to discuss the site of application of implants. In the following section the structure of the skin has been discussed, as it is a prominent site of application for implants (Govender et al., 2017).

6.1.1 Skin

Implantable systems essentially comprise a micropump containing a reservoir, an actuator, inlet valves, outlet valves, and a cannula or catheter. Implantable systems are implanted in subcutaneous tissue, uterus, vagina, and other body locations. This requires an overview of skin along with its physiology (Kuche et al., 2018).

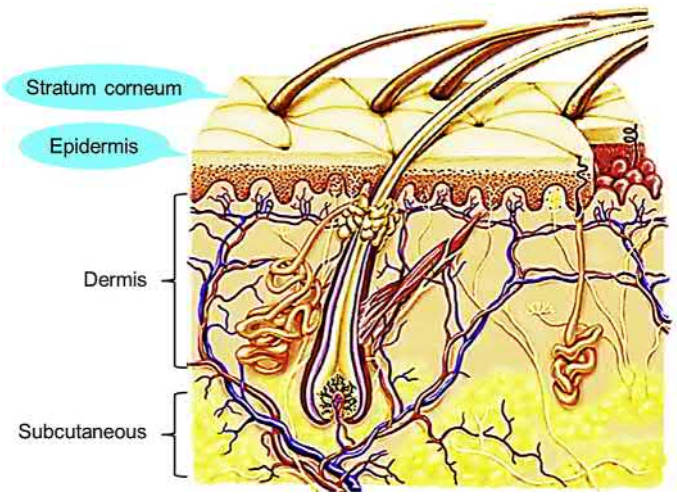

FIGURE 6.1 The human skin. Implantable systems specially designed to implant in the form of the pump in subcutaneous tissue.

Skin is the largest organ of the human body and covers 1.7 m^2. Stratum corneum, epidermis, dermis, and subcutaneous tissue altogether comprise the human skin. Hair follicles; apocrine, eccrine, and sweat glands; and nails are also present as appendages. The *epidermis*, which is composed of keratinocyte, is avascular. The outermost layer of the skin, *stratum corneum*, possesses a unique combination of intercellular lipids arranged as multiple stacked membrane layers in intercellular lipid lamellae (Russo et al., 2016) and hence represents a critical permeability barrier. *The dermis* comprises dense and irregular connective tissue along with collagen fibrils, hence providing support and elasticity to the skin. *The hypodermis* is a loose connective tissue layer that consists of lipocytes along with interconnected collagen fibers and elastin fibers. Drug transport through skin occurs majorily through two pathways: transappendageal route (sweat ducts, hair follicles, and associated sebaceous gland), and transepidermal route (through the stratum corneum; Fig. 6.1) (Maheshwari et al., 2012).

6.1.2 Implantable Drug Delivery System

Conventional drugs and proteins/peptides are susceptible to gastrointestinal tract conditions and hence are administered intravenously. Even upon administering intravenously, drug action duration is short for such drugs. As for topical drug administration, percutaneous absorption of drugs is limited owing to physical characteristics of drugs and highly impermeable nature of stratum corneum. Implantable drug delivery devices are devoid of such limitations. IDDSs, that is, these implantable drug delivery systems, are aimed to stock and carry minor, accurate quantities of the drug to the blood or particular tissues. This afterward replaces the regular instillation of drugs vital for relieving pain, and for management of various diseases like osteoporosis, diabetes, cardiac disease, age-linked macular degeneration, obstinate epilepsy, glaucoma, cystic fibrosis, and melanoma (Sutradhar and Sumi, 2016).

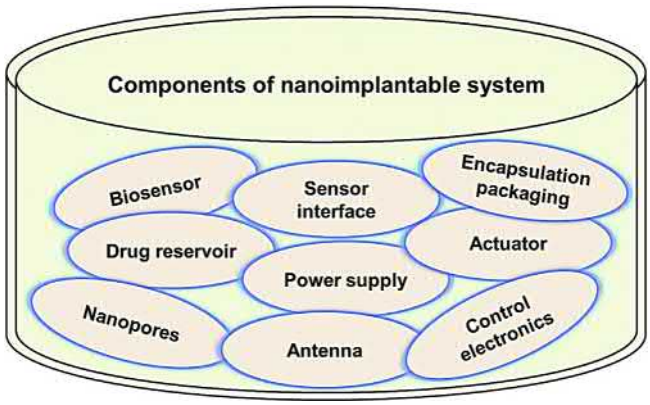

FIGURE 6.2 Major components of an efficient implantable system.

IDDS essentially comprise a micropump containing a reservoir, an actuator, inlet valves, outlet valves, and a cannula or catheter. The reservoir reserves therapeutic drug in either gaseous/liquid form, the actuator functions as a release/pump mechanism, and the cannula/catheter directs the drug to a target site (Kleiner et al., 2014). Components of implantable systems are represented in Fig. 6.2.

Implantable drug systems use various types of polymers and mechanisms for performing their functions hence they can be classified into various types (Fig. 6.3). These are biodegradable systems and nonbiodegradable systems. Biodegradable systems are further classified as reservoir and matrix controlled systems whereas nonbiodegradable systems are further classified into reservoir and monolithic systems.

6.2 BIODEGRADABLE AND NONBIODEGRADABLE IMPLANT SYSTEMS

IDDSs are divided into two broad classes: biodegradable systems and biodegradable systems. Nonbiodegradable systems are further classified as reservoir systems and matrix systems. Biodegradable arrangements are categorized as monolithic systems and reservoir systems. These systems follow different mechanisms like dissolution, diffusion, and activation to perform their action (Kleiner et al., 2014).

6.2.1 Nonbiodegradable Systems

Nonbiodegradable systems are basically classified into two forms: reservoir system and matrix system. A reservoir system comprises a dense drug core that is bounded by a nondegradable, permeable membrane. The polymers used for composing this membrane are explained in the next section. The thickness, as well as permeability of this membrane, control the diffusion of the drug into the body. The reservoir system follows zero-order release kinetics. It means that the driving force for the release of the drug is constant. The reservoir system carries a disadvantage with it that the outer membrane is

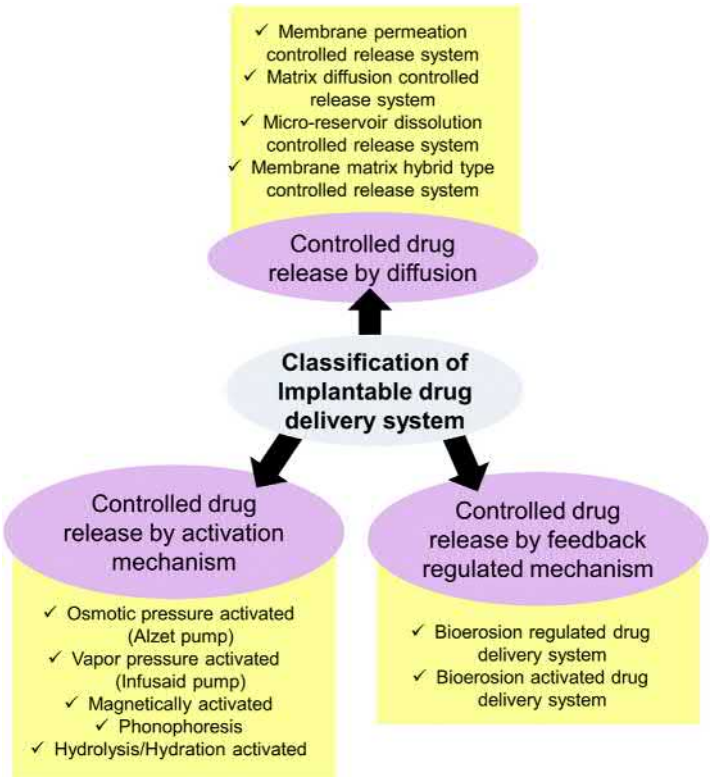
✓ Membrane permeation controlled release system
✓ Matrix diffusion controlled release system
✓ Micro-reservoir dissolution controlled release system
✓ Membrane matrix hybrid type controlled release system
Controlled drug release by diffusion
Classification of Implantable drug delivery system
Controlled drug release by activation mechanism
✓ Osmotic pressure activated (Alzet pump)
✓ Vapor pressure activated (Infusaid pump)
✓ Magnetically activated
✓ Phonophoresis
✓ Hydrolysis/Hydration activated
Controlled drug release by feedback regulated mechanism
✓ Bioerosion regulated drug delivery system
✓ Bioerosion activated drug delivery system

FIGURE 6.3 Classification of implantable drug delivery systems. Implantable drug delivery systems can be classified on the basis of the release mechanism followed by the system.

nonbiodegradable and hence needs to be removed via surgery. It may sometimes rupture during therapy leading to dose-dumping of the drug, causing toxic effects in the body (Joung, 2013).

As far as the matrix system is concerned, the drug is distributed into the matrix material homogeneously. The polymers used for preparing the matrix material are explained in the next section. The drug diffuses slowly across the polymeric matrix providing constant drug release from drug delivery arrangement. Unlike reservoir systems, drug's kinetic release is not constant, that is, it is governed by the volume portion of the drug in the matrix. The higher the amount of drug in the matrix, the greater will be the drug release from the arrangement (Kleiner et al., 2014).

6.2.1.1 Polymers Used in Nonbiodegradable Systems

A reservoir system comprises a dense drug core, which is bounded by a nondegradable, permeable membrane. Various polymers are used for preparing this membrane, some of which are explained as follows. Also, the matrix materials used in a matrix system also utilize a few of these polymers (Kim et al., 2016). All these polymers belong to the category of various polyurethanes and silicone rubber along with poly(ethylene vinyl acetate) (PEVA).

6.2.1.1.1 POLYURETHANES

Polyurethanes are the compounds formed by step-growth polymerization and contain urethane linkages in the backbone. Base polyurethanes are considered for drug delivery devices as they are nonbiodegradable. Being nonbiodegradable, they take a long time for thorough degradation. Also, the notch of degradation is insignificant as compared with the scale of complete release time. Base polyurethanes are biocompatible and stable in vivo. They are utilized in vivo in medical implants and other devices due to their favorable physical, mechanical properties, and biocompatibility. They are nondegradable and hence their use is limited to controlled drug delivery (Lamba, 2017).

6.2.1.1.2 SILICONE RUBBER

Polydimethylsiloxane (PDMS) comprises inorganic Si−O−Si units rather than hydrocarbon chains. PDMS is hydrophobic in nature, hence mostly hydrophobic drugs are loaded in PDMS-based drug delivery devices so as to attain prolonged release profiles. The drug release can be sustained to over a month. It can be also designed as reservoir and matrix type devices (Curtis and Colas, 2013).

6.2.1.1.3 POLY(ETHYLENE VINYL ACETATE)

PEVA is a copolymer of ethylene acetate and vinyl acetate. Controlled drug delivery systems are developed using PEVA by casting and freeze-drying methods. PEVA possesses good tissue compatibility and is available with a variety of vinyl acetate components. The release rate of drugs from these systems can be tailored to the desired value by changing membrane compositions (Genina et al., 2016).

6.2.2 Biodegradable Systems

Biodegradable systems are much more popular than the nonbiodegradable systems. The reason is the use of inert polymers in this system, which get ultimately absorbed and excreted from the body itself, hence eliminating the necessity of surgery for removing membrane as was the case with nonbiodegradable systems (Tekade et al., 2017b). Such inert polymers are explained in the next section. Biodegradable systems also occur in two forms: the reservoir type and the monolithic type.

In the reservoir type, the structure is similar to that described above but the peripheral membrane of polymer lowers at a slower rate as compared with the predictable diffusion rate of the drug across the membrane. Hence the membrane is unbroken until the drug releases entirely, after which the membrane degrades in vivo and gets eradicated. In a monolithic form, the drug is distributed into a polymer. This polymer erodes gradually by in vivo biological progressions in a controlled manner. Examples of such polymers include polyglycolic acid (PGA), polylactic acid (PLA), poly(lactic-*co*-glycolic acid) (PLGA), polyaspartic acid, and polycaprolactone (PCL) (Jeong et al., 2015).

6.2.2.1 Polymers Used in Biodegradable Systems

6.2.2.1.1 POLYGLYCOLIC ACID

PGA is a strong and crystal-like polymer having a melting point of 225°C along with 36°C glass transition temperature. PGA is not soluble in common polymer solvents. Also, it possesses excellent fiber-forming properties. Properties like less solubility and its extraordinary melting point confine its usage for applications in drug delivery. Due to this, it cannot be fabricated into films, rods, capsules, and microspheres by means of any solvent techniques or melt procedures. On the other hand, lactide/glycolide polymers show a wide range of hydrophilicity rendering them versatile for designing controlled release systems (Zambon et al., 2014).

6.2.2.1.2 POLYLACTIC ACID

PLA is a thermoplastic and a biodegradable polymer. It is created by polymerization of lactic acid molecules or cyclical lactide dimers. PLA hydrogels are used for developing a slow release drug delivery system of Mitomycin C and Dexamethasone sodium phosphate. These systems were developed for the prevention of tracheal wall fibroplasias (Tyler et al., 2016).

6.2.2.1.3 POLY(LACTIC-*CO*-GLYCOLIC ACID)

PLGA being a copolymer of PLA and PGA is the best biomaterial for drug delivery. PLGA consists of distorted α-carbon and is designated as Dextro- or Levo-arrangement. It can be developed in various size and shape and it can encapsulate any size molecules. It is soluble in various solvents including acetone, chlorinated solvents, tetrahedron, and ethyl acetate. Its physical properties depend on numerous factors including molecular weight, lactide to glycolide ratio, device size, exposure to water, and storage temperature (Muniswamy et al., 2018). Various nonsteroidal antiinflammatory drugs are incorporated in PLGA microspheres for treatment of rheumatoid arthritis. The examples include diflunisal and diclofenac sodium (Aparna et al., 2016).

6.2.2.1.4 POLYSACCHARIDES

Polysaccharides appear as ideal candidates for drug delivery because they are stable under physiological pH and temperature, not at extreme pH and temperatures. They can be obtained naturally. They can be subjected to various chemical and enzymatic reactions. They possess biodegradability, biocompatibility, and low immunogenicity. Polysaccharides go through dissolution in the aqueous system owing to solvent penetration effect, swelling, and polymer chain extrication. Hence polysaccharides based drug delivery systems can be dissolution and diffusion controlled. Various polysaccharides that can be used include hydroxypropyl methylcellulose (HPMC), cyclodextrin, dextran, and gellan gum (Alvarez-Lorenzo et al., 2013).

6.2.2.1.5 POLYCAPROLACTONE

PCL owns a regular structure, hence crystallizes readily. It is a tough and flexible with a melting point of 61°C and −60°C as its glass transition temperature. PCL is extremely penetrable to small molecular organisms at body temperature. Such features along with

biocompatibility designate PCL as a favorable entrant. PCL hydrolyzes slowly as compared with PLA and polylactic glycolic acid. Therefore it is considered very appropriate for long-time delivery (Tsang et al., 2015).

6.3 MECHANISM OF DRUG RELEASE FROM AN IMPLANTABLE DRUG DELIVERY SYSTEM

6.3.1 Diffusion-Controlled Release

Diffusion is an important mechanism of various controlled release systems. Molecules endure random collisions with other molecules owing to which they execute Brownian motion, that is, motion of a molecule is random at any point. This Brownian motion executed by drug molecules explains their passage from higher concentrations to the lower concentrations. Therefore diffusion of a substance takes place across the concentration gradient. Brownian movement of particles explains that average distance traveled by molecule through diffusion is proportional to the square root of time, that is, distance traveled is $\sim\sqrt{Dt}$. Here D is the diffusion coefficient and t is the time. Examples of diffusion controlled systems include intrauterine devices like progestasert. Progestasert uses silicon as the interior, reservoir saturated layer and ethylene vinyl acetate (EVA) copolymer (EVAc) as exterior rate-controlling layer. It releases progesterone at the rate of 65 μg/day for 1 year for treatment of endometrial proliferation. Intravaginal devices like etonogestrel-ethinylestradiol combination contraceptive intrvaginal rings (IVR) are founded on a coaxial fiber, which consists of EVA along with a spermicide IVR. Spermicide IVR uses an interior core of EVA/spermicide, which is bounded by a thin, porous layer of Silastic (Wang et al., 2014).

6.3.2 Chemically Controlled Release

The chemically controlled mechanism includes regulation of drug release rate via a chemical retort with the polymer. This system owns an advantage that the polymer is first liquefied and then absorbed by the body. Also, it eliminates the need for surgery for removing the device upon complete drug delivery. However, this mechanism of polymer fate should be observed carefully and be tested so as to ensure the safety of the polymer. The basic mechanisms involved in these systems are bioerosion and pendant chain, which are discussed in the subsequent section (Li et al., 2013).

6.3.2.1 Bioerosion

Erosion of polymeric monolithic devices happens when constituents of the release medium, specifically water, attack the covalent bonds present in the polymeric matrix. For hydrolytically labile bonds, water accessibility is a significant contributing factor in erosion rate. Hydrolysis of bonds can be acid catalyzed or base catalyzed. If it is so, then it is subjected to a confined concentration of proton donors and proton acceptors. For PLA, PLGA, and other polyesters or polyamides, the chain end provide acidic protons, hence the concentration of acid protons is inversely proportional to chain length (Harilall et al., 2015).

Bulk erosion appears due to the attack of water on the polymer in spite of hydrolysis. In such condition, water starts appearing all through the matrix and initiates chain scission progressions. Hydrolysis may be very slow in the beginning, but as a definite degree of hydrolysis has occurred, the progression may speed up.

6.3.2.2 Pendant Chain

Covalent binding of the drug to a polymeric carrier requires the use of an increasing number of linkages. These lead to the study of conjugation of metals by process of chelation along with chelated conjugates used for imaging. Pendant chain linkers are available in two types. One is peptidyl linkers, which remain stable in the bloodstream but get degraded by lysosomal enzymes and hence release drug intracellularly. Examples of peptidyl linkers include gold labeled β sheets, α-helix peptidyl linker for assembling quantum dot bioconjugates. Lys-tag and Gln-tag for selective Lys−Gln cross-linkage of different proteins are other examples of peptidyl linkers (Silna et al., 2016).

Other examples include acid labile, pH-dependent linkers, which are basically designed to be stable in plasma but they release drug intracellularly due to hydrolysis of endosome and lysosome at low pH. Examples of such linkers include pH controlled hydrazine linkage for cellular delivery of doxorubicin, azidomethyl-methyl maleic anhydride linker 3, PentyneMMan linker, 3-(azidomethyl)-4-methyl-2,5-furanone, and many more (Ang et al., 2017).

Hence, soluble polymer−drug conjugates are prepared using linkers other than those mentioned above. These conjugates increase the circulation time. The drug can be conjugated by chelation or by conjugating directly to the existing pendant chain or end group. The example includes conjugation of paclitaxel to the side chains of poly(L-glutamic acid). Another example includes conjugation of paclitaxel to the end groups of polyethylene glycol (Silna et al., 2016).

6.3.3 Swelling Controlled Release

Swelling concerns water uptake via a polymer arrangement along with a rise in polymer volume. Swelling occurs in three situations: first, when water and polymer are not compatible; second, when polymer chain length is large; and third, when cross-links have been presented for forming a polymer linkage. Swelling progression is synonymous with osmosis because water moves in rapidly to the polymer, but polymer dissolution in water is slow since the polymer chains need to be disentangled. The extent of swelling depends upon some factors such as polymer hydrophilicity and density of cross-links amid polymer chains (Danyuo et al., 2014).

Swelling is a mechanism that activates the discharge of confined drug. In case of rapid swelling, diffusion of the drug across the inflated polymer becomes the governing course for drug release. But if the swelling is slow, the process governing the degree of drug release assumes the role.

The swelling controlled drug release arrangements are the glassy polymers at room temperature and body temperature. The glassy polymer surface reduces to a pattern that is water compatible and swells. This leads to invasion of water into the system and

appearance of a moving front that separates the swollen outward layer from the dry central core. Hence swelling can be said to be complemented by a glass-to-rubber transition. If the drug is confined into the glass, it will be released once the polymer swells. If the drug diffuses across the relaxed matrix more rapidly than water invades, then the progression will be swelling controlled (Washington et al., 2017).

Also under proper conditions, all three—the dissolution of polymer chains, swelling, and drug release—can follow the same time. Example of such a system includes HPMC matrix systems such as METHOCEL K used for increasing the ionic strength of theophylline (Ibrahim and Fahmy, 2016).

6.3.4 Osmotically Controlled Release

Osmosis is a phenomenon that follows when a membrane separates the aqueous solutions of osmolytes. This membrane is absorptive to water but is not permeable to other solutes. Water flows through a semipermeable membrane for balancing the concentration of nonpermeable solutes on either side of the membrane. This water flow across the membrane occurs through diffusion in most of the cases. It may depend upon difference in the chemical potentials of water on either side of the membrane. The difference between chemical potentials depends upon the concentration of osmolytes and thermodynamic compatibility of water with them. If the osmolytes are small molecules like salts, then the osmotic pressure is determined by the concentration of osmolyte. If osmolytes are polymers, then the osmotic pressure will be accounted for by the concentration of polymer and compatibility of polymer with water (Hill et al., 2013).

In the case where individual drug particles are coated with a semipermeable polymer, they get released from the capsule when exposed to the gastric fluid. Water diffuses across the polymer membrane and dissolves the drug creating a gradient across the membrane that leads more water into the membrane. When sufficient osmotic forces get established, the polymer coating ruptures and releases the drug (Patra et al., 2013).

Examples of osmotically controlled systems include an Alzet mini osmotic pump, push–pull pump, and elementary osmotic pump (Fig. 6.4). Alzet mini pump is implanted in the animal's tissue. Here it delivers the drug in precise proportions. The drug is positioned in an impermeable flexible wall reservoir and this reservoir is enclosed via an osmotic agent. This surrounding is further closed in a rigid cellulose acetate membrane. In aqueous surroundings, water drives across the cellulose acetate membrane osmotically. This results in a stress on the reservoir walls, which navigates the agent out of the orifice (Zaher et al., 2015).

6.3.5 Magnetic Controlled Release

In these systems, the drug along with the magnetic beads is uniformly distributed into a semielastic polymer matrix. This semielastic polymer matrix is prepared out of a nonbiodegradable polymer like ethylene–vinyl acetate polymer. When positioned in a dissolution medium, the drug release from the device displays matrix diffusion control. On the other hand, when it is positioned in a magnetic field, the drug release occurs due to

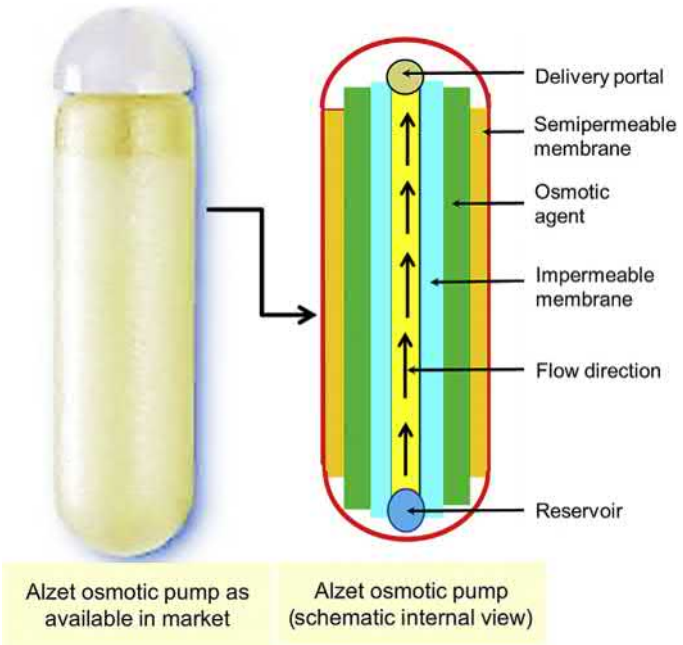

FIGURE 6.4 Composition of the Alzet osmotic pump, one of the various osmotic pumps available in the market and the most used one.

pulsatile flow of dissolution medium. In an oscillating magnetic field, the bead oscillates and compresses and therefore expands the polymer. This leads to a pulsatile movement of dissolution medium across the pores of the elastic polymer and also alongside the drug's concentration gradient. This results in an increased drug release rate (Zaher et al., 2015).

The consequence of the oscillating magnetic field can be improved by a rise in polymer elasticity and frequency and strength of the magnetic field. This system owns a major advantage of manipulating the drug's release kinetics by use of external magnetic stimuli. Such a system has been used for releasing of insulin and other macromolecular bioactive by embedding them in a carrier like EVAc (Genina et al., 2016).

6.4 IMPLANTABLE PUMP SYSTEM

6.4.1 Infusion Pumps

Infusion pumps are the devices that operate a fluorocarbon propellant for administering the drug in vivo. These systems were established for administering insulin to the diabetic patients. Examples of such systems include Infusaid, MiniMed, and SynchroMed. The Infusaid system comprises a disc-shaped canister made of titanium and comprises a collapsible welded bellow (Rauck et al., 2013). This bellow splits up the canister interior into two chambers out of which the first one holds fluorocarbon propellants and other contains the insulin formulation. The system also comprises a flow restrictor. The propellant's vapor pressure keeps creating a continuous pressure source at a stable temperature. Drug

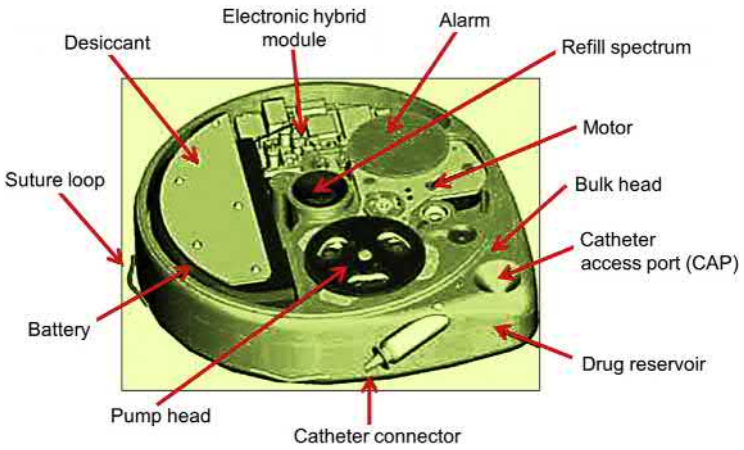

FIGURE 6.5 Synchromed system in synchroMed. The pump comprises an outer titanium casing that contains the pumping mechanism along with the controller, the drug solution reservoir, and the battery. It also contains a silicone rubber septum so that it can be refilled with a needle and syringe. A silicone catheter can be channeled to the intrathecal space.

delivery rate may be adjusted by altering the amount of drug in the pump reservoir. Examples of such devices include Codman and Synchromed infusion pumps. Battery life is 6–7 years. This system is employed for intrathecal delivery of opioids (pain management), baclofen (for severe spasticity), and other treatments as well (Spaan et al., 2014). A schematic of this type of system is represented in Fig. 6.5.

6.4.2 Peristaltic Pumps

Peristaltic pumps contain a rotary solenoid-driven system that operates through an exterior power source, namely a battery. These devices are packed through a silicone rubber septum. These devices may be used for numerous years, subjected to the extent of the battery-powered system. The system owns a benefit of controlling the drug administration rate by an outer remote control system. These pumps, being very costly, are not seen in regular practice to date (Kleiner et al., 2014).

A wide application of peristaltic pumps is found in microfluidic systems based on PDMS. PDMS is a biocompatible material resilient to many chemicals, versatile, and provides for ease of fabrication. A peristaltic pump has been developed comprising the fluid channels made in-between a thin PDMS layer along with a glass, silicon, or PDMS substrate (Portilla and Kim, 2013).

6.4.3 Osmotic Pumps

This device basically works on the principle of osmosis. Osmosis is a phenomenon that follows when a water permeable membrane, which is not permeable to other solutes, separates the aqueous solutions of osmolytes. A basic example of an osmotically driven system is represented in the figure. The device comprises a rigid housing that contains an osmotic agent and remains parted from the therapeutic agent by a piston. One wall of rigid covering is composed of a semipermeable membrane. When exposed to an aqueous surrounding, water moves osmotically through this semipermeable membrane and results in

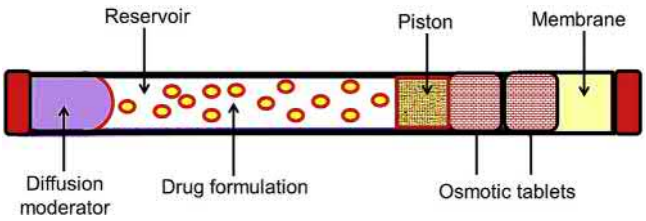

FIGURE 6.6 The DUROS implantable system. The system consists of an outer cylindrical reservoir. It is made of titanium alloy or a biocompatible rigid polymer. A rate-controlling membrane at one end, the "osmotic engine" (tablets containing primarily NaCl combined with other pharmaceutical excipients), is made up of a semi-permeable polyurethane polymer that has a specific water permeability and the ability to not to foul during the in vivo process.

increased volume within the osmotic compartment. This, in turn, exerts a pressure on the piston causing the release of drug from the device via a delivery orifice (Hill et al., 2013).

An example of such a system is the DUROS implantable osmotic system. This system is implanted subcutaneously. The system distributes drug at a continuous rate owing to the greater osmotic pressure of saturated sodium chloride solutions compared with the body tissue's osmotic pressure. The devices may be programmed for the duration of 1 month to 1 year. It had been used for delivery of gonadotropin-releasing hormone (GnRH) analog leuprolide for treating prostate cancer. It has been also investigated for delivering interferon, sufentanil, and other opioids (Kleiner et al., 2014). A typical example is shown in Fig. 6.6.

6.4.4 Positive Displacement Pumps

These pump systems employ the piezoelectric disk benders attached to the flexible tubing. Piezoelectric disk benders are used as AFM cantilevers, locating devices, and force sensors. They are of three types: the first one is the triple-layer bender embracing two piezoelectric layers, which act oppositely with a mechanically applicable intermediate passive layer; another one is the bimorph, having the same conformation without an intermediate layer; and the last one is the heterogeneous bimorph, embracing one piezoelectric layer and one passive. The piezoelectric layers are made up of various piezoelectric materials. Piezoelectric materials include quartz, piezoelectric ceramic materials like zinc oxide and PZT (lead-zirconate titanate). Moreover, piezoelectric polymers like polyvinylidene fluoride and its copolymers are also used (Zargarpour and Zarifi, 2015).

For preparing such pumps, the disks are first exposed to certain voltages to become spherical surfaces. The bellows-type arrangement then gets linked to the drug reservoir through a three-way solenoid driven valve. When exposed to the electrical pulses, a valve in the pump opens or closes according to the pulse. This act leads to a controlled drug release based on the electrical pulse rate (Dagdeviren et al., 2014).

A disposable piezoelectric micropump has been developed by Liu et al. for delivering insulin to diabetic patients and closed-loop monitoring of glucose concentration. It comprised four chambers in serial connection with a drug reservoir volume of 3.2 mL. A pressure of 22 kPa can be acquired by an applied voltage of 36 V along with a driving frequency of 200 Hz (Liu et al., 2014).

6.5 ATYPICAL IMPLANTABLE DRUG DELIVERY SYSTEMS

6.5.1 Micro/Nanofabricated Implantable Drug Delivery Systems

This technology has enabled miniaturization of individual components and whole systems, with minimally hostile implantable form (Tekade et al., 2017a). Surface modification methods and selection of biocompatible material provide a stable, inactive interface in-between implant and body. Also, this technology enhances drug release mechanisms to achieve programmable, cyclic, as well as pulsatile and continuous drug release profile (Zhang et al., 2015). One such system is being developed by MicroCHIPS.

In this system, minute microliter-sized reservoirs are engraved into the silicon wafer. These reservoirs are packed with one drug or more than one drug. The reservoirs are shielded by gold or another film. This film is by electronic means addressed on the chip. Postimplantation, a voltage is applied onto the gold foil, which results in electrochemical film dissolution leading to release of drug from the individual reservoir (Zhang et al., 2014).

An efficient example of this technology is nanoengineered titanium implants developed by Gulati et al. (2016). These implants appear as an efficient technology for the treatment of localized bone pathologies by delivering hormones or drugs locally to the trauma site. The implants are basically small titanium wires/needles along with nanoengineered oxide layer, which consists of an array of titania nanotubes (Fig. 6.7).

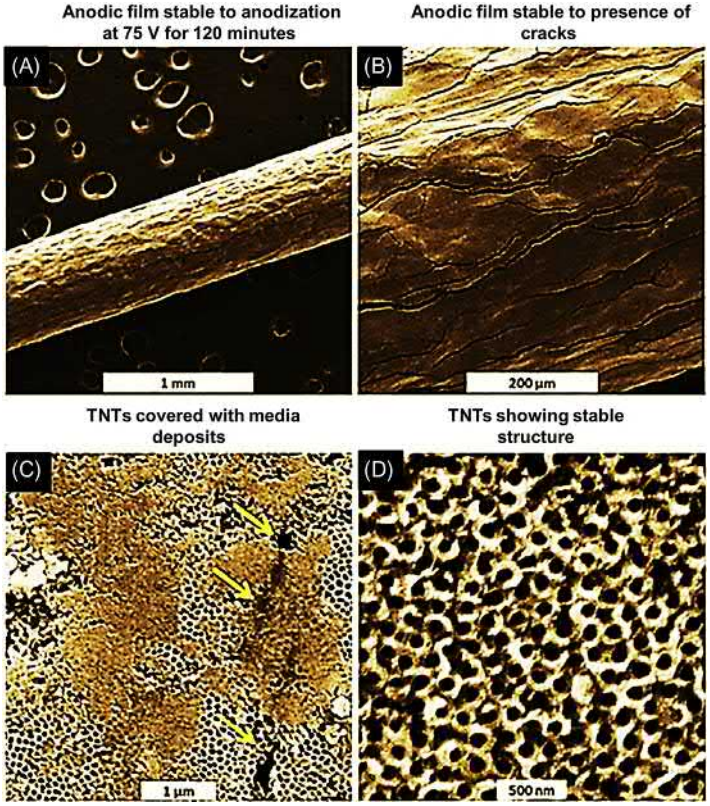

FIGURE 6.7 SEM images of the TNT after retrieval from the bovine trabecular bone core ex vivo. (A and B) The anodic film is seen as stable even for the presence of cracks and anodization performed at 75 V for 120 min (TNT-120), (C) high-magnification image showing TNTs covered with media depositions and possible extracellular secretions (arrows points towards the underlying cracks of the anodic film, which can be seen under the media deposits), and (D) close-up of the TNTs showing stable structure. *TNTs*, titania nanotubes. *Source: Adapted with permission from Gulati, K., Kogawa, M., Prideaux, M., Findlay, D.M., Atkins, G. J., Losic, D., 2016. Drug-releasing nanoengineered titanium implants: therapeutic efficacy in 3D cell culture model, controlled release and stability. Mater. Sci. Eng., C 69, 831–840.*

6.5.2 Ceramic Drug Delivery Systems

Bioceramics are inert materials that are used basically as bone-compatible materials. These materials can be used for replacement of bone or as fillers/coating, for correcting bony defects, periodontal effects, and also as ear and eye implants. Ceramics have also been utilized for the delivery of antibiotics, anticancer drugs, anticoagulants, analgesics, and so on. These ceramic devices can be easily modified for achieving desired release profiles. Ceramic devices are more compatible with the tissue and body fluids along with having great mechanical properties. These make it a suitable candidate for various biomaterial applications. Also, it had been found as a suitable candidate for drug delivery due to its nonimmunogenicity and extreme compatibility with the incorporated drugs/biologicals (Khan et al., 2014).

Ceramic drug delivery system uses five different types of ceramics for the delivery of drugs. This includes inorganic bone meal, aluminum calcium phosphorus oxides, hydroxyapatite, tricalcium phosphate, and ceramic−metal hybrids. One example of such system is silica-based ordered mesoporous materials, which are used as bone implants. These are considered as the best candidates for two reasons: one, the bioactive behavior on contact with body fluids; and two, ability as delivery systems for various biologically active molecules (Arcos and Vallet-Regí, 2013).

The mechanism of these systems includes a sequence of chemical reactions that occurs when silica-based ordered mesoporous materials get exposed to the physiological surroundings. This leads to the incorporation of the material into the biologically active tissue. These progressions are established through the nucleation and growth on the bioceramic surface. This bioceramic surface of a carbonated hydroxyapatite layer is similar to the mineral part of bone tissues (Argyo et al., 2013). Thus, this bioceramic would subsidize bone tissue regeneration. This type of system owns various advantages like site-specific delivery of drug at a precise frequency and the protection of drugs that are integrally not stable in vivo.

An example of this technology is Cermet ceramic composites developed by Dittmer et al. (2017) using a multilayer technology for creating conductive paths insulated from each other by embedding an electric conductor into a ceramic matrix. The Cermet capsules replaced the traditional pacemakers, which were heavier in weight, that is, about 300 g, and also used to occupy 240 cm^3. The Cermet capsules are lighter in weight (2 g) and occupy only 1 cm^3 volume, which makes them feasible for use in pediatric applications (Fig. 6.8). The Cermet capsules have more strength than the pure ceramics, high conductive properties, and they are biocompatible, chemically inert, and nonmagnetic. These capsules are used for cardiac arrhythmia, deafness, chronic pain, sleep apnea, Parkinson's syndrome, and other diseases.

6.6 MODELING OF AN IMPLANTABLE DRUG DELIVERY SYSTEM

Drug release is an important aspect of each and every type of drug delivery system. As for implantable systems, various modeling systems have been proposed by various scientists. Drug release is affected by various driving factors. These are composition, structure, swelling, and degradation of the material matrix, pH, temperature, ionic strength, and enzymes present in release medium and solubility, stability, charges, and interaction of drug compounds with the matrix.

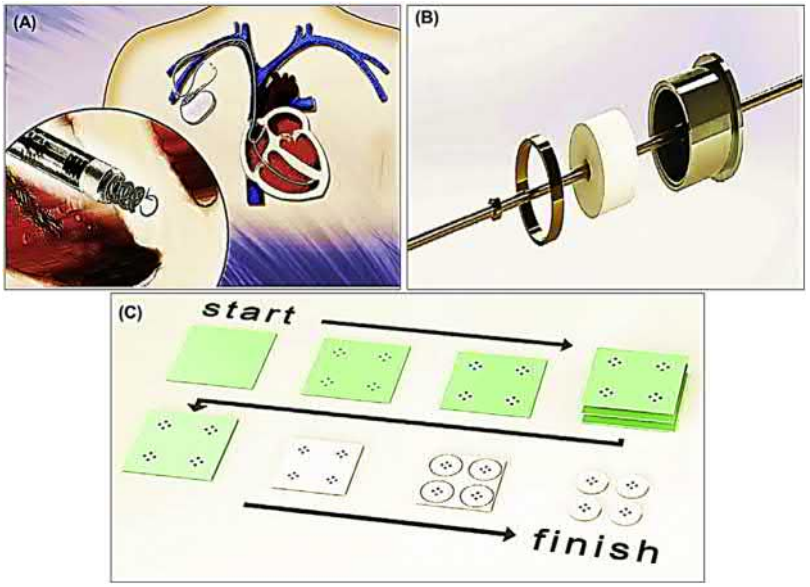

FIGURE 6.8 (A) Schematic of a cardiac pacemaker implanted into a human body. (B) Schematic assembly of a conventional feedthrough for one channel. (C) Schematic general HTCC process from top left to bottom right. *HTCC*, high-temperature co-fired ceramic. *Source: Adapted with permission from Dittmer, R., Schaefer, C.M., Fischer, J.-F., Hausch, U., Troetzschel, J., Specht, H., 2017. Advanced CerMet ceramic composites for medical applications. J. Mech. Behav. Biomed. Mater. 75, 206–211.*

It is suggested that basically solute diffusion, swelling of the polymeric matrix, and material degradation are the major driving forces for solute transport.

Particularly, Fick's laws are used fundamentally for describing the transport of solute from polymeric matrices. Solute transport can be described as Fickian diffusion and non-Fickian diffusion. This is based on polymer relaxation time (T_r) and solvent diffusion time (T_d). For Fickian diffusion, $T_r > T_d$ whereas for non-Fickian diffusion, $T_r \approx T_d$. Mathematical modeling is required for simplifying the complex release system and study release mechanism of a particular material system in detail. Various mathematical models are summarized below.

6.6.1 Empirical Models

These models were based on established empirical rules that may help in explaining the transport mechanism. Although these models are easy to use, they cannot take into account the physicochemical processes. Also, these models cannot explain the more complex transport mechanism. For example, the release of sodium salicylate from HPMC tablet, which indicates a non-Fickian drug release pattern, may be explained by using Ritger–Peppas and Peppas–Sahlin equations. Various law equations used for modeling of release kinetics have been proposed. These include:

6.6.1.1 Higuchi Model

The Higuchi model, which is used for explaining Fickian diffusion, is explained by the equation:

$$\frac{M_t}{M_\infty} = kt^{1/2} \tag{6.1}$$

where M_t = total drug released at time t, M_∞ = total drug mass loaded into the device, k = constant, and $t^{1/2}$ = half-life

6.6.1.2 Ritger–Peppas Model

The Ritger–Peppas model, which is used for explaining both Fickian and non-Fickian diffusions, is explained by the equation:

$$\frac{M_t}{M_\infty} = k_1 t^n \tag{6.2}$$

n is a diffusional exponent that explains the mechanism of release of the drug. For Fickian diffusion, the value of the diffusional exponent, n, limits to 0.5 or 1 whereas for non-Fickian diffusion, the value limits between 0.5 and 1.

This model was used for preliminary design purposes only. This is so because they can calculate up to the first 60% of the time release.

For Fickian diffusion, a value of n for the different systems was found to be as follows:

1. n shows 0.50 as value for thin films
2. n shows 0.45 as value for cylindrical samples
3. n shows 0.43 as value for spherical samples

As for swelling controlled-release systems, values of n were as follows:

1. n shows 1.0 as value for thin films
2. n shows 0.89 as value for cylindrical samples
3. n shows 0.85 as value for spherical samples

6.6.1.3 Peppas–Sahlin Model

Peppas–Sahlin model, which is used for explaining non-Fickian diffusion, is explained by the equation:

$$\frac{M_t}{M_\infty} = k_1 t^m + k_1 t^{2m} \tag{6.3}$$

6.6.1.4 Alfrey Model

The Alfrey model is also used for explaining non-Fickian diffusion and is explained by the equation:

$$\frac{M_t}{M_\infty} = k_1 t + k_1 t^{1/2} \tag{6.4}$$

6.6.1.5 Zero-Order Model

The zero-order model, which is used for explaining case 2 transport, is represented by the equation:

$$\frac{M_t}{M_\infty} = k_d t \tag{6.5}$$

6.6.2 Mathematical Models

Various mathematical models had been developed earlier for studying the release of drug from planar, spherical surfaces, and slab-like surfaces. These models were developed with respect to the mechanism of transport involved in drug releases like dissolution, diffusion, and erosion. These can be summarized as follows:

6.6.2.1 Mathematical Models for Diffusion-Based Drug Delivery System

These models were applied for devices with slab- and disk-like surfaces. Various assumptions were made in the case of diffusion based systems. These included diffusion to be unidirectional, constant drug diffusion coefficient, and nonappearance of degradation or matrix swelling. The release of the drug from these devices can be explained by following equations based on Fick's second law of diffusion.

$$\frac{M_t}{M_0} = 4\left(\frac{Dt}{\pi h^2}\right)^2 \tag{6.6}$$

This equation accounts for the first 60% of cumulative drug release, which means $0 \leq M_t/M_0 \leq 0.6$.

Another equation

$$\frac{M_t}{M_0} = 1 - \left(\frac{8}{\pi^2}\right)\exp\left[\frac{(-\pi^2 Dt)}{h^2}\right] \tag{6.7}$$

accounts for the remaining 40% of cumulative drug release, which means $0 \leq M_t/M_0 \leq 0.4$.

This model successfully explained the Fickian transport mechanism involved in drug release.

6.6.2.2 Mathematical Models for Dissolution Based Drug Delivery System

These models were applied for matrix devices with slab-, film-, and disk-like surfaces. Various assumptions were made in the case of dissolution based systems. This includes the presence of two moving interfaces: drug−membrane interface, and membrane−solvent interface, and constant drug diffusion coefficient and solvent diffusion coefficient. Drug release from this system can be either solute diffusion controlled or polymer dissolution controlled.

In case 1, that is, solute diffusion controlled, drug release can be stated by the following equation:

$$\frac{Q}{t} = \frac{K_{m/r}K_{a/m}D_dD_m}{K_{m/r}D_mh_d + K_{a/m}D_dh_m}C_R \tag{6.8}$$

where $K_{m/r}$ = partition coefficient, which represents the partitioning of drug molecules from the reservoir to the membrane, $K_{a/r}$ = partition coefficient, which represents the partitioning of drug molecules from the membrane to the aqueous diffusion layer, D_m = diffusion coefficient in membrane, D_d = diffusion coefficient in the aqueous diffusion layer, h_m = Thickness of membrane, h_d = thickness of the aqueous diffusion layer, and C_R = Concentration of drug in reservoir compartment

In case 2, that is, polymer dissolution controlled, drug release can be expressed by the equation proposed by Narsimhan and Peppas:

$$\frac{M_d}{M_{d,\infty}} = \frac{v_{d,eq} + V_d}{2l}\left(\sqrt{2At} + Bt\right) \tag{6.9}$$

where l = thickness of polymer, V_d = concentration of drug, $V_{d,eq}$ = equilibrium concentration of drug, and $A/B = \alpha$, case 2 behavior

This model successfully accounted for Fickian behavior and case 2 type behavior along with the transition state in between.

6.6.2.3 *Mathematical Models for Erosion Based Drug Delivery System*

Models have been proposed for explaining drug release from eroding polymeric matrices.

These models were applied for matrix devices like slab, sphere, cylinder, and disk. The models include Hopfenberg's model, Katzhendler's model, and Rothstein's model.

6.6.2.3.1 HOPFENBERG'S MODEL

This model was applied to matrix devices with slab, sphere, and cylinder. Various assumptions for this model were made including surface detachment of drug following zero order as rate-limiting step and constant material erosion rate. The cumulative drug fraction, which is released at time t, was given by using the following equation:

$$\frac{M_t}{M_\infty} = 1 - \left[\frac{1 - k_0 t}{C_L a}\right]^n \tag{6.10}$$

where K_0 = zero-order rate constant, C_L = initial drug loaded, a = half of the total width, that is, radius of a sphere or cylinder, and n = exponent; this differs according to the drug delivery system, that is, 1 for slab, 2 for sphere, and 3 for cylinder

6.6.2.3.2 KATZHENDLER MODEL

The next model in the queue for explaining drug discharge from the erodible matrix is the Katzhendler model, which accounts for radial and axial erosion along with assumptions of surface detachment of drug following zero order as rate-limiting step and constant material erosion rate. In the case of a tablet, the drug release may be explained by the following equation:

$$\frac{M_t}{M_\infty} = 1 - \left(1 - \frac{k_r \cdot t}{c_0 \cdot a_i}\right)\left(1 - \frac{2k_a t}{C_0 b_f}\right) \tag{6.11}$$

where k_r = radial erosion rate constant, k_a = axial erosion rate constant, a_i = initial radius of tablet, and b_f = final radius of tablet

6.6.2.3.3 ROTHSTEIN MODEL

This model was developed for surface eroding materials as well as for bulk eroding materials. The assumptions made for this model included the relation of D_{eff} to the matrix porosity and involvement of second-order polymer degradation kinetics. Rothstein developed this model for explaining the diffusion of drug through the bulk-eroding polymer

with effective diffusivity. Effective diffusivity referred to the product of polymer matrix porosity and maximum diffusivity through the matrix. The model accounted for the system's hydration kinetics, dissolution, and pore formation for computation of drug release and equations were framed for each of this.

For hydrolysis kinetics,

$$\frac{\partial M_w}{\partial t} = -kC_w M_w \tag{6.12}$$

For drug dissolution,

$$\frac{\partial C_s}{\partial x} = -k_{\text{dis}} C_{sn} C_{an} C_{wn} \tag{6.13}$$

For a cumulative fraction of drug release,

$$R_{(t)} = 1 - P_{(t)} \tag{6.14}$$

There are many more approaches acquired for explaining drug release form various types of controlled release drug delivery devices based on different polymers.

6.7 APPROACHES FOR DEVELOPMENT OF IMPLANTABLE THERAPEUTIC SYSTEMS

The development approaches for implantable systems include the application of various mechanisms like diffusion, dissolution, osmosis, and many more. This also involves the selection of appropriate polymers in the systems as polymers play a vital role in release rate, the extent of action, and stability (Kleiner et al., 2014). Implantable systems can be developed in many implantable forms like pumps, microneedles, transdermal patches, encapsulated capsules, cantilevers, etc. The various applications of wireless implantable systems are depicted in Fig. 6.9.

6.7.1 Controlled Drug release by Diffusion

Diffusion means activities of the drug particles to the external stimuli, which affect its external environment. In these systems, diffusion through a water-insoluble barrier is the rate-limiting step. These systems are either matrix-based systems or reservoir diffusion systems. Matrix-based systems comprise a drug mixed with a polymer, forming a matrix, which swells on water permeation. For effective diffusion, it is necessary that the pore size of the swollen matrix be greater than the size of the drug molecule and examples of this type of system include Nico400 and Nitro-Bid (Siepmann et al., 2002).

As for reservoir diffusion systems, the drug is captured into a polymer. It creates a porous barrier between the drug and its immediate surroundings. In these systems, the barrier coating permits water permeation and swells, whereas the inner components diffuse from the system. For effective diffusion, it is necessary that the pore size of the swollen matrix be greater than the size of the drug molecule. Example of such systems includes Wellbutrin XL, Glucotrol XL, and Procardia XL (Beckwith et al., 2004).

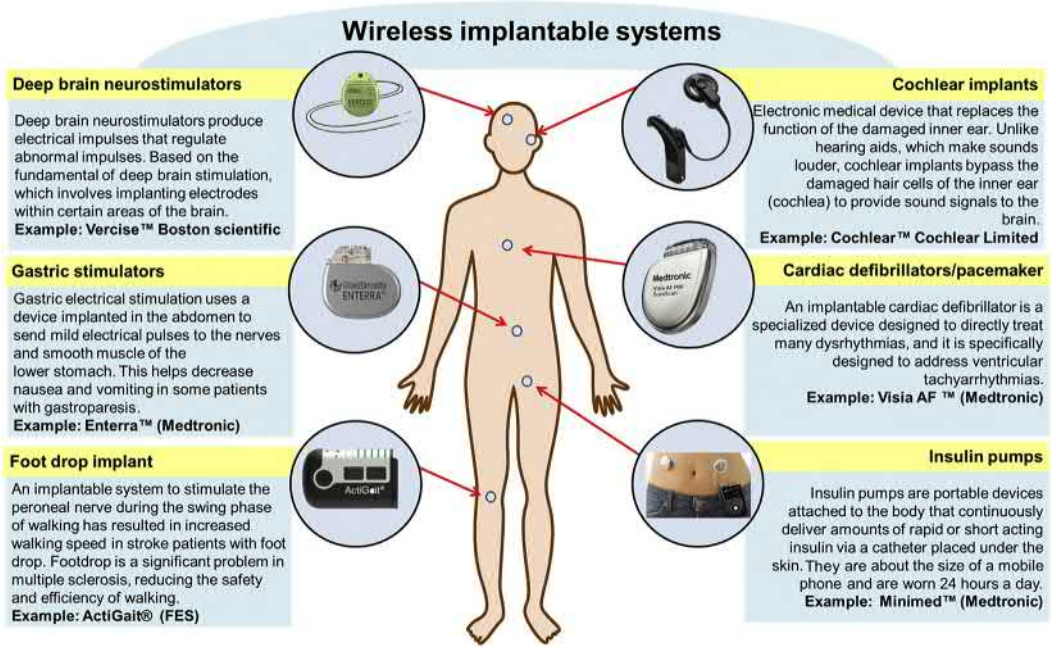
Wireless implantable systems
Deep brain neurostimulators
Deep brain neurostimulators produce electrical impulses that regulate abnormal impulses. Based on the fundamental of deep brain stimulation, which involves implanting electrodes within certain areas of the brain.
Example: Vercise™ Boston scientific
Gastric stimulators
Gastric electrical stimulation uses a device implanted in the abdomen to send mild electrical pulses to the nerves and smooth muscle of the lower stomach. This helps decrease nausea and vomiting in some patients with gastroparesis.
Example: Enterra™ (Medtronic)
Foot drop implant
An implantable system to stimulate the peroneal nerve during the swing phase of walking has resulted in increased walking speed in stroke patients with foot drop. Footdrop is a significant problem in multiple sclerosis, reducing the safety and efficiency of walking.
Example: ActiGait® (FES)
Cochlear implants
Electronic medical device that replaces the function of the damaged inner ear. Unlike hearing aids, which make sounds louder, cochlear implants bypass the damaged hair cells of the inner ear (cochlea) to provide sound signals to the brain.
Example: Cochlear™ Cochlear Limited
Cardiac defibrillators/pacemaker
An implantable cardiac defibrillator is a specialized device designed to directly treat many dysrhythmias, and it is specifically designed to address ventricular tachyarrhythmias.
Example: Visia AF ™ (Medtronic)
Insulin pumps
Insulin pumps are portable devices attached to the body that continuously deliver amounts of rapid or short acting insulin via a catheter placed under the skin. They are about the size of a mobile phone and are worn 24 hours a day.
Example: Minimed™ (Medtronic)

FIGURE 6.9 **Wireless implantable system.** The implantable drug delivery systems are utilized for various applications including brain targeting and diabetes control. Hence enlisting various types of implants with their location, function, and examples of IDDS system employed.

6.7.2 Controlled Drug Release by Activation

Activation refers to the utilization of any external mechanism for releasing drug from the IDDS. This set of drug delivery methods is facilitated by an energy brought about by an exterior source. The drug release rate is précised by regulation of applied process (Kamaly et al., 2016). The activation-based controlled drug delivery systems can be categorized into physical–chemical and biochemical. Physical activation method includes osmotic pressure, hydrodynamic pressure vapor pressure, mechanical force, magnetic field, sonophoresis, iontophoresis, and hydration, whereas, chemical activation methods include activated systems, ion activated systems, and hydrolysis activated systems (Talbi et al., 2018). Biochemical activation methods include enzyme activated systems and biochemical activated systems.

6.7.3 Lucentis in a New Vehicle

Of the various vision disorders, corneal disease is the second most common cause of nonrefractive visual impairment. Corneal disease is a common reason for blindness in people and appears due to an imbalance between pro- and antiangiogenic factors. This imbalance may occur as a result of inflammation, hypoxia, and trauma (Berg et al., 2016).

In the current scenario, administration of ranibizumab to the vitreous and retina has ocular risks, high patient-treatment liability, and compliance barriers. For preventing this, a new device was introduced that provided continued discharge of ranibizumab in the vitreous cavity for a period of a few months. The device consisted of thin films of nanoporous PCL, which surrounded the ranibizumab reservoir. These delivery systems provided a continuous release of the drug over 16 weeks in vitro, deprived of draining the initial drug payload. After implantation in vivo, the devices stayed well-accepted and did not display any signs of immune response (Andreoli et al., 2015).

Stevenson and Cheng reviewed the epidemiology, pathogenesis, and treatment of corneal neurovascularization along with the application of Lucentis (ranibizumab) and Avastin (bevacizumab) for treating corneal neurovascularization (Stevenson et al., 2012). Corneal neurovascularization is the second most prominent reason for visual impairment globally, and progresses in response to inflammation, hypoxia, trauma or due to limbal cell deficiency. Two open-label studies were performed with 30 patients, 10 patients for ranibizumab studies and 20 for bevacizumab studies. It was found that both appeared as an effective treatment for corneal neovascularization (NV) but ranibizumab showed a better decrease in corneal NV owing to its low molecular weight. The corneal penetration was high and therapeutic concentrations were achieved earlier in the treatment course making it more efficient than bevacizumab.

6.7.4 Biosilicon Technology

Biosilicon is a porous form of silicon that is both biocompatible and biodegradable in nature. It dissolves in the body, forming silicic acid, which gets excreted by the kidney (Receveur et al., 2007). It is an example of the top-down nanostructuring process, where elemental silicon is restructured to form nanopores within the material. Biosilicon permits drug molecules to be held in these nanosized pockets. This pocket releases the drug as it dissolves. These nanopores can be loaded with drugs, peptides, genes, proteins, and other therapeutics and vaccines. These systems possess various advantages such as:

- Biodegradability, biocompatibility, and semiconductivity
- Abundant low-cost element
- High drug loading protection from dose dumping
- High range of delivering formulations

These systems can be used for localized chemotherapy, transdermal delivery, and brachytherapy. An example of this system is BrachySil, that is., a novel phosphorus (^{32}P) brachytherapy device. This device was developed by Goh et al. (2007) for the treatment of hepatocellular carcinoma. The study was conducted with eight patients and the effect was measured in terms of target tumor response and overall tumor response. Target tumor response was observed within 12 weeks with a reduction in the size of tumors. Complete response, that is, 100% response was observed in 2 out of 8 patients. A graphic of this effect is shown in Fig. 6.10.

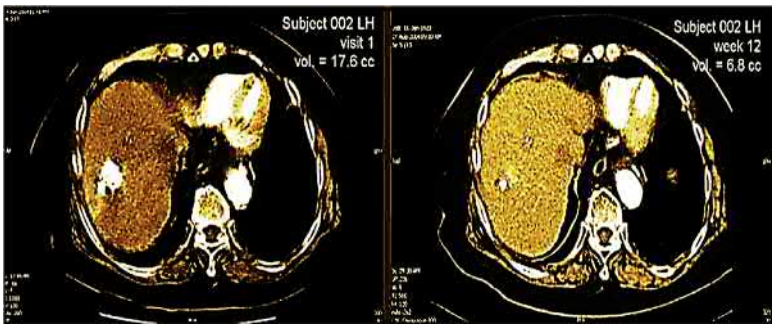

FIGURE 6.10 Significant tumor response over a 12-week period after implantation of 32P BioSilicon. Computed tomographic scan from the arterial phase. *Source: Adapted with permission from Goh, A.S.-W., Chung, A. Y.-F., Lo, R.H.-G., Lau, T.-N., Yu, S.W.-K., Chng, M., et al., 2007. A novel approach to brachytherapy in hepatocellular carcinoma using aphosphorous32 (32P) brachytherapy delivery device—a first-in-man study. Int. J. Radiat. Oncol. Biol. Phys. 67(3), 786–792.*

6.7.5 Replenish Mini Pump

Current approaches to ocular drug delivery possess various limitations like physiologic and anatomical obstructions, side effects, poor patient submission, etc. To prevent this, manually organized and electrically organized mini pumps were developed using MEMS engineering, that is, microelectromechanical systems. These systems consist of a refillable drug reservoir and transscleral cannula along with a check valve to regulate drug delivery (Saati et al., 2009). The pressure-sensitive check valve is placed at the cannula tip, which unlocks only after the internal reservoir pressure is greater than the extreme pressure of the check valve. Also, the valve consisted of an orifice sealed in contradiction of a valve seat. Above the extreme pressure, the orifice lifts away from the valve seat and creates a flow path. On removing the driving pressure, the orifice seals against the seat preventing backflow to the device. As the drug is exhausted, the reservoir can be replenished with the same or a different drug (Avery et al., 2010).

6.7.6 Encapsulated Cell Technology

The technology was developed for the treatment of central nervous system diseases and eye diseases. This implant consisted of living cells condensed in a semipermeable polymer membrane along with supporting matrices. The condensed living cells are genetically contrived so as to yield a definite therapeutic substance that targets a particular disease or condition. Upon implantation into CNS or eye, the semipermeable membrane performs two roles:

- Allowing outer movement of the therapeutic product along with shielding the condensed cells from elimination by a patient's immune system.
- Permitting access to oxygen and other nutrients.

The device is embedded via a small closed vitrectomy incision and is attached to the sclera through a small titanium wire loop. The device is secured outside the visual axis.

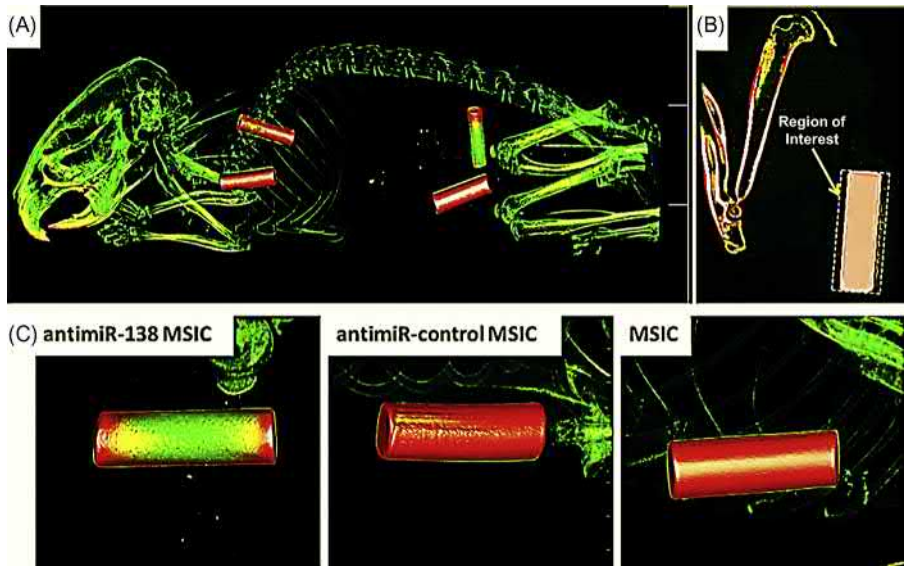

FIGURE 6.11 (A and C) 3D micro-CT images showing the newly formed bone around the implants after 8 weeks of subcutaneous implantation. (B) Region of interest is defined as a ring with a radius of 0.2 mm from the implant surface. *Source: Adapted with permission from Yan, J., Chang, B., Hu, X., Cao, C., Zhao, L., Zhang, Y., 2018. Titanium implant functionalized with antimiR-138 delivered cell sheet for enhanced peri-implant bone formation and vascularization. Mater. Sci. Eng., C 89, 52–64.*

Yan et al. (2018) developed a mesenchymal stem cell (MSC) sheet functionalized titanium implant with an inductive signal as a vital approach for mislaid tooth restoration. Authors developed an antimiR-138 delivered mesenchymal stem cell sheet-implant complex (MSIC) using an antimiR-138 MSC sheet to functionalize a Ti implant and studied the consequences on osteogenesis and angiogenesis coupling for treating the condition of lacking osseointegration during dental implant, in vitro, and in vivo. MSICs were planted subcutaneously in nude mice and assessed after 4 and 8 weeks. Fig. 6.11 shows the formation of ectopic periimplant bone with density similar to native bone.

These findings concluded that enhanced osteogenesis and angiogenesis coupling were observed in mice implanted with antimiR-138 delivered MSIC. The countenance of osteogenesis and angiogenesis-related genes and proteins was promoted along with improved alkaline phosphatase activity, extracellular matrix mineralization and collagen secretion in the mice as compared with antimiR control and nondelivered control group.

6.8 MANUFACTURING AND STERILIZATION PROTOCOLS

IDDSs need to be fabricated in suitable forms so as to improve the efficacy of drug release and delivery. Basically, microspheres are the form through which controlled drug delivery is achieved. The microsphere can be defined as a spherical particle that consists of polymeric or ceramic materials within the size range of 1–1000 μm in diameter (Morrison et al., 2015).

Various methods are used for fabrication of microspheres for delivery of the drug. Some of these methods are emulsion method, coacervation phase separation method, spray drying, air suspension method, solvent extraction method, and particle replication in nonwetting templates that is, PRINT method (Xu et al., 2013). Various parameters have critical importance like the selection of drug and polymeric material and the particle size of the fabrication process.

6.8.1 Coacervation Phase Separation

The method can use both aqueous and hydrophobic drugs to custom design a reservoir delivery system. The technique includes two phases: an organic phase, which is polymer-rich, and an aqueous drug phase. The drug is added to the organic phase in a continuous mode. This led to a steady exposure of the polymer to a hostile solvent environment. This, in turn, forms a coacervate with the aqueous drug units (or drug particles) undergoing high stirring to facilitate the regulation of the particle size. The phase separation leading to the development of the coacervate may be enhanced using salt, pH, or incompatible polymer (Glassman and Olsen, 2015).

6.8.2 Emulsion Phase Separation

This method comprises single-emulsion or double-emulsion techniques. The single-emulsion technique includes solubilization or dispersion of a polymeric constituent in the aqueous phase of a mixture. This is followed by adding an oil phase, which contains the drug. The dual phases are mixed with rapid stirring, which leads to cross-linking of either the polymeric component or the oil phase through means of heat or covalent linkages (Malavia and Kaiser, 2015).

The double-emulsion technique includes multiple emulsions surrounded by one another. For example, a water-in-oil-in-water (w/o/w) emulsion permits the therapeutic agent to be confined in either the aqueous phase, oil phase, or both. This can be accomplished by dissolving the aqueous solution of drug in an organic continuous phase, which in turn encloses a solvable polymer. The polymer present in the lipophilic phase encapsulates the drug present in the aqueous phase. The solution is then homogenized to disruption the emulsified particles. An aqueous polymer solution is then added to stabilize the emulsion particles being formed. The final step encompasses the evaporation of the organic phase, which yields the final phase of a w/o/w emulsion (Wood et al., 2018).

6.8.3 Spray Drying

This method includes the drying and stabilization of atomized polymer particles of drug molecules, which can be attained by liquefying the drug and polymer in a volatile organic solvent. Examples of such solvents are tetrahydrofuran, acetone, or methylene chloride. The solution is then homogenized until it is solubilized completely. The polymer–drug solution at that point is allowed to flow through an orifice, secured via an atomization tip (Yelles et al., 2017).

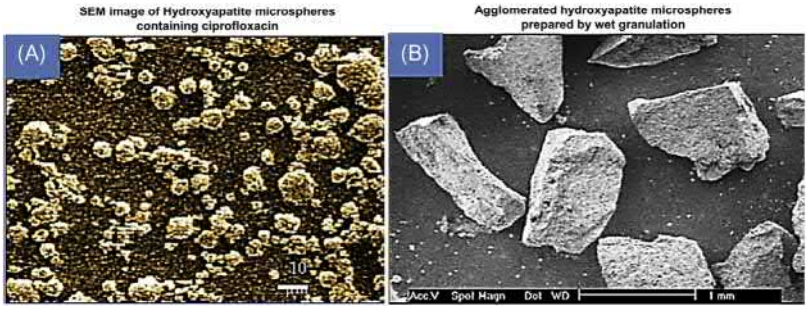

FIGURE 6.12 SEM photomicrographs. *Source: Adapted with permission from Pham, H.H., Luo, P., Génin, F., Dash, A.K. 2002. Synthesis and characterization of hydroxyapatite-ciprofloxacin delivery systems by precipitation and spray drying technique. AAPS PharmSciTech 3(1), 1–9.*

Pham et al. (2002) developed a hydroxyapatite–ciprofloxacin delivery system utilizing precipitation and spray-drying technique. The authors first prepared hydroxyapatite microspheres by chemical precipitation tailed by a spray-drying technique. These microspheres were then compressed on a Carver press for converting into implants. These implants were basically used for the treatment of bone infections. A precursor gel was prepared that contained calcium hydroxide and phosphoric acid in a ratio of 10:6 and ciprofloxacin (Fig. 6.12). The pH of this gel was adjusted to 10 using ammonium hydroxide. The suspension was mixed well by a magnetic stirrer at 25°C and 600 rpm. After adjusting the viscosity up to 2–3 cut with water, a spray-drying process was used to form hydroxyapatite microspheres. Atomization was carried out and atomized drops were dried by a coaxial flow of air. The inlet and outlet spraying temperatures were 25°C and 100°C. Agglomerated hydroxyapatite microspheres were prepared for improving compaction properties. These microspheres containing ciprofloxacin were mixed with water to create a gel that can be extruded at a pressure of 80 g/cm^3. The granules were air-dried for 12 hours and then compressed in a Carver press for preparing cylindrical implants.

6.8.4 Air Suspension

This method includes the drying of drug particles followed by suspending them in an air stream. The deferred particulates are spray-coated with a rapidly drying polymer solution. Since the particles constantly cycle across the system, the process permits for consecutive coating or layered coating. Although solid particles are normally cast off in this process, the casting of liquid particles and emulsions is possible as well (Chu et al., 2001).

6.8.5 Solvent Extraction

The solvent extraction method comprises the reducing of particulate formation by the extraction of the miscible organic solvent in an aqueous phase. The organic phase contains a polymer and should be miscible in water. The drug molecules are added to the organic phase, and then extracted by means of an aqueous solution. This leads to the formation of precipitated microspheres. Their size can be précised by the temperature of the water, the solubility of the polymer, and the ratio of the polymer to water and polymer to organic phases (Urist et al., 1973).

6.8.6 PRINT

The PRINT method was developed by DeSimone et al. This method involved the top-down creation of microparticles of different size, shape, strength, and surface functionality. The process begins with the creation of a master template by use of common lithographic etching technique. Liquid fluoropolymers are then added to the chief prototype and fixed by the photocross-linking procedure. As soon as the material solidifies after the cross-linking process, it is detached from the chief prototype, which results in an accurate mold. This accurate mold is utilized for the rest of the method. A liquefied drug–polymer solution was then added to the prototype, hard-pressed by a roller to confirm complete prototype filling devoid of bleed over, and permitted to set. The hardened mold at this point is moved to a harvesting film, which permits the superficial exclusion of cast materials (Perry et al., 2011). Perry et al. utilized this method for fabrication of particles ranging from 80 nm to 20 μm. These particles were composed of poly(D-lactic acid), polyethylene glycol, hydrogels, and proteins.

6.9 BENEFITS OF CONTROLLED DRUG ADMINISTRATION VIA IMPLANTATION

Techniques like encapsulated cell technology offer a substitute to the traditional means of management as it allows engineering of any therapeutic agent into the cells. The mammalian cell–produced protein factories are more effective as compared with the purified recombinant factors and hence decrease the dose requirement. It also allows direct delivery of proteins into the cerebrospinal fluid or eye. It allows retrieval of the cell-containing capsule. The advances in the area of micro/nanotechnologies led to the shortened delivery pathway of the drug, making it highly targeted (Yang, 2018).

Also, the miniaturization by these micro/nanotechnologies facilitates the integration of various constituents of the drug delivery device in a single micro/nanofluidic chip. These microdevices may be implanted in specific tissues or specific organs. They can be given either orally or externally through the skin. Drug delivery systems grounded on lab on chip (LOC) technologies facilitate administration of the precise quantity of drugs in a constant mode. Also the synthesis and delivery of drugs can both be included in a single device using this technology (Sutradhar and Sumi, 2016).

Nanofluidic devices that use techniques such as bulk nanomachining, surface nanomachining, buried channel technology, and nanoimprinted lithography have also been used to deliver drugs. Also, laser micromachining, a noncontact single-step technique is used to manufacture polymeric materials for application in drug delivery. These include the use unlike lasers for microfabrication that includes ultraviolet lasers, pulsated CO_2 lasers, and solid-state femtosecond lasers. Technologies like photolithography, micromolding, droplet-born air blowing, and layer-by-layer assembly have been used for the fabrication of microneedles (MNs) (Bruno et al., 2016).

Microreservoir-based drug delivery led to the design of drug delivery devices with smaller size and specific features for controlling rates of drug delivery to different target positions in a more specific manner. These reservoirs make accessible a well-controlled

environment for preparation of the drug to upsurge stability and delivery times of drug. Reservoir systems can be applied either externally or planted inside the body. These systems have the advantage of the selection of delivery methods including pulsatile release, on-demand dosing, and zero-order kinetics (Lee et al., 2014).

Polymer-based devices are extensively used for targeted and controlled drug delivery owing to their simplicity of fabrication and biocompatibility. Low-cost polymers have been successfully designed for administering biopharmaceuticals because of their properties such as biocompatibility, biodegradability, and they are easily acquired naturally or produced artificially. Biodegradable polymer-based microreservoirs are preferred for drug delivery because they can biodegrade entirely and discharge the drug at a precise rate on the site. Also, the necessity of surgically removing empty microreservoir device postrelease of the drug is eliminated (Qin et al., 2014).

Diffusion-controlled systems rely on the diffusion of the drug either out of a nonporous or microporous polymer layer or through the layer. Here the diffusion across the membrane structure is the rate-determining step and leads to drug transport through the inert aqueous diffusion layer. This technology had been extensively utilized for delivering the drug from reservoir-based oral systems and transdermal systems. Recently this technology has been improved for implants. A subcategory of diffusion-controlled systems possesses the benefit of a combining drug release from a polymer matrix via porosity plus polymer erosion (Lyndon et al., 2014).

6.10 COMMERCIALLY AVAILABLE ADVANCED IMPLANTABLE DEVICES

Vitrasert and Retisert are the two presently promoted, reservoir-based ocular implants that utilize drug distribution through polyvinyl alcohol (PVA) (Yasukawa, 2016). These products were industrialized by EyePoint Pharmaceuticals, Inc. (pSivida). The Vitrasert implant (accepted in 1996) containing 4.5 mg ganciclovir is used for treating cytomegalovirus (CMV) retinitis in AIDS patients. In this system, the ganciclovir tablet reservoir (3.5 mm) is covered with PVA as well as EVA polymers and then was attached to a tab. This tab is stitched to the inner eyewall. The PVA précises the release of drug whereas the EVA précises the devices' surface area over which the ganciclovir adsorbed. The system distributes the drug in the vitreous of the eye for a duration of about 5–8 months.

The Retisert implant was accepted in 2005 and it is a second generation Medidur technology. It contains 0.59-mg fluocinolone acetonide in a 1.5-mm tablet reservoir. The tablet is enclosed in an elastomeric silicone cup that contains a discharge orifice. Polyvinyl acetate membrane is placed amid the tablet and orifice. The elastomeric silicone cup is attached to the polyvinyl acetate suture tab with the help of a silicone adhesive. This silicone adhesive is surgically planted through a 3–4 mm incision (Bisht et al., 2018).

Another implant, the Iluvien implant, employs the third generation of Medidur technology and validates the technical ability to formulate minor devices (Jonas, 2018). Iluvien is introduced in the vitreous of the eye in the course of an outpatient procedure without being sutured to the eye as is the case of Vitrasert and Retisert. The implant comprises a polyimide tube reservoir that contains 190 μg fluocinolone in a polyvinyl acetate matrix.

The tube is covered with a rate-controlling membrane. During development, implants having two release rates were deliberated, one that was a higher dose implant with primary in vitro release rate 0.45 μg/day and one that was a lower dose implant with primary in vitro release rate 0.23 μg/day. These release rates of implants gradually declined in vitro and were almost the same, that is, ~0.15 μg/day, by the end of 18 months.

Durasert is another bioerodible reservoir implant for delivering latanoprost for the treatment of high intraocular pressure that is undergoing phase 2 clinical trials. pSivida is presently testing Tethadur for delivery of biomolecules and more than one therapeutic agent. Tethadur uses nanostructured pores to regulate the distribution of variously sized molecules. It can be directed to last around 6 months and is completely bioerodible (Jervis, 2017).

Debiotech industrialized a polymer-free nanocoating expertise which is centered on biocompatible as well as nanostructured ceramic coatings having variable porosities. These coatings can be worked to prepare drug reservoirs. The Debiostent loading capability can be précised by the dimensions of drug reservoirs in the lower coating layer. The upper coating layer lids the reservoir and hence précises the drug elution kinetics. The position and total figure of drug reservoirs can be pressed to emphasize the drug delivery from exact regions of the stent for maximum efficacy (Stevenson and Langer, 2015).

Endo Pharmaceuticals obtained the Hydron Implant Technology from Valera Pharmaceuticals. The Hydron technology is a cylindrical and nonbioerodible implant prepared of a hydrogel polymer blend called MedLaunch (comprised of 2-hydroxyethyl methacrylate, 2-hydroxypropyl methacrylate, trimethylol-propanetri methacrylate, benzoin methyl ether, Perkadox-16, Triton X-100) and is spun cast off into minute tube reservoirs. The implant is provided prehydrated and it comprises micropores that permit diffusion of the drug to follow a zero-order approach for a year or longer (Oimar, 2017).

Both Vantas for prostate cancer (accepted 2004) and Supprelin LA for precocious puberty (accepted in 2007) are implanted with a trocar and both contain 50 mg histrelin acetate. Both systems persist for 1 year owing to a release rate of 41 μg/day. Endo Pharmaceuticals also owns an octreotide implant (84 mg), which persisted for 6 months in phase 3 clinical trials performed for acromegaly.

iMEDD Inc. fabricated a small cylindrical titanium implant that continuously releases α-interferon for 3–6 months for treating hepatitis C. The implant can be injected beneath the skin and preserve drug plasma level above 50 pg/mL so as to sustain an antiviral effect deprived of any adjacent effects allied to higher doses. The NanoGATE implant, a titanium implant, is crowned at both ends and a nanopore membrane is fastened above a small bore, which opens in a cylindrical methacrylate inset carrier. The carrier is trim with two silicone O-rings and rooted inside the titanium case. Once the membrane is lined up with the titanium grate opening, the device is packed with drug formulation. The nanopore membrane regulates the drug diffusion from the reservoir (Stevenson and Langer, 2015).

The minimally invasive pocket (MIP) implantable pump was developed by Debiotech. It is a piezoactuated silicon micropump used for delivery of the drug. The pump comprises a pair of check valves along with a reciprocating pumping membrane, which guides liquid movement in the desired route from the reservoir to the targeted site. The device is designed from numerous attached films of silicon and glass, along with a piezoelectric

ceramic disk and titanium fluid connectors. The pump has a characteristic run rate of 1 mL/min. Burst release devices like the IRD3 (implantable rapid drug delivery device) devised at the Massachusetts Institute of Technology were developed for emergency care. They comprise three layers: a drug reservoir layer, a membrane that covers the drug reservoir, and an actuation layer where bubbles form. The device delivers around 20 μL of a vasopressin solution within 45 seconds (Lee et al., 2015).

6.11 FUTURE SCOPE AND CONCLUSION

In the current trade and industry, the combination product should likewise offer a discrete advantage over current treatments along with a lower price. Fabrication of effective drug delivery products necessitates foresight inside the governing bodies so as to obtain well-timed market acceptance. These embrace suitable shelf life stability and life stability for in vivo use to safeguard the efficacy of the concluding dosing period. The development of drug release tests are critical for a demonstration of the absence of dose dumping, total formulation percentage released from the delivery system, in vivo stability, and in-vitro in-vivo correlation (IVIVC) correlation. Extra attention should be paid to supply chain issues early during development. Drug excipients should bear generally regarded as safe status. Device constituents contacting with drug or patient must be of medical grade along with adequate physicochemical characteristics, biocompatibility, and leachable/extractable profile. These tests will as well be applicable to the raw materials and the final product. The selection of biocompatible device materials is critical, particularly significant for long-term implants or permanent implants. Here tissue adhesion or polymeric degradation products can lead to inflammation.

Acknowledgment

RKT would like to acknowledge Science and Engineering Research Board (Statutory Body Established Through an Act of Parliament: SERB Act 2008), Department of Science and Technology, Government of India for grant (grant #ECR/2016/001964) and N-PDF funding (PDF/2016/003329) for work on targeted cancer therapy in Dr. Tekade's Laboratory. RKT would also like to acknowledge the Department of Pharmaceuticals, Ministry of Chemicals and Fertilizers, India, for supporting research on cancer and diabetes at NIPER—Ahmedabad.

References

Alvarez-Lorenzo, C., Blanco-Fernandez, B., Puga, A.M., Concheiro, A., 2013. Cross-linked ionic polysaccharides for stimuli-sensitive drug delivery. Adv. Drug Delivery Rev. 65 (9), 1148–1171.

Andreoli, M.T., Pinnolis, M., Kieser, T., Sun, J., Andreoli, C.M., 2015. Feasibility and efficacy of a mass switch from ranibizumab (Lucentis) to bevacizumab (Avastin) for treatment of neovascular age-related macular degeneration. Digit. J. Ophthalmol. 21 (3), 1.

Ang, H.Y., Bulluck, H., Wong, P., Venkatraman, S.S., Huang, Y., Foin, N., 2017. Bioresorbable stents: current and upcoming bioresorbable technologies. Int. J. Cardiol. 228, 931–939.

Aparna, R., Prasad, R., Nirmal, N.P., 2016. An injectable in-situ conducting thermosensitive gel for controlled delivery of vancomycin in osteomyelitis treatment and bone regeneration. Sci. Adv. Mater. 8 (7), 1470–1477.

Arcos, D., Vallet-Regí, M., 2013. Bioceramics for drug delivery. Acta Mater. 61 (3), 890–911.

Argyo, C., Weiss, V., Bräuchle, C., Bein, T., 2013. Multifunctional mesoporous silica nanoparticles as a universal platform for drug delivery. Chem. Mater. 26 (1), 435–451.
Avery, R., Saati, S., Journey, M., Caffey, S., Varma, R., Tai, Y., et al., 2010. A novel implantable, refillable pump for intraocular drug delivery. Invest. Ophthalmol. Visual Sci. 51 (13), 3799.
Beckwith, M.C., Feddema, S.S., Barton, R.G., Graves, C., 2004. A guide to drug therapy in patients with enteral feeding tubes: dosage form selection and administration methods. Hosp. Pharm. 39 (3), 225–237.
Berg, K., Hadzalic, E., Gjertsen, I., Forsaa, V., Berger, L.H., Kinge, B., et al., 2016. Ranibizumab or bevacizumab for neovascular age-related macular degeneration according to the lucentis compared with avastin study treat-and-extend protocol: two-year results. Ophthalmology 123 (1), 51–59.
Bisht, R., Mandal, A., Jaiswal, J.K., Rupenthal, I.D., 2018. Nanocarrier mediated retinal drug delivery: overcoming ocular barriers to treat posterior eye diseases. Wiley Interdiscip. Rev. Nanomed. Nanobiotechnol. 10 (2), e1473.
Bruno, G., Canavese, G., Liu, X., Filgueira, C.S., Sacco, A., Demarchi, D., et al., 2016. The active modulation of drug release by an ionic field effect transistor for an ultra-low power implantable nanofluidic system. Nanoscale 8 (44), 18718–18725.
Chu, T.-M., Halloran, J., Hollister, S.J., Feinberg, S.E., 2001. Hydroxyapatite implants with designed internal architecture. J. Mater. Sci. Mater. Med. 12 (6), 471–478.
Curtis, J., Colas, A., 2013. Medical applications of silicones, Biomaterials Science, third ed. Elsevier.
Dagdeviren, C., Yang, B.D., Su, Y., Tran, P.L., Joe, P., Anderson, E., et al., 2014. Conformal piezoelectric energy harvesting and storage from motions of the heart, lung, and diaphragm. Proc. Natl. Acad. Sci. U.S.A. 111 (5), 1927–1932.
Danyuo, Y., Obayemi, J., Dozie-Nwachukwu, S., Ani, C., Odusanya, O., Oni, Y., et al., 2014. Prodigiosin release from an implantable biomedical device: kinetics of localized cancer drug release. Mater. Sci. Eng., C 42, 734–745.
Dittmer, R., Schaefer, C.M., Fischer, J.-F., Hausch, U., Troetzschel, J., Specht, H., 2017. Advanced CerMet ceramic composites for medical applications. J. Mech. Behav. Biomed. Mater. 75, 206–211.
Genina, N., Holländer, J., Jukarainen, H., Mäkilä, E., Salonen, J., Sandler, N., 2016. Ethylene vinyl acetate (EVA) as a new drug carrier for 3D printed medical drug delivery devices. Eur. J. Pharm. Sci. 90, 53–63.
Glassman, M.J., Olsen, B.D., 2015. Arrested phase separation of elastin-like polypeptide solutions yields stiff, thermoresponsive gels. Biomacromolecules 16 (12), 3762–3773.
Goh, A.S.-W., Chung, A.Y.-F., Lo, R.H.-G., Lau, T.-N., Yu, S.W.-K., Chng, M., et al., 2007. A novel approach to brachytherapy in hepatocellular carcinoma using aphosphorous32 (32P) brachytherapy delivery device—a first-in-man study. Int. J. Radiat. Oncol. Biol. Phys. 67 (3), 786–792.
Govender, T., Choonara, Y.E., Kumar, P., Bijukumar, D., du Toit, L.C., Modi, G., et al., 2017. Implantable and transdermal polymeric drug delivery technologies for the treatment of central nervous system disorders. Pharm. Dev. Technol. 22 (4), 476–486.
Gulati, K., Kogawa, M., Prideaux, M., Findlay, D.M., Atkins, G.J., Losic, D., 2016. Drug-releasing nanoengineered titanium implants: therapeutic efficacy in 3D cell culture model, controlled release and stability. Mater. Sci. Eng., C 69, 831–840.
Harilall, S.L., Choonara, Y.E., Tomar, L.K., Tyagi, C., Kumar, P., du Toit, L.C., et al., 2015. Development and in vivo evaluation of an implantable nanoenabled multipolymeric scaffold for the management of AIDS dementia complex (ADC). Int. J. Pharm. 496 (2), 863–877.
Hill, A., Geissler, S., Meyring, M., Hecht, S., Weigandt, M., Mäder, K., 2013. In vitro–in vivo evaluation of nanosuspension release from subcutaneously implantable osmotic pumps. Int. J. Pharm. 451 (1-2), 57–66.
Ibrahim, H.K., Fahmy, R.H., 2016. Localized rosuvastatin via implantable bioerodible sponge and its potential role in augmenting bone healing and regeneration. Drug Delivery 23 (9), 3181–3192.
Jeong, J., Bae, S.H., Min, K.S., Seo, J.-M., Chung, H., Kim, S.J., 2015. A miniaturized, eye-conformable, and long-term reliable retinal prosthesis using monolithic fabrication of liquid crystal polymer (LCP). IEEE Trans. Biomed. Eng. 62 (3), 982–989.
Jervis, L., 2017. A summary of recent advances in ocular inserts and implants. J. Bioequiv. Availab. 9 (1), 320–323.
Jonas, J.B., 2018. Reply to the letter by Hall Entitled "ILUVIEN in Diabetic Macular Edema: The Choice of Second-Line Corticosteroid Should Be Left to the Clinical Judgement of the Treating Physician". Ophthalmologica 239 (4), 237–238.

Joung, Y.-H., 2013. Development of implantable medical devices: from an engineering perspective. Int. Neurourol. J. 17 (3), 98.
Kamaly, N., Yameen, B., Wu, J., Farokhzad, O.C., 2016. Degradable controlled-release polymers and polymeric nanoparticles: mechanisms of controlling drug release. Chem. Rev. 116 (4), 2602–2663.
Khan, A.F., Saleem, M., Afzal, A., Ali, A., Khan, A., Khan, A.R., 2014. Bioactive behavior of silicon substituted calcium phosphate based bioceramics for bone regeneration. Mater. Sci. Eng., C 35, 245–252.
Kim, S.W., Petersen, R.V., Feijen, J., 2016. Polymeric drug delivery systems. Drug Des. 10, 193–250.
Kleiner, L.W., Wright, J.C., Wang, Y., 2014. Evolution of implantable and insertable drug delivery systems. J. Control. Release 181, 1–10.
Kuche, K., Maheshwari, R., Tambe, V., Mak, K.K., Jogi, H., Raval, N., et al., 2018. Carbon nanotubes (CNTs) based advanced dermal therapeutics: current trends and future potential. Nanoscale 10 (19), 8911–8937.
Lamba, N.K., 2017. Polyurethanes in Biomedical Applications. Routledge.
Lee, S.H., Park, M., Park, C.G., Kim, B.-H., Lee, J., Choi, S., et al., 2014. Implantable micro-chip for controlled delivery of diclofenac sodium. J. Control. Release 196, 52–59.
Lee, M.-S., Yao, D.-J., Hsu, W., 2015. An implantable drug-delivery system on a chip. Curr. Top. Med. Chem. 15 (15), 1516–1524.
Li, D., Guo, G., Fan, R., Liang, J., Deng, X., Luo, F., et al., 2013. PLA/F68/dexamethasone implants prepared by hot-melt extrusion for controlled release of anti-inflammatory drug to implantable medical devices: I. Preparation, characterization and hydrolytic degradation study. Int. J. Pharm. 441 (1-2), 365–372.
Liu, H., Rao, Z., Huang, X., Cheng, G., Tian, J., Ta, N., 2014. An incus-body driving type piezoelectric middle ear implant design and evaluation in 3D computational model and temporal bone. ScientificWorldJournal 2014, 121624.
Lyndon, J.A., Boyd, B.J., Birbilis, N., 2014. Metallic implant drug/device combinations for controlled drug release in orthopaedic applications. J. Control. Release 179, 63–75.
Maheshwari, R.G., Tekade, R.K., Sharma, P.A., Darwhekar, G., Tyagi, A., Patel, R.P., et al., 2012. Ethosomes and ultradeformable liposomes for transdermal delivery of clotrimazole: a comparative assessment. Saudi Pharm. J. 20 (2), 161–170.
Malavia, N., Kaiser, P.K., 2015. Overview of sustained-release drug-delivery systems. Retina Today 67–69.
Morrison, R.J., Kashlan, K.N., Flanangan, C.L., Wright, J.K., Green, G.E., Hollister, S.J., et al., 2015. Regulatory considerations in the design and manufacturing of implantable 3D-printed medical devices. Clin. Transl. Sci. 8 (5), 594–600.
Muniswamy, V.J., Raval, N., Gondaliya, P., Tambe, V., Kalia, K., Tekade, R.K., 2018. 'Dendrimer-Cationized-Albumin' encrusted polymeric nanoparticle improves BBB penetration and anticancer activity of doxorubicin. Int. J. Pharm. 555, 77–99.
Oimar, M., 2017. Hydroxyapatite precipitation with Hydron Blue dye. J. Environ. Manage. 203 (Pt 2), 807–810.
Patra, C.N., Swain, S., Sruti, J., Patro, A.P., Panigrahi, K.C., Beg, S., et al., 2013. Osmotic drug delivery systems: basics and design approaches. Recent Pat. Drug Deliv. Formul. 7 (2), 150–161.
Perry, J.L., Herlihy, K.P., Napier, M.E., DeSimone, J.M., 2011. PRINT: a novel platform toward shape and size specific nanoparticle theranostics. Acc. Chem. Res. 44 (10), 990–998.
Pham, H.H., Luo, P., Génin, F., Dash, A.K., 2002. Synthesis and characterization of hydroxyapatite-ciprofloxacin delivery systems by precipitation and spray drying technique. AAPS PharmSciTech 3 (1), 1–9.
Portilla, J.M., Kim, U., 2013. Low-power, self-contained, reciprocating micropump through electrolysis and catalyst-driven recombination toward drug delivery applications. In: Micro Electro Mechanical Systems (MEMS), 2013 IEEE 26th International Conference on. IEEE, pp. 1077–1080.
Pundir, S., Badola, A., Sharma, D., 2017. Sustained release matrix technology and recent advance in matrix drug delivery system: a review. Int. J. Drug Res. Technol. 3 (1), 8.
Qin, Y., Howlader, M.M., Deen, M.J., Haddara, Y.M., Selvaganapathy, P.R., 2014. Polymer integration for packaging of implantable sensors. Sens. Actuators, B: Chem. 202, 758–778.
Rauck, R., Deer, T., Rosen, S., Padda, G., Barsa, J., Dunbar, E., et al., 2013. Long-term follow-Up of a novel implantable programmable infusion pump. Neuromodulation 16 (2), 163–167.
Receveur, R.A., Lindemans, F.W., De Rooij, N.F., 2007. Microsystem technologies for implantable applications. J. Micromech. Microeng. 17 (5), R50.

Russo, A., Concia, E., Cristini, F., De Rosa, F., Esposito, S., Menichetti, F., et al., 2016. Current and future trends in antibiotic therapy of acute bacterial skin and skin-structure infections. Clin. Microbiol. Infection 22, S27–S36.
Saati, S., Lo, R., Li, P.-Y., Meng, E., Varma, R., Humayun, M.S., 2009. Mini drug pump for ophthalmic use. Trans. Am. Ophthalmol. Soc. 107, 60.
Siepmann, J., Rhodes, C., Banker, G.S., 2002. Sustained- and controlled-release drug-delivery systems, Modern Pharmaceutics, fourth ed. CRC Press.
Silna, E., Krishnakumar, K., Nair, S.K., Narayanan, A., Dineshkumar, B., 2016. Innovative Drug Discovery 6 (2), 87–93.
Spaan, N., Teplova, A., Stam, G., Spaan, J., Lucas, C., 2014. Systematic review: continuous intraperitoneal insulin infusion with implantable insulin pumps for diabetes mellitus. Acta Diabetol. 51 (3), 339–351.
Stevenson, C.L., Langer, R., 2015. Development of combination product drug delivery systems. In: Drug-Device Combinations for Chronic Diseases. John Wiley & Sons, Inc., p. 66.
Stevenson, W., Cheng, S.-F., Dastjerdi, M.H., Ferrari, G., Dana, R., 2012. Corneal neovascularization and the utility of topical VEGF inhibition: ranibizumab (Lucentis) vs bevacizumab (Avastin). Ocul. Surf. 10 (2), 67–83.
Sutradhar, K.B., Sumi, C.D., 2016. Implantable microchip: the futuristic controlled drug delivery system. Drug Delivery 23 (1), 1–11.
Talbi, Y., Campo, E., Brulin, D., Fourniols, J., 2018. Controllable and re-usable patch for transdermal iontophoresis drug delivery. Electron. Lett. 54 (12), 739–740.
Tekade, R.K., Maheshwari, R., Soni, N., Tekade, M., Chougule, M.B., 2017a. Nanotechnology for the development of nanomedicine A2—Mishra, Vijay. In: Kesharwani, P., Amin, M.C.I.M., Iyer, A. (Eds.), Nanotechnology-Based Approaches for Targeting and Delivery of Drugs and Genes. Academic Press.
Tekade, R.K., Maheshwari, R., Tekade, M., 2017b. 4—Biopolymer-based nanocomposites for transdermal drug delivery. Biopolymer-Based Composites. Woodhead Publishing.
Tsang, M., Armutlulu, A., Martinez, A.W., Allen, S.A.B., Allen, M.G., 2015. Biodegradable magnesium/iron batteries with polycaprolactone encapsulation: a microfabricated power source for transient implantable devices. Microsys. Nanoeng. 1, 15024.
Tyler, B., Gullotti, D., Mangraviti, A., Utsuki, T., Brem, H., 2016. Polylactic acid (PLA) controlled delivery carriers for biomedical applications. Adv. Drug Delivery Rev. 107, 163–175.
Urist, M.R., Iwata, H., Ceccotti, P.L., Dorfman, R.L., Boyd, S.D., McDowell, R.M., et al., 1973. Bone morphogenesis in implants of insoluble bone gelatin. Proc. Natl. Acad. Sci. U.S.A. 70 (12), 3511–3515.
Wang, Y., Gu, B., Burgess, D.J., 2014. Microspheres prepared with PLGA blends for delivery of dexamethasone for implantable medical devices. Pharm. Res. 31 (2), 373–381.
Washington, M.A., Swiner, D.J., Bell, K.R., Fedorchak, M.V., Little, S.R., Meyer, T.Y., 2017. The impact of monomer sequence and stereochemistry on the swelling and erosion of biodegradable poly(lactic-*co*-glycolic acid) matrices. Biomaterials 117, 66–76.
Wood, K., Szewczuk, M.R., Rousseau, D., Neufeld, R.J., 2018. Oseltamivir phosphate released from injectable Pickering emulsions over an extended term disables human pancreatic cancer cell survival. Oncotarget 9 (16), 12754.
Xu, J., Wong, D.H., Byrne, J.D., Chen, K., Bowerman, C., DeSimone, J.M., 2013. Future of the particle replication in nonwetting templates (PRINT) technology. Angew. Chem. Int. Ed. 52 (26), 6580–6589.
Yan, J., Chang, B., Hu, X., Cao, C., Zhao, L., Zhang, Y., 2018. Titanium implant functionalized with antimiR-138 delivered cell sheet for enhanced peri-implant bone formation and vascularization. Mater. Sci. Eng., C 89, 52–64.
Yang, G.-Z., 2018. Implantable Sensors and Systems: From Theory to Practice. Springer.
Yasukawa, T., 2016. Biomaterials for intraocular sustained drug delivery, Biomaterials and Regenerative Medicine in Ophthalmology, *second ed.* Elsevier.
Yelles, M.H.-B., Tan, V.T., Danede, F., Willart, J., Siepmann, J., 2017. PLGA implants: how poloxamer/PEO addition slows down or accelerates polymer degradation and drug release. J. Control. Release 253, 19–29.
Zaher, A., Li, S., Wolf, K., Pirmoradi, F., Yassine, O., Lin, L., et al., 2015. Osmotically driven drug delivery through remote-controlled magnetic nanocomposite membranes. Biomicrofluidics 9 (5), 054113.
Zambon, J.P., de Sá Barretto, L.S., Nakamura, A.N.S.E., Duailibi, S., Leite, K., Magalhaes, R.S., et al., 2014. Histological changes induced by polyglycolic-acid (PGA) scaffolds seeded with autologous adipose or muscle-derived stem cells when implanted on rabbit bladder. Organogenesis 10 (2), 278–288.

Zargarpour, N., Zarifi, M.H., 2015. A piezoelectric micro-electromechanical microphone for implantable hearing aid applications. Microsyst. Technol. 21 (4), 893–902.

Zhang, X.-S., Han, M.-D., Wang, R.-X., Meng, B., Zhu, F.-Y., Sun, X.-M., et al., 2014. High-performance triboelectric nanogenerator with enhanced energy density based on single-step fluorocarbon plasma treatment. Nano Energy 4, 123–131.

Zhang, H., Zhang, X.-S., Cheng, X., Liu, Y., Han, M., Xue, X., et al., 2015. A flexible and implantable piezoelectric generator harvesting energy from the pulsation of ascending aorta: in vitro and in vivo studies. Nano Energy 12, 296–304.

CHAPTER

7

Nanotechnology in Tissue Engineering

Neha Maheshwari[1], *Muktika Tekade*[1], *Yashu Chourasiya*[2], *Mukesh Chandra Sharma*[1], *Pran Kishore Deb*[3] *and Rakesh K. Tekade*[4]

[1]School of Pharmacy, Devi Ahilya Vishwavidyalaya, Takshila Campus, Indore, India [2]Department of Pharmacology, Shri Bherulal Pharmacy Institute, Indore, India [3]Faculty of Pharmacy, Philadelphia University, Amman, Jordan [4]National Institute of Pharmaceutical Education and Research (NIPER)—Ahmedabad, Gandhinagar, India

OUTLINE

7.1 Tissue Engineering: An Overview 226

7.2 Nanotechnology in Tissue Engineering 227

7.3 Strategies Related to the Formation of Scaffolds 231
7.3.1 Photolithography 231
7.3.2 Templating 231
7.3.3 Ionic Self-Complementary Peptide 231
7.3.4 Bionanotubes/Lipid Tubules 232
7.3.5 Miscellaneous 232

7.4 Natural Materials–Based Tissue Engineering Nanoscaffold 232
7.4.1 The Chitosan-Based Tissue Engineering Scaffold 233
7.4.2 The Albumin-Based Tissue Engineering Scaffold 233
7.4.3 The Alginate-Based Tissue Engineering Scaffold 235
7.4.4 The Silica-Based Tissue Engineering Scaffold 237

7.5 Synthetic Materials–Based Tissue Engineering Nanoscaffolds 238
7.5.1 The Dendrimer-Based Tissue Engineering Scaffold 238
7.5.2 Poly(Lactic Acid-co-Glycolic Acid)-Based Tissue Engineering Scaffold 240
7.5.3 Polylactic Acid–Based Tissue Engineering Scaffold 240
7.5.4 The Polyethylene Glycol–Based Tissue Engineering Scaffold 242

7.6 Applications 243
7.6.1 Nanotechnology in Cell Tissue Engineering 244

Biomaterials and Bionanotechnology
DOI: https://doi.org/10.1016/B978-0-12-814427-5.00007-X

© 2019 Elsevier Inc. All rights reserved.

7.6.2 *Nanotechnology-Based Tissue Engineering for Cell Labeling, Purification, Detection, and Suicide Bombing* 251
7.7 Recent Patents Overview 252
7.7.1 *Magnetic Pole Matrices* 253
7.7.2 *Differentiable Human Mesenchymal Stem Cells* 253
7.7.3 *Degradable Polyurethane Foams* 253
7.7.4 *Multilayer Polymer Scaffolds* 254
7.8 Clinical Trial Status 254
7.9 Conclusion 257
Acknowledgments 257
Abbreviations 257
References 257
Further reading 261

7.1 TISSUE ENGINEERING: AN OVERVIEW

The reliability and body function of the injured cells, tissues, and organs are preserved by the most vital and critical contrivance of the body, i.e., the self-repair mechanism. This mechanism slows down and recovery takes a long time with growing age, injury, or prevailing disease, and this process is limited to small localized tissue. Many times this natural mechanism is ineffective and therefore, more effective organ transplantation can be used in which the damaged organ is replaced via a healthier organ. Due to organ transplant, uncontrollable autoimmune suppression may occur, which increases the chances of graft rejection or often leads to the death of the patient. The development and progress of tissue engineering help to reconstitute artificial cells or tissues in place of damaged organs using cells of the recipient.

Therefore the definition of tissue engineering can be as the application of principles and methods of engineering and life sciences for the development of biological substitutes, to refurbish, sustain, or recover tissue function (Vacanti and Langer, 1999). Instead of replacing the tissues or organs the aim of this process, viz., tissue engineering is to regenerate injured tissues by developing biological surrogates that restore, maintain, or improve tissue function (O'Brien, 2011). The 1988 National Science Foundation workshop officially coined the term *tissue engineering* to decrypt the simple understanding of the assembly–purpose relationship in the development of biological substitutes and between normal and pathological mammalian tissue (O'Brien, 2011).

However, the first pioneering work in tissue engineering dates back to the 16th century when professor of surgery and anatomy at the University of Bologna Gasparo Tagliacozzi (1546–99) described a nose replacement that he had constructed from a forearm flap in his work *De Custorum Chirurigia per Insitionem* (*The Surgery of Defects by Implantation*), which was published in 1597 (O'Brien, 2011). Howard Green and his coworkers had a crucial contribution to the field of tissue engineering. The first mass production of normal human diploid cells (keratinocytes) was carried out by them in 1981. This was the first commercial product made by tissue engineering a living autologous human skin epithelium, which was used for burn patients (Peck et al., 2011).

Further, the work of Green was followed by Eugene Bell, who added a dermal component, finally developing "artificial skin," and this led to the foundation of Organogenesis Inc. in 1986. This was the first FDA approved plant for the mass-produced tissue-engineered product (Vacanti, 2006). Tissue and whole organ grafting are frequently used to replace the damaged/diseased tissues or organs of the body. Earlier this process solely depended on the transplanting of donated organs and decellularized tissues. However, graft rejection and less availability or unavailability of organ donors were the major problems that have been faced frequently. Tissue engineering techniques are emerging technologies and more robust and cheaper alternatives to such earlier techniques and deals with the improvement of the regenerative capability of tissues, and facilitate the development of new tissues or complete organ and replacement of damaged/diseased tissues.

Tissue engineering is different from biomimetic materials as biomimetic materials are substances that elicit one or more responses similar to that of the extracellular natural matrix (ECM) around the cells in tissue. Now they are extensively employed in the field of tissue engineering. Tissue engineering is at the frontier of material science, bioengineering, chemistry, biology, and medicine, controlled to meet the unmet clinical needs through the development of new technologies and enhancement of existing ones (Atala et al., 2012). The major advantage of tissue engineering is that it mimics the functional and anatomical features of innate tissues, so it can maintain the working and renovate the normal functioning of the injured tissues (Lee et al., 2016). The strategies of tissue engineering generally involve a combination of biomaterials, cells, and biologically active factors to effect tissue formation (Atala et al., 2012). Finally, tissue engineering leads to the foundation of organs that provide external support and nonimplantable structures in the situation where the convenience of a compatible donor is not possible (Martin et al., 2004).

7.2 NANOTECHNOLOGY IN TISSUE ENGINEERING

The branch of science that deals with the intent of making, classifying, and applying materials and devices at the molecular level with dimensions less than 100 nm is called nanotechnology (Lalu et al., 2017; Maheshwari et al., 2015a; Sharma et al., 2015; Tekade et al., 2017a). In medicine, the application of these materials can be programmed to interact with cells and tissues at a receptor level with the highest scale of specificity thus allowing a greater degree of incorporation of technology with biological systems not previously possible (Kuche et al., 2018; Tekade et al., 2017b). The question then arises: what is the importance of nanotechnology? The answer is that it provides an uncomplicated binding site and increases tissue production nanotechnology to help in developing cell bonding and vascularization. Also, nanotechnology ensures the controlled release (Danie Kingsley et al., 2013).

The ideal range of nanoparticles is 10−100 nm. (Walmsley et al., 2015). Nanotechnology ensures the formation of nanospheres, which imitate subjected body tissues like bone and cardiac tissues. After significant randomization difference in cell attachment, production

and separation were observed (Lamers et al., 2010). Nanosized scaffold also ensures good binding of a fibrin clot, which improves the movement of osteogenic cells to the engineered surface (Mager et al., 2011). They are also widely used as controlled drug release because of their small size, and thus high surface area; as a result, drug loading efficiency also increases (Maheshwari et al., 2012, 2015b).

The approaches for nanotechnology-based tissue engineering involved transplantation of harvested cells/tissues at the damaged site in the body; introduction of substances at the damaged site, which aids the cells to grow and repair; and implanting support matrices carrying cell seeds (e.g., stem cells, osteoblasts) (Langer and Vacanti, 1993). Tissue engineering trained in nanotechnology includes three components, namely scaffolds, cells, and growth factors (Krishnan and Sethuraman, 2013). Earlier efforts were made to choose the type of material that can be used in preparing the scaffold, but now attention has been paid in geometry and surface functionality of the scaffold chosen that mimics the topography of the extracellular matrix. Nanotechnology-enabled the integration of the nanostructures in the scaffold that showed better results than the two-dimensional cultures.

Growth factors are the crucial part of the tissue engineering as the cells must be provided with appropriate chemical factors at an appropriate time interval to acquire the native physiological, chemical, and the mechanical characters of the cell. When these growth factors were integrated as the nanocarriers the cell formed showed more resemblance in functional and physiological aspect as well. Cells that can be used are the stem cells, and the type of stem cell that should be employed depends upon the type of the cell that is needed to be engineered. The stem cells that can be employed for the tissue engineering of hepatocytes are human bone marrow stem cells (Raftery et al., 2016). The appropriate method for engineering the scaffold and the time interval used for the incorporation of the growth factors directly affects the function of the cell that has been engineered, so one must pay attention in this concern while employing nanotechnology in cell-based therapy. The triad of signal, scaffolds, and cells, which acts as a stencil for tissue engineering, is represented in Fig. 7.1.

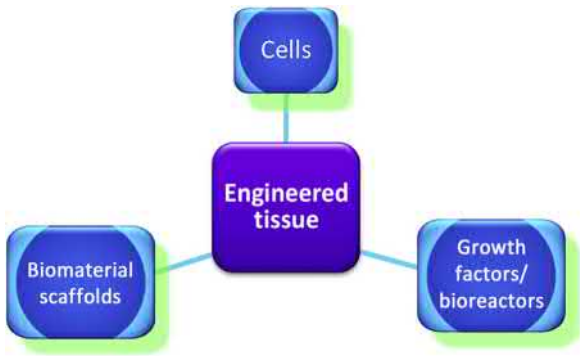

FIGURE 7.1 Triad of signal, scaffolds, and cells that act as a stencil for tissue engineering.

To form a microenvironment of the human body, an extracellular matrix (ECM) is embedded through support cells (mesenchymal cells) and functional cells (parenchymal cells); this forms the basis of every tissue or organ in the human body (Barnes et al., 2007). Mainly three approaches are used for designing of novel tissue: induced tissue, cell isolation and substitution, and cell matrices.

Induced tissue approach requires large-scale production of applicable signal molecules and their purification. It also includes a method for delivering these molecules. Cell isolation and substitution can avoid complications involved in surgery as it permits manipulation of the cell before infusion and replacement of specific cells. Immunological rejection is the limiting factor of this approach. Thirdly, in the cell matrices approach, cells are placed within the matrices, forming a closed system that includes isolation of cells by a semipermeable membrane, which allows molecules of low molecular weight, i.e., nutrients, and avoids high molecular weight molecules, which may lead to transplant destruction. Cells attached to matrices are termed as an open system. These are directly implanted, and further, can be integrated into the body (Langer and Vacanti, 1993).

Recent development has been seen in the approaches of tissue engineering that tend to be known as in situ tissue engineering, including assimilation of reformative stimuli into biomaterial scaffolds with the target of augmenting regenerative response of host cells. Along with a considerate approach toward cellular and molecular processes sustaining regenerative medicine, more radical methods of manipulating cells have emerged that can also allow RNA interference (RNAi) and a more integrated approach toward pharmacogenomics (Tekade et al., 2015; Maheshwari et al., 2017). The decisive aim of all these approaches is to empower the body to heal itself by familiarizing the body with tissue-engineered scaffolds and also to recognize them as an integral part of itself, as new innate tissues are regenerated (Barnes et al., 2007). The various advantages of using nanotechnology in tissue engineering are presented in Fig. 7.2.

The second strategy is frequently accompanied by the third. To grow cells efficiently in three-dimensional (3D) region, support matrices (scaffolds) play a very crucial role (Ma, 2004). Tissue engineering has become an emerging field since the 1980s (Chan and Leong, 2008) and is considered to be a field merging different disciplines like biology, engineering, and material science (Vacanti, 2006).

Fabrication of scaffolds with optimum attributes is a very important concern in the tissue engineering approach. Biomimetic materials are utilized in materialization of such scaffolds. Various types of biomimetic materials have been exploited and tailored for manufacturing of scaffolds, which may aid the tissue regeneration. Biomimetic materials to be used as scaffold should possess certain important properties to serve as temporary extracellular matrix (ECM) and to produce improved tissue growth compared with the natural EMC (Fig. 7.3).

It should be compatible with the biological system and microenvironment to which it has to be subjected as a scaffold. It should not produce any immunogenic stimulation or toxicity. The material should be such that the scaffold possesses sufficient porosity to facilitate the recruitment of cells and cell attachment (Ma, 2008).

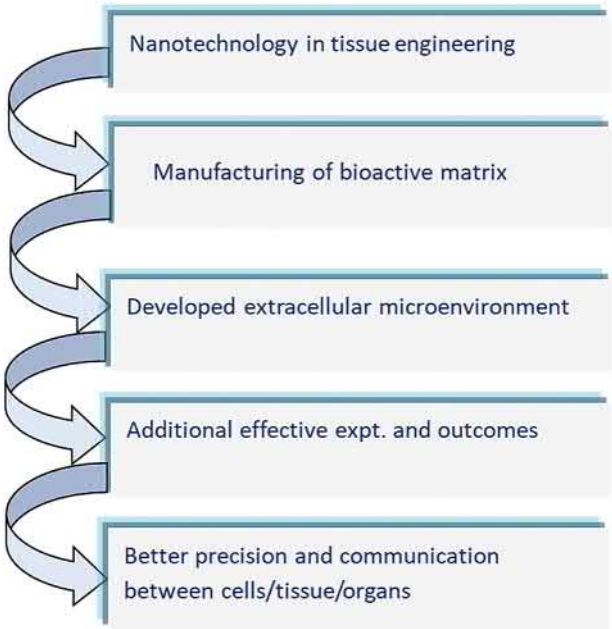
Nanotechnology in tissue engineering
Manufacturing of bioactive matrix
Developed extracellular microenvironment
Additional effective expt. and outcomes
Better precision and communication between cells/tissue/organs

FIGURE 7.2 Schematic representation of the advantages of nanotechnology in tissue engineering.

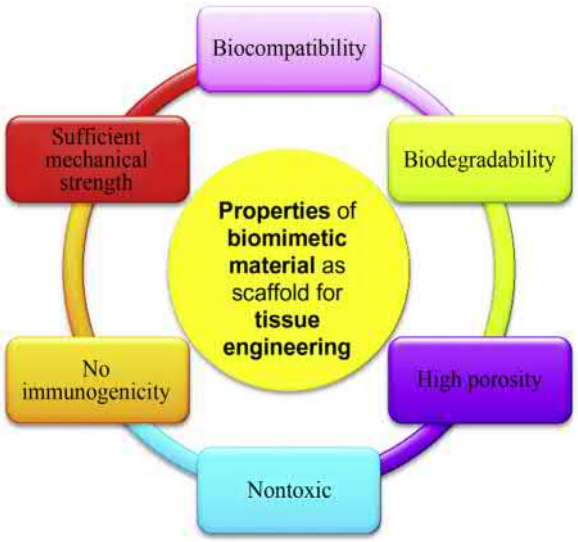

FIGURE 7.3 Properties of suitable scaffolds.

7.3 STRATEGIES RELATED TO THE FORMATION OF SCAFFOLDS

Scaffolds are structurally fabricated to be biodegradable and porous, which can be obtained either from natural material, e.g., collagen (George and Ravindran, 2010), fibrin, xanthan gum(Kumar et al., 2018), chitosan (CS), heparin (Rambhia and Ma, 2015), or synthetic polymers e.g., polyglycolide, polylactide, polylactide-*co*-glycolide (Kretlow and Mikos, 2008).

By using new material processing technologies, assembly can be made in the form of sponges; sheets, a highly complex structure with intricate channels and pores; or gels. The most important feature of scaffolds is that they tend to degrade after implantation and eventually get replaced by newer tissues (Griffith and Naughton, 2002).

7.3.1 Photolithography

Photolithography is the most prevailing technique of a top-down approach used by the semiconductor industry to generate the integrated circuits. When the lithographic technique of nanotechnology is used in cell biology, it is possible to set up cell cultures where neurons are put in one well and in another well there are astrocytes, and these two wells are conjoined by a channel that facilitates the diffusion of soluble factors (Takano et al., 2002).

7.3.2 Templating

Templating is an interesting phenomenon during the normal hard tissue development organic phase, in which collagen fibers work as a template to guide inorganic phase formation in bone and teeth. Bones and teeth are biocomposites that require controlled mineral deposition during their self-assembly to form tissues with unique mechanical properties. He et al. used dentin matrix protein 1, an acidic protein, to nucleate the formation of hydroxyapatite (Hap) in vitro in a multistep process (Shakiba et al., 2018). The nucleated amorphous calcium phosphate precipitates ripen and nanocrystals form. Pins et al. used a self-assembly process to form collagen fibers, guide the natural hard tissue formation, and engineer the bone tissue through this biomimetic approach (Pins et al., 1997).

7.3.3 Ionic Self-Complementary Peptide

Zhang et al. synthesized a 16-amino acid peptide, $\sim$5 nm in size, with an alternating polar and nonpolar pattern (Ghanghoria et al., 2016). The peptides can form a stable strand and sheet conformations, with side chains with one polar side and one nonpolar side, and then undergo self-assembly to form nanofibers. These nanofibers can form interwoven mats that form 3D hydrogels, with high water contents ($>$99.5%), which may be suitable for tissue engineering. The other feature of this peptide is that if the charge orientation is changed, entirely different molecules can be obtained.

7.3.4 Bionanotubes/Lipid Tubules

Rudolph et al. used amphiphilic molecules that contain distinct hydrophobic and hydrophilic segments, to form self-assembled lipid tubules (Pawar et al., 2016). These tubules can be used as microvials for long-term release of active agents. However, the lipid tubules are very weak regarding mechanical properties. Meanwhile, they have very low thermal stability, e.g., a few tens of degrees Celsius will destroy them.

To overcome these limitations, Rudolph et al. used the lipid tubule as a mold, pattern, or scaffolding to convert them into stronger objects with the same geometry (Pawar et al., 2016). For example, lipid tubules were subsequently coated with metals or inorganic materials to form scaffolds. This concept is very important for using self-assembly structures for realistic tissue regenerating applications. Using this concept, lipid tubules can be coated using sol–gels to fabricate ceramic rods or hollow cylinders with diameters down to 0.5 m, coated with silanes to change the chemical nature of the tubule's surface, or coated with metals. Modified tubules as microbials can be used for controlled release applications as well.

7.3.5 Miscellaneous

Premade porous cell-seeding scaffold techniques are one of the most basic techniques used for scaffold synthesis. The method comprises using pyrogens in biomaterials or use of solid free form or prototyping or use of woven or nonwoven fibers. Decellularized ECM cell-seeding technique utilizes the use of allogenic or xenogenic tissues with the help of decellularization technique. Self-secreted cell sheets ECM technique can be done by thermoresponsive culturing cells of a polymer such as poly(*N*-isopropylacrylamide) coated culture dish until convergence. The hydrogel matrix self-assembled cell encapsulation technique uses biomaterials that can self-assemble into hydrogels and are fabricated by self-assembling by using parameters such as temperature and humidity (Chan and Leong, 2008).

7.4 NATURAL MATERIALS–BASED TISSUE ENGINEERING NANOSCAFFOLD

Different types of biomimetic materials are used as starting material in the fabrication of support matrices. Various substances obtained from natural sources are used in tissue engineering. The versatile chemical compound can be employed for scaffold fabrication. These can be classified as natural and synthetic as presented in subsequent sections. There are various proteins, polypeptides, and polysaccharides that have been explored to be good scaffolding material in tissue engineering. Being substances from a natural source, they are likely to possess better compatibility and less antigenicity in the biological sites. Natural substances are more complex in structure orientation, which causes difficulty in the manufacturing of the scaffold while their complexity may be advantageous to mimic the extracellular milieu (Connor and Tirrell, 2007).

7.4.1 The Chitosan-Based Tissue Engineering Scaffold

Recently, CS, being the most promising natural polymer, has been used in many areas of medical science. It is a highly versatile biomaterial obtained from crustaceans. The property of CS with a special interest in tissue engineering is a minimal foreign-body response and high efficacy for fibrous encapsulation. In comparison to most of the synthetic polymers, CS possesses a hydrophilic surface with many amine-terminated groups that promote cell binding and proliferation. Moreover, being a natural polymer, the degradation products of CS are nontoxic.

Only a few materials can be classified as biologically active, biologically degradable, and osteoconductive. CS belongs in this category along with Hap and is most widely used for bone tissue engineering. Importantly, CS provides a platform for surface modification, which is also very useful for producing different 3D scaffolds. Moreover, being a biocompatible polymer, it can be combined with a variety of materials including ceramics and other polymers in conjugation to produce biocomposite materials with higher mechanical and physical characteristics.

When we talk about the methods for CS-based scaffold fabrication, the most commonly used techniques for producing CS-based scaffolds are phase separation and lyophilization, particulate leaching, gas foaming, and freeze gelation technique as depicted schematically in Fig. 7.4A–D (Levengood and Zhang, 2014).

7.4.2 The Albumin-Based Tissue Engineering Scaffold

Albumin is a naturally available serum protein that is reported to affect the binding of cells to different scaffold material with equal or better efficiency from collagen and fibronectin after slight modification. It can serve as an interface between cells and scaffold, thereby mediating the integration of these two components.

Lyu designed an investigation to study the potential of the albumin-based construct as tissue engineering nanoscaffolds for the regeneration of cartilaginous material (Guelcher et al., 2012). Briefly, authors seeded porcine knee chondrocytes followed by cultivation in a porous ternary matrix composed of different polymers with surface albumin. The outcomes found that the amount of albumin rarely influences the viability of porcine knee chondrocytes in the developed material. Although, a higher concentration of albumin preferentially improves the adhesion of porcine knee chondrocytes on the scaffolding pore surface. The staining image of the cultured scaffold (Fig. 7.5A and B) revealed that the purple dots were the stains of porcine knee chondrocytes. As indicated in Fig. 7.5C and D, the crimson stains denoted the secreted glycosaminoglycans. The red intensity in the albumin-grafted construct was stronger than that in the albumin-free construct, suggesting that albumin sustained a stable glycosaminoglycan secretion. As shown in Fig. 7.5E and F, the brown stains were the produced type II collagen.

Therefore it can be concluded that due to its nontoxic, biocompatible, and water-soluble properties, albumin can be used in the applications of tissue engineering.

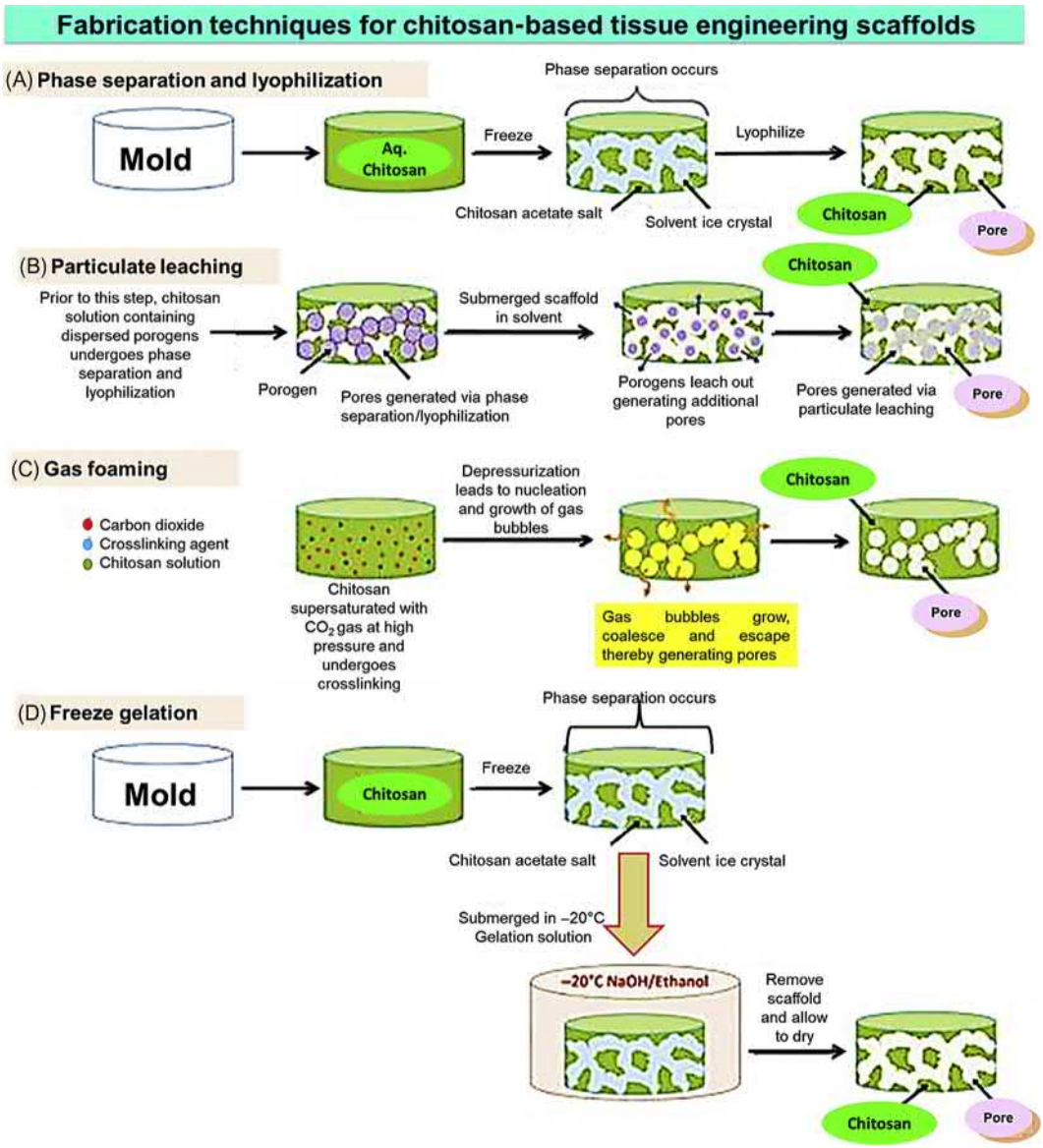

FIGURE 7.4 Schematic representation of four commonly used chitosan scaffold fabrication methods. (A) Phase separation and lyophilization technique where a chitosan solution is introduced into a mold, frozen to allow for phase separation of acetic acid solvent and chitosan acetate salt and then lyophilized. (B) Particulate leaching technique, which can be combined with phase separation to fabricate chitosan scaffolds. A porogen such as gelatin is mixed with chitosan solution prior to phase separation and lyophilization. The resultant scaffold is submerged in a solvent to allow for porogen leaching resulting in additional porosity. (C) Gas foaming technique where chitosan solution containing a cross-linker (glutaraldehyde) is supersaturated with carbon dioxide at high pressure while also undergoing cross-linking. When the system is depressurized, thermodynamic instability leads to nucleation and growth of gas bubbles. Gas bubbles grow and/or coalesce and escape the polymer solution thereby generating pores. (D) Freeze gelation technique, which initially involves phase separation due to freezing. The scaffold is placed in a gelation solution of sodium hydroxide and ethanol below the chitosan freezing temperature. Following gelation, the scaffold is air-dried to remove residual liquid. *Adapted with permission from Levengood, S.K.L., Zhang, M., 2014. Chitosan-based scaffolds for bone tissue engineering. J. Mater. Chem. B 2(21), 3161–3184.*

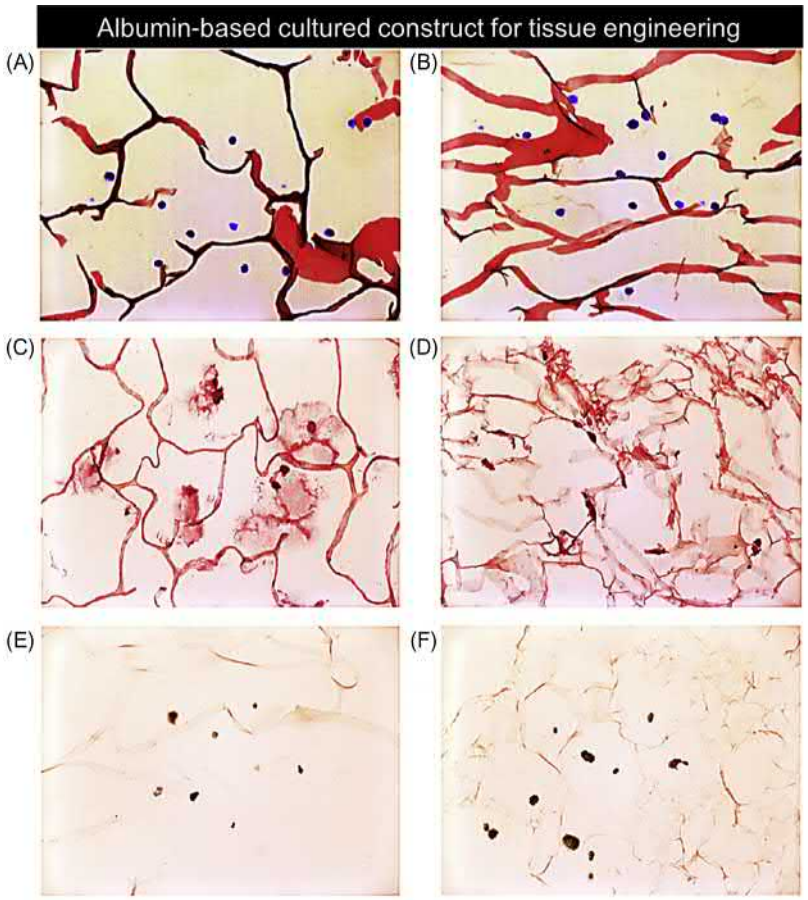

FIGURE 7.5 Stained photographs of the cultured constructs. (A) H&E stain, albumin-free construct; (B) H&E stain, albumin-grafted construct; (C) safranin-O stain, albumin-free construct; (D) safranin-O stain, albumin-grafted construct; (E) type II collagen stain, albumin-free construct; (F) type II collagen stain, albumin-grafted construct. Albumin-grafted constructs contained 150 g/mL of albumin. *Adapted with permission from Guelcher, S.A., Patel, V., Hollinger, J.O., Didier, J., 2012. Degradable Polyurethane Foams, Google Patents.*

7.4.3 The Alginate-Based Tissue Engineering Scaffold

Apart from albumin, sodium alginate also provides high water solubility and is known to be used in different biomedical applications such as drug delivery and wound dressings, including tissue engineering. In tissue engineering, the cross-linking ability of alginate that can be modified by altering the composition and molecular weight of the alginate chains is of prime importance.

Based on the fact that shorter degradation times may be more optimal for some tissue regeneration applications that aim to match tissue formation with polymer degradation rate, a group of investigators reported the alginate-based nanofibers made using two

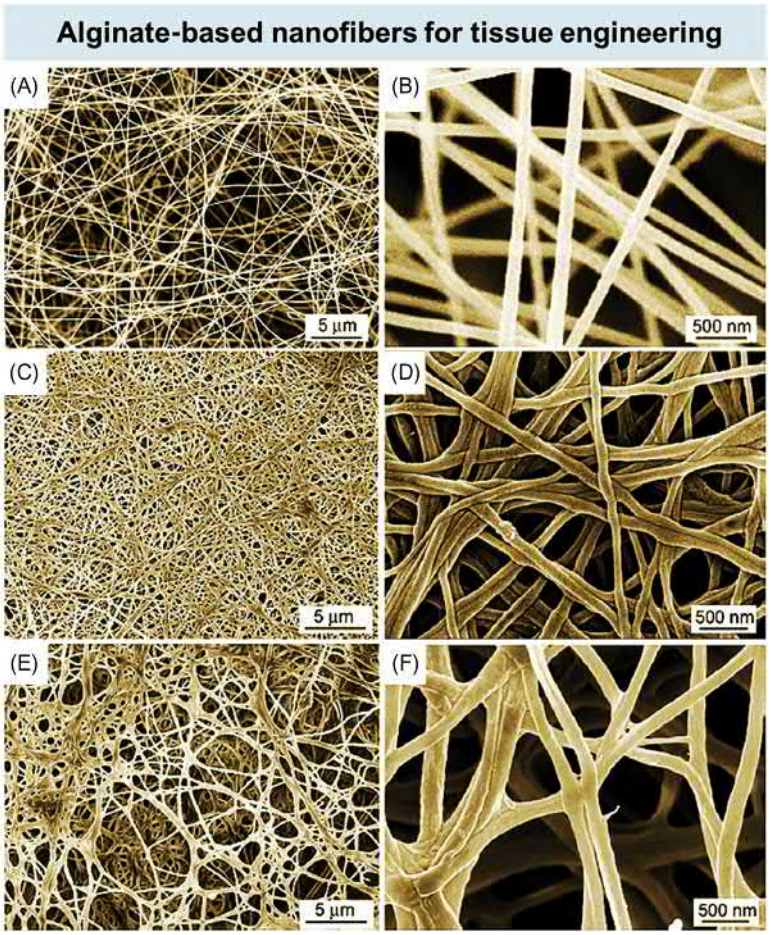

FIGURE 7.6 Scanning electron micrographs of nanofibers containing 37 kDa alginate/PEO/Pluronic F127 (8.0:1.6:2.0 wt.%) (A and B) prior to cross-linking. Nanofibers composed of 196 (C and D) and 37 kDa (E and F) alginate after cross-linking with calcium and soaking in water for 4 days to remove PEO. *Adapted with permission from Dwivedi, N., Shah, J., Mishra, V., Mohd Amin, M.C.I., Iyer, A.K., Tekade, R.K., et al., 2016. Dendrimer-mediated approaches for the treatment of brain tumor. J. Biomater. Sci. Polym. Ed. 27(7), 557–580.*

different molecular weights (37 and 196 kDa) for in vivo tissue scaffolds and investigated mechanical strength of the prepared scaffold (Dwivedi et al., 2016). Uniform nanofibers containing low molecular weight alginate, polyethylene oxide, and F127 surfactant were obtained (Fig. 7.6). It was the first study that reported alginate-based nanofibers from a low molecular weight alginate for scaffold application.

The ability to turn the structure and characteristics like biocompatibility, higher Young's modulus, cross-linking property, and cell affinity make the alginate valuable to be used in combination with other nanomaterials for tissue engineering applications.

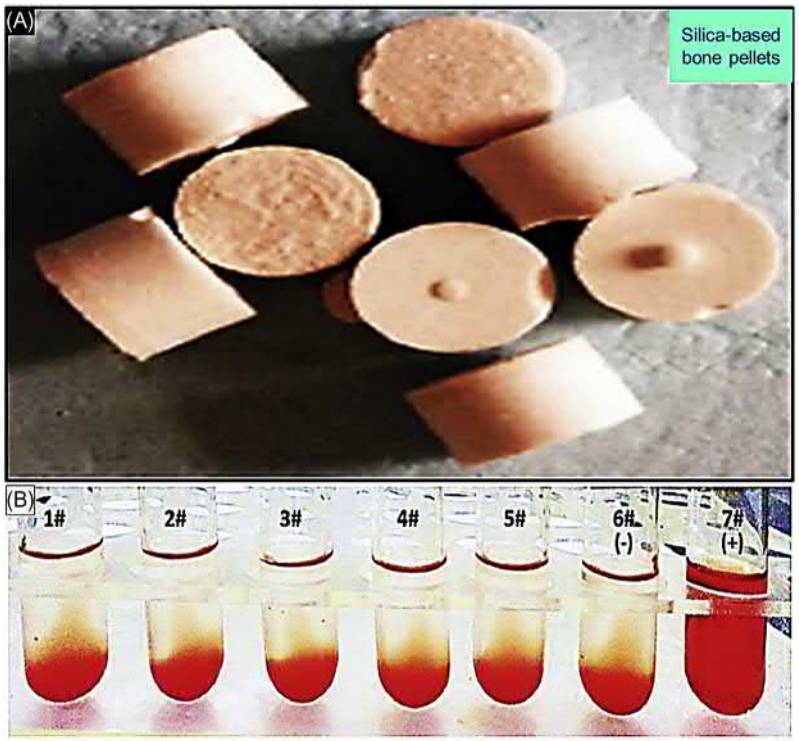

FIGURE 7.7 (A) Silica-based bone pellets. (B) Hemolysis of RBCs in the presence of silica-based developed formulation. + and − indicate distilled water and 0.9% saline solution as a positive and negative control, respectively. *Adapted with permission from Werani, J., Grünberg, M., Ober, C., Leuenberger, H., 2004. Semicontinuous granulation—the process of choice for the production of pharmaceutical granules?. Powder Technol., 140(3), 163–168.*

7.4.4 The Silica-Based Tissue Engineering Scaffold

Silica is a very favorable material from the tissue engineering point of view due to its porous nature. Apart from that, its surface modification ability also provides immense opportunities in tissue engineering applications.

Calcium sulfate α-hemihydrate (CSH) is widely used as the material for bone cement. However, the initial burst release of the loaded drug in the first few days greatly hindered its application. Werani et al. developed a novel bone cement pellet with sustained release of vancomycin by mixing vancomycin loaded mesoporous silica nanoparticle and CSH together (Werani et al., 2004). The developed bone pellets (Fig. 7.7A) revealed nonsignificant pyrogenicity and posed no potential adverse effects upon hemolytic test (Fig. 7.7B). These results imply that the silica-based bone pellets are a suitable candidate to replace CSH bone cement in the treatment of open fractures.

7.5 SYNTHETIC MATERIALS–BASED TISSUE ENGINEERING NANOSCAFFOLDS

Synthetic polymers are more frequently used with added advantages like ease for tailoring, improved mechanical attributes, low cost of production, and so on. These may be categorized as organic [polyesters like polylactic acid (PLA), polyglycolic acid (PGA), poly(lactic acid-*co*-glycolic acid) (PLGA)] and inorganic. Synthetic materials are widely used for tissue regeneration in the field of regenerative medicine. Synthetic materials have less structural complexity than natural substances and can be readily modified to obtain desired attributes (Sreejalekshmi and Nair, 2011). They can be manufactured in the form of the scaffold in a more economical way and are less immunogenic than natural materials.

Being a synthetic compound, they show diminished biological response compared with the natural extracellular matrix (O'Brien, 2011), but it is possible to tailor them easily, and the surface can be modified and attached with functional groups and biologically active moieties to impart such attribute into them to help enhance cell attachment and proliferation. The most commonly used synthetic polymers that can mimic the extracellular microenvironment and used in tissue engineering are polyesters, polyether esters, bioactive ceramics, etc.

They are inorganic compounds that have been explored for fabrication of support matrices for tissue regeneration. Commonly used bioceramics for this purpose are Hap, bioactive glasses, calcium phosphates, calcium sulfates, etc. Due to their rigid nature earlier bioceramics were used for bioengineering of hard tissues but recently their application in the regeneration of soft tissues has also been explored (Baino et al., 2016).

Bioceramics have higher biological responses as compared with other synthetic polymers. Calcium orthophosphate resembles the mineral component of bones and teeth and osteoconductivity, but brittleness limits its use in bone grafts, thus nanocrystallized form of calcium orthophosphates are used, which better mimic the component of mineralized tissues (Dorozhkin, 2010).

Another commonly used ceramic material is Hap, which is an apatite of calcium phosphate. Hap is also naturally present in the bone and teeth. It is osteoconductive and highly biocompatible. Moreover, it is used as bone cement for filling of bone and teeth (Baino et al., 2015). However, its tensile strength is not sufficient to be used as a scaffold. They are generally used as a composite scaffold with other biomimetic materials when subjected to tissue regeneration application (Barrere et al., 2006).

Polyesters are one amongst the most widely used synthetic polymers in tissue engineering. Linear aliphatic polyesters, PLA, PGA, and polycaprolactones are used either as single polymer or copolymers such as PLGA due to their tunable biodegradability and high biocompatibility (Chen and Ma, 2006).

7.5.1 The Dendrimer-Based Tissue Engineering Scaffold

The word *dendrimer* is obtained from the Greek word *dendron*, which means "tree," indicating that dendrimers are a tree-like structure (branched). Dendrimers are synthetic, highly branched, spherical, and monodisperse macromolecules with 3D nanometric structure.

In literature, they are also called cascade molecules, arborals, dendritic molecules, or because of their nanoscopic size and monodispersity they are often referred to as nanoscopic compounds (Svärd et al., 2013). Currently, dendrimers are proving their versatility in a number of fields, including biomedical sciences. The dendritic architecture is perhaps one of the most pervasive topologies observed.

The main objective in developing dendrimer-based tissue engineering scaffolds includes providing nontoxic constructs in the 3D scaffold surface where cells can grow in the provided native ECM with the necessary hormones, signaling molecules, and other growth factors.

The benefit of Poly(amidoamine) (PAMAM) dendrimers in scaffold engineering was investigated by two different research groups who studied the incorporation of dendrimers in tissue engineering. These authors employed an enhanced amount of alkaline phosphatase in, and mineralization characteristics of, the modified cellular microenvironment employing a dexamethasone carboxymethyl CS/PAMAM dendrimer. The study revealed enhancement in the ectopic early osteogenic differentiation of rat bone marrow stromal cells in the scaffold (Oliveira et al., 2009). Calcium deposition leading to higher mineralization was reported to be greater in the scaffold constructs exposed to a dexamethasone carboxymethyl CS/PAMAM dendrimer environment (Fig. 7.8).

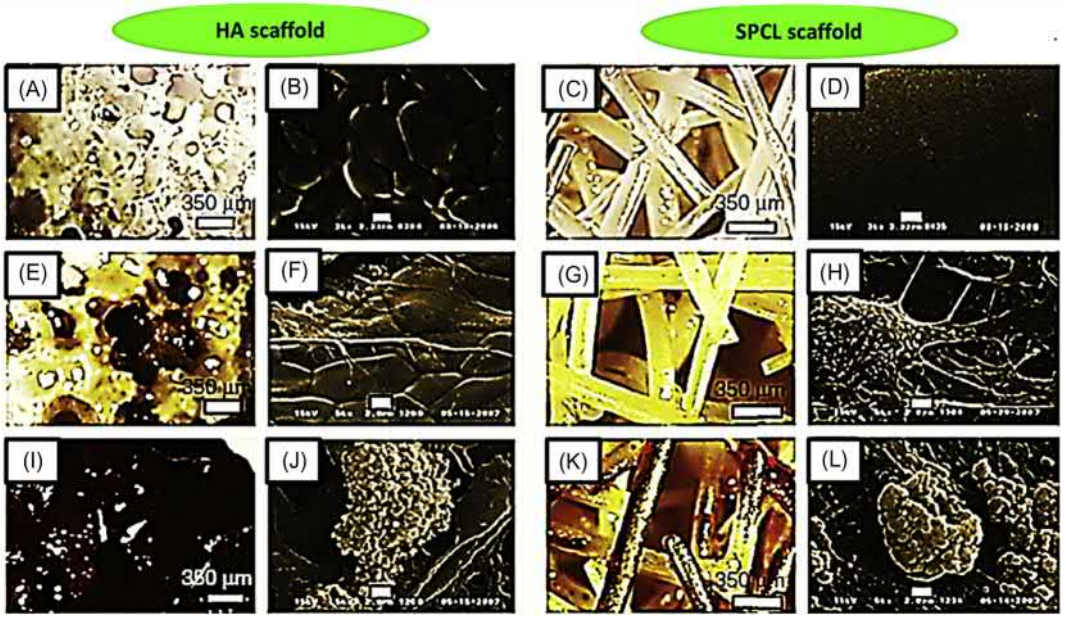

FIGURE 7.8 Microscopic images of dendrimer-based tissue engineering scaffolds. Optical microscopy and scanning electron microscope images of HA (left) and SPCL (right) scaffolds seeded with RBMSCs, stained with Alizarin red (mineralization) after culturing in different culture media for 14 days: (A–D) controls (scaffolds without RBMSCs); (E–H) complete Eagle's minimum essential medium; (I–L) MEM medium with Dex-loaded CMCht/PAMAM dendrimer nanoparticles. *HA*, Hydroxyapatite; *RBMSCs*, rat bone marrow stromal cells; *SPCL*, starch–polycaprolactone. *Adapted with permission from Oliveira, J.M., Sousa, R.A., Kotobuki, N., Tadokoro, M., Hirose, M., Mano, J.F., et al., 2009. The osteogenic differentiation of rat bone marrow stromal cells cultured with dexamethasone-loaded carboxymethylchitosan/poly(amidoamine) dendrimer nanoparticles. Biomaterials 30(5), 804–813.*

7.5.2 Poly(Lactic Acid-*co*-Glycolic Acid)-Based Tissue Engineering Scaffold

PLGA PGA is a polymer having rapid degradation that is suitable for fabrication of scaffold used for the short-term graft. However, it also has poor tensile strength. Thus it cannot be used for bioengineering of hard tissues like bones, tendon, and ligament (Bogan et al., 2016).

Recently, Kwak et al. (2016) developed micro/nanomultilayered scaffolds of PLGA and collagen by alternately electrospinning for bone tissue engineering. To fabricate the multilayered scaffolds having a sequential arrangement of microfibrous PLGA meshes and micro/nanomixed fibrous meshes of PLGA and collagen, the dual extrusion electrospinning technique was used (Fig. 7.9A). The simultaneous electrospinning parameters for PLGA and collagen solutions were optimized by individual electrospinning of PLGA and collagen solutions. The morphology and composition of mixed fibrous meshes in the multilayered scaffolds were controlled by varying electrospinning parameters of individual fibers (Fig. 7.9B). The results of this experiment showed that the dual extrusion electrospinning technique can be used further for designing 3D scaffolds with different topologies and compositions for drug delivery and bone tissue engineering in our ongoing programs for the applications of biomaterials in the fields of biomedical research.

7.5.3 Polylactic Acid–Based Tissue Engineering Scaffold

PLA has a slower degradation rate and better mechanical strength as compared with PGA, thus PLA is suitable for scaffolding for regeneration of bone and ligament (Venugopalan and Rajendran, 2015). PLA-based scaffold for cardiac tissue is also explored due to its sufficient elastic property. Carbon nanotubes (CNTs) are used with PLA and other polymers to improve conductivity and to make them useful for regeneration of skeletal muscle, cardiac muscle, and neuronal tissues (Ahadian et al., 2017). PLA can also be used as particle-based scaffolding such as microspheres, which undergo self-assembly in vivo to form 3D scaffold (Liu et al., 2011).

In a recent investigation, Wang et al. developed conductive nanofibrous scaffold by electrospinning considering its advantages for cardiomyocytes-based tissue engineering (Ghadiri et al., 2017). The investigators designed conductive nanofibrous sheets with electrical conductivity and nanofibrous structure made of poly(L-lactic acid) blending with polyaniline for cardiac tissue engineering and cardiomyocytes-based 3D actuators.

The outcomes of CX43 immunostaining analysis show the reason of how the conductivity of nanofibrous sheets influence the beating frequency and displacement of 3D actuators (Fig. 7.10). In comparison, both tubular shaped and folding shaped actuators formed by PLA nanofibrous sheets showed much weaker staining for CX43 (Fig. 7.10A and C). Strong positive staining for CX43, a gap junction protein responsible for cell–cell coupling and synchronous beating of cardiomyocytes (CMs), were exhibited on tubular and folding shaped actuators formed by PLA/PANI3 conductive nanofibrous sheets (Fig. 7.10B and D).

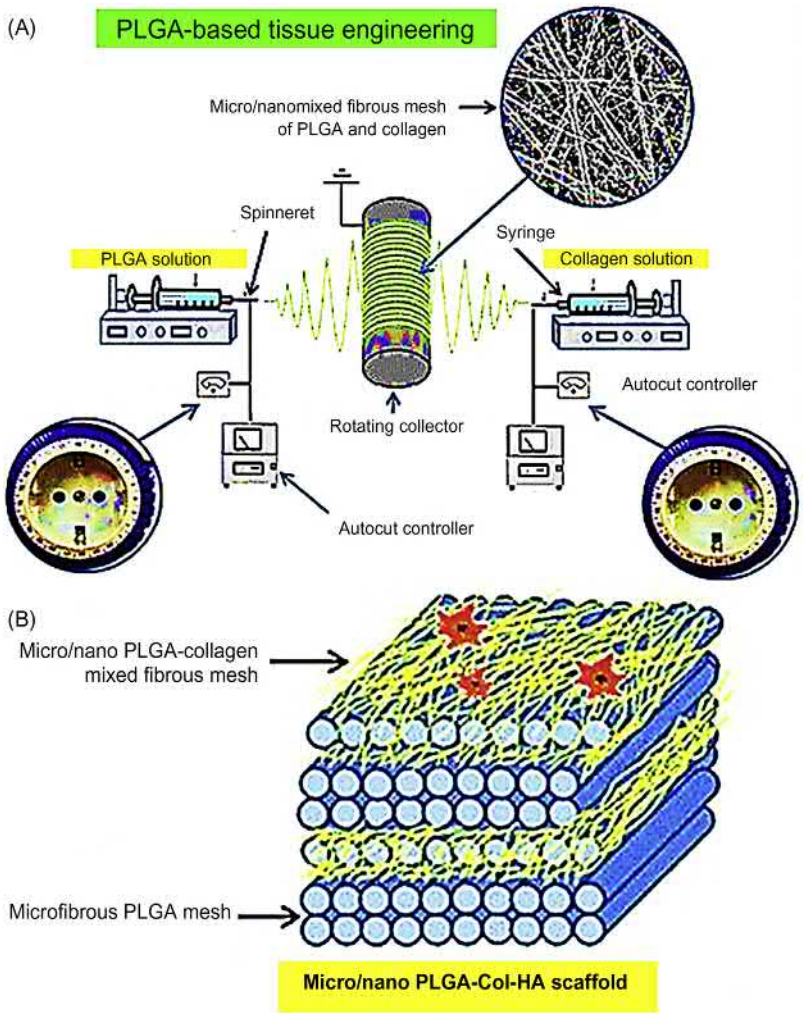

FIGURE 7.9 (A) Schematic representation of dual electrospinning technique for fabrication of multilayered 3D scaffolds. (B) structure and composition of multilayered scaffolds having micro/nanomixed fibrous PLGA and Col-HA mesh arranged in alternate fashion with microfibrous PLGA mesh as fabricated with dual extrusion electrospinning technique. *PLGA*, Poly(lactic acid-*co*-glycolic acid). *Adapted with permission from Kwak, S., Haider, A., Gupta, K.C., Kim, S., Kang, I.-K., 2016. Micro/nano multilayered scaffolds of PLGA and collagen by alternately electrospinning for bone tissue engineering. Nanoscale Res. Lett. 11(1), 323 with slight modification.*

The developed PLA and polyaniline conductive nanofibrous sheets with conductivity and extracellular matrix-like nanostructure revealed promising potential in cardiac tissue engineering and cardiomyocytes-based 3D actuators.

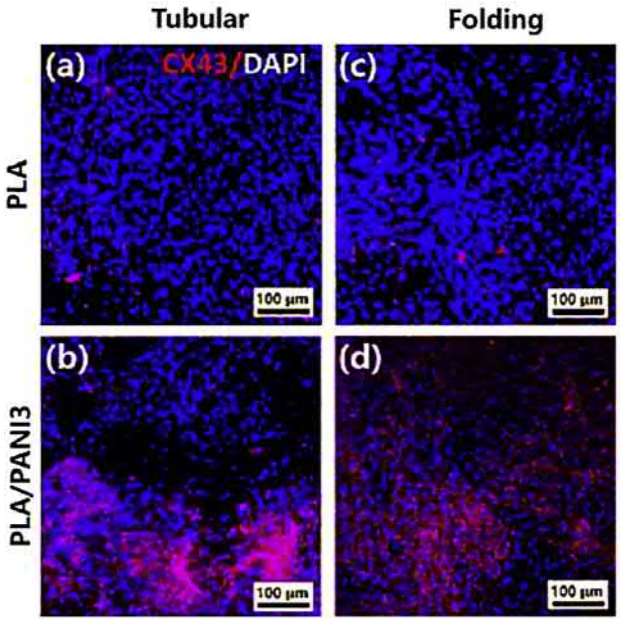

FIGURE 7.10 Representative fluorescence images of cardiomyocytes immunostained for CX43 (red) on tubular bioactuators formed by cardiomyocytes-laden PLA (A) and cardiomyocytes-laden PLA/PANI3 (B), and folding bioactuators formed by cardiomyocytes-laden PLA (C) and cardiomyocytes-laden poly(L-lactic acid)/polyaniline (D) after culture for 12 days. *PLA*, Polylactic acid. *Adapted with permission from Ghadiri, M., Vasheghani-Farahani, E., Atyabi, F., Kobarfard, F., Mohamadyar-Toupkanlou, F., Hosseinkhani, H., 2017. Transferrin-conjugated magnetic dextran-spermine nanoparticles for targeted drug transport across blood-brain barrier. J. Biomed. Mater. Res. A 105(10), 2851–2864.*

7.5.4 The Polyethylene Glycol–Based Tissue Engineering Scaffold

Polyether esters, which are generally used as scaffolding material, are polyethylene glycol (PEG) and polybutylene terephthalate (PBT). PEG is highly biocompatible and suitable for soft tissues (Elisseeff et al., 2002). However, it has a faster degradation rate. Degradation rate for PEG can be rendered to desirable extend by copolymerized with polyesters like PLA and PGA (Han and Hubbell, 1997). PEG is elastic in nature and PBT is stiff, their composite as PEG/PBT is generally used to combine their attributes, and their proportion can be tuned to obtain scaffold with the desired property.

Shakir et al. (2015) developed an interesting nanocomposite material containing nanohydroxyapatite, CS, and PEG (*n*-HAP/CS/PEG) using the coprecipitation method. The objective behind the development of this novel nanocomposite is to find suitable analog that can potentiate the natural formation of bone and therefore be applied to bone tissue engineering. The developed formulation was compared with the formulation lacking PEG (*n*-HAP/CS). The results of X-ray diffraction and TEM suggested that the crystallinity and thermal stability of the n-HAP/CS/PEG scaffold have decreased and increased respectively, relative to *n*-HAP/CS scaffold. The comparison of SEM images of both the scaffolds

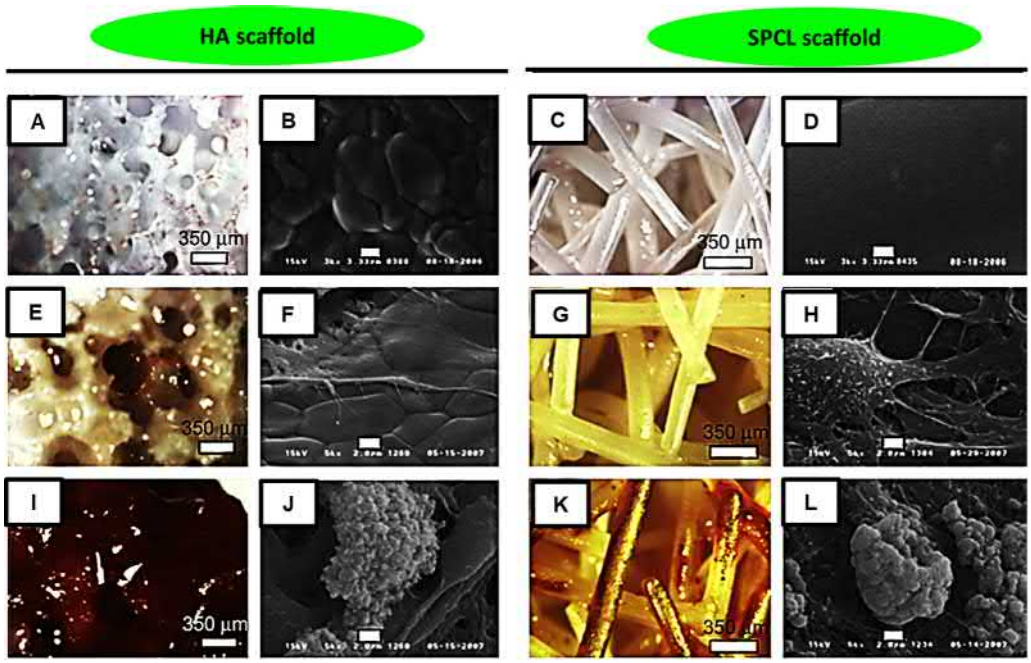

FIGURE 7.11 SEM micrographs of (A) n-HAP/CS and n-HAP/CS/PEG nanocomposites and their simulated body fluid studies after (B) 15 days and (C) 30 days. *CS*, Chitosan; *n-HAP*, nanohydroxyapatite; *PEG*, polyethylene glycol. *Adapted with permission from Shakir, M., Jolly, R., Khan, M.S., Iram, N.E., Sharma, T.K., Al-Resayes, S.I., 2015. Synthesis and characterization of a nano-hydroxyapatite/chitosan/polyethylene glycol nanocomposite for bone tissue engineering. Polym. Adv. Technol. 26(1), 41–48 with slight modifications.*

indicated that the incorporation of PEG influenced the surface morphology while a better in vitro bioactivity has been observed in *n*-HAP/CS/PEG than in *n*-HAP/CS-based on simulated body fluid study, referring a greater possibility for making direct bond to living bone if implanted (Fig. 7.11).

7.6 APPLICATIONS

Tissue engineering has a wide scope of applications and is a continuously developing field. It includes the development of artificial cartilage to the heart. The knowledge of tissue engineering is applied to develop soft tissue as well as hard tissue, helping to regenerate the damaged cells and increases the life of the patient.

Recent advances in developing scaffolds using various biomaterials have opened the doors for a large number of semisynthetic and synthetic polymers. Organ damage is a severe issue nowadays, and a proper and healthy donor organ is difficult to obtain; in such cases tissue engineering shows a wide area for development. Many industries are focusing on this thrust area for pursuing their further research. Since it includes the

intervention of humans and their cells, tissue engineering suffers many issues for regulatory approval. It is the most emerging field, and much development is accepted for this area. Further reading on the application of nanotechnology in tissue engineering is presented in following subsections.

7.6.1 Nanotechnology in Cell Tissue Engineering

Cellular engineering is the biological process that involves the principle of molecular biology to generate the cell products for the repair of tissue or organ. In the nanotechnology-driven era of research, new sophisticated techniques implicated in cell biology and nanotechnology do not only place emphasis on more complex in vivo–like extracellular environments but also consider the dynamic complex biological process at the receptor level. Eventually, the goal is to obtain a comprehensive knowledge of how the building blocks of humans, i.e., the cells, work at the molecular level (Mendes, 2013). Nanomaterials may be used as smart interfaces for additional understanding and controlling the complex relationship of actions and interactions that occur in the cell (Nikalje, 2015).

7.6.1.1 Nanotechnology in Bone Cells Tissue Engineering

Bone tissue transplantation is widely used in tissue transplantation in the world. Every year around 22 lakhs bone grafting take place worldwide (Saiz et al., 2013). Tissue engineering is widely used to produce, restore, and fix cells, tissues, or organs by using body cells with some bioadditives that help to construct the tissues similar to the body tissues. Tissue engineering combines the practice of engineering material science, medicine, and biology (Danie Kingsley et al., 2013).

For bone tissue engineering one must know bone functioning, rejuvenation, and healing. To create a tissue-engineered bone one must consider the following to get an effective outcome. Primarily, a bioactive matrix, i.e., scaffolds are required to maintain the interstitium of cellular integrity and tissue growth. Secondarily, the specialized phenotypic cells are then inculcated into the matrix and the matrix must have the ability to induce osteogenesis. Thirdly, the final product must match the basic functions of bone (Lyles et al., 2015).

In the body, osteoblasts and osteoclasts have the function of maintaining homeostasis of bone development (Tautzenberger et al., 2012). Osteoblasts promote cell formation, whereas osteoclasts cause bone breakage. In BTE, the osteoblast is supported by drug and growth factors, and osteoclasts are inhibited by specific inhibitors (Walmsley et al., 2015). Therapeutic agent, growth factor, or genetic material is encapsulated in the biodegradable or nonbiodegradable scaffold of nanosize. Both biodegradable and nonbiodegradable nanospheres are used here, but the biodegradable are generally the most preferred. The examples of nonbiodegradable nanoparticles are gold, dendrimer, and silica whereas degradable nanoparticles are PLA and PLGA (Jensen et al., 2011).

As mentioned earlier, the inner part is planned such that it improves cell binding and separation where the outer part promotes assimilation with adjacent tissue to prevent cell

extrusion and movement. In a few studies, it has been reported to use metallic plates and screws also for improved attachment in animals (Reichert et al., 2011). However, it is not a practical approach for a prolonged duration. Then the inner face is taken to micro- and nanosize, which resolves the major limitation of fixation and nearer tissue attachment. The other advantage of micro- and nanolevel scaffold is that they imitate extracellular matrix arrangement (Saiz et al., 2013).

Scaffold manufacturing techniques are solvent casting, particulate leaching, freeze-drying, gas forming, solution casting, phase separation, etc. (Ronca et al., 2016) and the various techniques used for bone tissue engineering through micro- and nanotechnology are soft lithography, photolithography, microcontact printing, and electrospinning (Ber et al., 2005). Although, more work is still required to be carried out as it is not clear between a nano or microscale, which one is better (Saiz et al., 2013).

BTE is a versatile approach to bone rejuvenation. However, still, the regeneration of large bones is a big challenge (Walmsley et al., 2015). A few new design concepts and techniques are required to be developed for a new bioactive scaffold (Saiz et al., 2013). The current strategy is based on the formation of 3D nanocomposite by the additive manufacturing method. The 3D technique has an advantage over the traditional method of scaffold formation in that it has replicable internal morphology, good structural management, and altered mechanical and mass transfer properties. Purposely, this method formulates the objects in layer-by-layer style (Ronca et al., 2016). This 3D-based nanocomposite scaffold has better bone rejuvenation in less time (Saiz et al., 2013).

In an investigation, a novel hybrid strategy involving the combination of mechanically strong, porous scaffolds and nanofeatured self-assembling peptide hydrogels as an osteoinductive scaffold system was reported (Igwe et al., 2014). In this strategy, the mechanically strong scaffold component would allow for mechanical stability of the load-bearing defect site; whereas, the hydrogel phase will allow for efficient cell delivery into the defect implantation site, cell niche establishment, and promotion of mineralization (Fig. 7.12).

Growth factors for the promotion of accelerated bone and vascularization may also be covalently tethered to the hydrogel phase to allow for enhanced effects upon implantation. The authors have incorporated the features described above and developed a hybrid system comprised of a mechanically load-bearing scaffold infused with a self-assembling peptide hydrogel with tethered bone morphogenetic proteins-2. Moreover, electrospun fiber is also widely used in bone repair and regeneration. Gelatin nanofibers mimic both physical architectures and chemical composition of bone. They show great biocompatibility and adhesion and are the best candidate for osteogenic activities (Aldana and Abraham, 2017).

The bone regeneration potential of CS−alginate scaffolds was determined using critical size rat calvarial defects. In all the experimental groups no significant bone formation occurred as shown in Fig. 7.13 (Levengood and Zhang, 2014).

7.6.1.2 Nanotechnology in Vascular Cells Tissue Engineering

Tissue engineering is defined as a process that improves the biological tissue with the help of a combination of cells, materials, methods, engineering, and other biochemical and

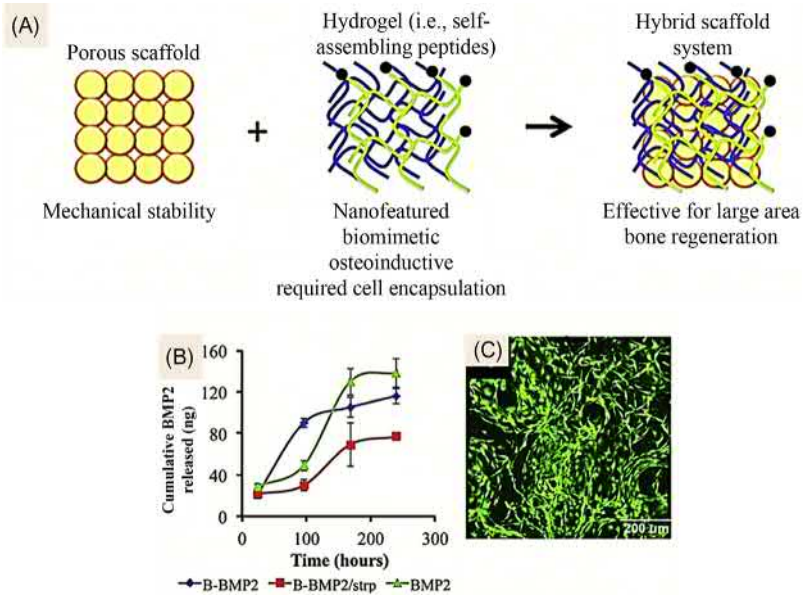

FIGURE 7.12 Development of a combination of mechanically strong, porous scaffolds and nanofeatured self-assembling peptide hydrogels for bone tissue engineering, (A) Illustration of hybrid scaffolds composed of a mechanically strong component, and a hydrogel phase for enhanced bone regeneration abilities. (B) In vitro release kinetics of biotinylated BMP2. Amount of BMP2 released over time was measured by ELISA. Results show the cumulative release of rhB-MP2 for untethered groups bone morphogenetic proteins (BMP-2-biotin, BMP-2) versus tethered group. (C) Survival of preosteoblastic MC3T3-E1 cells in the hybrid scaffold. Images show live and dead cells cultured on hybrid scaffolds; green represents live cells. *BMP2*, Bone morphogenetic proteins-2; *ELISA*, enzyme-linked immunosorbent assay. *Adapted with permission from Igwe, J.C., Mikael, P.E., Nukavarapu, S.P., 2014. Design, fabrication and in vitro evaluation of a novel polymer-hydrogel hybrid scaffold for bone tissue engineering. J. Tissue Eng. Regen. Med. 8(2), 131–142 with slight modifications.*

physiochemical factors. In vascular tissue engineering four approaches known for tissue assembly: a solid scaffold–based approach, in which cells seeded into a porous solid scaffold; a collagen-based approach, in which collagen matrix cells embedded; a cell sheet–based assembly approach, in which monolayers of cohesive cells rolled; and acellular type.

Drugs like heparin can load in electrospun nanofiber, which shows a great promise in vascular tissue repair (Aldana and Abraham, 2017). Electrospinning is the best modern cost-effective method for a variety of tissue engineering and drug delivery applications, does not cause an immunogenic reaction, and is biodegradable and compatible. However, the mechanism by which nanofiber affects cell behavior and tissue regeneration should be studied. Further study is needed to be carried out for selecting a drug loading capacity, loading and delivery method, dosage, and preclinical development (Aldana and Abraham, 2017).

Blood vessel replacement was the earliest application of tissue engineering by EC-seeded synthetic graft. Synthetic grafts approach for replacement of small diameter

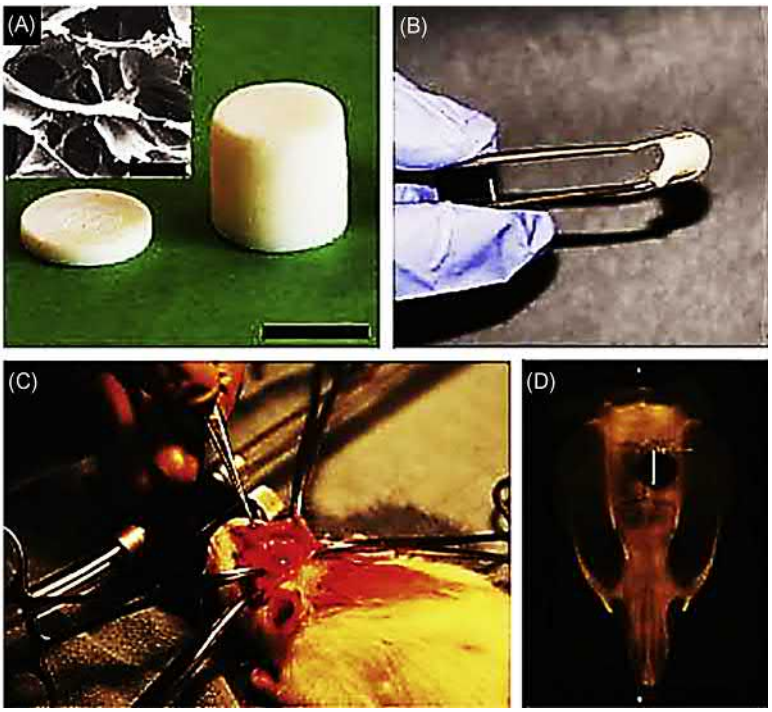

FIGURE 7.13 Use of CA scaffolds for cranial defect repair. (A) CA scaffolds were produced as cylinders and cut into slices (scale bar 1/4 10 mm); inset: SEM image of the scaffold showing the porous structure (scale bar 1/4 100 lm). (B) Cross-linked CA scaffolds are flexible and resilient. (C) The cranial defect model is shown during the procedure and (D) illustrated by MicroCT (line 1/4 5.0 mm). *CA*, Chitosan–alginate. *Adapted with permission from Levengood, S.K.L., Zhang, M., 2014. Chitosan-based scaffolds for bone tissue engineering. J. Mater. Chem. B 2(21), 3161–3184 with slight modifications.*

blood vessel is never used alone. The major limitation of the synthetic graft was there is thrombus formation in the blood and graft surface contact. In this approach, endothelial cells have been seeded onto the synthetic surface. On the graft surface seed, the endothelial cells are harvested from the patient. After harvesting, EC is seeded directly onto the biological sources, commonly dacron or ePTFE; during this process cells will attach to the synthetic material before implantation, and this EC monolayer after implantation with the natural antithrombogenic inner surface will provide the graft. Other limitations include the normal remodeling response of the vascular system blocked by the use of nonbiodegradable synthetic material (Nerem and Seliktar, 2001).

Moreover, the collagen-based approach aims to overcome the limitation of the EC-seeded synthetic graft approach. In this, in a reconstituted collagen gel matrix, a vascular cell being attached. Collagen gel is used for cell signaling and cell attachment. Benefits include that there is remodeling of the cell-mediated graft as well as vascular activity (Nerem and Seliktar, 2001). In cell sheet–based assembly approach, connective and

adipose tissue made up of cultured human adipose stem cells and endogenous extracellular matrix component secreted are reconstructed (Mironov et al., 2008). Advantages include immunological mismatch being eliminated, and withstanding the pressure during arterial implantation.

Also, in acellular methodology, a noncellular material is implanted and cells from host tissue are replenished. For example, in tissue engineering of acellular lung scaffold, the lung cells are exposed to harsh conditions, which leads to lysis, and the remaining cell debris is removed by a physical method, which acts as acellular lung scaffold from the existing one. The advantage of this kind of scaffold is that they grow as functional tissue cells as they assist the pluripotent stem cells (Nichols et al., 2012).

Much attention has been given to tissue-engineered vascular grafts in the last few years, and as an outcome, noteworthy progress has been reported regarding achieving the remodeling of the tissue in the *tissue*-engineered heart valve (TEHV) constructs similar to the native blood vessels, as presented in Fig. 7.14 (Yamamoto and Shao, 2017).

7.6.1.3 Nanotechnology in Hepatic Cells Tissue Engineering

Liver disease is a concern that needs clinical focus as there is an increase in patients suffering from liver disorders, and there is also the emergence of new kinds of diseases. Increase in the demand for donors for orthotopic liver transplantation led to cell-based therapy but due to certain limitations, nanotechnology in cell-based therapy has emerged. The liver has over 500 functions including protein, carbohydrate, and lipid metabolism; detoxification of endogenous and exogenous compounds; production of bile; and secretion of many serum proteins. Each year, over 30,000 people worldwide die due to liver disease, so liver disorder is one of the major concerns that needs special clinical focus.

Apart from existing disorders, there is the emergence of new disorders like nonalcoholic fatty liver disease and steatohepatitis (Bhatia et al., 2014), if left untreated these may lead to progressive liver failure, fibrosis, cirrhosis, hypertension in the portal vein, and even cancer. Though prevention and treatment of these conditions is possible, the only curative therapy in end-stage liver disease is orthotropic liver transplantation. The major limitation of this concern is lack of donors, high cost, and permanent immunosuppressive treatment (Pop and Mosteanu; Bhatia et al., 2014).

To overcome the major limitations encountered during orthotropic liver transplantation cell-based therapies have emerged. Cell-based therapy is the repair and restoration of cellular-based activity by using living cells, and this therapy has a wide range of advantages over orthotropic liver transplantation as this therapy is concerned with restoration of the damaged tissue by using living cells to produce the cells or tissue with properties mimicking the native tissue (Bhatia et al., 2014).

The cells regenerated by cell-based therapy can be cryopreserved, genetically handled to adjust inborn errors of metabolism, or infused so there is no need of surgery, and permanent immunosuppression can be overcome by acquiring cells from the same patient (Pop and Mosteanu). Even though it has a wide range of advantages it has certain limitations like lack of functional cells, low mechanical strength of the newly formed cells, and immune incompatibility with the host cell other than that hepatocyte have special

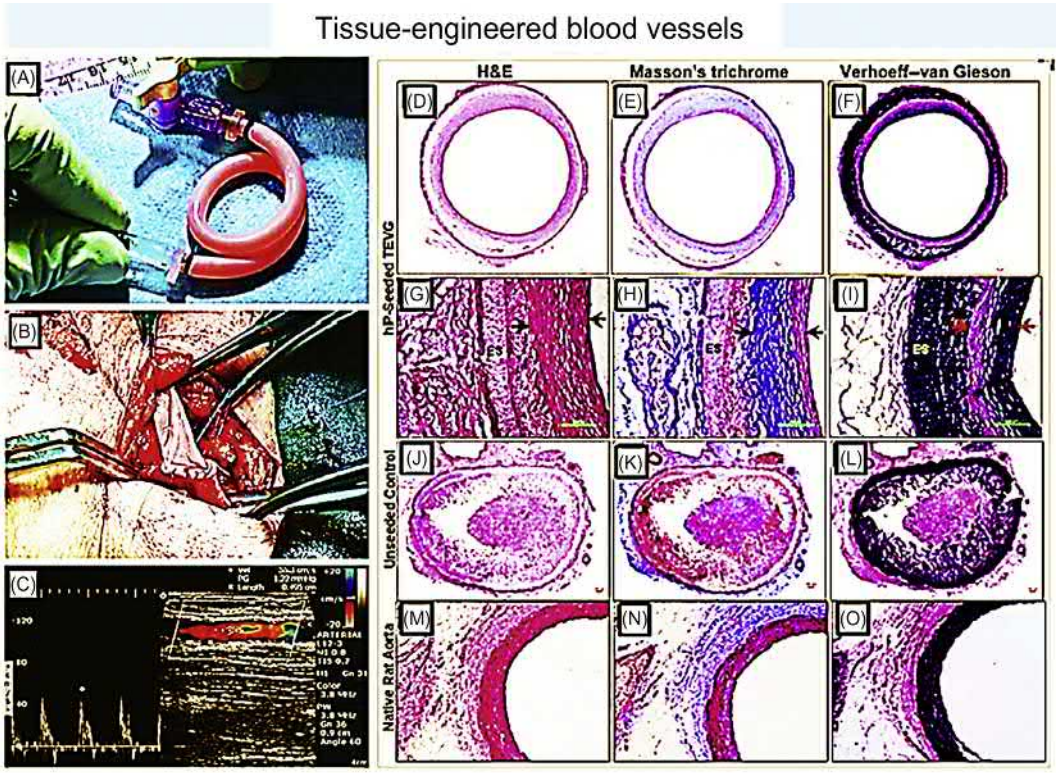

FIGURE 7.14 Tissue-engineered blood vessels. (A–C) The first clinically used sheet-based tissue-engineered blood vessel tested on three human patients for application as high-pressure arteries. (A) A tissue-engineered graft was implanted between the axillary vein and the humeral artery as an arteriovenous shunt, (B) the vessel exhibited normal suturing and surgical handling properties, (C) the shunt maintained high flow without signs of aneurysm restenosis even after 6 months. (D–O) A comparative histological analysis of human pericyte cell-seeded TEVGs (D–I), unseeded scaffolds (J–L), and native rat aorta (M–O). The H&E (D, G, J, and M), Masson's trichrome (E, H, K, and N), and Verhoeff–van Gieson (F, I, L and O) stainings demonstrated remodeling of the tissue in the TEHV construct enriched with collagen and elastin similar to the native aorta. (G–I) are magnified images for the wall cross-section of (D–F). Arrows indicate the remodeled tissue while ES stands for electrospun scaffold layer. *ES*, Embryonic stem; *TEVGs*, tissue-engineered vascular grafts. *(A–C) Reprinted from L'Heureux, N., Dusserre, N., Marini, A., Garrido, S., de la Fuente, L., McAllister, T., 2007. Technology insight: the evolution of tissue-engineered vascular grafts—from research to clinical practice. Nat. Clin. Pract. Cardiovasc. Med. 4, 389–395. (D–O) Adapted with permission from Yamamoto, K., Shao, Z.J., 2017. Process development, optimization, and scale-up: fluid-bed granulation. Developing Solid Oral Dosage Forms, second ed. Elsevier with slight modifications.*

limitation of trans diffusion to hepatocytes which leads to the loss of function and this lead nanotechnology to enter the field of health.

Nanotechnology has proven to be an effective method for reproducing and repairing the cells several times by improving cell properties and this can be achieved by providing

the cell with the 3D microenvironment with the help of the nanostructured collagen, matrix, elastin, and lamin; at this nanoscale level there is more evidence of interaction between the cell and the microenvironment provided and this helps the cells to differentiate from others (Montaser and Fawzy, 2015).

So, the scaffold of biochemical, mechanical, and electrical properties manipulating the native tissue is nanoengineered and this enhances the differentiation, proliferation, and maturation and fosters the cell growth and function; moreover the microenvironment provided by the nanotechnology prevents the hepatocytes from transdiffusing into the fibroblast and helps in retaining spheroidal morphology, which is the major challenge in the cell-based culture of hepatocytes (Krishnan and Sethuraman, 2013).

Commonly used in fabricating materials are graphene, CNTs, and molybdenum and tungsten. Electrospinning technique, self-assembly, cell printing technique, solvent casting, freeze-drying, particulate leaching, microsphere-based sintering, and phase separation are some of the techniques used for fabrication of nanofibers to provide a physiological environment that mimics the physiological environment of the native tissue (Krishnan and Sethuraman, 2013). However, the most commonly employed techniques are electrospinning technique and freeze-drying.

7.6.1.4 Nanotechnology for Stem Cell Engineering

The core triumph of engineered tissue by in vitro method is to use the patient's own primary cells (autologous cells), which are further introduced in scaffolds to reimplant, but this strategy can suffer from severe drawbacks like invasive nature of cells due to unhealthy conditions. Therefore, stem cells are given more emphasis, including bone marrow mesenchymal stem cells (MSCs), embryonic stem cells, and umbilical cord−derived MSCs (Howard et al., 2008).

The roots of cellular genetics can be modified by incorporating or eliminating one or the more genetic fragments in need of generating new and useful organisms. Currently, researchers are focusing on how they can engineer stem cells to increase the immune sensitization against a tumor and increase lifespan in animals (Aten et al., 2012).

The combination of genetic engineering with nanotechnology is proving to have good potential in the field of agriculture. Nanoinjection based on microelectromechanical systems (MEMS) fragment with moveable, nanometer-sized cut is reported to be able to hold DNA on the basis of its electrical charge. Nanotechnology is playing a vital role in genomics for improving crop features such as an increase in yield and resistance to infection, to overcome malnutrition and food insecurity (Coccia, 2012). Clinical practices in diagnostic therapies and therapeutics are exploring innovative applications by the convergence of the nanotechnology and other biomedical sciences.

In addition to microenvironmental control of MSC behaviors, MSCs have shown to modulate the microenvironmental characteristic via cell−cell contact and more interestingly, paracrine secretion of some cytokines and extracellular vesicles (Sui et al., 2019). Moreover, the reciprocal regulations between MSCs and microenvironments, particularly those connecting MSCs with diseased recipient microenvironmental factors, provide crucial mechanisms determining the efficacy of transplanted MSC-based bone regeneration (Fig. 7.15).

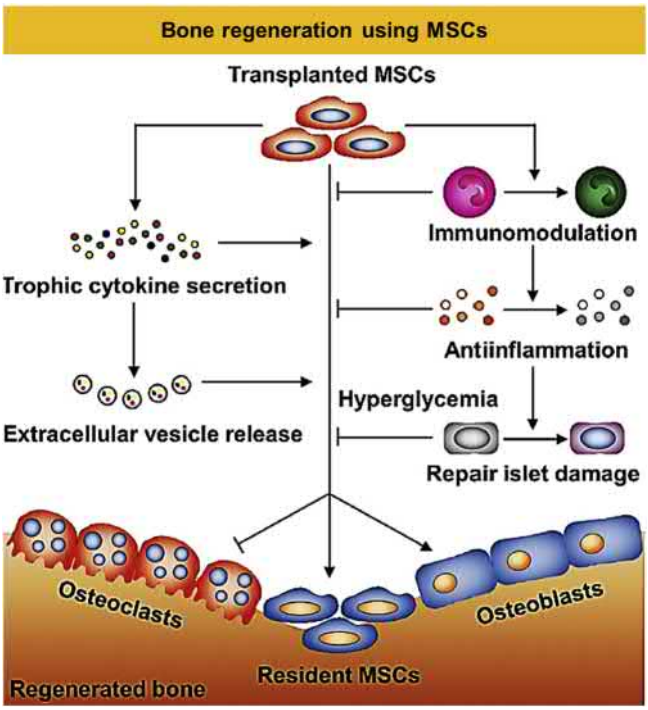

FIGURE 7.15 The interplay between MSCs and microenvironments in bone tissue engineering and cytotherapy. *MSCs*, Mesenchymal stem cells. *Adapted with permission from Sui, B.-D., Hu, C.-H., Liu, A.-Q., Zheng, C.-X., Xuan, K., Jin, Y., 2019. Stem cell-based bone regeneration in diseased microenvironments: challenges and solutions. Biomaterials 196, 18–30.*

7.6.2 Nanotechnology-Based Tissue Engineering for Cell Labeling, Purification, Detection, and Suicide Bombing

Nanoparticles, such as quantum dot (CdSe ~ 8 nm), can be used to label a variety of cellular targets. For example, allowing cells to ingest quantum dot dyes, the cell movement can be monitored for days without photobleaching the quantum dot dyes. Cell migration behavior can be studied by watching the quantum dot ingestion behavior, so that the cell types may be distinguished. Invasive cancerous cells and immotile nontumor cells can be differentiated by seeding them on a quantum dot bed. Cells ingest quantum dots and leave a so-called phagokinetic track behind. Cancer cells exhibit diverse uncertain behavior, and some nontumor cells show specific endocytosis and migration patterns. Quantum dots can also be used to trace cells for up to 10 generations because quantum dots are distributed during dividing. Therefore dots can be used to trace cancer cells and stem cells.

Moreover, nanotechnology -enabled measurement of the electric properties of a single individual cell, which is important in cell purification. The scientist is able to sort/purify cells through their different intrinsic electric properties. This application will be very

important in stem cell purification. Currently, we do not have the techniques to get purified stem cells; with the aid of nanotechnology, large quantities of purified stem cells may be obtained in the very near future.

Furthermore, cell detection is also possible by employing nanotechnology. About a thousand wires, each about 8 nm in diameter, coated with different antibody or nucleic acid, can be used to detect thousands of genes in a cell and proteins synthesized by a cell. Silicon nanowires tethered with biomolecules specifically bond to a protein expressed by cancer cells. When there is bonding, an electrical signal can be detected. The detectors made of nanowires are very sensitive and required minimal sample preparation; several bonds can be precisely detected. Moreover, the detectors are very cheap and patients can use them at home. However, the ions in the media for maintenance of the normal life of the cell may interfere with the biochemical reactions.

Despite significant progress of tissue engineering in both academic research and in industry, some issues have arisen that have forced the research progress and commercial procedures to slow down. The biggest setback that the field of tissue engineering faces now is the unknown fate of tissue-engineered analogs inside the human body. That is why the FDA has approved very few tissue-engineered products so far.

Before any further breakthroughs can be made, the following questions must be answered. Where will the transplanted cells go? How will they grow? What will they differentiate into? How will they be eliminated if an unexpected event occurs, such as tumor genesis? Unfortunately, most scientists are concentrating on regenerating all kinds of tissues and organs but are ignoring the control issues for proper regeneration and the fate of tissue-engineered grafts in vivo. Before these questions can be completely answered, one temporary solution called “suicide bombing” may be used. A “smart” agent in nanoscale can be taken up by all cells in the tissue-engineered grafts. The agent is inactive during a normal condition and is activated only by specific enzymes that are expressed in the cell under certain pathologic states. The activation of the agent will kill the abnormal cells. This idea is not only good for killing the abnormal cells but also suitable for the treatment of specific diseases if a particular therapeutic agent is used.

7.7 RECENT PATENTS OVERVIEW

Biotechnology-based tissue engineering is widely emerging field nowadays. Tissue engineering is engineering of cells using physicochemical and biochemical parameters to improve or replace biological tissue. The areas of application of tissue engineering are cartilage, heart, bone, cancer, pancreas, etc. (Castells-Sala et al., 2013). Bone scaffolds, cartilage scaffolds, heart scaffolds have been developed using biotechnology-based tissue engineering.

Recently, there has been a focus to produce regenerative heart valve as the mechanical heart valve has the limitation of thromboembolism, which can be overcome by a tissue-engineered regenerative valve (Zhu and Grande-Allen, 2018). Much biotechnology-based tissue engineering has been patented.

7.7.1 Magnetic Pole Matrices

This invention regards targeted treatment of cardiovascular system (CVS) disease by magnetic polymer nanoparticle drug. Aiming at a particular site of the body is a critical issue in drug administration. To achieve a therapeutic level at the target site, a high dose of the drug has to be administered as only part of it reaches the desired target site (Steinhoff et al., 2006). High dose may also cause side effects on sites other than the target site (Steinhoff et al., 2006). Targeted drug delivery may be the solution for the side effect because it reduces the concentration at other sites (Steinhoff et al., 2006).

Magnetic targeting is the one way of targeting the desired site of the organ. It involves the addition of magnetic particle into the drug carrier, and the drug is directed to the targeted site after being administered into the bloodstream using the external magnetic field (Steinhoff et al., 2006). Furthermore, these magnetic particles are compatible with the human body (Steinhoff et al., 2006). However, one of two limitations is that an accumulation of magnetic particle is affected by blood flow rate and the site having higher blood flow rate such as large arteries may require strong external magnetic field (Steinhoff et al., 2006). The second limitation is the site more than 2 cm deeper in the body is not easy to target with external magnetic field and there is also the chance of aggregate (Steinhoff et al., 2006). Biomedical devices with endothelial seeding can address the problem of thrombosis (Steinhoff et al., 2006). However, in vitro seeding is time-consuming and the risk of cell culture contamination is greater (Steinhoff et al., 2006).

In in vivo seeding of magnetically modified cell to the device, the surface has also a limitation of aggregation (Steinhoff et al., 2006). This invention utilizing magnetic polymer nanoparticle solved the issues described above (Steinhoff et al., 2006).

7.7.2 Differentiable Human Mesenchymal Stem Cells

This invention is related to the recipe and procedure of synthetic polymer's nanofiber matrix which is used for the delivery of human mesenchymal cells as a scaffold application of tissue engineering (Arinzeh et al., 2006). The isolated differentiable human mesenchymal cells are dispersed in the matrix prepared using the synthetic polymer nanofiber and it gives support to the maturing human mesenchymal cells (Arinzeh et al., 2006). The polymer used in the synthesis of nanofiber is 3D as well as biocompatible (Arinzeh et al., 2006). As per a different embodiment, the polymer contains poly D, L lactide−glycolide, and the preparation method is electrospinning (Arinzeh et al., 2006).

7.7.3 Degradable Polyurethane Foams

Allograft bone was mainly used to cure the bone defect. However, now its use is limited due to the spreading of disease and immune response (Guelcher et al., 2012). Here, one or more biocompatible polyol and water, one or more stabilizer, and one or more cell opener are used for the preparation of resin mix (Guelcher et al., 2012). The advantages of this invention are highly stable, very porous, nonharmful to a biological system, and most

importantly biodegradable. The binding and growth of cells in vitro is aided by the foams of the invention (Guelcher et al., 2012). This invention serves as a scaffold for the growth of the cell (Guelcher et al., 2012). Foam leakage is also present in this invention.

The biodegradability of this polyurethane foam is due to its ability to undergo hydrolysis and it does not form any noxious, harmful, injurious substance that would cause an immunological response (Guelcher et al., 2012). The application of this invention is very wide. It is used in an injectable scaffold for bone and in drug and gene delivery. In addition to that, it can be applied to the surface of bone that is damaged or has a hole, can be put into the two pieces of the bone, and can also be applied to skin that has been damaged (Guelcher et al., 2012). Moldability of this invention is very wide as it can be molded into a plate or screw (Guelcher et al., 2012).

7.7.4 Multilayer Polymer Scaffolds

This invention is a device and method applicable to tissue engineering (Hansford et al., 2005). The invention is a multilayer thermal plastic polymer scaffold, and helps in the curing of damaged tissue; in other words, this invention is useful for tissue regeneration (Hansford et al., 2005). The procedure for the fabrication of scaffolds is described in the patent (Hansford et al., 2005). The scaffold is 3D as well as multilayer or single layer (Hansford et al., 2005).

Various ongoing/completed patents in these fields have been discussed, providing a means for further developments and possible commercialization of these treatment modalities, in Table 7.1.

7.8 CLINICAL TRIAL STATUS

The loss of tissue or total organ failure is one frequent and costly proposition in healthcare. Millions of people worldwide are suffering from disability because of congenital deformity or organ loss either due to trauma, postoperatively after diseases like cancer, or pathological degeneration (Fisher and Mauck, 2013). Tissue engineering technology employing principles of bioengineering has revolutionized the treatment in such cases by providing methods to design and fabricate robust scaffolds from biocompatible materials having applications in tissue repair and regeneration.

Tissue engineering enables a substantial savings in treatment cost as the in vitro substitutes for in vivo tissue repair are much cheaper than organ transplantation (Aljohani et al., 2017). Today, there are many clinical trials being undertaken in this new and interdisciplinary field aiming to provide devices that functional substitutes that can replace a damaged organ or tissue with some successful attempts having achieved patentability. This section aimed to provide insight for scientists with research interest in the areas of tissue engineering and regenerative medicine employing novel nanoscaled scaffolds. Various ongoing/completed clinical trials in these fields have been discussed providing a means for further developments and possible commercialization of these treatment modalities in Table 7.2.

TABLE 7.1 Various Patents and Ongoing Clinical Trials in the Field of Tissue Engineering.

Patent No.	Publication Status	Publication Date	Original Assignee	Description of Patented Technology
US 9,012,415	Grant	April 21, 2015	Stemmatters, Biotechnologie Medicina Regenerativa (Barco, Portugal)	The patented invention comprises a gellan gum based photocross-linkable hydrogel that has applications in tissue regeneration in addition to drug delivery. A preferred embodiment narrates that the monomeric subunit of acyl gellan gum is substituted with a polymerizable moiety and a free radical based photoinitiator, which photopolymerizes in ultraviolet light. According to another embodiment, this hydrogel can also be formulated as a micro or a nanoparticle incorporating a bioactive agent in amounts that show a therapeutic effect. The invention has applications as an injectable hydrogel, biosensors, implants, medical procedures involving radio-frequency ablation, etc.
US 8,999,916	Grant	April 7, 2015	Hauser C, Seow WY	The scope of this patent includes an amphiphilic peptide or peptide that undergoes a conformational change for self-assembling to form a macromolecular 3D nanofibrous network, which entraps water and converts into a hydrogel consisting of at least one chemically cross-linked peptide. This hydrogel has applications in tissue replacement and regeneration, drug delivery, gene delivery, pharmaceutical formulations, cosmetic compositions, etc.
US 8,992,99	Grant	March 31, 2015	The Johns Hopkins University (Baltimore, MD, United States)	The scope of the appended claims includes the disclosed subject matter as well as some modifications therewith. The derived biodegradable multicomponent cationic polymer that gets self-assembled with DNA is devised as a nanoparticle with bioactive materials useful in tissue regeneration and cancer.
US8691974 B2	Grant	April 8, 2014	Virginia Tech Intellectual Properties, Inc.	This invention describes a novel technique for the production of BC via bacterial fermentation of culture medium using a microfluidic system. The medium flows into porous molds resulting in 3D-BC nanostructure of the desired shape. The porosity of the structure is controlled using 3D printing employing ink-jet printer technology. This structure can be used as biomedical implants or scaffolds supporting cell growth.
US8614189 B2	Grant	Dec 24, 2013	University of Connecticut	The claims of this investigation include a composite biocompatible material having sufficient mechanical strength. The scaffold consists of polar functionalized multiwalled carbon nanotubes to impart water dispersibility. PGLA is incorporated with one or a combination of the bioactive agent is the biodegradable polymer having the shape of a microsphere. The nanotubes are sintered on the microsphere at the junction of two microspheres. An embodiment therein mentions this scaffold bears suitable properties for cortical bone regeneration.

Refer https://clinicaltrials.gov for more details. *BC*, Biosynthetic cellulose.

TABLE 7.2 A Brief Insight Into Clinical Trials was Undertaken to Amalgamate Tissue Engineering and Nanotechnology.

Subject/NCT No.	Location/ Sponsor	Start Year/End Year	Type/Phase	Enrollment/ Eligibility	Gender/ Healthy Volunteer	Primary Outcome/ Secondary Outcome	Study
Nanostructured allogeneic artificial human cornea for corneal trophic ulcers in patients postconventional ophthalmic treatment/ NCT0176524	Spain/ Andalusian Initiative for Advanced Therapies	2014/2019	Interventional/ I and II	20/Adult, suffering from corneal Mackie third stage	All/No	Adverse events related to treatment/corneal stoma repair, visual acuity and corneal transparency.	Five patients implanted with the nanostructured artificial human cornea with allergenic cells of dead donors and other biomaterials for a duration of 5 years with first 36 months of inclusion and next 24 months of follow-up versus the randomized control group subjected to conventional transplantation of amniotic membrane.
Evaluation of nanobone, a nanocrystalline hydroxyapatite silica gel synthetic bone graft for the management of intrabony periodontal defects/NCT02507596	Egypt/Cairo University	2015/2017	Interventional/ Unavailable	30/30−55 years, bone loss with one or more pocket depth ≥ 6 mm, level of clinical attachment ≥ 5 mm detected by periapical radiographs	All/Yes	Shift from baseline in the level of clinical attachment in mm in patients with chronic periodontitis after an interval of 6 months/ estimation of pocket depth in mm and bone fill defects in mm^2 both at baseline and after the 6 months interval.	A comparison between the nanobone and conventional OFD surgical procedure as a negative control was conducted in 30 patients. Both the experimental and negative control groups were assigned an equal number of patients. Patients were assessed via clinical as well as radiographic parameters for a shift from baseline at 3 and 6 months interval postoperatively.
Chitosan nanoscaffolds seeded with mesenchymal stem cells derived from adipose tissue in the treatment of diabetic foot ulcer/ NCT03259217	Unavailable/ Assuit University	2017/2019	Interventional/ Phase I	40/Child, adult, senior, patients with grade 1 or 2 neuroischemic or neuropathic diabetic foot ulcer on Wagner scale and HbA1c $\leq 7.5\%$	All/No	Complete epithelialization of chronic ulcer/50% healing rate within 6 months and the rate of ulcer recurrence within 1 year.	Collagen−alginate consisting of curcumin loaded chitosan NP a biocompatible as well collagen as the biodegradable material may have applications in regenerative efficiency in diabetic foot ulcers and ischemic wound healing.

OFD, Open flap debridement.

7.9 CONCLUSION

The application of nanotechnology in tissue engineering is growing rapidly, as it can help to create, repair, and/or replace cells, tissues, and organs in combinations with nanoscale materials. By applying nanotechnology in tissue engineering based treatments/therapies millions of patients can benefit. As a general protocol in tissue engineering, firstly, cells are subjected to seeding on biomimicked platform providing adhesive surfaces, followed by the cellular deposition in their own protein to make them more compatible with biological substrates. For this purpose a variety of materials have been described in this chapter with diverse characteristics to support a particular type of regeneration of cells/tissues. These materials include CS, albumin, alginates, silica, dendrimers, PLGA, PEG, PLA, etc. This chapter successfully described that advantages of nanotechnology-based tissue engineering using electrospinning nanofibers, nanogels, and nanoparticles in comparison with traditional approaches and are employed in many of the fields for different purposes.

Acknowledgments

RKT would like to acknowledge Science and Engineering Research Board (statutory body established through an Act of Parliament: SERB Act 2008), Department of Science and Technology, Government of India for the grant (Grant #ECR/2016/001964) and N-PDF funding (PDF/2016/003329) for work on targeted cancer therapy in Dr. Tekade's Laboratory.

ABBREVIATIONS

CSH calcium sulfate α-hemihydrate
DMP1 dentin matrix protein 1
ECM extracellular natural matrix
Hap hydroxyapatite
ICs integrated circuits
PLGA poly(lactic acid-*co*-glycolic acid)
PBT polybutylene terephthalate
PGA polyglycolic acid
PLA polylactic acid
RNAi RNA interference

References

Ahadian, S., Davenport Huyer, L., Estili, M., Yee, B., Smith, N., Xu, Z., et al., 2017. Moldable elastomeric polyester-carbon nanotube scaffolds for cardiac tissue engineering. Acta Biomater. 52 (Supplement C), 81–91.

Aldana, A.A., Abraham, G.A., 2017. Current advances in electrospun gelatin-based scaffolds for tissue engineering applications. Int. J. Pharm. 523 (2), 441–453.

Aljohani, W., Ullah, M.W., Zhang, X., Yang, G., 2017. Bioprinting and its applications in tissue engineering and regenerative medicine. Int. J. Biol. Macromol. 107 (Pt A), 261–275.

Arinzeh, T., Jaffe, M., Shanmugasundaram, S., 2006. Substrate Recognition by Differentiable Human Mesenchymal Stem Cells, Google Patents.

Atala, A., Kasper, F.K., Mikos, A.G., 2012. Engineering complex tissues. Sci. Transl. Med. 4 (160), 160rv12.

Aten, Q.T., Jensen, B.D., Tamowski, S., Wilson, A.M., Howell, L.L., Burnett, S.H., 2012. Nanoinjection: pronuclear DNA delivery using a charged lance. Transgenic. Res. 21 (6), 1279–1290.
Baino, F., Novajra, G., Vitale-Brovarone, C., 2015. Bioceramics and scaffolds: a winning combination for tissue engineering. Front. Bioeng. Biotechnol. 3, 202.
Baino, F., Novajra, G., Miguez-Pacheco, V., Boccaccini, A.R., Vitale-Brovarone, C., 2016. Bioactive glasses: special applications outside the skeletal system. J. Non-Cryst. Solids 432 (Part A), 15–30.
Barnes, C.P., Sell, S.A., Boland, E.D., Simpson, D.G., Bowlin, G.L., 2007. Nanofiber technology: designing the next generation of tissue engineering scaffolds. Adv. Drug Deliv. Rev. 59 (14), 1413–1433.
Barrere, F., van Blitterswijk, C.A., de Groot, K., 2006. Bone regeneration: molecular and cellular interactions with calcium phosphate ceramics. Int. J. Nanomed. 1 (3), 317–332.
Ber, S., Torun Kose, G., Hasirci, V., 2005. Bone tissue engineering on patterned collagen films: an in vitro study. Biomaterials 26 (14), 1977–1986.
Bhatia, S.N., Underhill, G.H., Zaret, K.S., Fox, I.J., 2014. Cell and tissue engineering for liver disease. Sci. Transl. Med. 6 (245), 245sr2.
Bogan, S.L., Teoh, G.Z., Birchall, M.A., 2016. Tissue engineered airways: a prospects article. J. Cell. Biochem. 117 (7), 1497–1505.
Castells-Sala, C., Alemany-Ribes, M., Fernández-Muiños, T., Recha-Sancho, L., López-Chicón, P., Aloy-Reverté, C., et al., 2013. Current applications of tissue engineering in biomedicine. J. Biochip Tissue Chip (S2) (107), 1.
Chan, B.P., Leong, K.W., 2008. Scaffolding in tissue engineering: general approaches and tissue-specific considerations. Eur. Spine J. 17 (Suppl 4), 467–479.
Chen, V.J., Ma, P.X., 2006. The effect of surface area on the degradation rate of nanofibrous poly(L-lactic acid) foams. Biomaterials 27 (20), 3708–3715.
Coccia, M., 2012. Converging genetics, genomics and nanotechnologies for groundbreaking pathways in biomedicine and nanomedicine. Int. J. Healthcare Technol. Manage. 13 (4), 184–197.
Connor, R.E., Tirrell, D.A., 2007. Non-canonical amino acids in protein polymer design. Polym. Rev. 47 (1), 9–28.
Danie Kingsley, J., Ranjan, S., Dasgupta, N., Saha, P., 2013. Nanotechnology for tissue engineering: need, techniques and applications. J. Pharm. Res. 7 (2), 200–204.
Dorozhkin, S.V., 2010. Nanosized and nanocrystalline calcium orthophosphates. Acta Biomater. 6 (3), 715–734.
Dwivedi, N., Shah, J., Mishra, V., Mohd Amin, M.C.I., Iyer, A.K., Tekade, R.K., et al., 2016. Dendrimer-mediated approaches for the treatment of brain tumor. J. Biomater. Sci. Polym. Ed. 27 (7), 557–580.
Elisseeff, J.H., Lee, A., Kleinman, H.K., Yamada, Y., 2002. Biological response of chondrocytes to hydrogels. Ann. N. Y. Acad. Sci. 961, 118–122.
Fisher, M.B., Mauck, R.L., 2013. Tissue engineering and regenerative medicine: recent innovations and the transition to translation. Tissue Eng. Part B 19 (1), 1–13.
George, A., Ravindran, S., 2010. Protein templates in hard tissue engineering. Nano Today 5 (4), 254–266.
Ghadiri, M., Vasheghani-Farahani, E., Atyabi, F., Kobarfard, F., Mohamadyar-Toupkanlou, F., Hosseinkhani, H., 2017. Transferrin-conjugated magnetic dextran-spermine nanoparticles for targeted drug transport across blood-brain barrier. J. Biomed. Mater. Res. A 105 (10), 2851–2864.
Ghanghoria, R., Kesharwani, P., Tekade, R.K., Jain, N.K., 2016. Targeting luteinizing hormone-releasing hormone: a potential therapeutics to treat gynecological and other cancers. J. Control Release 269, 277–301.
Griffith, L.G., Naughton, G., 2002. Tissue engineering—current challenges and expanding opportunities. Science 295 (5557), 1009–1014.
Guelcher, S.A., Patel, V., Hollinger, J.O., Didier, J., 2012. Degradable Polyurethane Foams, Google Patents.
Han, D.K., Hubbell, J.A., 1997. Synthesis of polymer network scaffolds from L-lactide and poly(ethylene glycol) and their interaction with cells. Macromolecules 30 (20), 6077–6083.
Hansford, D., Yang, S., Ferrell, N., 2005. Multi-layer Polymer Scaffolds, Google Patents.
Howard, D., Buttery, L.D., Shakesheff, K.M., Roberts, S.J., 2008. Tissue engineering: strategies, stem cells and scaffolds. J. Anat. 213 (1), 66–72.
Igwe, J.C., Mikael, P.E., Nukavarapu, S.P., 2014. Design, fabrication and in vitro evaluation of a novel polymer-hydrogel hybrid scaffold for bone tissue engineering. J. Tissue Eng. Regen. Med. 8 (2), 131–142.
Jensen, T., Baas, J., Dolathshahi-Pirouz, A., Jacobsen, T., Singh, G., Nygaard, J.V., et al., 2011. Osteopontin functionalization of hydroxyapatite nanoparticles in a PDLLA matrix promotes bone formation. J. Biomed. Mater. Res. A 99 (1), 94–101.

Kretlow, J.D., Mikos, A.G., 2008. From material to tissue: biomaterial development, scaffold fabrication, and tissue engineering. AIChE J. 54 (12), 3048–3067.
Krishnan, U.M., Sethuraman, S., 2013. The integration of nanotechnology and biology for cell engineering: promises and challenges. Nanomater. Nanotechnol. 3, 19.
Kuche, K., Maheshwari, R., Tambe, V., Mak, K.K., Jogi, H., Raval, N., et al., 2018. Carbon nanotubes (CNTs) based advanced dermal therapeutics: current trends and future potential. Nanoscale 10 (19), 8911–8937.
Kumar, A., Rao, K.M., Han, S.S., 2018. Application of xanthan gum as polysaccharide in tissue engineering: a review. Carbohydr. Polym. 180 (Supplement C), 128–144.
Kwak, S., Haider, A., Gupta, K.C., Kim, S., Kang, I.-K., 2016. Micro/nano multilayered scaffolds of PLGA and collagen by alternately electrospinning for bone tissue engineering. Nanoscale Res. Lett. 11 (1), 323.
Lalu, L., Tambe, V., Pradhan, D., Nayak, K., Bagchi, S., Maheshwari, R., et al., 2017. Novel nanosystems for the treatment of ocular inflammation: current paradigms and future research directions. J. Control Release 268, 19–39.
Lamers, E., van Horssen, R., te Riet, J., van Delft, F.C., Luttge, R., Walboomers, X.F., et al., 2010. The influence of nanoscale topographical cues on initial osteoblast morphology and migration. Eur. Cell Mater. 20, 329–343.
Langer, R., Vacanti, J.P., 1993. Tissue engineering. Science 260 (5110), 920–926.
Lee, S.J., Yoo, J.J., Atala, A., 2016. Preface. In Situ Tissue Regeneration. Academic Press, Boston, MA.
Levengood, S.K.L., Zhang, M., 2014. Chitosan-based scaffolds for bone tissue engineering. J. Mater. Chem. B 2 (21), 3161–3184.
Liu, X., Jin, X., Ma, P.X., 2011. Nanofibrous hollow microspheres self-assembled from star-shaped polymers as injectable cell carriers for knee repair. Nat. Mater. 10, 398.
Lyles, M.B., Hu, J.C., Varanasi, V.G., Hollinger, J.O., Athanasiou, K.A., 2015. 5—Bone tissue engineering. Regenerative Engineering of Musculoskeletal Tissues and Interfaces. Woodhead Publishing.
Ma, P.X., 2004. Scaffolds for tissue fabrication. Mater. Today 7 (5), 30–40.
Ma, P.X., 2008. Biomimetic materials for tissue engineering. Adv. Drug Deliv. Rev. 60 (2), 184–198.
Mager, M.D., LaPointe, V., Stevens, M.M., 2011. Exploring and exploiting chemistry at the cell surface. Nat. Chem. 3 (8), 582–589.
Maheshwari, R.G., Tekade, R.K., Sharma, P.A., Darwhekar, G., Tyagi, A., Patel, R.P., et al., 2012. Ethosomes and ultradeformable liposomes for transdermal delivery of clotrimazole: a comparative assessment. Saudi Pharm. J. 20 (2), 161–170.
Maheshwari, R., Tekade, M., Sharma, P.A., Tekade, R.K., 2015a. Nanocarriers assisted siRNA gene therapy for the management of cardiovascular disorders. Curr. Pharm. Des. 21 (30), 4427–4440.
Maheshwari, R.G., Thakur, S., Singhal, S., Patel, R.P., Tekade, M., Tekade, R.K., 2015b. Chitosan encrusted nonionic surfactant based vesicular formulation for topical administration of ofloxacin. Sci. Adv. Mater. 7 (6), 1163–1176.
Maheshwari, R., Tekade, M., Gondaliya, P., Kalia, K., D'Emanuele, A., Tekade, R.K., 2017. Recent advances in exosome-based nanovehicles as RNA interference therapeutic carriers. Nanomedicine (Lond) 12 (21), 2653–2675.
Martin, I., Wendt, D., Heberer, M., 2004. The role of bioreactors in tissue engineering. Trends Biotechnol. 22 (2), 80–86.
Mendes, P.M., 2013. Cellular nanotechnology: making biological interfaces smarter. Chem. Soc. Rev. 42 (24), 9207–9218.
Mironov, V., Kasyanov, V., Markwald, R.R., 2008. Nanotechnology in vascular tissue engineering: from nanoscaffolding towards rapid vessel biofabrication. Trends Biotechnol. 26 (6), 338–344.
Montaser, L.M., Fawzy, S.M., 2015. Nano scaffolds and stem cell therapy in liver tissue engineering. SPIE Nanoscience + Engineering. International Society for Optics and Photonics, 95500M-95500M-8.
Nerem, R., Seliktar, D., 2001. Vascular Tissue Engineering. Annu. Rev. Biomed. Eng. 3, 225–243.
Nichols, J.E., Niles, J.A., Cortiella, J., 2012. Production and utilization of acellular lung scaffolds in tissue engineering. J. Cell. Biochem. 113 (7), 2185–2192.
Nikalje, A.P., 2015. Nanotechnology and its applications in medicine. Med. Chem. 5 (2), 185–189.
O'Brien, F.J., 2011. Biomaterials & scaffolds for tissue engineering. Mater. Today 14 (3), 88–95.
Oliveira, J.M., Sousa, R.A., Kotobuki, N., Tadokoro, M., Hirose, M., Mano, J.F., et al., 2009. The osteogenic differentiation of rat bone marrow stromal cells cultured with dexamethasone-loaded carboxymethylchitosan/poly (amidoamine) dendrimer nanoparticles. Biomaterials 30 (5), 804–813.

Pawar, J., Tayade, A., Gangurde, A., Moravkar, K., Amin, P., 2016. Solubility and dissolution enhancement of efavirenz hot melt extruded amorphous solid dispersions using combination of polymeric blends: a QbD approach. Eur. J. Pharm. Sci. 88 (Supplement C), 37–49.
Peck, M., Dusserre, N., McAllister, T.N., L'Heureux, N., 2011. Tissue engineering by self-assembly. Mater. Today 14 (5), 218–224.
Pins, G.D., Christiansen, D.L., Patel, R., Silver, F.H., 1997. Self-assembly of collagen fibers. Influence of fibrillar alignment and decorin on mechanical properties. Biophys. J. 73 (4), 2164–2172.
Pop, T., Mosteanu, O., 2013. Recent advances in tissue engineering for the therapy of liver diseases using nanotechnology and stem cells research. Medicine, 8, 12.
Raftery, R.M., Walsh, D.P., Castano, I.M., Heise, A., Duffy, G.P., Cryan, S.A., et al., 2016. Delivering nucleic-acid based nanomedicines on biomaterial scaffolds for orthopedic tissue repair: challenges, progress and future perspectives. Adv. Mater. 28 (27), 5447–5469.
Rambhia, K.J., Ma, P.X., 2015. Controlled drug release for tissue engineering. J. Control Release 219 (Supplement C), 119–128.
Reichert, J.C., Wullschleger, M.E., Cipitria, A., Lienau, J., Cheng, T.K., Schutz, M.A., et al., 2011. Custom-made composite scaffolds for segmental defect repair in long bones. Int. Orthop. 35 (8), 1229–1236.
Ronca, D., Langella, F., Chierchia, M., D'Amora, U., Russo, T., Domingos, M., et al., 2016. Bone tissue engineering: 3D PCL-based nanocomposite scaffolds with tailored properties. Procedia CIRP 49 (Supplement C), 51–54.
Saiz, E., Zimmermann, E.A., Lee, J.S., Wegst, U.G.K., Tomsia, A.P., 2013. Perspectives on the role of nanotechnology in bone tissue engineering. Dent. Mater. 29 (1), 103–115.
Shakiba, S., Mansouri, S., Selomulya, C., Woo, M.W., 2018. The role of the intermediate stage of drying on particle in-situ crystallization in spray dryers. Powder Technol. 323 (Supplement C), 357–366.
Shakir, M., Jolly, R., Khan, M.S., Iram, N.E., Sharma, T.K., Al-Resayes, S.I., 2015. Synthesis and characterization of a nano-hydroxyapatite/chitosan/polyethylene glycol nanocomposite for bone tissue engineering. Polym. Adv. Technol. 26 (1), 41–48.
Sharma, P.A., Maheshwari, R., Tekade, M., Tekade, R.K., 2015. Nanomaterial based approaches for the diagnosis and therapy of cardiovascular diseases. Curr. Pharm. Des. 21 (30), 4465–4478.
Sreejalekshmi, K.G., Nair, P.D., 2011. Biomimeticity in tissue engineering scaffolds through synthetic peptide modifications-altering chemistry for enhanced biological response. J. Biomed. Mater. Res. A. 96 (2), 477–491.
Steinhoff, G., Steinhoff, K., Li, W., Ma, N., 2006. Magnetic Pole Matrices Useful for Tissue Engineering and Treatment of Disease, Google Patents.
Sui, B.-D., Hu, C.-H., Liu, A.-Q., Zheng, C.-X., Xuan, K., Jin, Y., 2019. Stem cell-based bone regeneration in diseased microenvironments: challenges and solutions. Biomaterials 196, 18–30.
Svärd, M., Nordström, F.L., Hoffmann, E.-M., Aziz, B., Rasmuson, Å.C., 2013. Thermodynamics and nucleation of the enantiotropic compound p-aminobenzoic acid. CrystEngComm 15 (25), 5020–5031.
Takano, H., Sul, J.-Y., Mazzanti, M.L., Doyle, R.T., Haydon, P.G., Porter, M.D., 2002. Micropatterned substrates: approach to probing intercellular communication pathways. Anal. Chem. 74 (18), 4640–4646.
Tautzenberger, A., Kovtun, A., Ignatius, A., 2012. Nanoparticles and their potential for application in bone. Int. J. Nanomed. 7, 4545–4557.
Tekade, R.K., Maheshwari, R.G., Sharma, P.A., Tekade, M., Chauhan, A.S., 2015. siRNA therapy, challenges and underlying perspectives of dendrimer as delivery vector. Curr. Pharm. Des. 21 (31), 4614–4636.
Tekade, R.K., Maheshwari, R., Soni, N., Tekade, M., Chougule, M.B., 2017a. Chapter 1—nanotechnology for the development of nanomedicine A2—Mishra, Vijay. In: Kesharwani, P., Amin, M.C.I.M., Iyer, A. (Eds.), Nanotechnology-Based Approaches for Targeting and Delivery of Drugs and Genes. Academic Press.
Tekade, R.K., Maheshwari, R., Tekade, M., Chougule, M.B., 2017b. Chapter 8—solid lipid nanoparticles for targeting and delivery of drugs and genes A2—Mishra, Vijay. In: Kesharwani, P., Amin, M.C.I.M., Iyer, A. (Eds.), Nanotechnology-Based Approaches for Targeting and Delivery of Drugs and Genes. Academic Press.
Vacanti, C.A., 2006. The history of tissue engineering. J. Cell. Mol. Med. 10 (3), 569–576.
Vacanti, J.P., Langer, R., 1999. Tissue engineering: the design and fabrication of living replacement devices for surgical reconstruction and transplantation. Lancet 354 (Suppl 1), SI32–SI34.
Venugopalan, S., Rajendran, T., 2015. Role of polylactic acid in bone regeneration—a systematic review. J. Pharm. Sci. Res. 7(11), 960–966.

Walmsley, G.G., McArdle, A., Tevlin, R., Momeni, A., Atashroo, D., Hu, M.S., et al., 2015. Nanotechnology in bone tissue engineering. Nanomedicine 11 (5), 1253–1263.
Werani, J., Grünberg, M., Ober, C., Leuenberger, H., 2004. Semicontinuous granulation—the process of choice for the production of pharmaceutical granules? Powder Technol. 140 (3), 163–168.
Yamamoto, K., Shao, Z.J., 2017. Process development, optimization, and scale-up: fluid-bed granulation, Developing Solid Oral Dosage Forms, second ed. Elsevier.
Zhu, A.S., Grande-Allen, K.J., 2018. Heart valve tissue engineering for valve replacement and disease modeling. Curr. Opin. Biomed. Eng. 5, 35–41.

Further reading

Chaudhari, A.A., Vig, K., Baganizi, D.R., Sahu, R., Dixit, S., Dennis, V., et al., 2016. Future prospects for scaffolding methods and biomaterials in skin tissue engineering: a review. Int. J. Mol. Sci. 17 (12), 1974.
Gautam, S., Chou, C.-F., Dinda, A.K., Potdar, P.D., Mishra, N.C., 2014. Surface modification of nanofibrous polycaprolactone/gelatin composite scaffold by collagen type I grafting for skin tissue engineering. Mater. Sci. Eng. C 34, 402–409.
Mohamed, A., Xing, M.M., 2012. Nanomaterials and nanotechnology for skin tissue engineering. Int. J. Burns Trauma 2 (1), 29.

CHAPTER

8

Novel Therapeutic Approaches for the Treatment of Leishmaniasis

Vandana Soni[1], *Silki Chandel*[1], *Vikas Pandey*[1], *Saket Asati*[1], *Priyanka Jain*[1], *Aviral Jain*[2] *and Rakesh K. Tekade*[3]

[1]Department of Pharmaceutical Sciences, Dr. Hari Singh Gour University, Sagar, India
[2]Ravi Shankar College of Pharmacy, Bhopal, India [3]National Institute of Pharmaceutical Education and Research (NIPER)—Ahmedabad, Gandhinagar, India

OUTLINE

8.1 Introduction 264
8.1.1 The Causative Agent: Leishmania 265
8.1.2 Life Cycle of Leishmania 266
8.1.3 Clinical Manifestations 267
8.1.4 Pathology 267

8.2 Diagnosis 268
8.2.1 Parasitological Diagnosis 269
8.2.2 Serological Diagnosis 269
8.2.3 Molecular Diagnosis 269
8.2.4 Antibody Detection Diagnostic Tests 270

8.3 Currently Used Drugs for the Treatment of Leishmaniasis 270
8.3.1 Antimonial Agents 270
8.3.2 Pentamidine 270
8.3.3 Amphotericin B 271
8.3.4 Miltefosine 271
8.3.5 Paromomycin 271

8.4 Combined Therapy 271

8.5 Other Drugs Used for Leishmaniasis 273
8.5.1 Sitamaquine 273
8.5.2 8-Aminoquinolines 273
8.5.3 2-Substituted Quinolines 274
8.5.4 Buparvaquone and Its Derivatives 274

8.6 Macrophage-Targeted Drug Delivery Using Nanocarriers 275
8.6.1 Liposomes 275
8.6.2 Nanoparticles 277
8.6.3 Nanodisks 283
8.6.4 Niosomes 283
8.6.5 Emulsions 286
8.6.6 Carbon Nanotubes 287
8.6.7 Transfersomes 287
8.6.8 Other Drug Delivery Systems 288

Biomaterials and Bionanotechnology
DOI: https://doi.org/10.1016/B978-0-12-814427-5.00008-1

© 2019 Elsevier Inc. All rights reserved.

8.7 Prophylactic Vaccines for Leishmaniasis 290
8.7.1 *Leishmanization* 290
8.7.2 *First-Generation Aspirant Vaccines* 291
8.7.3 *Second-Generation Vaccines* 291
8.7.4 *Immunochemotherapy and Therapeutic Vaccines* 291
8.8 Conclusion 292
Abbreviations 292
References 293
Further reading 300

8.1 INTRODUCTION

Leishmaniasis, a vector-borne ailment affecting humans, is caused by different intracellular protozoan species of genus *Leishmania*, of which consequential effects include an infection of macrophages (Renslo and McKerrow, 2006). These parasite protozoans are spread through the bite of an infected female sand fly, *Phlebotomine* species in the Old World (Africa, Asia, the Middle East, and the Mediterranean) and the *Lutzomyia* genus in the New World (South America) that categorized the disease geographically. Such species transmit the blood meal of an infected individual to another person leading to disease transmission, where it replicates in macrophages of the mononuclear phagocytic system (MPS) (Berman, 2005; Mandell et al., 2005). Infection may also be blood borne, can transpire subsequent to organ transplantation, or may even be transmitted congenitally.

There are over 20 known species of *Leishmania* that infect human beings as discussed in Table 8.1. The consequences of infection are based on *Leishmania* parasite species and the host precise immune response (Roberts, 2006). Leishmaniasis is a public health issue worldwide and affects about 12 million people in 88 countries, where 350 million people live and are at the threat of infection mainly in sheltered rural areas (Maltezou, 2010). An average of 2 million new cases are reported yearly [1.5 million for cutaneous leishmaniasis (CL) and 500,000 for visceral leishmaniasis (VL)] all over the world with 90% of them in Asia (India, Bangladesh, and Nepal) (World Health Organization, 2010), Sudan, Ethiopia, and Brazil (Jean-Robert, 2008).

VL is considered to be the most widespread and deadliest form of the disease if left untreated, and therefore, it has been included in the top 10 life-threatening infective circumstances by the World Health Organization. In India, about 100,000 cases of VL are assessed annually and it has been noticed that it is changing epidemiology as a result of wide immigration of the population and human immunodeficiency virus (HIV)/VL coinfections. The Indian state of Bihar has the most prevalent cases of leishmaniasis accounting for about 50% of the total cases in the Indian subcontinent. *Leishmania* and HIV coinfection are considered to be an "emerging" infectious disease, which enhances the menace of VL development by 100-fold in endemic areas (Daher et al., 2009) with rising manifestation of drug resistance (Guerin et al., 2002). In certain countries, up to 70% of adults have coinfections of leishmaniasis associated with HIV/acquired immunodeficiency syndrome (Cruz et al., 2006).

TABLE 8.1 List of Various *Leishmania* Species and Associated Clinical Types.

	CL	VL	MCL
Old world	*L. major*	*L. donovani*	*L. infantum*
	L. aethiopica	*L. infantum*	*L. major*
	L. kilicki	*L. tropica*	*L. tropica*
	L. tropica		
New world	*L. pifanoi*	*L. infantum*	*L. braziliensin*
	L. panomensis	*L. chagasi*	*L. amazonensis*
	L. guyanensis		
	L. peruviana		
	L. mexicana		
	L. venezuelensis		

CL, Cutaneous leishmaniasis; *MCL*, mucocutaneous leishmaniasis; *VL*, visceral leishmaniasis.

TABLE 8.2 Taxonomy of *Leishmania*.

Kingdom	Protista
Phylum	Euglenozoa
Family	Tripanosomatidae
Order	Kinetoplastida

8.1.1 The Causative Agent: *Leishmania*

The *Leishmania* protozoan, responsible for leishmaniasis, is surrounded by a lipophosphoglycan (LPG) outer sheath. LPG is responsible for resisting the complement system by blocking the oxidative burst response (that takes place through abnormal activation of protein kinase C) and preventing its recognition by natural killer T cells. Subsequently, the macrophages infected by *Leishmania* lead to a reduction in phagocytic capacity of macrophages. These *Leishmania*-infected macrophages then modulate the host immune response and attack on antibodies and T-lymphocytes (Vinet et al., 2011).

The *Leishmania* parasites have adapted heterogeneous environments because of their capacity to alter gene expression that may arise either by amplification of specific gene or by tandem cycles (Singh et al., 2005a,b). This parasite has the ability to survive at varying temperature (from body temperature in the mammalian host to ambient temperature in the sand fly) and pH (neutral pH to highly acidic in the sand fly stomach). The taxonomy of leishmaniasis is shown in Table 8.2.

8.1.2 Life Cycle of *Leishmania*

Leishmania species essentially need two special hosts to complete their biological cycle:

1. An invertebrate insect vector: only the females of *Phlebotomine/Lutzomyia* sand fly species
2. A host: human, dog, or even a wild vertebrate (Balana-Fouce et al., 1998)

The life cycle of leishmaniasis is asexual and involves two stages (Fig. 8.1). The *Leishmania* protozoan is transformed into two forms: the replicative form known as amastigote and flagellar form known as promastigote. Amastigotes are ovoid, nonmotile, and exist in an intracellular stage, located within macrophages phagolysosomal compartments in humans or other vertebrate hosts. Promastigotes are characterized by an elongated shape, motile, and extracellular stage present in the midgut of the sand fly vector. The infection starts through the amastigote-infected blood of a vertebrate host taken by the sand fly during a blood meal. The transformation of amastigote to promastigote begins in the insect gut within hours of ingestion.

The amastigotes get converted to an active motile promastigotes form within 24–48 hours by means of binary division. After a week following ingestion of the infective blood meal, the promastigotes migrate into the sand fly midgut. As the sand fly bites a new host, promastigotes get transmitted to the blood circulation of the new host and rapidly penetrate into neutrophils and macrophages. At this point, the promastigotes are transformed into immotile and again alter in amastigote form.

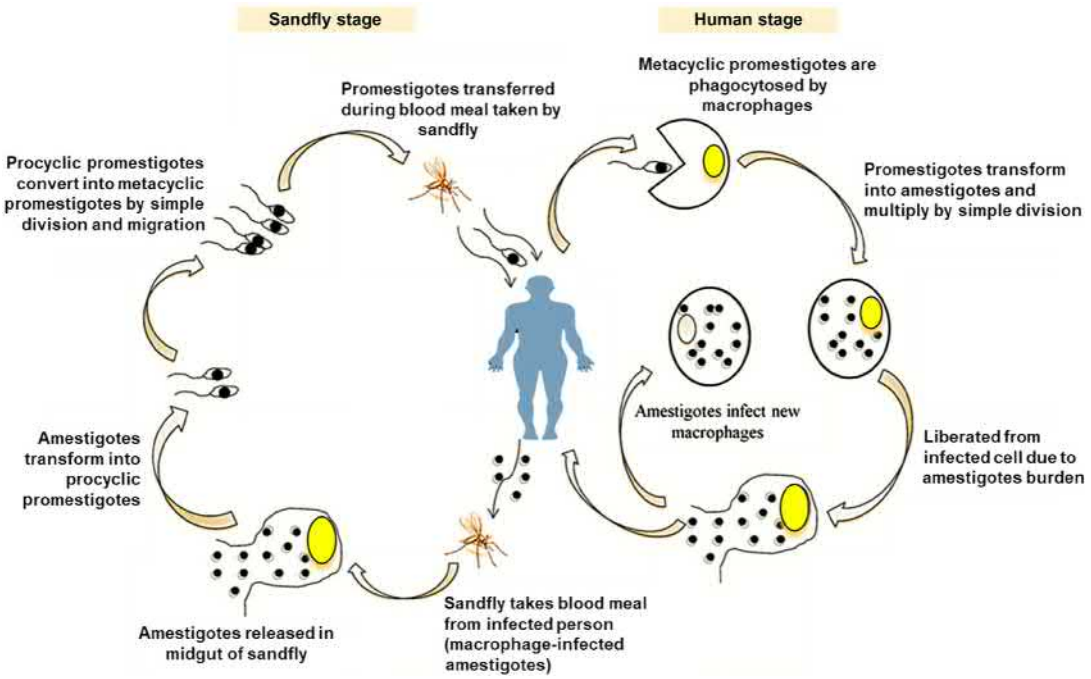
Sandfly stage
Human stage
Promestigotes transferred during blood meal taken by sandfly
Metacyclic promestigotes are phagocytosed by macrophages
Procyclic promestigotes convert into metacyclic promestigotes by simple division and migration
Promestigotes transform into amestigotes and multiply by simple division
Amestigotes infect new macrophages
Amestigotes transform into procyclic promestigotes
Liberated from infected cell due to amestigotes burden
Amestigotes released in midgut of sandfly
Sandfly takes blood meal from infected person (macrophage-infected amestigotes)

FIGURE 8.1 The life cycle of *Leishmania*.

The amastigote is liberated from infected cells less due to its burden and spreads to new cells and different organs, particularly the liver, spleen, and bone marrow. Failure of immune response is mainly as a result of impaired T helper cell type 1 (Th-1) response (Amprey et al., 2004). *Leishmania* parasites are capable to resist the microbiocidal action of acid hydrolases that are released from lysosomes, thus they stay alive and multiply within macrophages. This is a chronic stage that may persist from a few months to years, or even for a lifetime without any noticeable signs or symptoms. Presentation of symptoms and life-altering effects of the parasitic infection depends on the host susceptibility and immunity.

8.1.3 Clinical Manifestations

The protozoan parasite later known to be *Leishmania* was first reported by David D. Cuningham in 1885 (Vannier-Santos et al., 2002). Two independent reports were given by William Leishman and Charles Donovan in 1903 about the protozoan parasite. In addition, James Wright in 1903 proposed this parasite as the genus *Leishmania* (Vannier-Santos et al., 2002). Leishmaniasis has a broad spectrum of clinical manifestations that reveals the heterogeneity between the *Leishmania* species. Hence, leishmaniasis is categorized as VL (kala-azar, black fever, dumdum fever), post-kala-azar dermal leishmaniasis (PKDL), disseminated CL, diffuse CL, and mucocutaneous leishmaniasis (MCL) (Chappuis et al., 2007a,b).

8.1.4 Pathology

8.1.4.1 Visceral Leishmaniasis (Kala-Azar)

Reticuloendothelial hyperplasia develops as a result of leishmanial infection, which affects the liver, small intestinal mucosa, lymph nodes, bone marrow, or other lymphoid tissues and leads to insufficient lymphocytic infiltration. Liver functioning may be varied and production of prothrombin is decreased. Due to depletion of prothrombin, thrombocytopenia and mucosal hemorrhage may occur. The life span of leukocytes and erythrocytes are also decreased, thus leading to granulocytopenia and anemia. The *Leishmania* parasite can also affect the intestine and cause ulceration that may lead to diarrhea. At the crucial stage, death may occur with frequent infections, especially presenting with dysentery, pneumonia, and tuberculosis.

In VL, combined impairment of Th-1 and Th-2 responses takes place. The severity of VL is inversely associated with in vitro lymphoproliferative response. Treatment of such infection increases interferon (IFN)-γ and interleukin (IL)-12 while it decreases IL-10, at the same time altering the growth factor-β. It has been also reported that during effective therapy of active VL, $CD4^+$and $CD25^+$ T cells are increased and decreased, respectively.

8.1.4.2 Post-Kala-Azar Dermal Leishmaniasis

PKDL is a result of VL and is identified by a maculopapular, macular, or nodular rash with edema and proliferation of capillaries. In such circumstances, numerous parasites are shown by more frequent erythematous and nodular forms. During PKDL, the expression of IFN-α receptor 1 and tumor necrosis factor (TNF)-R1 and TNF-R2 receptors are

decreased, affecting the effective host response. Immunoglobulins (Ig)G3, IgG1, and IL-10 serum levels are increased in patients of PKDL. The level of IL-10 expressing $CD3^+CD8^+$ lymphocytes becomes reduced with treatment. In VL, the presence of high serum concentrations of IL-10 results in PKDL development. Using antiretroviral therapy during HIV coinfected leishmaniasis may also lead to PKDL.

8.1.4.3 Disseminated Cutaneous Leishmaniasis

A cell-mediated immunity, delayed-type hypersensitivity, and *Leishmania*-specific antibody production against *Leishmania* antigens are present in disseminated CL, but weaker when compared with localized CL.

8.1.4.4 Diffuse Cutaneous Leishmaniasis

In diffuse CL, there is lack of cell-mediated immunity, which may be recognized by severe dermal infiltration of vacuolated, parasite-burdened macrophages, the death of lymphocytes, necrosis, and ulceration. The treatment of such form of leishmaniasis is difficult with high chances of relapses following therapy.

8.1.4.5 Mucocutaneous Leishmaniasis

In the mucocutaneous form of this disease, lesions are similar to those observed in CL. But due to the nonspecific cellular reactions, ulceration that is different from the cutaneous form is observed in MCL. It may also cause infiltration of lymphocytes, macrophages, and plasmocytes. Rarely, necrotic and granulomatous reactions, which are responsible for the enlargement of a granuloma at the site of necrosis, take place along with degeneration of fibrinoids. Most important pathogenetic characteristics include coagulative necrosis of blood vessel walls. At this stage, lesions may induce an epithelioid granuloma (tuberculoid type) or relapse of exudation reaction.

The lesions mostly arise in the deep nasal mucosa because of the presence of amastigotes on proliferating vascular endothelium that is related to the perivascular cellular infiltrate and liquefaction of cartilage. Mucosal leishmaniasis is also related to the polymorphism in TNF-I promoter sequences. Therefore the TNF-I synthesis inhibitor, such as pentoxifylline, may be used along with antimonial agents for handling dermal leishmaniasis.

8.2 DIAGNOSIS

Leishmaniasis has broad clinical manifestations, which makes it more complicated to diagnose the various forms. Moreover, clinical manifestations of other disease conditions are also found similar to leishmaniasis. These similarly presenting disease conditions that are also frequently found in *Leishmania* endemic regions include leprosy, tuberculosis, skin cancers, cutaneous mycoses as CL, and schistosomiasis or malaria as VL (Silvestre et al., 2009). Thus specific and sensitive diagnostic tests are needed for successful diagnosis, treatment, and subsequent disease control.

8.2.1 Parasitological Diagnosis

Parasitological diagnosis of leishmaniasis is used due to high specificity. Giemsa or Leishman stain is generally used for histopathological diagnosis of malaria and other parasites that allow for differentiation of their types. In Giemsa- or Leishman-stained samples, the amastigote form of *Leishmania* protozoan parasite, also known as LD bodies, are found in tissue smears in cases of CL. Whereas in cases of VL, amastigotes are present in lymph nodes, spleen, or bone marrow aspirates. The sensitivity of this method is highest for the spleen (93.1%−98.7%), the bone marrow (53%−85%), or lymph node (52%−58%), respectively (Siddig et al., 1988).

8.2.2 Serological Diagnosis

Various serological diagnostic tests are used for the diagnosis of leishmaniasis based on their sensitivity, specificity, and the presence of specific humoral responses.

Some commonly used serological diagnostic tests are:

- Enzyme-linked immunosorbent assay (ELISA): This test has been used for diagnosis of VL. Its specificity and sensitivity are based on the type of antigen used. rK39 has mostly used antigen that shows their potential in the detection of leishmaniasis along with in HIV coinfected patients.
- Indirect fluorescent antibody test (IFAT): This test depends on the recognition of antibodies at early stages of infection. It indicates the possibility of relapse when a low number of antibody persistence is observed.
- Immunoblotting test: This test is much more sensitive than ELISA and IFAT in the diagnosis of VL by means of providing information about antibodies that respond to the various specific leishmaniasis antigens.
- Agglutination test: These tests are based on the agglutination of *Leishmania donovani* stained promastigotes in the presence of a serum containing antileishmanial antibodies.

The number of limitations that are associated with the *Leishmania* endemic regions may be improved by developing new diagnostic tests that are easy to perform, low cost, reproducible, and fast. As a result of research and development in the area of diagnostic tests, two serological tests have been validated and adapted for such situations: the fast agglutination screening test, which is a modified form of the direct agglutination test, and the rK39-immunochromatography or dipstick-based test (Silva et al., 2005; Farahmand et al., 2015).

8.2.3 Molecular Diagnosis

Molecular diagnostic tests are also used to identify *Leishmania* parasites. The most frequently used molecular diagnostic test is the polymerase chain reaction (PCR) test. PCR is a very specific and sensitive method for the recognition of *Leishmania* parasites, even when samples contain very low quantities of parasites (Garcia et al., 2005). This technique is more significant for the detention of *Leishmania* in HIV coinfected persons (De Doncker et al., 2005). This test also increases the chances of detection of the *Leishmania* species along

with providing a prediction of severity. The insights provided by PCR testing have implications for the selection of treatment options, which makes the method highly noteworthy in clinical disease management (Murray et al., 2005).

8.2.4 Antibody Detection Diagnostic Tests

The antibody detection diagnostic tests use antibodies and their cross-reactivity to detect leishmaniasis, however, these tests fail to distinguish between acute and asymptomatic disease. Therefore an antigen-based diagnostic test has been developed for the diagnosis of VL. These tests are based on the recognition of a thermostable, low molecular weight carbohydrate antigen in urine of patients suffering from VL (Attar et al., 2001; Sarkari et al., 2002).

8.3 CURRENTLY USED DRUGS FOR THE TREATMENT OF LEISHMANIASIS

Most of the medicines used for the treatment of leishmaniasis have many drawbacks, such as being expensive, difficult to administer, having toxicity, and most importantly the development of drug resistance in parasites. Drug resistance is generally associated with antimonial agents, making conventional therapies ineffective at controlling the diseases. Hence, there is an incredible requirement of developing novel and more efficient antileishmanial therapies that overcome all the drawbacks mentioned earlier (Mishra et al., 2007).

8.3.1 Antimonial Agents

Antileishmanial drugs that have the most valuable therapeutic applications at this time are recognized as antimonial agents, for example, sodium stibogluconate (Pentosam) and meglumine antimoniate (Glucantime). Therefore antimonial agents are the drug of choice for VL. The antimonial agents act by inhibiting various parasitic proteins, mainly enzymes that take part in glycolysis and oxidation of fatty acids (Moore et al., 2001). They may also cause serious side effects, such as pain at the injection site, gastrointestinal tract problems, cardiotoxicity, and stiff joints. Renal and hepatic insufficiencies may also be observed in some cases.

8.3.2 Pentamidine

Pentamidine is considered to be the first drug used in patients with disease intractable to sodium stibogluconate (Chakravarty and Sundar, 2010). It acts by inhibiting pathogen genome replication and transcription at the mitochondrial level. The pentamidine dose regimen consists of 4 mg/kg three times in a week until clinical treatment was achieved; however, its efficacy has been regularly declining over the years, possibly due to drug resistance. It effectively treats about 70% of patients and causes severe adverse events including hypoglycemia, shock, and may also be fatal in some cases (Jha et al., 1991).

8.3.3 Amphotericin B

Amphotericin B (AmB), a polyene antibiotic, is frequently used in the treatment of VL due to side effects and development of drug-resistant associated with antimonial therapy. AmB has a selective action against fungi and *Leishmania* protozoan parasite due to its greater affinity toward 24-substituted sterols like episterol and ergosterol. Regosterol and episterol are major components in the plasma membrane of eukaryotic microorganisms (Mishra et al., 2007). The National Expert Committee of India has suggested AmB as the first-line drug for the treatment of VL particularly in areas that show disease intractable to sodium stibogluconate or other antimonial agent therapies.

8.3.4 Miltefosine

Initially, miltefosine was developed as an antitumor agent but was additionally found to have significant efficacy against leishmaniasis. It was registered as the first orally administered antileishmanial drug and also approved in India as a VL treatment at a dose of 50−100 mg (∼2.5 mg/kg) for 4 weeks (Sundar et al., 2002). It is considered to be safe and effective in pediatric patients of VL (Bhattacharya et al., 2004). Its mode of action against *Leishmania* has been not well defined. Miltefosine is not only responsible for the cytotoxic effect on the parasite but also on the cellular immunity activation (Mishra et al., 2007).

8.3.5 Paromomycin

Paromomycin is an aminoglycoside antibiotic that possesses antileishmanial activity. It provides synergistic effects with antimonial drugs; thus it has been used effectively in India (Jha et al., 1998). Recently in India, phase III open-label clinical studies of this drug have found paromomycin as a superior drug compared with conventional therapies for the treatment of VL (Sundar et al., 2007).

8.4 COMBINED THERAPY

Combined therapies have been suggested to improve the efficacy of treatment along with the avoidance of drug resistance development in the parasite with the goal of ultimately decreasing the duration of therapy (Bryceson, 2001). For example, combined therapy of recombinant IFN-γ and pentavalent antimonial drugs have been clinically evaluated and were revealed as effective severe VL or pentavalent antimonial-intractable VL treatment in Brazil. But such combined therapy of recombinant IFN-γ and pentavalent antimonial drugs was not found as effective in a large randomized clinical study that was performed in India.

Combination therapies also include antileishmanial drugs and immunomodulators, which help in improving the complex manifestations of the disease. Seifert et al. proposed a DNA vaccine enriched with a T-cell epitope (LEISHDNAVAX) together with a standard

TABLE 8.3 List of Currently Used Antileishmanial Drugs.

Treatment	Mode of Action	Recommended Dose	Clinical Efficacy	Limitation
Pentavalent antimonials (sodium stibogluconate) (Pentostam)	Act by inhibiting the various parasitic proteins	20 mg/kg/day in two divided doses for 30 days, IM or IV	Standard pentavalent antimonial compounds show curative rate as high as 90%−100% in areas not plagued by resistance	Limited information regarding the chemistry and mode of action. Cardiotoxicity, renal insufficiency pancreatitis, anemia, leucopenia, a headache, nausea, vomiting, abdominal pain on long-term administration
Pentamidines [Dimedene analogs such as mepacrine, pentamidine isethionate (Pentam-300)]	Binds to tRNA and inhibits aminoacylation and translation of the replicating parasite	2−4 mg/kg every other day for up to 15 doses, IM	A study from Surinam found pentamidines have a 90% curative rate	Emergence of drug resistance, especially in HIV coinfections. Adverse reactions of injectable form of pentamidine are hypotension, hypoglycemia leucopenia, thrombocytopenia, cardiac arrhythmia, acute renal failure, elevated serum creatinine level, nausea, fever
Amphotericin B (polyene antibiotics)	Binds with the ergosterol of the parasitic cell membranes, thus forming a binary complex with the membrane sterols resulting in pores that cause changes in membrane permeability and ionic balance, leading to parasitic cell death	1 mg/kg every another day for up to 20 days, IV	N/A	Poor gastrointestinal absorption and negligible bioavailability. Also may react with mammalian cell membrane causing cellular dysfunction
Paromomycin (an aminocyclitol-aminoglycoside antibiotic)	Impairs the macromolecular synthesis and alters the membrane properties of *Leishmania*	16 mg/kg up to 21 days, IM	N/A	Mainly used in the CL and it has limited use in the treatment of VL
Miltefosine	Mechanism of action is uncertain, possibly inhibition by phosphatidyl online biosynthesis, signal transduction, and regulation of calcium homeostasis	2.5 mg/kg up to 4 weeks, orally	N/A	Development of quick drug resistance

CL, Cutaneous leishmaniasis; *HIV*, human immunodeficiency virus; *VL*, visceral leishmaniasis.

antileishmanial drug for the treatment of VL. This vaccine improved the efficacy of a single dose of liposomal AmB in C57BL/6 mice (Seifert et al., 2015). Another combined therapy of paromomycin and sodium stibogluconate was found to be most effective compared with others in patients residing in Sudan, Kenya, and India. On the basis of such clinical studies, the combined therapies are shown to be more successful and even decrease the duration of therapy required for clinical response (from 30 to 17–21 days) compared with a single therapy with sodium stibogluconate (Melaku et al., 2007). Trinconi et al. demonstrated the antileishmanial activity of tamoxifen and miltefosine combinations. The in vitro and in vivo studies in *Leishmania amazonensis*–infected BALB/c mice did not report any interaction between tamoxifen and miltefosine. Tamoxifen hindered the emergence of miltefosine resistance (Trinconi et al., 2016). A new combination of AmB liposomes and miltefosine has been recently assessed in India (Chappuis et al., 2007a,b). Currently used antileishmanial drugs are presented in Table 8.3.

8.5 OTHER DRUGS USED FOR LEISHMANIASIS

8.5.1 Sitamaquine

Sitamaquine is another orally administrated drug intended for handling leishmaniasis. It is in a developmental stage and so far, has not much evidence has been made available related to its efficacy and toxicity. It is responsible for the modification of parasite morphology. It has been shown to be well tolerated and efficacious at different dose levels under a randomized controlled open-label and multicenter phase II clinical trial in India (Jha et al., 2005) and Kenya (Wasunna et al., 2005).

8.5.2 8-Aminoquinolines

The 8-aminoquinolines (WR6026, lepidine) are antimalarial drugs, but they have also been shown to have activity against *Leishmanial* protozoan parasites. Another 8-aminoquinoline known as the (−) enantiomer NPC1161 had demonstrated promising activity against *L. donovani* in vivo similar to sitamaquine. In the same study, the stereoselective variations in drug performance and toxicity were found during assessment as racemate mixture of (−) or (+) enantiomers (Nanayakkara et al., 2008). In vitro performances of 8-aminoquinolines derivatives against *L. donovani* promastigotes along with their synthesis have been reported (Jain et al., 2005; Kaur et al., 2007). These derivatives involved substitution with a 5-(3-trifluoro methylphenoxy) on the quinoline ring (tafenoquine has antiparasitic activity) (Tekwani and Walker, 2006), as well as methyl-substituted, ethyl-substituted, or unsubstituted C4 positions (Fournet et al., 1993).

8.5.3 2-Substituted Quinolines

In the beginning, 2-substituted quinoline alkaloid was obtained from a Bolivian medicinal plant (*Galipea longiflora Kr*, Rutaceae) and was found to have promising activity in the treatment of New World CL in clinical trial stage (Fournet et al., 1993). Later, the performance of 2-substituted quinoline alkaloids in an *L. donovani* BALB/c mouse model was reported to be significantly active following oral administration of 2-*n*-propylquinoline, as well as with chimanine D following subcutaneous administration (Fournet et al., 1994). Current structure−activity relationship studies on 2-substituted quinolines resulted in the discovery that the substitution of the three-carbon alkenyl side chain with reactive electrophilic functions such as carbonyl, hydroxyl, or halogen have the most activity against and *L. amazonensis* and *Leishmania infantum* amastigotes in vitro (Fakhfakh et al., 2003). The selected compounds exhibited significant efficiency against *L. donovani*− and *L. amazonensis*−infected BALB/c mice after oral administration. A compound containing propenyl chain functionalized by an −OH group demonstrated acceptable activity in vivo (Nakayama et al., 2005).

8.5.4 Buparvaquone and Its Derivatives

Buparvaquone was more efficient against *L. donovani* amastigotes in vitro and in vivo in a BALB/mouse model (Croft et al., 1992). Chemical derivatization is an efficient approach to improve oral bioavailability of poorly soluble compounds. In vitro activity of water-soluble phosphate prodrugs of buparvaquone has been demonstrated against a variety of *Leishmania* species along with half-maximal effective concentration (EC_{50}) values. They showed potent in vitro activity against the intracellular amastigote stage of CL and VL caused by a variety of *Leishmania* species in micromolar to the nanomolar range (Mäntylä et al., 2004a). The oxime derivatives were also examined and show less in vitro activity against *L. donovani* in comparison to the parent compound (Mäntylä et al., 2004b). Topical application of buparvaquone and its prodrug (3-phosphono-oxymethyl-buparvaquone) were prepared and evaluated using in vitro human and mouse skin models, and using in vivo models of VL and CL (Garnier et al., 2007). A list of plants showing potent antileishmanial activity is presented in Table 8.4.

TABLE 8.4 List of Plants Shows Antileishmanial Activity.

Plants With Antileishmanial Activity	Plant Family	Part(s) Used	References
Tridax procumbens	Asteraceae	Whole plant	Martín-Sánchez et al. (2007), Martín-Quintal et al. (2009)
Urechites andrieuxii	Apocynaceae	Leaves and roots	Pulido and Serralta (1993), Argueta (1994), Chan-Bacab et al. (2003)
Desmodium gangeticum	Fabaceae	Whole plant	Iwu et al. (1992), Singh et al. (2005a,b)
Pseudelephantopus spicatus	Asteraceae	Leaves, aerial parts	Odonne et al. (2011)
Himatanthus sucuuba	Apocynaceae	Stem bark	Villegas et al. (1997), Castillo et al. (2007)
Azadirchta indica	Meliaceae	Stem bark	Tahir et al. (1998)

(*Continued*)

TABLE 8.4 (Continued)

Plants With Antileishmanial Activity	Plant Family	Part(s) Used	References
Maytenus senegalensis	Celasteraceae	Stem bark	Tahir et al. (1998)
Pseudocedrelakotsc ifye	Meliaceae	Stem bark	Tahir et al. (1998)
Balanites aegyptiaca	Balanitaceae	Seeds, stem bark	Tahir et al. (1998)
Eucalyptus globules	Myrtaceae	Seeds	Tahir et al. (1998)
Acanthospermum spidum	Asteraceae	Aerial parts	Bero et al. (2011)
Cymbopogon citratus	Poaceae	Leaves	Santin et al. (2009)
Peschiera australis	Apocynaceae	Stem	Delorenzi et al. (2001)
Lantana ukambensis	Verbenaceae	Stem, leaves	Sawadogo et al. (2012)
Chondodendrontom entosum	Menispermaceae	Bark and leaves	González-Coloma et al. (2012)
Cedrelaodorata L.	Meliaceae	Bark	González-Coloma et al. (2012)
Pentacaliadesidera bilis	Asteraceae	Leaves	Morais et al. (2012)
Drimysbrasiliensis miers	Winteraceace	Stem barks	Corrêa et al. (2011)
Polyalthia longifolia	Annonaceae	Leaves	Misra et al. (2010)
Valeriana wallichii	Valerianaceae	Roots	Ghosh et al. (2011)

8.6 MACROPHAGE-TARGETED DRUG DELIVERY USING NANOCARRIERS

Appropriate strategies are required for targeting antileishmanial drugs directly to where protozoan parasites exist, in the macrophages, for effective treatment of leishmanial infection. The improved therapeutic efficacy of drugs may be achieved along with minimal toxicity by using nanocarrier delivery systems. The concept of drug targeting to the macrophage cells using various antileishmanial agents have been used through the incorporation of drug delivery systems, such as nanoparticles, liposomes, multilamellar vesicles, microspheres, and emulsions. The use of bioactive molecules derived from plants may also be incorporated in various carrier systems as alternative strategies (Table 8.4). Various strategies implemented by modifying accomplishments for chemotherapeutic delivery of the antileishmanial drugs to the cells of the reticuloendothelial system (RES) through passive or active targeting are discussed later. These drug delivery systems should be able to deliver the drug with high efficiency, reduced dosing, and adequate safety (Ganeshpurkar et al., 2014).

8.6.1 Liposomes

Liposomes are well-established carriers for the delivery of a variety of bioactives (Maheshwari et al., 2012; Bansal et al., 2016). The major drawback associated with drug

delivery via liposomes is their rapid accumulation in the RES macrophages, which makes them unavailable for delivering their encapsulated bioactive cargo to their intended side of action (Soni et al., 2016). However, this drawback of liposomes has shown beneficial effects in antileishmanial therapy because the parasite resides in the RES macrophages. Alving et al. (1978) first confirmed the efficacy of drug delivery via liposomes in hamsters. The liposomal drug delivery systems provide effective treatment along with reduced toxicity associated with antileishmanial drugs, especially those associated with antimonial agents. Antimonial agents-loaded liposomes have been reported to be 700 times more effective than free drug (Date et al., 2007). Also, AmB-loaded liposomes have been found to be two to five times more active than free AmB drug, while 350−750 times more active compared with meglumine antimoniate in investigational leishmaniasis treatment. Several marketed formulations of AmB as Abelcet (AmB lipid complex), AmBisome (liposomal AmB), and Amphocil (AmB colloidal dispersions) are available. Of these, only AmBisome has proven maximum efficacy and received approval for leishmaniasis treatment (Mondal et al., 2010). Several strategies have attempted to enhance macrophage uptake of drugs and carriers. Surface modification of antileishmanial drug encapsulated liposomes by using mannose and fucose has been evaluated in a hamster model and has shown more effective antileishmanial drug delivery to phagocytic cells via functionalized liposomes compared with nonfunctionalized liposomes or free drug (Sinha et al., 2000).

Palmitoyl mannose and 4-SO4GalNAc modified AmB-loaded liposomes have also been reported for enhanced macrophage-specific targeting (Singodia et al., 2010a,b). Sinha et al. (2000) revealed that mannosylated andrographolide bearing liposomes lower the parasitic burden in the spleen, with less hepatic and renal toxicity than unmodified liposomes or free drug. In vitro antileishmanial activity of pentamidine isethionate and its analogs have been examined in mannose bearing liposomes (Banerjee et al., 1996). Date et al. demonstrated neoglycoprotein-altered liposomes to improve the targeting potential of hamycin to *Leishmania*-infected macrophages. Mannose and neoglycoprotein grafted hamycin-loaded liposomes were found to be more effective in reducing intracellular amastigotes burden up to 1.5−10 times higher than unconjugated liposomes and free drug (Date et al., 2007).

Cationic liposomes that consist of stearylamine and phosphatidylcholine decrease the hepatic parasite burden due to the reversible electrostatic interaction between parasite plasma membranes and cationic liposomes. As a result, the cell membrane and cellular organization of the *Leishmania* parasite get damaged (Dey et al., 2000). Cationic liposomes bearing oligonucleotides that are complementary to the *Leishmania*-specific mRNA sequences have been reported to reduce parasite burden. Cationic liposomes enhanced antisense oligonucleotide efficacy by about three times in comparison to uncoated oligonucleotides (Dasgupta et al., 2002). Cationic liposomes activate the CD8 + T-cell response when combined with *L. donovani* promastigote membrane antigens that shown successfully interaction with antigen-presenting cells (Bhowmick et al., 2010). Cationic and mannosylated liposomes were also examined for in vivo antileishmanial activity on *L. donovani*−infected golden hamsters. The results confirmed the maximum reduction in parasite load for the developed mannosylated cationic liposomes (Rathore et al., 2011).

Sinha et al. investigated a cationic liposomal delivery system bearing sodium stibogluconate designed for the treatment of sodium stibogluconate-sensitive and sodium stibogluconate-resistant *L. donovani* infections. Sodium stibogluconate encapsulated

cationic liposomes were found to be effective against both sodium stibogluconate-sensitive and sodium stibogluconate-resistant *L. donovani* infections in BALB/c mice (Sinha et al., 2015). Agrawal and Gupta (2000) revealed that liposomal surface modification with macrophage activating peptides, such as tuftsin, improves the antileishmanial activity of the liposomes as well as function as immunomodulators through MPS activation against infections. The immunoglobulin antibodies coupled liposomes containing antileishmanial drugs improved the macrophage targeting as well as antileishmanial activity (Kole et al., 1999). The bioactives derived from plant origin also possess antileishmanial activity, such as Bacopasaponin C from *Bacopa monniera* (Sinha et al., 2002) and amarogentin from *Swertia chirata* (Medda et al., 1999). The liposomal formulations of harmine and quercetin have been reported more efficient and not as toxic compared with free drugs (Sarkar et al., 2002; Lala et al., 2004). Basu (2005) investigated two native glycosides encapsulated together (i.e., acaciaside, which has glucose as an end sugar; and asiaticoside, which has rhamnose as an end sugar) in liposomes.

Carvalheiro et al. explored antileishmaniasis activity of dinitroaniline analogs incorporated into liposomal formulations. The dinitroaniline, trifluralin encapsulated liposomal formulation, has been found to be active against *Leishmania*-infected promastigotes as well as in intracellular amastigotes when studied in a murine model of VL with reduced cytotoxicity and hemolytic activity (Carvalheiro et al., 2015). Varikuti et al. (2017) evaluated the penetration of AmB encapsulated nanoliposomal formulation to the skin of *Leishmania mexicana*–infected mice in the nonulcerated (129SVE) and ulcerated (BALB/c) models. They found a transient decline in lesion sizes in 129SVE mice but found no decline in lesion sizes in BALB/c mice (Fig. 8.2) (Varikuti et al., 2017).

Wijnant et al. (2018) compared the efficiency of AmB liposomal formulations Fungisome (F) and AmBisome (A) on *Leishmania major* BALB/c murine model of CL. They found higher toxicity and lower efficacy of Fungisome (F) than AmBisome (A) (Fig. 8.3).

The major drawbacks of liposomal formulations are the drug leakage into the systemic circulation and long-lasting disposition that may cause unnecessary distracted accumulation of drugs leading to toxicity. To overcome these drawbacks, polymeric drug delivery systems as mentioned below have been promoted (Barratt and Bretagne, 2007).

8.6.2 Nanoparticles

In today's scenario, nanoparticles in the field of medicine have gained much attention (Asati et al., 2019; Tekade et al., 2017b; Pandey et al., 2015; Maheshwari et al., 2015a; Sharma et al., 2015). Polymeric nanoparticles have been planned for macrophage drug targeting due to their prolonged circulation time along from the plasma by the MPS. The antileishmanial action of AmB with biodegradable poly(ε-caprolactone)-based nanoparticulate carrier systems have improved and declined the toxicity related to AmB (Espuelas et al., 2002). AmB encapsulated in nanoparticles reduces the parasitic load in *Leishmania*-infected mice up to two to three times more efficiently compared with free AmB and reduces the side effects related to AmB administration.

Nicoletti et al. (2009) reported antileishmanial activity of AmB conjugated hydroxypropyl methacrylamide (HPMA). 8-Aminoquinoline formulated with HPMA as a copolymer

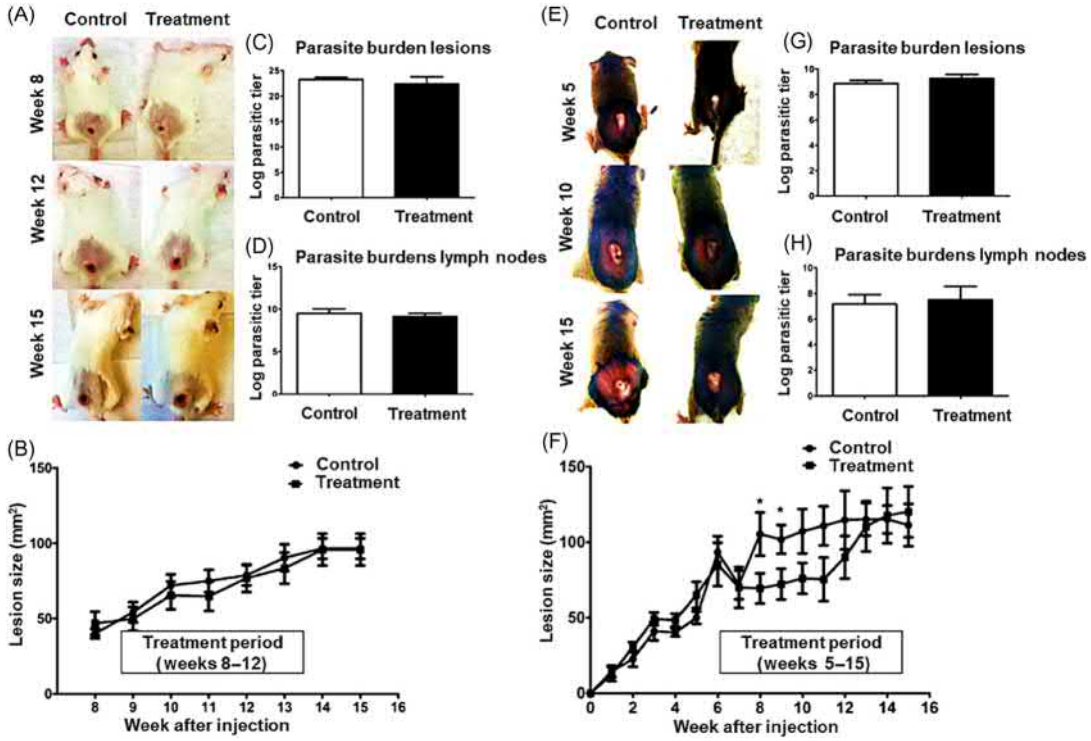

FIGURE 8.2 Evaluation of the efficacy of topical nanoliposomal amphotericin B treatment on *Leishmania mexicana*–infected BALB/c and 129SVE mice. BALB/c and 129SVE mice were infected with 5×10^6 stationary-phase *L. mexicana* promastigotes via subcutaneous injection in their shaven back rumps. After mice developed ulcerated lesions (BALB/c at week 8 and 129SVE at week 5), mice with similarly sized lesions were randomized and treated with SinaAmphoLeish 0.4% or Vaseline (control) twice a day. Representative images of BALB/c (A) and 129SVE (E) mice with back rump lesions from treatment and control groups. Lesion sizes of BALB/c (B) and 129SVE (F) mice expressed as mean lesion sizes (mm^2) ± SE. Parasitic loads expressed as the largest log dilution that represents live parasites in cultures obtained from lesions of BALB/c (C) and 129SVE (G) mice. Parasitic loads expressed as the largest log dilution that represents live parasites in cultures obtained from lymph nodes of BALB/c (D) and 129SVE (H) mice. Data represent the means ± SE from one of the two similar experiments ($n = 5$ mice per group). *$P < .05$ (student's unpaired *t*-test). *Source: Adapted with permission from Varikuti, S., Oghumu, S., Saljoughian, N., Pioso, M.S., Sedmak, B.E., Khamesipour, A., et al., 2017. Topical treatment with nanoliposomal amphotericin B reduces early lesion growth but fails to induce cure in an experimental model of cutaneous leishmaniasis caused by* Leishmania mexicana. *Acta Trop. 173, 102–108.*

was demonstrated to show antileishmanial activity. Gaspar et al. (1992) investigated polyalkyl cyanoacrylate (PACA) nanoparticles loaded with primaquine against *L. donovani* and reported that PACA nanoparticles were 21-fold more efficient as compared with free primaquine.

Similarly, in vitro studies have revealed that the pentamidine bearing methacrylate nanoparticles were 25-fold more efficient compared with the free drug while in vivo studies have shown that pentamidine nanoparticles were more effective at reducing the

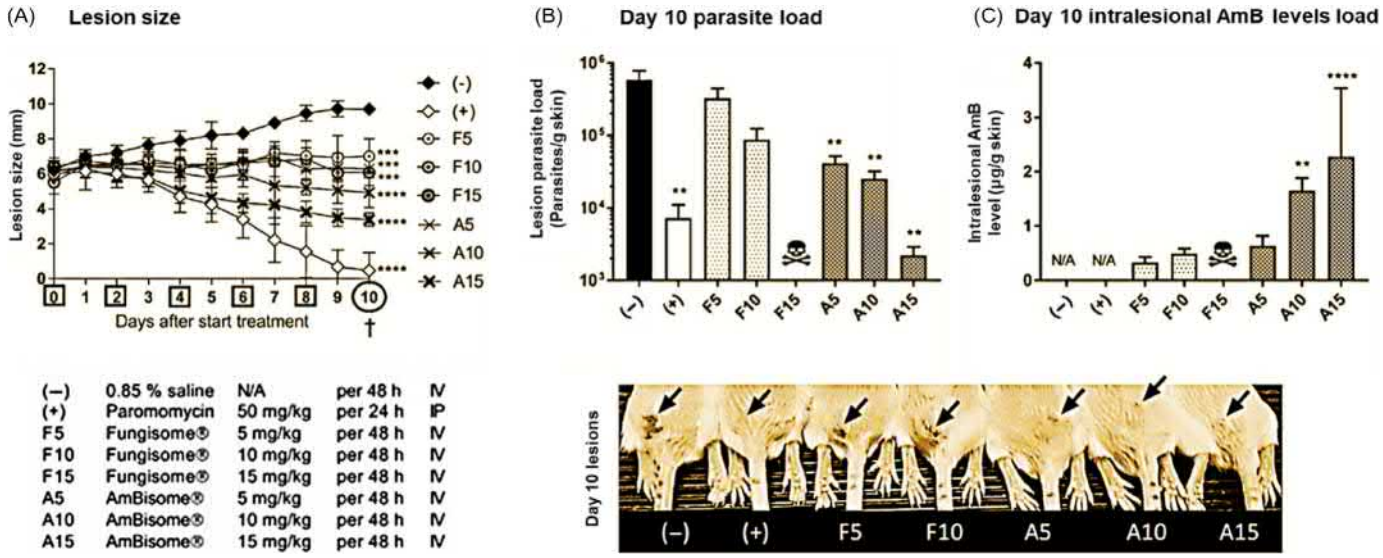
(A) Lesion size
Lesion size (mm)
Days after start treatment
(-)
(+)
F5
F10
F15
A5
A10
A15
(B) Day 10 parasite load
Lesion parasite load (Parasites/g skin)
(C) Day 10 intralesional AmB levels load
Intralesional AmB level (µg/g skin)
N/A
Day 10 lesions
(–) 0.85 % saline N/A per 48 h IV
(+) Paromomycin 50 mg/kg per 24 h IP
F5 Fungisome® 5 mg/kg per 48 h IV
F10 Fungisome® 10 mg/kg per 48 h IV
F15 Fungisome® 15 mg/kg per 48 h IV
A5 AmBisome® 5 mg/kg per 48 h IV
A10 AmBisome® 10 mg/kg per 48 h IV
A15 AmBisome® 15 mg/kg per 48 h IV

FIGURE 8.3 Comparative efficacy of the liposomal AmB formulations AmBisome (A) and Fungisome (F) in the *Leishmania major* BALB/c model of CL. Mice received 10 doses of 50 mg/kg paromomycin [IP, (+)] or five doses of either 0.85% saline [untreated negative control (–)] or 5, 10, and 15 mg/kg F and A (IV). During treatment, lesion size was measured daily (A). On day 10, lesion skin samples were collected and parasite load (B) and AmB levels (C) in the tissue were evaluated. The photo on the bottom shows the CL lesions (*arrow*) on the rump of the mice on day 10. Each point represents the mean ± SD ($n = 4–5$ per group). ANOVA (one-way for parasite load and intralesional AmB level, repeated measures for lesion size) followed by Tukey's multiple comparison tests were used to analyze differences between untreated controls and experimental groups. A P value $<.05$ was considered statistically significant ($^{*}P < .05$, $^{**}P < .001$, $^{***}P < .0005$, $^{****}P < .0001$), $P > .05$ not significant (no marking above bar). †Day of sacrifice. Skull: no data available due to lethal toxicity at this dose level. *AmB*, Amphotericin B; *CL*, cutaneous leishmaniasis; *N/A*, not applicable. *Source: Adapted with permission from Wijnant, G.J., Van Bocxlaer, K., Yardley, V., Harris, A., Alavijeh, M., Silva-Pedrosa, R., et al., 2018. Comparative efficacy, toxicity and biodistribution of the liposomal amphotericin B formulations Fungisome and AmBisome in murine cutaneous leishmaniasis. Int. J. Parasitol. Drugs Drug Resist. 8 (2), 223–228.*

parasite burden of liver along with decreasing adverse effects related to drugs (Paul et al., 1998). The cytotoxicity of poly(D,L-lactide) nanoparticles loaded with pentamidine on J774 macrophages cells was assessed and compared with the unloaded nanoparticles and free pentamidine isethionate. Pentamidine loaded nanoparticles showed a half-maximal inhibitory concentration (IC_{50}) value, which is considerably lower than the free drug (0.39 vs 6.5 g/mL) (Paul et al., 1998).

In a recent study, Pandya et al. reported the efficiency of nitric oxide (NO) against *L. donovani* by incorporating diethylenetriamine NO (prodrug) into poly(lactide-*co*-glycolide) nanoparticles with or without codelivery of AbB. Nanoparticles-encapsulated AmB and diethylenetriamine NO killed about 98% of promastigotes and about 76% of amastigotes compared with the nanoparticles bearing either diethylenetriamine NO or AmB alone, when tested in vitro. Nanoparticles encapsulated with both diethylenetriamine NO and AmB was found to be more effective than Ambisome. The results of the study revealed that delivery of NO to the cytosol of *Leishmania*-infected macrophages demonstrated intrinsic activity and is helpful in the effectiveness of AmB. Nanoparticles bearing only fluorescein isothiocyanate (FITC) were taken up keenly by J774 mouse macrophages in culture on exposing to 2 hours as compared with AmB bearing particles (Fig. 8.4A). J774 macrophages culture supernatants when exposed to a solution of diethylenetriamine NO or to

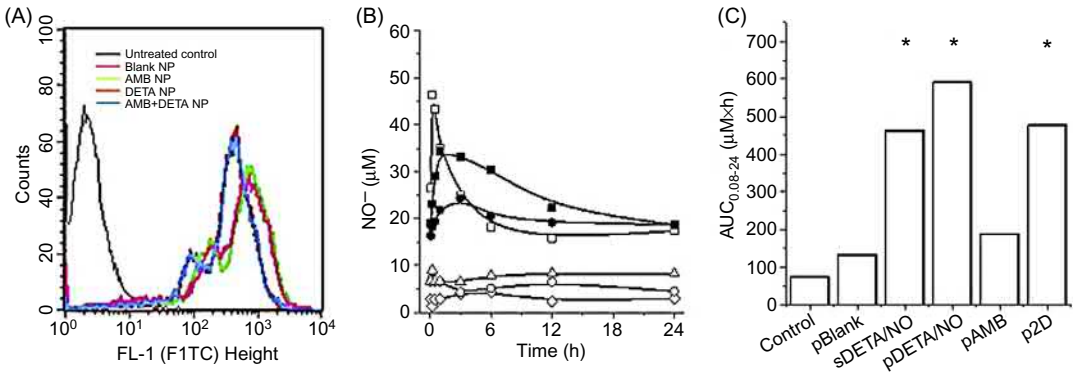

FIGURE 8.4 Uptake of particles and production of NO by J774 cells in 30 min of exposure. (A) Fluorescence acquired by cells exposed to (1) no particles, (2) blank particles, (3) AMB particles, (4) DETA/NO particles, and (5) two-drug particles. (B) Nitrite in culture supernatant following exposure to 50 μM DETA/NO in solution (*open squares*) or particles (*filled squares*). Particles containing both DETA/NO and AMB (*filled circles*) yielded a final theoretical concentration of 25 μM DETA/NO, generating a profile of lower levels of NO secretion. Particles containing AMB alone (*open triangles*) or no drug (*open circles*) did evoke NO release that was significantly different from untreated cells (*open diamonds*). Means ($N = 2$) of the data are shown. (C) Areas under the NO concentration−time curve ($AUC_{0.08-24}$) derived by integration. The suffixes and "p" added to *x*-axis labels indicate "solution" and "particles" respectively while p2D corresponds to two-drug particles. Means ($N = 2$) of the data is shown, significance at $P < .05$ compared with blank particles is denoted by an asterisk (*). *DETA*, Diethylenetriamine; *NO*, nitric oxide. *Source: Adapted with permission from Pandya, S., Verma, R.K., Khare, P., Tiwari, B., Srinivasarao, D.A., Dube, A., et al., 2016. Supplementation of host response by targeting nitric oxide to the macrophage cytosol is efficacious in the hamster model of visceral leishmaniasis and adds to efficacy of amphotericin B. Int. J. Parasitol. Drugs Drug Resist. 6 (2), 125–132.*

particles containing the diethylenetriamine NO were further observed for the next 12 hours to monitor the NO levels (Fig. 8.4B). The peaked level of NO produced by soluble diethylenetriamine NO was found to occur within 15 minutes and then reduced, whereas diethylenetriamine NO of particle had shown the NO levels increasing later and followed by a gradual decreasing. The data obtained from the difference of bioavailabilities calculated by the areas under the concentration–time curve of NO was found to be statistically insignificant also when the dose of diethylenetriamine NO had been decreased by half to that of particles bearing both diethylenetriamines NO and AmB (Fig. 8.4C) (Pandya et al., 2016).

In another study, Bose et al. developed hemoglobin tagged chitosan–chondroitin sulfate-based nanoparticles containing AmB to target the *Leishmania*-infected macrophage. It used the benefit of the highly auxotrophic nature of *Leishmania* for heme. Hemoglobin tagged nanoparticles decreased the toxicity level and lowered the median lethal dose value compared with conventional administration (Bose et al., 2016). Kumar and Bose (2015) also studied the site-specific delivery of encapsulated paromomycin through hemoglobin as a targeting moiety to the macrophage infected by *Leishmania*.

The antileishmanial agents from natural origins such as *Bacopasaponin C* (Sinha et al., 2002), *Quercetin* (Sarkar et al., 2002), and *Arjuna glucoside* (Tyagi et al., 2005) were found to be applicable either in free form or in encapsulated form in nanoparticles for treatment. At equivalent therapeutic concentrations of antileishmanial agents when encapsulated in nanoparticles produced the highest reduction of parasitic burden in the spleen than free drug or drug loaded in various colloidal carriers.

Two different formulations of lipid nanospheres were prepared that were loaded with piperine, one formulation containing stearylamine while the other formulation contained polyethylene glycol (PEG). Following intravenous administration of the above formulations in *L. donovani*–infected BALB/c mice revealed that lipid nanospheres containing stearylamine were reported as more effective in the reduction of the parasitic burden in liver and spleen than other formulations (Veerareddy et al., 2009).

To get better antileishmanial efficacy as well as to improve the bioavailability of a poorly soluble bioactive, andrographolide was nanoencapsulated in poly(D,L-lactide-*co*-glycolide) (PLGA). Antileishmanial drug releases in the surrounding area of the amastigotes by degradation of PLGA nanoparticles due to the acceleration of phagolysosomal acidic pH (Mundargi et al., 2008). Van de Ven et al. investigated antileishmanial in vitro activity of saponin β-aescin by incorporating in PLGA nanoparticles. β-aescin loaded nanoparticles had shown better results and more effective activity compared with free β-aescin (Van de Ven et al., 2011).

Kumar et al. developed two different formulations of PLGA–PEG nanoparticles to target *L. donovani*–infected macrophages. The first formulation encapsulated AmB and the other with miltefosine. After nanoencapsulation, the required dose of both drugs reduced by half to that of a conventional dose of AmB and miltefosine. The inhibition of amastigotes in the splenic tissue through nanoformulation was superior to conventional AmB and miltefosine. The mean cytotoxic assay of extracellular promastigote of PLGA–PEG encapsulated AmB was considerably lower than that of plain AmB (Kumar et al., 2015, 2016).

Asthana et al. reported the lactoferrin conjugated nanoreservoir bearing AmB for the treatment of VL and studied effects on VL models, toxicity, immunomodulatory potential, and biodistribution profile. The lactoferrin conjugated nanoreservoir produces the enhanced leishmaniasis activity by appreciably decreasing (~88%) the burden of splenic parasite--infected hamsters compared with commercial formulations. The uptake efficiency of nanoreservoirs bearing FITC in a macrophagic J774A.1 cell infected by promastigotes after a 6-hour incubation were studied. Lactoferrin-appended nanoreservoir administration leads to activation of macrophages, resulting in proinflammatory cytokine secretion. Fig. 8.6 shows various cytokines such as Th-1 (TNF-α, IFN-γ, IL-12) and Th-2 (IL-4, IL-10, and TGF-β) and their use in the immune response in *Leishmania*-infected hamsters when they are treated with drug-free and drug-bearing nanoreservoirs. IL-12 is considered to be the chief cytokine and acts as the main cause for the development of Th-1 cell-mediated immunity. Lactoferrin-appended nanoreservoirs have the ability to induce considerably enhanced release of IL-12, TNF-α, and IFN-γ cytokines (Asthana et al., 2015).

At present, various drugs like miltefosine and polymer-based drugs amBisome show high efficacy against VL but are associated with poor absorbance and severe side effects. Kumar et al. developed peptide (i.e., glycine) coated iron oxide nanoparticles of size range 10−15 nm to overcome these problems. AmB was used as a model drug against VL. In vitro study reveals the twofold higher efficacies of these glycine coated nanoparticles encapsulating AmB. The subcellular lysosomal compartments of infected cells have a pH < 5.0 while the pH of bloodstream is 7.4. The drug release studies have been performed to show the release pattern in these two different pH conditions under reservoir-sink conditions (Fig. 8.5), showing that the release profile strongly depends on the reservoir pH values. AmB encapsulated in glycine coated nanoparticles was found to be more significant than plain Amb or miltefosine as observed form the *L. donovani*−infected hamster. The 94.53% parasite inhibition was found in the case of glycine coated nanoparticles bearing AmB resulting in better protective result compared with 75.73% parasite inhibition with plain AmB (Fig. 8.6) (Kumar et al., 2017).

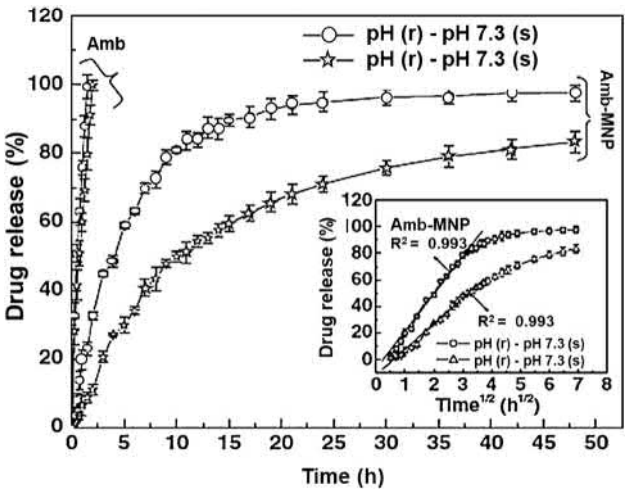

FIGURE 8.5 pH-dependent drug release profile of pure AmB and AmB GINPs in cell mimicking environment [reservoir (r): pH 5/pH 4 and sink (s): pH 7.3] at 37°C. *AmB*, Amphotericin B; *GINP*, glycine coated nanoparticles. *Source: Adapted with permission from Kumar, R., Pandey, K., Sahoo, G.C., Das, S., Das, V.N.R., Topno, R.K. et al., 2017. Development of high efficacy peptide coated iron oxide nanoparticles encapsulated amphotericin B drug delivery system against visceral leishmaniasis. Mater. Sci. Eng. C 75, 1465−1471.*

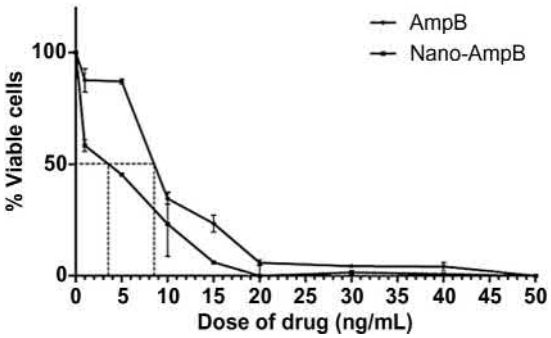

FIGURE 8.6 Drug sensitivity assay showing an IC_{50} value of 4 and 9 ng/mL was observed for nano-AmB and AmB, respectively. *AmB*, Amphotericin B; *IC_{50}*, half-maximal inhibitory concentration. *Source: Adapted with permission from Kumar, R., Pandey, K., Sahoo, G.C., Das, S., Das, V.N.R., Topno, R.K. et al., 2017. Development of high efficacy peptide coated iron oxide nanoparticles encapsulated amphotericin B drug delivery system against visceral leishmaniasis. Mater. Sci. Eng. C 75, 1465–1471.*

8.6.3 Nanodisks

Nanodisks are defined as self-assembled discoidal particles stabilized by a phospholipid bilayer that encircles a helical protein "belt" known as a membrane scaffold protein. The membrane scaffold protein helps to provide the solubility and biocompatibility attributable to its amphipathic nature (i.e., nonpolar part faces inward to attach with the phospholipids acyl chains, and polar and charged part at the aqueous interface) (Numata et al., 2013). These nanodisks could act as a vehicle for the delivery of hydrophobic drugs, such as all-trans retinoic acid and AmB (Ryan, 2008). Roy et al. formulated self-assembled nanoparticulate nanodisks that consisted of a phospholipid bilayer that were designed to be stabilized by an apolipoprotein scaffold. The structural design is significant for mimicking promising highly prolonged circulating properties of high-density lipoprotein (HDL) particles. HDL particles can be comprised by developing phospholipid vesicles having apolipoprotein (Roy et al., 2010).

In reconstituted HDL (rHDL) the phospholipids organize as a disk-shaped bilayer possessing two or more apolipoprotein molecules, which limit the edge of the disk. Recently, rHDL has come out as another opportunity to be used in the incorporation and transportation of various hydrophobic and amphipathic moieties. Yardley et al. reported the effect of AmB-loaded nanodisks on BALB/mice after intraperitoneal administration (Yardley and Croft, 2000). Complete clearance of the parasites was observed, without any lesions in experimental CL. Apolipoproteins, which could be modified through oxidization, acetylation, or other modifications, act as a ligand for scavenger receptors exposed on macrophages (Nelson et al., 2006).

Cole et al. prepared nanodisks of AmB and observed their effect on leishmaniasis infected mice and reported that the delivery system could be used for cutaneous therapy to treat leishmaniasis. The effect of nanodisks bearing AmB was observed on BALB/c mice infected with *L. major* parasites as shown in Fig. 8.7. The treatment of AmB nanodisks in *L. major* parasites infected mice lead to the reduced harshness of footpad lesions and reduced the parasite count locally in the feet as well as in popliteal lymph nodes (Cole et al., 2014).

8.6.4 Niosomes

Niosomes are similar to liposomes, except that they are made from nonionic surfactants and display better stability and shelf life compared with other vesicular systems

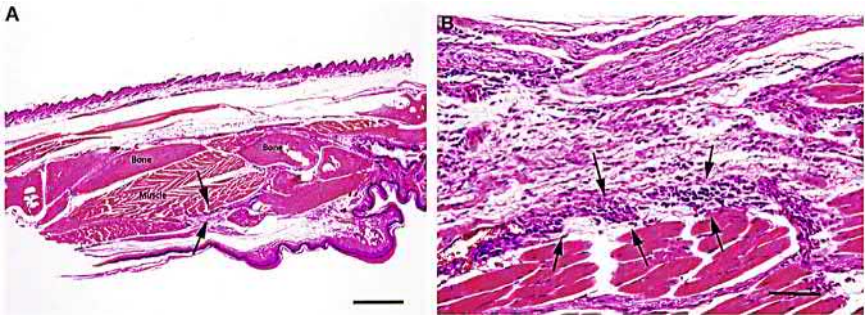

FIGURE 8.7 Sagittally sectioned foot of a representative BALB/c mouse sacrificed 25 days following inoculation with *Leishmania major* parasites and treatment with AmB nanodisks. (A) Note the mild inflammation in subcutaneous tissue (*arrows*). The footpad epidermis (bottom) is intact and bone and muscle have no lesions. H&E, bar = 500 μm. (B) The mild focal inflammatory cell infiltrate consists of mixed mononuclear cells (*arrows*). Normal skeletal muscle lies beneath these cells with normal loose connective above. H&E, bar = 500 μm. *AmB*, Amphotericin B. *Source: Adapted with permission from Cole, P.A., Bishop, J.V., Beckstead, J.A., Titus, R., Ryan, R.O., 2014. Effect of amphotericin B nanodisks on* Leishmania major *infected mice. Pharm. Anal. Acta. 5. ©2014 Cole et al.*

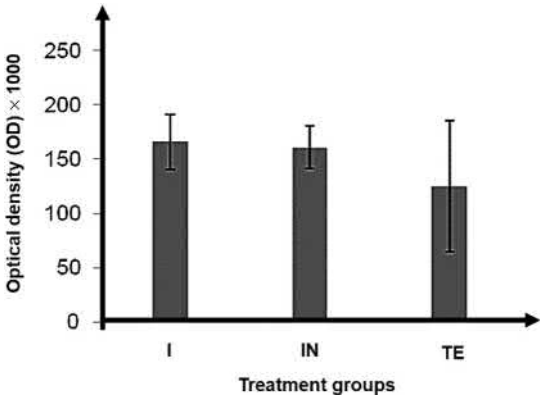

FIGURE 8.8 Comparison of the overall mean OD between itraconazole (I), IN, and TE in the susceptibility of *Leishmania tropica* promastigotes by MTT assay. *OD*, Optical density; *IN*, itraconazole niosome; *TE*, tartar emetic. *Source: Adapted with permission from Khazaeli, P., Sharifi, I., Talebian, E., Heravi, G., Moazeni, E., Mostafavi, M., 2014. Anti-leishmanial effect of itraconazole niosome on in vitro susceptibility of* Leishmania tropica. *Environ. Toxicol. Pharmacol. 38 (1), 205–211.*

(Jain et al., 2017). In vivo, niosomal retention capacity has been reported to be increased compared with liposomes due to the lack of lipids and smaller size (Maheshwari et al., 2015b). Therefore the therapeutic effects of certain antileishmanial agents have been enhanced by incorporating them in niosome delivery systems. Nieto et al. investigated the efficacy of sodium stibogluconate encapsulated niosomes in dogs. They found an enhanced antileishmanial activity that was further improved by dextran coating (Nieto et al., 2003). Other formulations of sodium stibogluconate loaded niosomes were assessed on BALB/c mice. Antileishmanial relative efficacies have been reported in the following manner: dextran-coated sodium stibogluconate loaded niosomes > sodium stibogluconate loaded niosomes > free sodium stibogluconate (Mullen et al., 1998). Khazaeli et al. prepared itraconazole niosomes and evaluated their in vitro susceptibility of *Leishmania tropica*. They found the highest overall mean optical density for *L. tropica* promastigotes treated with itraconazole followed by itraconazole bearing niosome and tartar emetic (Fig. 8.8). All of

these drugs were found to be effective in inhibiting the promastigotes growth, where the order of effectiveness from greatest to least was tartar emetic > itraconazole noisome > itraconazole (Khazaeli et al., 2014).

Nazari-Vanani et al. developed miltefosine and ketoconazole loaded nanoniosome formulations by using Span 65 and 80 as nonionic surfactants. They performed the 3-(4,5-dimethylthiazol-2-yl)-2,5-diphenyltetrazolium bromide (MTT) assay to test the cytotoxicity of miltefosine loaded nanoliposomes (M-Span 65 and M-Span 80) and ketoconazole loaded nanoniosome (K-Span 65 and K-Span 80) against *L. major*. They found that in the presence of drug-loaded nanoliposomes, the number of parasites decreased. M-Span 65 and K-Span 80 also caused higher blocking proliferation of the parasites, in comparison to other, even at higher concentration. Both of the formulations suppressed the growth of amastigote and promastigote forms of *L. major* in vitro following a 48 h incubation. The IC_{50} values were found to be 86.38 ± 0.07 and 53.39 ± 0.02 μg/mL for amastigote and promastigote forms, respectively (Fig. 8.9) (Nazari-Vanani et al., 2018).

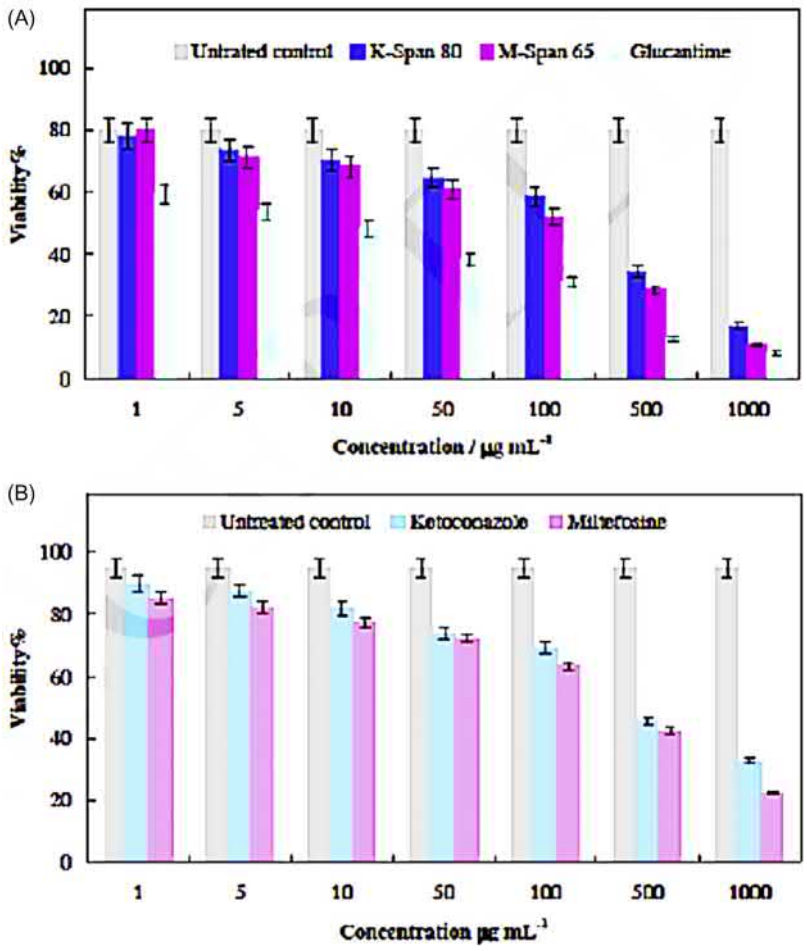

FIGURE 8.9 Cell viability of amastigotes of *Leishmania major* at different concentrations of M-Span 65, K-Span and Glucantime (A), miltefosine and ketoconazole (B), and for untreated control. *Source: Adapted with permission from Nazari-Vanani, R., Vais, R.D., Sharifi, F., Sattarahmady, N., Karimian, K., Motazedian, M.H., et al., 2018. Investigation of anti-leishmanial efficacy of miltefosine and ketoconazole loaded on nanoniosomes. Acta Trop. 185, 69–76.*

8.6.5 Emulsions

Veerareddy et al. (2009) developed the formulation of a water-insoluble drug, piperine, in a stearylamine containing oil in water (o/w) emulsion and observed a greater decline in parasitic load in macrophage-rich organs such as the spleen (85%) and liver (90%) compared with pegylated or plain formulations without any toxic effects. In addition, an *o*-palmitoyl mannan-coated formulation containing AmB known as trilaurin emulsomes was found to have a larger accumulation in the lungs, spleen, and liver, while having a higher reduction of the parasitic burden from the spleen in comparison with free AmB (Gupta et al., 2007).

Some researchers have been working on nanoemulsion systems for delivering medicinal plant extracts for the treatment of leishmaniasis. The fruit extract of the plant *Pterodon pubescens*, which exhibits antileishmanial activity, can be obtained by either a conventional method or a supercritical fluid method. The extract obtained from the supercritical fluid method had demonstrated higher cytotoxicity, superior selectivity index, and enhanced activity against the parasite *L. amazonensis* promastigotes and amastigotes when compared with the extract obtained from the conventional method. The smaller globules of the extract obtained from supercritical fluid method could be helpful for achieving easy penetration in the parasites, thus leading to reduced IC_{50} values in contrast to the other extract (da Silva Santos et al., 2016).

AmB-loaded nanoemulsions were prepared with different concentrations of stearylamine (a lipophilic amine) to determine the effect of stearylamine on the encapsulation efficiency, antileishmanial activity, and cytotoxicity. The study suggested that the encapsulation efficiency of the drug was found to be almost 100% without any impact from stearylamine concentration. As shown in Fig. 8.10, the in vitro study also exhibited that as the concentration of stearylamine increases, the higher the cytotoxicity and

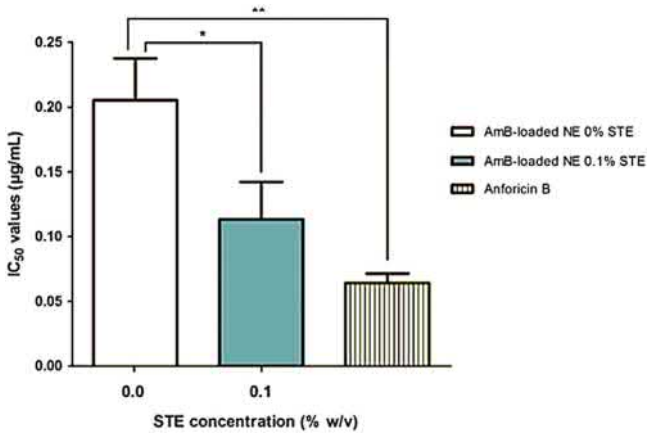

FIGURE 8.10 Comparison of IC_{50} values of different formulations of AmB. In vitro activity studies were performed against intracellular Leishmania *amazonensis* amastigotes after 24 h exposure. The AmB concentration capable of inhibiting 50% of parasite growth was expressed as IC_{50}. The results are mean values ± SD of three independent experiments. *AmB*, Amphotericin B; *IC_{50}*, half-maximal inhibitory concentration. *Source: Adapted with permission from Caldeira, L.R., Fernandes, F.R., Costa, D.F., Frézard, F., Afonso, L.C.C., Ferreira, L.A.M., 2015. Nanoemulsions loaded with amphotericin B: a new approach for the treatment of leishmaniasis. Eur. J. Pharm. Sci. 70, 125–131.*

antileishmanial activity present against the intracellular amastigotes with minimum toxicity to macrophages when compared with the conventional AmB (Caldeira et al., 2015).

8.6.6 Carbon Nanotubes

Carbon nanotubes (CNTs) are considered to be one of the major advanced nanocarriers for different types of bioactive delivery due to their great surface area and high loading capacity (Tekade et al., 2017a; Kuche et al., 2018). Prajapati et al. (2011) explored the activity of AmB conjugated CNTs with the J774A.1 macrophage cell line and showed that significant antileishmanial efficiency without any cytotoxic effects was achievable. Pruthi et al. demonstrated the potential of AmB loaded mannosylated multiwalled CNTs (MWCNTs) for site-specific delivery to macrophages in leishmaniasis. The data provided evidence that AmB-loaded MWCNTs showed better cellular uptake on J774 macrophages cells compared with AmB alone (Pruthi et al., 2012).

Betulin (BET), a triterpenoid metabolite, was attached to functionalized CNTs (f-CNTs) to prepare conjugated moiety of f-CNT−BET. The f-CNT−BET showed lesser toxicity to the J774 macrophage cell line compared with the plain BET as shown in Fig. 8.11. The f-CNT−BET conjugate exhibited higher antileishmanial activity against the *L. donovani* amastigotes with the minimal IC_{50} value (i.e., 0.69 ± 0.08 μg/mL) compared with the IC_{50} value of BET (8.33 ± 0.41 μg/mL), as shown in Fig. 8.12 (Saudagar and Dubey, 2014).

8.6.7 Transfersomes

Transfersomes have a unique characteristic of being an ultradeformable (ultraflexible) carrier due to their physical−structural properties that provide enhanced skin permeation. Singodia et al. formulated AmB-loaded transfersomes for treating sensitive, drug-resistant,

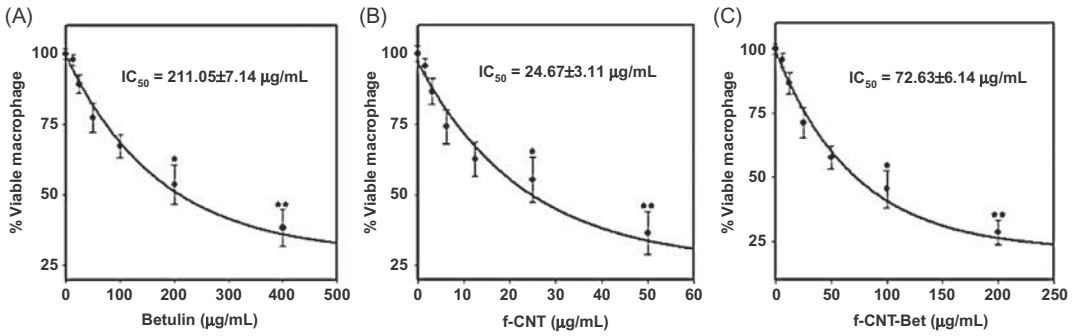

FIGURE 8.11 In vitro assessment of cytotoxicity studied on macrophage cells (J774A.1 cell line). (A) Cytotoxic effect of BET on macrophage cells and the IC_{50} value observed to be 211.05 ± 7.14 μg/mL. (B) Cytotoxic effect of f-CNTs on macrophage cells and the IC_{50} value observed to be 24.67 ± 3.11 μg/mL. (C) Cytotoxic effect of f-CNT−BET on macrophage cells and the IC_{50} value observed to be 72.63 ± 6.14 μg/mL. *BET*, Betulin; *f-CNT*, functionalized carbon nanotube; *IC_{50}*, half-maximal inhibitory concentration. *Source: Adapted with permission from Saudagar, P., Dubey, V.K., 2014. Carbon nanotube based betulin formulation shows better efficacy against* Leishmania *parasite. Parasitol. Int. 63 (6), 772−776.*

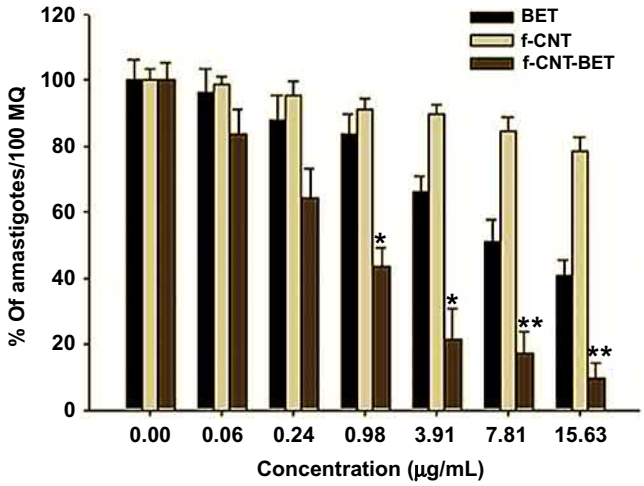

FIGURE 8.12 **In vitro antileishmanial activity on intracellular amastigote cells.** The antileishmanial activity of BET, f-CNTs, and f-CNT–BET was studied using microscopic counting of amastigote cell inside the infected macrophage cells. A dose-dependent response is observed with BET and f-CNT–BET, whereas the f-CNT did not show any antileishmanial effect on the parasite, revealing that the f-CNTs alone are not antileishmanial and the improved efficacy is due to the impact of the drug attached to f-CNT–BET. The IC_{50} value for BET and f-CNT–BET is found to be 8.33 ± 0.41 and 0.69 ± 0.08 µg/mL, respectively. *BET*, Betulin; *f-CNT*, functionalized carbon nanotube; *IC_{50}*, half-maximal inhibitory concentration. *Source: Adapted with permission from Saudagar, P., Dubey, V.K., 2014. Carbon nanotube based betulin formulation shows better efficacy against* Leishmania *parasite. Parasitol. Int. 63 (6), 772–776.*

and clinically isolated *L. donovani*. The given data revealed that the transfersomes penetrated 1.5 times higher as compared with conventional liposome formulations and therefore provided an enhanced activity of AmB (Singodia et al., 2010a,b).

Paromomycin sulfate encapsulated transferosomes also have been evaluated against promastigotes by MTT assay. The EC_{50} (ED_{50}) of the transferosomal formulation was reported to be 205.70 ± 10.05 g/mL. Topical application to *L. major* infected BALB/c mice using paromomycin sulfate encapsulated transferosome (T1, T4, T10, T13) reported smaller lesion size and decreased spleen parasitic burden as compared with control groups and paromomycin sulfate cream (Figs. 8.13 and 8.14) (Bavarsad et al., 2012).

8.6.8 Other Drug Delivery Systems

Numerous drug delivery systems are used for targeted delivery of antileishmanial drugs against leishmaniasis. Jain et al. developed muramyl dipeptide (MDP) conjugated 5.0 G multimeric poly(propylene imine) dendrimers that show the targeted delivery of AmB to macrophages. The formulation showed higher antiparasitic activity against parasite-infected macrophage cell lines. In vivo study carried out on BALB/c mice showed a significant reduction in hemolytic toxicity. It has also produced synergistic antiparasitic action, which may be due to the immune stimulation through developed MDP on dendrimers (Jain et al., 2015).

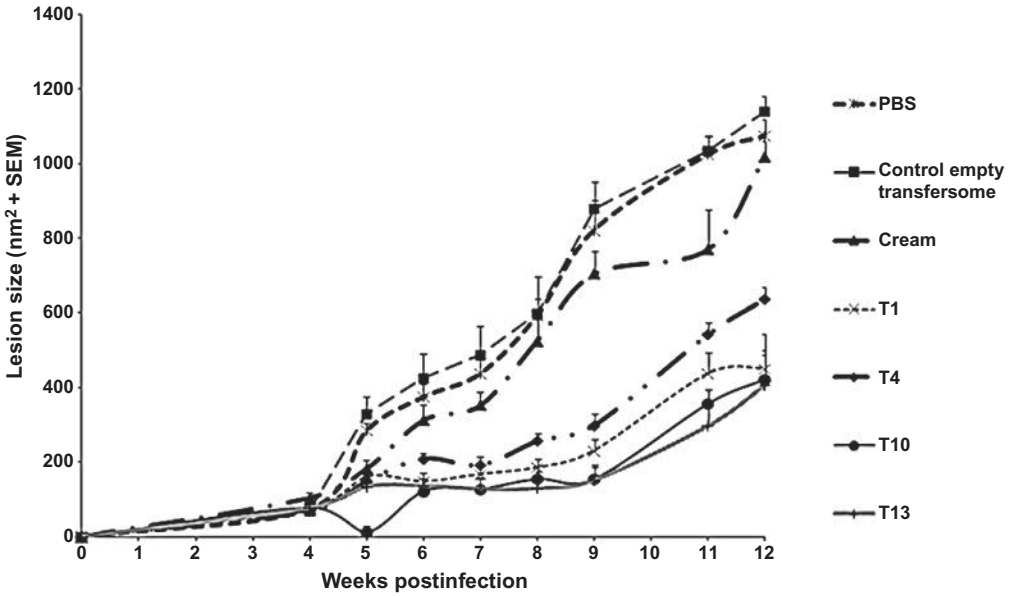

FIGURE 8.13 The progress of lesion size in *Leishmania major* infected BALB/c mice treated with different formulations of topical transfersomal paromomycin (PM). Female 6–8 weeks BALB/c mice were infected with subcutaneous injection of 3×106 stationary-phase *L. major* promastigotes at the base of the tail. At week 4 postinfection, the size of the lesions was measured in two dimensions using calipers, mean diameters determined, and mice were sorted into groups of 7. The lesions were treated topically with 50 mg formulations twice a day for 4 weeks. The lesion size was recorded weekly during the treatment and up to 8 weeks after termination of the treatment. *Source: Adapted with permission from Bavarsad, N., Bazzaz, B.S.F., Khamesipour, A., Jaafari, M.R., 2012. Colloidal, in vitro and in vivo anti-leishmanial properties of transfersomes containing paromomycin sulfate in susceptible BALB/c mice. Acta Trop. 124 (1), 33–41.*

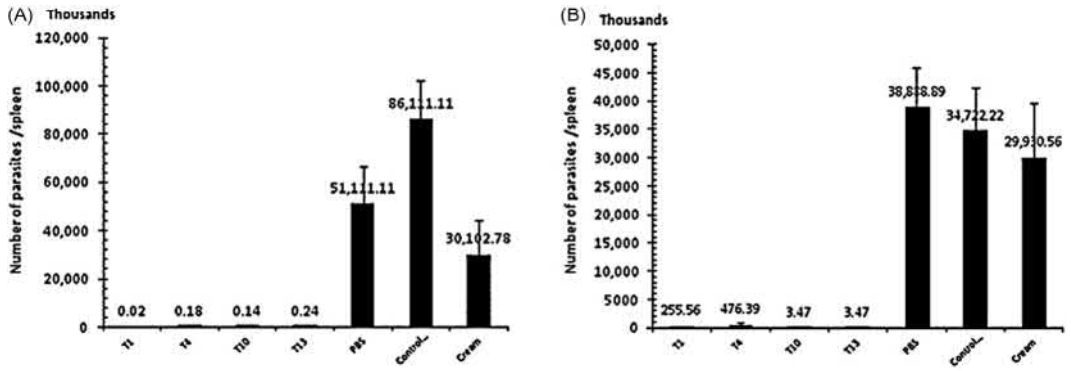

FIGURE 8.14 Splenic parasite burden in BALB/c mice treated with a topical transfersomal PM. The number of viable *Leishmania major* was quantified using limiting dilution assay in the spleen of different groups of mice at weeks 8 (A) and 12 (B) after infection with *L. major* promastigotes. The spleen was aseptically removed and homogenized in Roswell Park Memorial Institute - Fetal Calf Serum (RPMI-FCS), diluted with the same media in eight serial 10-fold dilutions in each well of flat-bottom 96-well microtiter plates containing a solid layer of blood agar. The plates were kept at 25°C for 1 week and they were ready to score the number of positive wells (containing one or more promastigotes). The final titer was the last dilution for which the well contained at least one parasite. (A) $n = 3$, mean ± SEM, there were significant ($P < .01$) differences between PM transfersomes and groups received control empty transfersomes or PBS; (B) mean ± SEM, there were significant differences between PM transfersomes and groups received either control empty transfersomes or conventional cream ($P < .01$) as well as PBS ($P < .001$). *Source: Adapted with permission from Bavarsad, N., Bazzaz, B.S.F., Khamesipour, A., Jaafari, M.R., 2012. Colloidal, in vitro and in vivo anti-leishmanial properties of transfersomes containing paromomycin sulfate in susceptible BALB/c mice. Acta Trop. 124 (1), 33–41.*

Veerareddy et al. (2009) assessed mannose-conjugated lipid nanospheres bearing AmB in *L. donovani* infected BALB/c mice. AmB-loaded nanospheres have enhanced activity by interacting with ergosterol but were not found to be effective for the resistant strain based on their characteristic of lacking ergosterol (Espuelas et al., 2002).

8.7 PROPHYLACTIC VACCINES FOR LEISHMANIASIS

Currently, there are no vaccines available against leishmaniasis, due to the lack of success in clinical phase trials. Therefore clinically approved adjuvants emphasize the need for safe and effective immunostimulants adjuvants in leishmaniasis vaccine development (Chappuis et al., 2007a,b). However, several strategies have been proposed for the development of a vaccine against intracellular parasites like *Leishmania* that induce cell-mediated immunity rather than by means of antibodies (Pashine et al., 2005). Development of vaccines based on recombinant proteins and plasmid DNA encoding leishmanial antigens are immunogenic and coadministered as an effective adjunct (O'Hagan and Valiante, 2003).

8.7.1 Leishmanization

Intradermal vaccination of live virulent promastigote form of *Leishmania* from a fresh culture, termed as leishmanization, has been used occasionally for many years to protect against the harmful effects of leishmanial infection. However, harsh cutaneous lesions were induced. Therefore their use has been hindered and should not generally be used in normal situations. Leishmanization is both useful and challenging to evaluate the aspirant vaccines for CL. On the other hand, the process should take place in a well-controlled environment, especially in high-risk volunteers without HIV infection (World Health Organization, 2010). The different types of vaccines used against leishmaniasis are represented in Fig. 8.15.

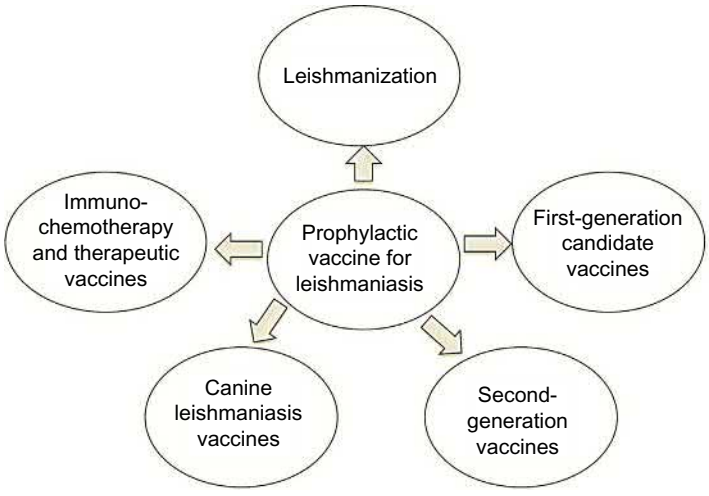

FIGURE 8.15 Types of vaccines used against leishmaniasis.

There are two commercialized canine vaccines against VL available in Brazil. The outcomes obtained from phase I and II studies of these vaccines proved their potential to decrease the severity of the disease in dogs, and therefore the Ministry of Agriculture issued a license for these vaccines. But these are not licensed by the Ministry of Health because of a lack of significant studies that reveals their potential outcome in the reduction of VL.

8.7.2 First-Generation Aspirant Vaccines

First-generation vaccines against leishmaniasis consist of either a fraction of the whole killed *Leishmania* or its extracts, with or without adjuvants. Various attempts have been made for the development of such vaccines in different countries, like Colombia, Brazil, Venezuela, Ecuador, and the Islamic Republic of Iran for CL and in Sudan for VL. A first-generation vaccine was first recorded in Brazil and was used as an adjunct to antimony therapy (Mayrink et al., 2006). These vaccines were successfully used along with chemotherapy in Venezuela (Convit et al., 1987) and Brazil (Mayrink et al., 2006).

- An *L. amazonensis* based vaccine resulting from the pentavalent vaccine in Brazil (Mayrink vaccine).
- Vaccine generated from *L. mexicana* used along with bacillus Calmette–Guérin (BCG) in Venezuela (Convit vaccine) (Convit et al., 1987).
- *L. major* derived vaccines that also used along with BCG (Razi Institute vaccine) in the Islamic Republic of Iran. Unfortunately, the outcomes have been doubtful for prophylaxis, apart from this it has been encouraged for curative indications.

8.7.3 Second-Generation Vaccines

Second-generation vaccines have been generated via live genetically modified bacteria, viruses, or parasites having *Leishmania* gene, like *L. major*, which expresses the herpes virus gene called ganciclovir sensitive thymidine kinase recombinant gene (Muyombwe et al., 1998). In addition, second-generation vaccines may be derived from native fractions such as the vaccinia virus having the *L. infantum* LACK antigen that shows the potential to protect the mice against *L. major* (Gonzalo et al., 2002). The various antigens are able to protect experimental animals when they are used with adjuvants, but only a Leish-111f vaccine as an adjuvant to monophosphoryl lipid A plus squalene has gone through clinical trials. This vaccine was assessed for immunotherapy of PKDL in Sudan and has gone through phase I and II clinical trials in Peru, and in phase I clinical trials in India.

8.7.4 Immunochemotherapy and Therapeutic Vaccines

In Venezuela, immunotherapy alone or in combination with chemotherapy has been used to treat CL. BCG along with three doses of injections of autoclaved *L. mexicana* is used when a patient does not respond to chemotherapy alone. This method has emerged as safe, with no adverse effects associated with conventional antimonials, except that lesions may form that can last for a few weeks. Daily repeated doses of killed

L. amazonensis vaccine, called the Mayrink vaccine, have been used along with low-dose antimonials at a dose of 8 mg/kg/day for four cycles of 10 daily injections, followed by rest of 10 days. These vaccines are registered in Brazil as a combined therapy with low-dose chemotherapy.

In Sudan, the cure rate in patients of persistent PKDL with immune-chemotherapy was much higher at 87% than chemotherapy alone, which was 53%. Therapeutic vaccines can be evaluated rapidly to provide a cost-effective therapy compared with already existing therapeutic, or immunochemotherapeutic, vaccines.

8.8 CONCLUSION

Leishmaniasis is considered to be a life-threatening disease of the modern world, and therefore its treatment remains ever important, although challenging, because of the development of drug resistance, toxicity linked with the existing drugs, adverse effects, and the nonavailability of new drugs. Thus the morbidity and mortality of leishmaniasis are rising constantly. Several efforts have been made to produce inexpensive drugs linked with minimal or no side effects. The most appropriate approach for significant management of leishmaniasis is to carry the drug cargo to the phagolysosomes of the macrophages, which have the amastigotes, which may be achieved by means of investigating various drug delivery techniques. The emerging trend of surface modified targeted delivery systems like liposomes, niosomes, nanoparticles, or nanospheres has been used to facilitate drug delivery and accumulation of the drug at the target site. These systems may deliver the drugs with significantly reduced toxicity to normal cells as well as improve tolerability and efficacy of antileishmanial drugs having a narrow therapeutic index. However, further exploration for control of leishmaniasis is required to develop cost-effective, novel, and efficient drug therapies.

Acknowledgments

The VP would like to acknowledge the Indian Council of Medical Research (ICMR), New Delhi for grant of SRF funding (45/01/2018-NAN/BMS) for research work. The PJ would like to acknowledge the UGC BSR [grant number F-25-1/2013-14(BSR)/7-57/2007(BSR)].

ABBREVIATIONS

AmB	amphotericin B
BCG	bacillus Calmette–Guérin
CL	cutaneous leishmaniasis
CNT	carbon nanotube
EC_{50}	half-maximal effective concentration
ELISA	enzyme-linked immunosorbent assay
HDL	high-density lipoprotein
HIV	human immunodeficiency virus
HPMA	hydroxypropyl methacrylamide
IC_{50}	half-maximal inhibitory concentration

IFAT	indirect fluorescent antibody test
IFN	interferon
Ig	immunoglobulin
IL	interleukin
LPG	lipophosphoglycan
MCL	mucocutaneous leishmaniasis
MDP	muramyl dipeptide
MPS	mononuclear phagocytic system
MWCNTs	multiwalled carbon nanotube
NO	nitric oxide
PACA	poly-alkyl cyanoacrylate
PCR	polymerase chain reaction
PEG	polyethylene glycol
PKDL	post-kala-azar dermal leishmaniasis
PLGA	poly(D,L-lactide-*co*-glycolide)
RES	reticuloendothelial system
rHDL	reconstituted high-density lipoprotein
Th-1	T helper cell type 1
TNF	tumor necrosis factor
VL	visceral leishmaniasis

References

Agrawal, A.K., Gupta, C.M., 2000. Tuftsin-bearing liposomes in the treatment of macrophage-based infections. Adv. Drug Deliv. Rev. 41 (2), 135–146.

Alving, C.R., Steck, E.A., Chapman, W.L., Waits, V.B., Hendricks, L.D., Swartz, G.M., et al., 1978. Therapy of leishmaniasis: superior efficacies of liposome-encapsulated drugs. Proc. Natl. Acad. Sci. U.S.A. 75 (6), 2959–2963.

Amprey, J.L., Im, J.S., Turco, S.J., Murray, H.W., Illarionov, P.A., Besra, G.S., et al., 2004. A subset of liver NK T cells is activated during *Leishmania donovani* infection by CD1d-bound lipophosphoglycan. J. Exp. Med. 200 (7), 895–904.

Argueta, V., 1994. Atlas Plants Traditional Mexican Medicine. National Indian Institute, Mexico City.

Asati, S., Pandey, V., Soni, V., 2019. RGD peptide as a targeting moiety for theranostic purpose: an update study. Int. J. Pept. Res. Ther. 25, 49–65.

Asthana, S., Gupta, P.K., Jaiswal, A.K., Dube, A., Chourasia, M.K., 2015. Targeted chemotherapy of visceral leishmaniasis by lactoferrin-appended amphotericin B-loaded nanoreservoir: in vitro and in vivo studies. Nanomedicine 10 (7), 1093–1109.

Attar, Z.J., Chance, M.L., el-Safi, S., Carney, J., Azazy, A., El-Hadi, M., et al., 2001. Latex agglutination test for the detection of urinary antigens in visceral leishmaniasis. Acta Trop. 78 (1), 11–16.

Balana-Fouce, R., Reguera, R.M., Cubria, J.C., Ordonez, D., 1998. The pharmacology of leishmaniasis. Gen. Pharmacol. 30, 435–443.

Banerjee, G., Nandi, G., Mahato, S.B., Pakrashi, A., Basu, M.K., 1996. Drug delivery system: targeting of pentamidines to specific sites using sugar grafted liposomes. J. Antimicrob. Chemother. 38 (1), 145–150.

Bansal, D., Yadav, K., Pandey, V., Ganeshpurkar, A., Agnihotri, A., Dubey, N., 2016. Lactobionic acid coupled liposomes: an innovative strategy for targeting hepatocellular carcinoma. Drug Deliv. 23 (1), 140–146.

Barratt, G., Bretagne, S., 2007. Optimizing efficacy of amphotericin B through nanomodification. Int. J. Nanomed. 2 (3), 301.

Basu, M.K., 2005. Liposomal delivery of antileishmanial agents. J. Appl. Res. 5, 221–236.

Bavarsad, N., Bazzaz, B.S.F., Khamesipour, A., Jaafari, M.R., 2012. Colloidal, in vitro and in vivo anti-leishmanial properties of transfersomes containing paromomycin sulfate in susceptible BALB/c mice. Acta Trop. 124 (1), 33–41.

Berman, J., 2005. Miltefosine to treat leishmaniasis. Expert. Opin. Pharmacother. 6, 1381–1388.

Bero, J., Hannaert, V., Chataigné, G., Hérent, M.F., Quetin-Leclercq, J., 2011. In vitro antitrypanosomal and antileishmanial activity of plants used in Benin in traditional medicine and bio-guided fractionation of the most active extract. J. Ethnopharmacol. 137 (2), 998–1002.

Bhattacharya, S.K., Jha, T.K., Sundar, S., Thakur, C.P., Engel, J., Sindermann, H., et al., 2004. Efficacy and tolerability of miltefosine for childhood visceral leishmaniasis in India. Clin. Infect. Dis. 38 (2), 217–221.
Bhowmick, S., Mazumdar, T., Sinha, R., Ali, N., 2010. Comparison of liposome based antigen delivery systems for protection against *Leishmania donovani*. J. Controlled Release 141 (2), 199–207.
Bose, P.P., Kumar, P., Dwivedi, M.K., 2016. Hemoglobin guided nanocarrier for specific delivery of amphotericin B to leishmania infected macrophage. Acta Trop. 158, 148–159.
Bryceson, A., 2001. A policy for leishmaniasis with respect to the prevention and control of drug resistance. Trop. Med. Int. Health 6 (11), 928–934.
Caldeira, L.R., Fernandes, F.R., Costa, D.F., Frézard, F., Afonso, L.C.C., Ferreira, L.A.M., 2015. Nanoemulsions loaded with amphotericin B: a new approach for the treatment of leishmaniasis. Eur. J. Pharm. Sci. 70, 125–131.
Carvalheiro, M., Esteves, M.A., Santos-Mateus, D., Lopes, R.M., Rodrigues, M.A., Eleutério, C.V., et al., 2015. Hemisynthetic trifluralin analogues incorporated in liposomes for the treatment of leishmanial infections. Eur. J. Pharm. Biopharm. 93, 346–352.
Castillo, D., Arevalo, J., Herrera, F., Ruiz, C., Rojas, R., Rengifo, E., et al., 2007. Spirolactone iridoids might be responsible for the antileishmanial activity of a Peruvian traditional remedy made with *Himatanthus sucuuba* (Apocynaceae). J. Ethnopharmacol. 112 (2), 410–414.
Chakravarty, J., Sundar, S., 2010. Drug resistance in leishmaniasis. J. Global Infect. Dis. 2 (2), 167.
Chan-Bacab, M.J., Balanza, E., Deharo, E., Muñoz, V., García, R.D., Peña-Rodríguez, L.M., 2003. Variation of leishmanicidal activity in four populations of *Urechites andrieuxii*. J. Ethnopharmacol. 86 (2), 243–247.
Chappuis, F., Sundar, S., Hailu, A., Ghalib, H., Rijal, S., Peeling, R.W., et al., 2007a. Visceral leishmaniasis: what are the needs for diagnosis, treatment and control. Nat. Rev. Microbiol. 5, 873–882.
Chappuis, F., Sundar, S., Hailu, A., Ghalib, H., Rijal, S., Peeling, R.W., et al., 2007b. Visceral leishmaniasis: what are the needs for diagnosis, treatment and control. Nat. Rev. Microbiol. 5 (11), 873–882.
Cole, P.A., Bishop, J.V., Beckstead, J.A., Titus, R., Ryan, R.O., 2014. Effect of amphotericin B nanodisks on *Leishmania major* infected mice. Pharm. Anal. Acta. 5, 311.
Convit, J., Rondon, A., Ulrich, M., Bloom, B., Castellanos, P., Pinardi, M., et al., 1987. Immunotherapy versus chemotherapy in localised cutaneous leishmaniasis. Lancet 329 (8530), 401–405.
Corrêa, D.S., Tempone, A.G., Reimão, J.Q., Taniwaki, N.N., Romoff, P., Fávero, O.A., et al., 2011. Anti-leishmanial and anti-trypanosomal potential of polygodial isolated from stem barks of *Drimys brasiliensis Miers* (Winteraceae). Parasitol. Res. 109 (1), 231–236.
Croft, S.L., Hogg, J., Gutteridge, W.E., Hudson, A.T., Randall, A.W., 1992. The activity of hydroxynaphthoquinones against *Leishmania donovani*. J. Antimicrob. Chemother. 30 (6), 827–832.
Cruz, I., Nieto, J., Moreno, J., Canavate, C., Desjeux, P., Alvar, J., 2006. *Leishmania*/HIV coinfections in the second decade. Indian J. Med. Res. 123, 357–388.
Daher, E.F., Fonseca, P.P., Gerhard, E.S., Silva, T.M.J., Silva, G.B., 2009. Clinical and epidemiological features of visceral leishmaniasis and HIV coinfection in fifteen patients from Brazil. J. Parasito. 95 (3), 652–655.
Dasgupta, D., Adhya, S., Basu, M.K., 2002. The effect of β-tubulin-specific antisense oligonucleotide encapsulated in different cationic liposomes on the suppression of intracellular *L. donovani* parasites in vitro. J. Biochem. 132 (1), 23–27.
Date, A.A., Joshi, M.D., Patravale, V.B., 2007. Parasitic diseases: liposomes and polymeric nanoparticles versus lipid nanoparticles. Adv. Drug Deliv. Rev. 59 (6), 505–521.
da Silva Santos, É., Garcia, F.P., Outuki, P.M., Hoscheid, J., de Goes, P.R.N., Cardozo-Filho, L., et al., 2016. Optimization of extraction method and evaluation of antileishmanial activity of oil and nanoemulsions of *Pterodon pubescens* benth. fruit extracts. Exp. Parasitol. 170, 252–260.
De Doncker, S., Hutse, V., Abdellati, S., Rijal, S., Singh Karki, B.M., Decuypere, S., et al., 2005. A new PCR-ELISA for diagnosis of visceral leishmaniasis in blood of HIV-negative subjects. Trans. R. Soc. Trop. Med. Hyg. 99 (1), 25–31.
Delorenzi, J.C., Attias, M., Gattass, C.R., Andrade, M., Rezende, C., da Cunha Pinto, Â., et al., 2001. Antileishmanial activity of an indole alkaloid from *Peschiera australis*. Antimicrob. Agents Chemother. 45 (5), 1349–1354.
Dey, T., Anam, K., Afrin, F., Ali, N., 2000. Antileishmanial activities of stearylamine-bearing liposomes. Antimicrob. Agents Chemother. 44 (6), 1739–1742.
Espuelas, M.S., Legrand, P., Loiseau, P.M., Bories, C., Barratt, G., Irache, J.M., 2002. In vitro antileishmanial activity of amphotericin B loaded in poly(ε-caprolactone) nanospheres. J. Drug Target. 10 (8), 593–599.

Fakhfakh, M.A., Fournet, A., Prina, E., Mouscadet, J.F., Franck, X., Hocquemiller, R., et al., 2003. Synthesis and biological evaluation of substituted quinolines: potential treatment of protozoal and retroviral coinfections. Bioorg. Med. Chem. 11 (23), 5013–5023.

Farahmand, M., Khalaj, V., Mohebali, M., Khalili, G., Naderi, S., Ghaffarinejad, P., et al., 2015. Comparison of recombinant A2-ELISA with rKE16 dipstick and direct agglutination tests for diagnosis of visceral leishmaniasis in dogs in Northwestern Iran. Rev. Soc. Bras. Med. Trop. 48 (2), 188–193.

Fournet, A., Barrios, A.A., Munoz, V., Hocquemiller, R., Cavé, A., Bruneton, J., 1993. 2-Substituted quinoline alkaloids as potential antileishmanial drugs. Antimicrob. Agents Chemother. 37 (4), 859–863.

Fournet, A., Gantier, J.C., Gautheret, A., Leysalles, L., Munos, M.H., Mayrargue, J., et al., 1994. The activity of 2-substituted quinoline alkaloids in BALB/c mice infected with *Leishmania donovani*. J. Antimicrob. Chemother. 33 (3), 537–544.

Ganeshpurkar, A., Ganeshpurkar, A., Pandey, V., Agnihotri, A., Bansal, D., Dubey, N., 2014. Harnessing the potential of bacterial ghost for the effective delivery of drugs and biotherapeutics. Int. J. Pharm. Investig. 4 (1), 1–4.

Garcia, A.L., Kindt, A., Quispe-Tintaya, K.W., Bermudez, H., Llanos, A., Arevalo, J., et al., 2005. American tegumentary leishmaniasis: antigen-gene polymorphism, taxonomy and clinical pleomorphism. Infect. Genet. Evol. 5 (2), 109–116.

Garnier, T., Mäntylä, A., Järvinen, T., Lawrence, M.J., Brown, M.B., Croft, S.L., 2007. Topical buparvaquone formulations for the treatment of cutaneous leishmaniasis. J. Pharm. Pharmacol. 59 (1), 41–49.

Gaspar, R., Opperdoes, F.R., Préat, V., Roland, M., 1992. Drug targeting with polyalkylcyanoacrylate nanoparticles: in vitro activity of primaquine-loaded nanoparticles against intracellular *Leishmania donovani*. Ann. Trop. Med. Parasitol. 86 (1), 41–49.

Ghosh, S., Debnath, S., Hazra, S., Hartung, A., Thomale, K., Schultheis, M., et al., 2011. *Valeriana wallichii* root extracts and fractions with activity against *Leishmania* spp. Parasitol. Res. 108 (4), 861–871.

González-Coloma, A., Reina, M., Sáenz, C., Lacret, R., Ruiz-Mesia, L., Arán, V.J., et al., 2012. Antileishmanial, antitrypanosomal, and cytotoxic screening of ethnopharmacologically selected Peruvian plants. Parasitol. Res. 110 (4), 1381–1392.

Gonzalo, R.M., del Real, G., Rodriguez, J.R., Rodriguez, D., Heljasvaara, R., Lucas, P., et al., 2002. A heterologous prime–boost regime using DNA and recombinant vaccinia virus expressing the *Leishmania infantum* P36/LACK antigen protects BALB/c mice from cutaneous leishmaniasis. Vaccine 20 (7), 1226–1231.

Guerin, P.J., Olliaro, P., Sundar, S., Boelaert, M., Croft, S.L., Desjeux, P., et al., 2002. Visceral leishmaniasis: current status of control, diagnosis, and treatment, and a proposed research and development agenda. Lancet Infect. Dis. 2, 494–501.

Gupta, S., Dube, A., Vyas, S.P., 2007. Antileishmanial efficacy of amphotericin B bearing emulsomes against experimental visceral leishmaniasis. J. Drug Target. 15 (6), 437–444.

Iwu, M.M., Jackson, J.E., Tally, J.D., Klayman, D.L., 1992. Evaluation of plant extracts for antileishmanial activity using a mechanism-based radiorespirometric microtechnique (RAM). Planta Medica 58 (05), 436–441.

Jain, K., Verma, A.K., Mishra, P.R., Jain, N.K., 2015. Characterization and evaluation of amphotericin B loaded MDP conjugated poly(propylene imine) dendrimers. Nanomedicine 11 (3), 705–713.

Jain, M., Khan, S.I., Tekwani, B.L., Jacob, M.R., Singh, S., Singh, P.P., et al., 2005. Synthesis, antimalarial, antileishmanial, and antimicrobial activities of some 8-quinolinamine analogues. Bioorg. Med. Chem. 13 (14), 4458–4466.

Jain, P., Rahi, P., Pandey, V., Asati, S., Soni, V., 2017. Nanostructure lipid carriers: a modish contrivance to overcome the ultraviolet effects. Egypt. J. Basic Appl. Sci. 4 (2), 89–100.

Jean-Robert, I., 2008. Natural products for neglected diseases: a review. Curr. Org. Chem. 12, 643–666.

Jha, S.N., Singh, N.K., Jha, T.K., 1991. Changing response to diamidine compounds in cases of kala-azar unresponsive to antimonial. J. Assoc. Physicians India 39 (4), 314–316.

Jha, T.K., Lockwood, D.N., Olliaro, P., Thakur, C.P.N., Kanyok, T.P., Singhania, B.L., et al., 1998. Randomised controlled trial of aminosidine (paromomycin) v sodium stibogluconate for treating visceral leishmaniasis in North Bihar, India. BMJ 316 (7139), 1200–1205.

Jha, T.K., Sundar, S., Thakur, C.P., Felton, J.M., Sabin, A.J., Horton, J., 2005. A phase II dose-ranging study of sitamaquine for the treatment of visceral leishmaniasis in India. Am. J. Trop. Med. Hyg. 73 (6), 1005–1011.

Kaur, K., Patel, S.R., Patil, P., Jain, M., Khan, S.I., Jacob, M.R., et al., 2007. Synthesis, antimalarial, antileishmanial, antimicrobial, cytotoxicity, and methemoglobin (MetHB) formation activities of new 8-quinolinamines. Bioorg. Med. Chem. 15 (2), 915–930.

Khazaeli, P., Sharifi, I., Talebian, E., Heravi, G., Moazeni, E., Mostafavi, M., 2014. Anti-leishmanial effect of itraconazole niosome on in vitro susceptibility of *Leishmania tropica*. Environ. Toxicol. Pharmacol. 38 (1), 205–211.
Kole, L., Das, L., Das, P.K., 1999. Synergistic effect of interferon-γ and mannosylated liposome-incorporated doxorubicin in the therapy of experimental visceral leishmaniasis. J. Infect. Dis. 180 (3), 811–820.
Kuche, K., Maheshwari, R., Tambe, V., Mak, K.K., Jogi, H., Raval, N., et al., 2018. Carbon nanotubes (CNTs) based advanced dermal therapeutics: current trends and future potential. Nanoscale 10 (19), 8911–8937.
Kumar, P., Bose, P.P., 2015. Targeted delivery of paromomycin to leishmania infected macrophage by hemoglobin tagged nanocarrier. J. App. Pharm. 8, 212.
Kumar, R., Sahoo, G.C., Pandey, K., Das, V.N.R., Das, P., 2015. Study the effects of PLGA-PEG encapsulated amphotericin B nanoparticle drug delivery system against *Leishmania donovani*. Drug Deliv. 22 (3), 383–388.
Kumar, R., Sahoo, G.C., Pandey, K., Das, V.N.R., Topno, R.K., Ansari, M.Y., et al., 2016. Development of PLGA–PEG encapsulated miltefosine based drug delivery system against visceral leishmaniasis. Mater. Sci. Eng. C 59, 748–753.
Kumar, R., Pandey, K., Sahoo, G.C., Das, S., Das, V.N.R., Topno, R.K., et al., 2017. Development of high efficacy peptide coated iron oxide nanoparticles encapsulated amphotericin B drug delivery system against visceral leishmaniasis. Mater. Sci. Eng. C 75, 1465–1471.
Lala, S., Pramanick, S., Mukhopadhyay, S., Bandyopadhyay, S., Basu, M.K., 2004. Harmine: evaluation of its antileishmanial properties in various vesicular delivery systems. J. Drug Target. 12 (3), 165–175.
Maheshwari, R.G., Tekade, R.K., Sharma, P.A., Darwhekar, G., Tyagi, A., Patel, R.P., et al., 2012. Ethosomes and ultradeformable liposomes for transdermal delivery of clotrimazole: a comparative assessment. Saudi. Pharm. J. 20 (2), 161–170.
Maheshwari, R.G., Tekade, M., Sharma, P.A., Tekade, R.K., 2015a. Nanocarriers assisted siRNA gene therapy for the management of cardiovascular disorders. Curr. Pharm. Des. 21 (30), 4427–4440.
Maheshwari, R.G., Thakur, S., Singhal, S., Patel, R.P., Tekade, M., Tekade, R.K., 2015b. Chitosan encrusted nonionic surfactant based vesicular formulation for topical administration of ofloxacin. Sci. Adv. Mater. 7 (6), 1163–1176.
Maltezou, H.C., 2010. Leishmaniasis. In: Maltezou, H.C., Gikas, A. (Eds.), Tropical and Emerging Infectious Diseases. Kerala: Research Signpost, India, pp. 163–185.
Mandell, G.L., Bennett, J.E., Dolin, R., 2005. Mandell, Douglas and Bennett's Principles and Practice of Infectious Diseases, sixth ed. Elsevier Churchill Livingstone, Philadelphia, PA.
Mäntylä, A., Garnier, T., Rautio, J., Nevalainen, T., Vepsälainen, J., Koskinen, A., et al., 2004a. Synthesis, in vitro evaluation, and antileishmanial activity of water-soluble prodrugs of buparvaquone. J. Med. Chem. 47 (1), 188–195.
Mäntylä, A., Rautio, J., Nevalainen, T., Vepsälainen, J., Juvonen, R., Kendrick, H., et al., 2004b. Synthesis and antileishmanial activity of novel buparvaquone oxime derivatives. Bioorg. Med. Chem. 12 (13), 3497–3502.
Martín-Quintal, Z., Moo-Puc, R., González-Salazar, F., Chan-Bacab, M.J., Torres-Tapia, L.W., Peraza-Sánchez, S.R., 2009. In vitro activity of *Tridax procumbens* against promastigotes of *Leishmania mexicana*. J. Ethnopharmacol. 122 (3), 463–467.
Martín-Sánchez, J., Acedo, C., Muñoz-Pérez, M., Pesson, B., Marchal, O., Morillas-Márquez, F., 2007. Infection by *Leishmania infantum* in cats: epidemiological study in Spain. Vet. Parasit. 145 (3), 267–273.
Mayrink, W., Botelho, A.C.D.C., Magalhães, P.A., Batista, S.M., Lima, A.D.O., Genaro, O., et al., 2006. Immunotherapy, immunochemotherapy and chemotherapy for American cutaneous leishmaniasis treatment. Rev. Soc. Bras. Med. Trop. 39 (1), 14–21.
Medda, S., Mukhopadhyay, S., Basu, M.K., 1999. Evaluation of the in-vivo activity and toxicity of amarogentin, an antileishmanial agent, in both liposomal and niosomal forms. J. Antimicrob. Chemother. 44 (6), 791–794.
Melaku, Y., Collin, S.M., Keus, K., Gatluak, F., Ritmeijer, K., Davidson, R.N., 2007. Treatment of kala-azar in southern Sudan using a 17-day regimen of sodium stibogluconate combined with paromomycin: a retrospective comparison with 30-day sodium stibogluconate monotherapy. Am. J. Trop. Med. Hyg. 77 (1), 89–94.
Mishra, J., Saxena, A., Singh, S., 2007. Chemotherapy of leishmaniasis: past, present and future. Curr. Med. Chem. 14 (10), 1153–1169.
Misra, P., Sashidhara, K.V., Singh, S.P., Kumar, A., Gupta, R., Chaudhaery, S.S., et al., 2010. 16α-Hydroxycleroda-3,13 (14)Z-dien-15, 16-olide from *Polyalthia longifolia*: a safe and orally active antileishmanial agent. Br. J. Pharmacol. 159 (5), 1143–1150.

Mondal, S., Bhattacharya, P., Ali, N., 2010. Current diagnosis and treatment of visceral leishmaniasis. Expert. Rev. Anti Infect. Ther. 8 (8), 919–944.
Moore, K.W., de Waal Malefyt, R., Coffman, R.L., O'Garra, A., 2001. Interleukin-10 and the interleukin-10 receptor. Annu. Rev. Immunol. 19 (1), 683–765.
Morais, T.R., Romoff, P., Fávero, O.A., Reimão, J.Q., Lourenço, W.C., Tempone, A.G., et al., 2012. Anti-malarial, anti-trypanosomal, and anti-leishmanial activities of jacaranone isolated from *Pentacalia desiderabilis* (Vell.) Cuatrec. (Asteraceae). Parasitol. Res. 110 (1), 95–101.
Mullen, A.B., Baillie, A.J., Carter, K.C., 1998. Visceral leishmaniasis in the BALB/c mouse: a comparison of the efficacy of a nonionic surfactant formulation of sodium stibogluconate with those of three proprietary formulations of amphotericin B. Antimicrob. Agents Chemother. 42 (10), 2722–2725.
Mundargi, R.C., Babu, V.R., Rangaswamy, V., Patel, P., Aminabhavi, T.M., 2008. Nano/micro technologies for delivering macromolecular therapeutics using poly(D,L-lactide-*co*-glycolide) and its derivatives. J. Controlled Release 125 (3), 193–209.
Murray, H.W., Berman, J.D., Davies, C.R., Saravia, N.G., 2005. Advances in leishmaniasis. Lancet 366 (9496), 1561–1577.
Muyombwe, A., Olivier, M., Harvie, P., Bergeron, M.G., Ouellette, M., Papadopoulou, B., 1998. Protection against *Leishmania major* challenge infection in mice vaccinated with live recombinant parasites expressing a cytotoxic gene. J. Infect. Dis. 177 (1), 188–195.
Nakayama, H., Loiseau, P.M., Bories, C., de Ortiz, S.T., Schinini, A., Serna, E., et al., 2005. Efficacy of orally administered 2-substituted quinolines in experimental murine cutaneous and visceral leishmaniases. Antimicrob. Agents Chemother. 49 (12), 4950–4956.
Nanayakkara, N.D., Ager, A.L., Bartlett, M.S., Yardley, V., Croft, S.L., Khan, I.A., et al., 2008. Antiparasitic activities and toxicities of individual enantiomers of the 8-aminoquinoline 8-[(4-amino-1-methylbutyl) amino]-6-methoxy-4-methyl-5-[3,4-dichlorophenoxy] quinoline succinate. Antimicrob. Agents Chemother. 52 (6), 2130–2137.
Nazari-Vanani, R., Vais, R.D., Sharifi, F., Sattarahmady, N., Karimian, K., Motazedian, M.H., et al., 2018. Investigation of anti-leishmanial efficacy of miltefosine and ketoconazole loaded on nanoniosomes. Acta Trop. 185, 69–76.
Nelson, K.G., Bishop, J.V., Ryan, R.O., Titus, R., 2006. Nanodisk-associated amphotericin B clears *Leishmania major* cutaneous infection in susceptible BALB/c mice. Antimicrob. Agents Chemother. 50 (4), 1238–1244.
Nicoletti, S., Seifert, K., Gilbert, I.H., 2009. *N*-(2-hydroxypropyl) methacrylamide–amphotericin B (HPMA–AmB) copolymer conjugates as antileishmanial agents. Int. J. Antimicrob. Agents 33 (5), 441–448.
Nieto, J., Alvar, J., Mullen, A.B., Carter, K.C., Rodríguez, C., San Andrés, M.I., et al., 2003. Pharmacokinetics, toxicities, and efficacies of sodium stibogluconate formulations after intravenous administration in animals. Antimicrob. Agents Chemother. 47 (9), 2781–2787.
Numata, M., Grinkova, Y.V., Mitchell, J.R., Chu, H.W., Sligar, S.G., Voelker, D.R., 2013. Nanodiscs as a therapeutic delivery agent: inhibition of respiratory syncytial virus infection in the lung. Int. J. Nanomed. 8, 1417.
O'Hagan, D.T., Valiante, N.M., 2003. Recent advances in the discovery and delivery of vaccine adjuvants. Nat. Rev. Drug Discov. 2 (9), 727–735.
Odonne, G., Herbette, G., Eparvier, V., Bourdy, G., Rojas, R., Sauvain, M., et al., 2011. Antileishmanial sesquiterpene lactones from *Pseudelephantopus spicatus*, a traditional remedy from the Chayahuita Amerindians (Peru). Part III. J. Ethnopharmacol. 137 (1), 875–879.
Pandey, V., Gajbhiye, K.R., Soni, V., 2015. Lactoferrin-appended solid lipid nanoparticles of paclitaxel for effective management of bronchogenic carcinoma. Drug Deliv. 22 (2), 199–205.
Pandya, S., Verma, R.K., Khare, P., Tiwari, B., Srinivasarao, D.A., Dube, A., et al., 2016. Supplementation of host response by targeting nitric oxide to the macrophage cytosol is efficacious in the hamster model of visceral leishmaniasis and adds to efficacy of amphotericin B. Int. J. Parasitol. Drugs Drug Resist. 6 (2), 125–132.
Pashine, A., Valiante, N.M., Ulmer, J.B., 2005. Targeting the innate immune response with improved vaccine adjuvants. Nat. Med. 11, S63–S68.
Paul, M., Durand, R., Boulard, Y., Fusai, T., Fernandez, C., Rivollet, D., et al., 1998. Physicochemical characteristics of pentamidine-loaded polymethacrylate nanoparticles: implication in the intracellular drug release in *Leishmania major* infected mice. J. Drug Target. 5 (6), 481–490.

Prajapati, V.K., Awasthi, K., Gautam, S., Yadav, T.P., Rai, M., Srivastava, O.N., et al., 2011. Targeted killing of *Leishmania donovani* in vivo and in vitro with amphotericin B attached to functionalized carbon nanotubes. J. Antimicrob. Chemother. 66 (4), 874–879.

Pruthi, J., Mehra, N.K., Jain, N.K., 2012. Macrophages targeting of amphotericin B through mannosylated multi-walled carbon nanotubes. J. Drug Target. 20 (7), 593–604.

Pulido, M., Serralta, L., 1993. Annotated List of Medicinal Plants Currently Used in the State of Quintana Roo, Chetumal, Quintana Roo, Mexico.

Rathore, A., Jain, A., Gulbake, A., Shilpi, S., Khare, P., Jain, A., et al., 2011. Mannosylated liposomes bearing amphotericin B for effective management of visceral leishmaniasis. J. Liposome. Res. 21 (4), 333–340.

Renslo, A.R., McKerrow, J.H., 2006. Drug discovery and development for neglected parasitic diseases. Nat. Chem. Biol. 2, 701–710.

Roberts, M.T.M., 2006. Current understandings on the immunology of leishmaniasis and recent developments in prevention and treatment. Br. Med. Bull. 75-76, 115–130.

Roy, P., Das, S., Bera, T., Mondol, S., Mukherjee, A., 2010. Andrographolide nanoparticles in leishmaniasis: characterization and in vitro evaluations. Int. J. Nanomed. 5, 1113.

Ryan, R.O., 2008. Nanodisks: hydrophobic drug delivery vehicles. Expert Opin. Drug Deliv. 5 (3), 343–351.

Santin, M.R., dos Santos, A.O., Nakamura, C.V., Dias Filho, B.P., Ferreira, I.C.P., Ueda-Nakamura, T., 2009. In vitro activity of the essential oil of *Cymbopogon citratus* and its major component (citral) on *Leishmania amazonensis*. Parasitol. Res. 105 (6), 1489–1496.

Sarkar, S., Mandal, S., Sinha, J., Mukhopadhyay, S., Das, N., Basu, M.K., 2002. Quercetin: critical evaluation as an antileishmanial agent in vivo in hamsters using different vesicular delivery modes. J. Drug Target. 10 (8), 573–578.

Sarkari, B., Chance, M., Hommel, M., 2002. Antigenuria in visceral leishmaniasis: detection and partial characterisation of a carbohydrate antigen. Acta Trop. 82 (3), 339–348.

Saudagar, P., Dubey, V.K., 2014. Carbon nanotube based betulin formulation shows better efficacy against *Leishmania* parasite. Parasitol. Int. 63 (6), 772–776.

Sawadogo, W.R., Le Douaron, G., Maciuk, A., Bories, C., Loiseau, P.M., Figadère, B., et al., 2012. In vitro antileishmanial and antitrypanosomal activities of five medicinal plants from Burkina Faso. Parasitol. Res. 110 (5), 1779–1783.

Seifert, K., Juhls, C., Salguero, F.J., Croft, S.L., 2015. Sequential chemoimmunotherapy of experimental visceral leishmaniasis using a single low dose of liposomal amphotericin B and a novel DNA vaccine candidate. Antimicrob. Agents Chemother. 59 (9), 5819–5823.

Sharma, P.A., Maheshwari, R., Tekade, M., Tekade, R.K., 2015. Nanomaterial based approaches for the diagnosis and therapy of cardiovascular diseases. Curr. Pharm. Des. 21 (30), 4465–4478.

Siddig, M., Ghalib, H., Shillington, D.C., Petersen, E.A., 1988. Visceral leishmaniasis in the Sudan: comparative parasitological methods of diagnosis. Trans. R. Soc. Trop. Med. Hyg. 82, 66–68.

Silva, E.S., Schoone, G.J., Gontijo, C.M., Brazil, R.P., Pacheco, R.S., Schallig, H.D., 2005. Application of direct agglutination test (DAT) and fast agglutination screening test (FAST) for sero-diagnosis of visceral leishmaniasis in endemic area of Minas Gerais, Brazil. Kinetoplastid Biol. Dis. 4 (1), 4.

Silvestre, R., Santarém, N., Teixeira, L., Cunha, J., Schallig, H., Cordeiro-da-Silva, A., 2009. Evaluation of *Leishmania* species reactivity in human serologic diagnosis of leishmaniasis. Am. J. Trop. Med. Hyg. 81 (2), 202–208.

Singh, N., Mishra, P.K., Kapil, A., Arya, K.R., Maurya, R., Dube, A., 2005a. Efficacy of *Desmodium gangeticum* extract and its fractions against experimental visceral leishmaniasis. J. Ethnopharmacol. 98 (1), 83–88.

Singh, S., Dey, A., Sivakumar, R., 2005b. Applications of molecular methods for *Leishmania* control. Expert Rev. Mol. Diagn. 5, 251–265.

Singodia, D., Gupta, G.K., Verma, A., Singh, V., Shukla, P., Misra, P., et al., 2010a. Development and performance evaluation of amphotericin B transfersomes against resistant and sensitive clinical isolates of visceral leishmaniasis. J. Biomed. Nanotechnol. 6 (3), 293–302.

Singodia, D., Gupta, G.K., Verma, A., Singh, V., Shukla, P., Misra, P., et al., 2010b. Development and performance evaluation of amphotericin B transfersomes against resistant and sensitive clinical isolates of visceral leishmaniasis. J. Biomed. Nanotechnol. 6 (3), 293–302.

Sinha, J., Mukhopadhyay, S., Das, N., Basu, M.K., 2000. Targeting of liposomal and rographolide to *L. donovani*-infected macrophages in vivo. Drug Deliv. 7 (4), 209–213.

Sinha, J., Raay, B., Das, N., Medda, S., Garai, S., Mahato, S.B., et al., 2002. Bacopasaponin C: critical evaluation of anti-leishmanial properties in various delivery modes. Drug Deliv. 9 (1), 55–62.
Sinha, R., Roychoudhury, J., Palit, P., Ali, N., 2015. Cationic liposomal sodium stibogluconate (SSG), a potent therapeutic tool for treatment of infection by SSG-sensitive and-resistant *Leishmania donovani*. Antimicrob. Agents Chemother. 59 (1), 344–355.
Soni, V., Chandel, S., Jain, P., Asati, S., 2016. Role of liposomal drug-delivery system in cosmetics. Nanobiomaterials in Galenic Formulations and Cosmetics 93–120.
Sundar, S., Jha, T.K., Thakur, C.P., Engel, J., Sindermann, H., Fischer, C., et al., 2002. Oral miltefosine for Indian visceral leishmaniasis. N. Engl. J. Med. 2002 (347), 1739–1746.
Sundar, S., Jha, T.K., Thakur, C.P., Sinha, P.K., Bhattacharya, S.K., 2007. Injectable paromomycin for visceral leishmaniasis in India. N. Engl. J. Med. 356 (25), 2571–2581.
Tahir, A.E., Ibrahim, A.M., Satti, G.M., Theander, T.G., Kharazmi, A., Khalid, S.A., 1998. The potential antileishmanial activity of some Sudanese medicinal plants. Phytother. Res. 12 (8), 576–579.
Tekade, R.K., Maheshwari, R., Soni, N., Tekade, M., 2017a. Chapter 12—Carbon nanotubes in targeting and delivery of drugs A2—Mishra, Vijay. In: Kesharwani, P., Amin, M.C.I.M., Iyer, A. (Eds.), Nanotechnology-Based Approaches for Targeting and Delivery of Drugs and Genes. Academic Press.
Tekade, R.K., Maheshwari, R., Soni, N., Tekade, M., Chougule, M.B., 2017b. Chapter 1—Nanotechnology for the development of nanomedicine A2—Mishra, Vijay. In: Kesharwani, P., Amin, M.C.I.M., Iyer, A. (Eds.), Nanotechnology-Based Approaches for Targeting and Delivery of Drugs and Genes. Academic Press.
Tekwani, B.L., Walker, L.A., 2006. 8-Aminoquinolines: future role as antiprotozoal drugs. Curr. Opin. Infect. Dis. 19 (6), 623–631.
Trinconi, C.T., Reimão, J.Q., Coelho, A.C., Uliana, S.R., 2016. Efficacy of tamoxifen and miltefosine combined therapy for cutaneous leishmaniasis in the murine model of infection with *Leishmania amazonensis*. J. Antimicrob. Chemother. 71 (5), 1314–1322.
Tyagi, R., Lala, S., Verma, A.K., Nandy, A.K., Mahato, S.B., Maitra, A., et al., 2005. Targeted delivery of arjunglucoside I using surface hydrophilic and hydrophobic nanocarriers to combat experimental leishmaniasis. J. Drug Target. 13 (3), 161–171.
Van de Ven, H., Vermeersch, M., Matheeussen, A., Vandervoort, J., Weyenberg, W., Apers, S., et al., 2011. PLGA nanoparticles loaded with the antileishmanial saponin β-aescin: factor influence study and in vitro efficacy evaluation. Int. J. Pharm. 420 (1), 122–132.
Vannier-Santos, M.A., Martiny, A., Souza, W., 2002. Cell biology of *Leishmania* spp.: invading and evading. Curr. Pharm. Des. 8 (4), 297–318.
Varikuti, S., Oghumu, S., Saljoughian, N., Pioso, M.S., Sedmak, B.E., Khamesipour, A., et al., 2017. Topical treatment with nanoliposomal amphotericin B reduces early lesion growth but fails to induce cure in an experimental model of cutaneous leishmaniasis caused by *Leishmania mexicana*. Acta Trop. 173, 102–108.
Veerareddy, P.R., Vobalaboina, V., Ali, N., 2009. Antileishmanial activity, pharmacokinetics and tissue distribution studies of mannose-grafted amphotericin B lipid nanospheres. J. Drug Target. 17 (2), 140–147.
Villegas, L.F., Fernández, I.D., Maldonado, H., Torres, R., Zavaleta, A., Vaisberg, A.J., et al., 1997. Evaluation of the wound-healing activity of selected traditional medicinal plants from Peru. J. Ethnopharmacol. 55 (3), 193–200.
Vinet, A.F., Jananji, S., Turco, S.J., Fukuda, M., Descoteaux, A., 2011. Exclusion of synaptotagmin V at the phagocytic cup by *Leishmania donovani* lipophosphoglycan results in decreased promastigote internalization. Microbiology 157, 2619–2628.
Wasunna, M.K., Rashid, J.R., Mbui, J., Kirigi, G., Kinoti, D., Lodenyo, H., et al., 2005. A phase II dose-increasing study of sitamaquine for the treatment of visceral leishmaniasis in Kenya. Am. J. Trop. Med. Hyg. 73 (5), 871–876.
Wijnant, G.J., Van Bocxlaer, K., Yardley, V., Harris, A., Alavijeh, M., Silva-Pedrosa, R., et al., 2018. Comparative efficacy, toxicity and biodistribution of the liposomal amphotericin B formulations Fungisome and AmBisome in murine cutaneous leishmaniasis. Int. J. Parasitol. Drugs Drug Resist. 8 (2), 223–228.
World Health Organization, 2010. Control of the Leishmaniases: Report of a Meeting of the WHO Expert Committee on the Control of Leishmaniases, Geneva, 22–26 March 2010.
Yardley, V., Croft, S.L., 2000. A comparison of the activities of three amphotericin B lipid formulations against experimental visceral and cutaneous leishmaniasis. Int. J. Antimicrob. Agents 13 (4), 243–248.

Further reading

Alavizadeh, S.H., Badiee, A., Khamesipour, A., Jalali, S.A., Firouzmand, H., Abbasi, A., et al., 2012. The role of liposome–protamine–DNA nanoparticles containing CpG oligodeoxynucleotides in the course of infection induced by *Leishmania major* in BALB/c mice. Exp. Parasitol. 132 (3), 313–319.

Badiee, A., Jaafari, M.R., Samiei, A., Soroush, D., Khamesipour, A., 2008. Coencapsulation of CpG oligodeoxynucleotides with recombinant *Leishmania major* stress-inducible protein 1 in liposome enhances immune response and protection against leishmaniasis in immunized BALB/c mice. Clin. Vaccine Immunol. 15 (4), 668–674.

Badiee, A., Khamesipour, A., Samiei, A., Soroush, D., Shargh, V.H., Kheiri, M.T., et al., 2012. The role of liposome size on the type of immune response induced in BALB/c mice against leishmaniasis: rgp63 as a model antigen. Exp. Parasitol. 132 (4), 403–409.

Coler, R.N., Hudson, T., Hughes, S., Po-wei, D.H., Beebe, E.A., Orr, M.T., 2015. Vaccination produces CD4 T cells with a novel CD154–CD40-dependent cytolytic mechanism. J. Immunol. 195 (7), 3190–3197.

Das, A., Ali, N., 2014. Combining cationic liposomal delivery with MPL-TDM for cysteine protease cocktail vaccination against *Leishmania donovani*: evidence for antigen synergy and protection. PLoS Negl. Trop. Dis. 8 (8), e3091.

Doroud, D., Zahedifard, F., Vatanara, A., Najafabadi, A.R., Taslimi, Y., Vahabpour, R., et al., 2011. Delivery of a cocktail DNA vaccine encoding cysteine proteinases type I, II and III with solid lipid nanoparticles potentiate protective immunity against *Leishmania major* infection. J. Controlled Release 153 (2), 154–162.

Heravi Shargh, V., Jaafari, M.R., Khamesipour, A., Jalali, S.A., Firouzmand, H., Abbasi, A., et al., 2012. Cationic liposomes containing soluble leishmania antigens (SLA) plus CpG ODNs induce protection against murine model of leishmaniasis. Parasitol. Res. 111 (1), 105–114.

LezamaDávila, C.M., 1999. Vaccination of C57BL/10 mice against cutaneous leishmaniasis. Use of purified gp63 encapsulated into niosomes surfactants vesicles: a novel approach. Mem. Inst. Oswaldo Cruz. 94 (1), 67–70.

Mazumder, S., Ravindran, R., Banerjee, A., Ali, N., 2007. Non-coding pDNA bearing immunostimulatory sequences co-entrapped with leishmanial antigens in cationic liposomes elicits almost complete protection against experimental visceral leishmaniasis in BALB/c mice. Vaccine 25 (52), 8771–8781.

Mazumder, S., Maji, M., Ali, N., 2011. Potentiating effects of MPL on DSPC bearing cationic liposomes promote recombinant GP63 vaccine efficacy: high immunogenicity and protection. PLoS Negl. Trop. Dis. 5 (12), e1429.

Mehravaran, A., Jaafari, M.R., Jalali, S.A., Khamesipour, A., Tafaghodi, M., Hojatizade, M., et al., 2015. The role of surface charge of ISCOMATRIX nanoparticles on the type of immune response generated against leishmaniasis in BALB/c mice. Nanomedicine 2 (4), 249–260.

Nagill, R., Kaur, S., 2010. Enhanced efficacy and immunogenicity of 78kDa antigen formulated in various adjuvants against murine visceral leishmaniasis. Vaccine 28 (23), 4002–4012.

Pardakhty, A., Shakibaie, M., Daneshvar, H., Khamesipour, A., Mohammadi-Khorsand, T., Forootanfar, H., 2012. Preparation and evaluation of niosomes containing autoclaved *Leishmania major*: a preliminary study. J. Microencapsul. 29 (3), 219–224.

Ravindran, R., Bhowmick, S., Das, A., Ali, N., 2010. Comparison of BCG, MPL and cationic liposome adjuvant systems in leishmanial antigen vaccine formulations against murine visceral leishmaniasis. BMC Microbiol. 10 (1), 181.

Santos, D.M., Carneiro, M.W., de Moura, T.R., Fukutani, K., Clarencio, J., Soto, M., et al., 2012. Towards development of novel immunization strategies against leishmaniasis using PLGA nanoparticles loaded with kinetoplastid membrane protein-11. Int. J. Nanomed. 7, 2115.

Shahbazi, M., Zahedifard, F., Saljoughian, N., Doroud, D., Jamshidi, S., Mahdavi, N., et al., 2015. Immunological comparison of DNA vaccination using two delivery systems against canine leishmaniasis. Vet. Parasit. 212 (3), 130–139.

Tafaghodi, M., Eskandari, M., Khamesipour, A., Jaafari, M.R., 2011. Alginate microspheres encapsulated with autoclaved *Leishmania major* (ALM) and CpG-ODN induced partial protection and enhanced immune response against murine model of leishmaniasis. Exp. Parasitol. 129 (2), 107–114.

Veerareddy, P.R., Vobalaboina, V., Nahid, A., 2004. Formulation and evaluation of oil-in-water emulsions of piperine in visceral leishmaniasis. Pharmazie 59 (3), 194–197.

Zarrati, S., Maleki, F., Mahdavi, M., Khabaz, N., Tabatabaie, F., 2014. Humoral immune responses in DNA vaccine formulated with poly(methyl methacrylate) against *Leishmania major*. J. Entomol. Zool. Stud. 2 (5), 201–206.

CHAPTER

9

Up-to-Date Implications of Nanomaterials in Dental Science

Muktika Tekade[1], *Neha Maheshwari*[1], *Hira Choudhury*[2], *Bapi Gorain*[3], *Pran Kishore Deb*[4], *Rakesh K. Tekade*[5] *and Mukesh Chandra Sharma*[1]

[1]School of Pharmacy, Devi Ahilya Vishwavidyalaya, Takshila Campus, Indore, India [2]Department of Pharmaceutical Technology, School of Pharmacy, The International Medical University, Kuala Lumpur, Malaysia [3]Faculty of Health and Medical Science, School of Pharmacy, Taylor's University, Subang Jaya, Malaysia [4]Faculty of Pharmacy, Philadelphia University, Amman, Jordan [5]National Institute of Pharmaceutical Education and Research (NIPER)—Ahmedabad, Gandhinagar, India

OUTLINE

9.1 Introduction: Understanding Dentistry and Underlying Problems in Dental Therapy 302

9.2 Medical Approaches to Resolve Dental Issues: Emergence of Nanotechnology in Dentistry 302

9.3 Various Nanomaterials Used in Dentistry 303

9.3.1 Chitosan Biopolymer-Based Formulations 303

9.3.2 Gelatin-Based Nanoformulations 306

9.3.3 Poly(Lactide-co-Glycolic Acid) 308

9.3.4 Liposomes 313

9.3.5 Silver Nanoparticles 314

9.3.6 Zinc Oxide Nanoparticles 317

9.3.7 Titanium Dioxide Nanoparticles 320

9.3.8 Nanoemulsion-Based Approach 324

9.3.9 Nanoemulgel Approach in Dentistry 327

9.4 Conclusion and Future Prospects 329

Abbreviations 329

References 330

Biomaterials and Bionanotechnology
DOI: https://doi.org/10.1016/B978-0-12-814427-5.00009-3

© 2019 Elsevier Inc. All rights reserved.

9.1 INTRODUCTION: UNDERSTANDING DENTISTRY AND UNDERLYING PROBLEMS IN DENTAL THERAPY

Dentistry is a branch of medicine that deals with the prevention, treatment, assessment, and diagnosis of diseases related to the oral cavity, maxillofacial area, as well as the adjacent/associated structures by surgical or nonsurgical means (Abrahamsson et al., 2017). The history of dentistry can be dated back as early as 5000 BC when tooth worms were described as the cause of dental decay in a Sumerian text. However, the development of the dentistry profession started only in the 18th century when Pierre Fauchard, the father of modern dentistry, published a book that described a comprehensive system for the practice of dentistry that included basic oral anatomy and function, operative and restorative techniques, and denture construction. Dental diseases, including dental caries (defined as decay or crumbling of a tooth), periodontal problems, and periimplantitis are among the prevalent oral diseases throughout the world (Ahrari et al., 2015; Abrahamsson et al., 2017).

Microorganism biofilms, composed of especially *Streptococcus*, *Lactobacillus*, *Candida*, *Escherichia coli*, and *Staphylococcus aureus*, as well as salivary dysfunction (xerostomia), and dietary carbohydrates serve as imperative etiologic factors in dental diseases. These bacterial biofilms produce lactic acid, which dematerializes enamel, and dentine, which leads to the creation of a carious lesion otherwise known colloquially as tooth decay or dental cavities (Nguyen et al., 2016).

9.2 MEDICAL APPROACHES TO RESOLVE DENTAL ISSUES: EMERGENCE OF NANOTECHNOLOGY IN DENTISTRY

Among the treatment modalities for dental issues, nanotechnology-based approaches are gaining interest. The application of nanotechnology to healthcare is called nanomedicine. Nanomedicine requires the intersection of many disciplines including chemistry, biology, physics, chemical and mechanical engineering, material science, and clinical medicine (Khurshid et al., 2015).

In the field of dentistry, nanomedicine can help to maintain oral health to improve the quality of life for patients through the employment of nanomaterials and biotechnology, including tissue engineering and nanorobotics (Tekade et al., 2017a). This may create limitless opportunities in dentistry, including dentition renaturalization, local anesthesia, permanent hypersensitivity cure, orthodontic treatment, and diagnosis of periodontal disease. The nanomedicines that have been applied in dentistry are composed of chitosan biopolymers, gelatin, poly(lactide-*co*-glycolic) acid (PLGA), phospholipids, silver, zinc oxide, and titanium dioxide (Kráľová and Jampílek, 2018).

The main objective of this chapter is to discuss the applications and potential of nanomedicine and nanotechnology in all specializations of dentistry. This includes the reported applications and emerging roles that would improve the diagnosis and treatment of diseases caused in the oral cavity, installation of biological autologous for tooth replacement, and the production of products that deliver subocclusal-dwelling nanorobotic dentifrices

that may patrol subgingival and supragingival surfaces. This chapter also focuses on the novel potential treatments in nanodentistry such as dentition renaturalization, local anesthesia, permanent hypersensitivity cures, cosmetic dentistry, covalently bonded diamondized enamel, continuous oral health maintenance, and complete orthodontic realignments.

9.3 VARIOUS NANOMATERIALS USED IN DENTISTRY

9.3.1 Chitosan Biopolymer-Based Formulations

Chitosan is a deacetylated derivative of chitin, which is the second most abundant natural polysaccharide after cellulose in terms of utilization and distribution. Chitin is the major structural component found in the exoskeleton of crustaceans, such as lobsters, crabs, and shrimp (Maheshwari et al., 2015). The free amino groups are known to contribute toward the cationic property of chitosan. Due to the insolubility of chitin, chitosan is generally more preferred for applications in different sectors of the medical and pharmaceutical fields. Besides, other important characteristics of chitin and chitosan are that they are nontoxic, biocompatible, biodegradable, and that they have hydrating and antimicrobial properties (Husain et al., 2017).

These polymeric components are also easily processed into gels, microparticles, microspheres, nanoparticles, scaffolds, beads, nanofibers, and sponges. Due to their special feature of having a relatively large pore size, these components have high efficiency in entrapping cargo molecules. Therefore chitosan has been perceived as a promising drug carrier and has been an interesting area to explore biomedical applications (Gohil et al., 2017). In dentistry, various approaches using chitosan have been ventured, such as the antimicrobial activity of chitosan, the potential drug delivery system using chitosan, and tissue engineering with chitosan as scaffolds (Elieh-Ali-Komi and Hamblin, 2016).

Before application of drug delivery using chitosan, chitosan itself had demonstrated a lot of amazing properties, one being its antimicrobial nature. The antimicrobial action of chitosan has been postulated by several mechanisms. First, with low molecular weight chitosan, it would dissociate into the solution and could bind with host deoxyribonucleic acid (DNA). Therefore synthesis of mRNA of the pathogenic microorganism is inhibited (Dobhal et al., 2017). Second, with high molecular weight chitosan, trace metals can be selectively bound by chelation, inhibiting microbial growth or toxin production. Furthermore, the cationic chitosan can interact with the anionic cell membrane of microorganisms, leading to leakage and disruption of the cell membrane (Cheung et al., 2015).

Bumgardner et al. evaluated bond strength of deacetylated chitosan using a mechanical tensile test, evaluated the dissolution in cell culture medium, and determined cytocompatibility in vitro UMR106 osteoblastic cells. They found that bond strength (1.5−1.8 MPa) of chitosan coatings were not affected by gas sterilization but bond strengths were less than that reported for calcium-phosphate coatings. Little dissolution was exhibited over 8 weeks in cell culture solution by gas sterilized chitosan, and growth of the UMR106

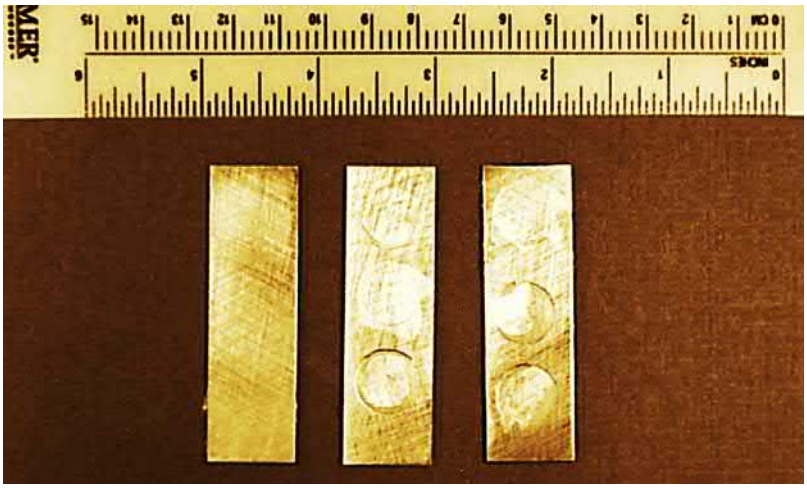

FIGURE 9.1 Photomicrograph showing representative chemically bonded chitosan coatings before and after tensile testing. The chitosan coating exhibited a yellow-gold color due to imine bond formation between the glutaraldehyde and chitosan molecules (left, before tensile testing). Chemically bonded chitosan coatings failed at the coating–substrate interface (middle and right). *Source: Adapted with permission from Bumgardner, J.D., Wiser, R., Gerard, P.D., Bergin, P., Chestnutt, B., Marini, M., et al., 2003. Chitosan: potential use as a bioactive coating for orthopaedic and craniofacial/dental implants. J. Biomater. Sci., Polym. Ed. 14(5), 423–438.*

osteoblast cells was greater on the chitosan-coated samples than on the uncoated titanium. Overall, the study concluded that chitosan has the potential to be used as a bioactive and biocompatible coating for orthopedic and craniofacial implant devices. Fig. 9.1 shows a photomicrograph of chemically bonded chitosan coatings before and after tensile testing and Fig. 9.2 shows a graph of the tensile bond strengths of chitosan coatings on titanium (Bumgardner et al., 2003).

Uraz et al. evaluated a 2% chitosan mouthwash and evaluated the formulation for clinical effects and antimicrobial action on plaque inhibition. The randomized clinical trial showed that there was no significant difference in the antiplaque effect between chlorhexidine gluconate with chitosan mouthwash and chitosan mouthwash alone (Uraz et al., 2012). Another in vitro study conducted by Costa et al. on the impact of chitosan mouthwash toward oral microorganism's biofilm formation proved that chitosan mouthwash was capable of interfering with microbial adherence, resulting in inhibition of biofilm formation. Besides, another great feature of chitosan mouthwash is that it is able to interact with and destroy mature biofilms, which is an ability that is normally lacking in conventional antimicrobial mouthwashes. Interestingly, there are currently no reports of known antimicrobial resistance toward chitosan (Costa et al., 2014).

In a study by Hayashi et al., the effects of chewing gum containing chitosan were evaluated by measuring its ability to inhibit the proliferation of cariogenic bacteria. The number of oral microorganisms was found to be significantly reduced in the chitosan group compared with the conventional chewing gum. This favorable result could be due to the direct antimicrobial effect of chitosan and the indirect mechanical effect of increasing salivary flow rate, hence washing out the bacteria (Hayashi et al., 2007).

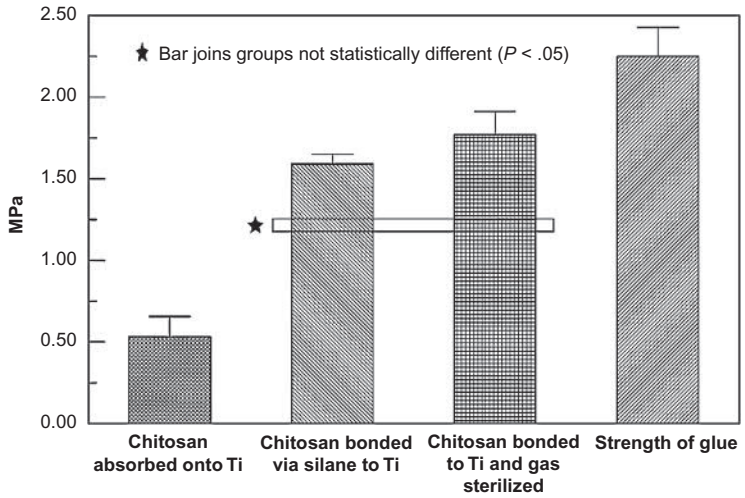

FIGURE 9.2 Bar graph of the tensile bond strengths of chitosan coatings on titanium. The silane bonded coatings exhibited bond strengths approximately three times that of the chitosan coatings absorbed (nonbonded) to the titanium. Ethylene oxide gas sterilization procedures did not affect the bond strength of the coatings. The strength of the Loctite 454 glue between the Al studs and uncoated titanium was greater than the strength of the bonded chitosan coatings. *Source: Adapted with permission from Bumgardner, J.D., Wiser, R., Gerard, P.D., Bergin, P., Chestnutt, B., Marini, M., et al., 2003. Chitosan: potential use as a bioactive coating for orthopaedic and craniofacial/dental implants. J. Biomater. Sci., Polym. Ed. 14(5), 423–438.*

In terms of drug delivery in dentistry, topical delivery remains the most appreciated approach to reduce unwanted systemic effects. When considering conventional therapy of mouthwash or gargle rinses, some limitations may be encountered, such as unpleasant taste and flushing action of saliva, which rapidly reduce the drug concentration. Therefore bioadhesive polymers have attracted great interest for drug delivery for intraoral administration in the past decade. In this context, chitosan has remained a great model polymer as it is an excellent natural mucoadhesive agent as well as permeabilizer (Meechan, 2000). The mucoadhesive property of chitosan is believed to be contributed by the electrostatic interactions between the cationic chitosan and anionic mucous membrane (Pitts et al., 2017).

In a study by Aksungur et al., nystatin was incorporated in chitosan to prepare gel and film formulations for the treatment of oral mucositis. In this study, chitosan demonstrated excellent properties as an occlusive dressing and drug carrier. The chitosan gel formulation also provided an extended drug retention time in the oral cavity above the minimum inhibitory concentration (MIC) when compared with a normal suspension formulation that did not contain chitosan (Aksungur et al., 2004).

In another study conducted by Ikinci et al., chlorhexidine gluconate was incorporated into chitosan to form gel and film formulations for treatment against *Porphyromonas gingivalis*. This combination of chitosan with chlorhexidine gluconate had demonstrated synergistic effect that was more efficacious than the drug alone. This can be advantageous to lower the concentration of the drug because it may, therefore, reduce the adverse effects

of the drug. In addition, the film formulation had demonstrated an extended release pattern when compared with gel formulation. In this study, it was proposed that chitosan in film and gel formulations can be a very promising drug delivery carrier for dental applications (Ikinci et al., 2002).

Tissue engineering is a field that focuses on rejuvenation and restoration of damaged or diseased tissue by using an artificial scaffold that mimics the natural environment of the cells. Chitosan has played an important role in the area of tissue engineering by having the ability to make well-interconnected porous scaffolds. Also, biological scaffold mimicking shapes can be constructed into the desired forms such as sponges, hydrogels, or three-dimensional (3D) porous structures. These structural properties ensure sufficient supply of nutrients and oxygen to improve cell viability to optimal levels. Furthermore, growth factors can be incorporated into chitosan that can potentiate its use in tissue engineering (O'brien, 2011; Trubiani et al., 2006). Lee et al. have demonstrated a significant increase in osteogenesis when treated with chitosan loaded with platelet-derived growth factor BB. It was postulated that while chitosan stimulates osteoblast activity, it inhibits fibroblasts. It has also been reported that chitosan potentiates the differentiation of osteoprogenitor cells (Lee et al., 2000).

In conclusion, chitosan has numerous biomedical applications and it is clear that chitosan has tremendous potential in novel dentistry drug delivery approaches due to its antimicrobial action and utility in tissue engineering.

9.3.2 Gelatin-Based Nanoformulations

Gelatin has been a tremendously used excipient for oral pharmaceutical drug delivery systems due to its unique Food and Drug Administration generally regarded as safe (GRAS) nature. The use of gelatin in pharmaceutical drug delivery system design is notably related to its ingestible characteristic as it is nontoxic. Its popularity in drug delivery design is also due to its biodegradability, low cost, availability, and flexibility in different types of alteration processes (Jacob et al., 2018). Nevertheless, its use has been extended into nanoformulations, which is particularly beneficial in providing local effects (De Jong et al., 2008). Hence, the current trend in the pharmaceutical field utilizes gelatin-based nanoformulation as a new tool to counter the common dental issues.

9.3.2.1 Delivery of Fibroblast Growth Factor-2 in Dental Pulp Therapy via Gelatin Hydrogel

Dental pulp, made up of living connective tissues and cells located in the center of the teeth, is often damaged due to microbiological or physical trauma. Currently, dentists carry out a procedure known as a pulpectomy to irreversibly remove the infected or diseased pulp followed by filling the tooth with biocompatible materials such as gutta-percha to prevent reinfection by bacteria (Morotomi et al., 2018). However, such therapy is unable to revive the natural defensive ability of the pulp. Thus the pulp is vulnerable to other infection, which might ultimately lead to tooth extraction. Thus fibroblast growth factor-2 (FGF-2) may be used as a modern treatment to induce dentinogenesis, which results in the growth of the tooth back to its healthy state (Anitua et al., 2018; Mehrvarzfar et al., 2018).

FGF-2 has been a good inducing factor of dentinogenesis; however, it has a short half-life due to rapid degradation via oral enzymes (Duncan et al., 2018). Thus many types of research have been utilizing gelatin hydrogels as a nanocarrier of FGF-2. Tabata et al. have used ^{125}I-labeled FGF-2 to study release patterns from gelatin hydrogels. They found that the release rate of ^{125}I-labeled FGF-2 is correlated with the degradation of gelatin hydrogel. As the type of calcified material formed in the new pulp is highly affected by the release pattern of FGF-2, the nanocarrier, which dictates the release pattern, has become enormously crucial. To produce dentin matrix protocol-1-positive calcified particles in the newly formed dental pulp, the ideal release mechanism should be controlled release, while to accelerate dentin formation, noncontrolled release mechanism should be used. After understanding the effects of different release patterns on dentinogenesis, researchers are interested in controlling the release rate of FGF-2 from gelatin hydrogels.

9.3.2.2 *Delivery of Hydroxyapatite in Remineralization of Tooth Enamel*

Caries in teeth are a common, but difficult, task to be managed by dentists. Formation of caries involves complex tooth demineralization and remineralization, which can be effectively reversed if the remineralization process dominates (Shahmoradi et al., 2018). Currently, besides casual preventive measures, caries prevention is done by incorporating hydroxyapatite (HA) into toothpaste. However, this method may remain ineffective due to the high affinity of free HA to bind with proteins, fragments of oral plaque, and bacteria. Thus approaches have been made by incorporating nano-HA in chitosan−gelatin bioglass scaffolds to tackle dental caries (Esteves-Oliveira et al., 2017).

HA is a bioactive bioceramic that has the molecular formula of $Ca_{10}(PO_4)_6 \cdot 2(OH)$, which presents as a major constituent in enamel (90%). To be a bioeffective functional unit in enamel remineralization, the nano-HA shall have a crystal dimension with the length of 50−100 nm and width of 20−40 nm (Pepla et al., 2014).

HA, when combined with chitosan−gelatin, gains the ability to closely mimic the natural bone matrix. Hence, it may be a very useful material to prepare bone scaffold. Chitosan is a partially deacetylated form of chitin that exhibits wound healing ability and is also structurally similar to the glycosamine glycan present in the extracellular bone matrix. Gelatin is derived from collagen and contains amino acid functional groups that are responsible for enhancing cell proliferation and growth. Chitosan, when linked with gelatin, exhibits superior plasticity, biocompatibility, and biodegradability that is useful in bone tissue engineering and dentistry (Mallick et al., 2015).

To make the chitosan−gelatin bioglass scaffold, chitosan solution was prepared and added to glutaraldehyde solution. Gelatin solution was also added, followed by bioglass addition. The mixture was sufficiently stirred and stored at −20°C. Then, the solidified mixture was lyophilized and washed with deionized water to remove the glutaraldehyde solution. The resultant solid material is the cross-linked chitosan−gelatin bioglass scaffold (Zhou et al., 2014).

Incorporation of the nano-HA into the scaffold together with the performance of chitosan−gelatin bioglass was tested in vitro. A study conducted by Han et al. had demonstrated the water-uptake ability and degradation profile of the generated scaffold. The water retention ability of this material was found to be strong, and it was observed to swell >100% of its own weight. It swells to its maximum size within the first hour of

administration. This excellent swelling property indicates that the release profile of the scaffold may be ideal to purposefully help in remineralization of damaged teeth (Thein-Han et al., 2009).

During the investigation of the degradation profile of chitosan–gelatin bioglass, researchers incubated the scaffold with lysozyme for 28 days. During that period, it was found that the scaffold had been drastically degraded within the first 7 days. It was postulated that the degradation of the scaffold was mainly due to the degradation of gelatin, the main scaffold ingredient. Further, it was understood that the scaffold degradation is often accompanied by drug release (Tangsadthakun et al., 2007). It was also shown that the gelatin-coated bioglass scaffold was capable of producing a controlled-release pattern, which is important in biomineralization of pulp (Maji et al., 2016). Therefore to control the degradation profile of the damaged tooth enamel, different concentrations of gelatin may be used to manipulate the degradation time of the scaffold material (Tangsadthakun et al., 2007).

The therapeutic potential of gelatin-based nanoformulations such as a gelatin-based scaffold or gelatin hydrogel in treating dental issues is undoubtedly beneficial. Currently, gelatin-based nanotechnologies are still subjected to extensive characterization studies together with in vitro studies to prove the efficacy of the developed formulation. Fortunately, the progress is optimistic as researchers are now able to control the performances of nanoparticles in biological tissues. In the near future, we hope these beneficial inventions will help in introducing useful products to the current market to treat such painful dental problems (Kráľová and Jampílek, 2018).

9.3.3 Poly(Lactide-*co*-Glycolic Acid)

PLGA, composed of lactic acid and glycolic acid, is one of the most biodegradable and biocompatible synthetic polymers. PLGA has gained great interest from scientists for its use in the development of novel drug delivery system due to its ability to be incorporated successfully in various formulations such as vaccines, peptides, and macromolecules (Jain, 2000; Kashi et al., 2012).

The PLGA polymer undergoes degradation by hydrolysis then breaks down into constituent monomers and gets excreted from the body as carbon dioxide and water (Jain, 2000; Ramchandani et al., 1997). The release of a drug is dependent on the degradation of PLGA polymer. There are several main mechanisms of drug release from the polymers, as it is either by erosion of polymer material or diffusion through polymer barrier or a mixture of both phenomena. The mechanisms are affected by factors such as pH, ionic strength, the temperature of the external bulk medium, molecular weights of polymer, crystallinity, and the presence of drug (Jain, 2000; Kashi et al., 2012; Ramchandani et al., 1997).

According to the World Oral Health Report 2003 done by the World Health Organization, oral diseases are major health problems in developing countries as periodontal and endodontic diseases are widespread among adults (Piñón-Segundo et al., 2005). Periodontal diseases result from dental plaque, multispecies biofilm that is structurally and functionally organized, which colonizes surfaces on the tooth and epithelial cells

lining the periodontal pocket, causing inflammation and subsequently gingivitis (Klepac-Ceraj et al., 2011). Current periodontal therapy utilizes mechanical root scaling and planing to remove bacterial plaque and systemic antibiotics to treat bacterial infections; however, high dose of antibiotics are required and therefore may result in more side effects (Kashi et al., 2012; Kimishima et al., 2016; Piñón-Segundo et al., 2005; Sousa et al., 2014). This PLGA delivery system showed promising results in treating various disease, ranging from bacterial infections, genetic disorders, and cancer. Therefore PLGA nanoparticles have been developed for local delivery of medicaments to treat various endodontics and periodontal diseases.

Nanoparticles are defined as solid colloidal particles with a size ranging from 10 to 1000 nm and may encapsulate or entrap active ingredient(s) (Klepac-Ceraj et al., 2011). The methods to prepare PLGA nanoparticles are coacervation or phase separation, spray drying, emulsion−solvent evaporation, and emulsification diffusion. The most common preparation method is solvent evaporation, in which polymer dissolved in organic solvent undergoes emulsification into the aqueous solution to create an oil-in-water emulsion with the use of poly(vinyl alcohol) (PVA) as a surfactant. The organic solvent is then subjected to high temperature under pressure to be evaporated. This preparation method of nanoparticles is dependent on the hydrophilicity/hydrophobicity of the active substance and its stability (Klepac-Ceraj et al., 2011).

One remarkable advantage of PLGA nanoparticles is their small size, which allows them to penetrate into areas such as alveolar bone trabeculae and gingival sulcus, inward to underlying connective tissue, and periodontal pocket areas below the gum line, which is not possible with other available drug delivery systems (Kashi et al., 2012). Furthermore, nanoparticles can protect the drug and are more stable in biological fluids compared with microspheres. In addition, PLGA nanoparticles are a potential periodontal carrier because they can continuously supply antibiotics over an extended period of time by modifying degradation rates of nanoparticles, therefore reducing the required dosage and frequency (Kashi et al., 2012).

Eslami et al. had synthesized PLGA/TiO_2 nanotubes (TNT) composite microspheres and characterized their 3D porous scaffolds. They found mechanical properties of PLGA/TNT microsphere sintered scaffold were increased by the incorporation of TNT. Experimental results from their study showed that PLGA scaffold, when sintered at 100°C for 3 hours, showed the relative best mechanical properties and pore structure for tissue engineering. In vivo results showed that bone formation for PLGA/TNT was approximately twice that of pure PLGA. They observed scanning electron microscopy (SEM) images of PLGA and PLGA/TNT composite at a basic molecule and when sintered at 100°C and 120°C for 3 hours, which are shown in Fig. 9.3 (Eslami et al., 2018).

Minocycline is commonly used to treat periodontal diseases as it has antimicrobial and anticollagenase effects that can reduce destruction of soft tissue and bone resorption (Kashi et al., 2012). In a study, minocycline-loaded nanoparticles prepared using the solid/oil/water ion pairing method doubled the antibacterial efficacy against *Aggregatibacter actinomycetemcomitans* compared with the free drug alone. This was because of the nanoparticle ability to penetrate into bacterial cells due to their nanosize and ability to be endocytosed by phagocytic cells to deliver the antibiotics to the infected site (Kashi et al., 2012).

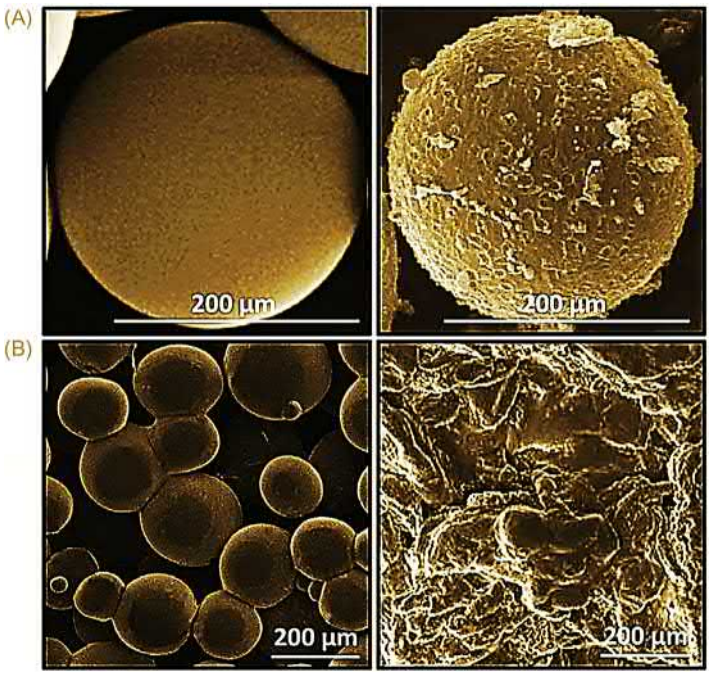

FIGURE 9.3 (A) SEM images from PLGA microsphere and PLGA/0.5% TNT composite, (B) SEM images of PLGA/0.5% TNT microspheres composite sintered at 100°C and 120°C for 3 hours. *PLGA*, poly(lactide-*co*-glycolic) acid; *SEM*, scanning electron microscopy; *TNT*, TiO_2 nanotubes. *Source: Adapted with permission from Eslami, H., Lisar, H.A., Kashi, T.S.J., Tahriri, M., Ansari, M., Rafiei, T., et al., 2018. Poly(lactic-co-glycolic acid)(PLGA)/TiO_2 nanotube bioactive composite as a novel scaffold for bone tissue engineering: in vitro and in vivo studies. Biologicals 53, 51–62.*

In addition, Piñón-Segundo et al. prepared triclosan nanoparticles composed of PLGA, polylactide, and chloroaluminum phthalocyanine (CAP) with PVA as a stabilizer via the emulsification–diffusion technique. Triclosan was chosen because it had demonstrated potential efficacy against some plaque-forming bacteria and resolved gingival lesions. Therefore it has been employed as a mouth rinse to slow down or to stop gingival inflammation (Piñón-Segundo et al., 2005). It was discovered that triclosan–PLGA nanoparticles led to reduced inflammation with less redness when compared with the control group in an in vivo study performed in dogs. Therefore it has been suggested that nanoparticles are able to play a role in reducing gingival inflammation (Piñón-Segundo et al., 2005).

In another study, Kimishima et al. investigated the efficacy of gatifloxacin-loaded PLGA and b-tricalcium phosphate (GFLX) composites to treat osteomyelitis. Interestingly, it was demonstrated that 10 wt.% GFLX composite was more effective than the 1 wt.% GFLX composite (Kimishima et al., 2016). This could be due to the pH decreasing the effect of GFLX, which further increases the degradation rate of PLGA. The release of glycolic and lactic acid leads to reduced pH and also kills the bacteria effectively by reducing the emergence of GFLX-resistant bacteria (Kimishima et al., 2016).

Another alternative treatment of periodontitis and elimination of subgingival species is photodynamic therapy (PDT). PDT utilizes a photosensitizer that would be embedded within targeted tissues and that has the ability to become activated when an appropriate wavelength of light reaches it in the presence of oxygen to cause oxidative stress to the cells by generating singlet oxygen and free radicals (Klepac-Ceraj et al., 2011; Pagonis et al., 2010). The use of methylene blue in PDT is well established to be effective in

staining Gram-negative and Gram-positive oral bacteria but recent studies showed that human dental plaque biofilm has reduced susceptibility to methylene blue PDT (Klepac-Ceraj et al., 2011; Pagonis et al., 2010).

Reduced susceptibility of biofilms is due to the restricted penetration of methylene blue and the expulsion of methylene blue from the bacterial cells by multidrug resistance pumps. Thus methylene blue–loaded PLGA nanoparticles were developed to overcome these problems, as they have nanosize, which can effectively penetrate into a bacterial cell and limit the ability of the cell to pump out drug molecules (Klepac-Ceraj et al., 2011; Pagonis et al., 2010). In addition, they have larger critical mass and the nanoparticle matrix did not elicit evidence of immunogenic responses. The release of the photosensitizer molecules to a targeted organ can be done by modifying the particle surface with poly(ethylene oxide) to enhance the biodistribution and biocompatibility of the carrier (Pagonis et al., 2010).

It has been suggested that cationic PLGA nanoparticles are more effective for applications in photodestruction of oral biofilms than anionic PLGA nanoparticles and free methylene blue. Results have shown that cationic methylene blue–loaded PLGA nanoparticles produced 1 $\log_{10}$ killing while free methylene blue and anionic nanoparticles produced 40% and 60% killing, respectively (Klepac-Ceraj et al., 2011). One possible explanation of this situation is due to the electrostatic interaction of cationic nanoparticles and negatively charged lipid bilayer residues leading to the formation of nanoscale holes in the outer bacterial cells' membranes (Klepac-Ceraj et al., 2011; Pagonis et al., 2010).

The activity of methylene blue might become enhanced by active or passive targeting by the nature of the charged surface of the nanoparticle. However, the negatively charged matrix may hinder the penetration of cationic nanoparticles due to strong ionic interactions (Klepac-Ceraj et al., 2011; Pagonis et al., 2010). Therefore it is hard to justify exactly the outcomes of the interplay of chemical composition of the matrix, physicochemical properties, and chemical reactivity of antimicrobial agents in affecting its effectiveness (Klepac-Ceraj et al., 2011).

On the other hand, PLGA nanoparticles can be incorporated with growth factors for bone grafting (Bessho et al., 2002; Hassan et al., 2015; Liu et al., 2012; Sousa et al., 2014). Bone morphogenetic proteins (BMPs) are osteoinductive factors that can induce the differentiation of osteoblasts from mesenchymal cells (Hassan et al., 2015; Zou et al., 2012). In a study done by Hassan et al., recombinant human BMP-2 was incorporated into depot injectable PLGA nanoparticles and effectiveness was studied. The study had shown that the nanoparticles had managed to maintain the increased plasma rhBMP-2 concentration longer than the liposomal in situ gel, which was a duration of 48 hours (Hassan et al., 2015).

The stiffness of nanoparticles formed by PLGA–polycaprolactone (PCL) mixture can be increased by increasing the ratio of PCL in the polymer matrix, resulting in higher viscosity and thus slowing down the release of the drug, reaching prolonged and controlled release of rhBMP-2 PLGA nanoparticles (Hassan et al., 2015). In addition, this study showed that the defects were 78% ossified with surrounding fibrovascular tissues containing numerous osteoblasts within 6 weeks. The bones formed had greater volume and maturity in the group using PLGA nanoparticles in comparison to liposomal in situ gel. These findings indicated that this method may have potential applications as an early grafting method for repair of alveoli defects (Hassan et al., 2015) (Table 9.1).

TABLE 9.1 Poly(Lactide-*co*-Glycolic) Acid (PLGA) Nanoparticles Applied in Dentistry.

Nanomaterial	The Objective of the Study	Method of Use	Application	Outcomes	Reference
Minocycline-loaded PLGA nanoparticles	To study different producing methods of minocycline-loaded PLGA nanoparticles for periodontal infections	Conjugated with PEG and used as a drug carrier for localized treatment	Periodontal infections	Minocycline PLGA nanoparticles prepared using ion pairing method had highest entrapment efficiency, drug loading, and higher in vitro antibacterial activity compared with other prepared nanoparticles	Kashi et al. (2012)
Triclosan-loaded PLGA nanoparticles	To produce and characterize triclosan-loaded nanoparticle by emulsification–diffusion process to be a delivery system to treat periodontal disease	Used as a drug carrier for localized treatment	Periodontal infections	Effectively reduce gingival inflammation	Piñón-Segundo et al. (2005)
GFLX	To study the effectiveness of different concentrations of GFLX in treating osteomyelitis	GFLX composites were implanted in bone defects secondary to osteomyelitis lesions caused by *Bacteroides fragilis* and *Streptococcus milleri*	Osteomyelitis treatment	10 wt.% GFLX composite is more effective than 1 wt.% GFLX for local treatment of osteomyelitis	Kimishima et al. (2016)
Methylene blue–loaded PLGA nanoparticles	To study the in vitro effects of methylene blue loaded PLGA nanoparticles and light against *Enterococcus faecalis*	PLGA nanoparticles incorporated with methylene blue are localized in certain tissues and get activated when light irradiated to kill bacteria	Endodontic treatment	There is a reduction of 2 and 1 $\log_{10}$ of colony-forming units in the planktonic phase and root canals respectively with the use of light and methylene blue loaded PLGA nanoparticles	Pagonis et al. (2010)
rhBMP-2 PLGA nanoparticles	To utilize the biocompatibility characteristics of PCL and PLGA to prepare sustained release depot injectable nanoparticles of bone morphogenetic protein-2 to repair alveolar bone defects in rabbits	Used as a delivery system incorporated with growth factor at the site of implantation	Alveolar bone defects treatment	There is 78% trabecular bone fill in bone defects within 6 weeks after treated with rhBMP-2	Hassan et al. (2015)

GFLX, Gatifloxacin-loaded PLGA; *PCL*, polycaprolactone; *PEG*, polyethylene glycol; *PLGA*, poly(lactide-*co*-glycolic) acid.

9.3.4 Liposomes

Liposomes are circular vesicles comprised of one or more phospholipid bilayers that can be made from cholesterol and natural nonharmful phospholipids. They are one of the promising systems for medication conveyance in view of their size as well as their hydrophobic and hydrophilic characteristics (Tekade et al., 2017b). Phospholipids form shut structures when they are hydrated in aqueous solutions. Such vesicles, which have one or more phospholipid bilayer films, can transport aqueous or lipidic drugs, depending upon the way those medications are loaded during the preparation process. Drug delivery with liposomes as transporter systems gives choices and opportunities for biostable and/or site particular medical treatments. They are amphiphilic, which allows a conceivable self-association in a fluid medium to frame liposomal structures (Allen and Cullis, 2013).

Liposomes, as a drug delivery system, have several advantages and disadvantages. The most attractive property is that lipid nanoparticles can combine with the bacterial outer membrane, conveying the antimicrobial agents specifically to the bacterial cells. In addition, by focusing on the nanoparticles to the biofilm, a high measurement of antimicrobial agents can be conveyed in the immediate vicinity of the bacterial cells, in this way boosting restorative advantages while diminishing undesirable reactions (Daraee et al., 2016).

Nguyen et al. investigated the in vitro adsorption and retention ability of liposomes on four types of dental restorative materials [conventional and silorane-based resin composites as well as conventional and resin-modified glass ionomer cement (GIC)]. They prepared and characterized uncoated liposomes (positively and negatively charged) and pectin coated liposomes (low and high methoxylated) in terms of their zeta potential and particle size. In this study, they found that positive liposomes, due to their attractive surface charge to negatively charged dental materials, showed the highest adsorption on all four types of dental materials. They also showed better retention on both conventional resin composite and GIC. However, pectin coated liposomes showed only an intermediate initial level of adsorption. Thereby the study concluded two new possible applications of liposomes in the preservation and dental restorations. Fig. 9.4 shows fluorescence images of different liposomes before and after adsorption (Nguyen et al., 2015). As a conclusion for this study, large unilamellar vesicles demonstrated better results and may be used as a drug delivery system for use on human dermal fibroblasts cell line since it appeared as noncytotoxic to the cell. The capability of liposomes as a drug delivery system for use in the oral cavity has been explored particularly focusing on the teeth, the in vitro adsorption of charged liposomes to HA, a typical model substance for dental finishes.

Many liposomal systems have been utilized as bearers to convey bactericides to restrain the development of biofilms. In vitro tests have demonstrated that liposomes adsorb to HA, a regularly acknowledged model substance for tooth enamel. Liposomes can be bioadhesive, as they have the ability to be held on enamel surfaces to increase the contact time in the oral cavity (Augustine et al., 2016). Notwithstanding its exemplifying capacity of active pharmaceutical ingredients, liposomes might protect the enamel against decay by physically covering the enamel surfaces. The preliminary adsorption of microorganisms to dental enamel is the premise for dental plaque arrangement, and if allowed to progress, can lead to plaque-related sicknesses in adulthood (Nguyen et al., 2017).

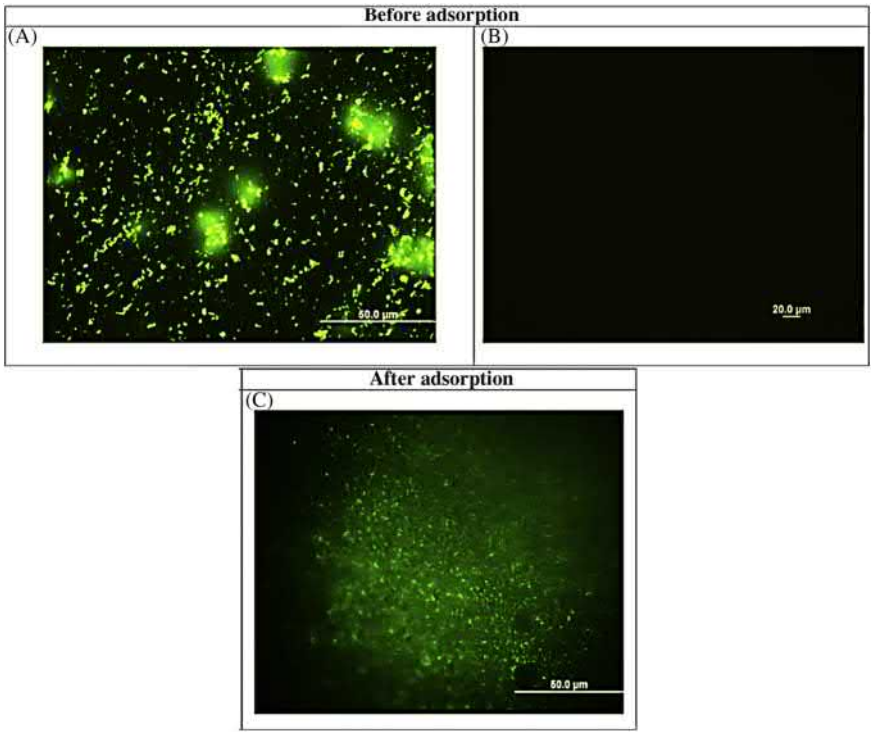

FIGURE 9.4 Fluorescence images of (A) positive liposomes alone at 100×, (B) the surface of the resin-modified glass ionomer FII LC at 40×, and (C) positive liposomes on FII LC at 100× (Nguyen et al., 2015).

We must consider the advantages of liposomes to embody fluid calcium chloride ($CaCl_2$) and to physically separate this reagent from an extravesicular inorganic phosphate solution. One procedure that might be more valuable in a clinical setting is to use liposomes intended to discharge their substance affected by a connected external stimulus, for example, light, heat, or an adjustment in pH (Chen et al., 2014). In a companion paper, we give an account of a thermally enacted liposomal mineralization system in which calcium discharge and mineral development are initiated by a temperature change. Authors recognize that such a system could be utilized to quickly shape calcium phosphates in situ for remineralization of dentin, enamel, or bone (Santheep et al., 2017).

9.3.5 Silver Nanoparticles

Microorganism biofilms, especially *Streptococcus* and *S. aureus*, act as an imperative causative element in dental diseases (Ahrari et al., 2015; Kasraei et al., 2014). The presence of bacteria leads to the colonization in the dental cavity and the bacterial microleakage between restoration and dental tissues. This is mainly associated with failure of restoration and results in secondary caries and recurrent caries (Kasraei et al., 2014; Sokołowski et al., 2014).

To prevent and control dental diseases, the applied materials should aim to eradicate the underlying microorganisms from the pulp cavity system to play an important role in achieving long-term successes in endodontic treatment (Ali et al., 2013; Lu et al., 2013). Thereby, the use of antimicrobial agents having minimal side effects that do not generate putative pathogenic resistance has resulted in decreasing the prevalence of such periodontal diseases (Ahrari et al., 2015; Ali et al., 2013; Lu et al., 2013).

Recent advances in the field of nanotechnology have demonstrated that nanostructured materials are considered to be a very promising tool due to their potential for achieving specific processes and selectivity, particularly in biological and pharmaceutical applications (De Giglio et al., 2013; Kasraei et al., 2014; Suganya et al., 2014). Among nanomaterials, silver has been employed most extensively to fight against infections and control spoilage (Ali et al., 2013; De Giglio et al., 2013; Suganya et al., 2014). Silver is a white shiny element with high ductility, electrical and thermal conductivity (Ali et al., 2013; Venkatesh et al., 2015). It has well-tolerated tissue response, low toxicity profile in human cells (Lu et al., 2013; Venkatesh et al., 2015; Suganya et al., 2014), and effective antimicrobial and inhibitory properties without inducing microbial resistance against a remarkable number of pathogens (De Giglio et al., 2013; Suganya et al., 2014).

Silver-containing materials are widely used in prostheses (Hsueh et al., 2015; Jerzy et al., 2014; Suganya et al., 2014), surgical devices (De Giglio et al., 2013; Hsueh et al., 2015; Jerzy et al., 2014), and wound dressing applications (Ali et al., 2013; De Giglio et al., 2013; Suganya et al., 2014). Meanwhile, silver nanoparticles (AgNPs) are commonly used as oral hygiene products in the dental field, such as toothpaste, antigingivitis agents, and restorative materials (Tunde Vig et al., 2008). Studies by Kasraei et al. suggested that AgNPs can effectively be applied against microorganisms with its antimicrobial properties and can prevent adhesion of bacteria to surfaces and formation of biofilms (Kasraei et al., 2014).

A study that compared AgNP with nanogold and nano−zinc oxide found that AgNP is the most effective antimicrobial agents against *Streptococcus mutans*, as it requires a lower concentration to inhibit *S. mutans* strain development compared with others (Hernández-Sierra et al., 2008). Another study by Cherif et al. (2015) In an another study, it was reported that the application of AgNP is more potent against Gram-negative bacteria compared with Gram-positive bacteria due to the thicker cell wall of Gram-negative bacteria that contains more peptidoglycan. Moreover, Ag^{+} ions were easily trapped by peptidoglycan of Gram-negative bacteria because Ag^{+} ions are positively charged, while peptidoglycan is negative (Cherif et al., 2015; Yamanaka et al., 2005).

Barbosa et al. showed that the predisposition to form particle aggregates is an important aspect that may hinder the action of nano-Ag against biofilm cultures. This aggregation may occur due to changes in ionic strength and interaction of nanoparticles with several substances present in the extracellular matrix produced by microorganisms. SEM images of clusters of AgNP in contact with mature *Candida albicans* biofilms and the enlarged view of this biofilm are shown in Fig. 9.5 (Barbosa et al., 2013).

Silver can modify the bacterial DNA synthesis and affect the enzymatic systems of the respiratory chain. The antimicrobial properties of AgNP are related to their size. The size reduction of the AgNP leads to an increase of surface area by releasing bioactive silver

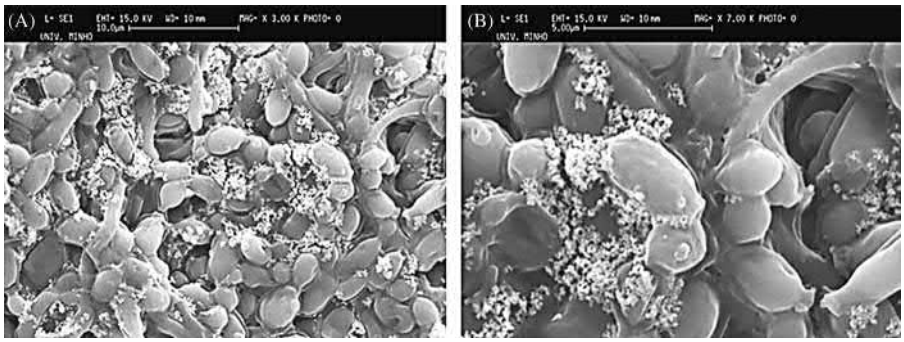

FIGURE 9.5 (A) Scanning electron microscopy images showing clusters of silver nanoparticles in contact with mature *Candida albicans* biofilm. (B) An enlarged view of part of biofilm displayed by Barbosa et al. (2013).

ions (Ag^+) (Fig. 9.10) (Ahrari et al., 2015; Ribeiro et al., 2013; Jerzy et al., 2014; Lu et al., 2013; Suganya et al., 2014). This exhibits antimicrobial activities and prevents the black staining of teeth after application of silver diamine fluoride (Ribeiro et al., 2013).

AgNP is sensitive to oxygen as they have been observed to oxidize in aqueous solution due to the presence of air (Lu et al., 2013; Suganya et al., 2014). Therefore oxidized silver results in the release of Ag^+ ions under acidic conditions and can lead to the structural damage of microorganisms, known as "oligodynamic action" of silver (Lu et al., 2013; Suganya et al., 2014).

Ag^+ ions are selectively toxic to prokaryotic cells with little effect on eukaryotic cells (Jerzy et al., 2014; Lu et al., 2013; Venkatesh et al., 2015; Suganya et al., 2014). They form metal-organic complexes and insoluble compounds with sulfhydryl groups in the cell walls of bacteria, which results in the inactivation of essential enzymes for energy metabolism and electron transport (Ahrari et al., 2015; Holla et al., 2012; Venkatesh et al., 2015; Yamanaka et al., 2005).

In addition, Ag^+ ions attach and rupture the outer membranes of bacterial cells. This then leads to lipid peroxidation, which damages the cell membrane, denatures the cellular protein, disrupts DNA replication, inhibits cell respiration, and eventually induces cell death. Thus a powerful antimicrobial activity that does not cause tooth discoloration and a low production cost may be achieved with the application of AgNP in the dental field, especially for the management or treatment of dental diseases (Kasraei et al., 2014; Aguiar et al., 2013; Chang et al., 2015).

Although there are many advantages of AgNP applications as dental therapies, a major limitation of using silver-containing materials is discoloration, thereby, losing aesthetic appeal to the users, which is an important criterion. Studies have shown that incorporating silver particles at more than 10% concentration into dental materials notably reduces compressive strength, elastic modulus, and tensile strength. However, the low concentration of AgNP might prevent severe staining (Hernández-Sierra et al., 2008; Kasraei et al., 2014; Jerzy et al., 2014).

In addition to the issue of tooth discoloration, a study conducted by Ahrari et al. observed that AgNPs are not highly effective against *S. mutans* due to the adherent properties of AgNPs (Ahrari et al., 2015). The AgNPs adhere to each other and form

micrometer aggregate particles at high concentration, which affects their antimicrobial activity (Ahrari et al., 2015). A few silver additives, including quaternary ammonium dimethacrylate (QADM), were synthesized and merged with AgNPs to reduce microorganism biofilm growth (Li et al., 2013). QADM inhibits the adherence on the surface of bacteria by forming a polymer network of covalent bonds to exert antiadherence properties, meanwhile, AgNP exhibits antimicrobial activates by releasing the Ag^{+} ions to destroy the microorganisms (Li et al., 2013).

AgNP can be prepared by the chemical reduction of silver nitrates, where reaction was conducted between the reducing agents, hydrazine hydrate and sodium citrate, sodium dodecyl sulfate as a stabilizer, or sodium tetrahydridoborate as reductant and polyvinylpyrrolidone as stabilizer (Hernández-Sierra et al., 2008; Jerzy et al., 2014; Targino et al., 2014). A quantity of 125 mL of 1 mM silver nitrate solution was heated and soon after boiling commenced, 5 mL of 1% sodium citrate solution was added. The heating was continued until the color changed to pale yellow. Then the solution was removed from the heating element and stirred until it had cooled down to room temperature. The formation of the synthetic AgNP was confirmed by examining using SEM (Dugal and Chakraborty, 2014).

In conclusion, AgNP is a promising new approach as a noninvasive dental caries preventive agent as it displayed good antimicrobial properties with low toxicity to human cells. It could inhibit the production of microorganism biofilms and prevent secondary dental caries in xerostomic patients. However, further studies on the dental application of modified denture base impregnated with AgNP and the potential impact of AgNP contamination on the ecosystems are needed to ensure the safety and efficacy of the use of AgNP in the dental field (Dugal and Chakraborty, 2014; Hsueh et al., 2015).

9.3.6 Zinc Oxide Nanoparticles

Zinc oxide (ZnO) is a functional and versatile inorganic material. ZnO-nanoparticles (ZnO-NPs) have high catalytic and photochemical activities contributing to their antibacterial and antifungal properties (Seil and Webster, 2012). ZnO-NPs can be synthesized by using any of the following methods: thermal evaporation of ZnO powders at 1400°C, hydrothermal synthesis, sol–gel technique, simple thermal sublimation, self-combustion polymerized complex method, vapor–liquid–solid technique, double jet precipitation, and solution synthesis. For example, flower-shaped ZnO-NPs were produced via the solution synthesis process at 90°C using zinc acetate dihydrate and sodium hydroxide (Wahab, 2007). Nanorods of hexagonal prismatic and pyramidal-like structures were synthesized by adding ZnO powder hydrothermally with different stabilizing agents and exhibited a prominent antibacterial effect toward the targeted bacteria. Different nanostructures are thought to add advantages to the production of antibacterial activity through modification of their mechanism of action.

Thus the morphology of ZnO-NPs plays an important role in their bactericidal action. For example, rods and wires are able to penetrate into the cell wall of the bacteria easier than spherical ZnO-NPs but have lower biocidal action against *S. aureus* and *E. coli* than flower-shaped ZnO-NPs (Yang et al., 2009). The antibacterial efficiency can be enhanced in

smaller sized ZnO-NPs because they can easily penetrate into bacterial membranes due to their large surface area. This characteristic is also beneficial for dentistry applications to ensure distribution of ZnO-NPs to the desired area to achieve therapeutic effect because of the small spaces present within the oral cavity and between the teeth (Hamouda, 2012).

The main mechanism that contributes to the antibacterial activity of ZnO-NPs is the generation of reactive oxygen species (ROS), which could be further enhanced when ZnO-NPs are exposed to ultraviolet (UV) sources (Brayner et al., 2006; Padmavathy, 2008; Sawai, 1998). Besides that, the number of polar surfaces of ZnO-NPs determines the oxygen vacancies, which will affect the photocatalytic action of ZnO-NPs, which leads to ROS generation. ROS, including superoxide anions, hydrogen peroxide, and hydroxide are involved in cellular component destruction due to their internalization into the bacterial cell membrane and subsequent bacterial cell death (Raghupathi et al., 2011).

ZnO-NPs have the ability to block additional antibacterial activity by remaining firmly adsorbed at the surface of the killed bacteria (Song et al., 2010). Other proposed mechanisms of action include metal ion uptake by translocation and particle internalization into cells followed by exhausting the intracellular adenosine triphosphate production and DNA replication disruption, as well as changes in bacterial membrane permeability and dissipation of the proton motive force, which leads to accumulation and dissolution of nanoparticles in the cell membrane (Amro et al., 2000).

ZnO-NPs are capable of inhibiting culturable oral bacteria and biofilm formation on glass and acrylic dentures, as well as cultured human epithelial cells. Conventional antibiotic treatments often result in chronic oral infections because of their subtherapeutic efficacy level following tooth extractions or implant removal. Biofilm formation due to complex polymicrobial communities in the human oral cavity is known to be associated with dental caries and periodontitis. Further, biofilm formation is found to be the main cause for the decline of antimicrobial treatment which eventually leads to multiple drug resistance in bacteria. Bacteria are less likely to be resistant toward metal nanoparticles because metal nanoparticles are able to control oral biofilm formation, thus making their use a novel approach to dental infection prophylaxis. Their exclusive physicochemical properties could prevent antimicrobial resistance by inhibiting rapid microbial adaptation and transformation (Hajipour et al., 2012; Rai et al.).

As metallic antibacterial nanoparticles have been shown to provide various advantages and antibiofilm efficacy when applied in infected root canals, Versiani et al. evaluated the influence of incorporating ZnO-NPs on physicochemical properties of Grossman sealer and found all groups had shown significant difference in setting time whereas, ZnO-Np decreased the setting time and dimensional changes characteristics of Grossman sealer. Fig. 9.6 represents SEM monographs and corresponding energy-dispersive X-ray spectra of the elements on the outer and inner surfaces of the control and experimental sealers with 50% and 25% of ZnO-NPs before and after the solubility test (Versiani et al., 2016).

Metal nanoparticles have the advantage of being able to endure high temperatures needed for fixation and are less toxic to mammalian cells when stabilized onto oral surfaces (Vargas-Reus, 2012). To prevent multidrug resistance and persistent biofilm formation, the implants can be coated with antimicrobial agents. Composite of ZnO-NPs and HA-nanoparticles (HA-NPs) showed the formation of a stable interface between bone and implant. In a biofilm analysis, the composite of ZnO-NP and HA-NP reduces 95% of

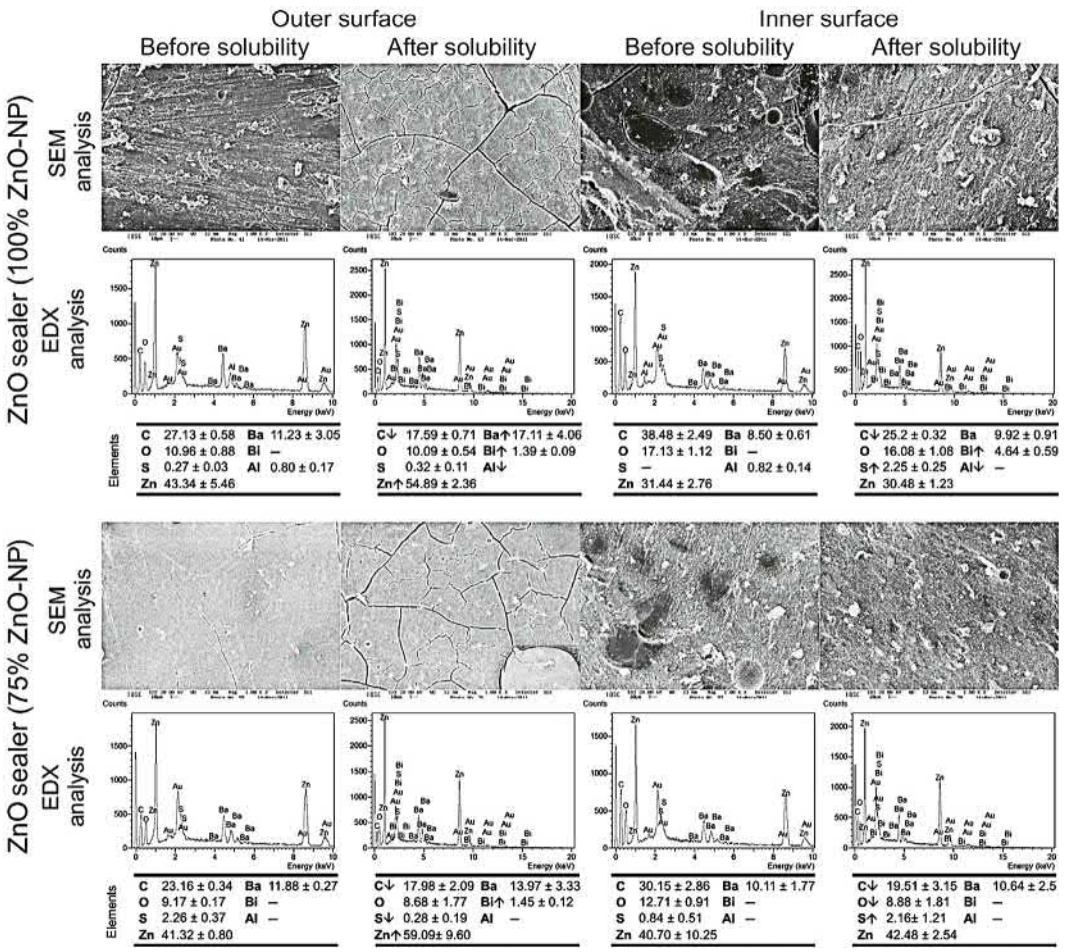

FIGURE 9.6 Representative scanning electron microscopic micrographs and corresponding energy-dispersive X-ray spectra of the elements on the outer and inner surfaces of the control and experimental sealers with 50% and 25% of ZnO-NPs before and after the solubility test. The down and up arrows in the energy-dispersive X-ray analysis mean decreasing and increasing in the average of the elemental constitution after the solubility test, respectively (Versiani et al., 2016).

Streptococcus spp. and 90% of aerobes while ZnO-NPs alone reduces only 92% of *Streptococcus* spp. and 64% of aerobes. This result clearly shows that the inhibition of microbial growth is closely related to the prevention of biofilm formation (Abdulkareem et al., 2015). Besides that, the latest studies prove ZnO-NPs promote bone growth in addition to enhanced osteoblast proliferation (Vargas-Reus et al., 2012).

Orthodontic treatment such as translating a tooth in the dental arch is often required due to undesired tooth movements. However, the sliding procedure produces a frictional force between the bracket and wire, which may affect the anchorage control (Kochoei et al., 2015). An excessive orthodontic force requires overcoming the friction force

produced, which poses the risk of anchorage loss. Orthodontic wires or brackets which are coated with ZnO-NPs have benefits such as (1) rolling effects, which enable two surfaces to slide on each other, and (2) functioning as spacers to prevent contact of two opposing surfaces (Kachoei et al., 2013, 2015).

In conclusion, nanoparticles have large surface area to volume ratios, which makes them effective antibacterial agents. ZnO-NPs could inhibit the bacterial activity in the oral cavity and thereby prevent the formation of biofilm, which makes them suitable as a novel approach in preventing dental infections. The long-term antibacterial physical and clinical effects of nanoparticles on dental fields should be studied more with the goal of benefiting the future generations by providing optimal dental care.

9.3.7 Titanium Dioxide Nanoparticles

Titanium is the fourth most abundant metallic element in the Earth's crust (Duraccio et al., 2015). Titanium dioxide (TiO_2) has been commonly used for many dental materials and applications (Padovani et al., 2015). For example, TiO_2 is used as inorganic nanobased materials in nanodentistry to improve the efficiency and stability of dental materials (Nayar et al., 2011; Padovani et al., 2015). Titanium dioxide nanoparticles (TiO_2NP) are proven to have antibacterial effects and have been observed to improve the performance of dental resins (Padovani et al., 2015). Hence, TiO_2NP may be coated onto other nanomaterials as well as can be incorporated with dental materials to serve as a drug delivery system for antibacterial activity and improve the quality of the dental material.

TiO_2NP can be synthesized by the sol–gel technique (Devi et al., 2014). In an example of this method, titanium tetra-isopropoxide should be mixed with deionized water, hydrochloride (HCl), and ethanol. The mixture at pH 1.5 is then stirred for 30 minutes. Stirring will be continued at room temperature for another 2 hours after deionized water addition. A powder may be obtained following the drying of the mixture at room temperature. Finally, heating of the powder at 120°C will result in the formation of TiO_2NP (Devi et al., 2014).

Like ZnO-NPs, TiO_2NPs carry out bactericidal activity via the production of ROS (Barnes et al., 2013; Kim et al., 2003; Maness et al., 1999). The process in which TiO_2NP produces ROS is known as the photocatalysis reaction (Blecher et al., 2011; Maness et al., 1999). TiO_2NPs undergo photocatalysis reaction when exposed to UV light radiation, where the photo energy generates an electron–hole pair on the TiO_2 surface (Blecher et al., 2011; Maness et al., 1999). The hole in the valence band is able to react with hydroxide ions or water molecules that are adsorbed on the surface to produce ROS. The ROS that is produced by TiO_2NP are hydrogen peroxide, superoxide ions, and singlet oxygen, and hydroxyl radical (Kim et al., 2003; Maness et al., 1999). The excessive ROS that is generated by TiO_2NP is able to disturb or damage the bacterial cell membrane and eventually cause bacterial cell death (Barnes et al., 2013).

There are many studies conducted by various scientists to prove the antibacterial activity of TiO_2NPs against both Gram-positive and Gram-negative bacteria. Studies have proven that TiO_2NP with UV illuminated suspension is able to produce bactericidal effect against Gram-positive *Bacillus subtilis*, *S. aureus*, and Gram-negative *E. coli* (Adams et al., 2006; Barnes et al., 2013). In the study by Barnes et al. (2013), it was demonstrated that 100% of

E. coli, 80% of *S. aureus*, and 100% *B. subtilis* were inactivated after exposure to 1 g/L of UV illuminated TiO_2NP suspension. Hence, it was inferred that TiO_2NPs were able to work against both Gram-negative and Gram-positive bacteria. Further, Ahrari et al. showed that TiO_2NP containing solution had the lowest MIC against *S. mutans* and *Streptococcus sanguis* compared with ZnO-NPs, copper oxide nanoparticles, AgNP, and chlorhexidine (Ahrari et al., 2015). These findings have proved that the antibacterial effects of TiO_2NP are more effective than other metal nanoparticles and chlorhexidine. Hence, there are clear advantages to eliciting the antibacterial effects of TiO_2NP for dental applications.

Garcia-Contreras et al. conducted a full-scale metabolomic analysis of human gingival fibroblast cells treated with IL-1b alone or in combination with TiO_2NPs to clarify the mechanism of TiO_2NPs-enhanced gingival inflammation. They found that TiO_2NPs enhanced the IL-1b-induced prostaglandin E2 production and COX-1 and COX-2 protein expression. The addition of TiO_2NPs further augmented these IL-1b-induced metabolic changes, recommending careful use of dental materials containing TiO_2NPs to patients with gingivitis or periodontitis. Fig. 9.7 shows the proinflammatory action of IL-1b and TiO_2NPs with different combinations and at different times (Garcia-Contreras et al., 2015).

In a study conducted by Adams et al. (2006), TiO_2NPs were found to inhibit the growth of *E. coli* and *B. subtilis* under dark conditions. This special outcome can be explained the effectiveness of the TiO_2NP in the absence of UV light. However, it has also been observed that the antibacterial activity of TiO_2NP is significantly reduced in absence of UV light (Adams et al., 2006). This might be due to the inability to produce photocatalytic ROS by the TiO_2NP without UV light. The possible mechanism for TiO_2NP to have antibacterial effect under dark conditions is explained by its nanoparticulate size as it is believed to disrupt the bacterial membrane integrity (Adams et al., 2006).

Thus TiO_2NPs are widely used in dental material due to such antibacterial activity and are able to improve the performance of the dental material. The two common dental materials that are used in dentistry are acrylic resins based on heat-cured poly(methylmethacrylate) and GIC (Acosta-Torres et al., 2010; Garcia-Contreras et al., 2015). Dental resins such as acrylic resins are widely used for orthodontic removable appliances and denture base (Mori et al., 2015; Shirkavand and Moslehifard, 2014). The dental resin containing TiO_2NP was shown to be effective against *E. coli*, *S. mutans*, *Staphylococcus epidermidis*, *Streptococcus pyogenes*, and *Enterococcus faecalis* (Cai et al., 2013).

The dental resin containing TiO_2NP was also reported to increase the tensile strength, shear bond strength, and flexural strength when compared with adding TiO_2NP dental resin (Shirkavand and Moslehifard, 2014; Sun et al., 2011; Xia et al., 2008). Surprisingly, a dental resin containing 0.1%−0.25% of TiO_2NP can simulate the opalescence of human enamel (Yu et al., 2009). Thus incorporation of TiO_2NP into dental resin could be effective against various types of bacteria as well as improve the quality and mechanical properties of the dental resin.

Besides that, GICs are commonly used as dental restorative materials in dentistry (Garcia-Contreras et al., 2015). Restorative GIC-containing 3% (w/w) TiO_2NP had shown better antibacterial activity against *S. mutans* than unmodified GIC (Elsaka et al., 2011; Garcia-Contreras et al., 2015). In addition, GIC-containing 3% and 5% (w/w) TiO_2NPs were able to improve the flexural strength, fracture toughness, and compressive strength compared with unmodified GIC (Elsaka et al., 2011). Hence, this demonstrated that

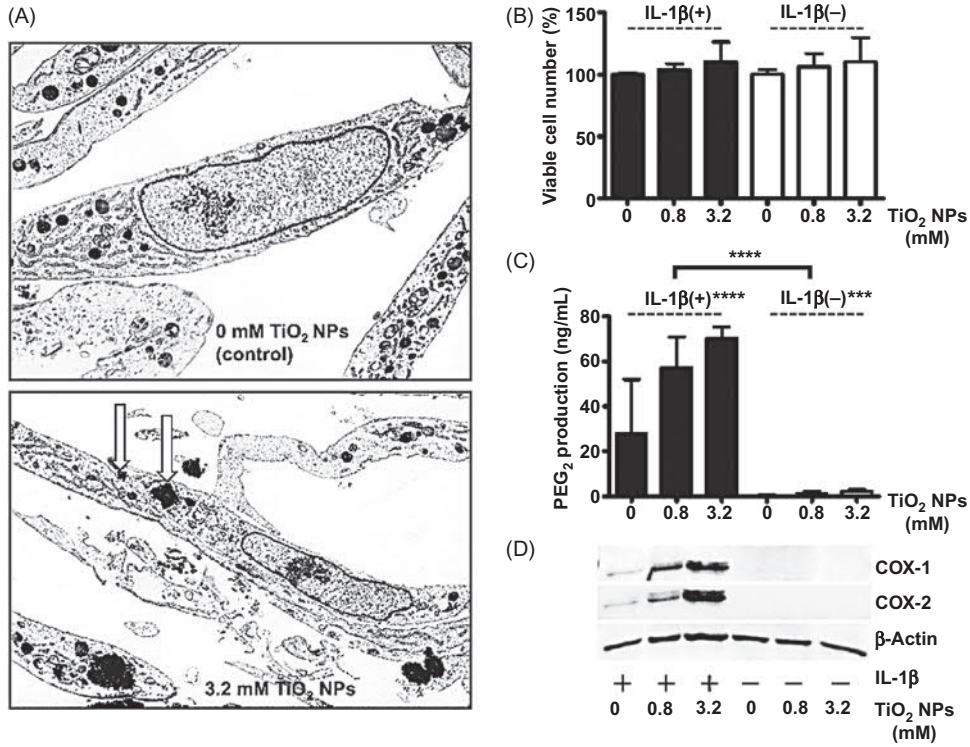

FIGURE 9.7 The proinflammatory action of IL-1b and TiO_2NPs. (A) Near-confluent HGF cells were incubated for 3 hours with 0 or 3.2 mM TiO_2NPs. The cells were then washed three times with cold PBS (A) and fixed for 1 hour with 2% glutaraldehyde in 0.1 M cacodylate buffer (pH 7.4) at 4°C for observation under transmission electron microscopy. Arrows indicate the agglomerated TiO_2NPs. The pictures with different concentrations of TiO_2NPs are shown in our previous chapter. (B) Viable cell number (absorbance at 540 nm with MTT method), (C) medium PGE2 level (with ELISA), and (D) COX-1 and COX-2 protein expression (with western blot analysis) after incubation for 24 hours. Similar reproducible results were obtained in another independent experiment. One-way ANOVA was conducted for the data with 0, 0.8, and 3.2 mg/mL of TiO_2NPs. Student's *t*-test (two-tailed) was used for the comparison of the data with and without IL-1b. ****$P < .0001$ and ***$P < .001$ (Garcia-Contreras et al., 2015). *HGF*, Human gingival fibroblast.

TiO_2NP incorporated with GIC was able to enhance the antibacterial effect and mechanical properties of GIC. There are studies that have also shown that orthodontic adhesive containing 1 wt.% of TiO_2NP does not result in additional health hazards compared with pure adhesives (Heravi et al., 2013). Thus it can be concluded that TiO_2NP is safe for intraoral application (Table 9.2).

In conclusion, TiO_2NPs are indeed able to bring many advantages to the dental material over other metallic nanoparticles. Also, TiO_2NP incorporated with the dental material can be used as a drug delivery system for long-term antibacterial activity. This can control the pronounced use of antibiotics in dentistry and the chance of developing antibiotic resistance. Finally, the addition of TiO_2NP into dental material can also enhance the mechanical properties and quality of the dental material.

TABLE 9.2 TiO_2NP Applied in Dentistry.

Nanomaterial	The Objective of the Study	Method of Use	Application	Outcomes	References
TiO_2NP	To determine the post-UV antibacterial property of the resin containing TiO_2NP tested on five bacterial strains including *Streptococcus mutans*, *Staphylococcus epidermidis*, *Streptococcus pyogenes*, *Enterococcus faecalis*, and *Escherichia coli* adhesion on the UV-treated resin containing TiO_2NP	TiO_2NP incorporated with resin composites	Dental resin	Resin-based composites containing 20% TiO_2NP provide a significant antibacterial effect against *S. mutans*, *S. epidermidis*, *S. pyogenes*, *E. faecalis*, and *E. coli* for p to 2 h post-UV	Cai et al. (2013)
TiO_2NP	To determine the tensile strength of heat-curing acrylic resin reinforced by added TiO_2NP into the resin matrix	TiO_2NP incorporated with acrylic resin nanocomposite	Dental resin	Nanocomposite with 1 wt.% TiO_2NP exhibited higher tensile strength by compared with the control group and other groups	Shirkavand and Moslehifard (2014)
TiO_2NP	To study the improvement of dental resins with the addition of TiO_2NP.	Acrylic acid modified TiO_2NP (AP25)	Dental resin	The mean shear bond strength using resins with 0.1% mass fraction of AP25 was approximately 30% higher than NP-free resin	Sun et al. (2011)
TiO_2NP	To determine the improvement of the mechanical properties of dental resin-based composites by adding TiO_2NP coated with an organosilane allytriethoxysilane	TiO_2NP coated with organosilane allytriethoxysilane incorporated dental resin-based composites	Dental resin	Composite resin with modified TiO_2NP have significantly better mechanical properties than the control group	Xia et al. (2008)
TiO_2NP	To determine the influence of TiO_2NP addition on the color, translucency, opalescence, and fluorescence of experimental resin composites	TiO_2NP incorporated with light curing resin matrix	Dental resin	Resin composites with 0.1%−0.25% TiO_2NP able to simulate the opalescence of human enamel	Yu et al. (2009)
TiO_2NP	To study the antibacterial activity, the physical properties, and the bond strength of base, core build up, and restorative GIC compared with GIC modified TiO_2NP at 3% and 5% (w/w)	TiO_2NP incorporated with GIC	GIC	GIC supplemented with TiO_2NP potential antibacterial activity and durable restoration to withstand the mastication force	Garcia-Contreras et al. (2015)
TiO_2NP	To evaluate the physical properties of conventional glass ionomer with the addition of TiO_2NP	TiO_2NP incorporated with glass ionomer	Glass ionomer	Glass ionomer-containing 3% and 5% (w/w) TiO_2NP enhanced the flexural strength, fracture, toughness, and compressive strength compared with the unmodified GI	Elsaka et al. (2011)
TiO_2NP	To evaluate the cytotoxicity of Transbond XT adhesive containing 1 wt.% TiO_2NP	TiO_2NP incorporated with orthodontic adhesive (Transbond XT)	Orthodontic adhesive	Incorporation of 1 wt.% TiO_2NP to the composite structure does not result in additional health hazards compared with the pure adhesive	Heravi et al. (2013)

GIC, Glass ionomer cement; *UV*, ultraviolet.

9.3.8 Nanoemulsion-Based Approach

Applications of nanoemulsions for the treatment of periodontic diseases are great approaches in the dentistry field. Nanoemulsions are thermodynamically stable, optically isotropic, transparent, and homogeneous/heterogeneous mixtures of oil and water, where the nanodroplets of the dispersing medium are stabilized by the thin layer of surfactant (Kikuchi et al., 2015). Use of nanoemulsions in several drug delivery systems have become popular due to nanosized droplets, stability, biocompatibility, safety (due to the incorporation of GRAS components), and protection of drug in the degradative physiological condition (Narang and Narang, 2015).

We have observed in our previous discussions that *S. mutans* is one of the pathogenic bacteria at the forefront of the global dental problem. Chlorhexidine acetate, an antiseptic agent, has been reported to be effective against such dental pathogens but the desirable antiinfective effect of the drug is limited due to its low aqueous solubility. Several studies conducted all over the world have suggested that nanoemulsions are a platform to enhance the solubility of poorly water-soluble drugs to improve their overall bioavailability. Li et al. (2015) have approached nanoemulsion delivery of the poorly water-soluble agent chlorhexidine acetate to improve its solubility. They prepared chlorhexidine acetate (0.5%) nanoemulsion with Tween 80 (19.2%), propylene glycol (4.8%), and isopropyl myristate (6%) by adopting a phase inversion technique (Foureaux et al., 2015).

MIC and minimum bactericidal concentration (MBC) of the formulated nanoemulsion decreased to 50% against *S. mutans* when compared with an aqueous solution chlorhexidine acetate. A slow release profile and fast acting antibacterial efficacy of nanoemulsion formulation can inhibit biofilm formation and enhance the damage of the cell membrane leading to improved antimicrobial activity, thereby helping to obtain improved oral hygiene (Foureaux et al., 2015).

Ramalingam et al. investigated the level and composition of bacterial contamination of dental chair syringe waterlines and also the efficacy of a cetylpyridinium chloride-containing nanoemulsion disinfectant in reducing bacterial loads. They exposed waterline biofilm to nanoemulsion for different time periods and observed a reduction of colonies. Their study showed that nanoemulsions improved efficacy against microorganisms more than unemulsified components. The results also indicated that the nanoemulsion was able to effectively disinfected waterlines to consistently meet the American Dental Association recommendations. Live/dead stained confocal micrograph sections of waterline tubing showing the effects on dental unit waterline biofilms of different groups at different time periods are shown in Fig. 9.8 (Ramalingam et al., 2013).

In addition, delivery of nanoemulsions may be highly advantageous when targeting resistant strains of bacteria that have been known to develop. Nanoemulsions are thought to cause nonspecific disruption of the bacterial cell membrane, thereby preventing the formation of resistant strains. Along with their bactericidal effect, nanoemulsions are also known to produce sporicidal and viricidal activity (Lacey, 2017). In their study, Ramalingam et al. reported that the formulated nanoemulsion resulted in decreased MIC and MBC against the tested strains of *S. mutans*, *L. casei*, *Actinomyces viscosus*, *C. albicans*, and mixed cultures. They formulated the oil-in-water nanoemulsion formulation with soybean oil (25%, v/v), Triton X100 (10%, v/v) in deionized water with cetylpyridinium

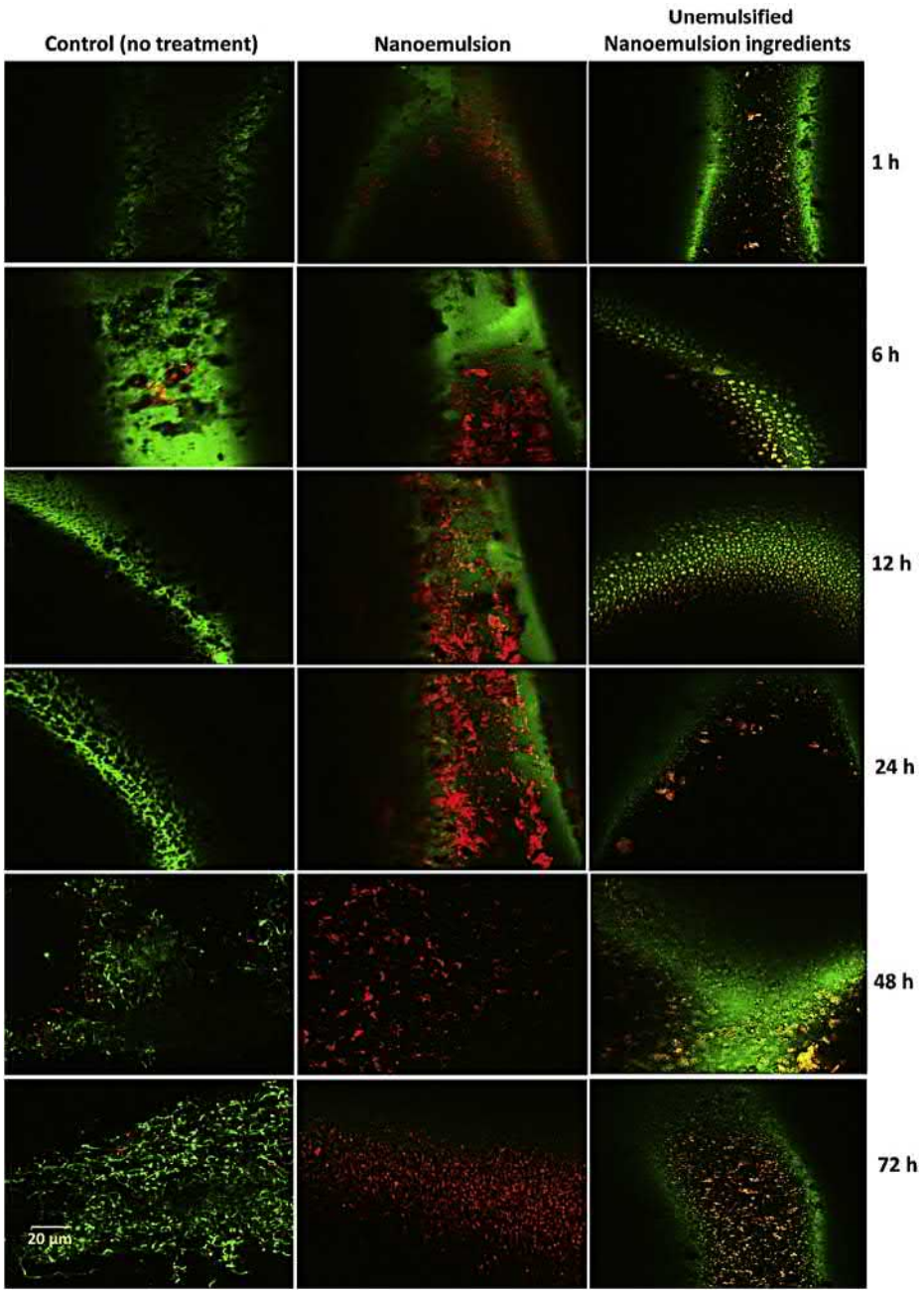

FIGURE 9.8 Live/dead stained confocal micrograph sections of waterline tubing show the effects on DUWL biofilms of controls (first column, no treatment), nanoemulsion (second column), and unemulsified nanoemulsion ingredients (third column) after 1, 6, 12, 24, 48, and 72 hours. The green color indicates live cells and the red color indicates dead cells (Ramalingam et al., 2013). *DUWL*, Dental unit waterline.

chloride (1%, w/v) as a cosurfactant by microfluidization method (Ramalingam et al., 2012). Previous reports by various scientists have hypothesized that the nanoemulsion formulation might fuse to the outer membrane of the microorganism, leading to destabilization of a lipid membrane by the action of surfactant to lead to the disruption of the microorganism cells (Hamouda et al., 2001).

Ramalingam et al. reported that their developed nanoemulsion could reduce biofilm formation and colonization ability of the tested microorganisms. It is important to note that the tested nanoemulsion was found to be 9- to 27-fold more active against oral biofilm than chlorhexidine (Hamouda et al., 2001). This team of researchers had reported earlier that such formulated nanoemulsion could be effective in the prevention of early dental caries caused by *S. mutans*.

Application of nanoemulsion delivery in PDT has also become popular for its advantages on high tissue penetration rate into the periodontal mucosa, increased stability, dose reduction, prevention of aggregation formation, reduction of side effect of the drugs, and retention of photodynamic efficacy (Paszko et al., 2011). Low concentration of surfactant present in the nanoemulsion produces less irritability to the buccal mucosa, which could further make it a safer choice for drug delivery in periodontal disease. Initial use of PDT has been limited as the agents were found to be less stable and have low solubility, therefore, solutions were prepared in situ with the use of organic solvent or have been administered with the help of another delivery system (Singh et al., 2017).

In this line, some investigators have also demonstrated CAP with the use of nanoemulsion to improve antimicrobial photodynamic activity. They formulated the nanoemulsion of CAP by spontaneous emulsification method with Miglyol 812N as the oil phase. The authors reported that encapsulated CAP in nanoemulsion could be able to reduce the colony-forming units/mL by more than 75% of methicillin-resistant and sensitive *S. aureus* following application of laser irradiation by an LED light source (Mantareva et al., 2016). In conjunction with our previous discussion on the negatively charged surface on Gram-positive bacteria due to the presence of teichoic acid on the thick peptidoglycan, cell membrane facilitates the binding of the cationic nanoemulsion.

In addition, another important parameter that was reported in this experiment was that the part of the drug that was able to penetrate into the bacterial cell was found to be effective, whereas the extracellular part of the nanoemulsion was washed away due to the opaque nature of the nanoemulsion, which hinders the photodynamic activity. Thus the authors concluded that delivery of CAP through cationic nanoemulsion could result in the promising photomediated killing of planktonic and biofilm cultures of tested organisms by offering greater permeation and stability for light-sensitive drugs.

Previous experiments by this group had reported that the cationic nanoemulsion of CAP was also able to effectively reduce the colony-forming units/mL (70%) of the fungus *C. albicans* as measured through XTT assay. Application of cationic nanoemulsion of zinc 2,9,16,23-tetrakis(phenylthio)-29*H*,31*H*-phthalocyanine (ZnPc) in three different fungal species has successfully been employed by Junqueira et al., 2012. They formulated the nanoemulsion containing soy lecithin/ZnPc/oily and aqueous phase by utilizing the simple spontaneous emulsification method.

Wangjit et al. have aimed to antimicrobial effectiveness of spearmint oil and coconut oil in the treatment of dental caries against *S. mutans*. They have chosen the nanoemulsion

delivery system to deliver those oils in dentistry because of the possible advantages of oil-in-water nanoemulsion in terms of compatibility with water, the ability for large incorporation of oil into the formulation, and easy removal ability (Wangjit et al., 2016). In due course of formulation development, they had noticed that the percentage of modified coconut oil in nanoemulsion formulation inversely affected the size of the dispersed droplet. They adopted a spontaneous method to formulate the nanoemulsion with those two oils.

9.3.9 Nanoemulgel Approach in Dentistry

It has been observed that nanoemulsion delivery often is unable to eliminate the formed biofilms of microorganisms completely due to the short exposure time of the oil-in-water nanoemulsion (Choudhury et al., 2017). To improve the retention time of the drug in the crevicular pocket, incorporation of a gelling agent is one of the most popular approaches elicited by various scientists. Thereby, incorporated polymers help the formulation to stick at the site of action for longer periods of time by forming a protective film on the application site. Among the polymers available for gelling, the buccoadhesive gels are prepared with hydroxyl propyl methyl cellulose, Carbopol 934P, and Poloxamer 407 to achieve controlled release of the drug and prolonging retention at the site of action (Koland and Charyulu, 2016).

Formulation of nanoemulgels was continued by the researchers after optimizing nanoemulsion formulation. Srivastava et al. prepared the nanoemulsion of ketoprofen, a nonsteroidal antiinflammatory drug, by an aqueous titration method using eugenol as the oil phase, cremophor EL as a surfactant, and Transcutol P as a cosurfactant. Here, the researchers prepared the nanoemulgel by addition of optimized nanoemulsion in the aqueous solution of Carbopol 934P and Poloxamer 407 while continuously stirring. In this experiment, the neutral pH (pH 6.67) of the formulation was maintained by the addition of the triethyl amine. During in vitro release studies of the gel formulation, it was observed that there was an initial burst of ketoprofen, due to the presence of nanodroplets of the drug in the outermost layer of the nanoemulgel, and thereafter, release pattern of the drug was modified to controlled manner. Further results of the optimized nanoemulgel formulation indicated low toxicity as evidenced by hen's egg test on the chorioallantoic membrane (Srivastava et al., 2016).

In vivo experimentation of the same nanoemulgel by Srivastava et al. revealed that the presence of eugenol and ketoprofen synergistically controlled periodontitis-related problems. The synergistic action of those two agents, which had returned cytokine levels to the normal level, reduced the inflammatory cell infiltration, cementum, and alveolar bone resorption significantly. They further reported that the nanoemulgel formulation significantly reduced gingival index, tooth mobility, and alveolar bone loss (Srivastava et al., 2016).

Aithal et al. prepared and characterized nanoemulgel composed of quercetin, cinnamon oil, Tween 80, carbitol, poloxamer, and water. In the sol–gel transition study, they found that the gel formation occurred at 53 ± 2 seconds at 37°C. The pH of quercetine nanoemulgel was measured by using pH paper in accordance with the pH of the gingival crevicular

fluid and was found to be 6.34 ± 0.5. Nanoemulsion also passed the syringeability test. The diffusion study showed that drug release from the quercetin-loaded gel (comprising of 23% Poloxamer 407 gel loaded with quercetin) was much less (<3% drug at the end of 6 hours), which may be due to poor solubility. In vitro drug diffusion profile and zero-order release kinetics for nanoemulgel are shown in Figs. 9.9 and 9.10, respectively (Aithal et al., 2018).

Application of nanoemulgels has now crossed the barrier of the laboratory, pertaining to its clinical application. Rabiya had detailed successful findings on periodontic patient case studies. This marketed formulation contains propolis, vitamin C, E, and herbs (which proved to have antiinflammatory, antioxidant, and antibacterial action) by incorporating biofusion of two newer technologies, that is, medical biotechnology and nanotechnology. Direct abruption from the application site and active biofilm formation of the formulation could protect the infected area, and direct absorption at the site of action could result in

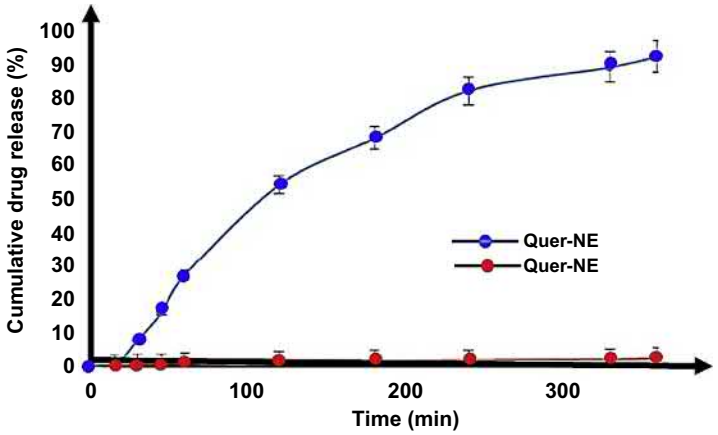

FIGURE 9.9 In vitro drug diffusion profile. *Source: Adapted from Aithal, G., Nayak, U., Mehta, C., Narayan, R., Gopalkrishna, P., Pandiyan, S., et al., 2018. Localized in situ nanoemulgel drug delivery system of quercetin for periodontitis: development and computational simulations. Molecules 23(6), 1363 (open access).*

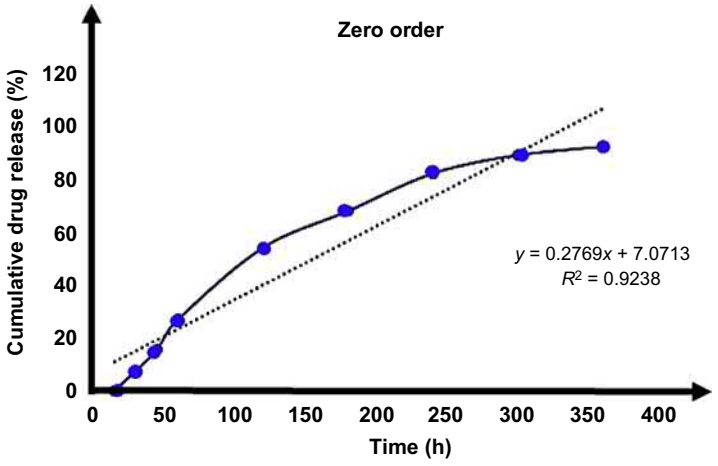

FIGURE 9.10 Zero-order release kinetics for nanoemulgel. *Source: Adapted from Aithal, G., Nayak, U., Mehta, C., Narayan, R., Gopalkrishna, P., Pandiyan, S., et al., 2018. Localized in situ nanoemulgel drug delivery system of quercetin for periodontitis: development and computational simulations. Molecules 23(6), 1363 (open access).*

rapid healing of the lesion. Application of NBF Gingival Gel on such patients resulted in significant reduction of inflammation with rapid healing devoid of any antibiotic and anti-inflammatory drug (Rabiya, 2013).

9.4 CONCLUSION AND FUTURE PROSPECTS

Despite promising results observed in several in vitro and in vivo studies, there are few dental nanoformulations that have been approved clinically. There are a few potential reasons causing such inability for breakthroughs. First of all, the manufacturing process of nanoformulations is a safety concern regarding the usage of nanoformulations in human beings. In the process of synthesizing the nanoformulation, one of the adjunct agents that aids in the synthesis process is the organic solvent, which is known to be toxic to humans. Even though the organic solvent will be removed in the final product, a certain amount of organic solvent residue will still be present on the formulation.

Furthermore, the tedious and time-consuming manufacturing process is also another limiting factor of producing nanoformulations on large scale. For instance, in synthesizing chitosan−gelatin bioglass scaffolds, the process involves the dissolution of materials, solidification, freezing, and freeze-drying, in which the whole process takes several hours to be completed. Moreover, the aspects of nanoformulation that have been studied are still incomplete. Currently, most of the literature is only focused on certain parameters of the nanoformulation such as the release pattern and the degradation profile, and studies on other aspects such as toxicological profile are scarce. Due to the reasons mentioned above, the progression of the research scope from animal studies to human studies is limited and commercial production is difficult.

Undeniably, the era of using nanoformulation in drug delivery has come and a promising progression of applying nanoformulations in dental issues is observed in the scientific community. However, the positive outcome of these studies must be supported by more concrete studies, and research on nanoformulations has to focus on different properties of the nanoformulation. A continuous effort is needed in the scientific community to bring the miraculous drug delivery system of the 21st century to the bedside of patients.

ABBREVIATIONS

AgNP	silver nanoparticles
BMP	bone morphogenetic protein
CAP	chloroaluminum phthalocyanine
DNA	deoxyribonucleic acid
FGF-2	fibroblast growth factor-2
GIC	glass ionomer cement
GFLX	gatifloxacin-loaded PLGA and b-tricalcium phosphate
GRAS	generally regarded as safe
HA	hydroxyapatite
HCl	hydrochloride
MBC	minimum bactericidal concentration
MIC	minimum inhibitory concentration

PCL	polycaprolactone
PDT	photodynamic therapy
PLGA	poly(lactide-*co*-glycolic) acid
PVA	poly(vinyl alcohol)
QADM	quaternary ammonium dimethacrylate
ROS	reactive oxygen species
SEM	scanning electron microscopy or scanning electron microscope
TiO_2NP	titanium dioxide nanoparticles
TNT	TiO_2 nanotubes
UV	ultraviolet
ZnO-NPs	zinc oxide nanoparticles
ZnPc	zinc 2,9,16,23-tetrakis(phenylthio)-29*H*,31*H*-phthalocyanine

References

Abdulkareem, E.H., Memarzadeh, K., Allaker, R.P., Huang, J., Pratten, J., Spratt, D., 2015. Anti-biofilm activity of zinc oxide and hydroxyapatite nanoparticles as dental implant coating materials. J. Dent. 43, 1462–1469. Available from: https://doi.org/10.1016/j.jdent.2015.10.010.

Abrahamsson, K.H., Wennström, J.L., Berglundh, T., Abrahamsson, I., 2017. Altered expectations on dental implant therapy: views of patients referred for treatment of peri-implantitis. Clin. Oral Implants Res. 28 (4), 437–442.

Acosta-Torres, L.S., López-Marín, L.M., Núñez-Anita, R.E., Hernández-Padrón, G., Castaño, V.M., 2010. Biocompatible Metal-Oxide Nanoparticles: Nanotechnology Improvement of Conventional Prosthetic Acrylic Resins. J. Nanomater. 2011, e941561. Available from: https://doi.org/10.1155/2011/941561.

Adams, L.K., Lyon, D.Y., Alvarez, P.J.J., 2006. Comparative eco-toxicity of nanoscale TiO2, SiO2, and ZnO water suspensions. Water Res. 40, 3527–3532. Available from: https://doi.org/10.1016/j.watres.2006.08.004.

Aguiar, P.H., Furtado, C., Repolês, B.M., Ribeiro, G.A., Mendes, I.C., Peloso, E.F., et al., 2013. Oxidative stress and DNA lesions: the role of 8-oxoguanine lesions in *Trypanosoma cruzi* cell viability. PLoS Negl. Trop. Dis. 7 (6), e2279.

Ahrari, F., Akbari, M., Mohammadpour, S., Forghani, M., 2015. The efficacy of laser-assisted in-office bleaching and home bleaching on sound and demineralized enamel. Laser Ther. 24 (4), 257–264.

Aithal, G., Nayak, U., Mehta, C., Narayan, R., Gopalkrishna, P., Pandiyan, S., et al., 2018. Localized in situ nanoemulgel drug delivery system of quercetin for periodontitis: development and computational simulations. Molecules 23 (6), 1363.

Aksungur, P., Sungur, A., Ünal, S., Iskit, A.B., Squier, C.A., Şenel, S., 2004. Chitosan delivery systems for the treatment of oral mucositis: in vitro and in vivo studies. J. Control. Release 98 (2), 269–279.

Allen, T.M., Cullis, P.R., 2013. Liposomal drug delivery systems: from concept to clinical applications. Adv. Drug Delivery Rev. 65 (1), 36–48.

Ali, K., Babak, T., Mandana, N., Omid, D., Soudabeh, T., 2013. In Vitro Comparison of Antibacterial Efficacy of a New Irrigation Solution Containing Nanosilver with Sodium Hypochlorite and Chlorhexidine. J. Dent. Sch. 31, 1–7.

Amro, N.A., Kotra, L.P., Wadu-Mesthrige, K., Bulychev, A., Mobashery, S., Liu, G., 2000. High-Resolution Atomic Force Microscopy Studies of the Escherichia coli Outer Membrane: Structural Basis for Permeability. Langmuir 16, 2789–2796. Available from: https://doi.org/10.1021/la991013x.

Anitua, E., Troya, M., Zalduendo, M., 2018. Progress in the use of dental pulp stem cells in regenerative medicine. Cytotherapy 20 (4), 479–498.

Augustine, R., Bhavanavenugopal, S.S., Kalarikkal, N., Thomas, S., 2016. Polyuronates and their application in drug delivery and cosmetics. Green Polymers and Environmental Pollution Control. CRC Press, p. 239.

Barbosa, D., Monteiro, D., Takamyia, A., Camargo, E., Agostinho, A., Delbem, A., et al., 2013. Silver and phosphate nanoparticles: antimicrobial approach and caries prevention application. Nanobiomaterials in Clinical Dentistry. Elsevier.

Barnes, R.J., Molina, R., Xu, J., Dobson, P.J., Thompson, I.P., 2013. Comparison of TiO2 and ZnO nanoparticles for photocatalytic degradation of methylene blue and the correlated inactivation of gram-positive and gram-negative bacteria. J. Nanoparticle Res. 15, 1–11.

Bessho, K., Carnes, D.L., Cavin, R., Ong, J.L., 2002. Experimental studies on bone induction using low-molecular-weight poly (DL-lactide-co-glycolide) as a carrier for recombinant human bone morphogenetic protein-2. J. Biomed. Mater. Res. 61, 61–65. Available from: https://doi.org/10.1002/jbm.10169.

Blecher, K., Nasir, A., Friedman, A., 2011. The growing role of nanotechnology in combating infectious disease. Virulence 2, 395–401. Available from: https://doi.org/10.4161/viru.2.5.17035.

Brayner, R., Ferrari-Iliou, R., Brivois, N., Djediat, S., Benedetti, M.F., Fiévet, F., 2006. Toxicological Impact Studies Based on Escherichia coli Bacteria in Ultrafine ZnO Nanoparticles Colloidal Medium. Nano Lett. 6, 866–870. Available from: https://doi.org/10.1021/nl052326h.

Bumgardner, J.D., Wiser, R., Gerard, P.D., Bergin, P., Chestnutt, B., Marini, M., et al., 2003. Chitosan: potential use as a bioactive coating for orthopaedic and craniofacial/dental implants. J. Biomater. Sci., Polym. Ed. 14 (5), 423–438.

Cai, Y., Strømme, M., Welch, K., 2013. Photocatalytic Antibacterial Effects Are Maintained on Resin-Based TiO2 Nanocomposites after Cessation of UV Irradiation: e75929. PLoS One 8. http://dx.doi.org.ezp.imu.edu.my/10.1371/journal.pone.0075929.

Chang, M.-C., Lin, L.-D., Wu, M.-T., Chan, C.-P., Chang, H.-H., Lee, M.-S., et al., 2015. Effects of camphorquinone on cytotoxicity, cell cycle regulation and prostaglandin E2 production of dental pulp cells: role of ROS, ATM/Chk2, MEK/ERK and hemeoxygenase-1. PLoS One 10 (12), e0143663.

Chen, W.-Y., Yang, C.-I., Lin, C.-J., Huang, S.-J., Chan, J.C., 2014. Characterization of the crystallization pathway of calcium phosphate in liposomes. J. Phys. Chem. C 118 (22), 12022–12027.

Cherif, A.M., Manal, R.A.-E., Rauesa, M.M.,H., 2015. The antibacterial and antifungal effect of Silver Nanoparticles and silver hydroxyapatite nanoparticles on Dental Ceramic. Rep Opin 7, 83–88.

Cheung, R.C.F., Ng, T.B., Wong, J.H., Chan, W.Y., 2015. Chitosan: an update on potential biomedical and pharmaceutical applications. Mar. Drugs 13 (8), 5156–5186.

Choudhury, H., Gorain, B., Pandey, M., Chatterjee, L.A., Sengupta, P., Das, A., et al., 2017. Recent update on nanoemulgel as topical drug delivery system. J. Pharm. Sci. 106 (7), 1736–1751.

Costa, E., Silva, S., Madureira, A., Cardelle-Cobas, A., Tavaria, F., Pintado, M., 2014. A comprehensive study into the impact of a chitosan mouthwash upon oral microorganism's biofilm formation in vitro. Carbohydr. Polym. 101, 1081–1086.

Daraee, H., Etemadi, A., Kouhi, M., Alimirzalu, S., Akbarzadeh, A., 2016. Application of liposomes in medicine and drug delivery. Artif. Cells Nanomed. Biotechnol. 44 (1), 381–391.

De Giglio, E., Cafagna, D., Cometa, S., Allegretta, A., Pedico, A., Giannossa, L.C., Sabbatini, L., Mattioli-belmonte, M., Iatta, R., 2013. An innovative, easily fabricated, silver nanoparticle-based titanium implant coating: development and analytical characterization. Anal. Bioanal. Chem. 405, 805–816. Available from: http://dx.doi.org.ezp.imu.edu.my/10.1007/s00216-012-6293-z.

de, Jong, 2008. Drug delivery and nanoparticles: Applications and hazards. International Journal of Nanomedicine 133.

Devi, R., Venckatesh, R., Sivaraj, R., 2014. Synthesis of Titanium Dioxide Nanoparticles by Sol-Gel Technique. Int. J. Innov. Res. Sci. Eng. Technol. 3, 15206–15211.

Dobhal, A., Bangde, P., Dey, A., Dandekar, P., Jain, R., 2017. Chitosan-based nanoparticulate systems: implication towards therapeutics application. Particulate Technology for Delivery of Therapeutics. Springer.

Duncan, H.F., Kobayashi, Y., Shimizu, E., 2018. Growth factors and cell homing in dental tissue regeneration. Curr. Oral Health Rep. 5 (4), 276–285.

Dugal, S., Chakraborty, S., 2014. Application of Nanosilver for Prevention of Recurrent Dental Caries in Patients Suffering From Xerostomia. Int. J. Pharm. Pharm. Sci. 6, 101–104.

Duraccio, D., Mussano, F., Faga, M.G., 2015. Biomaterials for dental implants: current and future trends. J. Mater. Sci. 50, 4779–4812. Available from: https://doi.org/10.1007/s10853-015-9056-3.

Elsaka, S.E., Hamouda, I.M., Swain, M.V., 2011. Titanium dioxide nanoparticles addition to a conventional glass-ionomer restorative: influence on physical and antibacterial properties. J. Dent. 39, 589–598. Available from: https://doi.org/10.1016/j.jdent.2011.05.006.

Elieh-Ali-Komi, D., Hamblin, M.R., 2016. Chitin and chitosan: production and application of versatile biomedical nanomaterials. Int. J. Adv. Res. 4 (3), 411.

Eslami, H., Lisar, H.A., Kashi, T.S.J., Tahriri, M., Ansari, M., Rafiei, T., et al., 2018. Poly(lactic-*co*-glycolic acid) (PLGA)/TiO_2 nanotube bioactive composite as a novel scaffold for bone tissue engineering: In vitro and in vivo studies. Biologicals 53, 51–62.

Esteves-Oliveira, M., Santos, N., Meyer-Lückel, H., Wierichs, R., Rodrigues, J., 2017. Caries-preventive effect of anti-erosive and nano-hydroxyapatite-containing toothpastes in vitro. Clin. Oral Invest. 21 (1), 291–300.

Foureaux, G., Franca, J.R., Nogueira, J.C., de Oliveira Fulgêncio, G., Ribeiro, T.G., Castilho, R.O., et al., 2015. Ocular inserts for sustained release of the angiotensin-converting enzyme 2 activator, diminazene aceturate, to treat glaucoma in rats. PLoS One 10 (7), e0133149.

Garcia-Contreras, R., Sugimoto, M., Umemura, N., Kaneko, M., Hatakeyama, Y., Soga, T., et al., 2015. Alteration of metabolomic profiles by titanium dioxide nanoparticles in human gingivitis model. Biomaterials 57, 33–40.

Gohil, S., Suhail, S., Rose, J., Vella, T., Nair, L., 2017. Polymers and composites for orthopedic applications. Materials for Bone Disorders. Elsevier.

Hajipour, M.J., Fromm, K.M., Ashkarran, A.A., Jimenez de Aberasturi, D., de Larramendi, I.R., Rojo, T., Serpooshan, V., Parak, W.J., Mahmoudi, M., 2012. Antibacterial properties of nanoparticles. Trends Biotechnol. 30, 499–511. Available from: https://doi.org/10.1016/j.tibtech.2012.06.004.

Hamouda, T., Myc, A., Donovan, B., Shih, A.Y., Reuter, J.D., Baker, J.R., 2001. A novel surfactant nanoemulsion with a unique nonirritant topical antimicrobial activity against bacteria, enveloped viruses and fungi. Microbiol. Res. 156 (1), 1–7.

Hamouda, I.M., 2012. Current perspectives of nanoparticles in medical and dental biomaterials. J. Biomed. Res. 26, 143–151. Available from: https://doi.org/10.7555/JBR.26.20120027.

Hassan, A.H., Hosny, K.M., Murshid, Z.A., Alhadlaq, A., Alyamani, A., Naguib, G., 2015. Depot injectable biodegradable nanoparticles loaded with recombinant human bone morphogenetic protein-2: preparation, characterization, and in vivo evaluation. Drug Des. Devel. Ther. 9, 3599–3606. Available from: https://doi.org/10.2147/DDDT.S79812.

Hayashi, Y., Ohara, N., Ganno, T., Yamaguchi, K., Ishizaki, T., Nakamura, T., et al., 2007. Chewing chitosan-containing gum effectively inhibits the growth of cariogenic bacteria. Arch. Oral Biol. 52 (3), 290–294.

Hernández-Sierra, J.F., Ruiz, F., Cruz Pena, D.C., Martínez-Gutiérrez, F., Martínez, A.E., de Jesús Pozos Guillén, A., Tapia-Pérez, H., Martínez Castañón, G., 2008. The antimicrobial sensitivity of Streptococcus mutans to nanoparticles of silver, zinc oxide, and gold. Nanomedicine Nanotechnol. Biol. Med. 4, 237–240. Available from: https://doi.org/10.1016/j.nano.2008.04.005.

Holla, G., Yeluri, R., Munshi, A.K., 2012. Evaluation of minimum inhibitory and minimum bactericidal concentration of nano-silver base inorganic anti-microbial agent (Novaron®) against streptococcus mutans. Contemp. Clin. Dent. 3, 288–293. Available from: https://doi.org/10.4103/0976-237X.103620.

Hsueh, Y.-H., Lin, K.-S., Ke, W.-J., Hsieh, C.-T., Chiang, C.-L., Tzou, D.-Y., Liu, S.-T., 2015. The Antimicrobial Properties of Silver Nanoparticles in Bacillus subtilis Are Mediated by Released Ag + Ions: e0144306. PLoS One 10. http://dx.doi.org.ezp.imu.edu.my/10.1371/journal.pone.0144306

Husain, S., Al-Samadani, K.H., Najeeb, S., Zafar, M.S., Khurshid, Z., Zohaib, S., et al., 2017. Chitosan biomaterials for current and potential dental applications. Materials 10 (6), 602.

Ikinci, G., Şenel, S., Akıncıbay, H., Kaş, S., Erciş, S., Wilson, C., et al., 2002. Effect of chitosan on a periodontal pathogen *Porphyromonas gingivalis*. Int. J. Pharm. 235 (1–2), 121–127.

Jacob, J., Haponiuk, J.T., Thomas, S., Gopi, S., 2018. Biopolymer based nanomaterials in drug delivery systems: a review. Mater. Today Chem. 9, 43–55.

Jain, R.A., 2000. The manufacturing techniques of various drug loaded biodegradable poly(lactide-co-glycolide) (PLGA) devices. Biomaterials, Orthopaedic Polymeric Biomaterials: Basic Aspects of Biodegradables 21, 2475–2490. Available from: https://doi.org/10.1016/S0142-9612(00)00115-0.

Jerzy, S., Małgorzata Iwona, S., Joanna, K., Zygmunt, K., Agnieszka, S.-K., Aleksandra, P., Krzysztof, S., Monika, Ł.-S., 2014. Evaluation of resin composites modified with nanogold and nanosilver. Acta Bioeng. Biomech. 16. Available from: https://doi.org/10.5277/abb140107.

Junqueira, J.C., Jorge, A., Barbosa, J., Rossoni, R., Vilela, S., Costa, A., et al., 2012. Photodynamic inactivation of biofilms formed by *Candida* spp., *Trichosporon mucoides*, and *Kodamaea ohmeri* by cationic nanoemulsion of zinc 2, 9, 16, 23-tetrakis (phenylthio)-29*H*, 31*H*-phthalocyanine (ZnPc). Lasers Med. Sci. 27 (6), 1205–1212.

Kachoei, M., Eskandarinejad, F., Divband, B., Khatamian, M., 2013. The effect of zinc oxide nanoparticles deposition for friction reduction on orthodontic wires. Dent. Res. J. 10, 499–505.

Kachoei, M., 2015. Deposition of ZnO Nano Particles on Stainless Steel Orthodontic Wires by Chemical Solution Method for Friction Reduction Propose. Research Journal of Pharmaceutical, Biological and Chemical Sciences 6 (3), 104–112.

Kasraei, S., Sami, L., Hendi, S., AliKhani, M.-Y., Rezaei-Soufi, L., Khamverdi, Z., 2014. Antibacterial properties of composite resins incorporating silver and zinc oxide nanoparticles on *Streptococcus mutans* and *Lactobacillus*. Restor. Dent. Endod. 39 (2), 109–114.

Kashi, T.S.J., Eskandarion, S., Esfandyari-Manesh, M., Marashi, S.M.A., Samadi, N., Fatemi, S.M., Atyabi, F., Eshraghi, S., Dinarvand, R., 2012. Improved drug loading and antibacterial activity of minocycline-loaded PLGA nanoparticles prepared by solid/oil/water ion pairing method. Int. J. Nanomedicine 7, 221–234. Available from: https://doi.org/10.2147/IJN.S27709.

Khurshid, Z., Zafar, M., Qasim, S., Shahab, S., Naseem, M., AbuReqaiba, A., 2015. Advances in nanotechnology for restorative dentistry. Materials 8 (2), 717–731.

Kikuchi, T., Mogi, M., Okabe, I., Okada, K., Goto, H., Sasaki, Y., et al., 2015. Adjunctive application of antimicrobial photodynamic therapy in nonsurgical periodontal treatment: a review of literature. Int. J. Mol. Sci. 16 (10), 24111–24126.

Kim, S.H., Kwak, S.-Y., Sohn, B.-H., Park, T.H., 2003. Design of TiO2 nanoparticle self-assembled aromatic polyamide thin-film-composite (TFC) membrane as an approach to solve biofouling problem. J. Membr. Sci. 211, 157–165. Available from: https://doi.org/10.1016/S0376-7388(02)00418-0.

Kimishima, K., Matsuno, T., Makiishi, J., Tamazawa, G., Sogo, Y., Ito, A., Satoh, T., 2016. Effects of gatifloxaine content in gatifloxacine-loaded PLGA and β-tricalcium phosphate composites on efficacy in treating osteomyelitis. Odontol. Soc. Nippon Dent. Univ. 104, 105–113. Available from: https://doi.org/10.1007/s10266-014-0187-9.

Klepac-Ceraj, V., Patel, N., Song, X., Holewa, C., Patel, C., Kent, R., Amiji, M.M., Soukos, N.S., 2011. Photodynamic effects of methylene blue-loaded polymeric nanoparticles on dental plaque bacteria. Lasers Surg. Med. 43, 600–606. Available from: https://doi.org/10.1002/lsm.21069.

Koland, M., Charyulu, N.R., 2016. Design and in vivo evaluation of buccoadhesive hydrophilic polymer matrix films of losartan potassium. Indian J. Pharm. Educ. Res. 50 (2), S115–S124.

Kráľová, K., Jampílek, J., 2018. Application of nanobioformulations for controlled release and targeted biodistribution of drugs. Nanobiomaterials. Apple Academic Press.

Lacey, J., 2017. Bioavailability of nanomaterials and interaction with cells. Emerging Nanotechnologies in Food Science. Elsevier.

Lee, Y.-M., Park, Y.-J., Lee, S.-J., Ku, Y., Han, S.-B., Klokkevold, P.R., et al., 2000. The bone regenerative effect of platelet-derived growth factor-BB delivered with a chitosan/tricalcium phosphate sponge carrier. J. Periodontol. 71 (3), 418–424.

Li, F., Weir, M.D., Chen, J., Xu, H.H.K., 2013. Comparison of quaternary ammonium-containing with nano-silver-containing adhesive in antibacterial properties and cytotoxicity. Dent. Mater. Off. Publ. Acad. Dent. Mater. 29, 450–461. Available from: https://doi.org/10.1016/j.dental.2013.01.012.

Li, Y.F., Sun, H.W., Gao, R., Liu, K.Y., Zhang, H.Q., Fu, Q.H., et al., 2015. Inhibited biofilm formation and improved antibacterial activity of a novel nanoemulsion against cariogenic *Streptococcus mutans* in vitro and in vivo. Int. J. Nanomed. 10, 447.

Liu, Y., Zheng, Z., Zara, J.N., Hsu, C., Soofer, D.E., Lee, K.S., Siu, R.K., Miller, L.S., Zhang, X., Carpenter, D., Wang, C., Ting, K., Soo, C., 2012. The antimicrobial and osteoinductive properties of silver nanoparticle/poly (DL-lactic-co-glycolic acid)-coated stainless steel. Biomaterials 33, 8745–8756. Available from: https://doi.org/10.1016/j.biomaterials.2012.08.010.

Lu, Z., Rong, K., Li, J., Yang, H., Chen, R., 2013. Size-dependent antibacterial activities of silver nanoparticles against oral anaerobic pathogenic bacteria. J. Mater. Sci. Mater. Med. 24, 1465–1471. Available from: http://dx.doi.org.ezp.imu.edu.my/10.1007/s10856-013-4894-5.

Maheshwari, R.G., Thakur, S., Singhal, S., Patel, R.P., Tekade, M., Tekade, R.K., 2015. Chitosan encrusted nonionic surfactant based vesicular formulation for topical administration of ofloxacin. Sci. Adv. Mater. 7 (6), 1163–1176.

Maji, K., Dasgupta, S., Pramanik, K., Bissoyi, A., 2016. Preparation and evaluation of gelatin-chitosan-nanobioglass 3D porous scaffold for bone tissue engineering. Int. J. Biomater. 2016, 9825659.

Mallick, S., Tripathi, S., Srivastava, P., 2015. Advancement in scaffolds for bone tissue engineering: a review. IOSR J. Pharm. Biol. Sci. 10, 37–54.

Maness, P.-C., Smolinski, S., Blake, D.M., Huang, Z., Wolfrum, E.J., Jacoby, W.A., 1999. Bactericidal Activity of Photocatalytic TiO2 Reaction: toward an Understanding of Its Killing Mechanism. Appl. Environ. Microbiol. 65, 4094–4098.

Mantareva, V., Kussovski, V., Durmuş, M., Borisova, E., Angelov, I., 2016. Photodynamic inactivation of pathogenic species *Pseudomonas aeruginosa* and *Candida albicans* with lutetium (III) acetate phthalocyanines and specific light irradiation. Lasers Med. Sci. 31 (8), 1591–1598.

Meechan, J., 2000. Intra-oral topical anaesthetics: a review. J. Dent. 28 (1), 3–14.

Mehrvarzfar, P., Abbott, P.V., Mashhadiabbas, F., Vatanpour, M., Tour Savadkouhi, S., 2018. Clinical and histological responses of human dental pulp to MTA and combined MTA/treated dentin matrix in partial pulpotomy. Aust. Endod. J. 44 (1), 46–53.

Mori, K., Tsuji, M., Ueda, T., Sakurai, K., 2015. Color and gloss evaluation of titanium dioxide coating for acrylic resin denture base. J. Prosthodont. Res. 59, 249–253. Available from: https://doi.org/10.1016/j.jpor.2015.06.001.

Morotomi, T., Washio, A., Kitamura, C., 2018. Current and future options for dental pulp therapy. Jpn. Dent. Sci. Rev. 55 (1), 5–11.

Narang, R.S., Narang, J.K., 2015. Nanomedicines for dental applications-scope and future perspective. Int. J. Pharm. Invest. 5 (3), 121.

Nayar, S., Bhuminathan, S., Muthuvignesh, J., 2011. Upsurge of nanotechnology in dentistry and dental implants. Indian J. Multidiscip. Dent. 1, 264.

Nguyen, S., Adamczak, M., Hiorth, M., Smistad, G., Kopperud, H.M., 2015. Interactions of liposomes with dental restorative materials. Colloids Surf., B: Biointerfaces 136, 744–751.

Nguyen, S., Smistad, G., Rykke, M., Hiorth, M., 2016. Nanoparticulate systems for dental drug delivery. Nanotechnol. Drug Delivery 2, 52–74.

Nguyen, S., Escudero, C., Sediqi, N., Smistad, G., Hiorth, M., 2017. Fluoride loaded polymeric nanoparticles for dental delivery. Eur. J. Pharm. Sci. 104, 326–334.

O'brien, F.J., 2011. Biomaterials & scaffolds for tissue engineering. Mater. Today 14 (3), 88–95.

Padovani, G.C., Feitosa, V.P., Sauro, S., Tay, F.R., Durán, G., Paula, A.J., Durán, N., 2015. Advances in Dental Materials through Nanotechnology: Facts, Perspectives and Toxicological Aspects. Trends Biotechnol. 33, 621–636. Available from: http://dx.doi.org.ezp.imu.edu.my/10.1016/j.tibtech.2015.09.005.

Padmavathy, N. Vijayaraghavan, R. Enhanced bioactivity of ZnO nanoparticles-an antimicrobial study. Sci. Technol. Adv. Mater. 9, 035004. Available from: https://doi.org/10.1088/1468-6996/9/3/035004.

Pagonis, T.C., Chen, J., Fontana, C.R., Devalapally, H., Ruggiero, K., Song, X., Foschi, F., Dunham, J., Skobe, Z., Yamazaki, H., Kent, R., Tanner, A.C.R., Amiji, M.M., Soukos, N.S., 2010. Nanoparticle-based endodontic antimicrobial photodynamic therapy. J. Endod. 36, 322–328. Available from: https://doi.org/10.1016/j.joen.2009.10.011.

Paszko, E., Ehrhardt, C., Senge, M.O., Kelleher, D.P., Reynolds, J.V., 2011. Nanodrug applications in photodynamic therapy. Photodiagn. Photodyn. Ther. 8 (1), 14–29.

Pepla, E., Besharat, L.K., Palaia, G., Tenore, G., Migliau, G., 2014. Nano-hydroxyapatite and its applications in preventive, restorative and regenerative dentistry: a review of literature. Ann. Stomatol. (Roma.) 5 (3), 108.

Pitts, N.B., Zero, D.T., Marsh, P.D., Ekstrand, K., Weintraub, J.A., Ramos-Gomez, F., et al., 2017. Dental caries. Nat. Rev. Dis. Primers 3, 17030.

Piñón-Segundo, E., Ganem-Quintanar, A., Alonso-Pérez, V., Quintanar-Guerrero, D., 2005. Preparation and characterization of triclosan nanoparticles for periodontal treatment. Int. J. Pharm. 294, 217–232. Available from: https://doi.org/10.1016/j.ijpharm.2004.11.010.

Rabiya, A., 2013. Treatment of periodontal disease with high functional paste made from nanoemulsion gel "NBF". Guident 7 (1), 102–103.

Rai, M.K., et al.: Silver nanoparticles: the powerful nanoweapon against multidrug-resistant bacteria. J. Appl. Microbiol. 112(5), 841-852.

Ramchandani, M., Pankaskie, M., Robinson, D., 1997. The influence of manufacturing procedure on the degradation of poly(lactide-co-glycolide) 85:15 and 50:50 implants. J. Controlled Release 43, 161–173. Available from: https://doi.org/10.1016/S0168-3659(96)01481-2.

Raghupathi, K.R., Koodali, R.T., Manna, A.C., 2011. Size-Dependent Bacterial Growth Inhibition and Mechanism of Antibacterial Activity of Zinc Oxide Nanoparticles. Langmuir 27, 4020–4028. Available from: https://doi.org/10.1021/la104825u.

Ramalingam, K., Amaechi, B.T., Ralph, R.H., Lee, V.A., 2012. Antimicrobial activity of nanoemulsion on cariogenic planktonic and biofilm organisms. Arch. Oral Biol. 57 (1), 15–22.

Ramalingam, K., Frohlich, N.C., Lee, V.A., 2013. Effect of nanoemulsion on dental unit waterline biofilm. J. Dent. Sci. 8 (3), 333–336.

Ribeiro, A., Oliveira, F., Boldrini, L., Leite, P., Falagan-Lotsch, P., Linhares, A., Zambuzzi, W., Fragneaud, B., Campos, A., Gouvêa, C., Archanjo, B., Achete, C., Marcantonio, E., Rocha, L., Granjeiro, J., 2015. Micro-arc oxidation as a tool to develop multifunctional calcium-rich surfaces for dental implant applications. Materials Science and Engineering: C 54, 196–206.

Santheep, P., Kumar, R., Simon, E.P., Ravi, S., 2017. Biomimetics in conservative dentistry and endodontics. Dent. Bites 32, 24–29.

Sawai, Jun S.S., 1998. Hydrogen peroxide as an antibacterial factor in zinc oxide powder slurry. J. Ferment. Bioeng. 86, 521–522. Available from: https://doi.org/10.1016/S0922-338X(98)80165-7.

Seil, J.T., Webster, T.J., 2012. Antimicrobial applications of nanotechnology: methods and literature. Int. J. Nanomedicine 7, 2767–2781. Available from: https://doi.org/10.2147/IJN.S24805.

Shahmoradi, M., Rohanizadeh, R., Sonvico, F., Ghadiri, M., Swain, M., 2018. Synthesis of stabilized hydroxyapatite nanosuspensions for enamel caries remineralization. Aust. Dent. J. 63 (3).

Shirkavand, S., Moslehifard, E., 2014. Effect of TiO_2 Nanoparticles on Tensile Strength of Dental Acrylic Resins. J. Dent. Res. Dent. Clin. Dent. Prospects 8, 197–203.

Song, W., Zhang, J., Guo, J., Zhang, J., Ding, F., Li, L., Sun, Z., 2010. Role of the dissolved zinc ion and reactive oxygen species in cytotoxicity of ZnO nanoparticles. Toxicol. Lett. 199, 389–397. Available from: https://doi.org/10.1016/j.toxlet.2010.10.003.

Singh, Y., Meher, J.G., Raval, K., Khan, F.A., Chaurasia, M., Jain, N.K., et al., 2017. Nanoemulsion: concepts, development and applications in drug delivery. J. Control. Release 252, 28–49.

Sokołowski, K., Szynkowska, M., Pawlaczyk, A., Łukomska-Szymańska, M., Sokołowski, J., 2014. The impact of nanosilver on element ions release form light cured dental composite and compomer into 0.9% NaCl. Acta Biochim. Pol. 61, 317–323.

Sousa, B.G.B. de, Pedrotti, G., Sponchiado, A.P., Cunali, R.S., Aragones, Á., Sarot, J.R., Zielak, J.C., Ornaghi, B.P., Leão, M.P., 2014. Analysis of tensile strength of poly(lactic-co- glycolic acid) (PLGA) membranes used for guided tissue regeneration [WWW Document]. RSBO Rev. Sul-Bras. Odontol. URL http://www.redalyc.org/articulo.oa?id = 153029831009 (accessed 2.20.16).

Srivastava, M., Kohli, K., Ali, M., 2016. Formulation development of novel in situ nanoemulgel (NEG) of ketoprofen for the treatment of periodontitis. Drug Delivery 23 (1), 154–166.

Suganya, S., Ahila, S., Kumar, B., Kumar, M., 2014. Evaluation and comparison of anti-Candida effect of heat cure polymethylmethacrylate resin enforced with silver nanoparticles and conventional heat cure resins: An in vitro study. Indian J. Dent. Res. 25, 204–207. Available from: http://dx.doi.org.ezp.imu.edu.my/10.4103/0970-9290.135923.

Sun, J., Forster, A.M., Johnson, P.M., Eidelman, N., Quinn, G., Schumacher, G., Zhang, X., Wu, W.-L., 2011. Improving performance of dental resins by adding titanium dioxide nanoparticles. Dent. Mater. Off. Publ. Acad. Dent. Mater. 27, 972–982. Available from: https://doi.org/10.1016/j.dental.2011.06.003.

Tangsadthakun, C., Kanokpanont, S., Sanchavanakit, N., Pichyangkura, R., Banaprasert, T., Tabata, Y., et al., 2007. The influence of molecular weight of chitosan on the physical and biological properties of collagen/chitosan scaffolds. J. Biomater. Sci., Polym. Ed. 18 (2), 147–163.

Targino, A.G., Ribeiro, Flores, M.A., Pelagio Dos Santos Junior, V.E., de Godoy Bené Bezerra, F., de Luna Freire, H., Galembeck, A., Rosenblatt, A., 2014. An innovative approach to treating dental decay in children. A new anti-caries agent. J. Mater. Sci. Mater. Med. 25, 2041–2047. Available from: http://dx.doi.org.ezp.imu.edu.my/10.1007/s10856-014-5221-5.

Tekade, R.K., Maheshwari, R., Soni, N., Tekade, M., Chougule, M.B., 2017a. Nanotechnology for the development of nanomedicine. Nanotechnology-Based Approaches for Targeting and Delivery of Drugs and Genes. Elsevier.

Tekade, R.K., Maheshwari, R., Tekade, M., Chougule, M.B., 2017b. Solid lipid nanoparticles for targeting and delivery of drugs and genes. Nanotechnology-Based Approaches for Targeting and Delivery of Drugs and Genes. Elsevier.

Thein-Han, W., Saikhun, J., Pholpramoo, C., Misra, R., Kitiyanant, Y., 2009. Chitosan–gelatin scaffolds for tissue engineering: physico-chemical properties and biological response of buffalo embryonic stem cells and transfectant of GFP–buffalo embryonic stem cells. Acta Biomater. 5 (9), 3453–3466.

Trubiani, O., Orsini, G., Caputi, S., Piattelli, A., 2006. Adult mesenchymal stem cells in dental research: a new approach for tissue engineering. Int. J. Immunopathol. Pharmacol. 19 (3), 451–460.

Tunde Vig, S., Irmgard, H.-G., Alma, U.D., Katharina, M.F., 2008. Silver coordinatio compounds as light-stable, nano-structured and anti-bacterial coatings for dental implant and restorative materials. J. Mater. Chem. 18, 5359–5362. Available from: https://doi.org/10.1039/b813026d.

Uraz, A., Boynueğri, D., Özcan, G., Karaduman, B., Uç, D., Şenel, S., et al., 2012. Two percent chitosan mouthwash: a microbiological and clinical comparative study. J. Dent. Sci. 7 (4), 342–349.

Vargas-Reus, M.A., Memarzadeh, K., Huang, J., Ren, G.G., Allaker, R.P., 2012. Antimicrobial activity of nanoparticulate metal oxides against peri-implantitis pathogens. Int. J. Antimicrob. Agents 40 (2), 135–139.

Vargas-Reus, K.M., 2012. Antimicrobial activity of nanoparticulate metal oxides against peri-implantitis pathogens. Int. J. Antimicrob. Agents 40, 135–139. Available from: https://doi.org/10.1016/j.ijantimicag.2012.04.012.

Venkatesh, N.S., Pranav, D., Smriti, J., Purna, P., 2015. Antibacterial Activity of Silver Nanoparticles Incorporated in Acrylic Resin - An In vitro Study. Int. J. Sci. Study 2. Available from: https://doi.org/10.17354/ijss/2015/58.

Versiani, M.A., Rached-Junior, F.J.A., Kishen, A., Pécora, J.D., Silva-Sousa, Y.T., de Sousa-Neto, M.D., 2016. Zinc oxide nanoparticles enhance physicochemical characteristics of Grossman sealer. J. Endod. 42 (12), 1804–1810.

Wahab, R., Ansari, S.G., Kim, Y.S., Seo, H.K., Kim, G.S., Gilson Khang, et al., 2007. Low Temperature Solution Synthesis and Characterization of ZnO Nano-Flowers. Mater. Res. Bull. 42, 1640–1648. Available from: https://doi.org/10.1016/j.materresbull.2006.11.035.

Wangjit, K., Limmatvapirat, C., Nattapulwat, N., Sutananta, W., Limmatvapirat, S., 2016. Factors affecting formation of nanoemulsions containing modified coconut oil and spearmint oil. Asian J. Pharm. Sci. 1 (11), 227–228.

Xia, Y., Zhang, F., Xie, H., Gu, N., 2008. Nanoparticle-reinforced resin-based dental composites. J. Dent. 36, 450–455. Available from: https://doi.org/10.1016/j.jdent.2008.03.001.

Yang, H., Liu, C., Yang, D., Zhang, H., Xi, Z., 2009. Comparative study of cytotoxicity, oxidative stress and genotoxicity induced by four typical nanomaterials: the role of particle size, shape and composition. J. Appl. Toxicol. JAT 29, 69–78. Available from: https://doi.org/10.1002/jat.1385.

Yu, B., Ahn, J.-S., Lim, J.I., Lee, Y.-K., 2009. Influence of TiO2 nanoparticles on the optical properties of resin composites. Dent. Mater. Off. Publ. Acad. Dent. Mater. 25, 1142–1147. Available from: https://doi.org/10.1016/j.dental.2009.03.012.

Zhou, Z., Lin, S., Yue, T., Lee, T.-C., 2014. Adsorption of food dyes from aqueous solution by glutaraldehyde cross-linked magnetic chitosan nanoparticles. J. Food Eng. 126, 133–141.

Zou, G.-K., Song, Y.-L., Zhou, W., Yu, M., Liang, L.-H., Sun, D.-C., Li, D.-H., Deng, Z.-X., Zhu, W.-Z., 2012. Effects of local delivery of bFGF from PLGA microspheres on osseointegration around implants in diabetic rats. Oral Surg. Oral Med. Oral Pathol. Oral Radiol. 114, 284–289. Available from: https://doi.org/10.1016/j.tripleo.2011.07.006.

CHAPTER

10

Current Research Perspectives of Orthopedic Implant Materials

Shantanu Bandopadhyay[1,*], *Nabamita Bandyopadhyay*[2,*], *Sarfaraz Ahmed*[3], *Vivek Yadav*[4] and *Rakesh K. Tekade*[5]

[1]Faculty of Pharmacy, Naraina Vidyapeeth Group of Institutions, Kanpur, Uttar Pradesh, India [2]Molecular Biology Division, National Institute of Malaria Research (NIMR), Dwarka, Delhi, India [3]Department of Pharmaceutical Chemistry, Global Institute of Pharmaceutical Education and Research, Kashipur, Uttarakhand, India [4]Department of Pharmacology, Institute of Pharmacy, Chhatrapati Shahu Ji Maharaj University, Kanpur, Uttar Pradesh, India [5]National Institute of Pharmaceutical Education and Research (NIPER)—Ahmedabad, Gandhinagar, India

OUTLINE

10.1 Introduction 338

10.2 History of Implant Materials 340
10.2.1 The Early Era or the Foundation Period 340
10.2.2 Trauma in the Postwar Era or the Premodern Era 341

10.3 Development of Implant Materials Through Various Generations 341
10.3.1 First Generation 342
10.3.2 Second Generation 345
10.3.3 Third Generation 347

10.4 Vital Properties for the Selection of Implant Material 348
10.4.1 Bulk Properties 348
10.4.2 Surface Properties 348
10.4.3 Biocompatibility 348

10.5 Implant Materials Used in Orthopedic 349
10.5.1 Metals 349
10.5.2 Polymers 350

* The authors have equal contributions as the first author.

Biomaterials and Bionanotechnology
DOI: https://doi.org/10.1016/B978-0-12-814427-5.00010-X

© 2019 Elsevier Inc. All rights reserved.

10.5.3 Ceramics 350

10.6 Orthopedic Implant Manufacturing: Design and Development 352
10.6.1 Design Process 352
10.6.2 Feasibility 352
10.6.3 Design 352
10.6.4 Design Verification 353
10.6.5 Manufacture 353
10.6.6 Design Validation 353
10.6.7 Design Transfer 353
10.6.8 Design Changes 354

10.7 Manufacturing Requirements for the Implant Materials 354
10.7.1 Mechanical Properties 354
10.7.2 Nonmechanical Requirements 355

10.8 Coating Technologies/Approaches for Orthopedic Implants 355
10.8.1 Electrostatic Spray Deposition 356
10.8.2 Fiber Laser Surface Engineering 356

10.9 Tissue-Implant Responses 356

10.10 Modeling Fracture Process in Orthopedic Implants 358

10.11 Complications Associated With the Performance of the Implant Materials 358
10.11.1 Sensitization, Irritation, and Intracutaneous (Intradermal) Reactivity 358
10.11.2 Systemic Toxicity (Acute Toxicity) and Subacute and Subchronic Toxicity 359
10.11.3 Genotoxicity 360
10.11.4 Carcinogenicity 360
10.11.5 Reproductive and Developmental Toxicity 360

10.12 Current Trends in the 21st Century 360
10.12.1 Titanium 360
10.12.2 Aluminum Base Alloys 361
10.12.3 Zirconia 361
10.12.4 Cross-Linked Polyethylene 361

10.13 Regulatory Approvals and Requirements 363
10.13.1 Directives 364

10.14 Clinical Applications of Orthopedic Implants 365
10.14.1 Osteosynthesis 365
10.14.2 Joint Replacement 365
10.14.3 Nonconventional Modular Tumor Implants 366
10.14.4 Spine Implants 366

10.15 Marketed Products: An Update 366
10.15.1 Medical Orthopedic Implants Market Segmentation 367

10.16 Conclusions 367

Abbreviations 368

References 368

10.1 INTRODUCTION

Clinically established for their endurance, human bones are one of the most rigid and strongest parts of the body vis-à-vis various musculatures of the body (Waugh and Grant, 2018). The skeletal system is vital for human life and thus, plays an essential role in homeostasis, "housing" the hematopoietic systems, providing mechanistic support to the

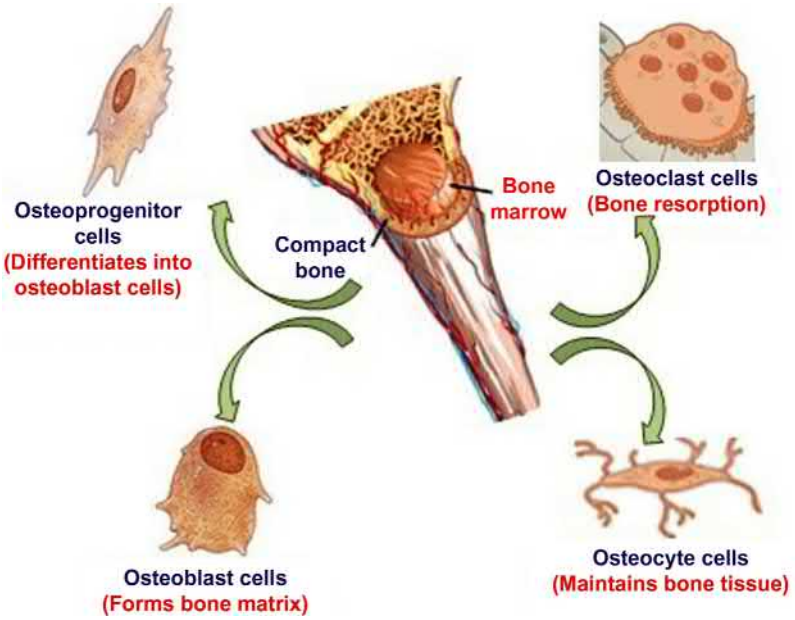

FIGURE 10.1 Functions of different types of cells present within the bone.

body (during movement, protecting the soft and delicate internal organs) and also determines the size and shape of the body (Ohman et al., 2013). The bones are made up of mainly osteoid (an organic matter) and mineral calcium (Ca). It is amazing to note that despite its hard texture, bone is a dynamic tissue that indulges in a continuous process of resorption, renewal, and remodeling (Boskey and Imbert, 2017). Bones have various cells that deliver these processes as depicted in Fig. 10.1 (Florencio-Silva et al., 2015):

1. Osteoprogenitor cells, when prompted by growth factors, produce cells that later differentiate into osteoblast cells
2. Osteoblast cells are located on the surface of bones and perform the function of mineralization and synthesis, transport of matrix proteins
3. Osteocyte cells help to control calcium and phosphate levels in the surrounding environment
4. Osteoclast cells perform the function of bone resorption

A collection of osteocytes, osteoblasts, and osteoclasts work as a unit to control bone formation and resorption. In the early life of a human being, the skeleton grows and bone formation predominates and upon reaching maturity the maintenance of the skeletal system, known as remodeling, takes place at fatigue sites (Florencio-Silva et al., 2015).

Bone and joint problems cause serious disabilities globally with the major causes being decalcification of bones, hereditary, fractures, abnormal growth, bacterial infection, cancers, etc. In most of the cases, there is a decrease in bone density, which causes fractures to the already porous bones. The healing process of bone is a complex process involving both mechanical and medical approach. The bone healing process goes through three stages: inflammation, bone production (callus formation) and bone remodeling. All bones

have the same healing process and this process is aided by a rich network of blood vessels (Hankenson et al., 2015; Marsell and Einhorn, 2011).

Orthopedic implants are devices used to replace or provide support/fixation of bone or to replace articulating surfaces of a joint. Simply put, orthopedic implants provide either assistance or replacement to damaged or troubled bones and joints. The substances that are used to manufacture implants are stainless steel and titanium (Ti) alloys mainly due to strength, and further, these are lined with plastic to act as cartilage so as to reduce the stress at the articulating surfaces. The implants may be fixed into place or pressed to fit so that the bone grows into the implant for strength. The implants can be in the form of plates, nails, and screws (Mantripragada et al., 2013).

10.2 HISTORY OF IMPLANT MATERIALS

Implants can be traced back to ancient Egyptian and South American civilizations where artificial teeth carved into the skull with stone have been discovered. A paper on the use of transplants as a tool for replacing missing teeth was also written by Albucasis de Condue, an Arabian surgeon (Saini et al., 2015).

10.2.1 The Early Era or the Foundation Period

During the 1860s, British surgeon Joseph Lister developed an aseptic surgical technique in combination with the general anesthesia administered by an American surgeon and pharmacist Crawford Long (Worboys, 2013). At the beginning of the 20th century, the efforts towards the manufacture of implants were minuscule, as the medical community was not committed to using metallic or nonmetallic artificial parts. The first surgical procedure towards the restoration of fractures in the long bones and their joints was performed by a British surgeon, Sir William Arbuthnot Lane along with a Belgian surgeon, Albin Lambotte, and Agnes Gwendoline Hunt, a British nurse. They developed a fracture plate that was based on stainless steel material for restoration purposes (Brand, 2009).

This method of Lane was modified by William Sherman of Pittsburgh and F. Pauwels in 1935 simultaneously. Instead of steel, they used a composition of vanadium–iron having the properties of elasticity and stamina. This combined property of the mixture diminished the acute angles in plates, which subsequently reduced the force generated by high pressure.

Satellite, an inert material, was introduced in 1924 by Adalbert Zierold and contained chromium (Cr) and cobalt (Co) (Markatos et al., 2016). Inertness is a prerequisite property of implantable device material. Molybdenum (Mo) containing stainless steel was introduced due to its resistivity towards reaction with organic compounds and biologic fluids. Vitallium, which is a mixture of both chromium and nickel, was also used for the same purpose (Saini et al., 2015).

Amidst the newer materials, stainless steel was the material of choice and was further improved by the Martin Kirschner, a German surgeon. He designed smooth pins and utilized them as wires for providing support to the implant and bone tractions. These implants are known by his name, that is, K-wire or Kirschner wire (Franssen et al., 2010).

In 1912, Ernest Hay Groves used metallic rods in the area of the intramedullary nailing for the first time. These rods had the advantage of inducing osteosynthesis process in small wounds sans the periosteum destruction (Markatos et al., 2016).

A unique and original type of external fixation method, that is, the "bone clamp," was developed by an American, Clayton Parkhill, in 1897. As per his observations, metal pins interlocked into the bone were well adjusted by the body (Hernigou, 2017).

10.2.2 Trauma in the Postwar Era or the Premodern Era

After the Second World War, more refined and advanced mixtures of materials began to be used ushering in a new era of implants and prostheses (Gaviria et al., 2014). This emerging era succeeded at the medical management of the orthopedic crisis. Antibiotics also helped the implantation procedures a great deal for carrying out prolonged operations without causing infection (Narsaria and Singh, 2017).

The development in visualizing techniques made it possible to have a closer look at the affected regions without the actual surgical cut or exposure. Gerhard Küntscher of Germany, a surgeon by profession, improved the materials required for the intramedullary nail implants. These were used in fractures of the long bones, for example, multifragment and metaphyseal fracture (Angadi et al., 2014). The materials used in orthopedic implants are also being refined continuously and may be divided into three generations, as discussed in the next section.

10.3 DEVELOPMENT OF IMPLANT MATERIALS THROUGH VARIOUS GENERATIONS

Throughout the 20th century, the materials used for implants were the same that were used in industrial applications (Narayan, 2010). The surgeons mostly went ahead with known materials used in chemistry and other mechanical fields that were proven to be safe and effective in other applications too. The human body shows specific reactions, that is, both in vitro and in vivo to the entry of any foreign material. As such it presents a very rough environment to the materials used in the implants, which have to pass various standards of in vitro and in vivo tests to ascertain their biological behavior.

Easily available materials that were basically used for industrial purposes formed the first generation of biomaterials with main emphasis on its inertness to prevent its corrosion upon implantation (Navarro et al., 2008). Mechanical properties associated with the materials are also significant criteria when selecting the perfect material for implant fabrication.

To gauge the evolution stages with respect to biomaterials used in implants during the past six decades, three different generations can be clearly seen. The first generation involved inert materials, the second generation comprised bioactive and biodegradable materials, and the third generation of materials are fabricated to stimulate specific cellular responses at the molecular and physiological level (Navarro et al., 2008). These generations are based only on the progression of the necessities and properties of the materials involved in the concept.

10.3.1 First Generation

For consideration of any material to function as a biomaterial, the biological requirements have to be appended along with other common requirements such as chemical, mechanical, and physical. Hence factors such as foreign body reaction and biocompatibility come into play for material selection. The selection of biomaterials for designing the implants depends upon the factors such as bioactivity and osteoinduction, that is, induction of osteogenesis and bone healing (Navarro et al., 2008; Wang and Yeung, 2017).

During the earlier stages, synthetic materials were used for biomedical applications and primarily focused on the physical properties of the material. The synthetic material must be inert with the tissue and cause minimum toxicity to the host, which subsequently aids in modulating the immunogenicity of tissue towards foreign material (Hench, 1980).

10.3.1.1 Metallic Materials

During the twentieth century, stainless steel and cobalt–chrome-based alloys were the first metallic materials that were successfully used in orthopedic applications (Gibon et al., 2017a,b). In the 1940s Ti and Ti alloys began to be used and by the 1960s nickel (Ni)-Ti alloys emerged due to their special mechanical behavior. The use of Ni was particularly hampered due to its allergenic effect (Oldani and Dominguez, 2012).

Owing to high Cr content, stainless steel materials proved to be very useful because of their noncorrosive nature when subjected to different microenvironments and they also allowed for the formation of corrosion resistant coating of their oxide (Godbol et al., 2016). Among the various types of stainless steels used austenitic stainless steel is most widely used for implants that contain Ni or Manganese (Mn) as stabilizing agents to make the material austenitic at room temperature (Yang and Ren, 2010). Owing to the economy, ease of availability, along with its processing viability, stainless steel is used in the manufacture of fracture plates, screws, and hip nails.

Alloys based on metals, for example, Ti, Co–Cr–Mo and Co–Cr, are known for their superior mechanical and corrosion properties. Owing to their different properties like medial elastic modulus (around 110 GPa), high noncorrodibility, and low density (around 4700 kg/m^3) Ti and its alloys are now the material of choice in the area of biomedical engineering. The stability and robustness of the Ti-based implant are considerably enhanced due to its strong bonding with the bones (Sulistioso et al., 2015). Fig. 10.2 illustrates an overview of metallic implants fixation.

10.3.1.2 Ceramic Materials

Alumina, zirconia, and several porous ceramics constitute the first-generation ceramic biomaterials (Piconi et al., 2003). Fabrication of ceramic-based implants depends mainly on the manufacturing process involving various factors such as temperature, material purity, dimension and distribution of the grains, and perviousness (Navarro et al., 2008).

Ceramic materials worked as a replacement for the metallic femoral heads of hip prostheses. Alumina has been in use for many years as it has less friction and constant wear, and zirconia's strength makes it suitable for medical use with negligible wear (Gamble et al., 2017).

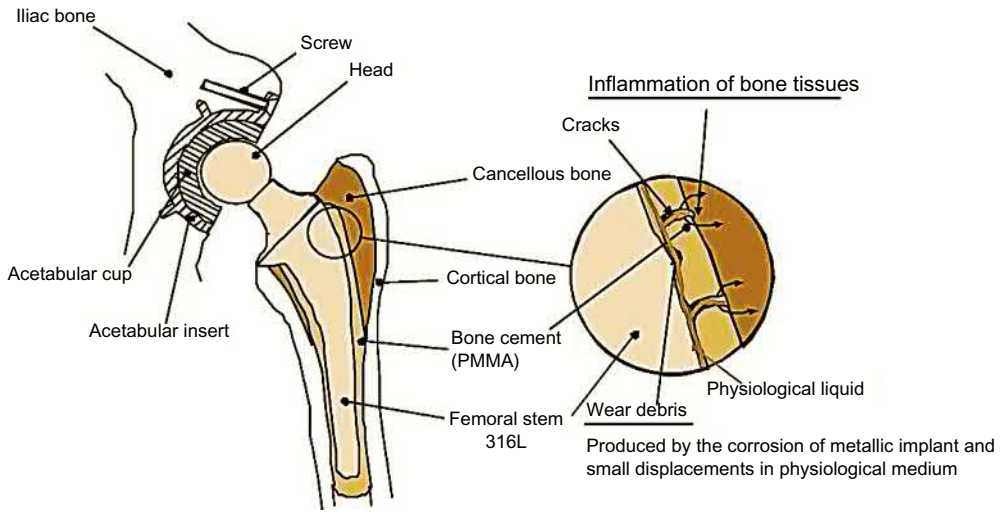

FIGURE 10.2 Metal alloy employed for implant during the first generation. Source: *Adapted with permission from Geringer, J., Forest, B., Combrade, P., 2005. Fretting-corrosion of materials used as orthopaedic implants. Wear 259, 943–951 (Geringer et al., 2005).*

Aluminum oxides and calcium phosphates (CaPs) are used as a ceramic material for implants (Bertoluzza et al., 1991). Ceramics are prepared by hot pressing wherein simultaneous application of pressure and temperature results in a product with high density, small size, and good mechanical properties (Thomas and Jones, 2014). The bioceramics have high modulus compared with bone, which may result in early loosening of ceramic acetabular sockets. Besides, alumina–alumina combination was also discontinued owing to low resilience to sudden impact. CaPs are used for implant coating because of its high biocompatibility (Baino et al., 2015).

10.3.1.3 Polymers

Owing to their flexible properties, that is, mechanical, electrical, chemical, and thermal, polymers can be easily fabricated. Besides, biocompatibility and their ability to get mixed with different materials as composites make it a suitable material for implants (Navarro et al., 2008). Polymeric materials must also have significant tensile strength and should be able to contain the device over the intended lifetime of the implant **(**Fig. 10.3**)**. For substrates, properties like structural properties and electrical properties would be of greater importance. Silicone rubber, acrylic resins, polyurethanes, polypropylene (PP), and polymethylmethacrylate (PMMA) constitute the first generation polymeric materials (Geetha et al., 2009; Bonilla and Perilla, 2011).

Several studies have evaluated the response of porous scaffolds. A study by Geetha et al. demonstrates that mouse preosteoblasts adhere and proliferate on both solid and porous poly(para-phenylene) (PPP) and polyether ether ketone (PEEK) scaffolds. The amorphous structure of PPP makes it relatively convenient to produce varying implant

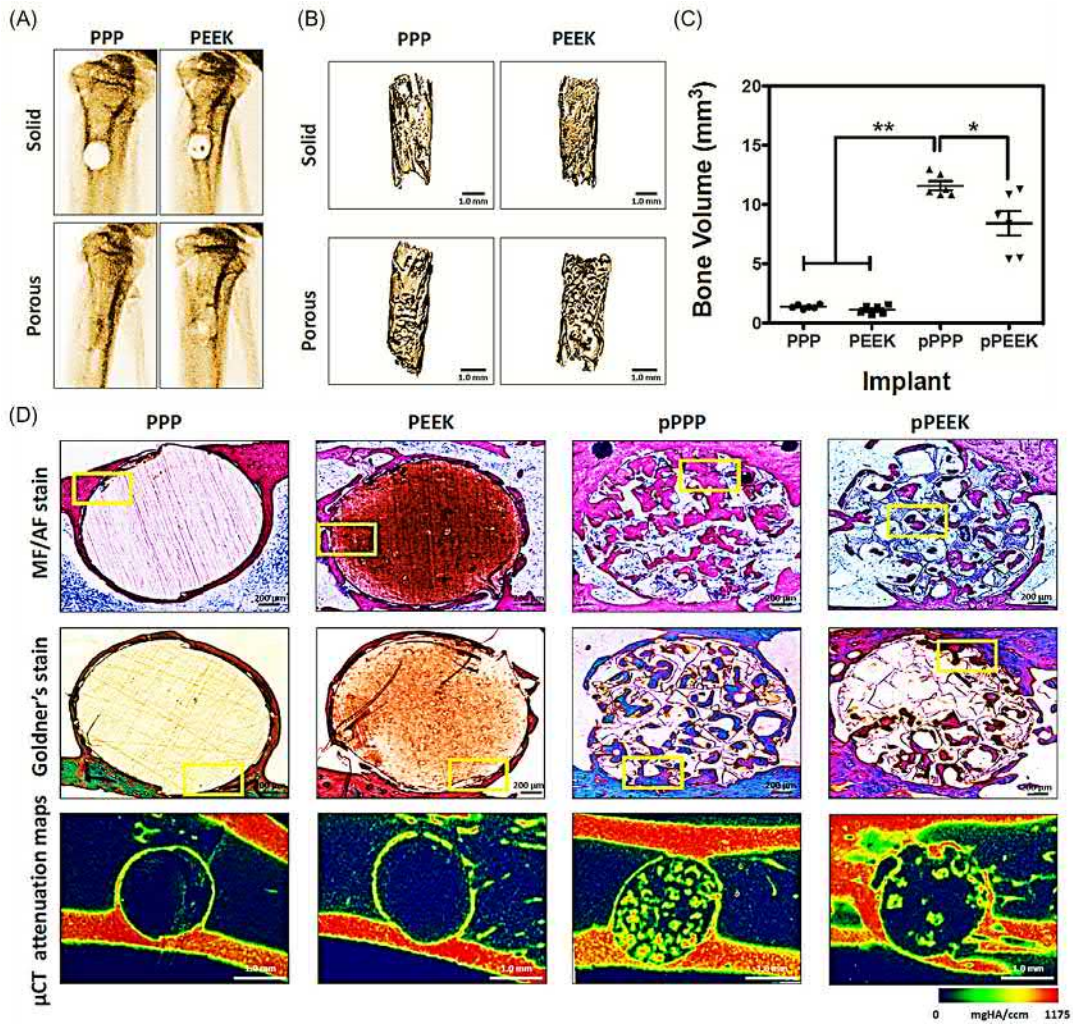

FIGURE 10.3 The polymer employed for implant during the first generation. (A) In vivo X-ray radiographs at 8-weeks postsurgical implantation; (B) micro-CT reconstructions of same specimens from X-ray images. (C) Quantitative measurement of the mineralized bone volume of implants. Solid scaffolds showed no significant difference of BV between groups, (D) osseointegration of implant and bone ingrowth in the coronal section of the implant with adjacent tissue. Notably, pPPP showed enhanced cellularization and substantial bone formation. *BM*, Bone marrow; *F*, fibrotic tissue (*black arrow*); *MB*, matured bone (stained *pink* from MF/AF staining or *purple* to *green* from Goldner's staining); *M*, material (stained *brown*); *OS*, osteoid seam (*red arrow*); *Osteocyte*, *yellow arrowhead*; *P*, inner pore structure. Source: *Adapted with permission from Ahn, H., Patel, R.R., Hoyt, A.J., Lin, A.S.P., Torstrick, F.B., Guldberg, R.E., et al., 2018. Biological evaluation and finite-element modeling of porous poly(para-phenylene) for orthopaedic implants. Acta Biomater. 72, 352–361 (Ahn et al., 2018).*

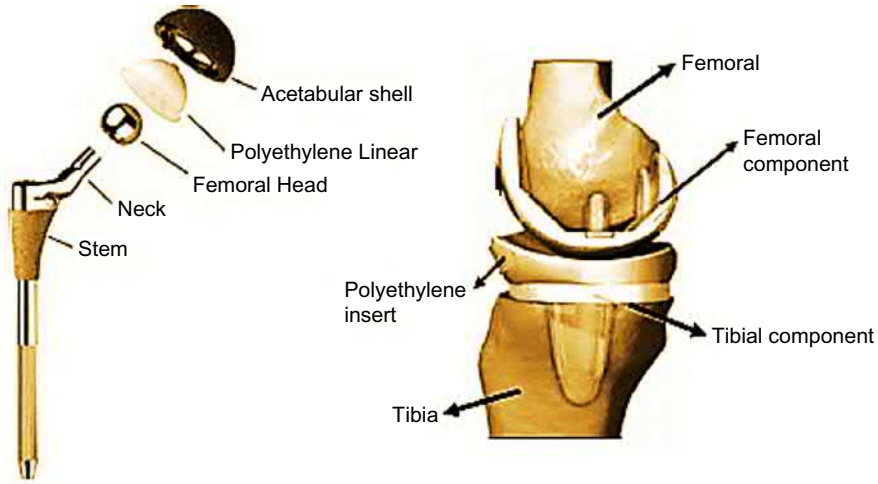

FIGURE 10.4 Ultrahigh molecular weight polyethylene-based implant. Source: *Adapted with permission from Geetha, M., Singh, A.K., Asokamani, R., Gogia, A.K., 2009. Ti based biomaterials, the ultimate choice for orthopaedic implants – a review. Prog. Mater. Sci. 54, 397–425.*

architectures while maintaining mechanical properties. PPP is promising as a potential orthopedic material for implants. It was found that the osteogenic potential was significantly increased in the porous PPP scaffold as assessed by calcium mineralization. The bone growth was notably high, within 420–500 μm pore size, throughout the porous networks **(**Fig. 10.4**)**.

The surface of PPP and PEEK were somewhat less rough than the osteoclast resorption surface; still, an insignificant difference was found in the coarseness of the two materials and mineralization on the two materials. A higher level of mineralization was noted in cases of porous scaffolds compared with the solid scaffolds, but the porous PPP additionally increased compared with porous PEEK. Additionally, porous PPP implants showed bone formation throughout the porous structure when observed via histology. Representative micro-CT attenuation heat maps also elicited the differences in new bone formation between porous groups **(**Fig. 10.5**)**. As evinced from Fig. 10.5, the porous PPP implants get filled with the mineralized bone cells, which is in line with the micro-CT attenuation maps. On the other hand, the porous PEEK showed significantly low mineralized bone ingrowth as determined by micro-CT analysis and histology that confirmed the presence of fibrotic tissue mass in the pores (Geetha et al., 2009).

10.3.2 Second Generation

The second generation heralded from 1980 and continued until 2000 with the main focus on developing bioactive materials that can amplify the biological response and enhanced bonding to tissue. The tissue bonding was achieved by developing bioabsorbable materials that undergo a progressive degradation along with new tissue regeneration. During this generation, mineralizations along with the bonding of the bone tissue

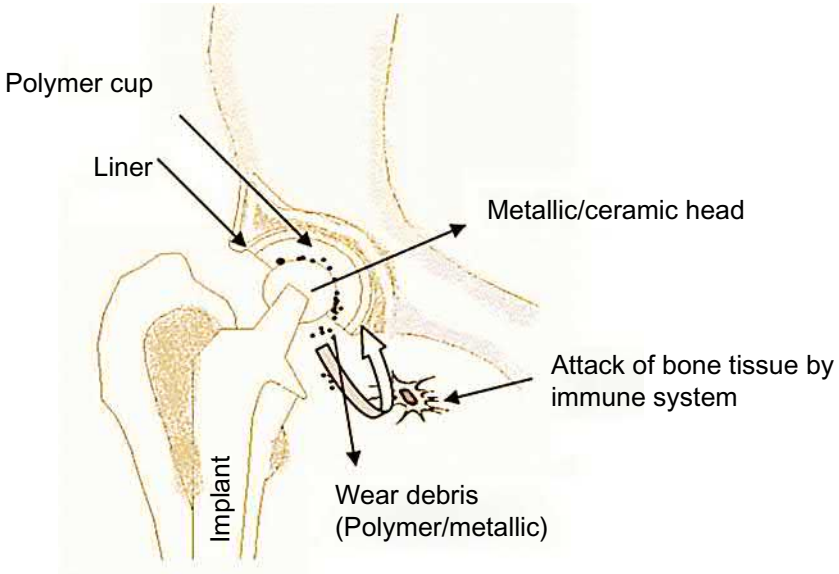

FIGURE 10.5 Schematic diagram representing wear of implant. Source: *Adapted with permission from Geetha, M., Singh, A.K., Asokamani, R., Gogia, A.K., 2009. Ti based biomaterials, the ultimate choice for orthopaedic implants – a review. Prog. Mater. Sci. 54, 397–425.*

with the implant are the two significant features to increase the bioactivity (Navarro et al., 2008).

The materials, that is, metal, ceramics, and polymers as used in the first generation were also used in the second generation with the added property of bioactivity. Glass ceramics and CaPs were used due to their resemblance with bone mineral and their constitutional and surface characteristics. Silicon is also used as an ingredient in ceramics due to its effect on the osteogenesis process (Bonilla and Perilla, 2011).

Although none of the metals can be labeled as a bioactive, coating them with bioactive ceramics or modifying their surface leading to in vivo deposition can make the metals worthy contenders for second generation implants. The coating will obviously take into account the other physical and thermal properties of both metals and coating material (Holloway et al., 2009).

Biomaterials having resorbable properties marked the second generation, which presented a chemical breakdown in an orderly manner along with reabsorption of the polymeric chains. Biodegradable polymers derived from nature and through synthesis were studied, for example, polyglycolide, polylactide (PLA), polydioxanone (PDS), poly (ϵ-caprolactone) (PCL), polyhydroxy butyrate (PHB), poly orthoester, chitosan, poly(2-hydroxyethyl-methacrylate) (PHEMA), hyaluronic acid, and other hydrogels (Kulkarni et al., 1971).

Materials having bioabsorbable characteristics came into light in the 1960s for use as a replacement for bone, in case of fracture of bone, meniscus, and intervertebral disc. Implants made up of the biodegradable material decrease the stress shielding effect,

completely removing the chance of further surgeries, which was previously required to remove the implant of metallic origin. It also enables a better visualization of the affected region as metallic interference is reduced (Triclot, 2011).

10.3.3 Third Generation

The third-generation biomaterials are newer materials that have the property to stimulate specific cellular responses at the molecular and physiological level. The concept of bioactivity and biodegradability is entwined for these biomaterials and can be used vice versa. The properties of these materials should be such that it can initiate any required particular cellular activity. Some transient three-dimensional structures having appropriate porosity activating attack, attachment, and growth by cells and specific surfaces with particular peptide sequences imitating the extracellular matrix (ECM) for eliciting cellular responses are also under the development stage (Navarro et al., 2008; Mantripragada et al., 2013).

The biomaterials belonging to the third generation came to the forefront simultaneously at the time when the frames for tissue engineering began developing. Tissue engineering and regenerative medicine are budding trends that explore the methods of repairing and regenerating organs and tissues by using the natural signaling pathways comprising of mechanisms such as stem cells and growth factors in combination with synthetic scaffolds (Henkel et al., 2013). Three-dimensional porous structures known as scaffolds should have the following properties for use in tissue engineering:

1. Biocompatibility and noncytotoxic by-products
2. Biodegradable nature of the scaffold having the same rate of resorption as the tissue being repaired
3. Highly interconnected porous network, consisting of macro- and micropores for proper tissue in-growth, vascularization, and nutrient uptake
4. Some mechanical properties that enable the scaffold to produce the tissue at the trauma site, helping in sharing of load and helping to maintain the structural stability during the initial stages of forming the new bone

The most relevant characteristics that are incorporated in the third-generation biomaterials are bioactivity and biodegradability combined with each other. Specific biomolecules used for the bioactivation of surfaces serve as a potent tool for stimulating a specific response from the cell and mimic ECM environment by coupling specific cues on the surface of the scaffold. Biomolecules that are attached to the material surface influence the cell behavior towards proper attachment, growth, and diversification (Hui et al., 2012).

Biodegradable scaffolds combining the properties of biodegradability and bioactivity offer a particular advantage in the biomedical engineering area. An inorganic phase, when introduced in a matrix of bioabsorbable polymer, affects the physical behavior, degradability pattern of the material and also enhances its bioactivity (Ghassemi et al., 2018).

10.4 VITAL PROPERTIES FOR THE SELECTION OF IMPLANT MATERIAL

For the lasting success of implants, the selection of implant biomaterial is an important factor of consideration. The biological nature of our body is prone to reject foreign material so the implants should be selected such that the negative biological response remains minimum and the requisite functions are maintained (Gibon et al., 2017a,b).

10.4.1 Bulk Properties

Modulus of elasticity: The modulus of elasticity of an implant should be similar to the bone to facilitate smooth and easy movement at the implant–bone surface (Hak et al., 2014).

Tensile, compressive, and shear strength: A high compressive and tensile strength material must be chosen for preventing fractures and improving its function (Mathieu et al., 2012).

Yield strength, fatigue strength: This property is required to prevent fracture due to load and materials having high value for these properties should be selected (Ducheyne et al., 1983).

Ductility: This property is essential for contouring and providing shape to the dental implants with a minimum of 8% ductility requirements (Saini et al., 2015).

Hardness and toughness: Hardness and toughness are the essential features of implant materials as hardness is required to reduce the rate of wear of implant material and toughness prevents the implant fracture (Saini et al., 2015).

10.4.2 Surface Properties

Surface tension and surface energy: Surface tension establishes the wetting ability of an implant and it finds implication in the cleanliness of the surface of the implant. Surface energy plays a role in protein adsorption on the surface of implants (Rupp et al., 2014).

Surface roughness: It determines and influences the response of cells and tissue. On the basis of various criteria, for example, roughness of the surface and its texture, implants have been classified as follows (Novaes Jr. et al., 2016):

1. On the basis of surface roughness as minimally rough, medially rough, and rough
2. Depending on the texture as concave texture obtained by the coating of hydroxyapatite (HA) and spray of titanium plasma, or convex texture obtained by etching and blasting method; and
3. Depending on irregularities on the surface as having similar surface and not dependent on a particular direction (isotropic surfaces); or having specified direction (anisotropic surfaces).

10.4.3 Biocompatibility

It determines the compatibility of the implant material with the biological environment. The biocompatibility depends on resistance against corrosion and cytotoxicity caused by the remnants of corroded material (Manam et al., 2017).

Corrosion and corrosion resistance: Corrosion takes place when the surface of metal loses its ion in the neighboring environment and it is of the following types (Gotman, 1997; Nagaraja et al., 2017):

- *Crevice corrosion*: This takes place in the constricted regions and occurs by an ionic environment created due to the dissolution of metals in the local environment., for example, interface of the screw−bone implant.
- *Pitting corrosion:* It is found in implants with pits (invariably of small size) on the surface containing dissolved metallic and chloride ions in combination. It generally leads to the irregular surface by formation of pits.
- *Galvanic corrosion*: Difference in the electrical gradients causes this type of corrosion.
- *Electrochemical corrosion*: It is characterized by metal deterioration that occurs due to anodic oxidation and cathodic reduction resulting in charge transfer via electrons as well. Application of the metal surface with a layer of passive oxide on metal surface prevents corrosion of the material.

Clinical significance of corrosion: Resistance to corrosion forms an important aspect for implant biomaterial. Corrosion results in irregularities in the surface, improper healing, and loss of ions and elements from the material, which can cause harmful toxic reactions. Discoloration and allergic reactions to adjacent tissues may result in patients due to the release of elements.

10.5 IMPLANT MATERIALS USED IN ORTHOPEDIC

Materials used in implants are basically divided into three categories: metals, polymers, and ceramics (Hasan et al., 2018).

10.5.1 Metals

Metals used in orthopedic implants comprise of stainless steel, Co−Cr alloys, and Ti and its alloys. Although stainless steel suffers from poor corrosion resistance and fatigue strength, it is still commonly used for nonpermanent implants such as internal fixation devices for fractures (Hamidi et al., 2017).

Prior to the use of Ti, Co, and Cr based alloys largely replaced stainless steel for permanent implants. These were more corrosion resistant but the in vivo ion release is still a concern. Another disadvantage is the proven carcinogenicity of chromium. Cobalt-based implants have been reported to fracture, which initiated the need of special forging process involving compression under high pressure (Madl et al., 2015).

Pure titanium along with its alloys are used in orthopedic implants and are known for their high biocompatibility. Titanium is corrosion resistant as it forms an oxide of titanium at the surface but its disadvantage is that it makes the layer porous and friable and its abrasion can release particles into the surrounding tissues, which may cause undesirable tissue responses. Many cobalt and titanium alloys are used as cement fewer implants (Kulkarni et al., 2015).

10.5.2 Polymers

The most popular polymer used in orthopedics is ultrahigh molecular weight polyethylene or high-density polyethylene (Fig. 10.4) (Alothman et al., 2014; Pokorny et al., 2016). Although polyethylene is the best material that can articulate with metals and ceramics it also suffers from a slow temperature-dependent deformation under load with time (creep) and progressive wear. Creep is subdued by backing up the polymer with metal. Wear of polyethylene is also a major concern because it releases debris into the tissue, which may cause bone lysis leading to aseptic prosthetic loosening. It is overcome by reinforcing the polymer with carbon fibers.

Some of the polymer materials are nylon, polyvinyl chloride (PVC), and polyetheretherketone (PEEK). The other advantages of using polymers are (Amini et al., 2011; Abdullah et al., 2015):

- Polymeric materials can be better alternatives as biomaterials looking into their varied and useful properties
- PEEK, PVC, polyethylene, nylon polymers are equally useful with similar good properties
- Polymers are highly corrosion resistant
- They are highly biocompatible with the human body, and thus suitable for implantation
- Their properties depend on the different types of material used as a biomaterial
- Owing to their good mechanical properties these polymers can be the best replacement materials
- Higher biocompatibility of ceramics and metals provides much better options as polymers for future applications
- These polymers can be used in different areas of medical field with enhanced future applications

Disadvantages of using the polymer as a material for implants include lack of adhesion to living tissues and surfaces, average mechanical properties, and specific adverse immunologic reactions.

10.5.3 Ceramics

Ceramics are the nonmetallic inorganic substances composed of various compounds. It is manufactured by mixing together all the particulates of the material together with an organic binder and water. A desirable shape is given to this mixture by pressing it into a mold. The organic binder and water are removed by thermal treatment and drying method respectively (Hamadouche and Sedel, 2000).

Sintering is a thermal process taking place at a very high temperature that increases the density of the resultant material and affects the final structure of the ceramic with respect to the temperature used and the time period for which it was subjected to such a high temperature (Hamadouche and Sedel, 2000).

Commonly available ceramics include glass, vitrified, plasma sprayed polycrystalline, solid-state sintered, and polycrystalline glass-ceramic. The mechanical and biological properties are dependent on porosity, purity of used powder, and the dimensions and distribution of the grains. Bioceramics owe their success as an implant material to their excellent biocompatibility (Kawanabe, 1996; Campbell, 2003; Vallittu et al., 2015).

Orthopedic surgery makes use of ceramics when implantation is needed in an osseous environment. On the basis of the tissue response, ceramics may be classified as bioactive or inert. An inert ceramic prompts a minor fibrous reaction and is applied as bearings in total joint replacements mainly due to its excellent resistance to wear and biological properties. Bioactive ceramics are used as coatings to help in the fixation of any device due to their osteoconductive properties (Navarro et al., 2008).

Total hip arthroplasty makes use of sliding ceramics in which femoral heads articulate with polyethylene. It is also used in the manufacture of cups in the combination of alumina-on-alumina. Due to its brittle nature along with its cost, the use is limited. However by improving the manufacturing process and refining the purity, density, size, and distribution of the grains the risk of fracture has been eliminated (Traina et al., 2013).

The powder of alumina is subjected to sintering at high temperatures (1600°C−1800°C) to produce alumina ceramic, which results in a material having thermodynamic stability along with chemical inertness and resistance to corrosion (Cutler et al., 1957).

Zirconia ceramic due to its higher strength and toughness was used for total hip replacements as femoral heads, which reduced the risk of fracture (von Schewelov et al., 2005). Pure zirconia occurs in three different crystalline phases which are monoclinic, tetragonal, and cubic. Zirconia as a material in a pure state is unstable and is stabilized by adding oxides to preserve the tetragonal phase (Abd El-Ghany and Sherief, 2016).

Mixed-oxide ceramics were developed by combining the tribological properties of alumina and the mechanical characteristics of yttrium-stabilized zirconia. Promising results have appeared during simulating it on hip joints, which have prompted further research to evaluate its long-term use (Denkena et al., 2017).

Bioactive ceramics are osteoconductive in nature serving as a frame on which the bone formation can occur. These types of ceramics have also been used to form a layer on various surfaces (Vallittu et al., 2015). CaP ceramics include HA and tricalcium phosphate and these have been extensively used in orthopedic implants (Yamada et al., 1997). Hench and Wilson introduced bioactive glasses having a vitrified morphology, which bond chemically to bone. 45S5 Bioglass is generally used for implants having a composition of 45% silicon dioxide (SiO_2), 24.5% calcium oxide (CaO), 6% phosphorous oxide (P_2O_5), and 24.5% sodium oxide (Na_2O) by weight (Islam et al., 2017). Hydroxycarbonate apatite layer results in a series of surface reactions attributed to the bonding mechanism between the material and bone (Kontonasaki et al., 2002). A layer of porous silica gel having a high surface area is a critical element necessary for its formation.

10.6 ORTHOPEDIC IMPLANT MANUFACTURING: DESIGN AND DEVELOPMENT

The environment of the surrounding biological system and various properties associated with the biodevices facilitate the process of the development of any product intended for the use inside the body. The state of specific medical requirement, effects of interaction with biological environment, proper selection of suitable biomaterial with appropriate physical (corrosion) and chemical properties, and suitable sterilization methods determine the factors to be considered from the initial development process, beginning with personnel from different disciplines forming the development team (Aitchison et al., 2009).

10.6.1 Design Process

The design process of any medical device may be divided into following key areas: market, design specification, concept and detailed design, manufacture, and sale (Cross, 2008).

10.6.2 Feasibility

The inputs for designing the implants are provided by the surgeons, medical engineers, and other interdisciplinary teams on the basis of the market or patient needs. A feasibility study may also be conducted at various levels to ascertain the needs to design any specific device. Proper planning in terms of achievable goals should be set and assessed at the end of definite periods during the manufacturing process. The planning process should also consider the human and financial resources required to realize a design. The regulatory requirements have to be met making it mandatory to identify the global standards applicable to the implants and devices being designed and manufactured (Sagbo et al., 2005).

There are certain requirements to implant design that should be addressed before venturing into the manufacturing process, viz., purpose of the implant, design attributes, material needed, manufacturing method and the instrumentation needed, testing, sterilization, packing and information supplied to the users from the manufacturer. A review is needed at every step of the design process for assessing and identifying the capability of the design and problems respectively (Bhoyar and Borade, 2015).

10.6.3 Design

Any concept for the design should be nurtured and the focus should be to generate as many ideas as possible. A simple sketch, computer-aided models by using Pro-Engineer and Unigraphics software, analytical calculations, and initial manufacture consultations are some of the tools to assist in the designing. The concept design evolves into detail design with the help of solid models developed through computers, engineering drawings, operative capabilities, and liaison with manufacturers to ascertain DFM, DFA, or DFMA (Syam et al., 2011).

10.6.4 Design Verification

Verification involves the confirmation that a medical device is being designed as per the requirement and it is absolutely necessary to follow this step at the start of the design process. The methods involved in the design verification include (Aitchison et al., 2009):

1. *Finite element analysis*: This method is used to verify the strength of the design and its ability to endure the conditions in the body.
2. *Risk analysis*: This method assesses the safety of the design so that the product does not interfere with the patient's health. Techniques involved in doing the risk analysis include failure mode effect analysis and fault tree analysis. Evaluation of hazards associated with the design process is carried out through bottom-up method.
3. *Rapid prototyping*: Analysis of risk is carried out through this method by developing models of implants through various techniques such as selective laser sintering, fused deposition modeling or three-dimensional printing. All these techniques help in communication between engineers and surgeons and aid in studying any anomaly in the bone to which the implant has to be fitted.

10.6.5 Manufacture

It should be ensured that any design that is being transferred to the manufacturing unit should be repeatable and reliable. The number, quality, and cleaning process needed for the product determine the choice of the manufacturing process (Aitchison et al., 2009).

10.6.6 Design Validation

This step is necessary before the final transfer of the design to the manufacturing unit. Validation is different from verification and ensures whether the right design has been processed. Validation includes mechanical testing of prototypes, clinical investigation, and validation of the sterilization method (Moiduddin et al., 2017).

The mechanical environment prevailing inside the body is reconstructed inside the laboratory during the examination, which warrants that the devices have sufficient strength and stiffness to perform the intended functions. Various standards are available as a guide to preclinical mechanical testing and in some cases, human cadavers have also been used (Moiduddin et al., 2017).

The guide for clinical testing is regulated and provided as standard BS EN ISO 14155-1. Ethics Committee approval is usually required for clinical investigation along with the information on the duration, an exact count of patients, along with the category of information to be collected (Aitchison et al., 2009).

10.6.7 Design Transfer

It involves all the requisite and related documents, for example, instructions for use, and instruction for training to surgeons, vendor requirements, process worksheets, and total cost bill of materials (Aitchison et al., 2009).

10.6.8 Design Changes

These are needed to ensure the safety of patients and results from the postmarket surveillance, which again will require complete documentation (Aitchison et al., 2009). It may be noted that the issue of loosening of joint replacements structures made of a metallic head as well as polymeric cup has been widely reported. Almost 20% of joint replacement surgeries need to be changed within >20 years of surgery. Notably, the loss of aseptic nature accounts for roughly 80% of the replacements. The limited biological life of artificial joint implants is becoming a growing concern for the healthcare sector. Currently, improving the surgical procedures to improve the lifespan and reduce the wear and tear attributes of joint components is a focused area of orthopedic research. The main reason reported to date for the failure of the joint implants is attributed to debris from the wear and tear process in the implant entering the surrounding environment. This event is marked by bone resorption, which finally results in relaxing (loosening) of the joint implant, and hence the implant has to be replaced by a new one (Fig. 10.5). It may be noted during this discussion that not only are the replacement surgical procedures costly, but also the diminishing success rate as compared with initial implantation is another prime issue. Moreover, the existence of foreign bodies, viz., metallic beads, bone cement particles, HA materials, etc. originated from coating raises the yield of debris at the joint interface. Reports inferred that the subjects undergoing total joint (hip or knee) replacements showed that buildup of wear/tear fragments in the spleen, liver, and lymph nodes.

10.7 MANUFACTURING REQUIREMENTS FOR THE IMPLANT MATERIALS

Biomaterials are those materials that are accepted by living tissues upon its introduction and can be utilized for tissue replacements. The required properties needed for the manufacture of implants may be divided into two categories (Saini et al., 2015):

10.7.1 Mechanical Properties

10.7.1.1 Bulk Properties

Modulus of elasticity: For ensuring even distribution of stress at the interface of implant and bone, materials having a modulus of elasticity greater than 18 GPa should be selected (Xue et al., 2012).

Tensile, compressive, and shear strength: To prevent fracture and improve functional stability the material should be of high tensile strength (Schulze et al., 2018).

Yield strength and fatigue strength: These properties must be of high-value fracture while loading (Mower and Long, 2016).

Ductility: At least a ductility of 8% is required. This property is used for contouring of the implants (Saini et al., 2015).

Hardness and toughness: With the increase in hardness and toughness there is a decrease in the wear and fracture of implant materials (Saini et al., 2015).

10.7.1.2 Surface Properties

Surface tension and surface energy: This property governs the ECM capability to maintain contact with implants and affects the absorption of proteins (Rupp et al., 2014).

Surface roughness: This property increases the surface area of the implant, which provides better cell attachment to the bone. Texture, roughness, and orientation of irregularities are some of the criteria on which implant surfaces may be classified (Turger et al., 2013).

10.7.2 Nonmechanical Requirements

These properties are not dependent on the mechanical aspects of the materials; instead they are more closely related to manufacturing aspects. Some of the requirements are the methods of fabrication employed in the manufacture of implants, consistency, and conformity of the materials, quality of the raw materials, sterilization techniques, and lastly the cost of production (Saini et al., 2015).

10.8 COATING TECHNOLOGIES/APPROACHES FOR ORTHOPEDIC IMPLANTS

Coating techniques have been applied to orthopedic implants to deal with various issues such as bacterial infection and sometimes to make the implant bioactive. The infections associated with biomaterial are a severe complication of modern orthopedic surgery, which is generally accompanied by prolonged patient pain and loss of function (Ribeiro et al., 2012).

Staphylococcus aureus is the leading cause of both surgical site infections and periprosthetic joint infection. Development of effective antibacterial surfaces may be one of the methods to prevent bacterial growth, which could prevent bacterial adhesion and proliferation into the surrounding tissues. The antibacterial coating should be biocompatible and must possess antiinfective efficiency in addition to other suitable properties (Romano et al., 2015; Gil et al., 2017).

The biomimetic coating is a flexible process for various orthopedic implant surfaces, which makes the implant bioactive, that is, helps in osseointegration irrespective of its biodegradability and nonbiodegradability. Apatite, a bone-like mineral, is composed of CaP, which is deposited on the surface of the implant thereby enhancing its bioactivity leading to osseointegration. By this process, a coating akin to bone known as calcium deficient carbonated HA is deposited on the surface of the implant facilitating osseointegration sans the fibrous tissue. The process involves prepping up the surface by treating it with alkali or acid before soaking at physiological conditions in the simulated body fluid during which various reactions occur (Goodman et al., 2013; Koju et al., 2017).

10.8.1 Electrostatic Spray Deposition

ESD is a recent technique in which CaP is coated upon the substrates. The organic solvents containing calcium and phosphate are propelled through a nozzle by applying a high voltage in between the nozzle and substrate resulting in the deposition of droplets coming out of the nozzle into a spray on the substrate. After the evaporation of the solvent, a layer of the coat is formed on the surface of the substrate. ESD also allows changes in coating composition and morphology. The surfaces are characterized by X-ray diffraction, Fourier transform infrared spectroscopy, a universal surface tester, scanning electron microscopy, and energy dispersive spectrometry (Iafisco et al., 2011; Sopcak et al., 2018).

10.8.2 Fiber Laser Surface Engineering

Orthopedic implants still face the challenge of bacterial infection, which contributes to about 30% of hip implant revision. There are two strategies to reduce bacterial adherence namely coating and noncoating methods. Coating methods involve coating of the whole implant with the antibacterial substance along with the possible limitation of cytotoxicity caused by the antibacterial materials. Noncoating methods include the modifications in the surface characteristics of implants to achieve antibacterial properties like creating surface nanofeatures, reducing surface hydrophobicity, and modifying surface chemistry (Chan et al., 2017).

Laser surface treatment is a recent noncoating method that has provided promising results in quashing the bacterial adherence. Laser technology encompasses various benefits which include high speed, tidiness, high precision, and repeatability, along with the flexibility to modify surfaces in selective areas. Fiber laser surface engineering technique is mostly used for antibacterial coating on the implants (Chan et al., 2017).

Commercially pure Ti (Grade 2), Ti6Al4 V (Grade 5), and Co−Cr−Mo alloy may be treated to enhance the antibacterial properties of the implants. Laser surface treatment is accomplished by a continuous wave fiber laser with a near-infrared wavelength of 1064 nm in a nitrogen-containing environment (Mantripragada et al., 2013; Chan et al., 2017).

S. aureus is used to evaluate the antibacterial characteristics of the laser-treated surfaces. The roughness of the surface and topography of the laser-treated materials is analyzed by a 2D roughness testing and by atomic force microscopy. Evaluation is done through the study of surface morphologies obtained by scanning electron microscope, and bacterial viability is determined with the help of live/dead staining (Jager et al., 2017).

10.9 TISSUE-IMPLANT RESPONSES

Biomaterials that are meant for use inside the human body elicit some kind of responses at the tissue level after the implantation. The following sequential steps take place when an implant is introduced inside the body (Amini et al., 2011):

- Injury
- Contact of blood and material

- Matrix formation
- Acute onsite inflammation
- Chronic inflammation
- Granulation tissue
- Foreign body reaction
- Fibrosis

The process of organization starts soon after the formation of fibrous tissue leading to the formation of a fibrous capsule at the interface of tissue and material. The capacity of cells to grow in any specific organ determines whether resolution or organization occurs. Implantation in vascularized tissues usually leads to organization and fibrosis (Kuboki et al., 2001).

Inflammatory responses are initiated with blood−material interaction, which presents the first reactions to injury. A provisional matrix develops when there is an injury to vascularized tissue during the implantation process at the site. This matrix is composed of fibrin, which is a product of the coagulation system, and the complement system generates inflammatory products. The duration of these events to occur is from minutes to hours immediately after introducing the medical device inside the body. Fibrin, which is released from the provisional matrix, initiates the resolution and repair processes. Inflammation is basically the reaction of vascularized living tissue to local injury and serves to contain, neutralize, or dilute the injurious agent or process. In most cases, the compatibility of a material with biological tissue depends on inflammatory responses, that is, either acute or chronic. This biocompatibility is also crucial during the various stages of fibrous capsule formation following implantation. Histological evaluation of adjoining tissue of the implanted material as a function of implant time is the most commonly used evaluation method for biocompatibility (Kuboki et al., 2001; Luttikhuizen et al., 2006).

Acute inflammation is of usually short duration and characterized by the release of fluid and plasma proteins (edema) and the emigration of leukocytes (predominantly neutrophils). The growth of blood vessels and connective tissue and the presence of monocytes, macrophages, and lymphocytes depicts the state of chronic inflammation (Bridges and Garcia, 2008).

The healing process starts within one day of the implantation due to the monocytes and macrophages and subsequent growth of fibroblasts and vascular endothelial cells taking place resulting in the granulation tissue (which is pink and softly granular in appearance) formation, which indicates healing. Granulation tissue becomes visible by three to five days after the implant is introduced into the body (Luttikhuizen et al., 2006; Xia and Triffitt, 2006).

Depending on the surface of the implant using the reaction involving foreign body consists of giant cells, granulation tissue consisting of macrophages, fibroblasts, and capillaries in varied amounts. The implants having smooth and even surfaces, are made up of macrophages layer of one to two cells in thickness whereas rough surfaces are composed of macrophages and foreign body giant cells at the surface. Fabric materials also have the same response in terms of macrophages, giant cells, and granulation tissue (Muldashev et al., 2005).

Fibrosis marks the completion of the healing process towards biomaterials. Cellular or tissue repair at the site of the implant occurs by regeneration, in which cells of parenchyma replace the damaged tissue and by replacement, in which the replacement takes place by connective tissue and a fibrous capsule is formed. Both regeneration and replacement are managed by either growing capability of cells at the site of implant and knowledge of the extent of injury or perseverance of the tissue at the same site (Luttikhuizen et al., 2006).

10.10 MODELING FRACTURE PROCESS IN ORTHOPEDIC IMPLANTS

It is not just the bones but sometimes the implant itself may fracture creating surfaces where the bonds are broken and its process is distinguished into fracture nucleation and propagation. Anatomical stress and strain analysis present a great deal of difficulty in its quantification. To prepare a model that combines both complexity of the implant site and implant fracture is very difficult (Amini et al., 2011).

According to the process energy consumption, fractures may be divided into two types, that is, plastic fractures occurring under the application of continuous external energy and preceded by significant plastic macrodeformation and brittle fracture, which requires low energy but develops very fast. As per the structural criteria, the fractures are of two types, that is, transcrystalline, in which the crack runs right through the grain, and intercrystalline, in which the crack spreads sideways with the boundaries of the grain.

Mechanics, metallurgy, and solid-state physics decide the material decohesion phenomenon. Mechanical properties preside over the selection of implant material by considering the parameters such as strength, elasticity, plasticity, hardness, and fragility. Modulus of elasticity, fracture resistance, and impact strength are some of the other features that are incorporated to understand the model (Chen et al., 2004).

10.11 COMPLICATIONS ASSOCIATED WITH THE PERFORMANCE OF THE IMPLANT MATERIALS

Normally there are no risks and complications involved in orthopedic implantation and nowadays surgeons are fully equipped, and properly trained to avoid any unfortunate incidence. Although the techniques have developed tremendously various complications, for example, blood loss, infections, coagulation, injury to nerves, restriction in movement, initiation of arthritis, and new injury at the same site still exist (Table 10.1) (Sambandam et al., 2013; Sansone et al., 2013).

10.11.1 Sensitization, Irritation, and Intracutaneous (Intradermal) Reactivity

All these complications arise due to the biomaterial and its leachable agents coming in contact with tissues, as shown in Table 10.2 (Fernandez et al., 2006).

TABLE 10.1 Complications due to Implantation of Orthopedic Materials.

Complication	Description
Postoperative infections	Such kinds of effects are addressed by the administration of antibiotics before, during and after the surgery. In the event of any previous infection, it needs to be treated prior to the operative procedure as any future infection might occur after some duration
Blood clots	These appear sporadically after the surgical procedure during knee replacement. Regular exercise and medication help in such cases
Damage to nerves or neuroparalytic	Nerves which are near to the implant site when severely damaged leads to such cases
Bone fracture	Delicate or brittle bones are more prone to this type of damage and it takes place during the insertion process
Implant failure	This is a combined result of inappropriate placement, dislocation, malfunction, and gradual detachment of the implant. It also arises due to wear and tear of the parts of the prosthesis
Allergic reactions	This is a reaction of the body to the material of the implant or other chemicals involved in the implantation process

TABLE 10.2 Reactions due to Different Orthopedic Materials.

Type of Implant	Described Allergic Reaction
Osteosynthesis material	Impaired wound healing, eczema, delayed fracture healing
Stainless steel	Impaired wound healing, eczema, sterile osteomyelitis, swelling
Arthroplasty	Eczema, swelling, effusion, loosening, pain
Bone cements	Fistula, pain, effusion, loosening

10.11.2 Systemic Toxicity (Acute Toxicity) and Subacute and Subchronic Toxicity

Systemic toxicity is mainly caused by the particulate debris produced by the implants falling in the range of 30–100 nm. This small size allows for its diffusion inside the cells (Sansone et al., 2013). Hemoglobin and hematocrit values are changed due to the use of Cr(VI) owing to its capacity to disturb iron utilization at the cellular level (Keegan et al., 2008).

Metals also modify the activities of immune-competent cells through various immune-stimulatory or immunosuppressive actions, which include disruption of T-cells, B-cells and macrophages functionalities, alteration in the release of cytokines, immunotoxicity, and generation of compounds causing an immune response (Sansone et al., 2013).

10.11.3 Genotoxicity

Metal particles are released from the implants through different mechanisms such as corrosion and certain electrochemical reactions resulting from the physical wear and stress. Ti alloy (Ti−6Al−4V) is a preferred and ideal metallic biomaterial for orthopedic implants but some of its components such as vanadium is known to cause osteomalacia and Alzheimer's disease due to the release of aluminum and vanadium ions (Gomes et al., 2011; Gibon et al., 2017a,b).

10.11.4 Carcinogenicity

Co is an important material used in the manufacture of orthopedic implants but at high concentration, its ions cause cytotoxicity and apoptosis by inducing necrosis with inflammation. On comparing the different metallic particles CoCr-alloy particles were found to cause the highest toxicity among the other particles, for example, CoCr alloy, Ti alloy, zirconium (Zr) oxide, and Zr alloy. The CoCr-alloy particles caused a significant decrease in viability and proliferation of human osteoblasts, fibroblasts, and macrophages. Higher concentration of metal in the body leads to an increase in hepatocellular necrosis. Cr when present in epithelial cells impairs the function of proximal renal tubules causing tubular necrosis and cause marked interstitial changes in experimental animals and humans (Sunderman, 1989; Maccauro et al., 2009).

10.11.5 Reproductive and Developmental Toxicity

Nickel, which is used in orthopedic implants, is a highly toxic metal and is known to cause systemic, immunologic, neurologic, reproductive, developmental, and carcinogenic effects (Keegan et al., 2007).

10.12 CURRENT TRENDS IN THE 21ST CENTURY

10.12.1 Titanium

The considerable success of titanium as an implant material on a commercial scale is due to its remarkable biocompatibility as a result of the formation of a stable oxide layer on its surface. As per ASTM Standard F1295 there are four grades of commercially pure titanium (cpTi) differing in their oxygen content. A maximum of 0.4% oxygen is present in Grade 4 while the least 0.18% is found in Grade 1 (Jorge et al., 2013).

Different grades of cpTi are based on the presence of small quantities of contaminants and this also leads to some mechanical differences. Iron and aluminum are added for resistance against corrosion, which increases strength and decreases the density respectively. Vanadium is also added to prevent corrosion and it acts by scavenging aluminum (ASTM Standard F, 2005).

At a temperature below 882.5°C Ti is found in α-hexagonal phase and above this temperature, it exists in β-cubic phase making it a dimorphic metal. A film of dense oxide at the surface is one of the characteristics of Ti along with its reactivity (Wang and Fenton, 1996).

Ti is the first material of choice for intraosseous applications for a variety of reasons such as inactivity caused by an unreactive thin inert surface layer of oxide, regulation on thickness, ability to self-repair, resistance to chemical attack, and similar modulus of elasticity as a bone. Due to its gray color, it is not very appealing as it shines through the thin mucosa at places where soft tissue is not thick (Branemark et al., 1969).

10.12.2 Aluminum Base Alloys

Endosteal plate and pin-type dental implants are some of the root forms made from aluminum, titanium, and zirconium oxides ceramics. Up to 3–5 times increase in tensile character, compressive nature, and bending strengths are observed in such material when compared with bones. Other properties such as a high modulus of elasticity along with fatigue and fracture strength result in special requirements in terms of design when this type of material is used (Saini et al., 2015).

10.12.3 Zirconia

Zirconia was commonly was used in the early 1990s for dental prosthetic surgery with endosseous implants as osseointegration ceramic implants were introduced at the same time. It offered less plaque accumulation, improved soft tissue management, and aesthetic appeal, so was considered a better option than titanium implants (Ozkurt and Kazazoglu, 2011).

Zirconia structure is present as three polymorphic crystals, that is, monoclinic (M), cubic (C), and tetragonal (T). Zirconia acquires a monoclinic structure at room temperature, at 1170°C changes into tetragonal, and then finally to a cubic structure at a temperature of 2370°C. The phases of zirconia are unstable at room temperature and when cooled it breaks into pieces (Manicone et al., 2007).

CaO, MgO, and Y_2O_3 (yttrium) stabilize the C-phase of pure zirconia, which leads to the formation of partially stabilized zirconia, which is a multiphase material consisting of the three phases as per the order of importance. Addition of yttrium at room temperature yields tetragonal zirconia polycrystal shaving properties like lower porosity, higher density, bending and compressive strength, which makes it apt for the biomedical application (Kelly and Denry, 2008; Pezzotti and Yamamoto, 2014).

Alloys containing titanium and zirconium with 13%–17% zirconium (TiZr1317) have acceptable mechanical qualities like high fatigue strength when compared with its pure form. Zirconium and titanium do not arrest the growth of osteoblasts, which is necessary for osseointegration (Chen et al., 2016).

10.12.4 Cross-Linked Polyethylene

Polyethylene such as cross-linked polyethylene (PEX/XLPE), consists of cross-linking in the structure. During the 1990s wear of polyethylene material was a cause of clinical

concern and hampered the life of hip replacements. Cross-linked polyethylene was introduced and due to its special features, it was instantly accepted by surgeons as an alternative for improving the wear resistance of hip arthroplasty, which makes it one of the most important progresses in articular technology characterized by the bonding together of polyethylene molecules, which leads to the formation of a stronger material. As a result, it significantly improves the wear resistance of the metals. Cross-linking occurs by the formation of covalent bonds, which inhibits the wear by restricting chain mobility and orientation (Chakravarty et al., 2015).

In general, cross-linking of polyethylene is achieved by (1) treatment with peroxide, (2) cross-linking by moisture, and (3) irradiation process.

10.12.4.1 Peroxide

The technique of cross-linking was used by the wire and cable industry for many years. In this method, the organic peroxide is required as an initiator along with cross-linking equipment. Low temperatures are requisite for the preparation of the compound and then considerably higher temperatures and pressures are needed in the equipment to complete the process of cross-linking. The peroxide is decomposed at high temperatures to liberate free radicals. The polymer chain gives away a hydrogen atom when subjected to these free radicals making the site a radical, which can cross-link with another radical of polyethylene. The reaction is repeated several times until all the peroxide is consumed or the decomposition point is reached by the falling temperatures. The use of antioxidants is restricted due to its main disadvantage of interfering with the reaction and hence, stabilization of the polymer is more difficult (Gul et al., 2017).

10.12.4.2 Moisture Cross-Linking

Cross-linking of polyethylene by moisture can be carried out by two basic methods using ethylene-vinyl-silane copolymers. There are two methods to produce these copolymers. The first method involves polymerizing ethylene with vinyl-silane, and the second method makes use of extruder grafting of polyethylene with vinyl-silane. The products are alike by both the methods with a few important differences (Atkinson and Cicek, 1983).

Silane copolymers are provided to the processor (polyethylene reactor) as the base component, which also consists of various other constituents. Catalysts and additives such as antioxidants and flame retardants are also added according to the requirement. Limited potential of the reactor to produce a variety of products is a major disadvantage of this process. The use of high pressure on the reactor also limits the production of high-density polymers (Yagi and Mantoku, 1985).

10.12.4.3 Irradiation

This method exploits the high energy electrons and its bombardment on polyethylene thereby liberating free radicals, which cause reactions leading to cross-linking. Chemicals are not required when this method is used; for example, polyethylene is cross-linked utilizing irradiation. Promoters are added to increase the speed of the reaction and efficiency of cross-linking. Its utility with respect to its cost and irregular cross-linking are some of the disadvantages of this method (Oral and Muratoglu, 2007).

During storage, mechanical properties and molecular weight are reduced owing to oxidative degradation. This occurs when oxygen present in the polyethylene and environmental oxygen that diffuses in the polyethylene react with the free radicals. For preventing degradation, the cross-linking of the material is done as blocks or prepregs and subsequently fabricated into cups. At the time of fabrication, the top layer, which is oxidized, is removed, leaving behind the cross-linked material. Cross-linking reportedly improves the wear characteristics in comparison to polyethylene, which is not cross-linked (Gomez-Barrena et al., 2009).

10.13 REGULATORY APPROVALS AND REQUIREMENTS

A medical device as defined by Council Directive 93/42/EEC on 14 June 1993 as "Any instrument, apparatus, appliance, material or another article, whether it is to be used alone or in combination, with the software, necessary for its proper application intended by the manufacturer to be used for human beings for the purpose of Diagnosis, prevention, monitoring, treatment or alleviation of disease:

- Diagnosis, monitoring, treatment, alleviation or compensation for any injury or handicap.
- The investigation, replacement or modification of the anatomy or of a physiological process.
- Control of conception, and which does not achieve its principal intended action by pharmacological, immunological or metabolic means, but which may be assisted in its function by such means" (Medical, Devices and Directive, 1993).

As per the US Food and Drug Administration (FDA), "A medical device is an instrument, apparatus, device, machine, appliance, implant, in vitro agent or other similar or related article, including a component part, or accessory which is

- Recognized in the official "National Formulary" or the "United States Pharmacopoeia," or any supplement to them.
- Intended for use in the diagnosis of disease or other conditions, or in the cure, mitigation, treatment or prevention of disease, in man or other animals.
- Intended to affect the structure or any function of the body of man or other animals and which does not achieve any of its primary purposes through chemical action within or on the body of man or other animals and which is not dependent upon being metabolized for the achievement of any of its primary intended purposes" (Van Norman, 2016).

Any strategy adopted during the product design will be deemed successful only if the issues relating to quality, safety, along with productivity are addressed. To ensure an answer to these issues, a set of basic safety and quality requirements have been assigned by different types of products manufacturers that must be met before they are approved (before duly recognized bodies) for receiving the "CE mark" and going to market in the European Union. An understanding of directive and standard is absolutely necessary for marketing the product in the European Union (obtaining the CE mark), while the others

(e.g., ISO standards) are needed for working in an organized manner. For safeguarding the interest of patients the design procedure for any medical devices is highly regulated (Labek et al., 2015).

In Europe, the Medical Device Directive is in place to control the process of development of such devices. This is a legal document containing law procedures and punishments in the event of noncompliance. Responsibility for the safety of medical devices in the United States lies with the FDA. In Japan, the Japanese Federation of Medical Device Associations in combination with the Ministry of Health, Welfare, and Labor is responsible for regulating the standards of medical devices. A quality management system is kept in order by the companies for strict adherence to these regulations during the whole process of designing (Altenstetter, 2012).

10.13.1 Directives

Three directives (with their associated amendments) are taken into consideration for any medical device to be considered to be marketed in the European Union (Medical, Devices and Directive, 1993):

10.13.1.1 Directive 93/42/EEC Regarding Medical Devices

Medical devices are classified in line with the classification standards laid down in Annex IX of the directive. The application of this type of classification standards is ruled by the device's intended use, the risks associated, the time and extent of contact with body tissue. Medical devices according to their increasing order of danger and responsibility and classified as "Class I," "Class II a," "Class II b," or "Class III."

10.13.1.2 Directive 90/385/EEC Regarding Active Implantable Medical Devices

This directive is for active implantable medical devices, which includes "any medical device that works on an electrical power supply (or any energy source not directly generated by the human body or by the force of gravity) and which is to be totally or partially inserted into the human body by surgical or medical means, or into a natural orifice by medical intervention and remain permanently installed after the procedure."

10.13.1.3 Directive 98/79/EC Regarding Medical Devices for In Vitro Diagnosis

This directive applies to in vitro devices used to examine the specimens and samples derived from the human body, reagents, instruments, and specimen receptacles linked to these tests. These devices are placed in the market after confirmation from the directive. The in vitro diagnostic medical device is "any medical device that includes reagents, calibres, control material, instruments, apparatus, equipment or systems which is used on its own or in combination are intended for in vitro use to examine specimens, including blood and tissue, obtained from the human body in order to gain information on: pathologies, congenital defects, safety and compatibility with potential receivers or therapeutic measurement monitoring."

10.13.1.4 Specific Regulations

- ISO Standard 10993 on the "biological evaluation of medical devices."
- ISO Standard 13485 on "sanitary products, quality management systems, and regulatory requirements."
- ISO Standard 13488 on "sanitary products, quality management systems and specific requirements for the implementation of ISO Standard 9002."
- ISO Standard 14971 on the "application of risk management to sanitary products."
- ISO Standard 15223 on the "symbols to be used with labels, labeling, and information to be supplied with medical devices."

The test procedures of the US Pharmacopeia, used for requesting product certification from the FDA, have various differences compared with ISO standards. By and large, ISO procedures are stricter, and the companies intending to market their products both in Europe and the United States must follow ISO requirements. Nevertheless, in both cases, after applying ISO methods and before placing products on the US market, the requirements of the FDA must be fulfilled and checked properly and additional testing may also be done. FDA reviewers may also be enlisted to clarify the matters (Aitchison et al., 2009).

10.14 CLINICAL APPLICATIONS OF ORTHOPEDIC IMPLANTS

With the advent of a newer generation of medical metallic materials and cross-linked polymers, an intense focus has been projected on biodegradability. Besides, circumventing the removal of implants postoperation has additionally increased the potential of these materials for surgical fixation of injured musculoskeletal tissues (Zhao et al., 2017).

10.14.1 Osteosynthesis

Implantable devices are mostly made up of metal, which causes the reduction and internal fixation of a bone fracture, that is, osteosynthesis. It is achieved by surgery through an open or percutaneous approach for the fractured bone. It aims to bring the ends of the fractured bone together and immobilize the site while healing takes place. A fracture that is rigidly immobilized heals by the process of intramembranous ossification (Xue et al., 2016).

10.14.2 Joint Replacement

Knee and hip replacement are the most important categories of joint replacement. The knee joint is made up of three bones, namely femur, tibia, and a patellar component, gliding over the femur. The prosthesis is placed over the junction of these three bones. While using fixed-bearing implants the metal part is inserted into the tibia, which is locked by a polyethylene tray. When using rotating platform implants the only difference is that the tray is placed on a circular stem which eases rotation during the knee movement (Banerjee et al., 2014).

Total hip replacement surgery has higher success rates and involves the replacement of the damaged joint by an implant. There are three approaches for the surgery (Knight et al., 2011):

- *Direct anterior approach*: It is a less disturbing approach and causes less harm to the musculature in the area adjacent to the hip joint and involves an incision made on the front of the hip. Fluoroscopy which is a type of X-ray along with customary operating table are the major requirements during this procedure.
- *Anterolateral approach*: This involves a side incision of the hip at the front.
- *Posterolateral approach*: This involves a side incision of the hip at the back.

10.14.3 Nonconventional Modular Tumor Implants

For longer life expectancy of patients suffering from metastatic cancer, treatment of bone metastases is crucial. A pathological fracture is a very common complication for long bone skeletal metastases, although long bones of the extremities are not the most common site of metastases. It leads to loss of function, pain, and loss of ambulation for the patient. Osteosynthesis, endoprostheses (joint replacement prostheses), or tumor endoprostheses (modular or conventional nonmodular components) are some of the options for surgical management (Henrichs et al., 2014).

10.14.4 Spine Implants

Almost 80 percent of adults in the world are affected by chronic lower back pain. The treatment usually involves physical therapy, medications, and exercise, but in severe cases, surgery and the placement of spinal implants become necessary. Implants for the spine have several roles to play and largely help to (Vaccaro and Madigan, 2002):

- Facilitate the fusion of two vertebrae
- Improve stability of the spine
- Provide strength to the spine
- Deformities correction

Spine implants may be used in complications such as arthritis of the spine, scoliosis and other deformities of the spine, broken vertebrae, spondylolisthesis, and herniated disks. In addition to many advantages, the spine implants come with the usual disadvantages including the risk of infection and other risk factors postsurgery (Wang et al., 2002; Hao et al., 2017; Cho et al., 2018).

10.15 MARKETED PRODUCTS: AN UPDATE

The market for orthopedic implants is anticipated to reach $116 billion by 2022. The orthopedic devices and implants had the biggest share in the world implants market in 2015, which can be credited to increase in the number of overweight people and an increase in fractures due to osteoporosis in all the age groups. There has been a

tremendous increase in patients belonging to the age group of 55 to over 80 who have started to opt for orthopedic implant surgeries. This has happened due to increased consciousness regarding the usefulness of such procedures and improvement in the quality of life. India and China now with their advancing healthcare system have now begun opting for surgical procedures involving orthopedic implants and devices. Advances in visualizing technology such as 3D and CAD have given a tremendous advantage over regular and ordinary implants especially in case of implants based on the specific needs of the patient, for example, knee arthroplasty. A rise in chronic diseases along with increased life expectancy would certainly require implants in the market in a higher number. According to a report by the National Institutes of Health, the number of people above 65 years of age will rise to 1.5 billion by 2050, which would be close to 16% of the world population. Breaking down the above data Japan, the United States, United Kingdom, Russia, and China will have around 27%, 16%, 24%, 17%, and 14% of the population above 65 years of age having chronic diseases such trauma related to old age and osteoarthritis (Wood, 2015).

10.15.1 Medical Orthopedic Implants Market Segmentation

- Orthopedic Implants
  - Reconstructive Joint Replacements
    - Knee Replacement Implants
    - Hip Replacement Implants
    - Extremities
  - Orthobiologics
  - Trauma & Craniomaxillofacial
- Spinal Implants
  - Interbody Fusion Devices
  - Thoracolumbar Devices
  - Cervical Fixation Devices
  - Spinal Electrical Stimulation
  - Vertebral Compression Fracture Devices
  - Motion Preservation Devices
- Dental Implants
  - Plate Form Dental Implants
  - Root Form Dental Implants
- Breast Implants
- Facial Implants

10.16 CONCLUSIONS

Implants have evolved dramatically in the past few decades with the focus now shifting to bioactive materials and targeting osteogenesis. The new technologies have opened up the possibility for controlling as well as modifying the microlevel surface properties,

accompanying the latest techniques and strategies to improve and stabilize the bone and implant attachment along with its interaction with the living system. Owing to various factors, patients of various ages are now opting for implants and they have been gaining popularity. The most important factors being an increase in life expectancy, increase in the number of old people, and the changed lifestyle. In the past decade, implants have overshadowed the other treatments available for the same ailment. With improvements in technology, new materials are also coming into light that may take the baton from the currently used implant materials and lead to the future generation of implants with same properties, characteristics, and function of a real bone.

ABBREVIATIONS

Ca	calcium
CaO	calcium oxide
CaP	calcium phosphate
Cr	chromium
Co	cobalt
PEX/XLPE	cross-linked polyethylene
ECM	extracellular matrix
FDA	Food and Drug Administration
HA	hydroxyapatite
Mn	manganese
Mo	molybdenum
Ni	nickel
P_2O_5	phosphorous oxide
PHEMA	poly(2-hydroxyethyl-methacrylate)
PLA	polylactide
PDS	polydioxanone
PCL	poly(ϵ-caprolactone)
PHB	polyhydroxybutyrate
PP	polypropylene
PVC	polyvinyl chloride
PEEK	polyetheretherketone
SiO_2	silicon dioxide
Na_2O	sodium oxide
Ti	titanium
Zr	zirconium

References

ASTM Standard F, 2005. Standard Specification for Wrought Titanium-6 Aluminum-7 Niobium Alloy for Surgical Implant Applications. ASTM International, West Conshohocken [ASTM International website]: (accessed 20.07.18).

Abd El-Ghany, O.S., Sherief, A.H., 2016. Zirconia based ceramics, some clinical and biological aspects: review. Future Dent. J. 2 (2), 55–64.

Abdullah, M.R., Goharian, A., Abdul Kadir, M.R., Wahit, M.U., 2015. Biomechanical and bioactivity concepts of polyetheretherketone composites for use in orthopedic implants-a review. J. Biomed. Mater. Res. A 103 (11), 3689–3702.

Ahn, H., Patel, R.R., Hoyt, A.J., Lin, A.S.P., Torstrick, F.B., Guldberg, R.E., et al., 2018. Biological evaluation and finite-element modeling of porous poly(para-phenylene) for orthopaedic implants. Acta Biomater. 72, 352–361.

Aitchison, G.A., Hukins, D.W., Parry, J.J., Shepherd, D.E., Trotman, S.G., 2009. A review of the design process for implantable orthopedic medical devices. Open Biomed. Eng. J. 3, 21–27.

Alothman, O.Y., Fouad, H., Al-Zahrani, S.M., Eshra, A., Al Rez, M.F., Ansari, S.G., 2014. Thermal, creep-recovery and viscoelastic behavior of high density polyethylene/hydroxyapatite nano particles for bone substitutes: effects of gamma radiation. Biomed. Eng. Online 13. Available from: https://doi.org/10.1186/1475-925X-13-125.

Altenstetter, C., 2012. Medical device regulation in the European Union, Japan and the United States. Commonalities, differences and challenges. Innov. Euro J. Soc. Sci. Res. 25 (4), 362–388.

Amini, A.R., Wallace, J.S., Nukavarapu, S.P., 2011. Short-term and long-term effects of orthopedic biodegradable implants. J. Long Term Eff. Med. Implants 21 (2), 93–122.

Angadi, D.S., Shepherd, D.E., Vadivelu, R., Barrett, T., 2014. Rigid intramedullary nail fixation of femoral fractures in adolescents: what evidence is available? J. Orthop. Traumatol. 15 (3), 147–153.

Atkinson, J.R., Cicek, R.Z., 1983. Silane cross-linked polyethylene for prosthetic applications Part I. Certain physical and mechanical properties related to the nature of the material. Biomaterials 4 (4), 267–275.

Baino, F., Novajra, G., Vitale-Brovarone, C., 2015. Bioceramics and scaffolds: a winning combination for tissue engineering. Front. Bioeng. Biotechnol. 3 (202). Available from: https://doi.org/10.3389/fbioe.2015.00202. eCollection 2015.

Banerjee, S., Kulesha, G., Kester, M., Mont, M.A., 2014. Emerging technologies in arthroplasty: additive manufacturing. J. Knee Surg. 27 (3), 185–191.

Bertoluzza, A., Simoni, R., Tinti, A., Morocutti, M., Ottani, V., Ruggeri, A., 1991. Calcium phosphate materials containing alumina: Raman spectroscopical, histological, and ultrastructural study. J. Biomed. Mater. Res. 25 (1), 23–38.

Bhoyar, P.K., Borade, A.B., 2015. The use of single point incremental forming for customized implants of unicondylar knee arthroplasty: a review. Res. Biomed. Eng. Available from: https://doi.org/10.1590/2446-4740.0705.

Bonilla, C.E.P., Perilla, J.E., 2011. The past, present and near future of materials for use in biodegradable orthopaedic implants. Ing. Inv 31 (2), 124–133.

Boskey, A.L., Imbert, L., 2017. Bone quality changes associated with aging and disease: a review. Ann. N. Y. Acad. Sci. 1410 (1), 93–106.

Brand, R.A., 2009. Sir William Arbuthnot Lane, 1856-1943. Clin. Orthop. Relat. Res. 467 (8), 1939–1943.

Branemark, P.I., Adell, R., Breine, U., Hansson, B.O., Lindstrom, J., Ohlsson, A., 1969. Intra-osseous anchorage of dental prostheses. I. Experimental studies. Scand. J. Plast. Reconstr. Surg. 3 (2), 81–100.

Bridges, A.W., Garcia, A.J., 2008. Anti-inflammatory polymeric coatings for implantable biomaterials and devices. J. Diabetes Sci. Technol. 2 (6), 984–994.

Campbell, A.A., 2003. Bioceramics for implant coatings. Mater. Today 6 (11), 26–30.

Chakravarty, R., Elmallah, R.D., Cherian, J.J., Kurtz, S.M., Mont, M.A., 2015. Polyethylene wear in knee arthroplasty. J. Knee Surg. 28 (5), 370–375.

Chan, C.-W., Carson, L., Smith, G.C., Morelli, A., Lee, S., 2017. Enhancing the antibacterial performance of orthopaedic implant materials by fibre laser surface engineering. Appl. Surf. Sci. 404, 67–81.

Chen, J., Browne, M., Taylor, M., Gregson, P.J., 2004. Application of an interface failure model to predict fatigue crack growth in an implanted metallic femoral stem. Comput. Methods Programs Biomed. 73 (3), 249–256.

Chen, Y.W., Moussi, J., Drury, J.L., Wataha, J.C., 2016. Zirconia in biomedical applications. Expert Rev. Med. Devices 13 (10), 945–963.

Cho, W., Job, A.V., Chen, J., Baek, J.H., 2018. A review of current clinical applications of three-dimensional printing in spine surgery. Asian Spine J. 12 (1), 171–177.

Cross, N., 2008. Engineering Design Methods: strategies for Product Design. J Wiley, Chichester.

Cutler, I.B., Bradshaw, C., Christensen, C.J., Hyatt, E.P., 1957. Sintering of alumina at emperatures of 1400°C and below. J. Am. Ceram. Soc. 40 (4), 134–139.

Denkena, B., Busemann, S., Gottwik, L., Grove, T., Wippermann, A., 2017. Material removal mechanisms in grinding of mixed oxide ceramics. Procedia CIRP 65, 70–77.

Ducheyne, P., Wevers, M., Meester, P.D., 1983. Fatigue properties of implant materials in hip prosthesis form: a standardized test. J. Biomed. Mater. Res. B: Appl. Biomater. 17, 45–57.

Fernandez, A.C., Mohanty, M., Varma, H.K., Komath, M., 2006. Safety and efficacy of Chitra-CPC calcium phosphate cement as bone substitute. Curr. Sci. 91 (12), 1678–1686.
Florencio-Silva, R., Sasso, G.R., Sasso-Cerri, E., Simoes, M.J., Cerri, P.S., 2015. Biology of bone tissue: structure, function, and factors that influence bone cells. Biomed. Res. Int. 2015, 421746. Available from: https://doi.org/10.1155/2015/421746.
Franssen, B.B., Schuurman, A.H., Van der Molen, A.M., Kon, M., 2010. One century of Kirschner wires and Kirschner wire insertion techniques: a historical review. Acta Orthop. Belg. 76 (1), 1–6.
Gamble, D., Jaiswal, P.K., Lutz, I., Johnston, K.D., 2017. The use of ceramics in total hip arthroplasty. Ortho. Rheum. Open Access. J. 4 (3). Available from: https://doi.org/10.19080/OROAJ.2017.04.555636.
Gaviria, L., Salcido, J.P., Guda, T., Ong, J.L., 2014. Current trends in dental implants. J. Korean Assoc. Oral Maxillofac. Surg. 40 (2), 50–60.
Geetha, M., Singh, A.K., Asokamani, R., Gogia, A.K., 2009. Ti based biomaterials, the ultimate choice for orthopaedic implants – a review. Prog. Mater. Sci. 54, 397–425.
Geringer, J., Forest, B., Combrade, P., 2005. Fretting-corrosion of materials used as orthopaedic implants. Wear 259, 943–951.
Ghassemi, T., Shahroodi, A., Ebrahimzadeh, M.H., Mousavian, A., Movaffagh, J., Moradi, A., 2018. Current concepts in scaffolding for bone tissue engineering. Arch. Bone Jt. Surg. 6 (2), 90–99.
Gibon, E., Amanatullah, D.F., Loi, F., Pajarinen, J., Nabeshima, A., Yao, Z., et al., 2017a. The biological response to orthopaedic implants for joint replacement: Part I: Metals. J. Biomed. Mater. Res. B: Appl. Biomater. 105 (7), 2162–2173.
Gibon, E., Cordova, L.A., Lu, L., Lin, T.H., Yao, Z., Hamadouche, M., et al., 2017b. The biological response to orthopedic implants for joint replacement. II: polyethylene, ceramics, PMMA, and the foreign body reaction. J. Biomed. Mater. Res. B: Appl. Biomater. 105 (6), 1685–1691.
Gil, D., Shuvaev, S., Frank-Kamenetskii, A., Reukov, V., Gross, C., Vertegel, A., 2017. Novel antibacterial coating on orthopedic wires to eliminate pin tract infections. Antimicrob. Agents Chemother. 61. Available from: https://doi.org/10.1128/AAC.00442-17.
Godbol, N., Yadav, S., Ramachandran, M., Belemkar, S., 2016. A review on surface treatment of stainless steel orthopedic implants. Int. J. Pharm. Sci. Rev. Res. 36 (1), 190–194.
Gomes, C.C., Moreira, L.M., Santos, V.J., Ramos, A.S., Lyon, J.P., Soares, C.P., et al., 2011. Assessment of the genetic risks of a metallic alloy used in medical implants. Genet. Mol. Biol. 34 (1), 116–121.
Gomez-Barrena, E., Medel, F., Puertolas, J.A., 2009. Polyethylene oxidation in total hip arthroplasty: evolution and new advances. Open Orthop. J. 3, 115–120.
Goodman, S.B., Yao, Z., Keeney, M., Yang, F., 2013. The future of biologic coatings for orthopaedic implants. Biomaterials 34 (13), 3174–3183.
Gotman, I., 1997. Characteristics of metals used in implants. J. Endourol. 11 (6), 383–389.
Gul, R.M., Fung, K., Doshi, B.N., Oral, E., Muratoglu, O.K., 2017. Surface cross-linked UHMWPE using peroxides. J. Orthop. Res. 35 (11), 2551–2556.
Hak, D.J., Mauffrey, C., Seligson, D., Lindeque, B., 2014. Use of carbon-fiber-reinforced composite implants in orthopedic surgery. Orthopedics 37 (12), 825–830.
Hamadouche, M., Sedel, L., 2000. Ceramics in orthopaedics. J. Bone Joint Surg. Br. 82 (8), 1095–1099.
Hamidi, M., Harun, W.S.W., Samykano, M., Ghani, S.A.C., Ghazalli, Z., Ahmad, F., et al., 2017. A review of biocompatible metal injection moulding process parameters for biomedical applications. Mater. Sci. Eng. C Mater. Biol. Appl. 78, 1263–1276.
Hankenson, K.D., Gagne, K., Shaughnessy, M., 2015. Extracellular signaling molecules to promote fracture healing and bone regeneration. Adv. Drug Deliv. Rev. 94, 3–12.
Hao, D.J., Duan, K., Liu, T.J., Liu, J.J., Wang, W.T., 2017. Development and clinical application of grading and classification criteria of lumbar disc herniation. Med. (Baltimore) 96 (47). Available from: https://doi.org/10.1097/MD.0000000000008676.
Hasan, A., Byambaa, B., Morshed, M., Cheikh, M.I., Shakoor, R.A., Mustafy, T., et al., 2018. Advances in osteobiologic materials for bone substitutes. J. Tissue Eng. Regen. Med. 12 (6), 1448–1468.
Hench, L.L., 1980. Biomaterials. Science 208 (4446), 826–831.
Henkel, J., Woodruff, M.A., Epari, D.R., Steck, R., Glatt, V., Dickinson, I.C., et al., 2013. Bone regeneration based on tissue engineering conceptions – a 21st century perspective. Bone Res. 1 (3), 216–248.

Henrichs, M.P., Krebs, J., Gosheger, G., Streitbuerger, A., Nottrott, M., Sauer, T., et al., 2014. Modular tumor endoprostheses in surgical palliation of long-bone metastases: a reduction in tumor burden and a durable reconstruction. World J. Surg. Oncol. 12. Available from: https://doi.org/10.1186/1477-7819-12-330.

Hernigou, P., 2017. History of external fixation for treatment of fractures. Int. Orthop. 41 (4), 845–853.

Holloway, I., Walter, W.L., Zicat, B., Walter, W.K., 2009. Osteolysis with a cementless second generation metal-on-metal cup in total hip replacement. Int. Orthop. 33 (6), 1537–1542.

Hui, J.H., Buhary, K.S., Chowdhary, A., 2012. Implantation of orthobiologic, biodegradable scaffolds in osteochondral repair. Orthop. Clin. North Am. 43 (2), 255–261.

Iafisco, M., Bosco, R., Leeuwenburgh, S.C.G., van den Beucken, J.J.J.P., Jansen, J.A., Prat, M., et al., 2011. Electrostatic spray deposition of biomimetic nanocrystalline apatite coatings onto titanium. Adv. Eng. Mater. 14 (3), B13–B20.

Islam, M.T., Felfel, R.M., Abou Neel, E.A., Grant, D.M., Ahmed, I., Hossain, K.M.Z., 2017. Bioactive calcium phosphate-based glasses and ceramics and their biomedical applications: a review. J. Tissue Eng. 8. Available from: https://doi.org/10.1177/2041731417719170.

Jager, M., Jennissen, H.P., Dittrich, F., Fischer, A., Kohling, H.L., 2017. Antimicrobial and osseointegration properties of nanostructured titanium orthopaedic implants. Materials (Basel) 10 (11). Available from: https://doi.org/10.3390/ma10111302.

Jorge, J.R., Barao, V.A., Delben, J.A., Faverani, L.P., Queiroz, T.P., Assuncao, W.G., 2013. Titanium in dentistry: historical development, state of the art and future perspectives. J. Indian Prosthodont. Soc. 13 (2), 71–77.

Kawanabe, K., 1996. Clinical application of A-W glass ceramic (dence and porous A-W glass ceramic). Nihon Geka Hokan. 65 (3), 97–98.

Keegan, G.M., Learmonth, I.D., Case, C.P., 2007. Orthopaedic metals and their potential toxicity in the arthroplasty patient: a review of current knowledge and future strategies. J. Bone Joint Surg. Br. 89 (5), 567–573.

Keegan, G.M., Learmonth, I.D., Case, C.P., 2008. A systematic comparison of the actual, potential, and theoretical health effects of cobalt and chromium exposures from industry and surgical implants. Crit. Rev. Toxicol. 38 (8), 645–674.

Kelly, J.R., Denry, I., 2008. Stabilized zirconia as a structural ceramic: an overview. Dent. Mater. 24 (3), 289–298.

Knight, S.R., Aujla, R., Biswas, S.P., 2011. Total hip arthroplasty – over 100 years of operative history. Orthop. Rev. (Pavia). 3 (2). Available from: https://doi.org/10.4081/or.2011.e16.

Koju, N., Sikder, P., Ren, Y., Zhou, H., Bhaduri, S.B., 2017. Biomimetic coating technology for orthopedic implants. Curr. Opin. Chem. Eng. 15, 49–55.

Kontonasaki, E., Zorba, T., Papadopoulou, L., Pavlidou, E., Chatzistavrou, X., Paraskevopoulos, K., et al., 2002. Hydroxy carbonate apatite formation on particulate bioglass in vitro as a function of time. Cryst. Res. Technol. 37 (11), 1165–1171.

Kuboki, Y., Jin, Q., Takita, H., 2001. Geometry of carriers controlling phenotypic expression in BMP-induced osteogenesis and chondrogenesis. J. Bone Joint Surg. Am. 83-A (Suppl 1(Pt 2)), S105–S115.

Kulkarni, M., Mazare, A., Gongadze, E., Perutkova, S., Kralj-Iglic, V., Milosev, I., et al., 2015. Titanium nanostructures for biomedical applications. Nanotechnology 26 (6), 062002. Available from: https://doi.org/10.1088/0957-4484/26/6/062002.

Kulkarni, R.K., Moore, E.G., Hegyeli, A.F., Leonard, F., 1971. Biodegradable poly(lactic acid) polymers. J. Biomed. Mater. Res. 5 (3), 169–181.

Labek, G., Schoffl, H., Meglic, M., 2015. New medical device regulations ahead - What does that mean for arthroplasty registers? Acta Orthop. 86 (1), 5–6.

Luttikhuizen, D.T., Harmsen, M.C., Van Luyn, M.J., 2006. Cellular and molecular dynamics in the foreign body reaction. Tissue Eng. 12 (7), 1955–1970.

Maccauro, G., Bianchino, G., Sangiorgi, S., Magnani, G., Marotta, D., Manicone, P.F., et al., 2009. Development of a new zirconia-toughened alumina: promising mechanical properties and absence of in vitro carcinogenicity. Int. J. Immunopathol. Pharmacol. 22 (3), 773–779.

Madl, A.K., Liong, M., Kovochich, M., Finley, B.L., Paustenbach, D.J., Oberdorster, G., 2015. Toxicology of wear particles of cobalt-chromium alloy metal-on-metal hip implants Part I: physicochemical properties in patient and simulator studies. Nanomedicine 11 (5), 1201–1215.

Manam, N.S., Harun, W.S.W., Shri, D.N.A., Ghani, S.A.C., Kurniawan, T., Ismail, M.H., et al., 2017. Study of corrosion in biocompatible metals for implants: a review. J. Alloys Compd. 701, 698–715.

Manicone, P.F., Rossi Iommetti, P., Raffaelli, L., 2007. An overview of zirconia ceramics: basic properties and clinical applications. J. Dent. 35 (11), 819–826.
Mantripragada, V.P., Lecka-Czernik, B., Ebraheim, N.A., Jayasuriya, A.C., 2013. An overview of recent advances in designing orthopedic and craniofacial implants. J. Biomed. Mater. Res. A 101 (11), 3349–3364.
Markatos, K., Tsoucalas, G., Sgantzos, M., 2016. Hallmarks in the history of orthopaedic implants for trauma and joint replacement. Acta Med. Hist. Adriat. 14 (1), 161–176.
Marsell, R., Einhorn, T.A., 2011. The biology of fracture healing. Injury 42 (6), 551–555.
Mathieu, V., Vayron, R., Barthel, E., Dalmas, D., Soffer, E., Anagnostou, F., et al., 2012. Mode III cleavage of a coin-shaped titanium implant in bone: effect of friction and crack propagation. J. Mech. Behav. Biomed. Mater. 8, 194–203.
Medical, Devices and Directive, 1993. Council Directive 93/42/EEC. European Union directive. <https://ec.europa.eu/growth/single-market/european-standards/harmonised-standards/medical-devices_en> (accessed 20.07.18.).
Moiduddin, K., Darwish, S., Al-Ahmari, A., ElWatidy, S., Mohammad, A., Ameen, W., 2017. Structural and mechanical characterization of custom design cranial implant created using additive manufacturing. Electron. J. Biotechnol. 29, 22–31.
Mower, T.M., Long, M.J., 2016. Mechanical behavior of additive manufactured, powder-bed laser-fused materials. Mater. Sci. Eng. A 651, 198–213.
Muldashev, E.R., Muslimov, S.A., Musina, L.A., Nigmatullin, R.T., Lebedeva, A.I., Shangina, O.R., et al., 2005. The role of macrophages in the tissues regeneration stimulated by the biomaterials. Cell Tissue Bank 6 (2), 99–107.
Nagaraja, S., Di Prima, M., Saylor, D., Takai, E., 2017. Current practices in corrosion, surface characterization, and nickel leach testing of cardiovascular metallic implants. J. Biomed. Mater. Res. B: Appl. Biomater. 105 (6), 1330–1341.
Narayan, R.J., 2010. The next generation of biomaterial development. Philos. Trans. R Soc. A 368, 1831–1837.
Narsaria, N., Singh, A.K., 2017. Role of prophylactic antibiotics in orthopaedics: current concepts. EC Orthopaediccs 7 (1), 1–2.
Navarro, M., Michiardi, A., Castano, O., Planell, J.A., 2008. Biomaterials in orthopaedics. J. R. Soc. Interface 5 (27), 1137–1158.
Novaes Jr., A.B., de Souza, S.L.S., de Barros, R.R.M., Pereira, K.K.Y., Iezzi, G., Piattelli, A., 2016. Influence of implant surfaces on osseointegration. Braz. Dent. J. 21 (6), 471–481.
Ohman, C., Zwierzak, I., Baleani, M., Viceconti, M., 2013. Human bone hardness seems to depend on tissue type but not on anatomical site in the long bones of an old subject. Proc. Inst. Mech. Eng. H 227 (2), 200–206.
Oldani, C., Dominguez, A., 2012. Titanium as a biomaterial for implants. Recent Advances in Arthroplasty S. Fokter. InTech Europe, Rijeka, Croatia.
Oral, E., Muratoglu, O.K., 2007. Radiation cross-linking in ultra-high molecular weight polyethylene for orthopaedic applications. Nucl. Instrum. Methods Phys. Res. B 265 (1), 18–22.
Ozkurt, Z., Kazazoglu, E., 2011. Zirconia dental implants: a literature review. J. Oral. Implantol. 37 (3), 367–376.
Pezzotti, G., Yamamoto, K., 2014. Artificial hip joints: the biomaterials challenge. J. Mech. Behav. Biomed. Mater. 31, 3–20.
Piconi, C., Maccauro, G., Muratori, F., Brach Del Prever, E., 2003. Alumina and zirconia ceramics in joint replacements. J. Appl. Biomater. Biomech. 1 (1), 19–32.
Pokorny, D., Sosna, A., Slouf, M., Fulin, P., Stefan, J., Landor, I., 2016. UHMWPE – polyethylene for articulating surfaces of joint replacements. Cas Lek Cesk 155 (8), 433–437.
Ribeiro, M., Monteiro, F.J., Ferraz, M.P., 2012. Infection of orthopedic implants with emphasis on bacterial adhesion process and techniques used in studying bacterial-material interactions. Biomatter 2 (4), 176–194.
Romano, C.L., Scarponi, S., Gallazzi, E., Romano, D., Drago, L., 2015. Antibacterial coating of implants in orthopaedics and trauma: a classification proposal in an evolving panorama. J. Orthop. Surg. Res. 10. Available from: https://doi.org/10.1186/s13018-015-0294-5.
Rupp, F., Gittens, R.A., Scheideler, L., Marmur, A., Boyan, B.D., Schwartz, Z., et al., 2014. A review on the wettability of dental implant surfaces I: theoretical and experimental aspects. Acta Biomater. 10 (7), 2894–2906.
Sagbo, S., Blochaou, F., Langlotz, F., Vangenot, C., Nolte, L.P., Zheng, G., 2005. New orthopaedic implant management tool for computer-assisted planning, navigation, and simulation: from implant CAD files to a standardized XML-based implant database. Comput. Aided Surg. 10 (5-6), 311–319.

Saini, M., Singh, Y., Arora, P., Arora, V., Jain, K., 2015. Implant biomaterials: a comprehensive review. World J. Clin. Cases 3 (1), 52–57.
Sambandam, B., Batra, S., Gupta, R., Agrawal, N., 2013. Blood conservation strategies in orthopedic surgeries: a review. J. Clin. Orthop. Trauma 4 (4), 164–170.
Sansone, V., Pagani, D., Melato, M., 2013. The effects on bone cells of metal ions released from orthopaedic implants. A review. Clin. Cases Miner. Bone Metab. 10 (1), 34–40.
von Schewelov, T., Sanzen, L., Onsten, I., Carlsson, A., Besjakov, J., 2005. Total hip replacement with a zirconium oxide ceramic femoral head: a randomised roentgen stereophotogrammetric study. J. Bone Joint Surg. Br. 87 (12), 1631–1635.
Schulze, C., Weinmann, M., Schweigel, C., Keßler, O., Bader, R., 2018. Mechanical properties of a newly additive manufactured implant material based on Ti-42Nb. Materials 11. Available from: https://doi.org/10.3390/ma11010124.
Sopcak, T., Medvecky, L., Zagyva, T., Dzupon, M., Balko, J., Balázsi, K., et al., 2018. Characterization and adhesion strength of porous electrosprayed polymer–hydroxyapatite composite coatings. Res. Disc. [Epub ahead of print] . Available from: http://dx.doi.org/10.1556/2051.2018.00057.
Sulistioso, G.S., Bandriyana, B., Siswanto, B., 2015. Sputtering of titanium in Co-Cr-Mo alloys for orthopedic implant materials. Adv. Mater. Res. 1123, 201–204.
Sunderman Jr., F.W., 1989. Carcinogenicity of metal alloys in orthopedic prostheses: clinical and experimental studies. Fundam. Appl. Toxicol. 13 (2), 205–216.
Syam, W.P., Mannan, M.A., Al-Ahmari, A.M., 2011. Rapid prototyping and rapid manufacturing in medicine and dentistry. J. Virt. Phys. Proto. 6 (2), 79–109.
Thomas, A.G., Jones, H.J., 2014. Hot pressing of ceramic powders. Powder Metallurgy 3 (6), 160–169.
Traina, F., De Fine, M., Di Martino, A., Faldini, C., 2013. Fracture of ceramic bearing surfaces following total hip replacement: a systematic review. Biomed. Res. Int. 2013. Available from: https://doi.org/10.1155/2013/157247.
Triclot, P., 2011. Metal-on-metal: history, state of the art (2010). Int. Orthop. 35 (2), 201–206.
Turger, A., Kohler, J., Denkena, B., Correa, T.A., Becher, C., Hurschler, C., 2013. Manufacturing conditioned roughness and wear of biomedical oxide ceramics for all-ceramic knee implants. Biomed. Eng. Online 12. Available from: https://doi.org/10.1186/1475-925X-12-84.
Vaccaro, A.R., Madigan, L., 2002. Spinal applications of bioabsorbable implants. J. Neurosurg. 97 (4 Suppl), 407–412.
Vallittu, P.K., Narhi, T.O., Hupa, L., 2015. Fiber glass-bioactive glass composite for bone replacing and bone anchoring implants. Dent. Mater. 31 (4), 371–381.
Van Norman, G.A., 2016. Drugs, devices, and the FDA: Part 2: an overview of approval processes: FDA approval of medical devices. JACC Basic Transl. Sci. 1 (4), 277–287.
Wang, R.R., Fenton, A., 1996. Titanium for prosthodontic applications: a review of the literature. Quintessence Int. 27 (6), 401–408.
Wang, W., Yeung, K.W.K., 2017. Bone grafts and biomaterials substitutes for bone defect repair: a review. Bioact. Mater. 2 (4), 224–247.
Wang, W.J., Zhou, J.N., Cao, S.J., 2002. Clinical application of interbody cage systems in the lumbar spine. Hunan Yi Ke Da Xue Xue Bao 27 (6), 547–550.
Waugh, A., Grant, A., 2018. Ross and Wilson Anatomy and Physiology in Health and Illness. Elsevier, Philadelphia, PA.
Wood, L., 2015. Global Orthopedic Prosthetic Implants Market 2015–2018 to 2022: Strategic Business Report – Spurt in Medical Tourism Offers Lucrative Market Growth Opportunities. Research and Markets.com <https://www.businesswire.com/news/home/20180702005895/en/Global-Orthopedic-Prosthetic-Implants-Market-2015-2018-2022> (accessed 20.07.18.).
Worboys, M., 2013. Joseph Lister and the performance of antiseptic surgery. Notes Rec. R. Soc. Lond. 67 (3), 199–209.
Xia, Z., Triffitt, J.T., 2006. A review on macrophage responses to biomaterials. Biomed. Mater. 1 (1), R1–R9.
Xue, X.-b, Wang, L.-q, Wang, M.-m, LÜ, W.-j, Zhang, D., 2012. Manufacturing, compressive behaviour and elastic modulus of Ti matrix syntactic foam fabricated by powder metallurgy. Trans. Nonferrous Met. Soc. China 22, s188–s192.

Xue, Z., Xu, H., Ding, H., Qin, H., An, Z., 2016. Comparison of the effect on bone healing process of different implants used in minimally invasive plate osteosynthesis: limited contact dynamic compression plate versus locking compression plate. Sci. Rep. 6. Available from: https://doi.org/10.1038/srep37902.

Yagi, K., Mantoku, H., 1985. Process for Preparation of Molecularly Oriented, Silane-Crosslinked Ultra-High-Molecular-Weight Polyethylene Molded Article. USPTO. USA, Mitsui Chemicals Inc. US4902460A.

Yamada, S., Heymann, D., Bouler, J.M., Daculsi, G., 1997. Osteoclastic resorption of calcium phosphate ceramics with different hydroxyapatite/beta-tricalcium phosphate ratios. Biomaterials 18 (15), 1037–1041.

Yang, K., Ren, Y., 2010. Nickel-free austenitic stainless steels for medical applications. Sci. Technol. Adv. Mater. 11 (1), 014105. Available from: https://doi.org/10.1088/1468-6996/11/1/014105. eCollection 2010 Feb.

Zhao, D., Witte, F., Lu, F., Wang, J., Li, J., Qin, L., 2017. Current status on clinical applications of magnesium-based orthopaedic implants: a review from clinical translational perspective. Biomaterials 112, 287–302.

CHAPTER

11

Biomaterials and Nanoparticles for Hyperthermia Therapy

Pran Kishore Deb[1], *Haifa'a Marouf Abdellatif Odetallah*[1], *Bilal Al-Jaidi*[1], *Raghuram Rao Akkinepalli*[2], *Amal Al-Aboudi*[3] *and Rakesh K. Tekade*[4]

[1]Faculty of Pharmacy, Philadelphia University, Amman, Jordan [2]National Institute of Pharmaceutical Education and Research, Mohali, India [3]Department of Chemistry, Faculty of Science, The University of Jordan, Amman, Jordan [4]National Institute of Pharmaceutical Education and Research (NIPER)—Ahmedabad, Gandhinagar, India

OUTLINE

11.1 Introduction 376
11.1.1 Hyperthermia: Historical Perspectives 377
11.1.2 Basic Principles of Hyperthermia 377
11.1.3 Thermotolerance 379
11.1.4 Human Body Temperature 380

11.2 Factors Affecting Hyperthermia Treatments 381

11.3 Classification of Hyperthermia 381
11.3.1 Local Hyperthermia 382
11.3.2 Regional-Deep Hyperthermia 383
11.3.3 Whole-Body Hyperthermia 383
11.3.4 Perfusion Therapy Hyperthermia 384
11.3.5 Interstitial and Indocavity Hyperthermia 384

11.4 Techniques Used for the Generation of Hyperthermia 385
11.4.1 Microwave 385
11.4.2 Radiofrequency 385
11.4.3 Near Infrared 386
11.4.4 Ultrasound 386

11.5 Biomaterials and Nanoparticle in Hyperthermia Therapy 387
11.5.1 Carbon Nanotubes for Hyperthermia Therapy 389
11.5.2 Graphene and Graphene Oxide 390
11.5.3 Gold Nanoshells 391
11.5.4 Gold Nanorods 392
11.5.5 Gold Nanoparticles 393
11.5.6 Magnetic Nanoparticles 394
11.5.7 Iron Oxide Nanoparticles 397
11.5.8 Silica Nanoparticles 397

Biomaterials and Bionanotechnology
DOI: https://doi.org/10.1016/B978-0-12-814427-5.00011-1

© 2019 Elsevier Inc. All rights reserved.

11.5.9 Small Molecules Used in Hyperthermia 398

11.6 Crosstalk on Various Application and Uses of Hyperthermia 400
11.6.1 Hyperthermia in the Treatment of Brain Tumor 400
11.6.2 Hyperthermia in the Treatment of Breast Cancer 400
11.6.3 Cervical Cancer 401
11.6.4 Melanoma 401
11.6.5 Neck Cancer 402
11.6.6 Hyperthermia in the Treatment of Arthritis 402
11.6.7 Hyperthermia in the Treatment of Wounds 402
11.6.8 Hyperthermia in the Treatment of Pain 403

11.7 Hyperthermia Combined Therapy 403
11.7.1 Hyperthermia Combined Chemotherapy 403
11.7.2 Hyperthermia Combined Gene Therapy 404
11.7.3 Hyperthermia Combined With Photodynamic Therapy 405

11.8 Conclusions and Future Perspectives 405

Abbreviations 405

References 406

Further reading 413

11.1 INTRODUCTION

Hyperthermia is a therapeutic technique that acts heating the target cells with sufficient temperature to destroy them without harming adjacent cells or tissues. This technique is mainly used nowadays for cancer treatment as an alternative to conventional chemotherapy and radiotherapy because it is found to be safer with lower side effects and most importantly tumor cells are very sensitive to heat as compared with normal cells which facilitate the successful application of this technique (McNamara and Tofail, 2015). Hyperthermia is applied by increasing body temperature to 40°C–43°C, which is considered to be injurious for cancer cells as compared with the normal noncancerous cells and the optimum effect of such technology on cancer is maintained when the tumor has been kept at 41°C for 1 hour (Kennedy et al., 2011).

The therapeutic action of hyperthermia on cancer is believed to be due to its direct cytotoxic effect as well as an immunological effect through the upregulation and overproduction of $CD4^+$ T-cells and IL-2, which play an essential role in the antitumor immunity (Zhang et al., 2009). Also, high temperature causes direct damage to the cancerous cells as well as increased sensitivity to other treatment modalities such as radiotherapy, gene therapy, and immunotherapy.

Many techniques have been used to apply heat to the tumor, including microwaves radiofrequency (RF), ultrasound, hot water perfusion, and infrared radiators (Chichel et al., 2007). Recently, nanoparticles and biomaterial are considered as the main materials for use in hyperthermia applications (www.regionalchemotherapy.com, accessed on September 11, 2017).

Hyperthermia has been applied for treating or controlling many types of cancer like liver, breast, prostate cancer, as well as glioblastoma and melanoma (Kennedy et al., 2011; McNamara and Tofail, 2015). This chapter covers the most important aspects of hyperthermia including fundamental techniques, current applications, and biomaterials and nanoparticles used in hyperthermia with special emphasize on hyperthermia as a treatment regimen for cancer.

11.1.1 Hyperthermia: Historical Perspectives

The application of heat to treat diseases, including cancer, has a long history. Ancient Greeks, Romans, and Egyptians have used heat to treat breast masses and the first report for the use of hyperthermia was in an Egyptian surgical papyrus dated from around 3000 BC (Shiyu et al., 2016). Medical practitioners in ancient India used regional and whole-body hyperthermia as a treatment for cancer as well.

In 1893, William Coley, a bone surgeon from New York Memorial Cancer Hospital (now known as Memorial Sloan-Kettering), induced hyperthermia in 38 advanced cancer patients through what is known as "Coley toxin," which is a mixture of bacterial vaccine that was the first specialized bacterial antitumor pyrogen with standard composition, which resulted in high fever in those patients, among whom 12 were cured completely, 19 showed improvement, and the other showed negligible effect. Interestingly, Coley found that 2 out of 10 patients with locally advanced sarcoma treated by Coley toxin showed complete remission (Roussakow, 2013). In 1898, Westermark, a Swedish gynecologist, was the first to show the ability to apply hyperthermia for the long term to treat cancers without harming noncancerous cells. In 1899, Gottschalk succeeded in applying hyperthermia with a higher temperature for less duration to treat cervical cancer. In 1903, Jensen was the first to realize that tumor tissues are more heat sensitive in comparison to the normal healthy ones (Roussakow, 2013). Wagner-Jauregg received the Nobel Prize because he made a breakthrough after achieving 30% remission rate using hyperthermic treatment in patients suffering from syphilis; he did so after intentionally infecting those patients with *Plasmodium falciparum*, which induced a high fever (Vertess et al., 2002).

During the 20th century, localization of hyperthermia was developed by using galvanocautery in patients with solid carcinoma; the fact that cancer cells in those patients were more sensitive to heat than normal tissues strongly indicated the usefulness of hyperthermia as a tool for cancer treatment. Hot water hyperthermia has also been used since the 20th century as localized hyperthermia for extremities, and technologies used for hyperthermia application and study developed widely (Roussakow, 2013; Kok et al., 2015). Nowadays, hyperthermia is being used in combination with chemotherapy and radiotherapy to target malignant disease in most of the body sites, especially cervical cancer, malignant melanoma, recurrent breast cancer, soft tissue sarcoma, and bladder cancer (Kok et al., 2015).

11.1.2 Basic Principles of Hyperthermia

Hyperthermia depends on the principle of converting energy into heat; these energies are produced through many sources, but magnetic nanoparticles, RF, microwave, and laser wavelength are the most used techniques as shown in Fig. 11.1 (McNamara and Tofail, 2015).

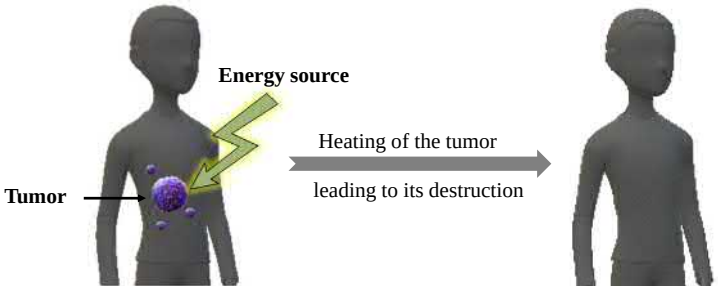

FIGURE 11.1 Diagrammatic illustration of the concept of hyperthermia therapy.

Hyperthermia is done by heating the body or a part of the body to a temperature within the range 40°C−43°C at which physiological and immunological changes will occur within cells leading to cell death (Bahman and Song, 1984). Hyperthermia is also known to induce a variety of cellular changes such as changes in cell membrane, nuclear and cytoskeletal structure, cellular metabolism, cytokines transduction, and the overexpression of heat shock proteins (HSPs). All these effects will be discussed in this section (Vertess et al., 2002).

11.1.2.1 Physiology of Hyperthermia

Hyperthermic physiological effect has been studied extensively to understand the cellular response upon heat exposure (Fajardo et al., 1980). Findings showed that mainly two physiological changes occur in response to heating. The first one is the microcirculation in tissues. It is well known that tumors have poor vascularization as compared with the normal tissues, which means that cancer tissues are hypoxic and after heat application, these vasculatures would not be able to provide enough blood, because of which the effect of hypoxia would increase, making these tissues weaker. Moreover, tumor vasculature also acts as a heat reservoir after heating, which could further amplify the effect of hypoxia (Siemann, 2015). Heat also increases blood volume and vascular permeability in normal tissues, which can increase the higher amount of drugs entry into the cell, and all these changes start when the temperature reaches 41°C−41.5°C (Fajardo et al., 1980; Song et al., 1980; Endrich et al., 1979). The second one is environmental factors, which affect oxygen, pH, and nutrients. Heating activates glycolysis, which leads to the accumulation of lactic acid within the tumor, as a result of which the intratumoral environment shifts to the acidic state and so for tumor vasculature, that leads erythrocytes to become rigid because of the acidity leading to the blockage of tumor capillaries and lowering of oxygen. The intratumoral acidity also leads to lysosomal membrane destabilization, because of which lysosomal enzymes can cause the destruction of tumor cells (Fajardo et al., 1980; Lee et al., 1986; Roussakow, 2013).

11.1.2.2 Mechanism of Hyperthermia Cytotoxicity

The therapeutic effects of hyperthermia are induced through a combination of directly induced cytotoxic effect and immunological effect, which differ in intensity based on the

temperature used, where higher temperature induces higher cytotoxicity (McNamara and Tofail, 2015; Zhang et al., 2009). The cytotoxic effect occurs because heat induces both microtubule and protein damage (McNamara and Tofail, 2015). It should be noted that the cytotoxicity starts when the temperature exceeds 41°C (Zhang et al., 2009).

Heating cells to a temperature between 41°C and 46°C will induce cell apoptosis (programmed cell death) (McNamara and Tofail, 2015) because of the breakdown of vital cell components by proteins called caspases, which then causes the production of enzymes that digest the DNA in the cell nucleus, leading to the destruction of the cell system followed by engulfment and digestion by macrophages (McNamara and Tofail, 2015).

Also heating the cell to such a temperature will cause the denaturation of proteins, which have vital functions in metabolism, building microskeleton, and plasma membrane and hence, this will lead to direct cell damage (Mustafa et al., 2013). Lysosomes are also destructed by heat to release enzymes leading to cell damage (Fajardo et al., 1980).

Heat also affects gene expression for many genes (HSP gene, TNF gene, caspases genes, IL-2 gene) either by their upregulation or downregulation. The most important gene found to be upregulated is that encoded for HSPs, which are a family of proteins showing many functions within cells and their primary function is to refold proteins that have been destroyed within the cell, especially those that are involved in DNA repair (Park and Seo, 2015). They are also involved in the immunological effect, where they are considered as "danger signals" because of their involvement in the presentation of tumor cell fragments. Also, HSP-peptide complexes are engulfed by antigen presenting cells, so their presence on major histocompatibility complex (MHC) class-I receptors can ease the recognition of tumor cells by cytotoxic T cells and natural killer cells (Schueller et al., 2003; Wust et al., 2002).

Elevation of temperature enhances the activity of T cells, macrophages, and natural killer cells (Valentina et al., 2005). When hyperthermia takes place at 43°C, it stimulates T cell activity and response by changing the ratio of CD_4/CD_8 cells and upregulation of IL-2 production from lymphocyte, which leads to immune-stimulatory action and thereby enhances the necrosis of tumor cells as depicted in Fig. 11.2 (Zhang et al., 2009; Valentina et al., 2005). In addition to the mentioned effects of hyperthermia on tumor cells metabolism and functions, it also worsens the tumor microenvironment by making a group of biochemical and microcirculatory changes such as acidosis, RBC stiffening and aggregation, increased vascular permeability, platelet aggregation, and intravascular clotting as discussed in the previous section (Idrees and Jebakumar, 2014).

11.1.3 Thermotolerance

Thermotolerance is "transient nonheritable adaptation to thermal stress that renders heated cells more resistant to additional heat stress" (Rice et al., 1982). It affects the response to hyperthermia (Dewhirst et al., 2003). As mentioned earlier, the recommended temperature for hyperthermia is reported to be 41°C–43°C, which is responsible for most of the physiological and immunological changes in tumor cells; high temperatures above 45°C can stimulate the overproduction of HSPs, which regulate this phenomenon (Liu et al., 2015;

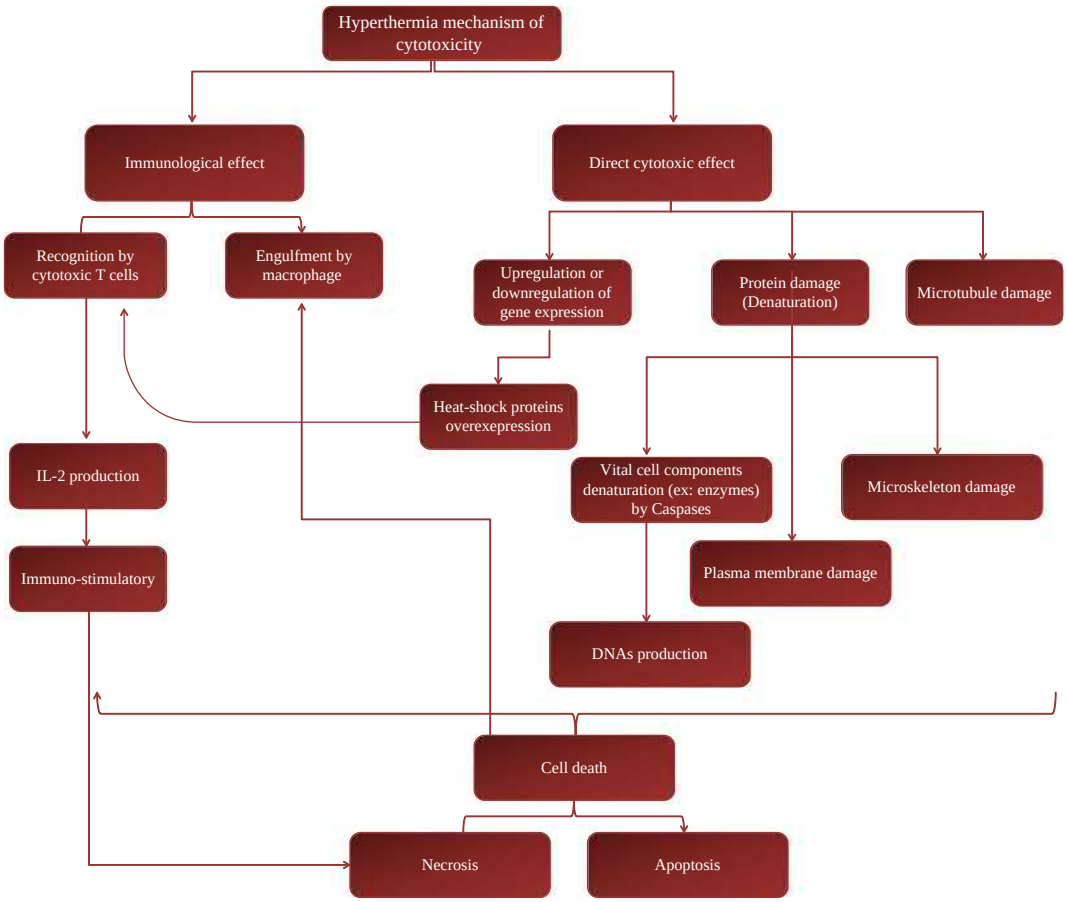

FIGURE 11.2 Hyperthermia mechanism of cytotoxicity.

Dewhirst et al., 2003). The occurrence of this phenomenon depends on the severity of the initial temperature exposure and the extent of time taken (Dewhirst et al., 2003). Fortunately, thermotolerance is able to decay, if the patient is not exposed to heat again and it takes 48–80 hours to decay (Singh, 2015; Dewhirst et al., 2003).

11.1.4 Human Body Temperature

In 1869, Wunderlich and Reeve established that 37.8°C is the value of normal human body temperature in healthy adults and in 1992, Mackowiak considered the baseline temperature as 36.7°C (Lu and Dai, 2008). The temperature of the therapeutic window is 37.5°C–41°C, which lies within the range of normal physiological fever (Kluger, 1986). The maximal temperature that can cause damage to body cells was reported to be 45°C (Kluger, 1986). For hyperthermia treatment, body temperature should rise to above 42°C

for less than 24 hours to give the intended results with minimal side effects; if patients are subjected to a temperature within the physiological range for short time, the mitotic cycle will be stimulated resulting in the enhancement of cancer growth (Roussakow, 2013).

11.2 FACTORS AFFECTING HYPERTHERMIA TREATMENTS

Many factors can affect the degree of cell death and the efficiency of hyperthermia in cancer treatment as mentioned below (Mallory et al., 2016; Otte, 1988):

- *Exposure of temperature and duration of heating:*
  Hyperthermia is applied with temperature in the range between 40°C and 45°C; as the temperature increases the therapeutic efficacy increases due to cytotoxicity enhancement (Mallory et al., 2016). Time duration is an important factor, for example, hyperthermia at 40°C for 30 minutes showed the enhanced oxygenation of tumor tissues, while heating at 43°C for 30 minutes resulted in reduction in tumor oxygenation, whereas heating at 45°C and above for 30 minutes is considered to be destructive to oxygenation as mentioned before (Otte, 1988). Also, it has been observed that heating tumors to 43°C for 1 hour led to the reduction of erythrocyte oxygenation especially in tumor capillaries, which could be one of the mechanisms of the cytotoxicity of hyperthermia as discussed earlier (Otte, 1988). An interesting finding showed that heating tumors to temperatures above 42.5°C−43°C can reduce exposure time by half with each 1°C increase with the same cell-damaging effect (Vernon et al., 1996; Mallory et al., 2016).
- *The rate of heating:*
  Heating tumors rapidly cause more cell membrane damage and induce cell death through necrosis while gradual heating causes apoptosis (Tang and McGoron, 2013).
- *Environmental factors such as pH and nutrients:*
  As mentioned previously, lowering the pH increases the rate of heating (Roussakow, 2013).

11.3 CLASSIFICATION OF HYPERTHERMIA

Hyperthermia is categorized either according to the method of heat application or based on the device being used for applying heat. According to the method of application, hyperthermia can be classified into local hyperthermia, regional deep hyperthermia, whole-body hyperthermia, perfusion hyperthermia, intraluminal and indocavity hyperthermia, and interstitial hyperthermia (Fig. 11.3). The choice of hyperthermia type for use depends upon the location and the tumor size in the body. In all the methods, the temperature for both cancer tissues and the surrounding normal tissues must be continuously monitored in order not to exceed the acceptable limits.

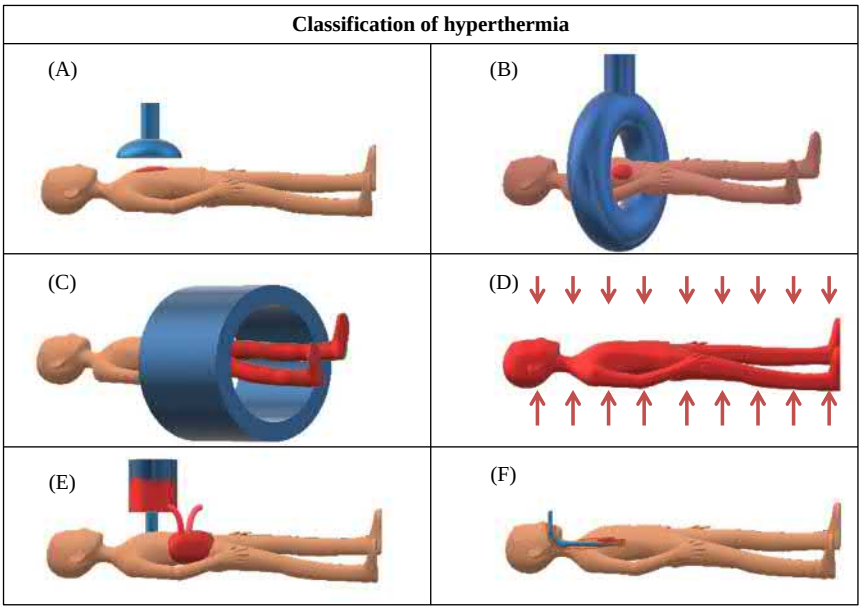

FIGURE 11.3 Illustration of hyperthermia classification. (A) Local hyperthermia application on the superficial tumor. (B) Regional deep hyperthermia application on the deep-seated tumor. (C) Part-body hyperthermia. (D) Whole-body hyperthermia. (E) Perfusion therapy hyperthermia. (F) Indocavity hyperthermia where the applicator is inserted in the esophagus to target superficial tumor there.

11.3.1 Local Hyperthermia

It is also known as superficial hyperthermia or external local hyperthermia, where it selectively heats tumor to a therapeutic temperature (39°C–45°C). The aim of this procedure is to target superficial tumors that are mainly invading skin or the nether layers, like those in lymph nodes. Heating is normally applied to a small area mainly by using a physical heating device like a microwave or radio wave and several types of applicators can be used here, all of them have similar major components such as the signal generator, amplifier, the applicator, bolus preceding the water path, and a feedback device.

The mechanism of local hyperthermia first includes the direct killing of the affected cell by changing cell membrane permeability and altering enzyme activity that could lead to cell apoptosis. Moreover, local hyperthermia has a serious effect on DNA replication through the rapid translocation of nucleon from the nucleolus into nucleoplasm; further heating can also cause inactivation of replication enzyme (Shiyu et al., 2016). An additional effect of local hyperthermia is the increase in vascular permeability and increase in oxygen pressure levels in a tumor, which has a great effect on altering the microenvironment; this change in tumor microenvironment will enhance the radiosensitivity of tumor tissues (Vidair and Dewey, 1991). The last possible mechanism of antitumor effect of local hyperthermia is called an antitumor immunity in which heating tumor tissues to 45°C will activate the overexpression of MHC class I ligand on the surface of the tumor, followed by

the activation of Natural Killer group 2 receptors that will either directly induce cytotoxicity or stimulate T-cell receptor signaling (Verneris et al., 2004; Toraya-Brown et al., 2014).

Local hyperthermia, on the other hand, has many limitations such as thermal dose control, and the target treatment regions in which local hyperthermia is not suitable to be applied such as head, neck, and supraclavicular regions. It has been applied as cancer treatment such as in laryngeal cancer (given twice a week in combination with chemotherapy), head and neck cancer along with the use of dendritic cell therapy (Takeda et al., 2014) as well as in tongue squamous cell carcinoma in which it decreased the size of tumor by 25% (Liang et al., 2010). Local hyperthermia has also been used to induce antiviral activity by interferon-dependent pathway (Zhu et al., 2010).

11.3.2 Regional-Deep Hyperthermia

It is also known as localized deep hyperthermia; the aim of this procedure is to selectively target the deep-seated tumor region rather than the whole body to reach a temperature of 42°C, causing thermal damage of the tumor cells. Part-body hyperthermia is a new generation technique, where scientists developed a more controlled heating pattern that is generated by the applicators to cover larger anatomical region like the complete peritoneal area for peritoneal cancer (www.biomedklinik.de, accessed on September 11, 2017).

Regional hyperthermia is generally used in diseases found in deeper tissues or when a large area of treatment is to be covered. This method can increase the perfusion of organs and limbs after heating blood by a noninvasive RF method (Mallory et al., 2016). In this method, tumor mass is heated by RF, microwave, or ultrasound. Regional hyperthermia has been used for many types of cancer such as ovarian cancer in which cisplatin was administered intraperitoneally at a temperature of 41.5°C (Leopard et al., 1993). Regional hyperthermia has been also tested in patients with locally advanced nonmetastatic rectal cancer along with radiotherapy, in which it improved the local control and survival (Hildebrandt et al., 2000).

11.3.3 Whole-Body Hyperthermia

The history of the use of whole-body hyperthermia started when the patient has been submerged in hot wax or liquid or wrapped in plastic or encased in a high-flow hot water jacket suit (Baronzio et al., 2014). It is also known as fever therapy. The aim here is to raise the temperature of the whole body to treat metastatic tumors, although it can be used for a localized therapy. The body temperature is raised to 39°C–40°C by using a heated bed. Under this temperature, the blood circulation increases, resulting in the increase in the permeability of the cancer cell membrane. Since the cancer cells are more sensitive to heat than normal cells, it will improve the access of the chemotherapeutic agents inside the tumor (McNamara and Tofail, 2015). A maximum temperature of 42°C can be maintained for about 1 hour with tolerable side effects (Wust et al., 2002); the patient here should be either under deep analgesia or general anesthesia (Wust et al., 2002). The method of

performing hyperthermia under these conditions is considered to be reproducible with no complications, although there could be certain systemic and local side effects (www.biomedklinik.de, accessed on September 11, 2017). Whole-body hyperthermia was applied in many types of cancer, especially in combination with chemotherapy. For example, in combination with carboplatin, whole-body hyperthermia was used in patients with recurrent ovarian cancer, where the study revealed that the whole-body hyperthermia at a temperature of 41.8°C in combination with carboplatin is an active salvage treatment, although significant hematological toxicity was also observed in patients (Atmaca et al., 2009). The most common approach to whole-body hyperthermia is the use of a flexible infrared chamber. Other methods may involve simply heating a patient's room or wrapping the patient within a heated blanket. The common side effects of the whole-body hyperthermia include nausea, vomiting, diarrhea, and rarely in severe cases, it may lead to problems in the heart, blood vessels, and major body organs.

11.3.4 Perfusion Therapy Hyperthermia

It is also known as intraperitoneal perfusion hyperthermia. The aim here is to treat a metastatic tumor in the abdominal region. The temperature is raised through infusing the abdomen with hot liquid to approximately raise the temperature up to 45°C enriched with cytostatics (www.biomedklinik.de, accessed on September 11, 2017). Hyperthermic intraperitoneal chemotherapy (HIPEC) is a subtype of intraperitoneal perfusion hyperthermia and it depends on the usage of chemotherapy during the application of the procedure, which will increase cellular death and induce apoptosis. HIPEC is mainly used after abdominal surgeries, where wound healing resulted from surgery would be delayed with more complications if chemotherapy is used alone, hence the combination therapy is preferred. This technique was applied effectively with colorectal and ovarian origin carcinoma (Boutros et al., 2010).

11.3.5 Interstitial and Indocavity Hyperthermia

These types of hyperthermia are sometimes considered as subtypes of local hyperthermia; the aim here is to target the superficial tumors by implanting the applicator within the tumor, which must be less than 5 cm in diameter and in a location achievable for implantation. For interstitial hyperthermia, the applicator is inserted in the interstitial space, while for indocavity the applicator is inserted in the natural opening of the hollow organs like esophagus, urethra, rectum, cervix, and vagina. Radiowave, microwave, and ultrasound can be used for this type of hyperthermia as a heat source (Jha et al., 2016); these heat sources were applied by using special antennas, the positioning of which could be very painful to the patient. Moreover, the placement of such antennas could be critical and experts must do that to avoid any complications. Interstitial hyperthermia has been used in many types of cancer such as prostate carcinoma (Vulpen et al., 2002), recurrent head and neck cancer (Geiger et al., 2002), and in breast carcinoma (Robinson et al., 1998).

11.4 TECHNIQUES USED FOR THE GENERATION OF HYPERTHERMIA

Different techniques and heat sources are used for hyperthermia application to the tumor. Heating sources for hyperthermia are usually placed outside the body to irradiate the tumor with electromagnetic waves or any other type of waves and frequencies (Wust et al., 2002; Deatsch and Evans, 2014).

Heat source selection for nanoparticle-mediated hyperthermia is dependent mainly on three factors, i.e., extrinsic heating of healthy tissues and of targeting nanoparticle containing tissues, adequate penetration depth to reach nanoparticles that settle within the cancer cells, and the chosen nanoparticle physicochemical properties (Kennedy et al., 2011).

11.4.1 Microwave

The application of microwaves is considered as a suitable hyperthermia technique for tumors in tissues with high water content or those with high resistance for electric current connection such as lung or bone tumors because it does not rely on electric current for ablation (Lubner et al., 2010). The wave frequency for the microwave is of the order of 1 GHz and the heating will be generated from dielectric relaxation and the energy deposition obtained from special applicators.

Microwave as a hyperthermia technique has attracted a lot of interest recently in clinical oncology (Shi et al., 2015; Du et al., 2015a,b) because of its advantages, which include fast intratumoral heat generation, deep penetration in tissue, large ablation volume for tumors, less pain during the procedure, and less susceptibility on the surrounding normal tissues (Wang et al., 2012, 2014; Liu et al., 2014).

Since microwave thermal ablation relies on the water content of the targeted tissues, materials with high polarity and high water content are necessary to induce high-temperature thermal ablation under microwave exposure and concentrate the resulted heat to the tumor, thus high treatment efficiency, as well as high protection of the healthy tissues from overheating, takes place surrounding the targeted tumor (Liang and Wang, 2007; Simon et al., 2005; Wright et al., 2005; Dou et al., 2016). These materials include ionic liquids, saline microcapsules, and saline solutions (Shi et al., 2015; Du et al., 2015a,b; Tan et al., 2016; Long et al., 2016; Tang et al., 2016). Microwave hyperthermia was used in many types of cancer especially the local ones such as breast cancer (Elkayal et al., 2015) and prostate cancer (Monotorsi et al., 1992) in which the intraprostatic temperature was kept around 43.5°C for 60 minutes.

11.4.2 Radiofrequency

RF electric field is another efficient hyperthermia technique. It was first known as a method for cauterizing blood vessels during surgery in the early 20th century, then its application for hyperthermia cancer treatment began during the same period of time (Kennedy et al., 2011). RF is unsuitable for heating specific tumor sites alone because the energy is attenuated by tissues although it has sufficient penetration depth, so using it

along with an absorptive agent like gold nanoparticles or carbon nanotube (CNT) has been found to increase RF induced hyperthermia specificity and protect healthy cells from its energy (Yanase et al., 1998; Kennedy et al., 2011).

Hyperthermia induced through nanoparticles and RF waves is better than other hyperthermia techniques because RF has high wavelength and low frequency with nondestructive effect on the excised tissue and appropriate penetration depth for the targeted tumors, especially solid tumors like a liver tumor. Patients prefer it because it is a safe technique with low cost (Nasseri et al., 2016; Kennedy et al., 2011).

Temperature, apoptosis, and necrosis of cells during RF induced hyperthermia can be manipulated by changing RF power and concentration of nanoparticles solution over time (Nasseri et al., 2016). The advantage of RF over microwave is that the former has the potential to achieve greater tissue penetration due to relatively lower frequency. RF waves are normally applied by the use of electromagnetic radiation applicators that will transmit energy as close as possible to tumor tissues and minimize the possibility of affecting surrounding normal tissues, making this method of heating a good alternative for the conventional methods of cancer treatment.

11.4.3 Near Infrared

Near infrared (NIR) is considered as a compatible technique for hyperthermia application in the biological system because tissue chromophores slightly absorb NIR, which protects healthy tissues from damage (Kennedy et al., 2011) and it has adequate penetration depth as compared with ultraviolet and visible ranges (Sohail et al., 2017). However, RF has better penetration as compared with NIR. Penetration of NIR in vivo is dependent upon several factors like the degree of light scattering and absorption within the tissue (Kennedy et al., 2011).

It is the most compatible wavelength for gold nanoparticle photothermal therapy, that when used together, energy attenuation for healthy tissues decreases. For NIR laser conjugated gold nanoparticle hyperthermia treatment, gold nanoparticles are loaded to accessible tumors such as superficial tumors (skin cancer) and then NIR laser is applied directly. On the other hand, for indirectly accessible tumors (their depth is greater than 1 cm), endoscopy or interstitial fiber-optic placement is used to deliver the tumor with NIR. But for nonaccessible tumors, alternative techniques should be used (Kennedy et al., 2011).

11.4.4 Ultrasound

When ultrasound is used, the technique is called high intensity focused ultrasound, sometimes also referred to as just focused ultrasound (www.cancer.org, accessed in October 11, 2017). Focused ultrasound is the most promising method for drug delivery because it is a highly penetrating, cheap, and precise method for drug delivery (Boissenot et al., 2017).

Ultrasound can induce mild hyperthermia because of its mechanical effects including its radiation forces, stable and inertial cavitation, leading to moderate enhancement of heating in focal zone; as blood flow increases along with vascular permeability, sensitivity

to cytotoxic drugs also increases (Boissenot et al., 2017). Ultrasound had been used for hyperthermia therapy in combination with thermosensitive liposome formulation of doxorubicin (DOX) (Thermodox) in the first clinical trial of combining heating stimulus with nanoparticles (Boissenot et al., 2017; Landon et al., 2011).

As ultrasound can induce mild hyperthermia, it is considered as an interesting method for targeting drug delivery during hyperthermia treatment for both available formulations and newly developed nanoparticle systems (Boissenot et al., 2017). On the other hand, some anatomical areas of the body could not be able to be targeted by ultrasound heating, which is considered as one of the disadvantages of this method, in addition to the seriousness of applying ultrasound around bones that could be harmed by ultrasound (Uysal, 2017).

11.5 BIOMATERIALS AND NANOPARTICLE IN HYPERTHERMIA THERAPY

Biomaterials are defined as "materials used in medical devices, provide a highly versatile tool to create defined macro- and microenvironments, and manipulate cells and tissues in vitro and in vivo" (Gu and Mooney, 2015). Biomaterials provide a base to mimic tumors (in vivo) for studying and understanding them as well as for screening of chemotherapeutic agents and other therapeutic agents for many diseases and conditions, as shown in Fig. 11.4 (Gu and Mooney, 2015). This will allow scientists to get a better understanding of cancers and help them to design effective therapeutic agents (Gu and Mooney, 2015).

Recently biomaterials have gained a lot of interest as a hyperthermia agent due to their unique properties including their strong NIR absorbance, excellent thermal conductivity,

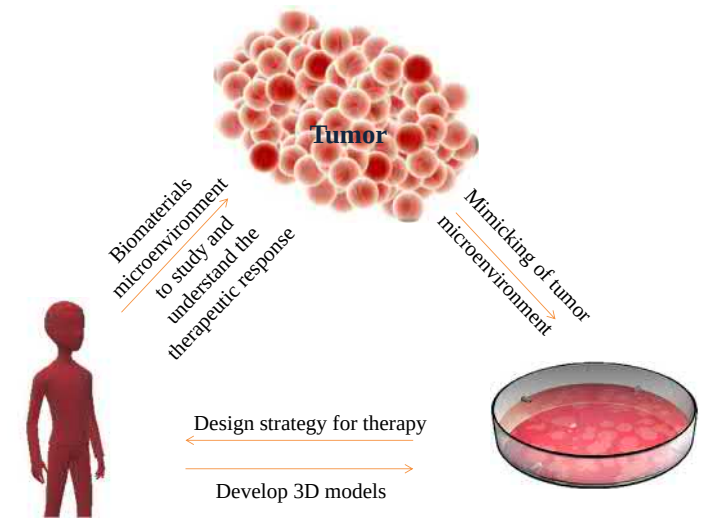

FIGURE 11.4 Use of biomaterials for creating new microenvironment both in vitro and in vivo.

high photothermal conversion efficiency, their cytocompatibility, and very low in vivo toxicity (Ma et al., 2016). Two properties of biomaterials, i.e., their type and size, can guide biomaterials-induced hyperthermia by involving in the effectiveness of signal transduction (Gu and Mooney, 2015).

Nanoparticles are particulate dispersions or solid particles of a size that exists in nanometer scale within the range of 10−1000 nm (Mohanraj and Chen, 2006). The advantage of using nanoparticles generally in biomedical applications lies on the property of a high surface to volume ratio because of the nanoscale system (McNamara and Tofail, 2015). For hyperthermia, nanoparticles offer promising advantages such as they can carry the chemotherapeutic agent to the tumor site selectively and noninvasively, can precisely target the tumor cells, and can intrude deeply into the tumor tissue without harming the healthy cells or tissues. They can be visualized and tracked by using MRI and they can manufacture huge numbers of binding sites for cancer cells (McNamara and Tofail, 2015; Sohail et al., 2017).

Nanoparticles for hyperthermia are combined with anticancer agents to improve their cytotoxicity and enhance their delivery of cancer cells (Alvarez-Berrios et al., 2014; Cherukuri et al., 2010). It should be noted that most of the anticancer agents have the problem of the narrow therapeutic index so they can easily cause acute or cumulative toxicity to noncancer cells (Cherukuri et al., 2010). The combination of anticancer cells with nanoparticles can enhance anticancer cytotoxicity due to the fact that hyperthermia can enhance the formation of misfolded protein causing the aggregation of these resulting proteins in the cytosol. The aggregation occurs because of microtubule damage that happens during hyperthermia, which further interrupts the transport of these aggregated proteins in the perinuclear area. The resulting misfolded aggregated proteins are normally degraded through the proteasome. To prevent the action of the proteasome as well as to ensure that misfolded proteins are accumulated causing the degradation of the whole cell, anticancer agents like bortezomib and carfilzomib that act as preferred proteasome inhibitors are combined with the nanoparticles (Alvarez-Berrios et al., 2014).

For successful hyperthermia therapy, adequate accumulation of nanoparticles inside the tumor cells along with sufficient penetration of excitation energy is required, so selecting the type of nanoparticle for the process is a key feature. Moreover, the size of particles, their maximum absorption wavelength, and their photothermal transduction efficiency (the portion of the incident light being converted into photothermal power by the nanoparticle) should also be considered (Kennedy et al., 2011; Cole et al., 2009).

Many nanoparticles have been used in preclinical studies to induce delivery of chemotherapeutic agents to tumors to reduce the toxicities and side effects of these agents on normal noncancerous cells. For example, nanoparticles loaded with docetaxel, 5-fluorouracil, and gemcitabine have been investigated in the preclinical studies for the treatment of lung, colon, and pancreatic cancers (Cherukuri et al., 2010). Nanoparticle surfaces had been modified by adding hydrophilic polymers like polyethylene glycol (PEG) so that their permeability to tumors and retention time within them are enhanced, and many nanomedicines are now available in the market that had been made based on this strategy such as Abraxane and Doxil (Boissenot et al., 2017).

Colloidal gold nanoparticles loaded with tumor necrosis factor (TNF)-α are under clinical investigation for hyperthermia cancer treatment and the preclinical trials have shown

TABLE 11.1 A Selection of FDA Approved Antibodies and Small Molecules That Can Be Conjugated With Nanoparticles for Cancer Therapy

Antibody/Small Molecule Name	Type	Target	Cancer Type	Brand Name
Bevacizumab	Antibody	VEGFR	Colorectal, nonsmall cell lung, breast	Avastin
Bortezomib	Molecule	Proteasome 26 s	Myeloma, lymphoma	Velcade
Gefitinib	Molecule	EGFR	Nonsmall cell lung	Iressa
Imatinib	Molecule	BCR-ABL	Leukemia, gastrointestinal	Gleevec
Rituximab	Antibody	CD20	Lymphoma	Rituxan
Sorafenib	Molecule	VEGFR, PDGFR	Kidney, liver	Nexavar
Tamoxifen	Molecule	Estrogen receptor	Breast	Nolvadex
Tositumomab	Antibody	CD20	Lymphoma	Bexxar
Trastuzumab	Antibody	HER2	Breast	Herceptin

BCR-ABL, Breakpoint cluster region-Abelson; *EGFR*, epithelial growth factor receptor; *HER2*, human epidermal growth factor receptor 2; *PDGFR*, platelet-derived growth factor receptor; *VEGFR*, vascular endothelial growth factor; *VEGFR*, vascular endothelial growth factor receptor.
Reprinted with permission from Cherukuri, P., Glazer, E.S., Curley, S.A., 2010. Targeted hyperthermia using metal nanoparticles. Adv. Drug Deliv. Rev. 62, 339–345.

promising results (Farma et al., 2007). Nanoparticles had been also studied for the delivery of targeting agents in gene therapy (Cherukuri et al., 2010). Nanoparticles were also conjugated with biomaterials such as antibodies and small molecules for cancer thermal ablation, as shown in Table 11.1.

Nanoparticles can also be used to enhance the detection and diagnosis of cancer. For example, magnetic iron nanoparticles have been used along with magnetic resonance imaging (MRI) to improve its diagnostic ability (Kou et al., 2008; Cherukuri et al., 2010) and if those magnetic iron nanoparticles are conjugated with antibodies that target cancer cells surface proteins, then the MRI process will be more accurate for diagnosis of early--stage tumors (Neumaier et al., 2008). Usage of nanoparticles in the field of cancer diagnosis will definitely continue to expand with time.

11.5.1 Carbon Nanotubes for Hyperthermia Therapy

CNTs have been known previously as a carrier of genes and proteins to deliver them to cancer cells through nonspecific endocytosis (Cherukuri et al., 2010; Al-Qattan et al., 2018; Shubhangi et al., 2018). CNTs are either metallic or semiconducting in nature based on the twist of graphitic carbon wall. Single-walled CNTs (SWNTs) have a structure of carbons arranged in a honeycomb pattern to form a thin seamless cylinder of carbons (Sohail et al., 2017; Kam et al., 2005); due to this structure SWNTs show a wide range of electromagnetic absorptions, and CNTs' absorption characteristics lead to their use as hyperthermia

enhancer by using NIR waves. The electromagnetic waves' conductivity in CNTs is defined by carbons of the cylindrical wall crystalline arrangement (Sohail et al., 2017).

Recently CNTs are coupled with RF field to treat deep tumors (Cherukuri et al., 2010; Gannon et al., 2008), studies had shown that the amount of heat released by CNTs under RF field is similar to that produced by gold nanoparticles under the same field, which is sufficient to cause apoptosis or necrosis for deep tumors. CNTs are able to be delivered and targeted to specific cell type by using them as a noncovalent wrap around targeting moieties or by direct covalent fictionalization (Cherukuri et al., 2010).

11.5.2 Graphene and Graphene Oxide

Graphene is one of the most promising carbon allotropes, and has gained much interest recently for the development of next-generation carbon-based materials. Graphene is found as colloidal dispersion and as a powder, and it is an important biomaterial as it is stable, with good thermal conductivity and impressive electronic and mechanical properties that are superior to CNT properties (Compton and Nguyen, 2010).

Large quantities of graphene can be produced easily by the reduction of graphene oxide—oxygenated graphene sheets covered with hydroxyl, epoxy, and carboxyl groups to be used for functionalized graphene-based materials (Fig. 11.5). Graphene can also be prepared from other graphite derivatives such as graphite fluoride and expandable graphite (Compton and Nguyen, 2010).

Graphene oxide is considered as a novel biomaterial for drug delivery and hyperthermia therapy, because of its many advantages including low cost; high surface to volume

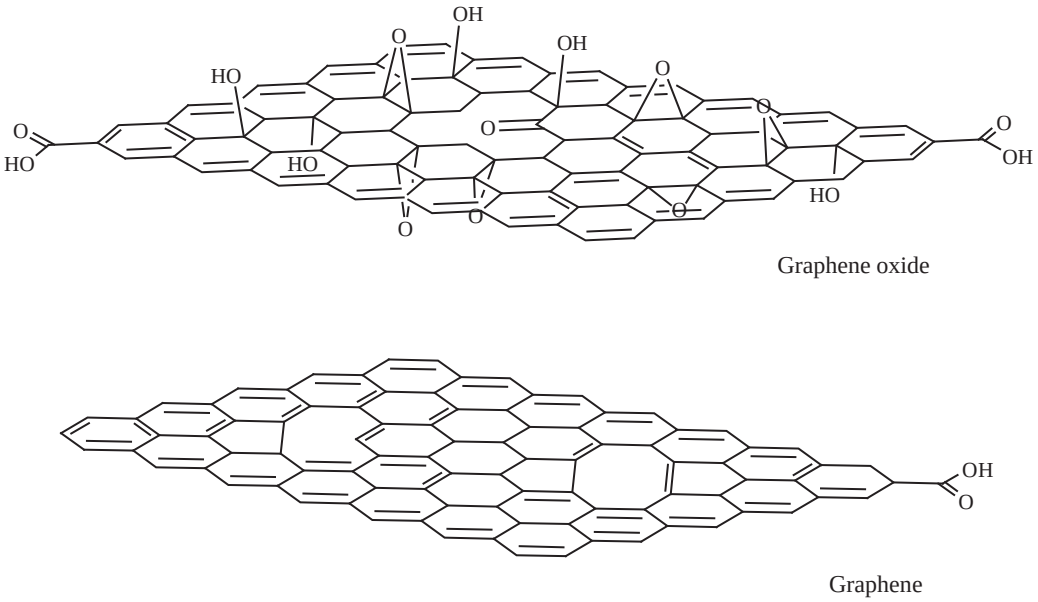

FIGURE 11.5 The structural difference between graphene and graphene oxide.

ratio, which provides a wide range of reactive surface-bound functional groups; high dispersibility in water and organic solvents; and ease of synthesis from graphite. Graphene oxide has the potential to be used in energy, molecular sensing areas, electronics, and catalysis, and as an agent for hyperthermia therapy. Both graphene and graphene oxide can be manipulated to produce a variety of novel biomaterials (Robinson et al., 2011).

Graphene oxide had been conjugated with PEG, which gave promising results in drug delivery and hyperthermia therapy under NIR laser field. It was found to be better than CNTs, but in comparison to CNT thermal ablation, the use of graphene oxide needed higher dose and higher NIR laser power because of the suboptimal absorption of NIR by graphene oxide (Robinson et al., 2011).

Recently nanographene oxide (NGO) was introduced to researchers of drug delivery and hyperthermia therapy. The hyperthermia agent NGO had shown superior sensitivity as compared with CNT under the same conditions (Zhang et al., 2011). Scientists had also produced pegylated NGO loaded with DOX (NGO−PEG−DOX) to deliver both heat and drug to the tumor cells; results of in vitro and in vivo studies of this functionalized biomaterial showed complete destruction of tumors without weight loss or recurrence of the tumor that was not accessible by the use of either DOX or NGO−PEG alone. Side effects of DOX were also reduced, so these results showed that the combination was superior as compared with chemotherapy or hyperthermia therapy alone (Zhang et al., 2011).

11.5.3 Gold Nanoshells

Gold nanoshells are nanospherical particles having a diameter that typically ranges from 10 to 200 nm and they are composed of a dielectric core mainly covered by a thin gold shell as shown in Fig. 11.6 (Erickson and Tunnell, 2009). They have a high ability to be used to detect and treat cancer because of their novel structure and their remarkable optical, physical, and chemical properties (Erickson and Tunnell, 2009). Due to their excellent physical characteristics, mainly thermal stability and benign toxicity profile, they are considered as one of the most important agents for biomedical applications (Erickson and Tunnell, 2009).

In particular, gold−silica nanoshell is composed of silica core covered by a thin layer of gold through seed-mediated growth formulation, where the silica core is attached to a "seed" of gold colloid, then additional gold is added to form the shell (Kennedy et al., 2011). In contrast to other gold nanostructures, the larger size of gold−silica nanoparticles provides an advantage in scattering based imaging but for drug delivery and for hyperthermia therapy it could be more challenging compared with smaller size particles. The size of the silica core and the thickness of the gold shell could be changed to span the resonance of these nanoshells from visible to NIR radiation (Kennedy et al., 2011).

Gold nanoshell was the first type of gold nanoparticle that is easily tunable to NIR (Erickson and Tunnell, 2009). Gold−silica nanoshells have been tested to treat human brain, liver, breast, and prostate cancer in vitro as a targeted therapy probe (Kennedy et al., 2011).

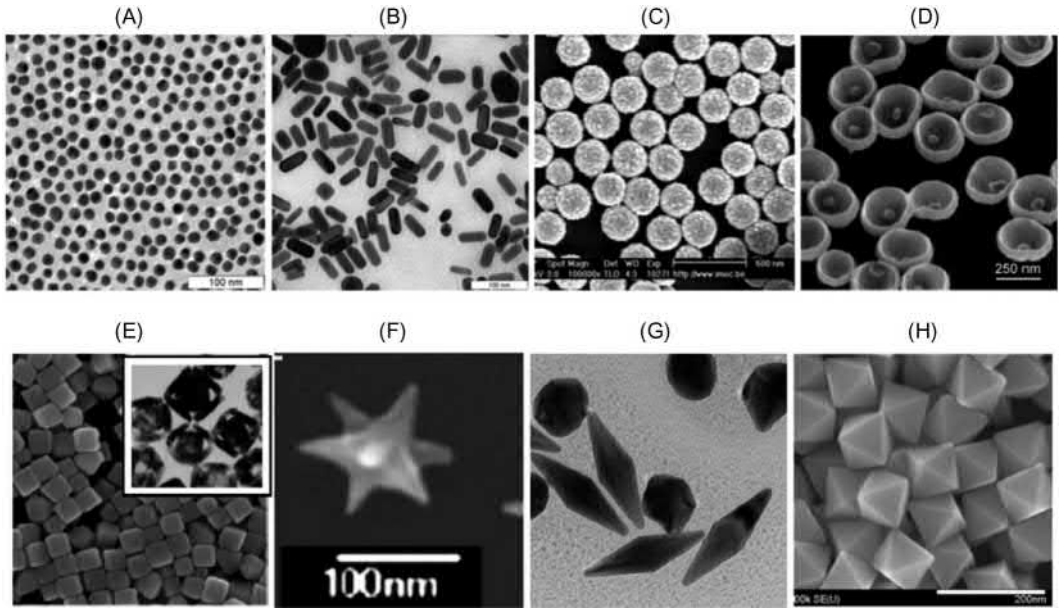

FIGURE 11.6 (A) TEM images of 15-nm colloidal gold, (B) 15 × 50-nm gold nanorods, (C) SEM 160(core)/17 (shell)-nm silica/gold nanoshells, (D) 250-nm gold nanobowls with 55-nm gold seed inside, (E) silver cubes and gold nanocages (inset), (F) nanostars, (F) bipyramids, and (H) octahedral. *SEM*, Scanning electron microscope; *TEM*, transmission electron microscope. Source*: Reprinted with permission from Khlebtsov, N.G., Dykman, L.A., 2010. J. Quant. Spectrosc. Radiat. Transfer, 111, 1–35 (Khlebtsov and Dykman, 2010).*

11.5.4 Gold Nanorods

Gold nanorods are biomaterials developed during the same period when gold nanoshells were developed. They show great potential for biomedical application due to their smaller size compared with gold nanoshells and they can also be easily synthesized (Fig. 11.6B). They also have high absorption coefficient especially within the NIR region where it is higher than other nanoparticles with narrow spectral bandwidths (Kennedy et al., 2011; Qiu et al., 2010; Huff et al., 2007).

Gold nanoparticles have been tested in vivo for the treatment of oral squamous cell carcinoma and colon cancer with promising results (Kennedy et al., 2011). During the hyperthermia process, gold nanorods can cause membrane breakdown, which in turn enhances the permeability, kinetics, and uptake of chemotherapeutic agents (Hauck et al., 2008).

Scientists found that the major challenge of using gold nanorods in hyperthermia therapy is their ability to change their conformation from nanorod shape into gold nanosphere under intense laser beam illumination, which leads to the loss of their absorption cross section efficiency under NIR region (Kennedy et al., 2011).

Gold nanorods have been covered with PEG to reduce the reshaping ability but results showed that during hyperthermia process PEG may either enhance or prevent reshaping, therefore coating with cetyltrimethylammonium bromide has been also tried and results showed enhanced heating efficiency, but caused reshaping of nanorods as well (Kennedy et al., 2011).

11.5.5 Gold Nanoparticles

Gold nanoparticles have been considered as an excellent agent for medical application based on the unique and high tunable optical properties provided by gold nanomaterials (Kennedy et al., 2011). Gold nanoparticles have been known for a long time because of their usage in the treatment of rheumatoid arthritis (Kennedy et al., 2011). It had been also used to deliver anticancer agents as well as an anticancer therapeutic agent. Gold nanoparticle with a diameter between 5 and 10 nm shows intrinsic antiangiogenic properties and they can bind to heparin-binding proangiogenic growth factors including VEGF165 and bFGF and inhibit their activity. Gold nanoparticles can inhibit the proliferation of multiple myeloma cells, and enhance apoptosis in chronic B cell leukemia (Cherukuri et al., 2010).

Gold nanoparticles have been introduced in the hyperthermia field as they can be easily synthesized with a well-defined structure, and they are nontoxic and able to respond to a variety of stimuli like RF, microwave, and visible light (Kabb et al., 2015; Dreaden et al., 2011).

During the initial in vivo testing of gold nanoparticles for hyperthermia therapy, direct intratumoral injection into subcutaneous tumors was given and it was very successful (Kennedy et al., 2011; Hirsch et al., 2003). Gold nanoparticles and gold nanomaterials are now administered systemically, where they are allowed to settle passively into the tumor after which the patient is subjected to the irradiation source like microwave, radio wave, or NIR laser (Kennedy et al., 2011; Hirsch et al., 2003).

After administration of nanoparticles, they undergo distribution throughout the body and tend to concentrate on tumor vasculature (Kennedy et al., 2011). Nanoparticles enter the tumor by passing from the blood through the fenestrations of the angiogenic tumor vasculature, which are malformed and more permeable in comparison to those supplying normal cells (Kennedy et al., 2011). So the passage of nanoparticles is dependent on the size of them and the tumor stage; the later the stage means larger and more permeable fenestrations. To optimize delivery and biodistribution as well as to ensure maximal nanoparticle accumulation within the tumor along with minimal accumulation in normal noncancerous cells, the smaller size of gold nanomaterials is preferred (Kennedy et al., 2011).

Like other nanoparticles, the selectivity of targeting could be enhanced by adding antibody or other molecules that corresponds with the targeted cancer cell type on the surface (Kennedy et al., 2011). In case of the usage of gold nanoparticle conjugates, coating them with biological agents enhanced their permeability and localization within tumor cells' endosomes, where the lower pH permits easy release and passage of the drug into its target (Sohail et al., 2017).

Here we will discuss different types of gold nanomaterials such as the smaller size of gold−gold sulfide (GGS) nanoparticles, hollow gold nanoshells (HAuNS), and gold colloidal nanospheres (Fig. 11.6), which give an advantage over larger gold nanoparticles in hyperthermia therapy.

11.5.5.1 Gold−Gold Sulfide Nanoparticles

GGS nanoparticles are described as either nanoparticles of a gold sulfide core with a thin layer coat of gold as a shell, or an aggregate of gold covered with thin coat of sulfur

on the surface with a diameter around 25 nm. They have been studied in vivo for thermal ablation of prostate cancer (Kennedy et al., 2011). These nanoparticles are applied simultaneously with a NIR laser for successful ablation therapy (Kennedy et al., 2011).

11.5.5.2 Hollow Gold Nanoshells

HAuNS are described as particles having hollow center covered with a thin layer of gold as a shell with a thickness of approximately 8 nm and diameter around 30 nm. They could be formulated by oxidizing a template of silver or cobalt followed by adding chloroauric acid and then used with NIR laser (Kennedy et al., 2011; Prevo et al., 2008; Schwartzberg et al., 2006).

HAuNS are conjugated with melanocyte stimulating hormone analogs for thermal ablation of xenografted subcutaneous murine melanoma tumors (Lu et al., 2009), or conjugated with antiepidermal growth factor receptor (EGFR) antibodies for thermal ablation of EGFR overproducing tumors (Melancon et al., 2008). Those agents could be conjugated to the hollow core of these nanoshells as other drugs and enzymes (Kennedy et al., 2011).

11.5.5.3 Gold Colloidal Nanospheres

Gold colloidal nanospheres are solid agents that were previously known as imaging probes, but because of their small size and simplicity of synthesis, they entered the hyperthermia field (Kennedy et al., 2011; El-Sayed et al., 2005; Boyd et al., 1986; Sokolov et al., 2003)

Although the absorbance peak of gold colloidal nanospheres is almost 530 nm, which belongs to the visible light region that makes it difficult to apply in vivo, thermal ablation using these particles had been applied by using NIR and visible wavelength (Kennedy et al., 2011; Abdulla-Al-Mamun et al., 2009; Li et al., 2009; Huang et al., 2007; El-Sayed et al., 2006).

Gold colloidal nanoparticles had been clustered or aggregated together to shift their absorbance from the visible region into the NIR region. The selectivity of these nanoparticles increased by this method, and has been approved after ablation of oral cancer cells by using 30 nm gold colloidal nanoparticles (El-Sayed et al., 2006). It had been observed that cancer cells were destroyed with 20 times lower laser power compared with noncancerous cells after the usage of gold colloidal nanoparticles clusters (Kennedy et al., 2011).

11.5.6 Magnetic Nanoparticles

Magnetic nanoparticles were introduced to the field of hyperthermia by a group headed by Andreas Jordan at Berlins Charité Hospital. This caused a lot of interest in the development two decades ago and they are still under improvement to date (Sohail et al., 2017). Hyperthermia that is induced through the usage of the magnetic nanoparticle is known as magnetic fluid hyperthermia. Fig. 11.7 shows the scanning electron microscope and transmission electron microscope images of magnetic nanoparticles (Alvarez-Berrios et al., 2013; Torres-Lugo and Rinaldi, 2013; Lee et al., 2011).

Magnetic nanoparticles are considered as an important tool for biomedical applications, especially for hyperthermia, because of their ability to react and to be modulated by the

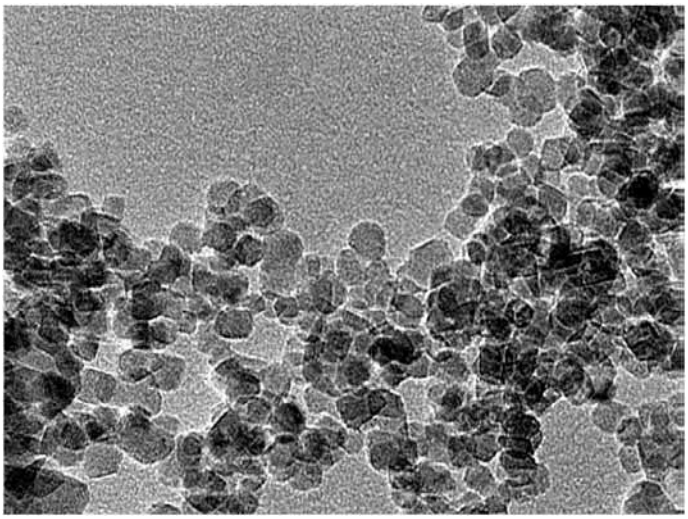

FIGURE 11.7 TEM image of iron oxide nanoparticles. *TEM*, Transmission electron microscope. Source*: Reprinted with permission from Chiemi, O., Kazunori, U., Nanao, H., Takeharu, T., Yoshitaka, K., 2015. Core–shell composite particles composed of biodegradable polymer particles and magnetic iron oxide nanoparticles for targeted drug delivery. J. Magn. Magn. Mater. 381, 278–284 (Chiemi et al., 2015).*

magnetic force, which gives them the potential to be used as a heating mediator in hyperthermia therapy (Sohail et al., 2017; McNamara and Tofail, 2015). Additionally, when magnetic nanoparticles are used as carriers they can enhance the drug penetration through the cancer cell membranes, thus they can avoid systemic administration and increase the therapeutic efficiency of the anticancer agents, as they are uptaken effectively by cancer cells while avoiding many side effects (McNamara and Tofail, 2015).

Magnetic hysteresis is done through magnetization/demagnetization cycles for heat generation using magnetic materials (Colombo et al., 2012; Wust et al., 2002; Tartaj et al., 2003). After administration of magnetic nanoparticle solution, the patient is subjected to alternating magnetic field, which causes Brownian rotation (rotation of the particles), internal reorientation, and Neel's relaxation (rotation of magnetic moment in the particle) of the nanoparticles, which leads to heat generation depending on the size of the nanoparticles as well as the strength of magnetic moment, and the resulted heat will deposit in the tissue that is adjacent to magnetic nanoparticles, raising its temperature above their normal degrees leading to cancer cell death (Fig. 11.8) (Alvarez-Berrios et al., 2014; McNamara and Tofail, 2015).

Magnetic nanoparticles can cause several cellular effects that can significantly enhance anticancer drug action and cell death; these cellular effects include an increase in membrane permeability, microtubule damage, and protein damage. The severity of these effects is temperature and time dependent (Fig. 11.9) (Alvarez-Berrios et al., 2014).

Magnetic nanoparticles are synthesized by several methods including coprecipitation method, microemulsifying, thermal decomposition, chemical vapor deposition, laser pyrolysis, solvothermal method, sonochemical, combustion, microwave-assisted, and carbon arc method (Sohail et al., 2017). Examples of magnetic nanoparticles that have been investigated for use in hyperthermia treatment of skin, breast, and cervical cancer are Fe–Co, Co–Fe_2O_4, Mn–Fe_2O_4, Ni–Co_2O_4, Fe–MgO, and Cu–Ni nanoparticles. Coating of all of these materials is required to ensure their biocompatibility and decrease

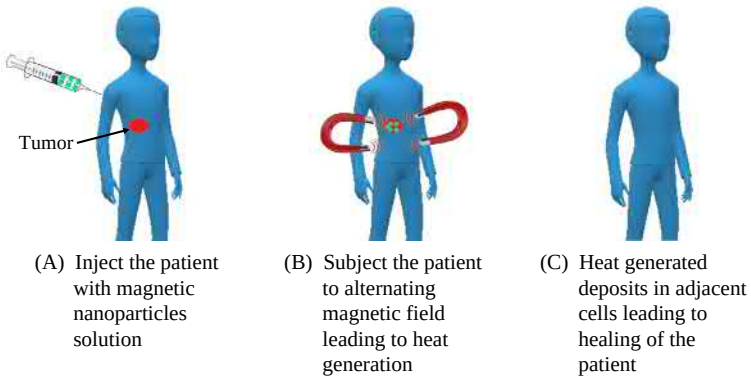
Tumor
(A) Inject the patient with magnetic nanoparticles solution
(B) Subject the patient to alternating magnetic field leading to heat generation
(C) Heat generated deposits in adjacent cells leading to healing of the patient

FIGURE 11.8 Representative figure of magnetic hysteresis steps.

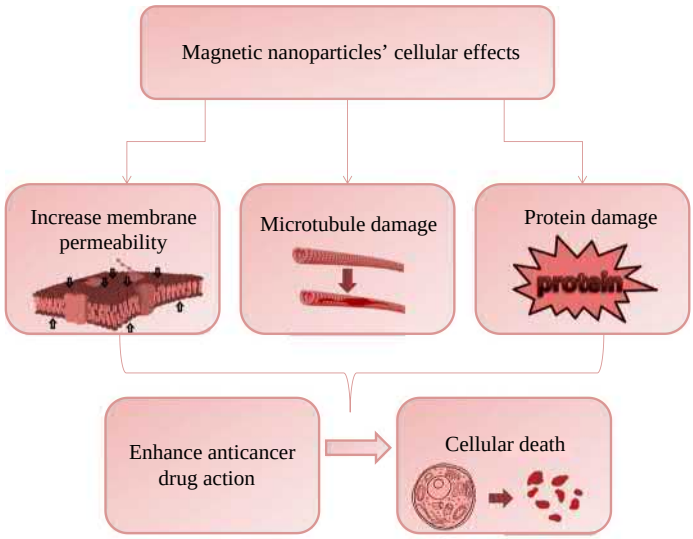

FIGURE 11.9 Schematic illustration of magnetic nanoparticles' cellular effects.

their agglomeration before being used for hyperthermia treatment (McNamara and Tofail, 2015).

When Cu−Ni nanoparticles were investigated the scientists found that they were able to be developed to have the desired Curie temperature for hyperthermia, which is 43°C−46°C (McNamara and Tofail, 2015). Curie temperature, also called Curie point, is the temperature at which certain magnetic materials undergo a sharp change in their magnetic properties (www.Britannica.com accessed on November 15, 2017). Scientists also found that Cu−Ni nanoparticles can be encapsulated in PEG to ensure their biocompatibility (McNamara and Tofail, 2015).

11.5.7 Iron Oxide Nanoparticles

Iron oxide nanoparticle is a type of magnetic nanoparticle that is widely investigated because of its promising properties such as the ease of synthesis, low cost, biocompatibility, and most importantly superparamagnetism (McNamara and Tofail, 2015). Although iron oxide nanoparticles are biocompatible, which makes them an efficient drug carrier for targeted therapy and for hyperthermia treatment, they are usually coated with biocompatible polymers, silica, or gold to protect them from oxidation before administration to patients for hyperthermia therapy. The oxidation tendency is higher with magnetite (Fe_3O_4), which is a mixed oxide of bivalent and trivalent iron that tends to oxidize, which is the most common form of iron oxide used (McNamara and Tofail, 2015; Sohail et al., 2017). Iron oxide nanoparticles are sometimes coated with a special coating to delay their recognition by the immune system, and thus prolong their half-life and ensure lower dose (Hergt et al., 1998).

Iron oxide nanoparticles have been investigated in vitro and in vivo for hyperthermia treatment of brain and breast tumors with promising results. The coated form of these nanoparticles has been tested clinically for brain and prostate tumor hyperthermia treatment. Scientists found that in hyperthermia iron oxide nanoparticles act by inducing cellular apoptosis, causing necrosis and inhibiting cellular growth; these effects are dependent on the concentration of iron oxide in the ferrofluid that is administered to the patients (McNamara and Tofail, 2015).

Superparamagnetic iron oxide nanoparticles are the most commercially available type of nanoparticles for hyperthermia treatment due to advantages like biocompatibility, magnetic ability, and their ability to be functionalized, although they are not the most efficient nanoparticles for heating in hyperthermia (McNamara and Tofail, 2015).

11.5.8 Silica Nanoparticles

Mesoporous silica nanoparticle (MSN) attracted a lot of interest in medical applications mainly as a drug or gene delivery agent because of its high surface area with the ability of surface fictionalization (Yang et al., 2013; Tao and Zhu, 2014). Fig. 11.10 represents field emission scanning electron microscopy images of silica nanoparticles (Naiara et al., 2017).

For hyperthermia therapy, MSN is usually conjugated with other materials to optimize their action, for example, MSN has been used to encapsulate magnetic nanoparticles to produce a platform for MRI as well as for chemotherapy and hyperthermia synergistic therapy with reduced risk (Tao and Zhu, 2014; Julián-López et al., 2007). A batch of γ-ferric oxide-mesoporous silica microspheres has been synthesized and tested for hyperthermia under low-frequency alternating magnetic field where it was able to provide sustained drug release and hence it may also be available for hyperthermia combined chemotherapy (Ruiz-Hernández et al., 2007). MSN has also been conjugated with gold nanorods in which gold nanorods serve as a heat generator to trigger drug release from MSN and induce hyperthermia (Liu et al., 2015). All MSN conjugates can be used for hyperthermia therapy either under NIR or magnetic field radiation (Yao et al., 2017).

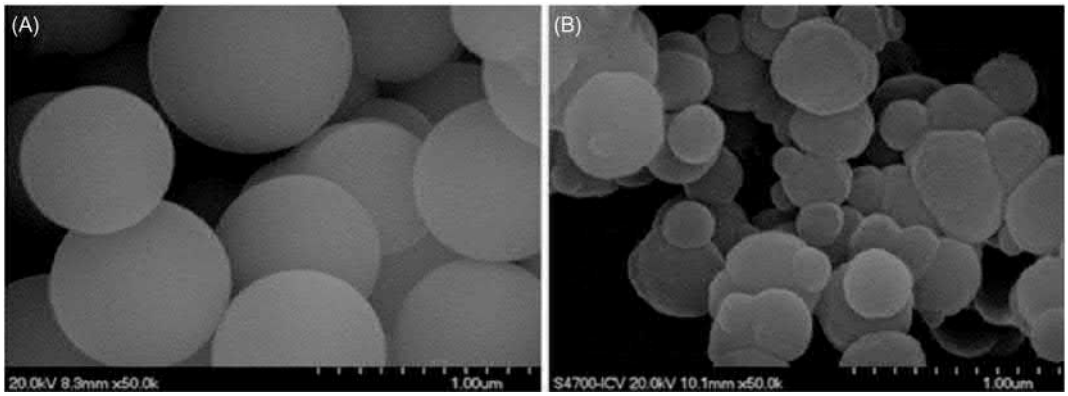

FIGURE 11.10 FESEM image of images of mesoporous silica particles (A) 0CTAB:45H_2O, (B) 0.1CTAB:45H_2O (Naiara et al., 2017). *CTAB*, Cetyltrimethylammonium bromide; *FESEM*, field emission scanning electron microscopy.

11.5.9 Small Molecules Used in Hyperthermia

There are many small molecules, in particular, organic dyes are being used in hyperthermia such as Indocyanine green (ICG), IR780, IR783, IR808, IR825, and PcBu4 as shown in Fig. 11.11. The following section will mainly discuss the importance of IR780 dyes in hyperthermia.

11.5.9.1 IR780 Dyes

Small organic NIR dyes (Fig. 11.11) were intensively synthesized and studied during the past decades for fluorescent imaging applications (because of their fluorescence emission) and as agents for hyperthermia due to their strong NIR absorbance in which it will be converted into heat; moreover their small molecular weight allows them to be excreted rapidly as a result of which the toxicity can be avoided (Song et al., 2014).

ICG as NIR dye is approved for clinical applications on patients by the United States Food and Drug Administration (FDA) and it has the ideal NIR absorption at 780 nm (Yang et al., 2013). But because of its concentration-dependent aggregation, its stability in aqueous solutions is limited, and also due to its low tumor specificity and nonspecific binding to proteins, nanocomplexes were formed to overcome those limitations (Song et al., 2014). Those nanocomplexes were synthesized through encapsulating, adsorbing, or covalently linking these dyes to liposomes, proteins, and most importantly micelles (Song et al., 2014).

ICG assembled with micelles generates a superior hyperthermic effect on cancer with sufficient efficacy, because of the fact that micelles can aid cellular uptake with efficient accumulation and retention within tumors with normal rapid elimination from nontumor cells (Yang et al., 2013). However, micelles themselves can facilitate photothermal damage of the tumor cells through destabilization of organelles (Yang et al., 2013). ICG has also

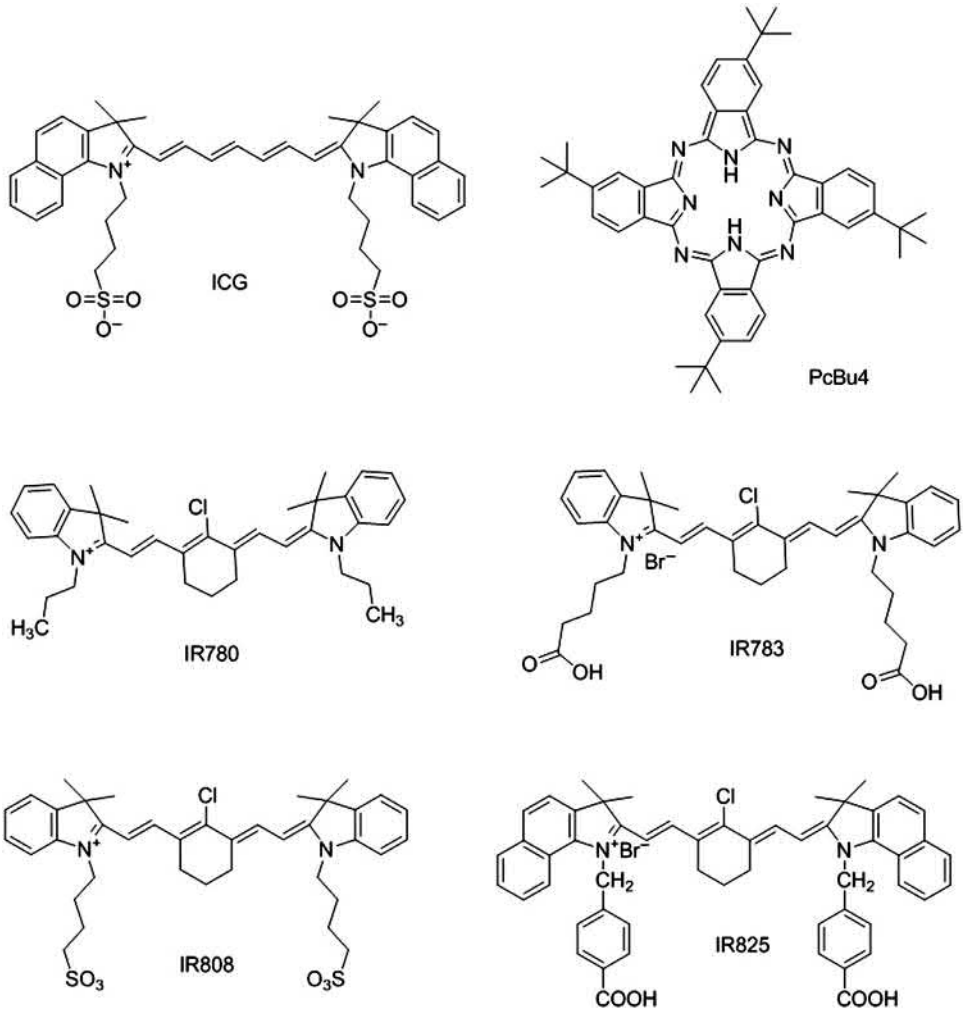

FIGURE 11.11 Some examples of organic NIR dyes. *NIR*, Near infrared.

assembled with phospholipid-PEG to enhance its stability with excellent hyperthermic tumor suppression efficacy (Song et al., 2014). This pegylated ICG micelles can be combined with chemotherapeutics like DOX to broaden their action to target multidrug-resistant tumors (Zheng et al., 2011).

IR780 have been assembled with heparin–folic acid conjugate to form heparin–folic acid-IR780 nanoparticles to target folate receptor-positive tumors under NIR laser irradiation hyperthermic therapy (Song et al., 2014). IR825 have been also assembled with PEG to form IR825–PEG nanoparticles with efficient tumor ablation under NIR with increased permeability and retention time (Song et al., 2014).

11.6 CROSSTALK ON VARIOUS APPLICATION AND USES OF HYPERTHERMIA

Hyperthermia can be generated through several methods to treat several illnesses alone or in combination (Mallory et al., 2016). Hyperthermia is an effective method for treating a wide range of tumors including brain, breast, head and neck, cervix, uterine, prostate, and even melanoma (Van der Zee, 2002; Gillette et al., 1992; Issels et al., 2010; Leopold et al., 1989a,b; Matsuda, 1993). Each of these diseases requires different thermal dose, for example, cancers in the central nervous system system are more sensitive compared with other tissues when it subjected to heat at 40°C–42°C for more than 40 minutes, while other types of tissues can tolerate heating for about 1 hour at 44°C (Mallory et al., 2016; Vernon et al., 1996).

11.6.1 Hyperthermia in the Treatment of Brain Tumor

A brain tumor is known to be difficult to treat as many chemotherapeutic agents can't cross the blood–brain barrier and radiotherapy can cause irreversible damage of normal brain cells because of which the survival percentage is almost 10%. So, there is a need for new treatment procedures to increase the percentage of survival, which include immunotherapy, gene therapy, and photodynamic therapy (Mahdavi et al., 2016; Cheng et al., 2013).

Hyperthermia has been introduced in brain tumor treatment in combination with radiotherapy and other techniques (Mahdavi et al., 2016). Combination therapy of hyperthermia–Navelbine and radiation gave positive results in increasing the therapeutic effect of Navelbine, hence lower doses can be used for the same purpose (Mahdavi et al., 2016). Photothermal therapy is hard to be applied because light can't penetrate skull bones, so light is applied during surgeries to the area of the tumor (Cheng et al., 2013).

Nanoparticles have been used for brain tumor hyperthermia therapy. Magnetic nanomaterials are known to cause hyperthermia under the alternative magnetic field, and silica–gold nanoshells have been investigated to treat glioma. RGD peptide is a biomaterial that is expressed in glioma, so it has been incorporated into some nanoparticles to induce their action, including gold nanoparticles and iron oxide nanoparticles. Titanium dioxide nanoparticles have been modified with anti-IL13Rα2 functionalized 3,4-dihydroxyphenilacetic acid to specifically target brain tumors (Cheng et al., 2013).

11.6.2 Hyperthermia in the Treatment of Breast Cancer

Breast cancer is one of the leading causes of death in women (Kikumori et al., 2009). Around 5%–10% of breast cancers diagnosed in the United States are locally advanced breast cancer (Vujaskovic et al., 2010). Patients with locally advanced breast cancer are at the risk for systemic diseases, so it is important to treat them efficiently, which has resulted in the development of many treatment strategies (Jones et al., 2004).

Hyperthermia is well known for the treatment of breast cancer (Mallory et al., 2016). The first use of hyperthermia in treating advanced primary and recurrent breast cancer

was from 1988 to 1991 with promising response of 59% of radiotherapy combined hyperthermia, but side effects were reported including brachial plexopathy, bone necrosis, and bone fracture associated with radiation injury (Vernon et al., 1996). Hyperthermia using RF is the most commonly used technique in the application of hyperthermia but there is a problem with a specificity of heating under RF electric field (Kikumori et al., 2009). To overcome this problem, magnetite nanoparticles have been used; in some studies, magnetic nanoparticles were combined with trastuzumab, which is a humanized monoclonal antibody that targets human EGFR-2 (hEGFR-2), which is overexpressed in breast cancer; thus enhanced targeting has been achieved with long lasting effect (Kikumori et al., 2009).

11.6.3 Cervical Cancer

Cervical cancer is the third most common cancer in women, causing 275,000 mortalities worldwide (Heijkoop et al., 2014). Hyperthermia is improving the local control and survival in patients with pelvic tumors in general (Van Der Zee et al., 2000; Mallory et al., 2016).

Hyperthermia has been considered as a standard method for treating cervical tumor since 1996. The standard therapy for cervical cancer is either platinum-based chemotherapy combined with hyperthermia for patients not treated with chemotherapy previously or hyperthermia combined radiotherapy for recurrent cases (Heijkoop et al., 2014; Wootton et al., 2011; Franckena and Van Der Zee, 2010; Van Der Zee et al., 2000; Harima et al., 2001; Datta et al., 2015; Sharma et al., 1989). Hyperthermia increases the uptake of cisplatin and its DNA adduct formation so hyperthermia combined with cisplatin has become standard therapy for recurrent cases (Heijkoop et al., 2014).

To apply hyperthermia to the uterine cervix intracavitary or interstitial RF electrode, catheter-based ultrasound devices or deep heating electromagnetic array are used (Diederich and Burdette, 1996; Diederich, 1996; Diederich et al., 2000; Wootton et al., 2011; Wust et al., 2002). Clinical hyperthermia delivery needs monitoring of heat to get favorable efficacy and toxicity, and the thermal dose should be increased with minimal temperature elevation (Wootton et al., 2011).

11.6.4 Melanoma

Melanoma is a typical cutaneous malignancy (Hulshof et al., 2010), which accounts for 5% of malignant tumors (Togni et al., 2009). Laser or cryoablation, simple surgical excision radiation therapy, and intralesional injection of biologically active agents are currently available strategies for the treatment of melanoma (Togni et al., 2009).

Hyperthermia combined with radiotherapy is one of the standard treatment strategies for melanoma. Hyperthermia application for melanoma has been proven to increase local control for melanoma (Hulshof et al., 2010). Isolated limb hyperthermia combined with TNF and melphalan gave a high rate of response (Hulshof et al., 2010).

11.6.5 Neck Cancer

Conventional treatment strategies have been used for years for treating neck cancer, but to decrease invasiveness of treatment, hyperthermia was introduced. Hyperthermia was used as palliative treatment to improve the patient's quality of life by decreasing the associated pain and preserving the patient's appearance and functions with avoidance of complex repetitive surgeries and reduction in procedural cost (Zhao et al., 2012).

53.3% of patients with head and neck cancer treated with hyperthermia in combination with radiotherapy totally survived with 5 years treatment compared with 0% of patients treated with radiotherapy alone due to the fact that hyperthermia can cause reoxygenation of hypoxic tumor tissues, which is known to cause radioresistance and chemoresistance. It should be noted that hypoxia causes chemoresistance because of inadequate blood perfusion (Datta et al., 2015; Huilgol et al., 2010; Valdagni and Amichetti, 1994; Mallory et al., 2016).

Hyperthermia combined with chemotherapy has also been used, and 55% patients of treated with hyperthermia and chemotherapy like cetuximab with radiotherapy have been survived totally with 3 years of treatment; adriamycin and bleomycin have been used in such treatment techniques too with favorable outcome (Huilgol et al., 2010). Iron oxide nanoparticles were used in local neck cancer hyperthermic treatment (Zhao et al., 2012)

11.6.6 Hyperthermia in the Treatment of Arthritis

Hyperthermia is used widely for motor system disorders in physical therapy (Takahashi et al., 2011). Hyperthermia is applied locally for arthritis physical rehabilitation in combination with therapeutic exercise. Heat causes increase in extensibility of collagen fibers and blood flow, acceleration in cellular metabolism, and gives an analgesic effect by increasing the pain threshold, which improves patient's daily life (Takahashi et al., 2011).

Hyperthermia is applied by RF method causing no structural modification on the treated area, but hyperthermia increases the production of HSPs involved in processes of chaperone-mediated autophagy, which is essential in the cellular homeostasis mechanism and so slows down the development of aging-related diseases including arthritis (Takahashi et al., 2011).

11.6.7 Hyperthermia in the Treatment of Wounds

Hippocrates once said, "Wounds love warmth; naturally, because they exist under shelter; and naturally they suffer from the opposite." People have treated wounds with hot packs since the beginning of medicine as heat can relieve pain and swelling (Rabkin et al., 1987), but when antibiotics were developed, the use of heat decreased, so it isn't used in large cutaneous lesions like cellulitis but is still considered for use in small ones (Rabkin et al., 1987).

Hyperthermia is known to increase oxygenation of tissues, which in turn is known to improve the inflammation associated with wounds so the application of local hyperemia therapy improves wound healing (Rabkin et al., 1987).

11.6.8 Hyperthermia in the Treatment of Pain

Patients with cancer are suffering from severe pain, which needs the use of narcotics or neurosurgical procedures for improvement. Unfortunately, narcotics are associated with lots of undesired side effects including loss of appetite, reduction of meaningful activity, and confinement to bed. Neurosurgical procedures are associated with fewer side effects but they represent an irreversible form of treatment (Estes et al., 1986).

RF hyperthermia used for treating patients with cancer is also known to decrease pain by increasing the pain threshold during the treatment (Takahashi et al., 2011).

11.7 HYPERTHERMIA COMBINED THERAPY

Nowadays, hyperthermia is significantly recommended for combination therapy because it can enhance immunity and immune response within the thermal range of 41°C−45°C (Rao et al., 2010).

11.7.1 Hyperthermia Combined Chemotherapy

Whole-body hyperthermia is usually combined with chemotherapy to target metastatic tumors and regional hyperthermia is applied with chemotherapy to target hypoxic tumors (Issels, 1999), and the application of the combination must be performed simultaneously (Datta et al., 2015).

Hyperthermia combined with chemotherapy will affect the sensitivity of the tumor to this technique without raising their associated side effects (Wust et al., 2002). When chemotherapeutic agents are to be used in combination with hyperthermia, it is better to be transformed into macromolecules by combining them with nanoparticles or liposome (Clavel et al., 2015). Magnetic nanoparticles are the most intensively used in this field where they are loaded with the chemotherapeutic agent and then functionalized with organic shells like cyclodextrin, dextran, or DNA and the agent is embedded with the shell (Tao and Zhu, 2014). Caelyx is an example of liposome loaded with adriamycin.

Hyperthermia can enhance the action of chemotherapeutics by increasing their uptake by tumors, and their accumulation weakens the cell (Rao et al., 2010), due to three mechanisms (Datta et al., 2015):

1. Hyperthermia can increase blood flow to tumors and oxygenation of tumors so the amount chemotherapeutic agent reaching to them increases (Datta et al., 2015), thus more drug can reach to the site of tumor, and so the dose may be decreased to minimize side effects of the chemotherapeutic agents and overcome chemoresistance (Wust et al., 2002; Issels, 1999). This is definitely beneficial especially for hypoxic tissues such as found in neck cancer because many chemotherapeutic agents are not effective on some tumors due to tissue hypoxia (Huilgol et al., 2010).
2. Hyperthermia inhibits DNA repair and hence play a key role in cell-damaging and enhancing the denaturation of cell proteins including cell membrane, thereby increasing the absorption of chemotherapeutic agents.
3. Hyperthermia blocks the cell cycle, so tumor cells are killed especially due to damaging G1 and S phases.

TABLE 11.2 The Interaction Between Heat and Chemotherapeutic Agents

The Interaction	The Chemotherapeutic Agents
Supraadditive	Alkylating agents platinum compound
Threshold behavior	Doxorubicin
Independent or additive	Fluorouracil, taxanes, vinca alkaloids

The effect of the combination of chemotherapy and hyperthermia varies according to the interaction between heat and the chemotherapeutic agent used, as shown in Table 11.2 (Wust et al., 2002).

As shown in Table 11.2, alkylating agents showed enhanced efficacy at a low temperature of 40.5°C for cyclophosphamide and nitrosourea and 41°C−43°C for cisplatin and all other platinum-based compounds (Datta et al., 2015; Issels, 1999), whereas 5-fluorouracil and other antimetabolites, taxanes, and Vinca alkaloid give the same effect whether in combination with hyperthermia or used alone (Datta et al., 2015).

11.7.2 Hyperthermia Combined Gene Therapy

Advanced cancers are difficult to treat, so use of combination therapy with them is critically important. In gene therapy combined with hyperthermia, mesenchymal stem cells (MSCs) are able to self-renew and differentiate into multiple cell lines even after systemic administration, thus including them in the treatment of cancer is an attractive alternative to conventional treatment strategies (Yin et al., 2016). Magnetic nanoparticles composed of highly magnetic zinc-doped iron oxide and mesoporous silica are used to deliver and activate heat-inducible gene vectors that induce the secretion of TNF from MSC, which leads to cellular apoptosis. After administration of these nanoparticles patients are subjected to mild magnetic hyperthermia (∼41°C) (Yin et al., 2016); these nanoparticles have been also applied to treat ovarian cancer (Yin et al., 2016).

Gene therapy is a method applied in many fields. The most important way to apply it is through controlling of gene expression (Ito et al., 2003). Suppression or induction of gene expression is needed according to the application; gene expression can be induced through radiation or heat shock (Ito et al., 2003). It is known that TNF can inhibit the growth of some human glioma cell types. TNF gene can be introduced to tumor cells under growth arrest and DNA damaged genes with hyperthermia can give extremely cytotoxic effect compared with ordinary effect when TNF is used alone (Ito et al., 2003).

HSPs are a group of proteins released when cells are under heat stress, so after hyperthermia therapy their amount within the targeted cells increases and facilitates their damage; based on that, some studies have been carried out to introduce HSP genes to tumor cells and then hyperthermia was applied, and a larger amount of HSP was produced, which enhanced patients' systemic immunity (Ito et al., 2003).

11.7.3 Hyperthermia Combined With Photodynamic Therapy

Photodynamic therapy is an approach developed to improve the efficacy and tolerability of drugs. Photosensitizers are agents developed for photodynamic therapy under clinical use; those agents can be encapsulated within magnetic nanoparticles and combined with liposomes to be combined with hyperthermia therapy to give dual therapy of photodynamic and hyperthermia (Di Corato et al., 2015)

11.8 CONCLUSIONS AND FUTURE PERSPECTIVES

Hyperthermia is an emerging therapeutic technique based on heating the target cells or tissue up to sufficient temperature to destroy them without affecting nearby normal cells. Hyperthermia is considered one of the promising choices not only for the treatment of cancer but also for arthritis, wounds, and pain. Several techniques have been employed for hyperthermia including superficial, whole-body, indocavity, deep, and part-body hyperthermia, respectively. Biomaterials are considered as excellent hyperthermia agents due to their significant thermal conductivity, high photothermal conversion efficacy, ability to accumulate inside tumor cells, and many other attractive properties.

Hyperthermia has been studied extensively but its clinical applications are still linked to trials and experiments. Recent technological advances aim to decrease operator dependence for hyperthermia application to provide more reproducible treatment and facilitate large-scale application of hyperthermia. 3D online hyperthermia therapy planning is now available, offering more consistent delivery. BSD Medical, Salt Lake City, UT has done many clinical trials that received FDA approval in 2011 for treating cervical cancer (Clavel et al., 2015; Franckena, 2012). Also, new systems are being developed for the real-time temperature monitoring with MRI, which was a hurdle previously (Bruggmoser et al., 2012).

New applications of hyperthermia include heat-controlled gene therapy and heat-enhanced immunotherapy; however, vaccinations must be studied and applied more. These applications rely on the principle that heat interferes with the regulation of cell cycle, DNA repair, and cell apoptosis (Wust et al., 2002). Thus, continuous research interest and technical advancement in hyperthermia may open up better therapeutic alternatives for the treatment of various diseases including cancer.

ABBREVIATIONS

BCR-ABL	breakpoint cluster region-Abelson
CNS	central nervous system
CNT	carbon nanotube
CTAB	cetyl trimethylammonium bromide
DNA	deoxyribonucleic acid
DOX	doxorubicin
EGFR	epidermal growth factor receptor
FDA	Food and Drug Administration
GGSNS	gold–gold sulfide nanoparticles
GHz	Gega hertz

HAuNS	hollow gold nanoparticles
HER2	human epidermal growth factor receptor 2
HIFU	high intensity focused ultrasound
HIPEC	hyperthermic intraperitoneal chemotherapy
HSP	heat shock protein
HWH	hot water hyperthermia
ICG	indocyanine green
IL	interleukin
MFH	magnetic fluid hyperthermia
MHC	major histocompatibility complex
MRI	magnetic resonance imaging
MSC	mesenchymal stem cell
MSH	melanocyte-stimulating hormone
MSN	mesoporous silica nanoparticles
NGO	nanographene oxide
NIR	near-infrared
PDGFR	platelet-derived growth factor receptor
PEG	polyethylene glycol
RBC	red blood cells
RF	radiofrequency
RNA	ribonucleic acid
SPOINS	superparamagnetic iron oxide nanoparticle
SWNTs	single-walled carbon nanotubes
TNF	tumor necrosis factor
UV	ultraviolet light
VEGFR	vascular endothelial growth factor receptor
WHO	World Health Organization

References

Abdulla-Al-Mamun, M., Kusumoto, Y., Mihata, A., Islam, M.S., Ahmmad, B., 2009. Plasmon-induced photothermal cell-killing effect of gold colloidal nanoparticles on epithelial carcinoma cells. Photochem. Photobiol. Sci. 8, 1125–1129.

Al-Qattan, M.N., Pran Kishore, D., Rakesh, K.T., 2018. Molecular dynamics simulation strategies for designing carbon nanotube-based targeted drug delivery. Drug Discov. Today 23 (2), 235–250.

Alvarez-Berrios, M.P., Castillo, A., Mendez, J., Soto, O., Rinaldi, C., Torres-Lugo, M., 2013. Hyperthermic potentiation of cisplatin by magnetic nanoparticle heaters is correlated with an increase in cell membrane fluidity. Int. J. Nanomed. 8, 1003–1013.

Alvarez-Berrios, M.P., Castillo, A., Merida, F., Mendez, J., Rinaldib, C., Torres-Lugo, M., 2014. Enhanced proteotoxic stress: one of the contributors for hyperthermic potentiation of the proteasome inhibitor Bortezomib using magnetic nanoparticles. Biomater. Sci. 3, 391–400.

Atmaca, A., Al-Batran, S.E., Neumann, A., Kolassa, Y., Jager, D., Knuth, A., et al., 2009. Whole-body hyperthermia (WBH) in combination with carboplatin in patients with recurrent ovarian cancer—a phase II study. Gynecol. Oncol. 112, 384–388.

Bahman, E., Song, C.W., 1984. Physiological mechanism in hyperthermia: a review. J. Radiat. Oncol. Biol. Phys. 10, 289–295.

Baronzio, G., Parmar, G., Ballerini, M., Szasz, A., 2014. A brief overview of hyperthermia in cancer treatment. J. Integr. Oncol. 3, 115.

Boissenot, T., Bordat, A., Larrat, B., Varna, M., Chacun, H., Paci, A., et al., 2017. Ultrasound-induced mild hyperthermia improves the anticancer efficacy of both Taxol and paclitaxel-loaded nanocapsules. J. Control. Release 28 (264), 219–227.

Boutros, C., Somasundar, P., Espat, N.J., 2010. Early results on the use of biomaterials as adjuvant to abdominal wall closure following cytoreduction and hyperthermic intraperitoneal chemotherapy. World J. Surg. Oncol. 8, 72.

Boyd, G.T., Yu, Z.H., Shen, Y.R., 1986. Photoinduced luminescence from the noble metals and its enhancement on roughened surfaces. Phys. Rev. B: Condens. Matter. 33 (12), 7923–7936.
Bruggmoser, G., Bauchowitz, S., Canters, R., Crezee, H., Ehmann, M., Gellermann, J., 2012. Guideline for the clinical application, documentation, and analysis of clinical studies for regional deep hyperthermia: quality management in regional deep hyperthermia. Strahlenther. Onkol. 188, 198–211.
Cheng, Y., Morshed, R., Auffinger, B., Tobias, A.L., Lesniak, M.S., 2013. Multifunctional nanoparticles for brain tumor diagnosis and therapy. Adv. Drug Deliv. Rev. 66, 42–57.
Cherukuri, P., Glazer, E.S., Curley, S.A., 2010. Targeted hyperthermia using metal nanoparticles. Adv. Drug Deliv. Rev. 62, 339–345.
Chichel, A., Janusz, S., Magda, K., Mark, K., 2007. Hyperthermia-description of a method and review of clinical applications. Rep. Pract. Oncol. Radiother. 12 (15), 267–275.
Chiemi, O., Kazunori, U., Nanao, H., Takeharu, T., Yoshitaka, K., 2015. Core-shell composite particles composed of biodegradable polymer particles and magnetic iron oxide nanoparticles for targeted drug delivery. J. Magn. Magn. Mater. 381, 278–284.
Clavel, C.M., Nowak-Sliwinska, P., Paunescu, E., Griffioen, A.W., Dyson, P.J., 2015. In vivo evaluation of small-molecule thermoresponsive anticancer drugs potentiated by hyperthermia. Chem. Sci. 6, 2795–2801.
Cole, J.R., Mirin, N.A., Knight, M.W., Goodrich, G.P., Halas, N.J., 2009. Photothermal efficiencies of nanoshells and nanorods for clinical therapeutic applications. J. Phys. Chem. C. 113 (28), 12090–12094.
Colombo, M., Carregal-Romero, S.S., Casula, M.F., Gutiérrez, L., Morales, M.P., Böhm, I.B., et al., 2012. Biological applications of magnetic nanoparticles. Chem. Soc. Rev. 41 (11), 4306–4334.
Compton, O.C., Nguyen, S.T., 2010. Graphene oxide, highly reduced graphene oxide, and graphene: versatile building blocks for carbon-based materials. Small 6, 711–723.
Datta, N.R., Ordonez, S.G., Gaipl, U.S., Paulides, M.M., Crezee, H., Gellermann, J., et al., 2015. Local hyperthermia combined with radiotherapy and-/or chemotherapy: recent advances and promises for the future. Cancer Treat. Rev. 41, 742–753.
Deatsch, A.E., Evans, B.A., 2014. Heating efficiency in magnetic nanoparticle hyperthermia. J. Magn. Magn. Mater. 354, 163–172.
Dewhirst, M.W., Viglianti, B.L., Lora-Michiels, M., Hanson, M., Hoopes, P.J., 2003. Basic principles of thermal dosimetry and thermal thresholds for tissue damage from hyperthermia. Int. J. Hyperthermia 19, 267–294.
Di Corato, R., Béalle, G., Kolosnjaj-Tabi, J., Espinosa, A., Clément, O., Silva, A.K.A., et al., 2015. Combining magnetic hyperthermia and photodynamic therapy for tumor ablation with photoresponsive magnetic liposomes. ACS Nano 9 (3), 2904–2916.
Diederich, C.J., 1996. Ultrasound applicators with integrated catheter-cooling for interstitial hyperthermia: theory and preliminary experiments. Int. J. Hyperthermia 12, 279–297.
Diederich, C.J., Burdette, E.C., 1996. Transurethral ultrasound array for prostate thermal therapy: initial studies. IEEE Trans. Ultrason. Ferroelectr. Freq. Control 43, 1011–1022.
Diederich, C.J., Nau, W.H., Burdette, E.C., Bustany, I.S., Deardorff, D.L., Stauffer, P.R., 2000. Combination of transurethral and interstitial ultrasound applicators for high-temperature prostate thermal therapy. Int. J. Hyperthermia. 16, 385–403.
Dou, J.P., Liang, P., Yu, J., 2016. Microwave ablation for liver tumors. Abdom. Radiol. 41, 650–658.
Dreaden, E.C., Mackey, M.A., Huang, X., Kang, B., El- Sayed, M.A., 2011. Beating cancer in multiple ways using nanogold. Chem. Soc. Rev. 40, 3391–3404.
Du, Q., Fu, C., Tie, J., Liu, T., Li, L., Ren, X., et al., 2015a. Gelatin microcapsules for enhanced microwave tumor hyperthermia. Nanoscale 7, 3147–3154.
Du, Q., Ma, T., Fu, C., Liu, T., Huang, Z., Ren, J., et al., 2015b. Encapsulating ionic liquid and Fe_3O_4. Nanoparticles in gelatin microcapsules as microwave susceptible. Agent for MR imaging-guided tumor thermotherapy. ACS Appl. Mater. Interfaces 7, 13612–13619.
El-Sayed, I.H., Huang, X., El-Sayed, M.A., 2005. Surface plasmon resonance scattering and absorption of anti-EGFR antibody conjugated gold nanoparticles in cancer diagnostics: applications in oral cancer. Nano Lett. 5, 829–834.
El-Sayed, I.H., Huang, X., El-Sayed, M.A., 2006. Selective laser photo-thermal therapy of epithelial carcinoma using anti-EGFR antibody conjugated gold nanoparticles. Cancer Lett. 239, 129–135.
Elkayal, H., Nour, I., Lotfy, M., 2015. Microwaves for breast cancer treatment. Alexandria Eng. J. 54 (4), 1105–1113.

Endrich, B., Zweifach, B.W., Reinhold, H.S., Intagleitta, M., 1979. Quantitative studies of microcirculation or microcirculator function in malignant tissue: influence of temperature on microvascular hemodynamics during the early growth of the BA-1112 rat sarcoma. Int. J. Radiat. Oncol. Biol. Phys. 5, 2021–2030.

Erickson, T.A., Tunnell, J.W., 2009. Gold nanoshells in biomedical applications. Nanomater. Life Sci. 3, 1–39.

Estes, N.C., Morphis, J.G., Homback, N.B., Jewell, W.R., 1986. Intraarterial chemotherapy and hyperthermia for pain control in patients with recurrent rectal cancer. Am. J. Surg. 152, 597–601.

Fajardo, L.F., Egbert, B., Marmor, J., Hahn, G.M., 1980. Effects of hyperthermia in a malignant tumor. Cancer 45 (3), 613–623.

Farma, J.M., Puhlmann, M., Soriano, P.A., Cox, D., Paciotti, G.F., Tamarkin, L., et al., 2007. Direct evidence for rapid and selective induction of tumor neovascular permeability by tumor necrosis factor and a novel derivative, colloidal gold-bound tumor necrosis factor. Int. J. Cancer 120, 2474–2480.

Franckena, M., 2012. Review of radiotherapy and hyperthermia in primary cervical cancer. Int. J. Hyperthermia 28, 543–548.

Franckena, M., Van Der Zee, J., 2010. Use of combined radiation and hyperthermia for gynecological cancer. Curr. Opin. Obstet. Gynecol. 22, 9–14.

Gannon, C.J., Patra, C.R., Bhattacharya, R., Mukherjee, P., Curley, S.A., 2008. Intracellular gold nanoparticles enhance non-invasive radiofrequency thermal destruction of human gastrointestinal cancer cells. J. Nanobiotechnol 6 (2), 1477–3155.

Geiger, M., Strnad, V., Lotter, M., Sauer, R., 2002. Pulsed-dose rate brachytherapy with concomitant chemotherapy and interstitial hyperthermia ion patients with recurrent head and neck cancer. Brachytherapy 1 (3), 149–153.

Gillette, S.M., Dewhirst, M.W., Gillette, E.L., Thrall, D.E., Page, R.L., Powers, B.E., et al., 1992. The response of canine soft tissue sarcomas to radiation or radiation plus hyperthermia: a randomized phase II study. Int. J. Hyperthermia 8 (3), 309–320.

Gu, L., Mooney, D.J., 2015. Biomaterials and emerging anticancer therapeutics: engineering the microenvironment. Nature Reviews Cancer 16, 56–66.

Harima, Y., Nagata, K., Harima, K., Ostapenko, V.V., Tanaka, Y., Sawada, S., 2001. A randomized clinical trial of radiation therapy versus thermoradiotherapy in stage IIIB cervical carcinoma. Int. J. Hyperthermia 17 (2), 97–105.

Hauck, T., Ghazani, A., Chan, W., 2008. Assessing the effect of surface chemistry on gold nanorod uptake, toxicity, and gene expression in mammalian cells. Small 4, 153–159.

Heijkoop, S.T., Van Doorn, H.C., Stalpers, L.J., Boere, I.A., Van Der Velden, J., Franckena, M., et al., 2014. Results of concurrent chemotherapy and hyperthermia in patients with recurrent cervical cancer after previous chemoradiation. Int. J. Hyperthermia 30, 6–10.

Hergt, R., Andra, W., d'Ambly, C.G., Hilger, I., Kaiser, W.A., Richter, U., et al., 1998. Physical limits of hyperthermia using magnetite fine particles. IEEE Trans Magn 34 (5), 3745–3754.

Hildebrandt, B., Wust, P., Rau, B., Schlag, P.M., Riess, H., 2000. Regional hyperthermia in rectal cancer. Lancet 356 (9231), 771–772.

Hirsch, L.R., Stafford, R.J., Bankson, J.A., Sershen, S.R., Rivera, B., Price, R.E., et al., 2003. Nanoshell-mediated near-infrared thermal therapy of tumors under magnetic resonance guidance. Proc. Natl. Acad. Sci. U.S.A. 100, 13549–13554.

Huang, X., Qian, W., El-Sayed, I.H., El-Sayed, M.A., 2007. The potential use of the enhanced nonlinear properties of gold nanospheres in photothermal cancer therapy. Lasers Surg. Med. 39, 747–753.

Huff, T.B., Tong, L., Zhao, Y., Hansen, M.N., Cheng, J.X., Wei, A., 2007. Hyperthermic effects of gold nanorods on tumor cells. Nanomedicine (London, England) 2 (1), 125–132.

Huilgol, N.G., Gupta, S., Dixit, R., 2010. Chemoradiation with hyperthermia in the treatment of head and neck cancer. Int. J. Hyperthermia 26, 21–25.

Hulshof, M.C., Van Haaren, P.M., Zum Vorde Sive Vording, P.J., Krishnadath, S., Marsman, W.A., Van Berge Henegouwen, M.I., et al., 2010. Radiotherapy combined with hyperthermia for primary malignant melanomas of the esophagus. Dis. Esophagus 23, E42–E47.

Idrees, M., Jebakumar, Z., 2014. A review on potential benefits of hyperthermia in the treatment of cancer. Acta Biomed. Sci. 1 (3), 98–104.

Issels, R., 1999. Hyperthermia combined with chemotherapy – biological rationale, clinical application, and treatment results. Onkologie 22, 374–381.

Issels, R.D., Lindner, L.H., Verweij, J., Wust, P., Reichardt, P., Schem, B.C., 2010. Neo-adjuvant chemotherapy alone or with regional hyperthermia for localised high-risk soft-tissue sarcoma: a randomized phase 3 multicentre study. Lancet Oncol. 11 (6), 561–570.

Ito, A., Matsuoka, F., Honda, H., Kobayashi, T., 2003. Heat shock protein 70 gene therapy combined with hyperthermia using magnetic nanoparticles. Cancer Gene Ther. 10, 918–925.
Jha, S., Sharma, P., Malviya, R., 2016. Hyperthermia: role and risk factor for cancer treatment. Achieve. Life Sci. 10, 161–167.
Jones, E.L., Prosnitz, L.R., Dewhirst, M.W., Kelly Marcom, P., Hardenbergh, P.H., Marks, L.B., et al., 2004. Thermochemoradiotherapy improves oxygenation in locally advanced breast cancer. Clin. Cancer Res. 10, 4287–4293.
Julián-López, B., Boissière, C., Chanéac, C., Grosso, D., Vasseur, S., Miraux, S., et al., 2007. Mesoporous maghemite–organosilica microspheres: a promising route towards multifunctional platforms for smart diagnosis and therapy. J. Mater. Chem. 17 (16), 1563–1569.
Kabb, C.P., Carmean, R.N., Sumerlin, B.S., 2015. Probing the surface-localized hyperthermia of gold nanoparticles in a microwave field using polymeric thermometers. Chem. Sci. 6, 5662–5669.
Kam, N.W., O'Connell, M., Wisdom, J.A., Dai, H., 2005. Carbon nanotubes as multifunctional biological transporters and near-infrared agents for selective cancer cell destruction. Proc. Natl. Acad. Sci. U.S.A. 102 (33), 11600–11605.
Kennedy, L.C., Bickford, L.R., Lewinski, N.A., Coughlin, A.J., Hu, Y., Day, E.S., et al., 2011. A new era for cancer treatment: gold-nanoparticle-mediated thermal therapies. Small 7 (2), 169–183.
Khlebtsov, N.G., Dykman, L.A., 2010. J. Quant. Spectrosc. Radiat. Transfer 111, 1–35.
Kikumori, T., Kobayashi, T., Sawaki, M., Imai, T., 2009. Anti-cancer effect of hyperthermia on breast cancer by magnetite nanoparticle-loaded anti-HER2 immunoliposomes. Breast Cancer Res. Treat. 113, 435–441.
Kluger, M.J., 1986. Is fever beneficial? Yale J. Biol. Med. 59, 89–95.
Kok, H., Wust, P., Stauffer, P., Bardati, F., Van Rhoon, G., Crezee, J., 2015. The current state of the art of regional hyperthermia treatment planning: a review. Radiat. Oncol. 10, 196–210.
Kou, G., Wang, S., Cheng, C., Gao, J., Li, B., Wang, H., et al., 2008. Development of SM5-1-conjugated ultrasmall super paramagnetic iron oxide nanoparticles for hepatoma detection. Biochem. Biophys. Res. Commun. 374, 192–197.
Landon, C.D., Park, J.Y., Needham, D., Dewhirst, M.W., 2011. Nanoscale drug delivery and hyperthermia: the materials design and preclinical and clinical testing of low temperature-sensitive liposomes used in combination with mild hyperthermia in the treatment of local cancer. Open. Nanomed. J. 3, 38–64.
Lee, J.S., Rodriguez-Luccioni, H.L., Mendez, J., Sood, A.K., Lpez-Berestein, G., Rinaldi, C., et al., 2011. Hyperthermia induced by magnetic nanoparticles improves the effectiveness of the anticancer drug cis-diamminedichloroplatinum. J. Nanosci. Nanotechnol. 11, 4153–4157.
Lee, S.Y., Ryu, K.H., Kang, M.S., Song, C.W., 1986. Effect of hyperthermia on the lactic acid and bet-hydroxybutyric acid content in the tumor. Int. J. Hyperthermia 2 (2), 213–222.
Leopard, K.A., Oleson, J.R., Pearson, D.C., Soper, J., Berchuck, A., Samulski, T.V., et al., 1993. Intraperitonial cisplatin and regional hyperthermia for ovarian carcinoma. Int. J. Radiat. Oncol. Biol. Phys. 27, 1245–1251.
Leopold, K.A., Harrelson, J., Prosnitz, L., Samulski, T.V., Dewhirst, M.W., Oleson, J.R., 1989a. Preoperative hyperthermia and radiation for soft tissue sarcomas: advantage of two vs one hyperthermia treatments per week. Int. J. Radiat. Oncol. Biol. Phys. 16, 107–115.
Leopold, K.A., et al., 1989b. Int. J. Radiat. Oncol. 16 (1), 107–115.
Li, J.L., Wang, L., Liu, X.Y., Zhang, Z.P., Guo, H.C., Liu, W.M., et al., 2009. In vitro cancer cell imaging and therapy using transferrin-conjugated gold nanoparticles. Cancer Lett. 274, 319–326.
Liang, P., Wang, Y., 2007. Microwave ablation of hepatocellular carcinoma. Oncology 72, 124–131.
Liang, X., Zhou, H., Liu, X., He, Y., Tang, Y., Zhu, G., et al., 2010. Effect of local hyperthermia on lymphangiogenic factors VEGF-C and -D in a nude mouse xenograft model of tongue squamous cell carcinoma. Oral Oncol. 46, 111–115.
Liu, T., Wang, C., Cui, W., Gong, H., Liang, C., Shi, X., et al., 2014. Combined photothermal and photodynamic therapy delivered by PEGylated MoS2 nanosheets. Nanoscale 6, 11219–11225.
Liu, T., Wei, Ye, Y., Zhu, A., Yang, Z., Fu, Y., Wei, C.Q., et al., 2015. Hyperthermia combined with 5-fluorouracil promoted apoptosis and enhanced thermotolerance in human gastric cancer line SGC-7901. OncoTargets Ther. 8, 1265–1270.
Long, D., Mao, J., Liu, T., Fu, C., Tan, L., Ren, X., et al., 2016. Highly stable microwave susceptible agents via encapsulation of Ti-mineral superfine powders in urea-formaldehyde resin microcapsules for tumor hyperthermia therapy. Nanoscale 8, 1144–1151.

Lu, W., Xiong, C., Zhang, G., Huang, Q., Zhang, R., Zhang, J.Z., et al., 2009. Targeted photothermal ablation of murine melanomas with melanocyte-stimulating hormone analog-conjugated hollow gold nanospheres. Clin. Cancer Res. 15, 876–886.
Lubner, M.G., Brace, C.L., Hinshaw, J.L., Lee, F.T., 2010. Microwave tumor ablation: mechanism of action, clinical results, and devices. J. Vasc. Intervent. Radiol. 8, S192–S203.
Ma, H., Jiang, C., Zhai, D., Luo, Y., Chen, Y., Lv, F., et al., 2016. A bifunctional biomaterial with photothermal effect for tumor therapy and bone regeneration. Adv. Funct. Mater. 26, 1197–1208.
Mahdavi, S.R., Yahyapour, R., Nikoofar, A., 2016. Cytotoxic effects of hyperthermia, chemotherapy (Navelbine) and radiation on glioma spheroids. Radiat. Phys. Chem. 123, 20–24.
Mallory, M., Gogineni, E., Jones, G., Greer, L., Simone II, C., 2016. Therapeutic hyperthermia: The old, the new and the upcoming. Crit. Rev. Oncol. Hematol. 97, 56–64.
Matsuda, H., Baba, K., Kitamura, K., Toh, Y., Ikeda, Y., Sugimachi, K., 1993. Hyperthermo-Chemo-Radiotherapy for patients with early carcinoma of the esophagus. Hepatogastroenterology 40, 217–221.
McNamara, K., Tofail, S.A.M., 2015. Nanosystems: the use of nanoalloys, metallic, bimetallic, and magnetic nanoparticles in biomedical applications. Phys. Chem. Chem. Phys 17, 27981–27995.
Melancon, M.P., Lu, W., Yang, Z., Zhang, R., Cheng, Z., Elliot, A.M., et al., 2008. In vitro and in vivo targeting of hollow gold nanoshells directed at epidermal growth factor receptor for photothermal ablation therapy. Mol. Cancer Ther. 7, 1730–1739.
Mohanraj, V.J., Chen, Y., 2006. Nanoparticles—a review. Trop. J. Pharm. Res. 5, 561–573.
Monotorsi, F., Guazzoni, G., Colombo, R., Galli, L., Bergamaschi, F., Rigatti, P., 1992. Transrectal microwave hyperthermia for advanced prostate cancer: long-term clinical results. J. Urol. 148 (2), 342–345.
Mustafa, T., Zhang, Y., Watanabe, F., Karmakar, A., Asar, M.P., Reginald Little, M., et al., 2013. Iron oxide nanoparticle-based radio-frequency thermotherapy for human breast adenocarcinoma cancer cells. Biomater. Sci. 1, 870–880.
Naiara, I.V., Zoilo, G., Begona, F., Yolanda, C., 2017. Synthesis of mesoporous silica nanoparticles by sol-gel as a nanocontainer for future drug delivery applications. Bol. Soc. Esp. Ceram. Vidr. 56, 139–145.
Nasseri, B., Yilmaz, M., Turk, M., Kocum, I.C., Piskin, E., 2016. Antenna-type radiofrequency generator in nanoparticle-mediated hyperthermia. RSC Adv. 6, 48427–48434.
Neumaier, C.E., Baio, G., Ferrini, S., Corte, G., Daga, A., 2008. MR and iron magnetic nanoparticles. Imaging opportunities in preclinical and translational research. Tumori 94, 226–233.
Otte, J., 1988. Hyperthermia in cancer therapy; a review. Eur. J. Pediatr. 147, 560–569.
Park, C.-J., Seo, Y.-S., 2015. Heat shock proteins: a review of the molecular chaperones for plant immunity. The Plant Path. J 31, 323–333.
Prevo, B.G., Esakoff, S.A., Mikhailovsky, A., Zasadzinski, J.A., 2008. Scalable routes to gold nanoshells with tunable size and response to near-infrared pulsed-laser irradiation. Small 4, 1183–1195.
Qiu, Y., Liu, Y., Wang, L., Xu, L., Bai, R., Ji, Y., et al., 2010. Surface chemistry and aspect ratio mediated cellular uptake of Au nanorods. Biomaterials 31, 7606–7619.
Rabkin, J.M., Hunt, T.K., 1987. Local heat increases blood flow and oxygen tension in wounds. Arch. Surg. 122 (2), 221–225.
Rao, W., Deng, Z.S., Liu, J., 2010. A review of hyperthermia combined with radiotherapy/chemotherapy on malignant tumors. Crit. Rev. Biomed. Eng. 38, 101–116.
Rice, L., Urano, M., Maher, J., 1982. The Kinetics of Thermotolerance in the Mouse Foot. Rad. Res 89 (2), 291–297.
Robinson, D., Parel, J.M., et al., 1998. Interstitial laser hyperthermia model development for minimally invasive therapy of breast carcinoma. J. Am. Coll. Surg. 186 (3), 284–292.
Robinson, J.T., Tabakman, S.M., Liang, Y., Wang, H., Casalongue, H.S., Vinh, D., et al., 2011. Ultrasmall reduced graphene oxide with high near-infrared absorbance for photothermal therapy. J. Am. Chem. Soc. 133 (17), 6825–6831.
Roussakow, S., 2013. The history of hyperthermia rise and decline. Conf. Pap. Med. 2013, 1–40.
Ruiz-Hernández, E., López-Noriega, A., Arcos, D., Izquierdo-Barba, I., Terasaki, O., Vallet-Regí, M., 2007. Aerosol-assisted synthesis of magnetic mesoporous silica spheres for drug targeting. Chem. Mater. 19, 3455–3463.
Schueller, G., Stift, A., Friedl, J., Dubsky, P., Bachleitner-Hofmann, T., Benkoe, T., et al., 2003. Hyperthermia improves cellular immune response to human hepatocellular carcinoma subsequent to co-culture with tumor lysate-pulsed dendritic cells. Int. J. Oncol. 22, 1397–1402.

Schwartzberg, A.M., Olson, T.Y., Talley, C.E., Zhang, J.Z., 2006. Synthesis, characterization, and tunable optical properties of hollow gold nanospheres. J. Phys. Chem. B 110 (40), 19935–19944.
Sharma, S., Patel, F.D., Sandhu, A.P., Gupta, B.D., Yadav, N.S., 1989. A prospective randomized study of localhyperthermia as a supplement and radiosensitizer in the treatment of carcinoma of the cervix with radiotherapy. Endocurietherapy/Hyperth. Oncol. 5, 151–159.
Shi, H., Niu, M., Tan, L., Liu, T., Shao, H., Fu, C., et al., 2015. Patterns of use of angiotensin-converting enzyme inhibitors/angiotensin receptor blockers among patients with acute myocardial infarction in China from 2001 to 2011: China PEACE-Retrospective AMI Study. Chem. Sci. 6, 5016–5026.
Shiyu, G., Min, Z., Xiaohua, R., Yaling, T., Xinhua, L., 2016. Local hyperthermia in head and neck cancer: mechanism, application, and advance. Oncotarget 7 (35), 57367–57378.
Shubhangi, M., Abhimanyu, P., Kaushik, K., Rahul, M., Pran Kishore, D., Kiran, K., et al., 2018. Functionalized carbon nanotubes as an emerging delivery system for the treatment of cancer. Int. J. Pharm. 548, 540–558.
Siemann, D. & Horsman, M. 2015. Modulation of the Tumor Vasculature and Oxygenation to Improve Therapy.
Simon, C.J., Dupuy, D.E., Mayo-Smith, W.W., 2005. Microwave ablation: principles and applications. Radiographics 25, S69–S83.
Sohail, A., Ahmad, Z., Bég, O.A., Arshad, S., Sherin, L., 2017. A review on hyperthermia via nanoparticle-mediated therapy. Bull. Cancer 104, 452–461.
Sokolov, K., Follen, M., Aaron, J., Pavlova, I., Malpica, A., Lotan, R., et al., 2003. Real-time vital optical imaging of precancer using anti-epidermal growth factor receptor antibodies conjugated to gold nanoparticles. Cancer Res. 63, 1999–2004.
Song, C.W., Kang, M.S., Rhee, J.G., Levitt, S.H., 1980. Effect of hyperthermia on vascular function, pH, and cell survival. Pathology 137, 795–803.
Song, X., Chen, Q., Liu, Z., 2014. Recent advances in the development of organic photothermal nano-agents. Nano Res. 8, 340–354.
Takahashi, K., Kurosaki, H., Hashimoto, S., Takenouchi, K., Kamada, T., Nakamura, H., 2011. The effects of radiofrequency hyperthermia on pain and function in patients with knee osteoarthritis: a preliminary report. J. Orthop. Sci. 16, 376–381.
Takeda, T., Takeda, H., Tanaka, C., Maruhashi, S., 2014. The effect of immunotherapy and hyperthermia for advanced or recurrent head and neck cancer-74 clinical cases. Gan To Kagaku Ryoho 41, 1283–1285.
Tan, L., Tang, W., Liu, T., Ren, X., Fu, C., Liu, B., et al., 2016. Biocompatible hollow polydopamine nanoparticles loaded ionic liquid enhanced tumor microwave thermal ablation in vivo. ACS Appl. Mater. Interfaces 8, 11237–11245.
Tang, W., Liu, B., Wang, S., Liu, T., Fu, C., Ren, X., et al., 2016. Doxorubicin-loaded ionic liquid–polydopamine nanoparticles for combined chemotherapy and microwave thermal therapy of cancer. RSC Adv. 6, 32434–32440.
Tao, C., Zhu, Y., 2014. Magnetic mesoporous silica nanoparticles for potential delivery of chemotherapeutic drugs and hyperthermia. Dalton Trans. 43, 15482–15490.
Tartaj, P., del Puerto Morales, M., Veintemillas-Verdaguer, S., Gonzalez-Carreno, T., Serna, C.J., 2003. The preparation of magnetic nanoparticles for applications in biomedicine. J. Phys. D: Appl. Phys. 36 (13), R182–R197.
Togni, P., Vrba, J., Vannucci, L., 2009. Water bolus influence on temperature distribution of applicator for small melanoma tumors. In: 2009 European Microwave Conference (EuMC), pp. 874–877.
Toraya-Brown, S., Sheen, M.R., Zhang, P., Chen, L., Baird, J.R., Demidenko, E., et al., 2014. Local hyperthermia treatment of tumors induces CD8+ T cell-mediated resistance against distal and secondary tumors. Nanomedicine 10, 1273–1285.
Torres-Lugo, M., Rinaldi, C., 2013. Thermal potentiation of chemotherapy by magnetic nanoparticles. Nanomedicine 8, 1689–1707.
Uysal, B., 2017. Hyperthermia and breast cancer: a short review. J. Radiol. Oncol. 1, 79–82.
Valdagni, R., Amichetti, M., 1994. Report of long-term follow-up in a randomized trial comparing radiation therapy and radiation therapy plus hyperthermia to metastatic lymph nodes in stage IV head and neck patients. Int. J. Radiat. Oncol. Biol. Phys. 28, 163–169.
Valentina, V.O., Tanaka, H., Miyano, M., Nishide, T., Nishide, H.U.I., Tanaka, Y., et al., 2005. Immune-related effects of local hyperthermia in patients with primary liver cancer. Liver 52 (65), 1502–1506.

Van Der Zee, J., González, D., Van Rhoon, G.C., Van Dijk, J.D.P., Van Putten, W.L.J., Hart, A.A.M., 2000. Comparison of radiotherapy alone with radiotherapy plus hyperthermia in locally advanced pelvic tumors: a prospective, randomized, multicentre trial. Lancet 355, 1119–1125.
Van der Zee, J., 2002. Heating the patient: a promising approach. Ann. Oncol. 13 (8), 1173–1184.
Verneris, M.R., Karimi, M., Baker, J., Jayaswal, A., Negrin, R.S., 2004. Role of NG2D signaling in the cytotoxicity of activated and expressed CD8 + T cells. Blood 103, 3065–3072.
Vernon, C.C., Hand, J.W., Field, S.B., Machin, D., Whaley, J.B., van der Zee, J., et al., 1996. Radiotherapy with or without hyperthermia in the treatment of superficial localized breast cancer: results from five randomized controlled trials. International Collaborative Hyperthermia Group. Int. J. Radiat. Oncol. Biol. Phys. 35, 731–744.
Vertess, R.A., Leeth, A., Girouard, M., Roach, J.D., Zwischenberger, J.B., 2002. Whole-body hyperthermia: a review of theory, design and application. Perfusion 17, 279–290.
Vidair, C.A., Dewey, W.C., 1991. Division-associated and division-independent hyperthermia cell death: comparison with other cytotoxic agents. Int. J. Hyperthermia 7, 51–60.
Vujaskovic, Z., Kim, D.W., Jones, E., Lan, L., Mccall, L., Dewhirst, M.W., et al., 2010. A phase I/II study of neoadjuvant liposomal doxorubicin, paclitaxel, and hyperthermia in locally advanced breast cancer. Int. J. Hyperthermia 26, 514–521.
Vulpen, M., Raamakers, B., Lagendijk, J., Crezee, J., Leeuw, A., 2002. Three dimensional controlled interstitial hyperthermia combined with radiotherapy for locally advanced prostate carcinoma-a feasibility study. Int. J. Radiat. Oncol. Biol. Phys. 53 (1), 116–126.
Wang, G., Gao, Z., Tang, S., Chen, C., Duan, F., Zhao, S., et al., 2012. Microwave absorption properties of carbon nanocoils coated with highly controlled magnetic materials by atomic layer deposition. ACS Nano 6, 11009–11017.
Wang, X., Liu, K., Yang, G., Cheng, L., He, L., Liu, Y., et al., 2014. Near-infrared light triggered photodynamic therapy in combination with gene therapy using upconversion nanoparticles for effective cancer cell killing. Nanoscale 6, 9198–9205.
Wootton, J.H., Prakash, P., Hsu, I.C., Diederich, C.J., 2011. Implant strategies for endocervical and interstitial ultrasound hyperthermia adjunct to HDR brachytherapy for the treatment of cervical cancer. Phys. Med. Biol. 56, 3967–3984.
Wright, A.S., Sampson, L.A., Warner, T.F., Mahvi, D.M., Lee, J.F.T., 2005. Pulmonary thermal ablation: comparison of radiofrequency and microwave devices by using gross pathologic and CT findings in a swine model. Radiology 236, 132–139.
Wust, P., Hildebrandt, B., Sreenivasa, G., Rau, B., Gellermann, J., Riess, H., et al., 2002. Hyperthermia in combined treatment of cancer. Lancet Oncol. 3 (8), 487–497.
Yanase, M., Shinkai, M., Honda, H., Wakabayashi, T., Yoshida, J., Kobayashi, T., 1998. Intracellular hyperthermia for cancer using magnetite cationic liposomes: an in vivo study. Cancer Sci. 89 (4), 463–470.
Yang, H., Mao, H., Wan, Z., Zhu, A., Guo, M., Li, Y., et al., 2013. Micelles assembled with carbocyanine dyes for theranostic near-infrared fluorescent cancer imaging and photothermal therapy. Biomaterials 34, 9124–9133.
Yao, X., Niu, X., Ma, K., Huang, P., Grothe, J., Kaskel, S., et al., 2017. Graphene quantum dots-capped magnetic mesoporous silica nanoparticles as a multifunctional platform for controlled drug delivery, magnetic hyperthermia, and photothermal therapy. Small 13 (2), 1602225.
Yin, P.T., Shah, S., Pasquale, N.J., Garbuzenko, O.B., Minko, T., Lee, K.-B., 2016. Stem cell-based gene therapy activated using magnetic hyperthermia to enhance the treatment of cancer. Biomaterials 81, 46–57.
Tang, Y., McGoron, A.J., 2013. Increasing the rate of heating: a potential therapeutic approach for achieving synergistic tumour killing in combined hyperthermia and chemotherapy. Int. J. Hyperthermia 29 (2), 145–155.
Zhang, W., Guo, Z., Huang, D., Liu, Z., Guo, X., Zhong, H., 2011. Synergistic effect of chemo-photothermal therapy using PEGylatedgraphene oxide. Biomaterials 32, 8555–8561.
Zhang, Y., Zhang, W., Geng, C., Lin, T., Wang, X., Zhao, L., et al., 2009. Thermal ablation versus conventional regional hyperthermia has greater anti-tumor activity against melanoma in mice by upregulating CD4 + cells and enhancing IL-2 secretion. Prog. Nat. Sci. 19, 1699–1704.
Zhao, Q., Wang, L., Cheng, R., Mao, L., Arnold, R.D., Howerth, E.W., et al., 2012. Magnetic nanoparticle-based hyperthermia for head & neck cancer in mouse models. Theranostics 2, 113–121.

Zheng, X., Xing, D., Zhou, F., Wu, B., Chen, W.R., 2011. Indocyanine green-containing nanostructure as near infrared dual-functional targeting probes for optical imaging and photothermal therapy. Mol. Pharmacol. 8, 447–456.
Zhu, L., Gao, X., Qi, R., Hong, Y., Li, X., Wang, X., et al., 2010. Local hyperthermia could induce antiviral activity by an endogenous interferon-dependent pathway in condyloma acuminate. Antiviral Res. 88, 187–192.

Further reading

Baeza, A., Guisasola, E., Ruiz-Hernández, E., Vallet-Regí, M., 2012. Magnetically triggered multidrug release by hybrid mesoporous silica nanoparticles. Chem. Mater. 24, 517–524.
Lu, S., Leasure, A., Dai, Y., 2010. A systematic review of body temperature variations in older people. J. Clin. Nurs. 19, 4–16.
Togni, P., Vrba, J., Vannucci, L., 2010. Microwave applicator for hyperthermia treatment on in vivo melanoma model. Med. Biol. Eng. Comput. 48, 285–292.

CHAPTER

12

Hyaluronic Acid as an Emerging Technology Platform for Silencing RNA Delivery

Kaushik Kuche, Pramina Kumari Pandey, Abhimanyu Patharkar, Rahul Maheshwari and Rakesh K. Tekade

National Institute of Pharmaceutical Education and Research (NIPER)—Ahmedabad, Gandhinagar, India

OUTLINE

12.1 Hyaluronic Acid: Emerging Technology Platform 416
12.1.1 History: A Brief Overview of Its Discovery 416
12.1.2 Properties and Features 417
12.1.3 Origin and Source of Hyaluronic Acid 418
12.1.4 Physiological Actions of Hyaluronic Acid 419
12.1.5 In Vivo Metabolism 419
12.1.6 Formulation Strategies for Hyaluronic Acid-Based Nanoplatforms 422

12.2 Introduction to RNA Interference 424
12.2.1 Structure of Silencing RNA 425
12.2.2 Silencing RNA Technology and Mechanism 426
12.2.3 Problems in the Delivery of Silencing RNA 428
12.2.4 Nanoparticles: The Salvager for the Silencing RNA Delivery 431

12.3 Hyaluronic Acid in Delivering Silencing RNA: Enhancing Target Specificity in Tumors 435
12.3.1 Role in Colon Cancer 437
12.3.2 Role in Ovarian Cancer 443
12.3.3 Role in Breast Cancer 445

12.4 Conclusion and Future Outlook 447

Acknowledgments 449

Abbreviations 449

References 450

Further reading 458

Biomaterials and Bionanotechnology
DOI: https://doi.org/10.1016/B978-0-12-814427-5.00012-3

© 2019 Elsevier Inc. All rights reserved.

12.1 HYALURONIC ACID: EMERGING TECHNOLOGY PLATFORM

Hyaluronic acid (HA) is a naturally occurring biodegradable, high molecular weight (105–107 Da) carbohydrate polymer named as hyaluronan. HA is basically a linear unbranched nonsulfated glycosaminoglycan (GAG) that possesses a repeating sequence of disaccharides [β-1,4-D-glucuronic acid (known as uronic acid) and β-1,3-*N*-acetyl-D-glucosamine], which are present in wide variety of species and has a wide sector of application. Regarding the structural interaction with water-based properties of HA, generally, when it is not bound to other molecules, it binds to water offering it a stiff viscous quality like Jello (Necas et al., 2008). HA is considered as a major element found in the extracellular matrix (ECM) of the vertebrate's animal tissues. Various body fluids like the vitreous humor of the eye, synovial fluid, and hyaline cartilage show a good level of HA (Falcone et al., 2006).

The body utilizes it in several important biological functions involving cell motility and regulation of cell, control of cell differentiation and proliferation, and implementing biomechanical properties of tissues (Shu et al., 2004). HA has also been described as a compatible biopolymer that can work as a scaffold, thereby bridging several other matrix molecules including aggrecan (Lam et al., 2014). Although, there are several issues like cytotoxicity associated with cross-linking techniques for scaffold fabrication and high viscosity of viscosupplements impede the development of products derived from HA. Hence, HA biomaterials for tissue engineering and enhanced properties of viscosupplements are in demand as well as viscosupplementation in the treatment of osteoarthritis, surgical aid in ophthalmology, and also in surgical wound regeneration in dermatology (Zhao et al., 2013).

Nanotechnology can be a pragmatic tool to address these needs (Lalu et al., 2017; Tekade et al., 2017a). In that context, HA is considered to be as the basic substrate for the following receptors: (1) CD44 (cluster of differentiation 44), (2) RHAMM (receptor for HA-mediated motility), and (3) intercellular adhesion molecule 1, thus by interaction with these receptors HA influences several cellular processes including morphogenesis, wound repair, inflammation, and metastasis (Cohen et al., 2009). Further, it is reported that HA is found during embryonic development, thereby pointing out that materials composed of HA may establish favorable conditions for tissue regeneration and growth (Collins and Birkinshaw, 2013). Currently, HA is being explored as a drug delivery agent for different routes such as nasal, pulmonary, ophthalmic, topical, and parenteral (Mero and Campisi, 2014). However, before getting into the applications of HA, it is recommended to have the gist of primary information related to HA, which will be described in the following sections, followed by its application in silencing RNA (siRNA) delivery.

12.1.1 History: A Brief Overview of Its Discovery

In 1934 Karl Meyer and his colleague John Palmer were the first investigators who discovered and isolated HA from the vitreous body of cows' eyes (Meyer and Palmer, 1934). Later the same group resolved the structure of the HA in the late 1950s; they declared that HA composed of two sugar molecules D-glucuronic was also known as

uronic acid and D-*N*-acetyl glucosamine and called it HA (hyaluronan). The word *hyalos* is Greek for "glass," and coupled with uric acid it led to the origination of the name "HA." The initially isolated HA behaved as salt in physiological conditions (Kim and Sykes, 2011). Soon after its discovery, it was first used as a substitute, in 1942. The preliminary biomedical application of HA took place in the late 1950s where it was utilized as a vitreous replacement for eye surgery. For medical applications, HA was primarily isolated from the umbilical cord and then from rooster combs (Shiedlin et al., 2004). Later on, there were further investigations done to obtain HA from other sources and characteristics of each were identified in detail in various laboratories (Kreil, 1995).

12.1.2 Properties and Features

HA is an ECM component, a high molecular weight GAG composed of disaccharide repeats of *N*-acetyl glucosamine and glucuronic acid. Thus this polymer is biocompatible and has an endogenous activity in the body and several chemical properties governing its type of action in the body.

12.1.2.1 Chemical Properties

Structural investigations revealed that two sugar molecules, D-glucuronic acid, and D-*N*-acetyl glucosamine, in the HA disaccharide structure are held together via alternate β-1,4 and β-1,3-glycosidic bonds (Tsepilov and Beloded, 2015). The backbone of HA is rigid, rather inflexible under physiological solution, and that is because of the chemical structure of the disaccharide, and the formation of certain internal hydrogen bond, which takes place due to interaction with solvents. The molecular investigations of HA indicated that the axial hydrogen atoms create a more polar face that is hydrophilic in nature and eventually leads to a twisted ribbon structure for HA, and is thus named as a coiled structure (Necas et al., 2008). Therefore the structural characteristics hooked onto this random coiled structure that is formed in solution.

At low concentration, chains tend to perplex with each other, leads to increase viscosity. Whereas, HA solutions with high concentration display more than the expected viscosity because of greater HA chain perplexities (entanglement), which are shear-dependent (Fakhari, 2012). Thus high molecular weight HA (>1000 kDa) generally behaves as a viscous fluid like jelly, but upon application of shear, the viscous fluid becomes shear thin and could be administrable with a needle. Thus such solutions are considered as having pseudoplastic nature. Other than the pseudoplastic behavior, another characteristic exhibited by HA is viscoelasticity, which is due to the self-association and entanglement of HA into random coils in solution (Mattheolabakis et al., 2015). It is predicted that self-assembly of HA nanoparticles is possible by forming parallel double helices, ropes, and bundles. The studies also propose that there could be hydrogen bonding between adjacent saccharides that may be adjacent to each other, and other interactions like electrostatic repulsion between carboxyl groups, thus establishing rigidity in the backbone (Burdick and Prestwich, 2011).

There were several evaluations done to observe the influence of several counterions on the rheological and hydrodynamic properties of HA. One such study done by Sheehan et al. (1983) explored the properties of HA solution with deionized water (D.I.), 0.5 M NaOH, and 0.5 M NaCl. The hydrodynamic radius of HA was obtained maximum in D.I. water followed by 0.5 M NaCl and 0.5 M NaOH. Thus results drawn from this investigation showed that specific changes in the properties of the solution bring about the changes in the electrostatic and hydrogen bonding properties of the solution with HA and eventually cause a change in the level of stiffness in HA (Garg and Hales, 2004).

12.1.2.2 Physiological Properties

It has been well established that HA performs various structural tasks in the ECM via a specific or nonspecific interaction with several biological components. There are several molecules such as neurocan, aggrecan, and versican, and many other receptors including RHAMM, CD44, LYVE-1, TSG6, and GHAP that usually interact with HA and bring out certain physiological actions via intracellular signal transduction. Out of the mentioned receptors, CD44 is the one that is being studied widely and has been a major area for researchers; along with CD44, another receptor that has been explored extensively is RHAMM, as both of them are associated with the metastases of carcinogenic tumors (Mele et al., 2017; Sironen et al., 2011; Toole, 2001; Yang et al., 2017). CD44 receptors are the primary receptor for HA, and structurally a glycoprotein that is expressed in many blood cells.

It has been studied that CD44 is responsible for regulating expression of genes in eosinophils, macrophages, endothelial cells, and other epithelial cells, but surprisingly the HA with low molecular weight can only cause the gene regulation and the HA with high molecular weight cannot (Jagannath and Ramachandran, 2010; Rayahin et al., 2015). Another intriguing fact is that HA has a vital role to play in case of curing of wounds and scar formation, but at the same time low molecular weight HA is observed to take part in the process of scar formation, and high molecular weight (HMW) HA tends to slow down the scar formation process. This observation clearly points out the importance of the molecular weight of HA and how crucial it is to consider the MW of HA for scar formation and wound healing (Choi et al., 2017; Neuman et al., 2015). Thus this study also shows that HMW HA is tentatively responsible for resting the cells and maintaining cell integrity, where the degradation of HA in small fragments leads to the generation of an inflammatory signal and also activates the respective response (Holstlaw et al., 2017; Neuman et al., 2015).

12.1.3 Origin and Source of Hyaluronic Acid

HA synthesis inside the cell is a highly controlled process; mainly the GAGs are synthesized inside the cell's Golgi body via various enzymatic processes. Specifically, cells present in tissues like cartilage and skin HA constitute a hefty chunk of the tissue mass. Thus HA synthesis tends to be high in these tissues. An integral membrane protein called hyaluronan synthase is the naturally available enzyme responsible for the synthesis of HA; it has subtypes HAS1, HAS2, and HAS3 (Lee and Spicer, 2000). The integral

membrane protein molecule is also regarded as the assembly of proteins that are mainly associated with or embedded into some biological membranes. Most of the time, the biological membrane is the plasma membrane onto which such proteins are associated or embedded as receptors, unlike those proteins that are dissolved in plasma or cytosol.

The synthesis of HA is the simultaneous addition of disaccharides or rather polymerization of disaccharides eventually yielding a polymer. The principal mechanism is the repetitive addition of glucuronic acid followed by *N*-acetyl glucosamine from the reducing end of sugar alternatively using Uridine diphosphate (UDP) glucuronic acid and UDP-*N*-acetylglucosamine as substrates. The molecular weight of one disaccharide (glucuronic acid-*N*-acetyl glucosamine) is roughly 400 D and length is 10 μm if measured linearly, which if compared is equal to that of the diameter of erythrocytes, and it is expected that in polymer the number of repeats could reach up to 10,000, which eventually takes the MW of HA to 4 million Da (Cowman and Matsuoka, 2005).

12.1.4 Physiological Actions of Hyaluronic Acid

There are several functions of HA. Not all have been understood completely, but the continuous and extensive clinical studies on HA have helped to understand a few. It has been observed that HA possesses some protective action and thus can be expected to show supplementary chondroprotective effects in the body thereby explaining its action on articular cartilage. When exposed for a longer period, HA showed protective effects on cartilage (Akmal et al., 2005; Huang et al., 2017).

The exogenously administered HA leads to the increase in HA content in chondrocytes, enhances the proteoglycan synthesis, and curtails the synthesis and the action of proinflammatory mediators and matrix metalloproteinase, which eventually revise the physiological actions of immune cells. Such functions demonstrate the role in oxygen scavenging action and inhibiting the adhesion of immune complexes to the blood cells (polymorphonuclear cells), thus leading to reticence of macrophage and leukocyte migration and aggregation (Kim et al., 2011) and the regulation of fibroblast proliferation, although many functions of the HA administered exogenously are molecular weight dependent (Rayahin et al., 2015).

It has been observed that HA is hygroscopic, which is considered essential for maintaining the hydration level and osmotic balance (Ashrafi et al., 2018; Dechert et al., 2006). Other than this HA also performs various signaling functions that involve surface receptor activation resulting in activation of several cascades of the signal that regulates migration, differentiation, cell proliferation, and gene expression. Thus HA is considered an essential component in embryo generation and carcinoma (Seton-Rogers, 2012).

12.1.5 In Vivo Metabolism

The in vivo metabolism of HA is considered to be a stepwise process that involves both enzymatic and nonenzymatic interaction. In enzymatic metabolism, there are three main enzymes: (1) hyaluronidase, (2) β-D-glucuronidase, and (3) β-*N*-acetyl-hexosaminidase involved and are also found in discrete form, in both intracellular regions, and in serum too. The enzyme hyaluronidase tends to break the glycosidic bond and is thereby

responsible for decreasing the molecular weight of HA, whereas the other enzymes are responsible for the degradation of HA fragments by the elimination of nonreducing terminal sugars (Stern et al., 2007; Volpi et al., 2009). It is interesting that enzymes not only get involved in the degradation of HA but also perform a vital role in exemplifying the HA action, like enzymes present in the cytosol region of the cell are basically involved in trimming of HA, which is required by HA to perform its basic biological process (Stern et al., 2007).

Considering nonenzymatic degradation, HA can be degraded due to either shear stress or thermal exposure; further exposure to certain chemical reactions involves acid/base catalyzed hydrolysis (Cho et al., 2017; Tokita and Okamoto, 1995) and oxidant based degradation (Burdick et al., 2005). It has been observed that the HMW HA will degrade slowly compared with that of low molecular weight HA when subjected to ultrasonication. Furthermore, whenever HA is exposed to ultrasonication, it tends to show random pathways for degradation. The temperature also has an inverse relation with the stability of HA; as we go on increasing the temperature, the viscosity goes on decreasing exponentially (Gibbs et al., 1968; Nicholls et al., 2018).

Similar to that in other polymers, HA is also sensitive toward acid and alkaline conditions. When the condition is acidic, the degradation occurs on glucuronic acid, whereas in the alkaline condition the hydrolytic degradation occurs on *N*-acetylglucosamine. Sometimes due to aerobic respiration there is generation of reactive oxygen species (ROS) like hydroxyl radicals, hypochlorite, and superoxide anions generated in the cells, which eventually leads to the degradation of HA. Such ROS are found to be vitally involved in various biodegenerative and inflammatory processes like arthritis (Esser et al., 2012). The schematic illustration of the entire in vivo metabolism of HA is well demonstrated in Figs. 12.1 and 12.2.

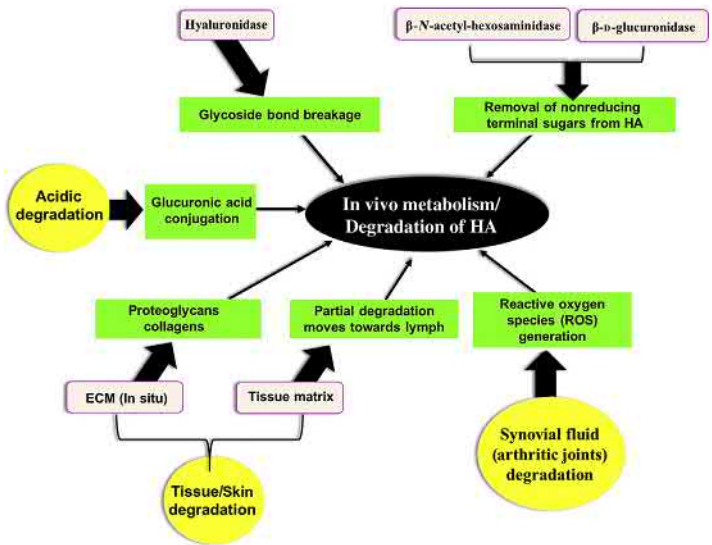

FIGURE 12.1 Scheme showing enzymatic metabolism/degradation of hyaluronic acid. The illustration briefly displays enzymatic degradation of HA along with other physiological sites like synovial fluid, liver, kidney lymph vessels, etc. where degradation of HA occurs at a prominent rate. *HA*, Hyaluronic acid.

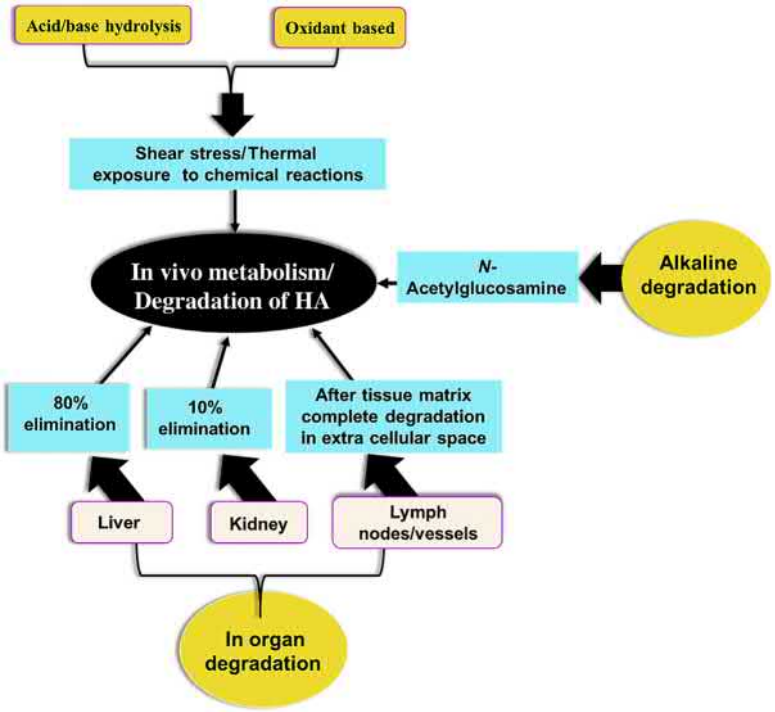

FIGURE 12.2 Scheme showing nonenzymatic metabolism/degradation of hyaluronic acid. The illustration briefly displays nonenzymatic degradation of HA along with other physiological sites like synovial fluid, liver, kidney lymph vessels, etc. where degradation of HA occurs at a prominent rate. *HA*, Hyaluronic acid.

As to the turnover and various possible pathways that are involved in elimination of HA in human body, the HA varies in different organs, starting from the highest containing sites like the umbilical cord (~4 g/kg) followed by 2–4 g/L in synovial fluid, nearly around 0.2 g/kg in dermis, and approximately 10 mg/L in thoracic lymph, although if we compare the concentration of HA in normal serum it is quite low, that is, 0.1–0.01 mg/L. Now depending upon the site where the HA is present, it determines its rate of metabolism. Through examination, it was concluded that the normal half-life of HA was around 1–3 weeks in inert tissues like joints, ligaments, bursae, cartilage, etc., and in the epidermis of the skin, the half-life observed was around 1–2 days, whereas only 2–5 minutes was observed in blood vessels (Hsieh et al., 2014). Other than the enzymatic and nonenzymatic degradation of HA there are two more significant pathways through which the degradation could occur, that is, internalization followed by degradation within the tissue, then release through the tissue matrix; another pathway is clearance through kidney, liver, and lymph nodes.

In the tissues where the lymphatic prevalence is quite low or scarce, like in the case of structural tissues, here the degradation of HA occurs in situ along with the other ECM molecules like proteoglycans and collagens. Approximately 50% of HA is present in skin, and since it mostly resides in the intercellular space, its half-life is longer, from several days to weeks (Volpi et al., 2009). Another route for the elimination of HA is via lymphatic

vessels, which drain the extracellular space of almost all the dense tissues. The process of HA degradation begins with the partial degradation of HMW HA in tissue matrix, after which it enters into the lymphatic system where the actual fragmentation or degradation of HA takes place (Fraser et al., 1997). Also, when the radiolabeled HA is administered via subcutaneous injection, the majority of HA is picked up by the lymphatic vessels, and the rest of the fragments continued to be in systemic circulation and eliminated via kidneys or sinusoidal epithelial cells of the liver. Out of the total circulation of HA in the body, almost 10% of HA from blood is eliminated by the kidney, and almost 80% is eliminated by the liver (Jeon et al., 2007).

As discussed earlier synovial fluid is the highest HA containing fluid in body, with 2−4 g/L of HA of MW of 6.5−7.5 MDa, in a healthy joint. For the healthy functioning of synovial fluids to provide proper lubrication and viscoelasticity, synoviocytes continuously secrete several macromolecules including HA. This continuous synthesis may sometimes lead to an increase in pressure in synovial joints. Thus to release that pressure, fluid is pushed out through microcapillaries embedded that are present around the synovium. Occasionally, HMW HA can progress to form a sheet at tissue−fluid called a shell, and thus cannot be drained out of the capillary. In case of arthritis, the level of HA goes down thereby inhibiting the normal function of synovial fluid; rather it has been reported that generation of ROS in arthritic joints degrades the HA (Jeon et al., 2007).

As HA has been extensively investigated for its in vivo compatibility, there are several nanoplatforms that have been developed (Cen et al., 2004). During our survey, we came across many reports wherein researchers have modified HA with several types of fatty acids, both linear and branched or with any lipophilic moiety (Ganesh et al., 2013b) that imparts amphiphilic property so that self-assembled nanovectors could be possible. Even several reports on cationization of HA were found to form complexes that can be employed as nanovectors (Liu et al., 2018). Thus such strategies are generally applied for preparing nanoplatforms using HA owing to its high biocompatibility.

12.1.6 Formulation Strategies for Hyaluronic Acid-Based Nanoplatforms

As mentioned, HA is hydrophilic in nature and under physiological conditions it shows a negative charge that is anionic nature, thus for the siRNA to be loaded they must be cationized with cationic polymers or any cationizing species (Al-Qadi et al., 2013; de la Fuente et al., 2008), which helps them to cross-link the HA to form nanoparticles. The species used are (1) adipic acid, (2) chitosan, (3) polyethyleneimine (PEI), and (4) Poly(amidoamine) (PAMAM) dendrimers; these not only help in cationization but also impart hydrophobicity onto the polymer, thus enabling self-assembly of HA nanoparticles. Another technique is via changing the suspension condition of HA, that is, changing ionic strength and pH of the electrolytic system containing HA. However, such particles would continue to be stable until they are exposed to these conditions; as conditions, change the particles lose their integral structure, hence chemical cross-linking with cationic species for self-assembled nanoparticles are more favored (Fakhari, 2012). The method of synthesizing HA nanoparticles using chemical cross-linking was explored less, but lately, there has been a rise in studies related to cross-linking of HA using various cross-linkers (Cho et al., 2003).

12.1.6.1 Desolvation Method

Desolvation is a common and rapid process of forming nanoparticles, and this phenomenon can also be observed in the case of atomic absorption spectroscopy. However, desolvation is a process wherein the polymer is completely dissolved in a primary solvent so as to form a homogeneous solution, then an antisolvent is added (a solvent or substance that has more solubility in primary solvent), which is more miscible with the primary solvent and thus displaces the polymer from the primary solvent under continuous agitation so as to get uniform-sized nanoparticles of the polymer.

The key process parameters here for getting uniform-sized particles are the rate and amount of antisolvent added, the rate of agitation, and MW of polymer used (Fonseca et al., 2017; Jun et al., 2011). Although plain HA cannot be solely used to form nanoparticles using desolvation, some modification to make it amphiphilic or by utilizing some cross-linkers like glutaraldehyde (Kutlusoy et al., 2017) and genipin (Nath et al., 2015) can assist the nanoparticle formation and stability via desolvation process.

Ghananeem et al. did one such study in which they created HA nanoparticle loaded with a drug wherein HA was first dissolved in water containing 2% Tween 20 at room temperature, then to completely solubilize HA the solution was heated to 40°C with stirring at 500 rpm. Then an organic phase of acetone containing the drug was poured into the above solution and then slowly the sodium sulfate solution was added dropwise until the solution went turbid indicating the formation of HA nanoparticles loaded with drug (paclitaxel). Further, glutaraldehyde was added as a cross-linker to prevent it from unwrapping followed by addition of sodium metabisulfite to terminate cross-linking and the particle size obtained with drug was in the range of 300 nm (Al-Ghananeem et al., 2009). Thus the authors developed much easier and effective method that can be employed for entrapping the free solubilized drug in the medium to get acceptable entrapment along with the desired size.

Discussing another method utilized by Figueroa et al. prepared cytochrome *C* and HA nanoparticles by simple desolvation method using acetonitrile and ethanol as a desolvating agent. Also, dithiobis(succinimidyl propionate) (DSP) was used as a cross-linker to prevent denaturation of particles formed (Figueroa et al., 2017).

Authors proposed that if the concentration of cross-linking agent increases, the size of the formed particles decreases as the same was observed with DSP concentration in case of HA-cyst C nanoparticles, that is, size was reduced from 542 ± 9 when DSP concentration was 3 mg/mL and the size was reduced to 504 ± 7 when DSP concentration was increased to 5 mg/mL. The formed nanoparticles showed cytotoxicity specifically toward A549 human lung adenocarcinoma cells, which overexpress HA receptor on their surface. Also, confocal microscopy proved the cytosolic delivery of cyst C, which proved to be an efficient model for cancer treatment (Figueroa et al., 2017). Thus desolvation could be a handy method for preparing HA nanoparticles with dynamic loading of the drug as well as biological therapeutics.

12.1.6.2 Self-assembling Hyaluronic Acid Nanoparticles

The self-assembling property in HA is not hereditary, thus, it can be imparted via specific modification done to the backbone of HA. Now there are several modifications

employed like fatty acids, cholesterol, bile acids, and oligomer. This makes HA an amphiphilic molecule that enables self-assembly.

One such study was performed by Vafaei et al. (2016) wherein the HA was modified using decaylamine, which is hydrophobic in nature, thereby imparting the self-assembling property, which led to the formation of particles of 173−293 nm in size. Also, modification with bioactive steroids also gives HA a self-assembling property as done by Quiñones et al. (2017), who conjugated HA with diosgenin and two brassinosteroids, that is, DI31 and S7, which led to formation self-assembled nanoparticles having a size range of 140−370 nm. Yet again, Choi et al. (2014) used cholesterol to impart the self-assembling property of HA and also to provide the hydrophobic core for the encapsulation of 2b RNA-binding protein and siRNA complex. Not only chemotherapeutic agents but also particles used as theragnostic agents can be prepared using HA as done by Lin et al. (2017) wherein they conjugated IR-780 with HA, which formed monodispersed nanospheres with a particle size of 170 nm, to show photothermal ablation in CD44 overexpressing cancer cells.

Furthermore regarding the theragnostic approach, Wang et al. (2017a,b) combined near-infrared (NIR) imaging and magnetic resonance imaging by forming HA-cyclodextrin conjugated biopolymer, which undergoes self-assembly when amantadine modified Gd-DOTAP and NIR cyanine dye Cy7 is brought in vicinity of the synthesized polymer with continuous stirring, thus creating an effective tumor imaging system with great potential for cancer diagnosis and treatment.

Although there are many such modifications possible that could be employed for desired effect and use, we found the majority of modifications to HA were done using PEI, dendrimers, adipic acid, and polyethylene glycol (PEG). PEI is nothing but an ethyl group with amine groups at both the carbons, which can be conjugated with a carboxylic acid group present on HA via EDC/NHS coupling. One study was done by Jiang et al. wherein PEI was conjugated with HA using EDC/NHS coupling reaction to cationize HA so that it could interact with negatively charged phosphate groups present on nucleic acids. Thus the cationized HA self-adheres around the siRNA to form 21-nm-sized nanoparticles that were able to deliver specifically toward CD44 overexpressing cancerous cells (Jiang et al., 2008).

Other than targeting cancer, drug resistance is yet another reason to worry. However, this problem was disentangled by Han et al. wherein doxorubicin-loaded PAMAM dendrimer was conjugated with HA and then self-assembled to form nanoparticles when incubated with major vault protein (MVP) siRNA. Thus such a dual delivery system could be efficiently utilized for delivering drugs to multidrug resistance (MDR) cancers caused due to MVP or *P*-glycoprotein (Pgp) mediated efflux (Han et al., 2012).

12.2 INTRODUCTION TO RNA INTERFERENCE

Gene silencing is nothing but the process of inhibiting the expression of certain genes and can be done at both the transcriptional and posttranscriptional level, and in the current scenario its use in therapeutics is booming for treating cancer, infection diseases, and neurodegenerative disorders (Tekade et al., 2015; Maheshwari et al., 2017).

There are several methods used for silencing a gene, that is, siRNA, RNA interference (RNAi), and CRISPR, which can lead to almost 65%−75% silencing of the gene and rather than complete silencing. There are three types of gene silencing: (1) transcriptional (Meister and Tuschl, 2004; Poulet et al., 2017), (2) posttranscriptional (Butel et al., 2017; Yu and Kumar, 2003), and (3) meiotic (Turner, 2015).

Moreover, the term *gene silencing* is nothing but an epigenetic method of regulating the gene. Silencing a gene means to switch off a gene without genetic modification and by turning off the machinery responsible for the gene transcription (TAT) and post-TAT (Yu and Kumar, 2003). The transcriptional silencing is brought about by altering the histone proteins thereby generating a heterochromatin environment and allowing the transcriptional machinery to access the gene. Similarly, in the case of posttranscriptional gene silencing there is blocking of mRNA, which eventually blocks the formation of active forms of the gene, that is, proteins; thus, this mechanism of posttranslational gene silencing is called RNAi (Chen et al., 2017; Murashov, 2010).

The term *RNAi* was previously called *cosuppression* and was first observed in transgenic plants from homology-dependent gene silencing process (Bernstein et al., 2001). As the work on RNAi technology progressed, it was observed that there was no RNAi activity seen upon delivery of sense and antisense strands; RNAi activity, that is, mRNA knockdown, was observed only upon delivery of dsRNA (double-stranded RNA) (Coffman et al., 2017; Fire et al., 1998).

RNAi is considered to be the most significant discovery in the field of molecular biology (Chen and Xie, 2012) and the discovery of nucleotides (NTs) silencing of approximately 22−25 bp termed as siRNA (small interference RNA) has been a groundbreaking discovery in the field of biology (Iki et al., 2017; Joseph et al., 2012). The mechanism of siRNA binding to the endogenous mRNA is being exploited in eukaryotic cells to inhibit the production of proteins at a posttranscriptional level, which is responsible for causing the diseased condition.

The asymmetric nature of siRNA duplex decides which strand would enter Dicer for RNA-interfering silencing complex (RISC) assembly induced mRNA breakdown. Several studies were conducted to verify the specificity of gene knockdown by siRNA and it was observed that selectivity was there but absolute specificity was absent (Chi et al., 2003; Jackson et al., 2003; Karikó et al., 2004); rather it was difficult to differentiate between an off-target effect, that is, knockdown of a wrong gene by siRNA. siRNA is considered to be an active intermediate formed when the long dsRNA is introduced in the cell followed by processing done by Dicer to form siRNA to guide RISC for mRNA degradation (Bantounas et al., 2004). The mechanism of miRNA is not exactly similar to that of siRNA but is almost similar.

12.2.1 Structure of Silencing RNA

Generally, siRNA is comprised of 20−22 bp that are double stranded with the phosphorylated group at 5′ end and the hydroxylated group at 3′ end with two extra unpaired NTs called an overhang region. Usually, the siRNA is formed by modification done to a long double-stranded siRNA by the DICER enzyme, which is an RNase type III

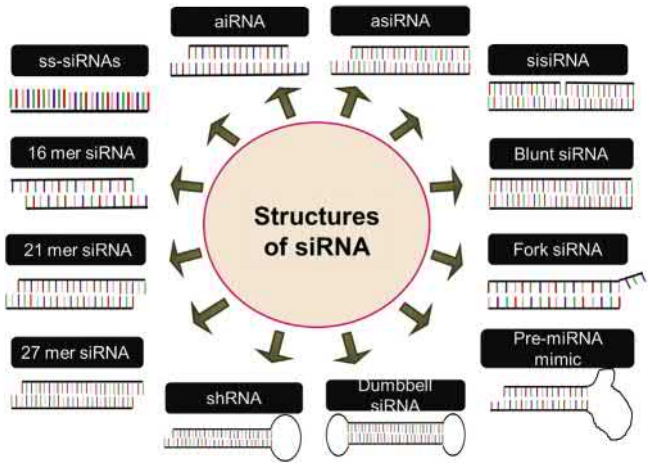

FIGURE 12.3 An illustrative diagram of several types of design of siRNA involved in gene therapy. *siRNA*, Silencing RNA.

endonuclease enzyme specific for dsRNA. Such siRNA could be administered exogenously to a cell by transfection or could be produced endogenously with the cell itself to regulate the epigenetic effects. Since the synthesis of synthetic siRNA is possible, use of such tools to silence any undesired gene is possible, hereby helping in resolving many diseases (Heale et al., 2005).

Due to the growing understanding of RNAi technology, a variety of siRNA types and design are available, and one can select the type depending upon individual need. The most widely used structure of siRNA is the design that mimics the dicer cleaved product comprising of 21 NTs with one RNA target and one passenger strand with 2–3 NTs at 3′ end call overhang region as shown in Fig. 12.3 (Elbashir et al., 2001a, 2001b).

Other designs like longer design type which includes moieties which mimics the Dicer substrates to increase its interference in RNA pathways (Takahashi et al., 2017). The shorter versions of siRNA are also gaining popularity, like 16-mer siRNA generally termed as shorter or truncated siRNA (Chu and Rana, 2008), short hairpin RNA (shRNA) with stem (containing $\leq$19 bp) (Siolas et al., 2005), blunt siRNA (with 19 bp) (Anton et al., 2017), asymmetrical siRNAs (siRNA) (Li, 2017), and asymmetric shorter-duplex siRNA (asiRNA) (Kim et al., 2017).

The very recent forms of siRNA therapeutics like fork siRNA, single-stranded siRNA (ss-siRNA), and dumbbell-shaped circular siRNA, bulge siRNA, and si-siRNA are yet to qualify for their clinical application and thus require extensive and long-term investigation to be used as a therapeutic agent. Thus out of the several mentioned designs of siRNA, the most widely used designed is the 21 mer siRNA. The mechanistic outlook of siRNA is well described in the preceding sections of this chapter.

12.2.2 Silencing RNA Technology and Mechanism

The siRNA could be present in the cell either endogenously by the process of TAT of both sense and antisense strand done from the same loci, or could be exogenously injected

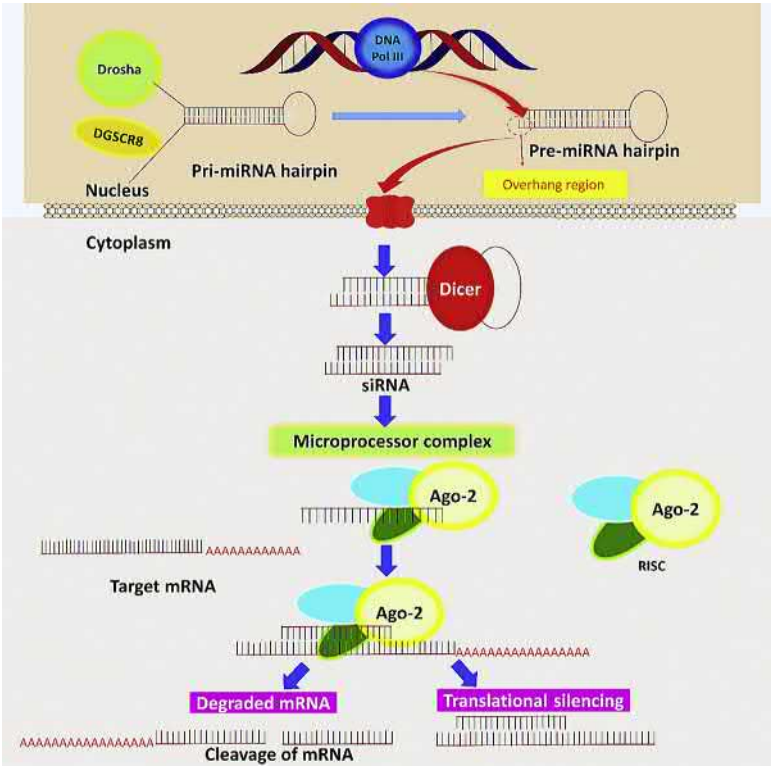

FIGURE 12.4 Schematic illustration genetic regulation of mRNA levels. Primarily the Pri-miRNA hairpin is converted to pre-miRNA by Drosha and DGSCR8, which then enters cytosol from the nucleus and is converted to siRNA by Dicer. Further microprocessor complex is formed upon binding of RISC, which causes silencing of targeted mRNA. *DGSCR8*, Di George Syndrome Critical Region 8; *RISC*, RNA-interfering silencing complex; *siRNA*, silencing RNA.

or transfected into the cell (Hou et al., 2013; Jensen et al., 2014). Now the dsRNA for silencing could be originated from any of the forms like hairpin loop-like or complementary RNA formed by RNA polymerase II, and thus called as the Pri-miRNA, which consists of 100−120 NTs. This long Pri-miRNA is recognized by a protein called Di George Syndrome Critical Region 8, which positions the endonuclease domain of Drosha (RNase endonuclease III enzyme) onto Pri-miRNA, and this complex formed is called a microprocessor complex, which then cleaves Pri-miRNA to form shRNA or pre-miRNA hairpins, which are dsRNA with one helical turn and 2 NT overhang region at 3′ prime end as shown in Fig. 12.4 (Bobbin et al., 2015).

The pre-miRNA hairpins can be spliced or transcribed from introns by RNA polymerase III, thus surpassing the formation of the microprocessor complex and are termed as mirtrons. These are then exported out of the nucleus into the cytoplasm through Exportin-5, which recognizes the pre-miRNA hairpin from the 2-NT overhang region. Once the pre-miRNA enters the cytoplasm, it is loaded onto Dicer (RNase III enzyme specific for dsRNA) (Kim et al., 2016; Lund and Dahlberg, 2006), which cleaves off the loop joining the 3′ and 5′ arms to form the siRNA. Once the siRNA is formed, it gets integrated with a protein complex named as RISC which is a complex formed of argonaute-2 (Ago2) and certain silencer proteins.

Ago2 is an RNase H type of endonuclease enzyme that hydrolytically cleaves only one strand and not both. Once the assembly is set then the PAZ domain of Argonaute-2 (Ago2)

(named because of the protein constituents like PIWI, AGO, and Zwille) attached to the 3′ end strand of siRNA acts as the guide strand, whereas the PIWI domain of Ago2 is responsible for cleaving and releasing the passenger strand. The RISC complex is then guided toward the mRNA as the guide strand is complementary to the mRNA that is to be silenced. Thus it leads to degradation of target mRNA or leads to transitional silencing, which provides the therapeutic effect.

12.2.3 Problems in the Delivery of Silencing RNA

As siRNA is considered as the potential therapeutic candidate, there are many more essential aspects that have kept siRNA away from clinical acceptance as mentioned in Table 12.1.

The exogenously administered siRNA could create competitive inhibition for endogenously present miRNA in processing pathways, thus resulting in several cytotoxicities, like hepatotoxicity (Kasuya et al., 2016). RNA can sometimes also activate certain inflammatory secretions in which the dsRNA that are longer in size possess higher tendency to stimulate the release of interferons by activating the machinery equipped for tackling viral pathogens, whereas the small dsRNA does not show such action (Tekade et al., 2015; Wang et al., 2010).

The stimulation of immune system via siRNA could be invalidated by adding guanosine or 2′-*O*-methyl uridine NTs in either of the siRNA strands (Judge et al., 2005, 2006). However, the most problematic issue with siRNA in its utility for therapeutics is deliverance at the therapeutic site because of their unfavorable properties as they possess negative charge, size of siRNA, the molecular weight of siRNA, short half-life, and endosomal degradation (Tekade et al., 2015, 2016). All of these factors are decrease the therapeutic efficiency of siRNA. Several factors that circumvent the siRNA delivery to target are well illustrated in Fig. 12.5.

Generally when naked siRNA is administered for in vivo delivery it is usually subjected to degradation and siRNA loaded carriers also have a tendency to liberate siRNA, and as siRNA are negatively charged, the carrier complex also tends to get eliminated from the body rapidly when compared with cationic or neutral particles (Buyens et al., 2008, 2012; Turner et al., 2006). Thus this issue points out the need for surface modification, and amongst many the most widely used surface modification is PEGylation, as PEGylation not only imparts stability but also imparts hydrophilicity thus making them difficult to be uptaken by reticuloendothelial system (RES) cells and also drastically decreasing the level of opsonization (Li et al., 2008; Tang et al., 2012).

Once locating the siRNA to the desired target, the siRNA-carrier complex undergoes extravasation, which is governed either by the makeup of the endothelial cells or depends on osmotic and hydrostatic pressure developed between blood vessels and interstitial space so that siRNA and the siRNA-carrier complex can diffuse through them (Wang et al., 2010). Thus the vascular endothelial surface also acts as a barrier that needs to be overcome by the siRNA-carrier complex to deliver the siRNA specific to an organ or tissue. Broadly the endothelium in a blood vessel can be classified as continuous (observed in normal arteries, arterioles, capillaries), fenestrated (observed in digestive mucosa), and

TABLE 12.1 Clinical Trials Involving Silencing RNA (siRNA) for Cancer Therapy

Name (Company)	Vehicle	Targeted Gene	Conditions	Clinical Trial Stage	ClinicalTrials.gov Identifier	Year
APN401 (Apeiron biologics)	PBMCs	E3 ubiquitin ligase Cbl-b	Multiple cancers	Phase I (completed)	NCT03087591	2017
DCR-MYC (Dicerna Pharmaceuticals)	LNP	Oncogene MYC	Solid tumors, multiple myeloma, non-Hodgkins lymphoma, pancreatic neuroendocrine tumors	Phase I (terminated)	NCT02110563	2014
DCR-MYC (Dicerna Pharmaceuticals)	LNP	MYC gene	Hepatocellular carcinoma	Phase I/II (terminated)	NCT02314052	2014
siRNA-EphA2-DOPC (M.D. Anderson Cancer Center and Cancer Prevention Research Institute of Texas)	Neutral Liposome (DOPC)	EphA2	Advanced cancer	Phase I (Recruiting)	NCT01591356	2012
siG12D LODER (Silenseed)	Biodegradable polymeric matrix	KRAS oncogene	Pancreatic ductal adenocarcinoma, pancreatic cancer	Phase I (completed)	NCT01188785	2011
TKM-080301 (Arbutus Biopharma)	LNP	PLK1 gene	Liver cancer	Phase I/II (completed)	NCT01437007	2010
Atu027 (Silence Therapeutics)	Liposome (cationic, AtuPlex)	Protein Kinase N3 (PKN3)	Advanced solid tumors	Phase I (completed)	NCT00938574	2009
ALN-VSP02 (Alnylam Pharmaceuticals Inc.)	LNP	KSP and VEGF	Solid tumors	Phase I (completed)	NCT00882180	2009
CALAA-01 (Arrowhead Research)	Polymeric nanoparticle	M2 subunit of ribonucleotide reductase (R2)	Cancer and solid tumor	Phase I (terminated)	NCT00689065	2008
Proteosome siRNA and tumor antigen RNA-transfected dendritic cells (Duke University)	Dendritic cells	Inducible immunoproteasome beta subunits LMP2, LMP7, and MECL1	Metastatic melanoma, absence of CNS Metastases	Phase I (completed)	NCT00672542	2008

LNP, Lipid nanoparticle; *PBMCs*, peripheral blood mononuclear cells; *PLK1*, polo like kinase-1.

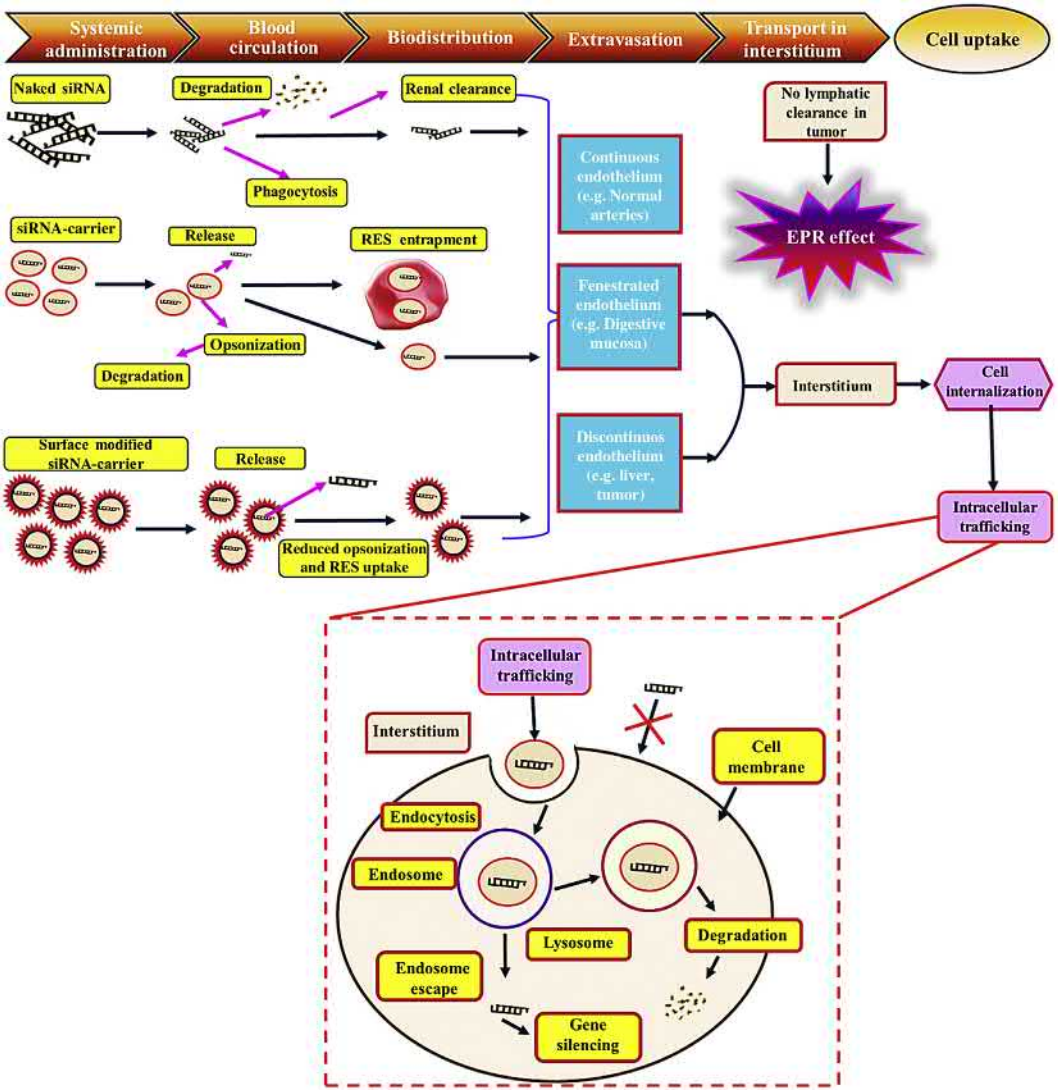

FIGURE 12.5 Schematic illustration of several barriers for siRNA in vivo delivery. Several barriers that circumvent the siRNA from its action onto its target are illustrated. *siRNA*, Silencing RNA.

discontinuous (observed in the liver). However, in the case of solid tumors, age-related macular diseases, and retinopathy vascular cells are not well developed due to abnormal neovascularization (Wang et al., 2010).

Following the extravasation into the target cell, the next barrier that arises is the interstitial transport. Mainly the small molecules in interstitial transits via diffusion and larger molecules transits via convection. As tumors have a poorly developed lymphatic system, the interstitial pressure inside the cells is high, and it creates a pressure-driven force

toward the outer direction of the tumor cell (Jain, 1987). The poorly developed lymphatic system in cancer cells also provides a property wherein there is enhanced permeability, but very slow draining into the lymphatic system and this effect is called an enhanced permeation and retention (EPR) effect (Jain, 1987).

Once the siRNA gets internalized into the cell via endosomal formation, chances are that the endosome will fuse with the lysosomal vacuole containing lysozyme and form and endolysosome that will degrade siRNA (Gilleron et al., 2013; Yezhelyev et al., 2008). Hence, it is very important for siRNA to show endosomal escape, otherwise it would undergo degradation, which eventually leads to a loss of its therapeutic action (Wang et al., 2010). Many other barriers and critical factors that contribute toward the degradation of siRNA are mentioned briefly in Fig. 12.5.

As there were many hindrances for siRNA to reach the target site and show its therapeutic action, researchers opted for nanoparticulate technology to cart the siRNA toward the cancer cell by using a suitable ligand. The reports that we found that employed nanoparticles for siRNA delivery have been discussed below, explaining its vital role.

12.2.4 Nanoparticles: The Salvager for the Silencing RNA Delivery

As there are many issues with the delivery of siRNA that have directed researchers to search for new avenues to deliver it, the nanoparticulate system was considered to be the typical choice, as they could be targeted easily by attaching ligands specific for receptors or via EPR effect. Nanoparticles can also protect siRNA from the systemic circulation and also prevent its degradation upon endosomal uptake termed as "endosomal escape" (Kanasty et al., 2013; Patil and Panyam, 2009; Whitehead et al., 2009). Nanocarriers that are mainly used for delivery of drugs and genetic materials are micelles, nanocapsules, nanospheres, macroemulsions, and liposomes.

These carriers size just below the capillary diameter, that is, below 100 nm, thus allowing easy penetration for cancer via passive targeting (Jang et al., 2003). However, administration of nanosized carriers in systemic circulation tends to show extensive interaction with various components in blood including immunoglobulins (a vital part of complement system). This increases the size and hydrophobicity of particles resulting in increased RES uptake and accumulation in spleen and liver. Such a phenomenon is being used to target siRNA RES organs (Morrissey et al., 2005).

However, there are several physicochemical aspects related to particles, that is, shape of particles (Huang et al., 2013), surface properties of particles (Whitehead et al., 2009), pH stability, thermal stability, size of particles (Resnier et al., 2013), and loading efficiency of siRNA on particles, which need to be optimized to benefit the delivery. Nanoparticles proffer advantages like (1) small size of particles enables easy penetration; (2) nonimmunogenic in nature; (3) some particles possess an ability to trigger the interferon-γ release thus, stimulating the natural killer cells and intensifying the antitumor therapy; (4) imaging and therapy both could be possible called as theragnostic agents; and (5) increased circulation time in systemic circulation (Maheshwari et al., 2015a,b; Sharma et al., 2015).

12.2.4.1 Cationic Carrier Conjugation With Hyaluronic Acid: Solving the Compatibility Issue

Cationic carriers are the gene delivery vehicles that fall under nonviral vectors. They interact with the negatively charged phosphate groups on the siRNA backbone thereby forming a complex that eventually gets internalized inside the cell. To serve this purpose several cationic carriers like cationic liposomes (Li et al., 2008), cationic chitosan nanoparticles (Tezgel et al., 2018), dendrimers (Xu et al., 2017), and protein transduction domain peptides (Divita et al., 2017) have been reported in the literature.

The majority of research articles that we found were based on liposomes because of their simplicity of production and relatively low immunogenicity; however, injecting cationic particles in vivo creates several complications involving hemotoxicity (Schlenk et al., 2017) and lack of targeting toward the oncogenic cells and protein binding. Also for in vitro application high degree of cationization leads to rupturing of cells eventually leading to failed transfection ability (Ranke et al., 2007). Thus such problems can be solved either by surface modification or synthesizing HA-conjugated block-copolymer, as HA is an indigenous biomaterial in the body and thus possesses minimal toxicity toward cells (Cortivo et al., 1991).

One such study was done by Wang et al. wherein they prepared nanostructured lipid carriers (NLCs) that were functionalized with D-α-tocopheryl succinate (TOS). The authors used etoposide (ETP) as a model drug, and HA and cell-penetrating peptide TAT factor as surface ligands enabling the NLCs' tumor specificity (Wang et al., 2017a,b). HA-PEG-TOS (HATOS) and TAT-PEG-TOS (TATTOS) was synthesized via ethylenediamine carbodiimide/N-hydroxy succinimide (EDC/NHS) coupling reaction, followed by this, ETP loaded NLCs were prepared using solvent injection method. The mean particle size of HATOS/TATOS-ETP-NLCs obtained was around 125 nm, and they were tested for cell uptake, wherein HATOS/TATOS-ETP-NLCs showed the highest cellular uptake when compared with other groups. Also, the ETP in vivo biodistribution was estimated, wherein HATOS/TATOS-ETP-NLCs showed the highest accumulation in the tumor region after 48 hours. The in vivo antitumor effect was also determined by checking the tumor volume wherein HATOS/TATOS-ETP-NLCs treated rat showed the minimum volume after 21 days. Also, the total body weight of the rat was found to be constant. Thus using HA, TAT, and TOS functionalized NLCs showed a great tumor targeting potential and could be further employed for siRNA delivery for the same.

Ran et al. studied the gene delivery efficiency of cationic liposomes coated with PEGylated HA for anti-Pgp siRNA. They found that in contrast to normal PEGylation, HA, and PEG, comodified PEG−HA−NP provided comparable cellular uptake and Pgp downregulation efficacy in MCF-7/ADR cells compared with Lipofectamine RNAiMAX and naked NP regardless of its anionic charged surface. And due to its better biocompatibility PEG−HA−NP possessed the best tumor accumulation, cellular uptake, and subsequently strongest Pgp silencing capability in tumor-bearing mice (Ran et al., 2014).

The PEG-HA coated siRNA liposomes showed better stability in FBS up to 24 hours as shown in Fig. 12.6A. PEG-HA covering proved to be better regarding internalization and reducing the expression of Pgp expression in MCF-7/ADR cells when compared with PEG naked liposomes and the marketed product, that is, RNAiMAX as shown in Fig. 12.6B.

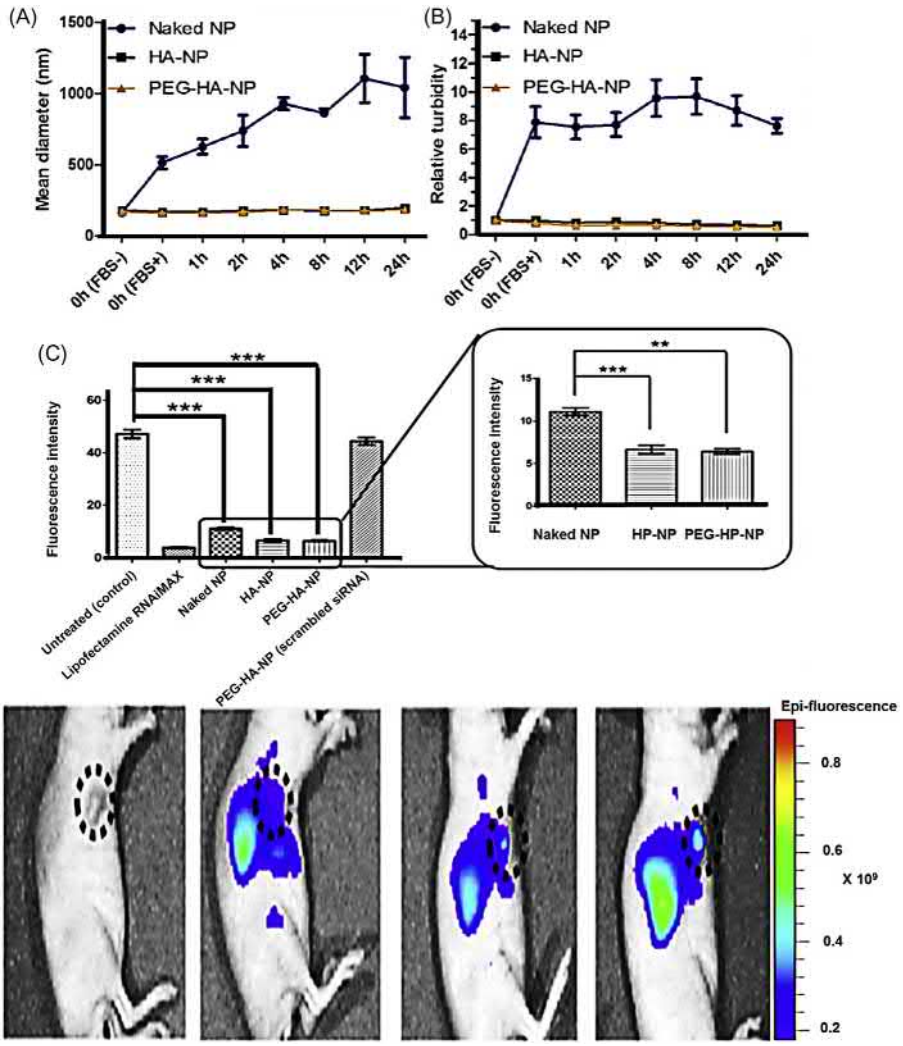

FIGURE 12.6 PEG-HA covering to enhance the transfecting efficiency of cationic liposomes. (A) Mean diameter and turbidity observations indicating the stability of PEG-HA coated liposomes in the presence of FBS. (B) Downregulation of Pgp expression showing PEG-HA-NP is significantly better than the naked NP. (C) In vivo distribution studies of DiD-labeled PEG-HA-NP showing higher targeting toward the induced tumor in nude female mice. *HA*, Hyaluronic acid; *PEG*, polyethylene glycol. Source*: Adapted with permission from Ran, R., Liu, Y., Gao, H., Kuang, Q., Zhang, Q., Tang, J., et al., 2014. Enhanced gene delivery efficiency of cationic liposomes coated with PEGylated hyaluronic acid for antiP-glycoprotein siRNA: a potential candidate for overcoming multi-drug resistance. Int. J. Pharm. 477 (1–2), 590–600, ©2014 Elsevier.*

Also, the in vivo application of DiD-labeled PEG-HA covered siRNA loaded liposomes showed a higher degree of targeting toward the tumor developed in female nude mice, which was confirmed using DiD fluorescence intensity as shown in Fig. 12.6C. Thus, an efficient transfection of Pgp in MCF-7/ADR cells could be possible with PEG-HA covering

of liposomes that may result into enhanced serum stability and in vivo targeting. These factors indicating its compatibility in physiological conditions (Ran et al., 2014).

Balbino et al. (2015) studied the capabilities of pseudoternary complexes formed between the plasmid DNA (pDNA), cationic liposomes, and HA, based on their electrostatic interaction. Then the in vitro transfection of the complexes on human epitheloid carcinoma (HeLa) cells showed equivalent transfection efficiency of the pseudoternary complex to that of binary pDNA/cationic complexes. Thus another proof explaining the rationale to use HA as a guiding tool for cationic species containing genetic payload (Balbino et al., 2015).

It is important to understand that there are several interactions possible between serum proteins and the formulated nanoparticles that can either increase the immunogenicity or could stimulate opsonization, which leads to reduced therapeutic activity. In such cases, HA could be used as good material in improving the physiological compatibility of the nanoformulation as done by Almalik et al. (2017). In their study, they found that HA modified chitosan nanoparticles showed the least surface absorption of proinflammatory proteins (clusterin) when compared with plain chitosan and alginate coated chitosan nanoparticles (Almalik et al., 2017), thus, providing a proof of concept that explains the utility of HA to improve compatibility of nanoformulations.

Fukushige et al. showed in their study that LPD induces hemolysis of murine red blood cells and cytotoxicity in human endothelial cells, whereas, when LPD is coated with the natural anionic polymers, HA (i.e., LPDH) reduces the hemolysis and cytotoxicity at the same concentration of siRNA. Fluorescently labeled LPD increases cellular uptake in comparison to LPDH. Hence, LPD and LPDH showed similar effects on gene silencing for luciferase gene on the luciferase-expressing B16F0 cancer cell line. The results conclude that LPDH have the capability to reduce cytotoxicity associated with LPD (Fukushige et al., 2017).

Hemolysis assay was done for the same using murine blood cells, and the cytotoxicity studies were performed using human endothelial cells (HUVEC). The hemolysis obtained was around tenfold less for the LPDH1 (HA at low concentration) and for LPDH5 (HA at high concentration) as compared with the LPD group as shown in Fig. 12.7A and no inflammatory response was observed for the LPDH group. Other groups with PEG coated LDP (LPD-PEG5 and LPD-PEG10) was also used as comparison groups, as pegylation is usually done to increase circulation time in the body (Fukushige et al., 2017).

The cytotoxicity observed was less for the LPDH group compared with the LPD group on HUVEC as shown in Fig. 12.7B. The drastic increase in the % cell survival for HUVEC was observed from 30% to 110% when LPDH was used. Gene silencing effect was studied using B16F0-Luc cells, and high gene silencing was observed for LPDH group compared with the LPD group. The results indicated that siRNA along with HA is highly compatible with the blood, and it is also cytotoxic only toward the cancerous cells and not toward the normal cells as shown in Fig. 12.7C and D.

Hence, HA, being an indigenously present biomaterial, has shown many successful attempts in improving the biocompatibility of cationic particles, thereby proving the efficiency of HA in resolving the issue related to biocompatibility and also enhanced targeting effect for tumors as described in the preceding sections of this chapter.

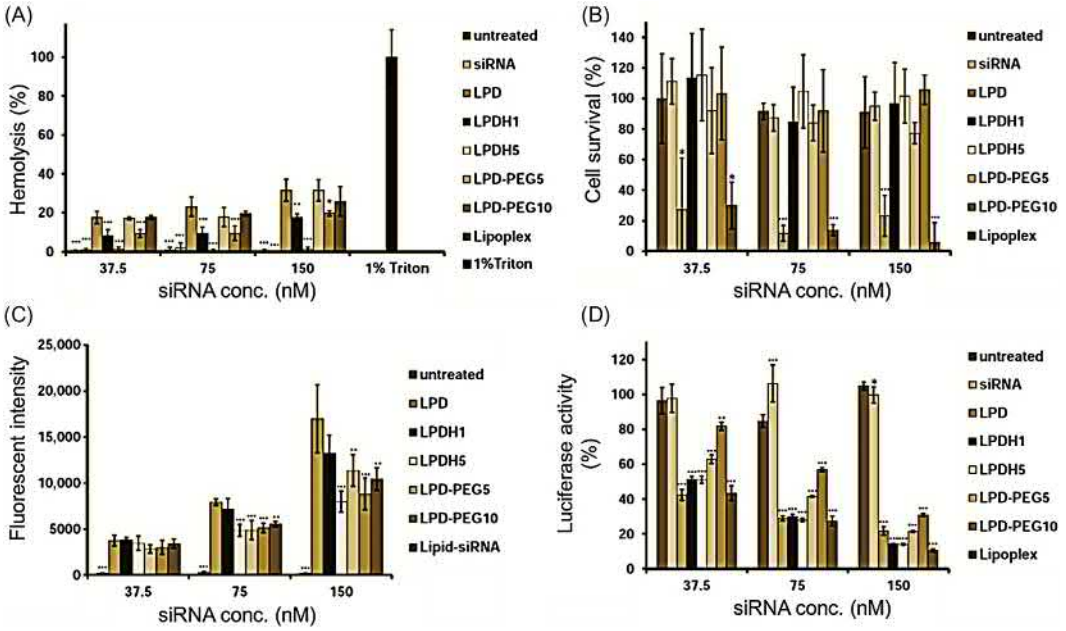

FIGURE 12.7 Elevated compatibility with HA coating on the siRNA loaded cationic lipidic carrier. (A) Hemolysis % was observed low in case of LPDH1 and in LPDH5 when compared with other groups at all concentrations. (B) Cytotoxicity study showed that LPDH1 and LDPH5 showed the least toxicity at all siRNA concentration when compared with other groups. (C) Intracellular uptake of fluorescently stained carriers showed no difference at low siRNA concentration, but at high concentration LPDH1 and LPDH5 showed lower uptake than LPD. (D) Gene silencing study in B16F0-Luc cells observed that LPDH is superior to LPD in the effective delivery of siRNA. *HA*, Hyaluronic acid; *siRNA*, silencing RNA. Source: *Adapted with permission from Fukushige, K., Tagami, T., Ozeki, T., 2017. The offset effect of a hyaluronic acid coating to cationic carriers containing siRNA: alleviated cytotoxicity and retained gene silencing in vitro. J. Drug Deliv. Sci. Technol. 39, 435–441, ©2017 Elsevier.*

12.3 HYALURONIC ACID IN DELIVERING SILENCING RNA: ENHANCING TARGET SPECIFICITY IN TUMORS

As we have discussed the issues related with siRNA delivery to target cells and organs and how nanotechnology helps in resolving some of its problems, one such method is by using HA nanoparticles (Fakhari, 2012). As in the early sections of this chapter, readers were updated with all physiological and physicochemical aspects of HA and explaining its potential to be used for targeting cancer (Almeida et al., 2014; Choi et al., 2009; Lokeshwar et al., 2014; Yang et al., 2013). HA was first used as a delivery agent by Kim Angela et al. in 2003 and siRNA being nonionic in nature enables it to form a self-assembled complex of HA nanoparticles, which can show CD44 receptor-mediated endocytosis specifically in cancerous cells (Jin et al., 2010). As already mentioned cancer cells express CD44 receptors in excess and thus could be used for targeting using HA (Naor et al., 2002) as described in Fig. 12.8.

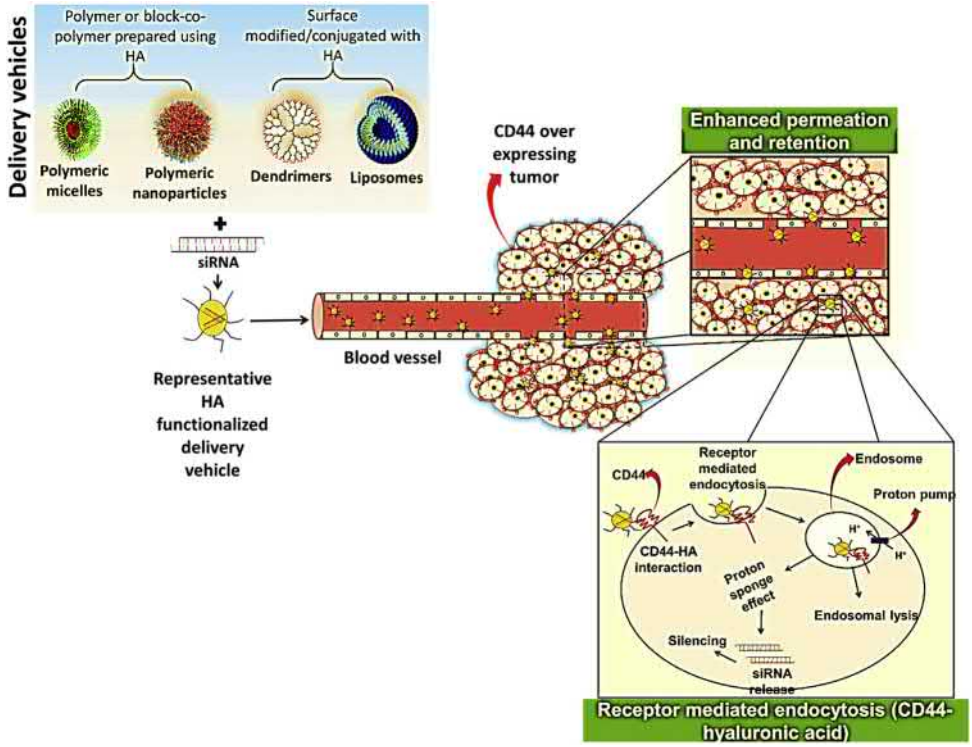

FIGURE 12.8 Diagrammatic illustration of several cationic delivery vehicles used for delivery of siRNA, which could be targeted toward CD44 overexpressing cancers either by conjugating the HA in the form of block-co-polymer or by surface modifying the vehicle with HA for enhanced internalization and thereby showing silencing effect. *CD44*, Cluster of differentiation 44; *HA*, hyaluronic acid; *siRNA*, silencing RNA.

The work done by Lee et al. supports the previously stated hypothesis. In this work, they prepared a layer-by-layer assembled cysteamine modified gold nanoparticles (AuCM)/siRNA/PEI/HA complex having a mean particle size of 37.3 ± 8.8 nm with a negative surface charge of -12 ± 1.5 mV. Various analysis methods like TEM, dark-field bioimaging, and inductively coupled plasma atomic emission spectroscopy (ICP-AES) confirmed the cellular uptake of the prepared complex to B16F1 cells by HA receptor-mediated endocytosis with 70%−80% targeting efficiency in the presence of 50% serum solution.

According to Lee et al. (2011) the higher targeting efficiency and serum stability of (AuCM)/siRNA/PEI/HA complex were due to the outer layer of HA. Yet again, in another study performed by Yoon et al. the targeting efficiency of HA has been proved. In this study, they developed a biodegradable HA-graft-poly (dimethylaminoethyl methacrylate) (HPD) conjugate that was complexed and chemically cross-linked with siRNA via a disulfide bond and showed high stability in a 50% serum solution compared with the free siRNA and unlinked siRNA-HPD complex. The cellular uptake of complexes was determined in two cell lines, that is, B16F10 and NIH3T3. The YOYO-1 labeled complexes

showed strong green fluorescent signals on CD44-positive B16F10 while undetectable signals were found on the NIH3T3 cells indicating the receptor-mediated cellular uptake of the complexes. Also in the in vitro study, high gene silencing effect was observed in RFP-B16F10 cells for the RFP-siRNA-HPD complexes compared with those of the control, free siRNA, and Lipofectamine-siRNA complexes. The in vivo gene silencing efficacy of complexes in RFP-B16F10 tumor-bearing mice evaluated using a real-time NIRF technique was also found to be excellent compared with control (Yoon et al., 2013).

Thus HA can either be coated or covered onto several particles like dendrimers, liposomes, and several other materials for improving targeting or could be synthesized as micelles or block copolymers to produce self-assembled siRNA loaded delivery vehicle. Such HA hybridized delivery vehicles are mainly used in delivering to four major cancers, that is, colon cancer, lung cancer, ovarian cancer, and breast cancer, as has been described in detail in the following section of this chapter.

12.3.1 Role in Colon Cancer

Colorectal cancer (CRC) is amongst the most often encountered diseases in industrialized countries, and the major reason for that is insidious onset, a lower rate of early diagnosis, and poor long-term prediction or treatment available for the condition (Jian et al., 2017). However, the primary treatment available for CRC is either surgical removal or chemotherapy using 5-fluorouracil, irinotecan, and oxaliplatin or both (Al-Keilani and Darweesh, 2017). However, eventually this first-line treatment began to fail due to the development of chemoresistance; this attracted several researchers to find a better alternative for treating CRC (Li et al., 2010; Longley et al., 2006).

The failure of first-line therapy led to the search for novel therapies involving RNAi technology, as this technique is well established for solving problems related to chemoresistance by silencing the gene causing the efflux of therapeutic. Again the problem was in vivo targeting, which was soon solved as CD44 was found to be overexpressed in CRC cells and was termed to be the hallmark for highly tumorigenic CRC cells (Dalerba et al., 2007). It was observed that CD44 gets expressed well and stays even after long-term expression and has self-renewable capacity thereby suggesting CD44 as the best suited therapeutic target for treating CRC (Karousou et al., 2017; Wang et al., 2012).

Hence in accordance to the abovementioned literature, an interesting study was reported by Lai et al. wherein they showed that HA and hyaluronic synthase (HAS) plays a vital role in tumor growth and by inhibiting the HAS3, the subcutaneously implanted colon tumor can be controlled efficiently (Kim, 2004). However, the proper mechanism of how HAS3 is distinctively involved for tumor growth in the case of colon tumor was projected by Teng et al. Authors' study involved silencing of HAS3 gene using HAS3 siRNA and employing it as a therapeutic model to control the tumor growth. In their study, they successfully showed a significant tumor reduction in subcutaneously induced tumorigenic HCT116 colon cancer cells (Teng et al., 2011). Thus along with this report, we found several other reports cementing the important role HA plays in the progression and growth of colon cancer (Kim et al., 2004; Kim, 2004; Kopp et al., 2009).

Park et al. prepared PEI-SS by cross-linking PEI with bisacrylamide (CBA) and further conjugated with HA to form a block copolymer complex [(PEI-SS)-bHA] and studied target-specific tumor treatment by this complex. They found that the prepared complex shows optimum complexation with Vascular endothelial growth factor (VEGF) siRNA and was able to show significant gene silencing activity in both conditions, that is, serum-free and serum conditions.

Fig. 12.9 shows the graphic representation of the effect of PEI–bisacrylamide–HA complex as a delivery vehicle for VEGF siRNA toward subcutaneously induced CT-26 colon cancer. In luciferase gene silencing assay only (PEI-SS)-*b*-HA showed prominent gene silencing in presence and absence of FBS (Fig. 12.9A), and siVEGF/(PEI-SS)-b-HA showed significant VEGF knockdown in the subcutaneously induced tumor in bulb/c mice (Fig. 12.9B).

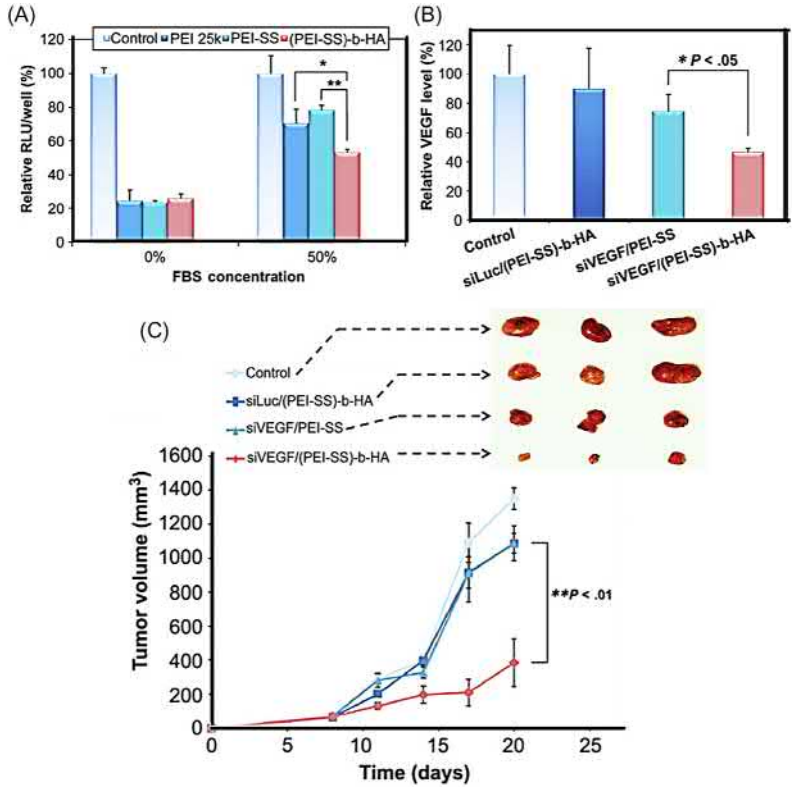

FIGURE 12.9 PEI–bisacrylamide–HA complex as a delivery vehicle for VEGF siRNA toward subcutaneously induced CT-26 colon cancer. (A) Luciferase gene silencing assay to check gene knockdown using siRNA along with several complexes out of which only (PEI-SS)-*b*-HA showed prominent gene silencing in absence and presence of FBS. (B) Relative % VEGF knockdown observed in the subcutaneously induced tumor in bulb/c mice wherein siVEGF/(PEI-SS)-*b*-HA showed significant VEGF knockdown. (C) Antitumor activity observed by calculating tumor volume showed that siVEGF/(PEI-SS)-*b*-HA showed the best antitumor activity. *HA*, Hyaluronic acid; *PEI*, polyethyleneimine; *siRNA*, silencing RNA. Source: *Adapted with permission from Park, K., Lee, M.-Y., Kim, K.S., Hahn, S.K., 2010. Target specific tumor treatment by VEGF siRNA complexed with reducible polyethyleneimine–hyaluronic acid conjugate. Biomaterials 31(19), 5258–5265, ©2010 Elsevier.*

Moreover, when siVEGF/(PEI-SS)-*b*-HA complex was injected via I.V. route in subcutaneously induced CT-26 colon cancer cell line it showed almost 60% decline in expression in VEGF expression when compared with control even after 20 days posttreatment as shown in Fig. 12.9C (Park et al., 2010). Thus efficient gene silencing by siVEGF/(PEI-SS)-*b*-HA led to an excellent tumor volume reduction as could be clearly observed from Fig. 12.9C. Thus it could be well concluded that the prepared siVEGF/(PEI-SS)-*b*-HA complex is a potential siRNA delivery agent that has proven to be biocompatible and shows targeted gene delivery specifically toward colon cancer, and could be considered for further studies (Park et al., 2010).

Another intriguing study was reported by Lee et al. wherein calcium phosphate (CAP) nanoparticles were prepared to surround the siRNA to form a CAP/siRNA complex. CAP has already been reported for transfecting siRNA into cells, but several issues like biocompatibility, lack of cell specificity, and uncontrolled crystal growth led to its clinical nonapplicability. Thus CP/siRNA prepared by Lee et al. was conjugated with HA via 3,4-dihydroxy-L-phenylalanine (dopa), which acts to be an adhesive agent between HA and CAP/siRNA (Lee et al., 2014). The gene expression studies were performed on human colon carcinoma cells stably expressing firefly luciferase (HT29-luc) cell line, which showed maximum gene knockdown using CAP/siRNA/dopa-HA with HA to siRNA weight ratio of 60 (siRNA of 100 nM was selected), with size near to 100 nm with a zeta potential of −50 mV. Although size showed and an inverse relation with HA concentration, zeta potential had a direct relation with HA concentration (Lee et al., 2014).

Also to prove that HA was involved in cancer-specific cell transfection, competition assay, also known as receptor blockade assay, was performed, wherein 10 mg/mL of free HA solution was incubated with cells followed by CAP/Cy5.5-labeled siRNA/dopa-HA. Thus CAP/siRNA/dopa-HA alone showed a higher degree of gene knockdown as compared with CAP/siRNA/dopa-HA administered in the presence of HA as shown in Fig. 12.10B and C. Also, the serum stability of the CAP/siRNA/dopa-HA was studied and proved to keep the siRNA well encapsulated within even after 24 hours and also showed a significant amount of gene knockdown in presence and absence of serum when compared with PEI and CAP/siRNA as shown in Fig. 12.10D and E. Thus such study concludes that CAP/siRNA/dopa-HA formulated could be further developed to act as a guided gene delivering the vehicle.

Thus the abovementioned studies clearly indicate that surface modified HA delivery vehicles not only improve the targeting efficiency but also improve the biocompatibility aspects of the delivery vehicle. The modification done using HA also enables serum stability and retained therapeutic action when studied in the presence and absence of serum. Hence, HA modified siRNA complex carriers serve to be a potential therapeutic for colon cancer.

In the current scenario, lung diseases are considered amongst the top 10 diseases with high mortality rate worldwide as mentioned by WHO. Thus there is ever-enhancing development and research being done to overcome the shortfalls of the currently available therapies. Usually, chemotherapy is used for treating lung cancer, but the specific cancer cell delivery remains the main problem to be solved, which eventually leads to serious toxicities (Yang et al., 2016). Although RNAi technology is usually employed as a general therapy to solve the unmet medical needs due to its high potential of suppressing the aggressively growing cells (Merkel et al., 2014).

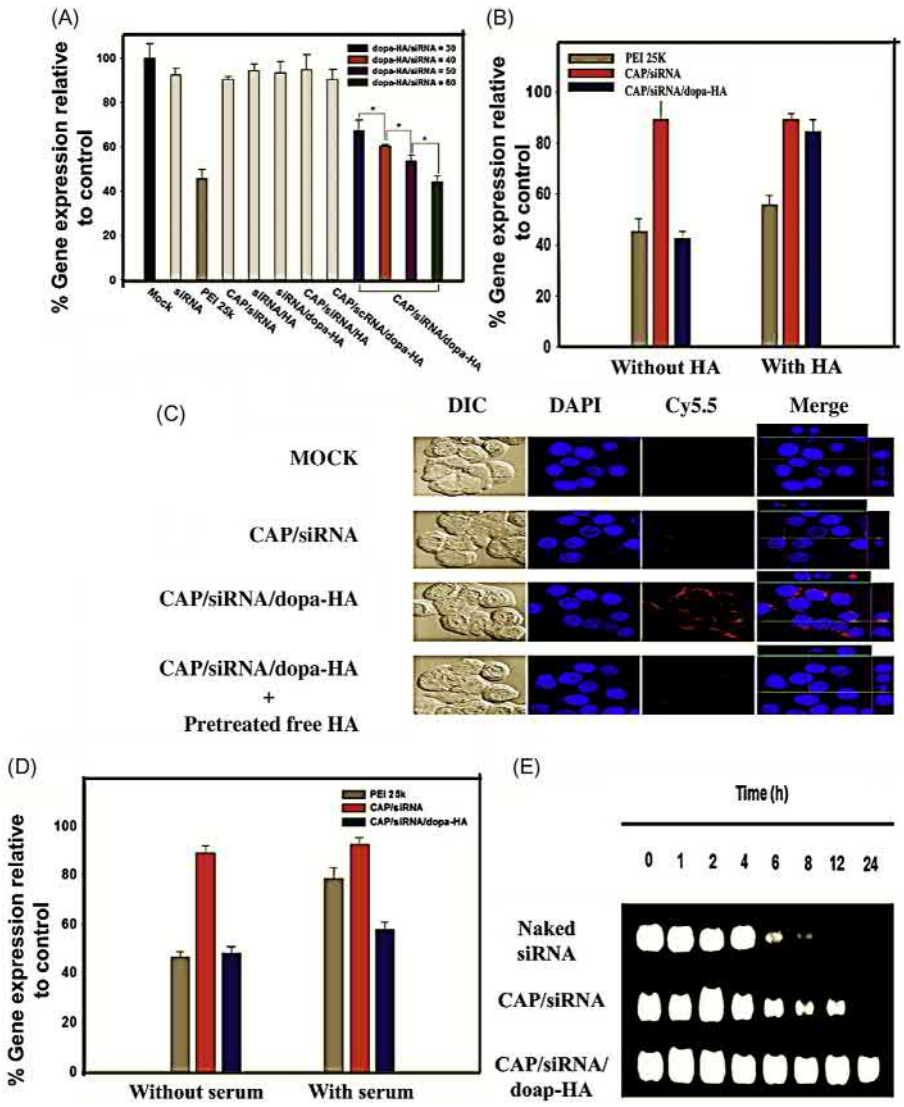

FIGURE 12.10 siRNA loaded calcium phosphate nanoparticles stabilized by HA. (A) Comparative analysis of gene knockdown using several groups, wherein CAP/siRNA/dopa-HA60 knockdown was equivalent with PEI25K, also was significantly lower that HA-30, 40, and 50. (B and C) Graphical representation of receptor blockade assay confirming the gene delivery is done mainly due to CD44 (HA acts as a primary substrate) receptor-mediated endocytosis, also confirmed by cell uptake study using DAPI and cy5.5 labeled siRNA via CLSM. (D) Graphical representation showing serum stability concerning % gene expression wherein CAP/siRNA/dopa-HA showed almost the same activity in both the scenario. (E) Representing the encapsulated siRNA stability with CAP/siRNA/dopa-HA60 to be the best in protecting for a longer period. *CLSM*, Confocal laser scanning microscopy; *CD44*, cluster of differentiation 44; *HA*, hyaluronic acid; *siRNA*, silencing RNA. Source*: Adapted with permission from Lee, M.S., Lee, J.E., Byun, E., Kim, N.W., Lee, K., Lee, H., et al., 2014. Target-specific delivery of siRNA by stabilized calcium phosphate nanoparticles using dopa–hyaluronic acid conjugate. J. Control. Release 192, 122–130, ©2014 Elsevier.*

Another benefit is that local delivery of siRNA into the lung enables noninvasive access and thereby avoids any kind of interactions with serum proteins as serum is absent on the air inside of the lung, and nuclease activity is comparably low, which tends to degenerate siRNA upon I.V. administration (Taratula et al., 2013). Although the pulmonary delivery of siRNA into the lung depends on the patient's pulmonary function and the aerodynamic diameter of the particle in which the siRNA is loaded (Lam et al., 2012). The optimal aerodynamic diameter considered to be efficient for deposition in the lung is assumed to be in the range of 1−5 μm (Lam et al., 2012).

Despite all advantages of the pulmonary route, the lung also imposes intrinsic anatomic, physiologic, immunologic, and metabolic hurdles to efficient siRNA delivery such as a cough and mucociliary clearance, the presence of the mucus and the clearance of particles by macrophages. Thus for I.V. delivery again the major problem that lies is targeting, which can be solved by employing HA. As CD44 expression on lung cancer is prominent and HA being a primary substrate it can be employed as a targeting ligand (Leung et al., 2010).

One such study discussing the use of HA was conducted by Wu et al. (2017) Docetaxel-loaded nanoparticles were prepared via nanoprecipitation method and was further coated with HA via covalent coating method, so as to obtain docetaxel-loaded PLGA nanoparticle coated with HA (DTX-HPLGA) of size 154 nm with zeta potential of −22.7 mV. DTX-HPLGA showed enhanced circulation time up to 24 hours, that is, showed 14-fold higher area under the curve when compared with DTX. Biodistribution study showed a 4.4-fold higher accumulation in lungs when compared with free DTX. The DTX-HPLGA exhibited better tumor volume restriction when compared with free DTX, and hence it helped to lower the morbidity level within the mice (Wu et al., 2017). Although the authors haven't included siRNA loading and its activity such mentioned delivery model creates new prospects in developing a similar delivery vehicle for siRNA delivery thereby enhancing its therapeutic efficiency by improving its targeting (Wu et al., 2017).

However, in another study involving siRNA, Nascimento et al. (2016) investigated the role of HA coating on the capacity to target CD44-overexpressing tumor cells via siRNA lipoplexes. The studies regarding the cellular uptake mechanism and its localization were done via flow cytometry and fluorescence microscopy. Both methods indicated that lipoplexes could get rapidly internalized as well as localized within the cytoplasm. The in vitro study was done for the same using anti-Luc siRNA to understand the luciferase expression inhibition in which 81% inhibition was observed in A549-luc-C8 Bioware cell line.

In case of in vivo luciferase inhibition in athymic nude mice bearing A549-luc metastatic cancer HA modified lipoplexes showed better knockdown of luciferase activity when compared with vehicle and non-HA-modified lipoplexes. The tissue analysis using rhodamine dye-labeled lipoplexes showed relative intensity in mouse lungs and as such very low or no intensity was observed in case of non-HA-modified lipoplexes thereby explaining the role that HA plays in imparting stability and targeting ligands for lung cancer (Nascimento et al., 2016).

A similar study was conducted by Ganesh et al. wherein they functionalized HA with various lipids and polyamines to screen the best material to be used for encapsulating siRNA so that it could deliver the SSB/PLK1 siRNA toward metastatic lung model. In the screening process, the PEI and PEG conjugated HA vehicle proved to show gene

knockdown in in vivo metastatic tumor induced using A549 cells in a dose-dependent manner when compared with B16F10 induced tumor as shown in Fig. 12.11A and B (Ganesh et al., 2013b).

Furthermore, the same group also studied NIR dye loaded HA-nanoparticles to study the whole-body localization of HA nanoparticles upon IV injection in cisplatin-resistant tumor-bearing mice (Ganesh et al., 2013a). The dye used was indocyanine green (ICG) to

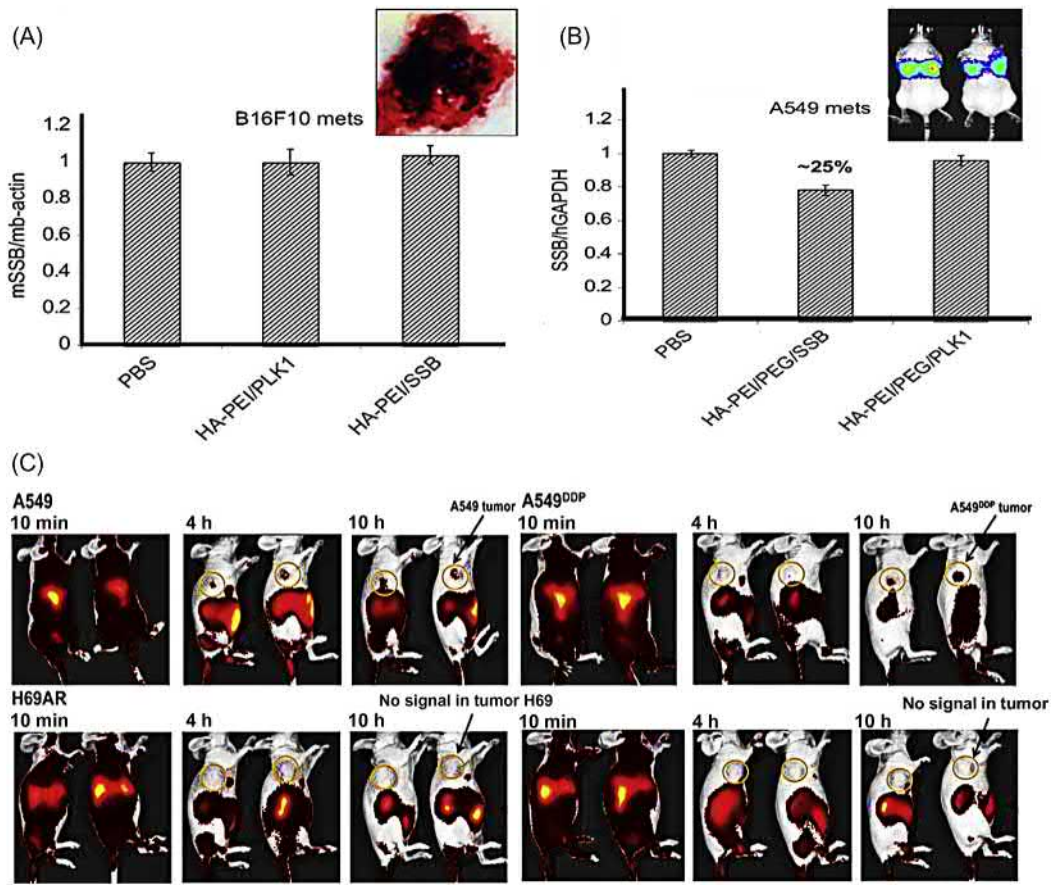

FIGURE 12.11 In vivo lung cancer targeting using HA/PEI/PEG conjugated delivery vehicle. (A) Gene knockdown of messenger SSB and PLK1 RNA upon delivery of SSB/PLK1 siRNA in B16F10 induced metastatic tumor and (B) in A549 influenced a metastatic tumor. (C) Whole-body optical imaging of ICG loaded HA nanoparticles (ICG/HA-PEI/PEG NP) in A549/ and H69/H69AR small cell lung cancer–bearing mice. *HA*, Hyaluronic acid; *PEI*, polyethyleneimine; *PEG*, polyethylene glycol; *siRNA*, silencing RNA. Source: *(A and B) Adapted with permission from Ganesh, S., Iyer, A.K., Morrissey, D.V., Amiji, M.M., 2013b. Hyaluronic acid based self-assembling nanosystems for CD44 target mediated siRNA delivery to solid tumors. Biomaterials 34(13), 3489–3502, ©2013 Elsevier. (C) Adapted with permission from Ganesh, S., Iyer, A.K., Gattacceca, F., Morrissey, D.V., Amiji, M.M., 2013a. In vivo biodistribution of siRNA and cisplatin administered using CD44-targeted hyaluronic acid nanoparticles. J. Control. Release 172 (3), 699–706, ©2013 Elsevier.*

get the whole-body distribution pattern in the live tumor of mice as it has very low background interference and is thus considered suitable for imaging applications. The authors observed that ICG dye loaded HA nanoparticles showed a higher degree of localization than in A549 and its resistant counterpart $A549^{DDP}$ induced tumors in mice, as A549 and $A549^{DDP}$ tend to have a higher degree of CD44 expression when compared with H69AR and H69 cell-induced tumor as shown in Fig. 12.11C.

This biodistribution study clearly indicates that this methodology of encapsulating siRNA along with a drug to get synergistic action or by using dye to locate tumors can be possible due to HA−CD44 interaction. Thus the abovementioned studies clearly point to the importance of HA as a targeting ligand and stabilizer, and its role in biocompatibility, which qualifies it to be employed for targeted lung cancer therapeutic.

12.3.2 Role in Ovarian Cancer

Ovarian cancer is considered amongst the most lethal types of cancer, as the data published for US population states that almost 21,980 women are diagnosed yearly and approximately 60% of them die every year (Siegel et al., 2014). The main reason for such high degree of mortality is due to the development of MDR (Coleman et al., 2013), as there is no well-established treatment for MDR ovarian cancer, thus, it continues to be a challenge for treatment (Lopez et al., 2013). The MDR gene-1 is the gene responsible, which transcripts for ATP-binding cassette (ABC) transporter Pgp, which is responsible for the drug resistance, as it is an ATP driven pump that pumps the therapeutic out of the cancerous cell thereby leading to MDR (Ali et al., 2012). Thus to overcome such complication, RNAi therapeutics could have a major role to play (Nieth et al., 2003). As CD44 is found to be overexpressed in ovarian cancer, HA could be employed as a targeting ligand for the same (Cheng et al., 2012).

It was observed that CD44 plays a vital role in ovarian cancer and thus, because of its involvement in progression and metastasis of cancer cells, it is found to be overexpressed in these cells. A study done by Shah et al. supports this statement as they prepared paclitaxel succinic acid conjugate that was attached on polypropylenimine dendrimer followed by conjugation of luteinizing hormone−releasing hormone peptide-PEG as a CD44 siRNA delivery vehicle (Shah et al., 2013). The developed vehicle showed a high degree of transfection and a significant level of CD44 knockdown was observed, which led to antitumor activity. This explains the importance of CD44 and supports that overexpression of CD44 on ovarian cancer could be employed as a potential strategy for delivering the payload while using HA as a targeting ligand (Shah et al., 2013).

A study showing the proof that HA could be used as a targeting ligand for ovarian cancer was reported by Vangara et al. (2013) wherein a compound SN-38 that failed clinical trial due to high hydrophobicity and low stability was loaded in HA decorated PLGA-PEGylated nanoparticle for specific targeting toward ovarian cancer. The formulation showed 8−16-fold higher cellular uptake in SKOV-3 and OVCAR-8 ($CD44^{+ve}$ cell lines) when compared with CHO cell line ($CD44^{-ve}$ cell line). This hinted that HA, which is a primary substrate of the CD44 receptor, could be employed as a targeting ligand for the treatment of ovarian cancer (Vangara et al., 2013). Although the study mentioned above

does not dictate about siRNA delivery this guided the path toward developing a delivery vehicle for siRNA toward ovarian cancer, and studies are mentioned below.

A report exploiting the HA−CD44 interaction for targeted delivery was done by Yang et al. wherein they conjugated PEG and PEI on HA so as to form HA−PEI/HA−PEG complex that will self-assemble upon addition of MDR1 siRNA to show MDR gene 1 knockdown (Yang et al., 2015). The developed system showed targeted delivery of MDR1 siRNA to ovarian cancer, which downregulated the Pgp and MDR1 expression as concluded from there transfection studies done on SKOV-3TR cells (which has a higher expression for MDR1 and Pgp) as shown in Fig. 12.12A and B. Also, the in vivo

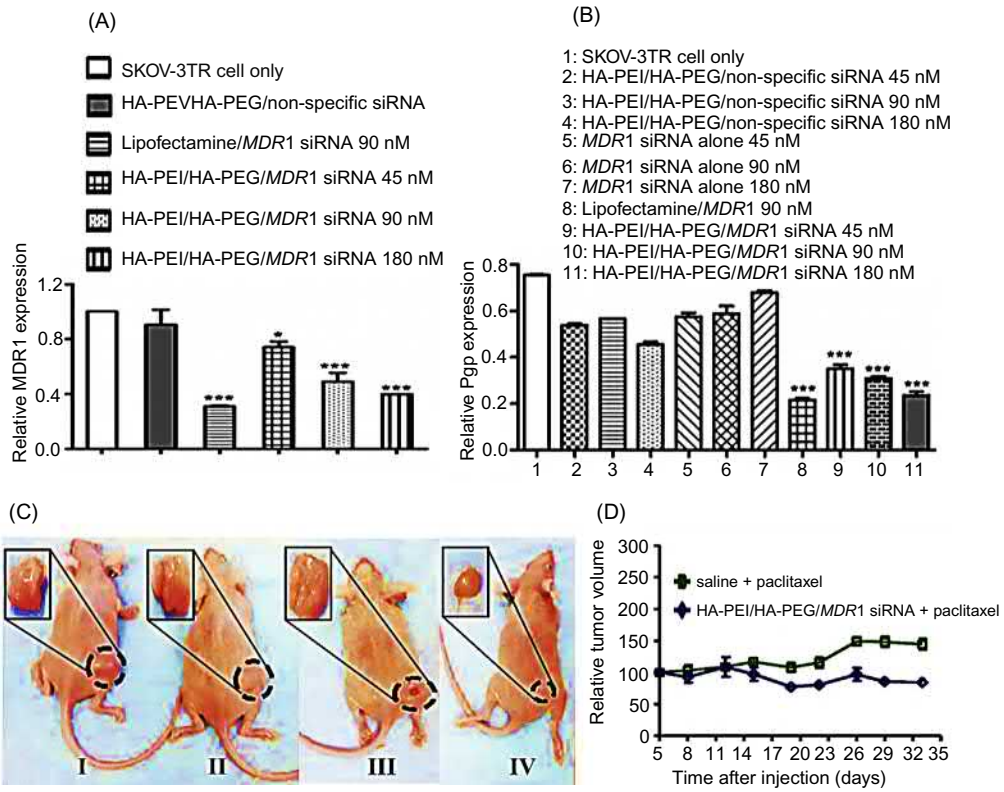

FIGURE 12.12 MDR1 and Pgp knockdown via HA functionalized nanoparticle assisting paclitaxel therapy for MDR resistant ovarian cancer. (A and B) MDR1 and Pgp expression were found to be significantly reduced when compared with plane SKOV-3TR cells and showed dose-dependent increment in target knockdown. (C) Photographic representation claiming that HA-PEI/HA−PEG/MDR1 siRNA + paclitaxel (IV) showed highest tumor volume reduction when compared with free paclitaxel (I), MDR1 siRNA alone + paclitaxel (II), HA-PEI/HA−PEG/nonspecific siRNA + paclitaxel (III). (D) Graphical representation claiming significant tumor volume reduction observed in mice model when treated with HA-PEI/HA−PEG/MDR1 siRNA + paclitaxel. *HA*, Hyaluronic acid; *MDR*, multidrug resistance; *Pgp*, *P*-glycoprotein; *PEI*, polyethyleneimine; *PEG*, polyethylene glycol; *siRNA*, silencing RNA. Source*: Adapted from Yang, X., Singh, A., Choy, E., Hornicek, F.J., Amiji, M.M., Duan, Z., 2015. MDR1 siRNA loaded hyaluronic acid-based CD44 targeted nanoparticle systems circumvent paclitaxel resistance in ovarian cancer. Sci. Rep. 5, 8509,* ©*2015 Springer Nature.*

applicability of the developed system was proved by treating xenografted MDR ovarian cancer model of mice with HA−PEG/MDR1 siRNA nanoparticles followed by paclitaxel treatment, which showed significantly higher tumor volume reduction when compared with paclitaxel alone as shown in Fig. 12.12C and D. Thus such HA modified delivery vehicle for MDR1 siRNA followed by paclitaxel delivery proved to be a significantly better therapy in treating the MDR ovarian cancer and thereby laid down a potential tool that could be employed for MDR cancer therapy (Yang et al., 2015).

Another report that employed HA as a targeting ligand was proposed by Kim et al. wherein they prepared PLXDC1 siRNA loaded chitosan nanoparticles coated with HA as the targeting ligand (Kim and Han, 2017). The prepared particles, that is, HA-chitosan nanoparticle complexed with siRNA (HA-CH-NP/siRNA) showed 2.1-fold enhanced gene silencing in $CD44^{+ve}$ endothelial cells when compared with CH-NP/siRNA. Also, HA-CH-NP/PLXDC1 siRNA showed significant ($P < .0001$) decrease in the level of mRNA essential for tumor angiogenesis when compared with the control group. Also, HA-CH-NP/siRNA showed significant decline in cell proliferation, microvessel density, and increase in cellular apoptosis (checked by TUNEL assay) when compared with CH-NP/siRNA (Kim and Han, 2017). Hence this study makes it evident that HA is responsible for targeting the siRNA loaded chitosan nanoparticles specifically toward ovarian cancer.

Thus from the compiled studies it has been prominent that HA−CD44 interaction can be employed toward developing gene delivery vehicles targeted toward ovarian cancer. However, in our literature search we didn't find extensive reports wherein researchers have employed delivery of siRNA toward ovarian cancer using HA, so this might create a new research avenue.

12.3.3 Role in Breast Cancer

Breast cancer is an often diagnosed cancer and the prominent cause of death from cancer in women. According to GLOBOCAN worldwide estimates of cancer incidence and mortality produced by the International Agency for Research on Cancer (IARC) for 2012, breast cancer alone accounts for 25% of all cancer cases and 15% of all cancer deaths among females altogether (Torre et al., 2015).

Treatment of early-stage breast cancer has been made easier by the accessibility of novel diagnostic tools and systemic therapeutics. Though, only slight progresses have been attained in the area of relapsed metastatic cancer that is thought to be a result of key cancer-causing genes that are usually considered "nondruggable," making it an urgent medical need for the exploration of new and effective therapeutics for the management of late-stage breast cancer (Shen et al., 2013). This problem has been resolved by introducing the siRNA, which is capable of rapidly and efficiently silencing the expression of any gene in any cell type, hence providing a novel tool to treat cancer by targeting range of oncogenic gene. Also, siRNA is being used to treat the drug-resistant breast cancer by silencing the genes responsible for drug resistance.

Although considerable research is going on regarding siRNA, there is a problem with the in vivo application of it due to the shortage of efficient carriers for systemic delivery. Several carriers that are applied as a delivering agent lack targeting and are also unstable.

So, the researchers are focusing on cargoes that can interact with the overexpressed receptors on breast cancer cells and hence can efficiently deliver siRNA to the targeted site. HA is the best example of it, which can selectively interact with the overexpressed transmembrane known as CD44 and assist with cellular uptake via endocytosis (Götte and Yip, 2006). Again, HA forms an ideal protective shell and enhances siRNA and drug stability, hiding it from the immune system and avoiding the damage to normal cells.

Yin et al. developed a redox-sensitive micellar system by conjugating cystamine modified HA with octandioic acid (OA) and branched PEI (bPEI) [HA-ss-(OA-*g*-bPEI), HSOP] for triple negative breast cancer (TNBC) targeted codelivery of AURKA (aurora kinase A) specific siRNA (si-AURKA) and paclitaxel (PTX). The simultaneous delivery of siRNA and paclitaxel into MDA-MB-231 cells through HA-receptor mediated endocytosis and siRNA transfection efficiency was confirmed by flow cytometer and confocal microscopy method. Further, in vivo study was done to confirm the antitumor activity. For this, the anticancer treatments were performed on tumors of BALB/c mice that were subcutaneously xenografted with MDA-MB-231 cells. The prepared formulation was compared with the marketed formulation Taxol for accumulation in tumors and antitumor efficacy, and it was found that HSOP micelles could effectively accumulate at the tumor site and also exhibited greater antitumor efficacy compared with Taxol. Fig. 12.13 shows the results of the investigations carried out. Intracellular uptake of HSOP micelles is highest compared with free-HA pretreated HSOP micelle at 4 hours (Fig. 12.13A); confocal microscopy shows the intracellular delivery of C6-loaded HSOP at various time points (Fig. 12.13B). In vivo imaging of tumor-bearing mice after administration of DiR/FAM-siRNA coloaded HSOP micelles at 2, 12, and 24 hours is shown in Fig. 12.13C and ex vivo fluorescence images of different tissues at different time are shown in Fig. 12.13D (Yin et al., 2015).

In another study, Parmar et al. formulated a siRNA delivery system using linoleic acid substituted PEI (PEI-LA) and HA at different ratios and by using additive and coating method for the treatment of TNBC. To evaluate HA-mediated siRNA uptake and transfection efficiency, MDA-MB-231 cells were transfected with the formulation containing HA in different ratios and without HA and flow cytometry, and confocal microscopy analysis was performed. Both of them showed higher uptake for siRNA/polymer complexes with HA as compared with without HA (Parmar et al., 2017).

Cellular uptake of siRNA/polymer complexes after transfection is analyzed by different methods, that is, flow cytometry and confocal microscopy. Fig. 12.14A–C shows uptake of siRNA:PEI-LA in 1:6 w/w ratio with different amounts of HA, uptake of FAM-siRNA/HA additive complex in different groups transfected with nonlabeled and labeled siRNA at different ratios, and cellular uptake of siRNA for HA coating with similar groups respectively.

Surace et al. (2009) have also performed a similar type of study, in which they proved that formulation containing HA as a targeting ligand has higher transfection efficiency on MDA-MB-231 cells expressing CD44 as compared with the MCF-7 line, which shows shallow levels of CD44. Further, enormous studies have been done by other research groups in which they have proved the role of HA in improving the transfection efficiency for the treatment of breast cancer (Ding et al., 2017; Ran et al., 2015). Thus we can conclude that HA has a very significant role in increasing the transfection efficiency of siRNA, which has a significant role in the treatment of metastatic and drug-resistant breast cancer.

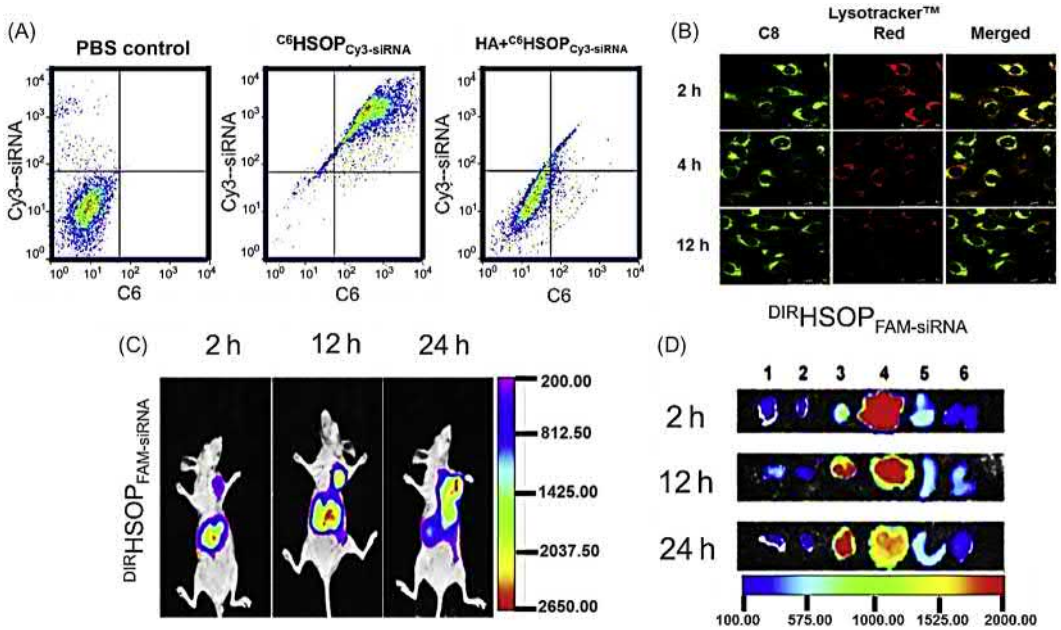

FIGURE 12.13 Redox-sensitive HA modified micellar system specific for breast cancer. (A) Flow cytometry investigation is showing the highest intracellular uptake of HSOP micelle compared with free-HA pretreated HSOP micelle at 4 h. (B) Confocal microscopy images of MDA-MB-231cells showing intracellular delivery of C6-loaded HSOP at various time points. (C) In vivo imaging of tumor-bearing BALB/c mice after administration of DiR/FAM-siRNA coloaded HSOP micelles at 2, 12, and 24 h. (D) Ex vivo fluorescence images of different tissues including (1) lung, (2) heart, (3) tumor, (4) liver, (5) spleen, and (6) kidneys collected at 2, 12, and 24 h postinjection of Dir/FAM-siRNA coloaded HSOP micelles showing highest uptake by tumor at 24 h. *HA*, Hyaluronic acid; *HSOP*, HA-ss-(OA-*g*-bPEI); *siRNA*, silencing RNA. Source*: Adapted with permission from Yin, T., Wang, L., Yin, L., Zhou, J., Huo, M., 2015. Co-delivery of hydrophobic paclitaxel and hydrophilic AURKA specific siRNA by redox-sensitive micelles for effective treatment of breast cancer. Biomaterials 61, 10–25, © 2015 Elsevier.*

12.4 CONCLUSION AND FUTURE OUTLOOK

In recent years, HA has emerged as a promising application for the tumor-targeted delivery of various therapeutic agents. Because of its biocompatibility, biodegradability, and receptor-binding properties, HA has been extensively investigated as a drug delivery carrier. In the early sections of this chapter, readers were updated with all physiological and physicochemical aspects of HA and its potential to be used for targeting cancer was explained. RNAi is considered to be the most significant discovery in the field of molecular biology, and the discovery of NTs silencing of approximately 22–25 bp termed as siRNA (small interference RNA) has been a groundbreaking discovery in the field of biology. As siRNA is considered as a potential therapeutic candidate, there are many more essential aspects that have kept siRNA away from clinical acceptance. We have discussed the issues related to siRNA delivery to target cells and organs and how nanotechnology helps in resolving some of its problems; one such method is by using HA nanoparticles.

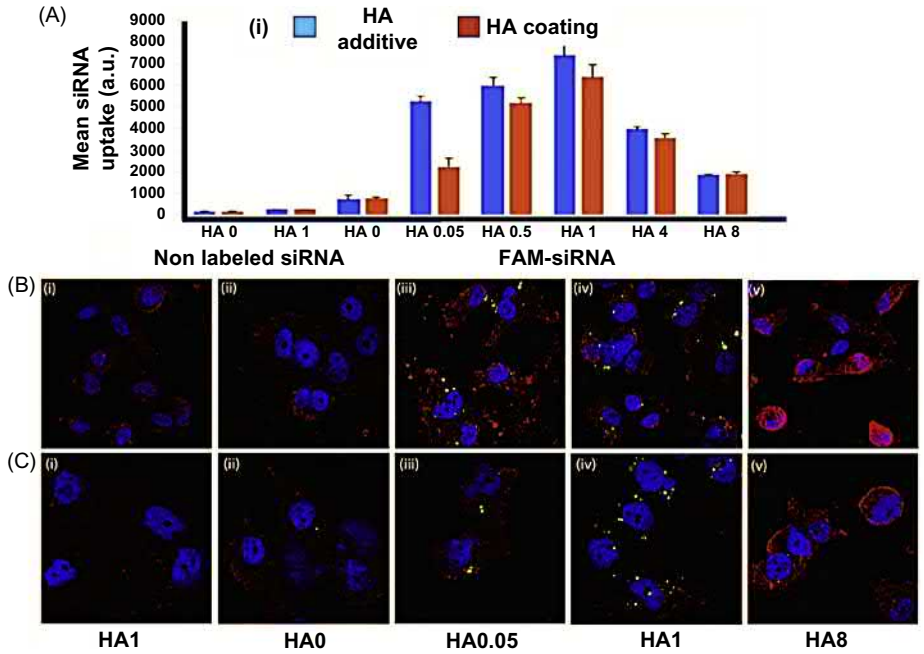

FIGURE 12.14 Cellular uptake of siRNA/polymer complexes after 24 h of transfection. (A) flow cytometry analysis is showing uptake of siRNA:PEI-LA in 1:6 w/w ratio with various amounts of HA. (B) Confocal microscopy images are showing uptake of FAM-siRNA/HA additive complex. Nonlabeled siRNA was transfected at 1:6:1 siRNA:PEI-LA:HA w/w/w ratio (i) as a negative control. Uptake of FAM-labeled siRNA was determined at 1:6:0 (ii), 1:6:0.05 (iii), 1:6:1 (iv), and 1:6:8 (v) siRNA:PEI-LA:HA w/w/w ratios. (C) Confocal microscopy images are showing cellular uptake of siRNA for HA coating with similar groups as in HA additive. Green color represents FAM-labeled siRNA complexes. FAM-Fluorescein. *HA*, Hyaluronic acid; *PEI*, polyethyleneimine; *siRNA*, silencing RNA. Source*: Adapted with permission from Parmar, M.B., Sundaram, D.N.M., KC, R.B., Maranchuk, R., Aliabadi, H.M., Hugh, J.C., et al., 2017. Combinational siRNA delivery using hyaluronic acid modified amphiphilic polyplexes against cell cycle and phosphatase proteins to inhibit growth and migration of triple-negative breast cancer cells. Acta Biomater. 66, 294–309, ©2017 Elsevier.*

This chapter successfully discussed HA-siRNA conjugate-based nanomedicines for diagnosis and treatment of different types of cancer. To develop a successful HA-siRNA conjugate, it is required to be prepared without significant deterioration of intrinsic property of HA. The chemical modification of HA with drugs or hydrophobic moieties may reduce the binding affinity of HA to the receptors. The investigations presented in the review revealed that the conjugation of siRNA to HA enhanced the resistance to RNase and facilitated the receptor-mediated endocytosis. In vitro gene silencing efficiency of HA–siRNA conjugates was in the range of 55%–80% in most of the studies.

Moreover, the cellular level targeting of HA–siRNA conjugates was also demonstrated to be effective in liver and breast cancer. Finally, the target-specific systemic delivery of HA–siRNA conjugates resulted in efficient downregulation of subjected genes. The target-specific HA–siRNA conjugate system can be effectively applied to the treatment of a variety of cancers and a promising futuristic approach as evident by the various clinical trials and patents presented in this review.

Acknowledgments

RKT would like to acknowledge Science and Engineering Research Board (Statutory Body Established Through an Act of Parliament: SERB Act 2008), Department of Science and Technology, Government of India for grant (Grant #ECR/2016/001964), and N-PDF funding (PDF/2016/003329) for work on targeted cancer therapy in Dr. Tekade's Laboratory. RKT also acknowledges Department of Pharmaceuticals, Ministry of Chemicals and Fertilizers, Government of India to support research program at NIPER-Ahmedabad.

ABBREVIATIONS

ABC	ATP-binding cassette
Ago2	argonaute-2
asiRNA	asymmetric shorter-duplex siRNA
ATP	adenosine triphosphate
AURKA	aurora kinase A
bPEI	branched polyethyleneimine
CAP	calcium phosphate
CBA	bisacrylamide
CD	cyclodextrin
CD44	cluster differentiating 44 receptors
CRC	colorectal cancer
CRISPER	clustered regularly interspaced short palindromic repeats
Cyt *C*	cytochrome *C*
Da	dalton
DGSCR8	Di George Syndrome Critical Region 8
Dopa	3,4-dihydroxy-L-phenylalanine
DSP	dithiobis (succinimidyl propionate)
dsRNA	double-stranded RNA
DTX	docetaxel
ECM	extracellular matrix
EDC	1-ethyl-3-(3-dimethylaminopropyl) carbodiimide
EPR	enhanced permeation and retention
ETP	etoposide
FAM	*Fluorescein* amidite
FBS	fetal bovine serum
GAG	glycosaminoglycan
HA	hyaluronic acid
HMW	high MW
HUVEC	human endothelial cells
IARC	International Agency for Research on Cancer
ICAM-1	intercellular adhesion molecule
ICG	indocyanine green
ICP-AES	inductively coupled plasma atomic emission spectroscopy
LHRH	luteinizing hormone−releasing hormone
MDR	multidrug resistance
MRI	magnetic resonance imaging
mRNA	messenger RNA
MVP	major vault protein
NHS	*N*-hydroxy succinimide
NIR	near infrared imaging
NIRF	near Infrared Fluorescence
NK	natural killer

NLC's	nanostructured lipid carriers
NP	nanoparticle
NT	nucleotide
OA	octandioic acid
PAMAM	poly amidoamine
PBMCs	peripheral blood mononuclear cells
pDNA	plasmid DNA
PEG	polyethylene glycol
PEI	poly ethylene imine
PEI-LA	linoleic acid substituted polyethyleneimine
Pgp	*P*-glycoprotein
PPI	polypropylenimin
PTX	paclitaxel
RES	reticuloendothelial system
RHAMM	receptor for HA-mediated motility
RISC	RNA-induced silencing complex
RISC	RNA-interfering silencing complex
RNAi	RNA interference
ROS	reactive oxygen species
shRNA	short hairpin RNA
si-AURKA	specific siRNA
siRNA	small interference RNA
siRNAs	silencing RNA
ss-siRNA	single-stranded siRNA
TEM	transmission electron microscopy
TNBC	triple negative breast cancer
TOS	D-α-tocopheryl succinate
VEGF	vascular endothelial growth factor
WHO	World Health Organization

References

Akmal, M., Singh, A., Anand, A., Kesani, A., Aslam, N., Goodship, A., et al., 2005. The effects of hyaluronic acid on articular chondrocytes. Bone Joint J. 87 (8), 1143–1149.

Al-Ghananeem, A.M., Malkawi, A.H., Muammer, Y.M., Balko, J.M., Black, E.P., Mourad, W., et al., 2009. Intratumoral delivery of paclitaxel in solid tumor from biodegradable hyaluronan nanoparticle formulations. AAPS PharmSciTech 10 (2), 410–417.

Ali, A.Y., Farrand, L., Kim, J.Y., Byun, S., Suh, J.Y., Lee, H.J., et al., 2012. Molecular determinants of ovarian cancer chemoresistance: new insights into an old conundrum. Ann. N. Y. Acad. Sci. 1271 (1), 58–67.

Al-Keilani, M., Darweesh, R., 2017. Sodium phenylbutyrate has an antineoplastic effect and enhances the cytotoxicity of 5-fluorouracil and irinotecan in colorectal cancer cell lines. In: AACR.

Almalik, A., Benabdelkamel, H., Masood, A., Alanazi, I.O., Alradwan, I., Majrashi, M.A., et al., 2017. Hyaluronic acid coated chitosan nanoparticles reduced the immunogenicity of the formed protein corona. Sci. Rep. 7 (1), 10542.

Almeida, P.V., Shahbazi, M.-A., Mäkilä, E., Kaasalainen, M., Salonen, J., Hirvonen, J., et al., 2014. Amine-modified hyaluronic acid-functionalized porous silicon nanoparticles for targeting breast cancer tumors. Nanoscale 6 (17), 10377–10387.

Al-Qadi, S., Alatorre-Meda, M., Zaghloul, E.M., Taboada, P., Remunán-López, C., 2013. Chitosan–hyaluronic acid nanoparticles for gene silencing: the role of hyaluronic acid on the nanoparticles' formation and activity. Colloids Surf., B: Biointerfaces 103, 615–623.

Anton, A.I.J., Fajardo, V.G., Palomar, V.R., 2017. SiRNA and Their Use in Methods and Compositions for the Treatment and/or Prevention of Eye Conditions. Google Patents.

Ashrafi, M., Hague, A., Baguneid, M., Alonso-Rasgado, T., Bayat, A., 2018. Wound healing and cutaneous scarring models of the human skin. Skin Tissue Models. Elsevier, pp. 201–221.
Balbino, T.A., Correa, G.S., Favaro, M.T., Toledo, M.A., Azzoni, A.R., Lucimara, G., 2015. Physicochemical and in vitro evaluation of cationic liposome, hyaluronic acid and plasmid DNA as pseudo-ternary complexes for gene delivery. Colloids Surf., A: Physicochem. Eng. Aspects 484, 262–270.
Bantounas, I., Phylactou, L., Uney, J., 2004. RNA interference and the use of small interfering RNA to study gene function in mammalian systems. J. Mol. Endocrinol. 33 (3), 545–557.
Bernstein, E., Denli, A.M., Hannon, G.J., 2001. The rest is silence. RNA 7 (11), 1509–1521.
Bobbin, M.L., Burnett, J.C., Rossi, J.J., 2015. RNA interference approaches for treatment of HIV-1 infection. Genome Med. 7 (1), 50.
Burdick, J.A., Prestwich, G.D., 2011. Hyaluronic acid hydrogels for biomedical applications. Adv. Mater. 23 (12), H41–56.
Burdick, J.A., Chung, C., Jia, X., Randolph, M.A., Langer, R., 2005. Controlled degradation and mechanical behavior of photopolymerized hyaluronic acid networks. Biomacromolecules 6 (1), 386–391.
Butel, N., Le Masson, I., Bouteiller, N., Vaucheret, H., Elmayan, T., 2017. sgs1: a neomorphic nac52 allele impairing post-transcriptional gene silencing through SGS3 downregulation. Plant J. 90 (3), 505–519.
Buyens, K., Lucas, B., Raemdonck, K., Braeckmans, K., Vercammen, J., Hendrix, J., et al., 2008. A fast and sensitive method for measuring the integrity of siRNA-carrier complexes in full human serum. J. Controlled Release 126 (1), 67–76.
Buyens, K., De Smedt, S.C., Braeckmans, K., Demeester, J., Peeters, L., van Grunsven, L.A., et al., 2012. Liposome based systems for systemic siRNA delivery: stability in blood sets the requirements for optimal carrier design. J. Controlled Release 158 (3), 362–370.
Cen, L., Neoh, K., Li, Y., Kang, E., 2004. Assessment of in vitro bioactivity of hyaluronic acid and sulfated hyaluronic acid functionalized electroactive polymer. Biomacromolecules 5 (6), 2238–2246.
Chen, J., Xie, J., 2012. Progress on RNAi-based molecular medicines. Int. J. Nanomed. 7, 3971.
Chen, X., Mangala, L.S., Rodriguez-Aguayo, C., Kong, X., Lopez-Berestein, G., Sood, A.K., 2017. RNA interference-based therapy and its delivery systems. Cancer Metastasis Rev. 37, 1–18.
Cheng, W., Liu, T., Wan, X., Gao, Y., Wang, H., 2012. MicroRNA-199a targets CD44 to suppress the tumorigenicity and multidrug resistance of ovarian cancer-initiating cells. FEBS J. 279 (11), 2047–2059.
Chi, J.-T., Chang, H.Y., Wang, N.N., Chang, D.S., Dunphy, N., Brown, P.O., 2003. Genomewide view of gene silencing by small interfering RNAs. Proc. Natl. Acad. Sci. U.S.A. 100 (11), 6343–6346.
Cho, K., Chung, T., Kim, B., Kim, M., Lee, J., Wee, W., et al., 2003. Release of ciprofloxacin from poloxamer-graft-hyaluronic acid hydrogels in vitro. Int. J. Pharm. 260 (1), 83–91.
Cho, S., Roh, K., Park, J., Park, Y.S., Lee, M., Cho, S., et al., 2017. Hydrolysis of hyaluronic acid in lymphedematous tissue alleviates fibrogenesis via TH 1 cell-mediated cytokine expression. Sci. Rep. 7 (1), 35.
Choi, K.Y., Min, K.H., Na, J.H., Choi, K., Kim, K., Park, J.H., et al., 2009. Self-assembled hyaluronic acid nanoparticles as a potential drug carrier for cancer therapy: synthesis, characterization, and in vivo biodistribution. J. Mater. Chem. 19 (24), 4102–4107.
Choi, K.-M., Jang, M., Kim, J.H., Ahn, H.J., 2014. Tumor-specific delivery of siRNA using supramolecular assembly of hyaluronic acid nanoparticles and 2b RNA-binding protein/siRNA complexes. Biomaterials 35 (25), 7121–7132.
Choi, J.U., Lee, S.W., Pangeni, R., Byun, Y., Yoon, I.-S., Park, J.W., 2017. Preparation and in vivo evaluation of cationic elastic liposomes comprising highly skin-permeable growth factors combined with hyaluronic acid for enhanced diabetic wound-healing therapy. Acta Biomater. 57, 197–215.
Chu, C.-Y., Rana, T.M., 2008. Potent RNAi by short RNA triggers. RNA 14 (9), 1714–1719.
Coffman, S.R., Lu, J., Guo, X., Zhong, J., Jiang, H., Broitman-Maduro, G., et al., 2017. *Caenorhabditis elegans* RIG-I homolog mediates antiviral RNA interference downstream of Dicer-dependent biogenesis of viral small interfering RNAs. mBio 8 (2), e00264-17.
Cohen, M.S., Cai, S., Xie, Y., Forrest, M.L., 2009. A novel intralymphatic nanocarrier delivery system for cisplatin therapy in breast cancer with improved tumor efficacy and lower systemic toxicity in vivo. Am. J. Surg. 198 (6), 781–786.
Coleman, R.L., Monk, B.J., Sood, A.K., Herzog, T.J., 2013. Latest research and treatment of advanced-stage epithelial ovarian cancer. Nat. Rev. Clin. Oncol. 10 (4), 211–224.

Collins, M.N., Birkinshaw, C., 2013. Hyaluronic acid based scaffolds for tissue engineering—a review. Carbohydr. Polym. 92 (2), 1262–1279.
Cortivo, R., Brun, P., Rastrelli, A., Abatangelo, G., 1991. In vitro studies on biocompatibility of hyaluronic acid esters. Biomaterials 12 (8), 727–730.
Cowman, M.K., Matsuoka, S., 2005. Experimental approaches to hyaluronan structure. Carbohydr. Res. 340 (5), 791–809.
Dalerba, P., Dylla, S.J., Park, I.-K., Liu, R., Wang, X., Cho, R.W., et al., 2007. Phenotypic characterization of human colorectal cancer stem cells. Proc. Natl. Acad. Sci. U.S.A. 104 (24), 10158–10163.
Dechert, T.A., Ducale, A.E., Ward, S.I., Yager, D.R., 2006. Hyaluronan in human acute and chronic dermal wounds. Wound Repair Regen. 14 (3), 252–258.
de la Fuente, M., Seijo, B., Alonso, M.J., 2008. Novel hyaluronic acid-chitosan nanoparticles for ocular gene therapy. Invest. Ophthalmol. Visual Sci. 49 (5), 2016–2024.
Ding, J., Liang, T., Zhou, Y., He, Z., Min, Q., Jiang, L., et al., 2017. Hyaluronidase-triggered anticancer drug and siRNA delivery from cascaded targeting nanoparticles for drug-resistant breast cancer therapy. Nano Res. 10 (2), 690–703.
Divita, G., Deshayes, S., Konate, K., Morris, M.C., 2017. Cell Penetrating Peptides for Intracellular Delivery of Molecules. Google Patents.
Elbashir, S.M., Harborth, J., Lendeckel, W., Yalcin, A., Weber, K., Tuschl, T., 2001a. Duplexes of 21-nucleotide RNAs mediate RNA interference in cultured mammalian cells. Nature 411 (6836), 494–498.
Elbashir, S.M., Martinez, J., Patkaniowska, A., Lendeckel, W., Tuschl, T., 2001b. Functional anatomy of siRNAs for mediating efficient RNAi in *Drosophila melanogaster* embryo lysate. EMBO J. 20 (23), 6877–6888.
Esser, P.R., Wölfle, U., Dürr, C., von Loewenich, F.D., Schempp, C.M., Freudenberg, M.A., et al., 2012. Contact sensitizers induce skin inflammation via ROS production and hyaluronic acid degradation. PLoS One 7 (7), e41340.
Fakhari, A., 2012. Biomedical Application of Hyaluronic Acid Nanoparticles. University of Kansas.
Falcone, S.J., Palmeri, D., Berg, R.A., 2006. Biomedical Applications of Hyaluronic Acid. ACS Publications.
Figueroa, C., Suárez, B., Molina, A., Fernández, J., Torres, Z., Griebenow, K., 2017. Smart release nanoformulation of cytochrome *C* and hyaluronic acid induces apoptosis in cancer cells. J. Nanomed. Nanotechnol. 8 (1), 427.
Fire, A., Xu, S., Montgomery, M.K., Kostas, S.A., Driver, S.E., Mello, C.C., 1998. Potent and specific genetic interference by double-stranded RNA in *Caenorhabditis elegans*. Nature 391 (6669), 806.
Fonseca, D.P., Khalil, N.M., Mainardes, R.M., 2017. Bovine serum albumin-based nanoparticles containing resveratrol: characterization and antioxidant activity. J. Drug Deliv. Sci. Technol. 39, 147–155.
Fraser, J., Laurent, T., Laurent, U., 1997. Hyaluronan: its nature, distribution, functions and turnover. J. Intern. Med. Suppl. 242 (1), 27–33.
Fukushige, K., Tagami, T., Ozeki, T., 2017. The offset effect of a hyaluronic acid coating to cationic carriers containing siRNA: alleviated cytotoxicity and retained gene silencing in vitro. J. Drug Deliv. Sci. Technol. 39, 435–441.
Ganesh, S., Iyer, A.K., Gattacceca, F., Morrissey, D.V., Amiji, M.M., 2013a. In vivo biodistribution of siRNA and cisplatin administered using CD44-targeted hyaluronic acid nanoparticles. J. Controlled Release 172 (3), 699–706.
Ganesh, S., Iyer, A.K., Morrissey, D.V., Amiji, M.M., 2013b. Hyaluronic acid based self-assembling nanosystems for CD44 target mediated siRNA delivery to solid tumors. Biomaterials 34 (13), 3489–3502.
Garg, H.G., Hales, C.A., 2004. Chemistry and Biology of Hyaluronan. Elsevier.
Gibbs, D.A., Merrill, E., Smith, K.A., Balazs, E., 1968. Rheology of hyaluronic acid. Biopolymers 6 (6), 777–791.
Gilleron, J., Querbes, W., Zeigerer, A., Borodovsky, A., Marsico, G., Schubert, U., et al., 2013. Image-based analysis of lipid nanoparticle–mediated siRNA delivery, intracellular trafficking and endosomal escape. Nat. Biotechnol. 31 (7), 638.
Götte, M., Yip, G.W., 2006. Heparanase, hyaluronan, and CD44 in cancers: a breast carcinoma perspective. Cancer Res. 66 (21), 10233–10237.
Han, M., Lv, Q., Tang, X.-J., Hu, Y.-L., Xu, D.-H., Li, F.-Z., et al., 2012. Overcoming drug resistance of MCF-7/ADR cells by altering intracellular distribution of doxorubicin via MVP knockdown with a novel siRNA polyamidoamine-hyaluronic acid complex. J. Controlled Release 163 (2), 136–144.
Heale, B.S., Soifer, H.S., Bowers, C., Rossi, J.J., 2005. siRNA target site secondary structure predictions using local stable substructures. Nucleic Acids Res. 33 (3), 1–10.

Holstlaw, T.A., Mahomed, M., Brier, L.W., Young, D.M., Boudreau, N.J., Jackson, W.M., 2017. biopolymer molecular weight can modulate the wound healing efficacy of multivalent sonic hedgehog–hyaluronic acid conjugates. Biomacromolecules 18 (8), 2350–2359.
Hou, K.K., Pan, H., Ratner, L., Schlesinger, P.H., Wickline, S.A., 2013. Mechanisms of nanoparticle-mediated siRNA transfection by melittin-derived peptides. ACS Nano 7 (10), 8605–8615.
Hsieh, C.-M., Huang, Y.-W., Sheu, M.-T., Ho, H.-O., 2014. Biodistribution profiling of the chemical modified hyaluronic acid derivatives used for oral delivery system. Int. J. Biol. Macromol. 64, 45–52.
Huang, C., Zhang, Y., Yuan, H., Gao, H., Zhang, S., 2013. Role of nanoparticle geometry in endocytosis: laying down to stand up. Nano. Lett. 13 (9), 4546–4550.
Huang, T.L., Yang, C.H., Yanai, G., Liao, J.Y., Sumi, S., Yang, K.C., 2017. Synergistic effect of L-ascorbic acid and hyaluronic acid on the expressions of matrix metalloproteinase-3 and -9 in human chondrocytes. J. Biomed. Mater. Res., B: Appl. Biomater. 106, 1809–1817.
Iki, T., Tschopp, M.-A., Voinnet, O., 2017. Biochemical and genetic functional dissection of the P38 viral suppressor of RNA silencing. RNA 23 (5), 639–654.
Jackson, A.L., Bartz, S.R., Schelter, J., Kobayashi, S.V., Burchard, J., Mao, M., et al., 2003. Expression profiling reveals off-target gene regulation by RNAi. Nat. Biotechnol. 21 (6), 635.
Jagannath, S., Ramachandran, K., 2010. Influence of competing metabolic processes on the molecular weight of hyaluronic acid synthesized by *Streptococcus zooepidemicus*. Biochem. Eng. J. 48 (2), 148–158.
Jain, R.K., 1987. Transport of molecules in the tumor interstitium: a review. Cancer Res. 47 (12), 3039–3051.
Jang, S.H., Wientjes, M.G., Lu, D., Au, J.L.-S., 2003. Drug delivery and transport to solid tumors. Pharm. Res. 20 (9), 1337–1350.
Jensen, K., Anderson, J.A., Glass, E.J., 2014. Comparison of small interfering RNA (siRNA) delivery into bovine monocyte-derived macrophages by transfection and electroporation. Vet. Immunol. Immunopathol. 158 (3–4), 224–232.
Jeon, O., Song, S.J., Lee, K.-J., Park, M.H., Lee, S.-H., Hahn, S.K., et al., 2007. Mechanical properties and degradation behaviors of hyaluronic acid hydrogels cross-linked at various cross-linking densities. Carbohydr. Polym. 70 (3), 251–257.
Jian, Y.-S., Chen, C.-W., Lin, C.-A., Yu, H.-P., Lin, H.-Y., Liao, M.-Y., et al., 2017. Hyaluronic acid–nimesulide conjugates as anticancer drugs against cD44-overexpressing hT-29 colorectal cancer in vitro and in vivo. Int. J. Nanomed. 12, 2315.
Jiang, G., Park, K., Kim, J., Kim, K.S., Oh, E.J., Kang, H., et al., 2008. Hyaluronic acid–polyethyleneimine conjugate for target specific intracellular delivery of siRNA. Biopolymers 89 (7), 635–642.
Jin, Y.-J., Ubonvan, T., Kim, D.-D., 2010. Hyaluronic acid in drug delivery systems. J. Pharm. Invest. 40 (spc), 33–43.
Joseph, B., Ajisha, S., Jeevitha, M., 2012. SiRNA mediated gene silencing: a mini review. ACEH Int. J. Sci. Technol. 1, 98–103.
Judge, A.D., Sood, V., Shaw, J.R., Fang, D., McClintock, K., MacLachlan, I., 2005. Sequence-dependent stimulation of the mammalian innate immune response by synthetic siRNA. Nat. Biotechnol. 23 (4), 457.
Judge, A.D., Bola, G., Lee, A.C., MacLachlan, I., 2006. Design of noninflammatory synthetic siRNA mediating potent gene silencing in vivo. Mol. Ther. 13 (3), 494–505.
Jun, J.Y., Nguyen, H.H., Chun, H.S., Kang, B.-C., Ko, S., 2011. Preparation of size-controlled bovine serum albumin (BSA) nanoparticles by a modified desolvation method. Food. Chem. 127 (4), 1892–1898.
Kanasty, R., Dorkin, J.R., Vegas, A., Anderson, D., 2013. Delivery materials for siRNA therapeutics. Nat. Mater. 12 (11), 967.
Karikó, K., Bhuyan, P., Capodici, J., Weissman, D., 2004. Small interfering RNAs mediate sequence-independent gene suppression and induce immune activation by signaling through toll-like receptor 3. J. Immunol. 172 (11), 6545–6549.
Karousou, E., Misra, S., Ghatak, S., Dobra, K., Götte, M., Vigetti, D., et al., 2017. Roles and targeting of the HAS/hyaluronan/CD44 molecular system in cancer. Matrix Biol. 59, 3–22.
Kasuya, T., Hori, S.-I., Watanabe, A., Nakajima, M., Gahara, Y., Rokushima, M., et al., 2016. Ribonuclease H1-dependent hepatotoxicity caused by locked nucleic acid-modified gapmer antisense oligonucleotides. Sci. Rep. 6, 30377.
Kim, H.L., 2004. Hyaluronan facilitates invasion of colon carcinoma cells in vitro via interaction with CD44 and hyaluronan synthesis is upregulated in metastatic colon carcinoma cells. Kor. Soc. Surg. Abstr. 33–35.

Kim, J.-E., Sykes, J.M., 2011. Hyaluronic acid fillers: history and overview. Facial Plast. Surg. 27 (06), 523–528.
Kim, G., Han, H., 2017. Targeted Delivery of Hyaluronic Acid-Labeled Chitosan Nanoparticles Against CD44 Overexpressed Endothelial Cell for Tumor Angiogenesis Therapy. AACR.
Kim, H.-R., Wheeler, M.A., Wilson, C.M., Iida, J., Eng, D., Simpson, M.A., et al., 2004. Hyaluronan facilitates invasion of colon carcinoma cells in vitro via interaction with CD44. Cancer Res. 64 (13), 4569–4576.
Kim, K., Park, S., Yang, J.-A., Jeon, J.-H., Bhang, S., Kim, B.-S., et al., 2011. Injectable hyaluronic acid–tyramine hydrogels for the treatment of rheumatoid arthritis. Acta Biomater. 7 (2), 666–674.
Kim, Y.-K., Kim, B., Kim, V.N., 2016. Re-evaluation of the roles of DROSHA, Exportin 5, and DICER in microRNA biogenesis. Proc. Natl. Acad. Sci. U.S.A. 113 (13), E1881–E1889.
Kim, Y., Kang, Y.G., Choe, J.Y., Lee, D., Shin, C., Hong, S.W., et al., 2017. RNA interference-mediated gene silencing by branched tripodal RNAs does not require dicer processing. Nucleic Acid Ther. 28, 44–49.
Kopp, R., Fichter, M., Schalhorn, G., Danescu, J., Classen, S., 2009. Frequent expression of the high molecular, 673-bp CD44v3, v8-10 variant in colorectal adenomas and carcinomas. Int. J. Mol. Med. 24 (5), 677–683.
Kreil, G., 1995. Hyaluronidases—a group of neglected enzymes. Protein Sci. 4 (9), 1666–1669.
Kutlusoy, T., Oktay, B., Apohan, N.K., Süleymanoğlu, M., Kuruca, S.E., 2017. Chitosan-co-hyaluronic acid porous cryogels and their application in tissue engineering. Int. J. Biol. Macromol. 103, 366–378.
Lalu, L., Tambe, V., Pradhan, D., Nayak, K., Bagchi, S., Maheshwari, R., et al., 2017. Novel nanosystems for the treatment of ocular inflammation: current paradigms and future research directions. J. Controlled Release 268, 19–39.
Lam, J.K.-W., Liang, W., Chan, H.-K., 2012. Pulmonary delivery of therapeutic siRNA. Adv. Drug Deliv. Rev. 64 (1), 1–15.
Lam, J., Truong, N.F., Segura, T., 2014. Design of cell–matrix interactions in hyaluronic acid hydrogel scaffolds. Acta Biomater. 10 (4), 1571–1580.
Lee, J.Y., Spicer, A.P., 2000. Hyaluronan: a multifunctional, megaDalton, stealth molecule. Curr. Opin. Cell Biol. 12 (5), 581–586.
Lee, M.-Y., Park, S.-J., Park, K., Kim, K.S., Lee, H., Hahn, S.K., 2011. Target-specific gene silencing of layer-by-layer assembled gold–cysteamine/siRNA/PEI/HA nanocomplex. ACS Nano 5 (8), 6138–6147.
Lee, M.S., Lee, J.E., Byun, E., Kim, N.W., Lee, K., Lee, H., et al., 2014. Target-specific delivery of siRNA by stabilized calcium phosphate nanoparticles using dopa–hyaluronic acid conjugate. J. Controlled Release 192, 122–130.
Leung, E.L.-H., Fiscus, R.R., Tung, J.W., Tin, V.P.-C., Cheng, L.C., Sihoe, A.D.-L., et al., 2010. Nonsmall cell lung cancer cells expressing CD44 are enriched for stem cell-like properties. PLoS One 5 (11), e14062.
Li, C.J., 2017. Asymmetric Interfering RNA Compositions That Silence k-ras and Methods of Uses Thereof. Google Patents.
Li, S.-D., Chono, S., Huang, L., 2008. Efficient gene silencing in metastatic tumor by siRNA formulated in surface-modified nanoparticles. J. Controlled Release 126 (1), 77–84.
Li, J., Hou, N., Faried, A., Tsutsumi, S., Kuwano, H., 2010. Inhibition of autophagy augments 5-fluorouracil chemotherapy in human colon cancer in vitro and in vivo model. Eur. J. Cancer 46 (10), 1900–1909.
Lin, T., Yuan, A., Zhao, X., Lian, H., Zhuang, J., Chen, W., et al., 2017. Self-assembled tumor-targeting hyaluronic acid nanoparticles for photothermal ablation in orthotopic bladder cancer. Acta Biomater. 53, 427–438.
Liu, J.-Y., Li, Y., Hu, Y., Cheng, G., Ye, E., Shen, C., et al., 2018. Hemostatic porous sponges of cross-linked hyaluronic acid/cationized dextran by one self-foaming process. Mater. Sci. Eng., C 83, 160–168.
Lokeshwar, V.B., Mirza, S., Jordan, A., 2014. Targeting hyaluronic acid family for cancer chemoprevention and therapy. Adv. Cancer Res. 123, 35–65.
Longley, D.B., Allen, W.L., Johnston, P.G., 2006. Drug resistance, predictive markers and pharmacogenomics in colorectal cancer. Biochim. Biophys. Acta, Rev. Cancer 1766 (2), 184–196.
Lopez, J., Banerjee, S., Kaye, S., 2013. New developments in the treatment of ovarian cancer—future perspectives. Ann. Oncol. 24 (suppl_10), x69–x76.
Lund, E., Dahlberg, J., 2006. Substrate selectivity of exportin 5 and Dicer in the biogenesis of microRNAs. Cold Spring Harbor Symposia on quantitative Biology. Cold Spring Harbor Laboratory Press, pp. 59–66.
Maheshwari, R., Tekade, M., Sharma, P.A., Tekade, R.K., 2015a. Nanocarriers assisted siRNA gene therapy for the management of cardiovascular disorders. Curr. Pharm. Des. 21 (30), 4427–4440.

Maheshwari, R.G., Thakur, S., Singhal, S., Patel, R.P., Tekade, M., Tekade, R.K., 2015b. Chitosan encrusted non-ionic surfactant based vesicular formulation for topical administration of ofloxacin. Sci. Adv. Mater. 7 (6), 1163–1176.

Maheshwari, R., Tekade, M., Gondaliya, P., Kalia, K., D'Emanuele, A., Tekade, R.K., 2017. Recent advances in exosome-based nanovehicles as RNA interference therapeutic carriers. Nanomedicine (London) 12 (21), 2653–2675.

Mattheolabakis, G., Milane, L., Singh, A., Amiji, M.M., 2015. Hyaluronic acid targeting of CD44 for cancer therapy: from receptor biology to nanomedicine. J. Drug. Target. 23 (7–8), 605–618.

Meister, G., Tuschl, T., 2004. Mechanisms of gene silencing by double-stranded RNA. Nature 431 (7006), 343.

Mele, V., Sokol, L., Kölzer, V.H., Pfaff, D., Muraro, M.G., Keller, I., et al., 2017. The hyaluronan-mediated motility receptor RHAMM promotes growth, invasiveness and dissemination of colorectal cancer. Oncotarget 8 (41), 70617.

Merkel, O.M., Rubinstein, I., Kissel, T., 2014. siRNA delivery to the lung: what's new? Adv. Drug Deliv. Rev. 75, 112–128.

Mero, A., Campisi, M., 2014. Hyaluronic acid bioconjugates for the delivery of bioactive molecules. Polymers 6 (2), 346–369.

Meyer, K., Palmer, J.W., 1934. The polysaccharide of the vitreous humor. J. Biol. Chem. 107 (3), 629–634.

Morrissey, D.V., Lockridge, J.A., Shaw, L., Blanchard, K., Jensen, K., Breen, W., et al., 2005. Potent and persistent in vivo anti-HBV activity of chemically modified siRNAs. Nat. Biotechnol. 23 (8), 1002.

Murashov, A.K., 2010. A brief introduction to RNAi and microRNAs in stem cells. RNAi and microRNA-Mediated Gene Regulation in Stem Cells. Springer, pp. 15–25.

Naor, D., Nedvetzki, S., Golan, I., Melnik, L., Faitelson, Y., 2002. CD44 in cancer. Crit. Rev. Clin. Lab. Sci. 39 (6), 527–579.

Nascimento, T.L., Hillaireau, H., Vergnaud, J., Rivano, M., Deloménie, C., Courilleau, D., et al., 2016. Hyaluronic acid-conjugated lipoplexes for targeted delivery of siRNA in a murine metastatic lung cancer model. Int. J. Pharm. 514 (1), 103–111.

Nath, S.D., Abueva, C., Kim, B., Lee, B.T., 2015. Chitosan–hyaluronic acid polyelectrolyte complex scaffold cross-linked with genipin for immobilization and controlled release of BMP-2. Carbohydr. Polym. 115, 160–169.

Necas, J., Bartosikova, L., Brauner, P., Kolar, J., 2008. Hyaluronic acid (hyaluronan): a review. Vet. Med. (Praha) 53 (8), 397–411.

Neuman, M.G., Nanau, R.M., Oruña-Sanchez, L., Coto, G., 2015. Hyaluronic acid and wound healing. J. Pharm. Pharm. Sci. 18 (1), 53–60.

Nicholls, M., Manjoo, A., Shaw, P., Niazi, F., Rosen, J., 2018. Rheological properties of commercially available hyaluronic acid products in the United States for the treatment of osteoarthritis knee pain. Clin. Med. Insights Arthritis Musculoskelet. Disord. 11, 1179544117751622.

Nieth, C., Priebsch, A., Stege, A., Lage, H., 2003. Modulation of the classical multidrug resistance (MDR) phenotype by RNA interference (RNAi). FEBS Lett. 545 (2–3), 144–150.

Park, K., Lee, M.-Y., Kim, K.S., Hahn, S.K., 2010. Target specific tumor treatment by VEGF siRNA complexed with reducible polyethyleneimine–hyaluronic acid conjugate. Biomaterials 31 (19), 5258–5265.

Parmar, M.B., Sundaram, D.N.M., KC, R.B., Maranchuk, R., Aliabadi, H.M., Hugh, J.C., et al., 2017. Combinational siRNA delivery using hyaluronic acid modified amphiphilic polyplexes against cell cycle and phosphatase proteins to inhibit growth and migration of triple-negative breast cancer cells. Acta Biomater. 66, 294–309.

Patil, Y., Panyam, J., 2009. Polymeric nanoparticles for siRNA delivery and gene silencing. Int. J. Pharm. 367 (1–2), 195–203.

Poulet, A., Duc, C., Voisin, M., Desset, S., Tutois, S., Vanrobays, E., et al., 2017. The LINC complex contributes to heterochromatin organisation and transcriptional gene silencing in plants. J. Cell. Sci. 130 (3), 590–601.

Quiñones, J.P., Brüggemann, O., Covas, C.P., Ossipov, D.A., 2017. Self-assembled hyaluronic acid nanoparticles for controlled release of agrochemicals and diosgenin. Carbohydr. Polym. 173, 157–169.

Ran, R., Liu, Y., Gao, H., Kuang, Q., Zhang, Q., Tang, J., et al., 2014. Enhanced gene delivery efficiency of cationic liposomes coated with PEGylated hyaluronic acid for antiP-glycoprotein siRNA: a potential candidate for overcoming multi-drug resistance. Int. J. Pharm. 477 (1–2), 590–600.

Ran, R., Liu, Y., Gao, H., Kuang, Q., Zhang, Q., Tang, J., et al., 2015. PEGylated hyaluronic acid-modified liposomal delivery system with anti-γ-glutamylcyclotransferase siRNA for drug-resistant MCF-7 breast cancer therapy. J. Pharm. Sci. 104 (2), 476–484.

Ranke, J., Müller, A., Bottin-Weber, U., Stock, F., Stolte, S., Arning, J., et al., 2007. Lipophilicity parameters for ionic liquid cations and their correlation to in vitro cytotoxicity. Ecotoxicol. Environ. Saf. 67 (3), 430–438.

Rayahin, J.E., Buhrman, J.S., Zhang, Y., Koh, T.J., Gemeinhart, R.A., 2015. High and low molecular weight hyaluronic acid differentially influence macrophage activation. ACS Biomater. Sci. Eng. 1 (7), 481–493.

Resnier, P., Montier, T., Mathieu, V., Benoit, J.-P., Passirani, C., 2013. A review of the current status of siRNA nanomedicines in the treatment of cancer. Biomaterials 34 (27), 6429–6443.

Schlenk, F., Werner, S., Rabel, M., Jacobs, F., Bergemann, C., Clement, J.H., et al., 2017. Comprehensive analysis of the in vitro and ex ovo hemocompatibility of surface engineered iron oxide nanoparticles for biomedical applications. Arch. Toxicol. 1–16.

Seton-Rogers, S., 2012. Metastasis: multitasking hyaluronic acid. Nat. Rev. Cancer 12 (4), 228-228.

Shah, V., Taratula, O., Garbuzenko, O.B., Taratula, O.R., Rodriguez-Rodriguez, L., Minko, T., 2013. Targeted nanomedicine for suppression of CD44 and simultaneous cell death induction in ovarian cancer: an optimal delivery of siRNA and anticancer drug. Clin. Cancer Res. 19 (22), 6193–6204.

Sharma, P.A., Maheshwari, R., Tekade, M., Tekade, R.K., 2015. Nanomaterial based approaches for the diagnosis and therapy of cardiovascular diseases. Curr. Pharm. Des. 21 (30), 4465–4478.

Sheehan, J., Arundel, C., Phelps, C., 1983. Effect of the cations sodium, potassium and calcium on the interaction of hyaluronate chains: a light scattering and viscometric study. Int. J. Biol. Macromol. 5 (4), 222–228.

Shen, H., Mittal, V., Ferrari, M., Chang, J., 2013. Delivery of gene silencing agents for breast cancer therapy. Breast Cancer Res. 15 (3), 205.

Shiedlin, A., Bigelow, R., Christopher, W., Arbabi, S., Yang, L., Maier, R.V., et al., 2004. Evaluation of hyaluronan from different sources: *Streptococcus zooepidemicus*, rooster comb, bovine vitreous, and human umbilical cord. Biomacromolecules 5 (6), 2122–2127.

Shu, X.Z., Liu, Y., Palumbo, F.S., Luo, Y., Prestwich, G.D., 2004. In situ cross-linkable hyaluronan hydrogels for tissue engineering. Biomaterials 25 (7–8), 1339–1348.

Siegel, R., Ma, J., Zou, Z., Jemal, A., 2014. Cancer statistics, 2014. CA Cancer J. Clin. 64 (1), 9–29.

Siolas, D., Lerner, C., Burchard, J., Ge, W., Linsley, P.S., Paddison, P.J., et al., 2005. Synthetic shRNAs as potent RNAi triggers. Nat. Biotechnol. 23 (2), 227–231.

Sironen, R., Tammi, M., Tammi, R., Auvinen, P., Anttila, M., Kosma, V., 2011. Hyaluronan in human malignancies. Exp. Cell Res. 317 (4), 383–391.

Stern, R., Kogan, G., Jedrzejas, M.J., Šoltés, L., 2007. The many ways to cleave hyaluronan. Biotechnol. Adv. 25 (6), 537–557.

Surace, C., Arpicco, S., Dufaÿ-Wojcicki, A.L., Marsaud, V.R., Bouclier, C.L., Clay, D., et al., 2009. Lipoplexes targeting the CD44 hyaluronic acid receptor for efficient transfection of breast cancer cells. Mol. Pharm. 6 (4), 1062–1073.

Takahashi, I., Yamada, S., Nata, K., 2017. Effects of heparan sulfate proteoglycan syndecan-4 on the insulin secretory response in a mouse pancreatic β-cell line, MIN6. Mol. Cell. Endocrinol.

Tang, Y., Li, Y.-B., Wang, B., Lin, R.-Y., van Dongen, M., Zurcher, D.M., et al., 2012. Efficient in vitro siRNA delivery and intramuscular gene silencing using PEG-modified PAMAM dendrimers. Mol. Pharm. 9 (6), 1812–1821.

Taratula, O., Kuzmov, A., Shah, M., Garbuzenko, O.B., Minko, T., 2013. Nanostructured lipid carriers as multifunctional nanomedicine platform for pulmonary co-delivery of anticancer drugs and siRNA. J. Controlled Release 171 (3), 349–357.

Tekade, R.K., Maheshwari, R., Sharma, P.A., Tekade, M., Chauhan, A.S., 2015. siRNA therapy, challenges and underlying perspectives of dendrimer as delivery vector. Curr. Pharm. Des. 21 (31), 4614–4636.

Tekade, R.K., Tekade, M., Kesharwani, P., D'Emanuele, A., 2016. RNAi-combined nano-chemotherapeutics to tackle resistant tumors. Drug Discov. Today 21 (11), 1761–1774.

Tekade, R.K., Maheshwari, R., Soni, N., Tekade, M., Chougule, M.B., 2017a. Chapter 1—Nanotechnology for the Development of Nanomedicine. In: Kesharwani, P., Amin, M.C.I.M., Iyer, A. (Eds.), Nanotechnology-Based Approaches for Targeting and Delivery of Drugs and Genes. Academic Press, pp. 3–61.

Teng, B.P., Heffler, M.D., Lai, E.C., Zhao, Y.-L., LeVea, C.M., Golubovskaya, V.M., et al., 2011. Inhibition of hyaluronan synthase-3 decreases subcutaneous colon cancer growth by increasing apoptosis. Anticancer Agents Med. Chem. 11 (7), 620–628.

Tezgel, Ö., Szarpak-Jankowska, A., Arnould, A., Auzély-Velty, R., Texier, I., 2018. Chitosan-lipid nanoparticles (CS-LNPs): application to siRNA delivery. J. Colloid. Interface. Sci. 510, 45–56.
Tokita, Y., Okamoto, A., 1995. Hydrolytic degradation of hyaluronic acid. Polym. Degrad. Stab. 48 (2), 269–273.
Toole, B.P., 2001. Hyaluronan in morphogenesis. Semin. Cell Dev. Biol. 12, 79–87.
Torre, L.A., Bray, F., Siegel, R.L., Ferlay, J., Lortet-Tieulent, J., Jemal, A., 2015. Global cancer statistics, 2012. CA Cancer J. Clin. 65 (2), 87–108.
Tsepilov, R., Beloded, A., 2015. Hyaluronic acid—an "old" molecule with "new" functions: biosynthesis and depolymerization of hyaluronic acid in bacteria and vertebrate tissues including during carcinogenesis. Biochemistry (Moscow) 80 (9), 1093–1108.
Turner, J.J., Jones, S.W., Moschos, S.A., Lindsay, M.A., Gait, M.J., 2006. MALDI-TOF mass spectral analysis of siRNA degradation in serum confirms an RNAse A-like activity. Mol. Biosyst. 3 (1), 43–50.
Turner, J.M., 2015. Meiotic silencing in mammals. Annu. Rev. Genet. 49, 395–412.
Vafaei, S.Y., Esmaeili, M., Amini, M., Atyabi, F., Ostad, S.N., Dinarvand, R., 2016. Self assembled hyaluronic acid nanoparticles as a potential carrier for targeting the inflamed intestinal mucosa. Carbohydr. Polym. 144, 371–381.
Vangara, K.K., Liu, J.L., Palakurthi, S., 2013. Hyaluronic acid-decorated PLGA-PEG nanoparticles for targeted delivery of SN-38 to ovarian cancer. Anticancer Res. 33 (6), 2425–2434.
Volpi, N., Schiller, J., Stern, R., Soltes, L., 2009. Role, metabolism, chemical modifications and applications of hyaluronan. Curr. Med. Chem. 16 (14), 1718–1745.
Wang, J., Lu, Z., Wientjes, M.G., Au, J.L.-S., 2010. Delivery of siRNA therapeutics: barriers and carriers. AAPS J. 12 (4), 492–503.
Wang, C., Xie, J., Guo, J., Manning, H.C., Gore, J.C., Guo, N., 2012. Evaluation of CD44 and CD133 as cancer stem cell markers for colorectal cancer. Oncol. Rep. 28 (4), 1301–1308.
Wang, H., Sun, D., Liao, H., Wang, Y., Zhao, S., Zhang, Y., et al., 2017a. Synthesis and characterization of a bimodal nanoparticle based on the host-guest self-assembly for targeted cellular imaging. Talanta 171, 8–15.
Wang, H., Sun, G., Zhang, Z., Ou, Y., 2017b. Transcription activator, hyaluronic acid and tocopheryl succinate multi-functionalized novel lipid carriers encapsulating etoposide for lymphoma therapy. Biomed. Pharmacother. 91, 241–250.
Whitehead, K.A., Langer, R., Anderson, D.G., 2009. Knocking down barriers: advances in siRNA delivery. Nat. Rev. Drug. Discov. 8 (2), 129.
Wu, J., Deng, C., Meng, F., Zhang, J., Sun, H., Zhong, Z., 2017. Hyaluronic acid coated PLGA nanoparticulate docetaxel effectively targets and suppresses orthotopic human lung cancer. J. Controlled Release 259, 76–82.
Xu, L., Yeudall, W.A., Yang, H., 2017. Folic acid-decorated polyamidoamine dendrimer exhibits high tumor uptake and sustained highly localized retention in solid tumors: Its utility for local siRNA delivery. Acta Biomater. 57, 251–261.
Yang, X.-Y., Li, Y.-X., Li, M., Zhang, L., Feng, L.-X., Zhang, N., 2013. Hyaluronic acid-coated nanostructured lipid carriers for targeting paclitaxel to cancer. Cancer Lett. 334 (2), 338–345.
Yang, X., Singh, A., Choy, E., Hornicek, F.J., Amiji, M.M., Duan, Z., 2015. MDR1 siRNA loaded hyaluronic acid-based CD44 targeted nanoparticle systems circumvent paclitaxel resistance in ovarian cancer. Sci. Rep. 5, 8509.
Yang, D., Feng, L., Dougherty, C.A., Luker, K.E., Chen, D., Cauble, M.A., et al., 2016. In vivo targeting of metastatic breast cancer via tumor vasculature-specific nano-graphene oxide. Biomaterials 104, 361–371.
Yang, C., Li, C., Zhang, P., Wu, W., Jiang, X., 2017. Redox responsive hyaluronic acid nanogels for treating RHAMM (CD168) over-expressive cancer, both primary and metastatic tumors. Theranostics 7 (6), 1719.
Yezhelyev, M.V., Qi, L., O'Regan, R.M., Nie, S., Gao, X., 2008. Proton-sponge coated quantum dots for siRNA delivery and intracellular imaging. J. Am. Chem. Soc. 130 (28), 9006–9012.
Yin, T., Wang, L., Yin, L., Zhou, J., Huo, M., 2015. Co-delivery of hydrophobic paclitaxel and hydrophilic AURKA specific siRNA by redox-sensitive micelles for effective treatment of breast cancer. Biomaterials 61, 10–25.
Yoon, H.Y., Kim, H.R., Saravanakumar, G., Heo, R., Chae, S.Y., Um, W., et al., 2013. Bioreducible hyaluronic acid conjugates as siRNA carrier for tumor targeting. J. Controlled Release 172 (3), 653–661.
Yu, H., Kumar, P., 2003. Post-transcriptional gene silencing in plants by RNA. Plant Cell Rep. 22 (3), 167–174.
Zhao, J.Y., Chai, J.K., Song, H.F., Zhang, J., Xu, M.H., Liang, Y.D., 2013. Influence of hyaluronic acid on wound healing using composite porcine acellular dermal matrix grafts and autologous skin in rabbits. Int. Wound. J. 10 (5), 562–572.

Further reading

Maheshwari, R.G., Tekade, R.K., Sharma, P.A., Darwhekar, G., Tyagi, A., Patel, R.P., et al., 2012. Ethosomes and ultradeformable liposomes for transdermal delivery of clotrimazole: a comparative assessment. Saudi Pharm. J. 20 (2), 161–170.

Soni, N., Tekade, M., Kesharwani, P., Bhattacharya, P., Maheshwari, R., Dua, K., et al., 2017. Recent advances in oncological submissions of dendrimer. Curr. Pharm. Des. 23 (21), 3084–3098.

Tekade, R.K., Maheshwari, R., Tekade, M., Chougule, M.B., 2017b. Chapter 8—Solid lipid nanoparticles for targeting and delivery of drugs and genes. In: Kesharwani, P., Amin, M.C.I.M., Iyer, A. (Eds.), Nanotechnology-Based Approaches for Targeting and Delivery of Drugs and Genes. Academic Press, pp. 256–286.

CHAPTER

13

Thiolated-Chitosan: A Novel Mucoadhesive Polymer for Better-Targeted Drug Delivery

Muktika Tekade[1], *Neha Maheshwari*[1], *Susanne R. Youngren-Ortiz*[2], *Vikas Pandey*[3], *Yashu Chourasiya*[4], *Vandana Soni*[3], *Pran Kishore Deb*[5] *and Mukesh Chandra Sharma*[1]

[1]School of Pharmacy, Devi Ahilya Vishwavidyalaya, Takshila Campus, Indore, India
[2]Research and Development, Akorn Pharmaceuticals, Inc., Vernon Hills, IL, United States
[3]Department of Pharmaceutical Sciences, Dr. Hari Singh Gour University, Sagar, India
[4]Department of Pharmacology, Shri Bherulal Pharmacy Institute, Indore, India
[5]Faculty of Pharmacy, Philadelphia University, Amman, Jordan

OUTLINE

13.1 Introduction 460

13.2 Polymers Used in Drug Delivery System 461

13.3 Mucoadhesive Polymers: Emerging Class of Novel Polymers 462
13.3.1 The Molecular Weight of the Polymer 463
13.3.2 Polymer Chain Length 463
13.3.3 Viscosity and Polymer Concentration 463
13.3.4 The Degree of Cross-Linking and Degree of Swelling 463
13.3.5 Flexibility of Polymer 463
13.3.6 Hydrogen Bonding 464

13.4 The Concept, Factors Affecting, and Theories of Mucoadhesion 464
13.4.1 Electronic Theory 465
13.4.2 Wetting Theory 465
13.4.3 Cohesive Theory 466
13.4.4 Adsorption Theory 466
13.4.5 Diffusion Theory 466
13.4.6 Mechanical Theory 467

13.5 Chitosan as a Mucoadhesive Polymer 468

Biomaterials and Bionanotechnology
DOI: https://doi.org/10.1016/B978-0-12-814427-5.00013-5

© 2019 Elsevier Inc. All rights reserved.

13.6 Mucoadhesive Thiolated Chitosan: Next Generation Polymer for Drug Delivery 468
13.6.1 Methods of Preparation 469
13.6.2 Techniques to Prepare Micro- and Nanoparticulate Thiolated Chitosan 472

13.7 Mucoadhesive Thiolated Chitosan: Effective Delivery Through Nanocarriers 476
13.7.1 Nanoparticles 476
13.7.2 Carbon Nanotubes 477
13.7.3 Liposomes 478
13.7.4 Niosomes 479

13.8 Applications 480
13.8.1 Thermosensitive Hydrogel Based on Thiolated Chitosan 480
13.8.2 As Coating Polymer for Stents 483
13.8.3 In Tissue Engineering 484
13.8.4 Matrix Tablet for Controlled Drug Delivery 487

13.9 Conclusion 488

Abbreviations 488

References 489

13.1 INTRODUCTION

Nanotechnology is serving various multidisciplinary fields and encompasses the design and application of objects in the nanometric range (Tekade et al., 2017b). Recent research studies have focused on the development of nanoformulations having biodegradable, biocompatible, and nonimmunogenic properties for safe and effective drug delivery (Tekade et al., 2017c). For this purpose, various synthetic, natural, plant- or animal-derived polymers are used for the encapsulation of different drug moiety (Ivanova et al., 2014).

Nanoformulations offer controlled or sustained release patterns of a drug moiety ideally at effective therapeutic levels for extended periods of time, leading to reduced toxicity and increased the efficacy of the drug moiety (Brigger et al., 2012). The targeted delivery of drug molecule is necessary to localize, target, and prolong the drug release and its subsequent effect. This helps to maintain the required drug plasma and tissue concentration of drug in the body, thus helps to prevent the side effect and damage to the healthy tissue. Also, nanocarriers allow the development for delivery at the target site, gene delivery, combined therapies, or systems for simultaneous therapeutics, observing applications, and diagnostics, which are collectively termed as nanomedicines (Agardan et al., 2016).

Besides several advantages, there are several drawbacks and challenges allied with nanotechnology. Some of these disadvantages are alterations in the stability, solubility, and pharmacokinetic aspects of the active drug cargo to undesirable levels. Material aspects such as aggregation, leakage, shelf-life, and toxicity are also important features to be considered in the preparation and manufacturing of several drug delivery systems. Structural features (1°/2°/3°/4°), structural conformation, solid state (crystalline, amorphous, solvates, hydrates), stability (chemical and physical), and general characteristics such as particles size are some major solid-state properties of material play an important role in the process of drug development (Maheshwari et al., 2018a; Soni et al., 2017).

High cost and scale-up problems are some other common issues. Nanocarriers remain in the body system for a long time when compared with free drug. In disease conditions, their high retention time serves as a beneficial tool for providing a higher bioavailability of the drug. Transportation of drug in a targeted site-specific manner leads to the accumulation of the drug molecule in the desired organ or area, resulting in minimum toxicity and improved efficacy (Torchilin, 2010).

The controlled and sustained release systems, the specific features of targeting take account of (1) availability of the desired concentration of drug at the target site, (2) interaction with target site, (3) shielding the molecule from the biochemical environment of the body system for minimizing degradation while providing maximum active drug delivered and available at the target site (Vhora et al., 2014).

The ability for chitosan to form electrostatic interactions with the residues that are present in mucin glycoprotein is due to their inherent mucoadhesive properties. Chitosan also has an excellent characteristic of temporarily interacting with the tight junctions between cells to enhance the paracellular transportation that leads to improved absorption (Yeh et al., 2011).

13.2 POLYMERS USED IN DRUG DELIVERY SYSTEM

The most important challenge that occurs in drug development and delivery is to ensure whether a delivery system is ably delivered to the candidate site of action to the right place, at the right time, and in an adequate amount. The effectiveness of various promising drug candidates could be influenced by drug degradation, rapid clearance from the body, drug toxicity, and low solubility, and hence would not elicit the desired response. To solve these challenges, various natural and synthetic polymers are valuable solutions to deliver small molecules, peptides, proteins, genes, or oligonucleotides. These polymers are used to prepare polymeric microparticles and nanoparticles as effective carriers to provide controlled as well as targeted drug delivery of various therapeutic agents. Hence, polymeric delivery systems may result in improvement of bioavailability and bioactivity of a delivered drug candidate (Muniswamy et al., 2019).

Bioavailability is necessary to get the required clinical effect. Bioavailability depends upon absorption, distribution, metabolism, and excretion (ADME) of the administered drug candidate. Any processing variables and clinical conditions such as physiological processes, physiology at the site, environmental pH, etc. that may affect bioavailability must be considered judicially during new drug development process (Maheshwari et al., 2018b).

Drug release kinetics and particle degradation rate are controlled by the physiochemical properties of the polymer used, such as hydrophobicity, molecular weight, and polydispersity. Some examples are poly(L-lactide) and poly(D,L-lactide) as polylactides and poly (lactide-*co*-glycolide) (PLGA). Natural polymers include chitosan and alginic acid sodium salt. Polymers have been found to be biodegradable, such as polylactide and polyglycolide, which include polylactic acid (PLA), polyglycolic acid, PLGA, chitosan, and RESOMER. Hydrophilic polymers include polyethylene (PE) glycols (PEGs), poly(2-oxazoline), and poly(*N*-isopropylacrylamide) (Raval et al., 2019; Mulas et al., 2019).

13.3 MUCOADHESIVE POLYMERS: EMERGING CLASS OF NOVEL POLYMERS

Polymers and their applications in mucoadhesive delivery systems have been explored to provide adequate concentration of drug at the desired site of action. The smart designing of the system through the incorporation of mucoadhesive polymers in the formulations provides properties that facilitate increased residence time of the therapeutic agent at the preferred site, thus helping to improve the localization of the active agents. Mucoadhesive polymers may be both water-soluble or water-insoluble in nature (Sosnik et al., 2014).

Mucoadhesive polymers are those polymers that bind to the mucin-epithelial surfaces with high efficiency. These polymers can be classified into three broad subcategories: (1) polymers that become gummy upon coming in contact with water, (2) polymers that bind following the formation of noncovalent (nonspecific) interactions that are predominantly electrostatic in nature, and (3) polymers that bind specifically to a receptor site. It may be noted that the mucoadhesive polymers bind to the mucous membranes by the two-stage process (wetting and consolidation) (Singh et al., 2017). Fig. 13.1 elaborates the two-stage model of mucoadhesion phenomenon. The first stage of this process is characterized by the initiation of interaction between the mucoadhesive polymeric and the mucous membrane, while the second stage is marked by the deposition of the polymeric membrane. It may be noted that the second stage is also promoted by the smoothness of the tissues to which the polymeric system is coming into contact (e.g., nasal, intestinal route).

Some examples of mucoadhesive polymers include lectins, thiolated polymers poly(acrylic acid)−cysteine, chitosan−iminothiolane, chitosan−thioglycolic acid, chitosan−thioethylamidine, alginate−cysteine, poly(acrylic acid)−homocysteine, poly (methacrylic acid)−cysteine and sodium carboxymethylcellulose−cysteine, poloxamer, pluronics and combination with poly(acrylic acid)s, alginate−PEG acrylate, and many more (Schattling et al., 2017).

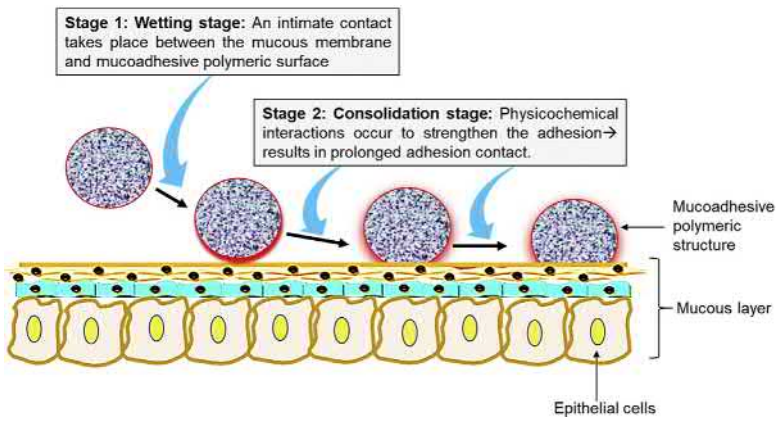
Stage 1: Wetting stage: An intimate contact takes place between the mucous membrane and mucoadhesive polymeric surface
Stage 2: Consolidation stage: Physicochemical interactions occur to strengthen the adhesion→ results in prolonged adhesion contact.
Mucoadhesive polymeric structure
Mucous layer
Epithelial cells

FIGURE 13.1 A two-stage model describing mucoadhesion phenomenon.

13.3.1 The Molecular Weight of the Polymer

An increase in polymer molecular weight leads to an increase in the mucoadhesive properties of a given polymer. As an example, the molecular mass of 100 kDa was found to show satisfactory mucoadhesive property for polymers to be used in biomedical applications. PEG having low molecular mass was demonstrated to not have much mucoadhesive property whereas an increase in molecular mass of PEG to 200 kDa has shown improved mucoadhesive property. PEG with a molecular mass of 400 kDa has shown tremendous mucoadhesiveness (Roy et al., 2009).

13.3.2 Polymer Chain Length

Mucoadhesive property depends upon the polymer chain length. The increase in mucoadhesive property of the polymer is observed as an increase in chain length of the polymers. Flexible chains of polymer help in better penetration and entanglement of the polymer in the mucosal layer. Hence, the bioadhesive property is improved. The hydration and cross-linking reactions influence the flexibility of polymer chains (Roy et al., 2009).

13.3.3 Viscosity and Polymer Concentration

An optimum concentration of polymer is required for providing the best mucoadhesive property. Increases in concentration beyond the optimum concentration lead to significant loss in adhesive strength. However, in a highly concentrated solution of polymer, the mucoadhesive property significantly decreases due to the poor solvent penetration of coiled molecules and unavailability of the chain. This concept is applicable for more or less liquid mucoadhesive formulations. However, in solid dosage forms like tablets, the higher concentration of the polymer is desirable to provide stronger mucoadhesion (Shaikh et al., 2011). In contrast, concentrations of the polymer chains that are lower than optimum lead to unstable and inadequate contact between the polymer and the mucosal layer, thus resulting in inadequate mucoadhesive properties (Maheshwari et al., 2015).

13.3.4 The Degree of Cross-Linking and Degree of Swelling

The cross-link density of a polymer is inversely proportional to the degree of swelling. The higher flexibility and hydration rate are related to lesser cross-link density, and larger surface area of the polymer, resulting in better mucoadhesiveness. A lightly cross-linked polymers had been used for achieving a high degree of swelling (Shaikh et al., 2011). The concept of high cross-linking density was used in the formulation of PEG−poly(acrylic acid) hydrogels, which results in better mucoadhesive properties (Lalu et al., 2017).

13.3.5 Flexibility of Polymer

Flexibility is a desired property in polymer chains as it helps in improving penetration of the polymer chains in the mucosal layer, thus facilitating mucoadhesiveness. Hydration

and cross-linking are the factors that affect the flexibility of the polymer. Elevated cross-linking density results in the production of the polymer of lower flexibility. The consequence of reduced flexibility of polymer chains is a reduction in diffusion of water in a cross-linked polymer matrix.

13.3.6 Hydrogen Bonding

Hydrogen bonds are another significant interaction produced between the various functional groups (such as −COOH, −OH, $-NH_2$ groups) of the polymers and a mucosal layer that affects mucoadhesive properties. The presence of functional groups is necessary to form hydrogen bonds. Examples of various polymers that can form hydrogen bonds include acrylic derivates, celluloses, poly(vinyl alcohol), poly(methacrylic acid), hydroxylated methacrylate, and starch (Boddupalli et al., 2010).

13.4 THE CONCEPT, FACTORS AFFECTING, AND THEORIES OF MUCOADHESION

Mucoadhesion is an intricate phenomenon that involves the resultant outcome of the chemical as well as the physical interaction between mucous membrane and polymeric surface. This event of mucoadhesion is greatly affected by diverse factors as depicted in Fig. 13.2. These factors primarily include molecular weight of the mucoadhesive polymer,

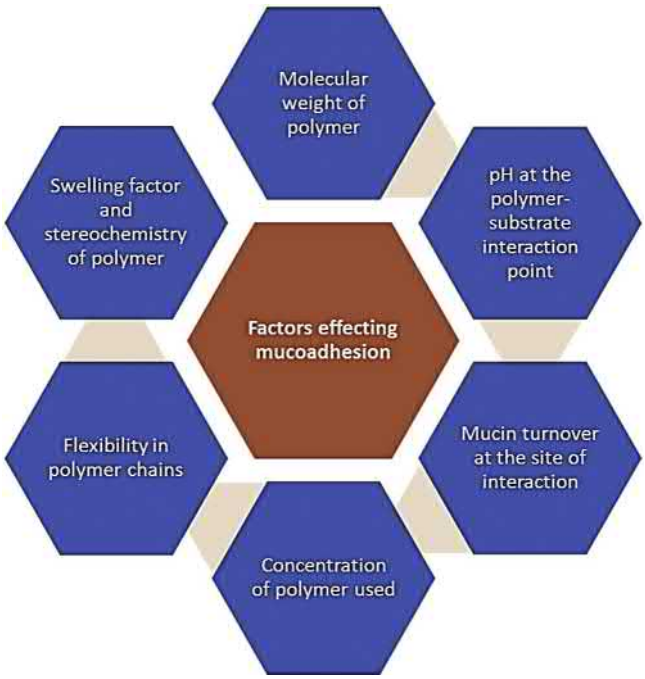
Molecular weight of polymer
pH at the polymer-substrate interaction point
Mucin turnover at the site of interaction
Concentration of polymer used
Flexibility in polymer chains
Swelling factor and stereochemistry of polymer
Factors effecting mucoadhesion

FIGURE 13.2 Major factors affecting mucoadhesion.

swelling index, the stereochemistry of mucoadhesive polymer, the concentration of polymers used, mucin turnover in the site of adherence, and most importantly the pH at the polymer substrate interaction point. To understand the mechanism of mucoadhesion in a better way, many theories have been put forward to provide an explanation of them. These theories include an explanation based on electronic, wetting, cohesive/fracture, adsorption, diffusion, and mechanical properties.

13.4.1 Electronic Theory

By considering the electronic theory, there is the establishment of attractive electrostatic force between a network of mucin glycoprotein and drug carrier. The fundamental principle of the electronic theory of mucoadhesion relies on the net difference between the electronegativities of adhering polymeric surface and the mucous membrane. The force of adhesion is usually the result of the transfer of electrons across the trans connection domain interface that creates the positive/negative charges, which attract each other. A diagrammatic representation of the electronic theory of mucoadhesion is shown in Fig. 13.3. Due to the difference in electronic properties of this both, there is electron transfer between these two surfaces. Hence the formation of a double layer at the interface and resulting adhesion occurs.

13.4.2 Wetting Theory

This theory is concerned with liquids or less viscous mucoadhesives. This theory mainly correlates mucoadhesiveness with spreadability. The mucoadhesive polymer should be capable of spreading and making intimate contact with the mucus layer. Positive spreading coefficient and zero contact angle are ideal requirements. The relation between the contact angle of the polymeric material elicited at the mucosal membrane interface and the magnitude of mucoadhesion is the imperative force governing the wetting phenomenon (Fig. 13.4). From an industrial point of view, the wetting characteristic is highly essential as it is straightforwardly associated with the coatings. Further, careful understanding of the wetting phenomenon is also very important toward attaining a stable polymeric film for vivid therapeutic applications. This property of polymer influences the film stability and ensures that the polymer is able to resourcefully wet the surface, which in turn requires the

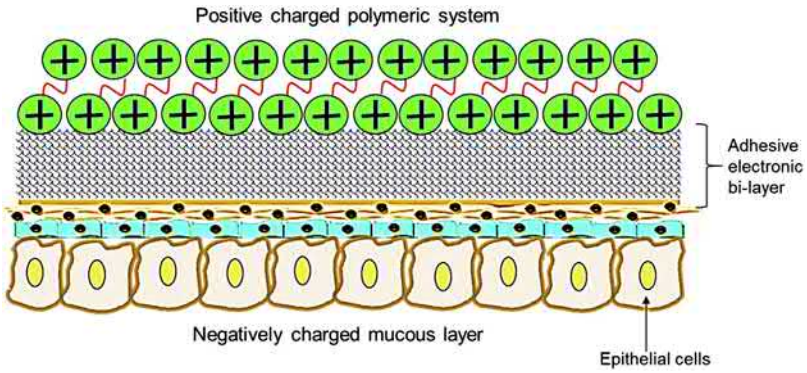

FIGURE 13.3 An electronic model of mucoadhesion. The principle of electronic theory of mucoadhesion involves the difference in the electronegativities of adhering polymeric materials. The force of adhesion results from the transfer of electrons across the interface, which creates positive/negative charges, which attract each other.

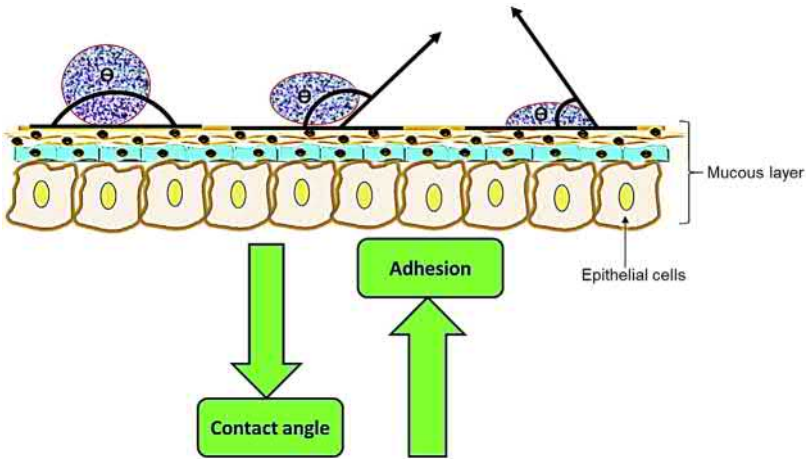

FIGURE 13.4 The relationship between the contact angle formed by the polymeric surface with the mucosal interface and the strength of adhesion.

understanding of the reverse phenomenon, that is, dewetting. Hence, the understanding of wetting and dewetting is very important toward using a polymer for pharmaceutical product development (Bassi da Silva et al., 2017).

The spreadability should be good and can be determined by:

$$\gamma(\text{solid}-\text{gas}) = \gamma(\text{solid}-\text{liquid}) + \gamma(\text{liquid}-\text{gas})$$
$$S = \gamma(\text{solid}-\text{gas}) - \left[\gamma(\text{solid}-\text{liquid}) - \gamma(\text{liquid}-\text{gas})\right]$$

where γ is the surface tension and S is the spreading coefficient

13.4.3 Cohesive Theory

Cohesive or fracture theory identifies the force necessary to part two separate particle surfaces following the establishment of adhesion. This theory does not consider diffusion or interpenetration of polymer chains since it is only concerned with the force required to separate the two surfaces. Therefore this theory is not suitable when studying the mucoadhesion of polymeric solids with mucous membranes (Smart, 2005).

13.4.4 Adsorption Theory

According to adsorption theory, hydrogen bonds and van der Waals forces are responsible for bioadhesion. Strong polymer forces such as covalent and metallic bonds are primary bonds, whereas ionic, hydrogen bonds and van der Waals forces are weak forces that form secondary bonds.

13.4.5 Diffusion Theory

Diffusion theory establishes that interpenetration and entrapment of bioadhesive material and mucin chains lead to mucoadhesion (Fig. 13.5). Its basic requirement is that

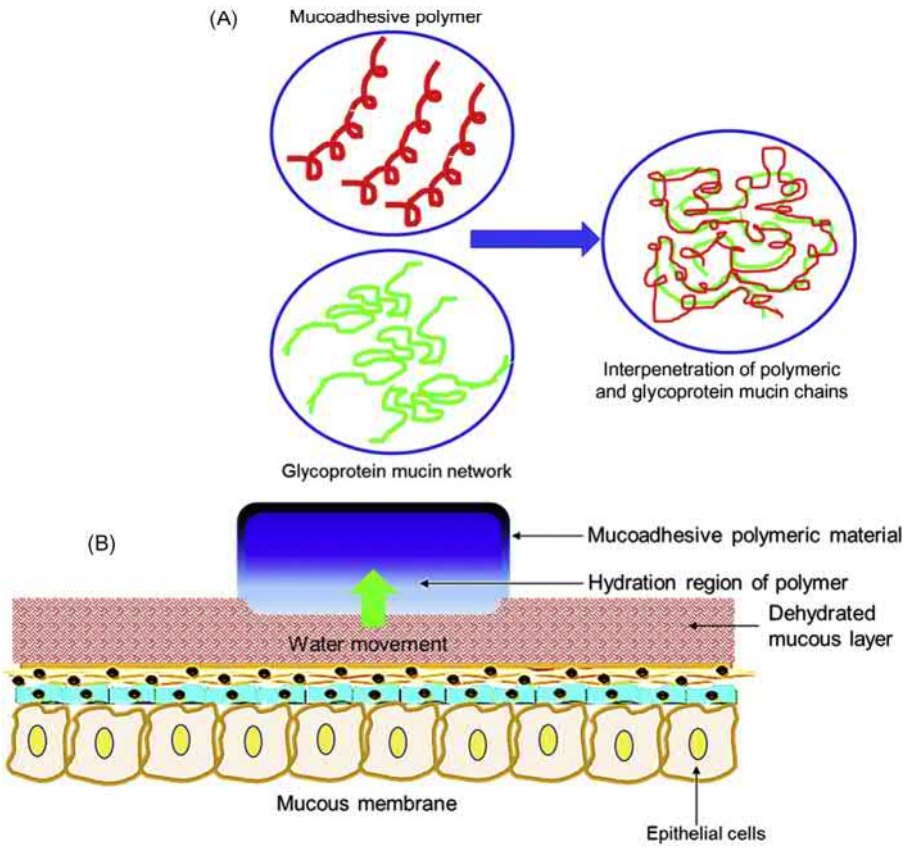

FIGURE 13.5 (A) Diffusion interlocking model for the mucoadhesion of polymers. (B) Dehydration theory of mucoadhesion.

mucoadhesive materials should be more structurally similar to the mucosa. Interpenetration is driven by contact time and diffusion coefficient, which are affected by molecular weight and flexibility of chain. Hence, we can establish a relation between these by the following equation:

$$t = \frac{L^2}{D}$$

where t is the time taken for maximum adhesion during interpenetration, L is the depth of interpenetration, and D is the diffusion coefficient.

13.4.6 Mechanical Theory

The mechanical theory proposes that adhesion is due to the filling of mucoadhesive liquid into the irregularities on the surface of the mucous membrane. The presence of more irregularities on the surface, the more area that is available for interaction (Mansuri et al., 2016).

13.5 CHITOSAN AS A MUCOADHESIVE POLYMER

Chitosan is a cationic polysaccharide that is a biocompatible and biodegradable mucoadhesive polymer fashioned by deacetylation of chitin (Roy et al., 2009). Chitin is the second most abundant polysaccharide present in the world after cellulose. Chitosan is a linear copolymer of β-(1−4)-linked D-glucosamine and *N*-acetyl-D-glucosamine. The presence of a basic amino group makes it hydrophilic, but the number of acetylated monomers and their distribution decides its solubility and conformation in an aqueous medium (Garcia-Fuentes and Alonso, 2012).

Chitosan exhibits excellent mucoadhesive properties, providing paracellular permeation due to improvement in the opening of tight junctions present in the intestinal epithelium (Ali and Ahmed, 2018). The primary amino functional groups present in chitosan and sialic acid interact ionically with sulfonic acid substructures of mucus, resulting mucoadhesion. Along with this, hydrogen bond formation takes place between the hydroxyl and amino groups of chitosan and mucus. The linear chain of chitosan molecules provides the information about the flexibility to improve the mucoadhesive property. This is helpful in controlling the release rate of the drug.

13.6 MUCOADHESIVE THIOLATED CHITOSAN: NEXT GENERATION POLYMER FOR DRUG DELIVERY

Thiomers are a hydrophilic macromolecule with free thiol groups in their structure. Normally, chitosan doesn't bear any thiol groups in its structural skeleton, but fortunately, the same structure provides opportunities to modify it chemically. In pharmaceutical science, when this natural polymer is thiolated it offers many benefits ranging from imparting mucoadhesive property to permeation enhancement of proteins. Certainly, thiolated chitosan has emerged as one of the most promising pharmaceutical polymers (Inamdar and Mourya, 2013). Thiolated chitosan is unique because it is the only cationic thiomer providing mucoadhesive property. Primary sites for chitosan thiolation are depicted in Fig. 13.6.

Chitosan is widely used in biomedical and pharmaceutical polymer science because of its versatility, but major drawbacks of using this polymer are its solubility constraints. It is only soluble in acidic condition (below pH 6.0) because chitosan is a cationic exchange proton in an acidic medium, which is not available in basic or neutral pH (Agarwal et al., 2015). To overcome this drawback, chitosan can undergo certain chemical modifications. Chitosan monomer contains primary amine and a primary or secondary hydroxyl group in its basic structure, which can be modulated chemically, which is helpful in increasing its solubility.

Various derivatives of chitosan like carboxylated, thiolated, acylated, and conjugates offer the best way to overcome the problem of solubility in chitosan. Chemical modification of *N*-substitution of the primary amino group with these groups has resulted in controlled release modification with prolongation of release, more patient compliance, and better absorption at basic and neutral pH.

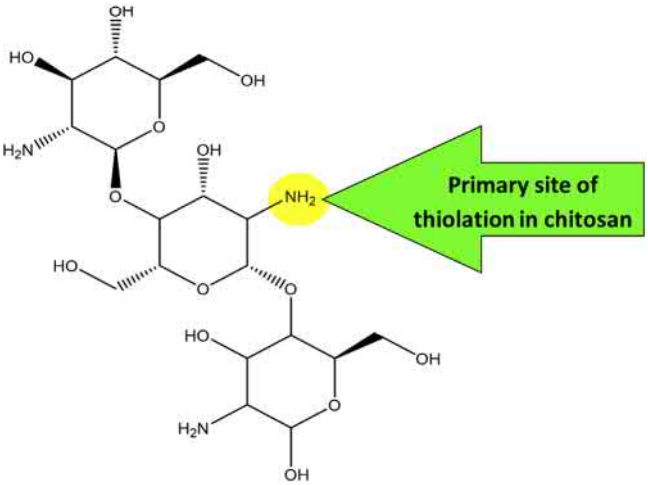

FIGURE 13.6 Chitosan is a linear polymer that contains a glucosamine ring and *N*-4 acetyl-D-glucosamine units in its structural skeleton. The primary site of thiolation is an amine group present in the glucosamine backbone.

Investigators also proposed a method to synthesize chitosan in water by using esterification technique of chitosan and maleic anhydride. However, with the passage of time, the solubility gets decreased because of change in morphology, physiochemical, or entrapment properties after 10−20 days. Entanglement means the knotting of the molecular chain and chemical chain of hydrogen bonding (Zhang et al., 2007).

13.6.1 Methods of Preparation

13.6.1.1 Thiolation Using Thioglycolic Acid and Cysteine

The primary amino group present in the glucosamine subunit of chitosan is a target for thiolation (addition of thiol group). Cysteine and thioglycolic acid carry sulfhydryl group (−SH) in their structure, which is shared with a primary group of chitosan leading to the formation of amide or amidine bond. This covalent bond is formed between an amino group of chitosan and a carboxylic acid group of sulfhydryl group-bearing agent. This reaction is facilitated by the presence of a hydrophilic group provided by the facilitator (carbodiimide). Air oxidation in the sulfhydryl group is prevented by performing the process below pH 5.0. At this pH, the concentration of thiolate anions in the reaction mixture is low, and the formation of the disulfide bond is prevented. The reaction can also perform in an inert condition (Kumar et al., 2004).

Dialysis is performed to isolate the thiolated compound. In an example of a purification method using dialysis, tubing with a molecular weight cutoff of 12 kDa was used for dialysis for three days at 10°C in dark condition against 5 mM HCl. The procedure was repeated twice in the same medium but with the addition of 1% NaCl to avoid interaction between the cationic polymer and anionic sulfur-containing the compound. The sample was dialyzed using 1 mM HCl to adjust the pH of the polymer at 4°C. The sample was lyophilized by freeze-drying aqueous solution at 4°C at 0.01 mbar and then stored at 4°C (Inamdar and Mourya, 2013). Thiolation using thioglycolic acid and cysteine is represented in Fig. 13.7.

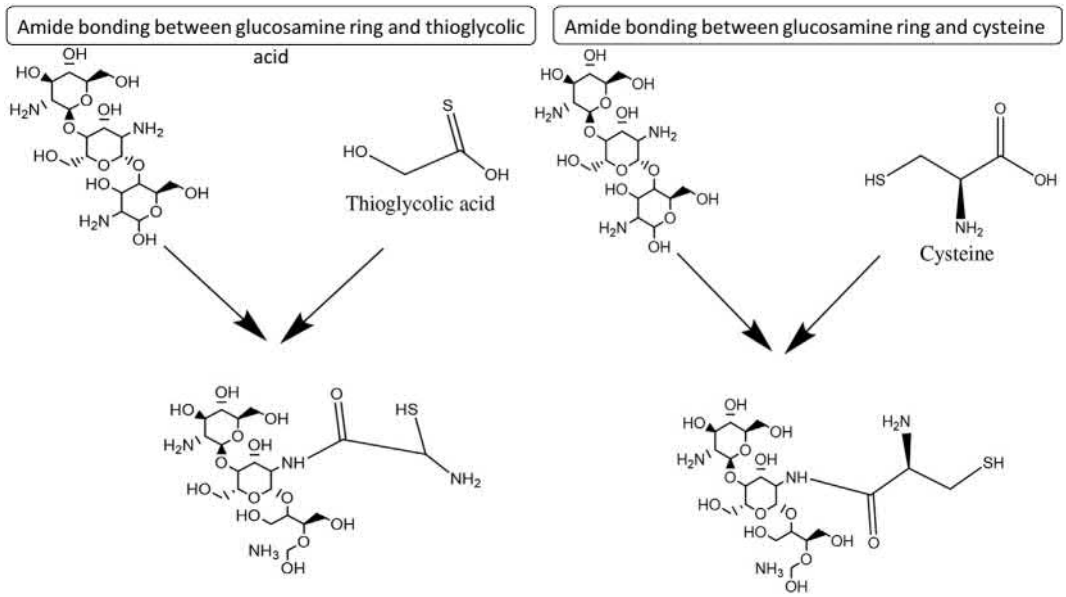
Amide bonding between glucosamine ring and thioglycolic acid
Thioglycolic acid
Amide bonding between glucosamine ring and cysteine
Cysteine

FIGURE 13.7 Thiolation using thioglycolic acid and cysteine.

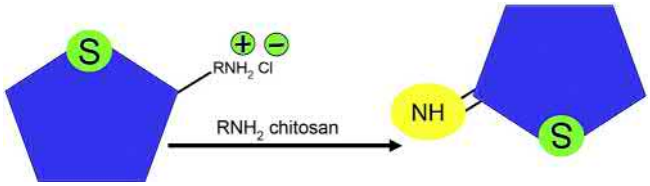

FIGURE 13.8 Thiolation using two imino thiolane (Traut's reagent).

13.6.1.2 Thiolation Using 2-Iminothiolane (Traut's Reagent)

The 2-iminothiolane, also known as Traut's reagent, is used as coupling reagent in this thiolation reaction. This is a very simple reaction in which the reaction is protected by the structure of the molecule. Thiolated chitosan shows a high degree of modification leading to increase in mucoadhesive property and permeation enhancing capability.

The nucleophilic nature of the amine group is protonation dependent making the reaction pH sensitive. 0.1% chitosan was added with 5% HCl with pH adjusted by 5 M NaOH with the addition of 0.1−0.4 g 2-iminothiolane for 24 hours at room temperature with continuous stirring. To avoid oxidation, 2-mercaptoethanol may be added in the final concentration of 3%. At pH 7.0 the highest percentage of thiolation was achieved as compared with pH 5.0 (Fig. 13.8) (Agarwal et al., 2015).

13.6.1.3 Thiolation Using 4 Mercaptobenzoic Acid

Covalent bonding formed between a 4-mercaptobenzoic acid and chitosan can be achieved by the amide bond formation between a carboxylic acid of mercaptobenzoic acid

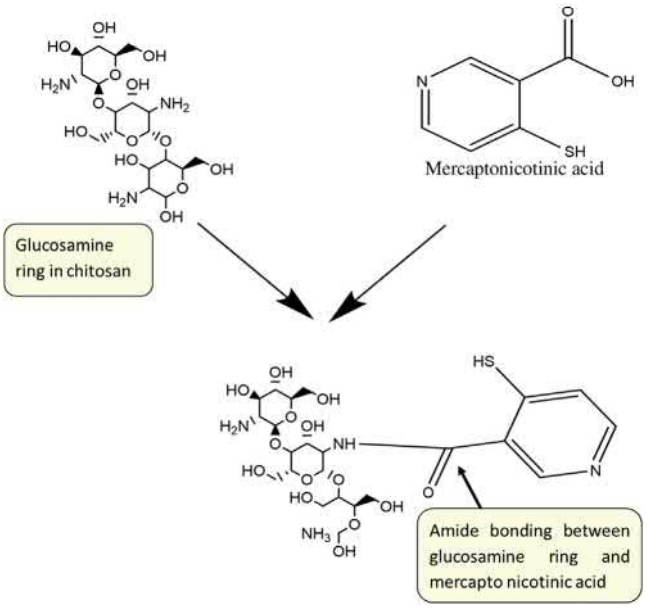
Mercaptonicotinic acid
Glucosamine ring in chitosan
Amide bonding between glucosamine ring and mercapto nicotinic acid

FIGURE 13.9 Thiolation of chitosan using four mercaptobenzoic acids.

and amine group of chitosan mediated by ethylenediamine modified succinylated caseinate. Increase in the reactivity of mercaptobenzoic acid leads to greater mucoadhesive property of chitosan, which will prolong the contact with the intestine and increase absorption of the drug. Due to this reaction, a unique type of thiolated chitosan may be prepared that exhibits full reactivity at intestinal pH with excellent in situ gelling property and better mucoadhesive property as compared with aliphatic thiolated chitosan. The methanolic solution of chitosan was treated with mercaptobenzoic acid and carbodiimide in the ratio of 1:3:0.1 in tetrahydrofuran for 24 hours. The −SH bond formation was protected by taking the product formed with 5% $NaHCO_3$ to obtain the pure product, which then can be purified with ethanol and treated with acetone after deionizing with water (Bernkop-Schnürch et al., 2004). A general scheme is represented in Fig. 13.9 for thiolation using 4-mercaptobenzoic acid.

13.6.1.4 Thiolation Using Thioethyl Amide

Most cationic thiomers are chitosan-based. The primary amino group at the 2-position of glucosamine subunit of chitosan is the primary target for thiolation. The simple amide or amidine bond formation occurs between chitosan and thioethanolamine. This method of thiolation improves the mucoadhesive property because of interaction between the cationic amidine conjugate and anionic mucus layer.

Chitosan thioethylamidine may be synthesized by using isopropyl-*s*-acetyl thioacetamide hydrochloride bearing protected thiol moiety. The modifier 2-iminothiolane is needed, and cyclic nonthiol ring production is discarded. The formed polymer shows 140 μmol free thiol group per gram, which improves the swelling property of the molecule (Kafedjiiski et al., 2005). A general procedure for thiolation using thioethyl amide is

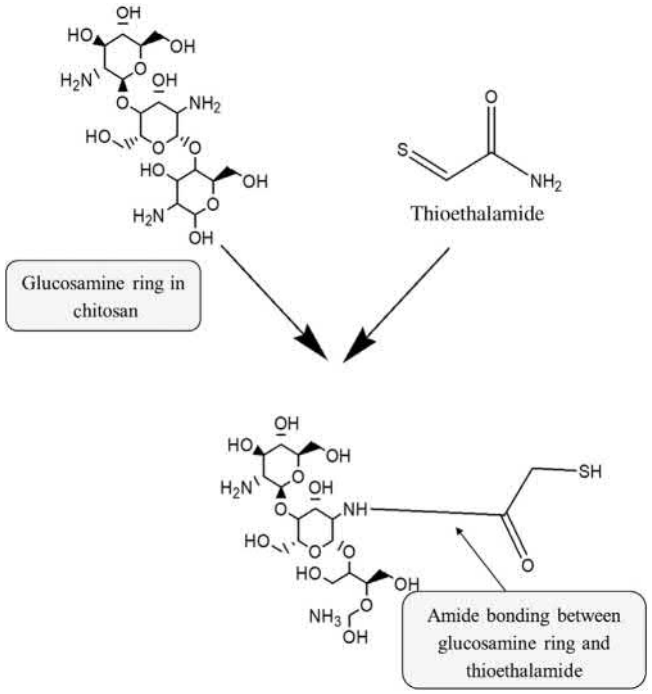

FIGURE 13.10 Thiolation of chitosan using thioethyl amide.

TABLE 13.1 The Importance of Thiolated Chitosan and How Thiolated Chitosan is Worth More Regarding the Degree of Modification and Improvement Ratio Than Polymer Chitosan Alone.

Polymer	The Degree of Modification (μg/mL)	Time (h)	Improvement Ratio
Chitosan alone	0	1.2 ± 0.8	1
Chitosan–thioglycolic acid	10	1.1 ± 0.1	0.9
	27	4.0 ± 0.1	5
Chitosan–thio-butyamidine	60	148 ± 25	123

presented in Fig. 13.10. Moreover, Table 13.1 signifies the importance of thiolated chitosan and how thiolated chitosan is worth more regarding the degree of modification and improvement ratio than polymer chitosan alone.

13.6.2 Techniques to Prepare Micro- and Nanoparticulate Thiolated Chitosan

13.6.2.1 Ionic Gelation

Ion-induced gelation is also known as ionic gelation. Due to this property, it results in the formation of microparticles and nanoparticles. However, these particles are formed

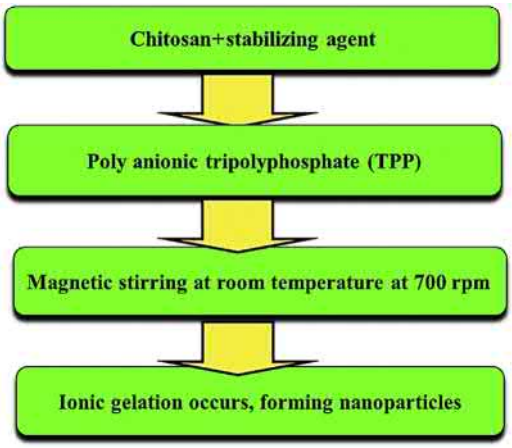
Chitosan+stabilizing agent
Poly anionic tripolyphosphate (TPP)
Magnetic stirring at room temperature at 700 rpm
Ionic gelation occurs, forming nanoparticles

FIGURE 13.11 Method for preparation of nanoparticles by ionic gelation.

with imperfections such as irregular surface morphology, delicate particulate system, high polydispersity index, and absence of proper surface alteration sites to confer various functional moieties (Kunjachan et al., 2010).

The capacity of thiolated chitosan to form the pH-dependent solution to gel changeover is caused due to the inter- and intramolecular disulfide bond formation amongst the thiol groups existing in the chitosan backbone. This also causes rheological transitions of the polymer. Due to this property of chitosan, there is more residence time of the polymer in the mucosal layer. Unchanged chitosan will not show any in situ gelling properties (Inamdar and Mourya, 2013). Within the pH range of 5−6.8 the process of cross-linking is seen. Due to this property of the in situ gelation at pH 5−6.8, this polymer is used in vaginal, nasal, and ocular mucosal formulations (Bernkop-Schnurch et al., 2004).

Chitosan nanoparticles can be formulated by this procedure as the tripolyphosphate (TPP) is multivalent and nonhazardous and has the ability to form gel by cross-linking with chitosan. By changing the pH of the formed combination, we can regulate the charge compactness of chitosan and TPP (Zhao et al., 2011). A general procedure is given in Fig. 13.11.

We can also prepare the magnetic nanoparticles of the chitosan−Fe_3O_4 by cross-linking with the TPP by the same method of ionic gelation (Fig. 13.12) (Wu et al., 2009).

13.6.2.2 *Emulsification or Solvent Evaporation*

Ohya et al. (1993) anticipated the intravenous route delivery of 5-fluorouracil, as an anticancer drug, conceded by chitosan nanoparticles gained by emulsification and cross-linking of the chitosan. Studies commenced that involved formulating chitosan nanoparticles via various methods. Some other research groups prepared chitosan nanoparticles with some modification in the formulation of the hydrophobic phase (i.e., liquid paraffin and petroleum ether) (Songjiang and Lixiang, 2009). This method has various disadvantages like the application of the hard cross-linkers and tedious procedure (Agnihotri et al., 2004). This method was used in the formulation of aspirin-loaded ethylcellulose nanoparticles and other such drug-loaded nanoparticles. This method is extensively used because of high biocompatibility, speed, and because it is properly scalable.

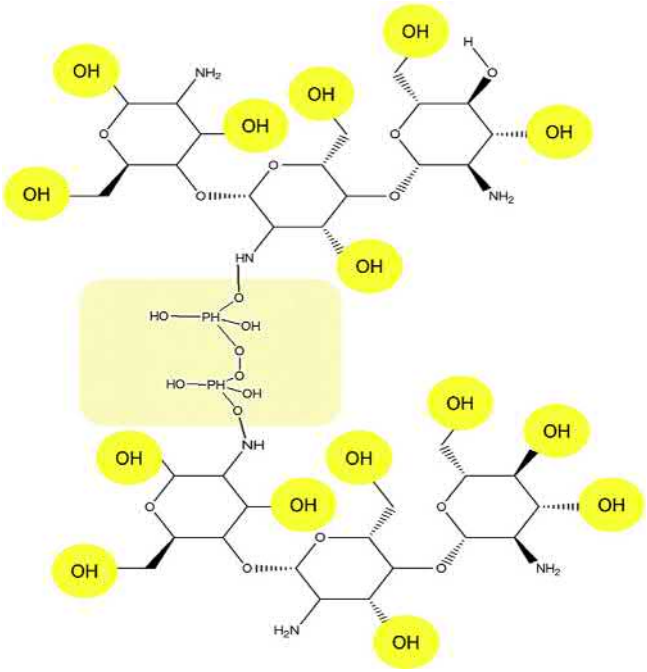

FIGURE 13.12 Schematic of cross-linking and ionic gelation.

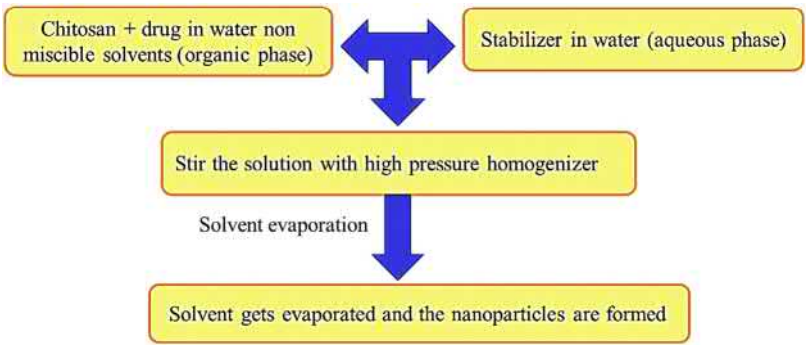
Chitosan + drug in water non miscible solvents (organic phase)
Stabilizer in water (aqueous phase)
Stir the solution with high pressure homogenizer
Solvent evaporation
Solvent gets evaporated and the nanoparticles are formed

FIGURE 13.13 Solvent evaporation method for nanoparticles formation.

Organic solvents that may be used to dissolve the chitosan include dichloromethane and ethyl acetate. Further, the organic phase can be mixed with the aqueous phase to obtain an oil-in-water (o/w) emulsion. The use of a suitable surfactant and stabilizer must be done acceptably to obtain uniform and small particles with the help of sonication or high-speed homogenizer (Fig. 13.13).

This method shows the advantages of thermal decomposition of the drugs and fast evaporation of organic solvents. This method is also associated with some disadvantages, such as high cost of preparation, and difficulty in removing the organic solvent from the mixture. For example, PLA containing testosterone nanoparticles were prepared by solvent evaporation using poloxamer 188 as the stabilizer.

13.6.2.3 Radical Emulsion Polymerization

Emulsion polymerization is a typical chemical process mostly applied for the formation of waterborne resins with different colloidal physicochemical parameters. The free radical emulsion polymerization involves emulsification reaction with the water-soluble component and o/w component emulsifier. This is then followed by the formation of the water-soluble initiator, also known as the oil insoluble initiator, in a process also known as an initiation reaction. The commonly used monomer in the emulsion polymerization reaction includes butadiene acrylonitrile styrene and ester vinyl acetate. Formation of the oil–water interfacial area around the particle nuclei then results in particle size growth (Chern, 2006).

The emulsification reaction involves effective ionic and nonionic surfactants used for stabilizing the reaction. Emulsion polymerization is a type of colloidal-like phenomena. An important feature of emulsion polymerization is segregation, and segregation leads to faster polymerization rate and polymers with increased molecular weight (Chern, 2006).

Water-borne resin formation was the first polymerization reaction that involved dissolving free radicals in the continuous water-soluble phase. This process results in the increased hydrophobicity of oil in water-soluble radicals. Addition of surfactant reduces the interfacial tension between monomer particles, increasing aqueous phase solubility (Chern, 2006). Moreover, Smith–Ewart kinetics may be used to calculate the rate of polymerization using the following equation.

$$R_p = K_p[M]_p\left(\frac{nN_p}{N_a}\right)$$

where K_p is the propagation rate constant, $[M]_p$ is the concentration monomer in the particle, n is the average number of free radicle per particle, N_a is the Avogadro's number, and N_p is the number concentration of particles (number of particles per unit volume)

13.6.2.4 Air Jet Milling

Air jet milling is used to produce fine particles having a particle size of 5 μm or below. This milling method has many advantages including size reduction with controlled size distribution and autogenous action produces low contamination. It was developed in the 19th century, but the original devices had many disadvantages such as contamination of the product. To overcome this led to new versions of fluidized bed jet mills (Chamayou and Dodds, 2007).

There are different types of air jet mills that include fluid impact mills, opposed jet mills, spiral jet mills, oval chamber jet mills, and fluidized bed jet mills. These are discussed below.

Fluid impact mills: These types of mills are generally used for industrial applications. Their mechanism for particle size reduction is through mechanical particle impact as the particles are projected against a fixed target by jet gas. These mills may work under the same principle of impact grinding and this method gives a change in particle size distribution and the impact of velocity (Chamayou and Dodds, 2007).

Opposed jet mills: The opposed jet mills were first introduced by Willoughby in 1917. This method also modified study impacts to opposed jets (Chamayou and Dodds, 2007). In opposed jet mills, the feed particles sweep around the chamber through nozzles until they impact the chamber and each other until the particles are small enough to escape through the centrifugal screen.

Spiral jet mills: This type of mill was introduced in 1934 by the Micronic Company. Spiral jet mills are also called pancake mills and tangential mills. These mills work by feeding particles placed into a flat disk-shaped vessel fed by high-speed peripheral inclined fluid jets. The particle size is reduced by impact and grinding upon the circular chamber. Particles may pass through a flat disk-chamber. The particle size of the particles is reduced due to the impact, while coarse and fine particles undergo separation via centrifugal force. Fine particles are removed from by the central outlet and coarse particles are retained for more grinding to form fine particles (Chamayou and Dodds, 2007).

Oval chamber jet mills: These mills are also known as torus chamber mills and they have many similarities with tangential jet mills. However, their main differences are that the grinding chamber is bean shaped in oval chamber jet mills, rather than circular. These mills contain fluid jets located at the base of the mill near the product entry port. Oval chamber mills were first introduced in 1941 by the Jet-O-Mizer company. The modern version was developed to a double side-by-side version that also added opposed jet impact to the fluid jet grinding action (Chamayou and Dodds, 2007).

Fluidized bed opposed jet mills: These mills are used to provide high impact between particles that are in suspension on a fluid bed. In this mill, high particle concentration in the grinding chamber is obtained. It is the most widely used mill for many pharmaceutical industrial applications and is available in standard sizes, namely chamber diameters of 10 cm with a capacity of 10 kg/h and up to 1.25-m-diameter chambers (Chamayou and Dodds, 2007).

13.7 MUCOADHESIVE THIOLATED CHITOSAN: EFFECTIVE DELIVERY THROUGH NANOCARRIERS

13.7.1 Nanoparticles

Thiolation of chitosan nanoparticles provides mucoadhesive characteristics, permeation enhancing, and antiprotease properties. Quantification of thiols group has been done by electromagnetic resonance spectroscopy, high-performance liquid chromatography (HPLC), liquid chromatography–mass (LC-MS) spectrometry, capillary electrophoresis, UV–visible spectroscopy, and other enzymatic methods. Thiolation of chitosan can be done by Ellman's reaction, whose scheme is given below:

Ellman's reaction is based on the reaction of the thiolated anion (R–S–) with Ellman's reagent [5,5-dithio-bis (2-nitrobenzoic acid)] (Bravo-Osuna et al., 2007).

$$RS^- + DTNB^{2-} \rightleftharpoons R-S-TNB^- + TNB^{2-}$$

$$R-S-TNB^- + RS^- \rightleftharpoons R-S-S-R + TNB^{2-}$$

Ellman's reaction has been presented in different pharmaceutical dosage forms like hydrogels, polymer solutions, and microgels. Based on structural characteristics there are four methods for preparation of nanoparticles:

- Covalently cross-linked nanoparticles
- Ion directed cross-linked nanoparticles
- Polyelectrolyte complexation
- Self-assembly of hydrophobically modified polysaccharides (Liu et al., 2008)

Nanoparticles consisting of trimetilchitosan have been prepared. In a recent study, tetanus toxoid nanoparticles were also prepared (Vila et al., 2002). Recombinant hepatitis-B surface antigen has also been formulated (Prego et al., 2010). By using the intranasal route, they were able to raise IgG levels, which are protective in the case of humans. A similar study using ovalbumin antigen demonstrated that it is a good candidate for nasal antigen delivery (Nagamoto et al., 2004).

So, it is clear formulating these antigens with trimetilchitosan in the form of nanocarriers will lead to the drastic increase in immunogenicity by intranasal administration. Vaccination efficacy can be further increased by various ways like the use of CpG oligodeoxynucleotide as a costimulant, which is complexed with chitosan−ovalbumin. It will increase the IgG and IgA levels comparable to results obtained from ovalbumin-loaded trimetilchitosan nanoparticles. A 10-fold increase in the IgG2a response was observed due to induction by CpG, and it also increases the ovalbumin (OVA)-specific IFN-gamma T cells in the lymphoid organ spleen (Slutter and Jiskoot, 2010). They have also prepared the single dose antigen delivery vehicles. Results obtained were comparable to those obtained after administration of alum-containing vaccine.

13.7.2 Carbon Nanotubes

Carbon nanotubes may be defined as the cylindrical structures made up of allotropes of carbon having a diameter in the nanoscale range. There are mainly two types: single-walled carbon nanotubes (SWCNTs) and multiwalled carbon nanotubes (MWCNTs). SWCNTs and MWCNTs have a diameter of about 0.8−2 and 5−20 nm, respectively. They have excellent optical, mechanical, and electrical properties.

13.7.2.1 Single-Walled Carbon Nanotubes

SWCNTs consist of a single graphite sheet rolled into a hollow cylinder with varying diameter and length. SWCNTs have appreciable mechanical strength (Young's modulus = 0.6−1.25 TPa), low electrical resistance (approximately two times lower than that of copper), and high thermal conductivity.

SWCNTs have many applications like drug delivery, biosensing, and targeting cancer cells. At a macroscopic level, there are several problems of achieving good a dispersion as well as stability. To overcome these problems, functionalization of SWCNTs has been done by several approaches.

- Functionalization involves the formation of defective sites, which leads to the loss of electrical, thermal, and optical properties.
- In another method, it was done by sonication and stabilizing with biocompatible surfactants, polymeric proteins, and DNA (De Volder et al., 2013).

In a recent study, multilayered cardiac patches made up of chitosan and gelatin hydrogel supported by a polycaprolactone (PCL) were developed. PCL provides suturability and adequate tensile strength while chitosan and gelatin hydrogel provide an extracellular matrix (ECM). A galactose biosensor was prepared by dispersion of SWCNTs into chitosan matrix, which is highly sensitive and selective. It allows the quick detection of galactose

with a sample-throughput of 150 per hour. They have used increased sonication time, of about 300 minutes, as compared with previous studies. Upon increasing sonication time from 60 to 170 minutes, it could lead to about 2.6-fold increase in sensitivity toward galactose (Tkac et al., 2007).

13.7.2.2 *Multiwalled Carbon Nanotubes*

Carbon nanotubes produce cytotoxicity in certain cell lines, which is mainly due to the use of metallic catalysts. However, they show improved biocompatibility when incorporated with biopolymers. Now researchers are focusing on the effect of carbon nanotubes on biological systems and the development of new methods for their use in biomedical engineering. Previously they have been used to improve the mechanical properties of various biomaterials like hydrogels.

MWCNTs have been demonstrated to have applications in biomedical engineering, including the development of novel biosensors (Tekade et al., 2017a; Kuche et al., 2018). If chitosan does not cross-link then it shows poor mechanical properties. Chitosan solution can bypass the need for surgical implantation of biomedical devices if its aqueous solution is used as an injectable gel for inducing new bone formation. If chitosan injectable gel is provided with bone marrow proteins, then it causes rapid new bone formation. Injectability and viscosity of chitosan solution play an important role in injectable gels. Apart from various nanomaterials, functionalized carbon nanotubes are one of the best approaches for biomedical tissue engineering.

Chitosan functionalized carbon nanotube composites were previously developed and characterized for their biocompatibility and mechanical properties. MWCNTs were developed to support a chitosan matrix that was fabricated using different chitosan concentrations.

13.7.3 Liposomes

Chitosan has a property of absorption on charged surfaces that leads to an increase in its efficiency to form a linear chain on the surface. As this effect reaches the maximum saturation concentration, above this concentration self-aggregation of the polymeric chains takes place and uneven loops appear that result in increasing the fluidity of liposomal membrane sheath and therefore deterioration of the liposomes (Laye et al., 2008). At physiological pH, chitosan's low solubility serves as a major disadvantage.

Chitosan has an important swelling degree in aqueous media leading to the instant discharge of the captured compounds, which serve as a barrier in the sustained release delivery systems (Azagury et al., 2014). Chemical modification of various reactive functional groups of chitosan may resolve the above mention limitations (Ahmed and Aljaeid, 2016).

Thiolated chitosan received major attention in recent years due to its mucoadhesive properties by its thiolation (Kast and Bernkop-Schnurch, 2001). The interaction between the thiol group and the cysteine-rich subdomains of mucus glycoproteins establishes a disulfide bridge that leads to excellent mucoadhesive properties (Bernkop-Schnürch, 2005). Another feature is the enhancement in permeation by temporary inhibition of protein tyrosine phosphate and thus increase in the permeation of the compound entrapped

in them by opening the tight junctions in a reversible manner via inhibition of this protein (Bernkop-Schnürch, 2005). They also have bioavailability properties of orally administered drugs by inhibiting the efflux pump of the intestine such as P-glycoprotein (Werle and Bernkop-Schnurch, 2008). Advantages of thiolated chitosan liposomes include:

- Increased mucoadhesive properties
- Enhanced permeation
- Increased bioavailability of orally administered drugs.

Due to all these advantages, thiolated chitosan serves as an excellent carrier for coating of liposomes designed to be used in various therapeutic sectors (Gradauer et al., 2012).

Some studies have shown that to overcome low water solubility, stability, and bioavailability of curcumin, it was loaded into thiolated liposomes with the encapsulation efficiency of 94.0%, drug loading of 7.95%, average particle size of 406 nm, and a positive zeta potential of 36.6 mV, which were all higher than that of the curcumin liposome (Li et al., 2017b). Thiolated chitosan liposomes were used for the effective delivery for the small interfering RNAi as therapy that resulted in lowered cytotoxicity, increased transfection, and subsequent silencing efficiency, with increased siRNA serum (Li et al., 2017b).

In some previous studies, it was shown that chitosan-coated liposomes prepared by solvent evaporation led to very effective changes in the transdermal delivery and increased the skin penetration efficiency of resveratrol, delaying the skin aging process (Park et al., 2014). A study by Li et al. (2009) had shown that the diclofenac sodium loaded liposomes coated with low molecular weight chitosan resulted in increased retention time as well as the penetration efficiency for the transcorneal delivery of the drug.

Thiomer-coated liposomes have shown effective delivery of peptides by the oral route of administration. In this, the drug was loaded in the liposomes that were coated with the chitosan thioglycolic acid. This coating leads to an increased particle size of 500 nm and a zeta potential between −40 and +44 mV, which demonstrated effective penetration of the intestinal membrane (Gradauer et al., 2013).

13.7.4 Niosomes

Niosomes are vesicle-type carrier particles that are similar to liposomes. Niosomes are composed of nonionic surfactants and thus may serve as a transporter for hydrophilic as well as lipophilic drugs. The nonionic surfactant used for the niosomes are assumed to be more chemically stable than the liposomes. Niosomes are compatible with the biological systems, biodegradable, nonimmunogenic, nontoxic, and can deliver various therapeutic agents, including proteins, to their target site of action (Moghassemi and Hadjizadeh, 2014).

Chitosan-based niosomes are used for the sustained release delivery of encapsulated compounds and to enhance intestinal permeability. They also have shown an increase in the aqueous solubility of the formulation. A major drawbacks of chitosan is that it is insoluble at physiological pH (Bowman and Leong, 2006). Although chitosan may function as a solubility enhancer, it is only soluble and active in an acidic medium where amino groups in chitosan are protonated. This positive charge becomes neutralized in alkaline and neutral pH surroundings and corresponds to the reduced solubility (Ahsan et al., 2017).

The studies performed by Moghassemi et al. (2015) demonstrated that niosomes loaded with insulin may be prepared by the reversed-phase evaporation method and coated with trimethyl chitosan by incubating the suspension in a solution of trimethyl chitosan. As a result, the permeation efficiency of insulin was found to be enhanced in the intestinal region. The prepared niosomes were evaluated for their entrapment efficiency and particle size.

Niosomes were used in some cases for delivery of vaccines, such as oral DNA vaccine as a transporter for inducing the immune system. Niosomes were prepared using span 60, cholesterol, and stearylamine as lipids and were coated by modified polysaccharide *o*-palmitoyl mannan for protecting them from bile salt and degradation from enzymes in the gastrointestinal tract to enhance affinity for antigen binding cells of Peyer's patches. The prepared niosomes were characterized by morphological characteristics, entrapment efficiency, ligand binding specificity and stability in simulated gastric fluid and simulated intestinal fluid. These niosomes were found to be more stable than previous formulations (Jain et al., 2005).

13.8 APPLICATIONS

13.8.1 Thermosensitive Hydrogel Based on Thiolated Chitosan

Chitosan is one of the most explored biopolymers for developing hydrogels. A hydrogel is a three-dimensional hydrophilic network that is highly swollen. Water and biological fluids may absorb in large quantity in the hydrogel. Physiochemical properties of hydrogel depend upon various factors such as gel structure, the degree of cross-linking, molecular structure, and also the content of water. Their rheological property analysis had shown thixotropic behavior during the development of in situ forming hydrogels and administered into the body, and therefore they have the probable clinical potential for use.

Hydrogels have a polymeric network and based on this network hydrogel can be classified into two types: chemical or physical hydrogels. Chemical hydrogels involve covalent bonds within the hydrophilic polymer chains. Physical hydrogels involve ionic bonds, hydrogen bonds, and intermolecular hydrophobic associations included in the secondary forces (Gyles et al., 2017).

Mechanisms involved in situ gel formation:

- Gelation in response to temperature or pH change,
- Ionic or covalent cross-linking,
- Solvent exchange or crystallization.

Thermosensitive hydrogel-based drug delivery systems are the formulations in which the drug can be encapsulated and released by the hydrogel in a temperature dependent manner. The thermosensitive hydrogel is the stimuli-responsive material. Interest and development in stimuli-responsive material-based drug delivery systems are rapidly increasing. In these, the drug is readily encapsulated and released by various stimuli such as heat, pH, and ionization. Thermogels undergo solution to gel transformations when the temperature changes. In thermal responsive delivery, there is no need of using an organic

solvent, chemical cross-linking, or any externally applied triggers. The solution state thermosensitive hydrogel can be injected together with the drug at the target site, which then quickly solidifies at 37°C. Thermosensitive hydrogels used for drug delivery applications include natural polymers and synthetic polymers, as well as their combinations. Chitosan alone is not thermosensitive, but when glycerophosphate is added to chitosan, the solution becomes thermosensitive.

Glycerophosphate forms strong hydrogen bonds with chitosan and then imparts the important thermosensitive functions, forming a gel. Thermosensitive hydrogels give less adverse effect on biological tissue. The main mechanism of thermosensitive hydrogels is that the solution is free-flowing at room temperature but is converted into a gel after administration in the body. They have the structure of the thermoresponsive polymer and a balance between the hydrophilic and hydrophobic group. However, when there is minute variation in temperature, they generate a new relationship between polymer and water interaction. Critical solution temperature (CST) is the temperature at which the formation of the polymer solution occurs. Polymers are soluble below lower CST. Polymers are insoluble and form a gel when they are above the lower CST. This as an important mechanism used in various biomedical applications (Matanović et al., 2014). There are various thermosensitive hydrogel formulations used for various diseases.

Chitosan-based thermosensitive hydrogels were prepared by using in situ gelling techniques and projected for the targeted delivery of paclitaxel to prevent tumor growth. This formulation provided prolonged action of therapeutic effects at the tumor site (Ruel-Gariépy et al., 2004). In this formulation, hydrophobic paclitaxel was used as an antineoplastic drug. While preparing the formulation, biodegradable materials such as chitosan were incorporated and it was also neutralized with glycerophosphate and then loaded with an antineoplastic drug. Thermosensitive chitosan-based hydrogels may be used to reduce severe side effects of chemotherapy and while this formulation was injected via intratumoral injection, it may be developed for different routes of administration. To evaluate the local action of a formulation, the author used BALB/c mice in which EMT-6 breast cancer cell line was implanted via subcutaneous route. This formulation was injected via intratumoral injection and gave the sustained release activity and inhibited the growth of EMT-6 cancer cell in mice. This investigation showed that single intratumoral injection formulation is very efficacious and found equivalent to four intravenous injections of taxol for inhibition of the growth of EMT-6 cancer cell in mice. The intratumoral injection when given to the animal produced no side effect but in the systemic treatment, it had various adverse effects such as weight loss and acute toxicity. To evaluate the ability of the formulation, the author performed in vitro release studies. These studies gave prolonged action over 1 month while giving a high loading dose of 64 mg/mL and inhibited all tumor growth. The advantage of the formulation was high local efficacy and low systemic toxicity (Ruel-Gariépy et al., 2004).

The number of diabetic patients has drastically increased worldwide. The most preferred route of administration of insulin is the subcutaneous route. For better patient compatibility, various noninvasive delivery methods may be used such as pulmonary, buccal, ocular, rectal, etc.

The main disadvantages of insulin include low permeation rate, unstable properties, and digestion degradation by the various proteolytic enzymes. Therefore delivery of

insulin is limited. To overcome this, injectable thermosensitive hydrogels based on chitosan were developed to give sustained release action of insulin. In a modified method, hydroxyl butyl chitosan had various advantages compared with the common injectable chitosan hydrogels. Hydroxyl butyl chitosan has a thermosensitive property and can be prepared by hydrogel at 25°C. Hydroxyl butyl chitosan is a viscous solution at room temperature, but when the temperature is increased it gets converted into hydrogel, as a reversible process. Insulin that was incorporated into the gel region demonstrated sustained release action (Gao et al., 2014).

Glaucoma is an ocular neuropathy disease that may lead to blindness if intraocular pressure remains uncontrolled. Various antiglaucoma agents are used such as prostaglandins and beta blockers. Latanoprost is the major preferred drug to treat glaucoma, but various side effects occur when used regularly. Eye drops contain antimicrobial preservatives that give a burning sensation, cause damage to the soft tissues of the eye, and other various side effects. Various methods are used to control these undesirable side effects. The industry is moving toward complete removal of antimicrobial agents in ophthalmic products to avoid side effects associated with them. In context, chitosan may help in eliminating the need for antimicrobials or simply reducing the dosing frequency to limit patient exposure to antimicrobials. One method is to develop thermosensitive chitosan hydrogels capable of solution to gel transitions, which occur without using any cross-linking method and only use of temperature and/or pH external stimuli. In recent years Agrawal et al. (2012) developed a long-term sustained-release drug for topical ocular administration using in situ forming hydrogel techniques. It had ideal gelling properties with important features such as prolonged retention time. Chitosan/gelatin/glycerophosphate based thermosensitive hydrogels were developed for the sustained release of latanoprost for controlling ocular hypertension. In this formulation, two important parameters, gelation temperature and time of gelation, were evaluated by using rheometers. The chitosan/gelatin/glycerophosphate hydrogel had desirable properties such as gelling strength and biocompatibility as compared with the chitosan/glycerophosphate hydrogel. The rheological properties reported suggested that the solution to gel transition temperature of the formulation was 34.18°C, which would be useful for administering in vivo for body temperatures of approximately 37°C.

There are various methods to analyze biocompatibility of latanoprost loaded hydrogels such as cell viability assay, hemolysis test, ocular irritation test, corneal fluorescein staining, and histological examination (Maheshwari, 2018, p. 1556). In this study, a rabbit glaucoma model induced by intravitreal injection of triamcinolone acetonide was used. Intraocular pressure decreased within 8 days following the subconjunctival injection of the given formulation. The author evaluated the sustained release action of latanoprost and long-term therapeutic effects. Also, they studied cytotoxicity, where assays resulted in the conclusion that no harmful effects were observed. In case of hemolysis assay, there was no hemolytic action while using the given formulation. This method may be highly beneficial for controlling ocular hypertension and providing long-term therapeutic effects, and this method is very useful for that patient who cannot apply the eye drop themselves (Cheng et al., 2016).

13.8.2 As Coating Polymer for Stents

Stents are devices that are used for opening cardiovascular vessels for the treatment of various cardiovascular diseases. Stents have a tube type structure that is inserted into the vessel or passageways to keep them open. Various types of stents are used such as a coronary stent, biliary stent, and vascular stent. There are various coating polymers used for coating stents (i.e., natural and synthetic polymer) and these coated stents may be used in a variety of biomedical applications such as cardiovascular disease devices, orthopedic materials, biosensors, and tissue engineering.

The main features of coating polymers are as follows:

- Electrical conductivity
- Mechanical strength
- Corrosion protection
- Surface chemistry
- Biocompatibility
- Antiwear characteristics

Various vasculature diseases such as ruptures, fistulas, and aneurysms may be treated by the membrane-covered device. Based on the natural polysaccharides such as chitosan the biodegradable membrane covered stent was developed (Tekade et al., 2017c). Chitosan was blended with PE oxide and the mechanical strength of the membrane was evaluated. Chitosan alone does not provide mechanical strength but when used with other polymers such as PEG, PE oxides have the ability to impart excellent mechanical strength. In these applications, synthetic polymers are not used because of various limitations such as low biocompatibility.

To overcome biocompatibility problems, natural polysaccharides such as chitosan and other biological polymers such as exogenous polymer collagen are used. For the inhibition of the cellular event, the bioactive drug, protein, oligonucleotides, DNA, and radionuclides are loaded into the chitosan–PE oxide membrane. In this study, sodium nitroprusside was used. In a biological environment, sodium nitroprusside readily converts into nitric oxide. The main function of nitric oxide is to reduce the blood pressure. In the treatment of restenosis, sodium nitroprusside is used. The author evaluated the fabrication and characterization of the chitosan–PE-based biodegradable membrane covered stent. In ex vivo assays they demonstrated excellent hemocompatibility of the chitosan–PE membrane (Thierry et al., 2005).

Obstructive jaundice is a disease caused by pancreatic or malignant biliary tumors and is treated by endoscopic insertion of plastic and metallic biliary stents. Elderly patients often cannot tolerate the pain associated with metallic stents, so instead the plastic stents are used. The plastic stents need to be placed every 3–5 months. Use of the metallic stent has a limitation because of greater cost and problems faced during removal. If PE tubing alone is used for the preparation of the plastic stent, then it will get occluded because of the bacteria. Therefore PE tubing is coated internally with chitosan. Chitosan has inherent antimicrobial properties and enhances the attachment of bacteria with prevention of occlusion. When PE tubing is coated internally with chitosan, there is an increase in the surface hydrophilicity (Lin et al., 2005).

13.8.3 In Tissue Engineering

Tissue engineering is an option for treating damaged tissues, and is a promising field comprising knowledge of biology and engineering to develop artificial tissues (Vacanti and Langer, 1999; Li et al., 2017a). The term *tissue engineering* was first used by Dr. Y.C. Fung in 1991 (Beck et al., 2017). Restoration, regeneration, and retention in defective or lost tissues are the most important goals of tissue engineering. Chitosan has been comprehensively used in the field of tissue engineering, since it has valuable and unique properties that include biocompatibility and biodegradability, acts as a blood thickener, and has significant activity against bacterial and fungal infections, as well as hypercholesterolemia. Chitosan is highly available in different forms such as hydrogels, sponges, fibers, sheets, films, and other structures (Rodriguez-Vazquez et al., 2015). The general phenomenon of tissue engineering is presented in Fig. 13.14.

Lyophilization, gas foaming, and electrospinning methods are used for molding chitosan into consistent porous scaffolds with the desired shape (Ahsan et al., 2017). The process for forming porous chitosan via lyophilization is depicted in Fig. 13.15.

A scaffold should have more than 80% porosity with an aperture size of more than 50 μm and less than 250 μm. For skin scaffolding, the pore size should be greater than 160 μm (Madihally and Matthew, 1999). Due to the porous structure of chitosan, cells may migrate into the pore to become incorporated in the structural scaffold and supplied with a generous quantity of nutrients (Kim et al., 2008). Chitosan has similar biological and mechanical properties to the natural ECM.

Chitosan makes a complex with anionic glycosaminoglycans (GAGs) such as heparin and chondroitin sulfate due to the cationic nature of chitosan (Ahsan et al., 2017). Chitosan encourages cell adhesion, proliferation, and differentiation activity due to hydrophilic groups on the surface of chitosan.

Chitosan is useful as a biomaterial in tissue engineering of bone, cartilage, liver, nerve, and cutaneous wound healing (Dash et al., 2011; Ho et al., 2015). Degradation of chitosan is a key parameter because of its important role in the performance of the engineered tissues.

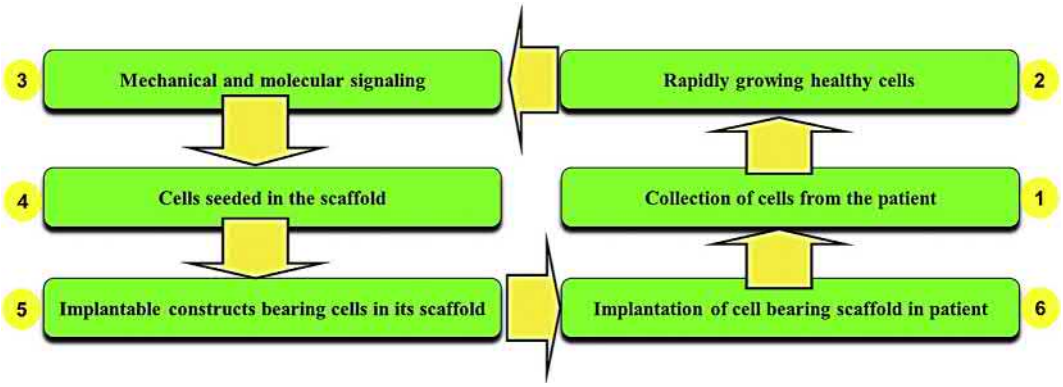

FIGURE 13.14 Theory of tissue engineering.

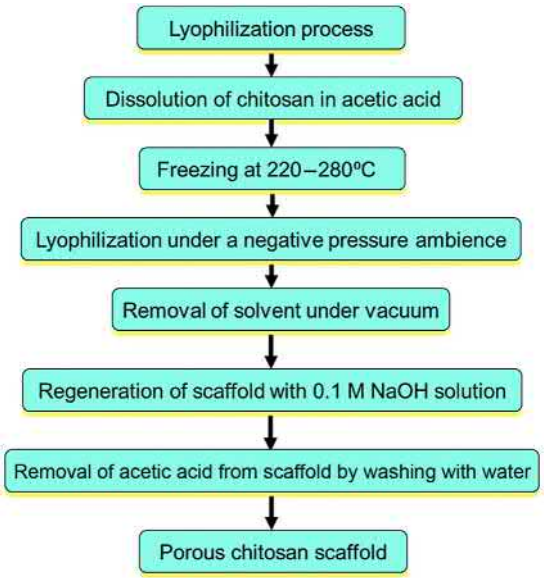
Lyophilization process
Dissolution of chitosan in acetic acid
Freezing at 220–280°C
Lyophilization under a negative pressure ambience
Removal of solvent under vacuum
Regeneration of scaffold with 0.1 M NaOH solution
Removal of acetic acid from scaffold by washing with water
Porous chitosan scaffold

FIGURE 13.15 Lyophilization process.

Chitosan scaffold should slowly degrade so that it can retain mechanical strength until the regeneration of tissue is complete. It is degraded by lysozyme enzymes due to the presence of β (1→4) glycosidic linkages (Kim et al., 2008). Biodegradation of chitosan mainly depends on crystallinity, the degree of deacetylation, distribution of acetyl residues, and molecular mass. Chitosan biodegradation rate increases when the degree of acetylation and crystallinity decreases (Croisier and Jérôme, 2013).

Applications of chitosan in tissue engineering are as follows:

- Skin tissue engineering
- Bone tissue engineering
- Cartilage tissue engineering
- Liver tissue engineering
- Nerve tissue engineering
- Blood vessel tissue engineering

13.8.3.1 Skin Tissue Engineering

Collagen, elastin, and GAGs are present in the dermis layer of skin, which forms the bulk of an important support system called the ECM. Hyaluronic acid, chondroitin sulfate, keratin sulfate, dermatan sulfate, heparin sulfate, and heparin are different types of GAGs present in the dermis.

Chitosan has been used in skin tissue engineering because it has a similar structure to GAGs, which are key components of the dermis of the skin and natural components of ECM (Romanova et al., 2015). It induces vascularization and generates adipose tissue, thereby providing skin regeneration and promoting its completion to the state of normal skin (Wu et al., 2007; Metcalfe and Ferguson, 2007).

13.8.3.2 Bone Tissue Engineering

When a bone is damaged it has significant self-healing capability. However, in cases of severe key bone defects, a graft (a piece of living tissue that is transplanted surgically) is used to prompt the physiological healing process. The grafts are obtained from a secondary site in the patient's body (autograft) or obtained from cadaver bones (allograft). Bone tissue engineering may use synthetic grafts as an alternative to autograft and allografts. Chitosan is comprehensively used in bone tissue engineering because of its unique characteristics such as biomechanical compatibility, biodegradability, and osteoconductivity to aid the formation of bone (Levengood and Zhang, 2014; Saravanan et al., 2016).

Chitosan is used either alone or in combined form with hydroxylapatite for bone tissue engineering (Levengood and Zhang, 2014). Chitosan's bone regeneration capabilities are increased by the addition of bone morphogenic protein and transforming factor beta-induced gene h3 (Kim et al., 2002). Chitosan and calcium phosphate composites are also used in tissue engineering. Some modified versions of chitosan such as quaternization, carboxyalkylation, and phosphorylation have a promising role in tissue engineering (LogithKumar et al., 2016). When bone morphogenetic proteins, which have a vital role in bone regeneration, were loaded in chitosan films, studies were performed to test their effects on MC3T3-E1 cell morphology and runt-related transcription factor 2 (RUNX2) expression. Results showed higher proliferation, reduced expression of RUNX2, and better bone growth (Li et al., 2017a).

The modified quaternized chitosan polymers *N*,*N*,*N*-trimethyl chitosan (TMC), *N*-(2-hydroxyl)propyl-3-trimethylammonium chitosan chloride (HTCC) were prepared by modification of chitosan side chain. When cortical bone coated with TMC-heparin polyelectrolyte was introduced, an increase in osteoblastic potential due to the periosteum mimics activity shown by TMC-heparin polyelectrolyte (LogithKumar et al., 2016).

Fibroblast growth factors that regulate cell proliferation and differentiation incorporated into chitosan−HTCC/glycerol phosphate thermosensitive hydrogel well improved new periodontal support tissues in dogs (Jana et al., 2014). Modified versions of chitosan have significant roles in bone tissue engineering. Hydroxylapatite deposition increased when chondroitin 4-sulfate was incorporated into chitosan matrix, which led to spreading of bone marrow stromal cells. Hydroxylapatite is used as filler to promote the growth of bone, but it has cytotoxicity on MC3T3-E1 cells. Some studies have found that when hydroxylapatite is incorporated with carboxymethyl chitosan it shows reduced cytotoxicity on MC3T3-E1 and high blood adsorbing capacity (Jayakumar et al., 2010). Chitosan increased alkaline phosphatase (ALP) activity and calcium deposition.

Nanohydroxyapatite is an inorganic material that has an important role in bone tissue engineering, but it is not widely used in this area because of some limitations such as intrinsic brittleness and very slow degradation. These limitations may be overcome by incorporating them into the proper biodegradable polymeric porous scaffold. So, chitosan is a good option for incorporation of nanohydroxyapatite because of its biodegradability. Chitosan−nanohydroxyapatite scaffolds were used for incorporation of phenol-formaldehyde resins, which have promising bioactivity in bone tissue engineering and results have shown that CHA-1RS nanocomposite scaffold has significant in vivo bioactivity, osteogenic activity, and ALP activity (Shakir et al., 2018).

Pigeonite is iron-containing ceramic. When pigeonite particles were incorporated into chitosan/calcium polyphosphate scaffolds, they produced better activity than chitosan/calcium polyphosphate alone because of increased protein adsorption and proliferation of mouse mesenchymal stem cells (Dhivya et al., 2017).

PLGA has been well-established in bone tissue engineering but when BMP-2 was loaded into PLGA microspheres, controlled release of BMP-2 was not observed due to the burst effect. There are many strategies for controlled release of protein; one of them is chitosan−PLGA microsphere, which shows promising controlled release of protein for 28 days (Boukari et al., 2017).

13.8.3.3 Cartilage Tissue Engineering

Articular cartilage can be found in all mobile joints of the human body and serves several important purposes. Most remarkably, articular cartilage acts as a protective surface to prevent wear at the end of bones (Beck et al., 2017). Articular cartilage is composed of distinctive cells called chondrocytes (Beck et al., 2017). In 1990 a cartilage defect was repaired by autologous chondrocytes transplantation (Brittberg et al., 1994). Mesenchymal stem/stromal cells become a useful source of cells for cartilage tissue engineering because they have a capacity for multilineage differentiation and self-renewal properties (Tuan et al., 2003; Wei et al., 2013).

Chitosan scaffolds have been shown to support cultured chondrocytes in vitro. These scaffolds help maintain their viability, round morphology, and support proliferation. This main feature of chitosan scaffolds in chondrocyte growth has led to wide use of chitosan in cartilage tissue engineering (Beck et al., 2017).

Graphene oxide has an epoxy functional group that can react with a primary amine group. The primary group of chitosan reacts with an epoxy group of graphene oxide and produces a complex via H-bond formation that is used for cartilage tissue engineering. Studies have reported that chondrocytes incorporated into reduced graphene oxide/chitosan films as cartilage tissue scaffolds. Cell viability tests of chondrocytes using MTT assay results showed elevated cell viabilities of chondrocytes after 14 days as compared with 1, 4, and 7 days, and demonstrated increased cell proliferation consistent with time (Cao et al., 2017).

Hyaluronic acid−based drug delivery reported a higher capacity of cartilage repair. Combination of hyaluronic acid−chitosan−based scaffold showed better cartilage repair activity. Hyaluronic acid−chitosan hydrogel showed higher seizing of water content, encapsulating cells, and retaining cell; due to these characteristics it is applicable in cartilage tissue engineering. In hyaluronic acid−chitosan gel and chondrocytes incorporated hyaluronic acid−chitosan gel it was observed that there was no any statistically significant difference in cartilage repair (Mohan et al., 2017).

13.8.4 Matrix Tablet for Controlled Drug Delivery

Conventional tablets do not show any modulated or extended drug release, which may be important to maintain a constant in vivo therapeutic plasma concentration of the drug. This major disadvantage of immediate release conventional tablets may be overcome by employing matrix tablets that provide steady pharmacological effects. Generally, cellulose

derivative polymers are used in the formulation of matrix tablets but polymers from other natural materials such as chitosan and alginate are used for matrix-based tablet formulations. Swellable polymers are used in the preparation of a matrix tablet; chitosan swelling property depends on molecular weight and salt form. The gravimetric technique is used for measurement of swelling and erosion rates of chitosan matrix tablets. Studies have shown that higher molecular weight (200 kDa) chitosan swelled greater than low molecular weight (40 kDa). The effect of salt form of chitosan on swelling property showed that chitosan glycolate based matrix tablet has the greatest swelling in both 0.1 N HCl and pH 6.8 Tris−HCl buffer than chitosan aspartate, chitosan lactate, and chitosan glutamate matrix tablets (Huanbutta et al., 2013).

Sodium alginate has swelling and erosion characteristics, therefore, it can be used in controlled release drug delivery. At a certain pH, sodium alginate is converted into alginic acid, which is insoluble. Due to this, lamination of matrix tablet may be observed and leads to burst drug release. This problem of sodium alginate is avoided by combining it with chitosan by polyelectrolyte complexation of chitosan−sodium alginate polymer. Conventional polyelectrolyte complex preparation is a long process. In situ chitosan−alginate polyelectrolyte complexation is an alternative way of polyelectrolyte complex for controlling drug release (Li et al., 2013). Interpenetrating polymer network (IPN) matrix chitosan tamarind seed polysaccharide tablets demonstrated an increased duration of action of aceclofenac to around 8 hours (Jana et al., 2014).

13.9 CONCLUSION

To fabricate mucoadhesive delivery systems, polymers have been explored to provide the desired effects. The main advantage of using mucoadhesive polymers is their ability to provide an enhanced residence time for the drug at the site of action as they adhere for a longer duration. Mucoadhesive polymers may be both water-soluble as well as water insoluble in nature. The mucoadhesive properties of chitosan can be improved using thiolation. Many methods of thiolation presented in this chapter revealed that thiolated chitosan may be effectively synthesized by using a variety of agents such as thioglycolic acid and cysteine. The thiolated chitosan can be implicated in many biomedical as well as pharmaceutical applications and serves as a good choice for formulation scientists for designing mucoadhesive systems.

Acknowledgment

The VP would like to acknowledge the Indian Council of Medical Research (ICMR), New Delhi for grant of SRFfunding (45/01/2018-NAN/BMS) for research work.

ABBREVIATIONS

PLGA poly(lactide-*co*-glycolide)
PLA polylactic acid
PEG polyethylene glycol
TPP tripolyphosphate

o/w	oil-in-water
SWCNT	single-walled carbon nanotube
MWCNT	multiwalled carbon nanotube
PCL	polycaprolactone
CST	critical solution temperature
PE	polyethylene
GAG	glycosaminoglycan
ECM	extracellular matrix
TMC	*N*,*N*,*N*-trimethyl chitosan
HTCC	*N*-(2-hydroxyl)propyl-3-trimethylammonium chitosan chloride
ALP	alkaline phosphatase

References

Agardan, N.B., Degim, Z., Yilmaz, S., Altintas, L., Topal, T., 2016. The effectiveness of raloxifene-loaded liposomes and cochleates in breast cancer therapy. AAPS PharmSciTech 17 (4), 968–977.

Agarwal, S., Leekha, A., Tyagi, A., Kumar, V., Moin, I., Verma, A., 2015. Versatality of Chitosan: A Short Review. J. Pharma Res. 4 (3), 125–134.

Agnihotri, S.A., Mallikarjuna, N.N., Aminabhavi, T.M., 2004. Recent advances on chitosan-based micro- and nanoparticles in drug delivery. J. Controlled Release 100 (1), 5–28.

Agrawal, A.K., Das, M., Jain, S., 2012. In situ gel systems as 'smart' carriers for sustained ocular drug delivery. Expert Opin. Drug Deliv. 9 (4), 383–402.

Ahmed, T.A., Aljaeid, B.M., 2016. Preparation, characterization, and potential application of chitosan, chitosan derivatives, and chitosan metal nanoparticles in pharmaceutical drug delivery. Drug Des. Devel. Ther. 10, 483–507.

Ahsan, S.M., Thomas, M., Reddy, K.K., Sooraparaju, S.G., Asthana, A., Bhatnagar, I., 2017. Chitosan as biomaterial in drug delivery and tissue engineering. Int. J. Biol. Macromol. 110, 97–109.

Ali, A., Ahmed, S., 2018. A review on chitosan and its nanocomposites in drug delivery. Int. J. Biol. Macromol. 109, 273–286.

Azagury, A., Khoury, L., Enden, G., Kost, J., 2014. Ultrasound mediated transdermal drug delivery. Adv. Drug Deliv. Rev. 72 (Suppl. C), 127–143.

Bassi da Silva, J., Ferreira, S.B.S., de Freitas, O., Bruschi, M.L., 2017. A critical review about methodologies for the analysis of mucoadhesive properties of drug delivery systems. Drug Dev. Ind. Pharm. 43 (7), 1053–1070. Available from: https://doi.org/10.1080/03639045.2017.1294600.

Beck, S.C., Jiang, T., Nair, L.S., Laurencin, C.T., 2017. 2—Chitosan for bone and cartilage regenerative engineering A2—Jennings, J. Amber. In: Bumgardner, J.D. (Ed.), Chitosan Based Biomaterials Volume 2. Woodhead Publishing.

Bernkop-Schnürch, A., 2005. Thiomers: a new generation of mucoadhesive polymers. Adv. Drug Deliv. Rev. 57 (11), 1569–1582.

Bernkop-Schnurch, A., Hornof, M., Guggi, D., 2004. Thiolated chitosans. Eur. J. Pharm. Biopharm. 57 (1), 9–17.

Bernkop-Schnürch, A., Krauland, A.H., Leitner, V.M., Palmberger, T., 2004. Thiomers: potential excipients for non-invasive peptide delivery systems. Eur. J. Pharm. Biopharm. 58 (2), 253–263.

Boddupalli, B.M., Mohammed, Z.N., Nath, R.A., Banji, D., 2010. Mucoadhesive drug delivery system: an overview. J. Adv. Pharm. Technol. Res. 1 (4), 381–387. Available from: https://doi.org/10.4103/0110-5558.76436.

Boukari, Y., Qutachi, O., Scurr, D.J., Morris, A.P., Doughty, S.W., Billa, N., 2017. A dual-application poly(DL-lactic-*co*-glycolic) acid (PLGA)-chitosan composite scaffold for potential use in bone tissue engineering. J. Biomater. Sci. Polym. Ed. 28 (16), 1966–1983.

Bowman, K., Leong, K.W., 2006. Chitosan nanoparticles for oral drug and gene delivery. Int. J. Nanomed. 1 (2), 117–128.

Bravo-Osuna, I., Teutonico, D., Arpicco, S., Vauthier, C., Ponchel, G., 2007. Characterization of chitosan thiolation and application to thiol quantification onto nanoparticle surface. Int. J. Pharm. 340 (1–2), 173–181.

Brigger, I., Dubernet, C., Couvreur, P., 2012. Nanoparticles in cancer therapy and diagnosis. Adv. Drug Deliv. Rev. 64 (Suppl.), 24–36.

Brittberg, M., Lindahl, A., Nilsson, A., Ohlsson, C., Isaksson, O., Peterson, L., 1994. Treatment of deep cartilage defects in the knee with autologous chondrocyte transplantation. N. Engl. J. Med. 331 (14), 889–895.
Cao, L., Lu, C., Wang, Q., Li, F., 2017. Biocompatibility and fabrication of RGO/chitosan film for cartilage tissue recovery. Environ. Toxicol. Pharmacol. 54 (Suppl. C), 199–203.
Chamayou, A., Dodds, J.A., 2007. Chapter 8—Air jet milling. In: Salman, A.D., Ghadiri, M., Hounslow, M.J. (Eds.), Handbook of Powder Technology. Elsevier Science B.V.
Cheng, Y.-H., Tsai, T.-H., Jhan, Y.-Y., Chiu, A.W., Tsai, K.-L., Chien, C.-S., et al., 2016. Thermosensitive chitosan-based hydrogel as a topical ocular drug delivery system of latanoprost for glaucoma treatment. Carbohydr. Polym. 144 (Suppl. C), 390–399.
Chern, C.S., 2006. Emulsion polymerization mechanisms and kinetics. Prog. Polym. Sci. 31 (5), 443–486.
Croisier, F., Jérôme, C., 2013. Chitosan-based biomaterials for tissue engineering. Eur. Polym. J. 49 (4), 780–792.
Dash, M., Chiellini, F., Ottenbrite, R.M., Chiellini, E., 2011. Chitosan—A versatile semi-synthetic polymer in biomedical applications. Prog. Polym. Sci. 36 (8), 981–1014.
De Volder, M.F., Tawfick, S.H., Baughman, R.H., Hart, A.J., 2013. Carbon nanotubes: present and future commercial applications. Science 339 (6119), 535–539.
Dhivya, S., Keshav Narayan, A., Logith Kumar, R., Viji Chandran, S., Vairamani, M., Selvamurugan, N., 2017. Proliferation and differentiation of mesenchymal stem cells on scaffolds containing chitosan, calcium polyphosphate and pigeonite for bone tissue engineering. Cell Prolif. 51 (1), e12408.
Gao, T.-T., Kong, M., Cheng, X.-J., Xia, G.-X., Gao, Y.-Y., Chen, X.-G., et al., 2014. A thermosensitive chitosan-based hydrogel for controlled release of insulin. Front. Mater. Sci. 8 (2), 142–149.
Garcia-Fuentes, M., Alonso, M.J., 2012. Chitosan-based drug nanocarriers: where do we stand? J. Controlled Release 161 (2), 496–504.
Gradauer, K., Vonach, C., Leitinger, G., Kolb, D., Frohlich, E., Roblegg, E., et al., 2012. Chemical coupling of thiolated chitosan to preformed liposomes improves mucoadhesive properties. Int. J. Nanomed. 7, 2523–2534.
Gradauer, K., Barthelmes, J., Vonach, C., Almer, G., Mangge, H., Teubl, B., et al., 2013. Liposomes coated with thiolated chitosan enhance oral peptide delivery to rats. J. Controlled Release 172 (3), 872–878.
Gyles, D.A., Castro, L.D., Silva, J.O.C., Ribeiro-Costa, R.M., 2017. A review of the designs and prominent biomedical advances of natural and synthetic hydrogel formulations. Eur. Polym. J. 88 (Suppl. C), 373–392.
Ho, M.H., Yao, C.J., Liao, M.H., Lin, P.I., Liu, S.H., Chen, R.M., 2015. Chitosan nanofiber scaffold improves bone healing via stimulating trabecular bone production due to upregulation of the Runx2/osteocalcin/alkaline phosphatase signaling pathway. Int. J. Nanomed. 10, 5941–5954.
Huanbutta, K., Cheewatanakornkool, K., Terada, K., Nunthanid, J., Sriamornsak, P., 2013. Impact of salt form and molecular weight of chitosan on swelling and drug release from chitosan matrix tablets. Carbohydr. Polym. 97 (1), 26–33.
Inamdar, N., Mourya, V.K., 2013. Thiolated chitosan: preparation, properties and applications. In: Advances in Drug Discovery and Developments, first ed.
Ivanova, E.P., Bazaka, K., Crawford, R.J., 2014. 2—Natural polymer biomaterials: advanced applications. New Functional Biomaterials for Medicine and Healthcare. Woodhead Publishing.
Jain, S., Singh, P., Mishra, V., Vyas, S.P., 2005. Mannosylated niosomes as adjuvant-carrier system for oral genetic immunization against hepatitis B. Immunol. Lett. 101 (1), 41–49.
Jana, S., Sen, K.K., Basu, S.K., 2014. In vitro aceclofenac release from IPN matrix tablets composed of chitosan-tamarind seed polysaccharide. Int. J. Biol. Macromol. 65, 241–245.
Jayakumar, R., Prabaharan, M., Nair, S.V., Tokura, S., Tamura, H., Selvamurugan, N., 2010. Novel carboxymethyl derivatives of chitin and chitosan materials and their biomedical applications. Prog. Mater. Sci. 55 (7), 675–709.
Kafedjiiski, K., Krauland, A.H., Hoffer, M.H., Bernkop-Schnürch, A., 2005. Synthesis and in vitro evaluation of a novel thiolated chitosan. Biomaterials 26 (7), 819–826.
Kast, C.E., Bernkop-Schnurch, A., 2001. Thiolated polymers—thiomers: development and in vitro evaluation of chitosan-thioglycolic acid conjugates. Biomaterials 22 (17), 2345–2352.
Kim, I.S., Park, J.W., Kwon, I.C., Baik, B.S., Cho, B.C., 2002. Role of BMP, betaig-h3, and chitosan in early bony consolidation in distraction osteogenesis in a dog model. Plast. Reconstr. Surg. 109 (6), 1966–1977.
Kim, I.Y., Seo, S.J., Moon, H.S., Yoo, M.K., Park, I.Y., Kim, B.C., et al., 2008. Chitosan and its derivatives for tissue engineering applications. Biotechnol. Adv. 26 (1), 1–21.

Kuche, K., Maheshwari, R., Tambe, V., Mak, K.K., Jogi, H., Raval, N., et al., 2018. Carbon nanotubes (CNTs) based advanced dermal therapeutics: current trends and future potential. Nanoscale 10 (19), 8911–8937.

Kumar, M.R., Muzzarelli, R.A., Muzzarelli, C., Sashiwa, H., Domb, A., 2004. Chitosan chemistry and pharmaceutical perspectives. Chem. Rev. 104 (12), 6017–6084.

Kunjachan, S., Jose, S., Lammers, T., 2010. Understanding the mechanism of ionic gelation for synthesis of chitosan nanoparticles using qualitative techniques. Asian J. Pharm. 4 (2), 148–153.

Lalu, L., Tambe, V., Pradhan, D., Nayak, K., Bagchi, S., Maheshwari, R., et al., 2017. Novel nanosystems for the treatment of ocular inflammation: current paradigms and future research directions. J. Controlled Release 268, 19–39.

Laye, C., McClements, D.J., Weiss, J., 2008. Formation of biopolymer-coated liposomes by electrostatic deposition of chitosan. J. Food Sci. 73 (5), N7–N15.

Levengood, S.L., Zhang, M., 2014. Chitosan-based scaffolds for bone tissue engineering. J. Mater. Chem. B Mater. Biol. Med. 2 (21), 3161–3184.

Li, J., Lin, J., Yu, W., Song, X., Hu, Q., Xu, J.H., et al., 2017a. BMP-2 plasmid DNA-loaded chitosan films—a new strategy for bone engineering. J. Craniomaxillofac Surg. 45, 2084–2091.

Li, L., Wang, L., Shao, Y., Ni, R., Zhang, T., Mao, S., 2013. Drug release characteristics from chitosan-alginate matrix tablets based on the theory of self-assembled film. Int. J. Pharm. 450 (1–2), 197–207.

Li, N., Zhuang, C., Wang, M., Sun, X., Nie, S., Pan, W., 2009. Liposome coated with low molecular weight chitosan and its potential use in ocular drug delivery. Int. J. Pharm. 379 (1), 131–138.

Li, R., Deng, L., Cai, Z., Zhang, S., Wang, K., Li, L., et al., 2017b. Liposomes coated with thiolated chitosan as drug carriers of curcumin. Mater. Sci. Eng. C Mater. Biol. Appl. 80, 156–164.

Lin, C.-H., Lin, J.-C., Chen, C.-Y., Cheng, C.-Y., Lin, X.-Z., Wu, J.-J., 2005. Feasibility evaluation of chitosan coatings on polyethylene tubing for biliary stent applications. J. Appl. Polym. Sci. 97 (3), 893–902.

Liu, Z., Jiao, Y., Wang, Y., Zhou, C., Zhang, Z., 2008. Polysaccharides-based nanoparticles as drug delivery systems. Adv. Drug Deliv. Rev. 60 (15), 1650–1662.

LogithKumar, R., KeshavNarayan, A., Dhivya, S., Chawla, A., Saravanan, S., Selvamurugan, N., 2016. A review of chitosan and its derivatives in bone tissue engineering. Carbohydr. Polym. 151, 172–188.

Madihally, S.V., Matthew, H.W., 1999. Porous chitosan scaffolds for tissue engineering. Biomaterials 20 (12), 1133–1142.

Maheshwari, R., Chourasiya, Y., Bandopadhyay, S., Katiyar, P.K., Sharma, P., Deb, P.K., et al., 2018a. Levels of solid state properties: role of different levels during pharmaceutical product development. Dosage Form Design Parameters. Elsevier.

Maheshwari, R., Kuche, K., Mane, A., Chourasiya, Y., Tekade, M., Tekade, R.K., 2018b. Manipulation of physiological processes for pharmaceutical product development. Dosage Form Design Considerations. Elsevier.

Maheshwari, R.G., Thakur, S., Singhal, S., Patel, R.P., Tekade, M., Tekade, R.K., 2015. Chitosan encrusted nonionic surfactant based vesicular formulation for topical administration of ofloxacin. Sci. Adv. Mater. 7 (6), 1163–1176.

Mansuri, S., Kesharwani, P., Tekade, R.K., Jain, N.K., 2016. Lyophilized mucoadhesive-dendrimer enclosed matrix tablet for extended oral delivery of albendazole. Eur. J. Pharm. Biopharm. 102, 202–213. Available from: https://doi.org/10.1016/j.ejpb.2015.10.015.

Matanović, M.R., Kristl, J., Grabnar, P.A., 2014. Thermoresponsive polymers: insights into decisive hydrogel characteristics, mechanisms of gelation, and promising biomedical applications. Int. J. Pharm. 472 (1), 262–275.

Metcalfe, A.D., Ferguson, M.W., 2007. Tissue engineering of replacement skin: the crossroads of biomaterials, wound healing, embryonic development, stem cells and regeneration. J. R. Soc. Interface 4 (14), 413–437.

Moghassemi, S., Hadjizadeh, A., 2014. Nano-niosomes as nanoscale drug delivery systems: an illustrated review. J. Controlled Release 185 (Suppl. C), 22–36.

Moghassemi, S., Parnian, E., Hakamivala, A., Darzianiazizi, M., Vardanjani, M.M., Kashanian, S., et al., 2015. Uptake and transport of insulin across intestinal membrane model using trimethyl chitosan coated insulin niosomes. Mater. Sci. Eng. C 46 (Suppl. C), 333–340.

Mohan, N., Mohanan, P.V., Sabareeswaran, A., Nair, P., 2017. Chitosan-hyaluronic acid hydrogel for cartilage repair. Int. J. Biol. Macromol. 104 (Part B), 1936–1945.

Mulas, K., Stefanowicz, Z., Oledzka, E., Sobczak, M., 2019. Current state of the polymeric delivery systems of fluoroquinolones - a review. J. Control Release. 294, 195–215. Available from: https://doi.org/10.1016/j.jconrel.2018.12.021. Epub 2018 Dec 13.

Muniswamy, V.J., Raval, N., Gondaliya, P., Tambe, V., Kalia, K., Tekade, R.K., 2019. Dendrimer-Cationized-Albumin' encrusted polymeric nanoparticle improves BBB penetration and anticancer activity of doxorubicin. Int. J. Pharm. 30 (555), 77–99. Available from: https://doi.org/10.1016/j.ijpharm.2018.11.035.

Nagamoto, T., Hattori, Y., Takayama, K., Maitani, Y., 2004. Novel chitosan particles and chitosan-coated emulsions inducing immune response via intranasal vaccine delivery. Pharm. Res. 21 (4), 671–674.

Ohya, Y., Takei, T., Kobayashi, H., Ouchi, T., 1993. Release behaviour of 5-fluorouracil from chitosan-gel microspheres immobilizing 5-fluorouracil derivative coated with polysaccharides and their cell specific recognition. J. Microencapsulation 10 (1), 1–9.

Park, S.N., Jo, N.R., Jeon, S.H., 2014. Chitosan-coated liposomes for enhanced skin permeation of resveratrol. J. Ind. Eng. Chem. 20 (4), 1481–1485.

Prego, C., Paolicelli, P., Diaz, B., Vicente, S., Sanchez, A., Gonzalez-Fernandez, A., et al., 2010. Chitosan-based nanoparticles for improving immunization against hepatitis B infection. Vaccine 28 (14), 2607–2614.

Raval, N., Kalyane, D., Maheshwari, R., Tekade, R.K., 2019. Chapter 5: copolymers and block copolymers in drug delivery and therapy. Basic Fund. Drug Deliv. 173–201.

Rodriguez-Vazquez, M., Vega-Ruiz, B., Ramos-Zuniga, R., Saldana-Koppel, D.A., Quinones-Olvera, L.F., 2015. Chitosan and its potential use as a scaffold for tissue engineering in regenerative medicine. Biomed. Res. Int. 2015, 821279.

Romanova, O.A., Grigor'ev, T.E., Goncharov, M.E., Rudyak, S.G., Solov'yova, E.V., Krasheninnikov, S.T., et al., 2015. Chitosan as a modifying component of artificial scaffold for human skin tissue engineering. Bull. Exp. Biol. Med. 159 (4), 557–566.

Roy, S., Pal, K., Anis, A., Pramanik, K., Prabhakar, B., 2009. Polymers in mucoadhesive drug-delivery systems: a brief note. Des. Monomers Polym. 12, 483–495.

Ruel-Gariépy, E., Shive, M., Bichara, A., Berrada, M., Le Garrec, D., Chenite, A., et al., 2004. A thermosensitive chitosan-based hydrogel for the local delivery of paclitaxel. Eur. J. Pharm. Biopharm. 57 (1), 53–63.

Saravanan, S., Leena, R.S., Selvamurugan, N., 2016. Chitosan based biocomposite scaffolds for bone tissue engineering. Int. J. Biol. Macromol. 93 (Pt B), 1354–1365.

Schattling, P., Taipaleenmäki, E., Zhang, Y., Städler, B., 2017. A polymer chemistry point of view on mucoadhesion and mucopenetration. Macromol Biosci. 17 (9). Available from: https://doi.org/10.1002/mabi.201700060.

Shaikh, R., Raj Singh, T.R., Garland, M.J., Woolfson, A.D., Donnelly, R.F., 2011. Mucoadhesive drug delivery systems. J. Pharm. Bioallied Sci. 3 (1), 89–100. Available from: https://doi.org/10.4103/0975-7406.76478.

Shakir, M., Jolly, R., Khan, A.A., Ahmed, S.S., Alam, S., Rauf, M.A., et al., 2018. Resol based chitosan/nano-hydroxyapatite nanoensemble for effective bone tissue engineering. Carbohydr. Polym. 179, 317–327.

Singh, I., Pawar, P., Sanusi, E.A., Odeku, O.A., 2017. Mucoadhesive polymers for drug delivery systems. Adhes. Pharm. Biomed. Dent. Fields 89.

Slutter, B., Jiskoot, W., 2010. Dual role of CpG as immune modulator and physical cross-linker in ovalbumin loaded *N*-trimethyl chitosan (TMC) nanoparticles for nasal vaccination. J. Controlled Release 148 (1), 117–121.

Smart, J.D., 2005. The basics and underlying mechanisms of mucoadhesion. Adv. Drug Deliv. Rev. 57 (11), 1556–1568.

Songjiang, Z., Lixiang, W., 2009. Amyloid-beta associated with chitosan nano-carrier has favorable immunogenicity and permeates the BBB. AAPS PharmSciTech 10 (3), 900–905.

Soni, N., Tekade, M., Kesharwani, P., Bhattacharya, P., Maheshwari, R., Dua, K., et al., 2017. Recent advances in oncological submissions of dendrimer. Curr. Pharm. Des. 23 (21), 3084–3098.

Sosnik, A., das Neves, J., Sarmento, B., 2014. Mucoadhesive polymers in the design of nano-drug delivery systems for administration by nonparenteral routes: a review. Prog. Polym. Sci. 39 (12), 2030–2075.

Tekade, R.K., Maheshwari, R., Soni, N., Tekade, M., 2017a. Chapter 12—Carbon nanotubes in targeting and delivery of drugs A2—Mishra, Vijay. In: Kesharwani, P., Amin, M.C.I.M., Iyer, A. (Eds.), Nanotechnology-Based Approaches for Targeting and Delivery of Drugs and Genes. Academic Press.

Tekade, R.K., Maheshwari, R., Soni, N., Tekade, M., Chougule, M.B., 2017b. Chapter 1—Nanotechnology for the development of nanomedicine A2—Mishra, Vijay. In: Kesharwani, P., Amin, M.C.I.M., Iyer, A. (Eds.), Nanotechnology-Based Approaches for Targeting and Delivery of Drugs and Genes. Academic Press.

Tekade, R.K., Maheshwari, R., Tekade, M., 2017c. 4—Biopolymer-based nanocomposites for transdermal drug delivery. Biopolymer-Based Composites. Woodhead Publishing.

Thierry, B., Merhi, Y., Silver, J., Tabrizian, M., 2005. Biodegradable membrane-covered stent from chitosan-based polymers. J. Biomed. Mater. Res. A 75, 556–566.

Tkac, J., Whittaker, J.W., Ruzgas, T., 2007. The use of single walled carbon nanotubes dispersed in a chitosan matrix for preparation of a galactose biosensor. Biosens. Bioelectron. 22 (8), 1820–1824.

Torchilin, V.P., 2010. Passive and active drug targeting: drug delivery to tumors as an example. Handb. Exp. Pharmacol. 197, 3–53.

Tuan, R.S., Boland, G., Tuli, R., 2003. Adult mesenchymal stem cells and cell-based tissue engineering. Arthritis Res. Ther. 5 (1), 32–45.

Vacanti, J.P., Langer, R., 1999. Tissue engineering: the design and fabrication of living replacement devices for surgical reconstruction and transplantation. Lancet 354 (Suppl. 1), SI32–SI34.

Vhora, I., Patil, S., Bhatt, P., Gandhi, R., Baradia, D., Misra, A., 2014. Receptor-targeted drug delivery: current perspective and challenges. Ther. Deliv. 5 (9), 1007–1024.

Vila, A., Sanchez, A., Tobio, M., Calvo, P., Alonso, M.J., 2002. Design of biodegradable particles for protein delivery. J. Controlled Release 78 (1–3), 15–24.

Wei, X., Yang, X., Han, Z.P., Qu, F.F., Shao, L., Shi, Y.F., 2013. Mesenchymal stem cells: a new trend for cell therapy. Acta Pharmacol. Sin. 34 (6), 747–754.

Werle, M., Bernkop-Schnurch, A., 2008. Thiolated chitosans: useful excipients for oral drug delivery. J. Pharm. Pharmacol. 60 (3), 273–281.

Wu, X., Black, L., Santacana-Laffitte, G., Patrick Jr., C.W., 2007. Preparation and assessment of glutaraldehyde-cross-linked collagen-chitosan hydrogels for adipose tissue engineering. J. Biomed. Mater. Res. A 81 (1), 59–65.

Wu, Y., Wang, Y., Luo, G., Dai, Y., 2009. In situ preparation of magnetic Fe_3O_4-chitosan nanoparticles for lipase immobilization by cross-linking and oxidation in aqueous solution. Bioresour. Technol. 100 (14), 3459–3464.

Yeh, T.H., Hsu, L.W., Tseng, M.T., Lee, P.L., Sonjae, K., Ho, Y.C., Sung, H.W., 2011. Mechanism and consequence of chitosan-mediated reversible epithelial tight junction opening. Biomaterials. 32 (26), 6164–6173. Available from: https://doi.org/10.1016/j.biomaterials.2011.03.056.

Zhang, W., Li, G., Fang, Y., Wang, X., 2007. Maleic anhydride surface-modification of cross-linked chitosan membrane and its pervaporation performance. J. Membr. Sci. 295 (1–2), 130–138.

Zhao, L.-M., Shi, L.-E., Zhang, Z.-L., Chen, J.-M., Shi, D.-D., Yang, J., et al., 2011. Preparation and application of chitosan nanoparticles and nanofibers. Braz. J. Chem. Eng. 28, 353–362.

CHAPTER

14

Recent Advances and Challenges in Microneedle-Mediated Transdermal Protein and Peptide Drug Delivery

Rubhan Chandran[1], *Eusni Rahayu Mohd. Tohit*[1], *Johnson Stanslas*[2] *and Tuan Mazlelaa Tuan Mahmood*[3]

[1]Haematology Unit, Department of Pathology, Faculty of Medicine and Health Sciences, Universiti Putra Malaysia, Selangor, Malaysia [2]Pharmacotherapeutics Unit, Department of Medicine, Faculty of Medicine and Health Sciences, Universiti Putra Malaysia, Serdang, Selangor, Malaysia [3]Faculty of Pharmacy, The National University of Malaysia (UKM), Kuala Lumpur, Malaysia

OUTLINE

14.1 Introduction to Transdermal Delivery of Protein and Peptides 496

14.2 Mechanism of Skin-Based Microneedle Systems: Entry Into the Blood Circulation 498

14.3 Skin Properties and Design of Microneedles: A Correlation 500

14.4 Challenges in Microneedle-Mediated Protein Drug Delivery 505

14.4.1 Skin Barrier 505

14.4.2 Limitations of Existing Microneedle Treatment 506

14.4.3 Physicochemical Instabilities of Protein Drugs 508

14.4.4 Immunogenicity After Treatment 509

14.5 Advances in Microneedle Technology in Protein Delivery 509

14.5.1 Solid Microneedles Technology 510

14.5.2 Coated Microneedles Technology 511

Biomaterials and Bionanotechnology
DOI: https://doi.org/10.1016/B978-0-12-814427-5.00014-7

© 2019 Elsevier Inc. All rights reserved.

14.5.3 *Hollow Microneedles Technology* 511
14.5.4 *Dissolving Microneedles Technology* 513
14.5.5 *Hydrogel/Swellable Microneedles Technology* 514
14.6 Current Status of Protein and Peptide Containing Microneedles in Clinical Trials and Marketed Microneedle Products 517
14.7 Conclusion 519
Abbreviations 519
Acknowledgments 520
References 520
Further reading 525

14.1 INTRODUCTION TO TRANSDERMAL DELIVERY OF PROTEIN AND PEPTIDES

The elucidation of the biological functions of many proteins and peptides including their roles in the pathophysiology of human illness has led to their widespread applications in biopharmaceutics (Adessi and Soto, 2002). Peptide- and protein-based drugs are considered as the best options for treatment of chronic diseases such as diabetes, cancer, leukemia, hemophilia, hepatitis, and rheumatoid arthritis due to their high specificity and potency compared with small compounds (Tan et al., 2010). In 2017, out of 369 biotechnology-based drugs approved by the US Food and Drug Administration (FDA), 239 were peptide and protein drugs. Most of the peptide drugs are targeted for replacement therapy or to facilitate existing pathways such as hematological and endocrine pathways. For instance, Epogen (erythropoietin) is administered to promote erythropoiesis in anemia caused by chronic kidney disease and Forteo [parathyroid hormone (PTH) residues] is administered to improve ossification in severe osteoporosis cases (Leader et al., 2008; Usmani et al., 2017). Due to the strong and continued development, worldwide market value for bioengineered protein drugs is expected to reach up to $228.4 billion by 2021 from $172.5 billion in 2016 (Dewan, 2017).

Drug delivery is the technique or process of administering a pharmaceutical agent to accomplish a therapeutic effect in humans or animals (Tiwari et al., 2012). According to Jitendra et al. (2011), the therapeutic effect of a drug is markedly influenced by the route of administration. Parenteral routes such as intravenous (IV), intramuscular (IM), and subcutaneous (SCT) are the most commonly adopted methods for protein and peptide drug administration (Jani et al., 2012). IV administration is the main choice for systemic delivery of proteins and peptides as 100% bioavailability can be achieved by this method. Almost 45% of protein drugs are delivered intravenously to prevent the drugs from being excessively metabolized by tissues at the site of IM or SCT and first-pass metabolism (Usmani et al., 2017; Desser et al., 2001; Lakshmi et al., 2017).

However, some of the therapeutic proteins have a very short in vivo half-life because they undergo rapid clearance or enzymatic degradation after parenteral injections

(Zalta et al., 2002; Bak et al., 2015). Macromolecular proteins in infusions are often recognized as "antigens" by the body, which leads to immunogenic response and necessitates frequent injections (Jani et al., 2012). In some serious conditions, as in severe hemophilia A, frequent lifelong injections practiced under clinical supervision require very expensive cumulative medical charges. The mean direct medical costs for severe hemophilia A patients receiving prophylactic treatment were estimated at $292,525 (Dalton, 2015). This is to say that, the cost for hemophilia A treatment is expensive and with advancement in technology, patients' life expectancy has increased and this leads to escalating cost of hemophilia management. Hypodermic injection also induces pain, needle phobia, phlebitis, and tissue necrosis issues (Bashyal et al., 2016). According to Duan and Mao (2010), optimal pharmacodynamics properties and rapid absorption of the applied drug into the bloodstream cannot be attained via SCT administration of biopharmaceuticals. Owing to these limitations, various noninvasive routes emerge as promising alternatives for the delivery of protein therapeutics (Mitragotri et al., 2014).

Tremendous efforts have been made to deliver biopharmaceuticals via noninvasive means such as pulmonary, nasal, oral, transdermal, vaginal, and ocular routes (Zelikin et al., 2016). Ideally, a noninvasive drug delivery system would be feasible for self-administration and painless, thus, increasing patient compliance (Mitragotri et al., 2014). Particularly, the transdermal route has undergone massive developments over the years because of its selective benefits over other noninvasive routes such as evasion of the first-pass metabolism, quick onset of action, the potential for sustained drug delivery, needle-free treatment, and adaptability for both small and macromolecular therapeutics administration. These advantages may result in a better therapeutic effect and improve patient compliance (Cao, 2016).

Vehicle- or carrier-based drug delivery is an approach to improve the bioavailability and stability of drug molecules. Vehicle-mediated sustained release systems considerably reduce the number of injections and extend the exposure period after a single administration, enabling a sustainable and cost-effective treatment (Okumu and Cleland, 2003). In transdermal drug delivery, vehicles provide a protection to the proteins and peptides from proteolytic enzymes and physiological changes, besides acting as a mediator for the transport of drugs across biological membranes (Cao, 2016). A broad range of materials are used as delivery vehicles including metals, microparticles (MPs), nanoparticles (NPs), liposomes, and a variety of polymers (e.g., hydrophilic mucoadhesive polymers, natural polymers, and hydrogels).

Microneedle (MN) patch, a transdermal drug delivery vehicle, is made up of arrays of microprojections formed with variable materials, ranging from 25 to 2000 μm in height, with different tip shapes and intervals. When applied to the skin, they penetrate the skin barrier-stratum corneum (SC) in the epidermis to reach the highly vascularized dermis. Compared with a hypodermic needle, this minimally invasive drug delivery technique is more patient-friendly especially among pediatrics (Ita, 2015). In this review, the advancement and limitations in MN-mediated protein and peptide drug delivery and mechanism of entry of proteins and peptide administered via MNs into circulation will be discussed.

14.2 MECHANISM OF SKIN-BASED MICRONEEDLE SYSTEMS: ENTRY INTO THE BLOOD CIRCULATION

Ideally, MNs are designed to penetrate the epidermis into the dermis especially the papillary layer where the blood and lymph capillary networks are present in abundance. Following MN administration, drugs enter into the bloodstream via two routes: direct entry into a blood vessel and/or entry into lymphatic vessel followed by clearance into bloodstream depending on their size and molecular weight (MW). Small molecules ($<$10 nm in size or $\sim$16–20 kDa for proteins) more readily diffuse into blood capillaries via transcellular (lipophilic drugs) (Fig. 14.1A) or paracellular (hydrophilic drug) ($<$600 Da) routes (Fig. 14.1B) due to the "leaky" property of capillary endothelium (Watson et al., 2001; Trevaskis et al., 2015; Ibrahim et al., 2012; Dowd et al., 2016; Harvey et al., 2011).

Conversely, macromolecules and proteins (10–100 nm in size) in the interstitium are too large to enter directly into blood capillaries but are able to enter into the lymphatic vessel by paracellular route via interendothelial junctions or dendritic cell–mediated uptake (Fig. 14.1C) or by transcellular route via passive diffusion or receptor-mediated uptake (Fig. 14.1D). Based on a two-slit theory model by Ibrahim et al. (2012), higher MW of large substances obstruct their diffusion through the slits of the endothelial wall of blood capillaries (with a diameter of $\sim$10–15 nm) preventing their systemic absorption. As MW is increased, lymph-mediated uptake is expected to increase because, in convection-based lymphatic uptake, the osmotic pressure of lymph flow serves as a major limiting factor, not the MW of the drug.

Harvey et al. (2011) reported that intradermal delivery of intracardiac green dye (ICG) (MW = 775 Da) by hollow MN resulted in instant uptake by the local lymphatic vessels using near infrared imaging studies. The dye could be identified within 20 seconds of administration in the neighboring inguinal lymph node and the signal strength continued to increase throughout the 3-minute observation period. Unlike in IV administration, peripheral vessels were not illuminated after MN administration although the potential uptake of low MW ICG from venous capillary cannot be neglected. Increase in interstitial pressure at the site of injection further enhances convective lymph absorption and transport of drug. This report shows that lymphatic uptake plays a significant role in the rapid pharmacokinetic and pharmacodynamic effects in MN-assisted delivery.

In a recent study, Kennedy et al. (2017) demonstrated the role of lymphatics in the biodistribution of rhodamine B (RhB) bound NPs delivered via dissolving MN in a murine model. Detection of RhB-associated fluorescence in lymph node, spleen, liver, and kidney following administration confirms that NPs (which are too large to enter blood capillaries) were drained into the lymphatic system before entering the systemic circulation. This study also supports previous findings, whereby, the rate of lymphatic uptake depends on the transport site of administration and the size of the drug delivered. It is expected that application sites closer to the neck will result in a faster distribution time for the NPs because the lymph will enter the cardiovascular system by flowing into subclavian veins at the base of the neck. This confirms the role of the lymphatic system in the absorption and transport of small and macromolecular proteins.

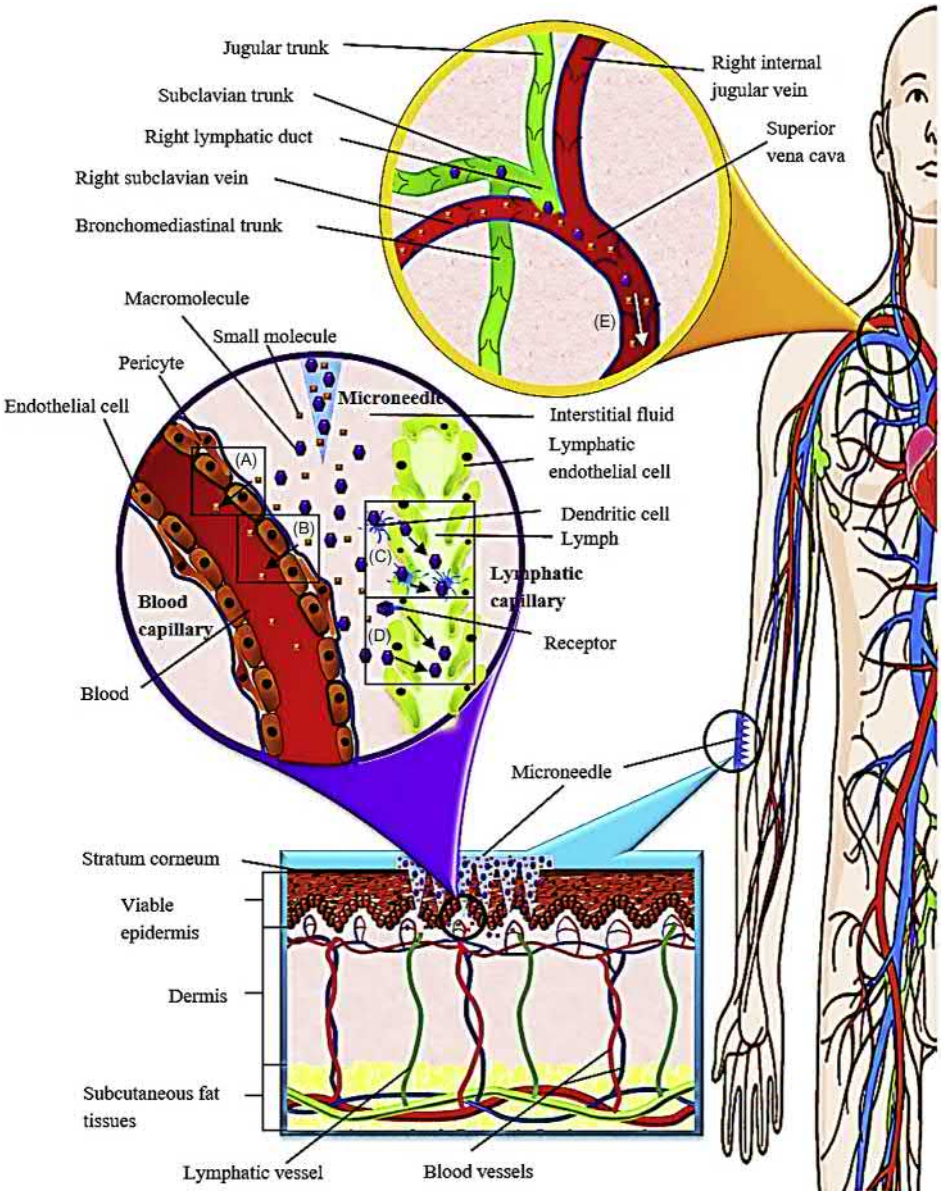

FIGURE 14.1 Mechanisms of entry of protein drugs administered via MNs into the circulation. A dissolving MN (encapsulated with small and macromolecular protein drug) administered in the arm of the patient pokes the SC and releases the drugs into the blood and lymphatic capillaries present in the dermal layer. Small proteins released in the interstitial space are mainly taken up by the blood capillaries by either (A) transcellular or (B) paracellular routes across endothelial cells. Macromolecular proteins have a greater tendency to be taken up by the lymphatic vessels with larger interendothelial junction diameter (~100 nm) compared with blood capillaries (~10–15 nm). The macromolecular protein may enter the lymphatic vessels by (C) paracellular route (through interendothelial junctions or dendritic cell–mediated uptake) or (D) transcellular route (passive diffusion or receptor mediated). In the lymphatic system, the protein drug flow is unidirectional due to the presence lymphatic valves acting similar to venous valves. At the base of the neck, the right lymphatic duct will drain the macromolecular protein drug present in the lymph at the junction of the right jugular and subclavian veins. Here (E) the macromolecular drug along with small molecular drug (which is already present in the circulatory system) will be transported to the heart via superior vena cava to be circulated throughout the body (Watson et al., 2001; Trevaskis et al., 2015; Ibrahim et al., 2012; Dowd et al., 2016; Harvey et al., 2011; Kennedy et al., 2017). Some sections of the figure created in the Mind the Graph platform (www.mindthegraph.com). *MN*, Microneedle; *SC*, stratum corneum.

14.3 SKIN PROPERTIES AND DESIGN OF MICRONEEDLES: A CORRELATION

The outermost layer of the epidermis, the SC, is made of 15 to 30 stacked dead and cornified cells that are mainly composed of lipid and keratin. This layer acts as a major barrier to drug delivery due to its innate role as a protective layer from the external environment. The inner layers of the SC consist of lamellar granules and serve as the permeability layers. The dermal layer is an integrated fibroelastic structure that gives mechanical strength to the skin and houses abundant blood capillaries and nerve receptors (Lambert and Laurent, 2008; Zaidi and Lanigan, 2010). Hence, MNs should be mechanically compatible to penetrate the rigid SC layer and successfully deliver drugs to the targeted sites without stimulating the pain-sensitive receptors in the dermis.

Kendall et al. (2007) studied the mechanical properties of murine skin with the insertion of micro and nanoprojections across intact SC and viable epidermis. They recorded a drop in mechanical properties with skin layers. Some mechanical test studies reported that the Young's modulus of the skin differs between 4.6 and 20 MPa. However, these factors vary with age, sex, race, body mass index, skin type, hydration, body sites, and between individuals (Kelchen et al., 2014; Márquez-Graña et al., 2017). Therefore the knowledge on the heterogeneous property of skin is vital in designing MN devices as it influences the insertion force required for MN application. Based on the inherent viscoelastic properties and structure of skin layers, parameters such as height, shape, sharpness, aspect ratio, center-to-center spacing, and patch area should be optimized when designing MN arrays.

Various ranges of materials have been explored for the fabrication of MNs such as metals, metalloids, carbohydrates, and synthetic polymers. Metals such as stainless steel, titanium, palladium, nickel, and metalloids such as silicon and aluminum were used for MN fabrication. Meanwhile, the nonmetals which have been utilized in MN development can be categorized into ceramics, glass, carbohydrates, and polymers (Larrañeta et al., 2016) (Fig. 14.2). In certain conditions, a mixture of natural and synthetic polymers such as polyvinyl-alcohol (PVA)−dextran−carboxymethyl cellulose (CMC) or PVA−gelatin have been used for the preparation of hydrogel MNs (Yang et al., 2012; Demir et al., 2013). Since each material has different chemical and physical properties, they require different preparation and application procedures. The biocompatibility of materials used is an important factor in MN fabrication as they should not cause any harm to the underlying viable tissues after SC penetration. For instance, allergy-causing substances such as nickel should be avoided in the preparation of MNs (Larrañeta et al., 2016).

The height of MNs is essential to create microconduits across the skin and achieve the desired drug flux. Generally, MNs are fabricated within a length of 100−1000 μm for complete SC permeation (Prausnitz, 2017). An increase in MN height facilitates diffusion of the drug into the dermal microcirculation by shortening the diffusion path. Donnelly et al. (2010) reported that a significant increase in the depth of MN penetration was achieved by increasing MN length from 350 to 600 and 900 μm at a constant application force of 11.0 N per array. Furthermore, Zhu et al. (2017) designed a solid polylactic acid (PLA) MNs aligned with rapidly dissolving drug loaded MNs at the tip and investigated the effect of MN length on drug insertion. They found that deeper penetration, complete insertion, and

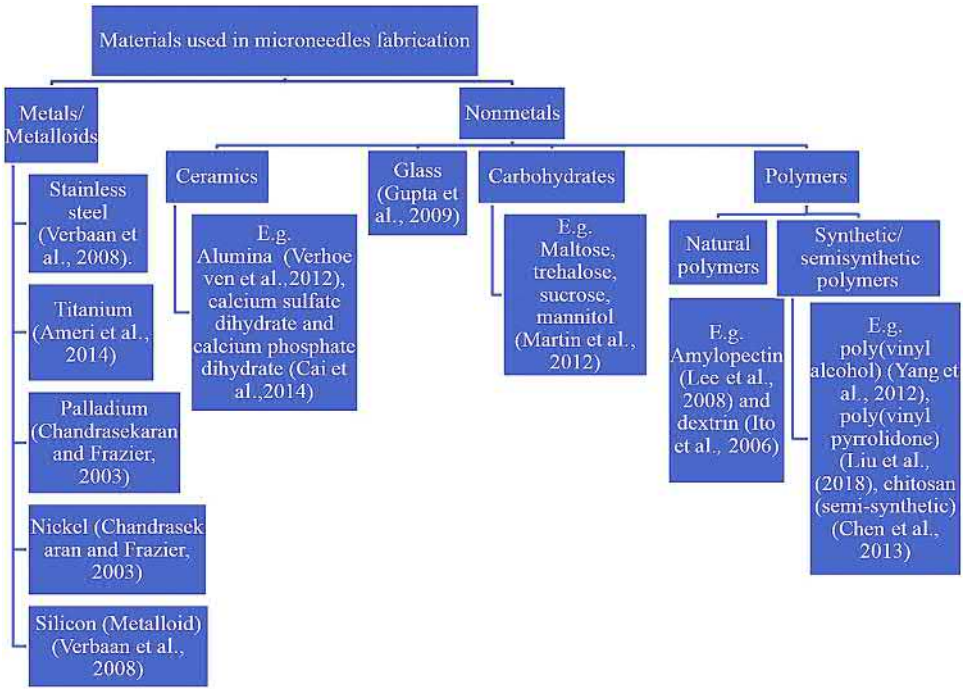
Materials used in microneedles fabrication
Metals/ Metalloids
Nonmetals
Stainless steel (Verbaan et al., 2008).
Titanium (Ameri et al., 2014)
Palladium (Chandrasekaran and Frazier, 2003)
Nickel (Chandrasekaran and Frazier, 2003)
Silicon (Metalloid) (Verbaan et al., 2008)
Ceramics
E.g. Alumina (Verhoeven et al.,2012), calcium sulfate dihydrate and calcium phosphate dihydrate (Cai et al.,2014)
Glass (Gupta et al., 2009)
Carbohydrates
E.g. Maltose, trehalose, sucrose, mannitol (Martin et al., 2012)
Polymers
Natural polymers
E.g. Amylopectin (Lee et al., 2008) and dextrin (Ito et al., 2006)
Synthetic/ semisynthetic polymers
E.g. poly(vinyl alcohol) (Yang et al., 2012), poly(vinyl pyrrolidone) (Liu et al., (2018), chitosan (semi-synthetic) (Chen et al., 2013)

FIGURE 14.2 Materials used for the preparation of MNs. *MN*, Microneedle.

effective drug delivery can be achieved by solid MNs with a length of 500 and 600 μm. PLA MNs with 400 μm in length deliver drugs up to just 80%, meanwhile, more than 95% drug delivery efficiency can be attained with 500- and 600-μm-long MNs. This is because shorter MNs (400 μm) are unable to completely implant the loaded drug due to the elastic deformation of the skin resulting in the incomplete dissolution of the drug (Fig. 14.3).

However, longer MNs cause more pain during administration. Gill et al. (2008) reported that a threefold increase in MN length increased the pain score by sevenfold. This is due to greater contact between the longer MNs and the nerve endings in the deeper layers of the dermis. (Yan et al., 2010). Thus, the skin's viscoelastic property and the possibility of pain stimulation should be considered when determining the length in MN design.

Wider base and smaller aspect ratios result in a better mechanical strength and higher fracture force for the MNs. These properties prevent the needle body from breaking or bending due to the action of lateral forces from the skin tissues during application. Usually, MN base width is within 50−300 μm and aspect ratios between 2:1 and 10:1 (Prausnitz, 2017). From a study by Gill et al. (2008), almost a threefold increase MN width did not have any significant effect on the pain scores. Davidson et al. (2008) studied the effect of MN design parameters on skin permeation using MN models in pyramidal, cylindrical, rectangular, conical, and arrowhead shapes each differing in tip dimensions and width (Fig. 14.4). From these studies, it can be concluded that longer, wider, and more densely packed MNs have better skin penetration property.

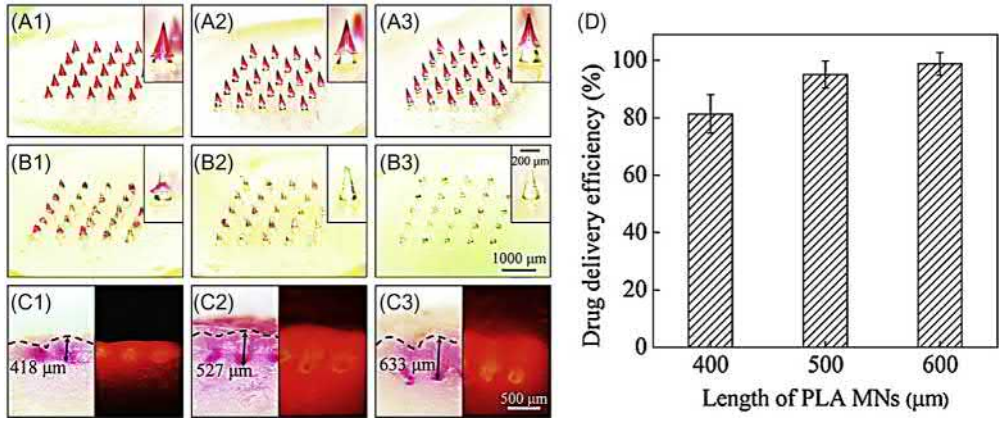

FIGURE 14.3 Images of MNs with the length of (A1) 400 mm, (A2) 500 mm, and (A3) 600 mm before (A1, A2, A3) and after insertion (B1, B2, B3). The drug penetration depth (C1, C2, C3) and delivery (D) increases with MN height. *MN*, Microneedle. Source: *Adapted with permission from Elsevier (Zhu, D.D., Chen, B.Z., He, M.C., Guo, X.D., 2017. Structural optimization of rapidly separating microneedles for efficient drug delivery. J. Ind. Eng. Chem. 51, 178–184).*

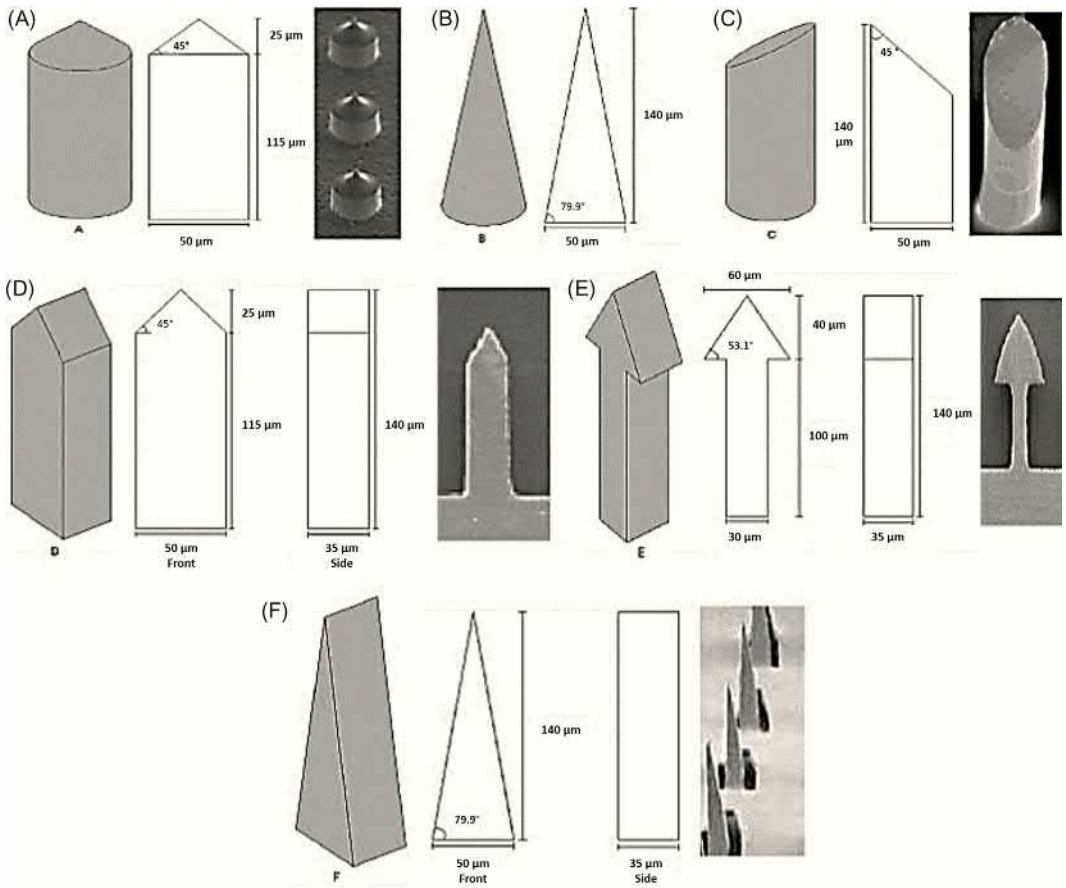

FIGURE 14.4 Various designs of MN model. *MN*, Microneedle. Source: *Adapted with permission from Elsevier (Davidson, A., Al-Qallaf, B., Das, D.B., 2008. Transdermal drug delivery by coated microneedles: geometry effects on effective skin thickness and drug permeability. Chem. Eng. Res. Des. 86 (11), 1196–1206).*

The sharpness or diameter of MN tips also affects the permeability and drug delivery across SC. Römgens et al. (2014) demonstrated that MN with sharper tips penetrate into the skin smoothly. Meanwhile, a sudden decrease in force was recorded during the application of MN with larger tips. These results suggest that sharper MNs are more suitable for controlled penetration depth. In an in vitro study by Cheung et al. (2015), higher bovine serum albumin (BSA) permeation was recorded in the case of sharp MNs compared with flat MNs. An approximate concentration of 120 μg/mL was achieved when sharp MN was applied to the full-thickness porcine skin. However, only 80 μg/mL concentration of BSA was measured after flat MN treatment. The results show that the amount of BSA delivered via sharp MNs was approximately 40 μg/mL greater than flat MNs over 5 hours suggesting sharp MN as better candidates for rapid onset of delivery. For successful penetration, MNs tips are between 1 and 10 μm in diameter, in some cases even below 1 μm (Prausnitz, 2017).

The shape of MNs also should be optimized to reach desired penetration depth upon application and better adherence to the skin tissues. Loizidou et al. (2016) reported a significantly higher penetration depth into ex vivo porcine skin for square and triangular MN as compared with hexagonal MN. Despite better mechanical properties of hexagonal MN with more vertices, sharper edges of triangular and square MNs were associated with enhanced SC penetration. In another study by Seong et al. (2017), bullet-shaped MNs with swellable tips provide better adhesion to the skin by distal swelling after insertion compared to cone-shaped MNs with the same base diameter (250 μm), height (750 μm), and polymer composition. They found that the bullet-shaped MNs showed significantly greater maximum adhesion strength on rat skin with an epidermal layer thickness of 20 μm compared with cone-shaped MNs (Fig. 14.5). This is an important aspect to prevent the extravasation of polymer MNs due to swelling and action of lateral forces from the skin during sustainable drug delivery for a long period.

Besides, designing MNs in the form of an array with higher needle density provides a larger surface area for transdermal drug delivery. With a large number of needles, the amount of drug loaded in coated and dissolving MN can be higher and greater volume of fluid can be obtained by swellable MNs. However, increasing the number of MNs in a patch with the fixed base area will shorten the center-to-center spacing between MNs. Data obtained by Zhang et al. (2018) explains that the maximal height difference of skin surface and stress applied on skin increase with increasing MN spacing. In other words, the shorter MN spacing causes smaller maximal height difference of skin surface leading to lower maximal stress for skin deformation. MN arrays with 20-μm interneedle spacing only produce stress at about 3.75×10^6 Pa but 7.5×10^6 Pa was recorded with 80-μm interneedle spacing (Fig. 14.6A). Fig. 14.6B shows that the relative height of the skin surface between two MN decreases with interneedle spacing. This condition results in a poor penetration due to "bed-of-nails" effect, whereby, the insufficient pressure is exerted by individual MN on the skin because the applied insertion force is dispensed among too many MNs. This effect can be prevented by applying greater force and designing sharper tips for patches with high needle density. At the same time, increasing MN number causes more stimulation to sensory nerves and increases the pain during application. A 10-fold increase in the MN quantity elevated the pain score just over two-fold (Gill et al., 2008).

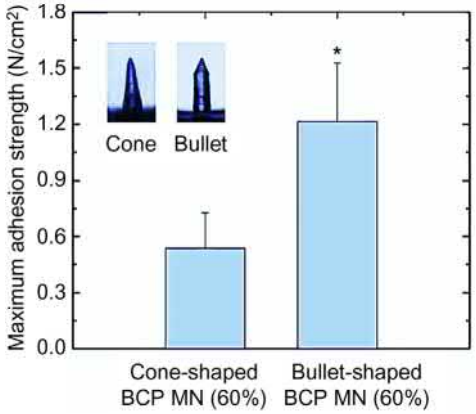

FIGURE 14.5 Comparison of maximum adhesion strength of cone-shaped and bullet-shaped MNs. Bullet-shaped MNs showed a significantly greater maximum adhesion strength (N/cm^3) compared with cone-shaped MNs. *MN*, Microneedle. Source: *Adapted with permission from Elsevier (Seong, K.Y., Seo, M.S., Hwang, D.Y., O'Cearbhaill, E.D., Sreenan, S., Karp, J.M., et al., 2017. A self-adherent, bullet-shaped microneedle patch for controlled transdermal delivery of insulin. J. Controlled Release 265, 48–56).*

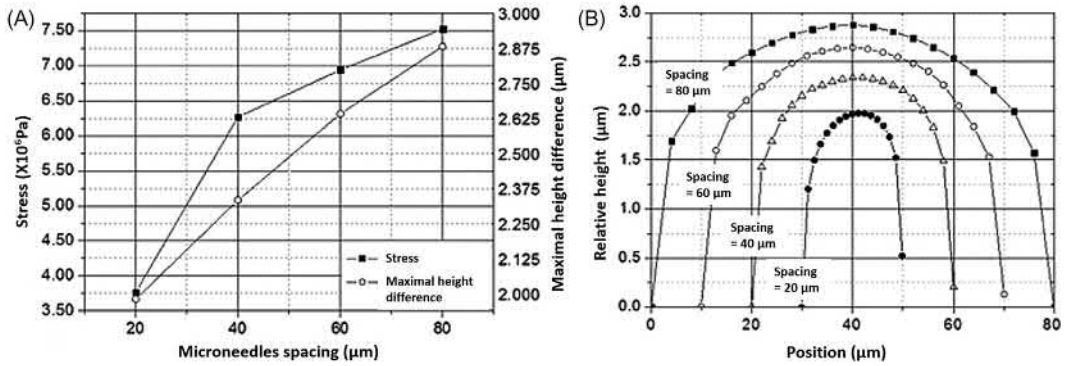

FIGURE 14.6 The effect of MNs spacing on the (A) skin's maximal height difference, stress applied to the skin and (B) relative height of the skin surface. An increase in MN spacing results in greater maximal height difference, the stress exerted on the skin, and relative height difference of skin between the MNs. *MN*, Microneedle. Source: *Adapted with permission from Springer Nature (Zhang, Y.H., Campbell, S.A., Karthikeyan, S., 2018. Finite element analysis of hollow out-of-plane HfO 2 microneedles for transdermal drug delivery applications. Biomed. Microdevices 20 (1), 19).*

Area of MN patch is often within a range of 1–10 cm^2. For convenience in handling and to provide a better adhesion to the skin, the size of the MN patch is generally larger than the MN array. However, the application and penetration will be less effective if the area of the MN patch is too large as the patch tends to deform and become nonplanar (Prausnitz, 2017). To sum up, in designing the MN the parameters mentioned previously need to be optimized for convenient administration and better performance. It is clear that these factors cannot be standardized for all MNs as different types of MNs work in a

different manner to deliver various types of drugs across the skin with heterogeneous properties. Therefore more studies need to be done to investigate the effects of MN application on subjects with different background and age groups.

14.4 CHALLENGES IN MICRONEEDLE-MEDIATED PROTEIN DRUG DELIVERY

14.4.1 Skin Barrier

The skin comprises of three primary layers: superficial epidermis, dermis, and hypodermis. The epidermis (50–200 μm in thickness) is composed of four sublayers: stratum spinosum, stratum basale, stratum granulosum, and SC. The dermal layer is composed of a thin papillary region and thick reticular region. The papillary region consists of loose connective tissue and dense blood capillaries, meanwhile, the reticular dermis consists of thicker blood and lymphatic vessels and connective tissues to provide support to the skin. The hypodermis mainly comprises fat tissues to provide insulation to the body (Fig. 14.7) (Van der Maaden et al., 2012; Zaidi and Lanigan, 2010).

SC with a thickness of about 15–20 μm is a poorly hydrated (10%–20% hydration) cell layer (Bensona and Watkinson, 2012). The corneocytes in SC are composed of cross-linked keratin fibers and held together by corneodesmosomes. The rigid brick and mortar structure of SC prevents most foreign substances from passing across it. Large molecules have lower permeability compared with small molecules (<75–100 Da), which seem to penetrate the barriers rapidly (Cleland and Langer, 1994). A molecule is able to diffuse into

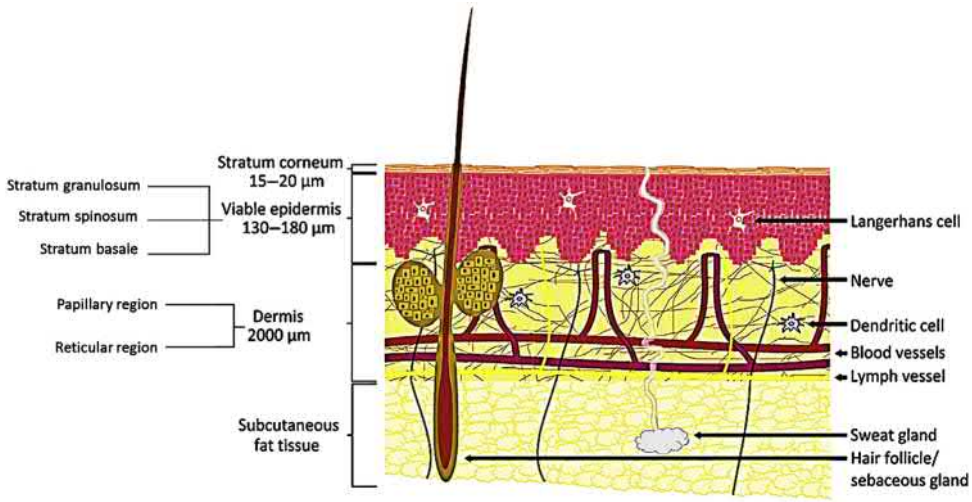

FIGURE 14.7 Representation of skin anatomy. Source: *Adapted with permission from Elsevier (Van der Maaden, K., Jiskoot, W., Bouwstra, J., 2012. Microneedle technologies for (trans) dermal drug and vaccine delivery. J. Controlled Release 161 (2), 645–655).*

blood circulation if it successfully transverses the SC. However, this diffusion process is limited by factors such as MW, concentration gradient, charge, partition coefficient, and solubility (Ita, 2014).

Proteins and only a few compounds with MW less than 500 Da can permeate the skin in sufficient quantities to produce therapeutic effects (Ita, 2014). This limitation is the major challenge for therapeutic macromolecular proteins with size exceeding 500 Da. Even though mechanical perturbation such as MN treatment enables the protein drug to pass across the SC layer, the bioavailability of the drug is limited by its capacity to diffuse into blood circulation. Moreover, the presence of acid−base side chains in proteins, which makes them polar/hydrophilic ($\log P$ values <0), further challenges the transport of proteins via a paracellular route across the epithelial cells (Frokjaer and Otzen, 2005).

14.4.2 Limitations of Existing Microneedle Treatment

Each type of MN has its limitations in terms of the delivery of protein drugs. In solid MNs, the expensive cost for the fabrication of metal-based MN and two-step application process is inconvenient for patients. These drawbacks can be overcome by using coated MNs. Nevertheless, in coated MNs the drug loading amount is very limited since the drug can only be applied onto the surface or tips of coated MNs. Potential biohazard due to the incautious disposal of sharp waste makes the solid and coated MN less preferable (Jacoby et al., 2015). If hollow MNs are broken in the skin, significant leakage or uncontrolled drug dose release may occur (Hong et al., 2014).

In dissolving MNs, the accumulation of polymeric residues following repeated applications may cause toxic effects in the body, thus limiting their application for repeated prophylactic treatment (Kim et al., 2012). The disadvantages from previous MN types can be overcome with hydrogel-forming MNs. Once applied to the skin, hydrogel MNs can be withdrawn intact from the tissue, leaving no polymeric residues behind, thus, increasing the patients' compliance compared with dissolving MN (Ita, 2015). Furthermore, they lose their structural integrity within several minutes after application, which makes them soft and thus they cannot be reused. This property hinders transmission of diseases between patients by preventing sharing of needles. Unlike hollow MNs, the needle tips swell in the skin to produce continuous conduits from adhesive drug reservoirs to the microcirculation in the dermis, enabling sustained transdermal drug administration (Hong et al., 2014). For example, PVA MNs do not dissolve in the skin but swell, opening diffusion channels to enable drug release (Yang et al., 2012).

Previous studies reported that MN treatment combined with permeation enhancers such as sonophoresis and iontophoresis markedly enhanced transdermal delivery of model proteins and peptides such as BSA, insulin, daniplestim, and leuprolide (Donnelly et al., 2014a; Katikaneni et al., 2009; Donnelly et al., 2010; Han and Das, 2013; Chen et al., 2010; Sachdeva et al., 2013). The mechanical perturbation of the skin barrier by MNs followed by application of physiologically acceptable electric current by iontophoresis drives the drug across the skin by electrorepulsion or electroosmosis (Guy et al., 2000).

Meanwhile, in sonophoresis, the low-frequency ultrasound waves create acoustic cavitation on the skin, which increases skin permeability toward the drug (Tang et al., 2002).

Chen et al. (2010) devised a Franz cell setup with hollow MN and low-frequency ultrasonic emitting ceramic membrane (lead zirconate titanate or PZT) and evaluated their synergistic effect on drug delivery. MNs were applied to poke the SC layer to create microfluidic pathways for drug transport; meanwhile, the ultrasonic energy from PZT creates acoustic cavitation on the skin, which further enhances the drug diffusion by increasing the depth and space for diffusion (Fig. 14.8).

However, it is expected that a combination of these techniques may result in more expensive manufacturing and treatment cost, and reduce patient compliance due to the added complexity in administration. In addition, skin irritation and pain limit the current applied and delivery rate because the effect of iontophoresis goes beyond SC (Prausnitz, 1996). Denaturation of proteins may occur when too much heat is produced in prolonged or uncontrolled iontophoresis and sonophoresis (Jani et al., 2012). Currently, there are no MN drug delivery devices in the market (Donnelly, 2017). Even with the latest technology 100% success of transdermal protein drug delivery via MN still cannot be achieved to replace parenteral administration.

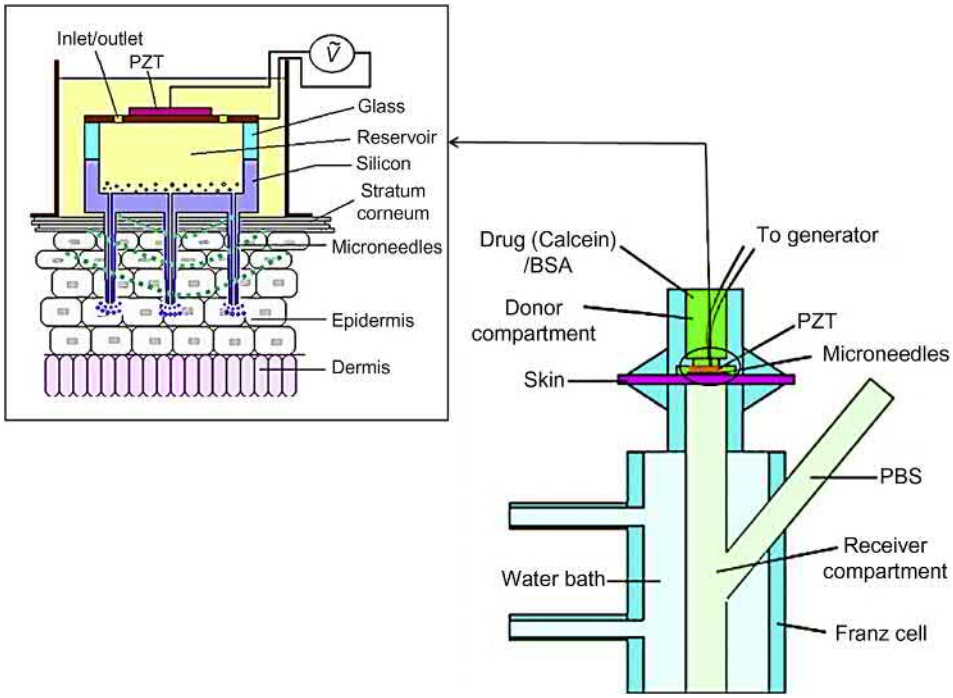

FIGURE 14.8 Illustration of the in vitro study on sonophoresis enhanced hollow MN-mediated drug delivery across the skin in Franz cell setup. Commercially available PZT ceramic membrane was used to emit ultrasound. *MN*, Microneedle; *PZT*, lead zirconate titanate. Source: *Adapted with permission from Elsevier (Chen, B., Wei, J., Iliescu, C., 2010. Sonophoretic enhanced microneedles array (SEMA)—improving the efficiency of transdermal drug delivery. Sens. Actuators, B: Chem. 145 (1), 54–60).*

14.4.3 Physicochemical Instabilities of Protein Drugs

In nature, proteins are prone to chemical and physical degradation in aqueous environments or organic solvents by several pathways depending on their type and property (Brown, 2005). Physical degradation involves changes in three-dimensional conformation by noncovalent aggregation and denaturation or precipitation. Meanwhile, chemical degradation refers to the covalent alteration of the primary protein structure by bond deformation or cleavage due to deamination, oxidation, and Maillard reaction (Werle and Bernkop-Schnürch, 2006).

Deamination is the formation of a free carboxylic acid due to hydrolysis of the side chain of an amino acid residue (Vyas and Khar, 2004). A nonenzymatic intramolecular deamination reaction in asparagine residues is one of the common deamination reactions that occur to proteins in drug formulations. Deamination has been mentioned in proteins such as human growth hormone, recombinant human interleukin (IL)-1 receptor antagonists, and recombinant bovine somatotropin (Lai and Topp, 1999).

Second, Maillard reaction is a series of complex of reactions that occur between amino acids/peptides and reducing sugars influenced by factors such as pH and temperature. In a stability study by Hamburger et al. (1975), glucose (excipient) in a lyophilized formulation of recombinant human relaxin led to formation of covalent adducts of glucose with amino groups on the side chains of the protein and using sugar (trehalose), or a polyhydric alcohol (mannitol) as an alternative improved the stability of relaxin.

Third, the oxidation reaction may occur if the proteins are exposed to unfavorable temperature, pH, or trace amount of metal ion and buffers at different phases of production, packaging, and storage (Maibach, 2017; Vyas and Khar, 2004). For instance, the presence of peroxide contaminant in formulation excipients such as polyethylene glycol (PEG) and surfactants results in oxidation of pharmaceutical products. Significant iron contamination may be caused by processing in stainless steel apparatus or presence of transition metal ions in excipients, which in turn leads to degradative oxidation of protein drugs. Even a low amount of oxygen (1%) in packaging leads to complete oxidation of certain proteins (Chang and Pikal, 2009). For example, aggregation and oxidation were found as the main pathway of chemical degradation in the development of PTH MNs for transdermal delivery. This issue was overcome by addition of excipient (0.03% ethylenediaminetetraacetic acid) to the drug formulation and optimization of package condition (Ameri et al., 2009).

Besides, the physical alteration may also result in loss of therapeutic effect and potency in protein drugs. Several processes such as precipitation, aggregation, denaturation, and adsorption to surfaces that may occur during manufacturing, storage, shipping, and administration cause physical degradation. Aggregation is considered the main issue with protein drugs (Lai and Topp, 1999; Ameri et al., 2009). Aggregation occurs when a denatured, unfolded protein rearranges to form hydrophobic amino acid residues or soluble oligomers or higher-molecular-weight precipitates (Vyas and Khar, 2004; Capelle et al., 2007). High temperature and protein concentration, shear stress, and changes in pH lead to aggregation result in low drug stability, shelf life, and negative

effects in drug potency, pharmacokinetics, and immunogenicity (Weiss et al., 2009; Lahiji et al., 2018a,b). Recently, Lahiji et al. (2018a,b) reported that optimization of the physicochemical conditions such as pH, temperature, and polymer–drug interaction in the MN formulation maintains the activity of encapsulated protein drug, Exendin-4 (used for the glycemic control in type 2 diabetic patients) up to 98.3% ± 1.5%.

14.4.4 Immunogenicity After Treatment

Most therapeutic proteins, even those having only human sequences, may induce immunogens such as neutralizing antibodies during administration in some patients (Dasgupta et al., 2008; Gouw et al., 2012). Generation of neutralizing antibody leads to rapid clearance or modified tissue distribution of the protein drug, which greatly reduces or negates its therapeutic effect toward the patient (Frokjaer and Otzen, 2005). For instance, almost 30% of severe hemophilia A patients undergoing replacement therapy with procoagulant factor VIII develop inhibitor and higher risk of severe hemorrhages (Gouw et al., 2012). This leads to low half-life and requires frequent administrations, which results in higher treatment costs (Werle and Bernkop-Schnürch, 2006). Therefore the efficacy of immunogenicity inducing protein therapeutics in patients should be determined in MN-mediated drug delivery in early clinical trials.

14.5 ADVANCES IN MICRONEEDLE TECHNOLOGY IN PROTEIN DELIVERY

Although MN was first patented by Gerstel et al. (1976), its application in transdermal drug delivery only began when MN arrays were fabricated using ion etching technique by Henry et al. (1998). A micromachining system was used to prepare the first MN from silicon. Since then, many novel microfabrication and drug loading technologies have been developed to widen the potential of this approach. Presently, MNs can be categorized into five types: solid MNs, coated MNs, hollow MNs, dissolving MNs, and swellable MNs. Each type of MN works using a different approach to transdermal drug delivery as shown in Fig. 14.9.

Solid MNs are used to poke the skin followed by removal of the MNs and application of the drug in the area (Fig. 14.9A). In coated MNs, the drug will be coated on the MNs and released upon insertion into skin followed by removal of MNs. The drug will be left remain under the skin to be absorbed into circulation (Fig. 14.9B). In hollow MNs, the drug formulation is channeled into the dermis through the bores in the MNs (Fig. 14.9C). Dissolving MNs are made up of biocompatible polymer formulations that encapsulate drugs within their matrix. After the insertion, the MNs dissolve in interstitial fluid and release the loaded drugs along with copresenting polymer leaving the drug-free baseplate (Fig. 14.9D). Hydrogel MNs are composed of biocompatible polymers that are cross-linked to prevent their dissolution in the skin. When applied, these MNs swell and

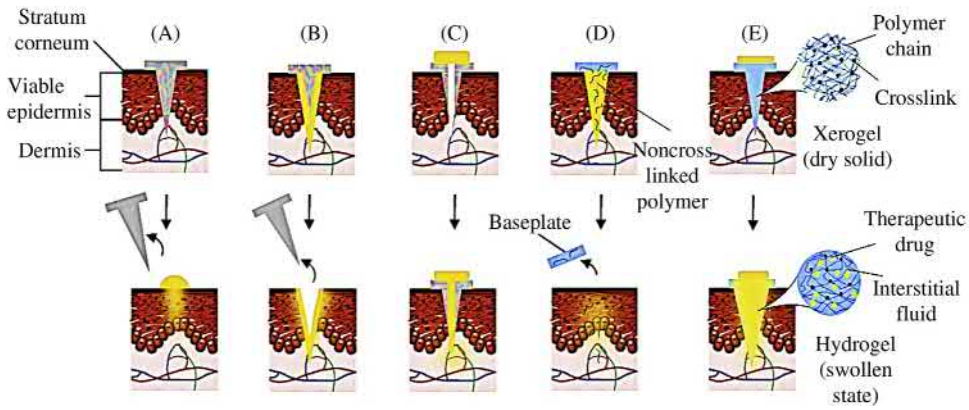

FIGURE 14.9 Drug (marked in yellow) delivery process with (A) *solid*, (B) *coated*, (C) *hollow*, (D) *dissolving*, and (E) *hydrogel* MNs. *MN*, Microneedle.

provide a continuous conduit for the drug to diffuse through interstitial space between cross-linked polymer networks and eventually enter into the skin (Fig. 14.9E).

14.5.1 Solid Microneedles Technology

Solid MNs work by "poke and patch" manner, where the rigid MNs are used to create microscale pores in the skin. Following the removal of solid MNs, the perforated area on the skin allows greater accessibility for the administered drugs (Fig. 14.9A). Results obtained from an in vitro study on the permeation of four model peptides with different MWs shows that peptide permeation was significantly enhanced by MN pretreatment but limited by the MW of the peptides. A good correlation between vehicle (deuterium oxide) flux and model peptide clearance proposes that MNs increase skin permeability of hydrophilic drugs by promoting convective flow (Zhang et al., 2014).

Li et al. (2017) fabricated a biodegradable solid MN array from PLA and investigated the effect of MN pretreatment in insulin permeation. Their in vivo study results show a remarkable decrease in glucose level in diabetic mice treated with PLA MNs but no significant difference in glucose level was recorded among a group where insulin was only applied on skin without any MN pretreatment. This data proves that the microchannels produced by solid MNs improve the drug permeation via the transdermal route. Furthermore, MN-mediated transdermal insulin delivery shows a gradual decrease in glucose level and maintains the level of glucose at approximately 29% lower from initial value over 5 hours unlike in SCT administration where a rapid drop of glucose level was recorded at initial 1.5 hours followed by a gradual increase to 100% after 1.5 hours. This is because the bulk release of systemically injected insulin will be rapidly cleared by the bloodstream. Therefore the sustainable release of insulin facilitated by solid MNs maintains an effective level of drug in the system for a prolonged duration.

14.5.2 Coated Microneedles Technology

In coated MNs, the drug is coated on the surface of the MN and released upon application as in the Macroflux MN patch consisting of thin titanium microprojection arrays with a polymeric adhesive back (Fig. 14.9B). The types of Macroflux MNs currently under development are Dry-Coated Macroflux: where drug or vaccine-coated MNs attached to a polymeric adhesive backing for bolus or short duration administration, D-TRANS Macroflux microarray: joined with a drug reservoir for prolonged passive delivery and E-TRANS Macroflux microarray: with an electron-transport system for pulsatile or on-demand delivery. For better drug incorporation and transport, the drug formulation is only coated on the tips of microprojections (Gupta and Sharma, 2014).

Shakya et al. (2017) reported a minimally invasive cutaneous immunotherapy by delivering ovalbumin via coated MN for the management of ovalbumin-induced airway allergy in mice. They coated a formulation containing CMC (viscosity enhancer), Lutrol F-68 NF (surfactant), and ovalbumin (model antigen) on MN arrays made from stainless steel. In vivo treatment with ovalbumin and CpG oligonucleotide (MNs-CIT) coated MNs modulated antiinflammatory cytokines IL-10 and Type 2 T helper cells (Th2) cytokines (IL-4, IL-5, and IL-13) in the bronchoalveolar fluid, interferon gamma and IL-2 and cytokines in restimulated splenocyte cultures. The MNs-CIT induced specific systemic immune response was similar to SCT delivery of ovalbumin via a hypodermic needle. This promising result suggests that cutaneous vaccination via coated MN can serve as an alternative to sublingual or SCT immunotherapy.

In a recent study, Caudill et al. (2018) used continuous liquid interface production (CLIP) technique to control the loading and spatial deposition of coated model proteins on MNs. They found that the CLIP method maintains the activity of lysozyme throughout the coating process and enables rapid transport of coated protein cargo into the porcine skin. In vivo results from the study showed that protein-coated CLIP MNs had better-sustained retention of BSA for 72 hours as compared with the SCT-treated mice (Fig. 14.10) suggesting coated MNs as useful delivery tools for treatment that requires sustainable drug release profile.

14.5.3 Hollow Microneedles Technology

Hollow MNs are like regular hypodermic needles but only a few micrometers in length. The drug formulation is channeled through bores in the MN (Fig. 14.9C). Compared with solid or coated MNs, pressure assisted injection enables hollow MN to have better regulation on drug quantity and timing, thus providing various types of drug delivery profiles (Kim et al., 2012). Designing a sideways opening at the tip of the MN prevents the clogging problem inside hollow MNs, maintains tip sharpness, and increases the area of drug exposure to the tissue (Griss and Stemme, 2003).

Du et al. (2018) investigated the intradermal delivery of nanoparticulated vaccines using hollow MNs to regulate the immune response of protein antigen (ovalbumin). Ovalbumin and polyinosinic:polycytidylic acid [poly(I:C)] (adjuvant) were loaded in different classes of NPs and delivered into the murine skin via hollow MNs. An applicator was used to control

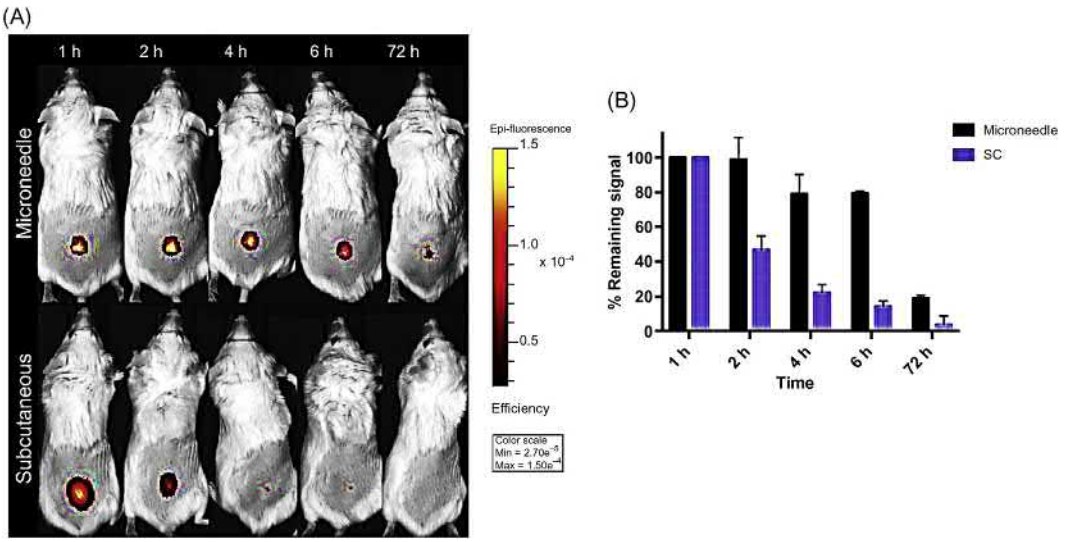

FIGURE 14.10 (A) Lumina in vivo imaging of in vivo delivery of BSA at 1, 2, 4, 6, and 72 h following AF680-BSA-coated MNs treatment (top) and SCT AF680-BSA injection (bottom). (B) BSA remains for a longer period in the coated MN treated rats compared with SCT treatment. *BSA*, Bovine serum albumin; *MN*, microneedle; *SCT*, subcutaneous. Source: *Adapted with permission from Elsevier (Caudill, C.L., Perry, J.L., Tian, S., Luft, J.C., DeSimone, J. M., 2018. Spatially controlled coating of continuous liquid Interface production microneedles for transdermal protein delivery. J. Controlled Release 284, 122–132).*

the depth of MN insertion for about 120 μm. High immunoglobulin G (IgG), IgG1, and IgG2a antibody titers were measured in murine treated with ovalbumin/poly(I:C)-loaded NPs. Moreover, ovalbumin/poly(I:C)-loaded liposomes induced the highest CD8 + and CD4 + T cell responses. To sum up, hollow MN delivery of nanoencapsulated vaccines in a precisely controlled depth produces detectable humoral and cellular immune responses.

Even low-dose influenza vaccine administration with hollow silicon MNs resulted in immunogenic responses similar to the full-dose IM vaccination (Van Damme et al., 2009). Several clinical trials by NanoPass Technologies Ltd. have validated the effectiveness, safety, and minimally invasiveness of intradermal delivery of insulin, local anesthetics, and influenza vaccine by MicronJet technology (Maibach, 2017).

Moreover, Van der Maaden et al. (2018) investigated the efficacy of a digitally controlled hollow MN injection system in the intradermal administration of a synthetic peptide derived from human papillomavirus, which was used as a therapeutic cancer vaccine. The main features of the digitally monitored microinjection system (DC-hMN-iSystem) are micrometer actuator, applicator controller unit, and a syringe pump to control the depth of microinjection. This system had delivery accuracy between 90% and 95% for 1–10 μL, and for volumes of 0.5 and 0.25 μL had a lower accuracy of 86% and 74%. In mice, this DC-hMN-iSystem induced remarkable functional cytotoxic and Th immune responses with therapeutically lower volumes of cancer vaccine compared with standard intradermal

immunization. Therefore this automated system is capable of delivering an accurate and low volume of vaccine that produces desired immune response in the mouse. Unlike traditional hypodermic injection, the depth of MN penetration in DC-hMN-iSystem can be controlled to provide minimally invasive cancer vaccination.

14.5.4 Dissolving Microneedles Technology

In dissolving MNs, the drug is encapsulated within the needle formulation itself, which will be fabricated into MNs. After insertion, the MNs dissolve in interstitial fluid and release the loaded drugs into the skin (Fig. 14.9D). In some studies, detachable support device was developed to insert the dissolving MN without baseplates, which enables complete penetration of MNs and improves the bioavailability of drug (Chu and Prausnitz, 2011; Lahiji et al., 2015; Chen et al., 2013). Results from these studies show that dissolving MNs are suitable vehicle candidates for rapid and bulk delivery of protein drugs, especially for on-demand therapy.

Furthermore, solid MN (DermaRoller) pretreatment, increasing the concentration of protein, MN length and quantity significantly improves the delivery of IgG-mediated by maltose MN across rat skin in vitro (Li et al., 2009, 2010). Liu et al. (2018) conducted an in vivo pharmacodynamic study using dissolving MNs prepared from insulin-loaded $CaCO_3$ MPs (INS-$CaCO_3$ MPs) and poly(vinyl pyrrolidone) (PVP) to determine the viability of the insulin-loaded dissolving MN treatment on diabetic rats in glucose regulation. The relative bioavailability and pharmacological availability of loaded insulin in MNs were very high (96.6% and 98.2% accordingly). This result proves that a sustainable and therapeutically effective insulin delivery is feasible with INS-$CaCO_3$/PVP MNs.

Although many methods have been developed for the fabrication of dissolving MNs, the selection of appropriate method and optimization of the procedures is crucial to preserve the stability and activity of encapsulated active pharmaceutical ingredients such as protein drugs. Lahiji et al. (2018a,b) evaluated the effects of concentration and type of polymer, preparation and storage temperature, and drying conditions on the activity of lysozyme (model protein) loaded in the dissolving MN. They reported that lower fabrication temperature (preferably at 4°C), natural drying process, specific polymer concentration, and presence of stabilizing agents such as trehalose help to preserve the activity of encapsulated lysozyme up to 99.8% ± 3.8% for 12 weeks.

Similarly, Mistilis et al. (2017) found that influenza vaccine in an optimized dissolving MN formulation containing arginine/heptagluconate did not show any significant loss of activity after exposure at 60°C up to four months, multiple freeze–thaw cycles, and electron beam. This finding further highlights the importance of optimal formulation in maintaining the drug's stability on the shelf. In addition, Huh et al. (2018) compared the effects of different fabrication methods [droplet-born air blowing (DAB) and centrifugal lithography (CL)] on the activity of epidermal growth factor (model protein) and ascorbic acid. The immunoreactivity of epidermal growth factor in CL and DAB decreased to 75.32% ± 19.40% and 41.75% ± 16.17% from a baseline value of 92.08% ± 2.86% and 80.67% ± 8.00%

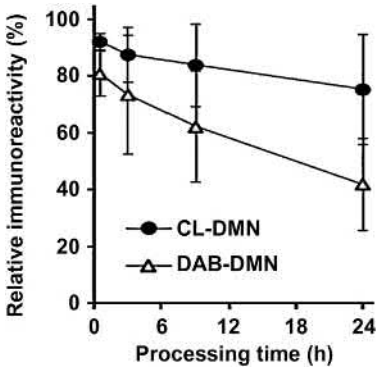

FIGURE 14.11 Immunoreactivity of epidermal growth factor after fabricated by DAB and CL methods into dissolving MNs. The initial activities of 92.08% ± 2.86% (in CL) and 80.67% ± 8.00% (in DAB) were decreased to 75.32% ± 19.40% and 41.75% ± 16.17%, respectively after 24 h incubation. *CL*, Centrifugal lithography; *DAB*, droplet-born air blowing; *MN*, microneedle. Source: *Adapted with permission from Elsevier (Huh, I., Kim, S., Yang, H., Jang, M., Kang, G., Jung, H., 2018. Effects of two droplet-based dissolving microneedle manufacturing methods on the activity of encapsulated epidermal growth factor and ascorbic acid. Eur. J. Pharm. Sci. 114, 285–292).*

accordingly after 24 hours. The study concluded that CL as a better method to minimize the activity loss of biological drugs as it exerts relatively lower temperature and drying stress during production (Fig. 14.11).

14.5.5 Hydrogel/Swellable Microneedles Technology

Hydrogels are polymeric networks composed of homopolymers or copolymers, insoluble due to the presence of chemical or physical cross-links. Their thermodynamic compatibility with water allows them to imbibe a large quantity of biological fluid and swell in aqueous media. Hydrogels are used to prepare contact lenses, biosensors membranes, artificial skins, and drug delivery devices such as MNs (Peppas et al., 2000). Hydrogel MN is easy to self-administer and nonreusable as it loses its structural integrity after one-time use. Recently, hydrogel MNs have been studied extensively for their ability to deliver high and low MW drugs, biotherapeutics, vaccines, and administration of body fluids (Hong et al., 2014).

Hydrogel MN arrays consist of MNs made of a swelling material composed of polymers with a drug reservoir attached externally to the baseplate (Fig. 14.9E). The polymers used to prepare hydrogel MNs should have notable biocompatibility, nontoxicity, degradability and generally approved by FDA (Park et al., 2006). For example, cross-linked polymethyl vinyl ether/maleic anhydride-PEG 10,000 and PVA, dextran, and CMC were produced as hydrogel/swelling MNs (Donnelly et al., 2012; Yang et al., 2012). These MNs are easy to fabricate, cost effective, and suitable for mass production (Tuan-Mahmood et al., 2013).

TABLE 14.1 Factors Affecting Transdermal Drug Delivery in Hydrogel Microneedles (MNs)

Factor	Preparation Strategies	References
Polymer content	The permeability of solutes is higher in the hydrogel with lower PMVE/MA content	Raj Singh et al. (2010)
MW of cross-linking agent	Polymers cross-linked with high-MW PEG (PEG 10,000) have better swelling ability favoring enhanced drug delivery	Garland et al. (2011)
The concentration of cross-linking agent	Hydrogels made from a lower concentration of pentaerythritol tetra-acrylate provide larger space for drug delivery	Wong et al. (2015)
Stimuli-responsive conjugate	Hydrogel with light-responsive 3,5-dimethoxybenzene conjugate deliver ibuprofen under the optical trigger	Hardy et al. (2016)
Presence of foaming agent	A pore-forming agent such as $NaHCO_3$ and $NaCO_3$ was added to the hydrogel formulation for experiments involving high-MW molecules	Raj Singh et al. (2012)
Iontophoresis	The combination of hydrogel MN and iontophoresis treatment accelerated FITC-BSA transdermal delivery	Donnelly et al. (2012, 2014a)

BSA, Bovine serum albumin; *FITC*, fluorescein isothiocynate; *MW*, molecular weight; *PEG*, polyethylene glycol; *PMVE/MA*, polymethyl vinylether/maleic anhydride.

Hydrogel MN technology has been investigated to enhance transdermal delivery of a large variety of molecules such as small hydrophilic drugs (methylene blue, caffeine, metronidazole, and theophylline) and model protein drugs (insulin and BSA). This system was shown to enable sustained percutaneous transport of pharmaceutical compounds in vitro in the porcine skin and in vivo in Sprague Dawley rats (Donnelly et al., 2012). Optical coherence tomography imaging results confirmed that skin treated with hydrogel MN became accustomed to the expansion of hydrogel MN. The increase in the volume of swelling hydrogel MN does not result in the extravasation of the MN from the skin. Following MN removal, skin barrier function was restored within 24 hours as confirmed by transepidermal water loss measurement, regardless of the duration of the MN treatment or swelling volume. There were no adverse reactions reported by the volunteers besides minor erythema, which was resolved within 48 hours after patch removal (Donnelly et al., 2014b,c). The amount of drug delivered is correlated to the hydrogel swelling and external enhancers, which can be tailored by different preparation strategies as outlined in Table 14.1.

Seong et al. (2017) fabricated double-layered MN arrays with swellable needle tips and nonswellable patch, which are able to interlock in a rat's skin upon insertion resulting in a firm adhesion. 60% of the insulin-loaded in the MN patch was released over 12 hours in vitro and 70% of the insulin delivered had a stable conformation (Fig. 14.12). Improved adhesion property of the patch displayed a sustainable release of insulin from MN patches, resulting in a gradual reduction in blood glucose levels. This technique could be tailored for the delivery of other protein therapeutics requiring sustainable release kinetics.

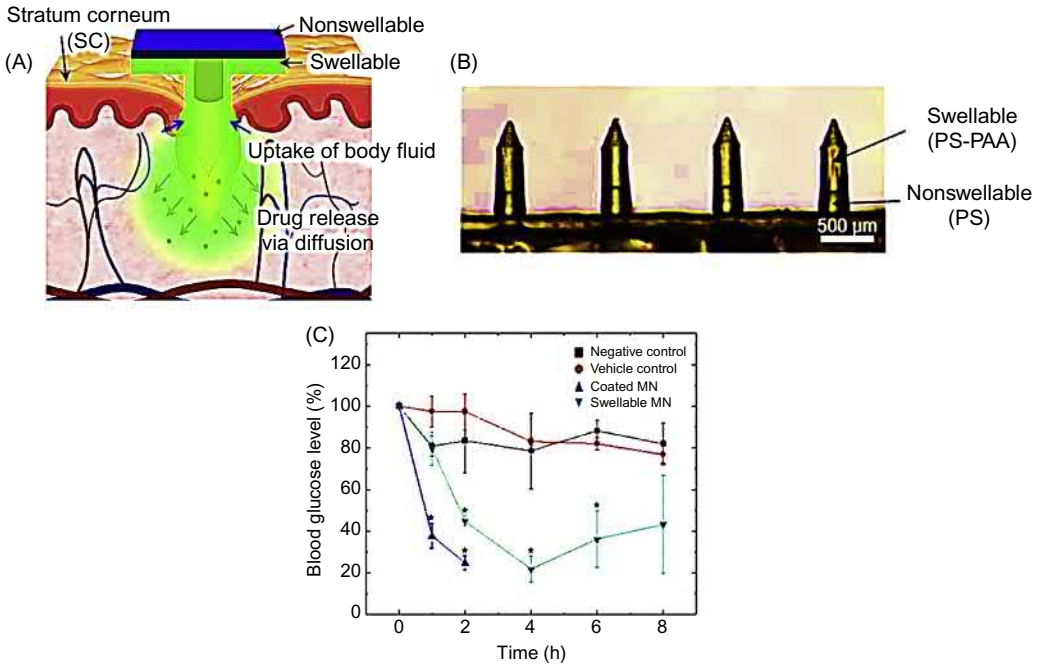

FIGURE 14.12 (A) The swelling behavior of fabricated double-layered MN arrays made of (B) swellable polymer tips and nonswellable base. (C) A gradual reduction in plasma glucose level was measured in vivo after transdermal application of MNs relative to normal mice. *MN*, Microneedle. Source: *Adapted with permission from Elsevier (Seong, K.Y., Seo, M.S., Hwang, D.Y., O'Cearbhaill, E.D., Sreenan, S., Karp, J.M., et al., 2017. A self-adherent, bullet-shaped microneedle patch for controlled transdermal delivery of insulin. J. Controlled Release 265, 48–56).*

Courtenay et al. (2018) studied the transdermal delivery of bevacizumab, a macromolecular (MW = 149,000 Da) anticancer drug with dissolving and hydrogel-forming MN. A dose-dependent increase in drug permeation was recorded in hydrogel MN-mediated drug delivery. They reported that higher antibody concentrations were delivered via hydrogel MN than dissolving MN aided by complete dissolution of antibody loaded patches that were observed in hydrogel MN. Conversely, almost 90% of antibody loaded in dissolving MN remained in the baseplate. Interestingly, the maximum concentration of bevacizumab in serum was achieved 24 hours after the hydrogel MN was removed from the system suggesting that controlled delivery via this system attributed to the ability of bevacizumab entering the microcirculation from the skin. This study shows that delivery of macromolecular proteins in high dose is possible via hydrogel MN but further optimization is necessary to achieve a clinically effective dose.

14.6 CURRENT STATUS OF PROTEIN AND PEPTIDE CONTAINING MICRONEEDLES IN CLINICAL TRIALS AND MARKETED MICRONEEDLE PRODUCTS

The global transdermal patch market currently approaches US$32 billion although it is based on only 20 drugs at present. According to Grand View Research, Inc. (2018), the worldwide transdermal drug delivery system market is forecasted to reach $81.4 billion by 2024. Lately, rising figures in the mechanical array and MN-based transdermal product launches by leading industry players represent the great growth potential of this industry. MN technology is expected to target not only the transdermal drug delivery but also global vaccine markets and global biologics market (Donnelly, 2017).

In the ClinicalTrial.gov database, there are 78 studies found for the keyword *microneedle* and 46 studies have been completed worldwide. The application of MNs in vaccine administration, particularly influenza vaccine, was studied the most, followed by diabetes, although generally, they are in early phase 1/2 stages. Overall, five studies have successfully completed phase 3 trial and two studies are in phase 4 trial. It is noteworthy that insulin is the only protein that has completed phase 3 clinical trial for MN-mediated delivery. It is estimated that the human insulin market will reach US$39.13 billion by 2020 (BusinessWire, 2016). Different types of MNs were assessed for their effectiveness in insulin delivery in clinical trials. These studies reported lower pain scores as compared with SCT administration and rapid onset pharmacokinetics (Bhatnagar et al., 2017). These convincing results further support the commercialization of MNs for patient-friendly insulin administration.

Zosano Pharma has completed phase 2 clinical trials for MN-assisted delivery of a 34−amino acid fragment of the PTH and also testing the delivery of another peptide hormone, glucagon with MN in phase 2 trials. Besides, Corium International (MicroCor) and Radius (Abaloparatide-TD) are also conducting phase 2 trials in MN-mediated PTH delivery (Zelikin et al., 2016). Intanza/IDflu is the first intradermal vaccine approved in European Union territory for the prevention of seasonal influenza. This trivalent inactivated vaccine was licensed by the European Medicines Agency for individuals aged 18 and above (Bragazzi et al., 2016).

Presently, there are no protein containing MN products in the market, but MN-based devices are commercially available for drug administration as listed in Table 14.2. The efficacy of these devices in protein and peptide drug delivery is being evaluated by their respective manufacturers. Companies such as LTS Lohmann Therapie-Systeme AG and Corium Inc. have now attained Good Manufacturing Practice licenses for MN patches. In the near future, there is a greater prospect for these companies to manufacture protein drug containing MN patches (Larrañeta et al., 2016; Donnelly, 2017; Richter-Johnson et al., 2018).

TABLE 14.2 Currently Marketed Microneedle (MN) Devices for Therapeutic Use

Product Type	Brand	Manufacturer	Features
Solid MN	Onvax	Becton Dickinson, United States	Consist of plastic microprojections of approximately 200 μm in length used as SC abrader for the delivery of vaccines (Laurent et al., 2010)
	AdminPen	AdminMed, United States	A pen injector device that allows injection of drugs in liquid formulation into the skin via micropores formed by AdminPatch MNs (Yuzhakov, 2010)
	MTS Roller	Clinical Resolution Laboratory Inc., United States	MN on the roller device pokes the skin to promote collagen production and increase skin's permeability toward therapeutics (Clinical Resolution Laboratory, Inc., 2015)
Coated MN	3M Solid Microstructured Transdermal System	3M	Wearable patch to deliver drugs formulations up to 300 μg. Improved stability of coated drug to exclude cold chain storage requirements (3M, 2018a,b)
	Macroflux	Zosano Pharma Inc., United States	Consist of 2.0 cm^2 array of titanium MN, which can be coated with a drug for bolus or sustainable delivery (Donnelly et al., 2009)
Hollow MN	MicronJet	NanoPass Inc., Israel	Comprises an array of 500-μm-long "micropyramids" to be used with any standard syringe for painless delivery of drugs (Van Damme et al., 2009)
	BD Soluvia	Becton Dickinson, United States	Short MN permanently affixed to the proximal end of the syringe with 1.5-mm-length needles (Laurent et al., 2007)
	Debioject	Debiotech	Delivery holes in MNs positioned at the side for specifically targeting intradermal site and regulating drug or vaccine distribution. The sharp tip can penetrate the skin at 90° angle (Debiotech, 2018)
	Intanza/Fluzone	Sanofi	Optimized from BD Soluvia Microinjection system for the delivery of influenza vaccine (Atmar et al., 2010)
	3M hMTS	3M	Consist of 1500-μm MNs and capable of delivering from 0.5 to 2 mL of liquid transdermally via a 1 cm^2 array (3M, 2018a,b)
Dissolving MNs	VaxMAT and DrugMAT	TheraJect Inc.	Enable transdermal delivery of small and large molecules (Market, TheraJect Inc., n.d.)
	MicroCor	Corium International Inc., United States	Uses drug-in-tip technology to formulate drugs with biodegradable polymer and excipients in solid-state microstructures (Corium, 2017)

Bariya et al. (2012) and Richter-Johnson et al. (2018). *hMTS*, Hollow Microstructured Transdermal System; *SC*, stratum corneum.

14.7 CONCLUSION

The limitation of the skin to selectively allow permeation of substances with certain physicochemical properties has been successfully overcome by MN technology. Over the past decades, various novel MN fabrication and drug loading methods have been developed with a goal to achieve a clinically effective drug delivery profile. However, there is still a high demand for a better MN system to replace the invasive delivery of high MW, high dose, and low potent protein therapeutics. It is clear that further optimization and advanced technology need to be employed in the preparation of MNs and protein drug formulation. This ensures the therapeutic protein has a prolonged shelf life and is apt for MN-based administration for a better treatment outcome. More pharmacokinetic reports on residues deposited in the skin due to the prolonged and repetitive application of MN are necessary to consider MN as a vehicle candidate for lifelong prophylactic treatment.

ABBREVIATIONS

BSA	bovine serum albumin
CL	centrifugal lithography
CMC	carboxymethyl cellulose
DC-hMN-iSystem	digitally monitored microinjection system
DAB	droplet-born air blowing
EDTA	ethylenediaminetetraacetic acid
FDA	Food and Drug Administration
FITC	fluorescein isothiocynate
ICG	intracardiac green dye
Ig	immunoglobulin
IL	interleukin
INS-$CaCO_3$ MPs	insulin-loaded $CaCO_3$ microparticles
IM	intramuscular
IFN	interferon
IV	intravenous
MN	microneedle
MNs-CIT	microneedles coated with ovalbumin and CpG oligonucleotide
MW	molecular weight
NP	nanoparticle
PEG	polyethylene glycol
PMVE/MA	polymethyl vinylether/maleic anhydride
Poly(I:C)	polyinosinic:polycytidylic acid
PTH	parathyroid hormone
PVA	polyvinyl-alcohol
PVP	poly(vinyl pyrrolidone)
PZT	lead zirconate titanate
RhB	rhodamine B
SC	stratum corneum
SCT	subcutaneous
Th2	type 2 T helper cells

Acknowledgments

We wish to thank the Ministry of Higher Education, Malaysia for financial assistance through the Fundamental Research Grant Scheme, and School of Graduate Studies, University Putra Malaysia for the services and facilities.

References

Adessi, C., Soto, C., 2002. Converting a peptide into a drug: strategies to improve stability and bioavailability. Curr. Med. Chem. 9 (9), 963–978.

Ameri, M., Daddona, P.E., Maa, Y.F., 2009. Demonstrated solid-state stability of parathyroid hormone PTH (1–34) coated on a novel transdermal microprojection delivery system. Pharm. Res. 26 (11), 2454–2463.

Atmar, R.L., Patel, S.M., Keitel, W.A., 2010. Intanza: a new intradermal vaccine for seasonal influenza. Expert Rev. Vaccines 9 (12), 1399–1409.

Bak, A., Leung, D., Barrett, S.E., Forster, S., Minnihan, E.C., Leithead, A.W., et al., 2015. Physicochemical and formulation developability assessment for therapeutic peptide delivery—a primer. AAPS J. 17 (1), 144–155.

Bariya, S.H., Gohel, M.C., Mehta, T.A., Sharma, O.P., 2012. Microneedles: an emerging transdermal drug delivery system. J. Pharm. Pharmacol. 64 (1), 11–29.

Bashyal, S., Noh, G., Keum, T., Choi, Y.W., Lee, S., 2016. Cell penetrating peptides as an innovative approach for drug delivery; then, present and the future. J. Pharm. Investig. 46 (3), 205–220.

Benson, H.A., Watkinson, A.C. (Eds.), 2012. Topical and Transdermal Drug Delivery: Principles and Practice. John Wiley & Sons.

Bhatnagar, S., Dave, K., Venuganti, V.V.K., 2017. Microneedles in the clinic. J. Controlled Release 260, 164–182.

Bragazzi, N.L., Orsi, A., Ansaldi, F., Gasparini, R., Icardi, G., 2016. Fluzone intra-dermal (Intanza/Istivac Intradermal): an updated overview. Hum. Vaccin. Immunother. 12 (10), 2616–2627.

Brown, L.R., 2005. Commercial challenges of protein drug delivery. Expert Opin. Drug Deliv. 2 (1), 29–42.

BusinessWire, 2016. Global Transdermal Drug Delivery Market Worth USD 95.57 Billion by 2025—Analysis, Technologies & Forecasts Report 2016-2025. Available from: <https://www.businesswire.com/news/home/20161111005701/en/Global-TransdermalDrug-Delivery-Market-Worth-USD>.

Cao, C., 2016. Advances in delivering protein and peptide therapeutics. Pharm. Technol. Available from: <http://www.pharmtech.com/advances-delivering-protein-and-peptide-therapeutics?pageID = 2>.

Capelle, M.A., Gurny, R., Arvinte, T., 2007. High throughput screening of protein formulation stability: practical considerations. Eur. J. Pharm. Biopharm. 65 (2), 131–148.

Caudill, C.L., Perry, J.L., Tian, S., Luft, J.C., DeSimone, J.M., 2018. Spatially controlled coating of continuous liquid Interface production microneedles for transdermal protein delivery. J. Controlled Release 284, 122–132.

Chang, L.L., Pikal, M.J., 2009. Mechanisms of protein stabilization in the solid state. J. Pharm. Sci. 98 (9), 2886–2908.

Chen, B., Wei, J., Iliescu, C., 2010. Sonophoretic enhanced microneedles array (SEMA)—improving the efficiency of transdermal drug delivery. Sens. Actuators, B: Chem. 145 (1), 54–60.

Chen, M.C., Huang, S.F., Lai, K.Y., Ling, M.H., 2013. Fully embeddable chitosan microneedles as a sustained release depot for intradermal vaccination. Biomaterials 34 (12), 3077–3086.

Cheung, K., West, G., Das, D.B., 2015. Delivery of large molecular protein using flat and short microneedles prepared using focused ion beam (FIB) as a skin ablation tool. Drug Deliv. Transl. Res. 5 (4), 462–467.

Chu, L.Y., Prausnitz, M.R., 2011. Separable arrowhead microneedles. J. Controlled Release 149 (3), 242–249.

Cleland, J.L., Langer, R., 1994. Formulation and Delivery of Proteins and Peptides. American Chemical Society, Washington, DC.

Clinical Resolution Laboratory, Inc., 2015. How Does "Microneedle Therapy System" Work? Available from: <http://www.clinicalresolution.com/main/whatismts.html>.

Corium, 2017. MicroCor. Available from: <http://www.coriumintl.com/home/technology/microcor/>.

Courtenay, A.J., McCrudden, M.T., McAvoy, K.J., McCarthy, H.O., Donnelly, R.F., 2018. Microneedle-mediated transdermal delivery of bevacizumab. Mol. Pharm. 15, 3545–3556.

Dalton, D.R., 2015. Hemophilia in the managed care setting. Am. J. Manag. Care 21 (6), S123–S130.

Dasgupta, S., Bayry, J., André, S., Dimitrov, J.D., Kaveri, S.V., Lacroix-Desmazes, S., 2008. Auditing protein therapeutics management by professional APCs: toward prevention of immune responses against therapeutic proteins. J. Immunol. 181 (3), 1609–1615.

Davidson, A., Al-Qallaf, B., Das, D.B., 2008. Transdermal drug delivery by coated microneedles: geometry effects on effective skin thickness and drug permeability. Chem. Eng. Res. Des. 86 (11), 1196–1206.

Debiotech, 2018. DebioJect: Successful and Accurate ID Injection. Available from: <https://www.debiotech.com/page/index.php?page = product_01&id = 1&id_prod = 4>.

Demir, Y.K., Akan, Z., Kerimoglu, O., 2013. Characterization of polymeric microneedle arrays for transdermal drug delivery. PLoS One 8 (10), e77289.

Desser, L., Holomanova, D., Zavadova, E., Pavelka, K., Mohr, T., Herbacek, I., 2001. Oral therapy with proteolytic enzymes decreases excessive TGF-β levels in human blood. Cancer Chemother. Pharmacol. 47 (1), S10–S15.

Dewan, S., 2017. Global markets for bioengineered protein drugs. BCC Res. Available from: <https://www.bccresearch.com/market-research/biotechnology/bioengineered-protein-drugs-report-bio009g.html>.

Donnelly, R.F., 2017. How can microneedles overcome challenges facing transdermal drug delivery? Ther. Deliv. 8 (9), 725–728.

Donnelly, R.F., Singh, T.R.R., Tunney, M.M., Morrow, D.I., McCarron, P.A., O'Mahony, C., et al., 2009. Microneedle arrays allow lower microbial penetration than hypodermic needles in vitro. Pharm. Res. 26 (11), 2513–2522.

Donnelly, R.F., Singh, T.R.R., Woolfson, A.D., 2010. Microneedle-based drug delivery systems: microfabrication, drug delivery, and safety. Drug Deliv. 17 (4), 187–207.

Donnelly, R.F., Singh, T.R.R., Garland, M.J., Migalska, K., Majithiya, R., McCrudden, C.M., et al., 2012. Hydrogel-forming microneedle arrays for enhanced transdermal drug delivery. Adv. Funct. Mater. 22 (23), 4879–4890.

Donnelly, R.F., Garland, M.J., Alkilani, A.Z., 2014a. Microneedle-iontophoresis combinations for enhanced transdermal drug delivery. Drug Delivery System. Humana Press, New York.

Donnelly, R.F., McCrudden, M.T., Alkilani, A.Z., Larrañeta, E., McAlister, E., Courtenay, A.J., et al., 2014b. Hydrogel-forming microneedles prepared from "super swelling" polymers combined with lyophilised wafers for transdermal drug delivery. PLoS One 9 (10), e111547.

Donnelly, R.F., Moffatt, K., Alkilani, A.Z., Vicente-Pérez, E.M., Barry, J., McCrudden, M.T., et al., 2014c. Hydrogel-forming microneedle arrays can be effectively inserted in skin by self-application: a pilot study centred on pharmacist intervention and a patient information leaflet. Pharm. Res. 31 (8), 1989–1999.

Dowd, F.J., Johnson, B., Mariotti, A., 2016. Pharmacology and Therapeutics for Dentistry-E-Book. Elsevier Health Sciences.

Du, G., Leone, M., Romeijn, S., Kersten, G., Jiskoot, W., Bouwstra, J.A., 2018. Immunogenicity of diphtheria toxoid and poly(I: C) loaded cationic liposomes after hollow microneedle-mediated intradermal injection in mice. Int. J. Pharm. 547 (1-2), 250–257.

Duan, X., Mao, S., 2010. New strategies to improve the intranasal absorption of insulin. Drug Discov. Today 15 (11–12), 416–427.

Frokjaer, S., Otzen, D.E., 2005. Protein drug stability: a formulation challenge. Nat. Rev. Drug Discov. 4 (4), 298–306.

Garland, M.J., Singh, T.R.R., Woolfson, A.D., Donnelly, R.F., 2011. Electrically enhanced solute permeation across poly(ethylene glycol)–cross-linked poly(methyl vinyl ether-*co*-maleic acid) hydrogels: effect of hydrogel cross-link density and ionic conductivity. Int. J. Pharm. 406 (1–2), 91–98.

Gerstel, M.S., Place, V.A., Alza Corp, 1976. Drug Delivery Device. US Patent 3,964,482.

Gill, H.S., Denson, D.D., Burris, B.A., Prausnitz, M.R., 2008. Effect of microneedle design on pain in human subjects. Clin. J. Pain 24 (7), 585.

Gouw, S.C., van den Berg, H.M., Oldenburg, J., Astermark, J., de Groot, P.G., Margaglione, M., et al., 2012. F8 gene mutation type and inhibitor development in patients with severe hemophilia A: systematic review and meta-analysis. Blood 119 (12), 2922–2934.

Grand View Research, Inc., 2018. The Transdermal Drug Delivery System Market is Driven by the High Demand for Highly Potent, New Generation Therapeutics. Available from: <www.grandviewresearch.com/industry-analysis/transdermal-drug-delivery-systems-industry>.

Griss, P., Stemme, G., 2003. Side-opened out-of-plane microneedles for microfluidic transdermal liquid transfer. J. Microelectromech. Syst. 12 (3), 296–301.

Gupta, H., Sharma, A., 2014. Recent trends in protein and peptide drug delivery systems. Asian J. Pharm. 3 (2), 69–75.
Guy, R.H., Kalia, Y.N., Delgado-Charro, M.B., Merino, V., Lopez, A., Marro, D., 2000. Iontophoresis: electrorepulsion and electroosmosis. J. Controlled Release 64 (1–3), 129–132.
Hamburger, R., Azaz, E., Donbrow, M., 1975. Autoxidation of polyoxyethylenic non-ionic surfactants and of polyethylene glycols. Pharm. Acta Helv. 50 (1–2), 10.
Han, T., Das, D.B., 2013. Permeability enhancement for transdermal delivery of large molecule using low-frequency sonophoresis combined with microneedles. J. Pharm. Sci. 102 (10), 3614–3622.
Hardy, J.G., Larrañeta, E., Donnelly, R.F., McGoldrick, N., Migalska, K., McCrudden, M.T., et al., 2016. Hydrogel-forming microneedle arrays made from light-responsive materials for on-demand transdermal drug delivery. Mol. Pharm. 13 (3), 907–914.
Harvey, A.J., Kaestner, S.A., Sutter, D.E., Harvey, N.G., Mikszta, J.A., Pettis, R.J., 2011. Microneedle-based intradermal delivery enables rapid lymphatic uptake and distribution of protein drugs. Pharm. Res. 28 (1), 107–116.
Henry, S., McAllister, D.V., Allen, M.G., Prausnitz, M.R., 1998. Microfabricated microneedles: a novel approach to transdermal drug delivery. J. Pharm. Sci. 87 (8), 922–925.
Hong, X., Wu, Z., Chen, L., Wu, F., Wei, L., Yuan, W., 2014. Hydrogel microneedle arrays for transdermal drug delivery. Nano-Micro Lett. 6 (3), 191–199.
Huh, I., Kim, S., Yang, H., Jang, M., Kang, G., Jung, H., 2018. Effects of two droplet-based dissolving microneedle manufacturing methods on the activity of encapsulated epidermal growth factor and ascorbic acid. Eur. J. Pharm. Sci. 114, 285–292.
Ibrahim, R., Nitsche, J.M., Kasting, G.B., 2012. Dermal clearance model for epidermal bioavailability calculations. J. Pharm. Sci. 101 (6), 2094–2108.
Ita, K., 2015. Transdermal delivery of drugs with microneedles—potential and challenges. Pharmaceutics 7 (3), 90–105.
Ita, K.B., 2014. Transdermal drug delivery: progress and challenges. J. Drug Deliv. Sci. Technol. 24 (3), 245–250.
Jacoby, E., Jarrahian, C., Hull, H.F., Zehrung, D., 2015. Opportunities and challenges in delivering influenza vaccine by microneedle patch. Vaccine 33 (37), 4699–4704.
Jani, P., Manseta, P., Patel, S., 2012. Pharmaceutical approaches related to systemic delivery of protein and peptide drugs: an overview. Int. J. Pharm. Sci. Rev. Res. 12 (1), 42–52.
Jitendra, P.K., Bansal, S., Banik, A., 2011. Noninvasive routes of proteins and peptides drug delivery. Indian J. Pharm. Sci. 73 (4), 367–375.
Katikaneni, S., Badkar, A., Nema, S., Banga, A.K., 2009. Molecular charge mediated transport of a 13 kD protein across microporated skin. Int. J. Pharm. 378 (1–2), 93–100.
Kelchen, M.N., Holdren, G.O., Farley, M.J., Zimmerman, M.B., Fairley, J.A., Brogden, N.K., 2014. Optimization of impedance spectroscopy techniques for measuring cutaneous micropore formation after microneedle treatment in an elderly population. Pharm. Res. 31 (12), 3478–3486.
Kendall, M.A., Chong, Y.F., Cock, A., 2007. The mechanical properties of the skin epidermis in relation to targeted gene and drug delivery. Biomaterials 28, 4968–4977.
Kennedy, J., Larrañeta, E., McCrudden, M.T., McCrudden, C.M., Brady, A.J., Fallows, S.J., et al., 2017. In vivo studies investigating biodistribution of nanoparticle-encapsulated rhodamine B delivered via dissolving microneedles. J. Controlled Release 265, 57–65.
Kim, Y.C., Park, J.H., Prausnitz, M.R., 2012. Microneedles for drug and vaccine delivery. Adv. Drug Deliv. Rev. 64 (14), 1547–1568.
Lahiji, S.F., Dangol, M., Jung, H., 2015. A patchless dissolving microneedle delivery system enabling rapid and efficient transdermal drug delivery. Sci. Rep. 5, 7914. Available from: https://doi.org/10.1038/srep07914.
Lahiji, S.F., Jang, Y., Huh, I., Yang, H., Jang, M., Jung, H., 2018a. Exendin-4–encapsulated dissolving microneedle arrays for efficient treatment of type 2 diabetes. Sci. Rep. 8 (1), 1170.
Lahiji, S.F., Jang, Y., Ma, Y., Dangol, M., Yang, H., Jang, M., et al., 2018b. Effects of dissolving microneedle fabrication parameters on the activity of encapsulated lysozyme. Eur. J. Pharm. Sci. 117, 290–296.
Lai, M.C., Topp, E.M., 1999. Solid-state chemical stability of proteins and peptides. J. Pharm. Sci. 88 (5), 489–500.
Lakshmi, P.K., Prasanthi, D., Veeresh, B., 2017. Noninvasive delivery of protein and peptide drugs: a review. Asian J. Pharm. Clin. Res. 10 (8), 25–33.

Lambert, P.H., Laurent, P.E., 2008. Intradermal vaccine delivery: will new delivery systems transform vaccine administration? Vaccine 26 (26), 3197–3208.
Larrañeta, E., Lutton, R.E., Woolfson, A.D., Donnelly, R.F., 2016. Microneedle arrays as transdermal and intradermal drug delivery systems: materials science, manufacture and commercial development. Mater. Sci. Eng., R: Rep. 104, 1–32.
Laurent, P.E., Bonnet, S., Alchas, P., Regolini, P., Mikszta, J.A., Pettis, R., et al., 2007. Evaluation of the clinical performance of a new intradermal vaccine administration technique and associated delivery system. Vaccine 25 (52), 8833–8842.
Laurent, P.E., Bourhy, H., Fantino, M., Alchas, P., Mikszta, J.A., 2010. Safety and efficacy of novel dermal and epidermal microneedle delivery systems for rabies vaccination in healthy adults. Vaccine 28 (36), 5850–5856.
Leader, B., Baca, Q.J., Golan, D.E., 2008. Protein therapeutics: a summary and pharmacological classification. Nat. Rev. Drug Discov. 7 (1), 21–39.
Li, G., Badkar, A., Nema, S., Kolli, C.S., Banga, A.K., 2009. In vitro transdermal delivery of therapeutic antibodies using maltose microneedles. Int. J. Pharm. 368 (1–2), 109–115.
Li, G., Badkar, A., Kalluri, H., Banga, A.K., 2010. Microchannels created by sugar and metal microneedles: characterization by microscopy, macromolecular flux and other techniques. J. Pharm. Sci. 99 (4), 1931–1941.
Li, Q.Y., Zhang, J.N., Chen, B.Z., Wang, Q.L., Guo, X.D., 2017. A solid polymer microneedle patch pretreatment enhances the permeation of drug molecules into the skin. RSC Adv. 7 (25), 15408–15415.
Liu, D., Yu, B., Jiang, G., Yu, W., Zhang, Y., Xu, B., 2018. Fabrication of composite microneedles integrated with insulin-loaded $CaCO_3$ microparticles and PVP for transdermal delivery in diabetic rats. Mater. Sci. Eng. C Mater. Biol. Appl. C 90, 180–188.
Loizidou, E.Z., Inoue, N.T., Ashton-Barnett, J., Barrow, D.A., Allender, C.J., 2016. Evaluation of geometrical effects of microneedles on skin penetration by CT scan and finite element analysis. Eur. J. Pharm. Biopharm. 107, 1–6.
3M, 2018. About 3M Hollow Microneedle Technology. Available from: <https://www.3m.com/3M/en_US/drug-delivery-systems-us/technologies/microneedle/hollow-needle/>.
3M, 2018. About 3M Hollow Microneedle Technology. Available from: <https://www.3m.com/3M/en_US/drug-delivery-systems-us/technologies/microneedle/solid/>.
Maibach, H.I. (Ed.), 2017. Percutaneous Penetration Enhancers Physical Methods in Penetration Enhancement. Springer.
Market, TheraJect Inc., n.d. Available from: <http://www.theraject.com/market/markethtml>.
Márquez-Graña, C., Bryan, K., Vucen, S., O'Sullivan, C., 2017. Development of a novel single-use microneedle design platform for increased patient compliance. Procedia Manuf. 13, 1352–1359.
Mistilis, M.J., Joyce, J.C., Esser, E.S., Skountzou, I., Compans, R.W., Bommarius, A.S., et al., 2017. Long-term stability of influenza vaccine in a dissolving microneedle patch. Drug Deliv. Transl. Res. 7 (2), 195–205.
Mitragotri, S., Burke, P.A., Langer, R., 2014. Overcoming the challenges in administering biopharmaceuticals: formulation and delivery strategies. Nat. Rev. Drug Discov. 13 (9), 655–672.
Okumu, F.W., Cleland, J.L., 2003. Implants and injectables. Modified-Release Drug Delivery Technology. Marcel Dekker Inc, pp. 633–638.
Park, J.H., Allen, M.G., Prausnitz, M.R., 2006. Polymer microneedles for controlled-release drug delivery. Pharm. Res. 23 (5), 1008–1019.
Peppas, N.A., Bures, P., Leobandung, W., Ichikawa, H., 2000. Hydrogels in pharmaceutical formulations. Eur. J. Pharm. Biopharm. 50 (1), 27–46.
Prausnitz, M.R., 1996. The effects of electric current applied to skin: a review for transdermal drug delivery. Adv. Drug Deliv. Rev. 18 (3), 395–425.
Prausnitz, M.R., 2017. Engineering microneedle patches for vaccination and drug delivery to skin. Annu. Rev. Chem. Biomol. Eng. 8, 177–200.
Raj Singh, T.R., Woolfson, A.D., Donnelly, R.F., 2010. Investigation of solute permeation across hydrogels composed of poly(methyl vinyl ether-*co*-maleic acid) and poly(ethylene glycol). J. Pharm. Pharmacol. 62 (7), 829–837.
Raj Singh, T.R., Garland, M.J., Migalska, K., Salvador, E.C., Shaikh, R., McCarthy, H.O., et al., 2012. Influence of a pore-forming agent on swelling, network parameters, and permeability of poly(ethylene glycol)-cross-linked poly(methyl vinyl ether-*co*-maleic acid) hydrogels: application in transdermal delivery systems. J. Appl. Polym. Sci. 125 (4), 2680–2694.

Richter-Johnson, J., Kumar, P., Choonara, Y.E., du Toit, L.C., Pillay, V., 2018. Therapeutic applications and pharmacoeconomics of microneedle technology. Expert Rev. Pharmacoecon. Outcomes Res. 18 (4), 359–369.
Römgens, A.M., Bader, D.L., Bouwstra, J.A., Baaijens, F.P.T., Oomens, C.W.J., 2014. Monitoring the penetration process of single microneedles with varying tip diameters. J. Mech. Behav. Biomed. Mater. 40, 397–405.
Sachdeva, V., Zhou, Y., Banga, A.K., 2013. In vivo transdermal delivery of leuprolide using microneedles and iontophoresis. Curr. Pharm. Biotechnol. 14 (2), 180–193.
Seong, K.Y., Seo, M.S., Hwang, D.Y., O'Cearbhaill, E.D., Sreenan, S., Karp, J.M., et al., 2017. A self-adherent, bullet-shaped microneedle patch for controlled transdermal delivery of insulin. J. Controlled Release 265, 48–56.
Shakya, A.K., Lee, C.H., Gill, H.S., 2017. Cutaneous vaccination with coated microneedles prevents development of airway allergy. J. Controlled Release 265, 75–82.
Tan, M.L., Choong, P.F., Dass, C.R., 2010. Recent developments in liposomes, microparticles and nanoparticles for protein and peptide drug delivery. Peptides 31 (1), 184–193.
Tang, H., Wang, C.C.J., Blankschtein, D., Langer, R., 2002. An investigation of the role of cavitation in low-frequency ultrasound-mediated transdermal drug transport. Pharm. Res. 19 (8), 1160–1169.
Tiwari, G., Tiwari, R., Sriwastawa, B., Bhati, L., Pandey, S., Pandey, P., et al., 2012. Drug delivery systems: an updated review. Int. J. Pharm. Investig. 2 (1), 2–11.
Trevaskis, N.L., Kaminskas, L.M., Porter, C.J., 2015. From sewer to saviour—targeting the lymphatic system to promote drug exposure and activity. Nat. Rev. Drug Discov. 14 (11), 781–803.
Tuan-Mahmood, T.M., McCrudden, M.T., Torrisi, B.M., McAlister, E., Garland, M.J., Singh, T.R.R., et al., 2013. Microneedles for intradermal and transdermal drug delivery. Eur. J. Pharm. Sci. 50 (5), 623–637.
Usmani, S.S., Bedi, G., Samuel, J.S., Singh, S., Kalra, S., Kumar, P., et al., 2017. THPdb: database of FDA-approved peptide and protein therapeutics. PLoS One 12 (7), e0181748. Available from: https://doi.org/10.1371/journal.pone.0181748.
Van Damme, P., Oosterhuis-Kafeja, F., Van der Wielen, M., Almagor, Y., Sharon, O., Levin, Y., 2009. Safety and efficacy of a novel microneedle device for dose sparing intradermal influenza vaccination in healthy adults. Vaccine 27 (3), 454–459.
Van der Maaden, K., Jiskoot, W., Bouwstra, J., 2012. Microneedle technologies for (trans) dermal drug and vaccine delivery. J. Controlled Release 161 (2), 645–655.
Van der Maaden, K., Heuts, J., Camps, M., Pontier, M., van Scheltinga, A.T., Jiskoot, W., et al., 2018. Hollow microneedle-mediated micro-injections of a liposomal HPV E743–63 synthetic long peptide vaccine for efficient induction of cytotoxic and T-helper responses. J. Controlled Release 269, 347–354.
Vyas, S.P., Khar, R.K., 2004. Targeted & Controlled Drug Delivery: Novel Carrier Systems. CBS Publishers & Distributors.
Watson, C.J., Rowland, M., Warhurst, G., 2001. Functional modeling of tight junctions in intestinal cell monolayers using polyethylene glycol oligomers. Am. J. Physiol. Cell Physiol. 281 (2), C388–C397.
Weiss, W.F., Young, T.M., Roberts, C.J., 2009. Principles, approaches, and challenges for predicting protein aggregation rates and shelf life. J. Pharm. Sci. 98 (4), 1246–1277.
Werle, M., Bernkop-Schnürch, A., 2006. Strategies to improve plasma half life time of peptide and protein drugs. Amino Acids 30 (4), 351–367.
Wong, R.S.H., Ashton, M., Dodou, K., 2015. Effect of cross-linking agent concentration on the properties of unmedicated hydrogels. Pharmaceutics 7 (3), 305–319.
Yan, G., Warner, K.S., Zhang, J., Sharma, S., Gale, B.K., 2010. Evaluation needle length and density of microneedle arrays in the pretreatment of skin for transdermal drug delivery. Int. J. Pharm. 391, 7–12.
Yang, S., Feng, Y., Zhang, L., Chen, N., Yuan, W., Jin, T., 2012. A scalable fabrication process of polymer microneedles. Int. J. Nanomed. 7, 1415–1422.
Yuzhakov, V.V., 2010. The AdminPen microneedle device for painless & convenient drug delivery. Drug Deliv. Technol. 10 (4), 32–36.
Zaidi, Z., Lanigan, S.W., 2010. Skin: structure and function. Dermatology in Clinical Practice. Springer, London, pp. 1–15.
Zalta, A.H., Sweeney, C.P., Zalta, A.K., Kaufman, A.H., 2002. Intracameral tissue plasminogen activator use in a large series of eyes with valved glaucoma drainage implants. Arch. Ophthalmol. 120 (11), 1487–1493.

Zelikin, A.N., Ehrhardt, C., Healy, A.M., 2016. Materials and methods for delivery of biological drugs. Nat. Chem. 8 (11), 997–1007.
Zhang, S., Qiu, Y., Gao, Y., 2014. Enhanced delivery of hydrophilic peptides in vitro by transdermal microneedle pretreatment. Acta Pharm. Sin. B 4 (1), 100–104.
Zhang, Y.H., Campbell, S.A., Karthikeyan, S., 2018. Finite element analysis of hollow out-of-plane HfO 2 microneedles for transdermal drug delivery applications. Biomed. Microdevices 20 (1), 19.
Zhu, D.D., Chen, B.Z., He, M.C., Guo, X.D., 2017. Structural optimization of rapidly separating microneedles for efficient drug delivery. J. Ind. Eng. Chem. 51, 178–184.

Further reading

Ameri, M., Kadkhodayan, M., Nguyen, J., Bravo, J.A., Su, R., Chan, K., et al., 2014. Human growth hormone delivery with a microneedle transdermal system: preclinical formulation, stability, delivery and PK of therapeutically relevant doses. Pharmaceutics 6 (2), 220–234.
Buckley, R.H., 1982. Long term use of intravenous immune globulin in patients with primary immunodeficiency diseases: inadequacy of current dosage practices and approaches to the problem. J. Clin. Immunol. 2 (2), 15S–21S.
Cai, B., Xia, W., Bredenberg, S., Engqvist, H., 2014. Self-setting bioceramic microscopic protrusions for transdermal drug delivery. J. Mater. Chem. B 2 (36), 5992–5998.
Chandrasekaran, S., Brazzle, J.D., Frazier, A.B., 2003. Surface micromachined metallic microneedles. J. Microelectromech. Syst. 12 (3), 281–288.
Gupta, J., Felner, E.I., Prausnitz, M.R., 2009. Minimally invasive insulin delivery in subjects with type 1 diabetes using hollow microneedles. Diabetes Technol. Ther. 11 (6), 329–337.
Ito, Y., Hagiwara, E., Saeki, A., Sugioka, N., Takada, K., 2006. Feasibility of microneedles for percutaneous absorption of insulin. Eur. J. Pharm. Sci. 29 (1), 82–88.
Lee, J.W., Park, J.H., Prausnitz, M.R., 2008. Dissolving microneedles for transdermal drug delivery. Biomaterials 29 (13), 2113–2124.
Martin, C.J., Allender, C.J., Brain, K.R., Morrissey, A., Birchall, J.C., 2012. Low temperature fabrication of biodegradable sugar glass microneedles for transdermal drug delivery applications. J. Controlled Release 158 (1), 93–101.
Verbaan, F.J., Bal, S.M., Van den Berg, D.J., Dijksman, J.A., Van Hecke, M., Verpoorten, H., et al., 2008. Improved piercing of microneedle arrays in dermatomed human skin by an impact insertion method. J. Controlled Release 128 (1), 80–88.
Verhoeven, M., Bystrova, S.N., Winnubst, L., Qureshi, H., de Gruijl, T.D., et al., 2012. Applying ceramic nanoporous microneedle arrays as a transport interface in egg plants and an ex-vivo human skin model. Microelectron. Eng. 98, 659–662. Available from: https://doi.org/10.1016/j.mee.2012.07.022.

CHAPTER

15

Synthesis, Characterization, and Applications of Metal Nanoparticles

Abeer Jabra Shnoudeh[1], *Islam Hamad*[2], *Ruwaida W. Abdo*[1], *Lana Qadumii*[3], *Abdulmutallab Yousef Jaber*[1], *Hiba Salim Surchi*[1] *and Shahd Z. Alkelany*[1]

[1]Faculty of Pharmacy, Philadelphia University, Amman, Jordan [2]Department of Pharmacy, Faculty of Health Sciences, American University of Madaba, Madaba, Jordan [3]Faculty of Science, Philadelphia University, Amman, Jordan

OUTLINE

15.1 Introduction 528
15.1.1 Introduction to Metals: General Properties 529
15.1.2 The Concept Behind Metallic Nanoparticles: Nanotechnology and Nanoscience 530
15.1.3 Advantages of Metallic Nanoparticles Over Polymeric Micro- and Nanostructures: Role in Pharmaceutical Systems 534

15.2 General Methods in Metal Nanoparticles Synthesis 534
15.2.1 Physical Approach 534
15.2.2 Chemical Approach 535
15.2.3 Biological Approach 536

15.3 Synthesis of Gold Nanoparticles 542

15.4 Synthesis of Silver Nanoparticles 543

15.5 Synthesis of Iron Nanoparticles 544

15.6 Synthesis of Zinc Oxide Nanoparticles 545

15.7 Synthesis of Copper Nanoparticles 546

15.8 Synthesis of Aluminum Nanoparticles 547

15.9 Synthesis of Platinum Nanoparticles 548

15.10 Synthesis of Ruthenium Nanoparticles 548

15.11 Synthesis of Bimetallic Nanoparticles 549

Biomaterials and Bionanotechnology
DOI: https://doi.org/10.1016/B978-0-12-814427-5.00015-9

© 2019 Elsevier Inc. All rights reserved.

15.12 Synthesis of Metalloid and Nonmetal Nanoparticles 550
15.12.1 Synthesis of Selenium Nanoparticles 550
15.12.2 Synthesis of Sulfur Nanoparticles 551

15.13 Surface Properties of Metal Nanoparticles 551

15.14 Methods Used in Metal Nanoparticles Characterization 552
15.14.1 Ultraviolet Visible Spectroscopy Studies and Plasmon Resonance 552
15.14.2 Fourier Transforms Infrared Spectroscopy 555
15.14.3 Scanning Electron Microscope 557
15.14.4 Environmental Scanning Electron Microscope 557
15.14.5 Transmission Electron Microscopy 558
15.14.6 X-Ray Crystallography 558
15.14.7 Energy-Dispersive X-Ray Spectroscopy 559
15.14.8 Fluorescence Correlation Spectroscopy 559
15.14.9 Surface-Enhanced Raman Spectroscopy 560
15.14.10 Tip-Enhanced Raman Spectroscopy 561
15.14.11 Zeta Potential 561
15.14.12 Circular Dichroism 562
15.14.13 Mass Spectroscopy 563
15.14.14 Dynamic Light Scattering 564
15.14.15 Scanning Tunneling Microscope 565
15.14.16 Atomic-Force Microscopy 566

15.15 Applications of Metal Nanoparticles 566
15.15.1 Applications in Drug Delivery 566
15.15.2 Application in Protein Delivery 572
15.15.3 Application in Peptide Delivery 572
15.15.4 Application in Gene Delivery 572
15.15.5 Application in Tissue Engineering 573
15.15.6 Application in Enzymology 574
15.15.7 Application in Surface Coating of Nanoparticles 575
15.15.8 Application in Biosensing Devices 576
15.15.9 Application in Diagnostics 578
15.15.10 Application in Theranostics 579
15.15.11 Other Application 580

15.16 Future Potential of Metallic Nanoparticles: Emerging Area of Biomedical Sciences 581

Conclusion 582

Acknowledgments 583

Abbreviations 583

References 585

15.1 INTRODUCTION

Nanoparticles (NPs) are part of a big scientific field of nanotechnology. NPs are used in many fields like chemistry, physics, biology, and many other areas (Murugan and Shanmugasundaram, 2014). Metallic NPs were introduced to the world ancient times, and they have been either synthesized by humans or were already present in nature. The Lycurgus Cup (exhibited at the British Museum, London) is a wonderful example of this;

it is a class of Roman vessel illuminated externally (green), or internally (red), containing silver (Ag) and gold (Au) NPs (Freestone et al., 2007; Castro et al., 2014). Faraday, in 1857, reported the synthesis of colloid Au NP in addition to other metals such as copper (Cu), zinc (Zn), iron (Fe), and stannum (Tin) and studied how they interact with light (Faraday, 1857; Alaqad and Saleh, 2016). Also, in 1975, Blakemore precipitated magnetite (Fe_3O_4) from the tissues of the various organisms including insects, algae, bacteria, mammals, and birds (Blakemore, 1975; Benelmekki, 2014).

During the last century, substantial development in this field (colloid science) has happened, including the introduction of breakthrough methodologies for the production of metals, metal oxides NPs, and organic products (Aitken, Creely, and Tran, 2004; Ostiguy, Cloutier and Boutin, 2006; Benelmekki, 2014). Several forms of NPs have been formulated in the last decades, and in 2010 more than 1000 products containing NPs in different sectors became commercially available (Ostiguy, Cloutier and Boutin, 2006; Benelmekki, 2014).

Metal NPs, in particular, played a major role in this field; for example, Au NPs are applied for the delivery of several drugs as doxorubicin (DOX), paclitaxel, and methotrexate (Rai et al., 2016). Also, they have been used for genetic disease, angiogenesis, genetic disorder diagnosis, tumor detection, photothermal therapy, and photoimaging. Whereas, iron oxide NPs have been applied in drug delivery, cancer, cell labeling, hyperthermia, targeting and immunoassays, tissue repair, magnetically responsive drug delivery therapy, and magnetic resonance (MR) imaging (MRI) (Huang et al., 2007; Khlebtsov and Dykman, 2011; Iv et al., 2015). Palladium (Pd) and Cu NPs are also applied in plastics, plasmonic waveguides, polymers, optical limiting devices, and batteries (Momeni and Nabipour, 2015; Nasrollahzadeh and Sajadi, 2015). Also, Ag NPs have been used for wound treatment, in various antimicrobial, antiinflammatory, and anticancer applications (Ahamed, Alsalhi and Siddiqui, 2010). Some of the applications and biological synthesis approaches of metal NPs are illustrated in Fig. 15.1.

This chapter discusses the science behind metal NPs and highlights the methods in their synthesis, characterization, as well as their potential applications. Also, some examples on the synthesis and applications of nonmetal NPs such as sulfur and metalloid NPs as selenium will be given.

15.1.1 Introduction to Metals: General Properties

Metals are elements that by losing electrons form positive ions during a chemical reaction. The main metals in the periodic table include Au, Ag, Cu, Fe, and Zn.

Metals are characterized by bright shine, solidity, ability to vibrate sound, and are excellent conductors of electricity and heat. In addition, metals can be formed into sheets or wires. Also, they have high melting and boiling points. These are considered as their physical properties. However, their chemical properties include electropositivity, as they form basic or amphoteric oxides with oxygen (oxidized). Alkali metals lose typically one electron, alkaline metals lose both electrons, whereas transition metals can lose one, two, or even three electrons from their orbitals. Metal oxides are usually basic oxides and can dissolve in water forming metal hydroxides. Whereas, they show their basic character when reacting with acids to form salts and water (Blaber, 2016).

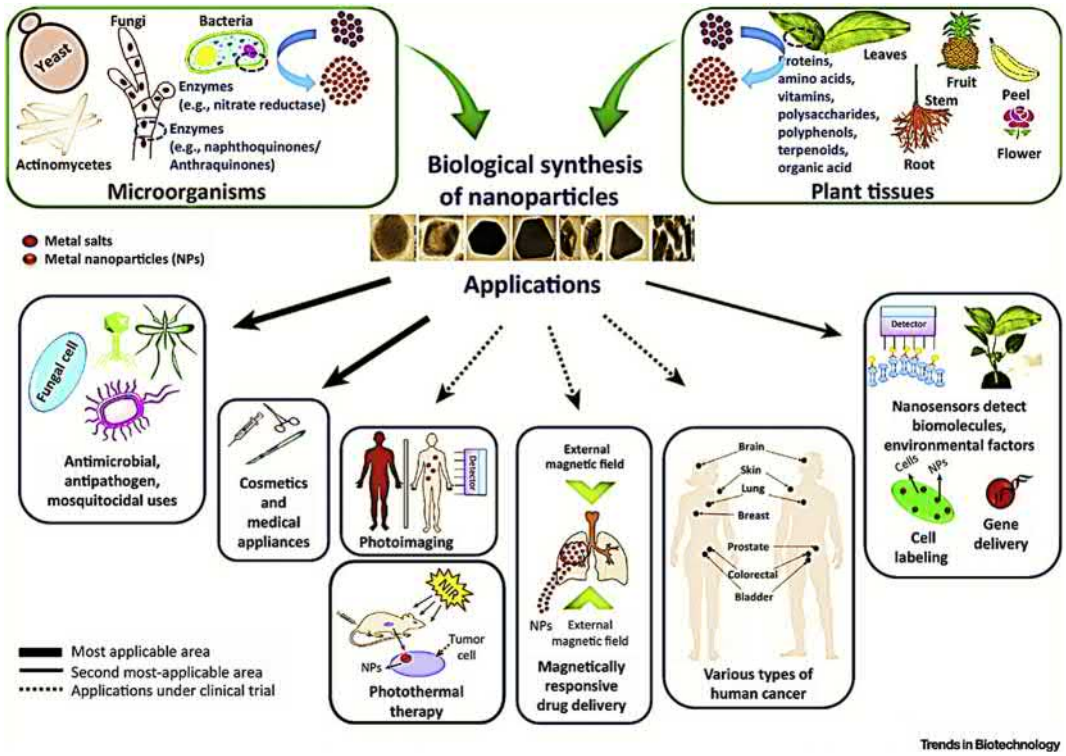

FIGURE 15.1 An illustration showing the biological synthesis of nanoparticles from microorganisms or plant tissue and several applications of metal nanoparticles (Singh et al., 2016).

It is worth noting that synthesis of metal NPs relies on either the physical or chemical characteristics of these metals, such as solidity, melting and boiling points, reactivity with acids, bases, and oxygen.

15.1.2 The Concept Behind Metallic Nanoparticles: Nanotechnology and Nanoscience

The concept of nanotechnology was introduced by Richard P. Feynman, a physics Nobel laureate, in his famous lecture titled "There's Plenty of Room at the Bottom" at the meeting of the American Physical Society in 1959 (Feynman, 1960).

Afterward, revolutionary developments in biology, chemistry, and physics have demonstrated his idea about atomic scale matter manipulation. Less than 20 years later, in 1974, a professor at Tokyo University, Norio Taniguchi, invented the term *nanotechnology* to describe extra and high precision ultrafine dimensions. Interestingly, by predicting enhancements and miniaturization in integrated circuits, computer memory devices, optoelectronic devices, and mechanical devices, he also introduced the "top-down approach," which includes physical and chemical methods to get atomic scale materials

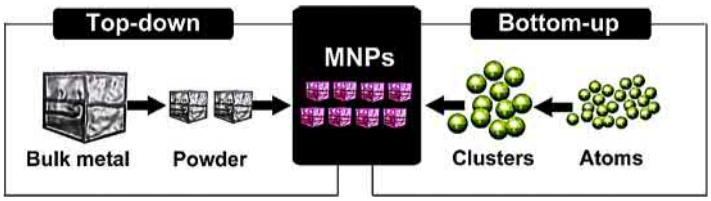

FIGURE 15.2 Illustration of bottom-up and top-down methods for metal nanoparticles. Source: *Reproduced from Domènech, B., Bastos-Arrieta, J., Alonso, A., Macanás, J., Muñoz, M., Muraviev, D.N., 2012. Bifunctional polymer-metal nanocomposite ion exchange materials, Ion Exchange Technologies, Ayben Kilislioğlu. IntechOpen. doi:10.5772/51579. Available from: <https://www.intechopen.com/books/ion-exchange-technologies/bifunctional-polymer-metal-nanocomposite-ion-exchange-materials>.*

from bulk materials. K. Eric Drexler, around 10 years later, introduced the "bottom-up approach" during his discussion of the formation of greater objects from their atomic and molecular constituents as becoming the potential of nanotechnology (Drexler, 1990; Benelmekki, 2014), shown in Fig. 15.2.

The importance of nanotechnology in the fields of science count on the synthesis and modulation of NPs, specifically metals, which involves substantial modification of their properties (Rao and Gan, 2015). Scientists were able to synthesize NPs using different methods relying on the top-down approach, which includes both physical and chemical approach, and bottom-up methods, which include biological and chemical methods. As both physical and chemical methods result in environmental contamination and toxicity, biological approaches using green synthesis were found to be environmentally friendly and less toxic. The approaches and methods of NPs synthesis are summarized in Fig. 15.3 (Keat et al., 2015; Ahmed et al., 2016).

NPs synthesized by plants have more stability and faster rate of synthesis than other organisms (Iravani and Zolfaghari, 2013). Biological methods for NPs synthesis have been used in different methods for their efficient cost and the requirement of little or no maintenance. The details of these approaches will be discussed in subsequent sections of this chapter.

15.1.2.1 Types of Nanoparticles: A Quick Look

There are many types of NPs including inorganic NPs, polymeric NPs, solid lipid NPs, liposomes, nanocrystals, nanotubes, and dendrimers. From the many types of NPs we are going to focus on metallic NPs, which are considered as inorganic NPs, and briefly explain the other types.

15.1.2.1.1 INORGANIC NANOPARTICLES

Inorganic NPs differs in their physical properties as size-dependent optical, catalytic, electronic, and magnetic properties, which depend on the type of NP and the synthetic approach that has been used. For example, biological approaches have been applied in the formulation of NPs including gold, iron oxides, silica, silver, quantum dots, etc. (Ladj et al., 2013).

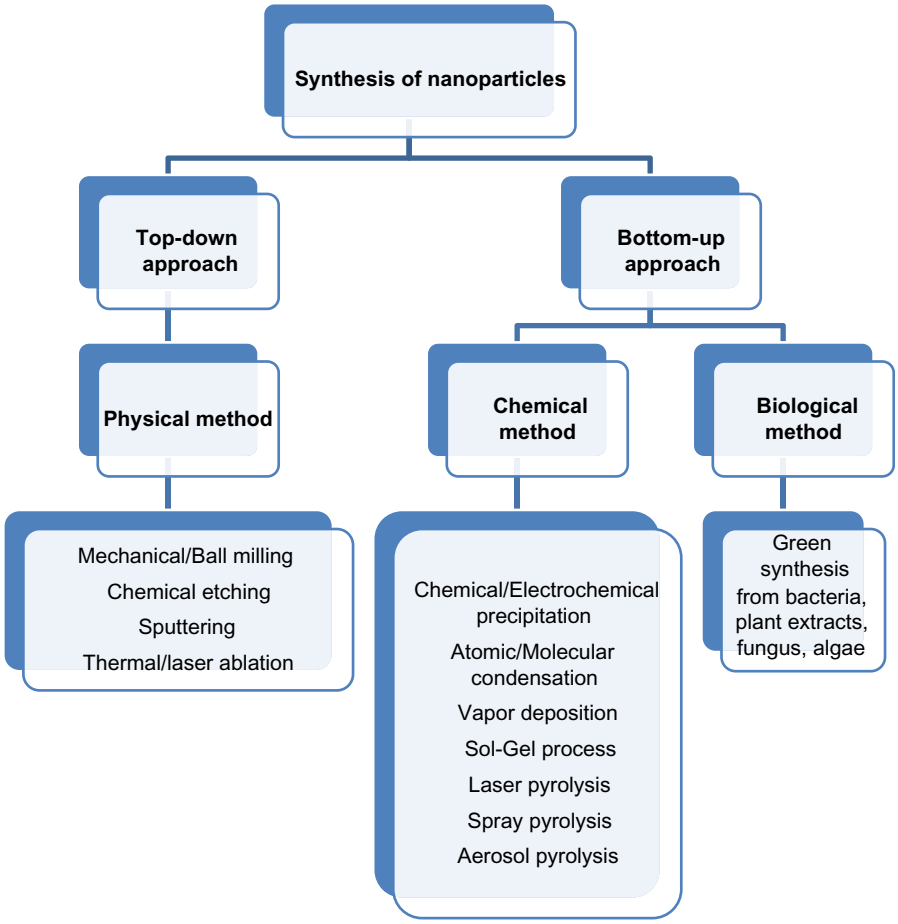

FIGURE 15.3 Illustration of synthesis of NPs using bottom-up and top-down method. *NPs*, Nanoparticles. Source: *Modified from: Ahmed, S., et al., 2016. A review on plants extract mediated synthesis of silver nanoparticles for antimicrobial applications: a green expertise. J. Adv. Res. 17–28. <http://dx.doi.org/10.1016/j.jare.2015.02.007> with permission.*

Types of inorganic NPs include:

- *Metallic Nanoparticles*

  Metallic NPs are considered flexible nanostructures because of the ability to control their composition, shape, size, structure, encapsulation, assembly, and their optical properties during synthesis.

  Metallic NPs have special surface properties such as plasmon excitation, shape, and dielectric properties, which give them high applicability in many fields as a platform for bimolecular ultrasensitive detection, protein, and cell labeling targeted delivery of therapeutic agents within the cells and hyperthermal treatment for cancer, a role in seed germination, and altered levels of micro-RNA expression, which controls various metabolic, physiological, and morphological processes in plants (Kumar et al., 2013).

- *Metal Oxide Nanoparticles*

  Metal oxide NPs have limited size and high density of corner edge surface sites. They also possess vital functions in the many areas of plant technology (Picó and Blasco, 2012), for example, silicon dioxide (SiO_2) NPs affect seeds germination (Siddiqui and Al-Whaibi, 2014), also alumina (Al) NPs increased the growth of roots in plants (Lin and Xing, 2007).
- *Quantum Dots*

  Structurally quantum dots are made of several metal complexes such as magnetic transition metals, semiconductors, and metal. In addition to their role in a plant system, quantum dots are used in the surface coating. They also fluoresce with different colors depending on their size, and quantum dots can give a secondary coating, which improves water solubility (Nair et al., 2011).

15.1.2.1.2 POLYMERIC NANOPARTICLES

Polymeric NPs are solid NPs in the range of 10−1000 nm, mainly lipid-based NPs (Nagavarma et al., 2012; Khan, Saeed and Khan, 2017), and are obtained from synthetic polymers, such as polycaprolactone, polyacrylamide, and polyacrylate, or natural polymers like albumin, which improve the pharmacodynamics and pharmacokinetics properties of different drugs (Bhatia et al., 2011).

15.1.2.1.2.1 SOLID LIPID NANOPARTICLES Solid lipid NPs (SNPs) played a major role in drug delivery in the 1990s. SNPs are considered alternative carrier systems to emulsions, polymeric NPs, and liposomes (Abhilash, 2010).

15.1.2.1.2.2 LIPOSOMES Liposomes are spherical vesicles made of one or more phospholipid bilayers. They are used extensively as carriers for numerous molecules in the pharmaceutical and cosmetic industries, and in the encapsulation of insoluble or unstable compounds in pharmaceutical, food, and farming industries (Akbarzadeh et al., 2013).

15.1.2.1.2.3 NANOCRYSTALS Nanocrystals are crystallized materials in nanosize, that is, smaller than 500 nm, which are composed of atoms in a single or polycrystalline organization (Junghanns and Müller, 2008). Nanocrystals are groups of up to thousands of molecules in a crystalline form, self-possessed of a drug within a thin coating.

15.1.2.1.2.4 NANOTUBES Nanotubes are tubes in nanometer scale that belong to the fullerene structural family. They possess a hollow structure that consists of walls made of one-atom-thick sheets of carbon (graphene). These sheets roll along at a particular angle and distinct chiral angles, the radius, and rolling angles decide the characteristics of the nanotube, that is., whether the nanotube shield is semiconductor or metal. They are classified into two types: single-walled nanotubes (SWNT) and multiwalled nanotubes (MWNT) (Malik et al., 2012).

For instance, carbon nanotubes (CNTs) can be SWNT and MWNT. CNTs are used to deliver chemicals to animal and plant cells, and increase the biomass and water-retaining capacity as well as the fruit yield in plants to 18% (Husen and Siddiqi, 2014).

15.1.2.1.2.5 DENDRIMERS Dendrimers have a well-defined shape, size, and molecular mass. They are three-dimensional globular, hyperbranched, monodisperse, nanoscale synthetic polymers. The well-defined feature has been exhibited by molecular and polymer chemistry (Malik et al., 2012).

Out of the several NPs discussed previously, the core focus of the following sections will be concerned with metallic NPs only.

15.1.3 Advantages of Metallic Nanoparticles Over Polymeric Micro- and Nanostructures: Role in Pharmaceutical Systems

Manufacturing carrier systems for biological, chemical, and medical applications face many challenges including stability, safety, and uniformity (Sengani, Grumezescu, and Rajeswari, 2017). Nanoparticulate carriers' success relies on the success of synthesis of biocompatible, stable, and selective NPs, which can be directed to specific sites in the body to be used for systemic administration with good safety and low toxicity (Mody, Nounou and Bikram, 2009). Due to the novel size-dependent behavior and properties of metallic NPs, they have gained great attention in some research fields, as they have been recommended as suitable, stable targeting tools for controlled and sustained release drugs (Sengani, Grumezescu, and Rajeswari, 2017). Besides, metallic NPs are biocompatible, inert, nontoxic, and can be synthesized easily with a different size range (1−150 nm), with low dispersity index and ease of surface functionalization. All these offer dense stacking of targeting ligand on the surface at the low core diameter size, which makes the metal NPs suitable and promising targets for drug delivery systems (Khan et al., 2013). Other advantages of metal NPs, mainly metal oxides, is that they have high catalytic activity, can be recycled, and have good selectivity in addition to a wide range of applications (Wang, Wang and Zha, 2009; Kharisov, Dias and Kharissova, 2014; Seabra and Durán, 2015).

On the other hand, polymeric nanomaterials' properties such as chemical composition, shape, size, surface structure, and charge in addition to solubility, agglomeration, and aggregation, can significantly affect their interactions with cells and biomolecules (Dong et al., 2012). Metallic nanostructures have the advantage over other nanomaterials owing to the probability of domineering the composition, structure, shape, size, encapsulation, assembly and tunable optical properties. Au NPs are most applied metal NPs in the medical field and showed great efficiency toward cancer therapy (Huang et al., 2007; Cobley et al., 2011; Kumar et al., 2013; Figueiredo et al., 2014, no date). Therefore polymeric and metallic NPs are beneficial for applications in drug delivery systems either in combination or alone (Ghosh et al., 2008; Hu et al., 2013).

15.2 GENERAL METHODS IN METAL NANOPARTICLES SYNTHESIS

15.2.1 Physical Approach

The physical approach is considered a top-down method for the synthesis of metal NPs, which is achieved by reducing the size of metal particles to nanosize by different

physical methods. Different physical methods, such as thermal evaporation, ball milling, lithography, and vapor phase preparation, can be used as physical methods for NP synthesis (Ghorbani, 2014).

15.2.1.1 Mechanical Methods

15.2.1.1.1 MECHANICAL BALL MILLING

This technique is used to produce nanosized powders. The powder here is subjected to high energy collision from the balls to reduce their size (Yadav, Yadav and Singh, 2012; Rajput, 2015).

15.2.1.1.2 MECHANOCHEMICAL SYNTHESIS

The concept of mechanochemistry, especially in NPs synthesis, means combining chemical and mechanical aspects of metal at its molecular level (Ghorbani, 2014). This technique depends on producing NPs by using a ball mill at room temperature and a reducing agent to complete the chemical reaction to get the required NPs. Several NPs are produced by using the previous method such as Co (cobalt), Ag, Cu, Cr (chromium), and Al (Paskevicius et al., 2009).

15.2.1.2 Vapor Methods

15.2.1.2.1 LASER ABLATION

Laser ablation method depends on laser pulses, which heat up the target to boiling point. The vapor atoms of the target are produced, then plasma expands adiabatically, and finally, NPs are produced by condensation (Ghorbani, 2014). Mg−Al and Zn−Al are examples of bimetallic NPs (BMNPs) produced using laser ablation (Hur, et al 2009).

15.2.1.2.2 EXPLODING WIRE

The resulting NPs produced by this method depend on the voltage, size, and shape of the wire and the electrical pulse nature. This method depends on a quick and powerful pulse that generates an electromagnetic field around the wire, which holds it together while it is superheated to tens of thousands of degrees. When the current stops, the electromagnetic field vanishes, and the wire divides into nanosized particles. Ag, Cu, Fe, Al, and Au NPs are produced by exploding wire (Sen et al., 2003, YAP et al., 2008).

15.2.1.2.3 GAS EVAPORATION

Gas evaporation depends on evaporating the metal from its molten state into a chamber occupied by an inert gas, where the gaseous metal condenses in nanosized particles (YAP et al., 2008).

15.2.2 Chemical Approach

Chemical approach is the most common approach in NPs synthesis, being a low cost and high yield approach. Generally, the chemical synthesis of NPs includes metal precursors, a reducing agent, and a stabilizing/capping agent. Synthesis via chemical

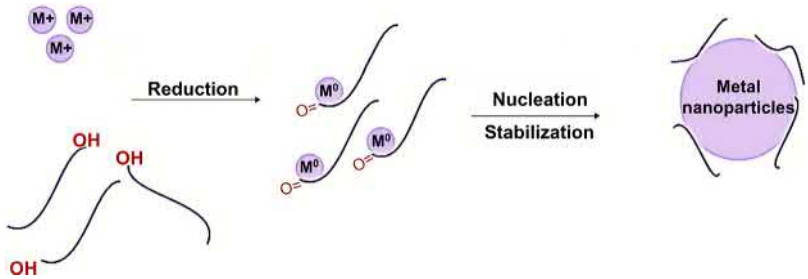

FIGURE 15.4 An illustration of chemical oxidation-reduction reaction of metal salts to produce metal NPs. *NPs*, Nanoparticles. Source: *Adapted with permission from Keat, C.L., et al., 2015. Biosynthesis of nanoparticles and silver nanoparticles. Bioresour. Bioprocess. 2 (1), 47. doi:10.1186/s40643-015-0076-2.*

process is an oxidation-reduction reaction; the reaction involves chemical reduction by organic and inorganic reducing agent, and different reducing agents can be used including sodium citrate, ascorbate, sodium borohydride ($NaBH_4$), elemental hydrogen, *N*,*N*-dimethylformamide, tollens reagent, and polyol process (Evanoff and Chumanov, 2004; Wiley et al., 2005; Merga et al., 2007). An illustration of the proposed reaction is shown in Fig. 15.4. In addition, using protective agents to stabilize dispersive NPs during metal NPs preparation is very important to protect NPs that can be absorbed on or bind onto NPs surfaces to avoid their agglomeration. Also, the addition of surfactants with different functionalities to interact with particles surface is recommended, to stabilize particle growth and to prevent particles from agglomeration, sedimentation, or even from losing their surface properties. Some of the surfactants that can be used are amines, thiols, alcohols, and acids (Oliveira et al., 2005; Khan, Saeed and Khan, 2017).

However, the use of chemically manufactured NPs has some restrictions in biomedical and clinical fields, because the synthesis procedure relates to the use of several nonpolar solvents and toxic chemicals. Part of these chemical approaches include the usage of toxic chemicals in later steps as capping agents and synthetic additives (Thakkar, Mhatre and Parikh, 2010; Ingale, 2013), which will end up in environmental compartments, such as water and soil and other toxic by-products (Das et al., 2017).

15.2.3 Biological Approach

Biogenic synthesis of NPs employs either biological microorganisms or plant extracts or exudates. Numerous bacteria, fungi, algae, yeasts, viruses, and plants are used to synthesize metallic NPs by employing vitamins, enzymes, microbial enzymes, biodegradable polymers, polysaccharides, microorganisms, and different biological systems (Korbekandi, Iravani and Abbasi, 2009; Iravani, 2011).

Biogenic metal NPs can be produced either by bioreduction, where metal ions are chemically reduced into their stable forms where the enzymes are oxidized (Deplanche et al., 2010), or by extracellular and intracellular extract of organisms, where the extracts are mixed with metal salts at room temperature, and within a few minutes the reaction is completed and the NPs are formed.

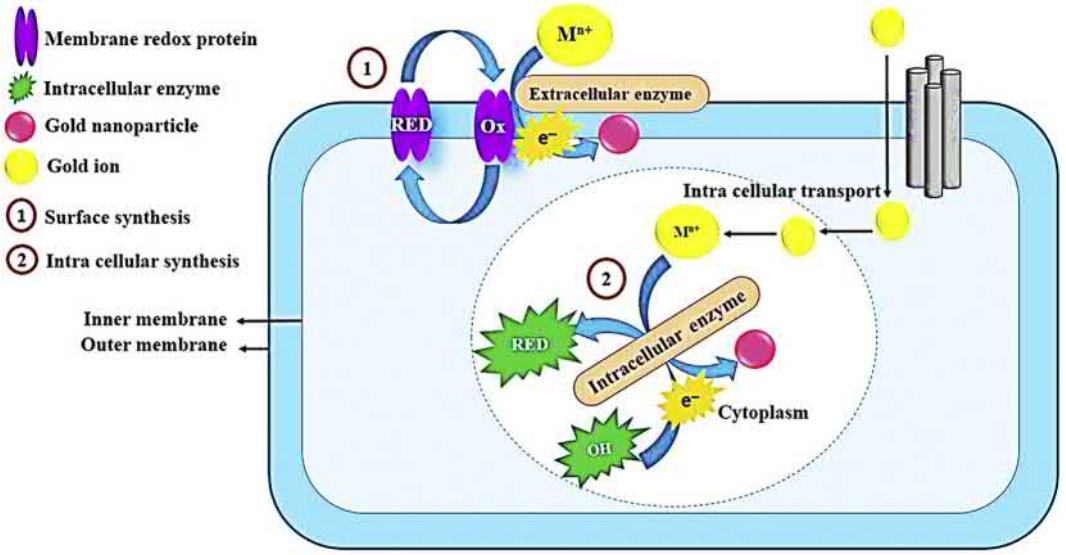

FIGURE 15.5 Intracellular synthesis of metal NPs. The illustration shows the synthesis of gold nanoparticles using the intracellular method. Synthesis can be done either at the surface by extracellular enzymes or by intracellular synthesis of oxidation-reduction reaction by intracellular enzymes. *NPs*, Nanoparticles. Source: *Adapted from Sengani, M., Grumezescu, A.M., Rajeswari, V.D., 2017. Recent trends and methodologies in Au nanoparticle synthesis—a prospective review on drug delivery aspect. OpenNano 37–46. <http://dx.doi.org/10.1016/j.onano.2017.07.001> with permission from Elsevier.*

The NPs produced by these green biologically based methods are inexpensive, safe, and environment-friendly as they reduce environmental pollution and recovering metals from industrial waste (Shah et al., 2015)

Illustrations of the intracellular method and extracellular methods are indicated in Figs. 15.5 and 15.6, respectively.

15.2.3.1 Nanoparticles via Actinomycetes

There are general reports on the intra- or extracellular synthesis of metallic NPs by actinomycetes such as *Rhodococcus* sp. and *Streptomyces* sp. LK-3 (Shah et al., 2015).

In the synthesis of Ag and Au NPs, for example by actinomycetes, nicotinamide adenine dinucleotide dependent nitrate reductase is the responsible enzyme for the reduction of Ag and Au to metallic Ag and Au by the electron transfer mechanism, and for the formation of stabilized NPs (Korbekandi, Iravani and Abbasi, 2009; Shah et al., 2015).

15.2.3.2 Nanoparticles via Algae

Several kinds of algae are known to hold heavy metals and can be used biologically to synthesize metallic NPs such as Ag, Au, and Au–Ag BMNPs, such as unicellular algae *Chlorella vulgaris* (Luangpipat et al., 2011), marine algae *Sargassum wightii* (Govindaraju et al., 2009), *S. wightii*, *Kappaphy cus alvarezii* (Rajasulochana et al., 2010), brown algae *Fucus*

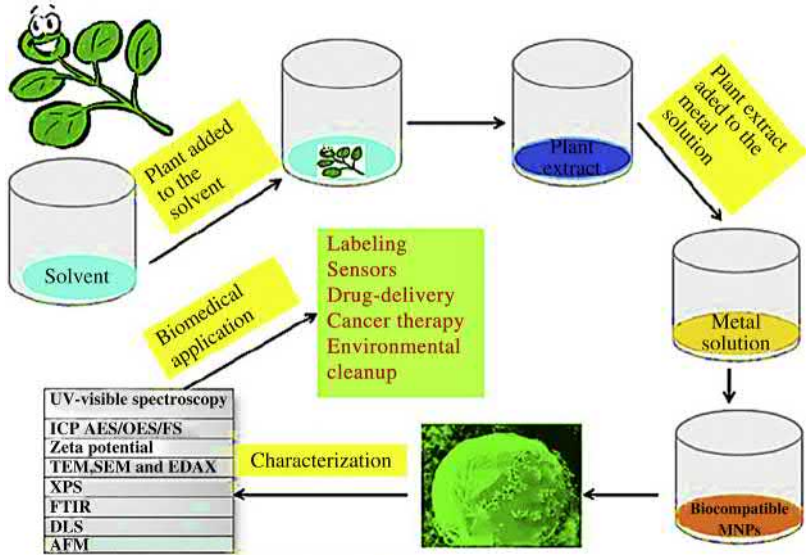

FIGURE 15.6 Illustration shows plants as a source of green nanosynthesis as an example of an extracellular method, and the characterization methods. The required part of the plant is soaked in a solvent; the plant extract is separated and added to the metal solution. Metal NPs formed are indicated by a change in the solution color. The NPs are separated, characterized, and then used. *NPs*, Nanoparticles. Source*: Adapted from Nath, D., Banerjee, P., 2013. Green nanotechnology—a new hope for medical biology. Environ. Toxicol. Pharmacol. 36 (3), 997–1014. doi:10.1016/j.etap.2013.09.002 (Nath and Banerjee, 2013) with permission from Elsevier.*

vesiculosus (Mata et al., 2009), *Tetraselmis kochinensis* (Senapati et al., 2012) red *Chondrus crispus*, and green algae *Spirogyra insignis* via extracellular synthesis (Castro et al., 2013).

15.2.3.3 Nanoparticles via Bacteria

In green nanotechnology, numerous bacteria species have been used to synthesize NPs such as *Thiobacillus ferrooxidans*, *Thiobacillus thiooxidans*, and *Sufolobus acido caldarium* (Brock and Gustafson, 1976), *Staphylococcus aureus*, *Bacillus subtilis*, *Escherichia coli*, *Pseudomonas aeruginosa* (Gudikandula and Charya Maringanti, 2016), and many others (Narayanan and Sakthivel, 2010).

The bacterium is considered a biofactory for metallic NPs syntheses such as Au, Ag, titanium, platinum, palladium, magnetite, cadmium sulfide, titanium dioxide, and many others; also bacteria have the ability to reduce heavy metal ions for synthesizing NPs (Narayanan and Sakthivel, 2010). The type of bacteria, temperature, pH, substrate concentration, the source of a compound of target NPs, reaction time, and irradiation and agitation, affect the size, morphology, shape, and monodispersity of NPs (Pantidos, 2014). It has been noted that the particle size increases with increasing pH value; pH at 3 is the best for the size below 10 nm (Gericke and Pinches, 2006; Li et al., 2011; Rac et al., 2014). Also, particle size and monodispersity were affected by the reaction time (Saifuddin, Wong and Yasumira, 2009). Smaller size and good monodispersity were observed with shorter cell exposure time to ion solution. Also, temperature and rate of reduction are

directly proportional, that is, increase in the synthesis of NPs as the increase in the rate of reduction has been observed at higher temperatures owing to the depletion of metal ions in the formation of nuclei (Vanaja et al., 2013).

15.2.3.4 Nanoparticles via Fungi

Production of metal NPs via fungi, such as *Aspergillus* sp., *Fusarium* sp., and *Penicillium* sp., has attracted scientists as this method proposes many advantages over the use of bacteria. The synthesis in fungi can be done via extracellular and intracellular methods; also the manifestation of mycelia offers an increased surface area allowing fungi to secrete higher amount of proteins than bacteria, which would highly increase the NPs synthesis and production. Some fungi possess high intracellular metal uptake volumes, which lead to smaller size for the particles synthesized (Volesky and Holan, 1995; Mukherjee et al., 2002; Kitching, Ramani and Marsili, 2015).

Some examples for NPs produced by fungi are silica and titania NPs that were produced by *Fusarium oxysporum* (Bansal et al., 2005), magnetite (Bharde et al., 2006), zirconia (Bansal et al., 2004), and oxide NPs (Bansal et al., 2006).

15.2.3.5 Nanoparticles via Viruses

Viruses are well known for their ability to deliver inorganic materials such as cadmium sulfide (CdS), silicon dioxide (SiO_2), zinc sulfide (ZnS), and iron oxide (Fe_2O_3) and convert them to nanosize (Shah et al., 2015). This is however, due to the viruses' dense surface which is covered by capsid proteins which is considered a reactive surface that have the potential to interact with metallic ions. For instance, tomato mosaic virus particle can have as many as 2130 capsid protein molecules covering its surface (Kowshik et al., 2002; Culver et al., 2015).

15.2.3.6 Nanoparticles via Yeasts

NPs synthesis via yeast is done either intracellularly or extracellularly. The synthesis can be done due to the ability of yeast to absorb and accumulate large amounts of toxic metals from the surroundings and through the processes of detoxification, bioprecipitation, chelation, extracellular sequestration and biosorption, the NPs are formed (Shah et al., 2015). Quantum dots of Cd (cadmium), Pb (lead), Au, and Ag are synthesized by yeasts (Dameron et al., 1989; Kowshik et al., 2002; Ung et al., 2012; Borovaya et al., 2015).

There are several kinds of yeasts used for NPs syntheses such as *Candida glabrata*, *Schizosaccharomyces pombe*, *Torulopsis* sp., *Pichia jadinii*, and MKY3 (Shah et al., 2015).

15.2.3.7 Nanoparticle via Plants

The green synthesis of metallic NPs using plants is the most environment-friendly route for synthesis and for detoxification applications. The ability of plants to be part of nanoscale material synthesis is due to plant extract components such as alkaloids, phenolic acids, polyphenols, proteins, sugar, and terpenoids, which are used to reduce metallic ions and stabilize them (Shah et al., 2015). The synthesis process is a straightforward method, done by mixing the metal salt solution with a plant extract at room temperature; this, however, will result in a change of the solution color indicating the creation of NPs in the reaction mixture (Malik et al., 2014).

The properties of plant extract as its concentration, reaction time, metal salt concentration, temperature, and reaction solution pH influence size, morphology, and quality of synthesized NPs (Pantidos, 2014; Shah et al., 2015). There are several metals that are produced in nanosize using plants such as Au, Ag, Cu, Cu oxide, palladium, platinum, titanium dioxide, and selenium, zinc oxide, lead, indium oxide, and iron oxide NPs (Shah et al., 2015).

Biological synthesis of some of metallic NPs by plants, bacteria, and fungi has been reviewed by Pantidos (2014), showing the method used, which is either intra- or extracellular Table 15.1.

TABLE 15.1 Synthesis of Metallic Nanoparticles by Different Microorganisms

Microorganism	Type of Nanoparticle	Location	Size Range (nm)
(A) BACTERIA			
Pseudomonas stutzeri	Ag	Intracellular	~200
Morganella sp.	Ag	Extracellular	20–30
Lactobacillus strains	Ag and Au	Intracellular	–
Plectonema boryanum (*Cyanobacteria*)	Ag	Intracellular	1–10
			1–100
Escherichia coli	CdS	Intracellular	2–5
Clostridium thermoaceticum	CdS	Intracellular and extracellular	–
Actinobacter spp.	Magnetite	Extracellular	10–40
Shewanella algae	Au	Intracellular, pH = 7	10–20
		Extracellular, pH = 1	50–500
Rhodopseudomonas capsulata	Au	Extracellular, pH = 7	10–20
		Extracellular, pH = 4	50–400
E. coli DH5α	Au	Intracellular	25–33
Thermomonospora sp.	Au	Extracellular	8
Rhodococcus sp.	Au	Intracellular	5–15
Klebsiella pneumoniae	Ag	Extracellular	5–32
Pseudomonas aeruginosa	Au	Extracellular	15–30
Shewanella oneidensis	Uranium (IV)	Extracellular	–
(B) YEAST			
MKY3	Ag	Extracellular	2–5
Candida glabrata and *Schizosaccharomyces pombe*	CdS	Intracellular	200

(*Continued*)

TABLE 15.1 (Continued)

Microorganism	Type of Nanoparticle	Location	Size Range (nm)
(C) FUNGI			
Phoma sp. 3.2883	Ag	Extracellular	71.06–74.46
Fusarium oxysporum	Au	Extracellular	20–40
Verticillium	Ag	Intracellular	25 ± 12
Aspergillus fumigatus	Ag	Extracellular	5–25
Trichoderma asperellum	Ag	Extracellular	13–18
Phanerochaete chrysosporium	Ag	Extracellular	50–200
F. oxysporum and *Verticillium* sp.	Magnetite	Extracellular	20–50
(D) PLANT AND PLANT EXTRACTS			
Azadirachta indica (Neem)	Ag, Au, and Ag/Au bimetallic	Extracellular	50–100
Geranium leaves plant extract	Ag	–	16–40
Lemongrass plant extract	Au	–	200–500
Avena sativa (Oat)	Au	Extracellular	5–85
Alfalfa sprouts	Ag	Intracellular	2–20
Aloe vera	Au	Extracellular	50–350
Cinnamomum camphora	Au and Ag	Extracellular	55–80
(E) ALGAE			
Sargassum wightii	Au	Extracellular	8–12
Chlorella vulgaris	Au	–	9–20

Adapted from Thakkar, K.N., Mhatre, S.S., Parikh, R.Y., 2010. Biological synthesis of metallic nanoparticles. Nanomedicine 6 (2), 257–262. doi:10.1016/j.nano.2009.07.002 with permission.

15.2.3.8 Nanoparticles via Animal Tissues

Animal tissues have many organic, inorganic, and biomolecules; they can be a likely source of capping and reducing agents for the biosynthesis of metal NPs. These include for example silk fibroin, which is produced for example from silkworms and spiders, some invertebrates' tissues such as starfish, and chitosan.

15.2.3.8.1 SILK PROTEINS (FIBROIN AND SERICIN)

NPs can be produced by using silk proteins, as they are natural semicrystalline biopolymers. The main compounds in silk fibroin include amino acids, such as alanine, glycine, and serine (Zhao, Li and Xie, 2015). Nano fibroin–TiO_2 has been produced by using fibroin, nanohydroxyapatite (nano-HA)/silk fibroin, and the obtained crystalline particles measured 100 nm in length (Feng et al., 2007).

Also, sericin, which is produced by silkworms, has been used in NPs production. The literature reported that the extracted sericin is reduced by rotation to attain a condensed sericin solution. The nanosericin powder is gained after ultrasonication for reduction of the particle size lyophilization (Gang et al., 2008; Agrawal and Bhushan, 2013), and these fibers were found to resist oxidation, had antimicrobial activity, and were ultraviolet (UV) resistant and biocompatible (Agrawal and Bhushan, 2013).

15.2.3.8.2 INVERTEBRATE

Nano-HA is being studied for medical purposes, for example, for osteogenesis. Nano-HA is synthesized from HA, a biological material found in sponges and starfish (Müller et al., 2009). Different species of worms are used to produce nano-red Au, by mixing the warm extract with $HAuCl_4$, for example earthworms, *Eisenia andrei*, and also marine worms (poly chaeta) have been used to produce Ag NPs (Wang et al., 2007; Djafari et al., 2018).

15.2.3.8.3 CHITOSAN

Chitosan is a peptide derived from invertebrate chitin. Nanofibers and nanocapsules can be produced from chitosan; these capsules are used to slow the release of vaccines and can be used for cancer treatment (Gunduz, 2014; Singh, Sahu and Thangaraj, 2014). Poly-hydroxyethyl-methacrylate-chitosan-MWCNT (multiwalled CNT) nanocomposite is used for pharmaceutical and industrial applications as carriers (Wijesena et al., 2015). ZnS/Chitosan nano-photocatalysts are used for photodegradation of dangerous organic contaminants that can be found in wastewater (Malathi et al., 2015). Also, chitosan-polyacrylic acid NPs of 50 nm were proved to have antifungal activity (Mahmoodian et al., 2015).

15.3 SYNTHESIS OF GOLD NANOPARTICLES

Au NPs have different properties other than their macro and micro size. They are an inert metal for various chemical reactions. Synthesizing Au in nanosize gives it many different exceptional properties such as electronic motion with spatial length scale, which is a special electronic property, and localized surface plasmon resonance (LSPR), (Pooja, Joginder, and Suresh, 2014; Vadlapudi and Kaladhar, 2014).

The Au NPs are important components for the biomedical and biotechnology fields as they have high electron conductivity and large surface area (Tedesco et al., 2010). They have been used as radiant enhancer (Khan, 2012) and in radiation therapy, labeling of protein biomolecular detection, biosensors, and for antimicrobial activity (He et al., 2007a, b; Hutter and Maysinger, 2013; Shevtsov et al., 2017) and anticancer activity especially for lung, colon, breast, prostate, an cardio cancers (Sharon, Oza and Pandey, 2012).

The Au NPs are wine-red in solution. Au (III) ion reduction to Au atom implicates binding of the atom to the surface of the cell. Au NPs can differ in size from 1 to 8 nm, and also have numerous shape, and structures such as suboctahedral, spherical ring, tetrahedral, icosahedra, octahedral, nanorods, decahedral (Sun, Mayers and Xia, 2002; Kamble, Jagdale and Kadam, 2010; Bandyopadhyay et al., 2018), Au nanorods (Au NRs),

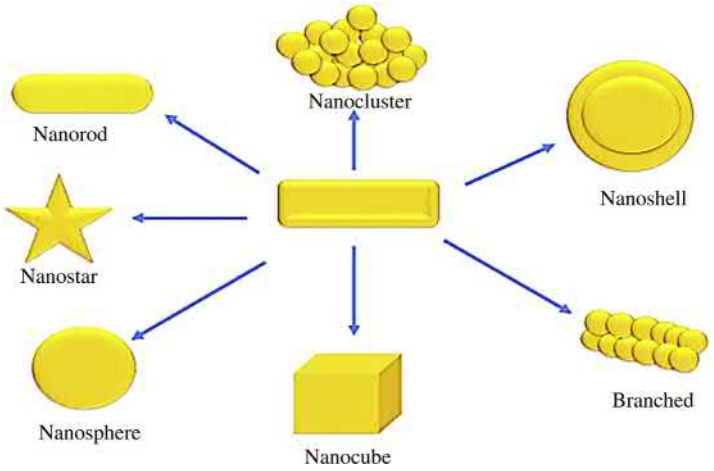

FIGURE 15.7 Different gold NP shapes (Alaqad and Saleh 2016). *NP*, Nanoparticle.

Au nanoshells (Murphy et al., 2005; D'Acunto, 2018), and hollow Au NPs (Oldenburg et al., 1998; Xiong et al., 2018). Different shapes of Au NPs are illustrated in Fig. 15.7.

Chemical synthesis of Au/NPs is done by the reduction process of different oxidizing agents such as $HAuCl_4$ through a solution of thiolated chitosan (Giljohann et al., 2010), or inositol hexa kis phosphate (IP6) (Amjadi and Farzampour, 2014) or trisodium citrate, and hydrogen tetrachloro cuprate III tetrahydrate (chloroauric acid) (Saleh, 2011b). Au NPs are made by employing peptide-biphenyl hybrids as a stabilizer for Au NPs (Pérez, Mann and Herradón, 2011).

Physical methods used for Au NPs synthesis include γ-irradiation technique, which leads to the synthesis of highly pure and uniform size of Au/NPs within the range 5−40 nm; this method includes the use of polysaccharide alginate as a stabilizer (Rezende et al., 2010). Also, microwave irradiation technique was utilized to prepare Au/NPs by using different reducing agents such as citric acid and cetyltrimethylammonium bromide (CTAB) as a binding agent (Guo et al., 2012).

Green method of Au/NPs synthesis can be done by different biomolecules, which replace the conventional stabilizing and reducing agents (green plants, algae, yeast, fungi, and bacteria). It was reported that $HAuCl_4$ was reduced by utilizing citrus fruit juice extracts (Tarnawski and Ulbricht, 2011). Moreover, the edible mushroom was used in the formulation of Au/NPs by light power (Nalawade, Mukherjee and Kapoor, 2012).

15.4 SYNTHESIS OF SILVER NANOPARTICLES

Ag NPs (Ag NPs) have gained significant attention because they also have the properties of LSPR, which gives them importance in medical applications. They also have unique broad-spectrum antimicrobial characteristic against fungi, virus, and bacteria (Jana and Pal, 2007; Monteiro et al., 2009; Stiufiuc et al., 2013; Franci et al., 2015). Ag NPs also have optical, electrical, and thermal properties that make them essential in the industrial application of electronics, catalysis, and photonics (Bosetti et al., 2002; Sondi, Goia and

Matijević, 2003; Li et al., 2008; Rahman et al., 2013; Behnam et al., 2018). They have been applied in surface-enhanced Raman spectroscopy (SERS) (Konrad, Doherty and Bell, 2013), chemical and biological sensors, and in biomedicine materials (Thanh and Green, 2010; Evtugyn et al., 2014; Shefi et al., 2014), in addition to biomarkers (Bu and Lee, 2012; Rivero et al., 2013; Luo et al., 2015). The most important use of Ag NPs is targeting of cells and treatment of diseases, such as interacting with HIV-1 virus and stopping it from binding to host cells in vitro (Tran, Nguyen and Le, 2013).

The antimicrobial activity of Ag NPs has benefited different applications such as (1) coatings (Aymonier et al., 2002; Ahamed, Alsalhi and Siddiqui, 2010); for example, coating vegetable oil with Ag NPs shows excellent antimicrobial properties (Kumar et al., 2008; Hazer and Kalaycı, 2017); (2) Ag NPs deposited in carbon filters reduced water-related diseases (Le Pape et al., 2002; Naeem et al., 2019); and (3) nanocrystalline Ag was used in wound dressing to treat ulcers (Bhattacharya and Mukherjee, 2008; Wang et al., 2018; Xu et al., 2018).

Chemical reduction is the most widely used method for chemical synthesis of Ag NPs. This method is considered simple, low cost, and high yield. The chemical reduction depends on these components: metal precursor; a reducing agent such as ethylene glycol, glucose, $NaBH_4$; and stabilizing/capping agents such as sodium oleate, polyvinylpyrrolidone (PVP), polyvinyl acetate. However, the shape and size of chemically synthesized Ag NPs depend on the components of the reaction in addition to the adjustment of the reaction parameters as temperature and pH (Evanoff and Chumanov, 2004; Chen and Zhang, 2012; Dang et al., 2012; Patil et al., 2012; Iravani et al., 2014).

Physical synthesis of Ag NPs can be achieved by different methods such as condensation, evaporation, and thermal decomposition methods (Jung et al., 2006; Iravani et al., 2014). The ceramic heating process is used to produce the monodisperse and uniform size of Ag NPs (Saleh, 2011a). Physical techniques utilized for the synthesis of Ag NPs resulted in uniform shape and size of Ag NPs (Sintubin, Verstraete and Boon, 2012; Saleh, 2013). However, primary costs for the investment of equipment, time consumption, and the requirement of high energy should be considered (Lee and Kang, 2004).

In green chemistry, the traditional stabilizing and reducing agents have been replaced by biomolecules. In the biological technique, Ag NPs are produced by using bacteria, yeast, fungi, algae, and plants as reducing agents and stabilizing agents (Suresh et al., 2010); for example, *Trichoderma ride* fungus was used for Ag NPs synthesis from $AgNO_3$ as a precursor (Fayaz et al., 2010). Also mixing *Fastia japonica* leaf extract with $AgNO_3$ produced Ag NPs with excellent antimicrobial activity (Zhang et al., 2017).

15.5 SYNTHESIS OF IRON NANOPARTICLES

The unique properties of iron oxide NPs like surface to volume ratio, superparamagnetism, ease of separation methodology, and high surface area are attractive for scientists. These special properties enabled the iron oxide NPs to be used in many scientific fields such as biomedicine, biomedical applications for protein immobilization as drug delivery, diagnostic MRI, thermal therapy, agriculture, and environment (Carvalho et al., 2013).

Iron oxides are found in different forms in nature, the most common ones include FeII $FeIII_2O_4$ ferromagnetic, Fe_3O_4 magnetite, α-Fe_2O_3 (weakly ferromagnetic or antiferromagnetic and hematite), γ-Fe_2O_3 (ferromagnetic, maghemite), FeO (wüstite, antiferromagnetic), ε-Fe_2O_3 and β-Fe_2O_3. When ferromagnetic materials form NPs with size less than 15 nm they are called superparamagnetic due to their unique magnetism.

Magnetic iron oxide NPs have advantages over other iron oxides such as large surface to volume ratios, which lead to high surface energies and the ability to aggregate to minimize the surface energies (Wu, He and Jiang, 2008).

Iron NPs are oxidized quickly as they are highly reactive, mainly in the presence of air. To overcome this disadvantage, proper surface coating should be applied to the naked iron oxide as well as provision of effective protection strategies to maintain the stability of magnetic iron oxide NPs. Different coating materials can be used for a thin coat for complete and permanent protection of the iron NPs from oxidation without affecting the magnetic property of the NPs (Wu, He and Jiang, 2008).

Different inorganic or organic molecules can be used for Fe_3O_4 NPs coating; these molecules include magnesium, gold, iron carbide, and silica, also adjoining the iron magnetic NPs with N_2 gas, that is, oxygen-free environment has a double effect on iron NPs, reducing the size and protecting the NPs from oxidation (Maity and Agrawal, 2007; Soenen et al., 2010).

Iron oxide NPs can be prepared by several physical methods including mechanochemical or vapor methods such as electrodeposition, pyrolysis, arc discharge, laser ablation, and combustion. Chemically synthesized iron oxide can be done through coprecipitation, sol–gel synthesis, reverse micelle, template-assisted synthesis, and hydrothermal methods. Many shapes of iron oxide NPs can be obtained by changing the iron salt precursor in different synthetic protocols; these shapes include nanocubes, porous spheres, nanorods, nanohusks, self-oriented flowers, and distorted cubes (Ali et al., 2016).

The size of the iron oxide NPs has a direct relation with the composition and magnetic behavior of these NPs (Carvalho et al., 2013). Iron oxide NPs within the size of 7–20 nm can be achieved by precipitation methods. The first method is done in a controlled atmosphere and the second one under air since it relies on reduction–precipitation; in some cases hydrothermal treatment can be used afterward. The advantage of reduction–precipitation method is the ability to produce the smallest NPs in size.

Green synthesis of iron NPs has shown ease and success in addition to lower time consumption; for instance, iron NPs have been synthesized by using *Camellia sinensis* leaves extract. Green tea extract polyphenols have properties for reducing the ferric cations and also act as capping agents (KSV, 2017).

15.6 SYNTHESIS OF ZINC OXIDE NANOPARTICLES

Zinc oxide (ZnO) NPs are well known for their large bandwidth and high excitation binding energy, which enable them to be used in biomedical applications; for example, ZnO absorbs a wide spectrum of radiation (UV, microwave, infrared, and at radio frequencies), so it can be used for the production of cosmetic ointments and creams (Kim et al., 2017). It is also used as sensors due to its semiconductivity (Bogutska, Sklyarov, and

Prylutskyy, 2013; Mittal, Chisti and Banerjee, 2013; Baskoutas, 2018). It also has antibacterial properties, so it is used in producing fabrics for clothing to prevent microbial and bacterial growth (Dastjerdi and Montazer, 2010).

Colloidal nanocrystalline quantum dots of CdSe/ZnS possess unique size-dependent optical properties, which make them an alternative to fluorescent organic dyes. Nanozinc (Zn NPs) compounds are also used for identifying antigens in malignant tumors and are used as immune markers (Sukhanova et al., 2004; Jiang, Pi and Cai, 2018).

There are several methods for ZnO synthesis; physically it can be prepared by colloidal dispersion, vapor condensation, and amorphous crystallization (Vidya et al., 2013; Aladpoosh and Montazer, 2015; Elumalai et al., 2015; Krupa and Vimala, 2016). Also, ZnO NPs synthesis can be done by nanosecond laser ablation of zinc by immersing the target in distilled water. Particle sizes of ZnO are usually in the range of 36 and 88 nm when ablated with 1064- and 532-nm lasers, respectively (Ismail et al., 2011).

In chemical methods such as reduction, ZnO NPs are synthesized by using zinc nitrate and KOH in aqueous solution resulting in particle size in the range of 30 ± 15 nm (Ghorbani et al., 2015).

For the biological synthesis of ZnO, plants, fungus, and bacteria are used to produce ZnO NPs (Agarwal, Venkat Kumar and Rajeshkumar, 2017). ZnO NPs synthesis via biological process can be achieved by combining zinc acetate, sodium hydroxide to plant extract such as leaves of *Catharanthus roseus* as they will interact with its biological components to produce spherical ZnO NP with an average size of 23–57 nm. The biological activity of these NPs was evaluated showing antibacterial activity against *Pseudomonas aeuroginosa* for instance. The advantages of this biological method for ZnO NP synthesis are ease of synthesis, cost-effectiveness, quick reaction, eco-friendliness in addition to the absence of side effects, so can be used in the preparation of antibacterial formulations (Savithramma and Bhumi, 2014).

15.7 SYNTHESIS OF COPPER NANOPARTICLES

There is an interest in synthesizing metallic copper and copper (I) oxide NPs due to their catalytic activity, sensing and surface properties. Copper NPs (Cu NPs) are used as antibacterial (Thirugnanasambandan and Alagar, 2011; Ramyadevi et al., 2012) and fungal agents when applied in coatings, plastics, and textiles, nanowires, and nanofibers (Nasirian, 2012).

Also, Cu NPs have the high surface area to volume ratio, low production cost, optical, and magnetic properties. So, Cu nanowires are used in nanoelectronics and have applications in magnetic devices, nanosensors, electron emitters, and other electronic applications. Cu NPs are also used as nanoprobes in medicines and bioanalytical areas (Toimil Molares et al., 2003; Din and Rehan, 2017).

Cu NP synthesis showed difficulties due to its high oxidation tendency and the higher stability of Cu oxides (Jeong et al., 2008; Balela and Amores, 2015), so the synthesis process must be prepared under inert atmosphere (Chen and Sommers, 2001; Mott et al., 2007; Suramwar, Thakare and Khaty, 2016); for that Cu NPs produced are usually protected with a capping agent in attempt to minimize oxidation. However, the stabilizers or

capping agents can reduce the oxidation but cannot solve the oxidation problem completely (Liu and Bando, 2003; Kobayashi et al., 2009; Tamilvanan et al., 2014). Also, different inert media such as nitrogen and argon have been used to overcome the oxidation drawback (Jana et al., 2000; Vanden Bout, 2002; Tamilvanan et al., 2014).

For Cu NPs synthesis, chemical and physical approaches are two basic techniques used for synthesis (Tamilvanan et al., 2014). Some of these methods include pulsed laser ablation (Yeh et al., 1999), vacuum vapor deposition (Wang, Chen, and Liu, 2006), microemulsion techniques (Pileni, 1993), sonochemical reduction (Kumar et al., 2001), electrochemical (Toimil Molares et al., 2001), microwave assisted (Felix, Chakkravarthy and Grace, 2015), and hydrothermal process (Liu et al., 2007).

Also biological or biosynthesis of Cu NPs have been achieved by using ascorbic acid as both protecting and reducing agent, which makes the procedure environment-friendly, economical, and nontoxic (Umer et al., 2012). Also, microwave-assisted synthesis can be combined with green synthesis as this method increases the yield of crystalline Cu NPs with better stability of about four months (Nasirian, 2012).

15.8 SYNTHESIS OF ALUMINUM NANOPARTICLES

The nanosized aluminum NPs (Al NPs) are more favorable and gained much attention for being active material with high reactivity, and having large specific surface area and high enthalpy of combustion and rapid kinetics (Paskevicius et al., 2009; Chaturvedi, Dave, and Shah, 2012).

The chemical and physical properties such as morphology, size, and stability of the metal NPs are strongly influenced by the experimental settings (Sharma, Yngard and Lin, 2009; Khan, Saeed, and Khan, 2017).

There are three main physical approaches for Al NPs synthesis, which include mechanical and mechanochemical approaches such as solid phase technique, laser ablation, explosive wire, and gas evaporation for liquid and gas-phase processes. Firstly, the solid phase synthesis of around 25−100 nm Al NPs requires a chemical reaction that originates inside the ball mill where sodium (Na) or lithium (Li) metals act as reducing agents to react with the unreduced aluminum such as aluminum chloride ($AlCl_3$) at room temperature, which is why the process is termed mechanochemical (Paskevicius et al., 2009).

Laser ablation using liquid and gas-phase techniques are used for Al NPs synthesis. Formation of NPs by laser ablation requires the Al target to be immersed in liquid and synthesized by this method as mentioned in the physical approach section. Al powder targets can be immersed in acetone, ethanol, and ethylene glycol. However, acetone media leads to finer NPs than using ethanol medium, with a mean diameter of 30 nm and with the narrower size of distribution (from 10 to 100 nm) (Ganeev et al., 2010).

Synthesis via exploding wire method requires the explosion of the respective wire, triggered by great current densities in the wires. The explosion should be performed in a dense medium, usually certain heavy alcohol or deionized water, which allows the particles to remain suspended and then collected (Sen et al., 2003; Ranjan et al., 2017).

Cryomelting, a modified gas evaporation method, is done by using an inert gas and can be used for Al NP synthesis. The method involves rapid condensation in the cooled region

of about 70K of the evaporated metal. 60% of the particles synthesized by this method are smaller than 70 nm while the remaining 40% will be in the range of 20–500 nm (Champion and Bigot, 1998; Ghorbani, 2014).

For the chemical reduction method for Al NPs synthesis, benzildiethylenetriamine in ethanol has been used as a reducing agent. Al NPs produced by this method fall in the range of 4–13 nm (Haber and Buhro, 1998), while the decomposition method generally yields Al particles of 50–200 nm in average size (Niaz et al., 2013).

15.9 SYNTHESIS OF PLATINUM NANOPARTICLES

Platinum (Pt) is well known for its catalytic activity especially in fuel cells, as Pt NPs are used in reformers for the production of hydrogen from the solid, liquid, or gaseous energy carrier, also Pt NPs are used as a biosensor (Lim, Lee, and Lee, 2008).

The active size of platinum NPs is 1–2 nm, while the shape of Pt NPs depends on the preparation method. These methods include colloidal systems (Pileni, 1997; Leong et al., 2014), reduction by formaldehyde and sodium borohydride (Wu and Chen, 2003), using bacteria cellulose as hydrophilic matrix (Evans et al., 2003), microemulsion (Sanchez-Dominguez, Boutonnet and Solans, 2009), sol–gel (Suffredini, Salazar-Banda and Avaca, 2009), sonochemical method (Angelucci, D'Villa Silva and Nart, 2007), and electrodeposition (Sieben, Duarte and Mayer, 2008).

15.10 SYNTHESIS OF RUTHENIUM NANOPARTICLES

Ruthenium (Ru) is one of the interesting transition metals because Ru can easily be reduced and only crystallizes in hexagonal compact structure, where other transition metals crystallizes in cubic structures in the absence of single axis which causes difficulty of the anisotropic growth in homogeneous solutions (Viau et al., 2003).

Ru NPs are also considered one of the most versatile catalysts in many reactions (Astruc, Lu and Aranzaes, 2005). They can play a role in many reactions, as double bond catalytic hydrogenation (Pelzer et al., 2003), arena (Choi et al., 2008) and carbonyl hydrogenation (Roucoux, Schulz and Patin, 2002; García-Peña et al., 2015), methane oxidation (Astruc, Lu and Aranzaes, 2005), ammonia synthesis (Seetharamulu et al., 2009), and in cross-coupling (Scholten, Leal and Dupont, 2012), and in carbenoid transfer reaction (Chen et al., 2006).

Chemical synthesis of ruthenium NPs is done by simple reduction of common cation solvent salts such as $RuCl_3$ (Patharkar, Nandanwar, and Chakraborty, 2013), or by decomposition of zero-valent compounds, such as $Ru_3(CO)_{12}$, or [Ru(cyclooctadiene) (cyclooctatetraene)] (Philippot, Lignier and Chaudret, 2014).

Physical synthesis of Ru NPs can be done by decomposition of Ru on thermally reduced graphite oxide in propylene carbonate by using microwave irradiation (Marcos Esteban et al., 2015)

Most Ru NPs are produced via chemical colloidal approach but this technique has disadvantages such as using the reducing agents and solvent in excess, size dependence on the intensity of the precursor salt, and high temperatures and long time of reaction

(Yang et al., 2004). In addition, the presence of molecular species was shown to be more stable than the zero-valent ones (Levason, Quirk and Reid, 1997; Garcia-Peña et al., 2013).

Mechanochemical synthesis of Ru NPs is applied to produce valent Ru NPs. This technique is designed to leave aside solvents and reduces reaction times of NPs preparation (Ricceri and Matteazzi, 2004), also it produces Ru NPs with a mean diameter of 1.8 nm and an SD of 0.40 nm. This method includes mixing ($RuCl_3$.n H_2O) with sodium borohydride and milling for few minutes in an agate mortar, after which a dark gray powder is obtained. Next steps are washing the powder with acetone or ethanol then centrifuging, whereby the supernatant is separated and contains Ru NPs (Garcia-Peña et al., 2013).

15.11 SYNTHESIS OF BIMETALLIC NANOPARTICLES

Metal NPs can be synthesized as bimetallic, trimetallic, or multimetallic (containing two, three, and more than three metals, respectively) (Khanal et al., 2014). Among these different metal NPs, BMNPs are favored over monometallic because for their better stability, selectivity, and catalytic activity (Stamenkovic et al., 2007; González, Arbiol, and Puntes, 2011). Also, BMNPs have a widespread application in various fields, specifically magnetic BMNPs are used for the modified drug delivery (Pankhurst et al., 2003) and conjugation of specific proteins (Sharma et al., 2017).

BMNPs have several architectures, that is, crown jewel, hollow, heterostructure, core−shell structure, or alloyed structures (Liu, Wang, and Li, 2012; Domènech et al., 2016).

Synthesis of BMNPs can be achieved by physical, chemical, electrical or biological methods. For physical methods, the BMNPs can be synthesized by a laser irradiation method where no chemical agents are used, the synthesis is done by using only laser irradiation of high intensity on aqueous solution. For example, Pt−Au BMNPs are synthesized by a laser irradiation method (Chau, Chen, and Yang, 2017).

For chemical synthesis of BMNPs, various synthesis methods are used via the chemical routes, such as, reverse metallic method, which is found in water or in oil microemulsions with certain composition such as nanosized droplets Fe−Co synthesized by using reverse metallic method (Uskoković and Drofenik, 2005; Sharma et al., 2017).

In the electrical method, the process is done at the electrode gap and constant current. Particles synthesized are kept in cooling liquid under the effect of gravitational force such as Cu−Ag (BMNP) (Yanık et al., 2013). The microwave irradiation is preferred for the synthesis of BMNP as microwave heating replaces the use of chemicals and reduces reaction time; Fe−Ru is produced by microwave irradiation (Du et al., 2009).

In the radiolytic coreduction method, NPs can be prepared with the use of ionization radiations such as UV, X-ray, as well as gamma radiation, in presence of a stabilizer such as Ag-Pd BMNPs are produced by using this method (Lee et al., 2007a,b; Karim et al., 2007). On the other hand, several other methods are used to produce other types of BMNP, such as the sol−gel method used to produce Cu−Ce BMNP, which is a process that occurs in four steps, that is, hydrolysis, condensation, growth, and agglomeration of particles (Rajput, 2015). Also, sonochemical coreduction method helps in synthesizing NPs of large surface area and small size; Au−Ru BMNPs are produced by using this method (Anandan, Grieser and Ashokkumar, 2008).

In the biological green method, NPs synthesis using living organisms such as plants and microbes has been used (Yamamoto et al., 2010; Kumar et al., 2012). Au_Ag are produced by using persimmon leaf extract (Song and Kim, 2008), while Au−Ag alloy was produced by mahogany leaves (Mondal et al., 2011), and Fe−Pd is produced by using green tea extract (Smuleac et al., 2011).

The BMNPs are used in electrochemical sensing; for example, (Pt/Ir-C) nanocomposites are used for the electrochemical sensing of hydrogen peroxide (Chang et al., 2014). Also, the mechanical effect of BMNPs reinforces composite coatings (Sharma et al., 2017).

15.12 SYNTHESIS OF METALLOID AND NONMETAL NANOPARTICLES

Metalloids are chemical elements found in group IVA, VA, VIA in the periodic table; their properties are a combination of metals and nonmetals. Some of these metalloids include silicon, germanium, antimony, arsenic, boron, and selenium, which is less commonly included in the metalloid group and exists as an oxyanion (Cutter, 2001; Cope, 2017).

Metalloids and nonmetals can also be used for the synthesis of NPs, such as selenium for metalloids and sulfur for nonmetals.

15.12.1 Synthesis of Selenium Nanoparticles

Selenium (Se) NPs have high photoconductivity, catalytic action in hydration and oxidation reactions (Stroyuk et al., 2008), and they have high piezoelectric, thermoelectric, and nonlinear optical responses (Chen et al., 2010a,b). Selenium NPs have been applied in many biomedical applications as drug delivery systems (Ren et al., 2013; Black et al., 2014), and as anticancer agents (Lan et al., 2013).

Se NPs chemical synthesis has been done by different methods including reduction of selenourea and peroxynitrite, also by decomposition of sodium selenosulfate (Mishra et al., 2005; Stroyuk et al., 2008). Also, Se NPs have been synthesized by reducing selenium tetrachloride in the presence of ascorbic acid. An optimization study with poly (sodium 4-styrenesulfonate) produced stable and spherical narrowly size-distributed NPs (46 nm), which are considered highly monodisperse (Gangadoo et al., 2017).

Many physical methods have been used for Se NPs syntheses like direct physical vapor decomposition process, hydrothermal process, and ultrasonic radiation (Cao et al., 2004; Chen et al., 2009, 2010a,b). Also, in a study conducted by Ju-Ying et al. (2011) it has been reported that the mixed approach was used where selenious acid was used as a source of Se, then was further reduced to spherical Se NPs using protein (silk fibroin) prepared from the cocoon under microwave radiation for 10 minutes (Chhabria and Desai, 2016).

Several green methods for elemental selenium NPs synthesis was reported to include the synthesis of Se NPs by bacteria, fungi, and plants, for example, (1) reduction of selenite was achieved using *P. aeruginosa*, under aerobic conditions (Kora and Rastogi, 2016);

(2) bacteria *Zooglea ramigera* have been used for mediated biosynthesis of selenium NPs, where the biosynthesized NPs were spheroids with a size range of 30−150 nm; and (3) *Vinifera* (raisin) extract was employed as a substrate for selenium NPs synthesis (Sharma et al., 2014). Garlic acid, which is considered as plant polyphenol, was also used as a substrate for Se NPs synthesis (Barnaby et al., 2013).

15.12.2 Synthesis of Sulfur Nanoparticles

Sulfur is considered a nonmetal and has a wide range of applications at the micro- and nanoscale in many industries such as sulfuric acid production, fertilizers, enamels, and the plastics, paper, and pulp industries; also it has antimicrobial and anticancer activities (Suleiman et al., 2015; Salem et al., 2016).

Sulfur NPs have different shapes and sizes that rely on the method used for preparation and parameters. Sulfur NPs have spherical, monoclinic, orthorhombic, rhombic, and nanowire shapes (Suleiman et al., 2013).

Sulfur NPs are prepared by many technologies, such as acid hydrolysis of sodium thiosulfate (Suleiman et al., 2015), oxidation-reduction of hydrogen sulfide H_2S gas by Fe−Chelate, resulting in small particle size distribution and nearly uniform average particle size 10 nm in comparison to that in aqueous surfactant systems, as examples of chemical methods (Deshpande et al., 2008).

For the synthesis of SNPs by physical approach, many methods have been used, for example (1) sulfur NPs were prepared by the ultrasonic method, which produced a particle size of a diameter of around 20 nm, uniform spherical shape, small size distribution, and good purity (Guo et al., 2006a,b; Suleiman et al., 2013); and (2) sulfur NPs can also be prepared by using electrochemical methods. The advantage of this method is that the particle size of sulfur NP can be adjusted to 35−65 nm by controlling the operation parameters. For example, by adjusting the initial sodium thiosulfate concentration, the use of cold water or hot alcohol as nonsolvent/solvent system alongside with 100 mL/min flow rate for comixing of nonsolvent resulted in the formation of sulfur NPs in an average size of 250 nm that are properly homogeneous in shape with a small particle size distribution (Shamsipur et al., 2011).

Also, sulfur NP can be synthesized by green approach by using plants; for example, sulfur NPs were produced by using *Melia azedarach* leaves aqueous extract and citric acid. The particles were crystalline in nature with a spherical shape, and the average particles size that was achieved by this method was around 20 ± 4 nm (Salem et al., 2016).

15.13 SURFACE PROPERTIES OF METAL NANOPARTICLES

Knowing the surface properties of metal NPs aids in the better determination of functional groups for surface functionalization and finding a proper application of metal NPs, Surface charge, morphology, and size are the main properties that can be easily determined through different characterization methods, which rely on advanced microscopic

techniques such as scanning electron microscopy (SEM), transmission electron microscopy (TEM), and atomic-force microscopy (AFM) (Bhatia, 2016).

Determination of the surface charge aids in proper prediction of the electrostatic interaction with bioactive compounds in addition to the interaction of NPs within the biological environment. For example, zeta potential (ZP) is an indirect method in measuring the surface charge (which will be explained in more detail in a later section) and aids in predicting the stability of colloidal material by evaluating the storage stability of materials. ZP aids in assuring stability to avoid aggregation of MNP. This is useful in the valuation of surface hydrophobicity along with the nature of the material that is encapsulated either inside the nanocapsules or coated on the surface (Pal et al., 2011). In addition, surface hydrophobicity measurement can be achieved by using other methods such as biphasic partitioning, contact angle measurements, hydrophobic interaction chromatography and adsorption of probes, etc. Moreover, modern techniques such as X-ray photon correlation spectroscopy have been recently used as a revolutionary tool for the analysis of surface NPs since this technique enables the identification of cations of specific chemical groups that are present on the surface of NPs (Scholes et al., 1999; Shpyrko, 2014; Jang et al., 2016; Lewis et al., 2018).

The next section will elaborate on various methods used in the characterization of metal NPs and surface properties.

15.14 METHODS USED IN METAL NANOPARTICLES CHARACTERIZATION

The basic properties that rely on the characterization of MNPs are optical properties, size, shape (morphology), and surface charge. Spectroscopy is used to study the optical properties. Fourier transform infrared spectroscopy (FTIR), X-ray crystallography (XRD), energy-dispersive X-ray (EDX) spectroscopy, and fluorescence correlation spectroscopy (FCS) are used for studying the basic molecular and chemical composition of metal NPs. Whereas SEM, TEM, scanning tunneling microscopy (STM), environmental SEM (ESEM), and tip-enhanced Raman spectroscopy (TERS) are used for imaging to study morphology and topography. This section will highlight these methods including their principal uses, advantages, and some of the disadvantages or limitations. The characterization methods used in NPs with their uses advantages and disadvantages are summarized in Table 15.2.

15.14.1 Ultraviolet Visible Spectroscopy Studies and Plasmon Resonance

Spectroscopy is the nondestructive study of the emission and absorption of light and other radiation by substances, as a function of the wavelength of the electromagnetic radiation. The UV−visible spectroscopy applications are generally concerned with UV (185−400 nm) and visible (400−700 nm) light. Using Beers−Lambert law, the concentration of various solutions can be calculated by measuring the absorbed light (Williams and Fleming, 1995b; Poole and Kalneniesks, 2000).

TABLE 15.2 Summary of Characterization Method and Their Uses, Advantages, and Disadvantages

Method	Physical and Chemical Properties	Advantages	Limitations
UV−visible	Optical properties, which depend on size and shape		
IR/Attenuated total reflection FTIR	Bioconjugate. Surface properties as structure and conformation	Rapid and cheap measurement Minimal or no need for sample preparation demands Superior reproducibility irrespective of sample thickness	Sample preparation (IR) is complex intrusion and efficient absorbance of water Sensitivity is comparatively low in nanoscale analysis
SEM ESEM	Size and size distribution. Shape. Aggregation. Dispersion	Simultaneous measurement of the shape and size navigation of NMs High resolution (below subnanometer) in natural status visualization of biomolecules supplied by the usage of ESEM technique	Constraint of conducting sample or coating conductive materials Need of dry samples In nonphysiological states, the sample analysis occurs. Size distribution is based on subjective statistics. Heterogeneous samples are required. Costly apparatus. For numerous, NP bioconjugates, cryogenic method is needed. ESEM resolution is decreased
TEM	Shape heterogeneity. Size and size navigation. Dispersion. Accumulation	With higher spatial resolution than SEM, direct measurement of the size transportation and shape of NMs occurs. For investigation of chemical composition and electronic structure of NMs. A lot of analytical techniques are paired with TEM	Ultrathin samples are needed. Requirement of samples in nonphysiological states Variations or damage or in sample Sampling is insufficient Expensive equipment
XRD	For crystalline materials, shape, size, and structure determination	Well-organized modalities. At atomic level, high spatial resolution	Usage in crystalline materials is reduced. Only one binding or conformation site for sample; accessibility compared with electron diffraction is low
FCS	Dimension, binding hydrodynamic kinetics	High temporal and spatial magnification. Uptake sample is low. For studying concentration effect, molecular diffusion, chemical kinetics, and conformation dynamics are specifically performed via fluorescent probe methods	Due to deficiency of proper methods, it causes limitation in fluorophore species and restriction in usage and inaccuracy

(*Continued*)

TABLE 15.2 (Continued)

Method	Physical and Chemical Properties	Advantages	Limitations
SERS, RS, TERS	Size distribution and hydrodynamic size. Conformational variations in structural, chemical, conjugate, and electronic characteristics	No need of sample preparation. Complementary data obtained from IR. Capability of detecting tissue abnormality. Improved Raman scattering signal. SERS. Enhanced spatial resolution of the NMs. Topological information	Compared with Rayleigh scattering, there is comparatively a weak single restricted spatial resolution, very minute cross-section. Disturbance of fluorescence irreproducible measurement
Zeta potential	Stability concerning to charge on surface	Concurrent measurement of numerous particles	Electroosmotic effect deficiency of accurate and repetition measurement
CD	In biomolecules. Structural and conformational variations (such as DNA and protein). Thermal constancy	Constructive and motivated methods	Conformational fluctuations are due to the involvement of nonspecific residual absorption. Absorption methods have higher sensitivity than CD. For nonchiral chromophores, CD signals are weak. Analysis of molecules consisting of multiple chiral chromophores is challenging
MS	Molecular weight. Composition. Structure. Surface properties (secondary ion MS)	High accuracy and precision in measurement. High sensitivity to detection (a very small amount of sample required)	Expensive equipment. Lack of complete databases for the identification of molecular species. Limited application to date in studying NM bioconjugates
DLS	Hydrodynamic size distribution	Rapid and consistent measurement Can be used for some liquid media, solvent of interest for monodisperse, exact determination of hydrodynamic sizes Moderate expenses on equipment	Used for particular composition, insensitive correlation of size fractions. Presence of small numbers of large particles in polydisperse sample Size restrictions Restricted size determination
STM	Shape heterogeneity. Size and size navigation. Dispersion. Accumulation	Sudden measurement at atomic level, high, spatial resolution takes place	Demand of conductive surfaces. Electronic structure and surface topography inevitably having an easy linkage with surface
AFM	Shape heterogeneity. Size and size navigation. Dispersion. Accumulation and sorption	Mapping of 3D sample surface resolution of subnanoscaled topographic samples. Direct measurement in dry state, ambient, or aqueous environment	Lateral dimensions over description. Sampling is poor and time consuming The exterior of NM analysis is generally restricted

AFM, Atomic-force microscopy; *CD*, circular dichroism; *DLS*, dynamic light scattering; *ESEM*, environmental scanning electron microscopy; *FTIR*, Fourier transform infrared spectroscopy; *FCS*, fluorescence correlation spectroscopy; *UV*, ultraviolet; *NM*, nanoparticles; *MS*, mass spectrometry; *RS*, Raman spectroscopy; *SEM*, scanning electron microscopy; *SERS*, surface-enhanced Raman spectroscopy; *TERS*, tip-enhanced Raman spectroscopy *XRD*, X-ray crystallography.

Adapted with permission from Lin, P.-C., et al., 2014. Techniques for physicochemical characterization of nanomaterials. Biotechnol. Adv. 32 (4), 711–726. <http://dx.doi.org/10.1016/J.BIOTECHADV.2013.11.006>.

TABLE 15.3 Color and the Wavelength Range of Different Metal Nanoparticles

Nanoparticles Material	Color	Wavelength (nm)	Reference
Au	Wine-red	520	Kamble, Jagdale and Kadam, (2010) and Kamble et al. (2010)
Silver	Gray	400	Mulfinger et al. (2007)
Copper	Black-green	280	Dang et al. (2011)
Ruthenium	Dark gray	–	García-Peña et al. (2015)
Sulfur	Yellow	–	Suleiman et al. (2015)
Selenium	Red	420 and 550	Kora and Rastogi (2016) and Rastogi (2016)

Generally, MNPs such as iron, selenium, and others are characterized by spectroscopy especially after synthesis as the color of the reaction mixture will change (Poinern, 2014). However, in MNPs, particularly gold and silver, absorption rises to intensive color solutions characterized by plasmon resonance. Each metal results in a different colored solution; to give a 20-nm gold particle, for example, there is a rise in red solution, which absorbs at 520 nm (Filipponi and Sutherland, 2010).

However, Martinez et al. (2012) have shown that visible spectra of gold colloids for sizes 5–80 nm results in redshift with an increase in NP diameter. Redshift is not only related to size but also can be correlated to shape as well. So UV–visible measurements are also employed to study the functionalization of Au NPs such as binding to antibodies (Nghiem et al., 2010) or aggregation (Raoof et al., 2012).

Table 15.3 summarizes the color and the wavelength range of different metal NPs.

15.14.2 Fourier Transforms Infrared Spectroscopy

FTIR spectroscopy method is used to record IR spectra of absorption or emission. Light covering the whole frequency range (5000–400 cm^{-1}) (Williams and Fleming, 1995a) may be used for studying the vibration of the functional groups associated with NPs as well as for the measurement of functional groups in plants prior to green metal NP synthesis, to investigate biological compounds responsible for the synthesis and stability (Sharma et al., 2014).

NPs of various natures have been characterized and defined by means of different spectroscopic techniques in the infrared range. NPs with characteristic infrared absorptions or functional groups exist at their surface may, therefore, be directly characterized by IR spectroscopy. In addition, FTIR allows a fast, precise, and nondestructive way to determine the different ligands attached to NPs, which relies on their vibrational signatures (López-Lorente and Mizaikoff, 2016). Some vibrations for iron oxide NPs are summarized in Table 15.4.

Also, a scheme of different roles of NPs in IR as analyte and tools is shown in Fig. 15.8.

TABLE 15.4 Some Vibration in for Iron Oxide Nanoparticles (Rahman, 2011)

Functional Group	Vibrations	Peak Value (cm^{-1})
Fe–O–Fe	Stretching vibration	462, 560
O = C = O		1481
O–H	Stretching	3354
O–H	Bending vibration	1680
O = C = O and H_2O, which nanomaterials absorbed from the environment due to their mesomorphous structure of some nanoparticles	Absorption bands	1481, 1680, 3354

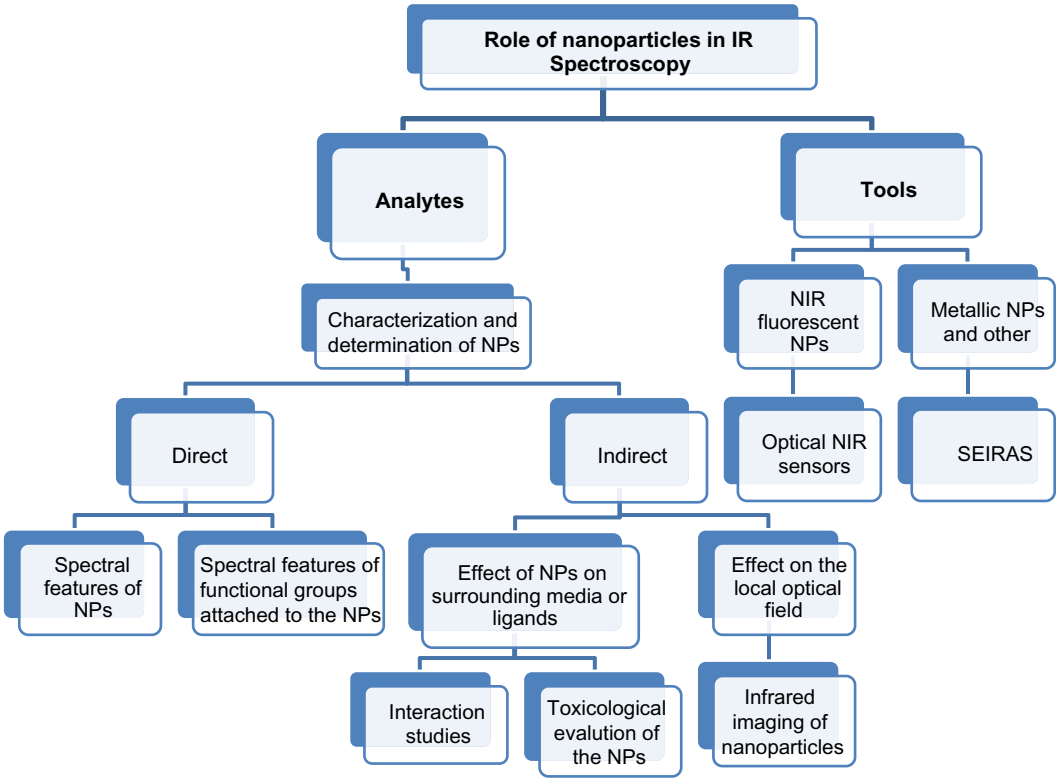

FIGURE 15.8 Schematic diagram of different roles of infrared in the characterization of nanoparticles, and NPs as a tool for determination of compounds and other NPs. *NPs*, Nanoparticles. Source: *Adapted from López-Lorente, Á.I., Mizaikoff, B., 2016. Recent advances on the characterization of nanoparticles using infrared spectroscopy. TrAC, Trends Anal. Chem. 84, 97–106. doi:10.1016/j.trac.2016.01.012 with permission.*

15.14.3 Scanning Electron Microscope

This technique has a similarity with the optical microscope, which utilizes light sources (photons) and a glass lens to create magnified images. Whereas, the electron microscope uses electrons where the incident beam of electrons transversely scans the sample (Filipponi and Sutherland, 2010), providing information on the composition of atoms along with the topographic details of samples (Johal, 2011).

SEM is a surface sensitive imaging procedure, which routinely uses three analysis modes: secondary electron (SE) mode, backscattered electron (BSE), mode, and X-ray energy dispersive spectroscopy as in TEM (Chekli et al., 2016). Among these modes, SE mode is the greatest used mode (<1 nm resolution) (Johal, 2011).

Many nonconductive biochemical materials acquire charge and refract the electron beam insufficiently, which leads to faults and artifacts in imaging. To overcome these artifacts, during the preparation of samples biomolecules are coated with an ultrathin layer of electrically conducting material (Suzuki, 2002; Hall et al., 2007). On the other hand, SEM cannot be used for cryogenic freeze materials such as in the case of imaging surface groups attached to NPs (Hall et al., 2007), where ESEM is used for such exceptional cases, in which samples are imaged in their ordinary state with no modifications (Tiede et al., 2008; Sapsford et al., 2011).

Most electron microscope methods possess disadvantages like sample destruction during preparation (Gmoshinski et al., 2013), and biased statistical analysis of size distribution, which is difficult to avoid in SEM (Bootz et al., 2004). However, sample preparation for SEM is less complicated as compared with TEM, as the former neither needs thin samples nor is it greatly affected by air exposure (Chekli et al., 2016).

15.14.4 Environmental Scanning Electron Microscope

ESEM is similar to SEM but with an advantage. Samples imaged by ESEM are observed under partial vapor pressure in the microscope specimen chamber, preserving the sample ambient conditions, which allows imaging samples in their ordinary state with no modification or preparation (Bogner et al., 2005; Tiede et al., 2008; Sapsford et al., 2011; Ponce, Mejía-Rosales and José-Yacamán, 2012). Tuoriniemi et al. (2014) found that ESEM with BSE detection was invaluable for imaging heavy elements such as Pt, Au, and Ag containing nanomaterial as small as 25 nm at very low concentrations (Tuoriniemi et al., 2014).

Also, ESEM is useful to image and impart elemental analysis for metal NPs such as nickel (50 nm), cobalt (50−200 nm), titanium (TiO_2 20−160 nm), silica (SiO_2 4−40 nm), in 10-μm-thick tissue segments, when placed over adhesive carbon discs inserted in the ESEM chamber (Gatti et al., 2008).

However, Wet-SEM is an alternative to ESEM. This technique uses a transparent electron membrane, which enables liquid sample imaging (NPs in their environmental matrices) by traditional SEM. Examples of metal NPs imaged by this technique are Au (50 nm), titanium dioxide TiO_2 (5 nm), ZnO (71 nm), and Fe_2O_3 (29 nm) in distilled and lake water and soil suspension (Tiede et al., 2009). Wet-SEM is a beneficial tool for investigations (in situ) that can be combined with EDX, but challenges are still there due to Brownian motion of NPs (Dudkiewicz et al., 2011).

15.14.5 Transmission Electron Microscopy

The principle of TEM operation differs from SEM, although it brings similar data type. In this technique, the ultrathin sample layer is transmitted and interacted with a beam of electrons. The transmitted electrons will lead to the formation of specimen image after being magnified and focused by an objective lens. The NPs are deposited onto supporting films or grid (Molpeceres and Aberturas, 2000; Joshi, Bhattacharyya and Ali, 2008). To facilitate handling and to create NPs that withstand the instrument vacuum, fixation with either plastic embedding or negative staining material, like uranyl acetate, phosphotungstic acid, or derivatives, for instance, is required. Alternatively, NPs sample is exposed to liquid nitrogen temperature after embedding in vitreous ice (Molpeceres and Aberturas, 2000).

TEM is widely implemented in contrast images of well-defined crystal planes (Canevarolo, 2004; Campos et al., 2015). The outcome information that can be given by TEM is dark and bright images regarding the microstructure and morphology of the sample, especially when combined with X-ray analysis of elemental composition (Mannheimer, 2002; Campos et al., 2015).

TEM is being used to image a variety of MNPs such as selenium NPs (Sharma et al., 2014), Ag NPs (Lee and Kang, 2004), Cu NPs (Rajeshkumar and Rinitha, 2018), iron NPs (Chekli et al., 2016), and other metal NPs to get information relevant to size, shape, and aggregation state.

It is worth noting that high-resolution TEM is an imaging mode of the transmission electron microscope that allows imaging of the crystallographic structure of a sample at the atomic scale (Joshi, Bhattacharyya and Ali, 2008). Also, wet TEM can be used for determination of dispersion, particle size, dynamic displacement, and aggregation of nanomaterials in an aqueous environment (Carlton and Ferreira, 2012; Chen and Wen, 2012; Hondow et al., 2012), such as Au NPs in aqueous solution (Chen and Wen, 2012).

15.14.6 X-Ray Crystallography

The principle of XRD is based on Bragg's law (Eq. 15.1)

$$(n\lambda = 2d \sin\theta) \tag{15.1}$$

where λ = wavelength of the X-rays,

n = order of diffraction,
d = spacing between sequential parallel planes of a crystal, and
θ = complementary angle of the X-ray incidence where monochromatic X-rays productively interfere with a crystalline sample and construct the diffracted X-rays (Klug and Alexander, 1954; Warren, 1969; Pope, 1997).

XRD is an adjustable, simple, nondestructive method for crystalline materials identification. XRD can be used for an extensive range of purposes including measurement of crystalline percentage, identification of fine spark minerals as in NPs and nanoclays, to resolve unit cell dimensions in addition to analysis of sample purity. The samples should

be pounded and homogenized for proper XRD analysis (Nurmi et al., 2005; Lin, Chang, and Chuang, 2008; Wang, Kanel, et al., 2009; Wang, Snyder, et al., 2009; Kim et al., 2010a,b; Wang and Hong, 2011).

In 1915, Bragg and Nishikawa identified the details of iron oxide crystallographic structures (hematite, maghemite, and magnetite), such as orthorhombic, cubic, hexagonal, tetrahedral, octahedral, in addition to the atomic coordinates of polymorphous iron oxides (Cornell, 2006).

XRD has been used to characterize many metal NPs such as Se NPs (Sharma et al., 2014), magnetite iron oxide NPs (Mahdavi et al., 2013), Ag NPs (Singh et al., 2015), Au NPs (Abbai et al., 2016), Cu NPs (Fathima et al., 2018), and many others.

15.14.7 Energy-Dispersive X-Ray Spectroscopy

EDX is an X-ray technique used to detect the elemental arrangement of materials. The EDX system can be attached to either TEM or SEM instruments as the ability of the microscope imaging distinguishes the specimen of concern. EDX analysis produces data that consist of spectra that show peaks related to the elements of the analyzed sample.

EDX is a nondestructive technique that can be used for qualitative, quantitative, and semiquantitative analysis, which provides the element distribution through mapping.

However, other techniques can be used in case of inadequate EDX data for specimen identification such as nuclear MR spectroscopy, Raman microscopy, FTIR microscopy, and for surface analysis time-of-flight secondary ion mass spectrometry (MS) or X-ray photoelectron spectroscopy.

EDX has the following benefits:

- Process optimization and amended quality control
- Quick identification of impurities and source
- Environmental factors can be fully controlled
- Higher production yield
- The problem source in the process chain can be identified [Energy Dispersive X-Ray Analysis (EDX) (no date)] (interteck.com)

The EDX spectroscopy analysis has been used by researchers to detect the related elemental constituents that might be present in metal NPs to confirm proper synthesis and purity, such as in the synthesis of Se NPs (Sharma et al., 2014), Cu NPs (Agarwal, Venkat Kumar and Rajeshkumar, 2017), and many others.

15.14.8 Fluorescence Correlation Spectroscopy

In this technique, statistical analysis is carried out to observe the fluctuations of fluorescence in a given system to interpret dynamic molecular measures, as conformational fluctuations or diffusion of biomolecules. Magde et al. were the first to introduce the FCS technique for the measurement of diffusion and binding of ethidium bromide onto double-stranded DNA. Since 1993, this technique is continuously undergoing revitalization with the implementation of confocal microscopy FCS. An overflow of experiments has applied FCS since then to characterize the rotational and translational mobility of

fluorescent molecules, the photochemistry of dyes, and also to perceive the conformational fluctuations of green fluorescent biomolecules as in DNA and proteins (Krichevsky and Bonnet, 2002).

In practice, the FCS uses specific fluorescence that is sensitive to chemical change to measure specified molecules (Elson and Magde, 1974; Lin et al., 2014). In NPs characterization, FCS has been used to follow the functionalization by probing the dynamics of the particles at the particular object level and illuminating desorption of fluorescent ligands that combine into greater objects. FCS is a useful tool for functionalized noble metal NPs characterization in solution under similar settings to those that are used in optical bioimaging (Loumaigne et al., 2010). The advantage of FCS as compared with dynamic light scattering (DLS) is that only a small amount of fluorescent probe particles are required (subnanomole to nanomole), which prevents interference by monitoring probe particles in the medium, in addition to the ability for nanomaterials to probe in the dimensions of nanometers to hundreds of nanometers (Boukari and Sackett, 2008). Recently FCS—near field scanning optical microscopy FCS-NSOM has been developed to overcome the disadvantage of FCS in its limits of application and accuracy (Vobornik et al., 2008).

15.14.9 Surface-Enhanced Raman Spectroscopy

Raman spectroscopy (RS) is a favorite technique for the analysis and identification of molecules in samples without the requirement of any modification or labeling. RS has been used for bioimaging and biofunctional analysis as its spectra provide information about intracellular and molecular distribution (Ando and Fujita, 2013). Whereas, SERS is considered as a powerful vibrational spectroscopy method, which also has been enhanced by using metallic nanostructures, which permit the detection of highly delicate structure of analytes at low concentration through the amplification of electromagnetic fields produced by the excitation of localized surface plasmons (LSPRs). Conventionally noble and coinage metals such as gold, silver, and copper with nanoscale features concentrate light in the gaps, cervices or the sharp features of these plasmonic metals (Camden et al., 2008; Sharma et al., 2012).

In addition to its powerfulness, SERS is a nondestructive technique for chemical and structural analysis for even small number of molecules. SERES experiment performance requires certain parameters for sample and optical setup to ensure maximum signal generation and enhancement. These parameters include choosing of the appropriate enhancing substrate (Camden et al., 2008) and considering proper excitation source (McFarland et al., 2005).

SERS success is extremely reliant on the interaction between the surface of the plasmonic nanostructures and the absorbed molecule; usually, the SERS substrates are silver, gold or copper. The most air-stable materials are gold and silver where copper is more reactive. The LSPRs of these three metals cover most of the visible and near-infrared range (Van Duyne, Hulteen, and Treichel, 1993; Boltasseva and Atwater, 2011; Kosuda et al., 2011).

SERS substrates development advances have been made (Fan, Andrade and Brolo, 2011), including Au and Ag NPs with coatings and various shapes resulting in structures

such as shell-isolated NP-enhanced Raman spectroscopy (Li et al., 2010a,b), 2D Au nanomushroom arrays (Naya et al., 2008), SiO_2-encapsulated Au particles (Wustholz et al., 2010), film over nanospheres (Biggs et al., 2009), polyhedral Ag mesocages (Fang, Liu and Li, 2011), Si wafers with Ag or Au coating (Dinish et al., 2011), and atomic layer deposition (ALD)−coated plasmonic NPs (Dieringer et al., 2006). The ALD coating on NPs is stimulating because it permits the determination of the distance dependence for SERS, provides temperature stability, protects the NP surface, and improves the stability of the surface for use with femtosecond pulses and enables functionalization of the NP (Dieringer et al., 2006; Kim et al., 2010a,b).

The uses of SERS include monitoring the conformational change in proteins conjugated to metal NPs, studying the surface functionalized metallic NPs, and tracking intracellular drug release from nanoplatform upon pH measurements of surrounding medium (Mannelli and Marco, 2010; Kumar and Thomas, 2011; Ando and Fujita, 2013; Huang et al., 2013).

15.14.10 Tip-Enhanced Raman Spectroscopy

TERS is a new emerging technique that was developed to overcome diffraction-limited resolution by modifying the perception of confining the light field in Raman near-field scanning optical microscopy. TERS employs an aperture devoid metallic tip instead of an optical fiber to gain the surface enhancement of the Raman signals (the SERS effect) (Hartschuh, 2008; Hayazawa et al., 2012; Ando and Fujita, 2013; Wang and Irudayaraj, 2013). TERS' advantages over the conventional RS and SERS are the provision of topological information along with information on the structural, chemical, and electronic properties of the nanomaterials provided by RS (Popović et al., 2011; Lee et al., 2013).

15.14.11 Zeta Potential

ZP is an analytical technique that is applied for the determination of surface charge of NPs in colloidal solution. The surface of a charged particle attracts a thin layer of opposite charge and firmly binds to it, forming a thin liquid layer named the Stern layer; when the particle diffuses in solution it will be involved by an outer diffuse layer that consists of loosely associated ions, as a result of which an electrical double layer is created (Clogston and Patri, 2011) (Fig. 15.9). ZP is named for the electrical potential of the double layer and determined through velocity measurement of the charged particles moving toward the electrode across the sample solution in the presence of an external electric field (Pons et al., 2006; Sapsford et al., 2011). ZP values are typically in the range of $+100$ to -100 mV. The magnitude of ZP gives a prediction of the colloidal stability. ZP of NPs with values $> +25$ mV or < -25 mV usually have high degree of stability. Lower dispersions ZP values will lead to aggregation, coagulation, or flocculation due to van der Waals interparticle attraction (Horie and Fujita, 2011; Sapsford et al., 2011).

ZP for metal NPs as ZnO has been used to study the effect of dispersant as water and ethylene glycol on particle size distribution (Marsalek, 2014). Metal NPs ZP must be

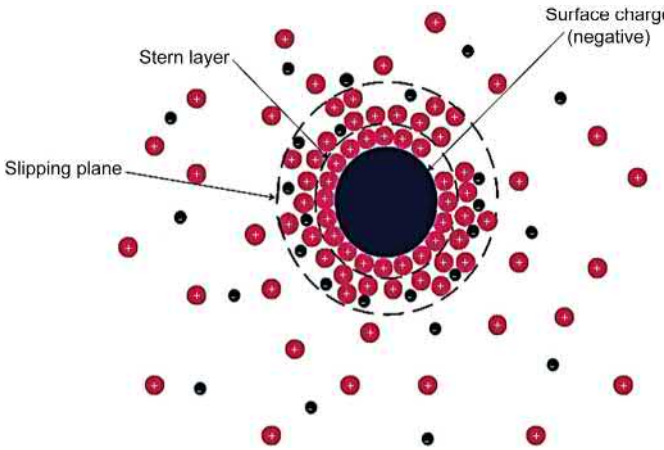

FIGURE 15.9 Illustration of zeta potential showing the surface charge, the Stern layer, and the slipping layer.

measured prior to functionalization to predict the particles behavior. Dougherty et al. (2008) studied ZP of palladium, Ag, and Au monometallic particles besides Au/Ag bimetallic particles for functionalization and found that the magnitude of the ZP is least at very low pH and most at moderate pH; on the other hand, acidic solutions should be avoided so as to minimize adhesion to PDMS surfaces or glass and aggregation, or to maximize electrokinetic mobility. Also, thiolated self-assembled monolayers coatings can have a dramatic effect on the ZP of the metallic NPs especial noble NPs (Dougherty et al., 2008).

ZP of NPs is also used to understand and predict the increase in susceptibility of aggregate formation when NPs interact with biomolecules. Once metal oxide NPs are dispersed in water, the ZP depends on the molecular species and the surface condition. However, the formation of aggregates does not depend on ZP only because of the presence of other interaction between particles with proteins such as van der Waals forces, hydrophobic, hydrophilic, structural, and steric interactions, which play an important role in the adsorption of material on proteins (Horie and Fujita, 2011).

15.14.12 Circular Dichroism

Circular dichroism (CD) (optical activity) is the rotation of the plane of plane-polarized light by a chiral molecule in a left-handed or right-handed direction; this can be observed either in chiral molecules or in molecule–ligand binding only if at least one of the interacting species is chiral. CD monitoring method has the following advantages:

- Monitoring induced CD, which occurs only as a result of interaction between the achiral molecule and chiral molecules.
- It is a selective spectroscopic technique in relation to absorption techniques.
- It can be used for structure determination in certain cases especially in an overall change in protein folding upon ligand interaction.
- It is nondestructive.

CD can be used for detection and characterization of chirality, determination of stereochemistry, enantiomeric purity, protein/peptide and nucleic acid secondary structure, binding interaction studies for drug/biopolymer or metal/ligand in addition to time-resolved studies and others. Regarding protein confirmation monitoring in solution, CD spectroscopy provides the most convenient method (Drake, 2001). After the emergence of NP science, CD techniques have been used to study the conformational changes behavior of biomolecules on NPs, drug-delivery nanocarriers structure, and to study the interactions of nanocarriers with biomolecules (Caminade, Laurent and Majoral, 2005; Ghosh et al., 2007; Liu and Webster, 2007; Ranjbar and Gill, 2009; Bhogale et al., 2014), interaction of DNA with metal NPs (Kaur et al., 2018), and protein interaction with Au NPs (Sen et al., 2011) and Ag NPs (Pandoli et al., 2011) in addition to the studies related to chiral Au nanoclusters (Zeng and Jin, 2017). Moreover, chiroptical properties of nanomaterials can be engineered using peptides as in the case of creating optically active Au NPs through NP−peptide interaction (Slocik, Govorov and Naik, 2011).

To improve biological structure measurements various CD based methods were developed such as X-ray magnetic CD (MCD), electronic CD, near-infrared CD, fluorescence detected CD, high-pressure liquid chromatography−circular dichroism, and vibrational CD (VCD) (Ranjbar and Gill, 2009; Lin et al., 2014). Bürgi has reviewed the CD methods that were used to study NPs including metal NPs in different conditions. For example, the use of VCD in the analysis of thiol-gold nanoclusters in addition to analysis for nanogold clusters protected by 3-mercaptophenylboronic acid (3-MPB) using MCD spectroscopy (Gautier and Bürgi, 2010).

15.14.13 Mass Spectroscopy

MS is one of the most useful analytical techniques that can offer significant elemental and molecular information on the structure, composition, and the chemical state of NPs, as well as to NP bioconjugates' analysis and quantification. It also can be used to obtain real-time information due to the compatibility of MS with any type of sample with high sensitivity and, can be easily coupled with separation techniques, which results in varied and novel insights into the nature of NPs and their final uses and applications (Fernández et al., 2010).

Following are various MS ionization coupled techniques for more informative characterization:

1. Inductive coupled plasma−MS (ICP-MS), which is used for elemental characterization and provides information about NPs size, size distribution, mass and concentration, detailed composition, or even the existence of impurities at a low level. Separation techniques that can be coupled to elemental MS are liquid chromatography, asymmetric flow field-flow fractionation, ion mobility, and electrophoretic techniques (Costa-Fernández et al., 2016). ICP-MS enabled a rapid characterization of multielemental trace impurities in high-purity metal NPs of ZnO, CeO_2, SiO_2, and TiO_2 (He et al., 2007a,b).

2. Introductive matrix-tolerant nebulizers of electrothermal vaporization (ETV) can be used for NP colloidal dispersion; ETV-ICP-MS is a particle size−independent method for quantification of metal (iron oxide) NPs, such as Ag, ZnO, TiO_2, SnO_2, and Sb_2O_3 NPs and their agglomerates in environmental samples (Duester et al., 2011).
3. The single particle ICP-MS (SP-ICP-MS) was developed for the detection of the model (alumina, rutile, and goethite) and natural (montmorillonite) colloids. The reported limits of NP detection number concentration are in the range of 10^4−10^6 L^{-1} (Majedi and Lee, 2016). The analytical potential of SP-ICP-MS in environmental samples and living organisms was used for the detection and quantification of Ag NPs (Laborda, Bolea, and Jiménez-Lamana, 2014). Further, the practicality of size analysis, measurement of NPs mass percent, their isotopic abundance and stability for Ag nanowires, TiO_2, ZnO, and CeO_2 NPs by SP-ICP-MS were studied by Reed et al. (2012).
4. Matrix-assisted laser desorption/ionization−MS (MALDI−MS) and electrospray ionization−MS (ESI−MS) have been used for the characterization and analysis of NPs functionalization. Especially, when NPs are intended to be used in bioanalytical applications, they have been conjugated to biological probes, including proteins, nucleic acids, small molecules, or antibodies. Molecular MS techniques (MALDI and ESI−MS) provide key information about the stoichiometry of these NPs (Costa-Fernández et al., 2016). NPs are advantageous over more conventional organic MALDI matrices, as NPs are outstanding laser energy−absorbing materials, because of their relatively high surface area (Z. Guo et al., 2006a,b; Lu et al., 2017).
5. As examples for the use of molecular MS, MALDI−MS has been used for the detection of fragments resulting from reagents adsorbed on the NPs surface identification as in Ag NPs synthesized with different surface capping reagents (that were able to interact with peptides and proteins such as heart cytochrome *c*, insulin, lysozyme, ubiquitin, homocysteine, and cysteine) (Shastri et al., 2015). However, electrospray ionization (ESI) might overcome the ionization vulnerability effect on some molecules by fragmenting themselves at the solid matrix (e.g., MALDI). ESI comprises a very popular ionization source for liquid samples. ESI−MS has proved to have unexpected capabilities and potential to analyze more convoluted samples containing NPs such as bimetallic protected NPs (e.g., Pd−Ag, Au−Ag, Cu−Au, Au−Pd, and core−shell NPs) and products from ligand exchange reactions (Fields-Zinna et al., 2009).

15.14.14 Dynamic Light Scattering

DLS is a light scattering method that can be used to study small particles' size distribution, even for polymers or molecules in the scale of submicron to one nanometer either in solution or suspension by using a monochromatic light source, for example, a laser (Patri et al., 2006; Sapsford et al., 2011). Lots of physicochemical characteristics of nanomaterials as structure, shape, hydrodynamic size, aggregation state, and even biomolecular conformation can be discovered through radiation scattering techniques (Sapsford et al., 2011; Inagaki, Ghirlando and Grisshammer, 2013). The DLS principle is to monitor the chronological changeability of the elastic scattering intensity of light, that is, Rayleigh scattering,

which is induced from the molecules or particles Brownian motion of very small size as much as smaller than the incident light wavelength, at a fixed scattering angle (Brar and Verma, 2011; Sapsford et al., 2011). The extent of the change in the scattered light by different particles can be derived from analysis of the motion-dependent autocorrelation function using the Stokes–Einstein equation (Pons et al., 2006; Brar and Verma, 2011; Sapsford et al., 2011).

DLS is a frequently used technique for physicochemical characterization of metal NP for the estimation of particle size and size distribution. DLS is reproducible, with short experiment duration, accurate in determining the hydrodynamic size of monodisperse samples, and can be used for measurement of particles in diluted samples, with different concentrations, to detect small amounts of higher molecular weight species (Filipe, Hawe and Jiskoot, 2010; Brar and Verma, 2011; Lim et al., 2013). Further, it is considered a noninvasive method, which is important for the recycling of MNPs, especially those with expensive surface coats (Lim et al., 2013).

DLS technique has been widely used for sizing metal NPs in a liquid phase like Fe NPs, Au NPs, and Ag NPs (Goon et al., 2009; Phenrat et al., 2009; Anandalakshmi, Venugobal and Ramasamy, 2016). There are several challenges of measuring metal NP size by DLS including (1) metal NPs are coated with macromolecules to enhance their colloidal stability in the applications of engineering, and (2) their presence of dipole–dipole magnetic interactions between the nonsuperparamagnetic NPs. Macromolecules that adsorb onto the surface of metal NPs particles have a tendency to increase the apparent RH of particles; this increase, however, is of convenience for the measurement of the thickness of the adsorbed macromolecules (Lim, Majetich and Tilton, 2009).

15.14.15 Scanning Tunneling Microscope

STM is scanning probe microscopy, which is based on the quantum mechanical nature of electrons on the subnanometer scale (Tiede et al., 2008). It is a fundamental tool in nanoscience and nanotechnologies and is used to obtain atomic-scale images of semiconducting surfaces and metals. It is used for surface detection and determination of size and conformation of molecules and aggregates (Filipponi and Sutherland, 2010).

In STM, a conducting tip (very thin needle) is brought into proximity of a metallic or semiconducting surface leaving a very small gap between the tip and the surface of the sample (less than 1 nm), where electrons can "tunnel" through this gap, creating a current. By scanning the tip through the surface and adjusting the height of the tip to maintain a constant tunneling current, the surface can be imaged (Tiede et al., 2008; Filipponi and Sutherland, 2010). Advantages of STM include that it can be used with environmental samples for imaging redox properties of resolution of around 1 nm or better (Tiede et al., 2008). Also, nonconductive samples such as biological molecules can be imaged by coating with a very thin layer of conductive material like gold (Filipponi and Sutherland, 2010). The spatial resolution of STM is benefited in the characterization of size, shape, structure, and state of dispersion and aggregation metal nanomaterials like gold and carbon. STM is the preferred tool for characterization of atomic structure like nanotubes (Wang and Chu, 2013).

15.14.16 Atomic-Force Microscopy

AFM is a physical scanning method that can measure particle size with high resolution upon sample scanning at submicron level by atomic-scale probe tip (zur Mühlen et al., 1996; Maver et al., 2016). Here the instrument provides a topographical map for the sample. The map result is based on the forces of the sample surface and the tip. There are two types of measurements: contact and noncontact modes. It is preferable to use contact mode for samples scanning as the topographical map is produced by tapping the probe onto the surface across the sample, whereas in the noncontact mode the probe hovers over the conducting surface. However, the use of contact or noncontact mode is dependent on the properties of the sample. There are several advantages for AFM, the ability to scan in a nonconducting mode without any specific sample treatment is the most important advantage in imaging sensitive biological samples; also polymeric micro- and nanostructure is allowable (Shi et al., 2003). The second advantage is the ability of AFM to provide the size and size distribution of the sample without the need of any mathematical handling in the most accurate description. In addition, the provision of a real picture of the particle size leads to a better understanding of various biological conditions effect (Polakovic et al., 1999; Maver et al., 2016).

AFM is a valid means to study and understand the interactions between nanomaterials/particles including metal NPs and biomolecules. AFM scanning has been used to characterize the dimensional and morphological characteristics of metal NPs as CdS nanocrystals and Au NPs prepared intentionally with designed properties and particulates collected in operational environments (Latterini and Tarpani, 2012). Also, AFM can be used to study the topography of other metal NPs such as Ag and Au (Alaqad and Saleh, 2016).

15.15 APPLICATIONS OF METAL NANOPARTICLES

As mentioned earlier there is a wide range of application fields for metal NPs. These applications include medical, biomedical, environmental, agricultural, catalysis, textiles, electronics, transportation, and many others. In this section, we are going to focus on the medical, pharmaceutical, and biomedical applications of metal NPs. Also, the general applications of different metal and some nonmetal NPs are summarized in Table 15.5.

15.15.1 Applications in Drug Delivery

Noble metal NPs such as Au NPs and Ag NPs are multipurpose agents that can serve as unique multidimensional scaffolds exhibiting desired characteristics, namely their distinctive morphology, surface functionalities, ease of synthesis, and other attractive properties, which are the main reasons for their application for medical purposes (Sperling et al., 2008; Sau et al., 2010). Optical applications are most focused on in this field, such as biosensors and medical imaging and tracing such as nanobiosensors for disease diagnosis and nanoprobes for in vivo sensing and imaging. In addition, noble

TABLE 15.5 Summary of the Applications of Nanoparticles (Metal, Nonmetal, and Metalloid) Mentioned in This Chapter

Nanoparticle	General Applications/Potential Applications	Reference
AgNPs	*Biomedical:* drug delivery, cell imaging, cancer therapy, and diagnosis	Keat et al. (2015)
	Health Care: Nutraceutical, UV protection, topical creams, and ointments	
	Environmental: Activated carbon filters, water disinfection, and wastewater treatments	
	Food Agriculture: Food quality analysis sensors, interactive food, and food packaging	
	Catalysis: Hydrogen production photocatalysts, fuel additive catalyst, and fuel cell catalyst	
	Textiles: medical textiles, antistain textiles, and UV blocking textiles	
AuNPs	*Biomedical*:	Khlebtsov and Dykman (2011)
	Diagnostics such as in plasmonic biosensors, analytical methods and visualization, and bioimaging	Siddiqi and Husen (2017)
	Therapy such as in photodynamic therapy, photothermal therapy, drug, and gene delivery	
	Immunology, adjuvants, biodistribution, and toxicity	
	Environmental: water remediation	
	Catalysis	
	Nanoelectronics	
	Nonlinear optics	
FeNPs	*Biomedical*: cancer therapy, cell labeling, drug delivery systems, and MRI contrast agents	Kornberg et al. (2017)
	Cosmetics: Pigment	
	Environmental: Biosensors, environmental catalysis, fuel cell catalysts, and wastewater cleanup	
	Materials: Coatings/Paints and pigmented thermoplastics	
	Electronics: Circuitry and in magnetic data storage	
	Transportation: As propellants and in brake systems	
ZnO NPs	*Biomedical*: Tissue repair, wound healing, antineoplastic (cancer therapy), antibacterial, angiogenesis	Kołodziejczak-Radzimska and Jesionowski (2014) and Anju Manuja (2015)
	Health care: UV protection (creams, powders, etc.)	
	Food agriculture: Food preservative, and feed additive	
	Catalysis: Photocatalyst	

(*Continued*)

TABLE 15.5 (Continued)

Nanoparticle	General Applications/Potential Applications	Reference
	Textiles: Absorber of UV radiation	
	Rubber industry: Activator of rubber compounds and as fillers	
	Electronics and electrotechnology industries: Sensors, photoelectronics, field emitters, solar cells, and UV lasers	
CuNPs	*Biomedical:* Biosensing and biolabeling	Ruparelia et al. (2008) and Ruparelia et al. (2008)
	Environmental: Disinfectant for wastewater	Mandal and De (2015)
	Industry: Effective antibacterial activity when stabilized on polymers, carbon, polyurethrane foam, and sepiolite	
	Catalysis: In nitroaromatics reduction.	
Pl and Pd NP and	*Biomedical*: Medical diagnostics, biosensors, and material sciences	Siddiqi and Husen (2016)
	Health care: Medicine and pharmaceutics, e.g., anticancer	
	Catalysis	
AlNPs	Plasmon-enhanced solar desalination	Zhou et al. (2016)
	Silicon solar cell applications	Temple and Bagnall (2011)
	Cooling application in modern buildings	Ravishankar Rai and Jamuna Bai (2011) and Kalaiselvam, Parameshwaran and Harikrishnan (2012)
	Antimicrobial and free radical scavenger	
RuNPs	*Catalysis*	Refer to Section 15.10
SeNPs	*Biomedical*: Antimicrobial, antioxidant, cancer prevention, has a role in immunomodulation and reproduction, improves growth performance, and helps in feed digestion, found to act as a treatment to cure fatty liver in animals	Sarkar et al. (2015)
SNPs	*Biomedical:* Anticancer and antibacterial	Suleiman et al. (2013)
	Catalysis	
	Electrochemistry: Lithium batteries	

metal NPs have been used in medical diagnosis and photothermal cancer therapy, in that they selectively target cancer cells with numerous pathways upon heating (Y. Zhang et al., 2012a,b). Other applications may include using them as delivery vectors for carrying and delivering biomolecular compounds (e.g., genes, probes, proteins) and drugs (Arvizo et al., 2012).

Generally, the aim of developing new and unique delivery systems is to ensure the delivery of drugs or other compounds to their desired sites in sufficient concentrations,

while maintaining the efficacy of the delivered drug along with minimizing toxicity and adverse effects of said drug (Anandhakumar, Nagaraja and Raichur, 2010; Anandhakumar et al., 2011, 2014).

NPs' surfaces can be functionalized with biocompatible polymeric materials (e.g., polyethylene glycol) to enable specific targeting of cells. Polymer functionalized NPs are biocompatible and have a high encapsulation capacity achieving delivery of genes and therapeutic proteins either by being dissolved or encapsulated resulting in an NP or a nanocapsule respectively (Tiwari et al., 2012). Likewise, surface modifications of noble metal NPs could be made to specifically target certain cells by functionalization with numerous biomolecular compounds, such as antibody conjugates, enzymes, peptides, and/or DNA/RNA, which sequentially will lead to prolong the in vivo circulation of the drug and will also let the NPs interact easily with biological systems (Sperling and Parak, 2010).

Surface NPs encapsulation of drug molecules is achieved through electrostatic interactions or drug conjugation by means of the coating surface of NPs with polyelectrolytes or other polymers. A study conducted by Chen et al. is an example; the reports showed that surface engineered Au NPs have potential to be applied as a DNA vaccine adjuvant for treatments of immunodeficiency virus (HIV) by exposing the Au NPs to near-infrared radiation (NIR) light that encourages the release of the DNA vaccine because of the LSPR effects (Xu et al., 2012).

Theranostics is an objectively new but innovative term in a tumor treatment and cancer therapies; it is an integrated diagnosis and therapeutic system that along with providing treatment, helps in the diagnosis and efficient therapy monitoring through imaging, also eliminating multistep procedures and improving patient care (Warner, 2004). This aids in determining the precise treatment plan for an individual patient (Fig. 15.10). Therefore using a single approach, the efficient diagnosis, treatment, and monitoring of the treatment progress can be accomplished (Jeelani et al., 2014). Metallic NPs, such as Au, Ag, Fe, Ti in addition to Zn are regarded as the most guaranteed theranostic mediators for the treatment of cancer, correspondingly owing to their decisive dual roles as diagnostic and active therapeutic agents (Sharma et al., 2015). Due to their intrinsic anticancer activity, metal NPs have advantages over other NPs as theranostic agents, which subdue the requirement of other carriers for the delivery of diagnostic and therapeutic agents (Gautier et al., 2013).

Furthermore, metal NPs are biocompatible and they can be straightforwardly eliminated from the body. Emphasizing their efficiency to serve as carriers of different therapeutic drugs through encapsulation or conjugation of these therapeutic moieties on the surface of the metal NPs, as previously mentioned, the metal NPs can be tailored to target cancerous cells. Integration of optical imaging technologies can further be considered as an innovative application for metal NPs in cancerous cell localization, where fluorescent dyes, radio isotopes, optical imaging agents, and others can be attached for the purpose of multimodal imaging (Fig. 15.11) (Gibson, Khanal and Zubarev, 2007; Thomas, Park and Jeong, 2013). In conclusion, as the necessity of applying tailored cancer therapies has emerged, metal NPs' theranostic applications offer an efficient technique for cancer diagnosis, therapy, and monitoring treatment response, which will result in perceptible fundamental improvements in the therapeutic outcome of anticancer treatment.

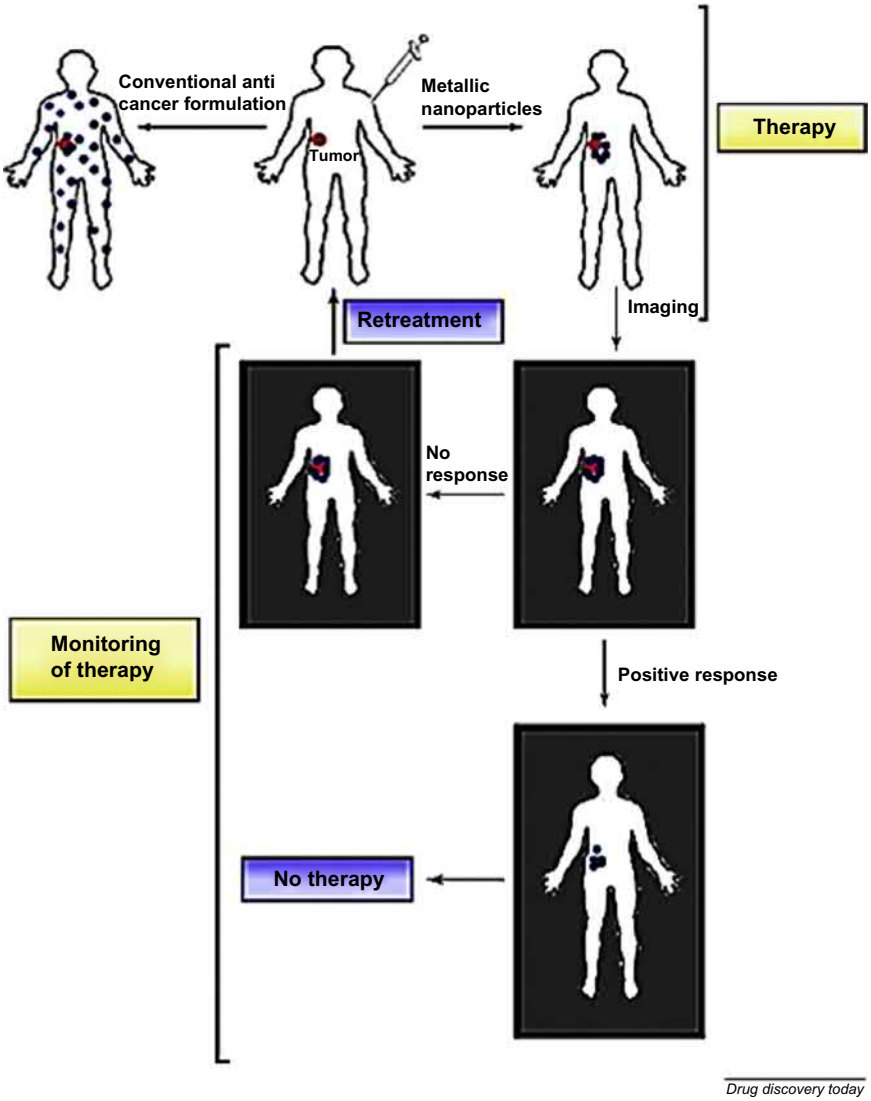

FIGURE 15.10 Theranostic appeal in cancer therapy. By using different methods, theranostic nanoparticles can be targeted toward the cancerous cells. These methods include active targeting using conjugated ligand nanoparticles, passive targeting, or by the use of the external magnetic field. The nanoparticles can induce therapeutic outcome after reaching the target, because of their inherent anticancer property or by delivering conjugated and or loaded chemotherapeutic agents. Therapy progress can be monitored by means of imaging properties of the metal nanoparticle. An alternate treatment can be specified if the patient is not responding. Source*: Adapted from Sharma, H., et al., 2015. Metal nanoparticles: a theranostic nanotool against cancer. Drug Discov. Today 20 (9), 1143–1151. doi:10.1016/j.drudis.2015.05.009.*

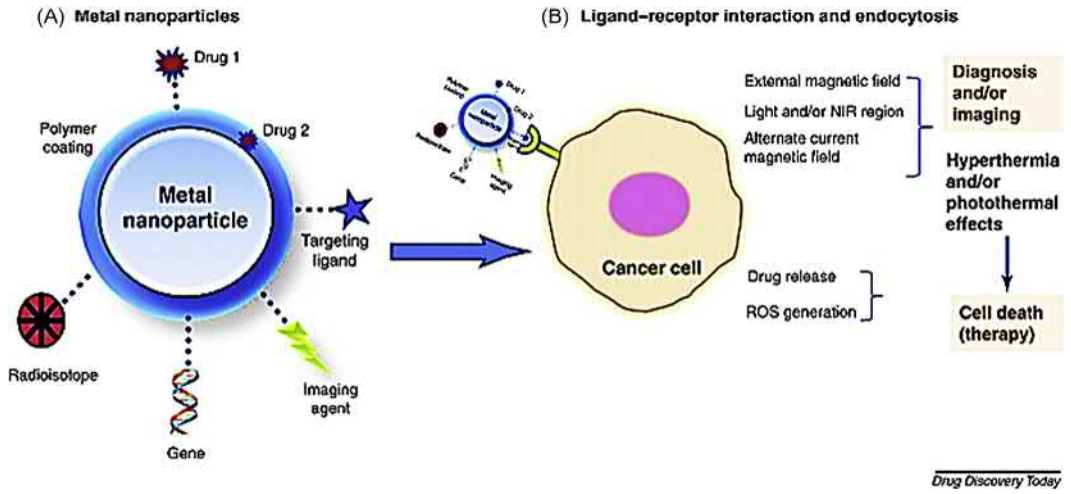

FIGURE 15.11 Multifunctional design of metal nanoparticles for cancer therapy. (A) Drug conjugation on the surface of NPs using the particles surface functional groups or through conjugation on the coated polymeric matrix or implantation of DNA and/or drugs in the polymeric matrix. Different imaging agents such as near-infrared dyes, fluorescent dyes, and radio isotopes can be loaded on the nanoparticles' surface, acting as a multifunctional theranostic agent. Targeting ligand or antibodies against exact receptor is achieved by its conjugation to NPs, leading to improvement of the specificity of the functionalized particles. (B) The particles will be internalized by cancer cells via endocytosis after ligand–receptor interaction. Tumor imaging can be done by applying magnetic field or light, which will also induce photothermal and hyperthermia effects; however, apoptosis will occur as a result of inherent activity of metal nanoparticles by ROS generation, and of loaded drug (chemotherapeutics). *NPs*, Nanoparticles; *ROS*, reactive oxygen species. Source*: Adapted from Sharma, H., et al., 2015. Metal nanoparticles: a theranostic nanotool against cancer. Drug Discov. Today 20 (9), 1143–1151. doi:10.1016/j.drudis.2015.05.009.*

Au NPs have been used as a potential delivery vehicle for anticancer drugs, improving their targeting and uptake into cells, such as paclitaxel- (Gibson, Khanal and Zubarev, 2007) or Pt-based drugs (e.g., cisplatin, oxaliplatin) (Dhar et al., 2009; Brown et al., 2010). Another example of the application of Au NPs in drug delivery is the photothermal drug delivery system developed through Au–Au sulfide nanoshells coated by a thermosensitive hydrogel matrix (Sershen et al., 2000). It has been found that NPs are particularly efficient in escaping the reticuloendothelial system (RES) (Hwu et al., 2009) (Fig. 15.11).

From numerous viewpoints, the brain is a challenging organ for drug delivery, mainly due to the presence of the blood–brain barrier (BBB), which halts the drug molecules from crossing it, and that is a major hurdle for the treatment of neurodegenerative conditions such as Alzheimer's and Parkinson's diseases. Many anti-Alzheimer's and anti-Parkinson's drugs lack brain targeting; this impedes their capability to attain essential maximum effective concentrations in the brain. On the other hand, NPs, on account of their small size, have the potential to cross various biological barriers in the body, particularly the BBB, which could lead to promising treatment outcomes for neurodegenerative disorders (Md et al., 2018).

15.15.2 Application in Protein Delivery

Proteins are macromolecules (also called biopharmaceuticals) that exert multiple biological actions in the human body and they have been known to be promising as treatment strategies for diverse diseases and disorders. Medical and pharmaceutical researchers sort protein drug delivery systems based on their various therapeutic applications (Raghvendra et al., 2010).

Several artificial proteins have been assembled via metal coordination site or specific mutations, which have important applications in catalysis, material, and biosupramolecular chemistry by mimicking naturally occurring proteins. One example is "protein cages," which Douglas et al. first introduced by modifying the exterior of the protein while maintaining its overall structure and properties. This artificial protein cage selectively binds to specific integrins that have a chief role in the initial phases of some cancers and rheumatoid arthritis (Schoonen and van Hest, 2014).

A new and innovative field of protein crystal engineering is gaining attention for developing solid biopharmaceuticals. Protein crystals, like natural protein assemblies, are densely packed monomeric proteins. These protein crystals can be modified and functionalized with metal ions or NPs via soaking or cocrystallization, creating new metal binding sites by site-specific mutations. Several metalloproteins have been developed where metal coordination has provided unnatural activity of metal ions and complexes in protein scaffolds, in efforts to understand natural functions of metalloproteins (Abe, Maity and Ueno, 2018).

15.15.3 Application in Peptide Delivery

Au NPs, due to their desirable properties, are particularly used as "transport vehicles" for various therapeutic agents and biomolecules including peptides (Abdelrasoul et al., 2015).

Antibiotic drug resistance is a global crisis that is driving the search for new treatment approaches. Antimicrobial peptides (AMPs) are small molecular weight proteins with varying number of amino acids found in both eukaryotes and prokaryotes. They have a broad spectrum of antibiotic activities and cytotoxic activity on cancer cells, and additionally antiinflammatory and immunomodulatory therapeutic actions. They have been recently discovered to have the potential to treat multiple drug−resistant infections. AMPs can be conjugated and functionalized with different materials such as antibiotics, polymers, DNA, salts, and phenolic derivatives. Using nanocarrier systems or nanoencapsulation for delivery has shown to improve the activity of the AMP (Faya et al., 2018).

15.15.4 Application in Gene Delivery

Gene therapies present an excellent stratagem for the treatment or prevention of genetic in addition to acquired diseases (Miller, 1992; Pan et al., 2018). Modern studies suggest that the ability to deliver the entire types of oligonucleotides such as single-stranded DNA, dual stranded DNA (dsDNA), single-stranded RNA, and plasmids could have outstanding therapeutic effects. Au NPs, in their diverse morphologies (e.g., nanospheres and nanorods), are potential candidates for DNA and RNA delivery as they protect nucleic

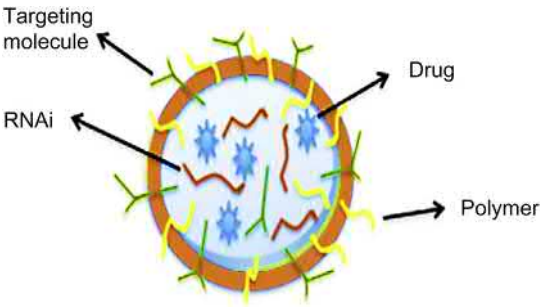

FIGURE 15.12 Illustration of therapeutic siRNA loaded nanoparticles. *siRNA*, Small interfering RNA. Source*: Adapted from Massadeh, S., Al Aamery, M., 2016. Nano-materials for gene therapy: an efficient way in overcoming challenges of gene delivery. J. Biosens. Bioelectron. 07 (01). doi:10.4172/2155-6210.1000195.*

acid and avert the molecules from nuclease degradation. In addition, Au NPs enhance targeting and help nucleic acid transfecting of cells. Conjugates of oligonucleotide-modified Au NPs have the potential to be used for intracellular gene regulatory agents. Au NPs functionalized with covalently bonding oligonucleotides are very capable of activating pathways in peripheral blood mononuclear cells and immune-related genes (Kim et al., 2012).

In attempts to overcome the disadvantages resulting from using traditional methods for genetic material delivery, different types of biocompatible NPs and new therapeutic approaches have been developed to deliver genetical moieties intended for gene therapy, such as the RNA interference therapy, which is a pathway that causes gene silencing and downregulation. Noncoding RNA may be considered a potent treatment for different diseases including cancer and viral diseases (Massadeh and Al Aamery, 2016). Moreover, research has found that small interfering RNA (siRNA) and microRNA could be used as restorative and curative agents alone due to their gene expression with high specificity. For instance, siRNA selectively increases the susceptibility of cells to low molecular weight anticancer agents housed in the same delivery system (Schiøtz et al., 2010; Kim et al., 2013; Lei et al., 2013; Deng et al., 2014; Takahashi and Carninci, 2014; Yan and Fu, 2014; Zhu et al., 2014; Chen, Gao and Huang, 2015; Rocha et al., 2015).

DNA-conjugated metal NPs have withdrawn the attention for their use in medical and biological applications, by which by combining these properties led to the development of highly sensitive and selective DNA detection technologies and development of extremely efficacious gene therapeutic agents. Researchers have established foremost effective methods to conjugate DNA with NPs to ensure the delivery of genes to the correct targeted cells. In a study, DNA−chitosan NPs have been synthesized to deliver DNA to the lungs, and based on the results, it seemed that DNA−chitosan NPs may be auspicious carriers for targeted gene delivery to the epithelial cell membranes of the lungs (Fig. 15.12) (Mohammadi et al., 2011; Das et al., 2014).

15.15.5 Application in Tissue Engineering

Tissue engineering is a rapidly developing field for the advancement of medicine. Its goal is to substitute or repair the anatomic scaffolds and functions of missing or damaged biological organs or tissues following any injury or pathological process by combining cells, tissue, biomaterials, and/or motivating the tissue microenvironment's mechanical

forces (Atala, 2000; Ibarra, Koski and Warren, 2000; Lanza et al., 2000; Miller and Patrick, 2003; Takezawa, 2003; Vats et al., 2003; Strobel et al., 2018; Zhang et al., 2019). Nanotechnology applications in tissue engineering mainly have three aspects: biomaterials scaffolding, cellular engineering, and biomolecular manipulation (Wen, Shi and Zhang, 2005). Fabrication and design of biocompatible scaffolds are achievable at the nanoscale in addition to control of the spatiotemporal biological and physiological factors release resembling natural behaviors of extracellular matrix to direct cell, and in the end leading to the development of implantable tissues (Abdelrasoul et al., 2015). In terms of cells for tissue engineering, nanotechnology can be used in two ways. One is to engineer cells for better regeneration, and the other is to study cell behavior, such as cell movement, proliferation, and tracing (Wen, Shi, and Zhang, 2005).

The chief function of a scaffold is to direct cell behaviors such as proliferation, differentiation, apoptosis, and maintenance of phenotype by facilitating sensing and responding to the environment via cell to cell communications and cell-matrix communications. Accordingly, for tissue engineering applications, several desired physical properties of biomaterial structures are required, such as huge surface area, high porosity, and homogeneously distributed interconnected porous structures in the matrix (Cima et al., 1991; Mikos et al., 1993; Edmondson et al., 2014). In nanotechnology, biomaterials may be assembled into specific geometrical and topological structures at a scale range of 1−100 nm and could be manipulated at the molecular, atomic, and macromolecular levels (West and Halas, 2000; Stix, 2001; Kricka and Fortina, 2002).

Au NP incorporation into biopolymer scaffolds is an effective pathway to produce nanostructures to deliver growth factors and medicinal agents directly into their target locations for tissue engineering applications. Polypropylene fumarate is a biodegradable, photocurable polymer resin, which can be functionalized with Au NPs to produce a hybrid resin to be straight exploited in stereolithography (SL) progressions. The Au NP nanofillers may be coated with PVP to enhance the stability of the colloidal particles. The produced resin was used to construct a new kind of complex structure via mask projection excimer laser SL (Abdelrasoul et al., 2015).

The use of artificial skin equivalents becomes great in cutaneous injuries and defects to avoid the cause of permanent infirmity or even death depending on the severity. Research using nanomaterials as in skin tissue transplant engineering is increasing to develop such biomaterials that mimic the native structure of extracellular matrices and offer a platformer base for cell attachment, proliferation, and differentiation (Fauzi et al., 2016; Sah and Rath, 2016). The biocompatibility of hydroxyethyl derivative of cellulose (HEC)/Ag NPs have been investigated and results showed significant scaffolds porosity, a high ability for water absorption, moderate degradation rate, and practical low toxicity. Therefore HEC/Ag NPs' scaffolds manifest ideal characteristics in skin tissue transplant engineering applications (Zulkifli et al., 2017).

15.15.6 Application in Enzymology

Application of metal NPs in enzymology is managed basically by using nanomaterials with the ability to mimic the protein enzymes' function. Several nanomaterials resemble

enzymes in size in addition to having catalytic activity. "Nanozyme" is a term used to focus on nanomaterials with intrinsic enzymatic properties. It has been found that simple metal oxide and metal NPs have catalytic action and essential ability in scavenging or generating active oxygen species and can take part in enzymatic reactions mirroring peroxidases, oxidases, superoxide dismutases, catalases, and laccases. In addition, NPs have been loaded with small inorganic catalysts to create other categories of nanozymes (He et al., 2014; Zhou et al., 2017).

Many NPs, especially those with enzyme-like activities, can be applied for commercial uses like in medical and pharmaceutical applications and the food industry. For example, peroxidase mimicking NPs may be used in wastewater treatment and detection of glucose in biological samples (He et al., 2014).

Iron oxide NPs' nanoscale physical properties such as magnetism/superparamagnetism, in addition to the assumption of being biologically inert, allow them to be used in a range of dissimilar fields. A good example of metal NPs' application in enzymology is that iron oxide NPs were found to hold enzyme-like activities, and are considered as novel enzyme mimetics (Gao, Fan, and Yan, 2017).

15.15.7 Application in Surface Coating of Nanoparticles

Surface alteration of NPs gives extraordinary properties and provides new potential for biomedical applications like drug targeting in terms of cell-specific binding, intracellular transport, and cellular uptake. For example, binding structural ligands of carbohydrate on the surface of biocompatible and biocomposable poly (D,L-lactic-*co*-glycolide) acid nanospheres were found to enhance carbohydrate cellular binding (Weissenböck, Wirth and Gabor, 2004). Another potential application is regarding the enhancement of immunologically directed targeting attained through coupling of certain proteins such as antibodies to a NP's surface, resulting in a more precise targeting (Nobs et al., 2004).

Numerous different types of NPs surface coatings have been shown in many studies to affect their properties, such as the production of improved biocompatible materials with significant stability against agglomeration. Among potential candidates for new biomedical applications are Ag NPs and maghemite (i.e., superparamagnetic iron oxide NPs or SPIONs), for which the inquiry into strict data concerning their behavior in a biological environment and physicochemical characteristics is maturing. There are Ag NPs and SPIONs under development in a number of sizes and surface coatings that can influence and improve the biocompatibility characteristics of those NPs. The biomedical applications of Ag NPs and SPIONs point toward enhanced cellular uptake into the body, which leads to interactions with protein-containing biological fluids (Jurašin et al., 2016).

Research has found that the combination of high adsorption strength of coating agents along with negative charge was demonstrated to be critical for effectively achieving great stability of metallic NPs in electrolyte-rich fluids. Moreover, the existence of proteins in biological fluids offers significant colloidal stabilization to metallic NPs irrespective of their chemical composition or their surface structure or surface charge (Gilbert et al., 2004; Zook et al., 2012).

15.15.8 Application in Biosensing Devices

Biosensors are analytical devices used for detection of various types of analytes, mainly biological, by translating a biological interaction by a physiochemical detector within the device into optical, electrochemiluminescent, electrochemical, gravimetric, or magnetic signals (Holzinger, Le Goff, and Cosnier, 2014). These analytes can be toxic substances, or biological compounds of importance for environmental monitoring biomedical diagnosis, and forensic analysis (Diamond, 1998). The biological compounds can be complex, such as antibodies, DNA, or different proteins, or simple like glucose (Holzinger, Le Goff, and Cosnier, 2014).

Generally, biosensors detectors rely on changes in color, UV−visible absorption, inelastic scattering, and fluorescence emission; the blue or redshift in plasmon resonance also can rely on solution properties such as conductivity, potential, and dielectric constant (Doria et al., 2012).

Due to the special physiochemical properties of nanoscale metals, they have been used in a wide range of biosensors applications, such as (1) nanoprobes for in vivo imaging/sensing, monitoring of disease pathology, or monitoring of therapy and cell tracking; (2) nanobiosensors for point of care disease diagnosis; and (3) other nanotechnology based tools for scientific research (Jain, 2007, 2008; Baptista, Doria and Conde, 2011; Zhao et al., 2011).

Different types of metals have shown good applicability in the biosensing area such as iron, heavy metals, and noble metals. However, in the past few years, great attention has been drawn toward noble NPs (mainly Au and Ag), as they have special physiochemical properties including high surface to volume ratio and simplicity of functionalization, in addition to their optical and spectral properties as SERS, LSPR, which made them better candidates to be used in biosensor devices (Wilcoxon, 2009; Doria et al., 2012).

Noble metal NPs development for biosensing applications requires functionalization with a different type of molecules or compounds such as antibodies, nucleic acids, enzymes, biocompatible polymers, and many different proteins to increase targeting specificity (Sperling and Parak, 2010; Subbiah, Veerapandian and Yun, 2010). Different types of conjugations between noble metal NPs and biomolecules have been introduced such as electrostatic interactions in the adsorption of negatively charged DNA to positively charged Au NPs (Sperling and Parak, 2010).

Many biological samples have been tested by noble metal NP biosensors using different types of methodologies such as colorimetric/scanometric, NIR, SERS, and fluorescence-based in addition to the electric/electrochemical method (Doria et al., 2012). Table 15.6 lists a summary of biological samples that have been tested by these methods relying on noble NP biosensors.

It's worth noting that not only noble metals have shown success in this field, as Wang et al. (2012) were able to modify electrodes with Au−Pt hybrid functionalized ZnO nanorods (Pt−Au@ZnONRs) in addition to fabrication of MWCNTs for use as a cholesterol biosensor.

TABLE 15.6 Some of the Biological Samples Tested Using Different Methodologies Relying on Metal NP Biosensors

Methodology	NP Type	Target/Samples (Reference)
Colorimetric/ Scanometric	Au	• SNPs in β-thalassemia gene in genomic DNA—mediated by PCR (Doria, Franco and Baptista, 2007; Li et al., 2010a,b) • SNPs in MBL2 gene in genomic DNA—mediated by PCR (Litos et al., 2007, 2009) • SNP associated with long QT syndrome (a physiological disorder that affect the repolarization of the heart after a heartbeat where Q and T referring to the heart's electrical cycle) in genomic DNA (Li and Rothberg, 2004) • SNP (rs2131877) in human DNA(Lee, Joo, et al., 2010) • Mutations in EGFR gene in genomic DNA (Lee, Kang, et al., 2010) • *Mycobacterium tuberculosis* DNA and associated drug-resistance SNPs in clinical samples (Baptista et al., 2006; Costa et al., 2010; Veigas et al., 2010) • Hepatitis C virus RNA (Shawky, Bald and Azzazy, 2010) • Fusion genes in K562 cell line (Kalogianni et al., 2007) • FSY1 mRNA in total RNA (Baptista et al., 2005) • BCR-ABL fusion transcript in clinical samples (Conde, de la Fuente and Baptista, 2010)
	Au	• PSA in human serum (Thaxton et al., 2009) • Mutations associated to methicillin resistance in *Staphylococcus aureus* and factor V Leiden mutants (Storhoff et al., 2004) • Melamine in whole milk (Wei et al., 2010) • Genetically modified organisms (Kalogianni et al., 2006) • CA15-3 breast cancer biomarker in human serum (ELISA) (Ambrosi, Airò and Merkoçi, 2010)
	Au/silver alloy	• BCR-ABL fusion genes (Baptista, Doria and Conde, 2011) • TP53 gene (Doria et al., 2010)
NIR	Au	• Lymph nodes in mouse (Pan et al., 2010) • Prostate cancer cells in mouse (Agarwal et al., 2007) • Brain vessels in mouse (Wang et al., 2004a,b; Yang et al., 2007; Lu et al., 2010) • HER2 cancer biomarker in breast adenocarcinoma cells (Loo et al., 2005; Bickford et al., 2008)
SERS	Au	• Deep-tissue imaging in living mouse (Zavaleta et al., 2009) • FCV antibody from cell culture media (Driskell et al., 2005) • Glucose in rat (Stuart et al., 2005) • Multiple pathogen DNA in clinical specimens (cerebrospinal fluid, stool, pus, and sputum) (Kang et al., 2010) • NAADP in cell extracts (Vitol et al., 2010) • Prostate-specific antigen in human serum (Grubisha et al., 2003)
	Silver	• Glucose in rat (Yuen et al., 2010) HIV-1 DNA in genomic DNA−PCR mediated (Wabuyele and Vo-Dinh, 2005)
	Au/silver core/shell	• Phospholipase Cγ1 biomarker protein in cancer cells (Lee et al., 2007a,b)

(*Continued*)

TABLE 15.6 (Continued)

Methodology	NP Type	Target/Samples (Reference)
Fluorescence-based	Au	• *Plasmodium falciparum* heat shock protein in infected blood cultures (Guirgis et al., 2012)
	Silver	• Cell membrane imaging in cell lines (Zhang et al., 2009; Zhang, Fu, Li, et al., 2010) • miRNA-486 expression levels in lung cancer cells (Zhang, Fu, Mei, et al., 2010)
Electric/ Electrochemical	Au	• Factor V Leiden DNA mutation in genomic DNA—mediated by PCR (Ozsoz et al., 2003) • *Escherichia coli* O157:H7 in food samples (Chen et al., 2008)
	Au	• Antihepatitis B virus antibodies and human IgG in human serum (de la Escosura-Muñiz, Maltez-da Costa and Merkoçi, 2009; de la Escosura-Muñiz et al., 2010) • Anti-*Toxoplasma gondii* immunoglobulins in rabbit blood and serum (Wang et al., 2004a,b) • HIV-1 protease and inhibitors in human serum (Mahmoud and Luong, 2008) • Human and goat IgG in serum (Leng et al., 2010) • Human and mouse IgG antibody in human and mouse serum (Lai et al., 2011) • Human IgG in human serum (Tian et al., 2009, 2010) • IL-6 cancer biomarker in calf serum (Dudkiewicz et al., 2011) • IL-8 cancer biomarker in human serum (Munge et al., 2011) • *P. falciparum* histidine-rich protein 2 in serum (Sharma et al., 2008) • *Salmonella* spp. in pork samples (Yang et al., 2009) • TNF-α in human serum (Yin et al., 2011)
	Silver	• AFP in human serum (Che et al., 2010)

AFP, α-1-Fetoprotein; *BCR-ABL*, breakpoint cluster region - Abelson murine leukemia; *EGFR*, epidermal growth factor receptor; *FCV*, Feline calicivirus; *IL-6*, Interleukin-6; *IL-8*, Interleukin-8; *PSA*, prostate-specific antigen; *NAADP*, nicotinic acid adenine dinucleotide phosphate; *SNP*, Solid lipid NP; *NP*, nanoparticle; *PCR*, polymerase chain reaction; *SERS*, surface-enhanced Raman spectroscopy; *TNF-α*, tumor necrosis factor-α.

Adapted with minimal modification from Doria, G., et al., 2012. Noble metal nanoparticles for biosensing applications. Sensors (Basel, Switzerland) 12 (2), 1657–1687. <http://dx.doi.org/10.3390/s120201657> open access distributed under the terms and conditions of the Creative Commons Attribution license (http://creativecommons.org/licenses/by/3.0/).

15.15.9 Application in Diagnostics

The optical properties of metallic nanocrystals such as high- or low-refractive index, high transparency, novel photoluminescence properties, photonic crystals, and plasmon resonance, have been of interest for decades. Biosynthetic methods have made it possible to prepare metal NPs of different sizes, shapes, and dielectric properties (Iskandar, 2009). Nanophotonics studies the behavior of light on the nanometer scale, where photons interact with particles smaller than their wavelength or nanostructures, for example, metallic NPs and CNTs, subsequently leading to novel phenomena, such as LSPR and a size-dependent semiconductor band gap (Talapin et al., 2010).

Au NPs have appeared to improve the specificity, sensitivity, turnaround times, and multiplexing of molecular diagnostics. Au NPs as molecular nanoprobes have widespread use in diagnostics, for example, Lu et al. have developed the foremost DNAzyme-based metal detectors for intracellular metal ion sensation, which are based on conjugating of a fluorescent DNAzyme onto Au NPs (Wu et al., 2013). In their work, adenosine triphosphate (ATP) aptamers and Ramos cell aptamers were covered on the surface of Au NPs, and showed a high specific target recognition ability for tumor sites. Also, various arrangements of the guanine–cytosine content pair (GC pairs represent the percentage of nitrogenous bases on a DNA or RNA molecule) into ATP aptamer dsDNA were designed to enhance the carrying ability of the DOX drug. Au nanocomposites have also been developed as ultrasensitive detectors for the carcinoembryonic antigen (Kong et al., 2011a,b;).

Hydrogen peroxide (H_2O_2) has been accepted as a diagnostic marker of oxidative stress, having an important role in asthma and chronic obstructive pulmonary disease (COPD). Wang et al. (2010) used the bacterial strain *B. subtilis* to create a hydrogen peroxide sensor based on biosynthesized Se NPs. The Se NPs produced were spherical and could be converted into one-dimensional trigonal wires, due to the proteins excreted from *B. subtilis* cells that act as a template. Cyclic voltammetry studies proved that Se NPs enhance the detection of H_2O_2 resulting in an 80-nM detection limit. Thus, Se NPs can be used for the detection of hydrogen peroxide in the exhaled breath of COPD patients (Wang et al., 2010).

15.15.10 Application in Theranostics

Recently, anisotropic noble metal NPs (ANPs) based theranostics have been developed, which hold the potential to revolutionize disease management and have promising therapeutic restorative potential because of their capacity in drug delivery along with their applicability in monitoring therapeutic responses and diagnosis.

Metallic ANPs have been studied as theranostics particularly for photochemotherapy in cancer therapy because of two important features. This first is their ease of attachment of chemotherapeutics and other useful ligands to ANPs through either capping agent thiol arbitrated binding or surface responsive groups (e.g., amino group and carboxyl group). The second important feature is the introduction of photothermal adaptation, by altering the absorbed photons to heat to eradicate cancer cells. The convenience of a wide range of metallic ANPs (e.g., nanoshells, nanocages, nanospheres), as well as cancer cells specific ligands (e.g., biomolecules, proteins, antibodies), make them promising theranostics in tumor targeting therapy (Paramasivam et al., 2017). Silica-coated AuNRs have been developed and shown to be multifunctional theranostics by liberating the loaded DOX upon exposure to NIR radiation. The rudimentary principle of theranostics has the title role of inquiry for both photon imaging and hyperthermia, even though silica coating accomplishes the role of a carrier and encapsulates the drug (DOX). Since the NPs have absorption properties at NIR range, the performances of the Au NRs–SiO_2–DOX system for hyperthermia and chemotherapy significantly have been influenced by changing of laser power density (Zhang et al., 2012a,b; Pandey et al., 2013; Zhang, Wang, and Chen, 2013).

Hong et al. prepared a multifunctional NP allowing two diverse groups to occur on each particle surface and called them Janus NPs, for example, Au NRs-mesoporous silica, and overloaded them with cancer therapies and/or imaging mediators for treating liver cancer cells. The presence of NRs in Janus NPs led them to produce heat when exposed to near-infrared light (NIR) light, thus, it is a promising theranostics system for combined photothermal and chemo cancer therapy (Wang et al., 2015).

It has been reported that colloidal green manufactured Ag nanoprisms (AgNPrs) can be generated by the reduction of Ag ions by *Olax scandens* leaf extract, which may be used for several purposes such as antibacterial and anticancer agents, drug delivery carriers, and imaging facilitators. The occurrence of imaging facilitators and anticancer effect in the NPs marks them as potential theranostics systems for cancer therapy (Mukherjee et al., 2014).

15.15.11 Other Application

15.15.11.1 Application in Cosmetics

Nanotechnology has now found applications in the area of nanocosmetics. Cosmetic manufacturers use nanoscaled ingredients to achieve deeper skin penetration, better UV protection, increased color, in addition to long-lasting effects, etc. Cosmetic manufacturers are coupling the enhanced antibacterial properties of nanosilver in several applications, for example, using it as a preservative in cosmetic products. Some manufacturers are producing deodorants with claims of the provision of up to 24-hour antibacterial protection due to the presence of Ag NPs in the product. Nanosized Au particles are also claimed to possess disinfecting effects against several strains of bacteria present in the mouth, therefore, they have been added to some toothpaste formulas (Raj et al., 2012).

15.15.11.2 Application of Au Nanoparticle–Based Molecular Imaging

Molecular imaging technologies have been undergoing increasing development in the past decade. Molecular imaging enables providing pathological and physiological information with high specificity and sensitivity for disease diagnosis. A range of imaging types such as computed tomography imaging, optical imaging, MRI, and ultrasound imaging have been developed for the diagnosis of diseases. In comparison with multiple other imaging techniques, SERS has the advantages of high accuracy, sensitivity, lack of damage, and no invasion for molecular identification. Au NPs typically have been used in the SERS technique, utilized as intracellular probes to monitor intracellular drug release as well as to probe molecules by targeting them at cellular compartments such as endosomes, cell nucleus, and mitochondria (Huefner et al., 2014).

15.15.11.3 Application in Wound Dressings

A wound is an external or internal breakage in or trauma to body tissue, typically involving the skin. Healing occurs over several complex stages including inflammation, proliferation, and remodeling. The dressing material is an important factor in maintaining the phases of healing. Dressings use different types of polymers whose origin is either synthetic or natural. Over the decades, various materials have been used, including cotton gauze, sponges, fins, etc. Nonetheless, commonly used synthetic dressings have disadvantages such as low mechanical strength and harmful degradation by-products. Therefore

the need for dressings made from natural polymers is increasing to decrease microbial infections as well as aiding in the healing process, for example, control of scar formation and extracellular matrix remodeling.

Extensive studies have been made on metal-based agents, and the incorporation of metallic NPs into chitosan scaffolds such as chitosan/nAg, chitosan/nAu, chitosan/nCu, chitosan/nZnO, and chitosan/n TiO. These dressing materials have been shown to have improved antimicrobial activity, modified cytotoxicity, in addition to the enhancement of healing by the incorporated metallic NPs through the regulation and control of reepithelialization and inflammation (Mohandas et al., 2018).

15.16 FUTURE POTENTIAL OF METALLIC NANOPARTICLES: EMERGING AREA OF BIOMEDICAL SCIENCES

Ongoing advancements in nanomedicine have created numerous opportunities for applications in a variety of medical and pharmaceutical disciplines. Metallic NPs' future applications for developing new generations of targeted drugs and diagnostics is under continuous research. For instance, in diagnosis, diseased cells' detection is faster and more specific, possibly at the point of a single ill cell, allowing diseased cells to be cured immediately before they spread into and/or affect other cells in other body parts (Fakruddin, Hossain and Afroz, 2012). Some drug delivery systems are still under clinical trial or are commercialized, for example, nanosystems and the American Pharmaceutical Partners have been developing drug delivery systems such as paclitaxel, which is the anticancer drug Taxol encapsulated in a polymer to make a nanosystem. Nonetheless, most therapeutics and medical agents are a decade or more away from being launched into the market. Furthermore, drug target manipulation requires complex technical infrastructure, that is, nanotechnology, which in turn needs constant regulatory management (Hamad-Schifferli et al., 2002).

Despite the controversies, nanotechnology provides optimism for the future. It provides eminent improvements in varying biomedical applications, from drug delivery and gene therapy to molecular imaging, biomarkers, and biosensors. Currently, the primary research objective is to achieve target-specific drug therapy and methods for early diagnosis and treatment of diseases (Sahoo and Labhasetwar, 2003).

Two key types of medical applications are emerging, both in R&D and in clinical trials; one is monitoring tissue activity at the cellular level and imaging, for example, semiconductor quantum dot technology, which is already licensed. The second major application type encompasses the development of highly sensitive and specific means of proteins and nucleic acids detection (Milunovich and Roy, 2001). In the years 2015–20, products are being tested in governmental laboratories and will be commercialized, for instance, molecular filtration and sparse cell isolation applications will be reaching the market.

Ag NP aptamers are used in single NP spectral analysis and intracellular protein imaging where Ag NPs act as aillumiophores and the aptamer as a biomolecule specific recognition unit, respectively (Chen et al., 2010a,b; Rosarin and Mirunalini, 2011).

Metallic NPs exhibit interesting and essential properties that can be harnessed for developing new generations of targeted-drug delivery systems, diagnoses, and treatments of a diverse range of life-threatening diseases. The biologically produced nanomaterials

are used for the management of microbial infections, cancer detection, and other diseases. Researchers have been recently focusing mainly on the development of the multifunctional nanoscale-sized platform with the highest targeting efficacy. Targeted delivery systems may exceptionally contribute to the in vitro and in vivo applications of nanobiomaterials in the field of nanomedicine. The techniques of these delivery systems, with a lack of toxicity, will enable the diagnosis of various types of cancers. The bionanomaterials for drug delivery may be potential natural nanocarriers and may have considerable significance for theranostic systems (Mittal and Banerjee, 2016).

Due to the reemergence of widespread infectious diseases and antibiotic-resistant strains, the need for alternative antimicrobial strategies has been rising. Several types of research have been conducted on metallic NPs, and remarkable results have been noted. Therefore they are being widely used as antibacterial agents and are currently regarded as the most effective antibacterial agents. One of the important efficient antibacterial metal NPs is Ag NPs, as it has been proven that colloidal Ag is a bactericidal and is a far more efficient antibiotic than any allopathic pharmaceutical agent. Colloidal Ag is effective in killing around 650 bacteria in a few minutes with concentrations ranging from 5 to 6 ppm. In four different preliminary studies, the solution of nanosilver embedded in water (ASAP) product has been effective at eradicating malaria from the bloodstream an average of 3 days after human ingestion. In a study at a US National Institutes of Health lab, using the ASAP nanosilver product orally on a daily basis on an animal model was able to boost the survival rate of mice by 100% against H5N1 bird flu virus. Moreover, this product was found to increase the T-lymphocyte number in seven patients with AIDS by an average of 40% within four months of administration a low oral daily dose. It is also worth noting that this product is patented capable of eradicating tuberculosis, methicillin-resistant *S. aureus*, hepatitis B, HIV, yeast, and several other pathogens (Rosarin and Mirunalini, 2011).

CONCLUSION

Metal NPs play a major role in nanotechnology and nanoscience. Using their metallic characteristics scientists were able to synthesize metal NPs using top-down and bottom-up approaches including physical, chemical, and biological methods. Biological methods were found to be the most environmentally friendly and least toxic methods.

Different analytical methods can be used to analyze and characterize the synthesized NPs, including, size, shape, the surface of the NP, functional groups, size distribution, aggregation, dispersion, structure, binding hydrodynamics, and confirmation to have enough information to find the proper application for these NPs or proper functionalization.

The main methods that can be used to determine the characteristics of NPs have been explained and summarized; they include optical, spectroscopic, and microscopic techniques such as UV spectroscopy, FTIR, SEM, ESEM, TEM, XRD, FCS, SERS, TERs, ZP, CD, MS, STM, DLS, and AFM.

Moreover, metal NPs have been found to play a major role in the medical, biomedical, and pharmaceutical applications of nanotechnology. They proved to be effective in drug delivery, protein, peptide, and gene delivery. Also, they have shown potential in tissue

engineering, enzymology, as well as usefulness in surface coatings. Furthermore, they have shown promising employability in biosensors, diagnostics, and theranostics, that is, the future of the medical sciences.

Acknowledgments

We acknowledge the Deanship of Research and Graduate Studies at Philadelphia University for funding the research project underlying this book chapter. The authors are also thankful to Dr. Pran Kishore Deb (Philadelphia University) and Prof. Rakesh K. Tekade (NIPER-Ahmedabad) for their valuable suggestions and guidance through the preparation of the manuscript.

ABBREVIATIONS

AFM	atomic-force microscopy
Ag	silver
$AgNO_3$	silver nitrate
Al	aluminum
$AlCl_3$	aluminum trichloride
ALD	atomic layer deposition
AMPs	antimicrobial peptides
ANPs	anisotropic noble metal nanoparticles
ASAP	solution of nanosilver embedded in water
ATP	adenosine triphosphate
Au NRs	Au nanorods
Au	gold
BBB	blood–brain barrier
BMNPs	bimetallic nanoparticles
BSE	backscattered electron
C	carbon
Cd	cadmium
CD	circular dichroism
CdS	cadmium sulfide
CdSeP	cadmium selenium phosphate
CeO_2	cerium dioxide
CNTs	carbon nanotubes
Co	cobalt
COPD	chronic obstructive pulmonary disease
Cr	chromium
CT	computed tomography
CTAB	cetyltrimethylammonium bromide
Cu	copper
DLS	dynamic light scattering
DOX	doxorubicin
dsDNA	dual stranded DNA
EDX	energy-dispersive X-ray
ESEM	environmental scanning electron microscopy
ESI–MS	electrospray ionization–mass spectrometry
ETV	introductive matrix-tolerant nebulizers of *electrothermal vaporization*
FCS	fluorescence correlation spectroscopy
Fe	iron

Fe_2O_3	iron oxide
Fe_3O_4	iron oxide magnetite
FeII $FeIII_2O_4$	iron oxides
FeII	ferrous (iron divalent oxidation state)
FeIII	ferric (iron trivalent oxidation state)
FeO	iron oxide, wüstite, antiferromagnetic
FTIR	Fourier transforms infrared spectroscopy
H_2O_2	hydrogen peroxide
H_2S	hydrogen sulfide
H5N1	bird flu virus
HA	hydroxyapatite
$HAuCl_4$	chloroauric (Au) acid tetrahydrate
HEC	hydroxyethyl derivative of cellulose
ICP-MS	inductive coupled plasma–mass spectrometry
IP6	inositol hexa kis phosphate
KOH	potassium hydroxide
Li	lithium
LSPR	localized surface plasmon resonance
MALDI–MS	matrix-assisted laser desorption/ionization–mass spectrometry
MCD	magnetic circular dichroism
Mg	magnesium
MKY3	silver-tolerant yeast strain
MR	magnetic resonance
MRI	magnetic resonance imaging
MS	mass spectroscopy
MWCNT	multiwalled carbon nanotube
MWNT	multiwalled nanotubes
Na	sodium
$NaBH_4$	sodium borohydride
NIR	near-infrared radiation
NMR	nuclear magnetic resonance spectroscopy
NPs	nanoparticles
NSOM	near-field scanning optical microscopy
Pb	lead
Pd	palladinum
Pt	platinum
PVP	polyvinylpyrrolidone
RES	reticuloendothelial system
Ru	ruthenium
SE	secondary electron
Se	selenium
SEM	scanning electron microscopy
SERS	surface-enhanced Raman spectroscopy
SiO_2	silicon dioxide
siRNA	small interfering RNA
SL	stereolithography
SPIONs	superparamagnetic iron oxide nanoparticles
***Streptomyces* sp. LK-3**	type of *Streptomyces* species
STM	scanning tunneling microscopy
SWNT	single-walled nanotube
TEM	transmission electron microscopy
TERS	tip-enhanced Raman spectroscopy
TiO_2	titanium dioxide

UV	ultraviolet
VCD	vibrational circular dichroism
XEDS	X-ray energy dispersive spectroscopy
XPS	X-ray photoelectron spectroscopy
XRD	X-ray crystallography
Zn	zinc
ZnO	zinc oxide
ZnS	zinc sulfide
ZP	zeta potential
α-Fe_2O_3	alpha phase iron oxide, hematite
β-Fe_2O_3	beta phase iron oxide
γ-Fe_2O_3	gamma phase iron oxide, maghemite
ε-Fe_2O_3	epsilon-phase iron oxide

References

Abbai, R., et al., 2016. Green synthesis of multifunctional silver and Au nanoparticles from the oriental herbal adaptogen: Siberian ginseng. Int. J. Nanomed. 11, 3131–3143. Available from: https://doi.org/10.2147/IJN.S108549.

Abdelrasoul, G.N., et al., 2015. Nanocomposite scaffold fabrication by incorporating Au nanoparticles into biodegradable polymer matrix: synthesis, characterization, and photothermal effect. Mater. Sci. Eng., C 56, 305–310. Available from: https://doi.org/10.1016/j.msec.2015.06.037.

Abe, S., Maity, B., Ueno, T., 2018. Functionalization of protein crystals with metal ions, complexes and nanoparticles. Curr. Opin. Chem. Biol. 43, 68–76. Available from: https://doi.org/10.1016/j.cbpa.2017.11.015.

Abhilash, M., 2010. Potential applications of nanoparticles. Int. J. Pharma Bio Sci. 1 (1), 379–386.

Agarwal, A., et al., 2007. Targeted Au nanorod contrast agent for prostate cancer detection by photoacoustic imaging. J. Appl. Phys. 102 (6), 064701. Available from: https://doi.org/10.1063/1.2777127.

Agarwal, H., Venkat Kumar, S., Rajeshkumar, S., 2017. A review on green synthesis of zinc oxide nanoparticles – an eco-friendly approach. Res.-Efficient Technol. 3 (4), 406–413. Available from: https://doi.org/10.1016/j.reffit.2017.03.002.

Agrawal, P., Bhushan, S., 2013. Preparation of sericin nano particles from waste of silk industry. Int. J. Sci. Res. 1 (3), 116–120. Available from: http://journal.tumkuruniversity.ac.in:8080/index.php/ijsr/article/viewFile/54/36.

Ahamed, M., Alsalhi, M.S., Siddiqui, M.K.J., 2010. Silver nanoparticle applications and human health. Clin. Chim. Acta 411 (23–24), 1841–1848. Available from: https://doi.org/10.1016/j.cca.2010.08.016.

Ahmed, S., et al., 2016. A review on plants extract mediated synthesis of silver nanoparticles for antimicrobial applications: a green expertise. J. Adv. Res. pp. 17–28. Available from: http://dx.doi.org/10.1016/j.jare.2015.02.007.

Aitken, R.J., Creely, K.S., Tran, C.L., 2004. Nanoparticles: an occupational hygiene review. Health Saf. Exec. 113.

Akbarzadeh, A., et al., 2013. Liposome: classification, preparation, and applications. Nanoscale Res. Lett. 8 (1), 102. Available from: https://doi.org/10.1186/1556-276X-8-102.

Aladpoosh, R., Montazer, M., 2015. The role of cellulosic chains of cotton in biosynthesis of ZnO nanorods producing multifunctional properties: mechanism, characterizations and features. Carbohydr. Polym. 126, 122–129. Available from: https://doi.org/10.1016/j.carbpol.2015.03.036.

Alaqad, K., Saleh, T.A., 2016. Au and silver nanoparticles: synthesis methods, characterization routes and applications towards drugs. J. Environ. Anal. Toxicol. 6 (4). Available from: https://doi.org/10.4172/2161-0525.1000384.

Ali, A., et al., 2016. Synthesis, characterization, applications, and challenges of iron oxide nanoparticles. Nanotechnol. Sci. Appl. Vol. 9, 49–67. Available from: https://doi.org/10.2147/NSA.S99986.

Ambrosi, A., Airò, F., Merkoçi, A., 2010. Enhanced Au nanoparticle based ELISA for a breast cancer biomarker. Anal. Chem. 82 (3), 1151–1156. Available from: https://doi.org/10.1021/ac902492c.

Amjadi, M., Farzampour, L., 2014. Fluorescence quenching of fluoroquinolones by Au nanoparticles with different sizes and its analytical application. J. Lumin. 145, 263–268. Available from: https://doi.org/10.1016/j.jlumin.2013.07.055.

Anandalakshmi, K., Venugobal, J., Ramasamy, V., 2016. Characterization of silver nanoparticles by green synthesis method using *Pedalium murex* leaf extract and their antibacterial activity. Appl. Nanosci. 6 (3), 399–408. Available from: https://doi.org/10.1007/s13204-015-0449-z.

Anandan, S., Grieser, F., Ashokkumar, M., 2008. Sonochemical synthesis of Au–Ag core–shell bimetallic nanoparticles. J. Phys. Chem. C 112 (39), 15102–15105. Available from: https://doi.org/10.1021/jp806960r.

Anandhakumar, S., et al., 2011. Polyelectrolyte microcapsules for sustained delivery of water-soluble drugs. Mater. Sci. Eng., C 31 (2), 342–349. Available from: https://doi.org/10.1016/j.msec.2010.10.005.

Anandhakumar, S., et al., 2014. Tailor-made hollow silver nanoparticle cages assembled with silver nanoparticles: an efficient catalyst for epoxidation. ACS Appl. Mater. Interfaces 6 (5), 3275–3281. Available from: https://doi.org/10.1021/am500229v.

Anandhakumar, S., Nagaraja, V., Raichur, A.M., 2010. Reversible polyelectrolyte capsules as carriers for protein delivery. Colloids Surf., B: Biointerfaces 78 (2), 266–274. Available from: https://doi.org/10.1016/j.colsurfb.2010.03.016.

Ando, J., Fujita, K., 2013. Metallic nanoparticles as SERS agents for biomolecular imaging. Curr. Pharm. Biotechnol. 14 (2), 141–149. Available from: https://doi.org/10.2174/1389201011314020003.

Angelucci, C.A., D'Villa Silva, M., Nart, F.C., 2007. Preparation of platinum–ruthenium alloys supported on carbon by a sonochemical method. Electrochim. Acta 52 (25), 7293–7299. Available from: https://doi.org/10.1016/j.electacta.2007.05.069.

Malik, A., Chaudhary, S., Garg, G., Tomar, A., 2012. Dendrimers: a tool for drug delivery. Adv. Biol. Res. 6 (4), 165–169. Available from: https://pdfs.semanticscholar.org/2b03/f81c5dc8cfa84071380f4d8e41200bb51944.pdf.

Anju Manuja, R.R., 2015. Zinc oxide nanoparticles: opportunities and challenges in veterinary sciences. Immunome Res. 11 (2). Available from: https://doi.org/10.4172/1745-7580.1000095.

Arvizo, R.R., et al., 2012. Intrinsic therapeutic applications of noble metal nanoparticles: past, present and future. Chem. Soc. Rev. 41 (7), 2943–2970. Available from: https://doi.org/10.1039/c2cs15355f.

Astruc, D., Lu, F., Aranzaes, J.R., 2005. Nanoparticles as recyclable catalysts: the frontier between homogeneous and heterogeneous catalysis. Angew. Chem. (Int. ed. English) 44 (48), 7852–7872. Available from: https://doi.org/10.1002/anie.200500766.

Atala, A., 2000. Tissue engineering of artificial organs. J. Endourol. 14 (1), 49–57. Available from: https://doi.org/10.1089/end.2000.14.49.

Aymonier, C., et al., 2002. Hybrids of silver nanoparticles with amphiphilic hyperbranched macromolecules exhibiting antimicrobial properties. Chem. Commun. (Cambridge, England) 24, 3018–3019. Available from: http://www.ncbi.nlm.nih.gov/pubmed/12536795.

Balela, M.D., Amores, K.L., 2015. Formation of oxidation-stable copper nanoparticles in water. Adv. Mater. Res. 1131, 255–259. Available from: https://doi.org/10.4028/www.scientific.net/AMR.1131.255.

Bandyopadhyay, S., et al., 2018. Growing Au nanostructures for shape-selective cellular uptake. Nanoscale Res. Lett. 13 (1), 254. Available from: https://doi.org/10.1186/s11671-018-2662-7.

Bansal, V., et al., 2004. Biosynthesis of zirconia nanoparticles using the fungus *Fusarium oxysporum*. J. Mater. Chem. 14 (22), 3303. Available from: https://doi.org/10.1039/b407904c.

Bansal, V., et al., 2005. Fungus-mediated biosynthesis of silica and titania particles. J. Mater. Chem. 15 (26), 2583. Available from: https://doi.org/10.1039/b503008k.

Bansal, V., et al., 2006. Room-temperature biosynthesis of ferroelectric barium titanate nanoparticles. J. Am. Chem. Soc. 128 (36), 11958–11963. Available from: https://doi.org/10.1021/ja063011m.

Baptista, P., et al., 2005. Colorimetric detection of eukaryotic gene expression with DNA-derivatized Au nanoparticles. J. Biotechnol. 119 (2), 111–117. Available from: https://doi.org/10.1016/j.jbiotec.2005.02.019.

Baptista P.V., Doria G. and Conde J., In: "Alloy metal nanoparticles for multicolor cancer diagnostics", In Proceeding SPIE 7909, Colloidal Quantum Dots/Nanocrystals for Biomedical Applications VI, 79090K (11 February 2011); doi: 10.1117/12.879025; https://doi.org/10.1117/12.879025

Baptista, P.V., et al., 2006. Au-nanoparticle-probe-based assay for rapid and direct detection of *Mycobacterium tuberculosis* DNA in clinical samples. Clin. Chem. 52 (7), 1433–1434. Available from: https://doi.org/10.1373/clinchem.2005.065391.

Barnaby, S., et al., 2013. The spontaneous formation of selenium nanoparticles on gallic acid assemblies and their antioxidant properties. Fordham Undergraduate Res. J. 1 (1), 1–6. Available from: http://fordham.bepress.com/furj/vol1/iss1/3/?utm_source = fordham.bepress.com/furj/vol1/iss1/3&utm_medium = PDF&utm_campaign = PDFCoverPages.

Baskoutas, S., 2018. Special issue: zinc oxide nanostructures: synthesis and characterization. Materials 11 (6), 873. Available from: https://doi.org/10.3390/ma11060873.

Behnam, M.A., et al., 2018. Novel combination of silver nanoparticles and carbon nanotubes for plasmonic photo thermal therapy in melanoma cancer model. Adv. Pharm. Bull. 8 (1), 49–55. Available from: https://doi.org/10.15171/apb.2018.006.

Benelmekki, M., 2014. An introduction to nanoparticles and nanotechnology. Des. Hybrid Nanopart. Available from: https://doi.org/10.1088/978-1-6270-5469-0ch1.

Bharde, A., et al., 2006. Extracellular biosynthesis of magnetite using fungi. Small (Weinheim an der Bergstrasse, Germany) 2 (1), 135–141. Available from: https://doi.org/10.1002/smll.200500180.

Bhatia, A., Shard, P., Chopra, D., Mishra, T., et al., 2011. Chitosan nanoparticles as carrier of immunorestoratory plant extract: synthesis, characterization and immunorestoratory efficacy. Int. J. Drug Deliv. 3, 381–385. ISSN: 0975-0215.

Bhatia, S., 2016. Nanoparticles types, classification, characterization, fabrication methods and drug delivery applications. Natural Polymer Drug Delivery Systems. Springer International Publishing, Cham, pp. 33–93. Available from: http://dx.doi.org/10.1007/978-3-319-41129-3-2.

Bhattacharya, R., Mukherjee, P., 2008. Biological properties of "naked" metal nanoparticles. Adv. Drug Deliv. Rev. 60 (11), 1289–1306. Available from: https://doi.org/10.1016/j.addr.2008.03.013.

Bhogale, A., et al., 2014. Comprehensive studies on the interaction of copper nanoparticles with bovine serum albumin using various spectroscopies. Colloids Surf., B: Biointerfaces 113, 276–284. Available from: https://doi.org/10.1016/j.colsurfb.2013.09.021.

Bickford, L., et al., 2008. Enhanced multispectral imaging of live breast cancer cells using immunotargeted Au nanoshells and two-photon excitation microscopy. Nanotechnology 19 (31), 315102. Available from: https://doi.org/10.1088/0957-4484/19/31/315102.

Biggs, K.B., et al., 2009. Surface-enhanced Raman spectroscopy of benzenethiol adsorbed from the gas phase onto silver film over nanosphere surfaces: determination of the sticking probability and detection limit time. J. Phys. Chem. A 113 (16), 4581–4586. Available from: https://doi.org/10.1021/jp8112649.

Blaber, M., 2016. Metals, nonmetals, and metalloids. Available from: <https://chem.libretexts.org/Textbook_Maps/General_Chemistry/Map%3A_Chemistry_-_The_Central_Science_(Brown_et_al.)/07._Periodic_Properties_of_the_Elements/7.6%3A_Metals%2C_Nonmetals%2C_and_Metalloids> (accessed 11.06.08).

Black, K.C.L., et al., 2014. Radioactive 198Au-doped nanostructures with different shapes for in vivo analyses of their biodistribution, tumor uptake, and intratumoral distribution. ACS Nano 8 (5), 4385–4394. Available from: https://doi.org/10.1021/nn406258m.

Blakemore, R., 1975. Magnetotactic bacteria. Science (New York, NY) 190 (4212), 377–379. Available at: http://www.ncbi.nlm.nih.gov/pubmed/170679.

Bogner, A., et al., 2005. Wet STEM: a new development in environmental SEM for imaging nano-objects included in a liquid phase. Ultramicroscopy. North-Holland 104 (3–4), 290–301. Available from: http://dx.doi.org/10.1016/J.ULTRAMIC.2005.05.005.

Bogutska, KI, Sklyarov, Y.P., Prylutskyy, Y.I, 2013. Zinc and zinc nanoparticles: biological role and application in biomedicine. Ukrain. Bioorg. Acta 1, 9–16.

Boltasseva, A., Atwater, H.A., 2011. Low-loss plasmonic metamaterials. Science 290–291. Available from: https://doi.org/10.1126/science.1198258.

Bootz, A., et al., 2004. Comparison of scanning electron microscopy, dynamic light scattering and analytical ultracentrifugation for the sizing of poly(butyl cyanoacrylate) nanoparticles. Eur. J. Pharm. Biopharm. 57 (2), 369–375. Available from: http://dx.doi.org/10.1016/S0939-6411(03)00193-0.

Borovaya, M.N., et al., 2015. Biosynthesis of quantum dots and their potential applications in biology and biomedicine. In: Fesenko, O., Yatsenko, L. (Eds.), Nanoplasmonics, Nano-Optics, Nanocomposites, and Surface Studies, Springer Proceedings in Physics. Springer International Publishing, Switzerland, pp. 339–362. Available from: http://dx.doi.org/10.1007/978-3-319-18543-9-24.

Bosetti, M., et al., 2002. Silver coated materials for external fixation devices: in vitro biocompatibility and genotoxicity. Biomaterials 23 (3), 887–892. Available from: http://www.ncbi.nlm.nih.gov/pubmed/11771707.

Boukari, H., Sackett, D.L., 2008. Fluorescence correlation spectroscopy and its application to the characterization of molecular properties and interactions. Methods Cell Biol. 84, 659–678. Available from: https://doi.org/10.1016/S0091-679X(07)84021-0.

Vanden Bout, D.A., 2002. Metal nanoparticles: synthesis, characterization, and applications. Edited by Daniel L. Feldheim (North Carolina State University) and Colby A. Foss, Jr. (Georgetown University). Marcel Dekker, Inc.: New York and Basel. 2002. x + 338 pp. $150.00. ISBN: 0-82. J. Am. Chem. Soc. 124 (26), 7874–7875. doi: 10.1021/ja015381a.

Brar, S.K., Verma, M., 2011. Measurement of nanoparticles by light-scattering techniques. TrAC, Trends Anal. Chem. 30 (1), 4–17. Available from: https://doi.org/10.1016/j.trac.2010.08.008.

Brock, T.D., Gustafson, J., 1976. Ferric iron reduction by sulfur- and iron-oxidizing bacteria. Appl. Environ. Microbiol. 32 (4), 567–571. Available from: http://www.ncbi.nlm.nih.gov/pubmed/825043.

Brown, S.D., et al., 2010. Au nanoparticles for the improved anticancer drug delivery of the active component of oxaliplatin. J. Am. Chem. Soc. 132 (13), 4678–4684. Available from: https://doi.org/10.1021/ja908117a.

Bu, Y., Lee, S., 2012. Influence of dopamine concentration and surface coverage of Au shell on the optical properties of Au, Ag, and Ag core Au shell nanoparticles. ACS Appl. Mater. Interfaces 4 (8), 3923–3931. Available from: https://doi.org/10.1021/am300750s.

Camden, J.P., et al., 2008. Probing the structure of single-molecule surface-enhanced Raman scattering hot spots. J. Am. Chem. Soc. 130 (38), 12616–12617. Available from: https://doi.org/10.1021/ja8051427.

Caminade, A.-M., Laurent, R., Majoral, J.-P., 2005. Characterization of dendrimers. Adv. Drug Deliv. Rev. 57 (15), 2130–2146. Available from: https://doi.org/10.1016/j.addr.2005.09.011.

Campos, E.A., et al., 2015. Synthesis, characterization and applications of iron oxide nanoparticles—a short review. J. Aerosp. Technol. Manage. 7 (3), 267–276. Available from: https://doi.org/10.5028/jatm.v7i3.471.

Canevarolo, J.S., 2004. Técnicas de caracterização de polímeros. Artliber, São Paulo.

Cao, X.B., et al., 2004. Ultra-thin trigonal selenium nanoribbons developed from series-wound beads. Adv. Mater. 16 (7), 649–653. Available from: https://doi.org/10.1002/adma.200306317.

Carlton, C.E., Ferreira, P.J., 2012. In situ TEM nanoindentation of nanoparticles. Micron 43 (11), 1134–1139. Available from: https://doi.org/10.1016/j.micron.2012.03.002.

Carvalho, M.D., et al., 2013. Iron oxide nanoparticles: the influence of synthesis method and size on composition and magnetic properties. J. Solid State Chem. 201, 144–152. Available from: https://doi.org/10.1016/j.jssc.2013.02.024.

Castro, L., et al., 2013. Biological synthesis of metallic nanoparticles using algae. IET Nanobiotechnol. 7 (3), 109–116. Available from: https://doi.org/10.1049/iet-nbt.2012.0041.

Castro, L., et al., 2014. Mechanism and applications of metal nanoparticles prepared by biomediated process. Rev. Adv. Sci. Eng. 3 (3), 199–216. Available from: https://doi.org/10.1166/rase.2014.1064.

Champion, Y., Bigot, J., 1998. Synthesis and structural analysis of aluminum nanocrystalline powders. Nanostruct. Mater. 10 (7), 1097–1110. Available from: https://doi.org/10.1016/S0965-9773(98)00149-4.

Chang, S.-H., et al., 2014. Bimetallic catalyst of PtIr nanoparticles with high electrocatalytic ability for hydrogen peroxide oxidation. Sens. Actuators, B: Chem. 190, 55–60. Available from: https://doi.org/10.1016/j.snb.2013.08.022.

Chaturvedi, S., Dave, P.N., Shah, N.K., 2012. Applications of nano-catalyst in new era. J. Saudi Chem. Soc. 16 (3), 307–325. Available from: https://doi.org/10.1016/j.jscs.2011.01.015.

Chau, J.L.H., Chen, C.-Y., Yang, C.-C., 2017. Facile synthesis of bimetallic nanoparticles by femtosecond laser irradiation method. Arabian J. Chem. 10, S1395–S1401. Available from: https://doi.org/10.1016/j.arabjc.2013.04.014.

Che, X., et al., 2010. Amperometric immunosensor for the determination of α-1-fetoprotein based on multiwalled carbon nanotube-silver nanoparticle composite. J. Colloid Interface Sci. 345 (2), 174–180. Available from: https://doi.org/10.1016/j.jcis.2010.01.033.

Chekli, L., et al., 2016. Analytical characterisation of nanoscale zero-valent iron: a methodological review. Anal. Chim. Acta. pp. 13–35. Available from: http://dx.doi.org/10.1016/j.aca.2015.10.040.

Chen, H., et al., 2010a. Selenium nanowires and nanotubes synthesized via a facile template-free solution method. Mater. Res. Bull. 45 (6), 699–704. Available from: https://doi.org/10.1016/j.materresbull.2010.02.016.

Chen, L.Q., et al., 2010b. Aptamer-based silver nanoparticles used for intracellular protein imaging and single nanoparticle spectral analysis. J. Phys. Chem. B 114 (10), 3655–3659. Available from: https://doi.org/10.1021/jp9104618.

Chen, S.-F., Zhang, H., 2012. Aggregation kinetics of nanosilver in different water conditions. Adv. Nat. Sci.: Nanosci. Nanotechnol. 3 (3), 35006. Available from: http://stacks.iop.org/2043-6262/3/i = 3/a = 035006.

Chen, S.-H., et al., 2008. Using oligonucleotide-functionalized Au nanoparticles to rapidly detect foodborne pathogens on a piezoelectric biosensor. J. Microbiol. Methods 73 (1), 7–17. Available from: https://doi.org/10.1016/j.mimet.2008.01.004.

Chen, S., Sommers, J.M., 2001. Alkanethiolate-protected copper nanoparticles: spectroscopy, electrochemistry, and solid-state morphological evolution. J. Phys. Chem. B 105 (37), 8816–8820. Available from: https://doi.org/10.1021/jp011280n.

Chen, W., et al., 2006. Carbene-functionalized ruthenium nanoparticles. Chem. Mater. 18 (22), 5253–5259. Available from: https://doi.org/10.1021/cm061595l.

Chen, X., Wen, J., 2012. In situ wet-cell TEM observation of Au nanoparticle motion in an aqueous solution. Nanoscale Res. Lett. 7 (1), 598. Available from: https://doi.org/10.1186/1556-276X-7-598.

Chen, Y., Gao, D.-Y., Huang, L., 2015. In vivo delivery of miRNAs for cancer therapy: challenges and strategies. Adv. Drug Deliv. Rev. 81, 128–141. Available from: https://doi.org/10.1016/j.addr.2014.05.009.

Chen, Z., et al., 2009. L-Cysteine-assisted controlled synthesis of selenium nanospheres and nanorods. Cryst. Growth Des. 9 (3), 1327–1333. Available from: https://doi.org/10.1021/cg800398b.

Chhabria, S., Desai, K., 2016. Selenium nanoparticles and their applications. Encyclopedia of Nanoscience and Nantotechnology. American Scientific Publishers.

Choi, M.K.-W., et al., 2008. A non-cross-linked soluble polystyrene-supported ruthenium catalyst for carbenoid transfer reactions. Chemistry 3 (8–9), 1256–1265. Available from: https://doi.org/10.1002/asia.200800144.

Cima, L.G., et al., 1991. Tissue engineering by cell transplantation using degradable polymer substrates. J. Biomech. Eng. 113 (2), 143–151. Available from: http://www.ncbi.nlm.nih.gov/pubmed/1652042.

Clogston, J.D., Patri, A.K., 2011. Zeta potential measurement. In: McNeil, S. (Ed.), Characterization of Nanoparticles Intended for Drug Delivery. Humana Press, pp. 63–70. Available from: http://dx.doi.org/10.1007/978-1-60327-198-1-6.

Cobley, C.M., et al., 2011. Au nanostructures: a class of multifunctional materials for biomedical applications. Chem. Soc. Rev. 40 (1), 44–56. Available from: https://doi.org/10.1039/B821763G.

Conde, J., de la Fuente, J.M., Baptista, P.V., 2010. RNA quantification using Au nanoprobes—application to cancer diagnostics. J. Nanobiotechnol. 8 (1), 5. Available from: https://doi.org/10.1186/1477-3155-8-5.

Cope, R., 2017. Metalloids. Veterinary Toxicology for Australia and New Zealand. Elsevier, pp. 255–277. Available from: http://dx.doi.org/10.1016/B978-0-12-420227-6.00014-1.

Costa-Fernández, J.M., et al., 2016. Mass spectrometry for the characterization and quantification of engineered inorganic nanoparticles. TrAC, Trends Anal. Chem. 84, 139–148. Available from: http://dx.doi.org/10.1016/j.trac.2016.06.001.

Costa, P., et al., 2010. Au nanoprobe assay for the identification of mycobacteria of the *Mycobacterium tuberculosis* complex. Clin. Microbiol. Infect. 16 (9), 1464–1469. Available from: https://doi.org/10.1111/j.1469-0691.2009.03120.x.

Culver, J.N., et al., 2015. Plant virus directed fabrication of nanoscale materials and devices. Virology 479–480, 200–212. Available from: https://doi.org/10.1016/j.virol.2015.03.008.

Cutter, G.A., 2001. Metalloids and oxyanions. Encyclopedia of Ocean Sciences. Elsevier, pp. 776–783. Available from: http://dx.doi.org/10.1016/B978-012374473-9.00283-6.

D'Acunto, M., 2018. Detection of intracellular Au nanoparticles: an overview. Materials 11 (6), 882. Available from: https://doi.org/10.3390/ma11060882.

Dameron, C.T., et al., 1989. Biosynthesis of cadmium sulphide quantum semiconductor crystallites. Nature 338 (6216), 596–597. Available from: https://doi.org/10.1038/338596a0.

Dang, T.M.D., et al., 2011. Synthesis and optical properties of copper nanoparticles prepared by a chemical reduction method. Adv. Nat. Sci.: Nanosci. Nanotechnol. 2 (1), 15009. Available from: http://stacks.iop.org/2043-6262/2/i = 1/a = 015009.

Dang, T.M.D., et al., 2012. Influence of surfactant on the preparation of silver nanoparticles by polyol method. Adv. Nat. Sci.: Nanosci. Nanotechnol. 3 (3), 35004. Available from: http://stacks.iop.org/2043-6262/3/i = 3/a = 035004.

Das, J., et al., 2014. Assessment of drug delivery and anticancer potentials of nanoparticles-loaded siRNA targeting STAT3 in lung cancer, in vitro and in vivo. Toxicol. Lett. 225 (3), 454–466. Available from: https://doi.org/10.1016/j.toxlet.2014.01.009.

Das, R.K., et al., 2017. Biological synthesis of metallic nanoparticles: plants, animals and microbial aspects. Nanotechnol. Environ. Eng. 2 (1), 18. Available from: https://doi.org/10.1007/s41204-017-0029-4.

Dastjerdi, R., Montazer, M., 2010. A review on the application of inorganic nano-structured materials in the modification of textiles: focus on antimicrobial properties. Colloids Surf., B: Biointerfaces 79 (1), 5–18. Available from: https://doi.org/10.1016/j.colsurfb.2010.03.029.

Deng, Y., et al., 2014. Therapeutic potentials of gene silencing by RNA interference: principles, challenges, and new strategies. Gene 538 (2), 217–227. Available from: https://doi.org/10.1016/j.gene.2013.12.019.

Deplanche, K., et al., 2010. Involvement of hydrogenases in the formation of highly catalytic Pd(0) nanoparticles by bioreduction of Pd(II) using *Escherichia coli* mutant strains. Microbiology (Reading, England) 156 (Pt 9), 2630–2640. Available from: https://doi.org/10.1099/mic.0.036681-0.

Deshpande, A.S., et al., 2008. Sulfur nanoparticles synthesis and characterization from H2S gas, using novel biodegradable iron chelates in W/O microemulsion. Nanoscale Res. Lett. 3 (6), 221–229. Available from: https://doi.org/10.1007/s11671-008-9140-6.

Dhar, S., et al., 2009. Polyvalent oligonucleotide Au nanoparticle conjugates as delivery vehicles for platinum (IV) Warheads. J. Am. Chem. Soc. 131 (41), 14652–14653. Available from: https://doi.org/10.1021/ja9071282.

Diamond, D. (Ed.), 1998. Principles of Chemical and Biological Sensors. Wiley.

Dieringer, J.A., et al., 2006. Surface enhanced Raman spectroscopy: new materials, concepts, characterization tools, and applications. Faraday Discuss. 132, 9–26. Available from: http://www.ncbi.nlm.nih.gov/pubmed/16833104.

Din, M.I., Rehan, R., 2017. Synthesis, characterization, and applications of copper nanoparticles. Anal. Lett. 50 (1), 50–62. Available from: https://doi.org/10.1080/00032719.2016.1172081.

Dinish, U.S., et al., 2011. Development of highly reproducible nanogap SERS substrates: comparative performance analysis and its application for glucose sensing. Biosens. Bioelectron. 26 (5), 1987–1992. Available from: https://doi.org/10.1016/j.bios.2010.08.069.

Djafari, J., et al., 2018. Synthesis of Au functionalised nanoparticles with the *Eranthis hyemalis* lectin and preliminary toxicological studies on *Caenorhabditis elegans*. Materials 11 (8), 1363. Available from: https://doi.org/10.3390/ma11081363.

Domènech, B., et al., 2016. Polyurethane foams doped with stable silver nanoparticles as bactericidal and catalytic materials for the effective treatment of water. New J. Chem. 40 (4), 3716–3725. Available from: https://doi.org/10.1039/C5NJ03202D.

Dong, L., et al., 2012. Applications of nanomaterials in biology and medicine. J. Nanotechnol. 2012, 1–2. Available from: https://doi.org/10.1155/2012/816184.

Doria, G., et al., 2010. Au–silver-alloy nanoprobes for one-pot multiplex DNA detection. Nanotechnology 21 (25), 255101. Available from: https://doi.org/10.1088/0957-4484/21/25/255101.

Doria, G., et al., 2012. Noble metal nanoparticles for biosensing applications. Sensors (Basel, Switzerland) 12 (2), 1657–1687. Available from: http://dx.doi.org/10.3390/s120201657.

Doria, G., Franco, R., Baptista, P., 2007. Nanodiagnostics: fast colorimetric method for single nucleotide polymorphism/mutation detection. IET Nanobiotechnol. 1 (4), 53–57. Available from: https://doi.org/10.1049/iet-nbt:20070001.

Dougherty, G.M., et al., 2008. The zeta potential of surface-functionalized metallic nanorod particles in aqueous solution. Electrophoresis 29 (5), 1131–1139. Available from: https://doi.org/10.1002/elps.200700448.

Drake, A., 2001. 'Circular dichroism'. In: Harding, Stephen E., Chowdhry, B.Z. (Eds.), Protein-Ligand Interactions: Structure and Spectroscopy, First ed. Oxford University Press, pp. 123–167.

Drexler, K.E., 1990. Engines of creation: the coming era of nanotechnology. *Oxford University Press, Oxford*.

Driskell, J.D., et al., 2005. Low-level detection of viral pathogens by a surface-enhanced Raman scattering based immunoassay. Anal. Chem. 77 (19), 6147–6154. Available from: https://doi.org/10.1021/ac0504159.

Du, J.-Q., et al., 2009. Microwave irradiation assisted rapid synthesis of Fe–Ru bimetallic nanoparticles and their catalytic properties in water-gas shift reaction. Mater. Res. Bull. 44 (6), 1347–1351. Available from: https://doi.org/10.1016/j.materresbull.2008.12.001.

Dudkiewicz, A., et al., 2011. Characterization of nanomaterials in food by electron microscopy. TrAC, Trends Anal. Chem. pp. 28–43. Available from: http://dx.doi.org/10.1016/j.trac.2010.10.007.

Duester, L., et al., 2011. Translocation of Sb and Ti in an undisturbed floodplain soil after application of Sb_2O_3 and TiO_2 nanoparticles to the surface. J. Environ. Monit.: JEM 13 (5), 1204–1211. Available from: https://doi.org/10.1039/c1em10056d.

Van Duyne, R.P., Hulteen, J.C., Treichel, D.A., 1993. Atomic force microscopy and surface-enhanced Raman spectroscopy. I. Ag island films and Ag film over polymer nanosphere surfaces supported on glass. J. Chem. Phys. 99 (3), 2101–2115. Available from: https://doi.org/10.1063/1.465276.

Edmondson, R., et al., 2014. Three-dimensional cell culture systems and their applications in drug discovery and cell-based biosensors. ASSAY Drug Dev. Technol. 12 (4), 207–218. Available from: https://doi.org/10.1089/adt.2014.573.

Elson, E.L., Magde, D., 1974. Fluorescence correlation spectroscopy. I. Conceptual basis and theory. Biopolymers 13 (1), 1–27. Available from: https://doi.org/10.1002/bip.1974.360130102.

Elumalai, K., et al., 2015. Retracted: green synthesis of zinc oxide nanoparticles using *Moringa oleifera* leaf extract and evaluation of its antimicrobial activity. Spectrochim. Acta, A: Mol. Biomol. Spectrosc. 143, 158–164. Available from: https://doi.org/10.1016/j.saa.2015.02.011.

Energy Dispersive X-Ray Analysis (EDX), no date. Available from: <http://www.intertek.com/analysis/microscopy/edx/> (accessed 05.05.18).

Evanoff, D.D., Chumanov, G., 2004. Size-controlled synthesis of nanoparticles. 2. Measurement of extinction, scattering, and absorption cross sections. J. Phys. Chem. B 108 (37), 13957–13962. Available from: https://doi.org/10.1021/jp0475640.

Evans, B.R., et al., 2003. Palladium-bacterial cellulose membranes for fuel cells. Biosens. Bioelectron. 18 (7), 917–923. Available from: https://doi.org/10.1016/S0956-5663(02)00212-9.

Evtugyn, G.A., et al., 2014. Cholinesterase sensor based on glassy carbon electrode modified with Ag nanoparticles decorated with macrocyclic ligands. Talanta 127, 9–17. Available from: https://doi.org/10.1016/j.talanta.2014.03.048.

Fakruddin, M., Hossain, Z., Afroz, H., 2012. Prospects and applications of nanobiotechnology: a medical perspective. J. Nanobiotechnol. 10 (1), 31. Available from: https://doi.org/10.1186/1477-3155-10-31.

Fan, M., Andrade, G.F.S., Brolo, A.G., 2011. A review on the fabrication of substrates for surface enhanced Raman spectroscopy and their applications in analytical chemistry. Anal. Chim. Acta 693 (1–2), 7–25. Available from: http://dx.doi.org/10.1016/J.ACA.2011.03.002.

Fang, J., Liu, S., Li, Z., 2011. Polyhedral silver mesocages for single particle surface-enhanced Raman scattering-based biosensor. Biomaterials 32 (21), 4877–4884. Available from: https://doi.org/10.1016/j.biomaterials.2011.03.029.

Faraday, M., 1857. The Bakerian lecture: experimental relations of Au (and other metals) to light author(s): Michael Faraday Source: Philosophical Transactions of the Royal Society of London, Vol. 147, No. (1857), pp. 145-181 Published by: The Royal Society. Philos. Trans. R. Soc. London, 147, 145–181. doi:10.1098/rstl.1857.0011.

Fathima, J.B., et al., 2018. Synthesis of eco-friendly copper nanoparticles for augmentation of catalytic degradation of organic dyes. J. Mol. Liq. 260, 1–8. Available from: https://doi.org/10.1016/j.molliq.2018.03.033.

Fauzi, M.B., et al., 2016. Ovine tendon collagen: extraction, characterisation and fabrication of thin films for tissue engineering applications. Mater. Sci. Eng., C: Mater. Biol. Appl. 68, 163–171. Available from: https://doi.org/10.1016/j.msec.2016.05.109.

Faya, M., et al., 2018. Conjugates and nano-delivery of antimicrobial peptides for enhancing therapeutic activity. J. Drug Deliv. Sci. Technol. 44, 153–171. Available from: https://doi.org/10.1016/j.jddst.2017.12.010.

Fayaz, A.M., et al., 2010. Biogenic synthesis of silver nanoparticles and their synergistic effect with antibiotics: a study against gram-positive and gram-negative bacteria. Nanomed. Nanotechnol. Biol. Med. 6 (1), 103–109. Available from: https://doi.org/10.1016/j.nano.2009.04.006.

Felix, S., Chakkravarthy, R.B.P., Grace, A.N., 2015. Microwave assisted synthesis of copper oxide and its application in electrochemical sensing. IOP Conf. Ser. Mater. Sci. Eng., 73, 012115. doi:10.1088/1757-899X/73/1/012115.

Feng, X.-X., et al., 2007. Preparation and characterization of novel nanocomposite films formed from silk fibroin and nano-TiO_2. Int. J. Biol. Macromol. 40 (2), 105–111. Available from: https://doi.org/10.1016/j.ijbiomac.2006.06.011.

Fernández, B., et al., 2010. Inorganic mass spectrometry as a tool for characterisation at the nanoscale. Anal. Bioanal. Chem. 396 (1), 15–29. Available from: https://doi.org/10.1007/s00216-009-2959-6.

Feynman, R.P., 1960. There's plenty of room at the bottom. Eng. Sci. 23 (5), 22–36.

Fields-Zinna, C.A., et al., 2009. Mass spectrometry of small bimetal monolayer-protected clusters. Langmuir 25 (13), 7704–7710. Available from: https://doi.org/10.1021/la803865v.

Figueiredo, S., et al., 2014. Conjugation of Au nanoparticles and liposomes for combined vehicles of drug delivery in cancer outline. Nanomedicine 48–82.

Figueiredo, S. et al., n.d. Integration of Au nanoparticles and liposomes for combined anti-cancer drug delivery. In: Seifalian, A., de Me, A. l, Kalaskar, M.D. (Eds.). Nanomedicine. Manchester: One Central Press (OCP).

Filipe, V., Hawe, A., Jiskoot, W., 2010. Critical evaluation of nanoparticle tracking analysis (NTA) by NanoSight for the measurement of nanoparticles and protein aggregates. Pharm. Res. 27 (5), 796–810. Available from: https://doi.org/10.1007/s11095-010-0073-2.

Filipponi, L., Sutherland, D., 2010. Chapter 6 – Characterisation methods. In: NANOYOU Teachers Training Kit in Nanotechnolgies, vol. January, . 1–13.

Franci, G., et al., 2015. Silver nanoparticles as potential antibacterial agents. Molecules 20 (5), 8856–8874. Available from: https://doi.org/10.3390/molecules20058856.

Freestone, I. *et al*., 2007. The Lycurgus cup – a Roman nanotechnology. Au Bull. Available from: <http://master-mcn.u-strasbg.fr/wp-content/uploads/2015/09/lycurgus.pdf>.

Ingale, A.G., 2013. Biogenic synthesis of nanoparticles and potential applications: an eco-friendly approach. J. Nanomed. Nanotechnol. 04 (02). Available from: https://doi.org/10.4172/2157-7439.1000165.

Ganeev, R.A., et al., 2010. Nanoparticle formation during laser ablation of metals at different pressures of surrounding noble gases. Appl. Phys. A: Mater. Sci. Process. 100, 119–123.

Gang, W., et al., 2008. Preparation of nano silk fibroin/hydroxyapatite biological composite by "one-step" method. Acta Mater. Compositae Sin. 6, 136–139. Available from: http://caod.oriprobe.com/articles/15178454/Preparation_of_nano_silk_fibroin_hydroxyapatite_biological_composite_b.htm.

Gangadoo, S., et al., 2017. The synthesis and characterisation of highly stable and reproducible selenium nanoparticles. Inorg. Nano-Metal Chem. 47 (11), 1568–1576. Available from: https://doi.org/10.1080/24701556.2017.1357611.

Gao, L., Fan, K., Yan, X., 2017. Iron oxide nanozyme: a multifunctional enzyme mimetic for biomedical applications. Theranostics 7 (13), 3207–3227. Available from: https://doi.org/10.7150/thno.19738.

Garcia-Peña, N.G., et al., 2013. Green solventless synthesis of ruthenium(0) nanoparticles. In: NANOCON 2013 - Conference Proceedings, Fifth International Conference, (0).

García-Peña, N.G., et al., 2015. Solventless synthesis of ruthenium nanoparticles. Appl. Surf. Sci. 340, 25–34. Available from: https://doi.org/10.1016/j.apsusc.2015.02.186.

Gatti, A.M., et al., 2008. ESEM evaluations of muscle/nanoparticles interface in a rat model. J. Mater. Sci.—Mater. Med. 19 (4), 1515–1522. Available from: https://doi.org/10.1007/s10856-008-3385-6.

Gautier, C., Bürgi, T., 2010. Vibrational circular dichroism of adsorbed molecules: BINAS on Au nanoparticles. J. Phys. Chem. C 114 (38), 15897–15902. Available from: https://doi.org/10.1021/jp910800m.

Gautier, J., et al., 2013. Recent advances in theranostic nanocarriers of doxorubicin based on iron oxide and Au nanoparticles. J. Controlled Release 169 (1–2), 48–61. Available from: https://doi.org/10.1016/j.jconrel.2013.03.018.

Gericke, M., Pinches, A., 2006. Biological synthesis of metal nanoparticles. Hydrometallurgy 83 (1–4), 132–140. Available from: https://doi.org/10.1016/j.hydromet.2006.03.019.

Ghorbani, H., 2014. A review of methods for synthesis of Al nanoparticles. Orient. J. Chem. 30 (4), 1941–1949. Available from: https://doi.org/10.13005/ojc/300456.

Ghorbani, H., et al., 2015. Synthesis of ZnO nanoparticles by precipitation method. Orient. J. Chem. 31 (2), 1219–1221. Available from: https://doi.org/10.13005/ojc/310281.

Ghosh, P., et al., 2008. Au nanoparticles in delivery applications. Adv. Drug Deliv. Rev. 60 (11), 1307–1315. Available from: https://doi.org/10.1016/j.addr.2008.03.016.

Ghosh, P.S., et al., 2007. Nanoparticles featuring amino acid-functionalized side chains as DNA receptors. Chem. Biol. Drug Des. 70 (1), 13–18. Available from: https://doi.org/10.1111/j.1747-0285.2007.00534.x.

Gibson, J.D., Khanal, B.P., Zubarev, E.R., 2007. Paclitaxel-functionalized Au nanoparticles. J. Am. Chem. Soc. 129 (37), 11653–11661. Available from: https://doi.org/10.1021/ja075181k.

Gilbert, B., et al., 2004. Nanoparticles: strained and stiff. Science (New York, NY) 305 (5684), 651–654. Available from: https://doi.org/10.1126/science.1098454.

Giljohann, D.A., et al., 2010. Au nanoparticles for biology and medicine. Angew. Chem. (Int. ed. English) 49 (19), 3280–3294. Available from: https://doi.org/10.1002/anie.200904359.

Gmoshinski, I.V., et al., 2013. Nanomaterials and nanotechnologies: methods of analysis and control. Russ. Chem. Rev. 82 (1), 48–76. Available from: https://doi.org/10.1070/RC2013v082n01ABEH004329.

González, E., Arbiol, J., Puntes, V.F., 2011. Carving at the nanoscale: sequential galvanic exchange and Kirkendall growth at room temperature. Science (New York, NY) 334 (6061), 1377–1380. Available from: https://doi.org/10.1126/science.1212822.

Goon, I.Y., et al., 2009. Fabrication and dispersion of Au–shell-protected magnetite nanoparticles: systematic control using polyethyleneimine. Chem. Mater. 21 (4), 673–681. Available from: https://doi.org/10.1021/cm8025329.

Govindaraju, K., et al., 2009. Extracellular synthesis of silver nanoparticles by a marine alga, *Sargassum wightii* Grevilli and their antibacterial effects. J. Nanosci. Nanotechnol. 9 (9), 5497–5501. Available from: http://www.ncbi.nlm.nih.gov/pubmed/19928252.

Grubisha, D.S., et al., 2003. Femtomolar detection of prostate-specific antigen: an immunoassay based on surface-enhanced Raman scattering and immunoAu labels. Anal. Chem. 75 (21), 5936–5943. Available from: https://doi.org/10.1021/ac034356f.

Gudikandula, K., Charya Maringanti, S., 2016. Synthesis of silver nanoparticles by chemical and biological methods and their antimicrobial properties. J. Exp. Nanosci. 11 (9), 714–721. Available from: https://doi.org/10.1080/17458080.2016.1139196.

Guirgis, B.S.S., et al., 2012. Au nanoparticle-based fluorescence immunoassay for malaria antigen detection. Anal. Bioanal. Chem. 402 (3), 1019–1027. Available from: https://doi.org/10.1007/s00216-011-5489-y.

Gunduz, O., 2014. A simple method of producing hydroxyapatite and tricalcium phosphate from coral (*Pocillopora verrucosa*). J. Aust. Ceram. Soc. 50 (2), 52–58. Available from: http://jglobal.jst.go.jp/en/public/20090422/201402281387335669.

Guo, W., et al., 2012. Layer-by-layer assembled Au nanoparticles modified anode and its application in microbial fuel cells. Colloids Surf., A: Physicochem. Eng. Aspects 415, 105–111. Available from: https://doi.org/10.1016/j.colsurfa.2012.09.032.

Guo, Y., et al., 2006a. Preparation and characterization of monoclinic sulfur nanoparticles by water-in-oil microemulsions technique. Powder Technol. 162 (2), 83–86. Available from: https://doi.org/10.1016/j.powtec.2005.12.012.

Guo, Z., et al., 2006b. Nanomaterials in mass spectrometry ionization and prospects for biological application. Anal. Bioanal. Chem. 384 (3), 584–592. Available from: https://doi.org/10.1007/s00216-005-0125-3.

Haber, J.A., Buhro, W.E., 1998. Kinetic instability of nanocrystalline aluminum prepared by chemical synthesis; facile room-temperature grain growth. J. Am. Chem. Soc. 120 (42), 10847–10855. Available from: https://doi.org/10.1021/ja981972y.

Hall, J.B., et al., 2007. Characterization of nanoparticles for therapeutics. Nanomedicine (London, England) 2 (6), 789–803. Available from: https://doi.org/10.2217/17435889.2.6.789.

Hamad-Schifferli, K., et al., 2002. Remote electronic control of DNA hybridization through inductive coupling to an attached metal nanocrystal antenna. Nature 415 (6868), 152–155. Available from: https://doi.org/10.1038/415152a.

Hartschuh, A., 2008. Tip-enhanced near-field optical microscopy. Angew. Chem. (Int. ed. English) 47 (43), 8178–8191. Available from: https://doi.org/10.1002/anie.200801605.

Hayazawa, N., et al., 2012. Tip-enhanced Raman spectroscopy. In: Kumar, C.S.S.R. (Ed.), Raman Spectroscopy for Nanomaterials Characterization. Springer Berlin Heidelberg, Berlin, Heidelberg, pp. 445–476. Available from: http://dx.doi.org/10.1007/978-3-642-20620-7_16.

Hazer, B., Kalaycı, Ö.A., 2017. High fluorescence emission silver nano particles coated with poly (styrene-*g*-soybean oil) graft copolymers: antibacterial activity and polymerization kinetics. Mater. Sci. Eng., C 74, 259–269. Available from: https://doi.org/10.1016/j.msec.2016.12.010.

He, S., et al., 2007a. Biosynthesis of Au nanoparticles using the bacteria *Rhodopseudomonas capsulata*. Mater. Lett. 61 (18), 3984–3987. Available from: https://doi.org/10.1016/j.matlet.2007.01.018.

He, W., et al., 2014. Enzyme-like activity of nanomaterials. J. Environ. Sci. Health., C 32 (2), 186–211. Available from: https://doi.org/10.1080/10590501.2014.907462.

He, X.-M., et al., 2007b. [Determination of trace impurities in high purity titanium dioxide by high resolution inductively coupled plasma mass spectrometry]. Guang pu xue yu guang pu fen xi = Guang pu 27 (6), 1192–1196. Available from: http://www.ncbi.nlm.nih.gov/pubmed/17763790.

Holzinger, M., Le Goff, A., Cosnier, S., 2014. Nanomaterials for biosensing applications: a review. Front. Chem. 2, 63. Available from: https://doi.org/10.3389/fchem.2014.00063.

Hondow, N. et al., 2012. TEM analysis of nanoparticle dispersions with application towards the quantification of in vitro cellular uptake. J. Phys. Conf. Ser. 371, 012020. doi:10.1088/1742-6596/371/1/012020.

Horie, M., Fujita, K., 2011. Toxicity of metal oxides nanoparticles. Adv. Mol. Toxicol. 145–178. Available from: https://doi.org/10.1016/B978-0-444-53864-2.00004-9.

Hu, H., et al., 2013. Preparation, characterization and in vitro release study of gallic acid loaded silica nanoparticles for controlled release. Die Pharm. 68 (6), 401–405. Available from: http://www.ncbi.nlm.nih.gov/pubmed/23875245.

Huang, J., et al., 2013. Tracking the intracellular drug release from graphene oxide using surface-enhanced Raman spectroscopy. Nanoscale 5 (21), 10591–10598. Available from: https://doi.org/10.1039/c3nr03264g.

Huang, X., et al., 2007. Au nanoparticles: interesting optical properties and recent applications in cancer diagnostics and therapy. Nanomedicine (London, England) 2 (5), 681–693. Available from: https://doi.org/10.2217/17435889.2.5.681.

Huefner, A., et al., 2014. Au nanoparticles explore cells: cellular uptake and their use as intracellular probes. Methods (San Diego, CA) 68 (2), 354–363. Available from: https://doi.org/10.1016/j.ymeth.2014.02.006.

Hur, T.-B., Phuoc, T.X., Chyu, M.K., 2009. Synthesis of Mg-Al and Zn-Al-layered double hydroxide nanocrystals using laser ablation in water. Opt. Lasers Eng. 47 (6), 695–700. Available from: https://doi.org/10.1016/j.optlaseng.2008.11.006.

Husen, A., Siddiqi, K.S., 2014. Carbon and fullerene nanomaterials in plant system. J. Nanobiotechnol. 12, 16. Available from: https://doi.org/10.1186/1477-3155-12-16.

Hutter, E., Maysinger, D., 2013. Au-nanoparticle-based biosensors for detection of enzyme activity. Trends Pharmacol. Sci. 34 (9), 497–507. Available from: http://dx.doi.org/10.1016/j.tips.2013.07.002.

Hwu, J.R., et al., 2009. Targeted paclitaxel by conjugation to iron oxide and Au nanoparticles. J. Am. Chem. Soc. 131 (1), 66–68. Available from: https://doi.org/10.1021/ja804947u.

Ibarra, C., Koski, J.A., Warren, R.F., 2000. Tissue engineering meniscus: cells and matrix. Orthop. Clin. N Am 31 (3), 411–418. Available from: http://www.ncbi.nlm.nih.gov/pubmed/10882467.

Inagaki, S., Ghirlando, R., Grisshammer, R., 2013. Biophysical characterization of membrane proteins in nanodiscs. Methods (San Diego, CA) 59 (3), 287–300. Available from: https://doi.org/10.1016/j.ymeth.2012.11.006.

Iravani, S., 2011. Green synthesis of metal nanoparticles using plants. Green Chem. 13 (10), 2638. Available from: https://doi.org/10.1039/c1gc15386b.

Iravani, S., et al., 2014. Synthesis of silver nanoparticles: chemical, physical and biological methods. Res. Pharm. Sci. 9 (6), 385–406. Available from: http://www.ncbi.nlm.nih.gov/pubmed/26339255.

Iravani, S., Zolfaghari, B., 2013. Green synthesis of silver nanoparticles using *Pinus eldarica* bark extract. BioMed Res. Int. 2013, 1–5. Available from: https://doi.org/10.1155/2013/639725.

Iskandar, F., 2009. Nanoparticle processing for optical applications – a review. Adv. Powder Technol. 20 (4), 283–292. Available from: https://doi.org/10.1016/j.apt.2009.07.001.

Ismail, R.A., et al., 2011. Preparation and characterization of colloidal ZnO nanoparticles using nanosecond laser ablation in water. Appl. Nanosci. 1 (1), 45–49. Available from: https://doi.org/10.1007/s13204-011-0006-3.

Iv, M., et al., 2015. Clinical applications of iron oxide nanoparticles for magnetic resonance imaging of brain tumors. Nanomedicine (London, England) 10 (6), 993–1018. Available from: https://doi.org/10.2217/nnm.14.203.

Jain, K.K., 2007. Applications of nanobiotechnology in clinical diagnostics. Clin. Chem. 53 (11), 2002–2009. Available from: https://doi.org/10.1373/clinchem.2007.090795.

Jain, K.K., 2008. Nanomedicine: application of nanobiotechnology in medical practice. Med. Princ. Pract. 17 (2), 89–101. Available from: https://doi.org/10.1159/000112961.

Jana, N. et al., 2000. Seed-mediated growth method to prepare cubic copper nanoparticles. *Curr. Sci.* 79 (9), 1367–1370.

Jana, S., Pal, T., 2007. Synthesis, characterization and catalytic application of silver nanoshell coated functionalized polystyrene beads. J. Nanosci. Nanotechnol. 7 (6), 2151–2156. Available from: https://doi.org/10.1166/jnn.2007.785.

Jang, W.-S., et al., 2016. The static structure and dynamics of cadmium sulfide nanoparticles within poly(styrene-block-isoprene) diblock copolymer Melts. Macromol. Chem. Phys. 217 (4), 591–598. Available from: https://doi.org/10.1002/macp.201500357.

Jeelani, S., et al., 2014. Theranostics: a treasured tailor for tomorrow. J. Pharm. Bioallied Sci. 6 (Suppl. 1), S6–S8. Available from: https://doi.org/10.4103/0975-7406.137249.

Jeong, S., et al., 2008. Controlling the thickness of the surface oxide layer on Cu nanoparticles for the fabrication of conductive structures by ink-jet printing. Adv. Funct. Mater. 18 (5), 679–686. Available from: https://doi.org/10.1002/adfm.200700902.

Jiang, J., Pi, J., Cai, J., 2018. The advancing of zinc oxide nanoparticles for biomedical applications. Bioinorg. Chem. Appl. 2018, 1–18. Available from: https://doi.org/10.1155/2018/1062562.

Johal, M., 2011. Understanding Nanomaterials. CRC Press, Boca Raton, FL. Available from: https://www.crcpress.com/Understanding-Nanomaterials/Johal/p/book/9781138441569#googlePreviewContainer.

Joshi, M., Bhattacharyya, A., Ali, S.W., 2008. Characterization techniques for nanotechnology applications in textiles. Indian J. Fibre Text. Res. 33 (3), 304–317.

Ju-Ying, Shi-Yun, A.I., Wei-Jie, S.H.I., 2011. Chem. Res. Chinese Univ. 27, 2006.

Jung, J.H., et al., 2006. Metal nanoparticle generation using a small ceramic heater with a local heating area. J. Aerosol Sci. 37 (12), 1662–1670. Available from: https://doi.org/10.1016/j.jaerosci.2006.09.002.

Junghanns, J.-U.A.H., Müller, R.H., 2008. Nanocrystal technology, drug delivery and clinical applications. Int. J. Nanomed. 3 (3), 295–309. Available from: http://www.ncbi.nlm.nih.gov/pubmed/18990939.

Jurašin, D.D., et al., 2016. Surface coating affects behavior of metallic nanoparticles in a biological environment. Beilstein J. Nanotechnol. 7, 246–262. Available from: https://doi.org/10.3762/bjnano.7.23.

Kalaiselvam, S., Parameshwaran, R., Harikrishnan, S., 2012. Analytical and experimental investigations of nanoparticles embedded phase change materials for cooling application in modern buildings. Renew. Energy 39 (1), 375–387. Available from: https://doi.org/10.1016/j.renene.2011.08.034.

Kalogianni, D.P., et al., 2006. Nanoparticle-based DNA biosensor for visual detection of genetically modified organisms. Biosens. Bioelectron. 21 (7), 1069–1076. Available from: https://doi.org/10.1016/j.bios.2005.04.016.

Kalogianni, D.P., et al., 2007. Dry-reagent disposable dipstick test for visual screening of seven leukemia-related chromosomal translocations. Nucleic Acids Res. 35 (4), e23. Available from: https://doi.org/10.1093/nar/gkl1097.

Kamble, V., Jagdale, D., Kadam, V., 2010. Solid lipid nanoparticles as drug delivery system. Int. J. Pharma Bio Sci. 1 (3), 1–9.

Kang, T., et al., 2010. Patterned multiplex pathogen DNA detection by Au particle-on-wire SERS sensor. Nano Lett. 10 (4), 1189–1193. Available from: https://doi.org/10.1021/nl1000086.

Karim, M.R., et al., 2007. Synthesis of core-shell silver–polyaniline nanocomposites by gamma radiolysis method. J. Polym. Sci. A: Polym. Chem. 45 (24), 5741–5747. Available from: https://doi.org/10.1002/pola.22323.

Kaur, G., et al., 2018. DNA interaction, antiproliferative effect of copper oxide nanocolloids prepared from metallosurfactant based microemulsions acting as precursor, template and reducing agent. Int. J. Pharm. 535 (1–2), 95–105. Available from: http://dx.doi.org/10.1016/j.ijpharm.2017.10.059.

Keat, C.L., et al., 2015. Biosynthesis of nanoparticles and silver nanoparticles. Bioresour. Bioprocess. 2 (1), 47. Available from: https://doi.org/10.1186/s40643-015-0076-2.

Khan, I., Saeed, K., Khan, I., 2017. Nanoparticles: properties, applications and toxicities. Arabian J. Chem. Available from: https://doi.org/10.1016/j.arabjc.2017.05.011.

Khan, M.S., Vishakante, G.D., Siddaramaiah, H., 2013. Au nanoparticles: a paradigm shift in biomedical applications. Adv. Colloid Interface Sci. 199–200, 44–58. Available from: https://doi.org/10.1016/j.cis.2013.06.003.

Khan, S., 2012. Solid lipid nanoparticles: a review. WJPPS 1, 96–115.

Khanal, S., et al., 2014. Highly monodisperse multiple twinned AuCu–Pt trimetallic nanoparticles with high index surfaces. Phys. Chem. Chem. Phys. 16 (30), 16278–16283. Available from: https://doi.org/10.1039/C4CP02208D.

Kharisov, B.I., Dias, H.V.R., Kharissova, O.V., 2014. Mini-review: ferrite nanoparticles in the catalysis. Arabian J. Chem. Available from: https://doi.org/10.1016/j.arabjc.2014.10.049.

Khlebtsov, N., Dykman, L., 2011. Biodistribution and toxicity of engineered Au nanoparticles: a review of in vitro and in vivo studies. Chem. Soc. Rev. 40 (3), 1647–1671. Available from: https://doi.org/10.1039/c0cs00018c.

Kim, E.-Y., et al., 2012. Au nanoparticle-mediated gene delivery induces widespread changes in the expression of innate immunity genes. Gene Ther. 19 (3), 347–353. Available from: https://doi.org/10.1038/gt.2011.95.

Kim, H.-S., et al., 2010a. Atmospherically stable nanoscale zero-valent iron particles formed under controlled air contact: characteristics and reactivity. Environ. Sci. Technol. 44 (5), 1760–1766. Available from: https://doi.org/10.1021/es902772r.

Kim, H., et al., 2010b. Resonance Raman and surface- and tip-enhanced Raman spectroscopy methods to study solid catalysts and heterogeneous catalytic reactions. Chem. Soc. Rev. 39 (12), 4820–4844. Available from: https://doi.org/10.1039/c0cs00044b.

Kim, J.E., et al., 2013. Combined RNA interference of adenine nucleotide translocase-2 and ganciclovir therapy in hepatocellular carcinoma. Nucl. Med. Biol. 40 (8), 987–993. Available from: https://doi.org/10.1016/j.nucmedbio.2013.08.004.

Kim, K.-B., et al., 2017. Risk assessment of zinc oxide, a cosmetic ingredient used as a UV filter of sunscreens. J. Toxicol. Environ. Health, B 20 (3), 155–182. Available from: https://doi.org/10.1080/10937404.2017.1290516.

Kitching, M., Ramani, M., Marsili, E., 2015. Fungal biosynthesis of Au nanoparticles: mechanism and scale up. Microb. Biotechnol. 8 (6), 904–917. Available from: https://doi.org/10.1111/1751-7915.12151.

Klug, H.P., Alexander, L.E., 1954. X-Ray Diffraction Procedure. Wiley-Interscience, New York.

Kobayashi, Y., et al., 2009. Synthesis of metallic copper nanoparticles coated with polypyrrole. Colloid Polym. Sci. 287 (7), 877–880. Available from: https://doi.org/10.1007/s00396-009-2047-7.

Kołodziejczak-Radzimska, A., Jesionowski, T., 2014. Zinc oxide—from synthesis to application: a review. Materials 7 (4), 2833–2881. Available from: https://doi.org/10.3390/ma7042833.

Kong, F.-Y., Xu, M.-T., et al., 2011a. A novel label-free electrochemical immunosensor for carcinoembryonic antigen based on Au nanoparticles-thionine-reduced graphene oxide nanocomposite film modified glassy carbon electrode. Talanta 85 (5), 2620–2625. Available from: https://doi.org/10.1016/j.talanta.2011.08.028.

Kong, F.-Y., Xu, Zhu, et al., 2011b. Au nanoparticle/DNA/methylene blue nanocomposites for the ultrasensitive electrochemical detection of carcinoembryonic antigen. Electrochim. Acta 56 (25), 9386–9390. Available from: https://doi.org/10.1016/j.electacta.2011.08.018.

Konrad, M.P., Doherty, A.P., Bell, S.E.J., 2013. Stable and uniform SERS signals from self-assembled two-dimensional interfacial arrays of optically coupled Ag nanoparticles. Anal. Chem. 85 (14), 6783–6789. Available from: https://doi.org/10.1021/ac4008607.

Kora, A.J., Rastogi, L., 2016. Biomimetic synthesis of selenium nanoparticles by *Pseudomonas aeruginosa* ATCC 27853: an approach for conversion of selenite. J. Environ. Manage. 181, 231–236. Available from: https://doi.org/10.1016/j.jenvman.2016.06.029.

Korbekandi, H., Iravani, S., Abbasi, S., 2009. Production of nanoparticles using organisms. Crit. Rev. Biotechnol. 29 (4), 279–306. Available from: https://doi.org/10.3109/07388550903062462.

Kornberg, T., et al., 2017. Potential toxicity and underlying mechanisms associated with pulmonary exposure to iron oxide nanoparticles: conflicting literature and unclear risk. Nanomaterials 7 (10), 307. Available from: https://doi.org/10.3390/nano7100307.

Kosuda, K.M., et al., 2011. Nanostructures and surface-enhanced Raman spectroscopy. Comprehensive Nanoscience and Technology. Elsevier, pp. 263–301. Available from: http://dx.doi.org/10.1016/B978-0-12-374396-1.00110-0.

Kowshik, M., et al., 2002. Microbial synthesis of semiconductor CdS nanoparticles, their characterization, and their use in the fabrication of an ideal diode. Biotechnol. Bioeng. 78 (5), 583–588. Available from: https://doi.org/10.1002/bit.10233.

Krichevsky, O., Bonnet, G., 2002. Fluorescence correlation spectroscopy: the technique and its applications. Rep. Prog. Phys. 65 (2), 251–297. Available from: https://doi.org/10.1088/0034-4885/65/2/203.

Kricka, L.J., Fortina, P., 2002. Nanotechnology and applications: an all-language literature survey including books and patents. Clin. Chem. 48 (4), 662–665. Available from: http://www.ncbi.nlm.nih.gov/pubmed/11901071.

Krupa, A.N.D., Vimala, R., 2016. Evaluation of tetraethoxysilane (TEOS) sol-gel coatings, modified with green synthesized zinc oxide nanoparticles for combating microfouling. Mater. Sci. Eng., C 61, 728–735. Available from: https://doi.org/10.1016/j.msec.2016.01.013.

Ksv, G., 2017. Green synthesis of iron nanoparticles using green tea leaves extract. J. Nanomed. Biother. Discov. 07 (01). Available from: https://doi.org/10.4172/2155-983X.1000151.

Kumar, A., et al., 2008. Silver-nanoparticle-embedded antimicrobial paints based on vegetable oil. Nat. Mater. 7 (3), 236–241. Available from: https://doi.org/10.1038/nmat2099.

Kumar, J., Thomas, K.G., 2011. Surface-enhanced Raman spectroscopy: investigations at the nanorod edges and dimer junctions. J. Phys. Chem. Lett. 2 (6), 610–615. Available from: https://doi.org/10.1021/jz2000613.

Kumar, R., et al., 2012. Agricultural waste *Annona squamosa* peel extract: biosynthesis of silver nanoparticles. Spectrochim. Acta, A: Mol. Biomol. Spectrosc. 90, 173–176. Available from: https://doi.org/10.1016/j.saa.2012.01.029.

Kumar, R.V., et al., 2001. Sonochemical synthesis of amorphous Cu and nanocrystalline Cu_2O embedded in a polyaniline matrix. J. Mater. Chem. 11 (4), 1209–1213. Available from: https://doi.org/10.1039/b005769j.

Kumar, V., et al., 2013. Au nanoparticle exposure induces growth and yield enhancement in *Arabidopsis thaliana*. Sci. Total Environ. 461–462, 462–468. Available from: http://dx.doi.org/10.1016/J.SCITOTENV.2013.05.018.

de la Escosura-Muñiz, A., et al., 2010. Au nanoparticle-based electrochemical magnetoimmunosensor for rapid detection of antihepatitis B virus antibodies in human serum. Biosens. Bioelectron. 26 (4), 1710–1714. Available from: https://doi.org/10.1016/j.bios.2010.07.069.

de la Escosura-Muñiz, A., Maltez-da Costa, M., Merkoçi, A., 2009. Controlling the electrochemical deposition of silver onto Au nanoparticles: reducing interferences and increasing the sensitivity of magnetoimmuno assays. Biosens. Bioelectron. 24 (8), 2475–2482. Available from: https://doi.org/10.1016/j.bios.2008.12.028.

Laborda, F., Bolea, E., Jiménez-Lamana, J., 2014. Single particle inductively coupled plasma mass spectrometry: a powerful tool for nanoanalysis. Anal. Chem. 86 (5), 2270–2278. Available from: https://doi.org/10.1021/ac402980q.

Ladj, R., et al., 2013. Individual inorganic nanoparticles: preparation, functionalization and in vitro biomedical diagnostic applications. J. Mater. Chem. B 1 (10), 1381. Available from: https://doi.org/10.1039/c2tb00301e.

Lai, G., et al., 2011. Ultrasensitive multiplexed immunoassay with electrochemical stripping analysis of silver nanoparticles catalytically deposited by Au nanoparticles and enzymatic reaction. Anal. Chem. 83 (7), 2726–2732. Available from: https://doi.org/10.1021/ac103283p.

Lan, M.-Y., et al., 2013. Induction of apoptosis by high-dose Au nanoparticles in nasopharyngeal carcinoma cells. Auris Nasus Larynx 40 (6), 563–568. Available from: https://doi.org/10.1016/j.anl.2013.04.011.

Lanza, Robert, Langer, Robert, Vacanti, J., 2000. Principles of Tissue Engineering, second ed. Academic Press. Available from: https://www.elsevier.com/books/principles-of-tissue-engineering/lanza/978-0-12-436630-5#.

Latterini, L., Tarpani, L., 2012. AFM measurements to investigate particulates and their interactions with biological macromolecules. Atomic Force Microscopy Investigations into Biology—From Cell to Protein. InTech, pp. 87–98. Available from: http://dx.doi.org/10.5772/36213.

Lee, D.K., Kang, Y.S., 2004. Synthesis of silver nanocrystallites by a new thermal decomposition method and their characterization. ETRI J. 26 (3), 252–256. Available from: https://doi.org/10.4218/etrij.04.0103.0061.

Lee, H., Kang, T., et al., 2010. Colorimetric detection of mutations in epidermal growth factor receptor using Au nanoparticle aggregation. Biosens. Bioelectron. 25 (7), 1669–1674. Available from: https://doi.org/10.1016/j.bios.2009.12.002.

Lee, H., Joo, S.-W., et al., 2010. Colorimetric genotyping of single nucleotide polymorphism based on selective aggregation of unmodified Au nanoparticles. Biosens. Bioelectron. 26 (2), 730–735. Available from: https://doi.org/10.1016/j.bios.2010.06.050.

Lee, J.-P., et al., 2013. Well-organized raspberry-like Ag@Cu bimetal nanoparticles for highly reliable and reproducible surface-enhanced Raman scattering. Nanoscale 5 (23), 11620–11624. Available from: https://doi.org/10.1039/c3nr03363e.

Lee, K.-P., et al., 2007a. Gamma radiation induced distribution of Au nanoparticles into carbon nanotube-polyaniline composite. Compos. Sci. Technol. 67 (5), 811–816. Available from: https://doi.org/10.1016/j.compscitech.2005.12.030.

Lee, S., et al., 2007b. Biological imaging of HEK293 cells expressing PLCgamma1 using surface-enhanced Raman microscopy. Anal. Chem. 79 (3), 916–922. Available from: https://doi.org/10.1021/ac061246a.

Lei, C., et al., 2013. Development of a gene/drug dual delivery system for brain tumor therapy: potent inhibition via RNA interference and synergistic effects. Biomaterials 34 (30), 7483–7494. Available from: https://doi.org/10.1016/j.biomaterials.2013.06.010.

Leng, C., et al., 2010. Au nanoparticle as an electrochemical label for inherently crosstalk-free multiplexed immunoassay on a disposable chip. Anal. Chim. Acta 666 (1–2), 97–101. Available from: https://doi.org/10.1016/j.aca.2010.03.060.

Leong, G.J., et al., 2014. Shape-directed platinum nanoparticle synthesis: nanoscale design of novel catalysts. Appl. Organomet. Chem. 28 (1), 1–17. Available from: https://doi.org/10.1002/aoc.3048.

Levason, W., Quirk, J.J., Reid, G., 1997. Trans-[$RuCl_2$ $(dmf)_4$]CF_3SO_3 CH_2Cl_2. Acta Crystallogr., Sect. C: Cryst. Struct. Commun. 53 (9), 1224–1226. Available from: https://doi.org/10.1107/S0108270197005349.

Lewis, R.M., et al., 2018. A new framework for X-ray photon correlation spectroscopy analysis from polycrystalline materials. Rev. Sci. Instrum. 89 (12), 123902. Available from: https://doi.org/10.1063/1.5051451.

Li, C., et al., 2011. Facile synthesis of concentrated Au nanoparticles with low size-distribution in water: temperature and pH controls. Nanoscale Res. Lett. 6 (1), 1–10. Available from: https://doi.org/10.1186/1556-276X-6-440.

Li, H., Rothberg, L.J., 2004. Label-free colorimetric detection of specific sequences in genomic DNA amplified by the polymerase chain reaction. J. Am. Chem. Soc. 126 (35), 10958–10961. Available from: https://doi.org/10.1021/ja048749n.

Li, J., et al., 2010a. Rolling circle amplification combined with Au nanoparticle aggregates for highly sensitive identification of single-nucleotide polymorphisms. Anal. Chem. 82 (7), 2811–2816. Available from: https://doi.org/10.1021/ac100336n.

Li, J.F., et al., 2010b. Shell-isolated nanoparticle-enhanced Raman spectroscopy. Nature 464 (7287), 392–395. Available from: https://doi.org/10.1038/nature08907.

Li, Q., et al., 2008. Antimicrobial nanomaterials for water disinfection and microbial control: potential applications and implications. Water Res. 42 (18), 4591–4602. Available from: https://doi.org/10.1016/j.watres.2008.08.015.

Lim, D.-H., Lee, W.-D., Lee, H.-I., 2008. Highly dispersed and nano-sized Pt-based electrocatalysts for low-temperature fuel cells. Catal. Surv. Asia 12 (4), 310–325. Available from: https://doi.org/10.1007/s10563-008-9059-z.

Lim, J., et al., 2013. Characterization of magnetic nanoparticle by dynamic light scattering. Nanoscale Res. Lett. 8 (1), 381. Available from: https://doi.org/10.1186/1556-276X-8-381.

Lim, J.K., Majetich, S.A., Tilton, R.D., 2009. Stabilization of superparamagnetic iron oxide core–Au shell nanoparticles in high ionic strength media. Langmuir 25 (23), 13384–13393. Available from: https://doi.org/10.1021/la9019734.

Lin, D., Xing, B., 2007. Phytotoxicity of nanoparticles: inhibition of seed germination and root growth. Environ. Pollut. (Barking, Essex: 1987) 150 (2), 243–250. Available from: https://doi.org/10.1016/j.envpol.2007.01.016.

Lin, K.-S., Chang, N.-B., Chuang, T.-D., 2008. Fine structure characterization of zero-valent iron nanoparticles for decontamination of nitrites and nitrates in wastewater and groundwater. Sci. Technol. Adv. Mater. 9 (2), 025015. Available from: https://doi.org/10.1088/1468-6996/9/2/025015.

Lin, P.-C., et al., 2014. Techniques for physicochemical characterization of nanomaterials. Biotechnol. Adv. 32 (4), 711–726. Available from: http://dx.doi.org/10.1016/J.BIOTECHADV.2013.11.006.

Litos, I.K., et al., 2007. Genotyping of single-nucleotide polymorphisms by primer extension reaction in a dry-reagent dipstick format. Anal. Chem. 79 (2), 395–402. Available from: https://doi.org/10.1021/ac061729e.

Litos, I.K., et al., 2009. Multianalyte, dipstick-type, nanoparticle-based DNA biosensor for visual genotyping of single-nucleotide polymorphisms. Biosens. Bioelectron. 24 (10), 3135–3139. Available from: https://doi.org/10.1016/j.bios.2009.03.010.

Liu, H., Webster, T.J., 2007. Nanomedicine for implants: a review of studies and necessary experimental tools. Biomaterials 28 (2), 354–369. Available from: https://doi.org/10.1016/j.biomaterials.2006.08.049.

Liu, X., Wang, D., Li, Y., 2012. Synthesis and catalytic properties of bimetallic nanomaterials with various architectures. Nano Today 7 (5), 448–466. Available from: https://doi.org/10.1016/j.nantod.2012.08.003.

Liu, Y., et al., 2007. Controlled synthesis of various hollow Cu nano/microstructures via a novel reduction route. Adv. Funct. Mater. 17 (6), 933–938. Available from: https://doi.org/10.1002/adfm.200600333.

Liu, Z., Bando, Y., 2003. A novel method for preparing copper nanorods and nanowires. Adv. Mater. 15 (4), 303–305. Available from: https://doi.org/10.1002/adma.200390073.

Loo, C., et al., 2005. Immunotargeted nanoshells for integrated cancer imaging and therapy. Nano Lett. 5 (4), 709–711. Available from: https://doi.org/10.1021/nl050127s.

López-Lorente, Á.I., Mizaikoff, B., 2016. Recent advances on the characterization of nanoparticles using infrared spectroscopy. TrAC, Trends Anal. Chem. 84, 97–106. Available from: https://doi.org/10.1016/j.trac.2016.01.012.

Loumaigne, M., et al., 2010. Fluorescence correlation spectroscopy reveals strong fluorescence quenching of FITC adducts on PEGylated Au nanoparticles in water and the presence of fluorescent aggregates of desorbed thiolate ligands. Phys. Chem. Chem. Phys. 12 (36), 11004. Available from: https://doi.org/10.1039/c004167j.

Lu, M., et al., 2017. Nanomaterials as assisted matrix of laser desorption/ionization time-of-flight mass spectrometry for the analysis of small molecules. Nanomaterials 7 (4), 87. Available from: https://doi.org/10.3390/nano7040087.

Lu, W., et al., 2010. Photoacoustic imaging of living mouse brain vasculature using hollow Au nanospheres. Biomaterials 31 (9), 2617–2626. Available from: https://doi.org/10.1016/j.biomaterials.2009.12.007.

Luangpipat, T., et al., 2011. Au nanoparticles produced in a microalga. J. Nanopart. Res. 13 (12), 6439–6445. Available from: https://doi.org/10.1007/s11051-011-0397-9.

Luo, Y., et al., 2015. SERS detection of dopamine using label-free acridine red as molecular probe in reduced graphene oxide/silver nanotriangle sol substrate. Nanoscale Res. Lett. 10 (1), 230. Available from: https://doi.org/10.1186/s11671-015-0937-9.

Rahman, M.M., et al., 2011. Iron oxide nanoparticles. Nanomaterials. InTech, pp. 43–66. Available from: http://dx.doi.org/10.5772/27698.

Mahdavi, M., et al., 2013. Green biosynthesis and characterization of magnetic iron oxide (Fe_3O_4) nanoparticles using seaweed (*Sargassum muticum*) aqueous extract. Molecules 18 (5), 5954–5964. Available from: https://doi.org/10.3390/molecules18055954.

Mahmoodian, H., et al., 2015. Enhanced removal of methyl orange from aqueous solutions by poly HEMA–chitosan-MWCNT nano-composite. J. Mol. Liq. 202, 189–198. Available from: https://doi.org/10.1016/j.molliq.2014.10.040.

Mahmoud, K.A., Luong, J.H.T., 2008. Impedance method for detecting HIV-1 protease and screening for its inhibitors using ferrocene-peptide conjugate/Au nanoparticle/single-walled carbon nanotube modified electrode. Anal. Chem. 80 (18), 7056–7062. Available from: https://doi.org/10.1021/ac801174r.

Maity, D., Agrawal, D.C., 2007. Synthesis of iron oxide nanoparticles under oxidizing environment and their stabilization in aqueous and non-aqueous media. J. Magn. Magn. Mater. 308 (1), 46–55. Available from: https://doi.org/10.1016/j.jmmm.2006.05.001.

Majedi, S.M., Lee, H.K., 2016. Recent advances in the separation and quantification of metallic nanoparticles and ions in the environment. TrAC, Trends Anal. Chem. 75, 183–196. Available from: https://doi.org/10.1016/j.trac.2015.08.009.

Malathi, B., et al., 2015. Immunopotentiating nano-chitosan as potent vaccine carter for efficacious prophylaxis of filarial antigens. Int. J. Biol. Macromol. 73, 131–137. Available from: https://doi.org/10.1016/j.ijbiomac.2014.11.014.

Malik, P., et al., 2014. Green chemistry based benign routes for nanoparticle synthesis. J. Nanopart. 2014, 1–14. Available from: https://doi.org/10.1155/2014/302429.

Mandal, S., De, S., 2015. Catalytic and fluorescence studies with copper nanoparticles synthesized in polysorbates of varying hydrophobicity. Colloids Surf., A: Physicochem. Eng. Aspects 467, 233–250. Available from: https://doi.org/10.1016/j.colsurfa.2014.11.026.

Mannelli, I., Marco, M.-P., 2010. Recent advances in analytical and bioanalysis applications of noble metal nanorods. Anal. Bioanal. Chem. 398 (6), 2451–2469. Available from: https://doi.org/10.1007/s00216-010-3937-8.

Mannheimer, W., 2002. Capitulo V Microscopia Eletrônicade Transmissão. In: Microscopia dos materiais: uma introdução , p. P.V.1-P.V.20.

Marcos Esteban, R., et al., 2015. Synthesis of ruthenium@graphene nanomaterials in propylene carbonate as reusable catalysts for the solvent-free hydrogenation of benzene. Nano-Struct. Nano-Objects 2, 28–34. Available from: https://doi.org/10.1016/j.nanoso.2015.07.002.

Marsalek, R., 2014. Particle size and zeta potential of ZnO. APCBEE Procedia. No longer published by Elsevier 9, 13–17. Available from: https://doi.org/10.1016/j.apcbee.2014.01.003.

Martínez, J.C., et al., 2012. Alternative methodology for Au nanoparticles diameter characterization using PCA technique and UV-vis spectrophotometry. Nanosci. Nanotechnol. 2 (6), 184–189. Available from: https://doi.org/10.5923/j.nn.20120206.06.

Massadeh, S., Al Aamery, M., 2016. Nano-materials for gene therapy: an efficient way in overcoming challenges of gene delivery. J. Biosens. Bioelectron. 07 (01). Available from: https://doi.org/10.4172/2155-6210.1000195.

Mata, Y.N., et al., 2009. Au(III) biosorption and bioreduction with the brown alga *Fucus vesiculosus*. J. Hazard. Mater. 166 (2–3), 612–618. Available from: https://doi.org/10.1016/j.jhazmat.2008.11.064.

Maver, U., et al., 2016. Recent progressive use of atomic force microscopy in biomedical applications. TrAC, Trends Anal. Chem. 80, 96–111. Available from: https://doi.org/10.1016/j.trac.2016.03.014.

McFarland, A.D., et al., 2005. Wavelength-scanned surface-enhanced Raman excitation spectroscopy. J. Phys. Chem. B 109 (22), 11279–11285. Available from: https://doi.org/10.1021/jp050508u.

Md, S., et al., 2018. Nano-carrier enabled drug delivery systems for nose to brain targeting for the treatment of neurodegenerative disorders. J. Drug Deliv. Sci. Technol. 43, 295–310. Available from: https://doi.org/10.1016/j.jddst.2017.09.022.

Merga, G., et al., 2007. Redox catalysis on "naked" silver nanoparticles. J. Phys. Chem. C 111 (33), 12220–12226. Available from: https://doi.org/10.1021/jp074257w.

Mikos, A.G., et al., 1993. Preparation of poly(glycolic acid) bonded fiber structures for cell attachment and transplantation. J. Biomed. Mater. Res. 27 (2), 183–189. Available from: https://doi.org/10.1002/jbm.820270207.

Miller, A.D., 1992. Human gene therapy comes of age. Nature 357 (6378), 455–460. Available from: https://doi.org/10.1038/357455a0.

Miller, M.J., Patrick, C.W., 2003. Tissue engineering. Clin. Plast. Surg., 30 (1), 91–103. vii. Available at: http://www.ncbi.nlm.nih.gov/pubmed/12636219.

Milunovich, J., Roy, S., 2001. The next small thing: an introduction to nanotechnology. In: Merrill Lynch Report.

Mishra, B., et al., 2005. Reactions of biological oxidants with selenourea: formation of redox active nanoselenium. J. Phys. Chem. B 109 (26), 12718–12723. Available from: https://doi.org/10.1021/jp051328n.

Mittal, A.K., Banerjee, U.C., 2016. Current status and future prospects of nanobiomaterials in drug delivery. Nanobiomaterials in Drug Delivery 147–170. Available from: http://dx.doi.org/10.1016/B978-0-323-42866-8.00005-8.

Mittal, A.K., Chisti, Y., Banerjee, U.C., 2013. Synthesis of metallic nanoparticles using plant extracts. Biotechnol. Adv. 31 (2), 346–356. Available from: http://dx.doi.org/10.1016/J.BIOTECHADV.2013.01.003.

Mody, V.V., Nounou, M.I., Bikram, M., 2009. Novel nanomedicine-based MRI contrast agents for gynecological malignancies. Adv. Drug Deliv. Rev. 61 (10), 795–807. Available from: https://doi.org/10.1016/j.addr.2009.04.020.

Mohammadi, Z., et al., 2011. Preparation and evaluation of chitosan-DNA-FAP-B nanoparticles as a novel non-viral vector for gene delivery to the lung epithelial cells. Int. J. Pharm. 409 (1–2), 307–313. Available from: https://doi.org/10.1016/j.ijpharm.2011.02.043.

Mohandas, A., et al., 2018. Chitosan based metallic nanocomposite scaffolds as antimicrobial wound dressings. Bioact. Mater. 3 (3), 267–277. Available from: https://doi.org/10.1016/j.bioactmat.2017.11.003.

Molpeceres, J., Aberturas, M., 2000. Biodegradable nanoparticles as a delivery system for cyclosporine: preparation and characterization. J. Microencapsulation 17 (5), 599–614. Available from: https://doi.org/10.1080/026520400417658.

Momeni, S., Nabipour, I., 2015. A simple green synthesis of palladium nanoparticles with sargassum alga and their electrocatalytic activities towards hydrogen peroxide. Appl. Biochem. Biotechnol. 176 (7), 1937–1949. Available from: https://doi.org/10.1007/s12010-015-1690-3.

Mondal, S., et al., 2011. Biogenic synthesis of Ag, Au and bimetallic Au/Ag alloy nanoparticles using aqueous extract of mahogany (*Swietenia mahogani* JACQ) leaves. Colloids Surf., B: Biointerfaces 82 (2), 497–504. Available from: https://doi.org/10.1016/j.colsurfb.2010.10.007.

Monteiro, D.R., et al., 2009. The growing importance of materials that prevent microbial adhesion: antimicrobial effect of medical devices containing silver. Int. J. Antimicrob. Agents 34 (2), 103–110. Available from: https://doi.org/10.1016/j.ijantimicag.2009.01.017.

Mott, D., et al., 2007. Synthesis of size-controlled and shaped copper nanoparticles. Langmuir 23 (10), 5740–5745. Available from: https://doi.org/10.1021/la0635092.

zur Mühlen, A., et al., 1996. Atomic force microscopy studies of solid lipid nanoparticles. Pharm. Res. 13 (9), 1411–1416. Available from: http://www.ncbi.nlm.nih.gov/pubmed/8893284.

Mukherjee, P., et al., 2002. Extracellular synthesis of Au nanoparticles by the fungus *Fusarium oxysporum*. ChemBioChem 3 (5), 461–463. Available from: https://doi.org/10.1002/1439-7633(20020503)3:5<461::AID-CBIC461>3.0.CO;2-X.

Mukherjee, S., et al., 2014. Potential theranostics application of biosynthesized silver nanoparticles (4-in-1 system). Theranostics 4 (3), 316–335. Available from: https://doi.org/10.7150/thno.7819.

Mulfinger, L., et al., 2007. Synthesis and study of silver nanoparticles. J. Chem. Educ. 84 (2), 322. Available from: https://doi.org/10.1021/ed084p322.

Müller, W.E.G., et al., 2009. Biosintering processes in hexactinellid sponges: fusion of biosilica in giant basal spicules from *Monorhaphis chuni*. J. Struct. Biol. 168 (3), 548–561. Available from: https://doi.org/10.1016/j.jsb.2009.08.003.

Munge, B.S., et al., 2011. Nanostructured immunosensor for attomolar detection of cancer biomarker interleukin-8 using massively labeled superparamagnetic particles. Angew. Chem. (Int. ed. English) 50 (34), 7915–7918. Available from: https://doi.org/10.1002/anie.201102941.

Murphy, C.J., et al., 2005. Anisotropic metal nanoparticles: synthesis, assembly, and optical applications. J. Phys. Chem. B 109 (29), 13857–13870. Available from: https://doi.org/10.1021/jp0516846.

Murugan, A., Shanmugasundaram, K.K., 2014. Biosynthesis and characterization of silver nanoparticles using the aqueous extract of *Vitex negundo linn*. World J. Pharm. Pharm. Sci. 3 (8), 1385–1393.

Naeem, H., et al., 2019. Facile synthesis of graphene oxide–silver nanocomposite for decontamination of water from multiple pollutants by adsorption, catalysis and antibacterial activity. J. Environ. Manage. 230, 199–211. Available from: https://doi.org/10.1016/j.jenvman.2018.09.061.

Nagavarma, B.V.N., et al., 2012. Different techniques for preparation of polymeric nanoparticles—a review. Asian J. Pharm. Clin. Res 5 (3), 16–23.

Nair, R., et al., 2011. Uptake of FITC labeled silica nanoparticles and quantum dots by rice seedlings: effects on seed germination and their potential as biolabels for plants. J. Fluoresc. 21 (6), 2057–2068. Available from: https://doi.org/10.1007/s10895-011-0904-5.

Nalawade, P., Mukherjee, T., Kapoor, S., 2012. High-yield synthesis of multispiked Au nanoparticles: characterization and catalytic reactions. Colloids Surf., A: Physicochem. Eng. Aspects 396, 336–340. Available from: https://doi.org/10.1016/j.colsurfa.2012.01.018.

Narayanan, K.B., Sakthivel, N., 2010. Biological synthesis of metal nanoparticles by microbes. Adv. Colloid Interface Sci. 156 (1–2), 1–13. Available from: https://doi.org/10.1016/j.cis.2010.02.001.

Nasirian, A., 2012. Synthesis and characterization of {Cu} nanoparticles and studying of their catalytic properties. Int. J. Nano Dimension 2 (3), 159–164. Available from: https://doi.org/10.7508/IJND.2011.03.002.

Nasrollahzadeh, M., Sajadi, S.M., 2015. Green synthesis of copper nanoparticles using *Ginkgo biloba* L. leaf extract and their catalytic activity for the Huisgen [3 + 2] cycloaddition of azides and alkynes at room temperature. J. Colloid Interface Sci. 457, 141–147. Available from: https://doi.org/10.1016/j.jcis.2015.07.004.

Nath, D., Banerjee, P., 2013. Green nanotechnology – a new hope for medical biology. Environ. Toxicol. Pharmacol. 36 (3), 997–1014. Available from: https://doi.org/10.1016/j.etap.2013.09.002.

Naya, M., et al., 2008. In: Stockman, M.I. (Ed.), 'Nanophotonics Biosensor Using Au Nanostructure'. p. 70321Q. Available from: http://dx.doi.org/10.1117/12.800900.

Nghiem, T.H.L., et al., 2010. Synthesis, capping and binding of colloidal Au nanoparticles to proteins. Adv. Nat. Sci.: Nanosci. Nanotechnol. 1 (2), 025009. Available from: https://doi.org/10.1088/2043-6254/1/2/025009.

Niaz, N.A., et al., 2013. Synthesis and characterization of Mg–Al alloys for hydrogen storage applications. Digest J. Nanomater. Biostructures 8, 423–431.

Nobs, L., et al., 2004. Poly(lactic acid) nanoparticles labeled with biologically active Neutravidin for active targeting. Eur. J. Pharm. Biopharm. 58 (3), 483–490. Available from: https://doi.org/10.1016/j.ejpb.2004.04.006.

Nurmi, J.T., et al., 2005. Characterization and properties of metallic iron nanoparticles: spectroscopy, electrochemistry, and kinetics. Environ. Sci. Technol. 39 (5), 1221–1230. Available from: http://www.ncbi.nlm.nih.gov/pubmed/15787360.

Oldenburg, S., et al., 1998. Nanoengineering of optical resonances. Chem. Phys. Lett. 288 (2–4), 243–247. Available from: https://doi.org/10.1016/S0009-2614(98)00277-2.

Oliveira, M.M., et al., 2005. Influence of synthetic parameters on the size, structure, and stability of dodecanethiol-stabilized silver nanoparticles. J. Colloid Interface Sci. 292 (2), 429–435. Available from: https://doi.org/10.1016/j.jcis.2005.05.068.

Ostiguy, C., Cloutier, Y., Boutin, M., 2006. Nanoparticles, actual knowledge about occupational health and safety risks and prevention measures, IRSST, p 1–86.

Ozsoz, M., et al., 2003. Electrochemical genosensor based on colloidal Au nanoparticles for the detection of Factor V Leiden mutation using disposable pencil graphite electrodes. Anal. Chem. 75 (9), 2181–2187. Available from: https://doi.org/10.1021/ac026212r.

Pal, S.L., et al., 2011. Nanoparticles—an overview of preparation and characterization. J. Appl. Pharm. Sci. 1 (6), 228–234. Available from: https://doi.org/10.7897/2230-8407.04408.

Pan, D., et al., 2010. Near infrared photoacoustic detection of sentinel lymph nodes with Au nanobeacons. Biomaterials 31 (14), 4088–4093. Available from: https://doi.org/10.1016/j.biomaterials.2010.01.136.

Pan, Y., et al., 2018. Therapeutic approaches targeting cancer stem cells. J. Cancer Res. Ther. 14 (7), 1469–1475. Available from: https://doi.org/10.4103/jcrt.JCRT_976_17.

Pandey, S., et al., 2013. Carbon dots functionalized Au nanorod mediated delivery of doxorubicin: tri-functional nano-worms for drug delivery, photothermal therapy and bioimaging. J. Mater. Chem. B 1 (38), 4972. Available from: https://doi.org/10.1039/c3tb20761g.

Pandoli, O., et al., 2011. Circular dichroism and UV-vis absorption spectroscopic monitoring of production of chiral silver nanoparticles templated by guanosine 5′-monophosphate. Analyst 136 (18), 3713–3719. Available from: https://doi.org/10.1039/c1an15288b.

Pankhurst, Q.A., et al., 2003. Applications of magnetic nanoparticles in biomedicine. J. Phys. D: Appl. Phys. 36, R167–R181.

Pantidos, N., 2014. Biological synthesis of metallic nanoparticles by bacteria, fungi and plants. J. Nanomed. Nanotechnol. 05 (05). Available from: https://doi.org/10.4172/2157-7439.1000233.

Le Pape, H., et al., 2002. Evaluation of the antimicrobial properties of an activated carbon fibre supporting silver using a dynamic method. Carbon 40 (15), 2947–2954. Available from: https://doi.org/10.1016/S0008-6223(02)00246-4.

Paramasivam, G., et al., 2017. Anisotropic noble metal nanoparticles: synthesis, surface functionalization and applications in biosensing, bioimaging, drug delivery and theranostics. Acta Biomater. 49, 45–65. Available from: https://doi.org/10.1016/j.actbio.2016.11.066.

Paskevicius, M., et al., 2009. Mechanochemical synthesis of aluminium nanoparticles and their deuterium sorption properties to 2kbar. J. Alloys Compd. 481 (1–2), 595–599. Available from: https://doi.org/10.1016/j.jallcom.2009.03.031.

Patharkar, R.G., Nandanwar, S.U., Chakraborty, M., 2013. Synthesis of colloidal ruthenium nanocatalyst by chemical reduction method. J. Chem. 2013, 1–5. Available from: https://doi.org/10.1155/2013/831694.

Patil, R.S., et al., 2012. One-pot synthesis of PVA-capped silver nanoparticles their characterization and biomedical application. Adv. Nat. Sci.: Nanosci. Nanotechnol. 3 (1), 15013. Available from: http://stacks.iop.org/2043-6262/3/i=1/a=015013.

Patri, A.K., et al., 2006. Preclinical characterization of engineered nanoparticles intended for cancer therapeutics. Nanotechnology for Cancer Therapy. CRC Press, pp. 105–138. Available from: https://www.crcpress.com/Nanotechnology-for-Cancer-Therapy/Amiji/p/book/9780849371943.

Pelzer, K., et al., 2003. Ruthenium nanoparticles in nanoporous alumina membranes: preparation, characterization and catalytic properties. Z. Anorganische Allg. Chem. 629 (78), 1217–1222. Available from: https://doi.org/10.1002/zaac.200300042.

Pérez, Y., Mann, E., Herradón, B., 2011. Preparation and characterization of Au nanoparticles capped by peptide–biphenyl hybrids. J. Colloid Interface Sci. 359 (2), 443–453. Available from: https://doi.org/10.1016/j.jcis.2011.04.029.

Phenrat, T., et al., 2009. Particle size distribution, concentration, and magnetic attraction affect transport of polymer-modified Fe0 nanoparticles in sand columns. Environ. Sci. Technol. 43 (13), 5079–5085. Available from: https://doi.org/10.1021/es900171v.

Philippot, K., Lignier, P., Chaudret, B., 2014. Organometallic ruthenium nanoparticles and catalysis,. Top. Organomet. Chem. Available from: https://doi.org/10.1007/3418_2014_83.

Picó, Y., Blasco, C., 2012. Nanomaterials in food, which way forward? Compr. Anal. Chem. 59, 305–353. Available from: http://dx.doi.org/10.1016/B978-0-444-56328-6.00009-8.

Pileni, M.P., 1993. Reverse micelles as microreactors. J. Phys. Chem. 97 (27), 6961–6973. Available from: https://doi.org/10.1021/j100129a008.

Pileni, M.P., 1997. Nanosized particles made in colloidal assemblies. Langmuir 13 (13), 3266–3276. Available from: https://doi.org/10.1021/la960319q.

Poinern, G.E.J., 2014. A Laboratory Course in Nanoscience and Nanotechnology, first ed. CRC Press Taylor & Francis, Boca Raton, FL.

Polakovic, M., et al., 1999. Lidocaine loaded biodegradable nanospheres II Modelling of drug release. J. Controlled Release 60 (2–3), 169–177. Available from: http://www.ncbi.nlm.nih.gov/pubmed/10425323.

Ponce, A., Mejía-Rosales, S., José-Yacamán, M., 2012. Scanning transmission electron microscopy methods for the analysis of nanoparticles. Methods in molecular biology (Clifton, N.J.) 906, 453–471. Available from: https://doi.org/10.1007/978-1-61779-953-2_37.

Pons, T., et al., 2006. Hydrodynamic dimensions, electrophoretic mobility, and stability of hydrophilic quantum dots. J. Phys. Chem. B 110 (41), 20308–20316. Available from: https://doi.org/10.1021/jp065041h.

Pooja, B., Joginder, S.D., Suresh, K.G., 2014. Biogenesis of nanoparticles: a review. Afr. J. Biotechnol. 13 (28), 2778–2785. Available from: https://doi.org/10.5897/AJB2013.13458.

Poole, R.K., Kalneniesks, U., 2000. Introduction to light absorption: visible and ultraviolet spectra. In: Gore, M.G. (Ed.), Spectrophotometry and Spectrofluorimetry. Oxford University Press, Oxford, pp. 1–32.

Pope, C.G., 1997. X-ray diffraction and the Bragg equation. J. Chem. Educ. 74 (1), 129. Available from: https://doi.org/10.1021/ed074p129.

Popović, Z.V., et al., 2011. Raman scattering on nanomaterials and nanostructures. Annalen der Physik 523 (1–2), 62–74. Available from: https://doi.org/10.1002/andp.201000094.

Rac, O., et al., 2014. Influence of stabilising agents and pH on the size of SnO_2 nanoparticles. Beilstein J. Nanotechnol. 5, 2192–2201. Available from: https://doi.org/10.3762/bjnano.5.228.

Raghvendra, et al., 2010. Clinical application of nanomedicines: a review. Int. J. Appl. Biol. Pharm. Technol. 1 (2), 660–665. Available from: http://www.ijabpt.com/pdf/8757-Tyagi[1].pdf.

Rahman, M.M., et al., 2013. Chemo-sensors development based on low-dimensional codoped Mn_2O_3-ZnO nanoparticles using flat-silver electrodes. Chem. Cent. J. 7 (1), 60. Available from: https://doi.org/10.1186/1752-153X-7-60.

Rai, M., et al., 2016. Strategic role of selected noble metal nanoparticles in medicine. Crit. Rev. Microbiol. 42 (5), 696–719. Available from: https://doi.org/10.3109/1040841X.2015.1018131.

Raj, S., et al., 2012. Nanotechnology in cosmetics: opportunities and challenges. J. Pharm. Bioallied Sci. 4 (3), 186. Available from: https://doi.org/10.4103/0975-7406.99016.

Rajasulochana, P., et al., 2010. Biosynthesis and characterization of Au nanoparticles using the alga *Kappaphycus alvarezii*. Int. J. Nanosci. 09 (05), 511–516. Available from: https://doi.org/10.1142/S0219581X10007149.

Rajeshkumar, S., Rinitha, G., 2018. Nanostructural characterization of antimicrobial and antioxidant copper nanoparticles synthesized using novel *Persea americana* seeds. OpenNano 3, 18–27. Available from: https://doi.org/10.1016/j.onano.2018.03.001.

Rajput, N., 2015. Methods of preparation of nanoparticles – a review. Int. J. Adv. Eng. Technol. 7 (4), 1806–1811. Available from: http://www.e-ijaet.org/media/23I24-IJAET0723754-v7-iss6-1806-1811.pdf.

Ramyadevi, J., et al., 2012. Synthesis and antimicrobial activity of copper nanoparticles. Mater. Lett. 71, 114–116. Available from: https://doi.org/10.1016/j.matlet.2011.12.055.

Ranjan, P. et al., 2017. Synthesis of γ-alumina nanoparticles by wire-explosion process: Characterisation and formation mechanism. In: 2017 International Conference on High Voltage Engineering and Power Systems (ICHVEPS), IEEE, pp. 301–306. doi:10.1109/ICHVEPS.2017.8225961.

Ranjbar, B., Gill, P., 2009. Circular dichroism techniques: biomolecular and nanostructural analyses—a review. Chem. Biol. Drug Des. 74 (2), 101–120. Available from: https://doi.org/10.1111/j.1747-0285.2009.00847.x.

Rao, P.V., Gan, S.H., 2015. Recent advances in nanotechnology-based diagnosis and treatments of diabetes. Curr. Drug Metab. 16 (5), 371–375. Available from: http://www.ncbi.nlm.nih.gov/pubmed/25429672.

Raoof, M., et al., 2012. Stability of antibody-conjugated Au nanoparticles in the endolysosomal nanoenvironment: implications for noninvasive radiofrequency-based cancer therapy. Nanomed. Nanotechnol. Biol. Med. 8 (7), 1096–1105. Available from: https://doi.org/10.1016/j.nano.2012.02.001.

Ravishankar Rai, V., Jamuna Bai, a, 2011. Nanoparticles and their potential application as antimicrobials. Formatex 197–209. Available from: https://doi.org/10.1016/j.jscs.2015.01.009.

Reed, R.B., et al., 2012. Overcoming challenges in analysis of polydisperse metal-containing nanoparticles by single particle inductively coupled plasma mass spectrometry. J. Anal. At. Spectrom. 27 (7), 1093. Available from: https://doi.org/10.1039/c2ja30061c.

Ren, Y., et al., 2013. Antitumor activity of hyaluronic acid-selenium nanoparticles in Heps tumor mice models. Int. J. Biol. Macromol. 57, 57–62. Available from: https://doi.org/10.1016/j.ijbiomac.2013.03.014.

Rezende, T.S., et al., 2010. Facile preparation of catalytically active Au nanoparticles on a thiolated chitosan. Mater. Lett. 64 (7), 882–884. Available from: https://doi.org/10.1016/j.matlet.2010.01.051.

Ricceri, R., Matteazzi, P., 2004. A fast and low-cost room temperature process for TiB_2 formation by mechanosynthesis. Mater. Sci. Eng., A 379 (1–2), 341–346. Available from: https://doi.org/10.1016/j.msea.2004.02.064.

Rivero, P.J., et al., 2013. A lossy mode resonance optical sensor using silver nanoparticles-loaded films for monitoring human breathing. Sens. Actuators, B: Chem. 187, 40–44. Available from: https://doi.org/10.1016/j.snb.2012.09.022.

Rocha, C.S.J., et al., 2015. RNA therapeutics inactivate PCSK9 by inducing a unique intracellular retention form. J. Mol. Cell. Cardiol. 82, 186–193. Available from: https://doi.org/10.1016/j.yjmcc.2015.03.009.

Cornell R. M., 2006. Crystal structure. In: The Iron Oxides: Structure, Properties, Reactions, Occurrences and Uses, second ed. John Wiley & Sons, pp. 9–37.

Rosarin, F.S., Mirunalini, S., 2011. Nobel metallic nanoparticles with novel biomedical properties. J. Bioanal. Biomed. 03 (04), 085–091. Available from: https://doi.org/10.4172/1948-593X.1000049.

Roucoux, A., Schulz, J., Patin, H., 2002. Reduced transition metal colloids: a novel family of reusable catalysts? Chem. Rev. 102 (10), 3757–3778. Available from: https://doi.org/10.1021/cr010350j.

Ruparelia, J.P., et al., 2008. Strain specificity in antimicrobial activity of silver and copper nanoparticles. Acta Biomater. 4 (3), 707–716. Available from: https://doi.org/10.1016/j.actbio.2007.11.006.

Sah, M.K., Rath, S.N., 2016. Soluble eggshell membrane: a natural protein to improve the properties of biomaterials used for tissue engineering applications. Mater. Sci. Eng., C 67, 807–821. Available from: https://doi.org/10.1016/j.msec.2016.05.005.

Sahoo, S.K., Labhasetwar, V., 2003. Nanotech approaches to drug delivery and imaging. Drug Discov. Today 8 (24), 1112–1120. Available from: http://www.ncbi.nlm.nih.gov/pubmed/14678737.

Saifuddin, N., Wong, C.W., Yasumira, A.A.N., 2009. Rapid biosynthesis of silver nanoparticles using culture supernatant of bacteria with microwave irradiation. E-J. Chem. 6 (1), 61–70. Available from: https://doi.org/10.1155/2009/734264.

Saleh, T.A., 2011a. Testing the effectiveness of visual aids in chemical safety training. J. Chem. Health Saf. 18 (2), 3–8. Available from: https://doi.org/10.1016/j.jchas.2010.03.012.

Saleh, T.A., 2011b. The influence of treatment temperature on the acidity of MWCNT oxidized by HNO_3 or a mixture of HNO_3/H_2SO_4. Appl. Surf. Sci. 257 (17), 7746–7751. Available from: https://doi.org/10.1016/j.apsusc.2011.04.020.

Saleh, T.A., 2013. A strategy for integrating basic concepts of nanotechnology to enhance undergraduate nano-education: statistical evaluation of an application study. J. Nano Educ. 4 (1), 1–7. Available from: https://doi.org/10.1166/jne.2012.1021.

Salem, N.M., et al., 2016. Sulfur nanoparticles improves root and shoot growth of tomato. J. Agric. Sci. 8 (4), 179. Available from: https://doi.org/10.5539/jas.v8n4p179.

Sanchez-Dominguez, M., Boutonnet, M., Solans, C., 2009. A novel approach to metal and metal oxide nanoparticle synthesis: the oil-in-water microemulsion reaction method. J. Nanopart. Res. 11 (7), 1823–1829. Available from: https://doi.org/10.1007/s11051-009-9660-8.

Sapsford, K.E., et al., 2011. Analyzing nanomaterial bioconjugates: a review of current and emerging purification and characterization techniques. Anal. Chem. 83 (12), 4453–4488. Available from: https://doi.org/10.1021/ac200853a.

Sarkar, B., et al., 2015. Selenium nanoparticles for stress-resilient fish and livestock. Nanoscale Res. Lett. 10 (1), 371. Available from: https://doi.org/10.1186/s11671-015-1073-2.

Sau, T.K., et al., 2010. Properties and applications of colloidal nonspherical noble metal nanoparticles. Adv. Mater. 22 (16), 1805–1825. Available from: https://doi.org/10.1002/adma.200902557.

Savithramma, N., Bhumi, G., 2014. Biological synthesis of zinc oxide nanoparticles from *Catharanthus roseus* (l) G Don leaf extract and validation for antibacterial activity. Int. J. Drug Dev. Res. 6 (1), 208–214.

Schiøtz, B.L., et al., 2010. Formation of autophagosomes and redistribution of LC3 upon in vitro infection with infectious salmon anemia virus. Virus Res. 151 (1), 104–107. Available from: https://doi.org/10.1016/j.virusres.2010.03.013.

Scholes, P.D., et al., 1999. Detection and determination of surface levels of poloxamer and PVA surfactant on biodegradable nanospheres using SSIMS and XPS. J. Controlled Release 59 (3), 261–278. Available from: http://www.ncbi.nlm.nih.gov/pubmed/10332059.
Scholten, J.D., Leal, B.C., Dupont, J., 2012. Transition metal nanoparticle catalysis in ionic liquids. ACS Catal. 2 (1), 184–200. Available from: https://doi.org/10.1021/cs200525e.
Schoonen, L., van Hest, J.C.M., 2014. Functionalization of protein-based nanocages for drug delivery applications. Nanoscale 6 (13), 7124–7141. Available from: https://doi.org/10.1039/c4nr00915k.
Seabra, A., Durán, N., 2015. Nanotoxicology of metal oxide nanoparticles. Metals 5 (2), 934–975. Available from: https://doi.org/10.3390/met5020934.
Seetharamulu, P., et al., 2009. Role of promoters on highly active nano-Ru catalyst supported on Mg–Al hydrotalcite precursor for the synthesis of ammonia. Catal. Today 141 (1–2), 94–98. Available from: https://doi.org/10.1016/j.cattod.2008.05.010.
Sen, P., et al., 2003. Preparation of Cu, Ag, Fe and Al nanoparticles by the exploding wire technique. J. Chem. Sci. 115 (5–6), 499–508. Available from: https://doi.org/10.1007/BF02708241.
Sen, T., et al., 2011. Interaction of Au nanoparticle with human serum albumin (HSA) protein using surface energy transfer. J. Phys. Chem. C 115 (49), 24037–24044. Available from: https://doi.org/10.1021/jp207374g.
Senapati, S., et al., 2012. Intracellular synthesis of Au nanoparticles using alga *Tetraselmis kochinensis*. Mater. Lett. 79, 116–118. Available from: https://doi.org/10.1016/j.matlet.2012.04.009.
Sengani, M., Grumezescu, A.M., Rajeswari, V.D., 2017. Recent trends and methodologies in Au nanoparticle synthesis – a prospective review on drug delivery aspect. OpenNano 37–46. Available from: http://dx.doi.org/10.1016/j.onano.2017.07.001.
Sershen, S.R., et al., 2000. Temperature-sensitive polymer-nanoshell composites for photothermally modulated drug delivery. J. Biomed. Mater. Res. 51 (3), 293–298. Available from: http://dx.doi.org/10.1002/1097-4636(20000905)51:3<293::AID-JBM1>3.0.CO;2-T.
Shah, M., et al., 2015. Green synthesis of metallic nanoparticles via biological entities. Materials 8 (11), 7278–7308. Available from: https://doi.org/10.3390/ma8115377.
Shamsipur, M., et al., 2011. Novel approach for electrochemical preparation of sulfur nanoparticles. Microchim. Acta 173 (3–4), 445–451. Available from: https://doi.org/10.1007/s00604-011-0581-8.
Sharma, B., et al., 2012. SERS: materials, applications, and the future. Mater. Today 15 (1–2), 16–25. Available from: http://dx.doi.org/10.1016/S1369-7021(12)70017-2.
Sharma, G., et al., 2014. Biomolecule-mediated synthesis of selenium nanoparticles using dried *Vitis vinifera* (raisin) extract. Molecules (Basel, Switzerland) 19 (3), 2761–2770. Available from: https://doi.org/10.3390/molecules19032761.
Sharma, G., et al., 2017. Novel development of nanoparticles to bimetallic nanoparticles and their composites: a review. J. King Saud Univ.—Sci. Available from: https://doi.org/10.1016/j.jksus.2017.06.012.
Sharma, H., et al., 2015. Metal nanoparticles: a theranostic nanotool against cancer. Drug Discov. Today 20 (9), 1143–1151. Available from: https://doi.org/10.1016/j.drudis.2015.05.009.
Sharma, M.K., et al., 2008. Highly sensitive amperometric immunosensor for detection of *Plasmodium falciparum* histidine-rich protein 2 in serum of humans with malaria: comparison with a commercial kit. J. Clin. Microbiol. 46 (11), 3759–3765. Available from: https://doi.org/10.1128/JCM.01022-08.
Sharma, V.K., Yngard, R.A., Lin, Y., 2009. Silver nanoparticles: green synthesis and their antimicrobial activities. Adv. Colloid Interface Sci. 145 (1–2), 83–96. Available from: https://doi.org/10.1016/j.cis.2008.09.002.
Sharon, M., Oza, G., Pandey, S., 2012. Extracellular synthesis of Au nanoparticles using *Pseudomonas* denitrificans and comprehending its stability. J. Microbiol. Biotech. Res 2, 493–499.
Shastri, L., et al., 2015. Synthesis, characterization and bifunctional applications of bidentate silver nanoparticle assisted single drop microextraction as a highly sensitive preconcentrating probe for protein analysis. RSC Adv. 5 (52), 41595–41603. Available from: https://doi.org/10.1039/C5RA04032A.
Shawky, S.M., Bald, D., Azzazy, H.M.E., 2010. Direct detection of unamplified hepatitis C virus RNA using unmodified Au nanoparticles. Clin. Biochem. 43 (13–14), 1163–1168. Available from: https://doi.org/10.1016/j.clinbiochem.2010.07.001.
Shefi, O., et al., 2014. Substrates coated with silver nanoparticles as a neuronal regenerative material. Int. J. Nanomed. 23. Available from: https://doi.org/10.2147/IJN.S45639.
Shevtsov, M., et al., 2017. Applicability of metal nanoparticles in the detection and monitoring of hepatitis B virus infection. Viruses 9 (7), 193. Available from: https://doi.org/10.3390/v9070193.

Shi, H.G., et al., 2003. Characterization of crystalline drug nanoparticles using atomic force microscopy and complementary techniques. Pharm. Res. 20 (3), 479–484. Available from: http://www.ncbi.nlm.nih.gov/pubmed/12669972.

Shpyrko, O.G., 2014. X-ray photon correlation spectroscopy. J. Synchrotron Radiat. 21 (5), 1057–1064. Available from: https://doi.org/10.1107/S1600577514018232.

Siddiqi, K.S., Husen, A., 2016. Green synthesis, characterization and uses of palladium/platinum nanoparticles. Nanoscale Res. Lett. 11 (1), 482. Available from: https://doi.org/10.1186/s11671-016-1695-z.

Siddiqi, K.S., Husen, A., 2017. Recent advances in plant-mediated engineered Au nanoparticles and their application in biological system. J. Trace Elem. Med. Biol. 40, 10–23. Available from: https://doi.org/10.1016/j.jtemb.2016.11.012.

Siddiqui, M.H., Al-Whaibi, M.H., 2014. Role of nano-SiO_2 in germination of tomato (*Lycopersicum esculentum* seeds Mill). Saudi J. Biol. Sci. 21 (1), 13–17. Available from: https://doi.org/10.1016/j.sjbs.2013.04.005.

Sieben, J.M., Duarte, M.M.E., Mayer, C.E., 2008. Supported Pt and Pt–Ru catalysts prepared by potentiostatic electrodeposition for methanol electrooxidation. J. Appl. Electrochem. 38 (4), 483–490. Available from: https://doi.org/10.1007/s10800-007-9462-6.

Singh, P., et al., 2015. Biosynthesis, characterization, and antimicrobial applications of silver nanoparticles. Int. J. Nanomed. 10, 2567–2577. Available from: https://doi.org/10.2147/IJN.S72313.

Singh, P., et al., 2016. Biological synthesis of nanoparticles from plants and microorganisms. Trends Biotechnol. 34 (7), 588–599. Available from: https://doi.org/10.1016/J.TIBTECH.2016.02.006.

Singh, R., Sahu, S.K., Thangaraj, M., 2014. Biosynthesis of silver nanoparticles by marine invertebrate (polychaete) and assessment of its efficacy against human pathogens. J. Nanopart. 2014, 1–7. Available from: https://doi.org/10.1155/2014/718240.

Sintubin, L., Verstraete, W., Boon, N., 2012. Biologically produced nanosilver: current state and future perspectives. Biotechnol. Bioeng. 109 (10), 2422–2436. Available from: https://doi.org/10.1002/bit.24570.

Slocik, J.M., Govorov, A.O., Naik, R.R., 2011. Plasmonic circular dichroism of peptide-functionalized Au nanoparticles. Nano Lett. 11 (2), 701–705. Available from: https://doi.org/10.1021/nl1038242.

Smuleac, V., et al., 2011. Green synthesis of Fe and Fe/Pd bimetallic nanoparticles in membranes for reductive degradation of chlorinated organics. J. Membr. Sci. 379 (1–2), 131–137. Available from: https://doi.org/10.1016/j.memsci.2011.05.054.

Soenen, S.J.H., et al., 2010. Intracellular nanoparticle coating stability determines nanoparticle diagnostics efficacy and cell functionality. Small (Weinheim an der Bergstrasse, Germany) 6 (19), 2136–2145. Available from: https://doi.org/10.1002/smll.201000763.

Sondi, I., Goia, D.V., Matijević, E., 2003. Preparation of highly concentrated stable dispersions of uniform silver nanoparticles. J. Colloid Interface Sci. 260 (1), 75–81. Available from: https://doi.org/10.1016/S0021-9797(02)00205-9.

Song, J.Y., Kim, B.S., 2008. Biological synthesis of bimetallic Au/Ag nanoparticles using Persimmon (*Diopyros kaki*) leaf extract. Korean J. Chem. Eng. 25 (4), 808–811. Available from: https://doi.org/10.1007/s11814-008-0133-z.

Sperling, R.A., et al., 2008. Biological applications of Au nanoparticles. Chem. Soc. Rev. 37 (9), 1896. Available from: https://doi.org/10.1039/b712170a.

Sperling, R.A., Parak, W.J., 2010. Surface modification, functionalization and bioconjugation of colloidal inorganic nanoparticles. Philos. Trans. R. Soc. London, Ser. A 368 (1915), 1333–1383. Available from: https://doi.org/10.1098/rsta.2009.0273.

Stamenkovic, V.R., et al., 2007. Improved oxygen reduction activity on Pt3Ni(111) via increased surface site availability. Science (New York, NY) 315 (5811), 493–497. Available from: https://doi.org/10.1126/science.1135941.

Stiufiuc, R., et al., 2013. SERS-active silver colloids prepared by reduction of silver nitrate with short-chain polyethylene glycol. Nanoscale Res. Lett. 8 (1), 47. Available from: https://doi.org/10.1186/1556-276X-8-47.

Stix, G., 2001. Little big science Nanotechnology. Sci. Am. 285 (3), 32–37. Available from: http://www.ncbi.nlm.nih.gov/pubmed/11524967.

Storhoff, J.J., et al., 2004. Au nanoparticle-based detection of genomic DNA targets on microarrays using a novel optical detection system. Biosens. Bioelectron. 19 (8), 875–883. Available from: http://www.ncbi.nlm.nih.gov/pubmed/15128107.

Strobel, H.A., et al., 2018. Targeted delivery of bioactive molecules for vascular intervention and tissue engineering. Front. Pharmacol. 9, 1329. Available from: https://doi.org/10.3389/fphar.2018.01329.

Stroyuk, A.L., et al., 2008. Structural and optical characterization of colloidal Se nanoparticles prepared via the acidic decomposition of sodium selenosulfate. Colloids Surf., A: Physicochem. Eng. Aspects 320 (1–3), 169–174. Available from: https://doi.org/10.1016/j.colsurfa.2008.01.055.

Stuart, D.A., et al., 2005. Glucose sensing using near-infrared surface-enhanced Raman spectroscopy: Au surfaces, 10-day stability, and improved accuracy. Anal. Chem. 77 (13), 4013–4019. Available from: https://doi.org/10.1021/ac0501238.

Subbiah, R., Veerapandian, M., Yun, K.S., 2010. Nanoparticles: functionalization and multifunctional applications in biomedical sciences. Curr. Med. Chem. 17 (36), 4559–4577. Available from: http://www.ncbi.nlm.nih.gov/pubmed/21062250.

Suffredini, H.B., Salazar-Banda, G.R., Avaca, L.A., 2009. Carbon supported electrocatalysts prepared by the sol–gel method and their utilization for the oxidation of methanol in acid media. J. Sol-Gel Sci. Technol. 49 (2), 131–136.

Sukhanova, A., et al., 2004. Biocompatible fluorescent nanocrystals for immunolabeling of membrane proteins and cells. Anal. Biochem. 324 (1), 60–67. Available from: http://www.ncbi.nlm.nih.gov/pubmed/14654046.

Suleiman, M., et al., 2013. Sulfur nanoparticles: synthesis, characterizations and their applications. J. Mater. Environ. Sci. 4 (6), 2028–2508.

Suleiman, M., et al., 2015. Synthesis of nano-sized sulfur nanoparticles and their antibacterial activities. J. Mater. Environ. Sci. 6 (2), 513–518.

Sun, Y., Mayers, B.T., Xia, Y., 2002. Template-engaged replacement reaction: a one-step approach to the large-scale synthesis of metal nanostructures with hollow interiors. Nano Lett. 2 (5), 481–485. Available from: https://doi.org/10.1021/nl025531v.

Suramwar, N.V., Thakare, S.R., Khaty, N.T., 2016. One pot synthesis of copper nanoparticles at room temperature and its catalytic activity. Arabian J. Chem. 9, S1807–S1812. Available from: https://doi.org/10.1016/j.arabjc.2012.04.034.

Suresh, A.K., et al., 2010. Silver nanocrystallites: biofabrication using *Shewanella oneidensis*, and an evaluation of their comparative toxicity on gram-negative and gram-positive bacteria. Environ. Sci. Technol. 44 (13), 5210–5215. Available from: https://doi.org/10.1021/es903684r.

Suzuki, E., 2002. High-resolution scanning electron microscopy of immunoAu-labelled cells by the use of thin plasma coating of osmium. J. Microsc. 208 (Pt 3), 153–157. Available from: http://www.ncbi.nlm.nih.gov/pubmed/12460446.

Takahashi, H., Carninci, P., 2014. Widespread genome transcription: new possibilities for RNA therapies. Biochem. Biophys. Res. Commun. 452 (2), 294–301. Available from: https://doi.org/10.1016/j.bbrc.2014.08.139.

Takezawa, T., 2003. A strategy for the development of tissue engineering scaffolds that regulate cell behavior. Biomaterials 24 (13), 2267–2275. Available from: http://www.ncbi.nlm.nih.gov/pubmed/12699663.

Talapin, D.V., et al., 2010. Prospects of colloidal nanocrystals for electronic and optoelectronic applications. Chem. Rev. 110 (1), 389–458. Available from: https://doi.org/10.1021/cr900137k.

Tamilvanan, A., et al., 2014. Copper nanoparticles: synthetic strategies, properties and multifunctional application. Int. J. Nanosci. 13 (02), 1430001. Available from: https://doi.org/10.1142/S0219581X14300016.

Tarnawski, R., Ulbricht, M., 2011. Amphiphilic Au nanoparticles: synthesis, characterization and adsorption to PEGylated polymer surfaces. Colloids Surf., A: Physicochem. Eng. Aspects 374 (1–3), 13–21. Available from: https://doi.org/10.1016/j.colsurfa.2010.10.027.

Tedesco, S., et al., 2010. Oxidative stress and toxicity of Au nanoparticles in *Mytilus edulis*. Aquat. Toxicol. (Amsterdam, Netherlands) 100 (2), 178–186. Available from: https://doi.org/10.1016/j.aquatox.2010.03.001.

Temple, T.L., Bagnall, D.M., 2011. Optical properties of Au and aluminium nanoparticles for silicon solar cell applications. J. Appl. Phys. 109 (8), 084343. Available from: https://doi.org/10.1063/1.3574657.

Thakkar, K.N., Mhatre, S.S., Parikh, R.Y., 2010. Biological synthesis of metallic nanoparticles. Nanomed. Nanotechnol. Biol. Med. 6 (2), 257–262. Available from: https://doi.org/10.1016/j.nano.2009.07.002.

Thanh, N.T.K., Green, L.A.W., 2010. Functionalisation of nanoparticles for biomedical applications. Nano Today 5 (3), 213–230. Available from: https://doi.org/10.1016/j.nantod.2010.05.003.

Thaxton, C.S., et al., 2009. Nanoparticle-based biobarcode assay redefines "undetectable" PSA and biochemical recurrence after radical prostatectomy. Proc. Natl. Acad. Sci. U.S.A. 106 (44), 18437–18442. Available from: https://doi.org/10.1073/pnas.0904719106.

Thirugnanasambandan, T., Alagar, M., 2011. Studies of copper nanoparticles effects on micro-organisms. Ann. Biol. Res. 2, 368–373.

Thomas, R., Park, I.-K., Jeong, Y.Y., 2013. Magnetic iron oxide nanoparticles for multimodal imaging and therapy of cancer. Int. J. Mol. Sci. 14 (8), 15910–15930. Available from: https://doi.org/10.3390/ijms140815910.

Tian, D., et al., 2009. Sandwich-type electrochemiluminescence immunosensor based on *N*-(aminobutyl)-*N*-ethylisoluminol labeling and Au nanoparticle amplification. Talanta 78 (2), 399–404. Available from: https://doi.org/10.1016/j.talanta.2008.11.037.

Tian, D., et al., 2010. Ultrasensitive electrochemiluminescence immunosensor based on luminol functionalized Au nanoparticle labeling. Biosens. Bioelectron. 25 (10), 2290–2295. Available from: https://doi.org/10.1016/j.bios.2010.03.014.

Tiede, K., et al., 2008. Detection and characterization of engineered nanoparticles in food and the environment. Food Addit. Contam., A 25 (7), 795–821. Available from: https://doi.org/10.1080/02652030802007553.

Tiede, K., et al., 2009. Imaging of engineered nanoparticles and their aggregates under fully liquid conditions in environmental matrices. Water Res. 43 (13), 3335–3343. Available from: http://dx.doi.org/10.1016/j.watres.2009.04.045.

Tiwari, G., et al., 2012. Drug delivery systems: an updated review. Int. J. Pharm. Invest. 2 (1), 2–11. Available from: https://doi.org/10.4103/2230-973X.96920.

Toimil Molares, M.E., et al., 2001. Single-crystalline copper nanowires produced by electrochemical deposition in polymeric ion track membranes. Adv. Mater. 13 (1), 62–65. Available from: http://dx.doi.org/10.1002/1521-4095(200101)13:1<62::AID-ADMA62>3.0.CO;2-7.

Toimil Molares, M.E., et al., 2003. Electrical characterization of electrochemically grown single copper nanowires. Appl. Phys. Lett. 82 (13), 2139–2141. Available from: https://doi.org/10.1063/1.1563741.

Tran, Q.H., Nguyen, V.Q., Le, A.-T., 2013. Silver nanoparticles: synthesis, properties, toxicology, applications and perspectives. Adv. Nat. Sci.: Nanosci. Nanotechnol. 4 (3), 033001. Available from: https://doi.org/10.1088/2043-6262/4/3/033001.

Tuoriniemi, J., et al., 2014. In situ characterisation of physicochemical state and concentration of nanoparticles in soil ecotoxicity studies using environmental scanning electron microscopy. Environ. Chem. 11 (4), 367. Available from: https://doi.org/10.1071/EN13182.

Umer, A., et al., 2012. Selection of a suitable method for the synthesis of copper nanoparticles. Nano 07 (05), 1230005. Available from: https://doi.org/10.1142/S1793292012300058.

Ung, T.D.T., et al., 2012. CdTe and CdSe quantum dots: synthesis, characterizations and applications in agriculture. Adv. Nat. Sci.: Nanosci. Nanotechnol. 3 (4), 043001. Available from: https://doi.org/10.1088/2043-6262/3/4/043001.

Uskoković, V., Drofenik, M., 2005. Synthesis of relatively highly magnetic nano-sized NiZn-ferrite in microemulsion at 45°C. Surf. Rev. Lett. 12 (01), 97–100. Available from: https://doi.org/10.1142/S0218625X05006822.

Vadlapudi, V., Kaladhar, D.S.V.G.K., 2014. Review: green synthesis of silver and Au nanoparticles. Middle-East J. Sci. Res. 19 (6), 834–842. Available from: https://doi.org/10.5829/idosi.mejsr.2014.19.6.11585.

Vanaja, M., et al., 2013. Kinetic study on green synthesis of silver nanoparticles using *Coleus aromaticus* leaf extract. Adv. Appl. Sci. Res. 4 (3), 50–55.

Vats, A., et al., 2003. Scaffolds and biomaterials for tissue engineering: a review of clinical applications. Clin. Otolaryngol. Allied Sci. 28 (3), 165–172. Available from: http://www.ncbi.nlm.nih.gov/pubmed/12755749.

Veigas, B., et al., 2010. Au-nanoprobes for detection of SNPs associated with antibiotic resistance in *Mycobacterium tuberculosis*. Nanotechnology 21 (41), 415101. Available from: https://doi.org/10.1088/0957-4484/21/41/415101.

Viau, G., et al., 2003. Ruthenium nanoparticles: size, shape, and self-assemblies. Chem. Mater. 15 (2), 486–494. Available from: https://doi.org/10.1021/cm0212109.

Vidya, C., et al., 2013. Green synthesis of ZnO nanoparticles by *Calotropis gigantea*. NCWSE 2012–2014.

Vitol, E.A., et al., 2010. Surface-enhanced Raman spectroscopy as a tool for detecting Ca^{2+} mobilizing second messengers in cell extracts. Anal. Chem. 82 (16), 6770–6774. Available from: https://doi.org/10.1021/ac100563t.

Vobornik, D., et al., 2008. Fluorescence correlation spectroscopy with sub-diffraction-limited resolution using near-field optical probes. Appl. Phys. Lett. 93 (16), 163904. Available from: https://doi.org/10.1063/1.2998602.
Volesky, B., Holan, Z.R., 1995. Biosorption of heavy metals. Biotechnol. Progr. 11 (3), 235–250. Available from: https://doi.org/10.1021/bp00033a001.
Wabuyele, M.B., Vo-Dinh, T., 2005. Detection of human immunodeficiency virus type 1 DNA sequence using plasmonics nanoprobes. Anal. Chem. 77 (23), 7810–7815. Available from: https://doi.org/10.1021/ac0514671.
Wang, C., et al., 2012. Highly-sensitive cholesterol biosensor based on platinum-Au hybrid functionalized ZnO nanorods. Talanta 94, 263–270. Available from: https://doi.org/10.1016/j.talanta.2012.03.037.
Wang, H., et al., 2004a. A piezoelectric immunoagglutination assay for *Toxoplasma gondii* antibodies using Au nanoparticles. Biosens. Bioelectron. 19 (7), 701–709. Available from: http://www.ncbi.nlm.nih.gov/pubmed/14709388.
Wang, H., et al., 2007. Biocompatibility and osteogenesis of biomimetic nano-hydroxyapatite/polyamide composite scaffolds for bone tissue engineering. Biomaterials 28 (22), 3338–3348. Available from: https://doi.org/10.1016/j.biomaterials.2007.04.014.
Wang, H., Chu, P., 2013. Surface characterization of biomaterials. In: Bandyopadhyay, A.S.B. (Ed.), Characterization of Biomaterials. Academic Press, Oxford, pp. 106–174. Available from: http://www6.cityu.edu.hk/appkchu/Publications/2013/13.42.pdf.
Wang, L.S., Hong, R.Y., 2011. Synthesis, surface modification and characterisation of nanoparticles'. In: Reddy, D. B. (Ed.), Advances in Nanocomposites—Synthesis, Characterization and Industrial Applications. InTech, pp. 289–322. Available from: http://dx.doi.org/10.5772/10540.
Wang, Q., Snyder, S., et al., 2009. Aqueous ethanol modified nanoscale zerovalent iron in bromate reduction: synthesis, characterization, and reactivity. Environ. Sci. Technol. 43 (9), 3292–3299. Available from: https://doi.org/10.1021/es803540b.
Wang, Q., Kanel, S.R., et al., 2009. Controllable synthesis, characterization, and magnetic properties of nanoscale zerovalent iron with specific high Brunauer–Emmett–Teller surface area. J. Nanopart. Res. 11 (3), 749–755. Available from: https://doi.org/10.1007/s11051-008-9524-7.
Wang, S., Wang, Z., Zha, Z., 2009. Metal nanoparticles or metal oxide nanoparticles, an efficient and promising family of novel heterogeneous catalysts in organic synthesis. Dalton Trans. 43, 9363. Available from: https://doi.org/10.1039/b913539a.
Wang, T., et al., 2010. Extracellular biosynthesis and transformation of selenium nanoparticles and application in H_2O_2 biosensor. Colloids Surf., B: Biointerfaces 80 (1), 94–102. Available from: https://doi.org/10.1016/j.colsurfb.2010.05.041.
Wang, Y.-S., et al., 2015. Au nanorods-silica Janus nanoparticles for theranostics. Appl. Phys. Lett. 106 (17), 173705. Available from: https://doi.org/10.1063/1.4919454.
Wang, Y., et al., 2004b. Photoacoustic tomography of a nanoshell contrast agent in the in vivo rat brain. Nano Lett. 4 (9), 1689–1692. Available from: https://doi.org/10.1021/nl049126a.
Wang, Y., et al., 2018. Biomedical potential of ultrafine Ag nanoparticles coated on poly (gamma-glutamic acid) hydrogel with special reference to wound healing. Nanomaterials 8 (5), 324. Available from: https://doi.org/10.3390/nano8050324.
Wang, Y., Chen, P., Liu, M., 2006. Synthesis of well-defined copper nanocubes by a one-pot solution process. Nanotechnology 17 (24), 6000–6006. Available from: https://doi.org/10.1088/0957-4484/17/24/016.
Wang, Y., Irudayaraj, J., 2013. Surface-enhanced Raman spectroscopy at single-molecule scale and its implications in biology. Philos. Trans. R. Soc. London, Ser. B 368 (1611), 20120026. Available from: https://doi.org/10.1098/rstb.2012.0026.
Warner, S., 2004. Diagnostics + therapy = theranostics. Scientist 18 (16), 38–39.
Warren, B.E., 1969. X-ray Diffraction. Courier Corporation. Available from: <https://books.google.jo/books/about/X_ray_Diffraction.html?id = wfLBhAbEYAsC&redir_esc = y>.
Wei, F., et al., 2010. Rapid detection of melamine in whole milk mediated by unmodified Au nanoparticles. Appl. Phys. Lett. 96 (13), 133702. Available from: https://doi.org/10.1063/1.3373325.
Weissenböck, A., Wirth, M., Gabor, F., 2004. WGA-grafted PLGA-nanospheres: preparation and association with Caco-2 single cells. J. Controlled Release 99 (3), 383–392. Available from: https://doi.org/10.1016/j.jconrel.2004.07.025.
Wen, X., Shi, D., Zhang, N., 2005. Handbook of nanostructured biomaterials and their applications in nanobiotechnology. In: Nalwa, H.S. (Ed.), J. Nanosci. Nanotechnol.

West, J.L., Halas, N.J., 2000. Applications of nanotechnology to biotechnology commentary. Curr. Opin. Biotechnol. 11 (2), 215–217. Available from: http://www.ncbi.nlm.nih.gov/pubmed/10753774.

Wijesena, R.N., et al., 2015. A method for top down preparation of chitosan nanoparticles and nanofibers. Carbohydr. Polym. 117, 731–738. Available from: https://doi.org/10.1016/j.carbpol.2014.10.055.

Wilcoxon, J., 2009. Optical absorption properties of dispersed Au and silver alloy nanoparticles. J. Phys. Chem. B 113 (9), 2647–2656. Available from: https://doi.org/10.1021/jp806930t.

Wiley, B., et al., 2005. Shape-controlled synthesis of metal nanostructures: the case of silver. Chemistry (Weinheim an der Bergstrasse, Germany) 11 (2), 454–463. Available from: https://doi.org/10.1002/chem.200400927.

Williams, D.H., Fleming, I., 1995a. Infrared spectra, Spectroscopic Methods in Organic Chemistry, fifth ed. McGraw-Hill, Berkshire, England, pp. 28–62.

Williams, D.H., Fleming, I., 1995b. Ultraviolet and visible spectra, Spectroscopic Methods in Organic Chemistry, fifth ed. McGraw-Hill, Berkshire, pp. 1–27.

Wu, P., et al., 2013. A DNAzyme-Au nanoparticle probe for uranyl ion in living cells. J. Am. Chem. Soc. 135 (14), 5254–5257. Available from: https://doi.org/10.1021/ja400150v.

Wu, S.-H., Chen, D.-H., 2003. Synthesis and characterization of nickel nanoparticles by hydrazine reduction in ethylene glycol. J. Colloid Interface Sci. 259 (2), 282–286. Available from: https://doi.org/10.1016/S0021-9797(02)00135-2.

Wu, W., He, Q., Jiang, C., 2008. Magnetic iron oxide nanoparticles: synthesis and surface functionalization strategies. Nanoscale Res. Lett. 3 (11), 397–415. Available from: https://doi.org/10.1007/s11671-008-9174-9.

Wustholz, K.L., et al., 2010. Structure-activity relationships in Au nanoparticle dimers and trimers for surface-enhanced Raman spectroscopy. J. Am. Chem. Soc. 132 (31), 10903–10910. Available from: https://doi.org/10.1021/ja104174m.

Xiong, C., et al., 2018. Cisplatin-loaded hollow Au nanoparticles for laser-triggered release. Cancer Nanotechnol. 9 (1), 6. Available from: https://doi.org/10.1186/s12645-018-0041-9.

Xu, L., et al., 2012. Surface-engineered Au nanorods: promising DNA vaccine adjuvant for HIV-1 treatment. Nano Lett. 12 (4), 2003–2012. Available from: https://doi.org/10.1021/nl300027p.

Xu, L., et al., 2018. A tiered experimental approach for characterization and silver release of silver-containing wound dressings. J. Biomed. Nanotechnol. 14 (3), 564–574. Available from: https://doi.org/10.1166/jbn.2018.2534.

Yadav, T., Yadav, R., Singh, D., 2012. Mechanical milling: a top down approach for the synthesis of nanomaterials and nanocomposites. Nanosci. Nanotechnol. 2 (3), 22–48. Available from: https://doi.org/10.5923/j.nn.20120203.01.

Yamamoto, T.A., et al., 2010. Bimetallic nanoparticles of PtM (M = Au, Cu, Ni) supported on iron oxide: radiolytic synthesis and CO oxidation catalysis. Appl. Catal., A: Gen. 387 (1–2), 195–202. Available from: https://doi.org/10.1016/j.apcata.2010.08.020.

Yan, F., Fu, Q., 2014. PLCε1: a potential target of RNA interference therapy for gastric cancer. Biochem. Biophys. Res. Commun. 448 (4), 409–413. Available from: https://doi.org/10.1016/j.bbrc.2014.04.119.

Yang, G.-J., et al., 2009. A reusable capacitive immunosensor for detection of *Salmonella* spp. based on grafted ethylene diamine and self-assembled Au nanoparticle monolayers. Anal. Chim. Acta 647 (2), 159–166. Available from: https://doi.org/10.1016/j.aca.2009.06.008.

Yang, J., et al., 2004. Preparation and characterization of positively charged ruthenium nanoparticles. J. Colloid Interface Sci. 271 (2), 308–312. Available from: https://doi.org/10.1016/j.jcis.2003.10.041.

Yang, X., et al., 2007. Photoacoustic tomography of a rat cerebral cortex in vivo with au nanocages as an optical contrast agent. Nano Lett. 7 (12), 3798–3802. Available from: https://doi.org/10.1021/nl072349r.

Yanık, B., et al., 2013. Synthesis and characterization of aluminium nanoparticles by electric arc technique. Arabian J. Sci. Eng. 38 (12), 3587–3592. Available from: https://doi.org/10.1007/s13369-013-0621-2.

Yap S.L., Lee Y.S., Tay W.H., Wong C.S., 2008, Exploding wire discharge for synthesis of nanoparticles, *in Proceedings of the International Workshop on Plasma Computations & Applications (IWPCA2008)*, pp. 60–64

Yeh, M.-S., et al., 1999. Formation and characteristics of Cu colloids from CuO powder by laser irradiation in 2-propanol. J. Phys. Chem. B 103 (33), 6851–6857. Available from: https://doi.org/10.1021/jp984163.

Yin, Z., et al., 2011. Electrochemical immunosensor of tumor necrosis factor α based on alkaline phosphatase functionalized nanospheres. Biosens. Bioelectron. 26 (5), 1890–1894. Available from: https://doi.org/10.1016/j.bios.2010.03.025.

Yuen, J.M., et al., 2010. Transcutaneous glucose sensing by surface-enhanced spatially offset Raman spectroscopy in a rat model. Anal. Chem. 82 (20), 8382–8385. Available from: https://doi.org/10.1021/ac101951j.
Zavaleta, C.L., et al., 2009. Multiplexed imaging of surface enhanced Raman scattering nanotags in living mice using noninvasive Raman spectroscopy. Proc. Natl. Acad. Sci. U.S.A. 106 (32), 13511–13516. Available from: https://doi.org/10.1073/pnas.0813327106.
Zeng, C., Jin, R., 2017. Chiral Au nanoclusters: atomic level origins of chirality. Chemistry 12 (15), 1839–1850. Available from: https://doi.org/10.1002/asia.201700023.
Zhang, J., et al., 2009. Fluorescent avidin-bound silver particle: a strategy for single target molecule detection on a cell membrane. Anal. Chem. 81 (3), 883–889. Available from: https://doi.org/10.1021/ac801932m.
Zhang, J., Fu, Y., Li, G., et al., 2010. Direct observation to chemokine receptor 5 on T-lymphocyte cell surface using fluorescent metal nanoprobes. Biochem. Biophys. Res. Commun. 400 (1), 111–116. Available from: https://doi.org/10.1016/j.bbrc.2010.08.020.
Zhang, J., Fu, Y., Mei, Y., et al., 2010. Fluorescent metal nanoshell probe to detect single miRNA in lung cancer cell. Anal. Chem. 82 (11), 4464–4471. Available from: https://doi.org/10.1021/ac100241f.
Zhang, J., et al., 2017. Antimicrobial effects of silver nanoparticles synthesized by fatsia japonica leaf extracts for preservation of citrus fruits. J. Food Sci. 82 (8), 1861–1866. Available from: https://doi.org/10.1111/1750-3841.13811.
Zhang, P.-X., et al., 2019. Tissue engineering for the repair of peripheral nerve injury. Neural Regen. Res. 14 (1), 51. Available from: https://doi.org/10.4103/1673-5374.243701.
Zhang, Y., et al., 2012a. Synthesis, properties, and optical applications of noble metal nanoparticle-biomolecule conjugates. Chin. Sci. Bull. 57 (2–3), 238–246. Available from: https://doi.org/10.1007/s11434-011-4747-x.
Zhang, Z., et al., 2012b. Mesoporous silica-coated au nanorods as a light-mediated multifunctional theranostic platform for cancer treatment. Adv. Mater. 24 (11), 1418–1423. Available from: https://doi.org/10.1002/adma.201104714.
Zhang, Z., Wang, J., Chen, C., 2013. Near-infrared light-mediated nanoplatforms for cancer thermo-chemotherapy and optical imaging. Adv. Mater. (Deerfield Beach, FL) 25 (28), 3869–3880. Available from: https://doi.org/10.1002/adma.201301890.
Zhao, W., et al., 2011. Bioengineering nanotechnology: towards the clinic. Nanotechnology 22 (49), 490201. Available from: https://doi.org/10.1088/0957-4484/22/49/490201.
Zhao, Z., Li, Y., Xie, M.-B., 2015. Silk fibroin-based nanoparticles for drug delivery. Int. J. Mol. Sci. 16 (3), 4880–4903. Available from: https://doi.org/10.3390/ijms16034880.
Zhou, L., et al., 2016. 3D self-assembly of aluminium nanoparticles for plasmon-enhanced solar desalination. Nat. Photonics 10, 393. Available from: https://doi.org/10.1038/nphoton.2016.75.
Zhou, Y., et al., 2017. Filling in the gaps between nanozymes and enzymes: challenges and opportunities. Bioconjugate Chem. 28 (12), 2903–2909. Available from: https://doi.org/10.1021/acs.bioconjchem.7b00673.
Zhu, X.-H., et al., 2014. Effect of RNA interference therapy on the mice eosinophils CCR3 gene and granule protein in the murine model of allergic rhinitis. Asian-Pacific J. Trop. Med. 7 (3), 226–230. Available from: https://doi.org/10.1016/S1995-7645(14)60026-2.
Zook, J.M., et al., 2012. Disentangling the effects of polymer coatings on silver nanoparticle agglomeration, dissolution, and toxicity to determine mechanisms of nanotoxicity. J. Nanopart. Res. 14 (10), 1165. Available from: https://doi.org/10.1007/s11051-012-1165-1.
Zulkifli, F.H., et al., 2017. A facile synthesis method of hydroxyethyl cellulose-silver nanoparticle scaffolds for skin tissue engineering applications. Mater. Sci. Eng., C 79, 151–160. Available from: https://doi.org/10.1016/j.msec.2017.05.028.

Further Reading

Al-Qattan, M.N., Deb, P.K., Tekade, R.K., 2018. Molecular dynamics simulation strategies of designing carbon-nanotube-based targeted drug delivery. Drug Discov. Today. 23, 235–250.
Deb, P.K., Al-Attraqchi, O., Jaber, A.Y., Amarji, B., Tekade, R.K., 2018. Chapter-2: Physicochemical aspects to be considered in pharmaceutical product development. In: Tekade, R.K. (Ed.), Dosage Form Design Considerations: Advances in Pharmaceutical Product Development and Research Series, Vol. I. Academic Press (Elsevier), pp. 57–83.

Deb, P.K., Abed, S.N., Jaber, A.Y., Tekade, R.K., 2018. Chapter-5: Particulate level properties and its implications on product performance and processing. In: Tekade, R.K. (Ed.), Dosage Form Design Considerations: Advances in Pharmaceutical Product Development and Research Series, Vol. II. Academic Press (Elsevier), pp. 155–220.

Abed, S.N., Deb, P.K., Surchi, H.S., Kokaz, S.F., Jamal, S.M., Bandopadhyay, S., Tekade, R.K., 2018. Chapter-17: nanocarriers in different preclinical and clinical stages. In: Tekade, R.K. (Ed.), Basic Fundamentals of Drug Delivery: Advances in Pharmaceutical Product Development and Research Series, Vol. III. Academic Press, pp. 668–731.

Deb, P.K., Kokaz, S.F., Abed, S.N., Paradkar, A., Tekade, R.K., 2018. Chapter-6: Pharmaceutical and biomedical applications of polymers. In: Tekade, R.K. (Ed.), Basic Fundamentals of Drug Delivery: Advances in Pharmaceutical Product Development and Research Series, Vol. III. Academic Press, pp. 204–255.

CHAPTER

16

Functionalized Carbon Nanotubes for Protein, Peptide, and Gene Delivery

Neha Maheshwari[1], *Muktika Tekade*[1], *Namrata Soni*[2], *Piyush Ghode*[3], *Mukesh Chandra Sharma*[1], *Pran Kishore Deb*[4] *and Rakesh K. Tekade*[5]

[1]School of Pharmacy, Devi Ahilya Vishwavidyalaya, Takshila Campus, Indore, India [2]Faculty of Health Sciences, Sam Higginbottom Institute of Agriculture, Technology and Sciences (Deemed University), Allahabad, India [3]School of Pharmacy and Technology Management, NMIMS, Shirpur, India [4]Faculty of Pharmacy, Philadelphia University, Amman, Jordan [5]National Institute of Pharmaceutical Education and Research (NIPER)—Ahmedabad, Gandhinagar, India

OUTLINE

16.1 Introduction to Nanotechnology 614

16.2 Carbon Nanotubes: Structure and Classification 615

16.3 Synthesis and Purification of Carbon Nanotubes 615
- *16.3.1 Carbon Arc-Discharge Technique* 615
- *16.3.2 Laser-Ablation Technique* 616
- *16.3.3 Chemical Vapor Deposition Technique* 616
- *16.3.4 Purification of Carbon Nanotubes* 616

16.4 Functionalization of Carbon Nanotubes 617
- *16.4.1 Covalent Functionalization* 617
- *16.4.2 Noncovalent Functionalization* 618

16.5 Functionalization of Carbon Nanotube With Protein, Peptide, DNA, and SiRNA 619

16.6 Role of Peptides in Cancer Management 621

16.7 Carbon Nanotube–Mediated Peptide and Vaccine Delivery 623

Biomaterials and Bionanotechnology
DOI: https://doi.org/10.1016/B978-0-12-814427-5.00016-0

© 2019 Elsevier Inc. All rights reserved.

16.8 Carbon Nanotube–Mediated Gene Delivery 626
16.9 Cellular Uptake and Cell Penetration Mechanism of Carbon Nanotubes 629
16.10 Toxicity Consideration of Carbon Nanotubes 630
16.11 Future Scope and Conclusion 632
Acknowledgments 633
References 633

16.1 INTRODUCTION TO NANOTECHNOLOGY

In the past few decades, there has been an incredible degree of optimism and opportunities surrounding nanotechnology-based effects on the advancement of different areas of medicine and pharmaceuticals (Tekade et al., 2017b). Nanotechnology deals with the manipulation of materials at nanoscale that helps to enhance existing functions and characteristics of materials in addition to adding new properties. Nanomaterials with a mean particle size of approximately 100 nm include nanoparticles from organic and inorganic origin, nanoparticulate ceramics, fullerenes, and carbon nanotubes (CNTs) (Al-Qattan et al., 2018; Maheshwari et al., 2015).

These nanomaterials are a considerable improvement over bulk raw material in optical, mechanical, electrical, structural, and magnetic properties. This could progressively impact the biomedical field, specifically biomedicine, through the development of novel sophisticated biosensors, diagnostics, and drug delivery systems. Reports are available estimating nanoparticle physical characteristics in relation to their biological compatibility, cytotoxicity, and clinical effectiveness (Sharma et al., 2015).

CNTs are among the most promising tools in the nanotechnological renaissance. In recent times, multiplicities of technologies have been projected resulting with biologically compatible CNTs (Tekade et al., 2017a). Their application in the pharmaceutical arena has extended much consideration in the past few years. The functionalization of CNTs by covalent and noncovalent approaches had permitted the initial direction of uses in the area of nanomedicines because it allowed for targeted drug delivery and targeting. In addition, CNT functionalization offers numerous advantages, including improved cellular internalization and improved stability within the biological milieu. These improved properties for diagnostic and therapeutic delivery have prospective implications in the biomedical and pharmaceutical research areas and industries. CNTs offer the opportunity to be utilized as an innovative depot system for the delivery of therapeutics including peptides and gene therapies (Mody et al., 2014).

CNTs have exclusive physicochemical properties, such as a high surface area, excellent encapsulation ability, low weight, and may be functionalized to impart biocompatibility, lower toxicity, and nonimmunogenicity.

16.2 CARBON NANOTUBES: STRUCTURE AND CLASSIFICATION

CNTs as well as carbon nanohorns, graphenes (GRs), carbon nanorods, and polyhydroxy fullerenes, are efficient systems capable of carrying payloads and may be equipped to employ a targeting strategy. The lengths of CNTs can be from a few nm to the μm range, depending upon their use and application. Their size also depends on the number of walls (whether single-walled or multiwalled) and is usually less than 100 nm in their longest dimension (Kuche et al., 2018).

Roger Bacon in 1960 first reported CNTs, and they were further explored by Sumio Iijima (Futaba et al., 2006). CNTs are large macromolecules composed of hollow long and thin cylinders of carbon, having an ultralight weight with a good aspect ratio (length/diameter), and good surface reactivity. They have exclusive physical characteristics, including morphological properties such as their dimension and geometry. They can be thought of as a sheet of graphite configured in a hexagonal lattice of carbon that is rolled into a cylinder. These can be modified to be smart nanoscale vehicles having biocompatible, nonimmunogenic, and photoluminescent properties for drug delivery with or without diagnostic agent utility (Iijima, 2002).

For in vivo detection, CNTs do not require any kind of fluorescent labeling since their inherent electron emission properties can be detected directly. CNTs have the same sp^2 hybridization as graphite. CNTs may be classified into four different groups on the basis of the configuration of their GR cylinders. Single monolayers of GR that form a cylinder are classified as single-walled CNTs (SWCNTs). When two GR layers are present, they are classified as double-walled CNTs. Three layers of GR cylinders are known as triple-walled CNTs. Multiwalled CNTs (MWCNTs) have many layers, up to around 50 (Abbas et al., 2016; Chen et al., 2001). CNT nanocarrier functionalization is a recognized strategy for surface modification of and may be linked with different bioactives. Therefore they have been employed to deliver both lipophilic and hydrophilic drugs. CNTs can cross different biological membranes and can also cross the plasma membrane thereby entering into the cytoplasm via the "tiny nanoneedle" mechanism (Mittal et al., 2015).

16.3 SYNTHESIS AND PURIFICATION OF CARBON NANOTUBES

Among the many available methods for synthesizing pure CNTs, carbon arc-discharge, laser ablation, and chemical vapor deposition (CVD) methods have gained the widest attention.

16.3.1 Carbon Arc-Discharge Technique

High-quality SWCNTs and MWCNTs were produced by the arc-discharge method. In the carbon arc-discharge method, two carbon electrodes are employed to produce an electric arc via direct current (DC). The electrodes are set side by side in a chamber in which a vacuum is created and space is backfilled with an inert gas, which influences the deposition speed of carbon. Carbon assembles when the pressure becomes stable and once the power supply is turned on, and supplies a DC of approximately 20 V (Berkmans et al., 2015).

The rods are separated by about a millimeter, and upon stabilized arc formation, CNTs deposit on the negative electrode. The power supply is turned off when a desired specific length of the CNTs is reached, and then the machine commences a chilling stage. The pressure of inert gas in the chamber and control of arcing current are the user-defined input parameters to be considered during formation of CNTs. In the production of MWCNTs, a catalyst for growth is not required, whereas SWCNTs can only be grown in the presence of a catalyst. Investigators also created high-quality MWCNTs with a diameter of 2−20 using a current of 18 V and helium inert gas at a pressure of 500 Torr. The MWCNTs manufactured using this technique were found to have crystalline morphological properties (Arora and Sharma, 2014).

16.3.2 Laser-Ablation Technique

In the laser ablation method, intense laser pulses ablating a solid carbon target are employed for the synthesis of CNTs. Investigators also synthesized SWCNTs with a diameter of 5−20 nm using the laser ablation method where graphite underwent pulsed laser ablation at 1200°C in the presence of an inert gas and catalyst. The type of catalyst, laser power, wavelength, temperature, pressure, type of inert gas present, and the fluid dynamics near the carbon target are the main parameters that determine the quantity of CNTs produced by this method (Chrzanowska et al., 2015).

16.3.3 Chemical Vapor Deposition Technique

CNTs are synthesized by CVD method using hydrocarbons, such as methane, ethylene, and acetylene, and a source of energy, which may be based on electron beam or resistive heating. The energy of the electron beam splits the hydrocarbon molecule into reactive radical species at a temperature range of 550°C−750°C (Shah and Tali, 2016).

José-Yacamán et al. (1993) synthesized CNTs with sizes within the micrometer range having a length of up to 50 μm by CVD method produced at the temperature of 700°C using the catalytic decomposition of acetylene over iron particles. Varadan and Xie synthesized MWCNTs having 26 layers and a particle size between 20 and 30 nm using the CVD technique at a temperature of 700°C, using microwave energy for catalytic decomposition of acetylene as the hydrocarbon and cobalt as the catalyst (Mubarak et al., 2016).

16.3.4 Purification of Carbon Nanotubes

In the CNT synthesis methods discussed above, a number of impurities, which depend on the techniques, may be formed, such as carbonaceous materials and metals present in CNT colloidal suspensions. CNT methods for purification include oxidation of carbonaceous impurities for the carbon arc-discharge method and microfiltration to remove amorphous carbon from crystalline CNTs. In the purification by oxidation normally two strategies are used: gas phase purification and liquid phase purification, since gas phase oxidation has low purification yields (Maio et al., 2014).

Dillon et al. (1999) obtained robust SWCNTs with diameters of less than 2 nm that were purified by nitric acid and sulfuric acid mixture, as well as by oxidation. Chiang et al. (2001) employed microfiltration that was ultrasonically assisted for purification of SWCNTs from amorphous and crystalline carbon impurities and metal particles. Dujardin et al. (1998) purified CNTs from amorphous carbon by boiling CNTs with nitric acid aqueous solutions.

16.4 FUNCTIONALIZATION OF CARBON NANOTUBES

Surface alteration or modification of CNTs is mainly done using chemical procedures that either introduce the new functional groups, or through the new bond formation. The obtained CNTs can be termed as functionalized CNTs. The main aim behind functionalizing the CNTs in cancer management is the development of biocompatibility, improvement of encapsulation affinity, and enhancement of solubility. Functionalization of CNTs can be achieved through covalent and noncovalent bonds (Cha et al., 2016).

16.4.1 Covalent Functionalization

The end caps of CNTs are highly reactive, in comparison to the side walls, due to the tendency to be made up of very curved and fullerene-like hemispheres. These sidewalls themselves have defect sites that are pentagon−heptagon pairs, which are known as Stone−Walls defects, sp^3-hybridized deformations, and vacancies in the CNTs lattice. Chemical functionalization is dependent on the formation of covalent bonds. Covalent functionalization by fluorination of CNTs occurs on end caps due to the inert nature of CNT sidewalls. Chemical functionalization of CNTs involves the covalent bond formation onto carbon with functional groups (Cha et al., 2016).

Chemical functionalization may be executed at the end caps or defective sidewalls of CNTs. Covalent functionalization on the sidewall directly is linked with modification of hybridization from sp^2 to sp^3 with simultaneous loss of p-conjugation system on the GR layer. Covalent functionalization may be executed by reaction with highly reactive molecules. In addition to cycloaddition, that is, Diels−Alder reaction, carbene and nitrene addition, chlorination, bromination, hydrogenation, and azomethineylides have been successfully employed (Voiry et al., 2015).

The most common CNT modification strategies include oxidation, using concentrated oxidizing agents to convert the most reactive sites on CNTs. A physical strain present on the sp^2 hybridized carbon atoms is implemented due to the curvature of the CNT, therefore dropping the energy barrier needed for converting the sp^2 hybridized bonds to sp^3 in comparison to GR. The sp^3 conversion in pristine CNTs also makes it more susceptible to many other reactions like the Bingel reaction (Naebe et al., 2014).

Covalent bonding provides a better chemical linkage, which is normally stable over wide pH range. However, the intrinsic physical characteristics of CNTs like luminescent behavior and Raman detection shift plots are reported to be reduced as a result of CNT structure distortion upon covalent attachment. This is a reason why covalently bonded

CNTs cannot as often be employed for photothermal or imaging applications (Fernández-García et al., 2016).

16.4.2 Noncovalent Functionalization

Considerable attention has recently been paid to the noncovalent surface tailoring of CNTs due to the noninvasive nature of this method (Chen et al., 2002). This method comprises of the only physical interaction of the functionalized molecules to the surface of CNTs (Mittal, 2011). This method of modification can be achieved without the destruction of the sp^2-hybridized skeleton of the graphitic sidewall. Thus it retains the original properties of the nanotube and does not cause any structural alterations in it (Chen et al., 2011). This type of surface functionalization involves weak interactions and adsorption forces like hydrophobic interactions, van der Waals forces, π−π stacking, and charge transfer (Trojanowicz, 2006) (Kayat et al., 2011; Mody et al., 2014). This approach involves the enveloping of polymer chains around the nanotubes or adsorption of several surfactant molecules onto the exterior of CNTs (Mittal, 2011). Noncovalent surface engineered CNTs with biomacromolecules like oligosaccharides (Gorityala et al., 2010), DNA (Sanz et al., 2011), and proteins (Oliveira et al., 2015) have also gained reasonable attention from scientists to prompt the exploration of their potential in nanotherapeutics.

The noncovalent surface modification of CNTs has been effectively accomplished by π−π stacking interactions. Compounds with poly-aromatic hydrocarbons moieties such as pyrene, naphthalene, and phenanthrene have been explored to exhibit π−π stacking with CNTs with considerable binding energies (Wurm et al., 2010; Paloniemi et al., 2005; Yang et al., 2006). A derivative of pyrene like *N*-succinimidyl-1-pyrenebutanoate, which is a bifunctional molecule, has been reported for irreversible adsorption on the hydrophobic exterior of SWCNTs via π−π stacking interaction. Due to the highly aromatic nature of the pyrenyl group it has been shown to react significantly with the graphitic plane of CNTs and the sidewalls as well.

The succinimidyl ester group present on this bifunctional molecule undergoes nucleophilic substitution by primary (1°) and secondary (2°) amines present on the surface of several proteins. The high reactivity of succinimidyl esters thus suggests the enormous prospects of immobilization of numerous biomolecules onto CNTs with selectivity and precision (Chen et al., 2001).

Pyrene derivatives were also investigated to design DNA fabricated SWCNTs. 1-Pyrenemethylamine (PMA) has been studied as a connecting moiety to anchor SWCNTs and DNA molecules. The study was based on the electrostatic interaction of amine group of the PMA with the phosphate backbone of DNA, which is negatively charged, along with the pyrenyl group of the PMA exhibiting pi-stacking interaction with SWCNT surfaces (Xin and Woolley, 2003).

In another investigation, DNA oligonucleotides were noncovalently and selectively linked to CNTs using the pyrene functional group (Taft et al., 2004). Similarly, the enzyme glucose oxidase and gold nanoparticles were immobilized onto CNTs by using the same strategy of involving linkers having a pyrene moiety (Besteman et al., 2003; Liu et al., 2003).

16.5 FUNCTIONALIZATION OF CARBON NANOTUBE WITH PROTEIN, PEPTIDE, DNA, AND SIRNA

CNTs have been functionalized with different peptides, proteins, DNA, RNA aptamer, siRNA, and other large molecules. Protein or peptide immobilization through functionalization with CNTs often involves covalent bonding.

Protein can be functionalized on different reactive groups present on the surface of CNTs, such as hydroxyl, amines, thiols, in addition to carboxylic acids (Oliveira et al., 2015). The proteins that have been studied in functionalization onto CNTs via covalent bonding include chymotrypsin, ferritin, fibrinogen, hemoglobin, and streptavidin. Covalent functionalization with proteins onto CNTs employs a cross-linking agent such as 1-ethyl-3-(3-dimethylaminopropyl) carbodiimide.

The biochemical functionalization of peptide CNTs might have created prospects in fundamental studies in addition to numerous biomedicinal applications. Biochemically functionalized CNTs are spontaneously assembled carbon nanostructures prepared from peptides. The phage-display peptides are revealed to distinguish peptide nanotubes, which permit for the expansion of bifunctional peptides for the capturing bacteria and the self-assembly of silver particle peptide nanotubes (Mehra et al., 2015).

As per the results of confocal microscopy, Hazani et al. (2003) have demonstrated that the functionalization of SWCNTs with DNA involve covalent cross-linking and minimum nonspecific interactions with noncomplementary sequences. Chen et al. (2001) prepared succinimidyl ester groups functionalized CNTs employing noncovalent interactions, and they found that these groups are highly reactive with 1° and 2° amines, and moreover, this strategy may be employed for binding different kinds of biomolecules onto the modified nanotubes.

Protein functionalized CNTs were synthesized by covalent bonding between SWCNTs or MWCNTs and bovine serum albumin (BSA). BSA itself is colorless in solution, but when reacted with either type of CNTs a dark color is produced. The functionalization of SWCNTs with an amine can be performed by employing two different methods involving modification of the carboxylic moiety through amide formation. The first method involved the coupling of EDTA with the carboxylic acid (−COOH) groups directly to introduce amide ($-NH_2$) groups. The second method involved the reduction of the carboxyl group to hydroxymethyl, then transforming the aminomethyl group. In another study, amino functionalization of SWCNTs was done by covalent attachment (Marchesan et al., 2015).

Protein functionalization of CNTs using different moieties may facilitate them to infiltrate into cells and deliver payloads more effectively. Functionalized CNTs infiltrate into cells either by passive diffusion or active mechanisms to cross the lipid bilayer. Functionalized CNTs with surface amines were previously developed as targeted delivery systems for DNA and gene delivery (Oliveira et al., 2015).

The interaction between plasmid DNA and amino-functionalized SWCNTs and MWCNTs were reported. A complex of DNA and CNTs were obtained by dissolving functionalized CNTs in water and then this mixture was combined with different ratios of plasmid DNA at room temperature. It was found that ammonia functionalized CNTs have a greater affinity for DNA due to the presence of positive charge and large surface area of

the CNTs, which leads to strong interaction with negatively charged DNA. For effective genetic knockdown and siRNA delivery, Krajcik et al. created a complex of hexamethylenediamine functionalized CNTs, as well as poly(diallyldimethylammonium)chloride, functionalized CNTs complexed with siRNAs by mixing siRNA in an aqueous solution of hexamethylenediamine functionalized CNTs. They found that the mixture involved noncovalent interaction and hexamethylenediamine and poly(diallyldimethylammonium)chloride functionalized CNTs were an appropriate candidate for the formation of complexes with siRNA (Krajcik et al., 2008).

Peptides are products of proteolysis and may be created by dehydration condensation reactions of amino acids. Peptides are composed of different amino acids bonded together by peptide linkages. Peptides might be obtained by direct synthesis in the body or by artificial synthesis. Peptides impart a major position in the management of different diseases such as allergic diseases, infectious diseases, autoimmune diseases, fibrosis, neurological diseases, and asthma. Peptide-based treatment has been indicated and evaluated in vitro and in vivo experimental models for a variety of diseases (Firer et al., 2015).

The fundamental mechanisms and viability of peptide treatment for diseases due to allergy have been studied. Anti-DNA immunoglobulin peptide therapy has been applied for systemic lupus erythematosus, which is an autoimmune disease, using murine models. Peptides are typically simple, synthetically diverse, and ideally nonimmunogenic (Yan et al., 2018).

Recently, in the area of peptide-based drug delivery, numerous developments have been found, especially for cancer therapy, as they may be employed to avoid nontarget adverse effects, reducing mortality due to frequent large-dose conventional chemotherapy administration. The blood–brain barrier (BBB) is an active and complex barrier created by endothelial cells that can obstruct the access of potentially harmful exogenous substances, such as pathogens and therapeutic molecules alike into the central nervous system from the blood circulation (Ruoslahti, 2017).

Numerous neurological diseases stay beyond the reach of conventional therapies, but due to immense advancements in medical technology, the BBB may be overcome (Kumar et al., 2018). By the use of cell-penetrating peptides (CPPs), delivery systems demonstrate an enormous aptitude in the transportation of macromolecules to cross cellular membranes, with a low cellular toxicity and higher efficiency. CPP has a small size of up to 30 amino acids, are cationic, amphipathic, and have better potential to enter the BBB in comparison to other transport systems. CPP containing delivery systems may be employed as extremely useful tools for therapeutic rationale (Copolovici et al., 2014).

The trans-activator of transcription (TAT) peptide, obtained from human immunodeficiency virus-1, was the earliest identified and studied CPP. Smith (1991) described the development of genetically engineered filamentous bacteriophages in 1985, that expressed foreign peptide sequences on their surface (protein coat), which resulted in the expansion of the phage library of which every clone represents a peptide having a combinatorial sequence. The authors also explained the development of peptide-based functionalized CNTs for targeted delivery of chemotherapeutics and their clinical applications (Gilad et al., 2016). Fig. 16.1 shows different groups of peptides.

Molecular modeling studies have suggested that DNA having a single strand is able to attach to CNTs via pi-stacking and leads to helical folding on the CNT surface. Many

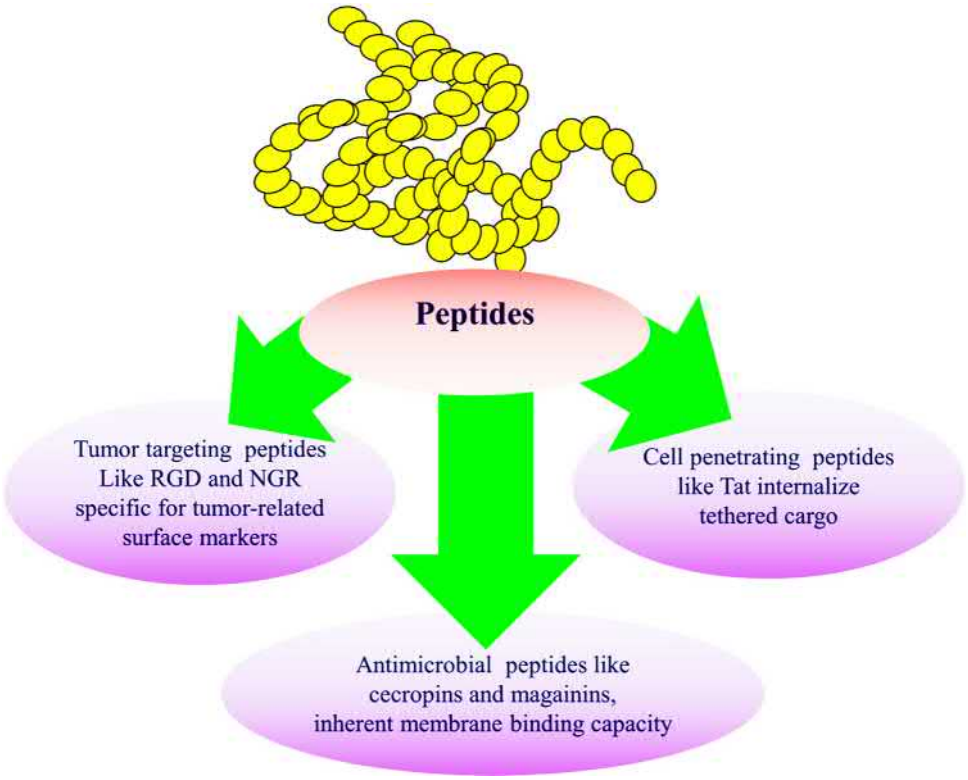

FIGURE 16.1 Different groups of peptides such as TTP specific for tumor-related surface markers, CPP internalized tethered cargo, and antimicrobial pore-forming peptides. *CPP*, Cell-penetrating peptide; *TTP*, tumor-targeting peptide.

multistep strategies were employed for binding of MWCNTs and DNA covalently according to their electronic properties. DNA might be linked at the sidewalls and ends equally. End exposed CNTs with −COOH groups have been loaded with DNA (Amirani and Tang, 2015).

Peptide-functionalized CNTs involved covalent linkage to free amino groups with about 0.2−0.4 mmol/g of functional groups occupied per gram of the CNTs (Gilad et al., 2016). Fig. 16.2 contains the schematic representation of peptide, DNA, and amino acid functionalization of CNTs.

16.6 ROLE OF PEPTIDES IN CANCER MANAGEMENT

Cancer can be defined as the abnormal growth of cells that occurs due to a sequence of mutations that originate from abnormal expression of gene products vital for regulating proliferation, survival, and growth activities of cells (Soni et al., 2017). Currently, various novel strategies are utilized for cancer management and among these novel techniques,

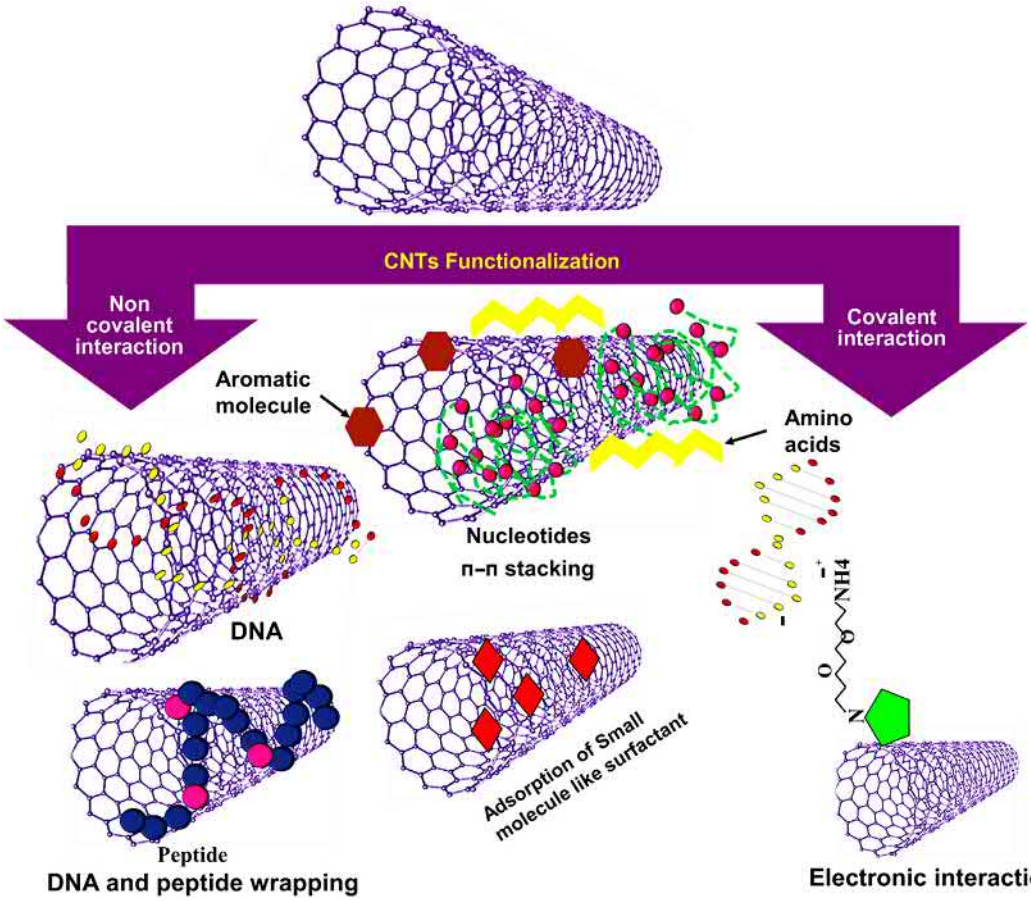

FIGURE 16.2 Schematic representation of CNTs functionalization with peptide, DNA, nucleotide, and amino acid molecules. Noncovalent interactions involve DNA and peptide wrapping, π−π stacking, adsorption, as well as an electronic interaction that may be a precursor to later covalent interaction. *CNT*, Carbon nanotube.

peptide chemotherapeutics is a highly regarded field due to the distinctive properties and abilities of peptides such as being naturally occurring, and having inherent membrane binding capacity, ability to form pores or disrupt membranes, inherent cytotoxicity to tumor cells, tumor targeting properties, and antimicrobial properties (Tekade et al., 2015a).

There are various tumor-targeting peptides (TTPs) that may link to molecules on tumor vasculature that are reachable and expressed in vivo. Various TTPs were recognized and characterized by the screening of phage-display peptide libraries and antibodies against tumor markers (Dissanayake et al., 2017).

Numerous therapeutic agents deliver to tumors via TTPs, and these TPPs can be divided into two basic groups. The first group of TTPs that nonspecifically bind to cell membranes and permit transport through the cell membrane are known as CPPs. The

second group comprises TPPs that can link directly to a tumor marker. TAT peptide, penetratin (Antp), transportan and its variant TP10, and repeating units of arginine, R8 and R9, are pH-responsive TPPs (Robbins et al., 2015). Their amphiphilic helices are due to cationic residues, which can, in some instances, be separated by hydrophobic residues that have the ability to penetrate membranes due to hydrophobicity. The PFDYLI peptides are an example of extremely hydrophobic CPPs (Aryasomayajula and Torchilin, 2016).

HIV-Tat, which is a CPP with the Tat sequence (GRKKRRQRRRPPQ) that could facilitate the internalization of cargo from the surrounding media by numerous cell types, was previously discovered. RGD (arginine/glycine/aspartic acid) or NGR (asparagine/glycine/arginine) peptides have intrinsic tumor targeting ability. The development of several anticancer hybrids of TPPs was a result of effective design and use of TAT-like and RGD-like sequences to deliver therapeutics to tumors in biochemical studies. RGD may distinguish tumors linked with a group of integrins, particularly overexpressed $\alpha v\beta 3$, and $\alpha v\beta 5$ integrins, on angiogenic blood vessels. Moreover, NGR peptides distinguish as well as link with an overexpressed aminopeptidase *N* (also known as CD13) located on the endothelial cells of numerous tumors, which results in improved tumor specificity (Rizzuti et al., 2015).

16.7 CARBON NANOTUBE–MEDIATED PEPTIDE AND VACCINE DELIVERY

Peptide CNTs have attracted recent attention for numerous biomedicinal applications due to their physicochemical stability and antimicrobial activity in addition to antiviral activities. Peptide-functionalized CNTs may be used for various types of delivery systems, including sensors and biosensors, nanoelectronics, energy storage devices, drug delivery, as well as tissue engineering (Hassan et al., 2016).

Functionalization of peptide CNTs with selective binding ornamentation for improved performance of CNTs broadens their applications. The encouraging observations of the interaction between functionalized CNTs with mammalian cells permitted additional investigations on their ability for therapeutic usefulness. Synthetic vaccines for immunization based on peptide examples are able to elicit abridged immune responses in comparison to natural pathogens. Functionalized CNTs may be an ideal delivery system for peptide antigens, by means of high loading capacity of potential cargo molecules. Therefore synthetic peptides were conjugated to CNTs and tested for their abilities as efficient vaccine candidates by studying their immunological effects (Zhao et al., 2014). Fig. 16.3 illustrates CNT-mediated immunization.

Villa et al. (2011) used SWCNTs for delivery of a peptide antigen, Wilm's tumor protein (WT1), to enhance immune responses to tumor linked antigen into the dendritic cells of Balb/c mice. They found that peptide-conjugated SWCNT nanoconstructs were rapidly internalized into professional antigen presenting cells, such as dendritic cells and macrophages, within minutes in a dose-dependent approach in vitro. Vaccination of BALB/c mice with a mixture of peptide conjugated SWCNTs and immunological adjuvant augment specific IgG immune responses in the counter of the peptides, whereas only peptide or a mixture of peptide and the adjuvant did not persuade such response. In human and

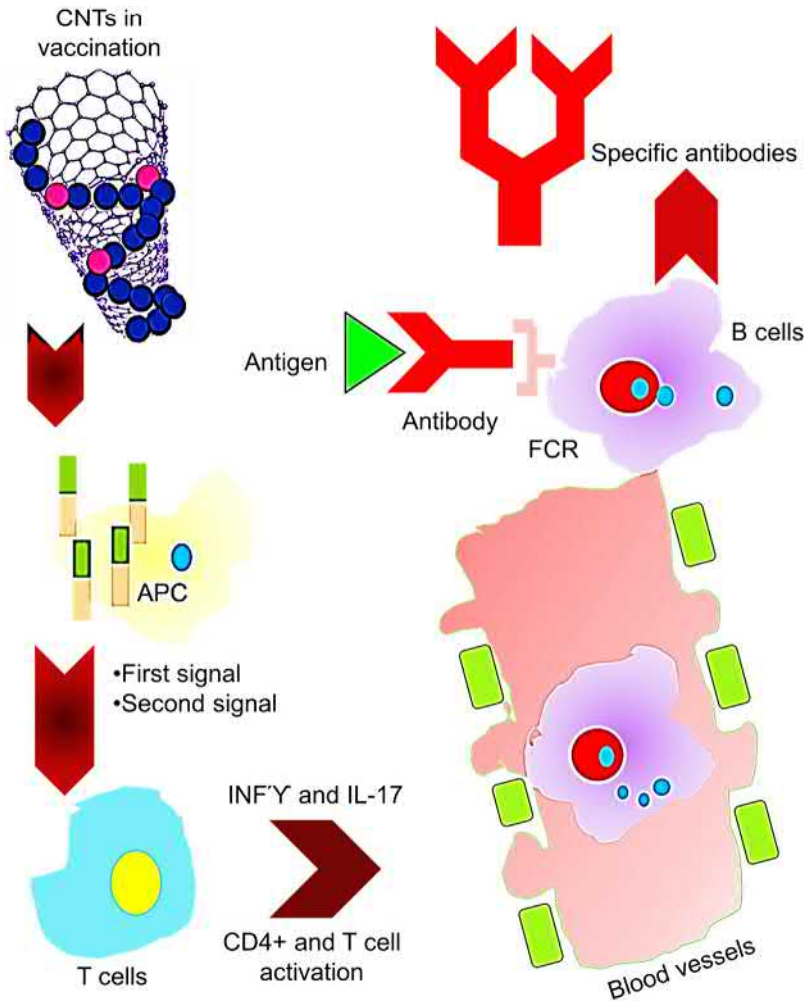

FIGURE 16.3 Schematic representation of CNTs mediated peptide delivery for immunization, which showed that vaccination by peptide leads to activated T cell response, which is responsible for specific antibodies. *CNT*, Carbon nanotube.

mouse cells, the peptide conjugated SWCNT did not augment peptide-specific CD4 T cell response. They found that solubilized SWCNTs were harmless in vitro, and in vivo antibody responses to SWCNT were not identified. Hence, they suggested that SWCNTs acting as antigen carriers improve immune responses in the counter of weak tumor antigens.

De Faria et al. (2014) demonstrated a CNT-based supramolecular hybrid for vaccination of testis cancer in the counter of cancer testis antigen NY-ESO-1, which is a Toll-like receptor agonist. The internalization of CNTs was quick in dendritic cells, both equally in vitro and in vivo. The nanoconstruct acted as an antigen depot intracellularly, therefore producing induction of $CD4^+$ T and $CD8^+$ T cell-mediated immune responses against the NY-ESO-1. They suggested that vaccination with CNTs offers superior immunogenicity and strong protection against cancer, as demonstrated by deferred tumor expansion and improved survival in a mouse model.

Versiani et al. (2017) synthesized a nanoconjugate of recombinant Dengue envelope proteins (DENV3E) and MWCNTs by a process known as diimide-activated amidation. They compared the immune response of developed immunogen with IgG responses in relation to the immunization with non–Dengue-specific splenocyte proliferation of conjugated proteins in mice. They also evaluated cell-mediated responses and found that mice immunized with DENV3E conjugated MWCNTs have higher Dengue-specific splenocyte proliferation.

Bhirde et al. (2009) constructed a bioconjugate of the anticancer agent cisplatin, peptide epidermal growth factor (EGF), and SWCNTs (SWCNT-EGR) for the targeting of squamous cell cancer and compared the treatment with a nontargeted control of SWCNT-cisplatin without EGF in vitro. After the imaging of head and neck squamous carcinoma cells (HNSCC) with SWCNT-EGF bioconjugates, they found that the bioconjugate is internalized rapidly into the cancer cells that overexpress EGF receptors (EGFR) via EGF-EGFR binding while control cells without EGF had limited uptake. In vivo video imaging in live mice revealed that injected SWCNT-EGF was selectively taken up by HNSCC, whereas SWCNT controls with no EGF were rapidly cleared from the tumor region. The schematic representation of EGF peptide-SWCNTs mediated delivery of cisplatin to squamous cancer cells is shown in Fig. 16.4.

Pantarotto et al. (2004a) demonstrated peptide functionalized SWCNT conjugates produce marked antipeptide antibody responses in mice with no visible cross-reactivity to the CNTs. In this study, a water-soluble SWCNT conjugate was modified by means of a

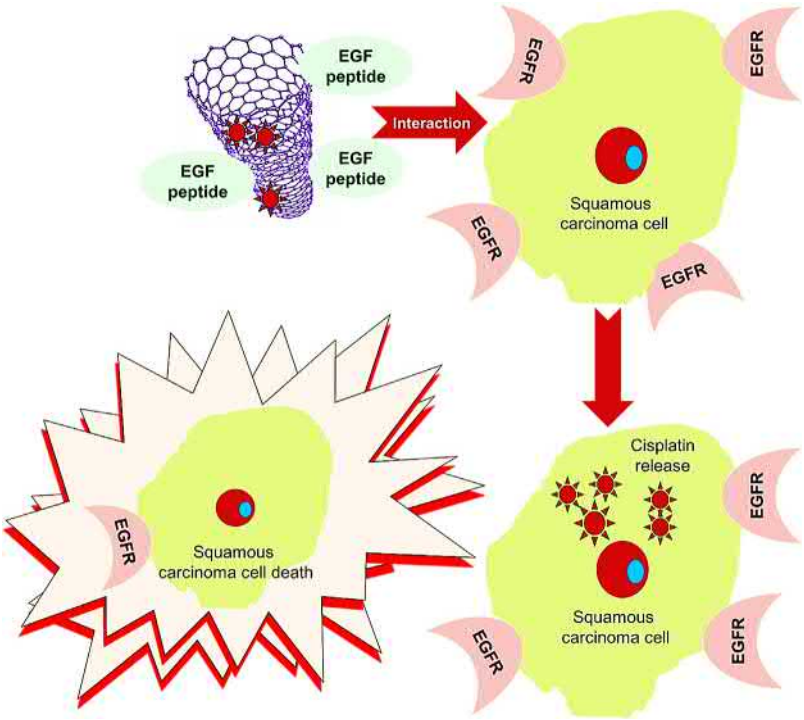

FIGURE 16.4 Schematic representation of EGF-SWCNT-mediated delivery of cisplatin for treatment of squamous cancer cells in which EGF peptide interacts with EGFR leading to endocytosis. *EGF*, Epidermal growth factor; *EGFR*, EGF receptor; *SWCNT*, single-walled CNT.

fluorescent probe, which is capable of translocating cell membranes transversely. The peptide related to G protein function is concerned with signal transduction. FITC-labeled SWCNT derivative I in addition to the peptide SWCNT conjugate II were synthesized and compared with fluorescein alone and free FITC-peptide by epifluorescence and confocal microscopy on human 3T6 and murine 3T3 fibroblasts. They found that the derivative I concentrated primarily in the cytoplasm of the cells.

In another investigation, the same group of researchers developed foot-and-mouth disease virus peptide functionalized CNTs bis FMDV peptide-CNT and studied both in vitro and in vivo applications for vaccine delivery. FMDV 141−159 peptide only and FMDV 141−159 peptide functionalized CNTs together with ovalbumin complete Freund's adjuvant was intraperitoneally injected in female BALB/c mice and were found to be nonimmunogenic. They also gave a booster dose intraperitoneally after 21 days in incomplete Freund's adjuvant and then obtained blood samples for testing by ELISA for the detection of antibody using the BSA-conjugated FMDV 141−159 peptide as the solid-phase antigen. They found significant enhancement in antipeptide antibody titers when treated with bis FMDV peptide CNTs and a lack of reactivity of serum antibodies when compared with a control peptide conjugated to BSA (Pantarotto et al., 2003).

Zhang et al. synthesized and functionalized SWCNTs with biodegradable and biocompatible chitosan in an effort to decrease their toxicity and to impart efficient peptide and DNA delivery. The chitosan functionalized CNTs were complexed with DNA and peptide encoding for EGFP reporter protein was administered to mice. They found that chitosan functionalized CNTs were more effective in the intracellular delivery of peptide compared with chitosan. Chitosan functionalized CNTs significantly increased DNA and peptide delivery to the cells (Zhang et al., 2006).

16.8 CARBON NANOTUBE−MEDIATED GENE DELIVERY

Gene delivery to target cells has been considered to be one of the most significant barriers to flourishing genetic intervention modalities. Definitely, a proficient delivery system is necessary for successful gene therapy. This will permit therapeutic gene transfer and expression in the target organ as well as tissue. Functionalized CNTs should have the ability to be distributed and internalized within whole mammalian cells, which has resulted in their exploration as novel nonviral vectors for the delivery of plasmid DNA. Complexes of functionalized CNTs and plasmid DNA can comprise a new class of nonviral gene delivery systems (Pantarotto et al., 2004b). Fig. 16.5 illustrates CNT-mediated gene delivery.

Zhang et al. (2006) prepared a complex of siRNA with $-CONH-(CH_2)_6-NH_3^+Cl^-$ functionalized SWCNTs for delivery of siRNA to silence the targeted mRNA and protein in lung tumors of nude mice. They used telomerase reverse transcriptase (TERT) for the conjugation of siRNA to SWCNTs. They suggested that complexes of siRNA with $-CONH-(CH_2)_6-NH_3^+Cl^-$ functionalized SWCNTs have target specificity to murine TERT expression. They found that complexes of siRNA with $-CONH-(CH_2)_6-NH_3^+Cl^-$ functionalized SWCNTs were rapidly internalized in three murine cancer cell lines and caused suppression in mTERT expression growth arrest. Finally, they concluded that

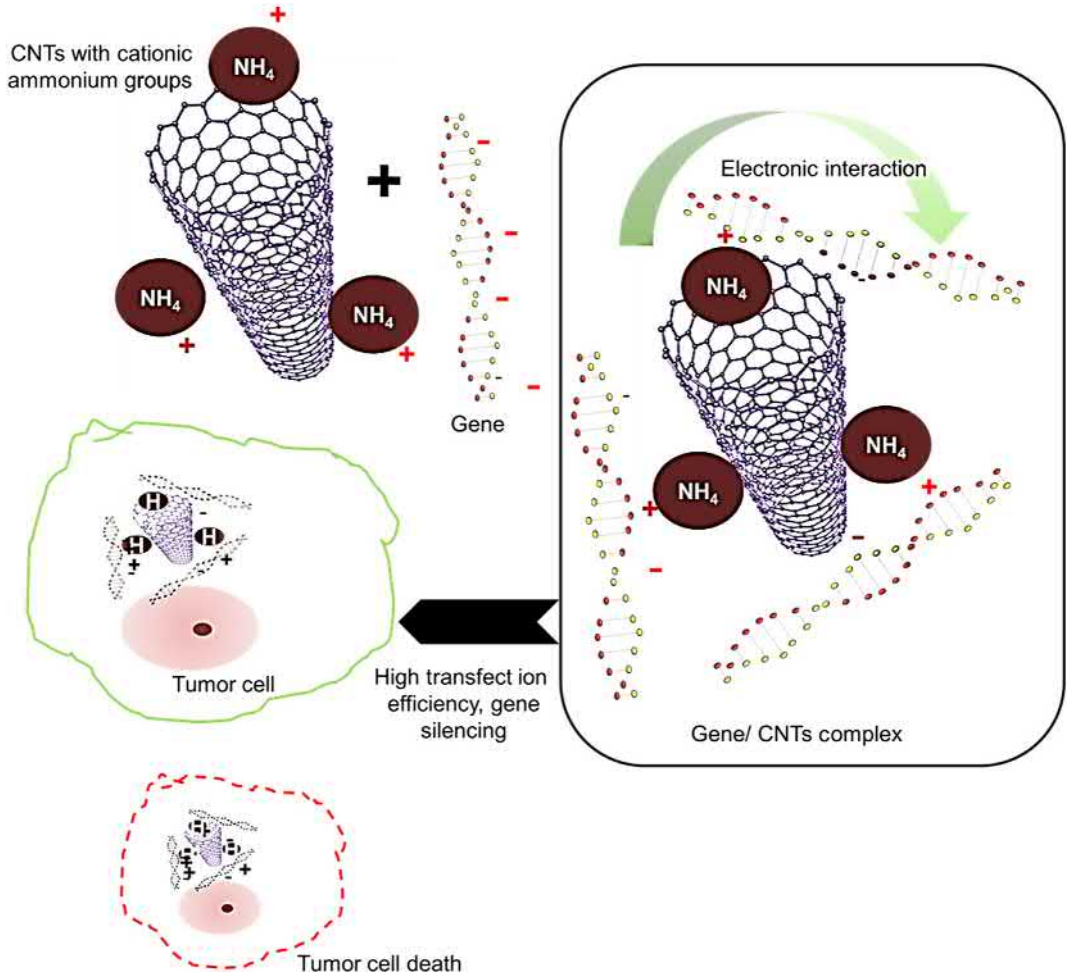

FIGURE 16.5 Schematic presentation of CNT-mediated gene delivery that demonstrates that electronic interaction between negatively charged DNA or gene and positively charged SWCNTs leads to close electronic interactions, which allows for improved gene delivery at the cancer cells that modify gene expression, causing cancer cell death or inhibiting proliferation. *CNT*, Carbon nanotube; *SWCNT*, single-walled CNT.

siRNA with $-CONH-(CH_2)_6-NH_3^+Cl^-$ functionalized SWCNTs deliver siRNA into tumor cells to silence the targeted mRNA and therefore these developed SWCNT complexes may be used as molecular transporters for siRNA therapeutics. Liu et al. (2011) reported delivery of siRNA via a targeted mechanism to cell-surface receptors of CXCR4, by SWCNTs to human T cells as a novel HIV infection therapy.

Taghavi et al. reported polyethyleneimine grafted SWCNT mediated codelivery of shRNA and a chemotherapeutic agent doxorubicin for the treatment of gastric cancer, which overexpresses nucleolin receptors. The synthesized conjugates were attached with an aptamer AS1411 nucleolin ligand and were examined by MTT cytotoxic assay, GFP

expression, and transfection efficiency against L929 (−nucleolin) and AGS (+nucleolin) cells. They found that the conjugate had marked cell selectivity and inhibited the growth of nucleolin-abundant gastric cancer cells with excellent tumoricidal efficacy and high transfection efficiency. Finally, they suggested that SWCNT mediated targeted codelivery of shRNA in combination with the chemotherapeutic agent doxorubicin may be used for gastric cancer treatment (Taghavi et al., 2017).

Pantarotto et al. prepared complexes of DNA and ammonium-functionalized CNTs by electrostatic interaction. They determined their cellular uptake and efficacy using mammalian HeLa cells. They incubated HeLa cells with ammonium-functionalized SWCNTs and ammonium-functionalized MWCNTs at a concentration of 2.5 mg. They found that ammonium-functionalized CNTs reach the HeLa cell nuclei and may be potentially used as a vector for cellular delivery of plasmid DNA. They found that the complexes have low cytotoxicity and have the potential to deliver the DNA into the cells. They observed that the transfected cells expressed genes 10-fold higher than those cells treated with DNA only (Pantarotto et al., 2004b).

Pan et al. (2007) designed PAMAM dendrimer modified MWCNTs conjugated with FITC-labeled antisense c-myc oligonucleotides (as ODN) termed as ODN−dMNTs. The conjugated ODN−dMNTs were evaluated and their cellular uptake was compared with antisense c-myc oligonucleotides (asODN) CNT conjugate and antisense c-myc oligonucleotides (asODN) 5.0G dendrimer conjugate, in the human breast cancer cell lines MCF-7 cells and MDA-MB-435 cells, and liver cancer cell line HepG2 cells, using laser confocal microscopy. They found that the nanocomposite subdued the cell growth in a time- and dose-dependent means, and downregulated the expression of the c-myc gene and C-Myc protein. Finally, they suggested that ODN−dMNTs have high transfection efficiency and inhibit tumor cell growth.

Singh et al. (2005) reported SWCNTs functionalized with ammonium for delivery of plasmid DNA leading to the expression of marker genes in human and murine cells. They studied ammonium-functionalized SWCNTs, ammonium-functionalized MWCNTs, and lysine-functionalized SWCNTs complexed with plasmid DNA. They found that all positively charged CNTs have the proficiency to complex DNA molecules in various degrees, which demonstrates that the surface area of CNTs and charge density are involved in the electrostatic complex formation of functionalized CNTs with DNA. Cells treated with positively charged CNTs show upregulation of marker gene expression in human cell line when compared with the cells treated with naked DNA.

Pan et al. investigated the potential of dendrimer grafted CNTs for the delivery of antisense survivin oligonucleotide into MCF-7 cells and its effect on tumor growth was evaluated by MTT cytotoxic assay. They observed the distribution of the dendrimer CNT complexed with antisense survivin oligonucleotide at different sites within MCF-7 cells by TEM and found that it was concentrated in the cytoplasm, endosome, and lysosome within MCF-7 cells. They suggested that the dendrimer CNT complex with antisense survivin oligonucleotide inhibited MCF-7 cells at a concentration of 3.0 μmol/L. Finally, they concluded that the dendrimer CNT complex with antisense survivin oligonucleotide has higher transfection efficiency and inhibited tumor cell proliferation markedly, and therefore it may be used as a vector for oligonucleotide delivery (Pan et al., 2007).

Behnam et al. (2013) reported polyethyleneimine-functionalized SWCNTs for delivery of DNA and other biomolecules into various cells. They used three different molecular weights of polyethyleneimines (25, 10, and 1.8 kDa) and they found that all polyethyleneimine-functionalized SWCNTs demonstrated good stability in addition to dispersibility in biological media. They found that polyethyleneimines functionalized SWCNTs have the potential to condense plasmid DNA completely at low nitrogen/phosphate (N/P) ratios in addition to substantial buffering capacity in the endosomal pH range. Polyethyleneimine-functionalized SWCNTs have marked transfection efficiency at 19-fold higher in comparison to unfunctionalized polyethyleneimines. Finally, they concluded that polyethyleneimine-functionalized SWCNTs may potentially be employed as vectors for gene delivery in vivo.

Liu et al. synthesized MWCNTs functionalized with polyamidoamine as a novel gene delivery system by amide bond creation between polyamidoamine and chemically oxidized MWCNTs. They found that polyamidoamine functionalized MWCNTs have marked transfection potential in comparison to polyamidoamine and polyethyleneimine at optimal weight ratios. They found that after a 24-hour incubation with polyamidoamine functionalized MWCNTs, a large number of Cy3-labeled pGL-3 were attached to the nuclear membrane in intracellular trafficking of Cy3-labeled pGL-3. Finally, they suggested polyamidoamine functionalized MWCNTs facilitated higher DNA uptake and gene expression in vitro, therefore they may be used as a novel gene−drug delivery system having high transfection efficiency and low cytotoxicity.

Guo et al. developed a genetic inhibitory approach for gene therapy in lung cancer. They synthesized cationic MWCNTs siPLK1:MWCNT-$NH_3$for siRNA delivery against the PLK1 protein (siPLK1) in Calu6 tumor xenografts and administered by direct intratumoral injections, and compared with cationic liposomes (Guo et al., 2015). They analyzed biological tumors treated with siPLK1:MWCNT-NH_3^+ via qRT-PCR and western blot assay. They also analyzed TUNEL staining to identify the biological functionality of the intratumorally administered siRNA. They suggested significant improvement in therapeutic efficacy observed for siPLK1:MWCNT-NH_3 in the delivery of siRNA and it was directly proportional to enhanced retention of siRNA in the solid tumors. In addition, following local administration in vivo, the enhanced siRNA retention within the tumor microenvironments led to consequent uptake by tumor cells. Finally, they concluded that cationic MWCNTs siPLK1:MWCNT-NH_3 for siRNA delivery to tumor cancer tissues significantly improved survival.

16.9 CELLULAR UPTAKE AND CELL PENETRATION MECHANISM OF CARBON NANOTUBES

CNTs have an efficient cell-penetrating mechanism that inspires researchers to investigate the use of CNTs as a device for delivering drugs and other therapeutic agents. To understand the underlying mechanism by which these CNTs deliver drugs to the targeted site, there is a need to study the internalization and cell-penetrating mechanism of CNTs. Several strategies can be utilized to explore and understand the exact mechanisms of cellular uptake such as tracking of fluorescent labeled CNTs using confocal microscopy and flow cytometry (Wong Shi Kam and Dai, 2006; Pantarotto et al., 2004a; Kosuge et al., 2012).

The mechanisms of cellular internalization can be endocytosis-dependent or -independent (Lee and Geckeler, 2010; Fisher et al., 2012). The mediation of endocytosis-dependent pathway could be either through receptor or nonreceptor mechanisms. This pathway also depends upon energy and temperature in transporting and the engulfment of drug molecules into the cellular membrane.

Moreover, the endocytosis involves several mechanisms as shown in Fig. 16.6. One of the important mechanisms is via clathrin-dependent endocytosis (<250 nm) for entry of CNTs inside the cells (Al-Qattan et al., 2018).

Briefly, this method involves the bending of the cell membrane as initial step via the ligand present at the periphery. This further stimulates the creation of coated pits because of the assembly of several cytoplasmic proteins, which again leads to the creation of clathrin cage (Fig. 16.7). This clathrin-dependent endocytosis is often synonymous with receptor-dependent endocytosis (Nel et al., 2009).

Raffa et al. (2010) discussed several unique physicochemical properties of CNTs that affect cellular uptake such as the degree of dispersion, the length of CNTs, and formation of supramolecular complexes. Furthermore, the experiments have confirmed that pluronic stabilized SWCNTs only enter the cell membrane through the endocytosis-dependent pathways and not through direct membrane penetration. The measurements were performed using a Langmuir monolayer film balance and electrochemical impedance spectroscopy (Yaron et al., 2011).

16.10 TOXICITY CONSIDERATION OF CARBON NANOTUBES

Studies of the interaction of CNTs with biological systems most often have resulted in cytotoxicity in early stages of their development, and therefore issues relevant to the protection and biological compatibility of CNTs are of prime importance (Bellucci, 2009). Reports are available pertaining to the toxicity of CNTs (Chatterjee et al., 2016). Carbon materials, as well as pyrolytic carbon, diamond-like carbon, are commonly employed as treatment modalities. Then again, high-virtue carbon black has been accounted to increase oxidation reactions in human lung cells in vitro (Stone et al., 1998; Chougule et al., 2014).

There are many investigations on CNTs' toxicity, such as those that focus on their toxicity towards individual cells, some CNTs have been shown to harm human keratinocyte (skin) cells, and the demonstration that SWCNTs have low lethality to human lung cells (Shvedova et al., 2003; Tekade et al., 2015b). The toxicity of functionalized SWCNTs has been shown to be significantly less than that of nonfunctionalized CNTs (Sayes et al., 2006; Davoren et al., 2007).

Biocompatibility and biodegradability are important properties for carbon-based nanosystems. Researchers are accordingly utilizing functionalized CNTs while avoiding virulent properties (Vega-Estrada et al., 2016). Biodegradability of CNTs is among the main problems facing their biological application. Nonbiodegradable nanoparticles may accumulate in a few organs and prompt serious undesirable effects. In context, functionalization is a way to develop biodegradable CNTs for biomedical applications (Liu et al., 2016).

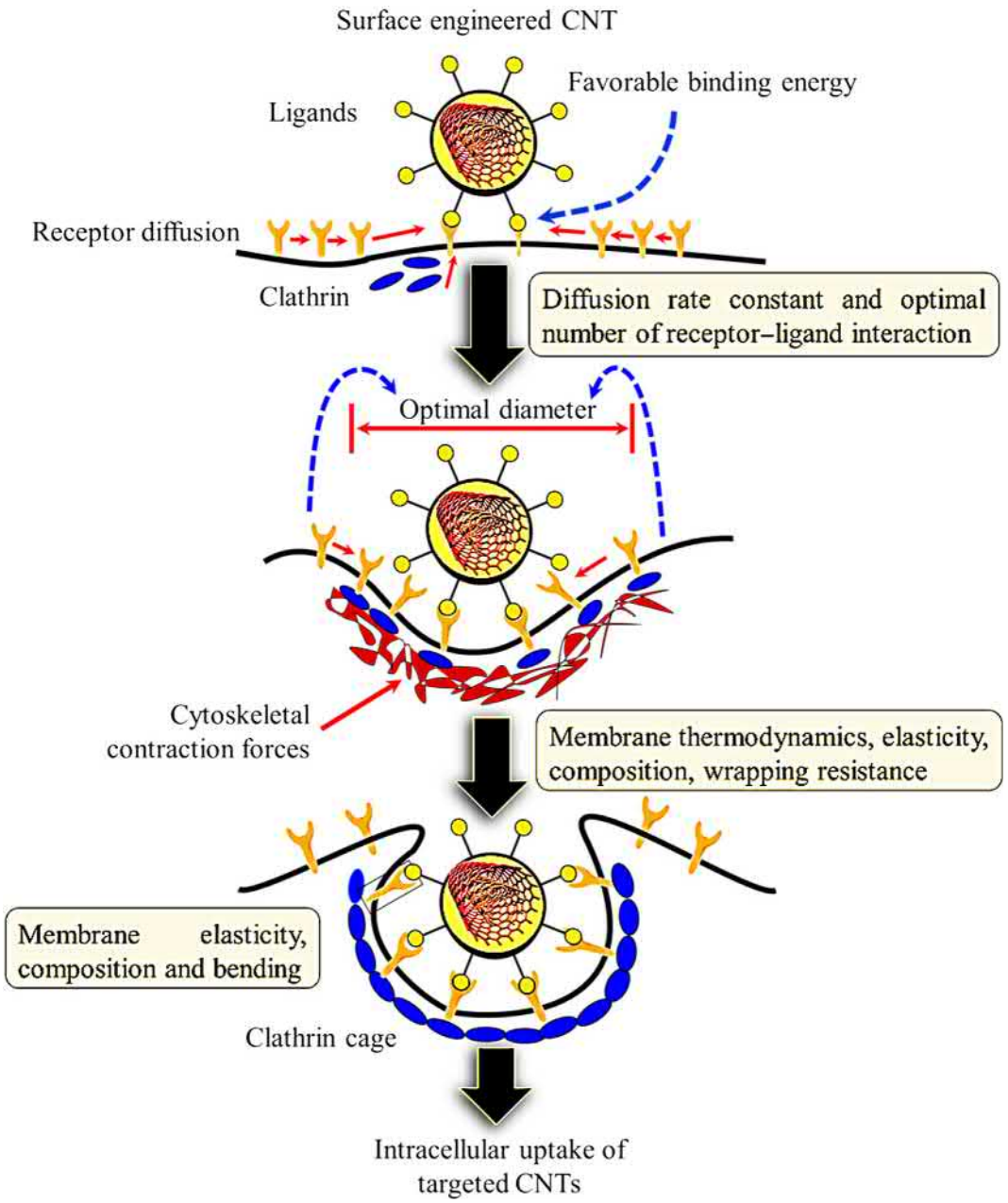

FIGURE 16.6 **Schematic showing clathrin-dependent pathway for internalization.** The blue globules represent clathrin; red represents particles that undergo uptake through interaction between ligands (*yellow dots*) on the particle surface and membrane receptors (Y-shaped). Source*: Adapted with permission from Al-Qattan, M.N., Deb, P.K., Tekade, R.K., 2018. Molecular dynamics simulation strategies for designing carbon-nanotube-based targeted drug delivery. Drug Discov. Today 23, 235–250.*

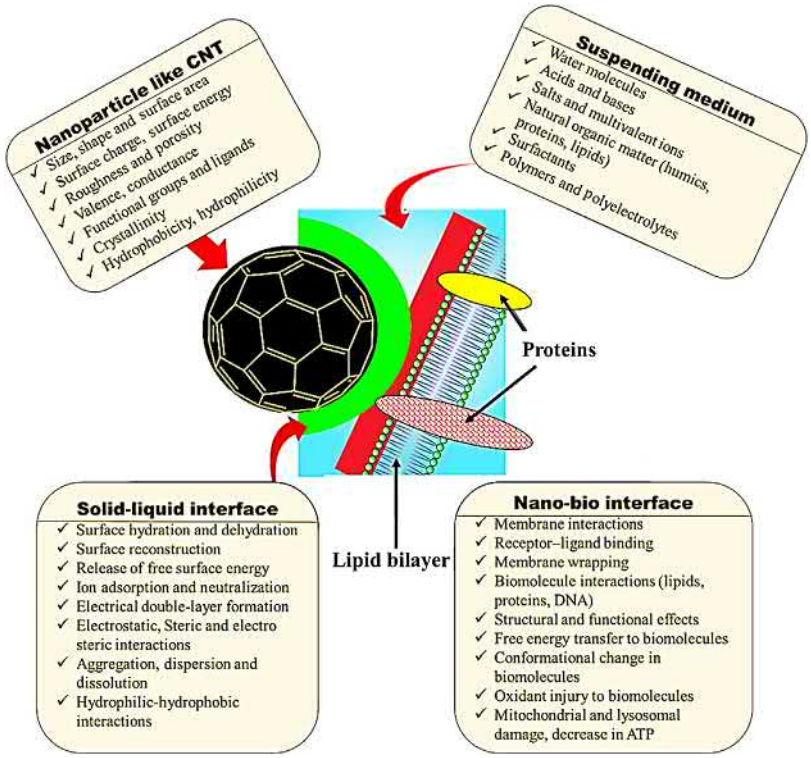
Nanoparticle like CNT
✓ Size, shape and surface area
✓ Surface charge, surface energy
✓ Roughness and porosity
✓ Valence, conductance
✓ Functional groups and ligands
✓ Crystallinity
✓ Hydrophobicity, hydrophilicity
Suspending medium
✓ Water molecules
✓ Acids and bases
✓ Salts and multivalent ions
✓ Natural organic matter (humics, proteins, lipids)
✓ Surfactants
✓ Polymers and polyelectrolytes
Proteins
Lipid bilayer
Solid-liquid interface
✓ Surface hydration and dehydration
✓ Surface reconstruction
✓ Release of free surface energy
✓ Ion adsorption and neutralization
✓ Electrical double-layer formation
✓ Electrostatic, Steric and electro steric interactions
✓ Aggregation, dispersion and dissolution
✓ Hydrophilic-hydrophobic interactions
Nano-bio interface
✓ Membrane interactions
✓ Receptor–ligand binding
✓ Membrane wrapping
✓ Biomolecule interactions (lipids, proteins, DNA)
✓ Structural and functional effects
✓ Free energy transfer to biomolecules
✓ Conformational change in biomolecules
✓ Oxidant injury to biomolecules
✓ Mitochondrial and lysosomal damage, decrease in ATP

FIGURE 16.7 Schematic of the interface between a nanoparticle and a lipid bilayer. The factors that affect the nanoparticle internalization belong to the nanoparticle surface, suspending medium, and the dynamic interactions between the solid−liquid interface and the biomolecules and cellular compartments. Source: *Adapted with permission from Nel, A.E., Mädler, L., Velegol, D., Xia, T., Hoek, E.M., Somasundaran, P., et al., 2009. Understanding biophysicochemical interactions at the nano−bio interface. Nat. Mater. 8(7), 543; Al-Qattan, M.N., Deb, P.K., Tekade, R.K., 2018. Molecular dynamics simulation strategies for designing carbon-nanotube-based targeted drug delivery. Drug Discov. Today 23, 235−250.*

16.11 FUTURE SCOPE AND CONCLUSION

During recent years peptide-mediated CNT delivery has attained a widespread interest in therapeutic research and development. Currently, around 60 peptide-based formulations have entered into the commercial market. In addition, numerous novel peptide-based formulations have entered into preclinical and clinical levels. The most important feature of CNT-based peptide delivery is their potent and specific mechanisms of action.

CNTs are nowadays becoming one of the most intensively researched nanosystems. Their exclusive properties present great assurance for the expansion to numerous CNT-based systems in applications ranging from electronics, biosensor composites, to biomedicine. We are still in a promising phase of CNT technology advancement, mainly in sight of biomedically associated applications. The conversion of CNTs from new, biologically incompatible materials to valuable, effective, and safe biotechnological implements entails many attempts to recover different CNT features to promote improved efficiency, production, processing, and biosafety.

Acknowledgments

The authors would like to acknowledge the Science and Engineering Research Board (Statutory Body Established Through an Act of Parliament: SERB Act 2008), Department of Science and Technology (DST), Government of India for a grant (#*ECR/2016/001964*) allocated to Dr. Tekade for research work on drug and gene delivery. The authors also acknowledge DST-SERB for N-PDF funding (*PDF/2016/003329*) to Dr. Rahul Maheshwari in Dr. Tekade's lab for work on targeted cancer therapy. Authors would also like to acknowledge the Department of Pharmaceuticals, Ministry of Chemicals and Fertilizers, India, for supporting research on cancer and diabetes at NIPER–Ahmedabad.

References

Abbas, A., Al-Amer, A.M., Laoui, T., Al-Marri, M.J., Nasser, M.S., Khraisheh, M., et al., 2016. Heavy metal removal from aqueous solution by advanced carbon nanotubes: critical review of adsorption applications. Sep. Purif. Technol. 157, 141–161.

Al-Qattan, M.N., Deb, P.K., Tekade, R.K., 2018. Molecular dynamics simulation strategies for designing carbon-nanotube-based targeted drug delivery. Drug Discov. Today 23, 235–250.

Amirani, M.C., Tang, T., 2015. A QM: MM model for the interaction of DNA nucleotides with carbon nanotubes. Phys. Chem. Chem. Phys. 17 (11), 7564–7575.

Arora, N., Sharma, N., 2014. Arc discharge synthesis of carbon nanotubes: comprehensive review. Diamond Relat. Mater. 50, 135–150.

Aryasomayajula, B., Torchilin, V.P., 2016. Nanoformulations: a lucrative tool for protein delivery in cancer therapy. Nanobiomaterials in Cancer Therapy. Elsevier.

Behnam, B., Shier, W.T., Nia, A.H., Abnous, K., Ramezani, M., 2013. Non-covalent functionalization of single-walled carbon nanotubes with modified polyethyleneimines for efficient gene delivery. Int. J. Pharm. 454 (1), 204–215.

Bellucci, S., 2009. Carbon nanotubes toxicity. In: Bellucci, S. (Ed.), Nanoparticles and Nanodevices in Biological Applications: The INFN Lectures—Vol I. Springer Berlin Heidelberg, Berlin, Heidelberg.

Berkmans, J., Jagannatham, M., Reddy, R., Haridoss, P., 2015. Synthesis of thin bundled single walled carbon nanotubes and nanohorn hybrids by arc discharge technique in open air atmosphere. Diamond Relat. Mater. 55, 12–15.

Besteman, K., Lee, J.-O., Wiertz, F.G., Heering, H.A., Dekker, C., 2003. Enzyme-coated carbon nanotubes as single-molecule biosensors. Nano Lett. 3 (6), 727–730.

Bhirde, A.A., Patel, V., Gavard, J., Zhang, G., Sousa, A.A., Masedunskas, A., et al., 2009. Targeted killing of cancer cells in vivo and in vitro with EGF-directed carbon nanotube-based drug delivery. ACS Nano 3 (2), 307–316.

Cha, J., Jin, S., Shim, J.H., Park, C.S., Ryu, H.J., Hong, S.H., 2016. Functionalization of carbon nanotubes for fabrication of CNT/epoxy nanocomposites. Mater. Des. 95, 1–8.

Chatterjee, N., Yang, J., Kim, S., Joo, S.W., Choi, J., 2016. Diameter size and aspect ratio as critical determinants of uptake, stress response, global metabolomics and epigenetic alterations in multi-wall carbon nanotubes. Carbon 108, 529–540.

Chen, J., Liu, H., Weimer, W.A., Halls, M.D., Waldeck, D.H., Walker, G.C., 2002. Noncovalent engineering of carbon nanotube surfaces by rigid, functional conjugated polymers. J. Am. Chem. Soc. 124 (31), 9034–9035.

Chen, L., Xie, H., Yu, W., 2011. Functionalization Methods of Carbon Nanotubes and Its Applications. INTECH Open Access Publisher.

Chen, R.J., Zhang, Y., Wang, D., Dai, H., 2001. Noncovalent sidewall functionalization of single-walled carbon nanotubes for protein immobilization. J. Am. Chem. Soc. 123 (16), 3838–3839.

Chiang, I., Brinson, B., Smalley, R., Margrave, J., Hauge, R., 2001. Purification and characterization of single-wall carbon nanotubes. J. Phys. Chem. B 105 (6), 1157–1161.

Chougule, M., Tekade, R., Hoffmann, P., Bhatia, D., Sutariya, V., Pathak, Y., 2014. Nanomaterial-based gene and drug delivery: pulmonary toxicity considerations. Biointeractions of Nanomaterials. CRC Press.

Chrzanowska, J., Hoffman, J., Małolepszy, A., Mazurkiewicz, M., Kowalewski, T.A., Szymanski, Z., et al., 2015. Synthesis of carbon nanotubes by the laser ablation method: effect of laser wavelength. Phys. Status Solidi B 252 (8), 1860–1867.

Copolovici, D.M., Langel, K., Eriste, E., Langel, U., 2014. Cell-penetrating peptides: design, synthesis, and applications. ACS Nano 8 (3), 1972–1994.
Davoren, M., Herzog, E., Casey, A., Cottineau, B., Chambers, G., Byrne, H.J., et al., 2007. In vitro toxicity evaluation of single walled carbon nanotubes on human A549 lung cells. Toxicol. In vitro 21 (3), 438–448.
Dillon, A.C., Gennett, T., Jones, K.M., Alleman, J.L., Parilla, P.A., Heben, M.J., 1999. A simple and complete purification of single-walled carbon nanotube materials. Adv. Mater. 11 (16), 1354–1358.
Dissanayake, S., Denny, W.A., Gamage, S., Sarojini, V., 2017. Recent developments in anticancer drug delivery using cell penetrating and tumor targeting peptides. J. Control. Release 250, 62–76.
Dujardin, E., Ebbesen, T.W., Krishnan, A., Treacy, M.M., 1998. Purification of single-shell nanotubes. Adv. Mater. 10 (8), 611–613.
De Faria, P.C.B., Santos, L.Id, Coelho, Jo.P., Ribeiro, H.Bc, Pimenta, M.Aao, Ladeira, L.O., et al., 2014. Oxidized multiwalled carbon nanotubes as antigen delivery system to promote superior CD8 + T cell response and protection against cancer. Nano Lett. 14 (9), 5458–5470.
Fernández-García, L., Blanco, M., Blanco, C., Álvarez, P., Granda, M., Santamaría, R., et al., 2016. Graphene anchored palladium complex as efficient and recyclable catalyst in the Heck cross-coupling reaction. J. Mol. Catal. A: Chem. 416, 140–146.
Firer, M., Luboshits, G., Gilad, J., Gellerman, G., 2015. Design and selection of appropriate peptide-drug conjugates for targeted drug delivery. Int. J. Mol. Med. 36, S32.
Fisher, C., Rider, A.E., Han, Z.J., Kumar, S., Levchenko, I., Ostrikov, K., 2012. Applications and nanotoxicity of carbon nanotubes and graphene in biomedicine. J. Nanomater. 2012 (3).
Futaba, D.N., Hata, K., Yamada, T., Hiraoka, T., Hayamizu, Y., Kakudate, Y., et al., 2006. Shape-engineerable and highly densely packed single-walled carbon nanotubes and their application as super-capacitor electrodes. Nat. Mater. 5 (12), 987.
Gilad, Y., Firer, M., Gellerman, G., 2016. Recent innovations in peptide based targeted drug delivery to cancer cells. Biomedicines 4 (2), 11.
Gorityala, B.K., Ma, J., Wang, X., Chen, P., Liu, X.-W., 2010. Carbohydrate functionalized carbon nanotubes and their applications. Chem. Soc. Rev. 39 (8), 2925–2934.
Guo, C., Al-Jamal, W.T., Toma, F.M., Bianco, A., Prato, M., Al-Jamal, K.T., et al., 2015. Design of cationic multiwalled carbon nanotubes as efficient siRNA vectors for lung cancer xenograft eradication. Bioconjugate Chem. 26 (7), 1370–1379.
Hassan, H.A., Smyth, L., Rubio, N., Ratnasothy, K., Wang, J.T.-W., Bansal, S.S., et al., 2016. Carbon nanotubes' surface chemistry determines their potency as vaccine nanocarriers in vitro and in vivo. J. Controlled Release 225, 205–216.
Hazani, M., Naaman, R., Hennrich, F., Kappes, M.M., 2003. Confocal fluorescence imaging of DNA-functionalized carbon nanotubes. Nano Lett. 3 (2), 153–155.
Iijima, S., 2002. Carbon nanotubes: past, present, and future. Physica B: Condens. Matter 323 (1–4), 1–5.
José-Yacamán, M., Miki-Yoshida, M., Rendon, L., Santiesteban, J., 1993. Catalytic growth of carbon microtubules with fullerene structure. Appl. Phys. Lett. 62 (6), 657–659.
Kayat, J., Gajbhiye, V., Tekade, R.K., Jain, N.K., 2011. Pulmonary toxicity of carbon nanotubes: a systematic report. Nanomed: nanotechnol. 7, 40–49.
Kosuge, H., Sherlock, S.P., Kitagawa, T., Dash, R., Robinson, J.T., Dai, H., et al., 2012. Near infrared imaging and photothermal ablation of vascular inflammation using single-walled carbon nanotubes. J. Am. Heart Assoc. 1 (6), e002568.
Krajcik, R., Jung, A., Hirsch, A., Neuhuber, W., Zolk, O., 2008. Functionalization of carbon nanotubes enables non-covalent binding and intracellular delivery of small interfering RNA for efficient knock-down of genes. Biochem. Biophys. Res. Commun. 369 (2), 595–602.
Kuche, K., Maheshwari, R., Tambe, V., Mak, K.K., Jogi, H., Raval, N., et al., 2018. Carbon nanotubes (CNTs) based advanced dermal therapeutics: current trends and future potential. Nanoscale 10 (19), 8911–8937.
Kumar, M., Sharma, P., Maheshwari, R., Tekade, M., Shrivastava, S.K., Tekade, R.K., 2018. Beyond the blood–brain barrier: facing new challenges and prospects of nanotechnology-mediated targeted delivery to the brain. Nanotechnology-Based Targeted Drug Delivery Systems for Brain Tumors. Elsevier.
Lee, Y., Geckeler, K.E., 2010. Carbon nanotubes in the biological interphase: the relevance of noncovalence. Adv. Mater. 22 (36), 4076–4083.

Liu, L., Wang, T., Li, J., Guo, Z.-X., Dai, L., Zhang, D., et al., 2003. Self-assembly of gold nanoparticles to carbon nanotubes using a thiol-terminated pyrene as interlinker. Chem. Phys. Lett. 367 (5), 747–752.
Liu, M., Chen, B., Xue, Y., Huang, J., Zhang, L., Huang, S., et al., 2011. Polyamidoamine-grafted multiwalled carbon nanotubes for gene delivery: synthesis, transfection and intracellular trafficking. Bioconjugate Chem. 22 (11), 2237–2243.
Liu, Z., Liu, Y., Peng, D., 2016. Hydroxylation of multi-walled carbon nanotubes: Enhanced biocompatibility through reduction of oxidative stress initiated cell membrane damage, cell cycle arrestment and extrinsic apoptotic pathway. Environ. Toxicol. Pharmacol. 47, 124–130.
Maheshwari, R., Tekade, M., Sharma, P.A., Tekade, R.K., 2015. Nanocarriers assisted siRNA gene therapy for the management of cardiovascular disorders. Curr. Pharm. Des. 21 (30), 4427–4440.
Maio, A., Botta, L., Tito, A.C., Pellegrino, L., Daghetta, M., Scaffaro, R., 2014. Statistical study of the influence of CNTs purification and plasma functionalization on the properties of polycarbonate-CNTs nanocomposites. Plasma Process. Polym. 11 (7), 664–677.
Marchesan, S., Kostarelos, K., Bianco, A., Prato, M., 2015. The winding road for carbon nanotubes in nanomedicine. Mater. Today 18 (1), 12–19.
Mehra, N.K., Jain, K., Jain, N.K., 2015. Pharmaceutical and biomedical applications of surface engineered carbon nanotubes. Drug Discov. Today 20 (6), 750–759.
Mittal, G., Dhand, V., Rhee, K.Y., Park, S.-J., Lee, W.R., 2015. A review on carbon nanotubes and graphene as fillers in reinforced polymer nanocomposites. J. Ind. Eng. Chem. 21, 11–25.
Mittal, V., 2011. Carbon nanotubes surface modifications: an overview. Surf. Modif. Nanotube Fillers (1), 1–23.
Mody, N., Tekade, R.K., Mehra, N.K., Chopdey, P., Jain, N.K., 2014. Dendrimer, liposomes, carbon nanotubes and PLGA nanoparticles: one platform assessment of drug delivery potential. AAPS PharmSciTech 15 (2), 388–399.
Mubarak, N.M., Sahu, J.N., Abdullah, E.C., Jayakumar, N.S., 2016. Rapid adsorption of toxic Pb (II) ions from aqueous solution using multiwall carbon nanotubes synthesized by microwave chemical vapor deposition technique. J. Environ. Sci. 45, 143–155.
Naebe, M., Wang, J., Amini, A., Khayyam, H., Hameed, N., Li, L.H., et al., 2014. Mechanical property and structure of covalent functionalised graphene/epoxy nanocomposites. Sci. Rep. 4, 4375.
Nel, A.E., Mädler, L., Velegol, D., Xia, T., Hoek, E.M., Somasundaran, P., et al., 2009. Understanding biophysicochemical interactions at the nano–bio interface. Nat. Mater. 8 (7), 543.
Oliveira, S.F., Bisker, G., Bakh, N.A., Gibbs, S.L., Landry, M.P., Strano, M.S., 2015. Protein functionalized carbon nanomaterials for biomedical applications. Carbon 95, 767–779.
Paloniemi, H., Ääritalo, T., Laiho, T., Liuke, H., Kocharova, N., Haapakka, K., et al., 2005. Water-soluble full-length single-wall carbon nanotube polyelectrolytes: preparation and characterization. J. Phys. Chem. B 109 (18), 8634–8642.
Pan, B.-f, Cui, D.-x, Xu, P., Chen, H., Liu, F.-t, Li, Q., et al., 2007. Design of dendrimer modified carbon nanotubes for gene delivery. Chin. J. Cancer Res. 19 (1), 1–6.
Pantarotto, D., Partidos, C.D., Hoebeke, J., Brown, F., Kramer, E., Briand, J.-P., et al., 2003. Immunization with peptide-functionalized carbon nanotubes enhances virus-specific neutralizing antibody responses. Chem. Biol. 10 (10), 961–966.
Pantarotto, D., Briand, J.-P., Prato, M., Bianco, A., 2004a. Translocation of bioactive peptides across cell membranes by carbon nanotubes. Chem. Commun. 1, 16–17.
Pantarotto, D., Singh, R., McCarthy, D., Erhardt, M., Briand, J.P., Prato, M., et al., 2004b. Functionalized carbon nanotubes for plasmid DNA gene delivery. Angew. Chem. 116 (39), 5354–5358.
Raffa, V., Ciofani, G., Vittorio, O., Riggio, C., Cuschieri, A., 2010. Physicochemical properties affecting cellular uptake of carbon nanotubes. Nanomedicine 5 (1), 89–97.
Rizzuti, M., Nizzardo, M., Zanetta, C., Ramirez, A., Corti, S., 2015. Therapeutic applications of the cell-penetrating HIV-1 Tat peptide. Drug Discov. Today 20 (1), 76–85.
Robbins, S.M., Rahn, J., Senger, D.L., 2015. Brain Tumor Targeting Peptides and Methods. Google Patents.
Ruoslahti, E., 2017. Tumor penetrating peptides for improved drug delivery. Adv. Drug Deliv. Rev. 110, 3–12.
Sanz, V., Borowiak, E., Lukanov, P., Galibert, A.M., Flahaut, E., Coley, H.M., et al., 2011. Optimising DNA binding to carbon nanotubes by non-covalent methods. Carbon 49 (5), 1775–1781.
Sayes, C.M., Liang, F., Hudson, J.L., Mendez, J., Guo, W., Beach, J.M., et al., 2006. Functionalization density dependence of single-walled carbon nanotubes cytotoxicity in vitro. Toxicol. Lett. 161 (2), 135–142.

Shah, K.A., Tali, B.A., 2016. Synthesis of carbon nanotubes by catalytic chemical vapour deposition: a review on carbon sources, catalysts and substrates. Mater. Sci. Semicond. Process. 41, 67–82.
Sharma, P.A., Maheshwari, R., Tekade, M., Tekade, R.K., 2015. Nanomaterial based approaches for the diagnosis and therapy of cardiovascular diseases. Curr. Pharm. Des. 21 (30), 4465–4478.
Shvedova, A.A., Castranova, V., Kisin, E.R., Schwegler-Berry, D., Murray, A.R., Gandelsman, V.Z., et al., 2003. Exposure to carbon nanotube material: assessment of nanotube cytotoxicity using human keratinocyte cells. J. Toxicol. Environ. Health A 66 (20), 1909–1926.
Singh, R., Pantarotto, D., McCarthy, D., Chaloin, O., Hoebeke, J., Partidos, C.D., et al., 2005. Binding and condensation of plasmid DNA onto functionalized carbon nanotubes: toward the construction of nanotube-based gene delivery vectors. J. Am. Chem. Soc. 127 (12), 4388–4396.
Smith, G.P., 1991. Surface presentation of protein epitopes using bacteriophage expression systems. Curr. Opin. Biotechnol. 2 (5), 668–673.
Soni, N., Tekade, M., Kesharwani, P., Bhattacharya, P., Maheshwari, R., Dua, K., et al., 2017. Recent advances in oncological submissions of dendrimer. Curr. Pharm. Des. 23 (21), 3084–3098.
Stone, V., Shaw, J., Brown, D.M., MacNee, W., Faux, S.P., Donaldson, K., 1998. The role of oxidative stress in the prolonged inhibitory effect of ultrafine carbon black on epithelial cell function. Toxicol. In Vitro 12 (6), 649–659.
Taft, B.J., Lazareck, A.D., Withey, G.D., Yin, A., Xu, J., Kelley, S.O., 2004. Site-specific assembly of DNA and appended cargo on arrayed carbon nanotubes. J. Am. Chem. Soc. 126 (40), 12750–12751.
Taghavi, S., Nia, A.H., Abnous, K., Ramezani, M., 2017. Polyethylenimine-functionalized carbon nanotubes tagged with AS1411 aptamer for combination gene and drug delivery into human gastric cancer cells. Int. J. Pharm. 516 (1–2), 301–312.
Tekade, R., GS Maheshwari, R., Sharma, P.A., Tekade, M., Singh Chauhan, A., 2015a. siRNA therapy, challenges and underlying perspectives of dendrimer as delivery vector. Curr. Pharm. Des. 21 (31), 4614–4636.
Tekade, R.K., Tekade, M., Kumar, M., Chauhan, A.S., 2015b. Dendrimer-stabilized smart-nanoparticle (DSSN) platform for targeted delivery of hydrophobic antitumor therapeutics. Pharm. Res. 32 (3), 910–928.
Tekade, R.K., Maheshwari, R., Soni, N., Tekade, M., 2017a. Chapter 12—Carbon nanotubes in targeting and delivery of drugs A2—Mishra, Vijay. In: Kesharwani, P., Amin, M.C.I.M., Iyer, A. (Eds.), Nanotechnology-Based Approaches for Targeting and Delivery of Drugs and Genes. Academic Press.
Tekade, R.K., Maheshwari, R., Soni, N., Tekade, M., Chougule, M.B., 2017b. Chapter 1—Nanotechnology for the development of nanomedicine A2—Mishra, Vijay. In: Kesharwani, P., Amin, M.C.I.M., Iyer, A. (Eds.), Nanotechnology-Based Approaches for Targeting and Delivery of Drugs and Genes. Academic Press.
Trojanowicz, M., 2006. Analytical applications of carbon nanotubes: a review. TrAC, Trends Anal. Chem. 25 (5), 480–489.
Vega-Estrada, A., Silvestre-Albero, J., Rodriguez, A.E., Rodriguez-Reinoso, F., Gomez-Tejedor, J.A., Antolinos-Turpin, C.M., et al., 2016. Biocompatibility and biomechanical effect of single wall carbon nanotubes implanted in the corneal stroma: a proof of concept investigation. J. Ophthalmol. 2016, 4041767.
Versiani, A.F., Astigarraga, R.G., Rocha, E.S., Barboza, A.P.M., Kroon, E.G., Rachid, M.A., et al., 2017. Multi-walled carbon nanotubes functionalized with recombinant dengue virus 3 envelope proteins induce significant and specific immune responses in mice. J. Nanobiotechnol. 15 (1), 26.
Villa, C.H., Dao, T., Ahearn, I., Fehrenbacher, N., Casey, E., Rey, D.A., et al., 2011. Single-walled carbon nanotubes deliver peptide antigen into dendritic cells and enhance IgG responses to tumor-associated antigens. ACS Nano 5 (7), 5300–5311.
Voiry, D., Goswami, A., Kappera, R., e Silva, Cd.C.C., Kaplan, D., Fujita, T., et al., 2015. Covalent functionalization of monolayered transition metal dichalcogenides by phase engineering. Nat. Chem. 7 (1), 45.
Wong Shi Kam, N., Dai, H., 2006. Single walled carbon nanotubes for transport and delivery of biological cargos. Phys. Status Solidi B 243 (13), 3561–3566.
Wurm, F., Hofmann, A.M., Thomas, A., Dingels, C., Frey, H., 2010. α, ωn-Heterotelechelic hyperbranched polyethers solubilize carbon nanotubes. Macromol. Chem. Phys. 211 (8), 932–939.
Xin, H., Woolley, A.T., 2003. DNA-templated nanotube localization. J. Am. Chem. Soc. 125 (29), 8710–8711.
Yan, J., He, W., Yan, S., Niu, F., Liu, T., Ma, B., et al., 2018. Self-assembled peptide–lanthanide nanoclusters for safe tumor therapy: overcoming and utilizing biological barriers to peptide drug delivery. ACS Nano 12 (2), 2017–2026.

Yang, K., Wang, X., Zhu, L., Xing, B., 2006. Competitive sorption of pyrene, phenanthrene, and naphthalene on multiwalled carbon nanotubes. Environ. Sci. Technol. 40 (18), 5804–5810.
Yaron, P.N., Holt, B.D., Short, P.A., Lösche, M., Islam, M.F., Dahl, K.N., 2011. Single wall carbon nanotubes enter cells by endocytosis and not membrane penetration. J. Nanobiotechnol. 9 (1), 45.
Zhang, Z., Yang, X., Zhang, Y., Zeng, B., Wang, S., Zhu, T., et al., 2006. Delivery of telomerase reverse transcriptase small interfering RNA in complex with positively charged single-walled carbon nanotubes suppresses tumor growth. Clin. Cancer Res. 12 (16), 4933–4939.
Zhao, L., Seth, A., Wibowo, N., Zhao, C.-X., Mitter, N., Yu, C., et al., 2014. Nanoparticle vaccines. Vaccine 32 (3), 327–337.

CHAPTER

17

Surface Modifications of Biomaterials and Their Implication on Biocompatibility

Nidhi Raval, Dnyaneshwar Kalyane, Rahul Maheshwari and Rakesh K. Tekade

National Institute of Pharmaceutical Education and Research (NIPER)—Ahmedabad, Gandhinagar, India

OUTLINE

17.1 Introduction to Biomaterials 640

17.2 Compatibility of the Biomaterial With Biological Surfaces: Challenges and Opportunity 640

17.2.1 The Need for Surface Modification of Biomaterials 643

17.2.2 Nonfouling Surfaces 645

17.3 Approaches for Surface Modification and Influences on Biocompatibility 646

17.3.1 Cationization 646

17.3.2 Carboxylation 646

17.3.3 Polyethylene Oxide and Derivatives 647

17.3.4 Polyoxazoline Conjugation 649

17.3.5 Albumin coating 650

17.3.6 Phospholipidic Coating 651

17.3.7 Chitosan Coating 654

17.4 Immobilization of Biomolecule on a Surface of Biomaterials 658

17.4.1 Physical Adsorption 658

17.4.2 Chemical Bonding With Biomolecules 658

17.4.3 Physical Entrapment 659

17.4.4 Chemical Modification 659

17.5 Techniques to Assess the Biocompatibility of Polymers 660

17.5.1 In Vitro Testing 660

17.5.2 Ex Vivo Testing 660

17.5.3 In Vivo Techniques to Assess the Biocompatibility of Polymers 663

Biomaterials and Bionanotechnology
DOI: https://doi.org/10.1016/B978-0-12-814427-5.00017-2

© 2019 Elsevier Inc. All rights reserved.

17.6 Effect of Surface Modification of Biomaterials for Biocompatibility 665
17.6.1 Influence of Protein-Modified Surface 665
17.6.2 Influence of Surface Functional Groups on Cellular Responses 666
17.6.3 Carboxyl (−COOH) Functional Group-Bearing Surface 667
17.6.4 Hydroxyl (−OH) Functional Group−Coated Surfaces 667
17.6.5 Amine ($-NH_2$) Functional Group-Rich Surfaces 667
17.6.6 Methyl ($-CH_3$) Functional Group-Bearing Surfaces 668
17.6.7 Surfaces With Mixed Functionality 668
17.7 Conclusion 668
Acknowledgment 669
References 669

17.1 INTRODUCTION TO BIOMATERIALS

Biomaterials are commonly defined as a nonviable substance that interacts with biosystem and is utilized for many biomedical and pharmaceuticals purposes such as drug delivery and tissue repair. It represents an interdisciplinary field between chemical engineering, chemistry, surface science, plastic surgery, drug delivery devices, medical implants, biology, and bioengineering. The global market of biomaterials projected to reach USD 139 billion by 2022, from USD 70.90 billion in 2016. This can be ascribed to the enhanced market demand and availability of funds for biomaterial research as well as deciphers the expectations from biomaterials.

Initially, biomaterials were used for biomedical applications but nowadays the use of biomaterials has more relevance for extended applications from nonmedicinal to medicinal indications (Fig. 17.1**)**. Table 17.1 shows applications of biomaterials in both therapeutic and nontherapeutic areas. The interaction of tissues with either modified natural biomaterial or synthetic biomaterial may improve the functioning ability of diseased tissue or organs, depending upon the nature, activity, as well as the rationale for the selected biomaterial (Cooper et al., 2018). Hence, the use of biomaterials must be in accordance with the regulation by government organizations (which may vary from country to country) (Othman et al., 2018). A diverse range of polymers are available to be utilized for the casting of biomaterials. For example, the elastomer of polyurethane was among the first utilized as bioprosthetics for complete artificial heart transplantation with end-stage dilated cardiomyopathy (Carpentier et al., 2015).

17.2 COMPATIBILITY OF THE BIOMATERIAL WITH BIOLOGICAL SURFACES: CHALLENGES AND OPPORTUNITY

The utilization of biomaterials or biomaterial based implants is not new for medical purposes, however, most of them have failed due to the adverse interaction with the

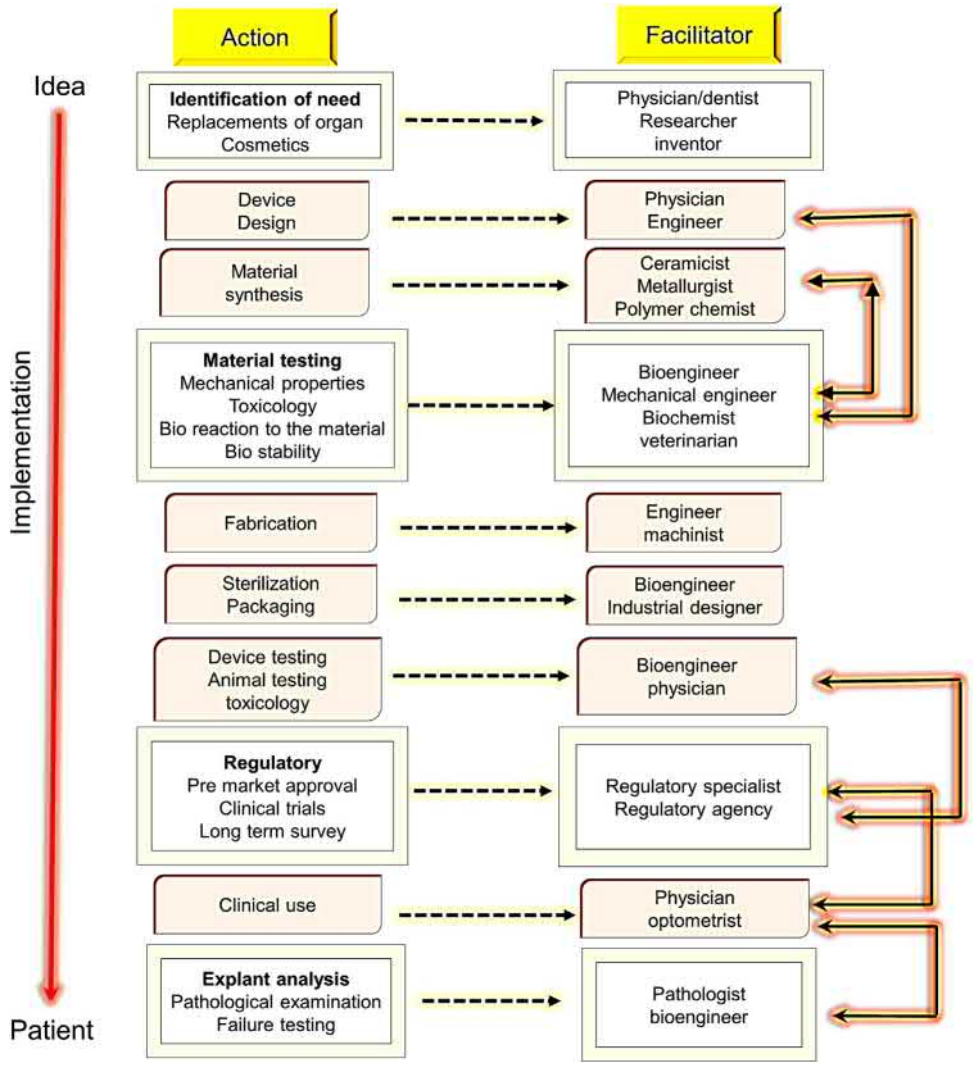

FIGURE 17.1 Suggestive hierarchy involved in the manufacturing of the biomedical device and biomaterials.

biological surface and consequently resulted in infection or an associated side effect of biomaterials (Robeson and Rothrock, 2015). This statement is important and can be understood using a simple example of events associated with tissue injury recovery. For instance, after tissue injury, the normal process of healing is started using numerous complicated events comprised of acute inflammation, the development of granulation tissue, and ultimate scar formation. The reaction takes place in the abundance of blood at the injured area (Martin and Nunan, 2015).

TABLE 17.1 Application of Biomaterials based on Its Therapeutic and Nontherapeutic Utilization

Therapeutic	Nontherapeutic
Cardiovascular implant: artery graft	DNA
Substitute of heart valve	Diagnostic array
Left ventricular assisted device	
Pacemaker	
Stent	
Artificial hip joint	Bioremediation substance
Dental implants	Biosensors
Eye implant:	Bioseparation
Intraocular lenses Glaucoma drainage tube Ophthalmic drug delivery device	
Breast implants	Chromatography
Cochlear implants	Biofouling resistant substance
Ear drainage tube	Cell culture studies
Feeding tube	Control release agriculture product
Renal implants:	Electrophoresis material
Renal dialyzer Urinary catheter	
Hydrocephalous shunt	Biomass
Joint implant:	Microelectrochemical systems
Hip implant Knee implant Shoulder implant Zirconium knee joint	
Keratoprosthesis	Nonmicroelectrochemical systems
Nerve guidance tube	Biocomputing system
Wound dressing	Biowarfare
X-ray guide	Bacterial array chip
Nanofabrication	

Fibrinogen present in the blood is converted into fibrin for the formation of a blood clot following platelet adhesion and aggregation process. Other supportive chemokines also get released during this event such as cytokines and growth factors, which tend to release

white blood cells, largely neutrophils. After that monocytes gather at the site of injury (Zuliani-Alvarez and Midwood, 2015). They transform the fibrin clot into a greatly vascularized granulation tissue. The process of blood vessel formation is necessary to heal the wound and to restore the tissue. Lastly, the macrophages clean the injured site, which primarily comprises an extraneous substance such as bacteria, dead cells, as well as fibroblasts and endothelial cells. Furthermore, an extracellular matrix (ECM) develops in place of granulation tissue. Normal tissue regeneration is also possible in several cases, and in absence of this, the granulation tissues get converted into scar tissue mass (Gensel and Zhang, 2015).

Generally, after implantation, biomaterial provokes broad-spectrum adsorption of proteins. Numerous dissimilar proteins adhere to the surface of biomaterial, which may denature the biomaterial. For instance, monocytes, leukocytes, and platelets mainly get adsorbed on the surface of biomaterial, which concomitantly results in an amplified abundance of cytokines and succeeding proinflammatory mediators in the body (Banerjee and Azevedo, 2017). The implanted biomaterial may also tend to develop diverse response called foreign body reaction depending upon the foreignness of its architect (Fig. 17.2**)**. In most of cases, implanted biomaterials are considerably bigger than the attached macrophages, which avoid phagocytosis of the foreign body. Accumulation of cytokines leads to chronic inflammation at the biomaterial interface and the exasperated macrophages form multinucleated foreign body giant cells, which may remain at the implant site permanently. The removal of an outer layer of biomaterial uses an avascular, collagenous fibrous tissue that is usually 50−200 μm dense (Saleh and Bryant, 2018)

As a concluding remark, it can be stated that the biomaterials developed by conventional means do not have the capability to regulate a sudden and inadvertent biological reaction aroused following their administration/implantation. Evidently, a modified approach is warranted to normalize the biomaterials' interfacial response, and therefore, there is an urgent need for the development of a next-generation biomaterials class. The following section of the chapter specifically deals with the need for surface modification of biomaterials in further detail (Chen and Liu, 2016).

17.2.1 The Need for Surface Modification of Biomaterials

Generally, the utilized biomaterials have a greater affinity to a wide variety of proteins and hence get enclosed with a plasma protein, mainly albumin, fibrinogen, IgG, fibronectin, and von Willebrand factor after administration. The protein interaction and adsorption process alter the conformation of developed biomaterial (Ren et al., 2015). Upon interaction of biological tissue with the biomaterial or implant surfaces, fibrinogen turns out to be increasingly more adherent and employs denaturation of biomaterials. Therefore, to protect the biomaterial throughout its predicted shelf life, there is an urgent need to modify the biomaterial surface to decrease the degree of neoepitopes exposure following cell and tissue reactions (Ramalingam et al., 2016).

The surface chemistry and structure of a biomaterial are of a pivotal importance that impacts protein adsorption, cell interference, as well as the host reaction. For instance, in vitro cell adsorption can be achieved by modification in the surface chemistry of

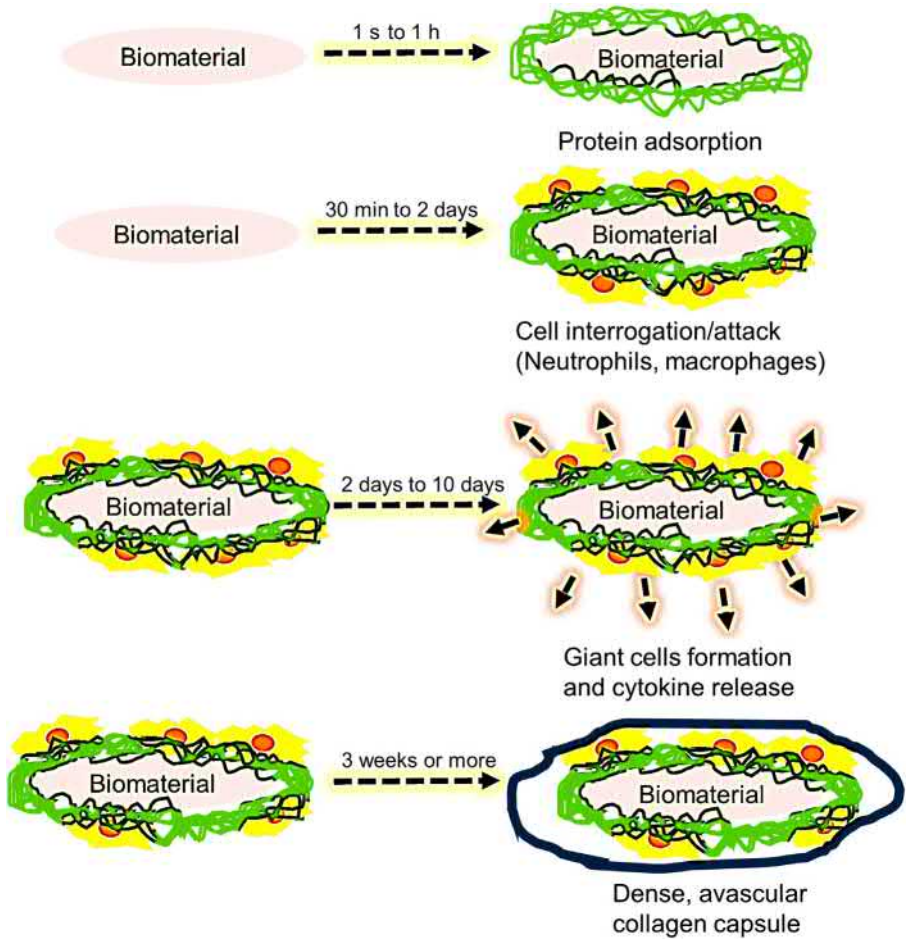

FIGURE 17.2 The reaction of the foreign body as shown here is the normal reaction of the cells by means of the higher organism toward implanted synthetic biomaterial.

biomaterial. Nevertheless, in vivo mechanism of externally applied biomaterial does not depend on conventional chemistry. For example, biomaterials are generally polymer, ceramic, metal-based, etc. and display diverse surface properties starting from hydrophilic to hydrophobic, tough to soft, and all provoke equal reaction in vivo. It may lead to nonspecific protein adsorption (Abdallah et al., 2017). The surface modification of these biomaterials aids in controlling their protein interaction behavior. Precisely, a substantial quantity of outcomes have been discovered and surfaces that are unaffected by protein adsorption are termed as nonfouling surfaces (Kulkarni et al., 2014).

Hence, to obtain a highly biocompatible biomaterial architect, the literature demonstrates a surface modification of biomaterial using a wide range of techniques including physical modifications, chemical modifications, and radiation. Generally, biomaterial surface modification such as the modifying chemistry of polymer, wetting ability, domain

arrangement, and morphology has broadly affected the protein adsorption and cellular reactions in vitro (He and Benson, 2017). For generating modified surfaces, some techniques are suggested in the literature such as self-assembled monolayer methods, chemical graft alteration, and plasma medication, and are utilized in various topical experimentations (Pelaz et al., 2015).

17.2.2 Nonfouling Surfaces

For cellular resistance and protein nonadsorption the most extensively explored polymer is poly(ethylene glycol) (PEG) or poly(ethylene oxide) (PEO). Numerous approaches have been established for the conjugation of biomaterials with PEG to avoid nonfouling. For example, nonfouling was employed using covalent immobilization, adsorption, or interpenetration of protein. A current new tactic to avoid nonfouling is taking benefit of the extremely adhesive fauna of mussel adhesive protein (Horbett, 2018). However, the mussel adhesive protein was covalently attached with PEG to develop copolymer revealing a nonfouling section as well as a sticky part. Literature reveals that the PEG anchored gold and titanium surface provided resistance toward cell adhesion over two weeks. To avoid nonspecific interactions with the blood proteins, PEG has been utilized. In this meadow, the PEG protection efficiency depends on its chain density on the surface (Jiang et al., 2017).

As a substitute, Zhang et al. developed PEG-like surfaces using radio frequency plasma deposition method using tetraethylene glycol dimethyl ether (tetraglyme), which is known to produce extremely nonfouling cross-linked assemblies. In case of tetraglyme, not more than three tetramethylene glycol subunits are connected together and the resultant modified surfaces show minute protein adsorption around at 2 ng/cm^2 concentration. Also, it was able to expressively reduce blood platelet and monocyte adhesion in vitro (Zhang et al., 2018). Moreover, another group of researchers also revealed that when untreated fluorinated ethylene propylene (FEP) copolymer and FEP treated with plasma-polymerized tetraglyme were implanted in vivo via subcutaneous route in the backbone of mice, 4 weeks later a fibrous capsule had developed surrounding the implant. However, the thickness of the capsule was found to be the same irrespective of treatment. More interestingly, adhesion of macrophage was found to be considerably greater in case of tetraglyme-treated models over the untreated samples (Ramkumar et al., 2018).

The work done by Ramkumar et al. was further proved by Steckbeck et al. by reporting the variation among in vitro and in vivo reactions. Hence, the researchers assumed that the tetraglyme comprised surface of biomaterials adhered to a host protein in vitro and in vivo. However, sometimes it may change conformation and therefore, the little-adsorbed protein might induce little foreign body response, e.g., tetraglyme provides less or negligible protein adsorption, which increases the availability of active sites vacant for cell adhesion (Steckbeck, 2014).

On the other hand, in case of withdrawal of the tetraglyme surface, the successive loss of the nonfouling effect was taken care of in in vivo conditions by the PEG (Park et al., 2018). Understanding nonfouling properties is significant for the protein adsorption phenomenon and it is discovered theoretically and experimentally through studies. Generally,

several modifications in the surface of biomaterials make them able to reduce protein adsorption in vitro, but it was found dissimilar in the case of in vivo implantation. Therefore, there is a need for a better ex vivo model to evaluate a long-term nonfouling surface for biomaterial (Cross et al., 2016).

17.3 APPROACHES FOR SURFACE MODIFICATION AND INFLUENCES ON BIOCOMPATIBILITY

17.3.1 Cationization

Surface modification significantly affects attachment and development of cells on biomaterials. For the purpose of modification, biologically degradable polymers are extensively utilized as scaffold materials for tissue engineering (Nogués et al., 2018). Modifications of the surface of biomaterial commonly include elevating the materials with ECM molecules and their resultant derivatives, for example, collagen, chitosan, and gelatin were considered as surface modifiers, which tended to considerably expand the cytocompatibility of polymers (Saini et al., 2016).

In context, Shen et al. modified poly(L-lactide-*co*-glycolide) (PLGA) through combined oxygen plasma treatment and surface conjugated with cationized gelatin. Predecided oxygen treatment was given up to 10 min, defined by 50 W power and 20 Pa oxygen pressure. Based on the stability study through XPS, ATR-FTIR, surface energy determination, as well as contact angles it was found that cationized gelatin comprised PLGA is more stable than plain gelatin. Cellular affinity was also found more in case of cationized gelatin comprised of PLGA on NIH 3T3 fibroblast cells. Therefore, surface modification using cationization by gelatin proved biocompatible and had greater cellular affinity and cellular attachment (Shen et al., 2007).

17.3.2 Carboxylation

Over the past few years, huge efforts have been made for the development of modified biomaterials that can imitate natural tissues by virtue of their physical or molecular properties. Nowadays, very few synthetically tailored biomaterials are available for use in tissue engineering (Illés et al., 2015). The exact causes behind biological incompatibility of biomaterial in vivo might be due to their synthetic nature and nonmodified surfaces. Liang et al. developed poly(glycerol sebacate) (PGS)-Bioglass elastomer through carboxylation method. In this investigation, PGS alone was found less useful owing to cytotoxicity caused by acidic degradation under in vivo conditions. Moreover, researchers developed the PGS/Bioglass composite through metallic carboxylate bridges and further evaluated its mechanical properties, swelling factor in water and tetrahydrofuran, and tensile strength. Conclusively, this composite was found have higher Young's modulus. Further, it was observed that under in vivo experimental condition it was not getting hard enough, and was found to be less cytotoxic, more biocompatible, and provide desirable mechanical support. Hence, such materials were recommended by the investigators to be fit for the purpose of soft tissue engineering (Liang et al., 2010).

Similarly, Senthilkumar et al. formulated polyacrylonitrile (PAN) membranes and modified them using carboxylated polyetherimide. For this, polyethyleneimine (PEI) was modified using carboxylation and further utilized for preparation of PAN membrane through hydrophilic alteration. The casting of the membrane was achieved by taking similar ratios of carboxylated PEI and PAN (Figs. 17.3 and 17.4). The result of biocompatibility studies revealed that it reduced the absorption of plasma protein, adhesion of platelets, and formation of thrombus. Moreover, a complete blood count was also found in the normal range and membrane was found to be less cytotoxic to mononuclear cells (Senthilkumar et al., 2013).

17.3.3 Polyethylene Oxide and Derivatives

Adsorption of nonspecific protein or microbial matter on the surface of biomaterials shows unfavorable effect in vivo. This problem associated with adsorption of protein or

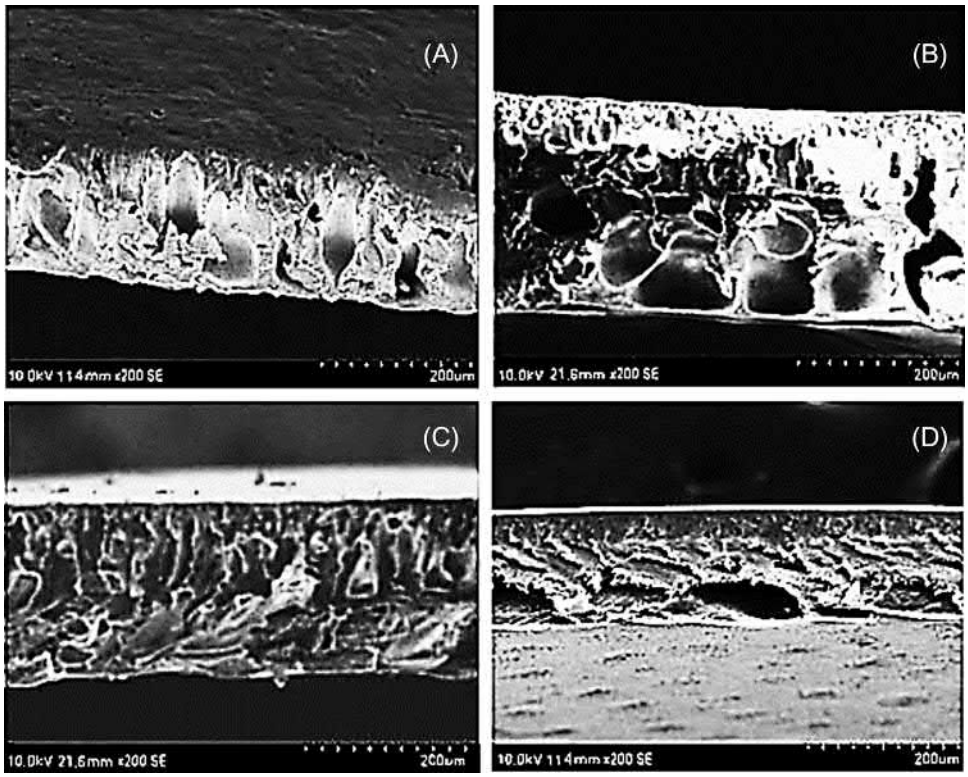

FIGURE 17.3 Scanning electron microscope (SEM) images of membrane at different ratio of cationized PEI: PAN (A) 100:0, (B) 90:10, (C) 80:20, and (D) 70:30 (The image represents cationized PEI and PAN membrane bland 2.5 %w/w additive). *PAN*, Polyacrylonitrile; *PEI*, polyethyleneimine. Source*: Adapted with permission from Senthilkumar, S., Rajesh, S., Jayalakshmi, A., Mohan, D., 2013. Biocompatibility studies of polyacrylonitrile membranes modified with carboxylated polyetherimide. Mater. Sci. Eng.: C 33 (7), 3615–3626.*

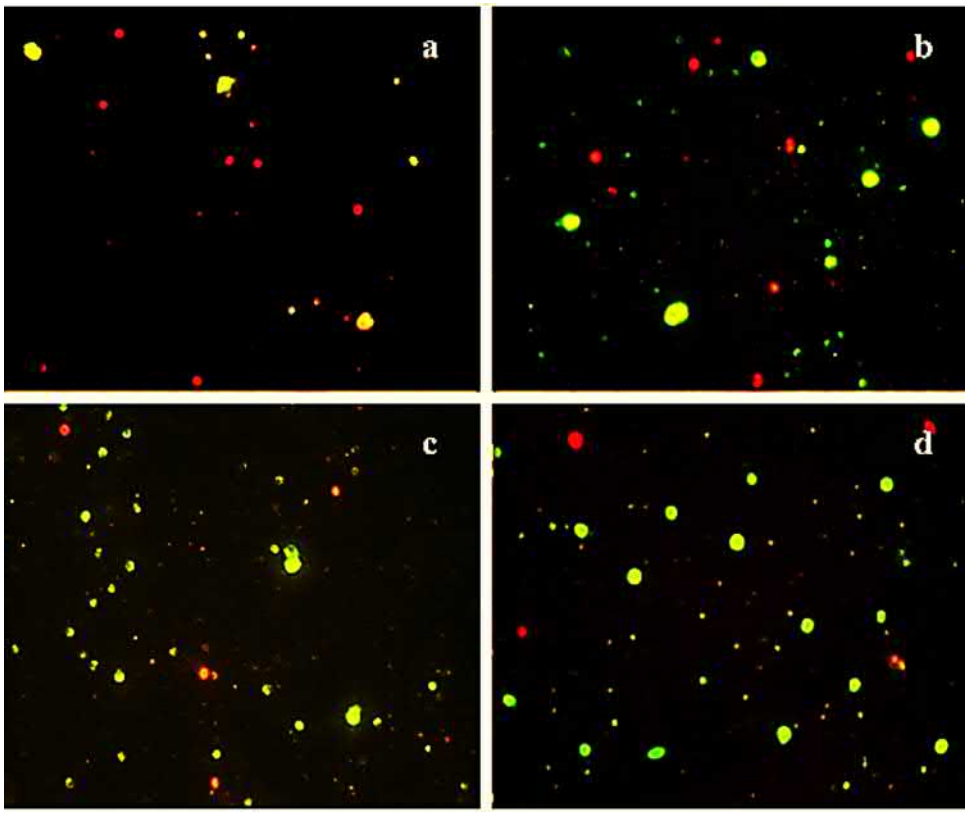

FIGURE 17.4 Apoptotic effect of monocytes observed by fluorescence microscopy on cationized PEI:PAN membrane in presence of additives (A) 100:0, (B) 90:10, (C) 80:20, and (D) 70:30. *PAN*, Polyacrylonitrile; *PEI*, polyethyleneimine. Source*: Adapted with permission from Senthilkumar, S., Rajesh, S., Jayalakshmi, A., Mohan, D., 2013. Biocompatibility studies of polyacrylonitrile membranes modified with carboxylated polyetherimide. Mater. Sci. Eng.: C 33 (7), 3615–3626.*

microbial matter can be resolved by coating antibiofouling or nonfouling polymer on the surface of medical device or nanoparticles which possesses protein and microbial repelling ability (Tekade et al., 2017). The extensively utilized antifouling polymers such as PEG or PEO are studied together with numerous favorable substitutes, comprising zwitterionic polymers, poly(hydroxy functional acrylates), poly(2-oxazoline)s, poly(vinylpyrrolidone), poly(glycerol), peptides, and peptoids (Xu et al., 2016).

Toskas et al. developed hybrid nanofibers comprised of silica and chitosan and further modified them with PEO (3.6 %w/w) using electrospinning. The prepared solution for nanofiber comprised of a sol–gel particle of tetraethoxysilane and the organosilane 3-glycidyloxy propyl triethoxysilane. Results showed that the prepared nanofiber was biocompatible and biologically active on 7F2-cells, which allowed attachment and growth of cells up to 7 days (Toskas et al., 2013).

In a similar line, Han et al. modified polyurethanes using sulfonated PEO utilized as heart valve and vascular graft in vivo. Nontreated and sulfonated PEO-polyurethanes were implanted in vivo over 39 days for deposition of calcium and were also evaluated for biological stability and compatibility with blood. Results were found that deposition of calcium of sulfonated PEO-polyurethanes was much less compared with untreated polyurethanes, and were found biocompatible and biologically stable in vivo upon contact with tissues (Han et al., 2006).

Xu et al. developed scaffold as coaxial microfibers of poly(butylene succinate) and PEG using electrospinning. The dissimilar composition of the polymer at the core and shell region was found in coaxial microfiber. PEG comprised microfibers were easily solubilized in an aqueous medium and resulted in enhancement of the porosity of scaffold. Therefore, solubilization of fibers was found to rely on the distribution of PEG whereas in coaxial fibers retention of PEG was found to be higher at the core region in comparison to the shell (Xu et al., 2016).

Triclosan and curcumin type therapeutic agents can be easily be loaded inside the fiber and are also found to be biocompatible in physiological condition (Llorens et al., 2015). Similarly, Cui et al. prepared a sensitive biomarker for tumor. Here, polymerization of poly(3,4-ethylene dioxythiophene) (PEDOT) and a thiol group comprised of PEG was carried out employing electrochemical polymerization method, where PEG was doped onto the PEDOT, and resulting formulation was found to display flake-like nanoarchitect with improved stability as well as surface area. For incorporation of alpha-fetoprotein antibodies, gold nanoparticles were employed and it was found that casted biosensor had greater selectivity toward liver cancer tumor with a low detection limit (Cui et al., 2016).

Xu et al. functionalized graphene oxide (GO) via PEG for the delivery of an anticancer drug (paclitaxel). In this experiment, 6-armed PEG was covalently bound with GO sheet using facile amidation and formed stable and biocompatible conjugates. It was found that GO-PEG-FITC was easily uptaken by A549 human adenocarcinoma and MCF-7 breast cancer cells as shown in Fig. 17.5. Cytotoxicity study on A549 human adenocarcinoma and MCF-7 breast cancer cells revealed that more than 85% of cells were found viable at even 100 mg/L concentration (Xu et al., 2014).

17.3.4 Polyoxazoline Conjugation

Polyoxazoline, which is a hydrophilic polymer in nature, comprised of *N*-acyl ethyleneimine. However, its affinity toward water can be controlled using an appropriate selection of the alkyl substituent at the C2 position. It varied from extremely water-soluble methyl oxazoline to highly hydrophobic fluoro-alkyl substituted polyoxazolines. It is an amphiphilic polymer and could easily self-assemble in the presence of water (Zanini et al., 2016). Polyoxazoline holds greater biocompatibility and it is already proved by researchers. Polyoxazoline is also known as pseudopeptide due to its similarity with polypeptides. It is possible to link polyoxazolines with protein, small therapeutic agents, liposomes, and micelles as well. Functionalizing these molecules with polyoxazoline may help in producing antifouling surfaces (Dworak et al., 2014).

In context, Morgese et al. prepared polyoxazoline conjugated ZnO Single nanocrystals characterized as ultrastable suspension. Prepared nanocrystal was formulated using w/o

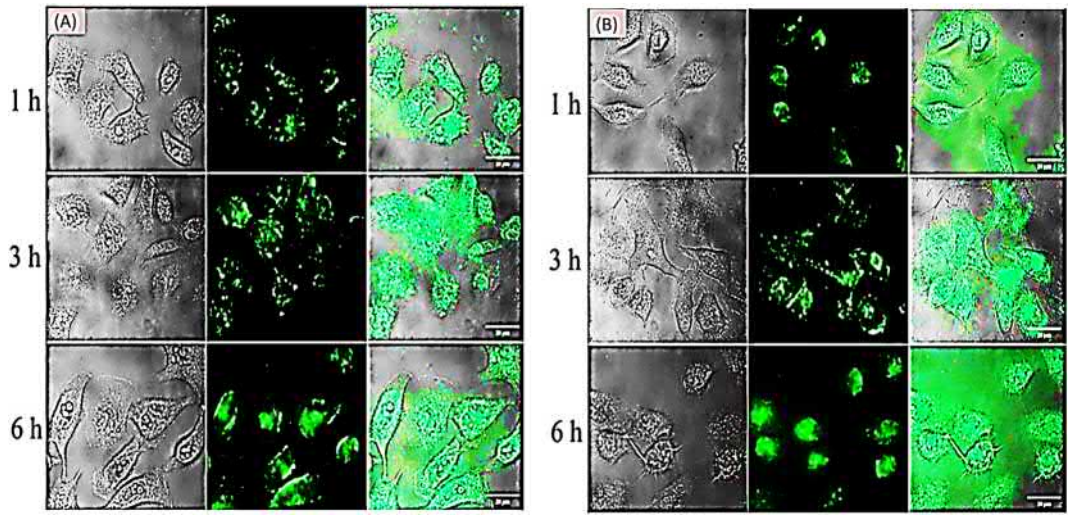

FIGURE 17.5 Fluorescent images of cellular uptake assay (A) A547 cells and (B) MCF-7 cells after treatment with GO-PEG-FITC after different time periods (1, 3, and 6 h). Source: *Adapted with permission from Xu, Z., Wang, S., Li, Y., Wang, M., Shi, P., Huang, X., 2014. Covalent functionalization of graphene oxide with biocompatible poly(ethylene glycol) for delivery of paclitaxel. ACS Appl. Mater. Interfaces 6 (19), 17268–17276.*

microemulsion method in the presence of surfactants, which were simultaneously exchanged by polyoxazoline-ZnO with nitrodopamine. It was found that the stability of the nanocrystal formulation relied on the chain length of the polymer and resultant single nanocrystal presents as similar platelet morphology. Derivatization of nanocrystal with ZnO enables it to protect the nanocrystal from chemical oxidation and provide excellent stability for up to 9 months (Morgese et al., 2015).

Furthermore, Bissadi and Weberskirch developed polyoxazoline comprised silica nanoparticles using surface introduced cationic polymerization technique. The reverse microemulsion was utilized for nanoparticle hybrid preparation. Further, FITC as a fluorophore and folic acid as a therapeutic agent for targeting cancer was also found biocompatible when delivered using a developed system (Bissadi and Weberskirch, 2016).

17.3.5 Albumin coating

In tissue engineering or tissue regeneration, it is essential to offer an environment to cells that would control and enhance the proliferation and differentiation of cells for the revival of tissue. Biomaterial scaffolding is useful to provide additional physical support as well as the chemical and biological evidence for functional tissue generation (Petros and DeSimone, 2010). Protein originated biomaterials such as albumin, fibronectin, laminin, collagen, elastin, casein, vitronectin, and zein deliver appropriate surroundings for the development of cells. Due to their biodegradable property, proteins utilized for surface modifications of biomaterials are gaining attention in tissue engineering (Preiss-Bloom, 2015).

Albumin is found in greater proportion in the body as a human serum protein, and has been thought to affect the response of cells to various scaffold materials such as collagen and fibronectin upon treatment. It aided as an intermediate among cells and scaffold, thus facilitating the integration of these two substitutes. Albumin has supported cellular connection to the scaffold in bone, cardiac, and neural tissue engineering (Guidoin et al., 1984).

Horvath et al. coated albumin to the demineralized bone matrix for bone cell regeneration and strong bone formation and investigated stem cell adherence on bone in vitro using calvaria defect rat model. From the results of the experiment, it was shown that adherence ratio of the cell toward albumin coated demineralized bone matrix enhanced with respect to time. The defect was continuously observed up to 11 weeks; the 7-week defect was seemed only $3.0 \pm 2.3\%$, whereas $40.2 \pm 9.1\%$ in the case of the uncoated demineralized bone matrix and $52.4 \pm 8.9\%$ for control. Density was also enhanced in the presence of albumin demineralized bone matrix. MicroCT analysis showed greater breaking force, which was found to be 46.1 ± 11 N for albumin coated demineralized bone matrix, 15.7 ± 4 N for uncoated matrix and stiffness over the uncoated and control group. It was also found that required healing time in albumin coated matrix was decreased by threefold in comparison to control and therefore resulted in successful implantation of the matrix (Horvathy et al., 2016).

Zhu et al. prepared L-3,4-dihydroxyphenylalanine and albumin comprised tissue adhesive for application in tissue regeneration. From the experimental results, it was shown that immediately after 30 minutes, the developed tissue adhesive provided 10-fold enhanced adhesion stress in comparison to the marketed glue. When it was applied internally and found with higher gelation kinetics and swelling fate, it was less cytotoxic and showed biocompatible behavior. In vitro cytocompatibility was checked on 3T3 and porcine chondrocyte cells (PCC) and employed significant cellular proliferation as shown in Fig. 17.6. Biodegradation study depicted that after 15 days of implantation, it was completely degraded, where merely $26.98 \pm 15.92\%$ gel remained, but after 30 days no gel sample was found as shown in Fig. 17.7 (Zhu et al., 2017).

17.3.6 Phospholipidic Coating

Phospholipid polymers can be used as biomaterials with numerous possible applications in therapeutics and diagnosis. The improvement of biomaterials using these compounds is reported to show identical behavior to cellular membrane. Several polymeric materials are utilized as biomaterials for engineering biomedical expedients comprising artificial organs that may remain in close contact with blood (Rieffel et al., 2015). Nevertheless, the available polymeric material used to modify the surface of biomaterials includes poly(vinyl chloride), polyethylene, poly(methyl methacrylate), segmented polyether urethane, poly(dimethylsiloxane), poly(tetrafluoroethylene) (PTFE), cellulose, and polysulfone (PS). These polymers possess greater hemocompatibility as well as biocompatibility (Gallagher et al., 2014).

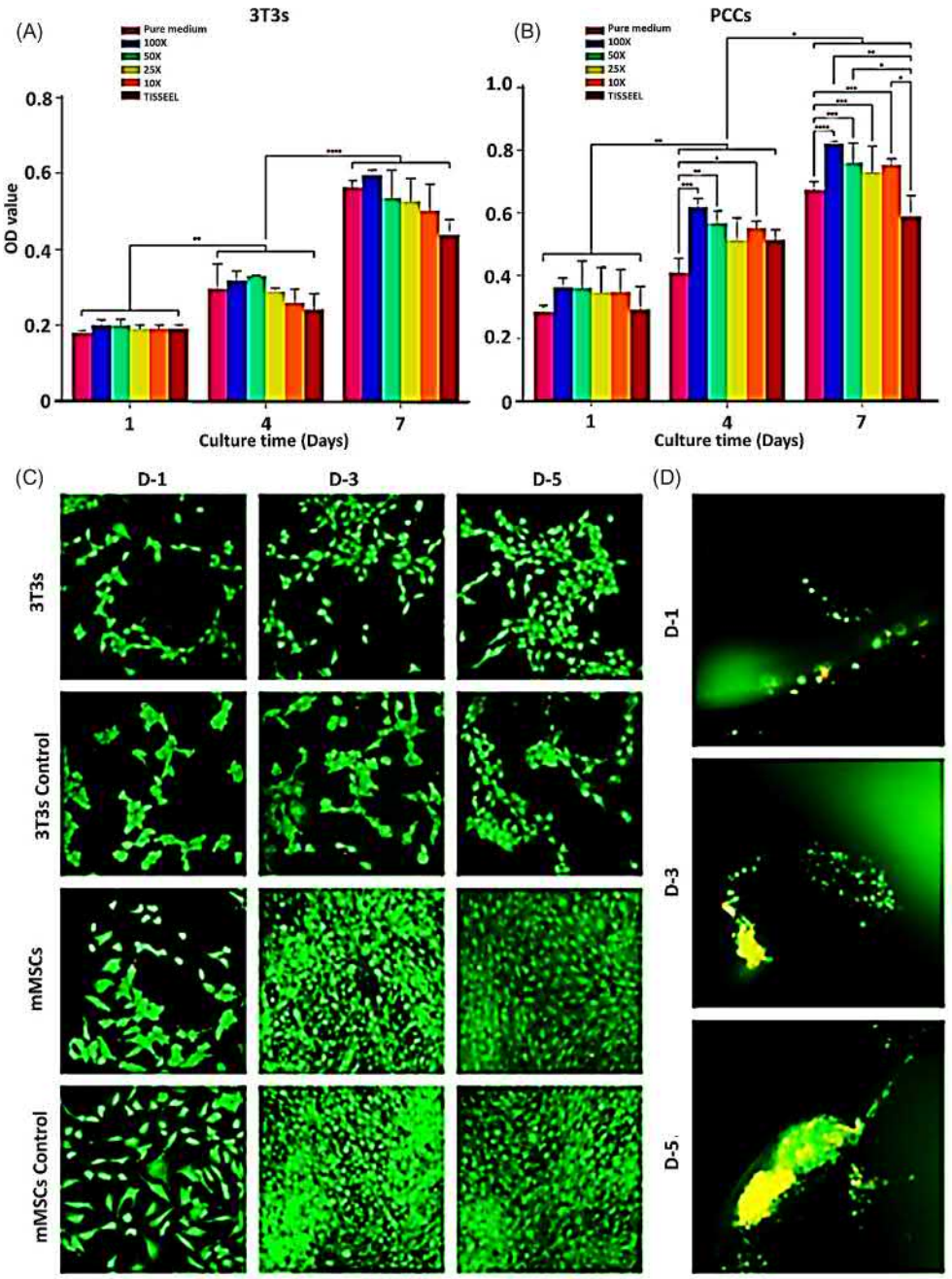

FIGURE 17.6 Cytocompatibility evaluation data in vitro of albumin comprised tissue adhesive and fibrin glue (A) 3T3 cells; (B) PCC; (C) analysis of live and dead cells on 2D culture of 3T3 cells as well as mMSC after implantation of 50× solution day 1, day 3 and day 5; (D) live or dead cell analysis after seeding of mMSC on albumin comprised gel at day 1, day 3, and day 5. Source: *Adapted with permission from Zhu, W., Peck, Y., Iqbal, J., Wang, D.-A., 2017. A novel DOPA-albumin based tissue adhesive for internal medical applications. Biomaterials 147, 99–115.*

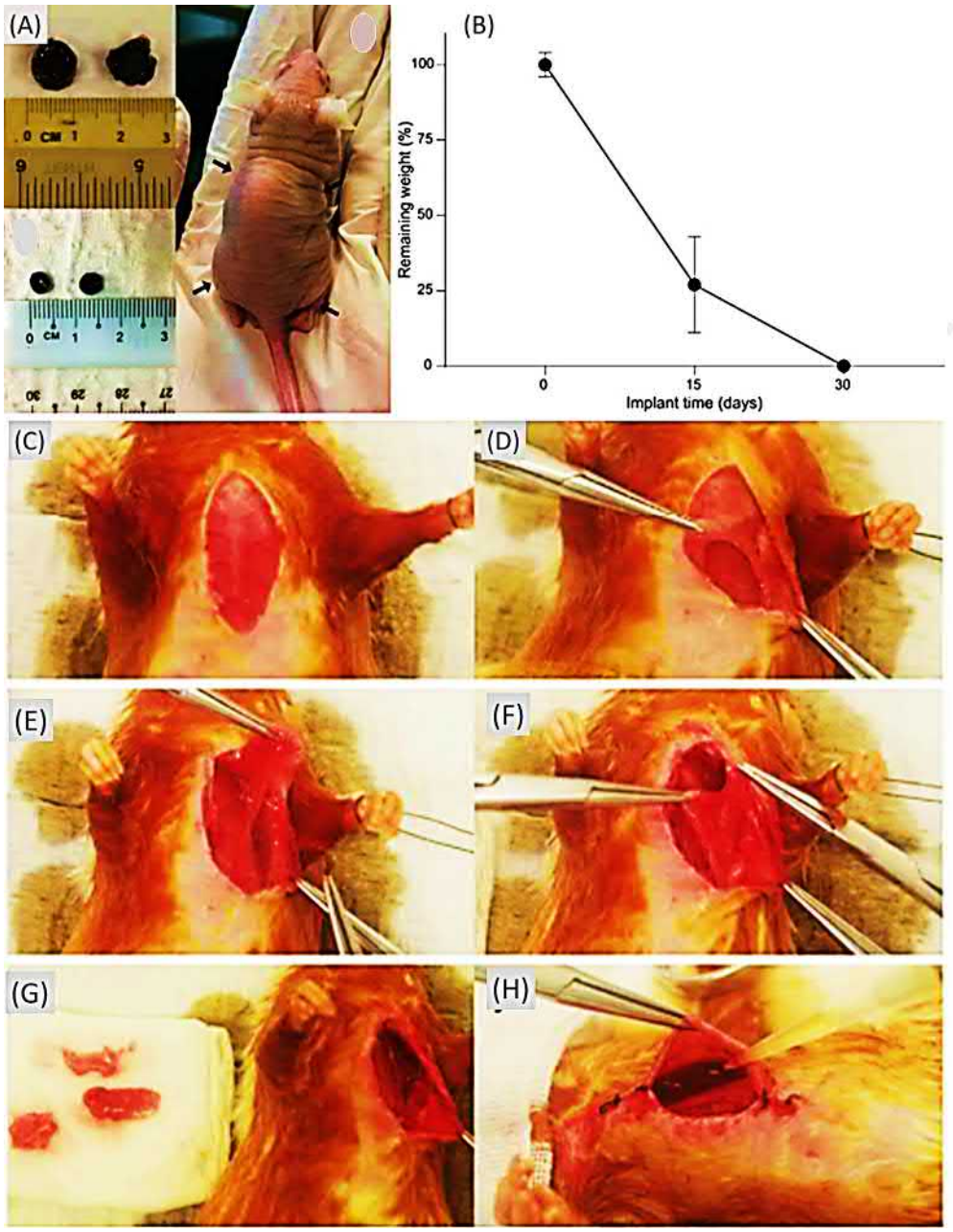

FIGURE 17.7 Representation of cross-linked tissue glue of albumin comprised glue. (A) Upper; before implantation; lower: after implantation. (B) In vivo degradation pattern after implantation. (C) Middle incision was created. (D) Muscular tissue was separated from skin. (E) Muscular tissue removal in sequential manner. (F) Subcutaneously deposited adipose tissue removal. (G) Lymphovascular disruption. (H) For treatment implantation of albumin comprised adhesive glue or fibrin glue or saline as control. Source*: Adapted with permission from Zhu, W., Peck, Y., Iqbal, J., Wang, D.-A., 2017. A novel DOPA-albumin based tissue adhesive for internal medical applications. Biomaterials 147, 99–115.*

Thus, administration of an anticoagulant is essential through medical treatments using biomedical devices to evade clot development. Novel biomaterials imitate the constituent existing on the external cell surface of the lipid bilayer, which form the matrix cells, that is, the phosphorylcholine part of phosphatidylcholine and sphingomyelin (Leslie et al., 2017). Phosphorylcholine is an electrically neutral zwitterionic crown part that signifies the characteristics of the phospholipidic head portion situated on the exterior part of cells. Blood clotting time may be prolonged using the phospholipid-based surface of biomaterial associated with the nonmodified substrate (Laschewsky and Rosenhahn, 2019).

Yang et al. developed a phospholipidic based nanoparticulate architect for the treatment of inner ear diseases. They prepared four types of phospholipidic nanoparticles based on charge and hydrophilicity: neutral, anionic, cationic, and cationic-PEG. These were evaluated on the artificial mucosa of 100 μm round window membrane and HEI-OC1 cells. Ototoxicity was found after intratympanic injection of dexamethasone comprised nanoparticles. Hearing loss was improved upon administering nanoparticles in comparison to available dexamethasone sodium sulfate solution as confirmed by auditory brainstem response measurement (Figs. 17.8 and 17.9). Level of proinflammatory cytokines was also reduced and displayed antiinflammatory effect over the marketed solution. In addition, charged based nanoparticles employed an essential role in distribution and permeation of nanoparticles (Yang et al., 2018).

17.3.7 Chitosan Coating

Chitosan is a mucoadhesive polysaccharide obtained mainly from outer shells of crustaceans, corals, or jellyfish. Owing to its biological compatibility and a variety of remarkable properties, such as antimicrobial, antitumor, antiinflammatory, and immunity improving potential, it could aid a multifunctional drive in biomedicine. Though, the cationic nature of chitosan could compromise the integrity of cellular membrane and stimulate cytotoxicity. It could encourage thrombosis; due to this it may not be utilized for extensive applications (Luo et al., 2015).

Hsueh et al. prepared chitosan-coated conduit for the delivery of neurosphere cells obtained from adipose-derived cells to attain the regeneration of the sciatic nerve. For this, the authors applied the chitosan coated conduit on the adipose tissue−derived stem cells. The silicon tubing was utilized for making a bridge of 10 mm in rat sciatic nerve for aiding the application. Using this implant, myelin sheath generation along with regeneration of glial scar was observed. This event was associated with a marked recovery of nerve gap following 6 weeks of treatment. An improvement in nerve regeneration was attributed to the enhancement of myelin axon density and thickness through the chitosan-coated conduit and neurosphere cells (Fig. 17.10). It was also revealed that in the presence of chitosan-coated conduit inflammatory marker such as IL-1β and leukotriene B4-1 receptor at intraneuronal site decreased. Hence, it was observed that the use of chitosan in improving the biomaterial property was proved to have excellent biocompatibility for nerve cell regeneration (Hsueh et al., 2014).

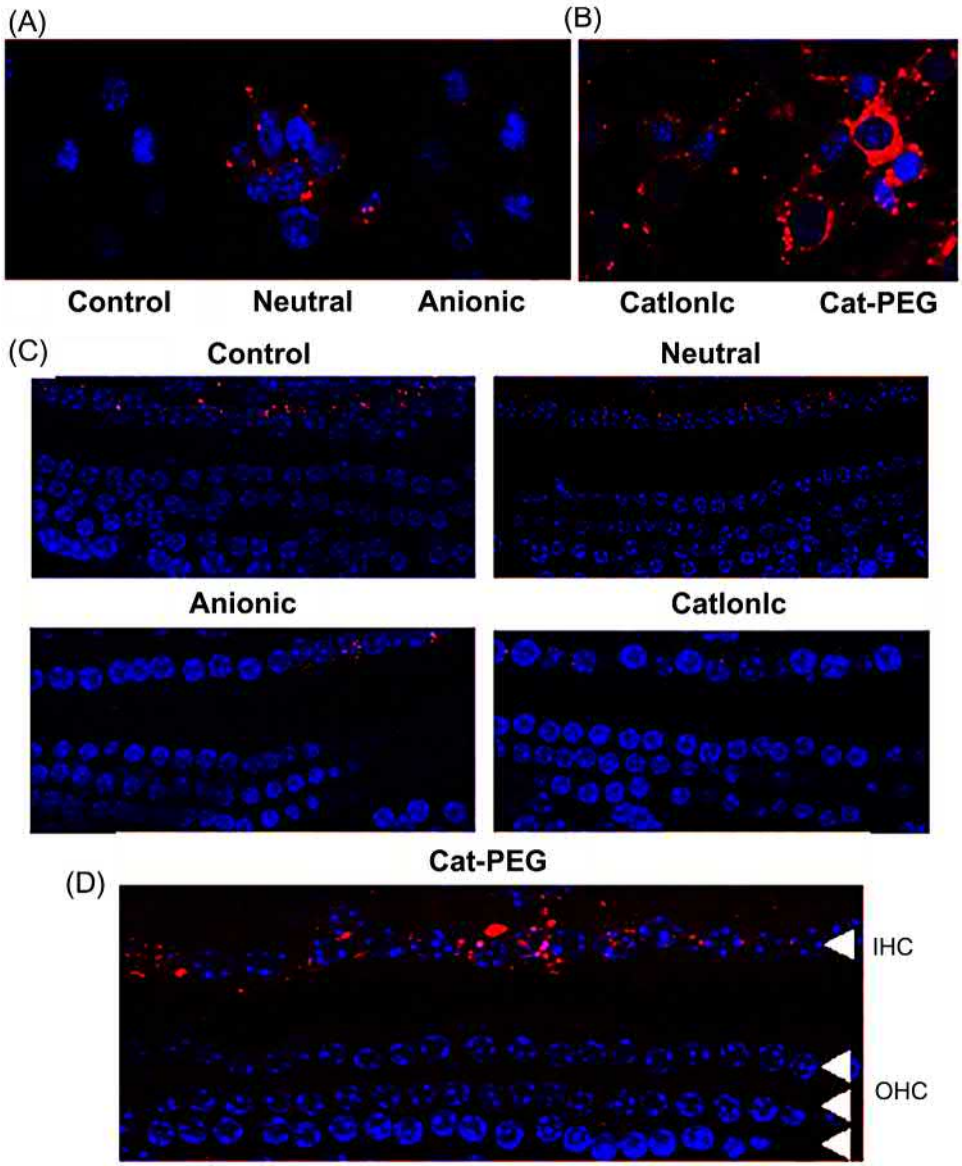

FIGURE 17.8 (A, B) Cellular uptake of different nanoparticle in HEI-OC1 cells. Among them, Cat-PEG nanoparticle found high cellular uptake. (C) In vivo image of the organ of Corti after 24 h. (D) Confocal image of the organ of Corti after application of cat-PEG. Source*: Adapted with permission from Yang, K.-J., Son, J., Jung, S.Y., Yi, G., Yoo, J., Kim, D.-K., et al., 2018. Optimized phospholipid-based nanoparticles for inner ear drug delivery and therapy. Biomaterials 171, 133–143.*

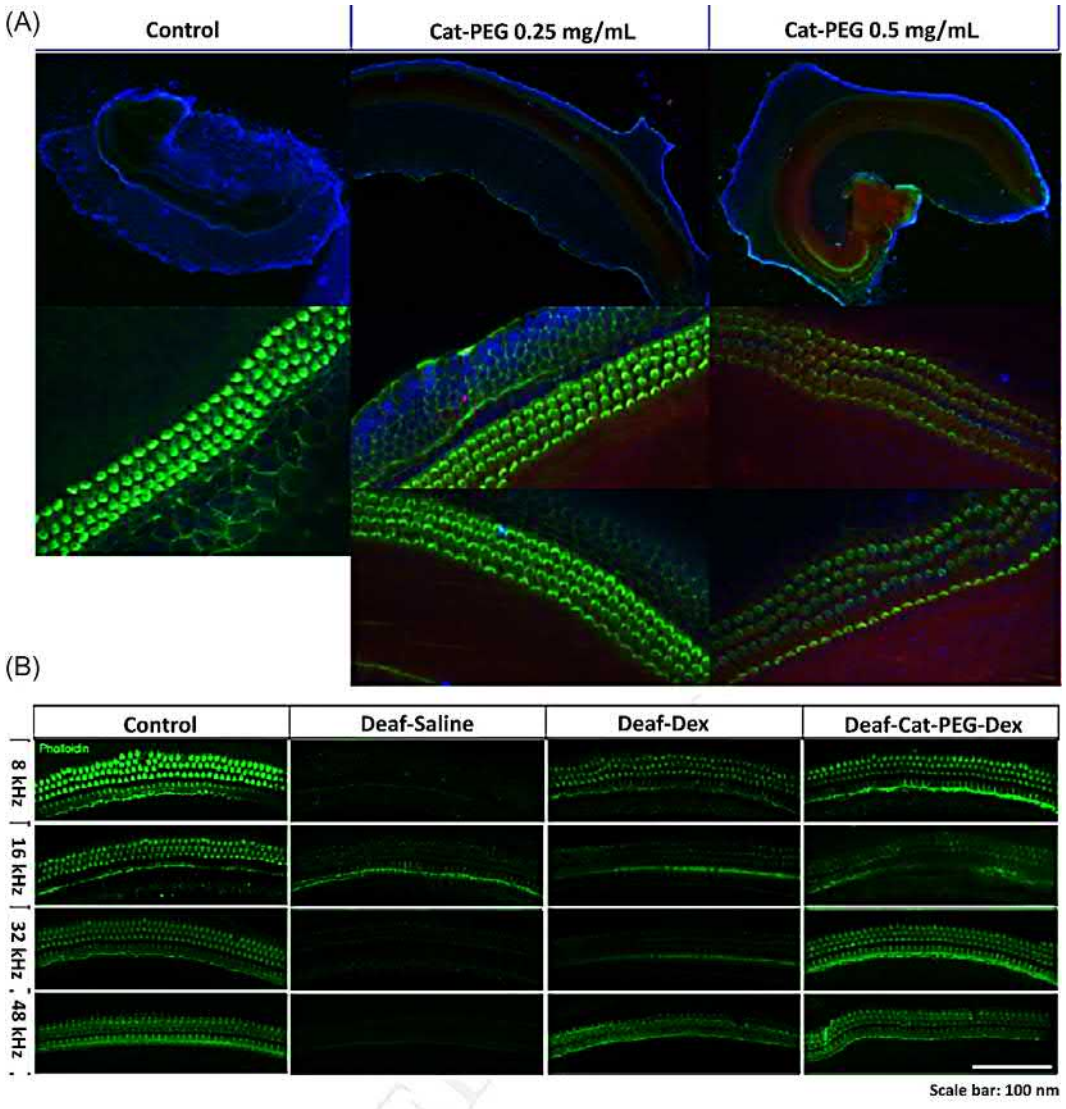

FIGURE 17.9 (A) Cat-PEG nanoparticle absorption through organoleptic culture after 24 h of implantation. Morphology of cilia of the hair cell remained intact after treatment. Nile red dye was absorbed more by 0.5 mg/mL than by the 0.25 mg/mL group and improved absorption of dye on organotypic cell culture. (B) Loss of stereocilia and hair cells in whole-mount organs of Corti of the Deaf-saline group but in Deaf-Cat-PEG-Dexamethasone group showed little damage at the 16-kHz site, and the other sites were as well conserved as those of the control group. Source*: Adapted with permission from Yang, K.-J., Son, J., Jung, S.Y., Yi, G., Yoo, J., Kim, D.-K., et al., 2018. Optimized phospholipid-based nanoparticles for inner ear drug delivery and therapy. Biomaterials 171, 133–143.*

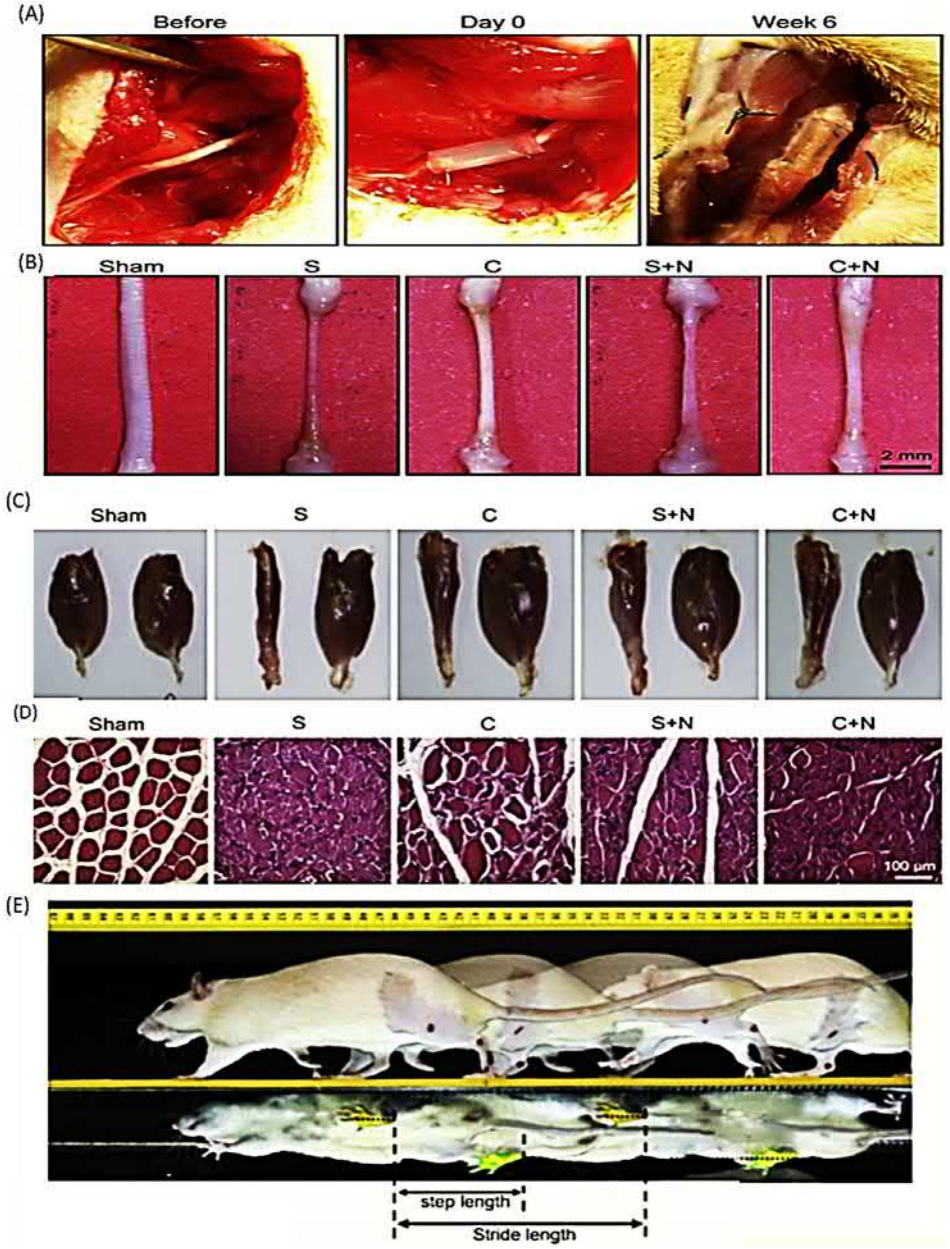

FIGURE 17.10 Renewal in rat model of sciatic nerve transection. (A) (Left) Exploration of sciatic nerve from spinal cord to sciatic notch, (middle) 10-mm gap was generated chitosan coated silicon conduit was inserted, (right) after 6-week nerve generation was observed. (B) Sciatic nerve regeneration model sham as a control, silicon as S conduit, chitosan coated conduit as C, neurosphere cells and silicon conduit as a S + N, neurosphere cells, and chitosan coated silicon conduit denoted as a C + N. (C) The gastrocnemius muscles of both hindlimbs were collected 6 weeks after implantation. (D) H&E staining exposed that the muscle fiber atrophied in the S group. (E) Dynamic gait analysis through functional assessment. The step and stride lengths were attained by means of a high-speed video recording system to detect the rats during various treatments for 1, 3, and 6 weeks. Source: *Adapted with permission from Hsueh, Y.-Y., Chang, Y.-J., Huang, T.-C., Fan, S.-C., Wang, D.-H., Chen, J.-J.J., et al., 2014. Functional recoveries of sciatic nerve regeneration by combining chitosan-coated conduit and neurosphere cells induced from adipose-derived stem cells. Biomaterials 35 (7), 2234–2244.*

17.4 IMMOBILIZATION OF BIOMOLECULE ON A SURFACE OF BIOMATERIALS

Immobilization of biomolecules can be done via hydrophobic interaction, ionic interaction or covalent interaction where the attachment occurs at the activated groups. The noncovalent interaction may also occur but has a major limitation of passive adsorption (Zhou et al., 2016). Thus, the best technique is covalent interaction as it leads to higher stability as well as reduces the chances of nonspecific adsorption. Immobilization reactions possess several characteristics wherein the reaction required should occur rapidly and hence requires a lower amount of reagent (Guo et al., 2004). The chemistry used should maximize the number of compounds that can be generated by solid phase synthesis and the ligands chosen should have a proper orientation and should be homogeneous. This process should occur in the presence of common functional groups like amines, thiols, carboxylic acids, and alcohols.

17.4.1 Physical Adsorption

Physical adsorption occurs with the help of covalent modification, which helps in the efficient coating of biomolecules through their attachment to the scaffold surface exposing the specific functional groups (Repka and McGinity, 2000). Thus, first there is exposure of functional group, and then covalent binding of biomolecules to the functional group occurs. Mostly for this carboxyl, as well as amine groups, are used. Polymers like PLLA and PCL have carboxyl groups that tend to undergo hydrolysis (Siparsky et al., 1998).

Apart from covalent binding, other forces like electrostatic interaction, van der Waals interaction, hydrophobic interaction, as well as hydrogen bonds can also be observed. For this purpose, the material should be exposed to air first to increase its hydrophilicity (Zhang et al., 2002). The main advantage of the physical adsorption method is its simplicity; also there is limited damage to the fragile material (Katti et al., 2008). Noncovalent immobilization can also occur based on electrostatic interactions.

For example, the ionic complex of gelatin and transforming growth factor-1 (TGF-1) can be obtained when gelatin microparticles loaded with TGF-1 are encapsulated in oligo (PEG fumarate) hydrogels at pH 7.4. The interactions between gelatin and TGF-1 occur because of negatively charged chemical groups on the gelatin surface and TGF-1 positive charge (Niu et al., 2009; Li et al., 2012).

17.4.2 Chemical Bonding With Biomolecules

Chemical bonding occurs through relatively weak and nonspecific interactions as well as covalent binding to the specific functional groups. This process can lead to permanent immobilization at high density and in a specific orientation (Yoshida et al., 2000; Costa et al., 2011). It is one of the most widely used methods for immobilization. Chemical binding provides a powerful link and allows reuse of material more often than with other available immobilization methods and prevents biomolecules from being released into the reaction environment (Gentile et al., 2014).

The method also increases the half-life and thermal stability of molecules when coupled with different supports like mesoporous silica, chitosan, etc. (Gaur et al., 2006). The conferred stability comes from unlimited covalent binding, which occurs as well as localization of the biomolecule on the surface of the support, further enhancing its attachment as well as binding. Activity after covalent bonding depends on the size and shape of the carrier material, the nature of the coupling method, composition of the carrier material, and specific conditions during coupling (Karplus, 2014). The coupling can be done in two ways: the addition of reactive functional groups to the support without modifications or the modification of the matrix to generate activated groups. In both cases, it is anticipated that the electrophilic groups generated on the support would react with strong nucleophiles on the protein (Bickerstaff, 1997).

17.4.3 Physical Entrapment

This is an irreversible method of enzyme immobilization where entrapping is done in the support or inside of the fibers, either in the lattice structure of the material or the membrane (Diaz and Balkus Jr, 1996). This method allows the substrate and products to pass through easily, but it retains the molecule. It is a restriction done within a confined space or network. Typically, entrapment can improve mechanical stability and helps in reducing the denaturing of the material (Svenson, 2015). Thus, encapsulating the material by this method becomes easy and more fruitful. Entrapment is done through a variety of materials including polymers, sol−gels, polymer/sol−gel composites, and other inorganic materials (Wang, 1999). The pore size of support material should be small for proper adsorption. Gelation of polyanionic or polycationic polymers can be done to increase the feasibility of this method (Won et al., 2005).

It is possible to use the following polymers as a matrix: alginate, carrageenan, collagen, polyacrylamide, gelatin, silicon rubber, polyurethane and polyvinyl alcohol with styrylpyridinium group. However, this method causes mass transfer of substrate or analytes and can cause leakage when the pores of the support matrix are too large. Apart from this, deactivation, low loading capacity, and abrasion of support material are other disadvantages of this method. Also, the ratio of immobilized particle size to the support material pore size is a significant factor to be considered for the usability of ready probes (Zhu et al., 2005).

17.4.4 Chemical Modification

Surface modification can be also done via chemical methods that involve the physicochemical interactions between the biomaterial and the biomolecule (Nanci et al., 1998). Currently, it is one of the most useful techniques for immobilization. This type of modification helps to change the physical as well as chemical properties of surfaces to improve the functionality of the original material. Surface hydrophobicity or hydrophilicity of a material can be altered via this method. Addition of various functional groups like −COOH, −OH, $-CH_3$, etc. helps in altering the chemical properties of the biomaterial. However, for this type of modification, the surface must itself be able to be chemically modified so that it can provide reactive groups for the subsequent immobilization steps (Kam et al., 2002).

17.5 TECHNIQUES TO ASSESS THE BIOCOMPATIBILITY OF POLYMERS

17.5.1 In Vitro Testing

As the current market for biomaterials is on the rise and to fulfill the ever-increasing demand many preclinical studies have been done (Jandt, 2007). However, in doing so to implement Russell and Burch's 3R aspect, reliable in vitro tests are to be done, so that significant amount of animal numbers could be reduced (Noviana et al., 2016). Most of the time a poor in vitro and in vivo correlation leads to heavy losses and thus calls for a suitable in vitro test (Hulsart-Billström et al., 2016).

However, in the present scenario, the classic standard to assess the material-induced native tissue responses which are observed after grafting a biomaterial is based on preclinical studies [ISO 10993−6:2007, Part 6] (Geetha et al., 2012; Walker et al., 2013). On the other hand, in vitro tests requires a short-term screening to observe any probable acute effects of blood−biomaterial interaction [ISO 10993−4:2002, Part 4] (Bian et al., 2018). However, a scanty test condition results in a poor in vitro in vivo correlation. Also, during in vitro studies it must be ensured that obtained results are not biased by the test conditions or performance of the experimental setup.

One study was done by Jannasch et al. wherein the aim was to identify testing that could be more reliable and could be effective in cutting down the cost as well as time (Jannasch et al., 2017). Authors showed how critically sensitive in vitro biomaterial evaluation is based on human primary macrophages and also depends on test conditions. Authors employed glass, titanium, PTFE, silicone, and polyethylene material on behalf of a specific material that has a tendency to induce fibrotic response. Under the native plasma test conditions, authors claimed to have higher accuracy when compared with in vivo assessments, strengthening a biomimetic three-dimensional in vitro test platform (Jannasch et al., 2017).

17.5.2 Ex Vivo Testing

As mentioned, before the use of a biomaterial it is important to check for its in vitro applicability in cell line so that a good prediction can be made for its in vivo applicability. Thus, to further mimic the in vivo conditions ex vivo studies could also be employed. Ex vivo studies are nothing but the organ/tissue of the desired, or targeted organism isolated and employed for study purposes under the same physiological conditions mimicked in in vitro conditions (Kutty et al., 2015). In Ex vivo studies, the biomaterial actually comes in contact with the tissues, thereby moving a step ahead in mimicking the in vivo conditions, which helps in making an even clearer judgment whether to proceed with the material for in vivo application or not (Roque et al., 2018).

The most widely employed evaluation parameters to check the compatibility of the biomaterials for in vivo applications are the cellular cytotoxicity, hemocompatibility, and blood clotting time. These will be discussed in the following sections.

17.5.2.1 Cytotoxicity Test

It is mandatory for the biomaterial employed for constructing any in vivo inserts or devices to be compatible with the physiological system, that is, it should not elicit any signs of inflammation, cytotoxicity, or others signs of noncompliance (Bélanger and Marois, 2001). The situation becomes more critical in the case of metallic biomaterials like Ti alloys. One such study was performed by Donato et al., who developed an in vitro experiment to check the cytotoxicity as well as guide the selection of Ti-alloys as per the outcome of cytotoxicity assay done using 3-(4,5-dimethylthiazol-2-yl)-2,5-diphenyltetrazolium bromide (MTT) (Donato et al., 2009).

In this, two types of determination were done, that is, by direct method and indirect method. In the direct method, Vero cells with a density of 2×105 cell/well were seeded on Ti discs alloys, which were already placed in a 96-well microplate, followed by 48 hours of incubation. In the indirect method an extract of alloys obtained from 1 g of material was incubated with 10 mL of culture media followed by 48 hours incubation, followed by seeding in 96-well plates (Donato et al., 2009). Using both methods MTT test was performed and the results obtained are shown in Fig. 17.11A and B. Also, scanning electron microscope (SEM) analysis of the Vero cells was done, which were incubated with two alloys, that is, TNZ (Ti−13Nb−13Zr) alloy and TNZT (Ti−35Nb−7Zr−5Ta) alloy and cell morphology was observed for any kind of debris as shown in Fig. 17.11C−H.

Thus, Donato et al. concluded that both indirect and direct cytotoxicity tests showed no toxic effects for any of the alloy. Moreover, the biocompatibility testing done using SEM for TNZ (Ti−13Nb−13Zr) alloy and TNZT (Ti−35Nb−7Zr−5Ta) alloy showed complete compatibility with no changes in morphology (Donato et al., 2009).

Ghorbani et al. checked the biocompatibility of injectable hydrogel as a newly developed biomaterial to be used as a scaffold for intervertebral disc regeneration. The toxicity of the gel comprising of Chitosan-β glycerophosphate−hyaluronic acid, Chondroitin-6-sulfate, type 2 collagen, gelatin, fibroin silk, which is commonly termed NP (nucleus pulpous) hydrogel, as well as several other parameters were evaluated such as storage modulus, gelation time, and rheological properties (Ghorbani et al., 2017).

However, the cytotoxicity tests, that is, MTT and trypan blue test showed the good compatibility of developed hydrogel with NP human cells. Thereby suggesting that NP hydrogel could be a choice as an injectable scaffold to be used for intervertebral disc regeneration. Thus cytotoxicity studies are considered to be amongst the most widely recognized investigations as to compatibility issue that is usually associated with the use of biomaterial (Ghorbani et al., 2017).

17.5.2.2 Hemocompatibility

Hemocompatibility is an essential aspect for the biomaterials intended to be delivered inside the body, primarily when the material is meant to come in contact with blood for a long period (Mao et al., 2004). As there are many elements residing in the blood that can either get ruptured or activated, leading to coagulation emboli formation and eventually

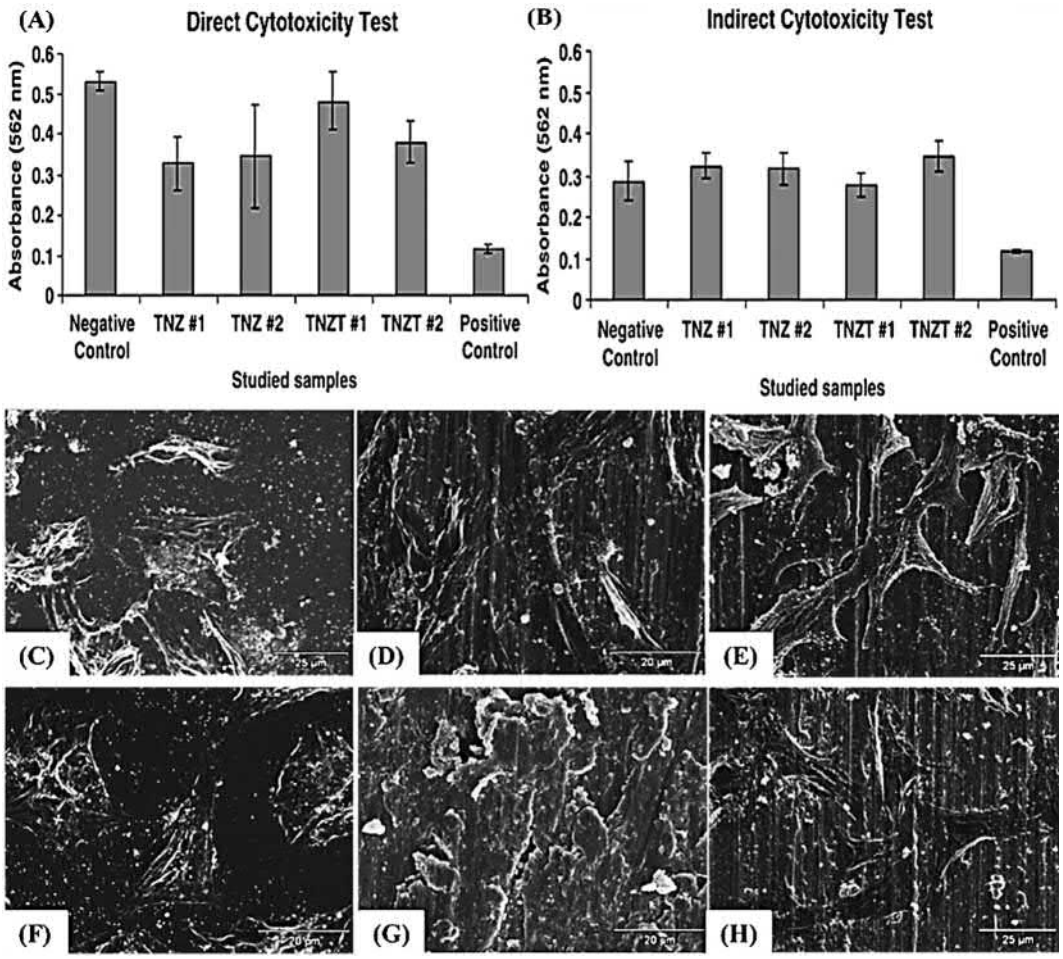

FIGURE 17.11 Cytotoxicity estimation of Ti alloys using MTT. (A) Absorbance of the formazan crystals obtained after MTT using the direct method as mentioned. (B) The absorbance is seen in the MTT assay using an indirect method to detect cytotoxicity. (C–E) SEM images of TNZ (Ti–13Nb–13Zr) alloy surface after 48 h where (C) is the control (glass plate), (D) is the as-received sample, and (E) is the sample after heat treatment. Analysis to check for any change in cell morphology. (F–H) SEM images of TNZT (Ti–35Nb–7Zr–5Ta) alloy; (F) is the control (glass plate), (G) is the as-received sample, (H) is the after heat treatment sample. *MTT*, 3-(4,5-Dimethylthiazol-2-yl)-2,5-diphenyltetrazolium bromide. Source*: Adapted with permission from Donato, T.A., de Almeida, L.H., Nogueira, R.A., Niemeyer, T.C., Grandini, C.R., Caram, R., et al., 2009. Cytotoxicity study of some Ti alloys used as biomaterial. Mater. Sci. Eng.: C 29 (4), 1365–1369 © Elsevier 2009.*

death (Seyfert et al., 2002), thus, it is recommended to incorporate hemocompatibility tests for the majority of biomaterials. For example, Sezer et al. developed a core–shell electrospun structure made of PS at the core and sulfonated PS in the shell and checked its hemocompatibility first to further process the development of electrospun construct (Sezer et al., 2018).

Although PS has been used in several components, its hemocompatibility is yet not well defined, thus an attempt was made by the authors to check its hemocompatibility. The authors assessed % hemolysis, platelet adhesion via SEM analysis, plasma recalcification profile, and turnaround time values to estimate the thrombin generation levels as shown in Fig. 17.12 (Sezer et al., 2018).

17.5.3 In Vivo Techniques to Assess the Biocompatibility of Polymers

17.5.3.1 Alanine Aminotransferase

Alanine aminotransferase (ALT) is an enzyme found mostly in liver cells. Apart from the liver, it is also found in heart and muscle cells. The function of ALT is to convert

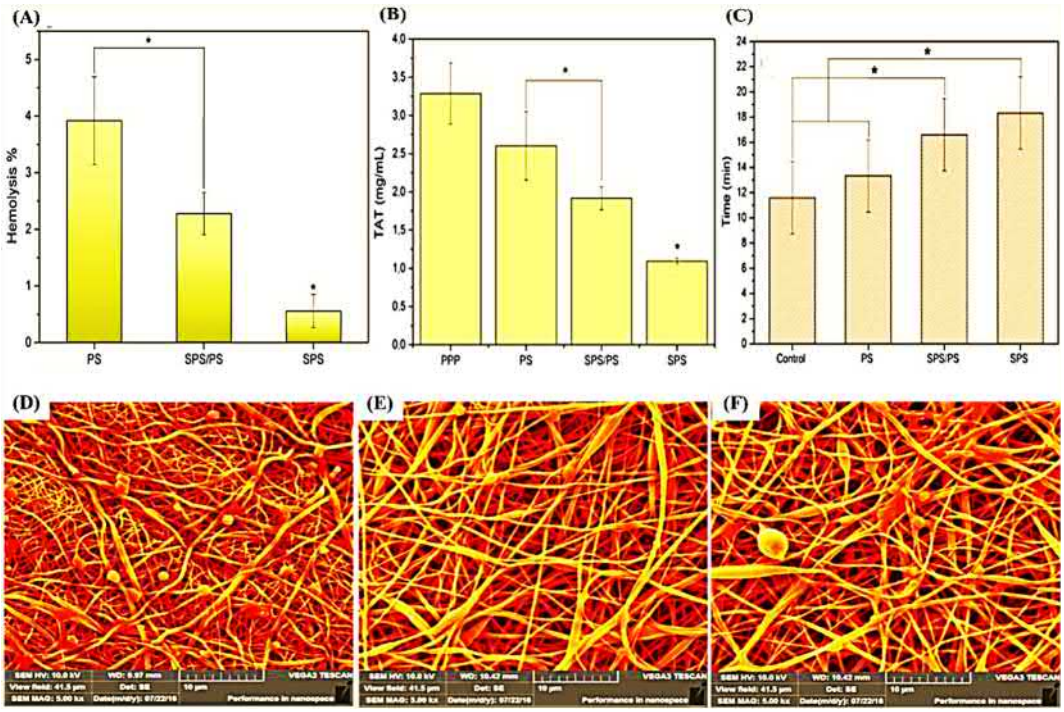

FIGURE 17.12 Hemocompatibility testing for electrospun fibers of PS. (A) % Hemolysis seen for SPS was lowest although no significant difference between SPS/SP and SPS was observed. (B) Least TAT value was observed only for SPS when compared with PS and SPS/PS, but SPS/PS showed lower TAT regeneration value when compared with PS, although PS showed the nonsignificant difference with PPP. (C) Plasma recalcification was observed to be similar with no significant difference between SPS/PS and PS, and thus, less coagulative than PS. (D–F) SEM images with color showing. (D) Most intensive pellet adhesion was observed with PS. (E and F) No significant pellet adhesion was observed with SPS/PS and SPS respectively. Thus, surface hydrophilicity can remarkably reduce the platelet adhesion. *PPP*, Platelet poor plasma; *SPS*, sulfonated polysulfone; *TAT*, turnaround time. Source: *Reproduced with permission from Sezer, U.A., Ozturk, K., Aru, B., Demirel, G.Y., Sezer, S., 2018. A design achieved by coaxial electrospinning of polysulfone and sulfonated polysulfone as a core-shell structure to optimize mechanical strength and hemocompatibility. Surf. Interfaces 10, 176–187* © *Elsevier 2018.*

alanine into pyruvate, for cellular energy production (Chen et al., 2004). Thus, the ALT test is performed to measure its level, particularly in the case when biopolymer is applied within the body. Generally, the ALT level is quite low in the case of healthy individuals. In case of illness of liver like jaundice or hepatitis, ALT gets released into the blood. Thus, ALT is considered to be a useful test for early detection of liver damage (Lin et al., 2008).

ALT is commonly tested in conjunction with aspartate-aminotransferase (AST), another liver enzyme, as a part of a liver panel. Both ALT and AST levels usually rise whenever the liver is being damaged, although ALT is more specific for the liver and, in some cases, may be the only one of the two to be increased. An AST/ALT ratio may be calculated to aid in distinguishing between different causes and severity of liver injury and to help distinguish liver injury from damage to heart or muscles (Lin et al., 2008; Sagir et al., 2008).

The level of ALT in healthy males is 7–55 U/L, and for females, it is 7–45 U/L. Elevated ALT values are seen in liver diseases characterized by hepatocyte destruction. 10 times increment in the values is observed. Levels may reach values as high as 100 times the upper reference limit, although 20- to 50-fold elevations are most frequently encountered (Lai et al., 2007). Thus, it helps to measure the damage caused by the liver when the body is exposed to a polymeric material. If huge increment in the ALT level is observed, then critical measures are required before giving it to the individual (Ohgo et al., 2009).

17.5.3.2 *Alanine Transaminase*

Aspartate aminotransferase (AST) is an enzyme found mostly in the liver, but it is present in muscles also. When the liver is damaged, it releases AST into the bloodstream. An AST blood test measures the amount of AST in the blood and hence is useful in finding liver damage (Giboney, 2005). During the AST test, a blood sample is withdrawn from the vein in the arm, using a small needle. After the needle inserted, a small amount of blood will be collected into a test tube or vial. High levels of AST in the blood may indicate hepatitis, cirrhosis, mononucleosis, or other liver diseases. High AST levels can also indicate heart problems or pancreatitis (Tenner et al., 1994). The results of the test are generally constant, but can change due to age, gender, diet, as well as the medicines taken by the person. The ratio of ALT:AST is also calculated to identify liver damage. The value is generally higher in case of liver disorder. Thus, in the case of external applications of any kind of biopolymer, the levels of AST get increased, which indicates its direct effect on the liver (Nyblom et al., 2004).

17.5.3.3 *Blood Urea Nitrogen*

Blood urea nitrogen (BUN) is used to find the effective functioning of kidneys. Increased BUN may be due to prerenal causes comprising of cardiac decompensation, water depletion due to decreased intake or due to excessive loss of water. It may also be due to renal causes like acute glomerulonephritis, chronic nephritis, polycystic kidney disease, nephrosclerosis, and tubular necrosis and due to some postrenal causes like stones or tumors. Generally, the reference value for the same in the case of both males and females is 7–20 mg/dL. This test is quite sensitive and is used in adjunct to the normal serum

creatinine test to determine the kidney function (Aronson et al., 2004). This test again plays a very significant role in determining the effective kidney functioning as the value can get altered when biopolymers are used. If the value occurs in the normal range, then it clearly indicates the biocompatibility of the polymer within the human body (Karadağ et al., 1996).

17.6 EFFECT OF SURFACE MODIFICATION OF BIOMATERIALS FOR BIOCOMPATIBILITY

Modification of the surface of the biomaterial is done for alteration in its nature to improve its use in biomedical applications as well as biocompatibility (Bose et al., 2018).

17.6.1 Influence of Protein-Modified Surface

Protein adsorption is the first event that happens after implantation of the biomaterial. The protein adsorbed surface mediates the surface for easy anchoring as well as determines the type of tissue that ultimately develops (Schmidt et al., 2009). This type involves the fundamentals of physicochemical interactions between the biomaterial and the physiological environment at the molecular, cellular, and tissue levels. Currently, there are various methods available for the surface modification of biomaterials, the applications of which are primarily based on the fundamental properties of the surface modifying material. Protein surface modification of different types of biomaterials (ceramics, polymers, metals, composites) is performed to increase biocompatibility of the material ultimately and to interact as a bioactive material for specific applications (Randon et al., 1995; Kenausis et al., 2000; Eitan et al., 2003). In various biomedical applications of developing implantable medical devices (such as pacemakers and stents), surface properties/interactions of proteins with a specific material must be evaluated with regard to biocompatibility as it plays a major role in determining a biological response (Eitan et al., 2003). For instance, surface hydrophobicity or hydrophilicity of a material can be altered. Engineering biocompatibility between the physiological environment and the surface material allows development of new medical products with additional biofunctionality (Bauer et al., 2013).

Surface modification of biomaterials also improves the possible physicochemical interactions between the biomaterials and the physiological environment at the molecular, cellular, and tissue levels (Walkey and Chan, 2012). However, the major functions of protein modification on biomaterials are to improve cell adhesion and to suffice other properties like preventing corrosion, elemental functionalization with calcium, nitrogen, and sodium to improve the biocompatibility of the material (Shen and Horbett, 2001).

One such study was done by Khan et al. wherein stainless steel was coated with bovine serum albumin (BSA) to improve its biocompatibility (Khan et al., 2007). In this process, authors produced monomer by hydrolyzing 1-(2-cyanoethyl) pyrrole so as to form 1-(2-carboxyethyl) pyrrole, which was further activated using *N*-hydroxysuccinimide to *N*-succinimidyl ester pyrrole, which was electrosprayed on the steel plate to form

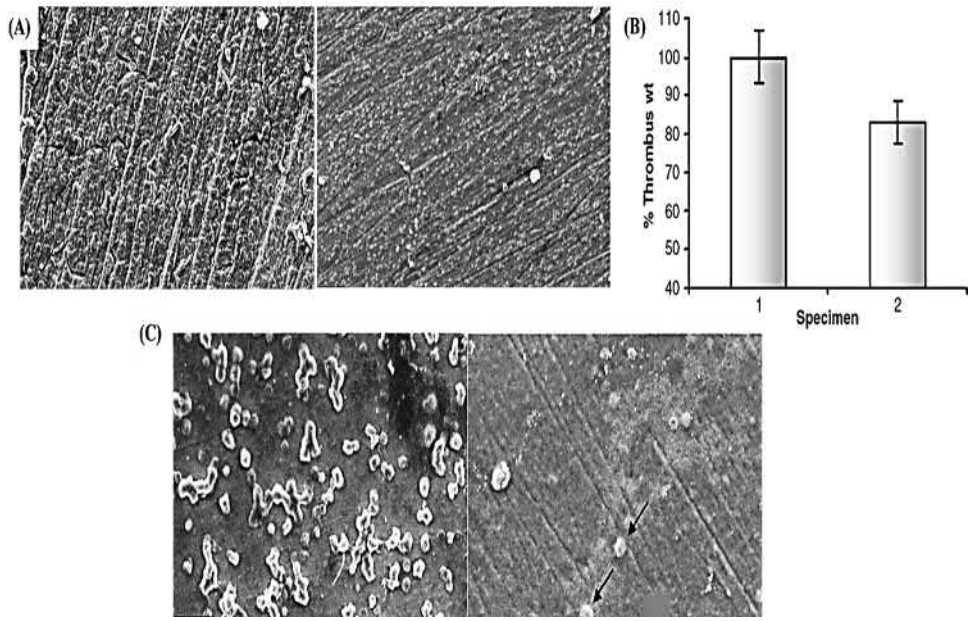

FIGURE 17.13 Stainless steel surface modification with bovine serum albumin to increase compatibility. (A) SEM image of unmodified stainless steel (316 L) rough surface and BSA modified the smooth surface of the same. (B) Percentage of thrombus formation upon administration of uncoated (specimen 1) and coated stainless steel (specimen 2). (C) SEM images of platelets adhered on the uncoated and BSA coated stainless steel surfaces. *BSA*, Bovine serum albumin. Source*: Adapted with permission from Khan, W., Kapoor, M., Kumar, N., 2007. Covalent attachment of proteins to functionalized polypyrrole-coated metallic surfaces for improved biocompatibility. Acta Biomater. 3 (4), 541–549* © *Elsevier 2007.*

adherent surface. Onto this adherent surface, BSA was attached, which was confirmed through SEM and IR spectroscopy. The resulting functionalized formulation showed a higher degree of compatibility regarding enhanced hemocompatibility, less thrombus formation, and less platelet adhesion on the surface, as shown in Fig. 17.13 (Khan et al., 2007).

Modification of the surface of the biomaterial helps in improving its use in biomedical applications as well as its biocompatibility. For this modification, various physical as well as chemical methods are used as well as explored. The chemical modifications are mainly used (Webster et al., 2000) and are described in below in this section.

17.6.2 Influence of Surface Functional Groups on Cellular Responses

Activation of the immune system in the body is the first thing that happens after insertion of biomaterial in the body. The proteins surround the implant try to hide it from the innate immune system (Tang et al., 2008). However, if the protein is allergenic, then adaptive immunity in the patient gets initiated. Acute inflammation gets initiated, which results in redness, swelling, heat, pain, and loss of function. Hemorrhaging can also occur due to

the presence of latent mast cells. The mast cells release chemokines, which activate blood vessel endothelium. Dilation of the blood vessels happens, which makes them leaky, producing the redness and swelling associated with acute inflammation (Franz et al., 2011). The activated endothelium releases macrophages, which release oxidants to combat the foreign body. However, if the antioxidants don't get activated, then chronic inflammation begins (Franz et al., 2011). Implantation of nondegradable materials will eventually result in chronic inflammation and fibrous capsule formation (Franz et al., 2011; Daghighi et al., 2013). Macrophages that fail to destroy pathogens will merge to form a foreign-body giant cell that quarantines the implant. High levels of oxidants cause fibroblasts to secrete collagen, forming a layer of fibrous tissue around the implant (Ravi and Aliyar, 2006).

17.6.3 Carboxyl (−COOH) Functional Group-Bearing Surface

Biomaterial-bearing −COOH brings negative charge to the surface of biomaterials (Lee et al., 2006). It has been proven that fibronectin and albumin are more easily eluted from surfaces coated with −COOH (Tang et al., 2008). Apart from this, the surfaces with −COOH terminals show a marked increment in cell growth. However, this phenomenon depends on the concentration of −COOH on the surface based on the fact that increment of functional group density results in a higher negative charge on the surface, which helps to inhibit cell growth. On the other hand, −COOH also mediates and inhibits osteoblast differentiation and mineralization. −COOH surfaces decrease the myoblast differentiation through cell proliferation levels were high (Hudson et al., 2008).

17.6.4 Hydroxyl (−OH) Functional Group−Coated Surfaces

The hydroxyl group functionality (−OH) represents a neutral and hydrophilic surface. This type of surface functionality gives an idea that increment of the oxygen-containing groups is directly proportional to cell growth (Sperling et al., 2005). −OH, functional groups also increase cell adhesion strength as well as increase levels of structural signaling components related to focal adhesions (Barrias et al., 2009; Faucheux et al., 2004). Further investigation with osteoblasts showed high levels of differentiation and mineralization with −OH functionality as opposed to other functional groups. Rather contradictory, −OH functionality has been shown to have reduced plasma protein adsorption and thus higher platelet compatibility. The charge neutrality as well as the hydrophilic nature of the −OH functionality decreases its affinity toward proteins and thus shows protein repelling properties (Archambault and Brash, 2004; Konradi et al., 2008).

17.6.5 Amine ($-NH_2$) Functional Group-Rich Surfaces

Amine group ($-NH_2$) functionality displays a positive charge to the biomaterial surface. Studies have proven that $-NH_2$ surfaces promote the exposure of high density bound receptors as well as focal adhesion components by adsorbed fibronectin. This helps to increase the endothelial cell growth and also helps in enhancing the differentiation as well as mineralization of osteoblast cells. The adhesion, growth, as well as cell differentiation of

fibroblasts on $-NH_2$ surfaces was observed more as compared with other coatings. Formation of focal adhesion plaques that are linked to the cellular surfaces occur later on due to this phenomenon (Lim et al., 2018).

17.6.6 Methyl ($-CH_3$) Functional Group-Bearing Surfaces

The $-CH_3$ group is highly used in the polymeric materials as it provides a hydrophobic surface on biomaterials (Raynor et al., 2009; Polesel-Maris et al., 2012). This type of hydrophobic moiety promotes protein adsorption, which is highly used for desired cellular interactions. It also increases fibrinogen binding and platelet accumulation, and so there are compatibility related issues (Chang et al., 2006; Tegoulia and Cooper, 2002). Fibrinogen, albumin, and IgG bind with the highest strength to the $-CH_3$ bearing surfaces. Overall, these results suggest that CH_3 surfaces can cause surface reactions that may generate several inflammatory cells (Boccafoschi et al., 2014).

17.6.7 Surfaces With Mixed Functionality

Evaluation of mixed functional groups on surfaces is a new area of interest, particularly where the surface is required to be modified for biomedical or therapeutic purposes. Thus, under this phenomenon, favorable properties of different functional groups help in enhancing the overall biocompatibility of the biomaterial composite (Bulpitt and Aeschlimann, 1999). The associated properties of each functional group have equal impact on the properties of the surface. The equimolar ratio of $-NH_2$ (positive charge) and $-COOH$ (negative charge) shows lowest platelet adsorption (Ishihara et al., 1994). This equal proportion of the functionalities brings the neutral charge to the surface of the biomaterials. Thus, in this way, it will help in increasing the hemocompatibility of the utilized polymer with the blood (Holmlin et al., 2001; Motlagh et al., 2006).

17.7 CONCLUSION

Despite the advances made in biomedical engineering, the degree of biocompatibility is quite a significant topic for research and development and is still facing a number of challenges for biomaterials research. To eliminate hurdles in setting up biocompatibility, strategies must be developed that do not cause any harmful reactions such as chronic inflammatory reaction or development of unfamiliar tissues upon interaction of biomaterials with biosurfaces. Thus, the significance of biomaterials with suitable surface characteristic is apparently crucial. Altogether, precise bulk characteristics are vital, mainly mechanical properties for biomaterials to achieve specific effects in the biological environment. The situation manifests that tailoring of biomaterials that accomplish dual requirements might be moderately problematic.

For that, an available method is to construct biomaterials with acceptable bulk characteristics, and subsequent alteration of surface properties using numerous actions. Nevertheless, there is no one method for surface modification approved entirely to

regulate the polymerization as well as biocompatible polymer generation. Plasma and laser ablation methods have been engaged for modification of the surface of polymers, which allows biologically compatible properties in biomaterial. Tissue engineering will alter the fate of biomaterials, using utilization of biomaterials. Also, the regenerative approach of biomaterial will decrease the necessity for synthetic substances for treatment. Though numerous solicitations will need synthetics, we foresee the requirement for biomaterials for several medical applications.

Acknowledgment

The authors would like to acknowledge Science and Engineering Research Board (Statutory Body Established Through an Act of Parliament: SERB Act 2008), Department of Science and Technology, Government of India for grant (Grant # *ECR/2016/001964*) allocated to Dr. Tekade for research work on gene delivery and N-PDF funding to Dr. Maheshwari (PDF/2016/003329) for work on targeted cancer therapy in Dr. Tekade's Laboratory. The authors also acknowledge the support by Fundamental Research Grant (FRGS/1/2015/TK05/IMU/03/1) scheme of Ministry of Higher Education, Malaysia to support research on gene delivery.

References

Abdallah, M.-N., Tran, S.D., Abughanam, G., Laurenti, M., Zuanazzi, D., Mezour, M.A., et al., 2017. Biomaterial surface proteomic signature determines interaction with epithelial cells. Acta Biomater. 54, 150–163.

Archambault, J.G., Brash, J.L., 2004. Protein repellent polyurethane-urea surfaces by chemical grafting of hydroxyl-terminated poly(ethylene oxide): effects of protein size and charge. Colloids Surf. B: Biointerfaces 33 (2), 111–120.

Aronson, D., Mittleman, M.A., Burger, A.J., 2004. Elevated blood urea nitrogen level as a predictor of mortality in patients admitted for decompensated heart failure. Am. J. Med. 116 (7), 466–473.

Banerjee, J., Azevedo, H.S., 2017. Crafting of functional biomaterials by directed molecular self-assembly of triple helical peptide building blocks. Interface Focus 7 (6), 20160138.

Barrias, C.C., Martins, M.C.L., Almeida-Porada, G., Barbosa, M.A., Granja, P.L., 2009. The correlation between the adsorption of adhesive proteins and cell behaviour on hydroxyl-methyl mixed self-assembled monolayers. Biomaterials 30 (3), 307–316.

Bauer, S., Schmuki, P., von der Mark, K., Park, J., 2013. Engineering biocompatible implant surfaces: Part I: Materials and surfaces. Prog. Mater. Sci. 58 (3), 261–326.

Bélanger, M.C., Marois, Y., 2001. Hemocompatibility, biocompatibility, inflammatory and in vivo studies of primary reference materials low-density polyethylene and polydimethylsiloxane: a review. J. Biomed. Mater. Res., A 58 (5), 467–477.

Bian, Y.-Y., Zhou, L., Zhou, G., Jin, Z.-M., Xin, S.-X., Hua, Z.-K., et al., 2018. Study on biocompatibility, tribological property and wear debris characterization of ultra-low-wear polyethylene as artificial joint materials. J. Mech. Behav. Biomed. Mater. 82, 87–94.

Bickerstaff, G.F., 1997. Immobilization of enzymes and cells. Immobilization of Enzymes and Cells. Springer.

Bissadi, G., Weberskirch, R., 2016. Formation of polyoxazoline-silica nanoparticles via the surface-initiated cationic polymerization of 2-methyl-2-oxazoline. Polym. Chem. 7 (32), 5157–5168.

Boccafoschi, F., Mosca, C., Cannas, M., 2014. Cardiovascular biomaterials: when the inflammatory response helps to efficiently restore tissue functionality? J. Tissue Eng. Regenerative Med. 8 (4), 253–267.

Bose, S., Robertson, S.F., Bandyopadhyay, A., 2018. Surface modification of biomaterials and biomedical devices using additive manufacturing. Acta Biomater. 66, 6–22.

Bulpitt, P., Aeschlimann, D., 1999. New strategy for chemical modification of hyaluronic acid: preparation of functionalized derivatives and their use in the formation of novel biocompatible hydrogels. J. Biomed. Mater. Res., A 47 (2), 152–169.

Carpentier, A., Latrémouille, C., Cholley, B., Smadja, D.M., Roussel, J.-C., Boissier, E., et al., 2015. First clinical use of a bioprosthetic total artificial heart: report of two cases. Lancet 386 (10003), 1556–1563.

Chang, Y., Chen, S., Zhang, Z., Jiang, S., 2006. Highly protein-resistant coatings from well-defined diblock copolymers containing sulfobetaines. Langmuir 22 (5), 2222–2226.
Chen, F.-M., Liu, X., 2016. Advancing biomaterials of human origin for tissue engineering. Prog. Polym. Sci. 53, 86–168.
Chen, H.-T., Neerman, M.F., Parrish, A.R., Simanek, E.E., 2004. Cytotoxicity, hemolysis, and acute in vivo toxicity of dendrimers based on melamine, candidate vehicles for drug delivery. J. Am. Chem. Soc. 126 (32), 10044–10048.
Cooper, B.G., Nazarian, A., Snyder, B.D., Grinstaff, M.W., 2018. Active agents, biomaterials, and technologies to improve biolubrication and strengthen soft tissues. Biomaterials 181, 210–226.
Costa, F., Carvalho, I.F., Montelaro, R.C., Gomes, P., Martins, M.C.L., 2011. Covalent immobilization of antimicrobial peptides (AMPs) onto biomaterial surfaces. Acta Biomater. 7 (4), 1431–1440.
Cross, M.C., Toomey, R.G., Gallant, N.D., 2016. Protein-surface interactions on stimuli-responsive polymeric biomaterials. Biomed. Mater. 11 (2), 022002.
Cui, M., Song, Z., Wu, Y., Guo, B., Fan, X., Luo, X., 2016. A highly sensitive biosensor for tumor maker alpha fetoprotein based on poly(ethylene glycol) doped conducting polymer PEDOT. Biosens. Bioelectron. 79, 736–741.
Daghighi, S., Sjollema, J., van der Mei, H.C., Busscher, H.J., Rochford, E.T., 2013. Infection resistance of degradable versus nondegradable biomaterials: an assessment of the potential mechanisms. Biomaterials 34 (33), 8013–8017.
Diaz, J.F., Balkus Jr, K.J., 1996. Enzyme immobilization in MCM-41 molecular sieve. J. Mol. Catal. B: Enzym. 2 (2–3), 115–126.
Donato, T.A., de Almeida, L.H., Nogueira, R.A., Niemeyer, T.C., Grandini, C.R., Caram, R., et al., 2009. Cytotoxicity study of some Ti alloys used as biomaterial. Mater. Sci. Eng.: C 29 (4), 1365–1369.
Dworak, A., Trzebicka, B., Kowalczuk, A., Tsvetanov, C., Rangelov, S., 2014. Polyoxazolines-mechanism of synthesis and solution properties. Polimery 59 (1), 88–94.
Eitan, A., Jiang, K., Dukes, D., Andrews, R., Schadler, L.S., 2003. Surface modification of multiwalled carbon nanotubes: toward the tailoring of the interface in polymer composites. Chem. Mater. 15 (16), 3198–3201.
Faucheux, N., Schweiss, R., Lützow, K., Werner, C., Groth, T., 2004. Self-assembled monolayers with different terminating groups as model substrates for cell adhesion studies. Biomaterials 25 (14), 2721–2730.
Franz, S., Rammelt, S., Scharnweber, D., Simon, J.C., 2011. Immune responses to implants—a review of the implications for the design of immunomodulatory biomaterials. Biomaterials 32 (28), 6692–6709.
Gallagher, E.S., Adem, S.M., Bright, L.K., Calderon, I.A., Mansfield, E., Aspinwall, C.A., 2014. Hybrid phospholipid bilayer coatings for separations of cationic proteins in capillary zone electrophoresis. Electrophoresis 35 (8), 1099–1105.
Gaur, R., Pant, H., Jain, R., Khare, S., 2006. Galacto-oligosaccharide synthesis by immobilized Aspergillus oryzae β-galactosidase. Food Chem. 97 (3), 426–430.
Geetha, C., Sabareeswaran, A., Mohanan, P., 2012. Pre-clinical evaluation of titanium nitride coated titanium material. Toxicol. Mech. Methods 22 (2), 144–150.
Gensel, J.C., Zhang, B., 2015. Macrophage activation and its role in repair and pathology after spinal cord injury. Brain Res. 1619, 1–11.
Gentile, P., Chiono, V., Carmagnola, I., Hatton, P.V., 2014. An overview of poly(lactic-*co*-glycolic) acid (PLGA)-based biomaterials for bone tissue engineering. Int. J. Mol. Sci. 15 (3), 3640–3659.
Ghorbani, M., Ai, J., Nourani, M.R., Azami, M., Beni, B.H., Asadpour, S., et al., 2017. Injectable natural polymer compound for tissue engineering of intervertebral disc: in vitro study. Mater. Sci. Eng.: C 80, 502–508.
Giboney, P.T., 2005. Mildly elevated liver transaminase levels in the asymptomatic patient. Am. Fam. Phys. 71 (6), 1105–1110.
Guidoin, R., Snyder, R., Martin, L., Botzko, K., Marois, M., Awad, J., et al., 1984. Albumin coating of a knitted polyester arterial prosthesis: an alternative to preclotting. Ann. Thorac. Surg. 37 (6), 457–465.
Guo, M., Chen, J., Liu, D., Nie, L., Yao, S., 2004. Electrochemical characteristics of the immobilization of calf thymus DNA molecules on multi-walled carbon nanotubes. Bioelectrochemistry 62 (1), 29–35.
Han, D.K., Park, K., Park, K.D., Ahn, K.D., Kim, Y.H., 2006. In vivo biocompatibility of sulfonated PEO-grafted polyurethanes for polymer heart valve and vascular graft. Artif. Organs 30 (12), 955–959.
He, W., Benson, R., 2017. Polymeric biomaterials, Applied Plastics Engineering Handbook, second edition Elsevier.

Holmlin, R.E., Chen, X., Chapman, R.G., Takayama, S., Whitesides, G.M., 2001. Zwitterionic SAMs that resist nonspecific adsorption of protein from aqueous buffer. Langmuir 17 (9), 2841–2850.
Horbett, T.A., 2018. Fibrinogen adsorption to biomaterials. J. Biomed. Mater. Res., A 106, 2777–2788.
Horvathy, D.B., Vacz, G., Szabó, T., Szigyarto, I.C., Toro, I., Vamos, B., et al., 2016. Serum albumin coating of demineralized bone matrix results in stronger new bone formation. J. Biomed. Mater. Res., B: Appl. Biomater. 104 (1), 126–132.
Hsueh, Y.-Y., Chang, Y.-J., Huang, T.-C., Fan, S.-C., Wang, D.-H., Chen, J.-J.J., et al., 2014. Functional recoveries of sciatic nerve regeneration by combining chitosan-coated conduit and neurosphere cells induced from adipose-derived stem cells. Biomaterials 35 (7), 2234–2244.
Hudson, S.P., Padera, R.F., Langer, R., Kohane, D.S., 2008. The biocompatibility of mesoporous silicates. Biomaterials 29 (30), 4045–4055.
Hulsart-Billström, G., Dawson, J., Hofmann, S., Müller, R., Stoddart, M., Alini, M., et al., 2016. A Surprisingly Poor Correlation Between In Vitro and In Vivo Testing of Biomaterials for Bone Regeneration: Results of a Multicentre Analysis.
Illés, E., Tombácz, E., Szekeres, M., Tóth, I.Y., Szabó, Á., Iván, B., 2015. Novel carboxylated PEG-coating on magnetite nanoparticles designed for biomedical applications. J. Magn. Magn. Mater. 380, 132–139.
Ishihara, K., Inoue, H., Kurita, K., Nakabayashi, N., 1994. Selective adhesion of platelets on a polyion complex composed of phospholipid polymers containing sulfonate groups and quarternary ammonium groups. J. Biomed. Mater. Res., A 28 (11), 1347–1355.
Jandt, K.D., 2007. Evolutions, revolutions and trends in biomaterials science—a perspective. Adv. Eng. Mater. 9 (12), 1035–1050.
Jannasch, M., Gaetzner, S., Weigel, T., Walles, H., Schmitz, T., Hansmann, J., 2017. A comparative multiparametric in vitro model identifies the power of test conditions to predict the fibrotic tendency of a biomaterial. Sci. Rep. 7 (1), 1689.
Jiang, S., Zhang, Z., Chen, S., Vaisocherova, H. 2017. Dual-Functional Nonfouling Surfaces Comprising Target Binding Partner Covalently Coupled to Polymer Attached to Substrate. Google Patents.
Kam, L., Shain, W., Turner, J., Bizios, R., 2002. Selective adhesion of astrocytes to surfaces modified with immobilized peptides. Biomaterials 23 (2), 511–515.
Karadağ, E., Saraydin, D., Çetinkaya, S., Güven, O., 1996. In vitro swelling studies and preliminary biocompatibility evaluation of acrylamide-based hydrogels. Biomaterials 17 (1), 67–70.
Karplus, M., 2014. Development of multiscale models for complex chemical systems: from H + H2 to biomolecules (Nobel lecture). Angew. Chem. Int. Ed. 53 (38), 9992–10005.
Katti, D.S., Vasita, R., Shanmugam, K., 2008. Improved biomaterials for tissue engineering applications: surface modification of polymers. Curr. Topics Med. Chem. 8 (4), 341–353.
Kenausis, G.L., Vörös, J., Elbert, D.L., Huang, N., Hofer, R., Ruiz-Taylor, L., et al., 2000. Poly(L-lysine)-*g*-poly (ethylene glycol) layers on metal oxide surfaces: attachment mechanism and effects of polymer architecture on resistance to protein adsorption. J. Phys. Chem. B 104 (14), 3298–3309.
Khan, W., Kapoor, M., Kumar, N., 2007. Covalent attachment of proteins to functionalized polypyrrole-coated metallic surfaces for improved biocompatibility. Acta Biomater. 3 (4), 541–549.
Konradi, R., Pidhatika, B., Mühlebach, A., Textor, M., 2008. Poly-2-methyl-2-oxazoline: a peptide-like polymer for protein-repellent surfaces. Langmuir 24 (3), 613–616.
Kulkarni, M., Mazare, A., Schmuki, P., Iglič, A., 2014. Biomaterial surface modification of titanium and titanium alloys for medical applications. Nanomedicine 111, 111.
Kutty, R.V., Chia, S.L., Setyawati, M.I., Muthu, M.S., Feng, S.-S., Leong, D.T., 2015. In vivo and ex vivo proofs of concept that cetuximab conjugated vitamin E TPGS micelles increases efficacy of delivered docetaxel against triple negative breast cancer. Biomaterials 63, 58–69.
Lai, M., Hyatt, B.J., Nasser, I., Curry, M., Afdhal, N.H., 2007. The clinical significance of persistently normal ALT in chronic hepatitis B infection. J. Hepatol. 47 (6), 760–767.
Laschewsky, A., Rosenhahn, A., 2019. Molecular design of zwitterionic polymer interfaces: searching for the difference. Langmuir 35, 1056–1071.
Lee, M.H., Ducheyne, P., Lynch, L., Boettiger, D., Composto, R.J., 2006. Effect of biomaterial surface properties on fibronectin–α5β1 integrin interaction and cellular attachment. Biomaterials 27 (9), 1907–1916.

Leslie, D.C., Waterhouse, A., Ingber, D.E., 2017. New anticoagulant coatings and hemostasis assessment tools to avoid complications with pediatric left ventricular assist devices. J. Thorac. Cardiovasc. Surg. 154 (4), 1364–1366.
Li, Y., Rodrigues, J., Tomas, H., 2012. Injectable and biodegradable hydrogels: gelation, biodegradation and biomedical applications. Chem. Soc. Rev. 41 (6), 2193–2221.
Liang, S.-L., Cook, W.D., Thouas, G.A., Chen, Q.-Z., 2010. The mechanical characteristics and in vitro biocompatibility of poly(glycerol sebacate)-Bioglass elastomeric composites. Biomaterials 31 (33), 8516–8529.
Lim, W.-G., Jo, C., Lee, J., Hwang, D.S., 2018. Simple modification with amine-and hydroxyl-group rich biopolymer on ordered mesoporous carbon/sulfur composite for lithium-sulfur batteries. Korean J. Chem. Eng. 35 (2), 579–586.
Lin, C.-S., Chang, C.-S., Yang, S.-S., Yeh, H.-Z., Lin, C.-W., 2008. Retrospective evaluation of serum markers APRI and AST/ALT for assessing liver fibrosis and cirrhosis in chronic hepatitis B and C patients with hepatocellular carcinoma. Intern. Med. 47 (7), 569–575.
Llorens, E., Ibañez, H., Del Valle, L., Puiggalí, J., 2015. Biocompatibility and drug release behavior of scaffolds prepared by coaxial electrospinning of poly(butylene succinate) and polyethylene glycol. Mater. Sci. Eng.: C 49, 472–484.
Luo, Y., Teng, Z., Li, Y., Wang, Q., 2015. Solid lipid nanoparticles for oral drug delivery: chitosan coating improves stability, controlled delivery, mucoadhesion and cellular uptake. Carbohydr. Polym. 122, 221–229.
Mao, C., Qiu, Y., Sang, H., Mei, H., Zhu, A., Shen, J., et al., 2004. Various approaches to modify biomaterial surfaces for improving hemocompatibility. Adv. Colloid Interface Sci. 110 (1-2), 5–17.
Martin, P., Nunan, R., 2015. Cellular and molecular mechanisms of repair in acute and chronic wound healing. Br. J. Dermatol. 173 (2), 370–378.
Morgese, G., Causin, V., Maggini, M., Corrà, S., Gross, S., Benetti, E.M., 2015. Ultrastable suspensions of polyoxazoline-functionalized ZnO single nanocrystals. Chem. Mater. 27 (8), 2957–2964.
Motlagh, D., Yang, J., Lui, K.Y., Webb, A.R., Ameer, G.A., 2006. Hemocompatibility evaluation of poly(glycerol-sebacate) in vitro for vascular tissue engineering. Biomaterials 27 (24), 4315–4324.
Nanci, A., Wuest, J., Peru, L., Brunet, P., Sharma, V., Zalzal, S., et al., 1998. Chemical modification of titanium surfaces for covalent attachment of biological molecules. J. Biomed. Mater. Res., A 40 (2), 324–335.
Niu, X., Feng, Q., Wang, M., Guo, X., Zheng, Q., 2009. Preparation and characterization of chitosan microspheres for controlled release of synthetic oligopeptide derived from BMP-2. J. Microencapsul. 26 (4), 297–305.
Nogués, C., Blanquer, A., Barrios, L., Ibañez, E., 2018. Assessment of metallic alloys biocompatibility. Biomaterials in Clinical Practice. Springer.
Noviana, D., Estuningsih, S., Ulum, M.F., 2016. Animal study and pre-clinical trials of biomaterials. Biomaterials and Medical Devices. Springer.
Nyblom, H., Berggren, U., Balldin, J., Olsson, R., 2004. High AST/ALT ratio may indicate advanced alcoholic liver disease rather than heavy drinking. Alcohol Alcohol 39 (4), 336–339.
Ohgo, H., Yokoyama, H., Hirose, H., Kawabe, H., Saito, I., Tomita, K., et al., 2009. Significance of ALT/AST ratio for specifying subjects with metabolic syndrome in its silent stage. Diab. Metab. Syndr.: Clin. Res. Rev. 3 (1), 3–6.
Othman, Z., Pastor, B.C., van Rijt, S., Habibovic, P., 2018. Understanding interactions between biomaterials and biological systems using proteomics. Biomaterials 167, 191–204.
Park, J., Andrade, B., Seo, Y., Kim, M.-J., Zimmerman, S.C., Kong, H., 2018. Engineering the surface of therapeutic "living" cells. Chem. Rev. 118 (4), 1664–1690.
Pelaz, B., del Pino, P., Maffre, P., Hartmann, R., Gallego, M., Rivera-Fernandez, S., et al., 2015. Surface functionalization of nanoparticles with polyethylene glycol: effects on protein adsorption and cellular uptake. ACS Nano 9 (7), 6996–7008.
Petros, R.A., DeSimone, J.M., 2010. Strategies in the design of nanoparticles for therapeutic applications. Nat. Rev. Drug Discov. 9 (8), 615.
Polesel-Maris, J., Legrand, J., Berthelot, T., Garcia, A., Viel, P., Makky, A., et al., 2012. Force spectroscopy by dynamic atomic force microscopy on bovine serum albumin proteins changing the tip hydrophobicity, with piezoelectric tuning fork self-sensing scanning probe. Sens. Actuators B: Chem. 161 (1), 775–783.
Preiss-Bloom, O. 2015. Cross-Linked Compositions. Google Patents.

Ramalingam, M., Kumar, T.S., Ramakrishna, S., Soboyejo, W.O., 2016. Biomaterials: A Nano Approach. CRC Press.
Ramkumar, M., Cools, P., Arunkumar, A., De Geyter, N., Morent, R., Kumar, V., et al., 2018. Polymer coatings for biocompatibility and reduced nonspecific adsorption. Functionalised Cardiovascular Stents. Elsevier.
Randon, J., Blanc, P., Paterson, R., 1995. Modification of ceramic membrane surfaces using phosphoric acid and alkyl phosphonic acids and its effects on ultrafiltration of BSA protein. J. Membr. Sci. 98 (1-2), 119–129.
Ravi, N., Aliyar, H.A., 2006. Tissue reaction to prosthetic materials. The Bionic Human. Springer.
Raynor, J.E., Capadona, J.R., Collard, D.M., Petrie, T.A., García, A.J., 2009. Polymer brushes and self-assembled monolayers: versatile platforms to control cell adhesion to biomaterials. Biointerphases 4 (2), FA3–FA16.
Ren, X., Feng, Y., Guo, J., Wang, H., Li, Q., Yang, J., et al., 2015. Surface modification and endothelialization of biomaterials as potential scaffolds for vascular tissue engineering applications. Chem. Soc. Rev. 44 (15), 5680–5742.
Repka, M.A., McGinity, J.W., 2000. Physical–mechanical, moisture absorption and bioadhesive properties of hydroxypropylcellulose hot-melt extruded films. Biomaterials 21 (14), 1509–1517.
Rieffel, J., Chen, F., Kim, J., Chen, G., Shao, W., Shao, S., et al., 2015. Hexamodal imaging with porphyrin-phospholipid-coated upconversion nanoparticles. Adv. Mater. 27 (10), 1785–1790.
Robeson, L.M., Rothrock, G.D. 2015. Nanostructured Surfaces for Biomedical/Biomaterial Applications and Processes Thereof. Google Patents.
Roque, L., Castro, P., Molpeceres, J., Viana, A.S., Roberto, A., Reis, C., et al., 2018. Bioadhesive polymeric nanoparticles as strategy to improve the treatment of yeast infections in oral cavity: in vitro and ex vivo studies. Eur. Polym. J. 104, 19–31.
Sagir, A., Erhardt, A., Schmitt, M., Häussinger, D., 2008. Transient elastography is unreliable for detection of cirrhosis in patients with acute liver damage. Hepatology 47 (2), 592–595.
Saini, S., Falco, Ç.Y., Belgacem, M.N., Bras, J., 2016. Surface cationized cellulose nanofibrils for the production of contact active antimicrobial surfaces. Carbohydr. Polym. 135, 239–247.
Saleh, L.S., Bryant, S.J. 2018. In vitro and in vivo models for assessing the host response to biomaterials. Drug Discov. Today: Dis. Models 24, 13–21.
Schmidt, D.R., Waldeck, H., Kao, W.J., 2009. Protein adsorption to biomaterials. Biological Interactions on Materials Surfaces. Springer.
Senthilkumar, S., Rajesh, S., Jayalakshmi, A., Mohan, D., 2013. Biocompatibility studies of polyacrylonitrile membranes modified with carboxylated polyetherimide. Mater. Sci. Eng.: C 33 (7), 3615–3626.
Seyfert, U.T., Biehl, V., Schenk, J., 2002. In vitro hemocompatibility testing of biomaterials according to the ISO 10993-4. Biomol. Eng. 19 (2-6), 91–96.
Sezer, U.A., Ozturk, K., Aru, B., Demirel, G.Y., Sezer, S., 2018. A design achieved by coaxial electrospinning of polysulfone and sulfonated polysulfone as a core-shell structure to optimize mechanical strength and hemocompatibility. Surf. Interfaces 10, 176–187.
Shen, H., Hu, X., Yang, F., Bei, J., Wang, S., 2007. Combining oxygen plasma treatment with anchorage of cationized gelatin for enhancing cell affinity of poly(lactide-*co*-glycolide). Biomaterials 28 (29), 4219–4230.
Shen, M., Horbett, T.A., 2001. The effects of surface chemistry and adsorbed proteins on monocyte/macrophage adhesion to chemically modified polystyrene surfaces. J. Biomed. Mater. Res., A 57 (3), 336–345.
Siparsky, G.L., Voorhees, K.J., Miao, F., 1998. Hydrolysis of polylactic acid (PLA) and polycaprolactone (PCL) in aqueous acetonitrile solutions: autocatalysis. J. Environ. Polym. Degradation 6 (1), 31–41.
Sperling, C., Schweiss, R.B., Streller, U., Werner, C., 2005. In vitro hemocompatibility of self-assembled monolayers displaying various functional groups. Biomaterials 26 (33), 6547–6557.
Steckbeck, S. 2014. Experimental Analysis of Interactions Between Biomolecules and Inorganic Surfaces. Staats- und Universitätsbibliothek Bremen.
Svenson, S., 2015. The dendrimer paradox–high medical expectations but poor clinical translation. Chem. Soc. Rev. 44 (12), 4131–4144.
Tang, L., Thevenot, P., Hu, W., 2008. Surface chemistry influences implant biocompatibility. Curr. Topics Med. Chem. 8 (4), 270–280.
Tegoulia, V.A., Cooper, S.L., 2002. Staphylococcus aureus adhesion to self-assembled monolayers: effect of surface chemistry and fibrinogen presence. Colloids Surf. B: Biointerfaces 24 (3-4), 217–228.

Tekade, R.K., Maheshwari, R., Tekade, M., 2017. 4 – Biopolymer-based nanocomposites for transdermal drug delivery. Biopolymer-Based Composites. Woodhead Publishing.
Tenner, S., Dubner, H., Steinberg, W., 1994. Predicting gallstone pancreatitis with laboratory parameters: a meta-analysis. Am. J. Gastroenterol. 89 (10), pp.
Toskas, G., Cherif, C., Hund, R.-D., Laourine, E., Mahltig, B., Fahmi, A., et al., 2013. Chitosan (PEO)/silica hybrid nanofibers as a potential biomaterial for bone regeneration. Carbohydr. Polym. 94 (2), 713–722.
Walker, J., Shadanbaz, S., Woodfield, T., Staiger, M., Dias, G., 2013. The in vitro and in vivo evaluation of the biocompatibility of Mg alloys. Biomed. Mater. 9 (1), 015006.
Walkey, C.D., Chan, W.C., 2012. Understanding and controlling the interaction of nanomaterials with proteins in a physiological environment. Chem. Soc. Rev. 41 (7), 2780–2799.
Wang, J., 1999. Sol–gel materials for electrochemical biosensors. Anal. Chim. Acta 399 (1-2), 21–27.
Webster, T.J., Ergun, C., Doremus, R.H., Siegel, R.W., Bizios, R., 2000. Specific proteins mediate enhanced osteoblast adhesion on nanophase ceramics. J. Biomed. Mater. Res., A 51 (3), 475–483.
Won, K., Kim, S., Kim, K.-J., Park, H.W., Moon, S.-J., 2005. Optimization of lipase entrapment in Ca-alginate gel beads. Process Biochem. 40 (6), 2149–2154.
Xu, M., Zhu, J., Wang, F., Xiong, Y., Wu, Y., Wang, Q., et al., 2016. Improved in vitro and in vivo biocompatibility of graphene oxide through surface modification: poly(acrylic acid)-functionalization is superior to PEGylation. ACS Nano 10 (3), 3267–3281.
Xu, Z., Wang, S., Li, Y., Wang, M., Shi, P., Huang, X., 2014. Covalent functionalization of graphene oxide with biocompatible poly(ethylene glycol) for delivery of paclitaxel. ACS Appl. Mater. Interfaces 6 (19), 17268–17276.
Yang, K.-J., Son, J., Jung, S.Y., Yi, G., Yoo, J., Kim, D.-K., et al., 2018. Optimized phospholipid-based nanoparticles for inner ear drug delivery and therapy. Biomaterials 171, 133–143.
Yoshida, Y., Van Meerbeek, B., Nakayama, Y., Snauwaert, J., Hellemans, L., Lambrechts, P., et al., 2000. Evidence of chemical bonding at biomaterial-hard tissue interfaces. J. Dent. Res. 79 (2), 709–714.
Zanini, S., Zoia, L., Dell'Orto, E.C., Natalello, A., Villa, A.M., Della Pergola, R., et al., 2016. Plasma polymerized 2-ethyl-2-oxazoline: chemical characterization and study of the reactivity toward different chemical groups. Mater. Des. 108, 791–800.
Zhang, C., Yuan, J., Lu, J., Hou, Y., Xiong, W., Lu, H., 2018. From neutral to zwitterionic poly(α-amino acid) nonfouling surfaces: effects of helical conformation and anchoring orientation. Biomaterials 178, 728–737.
Zhang, M., Li, X., Gong, Y., Zhao, N., Zhang, X., 2002. Properties and biocompatibility of chitosan films modified by blending with PEG. Biomaterials 23 (13), 2641–2648.
Zhou, T., Zhu, Y., Li, X., Liu, X., Yeung, K.W., Wu, S., et al., 2016. Surface functionalization of biomaterials by radical polymerization. Prog. Mater. Sci. 83, 191–235.
Zhu, H., Srivastava, R., Brown, J.Q., McShane, M.J., 2005. Combined physical and chemical immobilization of glucose oxidase in alginate microspheres improves stability of encapsulation and activity. Bioconjug. Chem. 16 (6), 1451–1458.
Zhu, W., Peck, Y., Iqbal, J., Wang, D.-A., 2017. A novel DOPA-albumin based tissue adhesive for internal medical applications. Biomaterials 147, 99–115.
Zuliani-Alvarez, L., Midwood, K.S., 2015. Fibrinogen-related proteins in tissue repair: how a unique domain with a common structure controls diverse aspects of wound healing. Adv. Wound Care 4 (5), 273–285.

Index

Note: Page numbers followed by "*f*" and "*t*" refer to figures and tables, respectively.

A

7-AAD. *See* 7-Amino actinomycin D (7-AAD)
a-SMA. *See* Alpha-smooth muscle actin (a-SMA)
Abbreviated new drug application (ANDA), 13
ABC. *See* ATP-binding cassette (ABC)
Abraxane, 21
Absorption, 165
Acceptance criteria, 3
D-*N*-Acetyl glucosamine, 416–417
Acid-sensitive hydrazone-based nanosystems, 113–114
Acid–base side chains, 506
ACNs. *See* Anti-biotic cement nails (ACNs)
Acrylamide based DNA hydrogel networks, 125–126
Acrylic resins, 321, 343
Actinomycetes, NPs via, 537
Activation-based controlled drug delivery systems, 211
Acute inflammation, 357
Adenosine triphosphate (ATP), 579
Adhesion, 66
Adsorption
  of nonspecific protein, 647–648
  theory, 466
Advanced implantable devices, 218–220
Advanced microscopic techniques, 551–552
Aerosolized powder inhalers, 99
Affinity chromatography, 162, 163*f*
Affinity-based drug delivery systems, 117–119
  recognition molecular systems, 117–119
AFM. *See* Atomic-force microscopy (AFM)
Ag^{+} ions, 316
Agglutination test, 269
Aggregatibacter actinomycetemcomitans, 309
AGM. *See* Aminoglutethimide (AGM)
Ago2. *See* Argonaute-2 (Ago2)
Air
  jet milling, 475–476
  suspension method, 216
Air plasma spraying (APS), 73
Al NPs. *See* Aluminum nanoparticles (Al NPs)
Alanine, 541
Alanine aminotransferase (ALT), 663–664
Alanine transaminase, 664
Albumin, 166–167, 650
  albumin-based tissue engineering scaffold, 233–234
  coating, 650–651
  cross-linked tissue glue of albumin comprised glue, 653*f*
  cytocompatibility evaluation data in vitro of, 652*f*
Alfrey model, 207
Algae, NPs via, 537–538
Alginate-based tissue engineering scaffold, 235–236
Alkali metals, 529
Alkaline phosphatase (ALP), 486
All-*trans*-retinoic acid (ATRA), 30
Allergic/allergy
  allergy-causing substances, 500
  reactions, 359*t*
ALP. *See* Alkaline phosphatase (ALP)
Alpha-smooth muscle actin (a-SMA), 27
D-α-Tocopheryl succinate (TOS), 432
Alpha1-acid glycoprotein, 166–167
ALT. *See* Alanine aminotransferase (ALT)
Alumina ceramic, 351
Aluminum base alloys, 361
Aluminum chloride ($AlCl_3$), 547
Aluminum nanoparticles (Al NPs), 547, 567*t*
  synthesis, 547–548
Aluminum oxides, 343
Alzet osmotic pump, 200, 201*f*
Amastigote, 266–267
AmB. *See* Amphotericin B (AmB)
AmBisome (A), 275–277, 279*f*, 282
American National Institute of Health, 58
Amikacin, 100
Amine functional group-rich surfaces ($-NH_2$ functional group-rich surfaces), 667–668
Amino acid, 169, 170*f*
7-Amino actinomycin D (7-AAD), 31
6-Amino penicillanic acid (6-APA), 173
Aminoglutethimide (AGM), 115
Aminopeptidase *N*, 623
8-Aminoquinoline, 273, 277–278
Ammonia functionalized CNTs, 619–620
Amphiphilic
  CS/silica hybrid hydrogel system, 125
  molecules, 232

Amphocil, 275–276
Amphotericin B (AmB), 271, 272*t*
  AmB-loaded
    nanoemulsions, 286–287
    nanospheres, 290
    transfersomes, 287–288
AMPs. *See* Antimicrobial peptides (AMPs)
ANDA. *See* Abbreviated new drug application (ANDA)
Animal tissues, NPs via, 541–542
  chitosan, 542
  invertebrate, 542
  silk proteins, 541–542
Anisotropic noble metal NPs (ANPs), 579
Annealing polymerization, 60
Anodic spark deposition. *See* Microarc oxidation (MAO)
ANPs. *See* Anisotropic noble metal NPs (ANPs)
Anterolateral approach, 366
Anti-biotic cement nails (ACNs), 104
Anti-DNA immunoglobulin peptide therapy, 620
Antibacterial metal NPs, 582
Antibiotic(s), 172–173, 341
  drug resistance, 572
Antibody
  detection diagnostic tests, 270
  structure, 177–178, 178*f*
Anticancer drug delivery system, 42, 97
Antileishmanial drugs, 270–273, 272*t*
Antileishmaniasis activity of dinitroaniline analogs, 277
Antimicrobial activity of Ag NPs, 544
Antimicrobial peptides (AMPs), 572
AntimiR-138 delivered MSIC, 214
Antimonial agents, 270
Antisense c-myc oligonucleotides (asODN), 628
Antitumor immunity, 382–383
6-APA. *See* 6-Amino penicillanic acid (6-APA)
Apatite, 355
Apolipoproteins, 283
APS. *See* Air plasma spraying (APS)
Aqueous media, 71
Aqueous solubility change materials, 105
Arginine-glycine-aspartic acid-cystine (RGDC), 129
Arginine/glycine/aspartic acid peptides (RGD peptides), 129, 623
Argonaute-2 (Ago2), 427
Arjuna glucoside, 281
Arthritis, hyperthermia in treatment of, 402
Artificial proteins, 572
Artificial skin, 227, 574
Asialoglycoprotein receptors, 60–61
asODN. *See* Antisense c-myc oligonucleotides (asODN)
Asparagine/glycine/arginine peptides (NGR peptides), 623
Aspartate-aminotransferase (AST), 664
  AST/ALT ratio, 664
Aspirin-loaded ethylcellulose nanoparticles, 473
AST. *See* Aspartate-aminotransferase (AST)
Atomic-force microscopy (AFM), 551–552, 566
ATP. *See* Adenosine triphosphate (ATP)
ATP-binding cassette (ABC), 443
ATRA. *See* All-*trans*-retinoic acid (ATRA)
AuCM. *See* Cysteamine modified gold nanoparticles (AuCM)
Au–Pt hybrid functionalized ZnO nanorods (Pt–Au@ZnONRs), 576

B

Bacillus Calmette–Guérin (BCG), 291
Backscattered electron mode (BSE mode), 557
Bacopasaponin C, 281
Bacteria(l)
  infection, 130–131
  NPs via, 538–539
  plasmid, 158
Bacterium, 538–539
Ball milling, 534–535
  mechanical, 535
BBB. *See* Blood–brain barrier (BBB)
BCG. *See* Bacillus Calmette–Guérin (BCG)
Beers–Lambert law, 552
BET. *See* Betulin (BET)
β-D-glucuronidas, 419–420
β-*N*-acetyl-hexosaminidase, 419–420
Beta-tricalcium phosphates (Beta-TCPs), 75
Betulin (BET), 287
Bevacizumab, 516
Bimetallic nanoparticles (BMNPs), 535, 549–550
Bimolecular ultrasensitive detection, 532
Binary pDNA/cationic complexes, 434
Bio-Raman spectroscopy, 133
Bioactive ceramics, 351
Bioactive materials, 92
Bioadhesion enhancement, 63
Bioavailability, 104–105, 461
Bioceramics, 94–95, 205, 238, 343
Biochemical activation methods, 211
Biocompatibility, 66, 129, 348–349, 630
  biomaterials influencing on, 646–657
  system, 91

Biodegradability, 127, 218, 630
  polymers, 77, 81, 346
    polymer-based microreservoirs, 218
  scaffolds, 347
  systems, 91, 194
Biodegradable implant system, 194, 196–198. *See also* Nonbiodegradable implant system
  polymers in
    PCL, 197–198
    PGA, 197
    PLA, 197
    PLGA, 197
    polysaccharides, 197
Biodegradation, 131, 485
Biodistribution, 20
Bioerosion, 198–199
Biogenic metal NPs, 536
Biogenic synthesis of NPs, 536
Bioglass(es), 94–95, 351
Bioinert materials, 92
Biological approach, 536–542
  NPs
    via actinomycetes, 537
    via algae, 537–538
    via animal tissues, 541–542
    via bacteria, 538–539
    via fungi, 539
    via plants, 539–540
    via viruses, 539
    via yeasts, 539
Biological assays, 164
Biological assessment tests, 132–134
Biological events upon host–biomaterial interaction and solutions
  bacterial infection, 130–131
  biocompatibility, 129
  biodegradation, 131
  hemocompatibility, 129–130
  protein adsorption, 128–129
Biological materials, 102–103
Biological stimuli-responsive
  biomolecular-responsive biomaterials, 114–115
  enzyme-responsive biomaterials, 115
Biomaterials, 58–59, 58*f*, 346, 354, 356–357, 640. *See also* Implant materials
  advancements in, 107–126
    intelligent drug delivery systems, 116–126
    smart components, 108–116
  application, 642*t*
    for sustained and controlled release, 96–107
  biomaterials-based
    drug delivery, 126
    immunoassays, 107
  ceramics and glasses, 94–95
  challenges in using biomaterials for drug delivery, 126–134
  compatibility with biological surfaces, 640–646
  composites, 96
  hierarchy involved in biomaterial science, 641*f*
  in hyperthermia therapy, 387–399
  immobilization of biomolecule on surface of, 658–659
  instability, 59–60
  mechanical properties, biomaterials, 93
    tensile and shear properties, 93
  metals, 94
  nonfouling surfaces, 645–646
  polymers, 94
  reaction of foreign body, 644*f*
  regulatory and patent aspect, 134–135, 135*t*
  requirements for, 92, 92*f*
  science and biomaterials, 91
  surface modification
    approaches for, 646–657
    effect for biocompatibility, 665–668
    need for, 643–645
  synthesis (additive manufacturing) and properties, 92–93
  techniques to assessing of polymer biocompatibility, 660–665
Biomicroelectron mechanical systems, 105
Biomimetic(s), 72
  coatings, 80–81, 355
  materials, 229, 232
  nanofibers, 119
Biomolecular/biomolecules, 155, 161–162, 347, 543
  biomolecular-responsive biomaterials, 114–115
  biomolecular/protein corona, 128
  chemical bonding with, 658–659
  compounds, 566–568
Bionanotubes, 232
Biosensing devices, MNPs applications in, 576–577, 577*t*
Biosilicon technology, 212
Biotechnology-based pharmaceutical products, 172–179, 180*t*
  commercially available leading, 179–180
  in comparison with conventional drugs, 155
  gene therapy, 181–182
  nanobiotechnology, 180–181
  pharmacogenomics, 182
  pharmacokinetics of pharmaceutical, 164–168
  problems associating with, 168–172

Biotechnology-based pharmaceutical products (*Continued*)
ethical and regulatory concerns of biotechnology, 171–172
formulation stability of, 169–171
immunogenicity, 171
production process for, 155–164
stem cell therapy, 182–183
Biotechnology-based tissue engineering, 252
Biotolerant materials, 92
Blood
blood–cerebrospinal fluid barrier, 101
blood–material interaction, 357
circulation, 498–499
clots, 359*t*
clotting factors, 175–176
heparinization to improving blood compatibility, 67–69
plasma half-life, 63–64
toxicity reduction, 62
vessel replacement, 246–247
Blood urea nitrogen (BUN), 664–665
Blood–brain barrier (BBB), 28, 37, 38*f*, 101, 571, 620
BMNPs. *See* Bimetallic nanoparticles (BMNPs)
Boc. *See t*-butoxy carbonyl (Boc)
Bolivian medicinal plant (*Galipea longiflora*), 274
Bone
cancer, 39–42
clamp, 341
fracture, 359*t*
marrow–derived MSCs, 29–30
nanotechnology in bone cells tissue engineering, 244–245
tissue engineering, 486–487
Bovine serum albumin (BSA), 503, 619, 665–666
Bragg's law, 558
Brain, 101–102
cancer, 34–39
enhanced drug delivery to, 61
hyperthermia in treatment of brain tumor, 400
Breast cancer, 445–446, 447*f*
cells, 112
hyperthermia in treatment of, 400–401
management, 30
Brentuximab vedotin, 21
BSA. *See* Bovine serum albumin (BSA)
BSE mode. *See* Backscattered electron mode (BSE mode)
BTE, 245
Buccal mucosa, 326
Bulk properties for implant materials, 348, 354
BUN. *See* Blood urea nitrogen (BUN)
Buparvaquone and derivatives, 274

C

Cadmium (Cd), 539
Cadmium sulfide (CdS), 539
Caffeine, 515
CAFs. *See* Carcinoma-associated fibroblasts (CAFs)
Calcium chloride ($CaCl_2$), 314
Calcium orthophosphate, 238
Calcium phosphate (CAP), 72, 80, 343, 346, 439
CAP/siRNA/dopa-HA, 439, 440*f*
coating, 77
deposition, 72
Calcium phosphate coating techniques, 72
Calcium sulfate α-hemihydrate (CSH), 237
Cancer, 107, 154
breast, 400–401, 445–446
cells, 251
disease management, 20–22, 22*t*
enhanced uptake by cancer and inflamed tissues, 62–63
novel formulation strategy in cancer treatment, 27–46
bone cancer, 39–42
brain cancer, 34–39
lung cancer, 31–34
MSC nanoparticles in, 42–46
nanoparticles engineered MSCs in breast cancer management, 30
ovarian cancer, 42
peptides in cancer management, 621–623
vaccines, 181
Cancer stem cell (CSC), 24, 27
CAP. *See* Calcium phosphate (CAP); Chloroaluminum phthalocyanine (CAP)
Capacity of tissue bonding, 95, 96*t*
Carbon arc-discharge technique, 615–616
Carbon nanofiber/gelatin hydrogel scaffold, 103
Carbon nanotubes (CNTs), 96, 121, 240, 287, 385–386, 477–478, 533, 614
cellular uptake and cell penetration mechanism, 629–630
CNT-based supramolecular hybrid for vaccination of testis cancer, 624
CNT–mediated gene delivery, 626–629
CNT–mediated peptide and vaccine delivery, 623–626
functionalization, 614, 617–618
covalent, 617–618
noncovalent, 618
with protein, peptide, DNA, and siRNA, 619–621
for hyperthermia therapy, 389–390
liposomes, 478–479
MWCNTs, 478
niosomes, 479–480

structure and classification, 615
SWCNTs, 477–478
synthesis and purification, 615–617
toxicity consideration, 630–631
Carbonate-substituted apatite, 78
Carbopol 934P, 327
1-(2-Carboxyethyl) pyrrole, 665–666
Carboxyl functional group-bearing surface (–COOH functional group-bearing surface), 667
Carboxylation, 646–647
Carboxymethyl cellulose (CMC), 500
Carcinogenicity, 360
Carcinoma-associated fibroblasts (CAFs), 27
Cardiovascular
biomaterial, 102–103, 103*t*, 104*f*
diseases, 105–106
drug delivery, 102–103
system, 102
Carrier-based drug delivery, 497
Cartilage tissue engineering, 487
Casein, 169, 650
Caspases, 379
Cationic
carrier conjugation with HA, 432–434
chitosan, 303
nanoparticles, 432
liposomes, 276
particles, 434
polysaccharide, 468
Cationization, 646
CBA. *See* Cross-linking PEI with bisacrylamide (CBA)
CCL5. *See* Chemokine C–C motif ligand 5 (CCL5)
CD. *See* Circular dichroism (CD); Cytosine deaminase (CD)
CD13. *See* Aminopeptidase N
$CD4^+$ T-cells, 376
CD44. *See* Cluster of differentiation 44 (CD44)
CDER. *See* Centre for Drug Evaluation or Research (CDER)
cDNA. *See* Complementary DNA (cDNA)
Cell-penetrating peptides (CPPs), 620, 622–623
Cell(ular)
adhesion molecules, 27
affinity, 646
behavior, 574
cell-based therapy, 248
cell–cell receptors, 26
labelling
purification, detection, nanotechnology-based tissue engineering, 251–252
targeted delivery, 532
matrices approach, 229
nanotechnology in cell tissue engineering, 244–250
bone cells tissue engineering, 244–245
for cell labeling, purification, detection, and suicide bombing, 251–252
hepatic cells tissue engineering, 248–250
stem cell engineering, 250
vascular cells tissue engineering, 245–248
penetration mechanism of carbon nanotubes, 629–630
sheet–based assembly approach, 247–248
uptake
of carbon nanotubes, 629–630
of siRNA/polymer complexes, 446
Cellulose, 100–101, 651
dialysis membranes, 68
Central nervous system drug delivery, 101–102
Centre for Drug Evaluation or Research (CDER), 13
Centrifugal lithography (CL), 513–514
Cephalosporins, 172–173, 172*f*
Ceramic(s), 94–95, 95*t*, 350–351
drug delivery systems, 205
heating process, 544
implants, 105–106
materials, 342–343
and metals, 91
Cerebral cortex, 61
Cermet capsules, 205
Cervical cancer, 401
Cesium lead halide, 62
Cetyltrimethylammonium bromide (CTAB), 543
Chemical approach, 531, 535–536
Chemical bonding with biomolecules, 658–659
Chemical colloidal approach, 548–549
Chemical degradation, 169
Chemical derivatization approach, 274
Chemical functionalization of CNTs, 617
Chemical modification, 659
Chemical stimuli-responsive, 113–114
pH-responsive biomaterials, 113–114
redox-responsive biomaterials, 114
Chemical vapor deposition technique (CVD technique), 615–616
Chemically controlled release mechanism, 198–199
bioerosion, 198–199
pendant chain, 199
Chemoattractant inflammatory cytokines, 27
Chemokine C–C motif ligand 5 (CCL5), 27
Chemokine(s), 27
receptors, 26
Chemotherapy, 28, 47, 47*f*, 439
Chinese hamster ovary cells (CHO cells), 159
Chitin, 303

Chitosan (CS), 96, 231, 542
biopolymer-based formulations, 303–306
chitosan-based thermosensitive hydrogels, 481
chitosan–DNA NPs, 45–46
coating, 654–657
renewal in rat model of sciatic nerve transaction, 657*f*
CS-based tissue engineering scaffold, 233, 234*f*
functionalized carbon nanotube composites, 478, 626
mouthwash, 304
as mucoadhesive polymer, 468, 469*f*
thioethylamidine, 471–472
Chlorhexidine acetate, 324
Chlorhexidine gluconate, 305–306
Chloroaluminum phthalocyanine (CAP), 310
Chlorotoxin, 28
CHO cells. *See* Chinese hamster ovary cells (CHO cells)
Cholesterol, 102
biosensors, 105–106
Chromatographic methods, 7–9
Chromium (Cr), 340
Chronic diseases, 496
Chronic obstructive pulmonary disease (COPD), 579
Ciprofloxacin, 100
Circular dichroism (CD), 562–563
CL. *See* Centrifugal lithography (CL); Cutaneous leishmaniasis (CL)
Clathrin-dependent pathway for internalization, 630, 631*f*
Clinical trial status in tissue engineering, 254–256
to amalgamate tissue engineering and nanotechnology, 256*t*
patents and, 255*t*
CLIP technique. *See* Continuous liquid interface production technique (CLIP technique)
Cluster of differentiation 44 (CD44), 416
receptor, 26
receptor-mediated endocytosis, 435
CMC. *See* Carboxymethyl cellulose (CMC)
CNTs. *See* Carbon nanotubes (CNTs)
Coacervation phase separation, 215
Coated/coating
MNs technology, 511
polymer for stents, 483
technologies/approaches for orthopedic implants, 355–356
ESD, 356
fiber laser surface engineering, 356
Cobalt (Co), 340
cobalt-based implants, 349
cobalt–chrome-based alloys, 342, 360
Cohesive theory, 466
Coley toxin, 377
Collagen, 650
collagen-based approach, 247–248
gel, 247–248
Colloidal Ag, 582
Colon cancer, 437–443
Colorectal cancer (CRC), 437
Combined therapy, 271–273, 272*t*
"Combo" nanomedicine, 46
Commercially available leading biotechnology-based products, 179–180
Commercially pure titanium (cpTi), 360
Competition assay, 439
Complementary DNA (cDNA), 159–160, 160*f*
Composites, 96
Compression testing, 93
Compressive material, 348, 354
Configurational biomimetic imprinting polymers, 119
Continuous liquid interface production technique (CLIP technique), 511
Controlled drug
administration benefits by implantation, 217–218
delivery systems, 90, 192, 196, 487–488
release
by activation, 211
by diffusion, 210
Controlled-release pattern, 308
Conventional drugs, 193
biotechnology-based products in comparison with, 155
release system, 108
COPD. *See* Chronic obstructive pulmonary disease (COPD)
Copolymers, 514
Copper (Cu), 528–529
copper-free click chemistry principles, 125
Cu–Ni nanoparticles, 396
Copper nanoparticles (CuNPs), 546–547, 567*t*
Corneal disease, 211
Correlation, 500–505
Corrosion, 349
clinical significance, 349
resistance, 349
technique, 80–81
Cosmetics, MNPs applications in, 580–581
Cosuppression, 425
Covalent
approach, 69–71
bonding, 617–618
of heparin, 68–69
functionalization, 617–618
CpG oligo-deoxynucleotide, 477
CPPs. *See* Cell-penetrating peptides (CPPs)
cpTi. *See* Commercially pure titanium (cpTi)

CRC. *See* Colorectal cancer (CRC)
Cremophor EL, 327
Crevice corrosion, 349
Critical quality attribute, 4–5
Critical solution temperature (CST), 481
Cross-linked polyethylene (PEX/XLPE), 361–363
  irradiation, 362–363
  moisture cross-linking, 362
  peroxide, 362
Cross-linking PEI with bisacrylamide (CBA), 438
Cryotherapy, 109–110
CS. *See* Chitosan (CS)
CSC. *See* Cancer stem cell (CSC)
CSH. *See* Calcium sulfate α-hemihydrate (CSH)
CST. *See* Critical solution temperature (CST)
CTAB. *See* Cetyltrimethylammonium bromide (CTAB)
CuNPs. *See* Copper nanoparticles (CuNPs)
Curcumin type therapeutic agents, 649
Curie point. *See* Curie temperature
Curie temperature, 396
Cutaneous leishmaniasis (CL), 264. *See also* Prophylactic vaccines for leishmaniasis
  diffuse, 268
  disseminated, 268
CVD technique. *See* Chemical vapor deposition technique (CVD technique)
Cy3-labeled pGL-3, 629
1-(2-Cyanoethyl) pyrrole, 665–666
Cyclic voltammetry, 579
Cyclodextrins (CyDs), 97
CySH/CySSCy. *See* Cysteine/cystine (CySH/CySSCy)
Cysteamine modified gold nanoparticles (AuCM), 436
Cysteine, 469, 470*f*
Cysteine/cystine (CySH/CySSCy), 114
Cystic fibrosis, 99
Cytokines, 164–165, 176–177, 282, 642–643
  interferons, 176–177
  interleukins, 177
  receptors, 26
Cytosine deaminase (CD), 36–37
Cytotoxic(ity)
  ability of nanoengineered MSCs, 31, 33*f*
  effect, 378–379
  test, 661, 662*f*

D

DAB. *See* Droplet-born air blowing (DAB)
Danger signals, 379
DaunoXome, 21
DC. *See* Direct current (DC)
DDS. *See* Drug delivery systems (DDS)
Deamination, 508
Debiotech, 219
Decaylamine, 424
Decellularized ECM cell-seeding technique, 232
Decidua-derived mesenchymal stem cells (DMSCs), 30
Degradable polyurethane foams, 253–254
Degradation of chitosan, 484
Degree of cross-linking, 463
Degree of swelling, 463
Denaturation, 169–171
  of proteins, 379
Dendrimers, 20, 534
  dendrimer-based biomaterials, 98
  dendrimer-based tissue engineering scaffold, 238–239, 239*f*
Dental therapy
  FGF-2 delivery in dental pulp therapy, 306–307
  problems in, 302
Dentinogenesis, 306
Dentistry, 302
  emergence of nanotechnology in, 302–303
  nanomaterials in, 303–329
    chitosan biopolymer-based formulations, 303–306
    gelatin-based nanoformulations, 306–308
    liposomes, 313–314
    nanoemulgel approach, 327–329
    nanoemulsion-based approach, 324–327
    PLGA, 308–312
    silver nanoparticles, 314–317
    TiO_2NP, 320–323
    ZnO-NPs, 317–320
DENV3E (Dengue envelope proteins), 625
Deoxyribonucleic acid (DNA), 154, 159, 303
  DNA-based nanostructures, 124
  DNA-conjugated metal NPs, 573
  DNA/aptamer-based hydrogels, 125
  DNA–chitosan NPs, 573
  functionalization of CNTs with, 619–621
  libraries, 159–160
    cDNA, 159–160
    genomic DNA, 159
  oligonucleotides, 618
Dermis, 193, 505
Desolvation method, 423
Developmental toxicity, 360
Dexamethasone loaded nanocomposite film, 110
Diabetes, 154, 173–174
DICER enzyme, 425–426
Diethylenetriamine NO, 280–281
Differentiable human MSCs, 253
Diffuse CL, 268
Diffusion

Diffusion (*Continued*)
diffusion-controlled release, 198, 218
mathematical models for diffusion-based drug delivery system, 208
theory, 466–467, 467*f*
Digitally monitored microinjection system (DC-hMN-iSystem), 512–513
L-3,4-Dihydroxyphenylalanine, 651
Diimide-activated amidation, 625
3-(4,5-Dimethylthiazol-2-yl)-2,5-diphenyltetrazolium bromide assay (MTT assay), 285, 661
Direct anterior approach, 366
Direct current (DC), 615
Direct physical vapor decomposition process, 550
Directives, 364–365
Directive 90/385/EEC Regarding Active Implantable Medical Devices, 364
Directive 93/42/EEC Regarding Medical Devices, 364
Directive 98/79/EC Regarding Medical Devices for In Vitro Diagnosis, 364
specific regulations, 365
Disposable piezoelectric micropump, 203
Disseminated CL, 268
Dissolution based drug delivery system, mathematical models for, 208–209
Dissolving microneedles technology, 513–514
Distribution, 165–167
Disulfide bonds, 173
Dithiobis(succinimidyl propionate) (DSP), 423
DLS. *See* Dynamic light scattering (DLS)
DMSCs. *See* Decidua-derived mesenchymal stem cells (DMSCs)
DNA. *See* Deoxyribonucleic acid (DNA)
Docetaxel-loaded PLGA nanoparticle coated with HA (DTX-HPLGA), 441
Double-emulsion technique, 215
Double-stranded RNA (dsRNA), 176–177, 425
Downstream process(ing), 155–156, 161–164
characterization of biotechnology-based products, 164
isolation and purification of biotechnology-based products, 161–163
Doxil, 21
Doxorubicin (DOX), 30, 43, 97, 113, 123, 386–387, 529, 627–628
doxorubicin-loaded liposomes, 102
Droplet-born air blowing (DAB), 513–514, 514*f*
Drug delivery systems (DDS), 20, 21*f*, 288–290, 460–461, 496, 581. *See also* Erosion based drug delivery system; Implantable drug delivery system (IDDSs)
biomaterial applications for sustained and controlled release for, 96–107
cardiovascular, 102–103
central nervous system, 101–102
drug delivery for wound closure, 106
drug delivery to ear, 98–99
implantable, 105–106
injectable, 104–105
localized drug targeting, 107
ocular, 97–98
oral, 96–97
orthopedic, 104
pulmonary, 99–100
transdermal, 100–101
biomaterials for, 126–134
biological assessment tests, 132–134
biological events upon host–biomaterial interaction and solutions, 128–131
biological outcomes to host–biomaterial interactions, 127*f*
challenges and advantages of diverse biomaterial, 127*t*
examples of smart biomaterial challenges and toxicities, 131–132
enhancing to brain, 61
MNPs applications in, 566–571
multifunctional design of MNPs for cancer therapy, 571*f*
theranostics appeal in cancer therapy, 570*f*
polymers in drug, 461
Drug release, 205
mechanism from IDDS
chemically controlled release, 198–199
diffusion-controlled release, 198
magnetic controlled release, 200–201
osmotically controlled release, 200
swelling controlled release, 199–200
Drug(s). *See also* Conventional drugs
degradation, 461
development process, 460–461
drug-loaded NPs, 21
drug–drug interactions, 182
drug–polymer conjugates, 20
for leishmaniasis treatment, 270–271
AmB, 271
antimonial agents, 270
miltefosine, 271
paromomycin, 271
pentamidine, 270
loading enhancement, 60
product, 2–3, 7*f*, 8*t*
resistance, 270

stability enhancement, 62
substance, 2–4, 7*f*, 8*f*, 8*t*
drug substance/drug product, 5–9
justification for specification, 5–6
pharmacopoeial test and evolving methodology, 6–9
dsDNA. *See* Dual stranded DNA (dsDNA)
DSP. *See* Dithiobis(succinimidyl propionate) (DSP)
dsRNA. *See* Double-stranded RNA (dsRNA)
DTX-HPLGA. *See* Docetaxel-loaded PLGA nanoparticle coated with HA (DTX-HPLGA)
Dual electrospinning nozzle system, 123
Dual stranded DNA (dsDNA), 572–573
Dual/multiple stimuli-responsive biomaterial systems, 115–116
tristimuli/multiple responsive systems, 116
Ductility, 348, 354
Durasert, 219
DUROS implantable system, 203*f*
Dynamic light scattering (DLS), 560, 564–565
Dynamic photooxidation, 111
Dysplastic stroma, 63

E

E-TRANS Macroflux microarray, 511
EAPs. *See* Electroactive/conducting polymers (EAPs)
Ear, drug delivery to, 98–99
ECM. *See* Extracellular matrix (ECM)
EDC. *See* 1-Ethyl-3-(3-dimethyl aminopropyl) carbodiimide (EDC)
EDX spectroscopy. *See* Energy-dispersive X-ray spectroscopy (EDX spectroscopy)
EGF. *See* Epidermal growth factor (EGF)
Elastin, 650
Electrical-responsive biomaterials, 110
Electroactive/conducting polymers (EAPs), 110
Electrochemical
corrosion, 349
deposition, 77–78
Electrolytic solution composition, 77
Electron microscope methods, 557
Electronic theory, 465, 465*f*
Electrophoretic deposition, 77
Electroporation, 158–159
Electrospinning, 246
Electrospray ionization–MS (ESI–MS), 564
Electrostatic
interactions, 461
repulsion, 417
Electrostatic spray deposition (ESD), 356
Electrothermal vaporization (ETV), 564
ELISA. *See* Enzyme-linked immunosorbent assay (ELISA)
Emulsification, 473–474
Emulsion(s), 286–287
phase separation, 215
polymerization, 475
Enantiomers, 118–119
Encapsulated cell technology, 213–214, 217
Endocytosis, 630
Endosomal escape, 431
Endosteal plate dental implants, 361
Energy-dispersive X-ray spectroscopy (EDX spectroscopy), 552, 559
Engineered MSCs
hMSCs, 25–27
MSCs, 23–25
multifunctional stem cell platform, 46–47
nanotechnology as emerging platform, 20–22
as novel formulation strategy in cancer treatment, 27–46
Enhanced permeability and retention (EPR), 62–63, 430–431
Environmental SEM (ESEM), 552, 557
Enzymatic/enzymes, 175
beta-glucocerebrosidase, 175
degradation, 496–497
enzyme-responsive biomaterials, 115
Enzyme-linked immunosorbent assay (ELISA), 269
Enzymology, MNPs applications in, 574–575
EOEOVE. *See* 2-(2-Ethoxy) methoxyethyl vinyl ether (EOEOVE)
Epidermal growth factor (EGF), 625. *See also* Fibroblast growth factor (FGF)
Epidermis, 193
Episterol, 271
Epogen, 496
EPR. *See* Enhanced permeability and retention (EPR)
Erosion based drug delivery system. *See also* Drug delivery systems (DDS)
Hopfenberg's model, 209
Katzhendler's model, 209
mathematical models for, 209–210
Rothstein's model, 209–210
Erythropoietin, 496
Escherichia coli, 159
ESD. *See* Electrostatic spray deposition (ESD)
ESEM. *See* Environmental SEM (ESEM)
ESI–MS. *See* Electrospray ionization–MS (ESI–MS)
Esterification technique, 469
2-(2-Ethoxy) methoxyethyl vinyl ether (EOEOVE), 109
Ethyl cyano(hydroxyamino) acetate, 70–71
1-Ethyl-3-(3-dimethyl aminopropyl) carbodiimide (EDC), 68
Ethylene vinyl acetate copolymer (EVAc), 198
Etoposide (ETP), 432

ETV. *See* Electrothermal vaporization (ETV)
Eugenol, 327
EVAc. *See* Ethylene vinyl acetate copolymer (EVAc)
Ex vivo testing, 660–663
Excretion, 167
Exploding wire, 535
External local hyperthermia. *See* Local hyperthermia
Extracellular matrix (ECM), 102–103, 227, 229, 347, 416, 477–478, 642–643
Extracellular methods, 537, 538*f*

F

f-CNTs. *See* Functionalized CNTs (f-CNTs)
Fast agglutination screening test, 269
Fatigue strength, 348, 354
Fatty acids, 102, 422–424
5-FC. *See* 5-Fluorocytosine (5-FC)
FCS. *See* Fluorescence correlation spectroscopy (FCS)
FCS-NSOM. *See* Fluorescence correlation spectroscopy–near field scanning optical microscopy (FCS-NSOM)
FDA. *See* United States Food and Drug Administration (FDA)
Feasibility, 352
FEP. *See* Fluorinated ethylene propylene (FEP)
2-Ferrocenyl-1,1-bis(4-hydroxyphenyl)-but-1-one, 35–36
Ferrociphenol (Fc-diOH), 35–36
Fever therapy. *See* Whole-body hyperthermia
FGF. *See* Fibroblast growth factor (FGF)
Fiber laser surface engineering, 356
Fibrin, 357
Fibrinogen, 642–643
Fibroblast growth factor (FGF), 133, 486
  FGF-2, 306
    delivery in dental pulp therapy, 306–307
Fibroblast surface protein (FSP), 27
Fibroin, 541–542
Fibronectin, 650
Fibrosis, 358
Fick's laws, 206
Finite element analysis, 353
First generation
  aspirant vaccines for leishmaniasis, 291
  implant materials, 342–345, 343*f*
    ceramic materials, 342–343
    metallic materials, 342
    polymers, 343–345, 344*f*
Fluid impact mills, 475
Fluidized bed opposed jet mills, 476
Fluorenyl methoxycarbonyl (Fmoc), 70
Fluorescence correlation spectroscopy (FCS), 552, 559–560
Fluorescence correlation spectroscopy–near field scanning optical microscopy (FCS-NSOM), 560
Fluorescent core–shell PMMA NPs (FNPs), 39–40, 40*f*
Fluorinated ethylene propylene (FEP), 645
5-Fluorocytosine (5-FC), 36–37
Fmoc. *See* Fluorenyl methoxycarbonyl (Fmoc)
FNPs. *See* Fluorescent core–shell PMMA NPs (FNPs)
Focused ultrasound, 386
Foot-and-mouth disease virus peptide functionalized CNTs, 626
Formulation
  stability of pharmaceutical biotechnology-based products, 169–171
    chemical degradation, 169
    physical degradation, 169–171
  strategies for HA-based nanoplatforms, 422–424
    desolvation method, 423
    self-assembling HA nanoparticles, 423–424
Fourier transform infrared spectroscopy (FTIR spectroscopy), 552, 555–556
  vibration in for iron oxide nanoparticles, 556*t*
Fracture process modeling in orthopedic implants, 358
Free radicals, 66, 310–311, 362
FSP. *See* Fibroblast surface protein (FSP)
FTIR spectroscopy. *See* Fourier transform infrared spectroscopy (FTIR spectroscopy)
Functionalized CNTs (f-CNTs), 287
Fungi, NPs via, 539
Fungisome (F), 277, 279*f*
Fusarium oxysporum, 539

G

GAGs. *See* Glycosaminoglycans (GAGs)
Galvanic corrosion, 349
Gamma-interferon$_{1b}$, 177
γ-irradiation technique, 543
Ganciclovir sensitive thymidine kinase recombinant gene, 291
Gas
  evaporation, 535
  gas-phase technique, 547
Gas chromatography (GC), 7–9
Gastric/enzymatic drug degradation, 100
Gastrointestinal tract (GIT), 155
Gastroretentive drug delivery systems, 97
Gatifloxacin-loaded PLGA and b-tricalcium phosphate composite (GFLX composite), 310, 312*t*
GC. *See* Gas chromatography (GC)
GC pairs. *See* Guanine–cytosine content pair (GC pairs)
Gel electrophoresis, 164
Gel filtration. *See* Size exclusion chromatography

Gelatin nanofibers, 245
Gelatin-based nanoformulations, 306–308
  fibroblast growth factor-2 delivery in dental pulp therapy, 306–307
  HA delivery in remineralization of tooth enamel, 307–308
Gelfoam (biodegradable gelatin polymer), 98–99
Gene
  cloning, 156
  MNPs applications in gene delivery, 572–573
  therapy, 171–172, 181–182, 404, 572–573
  transfer process, 181–182
Gene silencing, 424
  effect, 434
  mechanism of posttranslational, 425
  in vitro gene silencing efficiency, 448
Generally regarded as safe (GRAS), 306
Genomic DNA libraries, 159
Genotoxicity, 360
Genotropin, 174
GFLX composite. *See* Gatifloxacin-loaded PLGA and b-tricalcium phosphate composite (GFLX composite)
GGS nanoparticles. *See* Gold–gold sulfide nanoparticles (GGS nanoparticles)
GIC. *See* Glass ionomer cement (GIC)
GIT. *See* Gastrointestinal tract (GIT)
Glass ionomer cement (GIC), 313, 321
Glass(es), 94–95, 95*t*
  ceramics, 346
  vessels, 66–67
Glaucoma, 482
Global Society for Cell Therapy, 23
Glucose-responsive insulin delivery systems, 114
Glucuronic acid, 419
  degradation on, 420
  glucuronic acid-*N*-acetyl glucosamine, 419
Glycerol distearate, 99
Glycerophosphate, 481
Glyceryl behenate, 99
Glycine, 169, 541
Glycolysis, 270, 378
Glycosaminoglycans (GAGs), 416, 484
Glycosylated polypeptide, 177
Glycosylated protein, 179
GO. *See* Graphene oxide (GO)
Gold (Au)
  gold–silica nanoshell, 391
  nanorods, 392
  nanoshells, 391
  nanostructures, 111
Gold NPs (AuNPs), 393–394, 528–529, 566–568, 567*t*, 571–574, 579–580
  AuNPs–based molecular imaging, 580
  GGS nanoparticles, 393–394
  gold colloidal nanospheres, 394
  HAuNS, 394
  synthesis, 542–543, 543*f*
Gold–gold sulfide nanoparticles (GGS nanoparticles), 393–394
Graphene oxide (GO), 122, 390–391, 487, 649
Graphenes (GRs), 390–391, 615
Graphite benzalkonium-heparin, 68
GRAS. *See* Generally regarded as safe (GRAS)
Green biologically based methods, 537
Green method of Au/NPs synthesis, 543
Green nanotechnology, 538
Growth disorders, 154
Growth factors, 228, 642–643
  for bone grafting, 30
  receptors, 26
GRs. *See* Graphenes (GRs)
Guanine–cytosine content pair (GC pairs), 579

H

HA. *See* Hyaluronic acid (HA); Hydroxyapatite (HA)
HA coated mesoporous silica NPs (HA-MSNs), 35
HA-graft-poly (dimethylaminoethyl methacrylate) (HPD), 436–437
HA-MSNs. *See* HA coated mesoporous silica NPs (HA-MSNs)
HA-nanoparticles (HA-NPs), 318–319
Hafnium oxide (HfO_2), 120
Half-maximal inhibitory concentration value (IC_{50} value), 278–280
Hap. *See* Hydroxyapatite (Hap)
Hardness, 348, 354
HAS. *See* Hyaluronic synthase (HAS)
HAuNS. *See* Hollow gold nanoshells (HAuNS)
HCl. *See* Hydrochloride (HCl)
HDL. *See* High-density lipoprotein (HDL)
Head and neck squamous carcinoma cells (HNSCC), 625
Healing process of bone, 339–340
Heat shock proteins (HSPs), 379, 404
HEC. *See* Hydroxyethyl derivative of cellulose (HEC)
hEGFR-2. *See* Human EGFR-2 (hEGFR-2)
HeLa. *See* Human epitheloid carcinoma (HeLa)
HEMA. *See* 2-Hydroxyethyl methacrylate (HEMA)
Hematopoietic stem cells (HSCs), 25
Hemocompatibility, 129–130, 661–663, 663*f*
Hemoglobin tagged chitosan–chondroitin sulfate-based nanoparticles, 281
Hemolysis assay, 434, 482

Heparin, 246
  covalent binding, 68–69
  ionic binding, 68
  molecule, 67–68
Heparinization to improving blood compatibility, 67–69
  covalent binding of heparin, 68–69
  ionic binding of heparin, 68
  physical blending of heparin for controlled release, 69
Hepatic cells tissue engineering, nanotechnology in, 248–250
HER2. *See* Human epidermal growth factor receptor 2 (HER2)
Hexamethylenediamine functionalized CNTs, 619–620
hGH. *See* Human growth hormone (hGH)
High affinity hydrogen bonding based supramolecules, 108
High intensity focused ultrasound, 386
High MW (HMW), 418
High-density lipoprotein (HDL), 283
High-performance liquid chromatography (HPLC), 7–9
High-resolution TEM, 558
High-velocity oxy-fuel spray deposition, 73
High–molecular weight nontargeted drugs, 62–63
Higuchi model, 206
HIP. *See* Hot isostatic pressing (HIP)
Hip replacement, 365
HIPEC. *See* Hyperthermic intraperitoneal chemotherapy (HIPEC)
HIV. *See* Human immunodeficiency virus (HIV)
hMSCs. *See* Human mesenchymal stem cells (hMSCs)
HMW. *See* High MW (HMW)
HNSCC. *See* Head and neck squamous carcinoma cells (HNSCC)
Hollow gold nanoshells (HAuNS), 393–394
Hollow MNs technology, 511–513
Homopolymers, 514
Hopfenberg's model, 209
Hormones, 173–174
  blood clotting factors, 175–176
  cytokines, 176–177
  enzymes, 175
  hGH, 174
  insulin hormone, 173–174
  monoclonal antibodies, 177–178
  vaccines, 178–179
Host
  cells, 159
  host–guest complex systems, 108
Hot isostatic pressing (HIP), 79–80
HPD. *See* HA-graft-poly (dimethylaminoethyl methacrylate) (HPD)
HPLC. *See* High-performance liquid chromatography (HPLC)
HPMA. *See* Hydroxypropyl methacrylamide (HPMA)
HPMA copolymer-cyclopamine conjugate (P-CYP), 42
HPMA copolymer-docetaxel (PDTX), 42
HPMC. *See* Hydroxyl propyl methyl cellulose (HPMC)
HSCs. *See* Hematopoietic stem cells (HSCs)
HSPs. *See* Heat shock proteins (HSPs)
HTCC. *See N*-(2-Hydroxyl)propyl-3-trimethylammonium chitosan chloride (HTCC)
Human
  autologous MIMIC, 134
  beta-interferon-based product, 177
  body temperature, 380–381
  bones, 338–339
  colon carcinoma cell, 45–46
  insulin, 173
  ovarian carcinoma cell, 45–46
  papillomavirus, 512–513
Human EGFR-2 (hEGFR-2), 400–401
Human endothelial cells (HUVEC), 434
Human epidermal growth factor receptor 2 (HER2), 21
Human epitheloid carcinoma (HeLa), 434
Human growth hormone (hGH), 173–174
Human immunodeficiency virus (HIV), 264
  coinfected leishmaniasis, 267–268
  HIV-Tat, 623
Human mesenchymal stem cells (hMSCs), 25–27
HUVEC. *See* Human endothelial cells (HUVEC)
Hyaluronan. *See* Hyaluronic acid (HA)
Hyaluronic acid (HA), 26–27, 416–417, 420*f*
  in delivering silencing RNA, 435–446, 436*f*
    breast cancer, 445–446
    colon cancer, 437–443
    ovarian cancer, 443–445
  emerging technology platform, 416–424
  hyaluronic acid–based drug delivery, 487
  properties and features, 417–418
    chemical properties, 417–418
    formulation strategies for HA-based nanoplatforms, 422–424
    origin and source, 418–419
    physiological actions, 419
    physiological properties, 418
    in vivo metabolism, 419–422
  RNAi, 424–434
  synthase, 418–419
Hyaluronic synthase (HAS), 437
Hyaluronidase, 419–420
Hybridoma technology, 178, 179*f*

Hydrochloride (HCl), 320
Hydrogels, 98–99, 107, 124–126, 480
  hydrogel/swellable microneedles technology, 514–516, 515*t*
  matrix self-assembled cell encapsulation technique, 232
Hydrogen bonding, 464, 466
Hydrogen peroxide (H_2O_2), 579
Hydrolysis of bonds, 198
Hydron technology, 219
Hydrophilic monomers, 114
Hydrophobic drugs, 283
  aqueous and, 215
  hydrophobic drug-loaded Pluronic-F127 micelles, 110
Hydrothermal process, 547, 550
Hydroxyapatite (HA), 72, 91, 307, 348
  delivery in remineralization of tooth enamel, 307–308
  hydroxyapatite–ciprofloxacin delivery system, 216
Hydroxyapatite (Hap), 231, 238
Hydroxycarbonate apatite layer, 351
Hydroxyethyl derivative of cellulose (HEC), 574
2-Hydroxyethyl methacrylate (HEMA), 93
Hydroxyl (–OH) functional group–coated surfaces, 667
Hydroxyl butyl chitosan, 481–482
Hydroxyl propyl methyl cellulose (HPMC), 100–101, 197
  matrix systems, 200
N-(2-Hydroxyl)propyl-3-trimethylammonium chitosan chloride (HTCC), 486
Hydroxypropyl methacrylamide (HPMA), 101–102, 115, 277–278
N-Hydroxysuccinimide, 665–666
Hyperthermia, 376, 378*f*, 381–384, 382*f*
  basic principles, 377–379
  biomaterials and nanoparticle in hyperthermia therapy, 387–399
  combined chemotherapy, 403–404
  combined gene therapy, 404
  combined therapy, 403–405
  combined with photodynamic therapy, 405
  crosstalk on application and uses of, 400–403
  factors affecting hyperthermia treatments, 381
  historical perspectives, 377
  human body temperature, 380–381
  mechanism of cytotoxicity, 378–379, 380*f*
  physiology, 378
  techniques used for generation of, 385–387
  thermotolerance, 379–380
Hyperthermic intraperitoneal chemotherapy (HIPEC), 384
Hypodermis, 193, 505

I

^{125}I-labeled FGF-2, 306
IARC. *See* International Agency for Research on Cancer (IARC)
Ibuprofen, 60
IC. *See* Integrated circuit (IC)
ICG. *See* Indocyanine green (ICG); Intracardiac green dye (ICG)
ICHQ6, 2–3
ICP-AES. *See* Inductively coupled plasma atomic emission spectroscopy (ICP-AES)
ICP-MS. *See* Inductive coupled plasma–MS (ICP-MS)
IDDSs. *See* Implantable drug delivery system (IDDSs)
IDO. *See* Indoleamine 2,3-dioxygenase (IDO)
IFAT. *See* Indirect fluorescent antibody test (IFAT)
IL. *See* Interleukin (IL)
Iluvien implant, 218–219
IM. *See* Intramuscular (IM)
Imaging probes, 394
2-Iminothiolane, 470, 470*f*
Immobilization of biomolecule on biomaterial surface, 658–659
  chemical bonding with biomolecules, 658–659
  chemical modification, 659
  physical adsorption, 658
  physical entrapment, 659
Immune disease, 23
Immunoblotting test, 269
Immunochemotherapy, 291–292
Immunogenicity, 168, 174
  of biotechnology-based pharmaceutical products, 171
  after treatment, 508–509
Immunoglobulin antibodies, 276–277
Immunological effect, 378–379
Immunomodulating receptors, 26–27
Immunomodulatory, 26
Immunotherapy, 107
  of PKDL, 291
  tumor, 181
Implant failure, 359*t*
Implant materials
  complications associated with performance, 358–360, 359*t*
  current trends in 21st century, 360–363
  through generations, 341–347
  history, 340–341
    early era or foundation period, 340–341
    trauma in postwar or premodern era, 341
  manufacturing requirements for, 354–355
    mechanical properties, 354–355
    nonmechanical requirements, 355
  in orthopedic, 349–351

Implant materials (*Continued*)
regulatory approvals and requirements, 363–365
directives, 364–365
tissue-implant responses, 356–358
vital properties for selection, 348–349
biocompatibility, 348–349
bulk properties, 348
surface properties, 348
Implantable drug delivery, 105–106
Implantable drug delivery system (IDDSs), 193–194, 194*f*, 195*f*, 214
drug release mechanism from, 198–201
cardiac pacemaker, 206*f*
ceramic drug delivery systems, 205
micro/nanofabricated IDDSs, 204
modeling, 205–210
empirical models, 206–207
mathematical models, 208–210
Implantable pump system
infusion pumps, 201–202
osmotic pumps, 202–203
peristaltic pumps, 202
positive displacement pumps, 203
Implantable rapid drug delivery device (IRD3), 219–220
Implantable therapeutic systems
approaches for development, 210–214
Biosilicon technology, 212
controlled drug release by activation, 211
controlled drug release by diffusion, 210
encapsulated cell technology, 213–214
lucentis in new vehicle, 211–212
replenish mini pump, 213
biodegradable and nonbiodegradable implant systems, 194–198
commercially available advanced implantable devices, 218–220
controlled drug administration benefits by implantation, 217–218
IDDSs, 193–194, 194*f*, 204–205
drug release mechanism from, 198–201
modeling, 205–210
implantable pump system, 201–203
manufacturing and sterilization protocols, 214–217
air suspension, 216
coacervation phase separation, 215
emulsion phase separation, 215
PRINT method, 217
solvent extraction method, 216
spray drying method, 215–216
skin, 192–193
In situ chitosan–alginate polyelectrolyte complexation, 488
In situ tissue engineering, 229
In vitro
drug diffusion profile, 327–328, 328*f*
testing, 660
In vivo
biocompatibility assay, 133
biodistribution, 31–33, 34*f*
biological mechanisms, 22
metabolism, 419–422
targeting, 437
techniques, 663–665
tumor delivery, 35
In-process specification, 4
Indirect fluorescent antibody test (IFAT), 269
Indocavity hyperthermia, 384
Indocyanine green (ICG), 398, 442–443
Indoleamine 2,3-dioxygenase (IDO), 26–27
Induced tissue approach, 229
Inductive coupled plasma–MS (ICP-MS), 563
Inductively coupled plasma atomic emission spectroscopy (ICP-AES), 436
Inert gas, 615
Inertness, 340–341
Infection-resistant slippery surface, 131
Infectious diseases, 154
Inflammatory responses, 357
Infusion pumps, 201–202
Injectable drug delivery, 104–105
Inorganic NPs, 531–533
INS-$CaCO_3$ MPs. *See* Insulin-loaded $CaCO_3$ MPs (INS-$CaCO_3$ MPs)
Insulin, 164–165, 173
aerosolized liposomes mediated delivery, 100
hormone, 154, 173–174
Insulin-loaded $CaCO_3$ MPs (INS-$CaCO_3$ MPs), 513
Integral membrane protein molecule, 418–419
Integrated circuit (IC), 66
Intelligent drug delivery systems, 116–126
affinity-based drug delivery systems, 117–119
reservoir-based drug delivery system, 119–126
Intelligent stimuli-responsive hydrogels, 125
Interferons (IFN), 176–177
IFN-γ, 267
interferon-$beta_{1b}$, 177
Interleukin (IL), 176–177, 267, 508
IL-1b, 321
IL-2, 376
IL-12, 267
Internalization process, 30

International Agency for Research on Cancer (IARC), 445
International Standard Organization, 72
Interstitial hyperthermia, 384
Intracardiac green dye (ICG), 498
Intracellular method, 537
Intracutaneous reactivity, 358
Intradermal reactivity. *See* Intracutaneous reactivity
Intramuscular (IM), 496
  injection, 165
Intraperitoneal perfusion hyperthermia. *See* Perfusion therapy hyperthermia
Intratumoral interstitial fluid pressure (IT interstitial fluid pressure), 21
Intravascular injections, 29–30
Intravenous (IV), 29–30, 496
  administration, 281
  injection, 165
Invertebrate, 542
IO-NPs. *See* Iron oxide NPs (IO-NPs)
Ion beam assisted deposition, 74
Ion exchange chromatography, 161–162, 163*f*
Ion-induced gelation. *See* Ionic—gelation
Ionic
  binding of heparin, 68
  gelation, 472–473, 473*f*, 474*f*
  self-complementary peptide, 231
Ionization radiations, 549
Iontophoresis, 506
IR780 dyes, 398–399
IR825 dyes, 399
IRD3. *See* Implantable rapid drug delivery device (IRD3)
Iron (Fe), 528–529
  nanoparticles synthesis, 544–545
Iron oxide (Fe_2O_3), 539
  crystallographic structures, 559
Iron oxide NPs (IO-NPs), 43, 397, 575
Irradiation, 362–363
Irritation, 358
Isolation and purification of biotechnology-based products, 161–163
Isomers, 118–119
N-Isopropylacrylamide (NIPAAm), 97–98
Isotropy, 93
IT interstitial fluid pressure. *See* Intratumoral interstitial fluid pressure (IT interstitial fluid pressure)
IV. *See* Intravenous (IV)

J

Janus kinase/signal transducers pathway, 27
Janus NPs, 580
Joint replacement, 365–366

K

Kala-Azar. *See* Visceral Leishmaniasis (VL)
Kaplan–Meier survival curves, 36–37
Katzhendler model, 209
Ketoconazole loaded nanoniosome, 285
Ketoprofen, 327
Knee replacement, 365

L

Labeling, 14
Lactate dehydrogenase (LDH), 30, 31*f*
Lactic acid, 302
Lactoferrin, 282
Laminin, 650
Laser
  micromachining technique, 217
  surface treatment, 356
Laser ablation, 535, 547
  nanosecond, 546
  pulsed, 547
  technique, 616
Latanoprost, 482
LCST. *See* Lower critical solution temperature (LCST)
LDH. *See* Lactate dehydrogenase (LDH)
Lead (Pb), 539
Lead zirconate titanate (PZT), 506–507
Leishmania, 264–265
  L. donovani BALB/c mouse model, 274
  species and associated clinical types, 265*t*
  taxonomy, 265*t*
Leishmaniasis, 264
  8-aminoquinolines, 273
  buparvaquone and derivatives, 274
  combined therapy, 271–273
  currently using drugs for treatment, 270–271
  diagnosis, 268–270
    antibody detection diagnostic tests, 270
    molecular diagnosis, 269–270
    parasitological diagnosis, 269
    serological diagnosis, 269
  Leishmania, 265
    clinical manifestations, 267
    life cycle, 266–267, 266*f*
    pathology, 267–268
    species and associated clinical types, 265*t*
    taxonomy, 265*t*
  macrophage-targeted drug delivery using nanocarriers, 275–290
  prophylactic vaccines for, 290–292
  sitamaquine, 273
  2-substituted quinolines, 274
Leishmanization, 290–291
Lenticular liposomes, 112

Leukocytes, 176, 267, 643
LEWIS lung carcinoma cells (LLC), 45–46
Ligase enzymes, 156, 158*f*
Light-responsive biomaterials, 110–112
Linear aliphatic polyesters, 238
Linoleic acid, 446
Lipid
  nanocapsules, 98
  tubules, 232
Lipid NC (LNC), 34–35
Lipiodol liposomes, 62–63
Lipophilic
  drugs, 498
  moiety, 422
Lipophosphoglycan (LPG), 265
Lipoproteins, 166–167
Lipoquin, 100
Liposomes, 20, 168, 275–277, 313–314, 478–479, 533
Liquid
  fluoropolymers, 217
  liquid-phase technique, 547
Lithium (Li), 547
Lithography, 534–535
  centrifugal, 513–514
  nanoimprinted, 217
Liver disease, 248
LLC. *See* LEWIS lung carcinoma cells (LLC)
LNC. *See* Lipid NC (LNC)
Local hyperthermia, 382–383
Localized deep hyperthermia. *See* Regional-deep hyperthermia
Localized drug targeting, 107
Localized surface plasmon resonance (LSPR), 542
Lower critical solution temperature (LCST), 105
LPG. *See* Lipophosphoglycan (LPG)
LSPR. *See* Localized surface plasmon resonance (LSPR)
Lucentis in vehicle, 211–212
Luciferase gene silencing assay, 438–439
Lung cancer, 31–34
Lutzomyia genus, 264
Lycurgus Cup, 528–529
Lymphocyte, 379
Lyophilization, 233, 484, 485*f*
Lysosomes, 35, 267, 379

M

MAA. *See* Marketing authorization application (MAA)
Macromolecular proteins, 496–498
Macromolecules, 63, 169, 498
Macrophage targeting, 61
Macrophage-targeted drug delivery using nanocarriers, 275–290
  carbon nanotubes, 287
  drug delivery systems, 288–290
  emulsions, 286–287
  liposomes, 275–277
  nanodisks, 283
  nanoparticles, 277–282
  niosomes, 283–285
  transfersomes, 287–288
Maghemite, 575
Magnetic
  controlled release, 200–201
  hysteresis, 395, 396*f*
  iron oxide NPs, 545
  magnetic-responsive biomaterials, 110
  nanomaterials, 400
  NPs, 394–396
  pole matrices, 253
Magnetic CD (MCD), 563
Magnetic resonance (MR), 529
Magnetic resonance imaging (MRI), 31, 389, 529
Magnetite (Fe_3O_4), 397
Magnetron sputtering deposition, 76
Maillard reaction, 508
Major histocompatibility complex (MHC), 379
Major vault protein (MVP), 424
MALDI–MS. *See* Matrix-assisted laser desorption/ionization–MS (MALDI–MS)
Malignant glioma, 35–36
Mannose-conjugated lipid nanospheres, 290
MAO. *See* Microarc oxidation (MAO)
MAPCs. *See* Multipotent adult progenitor cells (MAPCs)
Marketed MN products, 517–518, 518*t*
Marketed products for orthopedic implants, 366–367
Marketing authorization application (MAA), 3
Marqibo, 21, 22*t*
Marrow-isolated adult multilineage inducible (MIAMI), 29–30, 38*f*
Mass spectrometry (MS), 559, 563–564
Materials and product specifications
  designing of specification, 5–11
  handling of OOS, 11–12
  objectives and scope, 2–3
  pharmaceutical product, 12–15
  on pharmaceutical quality system, 15
Mathematical models, 208–210
  for diffusion-based drug delivery system, 208
  for dissolution based drug delivery system, 208–209
  for erosion based drug delivery system, 209–210
Matrix metalloproteinase (MMP), 115
Matrix tablet for controlled drug delivery, 487–488

Matrix-assisted laser desorption/ionization–MS (MALDI–MS), 564
Matrix-based systems, 210
Mayrink vaccine, 291–292
MBC. *See* Minimum bactericidal concentration (MBC)
MCD. *See* Magnetic CD (MCD)
MCF-7 cells, 628
MCL. *See* Mucocutaneous leishmaniasis (MCL)
MDP. *See* Muramyl dipeptide (MDP)
MDR. *See* Multidrug resistance (MDR)
Mechanical ball milling, 535
Mechanical methods
  mechanical ball milling, 535
  mechanochemical synthesis, 535
Mechanical theory, 467
Mechanical-responsive biomaterials, 112
Mechanochemical
  method, 545
  synthesis, 535
    of RuNPs, 549
Medical device, 363
Medical orthopedic implants market segmentation, 367
MedLaunch, 219
Melanoma, 401
Memorial Sloan-Kettering, 377
4-Mercaptobenzoic acid, 470–471, 471*f*
3-Mercaptophenylboronic acid (3-MPB), 563
Mesenchymal stem cells (MSCs), 20–21, 23–25, 24*t*, 25*f*, 26*f*, 214, 250, 251*f*, 404
  differentiable human, 253
  mouse, 487
  NPs in cancer treatment, 42–46
Mesengenic process, 24
Meso-tetrakis (4-sulfonatophenyl) porphyrin (TPPS), 39–40
Mesoporous silica nanoparticles (MSNs), 113–114, 397
Messenger ribonucleic acid (mRNA), 159–160
Metabolism, 167
Metal NPs (MNPs), 318–319, 529, 536*f*, 555, 569
  applications, 566–581
    Au nanoparticle–based molecular imaging, 580
    in biosensing devices, 576–577
    in cosmetics, 580–581
    in diagnostics, 578–579
    in drug delivery, 566–571
    in enzymology, 574–575
    in gene delivery, 572–573
    of nanoparticles, 567*t*
    in peptide delivery, 572
    in protein delivery, 572
    in surface coating of nanoparticles, 575
    in theranostics, 579–580
    in tissue engineering, 573–574
    in wound dressings, 580–581
  color and wavelength range, 553*t*
  future potential, 581–582
  methods in metal NPs synthesis, 534–542
    biological approach, 536–542
    chemical approach, 535–536
    physical approach, 534–535
  methods used in characterization, 552–566, 553*t*
    AFM, 566
    CD, 562–563
    DLS, 564–565
    EDX spectroscopy, 559
    ESEM, 557
    FCS, 559–560
    FTIR spectroscopy, 555–556
    MS, 563–564
    SEM, 557
    SERS, 560–561
    STM, 565
    TEM, 558
    TERS, 561
    UV visible spectroscopy studies and plasmon resonance, 552–555
    X-ray crystallography, 558–559
    ZP, 561–562
  nanotechnology and nanoscience, 530–534
  properties, 529–530
  role in pharmaceutical systems, 534
  surface properties, 551–552
  synthesis
    of AgNPs, 543–544
    of AlNPs, 547–548
    of AuNPs, 542–543
    of bimetallic NPs, 549–550
    of CuNPs, 546–547
    of iron NPs, 544–545
    of metalloid and non-metal NPs, 550–551
    of PtNPs, 548
    of ruthenium NPs, 548–549
    of ZnONPs, 545–546
Metal oxide NPs, 533
Metallic
  ANPs, 579
  antibacterial nanoparticles, 318
  materials, 342
  nanocrystals, optical properties of, 578
  Metallic nanostructures, 534
  NPs, 528–529, 532, 581–582
    by different microorganisms, 540*t*
    future potential, 581–582
    over polymeric micro-and nanostructures, 534
  rods, 341

Metalloid NPs, 550–551
  synthesis
    of Se NPs, 550–551
    of sulfur NPs, 551
Metalloproteins, 572
Metals, 94, 349, 529
  biomaterial, 102–103
  ion–ligand coordination systems, 108
Methyl ($-CH_3$) functional group-bearing surfaces, 668
Methylene blue, 515
  assay, 40
  methylene blue–loaded PLGA nanoparticles, 312*t*
Metronidazole, 515
MHC. *See* Major histocompatibility complex (MHC)
MI. *See* Myocardial infarction (MI)
MIAMI. *See* Marrow-isolated adult multilineage inducible (MIAMI)
MIC. *See* Minimum inhibitory concentration (MIC)
Micro-and nanoparticulate thiolated chitosan
  air jet milling, 475–476
  emulsification or solvent evaporation, 473–474
  ionic gelation, 472–473
  radical emulsion polymerization, 475
Micro-RNA expression, 532
Micro/nanofabricated IDDSs, 204
Microarc discharge oxidation. *See* Microarc oxidation (MAO)
Microarc oxidation (MAO), 75–76
Microbubble-based US/magnetic/glucose tristimuli-responsive system, 116
Microcirculation in tissues, 378
Microfabrication, 120
Microneedle-mediated protein drug delivery
  immunogenicity after treatment, 508–509
  limitations of existing MN treatment, 506–507
  physicochemical instabilities of protein drugs, 508–509
  skin barrier, 505–506
Microneedles (MNs), 497, 499*f*, 501*f*, 502*f*, 504*f*
  advances in MN technology in protein delivery, 509–516
  in clinical trials and marketed MN products, 517–518
  patches, 100
  skin properties and design, 500–505
Microorganism biofilms, 302
Microparticles (MPs), 497
Microreservoir-based drug delivery, 217–218
Microspheres, 168, 214
Microwave, 385
Miltefosine, 271, 272*t*, 282, 285
MIMIC. *See* Modular immune in vitro construct (MIMIC)
Mineralized bone cells, 345
Minimally invasive drug delivery technique, 497
Minimum bactericidal concentration (MBC), 324
Minimum inhibitory concentration (MIC), 305, 324
Minocycline, 309, 312*t*
MINPs. *See* Molecularly imprinted nanoparticles (MINPs)
MIPs. *See* Molecularly imprinted polymers (MIPs)
Mixed functionality, surfaces with, 668
Mixed-oxide ceramics, 351
MMP. *See* Matrix metalloproteinase (MMP)
MNPs. *See* Metal NPs (MNPs)
MNs. *See* Microneedles (MNs)
Modular immune in vitro construct (MIMIC), 133
Modulus of elasticity, 348, 354
Moisture
  cross-linking, 362
  moisture-insensitive, 80–81
Molecular
  crowding technique, 119
  diagnostic tests, 269–270
  imaging technologies, 580
  modeling studies, 620–621
  MS techniques, 564
Molecular weight (MW), 63, 498
  of polymer, 463
Molecularly imprinted nanoparticles (MINPs), 117
Molecularly imprinted polymers (MIPs), 118–119
  implantable pump, 219–220
Molybdenum (Mo), 340
Monoclonal antibodies, 154, 177–178
Monocytes, 642–643
  apoptotic effect, 648*f*
Mononuclear phagocytic system (MPS), 264
3-MPB. *See* 3-Mercaptophenylboronic acid (3-MPB)
MPs. *See* Microparticles (MPs)
MPS. *See* Mononuclear phagocytic system (MPS)
MR. *See* Magnetic resonance (MR)
MRI. *See* Magnetic resonance imaging (MRI)
mRNA. *See* Messenger ribonucleic acid (mRNA)
MS. *See* Mass spectrometry (MS)
MSCs. *See* Mesenchymal stem cells (MSCs)
MSNs. *See* Mesoporous silica nanoparticles (MSNs)
MTT assay. *See* 3-(4,5-Dimethylthiazol-2-yl)-2,5-diphenyltetrazolium bromide assay (MTT assay)
Mucin-epithelial surfaces, 462

Mucoadhesion theories, 464–467, 464*f*
adsorption theory, 466
cohesive theory, 466
diffusion theory, 466–467
electronic theory, 465
mechanical theory, 467
wetting theory, 465–466
Mucoadhesive polymers, 462–464, 462*f*
chitosan as, 468
degree of cross-linking and degree of swelling, 463
flexibility of polymer, 463–464
hydrogen bonding, 464
molecular weight of polymer, 463
polymer chain length, 463
viscosity and polymer concentration, 463
Mucoadhesive thiolated chitosan, 468–480
methods of preparation
thiolation using 2-iminothiolane, 470
thiolation using 4 mercaptobenzoic acid, 470–471
thiolation using thioethyl amide, 471–472
thiolation using thioglycolic acid and cysteine, 469
micro-and nanoparticulate thiolated chitosan, 472–476
Mucocutaneous leishmaniasis (MCL), 267–268
Multicompartment microparticles, 120
Multidrug resistance (MDR), 113–114, 424
MDR1, 29–30, 444–445, 444*f*
Multifunctional
NP, 580
stem cell platform, 46–47
Multilayer polymer scaffolds, 254
Multilayered nano/microfibers, 123
Multiple drug release via layer-by-layer approach, 64–65
Multipotent adult progenitor cells (MAPCs), 29–30
Multiwalled carbon nanotubes (MWCNTs), 287, 477–478, 533, 542, 615
Muramyl dipeptide (MDP), 288
MVP. *See* Major vault protein (MVP)
MW. *See* Molecular weight (MW)
MWCNTs. *See* Multiwalled carbon nanotubes (MWCNTs)
Myeloma cells, 178, 393
Myocardial infarction (MI), 103

N

n-HAP/CS/PEG. *See* Nanohydroxyapatite, CS, and PEG (*n*-HAP/CS/PEG)
N/P ratios. *See* Nitrogen/phosphate ratios (N/P ratios)
Nano-HA. *See* Nanohydroxyapatite (nano-HA)
Nanobiomaterials, 120–124
CNTs, 121
DNA-based nanostructures, 124
nanofibrous scaffolds, 121–124
Nanobiosensors, 576
Nanobiotechnology, 180–181
Nanocarriers, 20, 47*f*, 460–461
effective delivery through
CNTs, 477–478
NPs, 476–477
macrophage-targeted drug delivery using, 275–290
Nanocarriers, effective delivery through, 476–480
Nanocomposites, 124–125
Nanocrystals, 533
Nanodisks, 283
Nanoemulgel approach in dentistry, 327–329
Nanoemulsion
nanoemulsion-based approach, 324–327
systems, 286
Nanoengineered MSCs, 33–34
Nanoengineered titanium implants, 204
Nanofibers, 122–123
Nanofibrous scaffolds, 121–124
Nanofluidic devices, 217
Nanoformulations, 460
biomaterial-based, 99
gelatin-based, 306–308
NanoGATE implant, 219
Nanographene oxide (NGO), 391
Nanohybrids, 124–125
Nanohydroxyapatite (nano-HA), 486, 541
Nanohydroxyapatite, CS, and PEG (*n*-HAP/CS/PEG), 242–243
Nanomaterials, 23
in dentistry, 303–329
mesoporous silica, 114
Nanomedicine, 20, 28, 302, 460, 581
Nanoparticles (NPs), 20, 29*f*, 32*f*, 37–39, 39*f*, 101, 168, 227–228, 251, 277–282, 309, 431–434, 476–477, 497, 528–529, 532*f*, 555, 569
via actinomycetes, 537
via algae, 537–538
via animal tissues, 541–542
via bacteria, 538–539
compatibility issue, 432–434, 435*f*
engineered MSCs in breast cancer management, 30
via fungi, 539
in hyperthermia therapy, 387–399
MNPs applications in NPs surface coating, 575
nanoparticles-based oral delivery, 97
nanoparticles. β-aescin loaded nanoparticles, 281

Nanoparticles (NPs) (*Continued*)
via plants, 539–540
types, 531–534
inorganic NPs, 531–533
polymeric NPs, 533–534
via viruses, 539
via yeasts, 539
Nanoparticulate thiolated chitosan, 472–476
Nanopharmacology, 20–21
Nanoprobes, 576
Nanoscience, 530–534
Nanoscopic compounds, 239
Nanosized scaffold, 227–228
Nanostructured lipid carriers (NLCs), 432
Nanotechnology, 416, 460, 528–534, 580, 614
in cell tissue engineering, 244–250
in dentistry, 302–303
as emerging platform in cancer disease management, 20–22
in tissue engineering, 227–230
advantages, 230*f*
properties of suitable scaffolds, 230*f*
triad of signal, scaffolds, and cells that act as a stencil, 228*f*
types, 531–534
Nanotubes, 533
"Nanozyme", 574–575
Natural
polymers, 63
substances, 232
Natural killer (NK), 27
Natural materials–based tissue engineering nanoscaffold, 232–237. *See also* Synthetic materials–based tissue engineering nanoscaffolds
albumin-based tissue engineering scaffold, 233–234
alginate-based tissue engineering scaffold, 235–236
CS-based tissue engineering scaffold, 233, 234*f*
silica-based tissue engineering scaffold, 237
NBF Gingival Gel, 328–329
NDDS. *See* Novel drug delivery systems (NDDS)
Near infrared (NIR), 386
imaging, 424
light, 580
radiation, 569
regions, 110–111
Neck cancer, 402
Neoglycoprotein-altered liposomes, 276
Neurodegenerative disorders, 424
Neurological disorders, 101
Neuron, 61
Neutralizing antibodies, 509
Neutrophils, 642–643
Next generation polymer for drug delivery, 468–476
NGO. *See* Nanographene oxide (NGO)
NGR peptides. *See* Asparagine/glycine/arginine peptides (NGR peptides)
Nickel, 360
Niosomes, 283–285, 479–480
NIPAAm. *See N*-Isopropylacrylamide (NIPAAm)
NIR. *See* Near infrared (NIR)
Nitric oxide (NO), 280–281
Nitrogen/phosphate ratios (N/P ratios), 629
NK. *See* Natural killer (NK)
NLCs. *See* Nanostructured lipid carriers (NLCs)
Noble metal NPs, 566–568
Noble NPs, 576
Non-metal NPs, 550–551
synthesis
of SeNPs, 550–551
of sulfur NPs, 551
Nonbiodegradable implant system, 194–196. *See also* Biodegradable implant system
polymers in, 195–196
PEVA, 196
polyurethanes, 196
silicone rubber, 196
Nonbiodegradable nanoparticles, 630
Noncoating
methods, 356
RNA, 573
Nonconventional modular tumor implants, 366
Noncovalent functionalization, 618
Nonenzymatic degradation, 420, 421*f*
Nonfouling surfaces, 645–646
Nonglycosylated protein, 179
Nonimmune disease, 23
Noninvasive delivery methods, 481
Noninvasive drug delivery system, 497
Nonsteroidal antiinflammatory drugs, 197
Non–surface damaging processes, 80–81
Novel biomaterial-based nanomedicines, 98
Novel drug delivery systems (NDDS), 90
Novel formulation strategy in cancer treatment, 27–46
Novel polymers, emerging class of, 462–464
NPs. *See* Nanoparticles (NPs)
Nucleotides, 157
Numerous biomaterial linked toxicities, 132
Numerous drug delivery systems, 288
NY-ESO-1 (cancer testis antigen), 624

O

O-acyl urea, 70–71
o/w emulsion. *See* Oil-in-water emulsion (o/w emulsion)
OA. *See* Octandioic acid (OA)

Obstructive jaundice, 483
Octandioic acid (OA), 446
Octreotide conjugated paclitaxel (OCT-PTX), 30
Ocular drug delivery, 97–98
Office of Generic Drugs (OGD), 13
Oil insoluble initiator. *See* Water-soluble initiator
Oil-in-water emulsion (o/w emulsion), 474
Olax scandens leaf extracts, 580
"Oligodynamic action" of silver, 316
Oligonucleotides, 483, 572–573
One-step functionalization, 71, 72*t*
OOS. *See* Out-of-specification (OOS)
Opposed jet mills, 475
Optical properties of metallic nanocrystals, 578
Optimal therapeutic effect, 21
Oral diseases, 308–309
Oral drug delivery, 96–97
Oral liquid drug product, 7, 9*f*
Oral route of administration, 165
Oral solid drug product, 7, 9*f*
Organ damage, 243–244
Organic solvents, 71, 474
Orthodontic treatment, 302, 319–320
Orthopedic implants, 340
  clinical applications, 365–366
  coating technologies/approaches for, 355–356
  manufacturing, 352–354
    design changes, 354
    design process, 352
    design transfer, 353
    design validation, 353
    design verification, 353
    feasibility, 352
  marketed products, 366–367
  materials in, 349–351
  modeling fracture process in, 358
Orthopedics, 91
  drug delivery, 104
  surgery, 351
OS. *See* Osteosarcoma (OS)
Osmosis, 202–203
Osmotic pumps, 202–203
Osmotically controlled release, 200
Osseointegration, 92
Osteoblasts, 244
  cells, 339
Osteoclasts, 244
  cells, 339
Osteocyte cells, 339
Osteogenesis, 306
Osteogenic phenotype, 72
Osteoprogenitor cells, 339
Osteosarcoma (OS), 39–40, 41*f*
Osteosynthesis, 365
Out-of-specification (OOS), 7, 11–12
  phase I investigation, 12
  phase II investigation, 12
Oval chamber jet mills, 476
Ovalbumin, 511–512
  ovalbumin-induced airway allergy, 511
Ovarian cancer, 42, 443–445
Oxidation-reduction reaction, 535–536, 537*f*

P

p-hydroxybenzoic acid, 61
PACA. *See* Poly-alkyl cyanoacrylate (PACA)
Packaging material, designing specification for, 10–11, 11*f*
  justification for specification, 10
  pharmacopoeial tests and evolving methodology, 10–11
Paclitaxel (PTX), 446, 581
Pain, hyperthermia in treatment of, 403
Palladium (Pd), 529
Palmitoyl mannose, 276
PAMAM, 239
PAN. *See* Polyacrylonitrile (PAN)
Parasitological diagnosis of leishmaniasis, 269
Parathyroid hormone (PTH), 496
Parenteral drug product, 7
Paromomycin, 271, 272*t*
Paromomycin sulfate, 288
Partially stabilized zirconia, 361
Particle replication in nonwetting templates (PRINT method), 215, 217
PBT. *See* Polybutylene terephthalate (PBT)
PCL. *See* Polycaprolactone (PCL)
PCLA. *See* Poly(ε-caprolactone-co-lactide) (PCLA)
PCR. *See* Polymerase chain reaction (PCR)
PDADMAC. *See* Poly(diallyldimethylammonium chloride) (PDADMAC)
PDGF-BB. *See* Platelet-derived growth factor-BB (PDGF-BB)
PDMS. *See* Polydimethylsiloxane (PDMS)
pDNA. *See* Plasmid DNA (pDNA)
PdNP, 567*t*
PDS. *See* Polydioxanone (PDS)
PDT. *See* Photodynamic therapy (PDT)
PE. *See* Polyethylene (PE)
Pectin, 101
PEDOT. *See* Poly(3,4-ethylene dioxythiophene) (PEDOT)
PEEK. *See* Polyether ether ketone (PEEK)

PEG. *See* Polyethylene glycol (PEG)
PEGA. *See* Poly(ethyleneglycol acrylamide) copolymer (PEGA)
PEGylation, 63–64
PEI. *See* Polyethyleneimine (PEI)
Pendant chain, 199
Penicillins, 172–173, 172*f*
Pentagon–heptagon pairs, 617
Pentamidine, 270, 272*t*
Pentavalent antimonials, 272*t*
PEO. *See* Polyethylene oxide (PEO)
Peppas–Sahlin model, 206–207
Peptide(s), 165, 167
  in cancer management, 621–623
  CNTs, 623
  functionalization, 69–71
    covalent approach, 69–71
    one-step functionalization, 71
  functionalization of CNTs with, 619–621
  functionalized SWCNT conjugates, 625–626
  MNPs applications in peptide delivery, 572
Peptides, 193
  containing MNs in clinical trials and marketed MN products, 517–518
  transdermal delivery of, 496–497
Perfluoropentane (PFP), 112–113
Perfusion therapy hyperthermia, 384
Periodontal diseases, 308–309
Peristaltic pumps, 202
Permeability, 66
Peroxide, 362
PET. *See* Polyethylene terephthalate (PET)
PEVA. *See* Poly(ethylene vinyl acetate) (PEVA)
PEX/XLPE. *See* Cross-linked polyethylene (PEX/XLPE)
PFDYLI peptides, 622–623
PFP. *See* Perfluoropentane (PFP)
PGA. *See* Polyglycolic acid (PGA)
PGS. *See* Poly(glycerol sebacate) (PGS)
PGS-Bioglass elastomer, 646
pH-responsive biomaterials, 113–114
Phagocytosis, 35
Pharmaceutical biotechnology-based products
  formulation stability, 169–171
  pharmacokinetics, 164–168
Pharmaceutical industries, 2, 12–13, 91
Pharmaceutical manufacturer, 5
Pharmaceutical product
  associated terminologies, 4
  development, 59*f*
    biomaterials, 58–59
    surface modification of biomaterials, 59–81
  finishing
    critical labeling requirements of finished product, 14*f*
    labeling, 14
    quality parameters of finished product, 14*t*
    regulatory requirements, 12–13
    schematic plan for verification of specification, 14
    shelf-life and storage, 14–15
  rationale for designing specifications, 3–4
  specification, 3–5
    types, 4–5
Pharmaceutical quality system, specification on, 15
Pharmaceutical sector, 90
Pharmaceutical systems, 534
Pharmacogenomics, 154–155, 182, 183*f*
Pharmacokinetics, 20
  of pharmaceutical biotechnology-based products, 164–168
    absorption, 165
    distribution, 165–167
    metabolism and excretion, 167
    profile of biotechnology-based pharmaceutical products, 167–168
Pharmacopeia, 3, 6–7
Pharmacopoeial harmonization policy, 6–7
Pharmacopoeial test and evolving methodology, 6–11
PHB. *See* Polyhydroxy butyrate (PHB)
PHEMA. *See* Poly(2-hydroxyethyl-methacrylate) (PHEMA)
Phenol-formaldehyde resins, 486
Phlebotomine species, 264
Phosphodiester bond, 157
Phospholipase A2 (PLA2), 115
Phospholipidic coating, 651–654
Phospholipids, 102, 313
Phosphorylcholine, 654
Photoabsorption, 111
Photocrosslinkable hyperbranched polyesters hydrogels, 125
Photodynamic therapy (PDT), 47, 310–311, 405
Photoisomerization, 111
Photolithography, 231
Photosensitizer, 46
Photothermal adaptation, 579
Physical adsorption, 658
Physical approach, 531, 534–535
  mechanical methods, 535
  vapor methods, 535
Physical blending of heparin for controlled release, 69
Physical degradation, 169–171

Physical entrapment, 659
Physical stimuli-responsive biomaterials
  electrical-responsive biomaterials, 110
  light-responsive biomaterials, 110–112
  magnetic-responsive biomaterials, 110
  mechanical-responsive biomaterials, 112
  thermoresponsive biomaterials, 109–110
  ultrasound-responsive biomaterials, 112–113
Physical vapor deposition, 74
Physicochemical instabilities of protein drugs, 508–509
Physiological actions of hyaluronic acid, 419
Piezoelectric ceramic materials, 203
Piezoelectric materials, 203
Pigeonite, 487
Pin-type dental implants, 361
Pinocytosis, 35
Piperine, 286
Pitting corrosion, 349
PKDL. *See* Post-kala-azar dermal leishmaniasis (PKDL)
PLA. *See* Polylactic acid (PLA)
PLA2. *See* Phospholipase A2 (PLA2)
Plants
  with antileishmanial activity, 274, 274*t*
  NPs via, 539–540
Plasma
  electrolytic oxidation. *See* Microarc oxidation (MAO)
  polymerization, 65–67
  protein binding, 166–167
  spraying techniques, 72
Plasmid, 158
Plasmid DNA (pDNA), 434
Plasmodium falciparum, 377
Plasmon
  excitation, 532
  resonance, 552–555
Plasticizer-free polymers, 132
Platelet-derived growth factor-BB (PDGF-BB), 125–126
Platelets, 643
Platinum (Pt), 548
  Pt-based drugs, 571
Platinum nanoparticles (PtNPs), 548
  synthesis, 548
PLGA. *See* Poly(lactic acid-*co*-glycolic acid) (PLGA)
PLGA-MPs. *See* Poly (lactide-*co*-glycolide) microparticles (PLGA-MPs)
PlNP, 567*t*
Pluronic-F127 micelles, 120–121
PMA. *See* 1-Pyrenemethylamine (PMA)
PMAA-Polysorbate 80 grafted starch (PMAA-PS80-*g*-St), 113–114
PMMA. *See* Polymethyl methacrylate (PMMA)
PNIPAAMs. *See* Poly(*N*-isopropylacrylamide) (PNIPAAMs)
Poloxamer 407, 327
Poly (lactide-*co*-glycolide) microparticles (PLGA-MPs), 43, 45*f*
Poly-alkyl cyanoacrylate (PACA), 277–278
Poly(2-hydroxyethyl-methacrylate) (PHEMA), 346
Poly(2-oxazolines) (POxs), 109
Poly(3,4-ethylene dioxythiophene) (PEDOT), 649
Poly(diallyldimethylammonium chloride) (PDADMAC), 123
Poly(dimethylsiloxane), 651
Poly(ethylene vinyl acetate) (PEVA), 195–196
Poly(ethyleneglycol acrylamide) copolymer (PEGA), 70
Poly(glycerol sebacate) (PGS), 646
Poly(lactic acid-*co*-glycolic acid) (PLGA), 97–98, 111, 120, 196–197, 238, 281, 302, 308–312, 461, 646
  nanoparticles applied in dentistry, 312*t*
  PGA, 240
  PLGA-based tissue engineering scaffold, 240
Poly(maleic anhydride-alt-1-octadecene), 62
Poly(methyl methacrylate), 651
Poly(*N*-isopropylacrylamide) (PNIPAAMs), 97–98
Poly(para-phenylene) (PPP), 343–345
Poly(pyrrole) (PPy), 110
Poly(sodium 4-vinylbenzene sulfonate) (PSS), 110, 123
Poly(tetrafluoroethylene) (PTFE), 651
Poly(ε-caprolactone-co-lactide) (PCLA), 116
Poly[bis(*p*-carboxy-phenoxy)propane-sebacic acid copolymer (p(CPP:SA)), 107
Polyacrylamide, 533
Polyacrylate, 533
Polyacrylonitrile (PAN), 647
Polyamidoamine functionalized MWCNTs, 629
Polyaspartic acid, 196
Polybutylene terephthalate (PBT), 242
Polycaprolactone (PCL), 77, 100, 122, 196–198, 311, 346, 477–478, 533
Polydimethylsiloxane (PDMS), 196, 202
Polydioxanone (PDS), 346
Polyesters, 238
Polyether ether ketone (PEEK), 343–345, 350
Polyethylene (PE), 461
Polyethylene, 60, 350, 651
Polyethylene glycol (PEG), 63–64, 97–98, 167–168, 242, 281, 388, 424, 461, 508, 645, 647–648
  PEG-HA coated siRNA liposomes, 432–434
  PEG–based tissue engineering scaffold, 242–243

Polyethylene oxide (PEO), 68–69, 645, 647–648
and derivatives, 647–649
Polyethylene terephthalate (PET), 80
Polyethyleneimine (PEI), 422, 438*f*
grafted SWCNT mediated codelivery of shRNA, 627–628
polyethyleneimine-functionalized SWCNTs, 629
Polyglycolic acid (PGA), 101–102, 196–197, 238
Polyhydroxy butyrate (PHB), 346
Polylactic acid (PLA), 34–35, 60–61, 81, 101–102, 196–197, 238, 346, 461, 500–501
PLA–based tissue engineering scaffold, 240–241
Polylactide. *See* Polylactic acid (PLA)
Polymerase chain reaction (PCR), 159–160, 269–270
Polymeric/polymers, 76, 78–79, 94, 95*t*, 102–103, 193, 343–345, 350
biocompatibility
ex vivo testing, 660–663
in vitro testing, 660
in vivo techniques, 663–665
in biodegradable systems, 197–198
chain length, 463
concentration, 463
in drug delivery system, 461
flexibility, 463–464
functionalized NPs, 569
micelles, 20
micro-and nanostructures, 534
molecular weight, 463
in nonbiodegradable systems, 195–196
NPs, 533–534
dendrimers, 534
liposomes, 533
nanocrystals, 533
nanotubes, 533
SNPs, 533
polymer-based devices, 218
surface modification, 60, 64
systems, 117
Polymethyl methacrylate (PMMA), 91, 94, 343
Polymorphonuclear cells, 419
Polyoxazoline conjugation, 649–650
Polypropylene (PP), 343
fumarate, 574
Polypropylenimine dendrimer, 443
Polysaccharides, 197
Polystyrene, 69–70
Polysulfone (PS), 651, 661–663, 663*f*
Polyurethane (PU), 104, 196, 343
catheters, 68
Polyvinyl alcohol (PVA), 218, 500
Polyvinyl chloride (PVC), 350
Polyvinylidene fluoride, 94
Polyvinylpyrrolidone (PVP), 544
Porcine dermis, 106
Porphyromonas gingivalis, 305–306
Positive displacement pumps, 203
Post-kala-azar dermal leishmaniasis (PKDL), 267–268
Posterolateral approach, 366
Posttranslational modification processes, 159
POxs. *See* Poly(2-oxazolines) (POxs)
PP. *See* Polypropylene (PP)
PPP. *See* Poly(para-phenylene) (PPP)
PPy. *See* Poly(pyrrole) (PPy)
Pre-miRNA hairpins, 427
Premade porous cell-seeding scaffold techniques, 232
Pri-miRNA, 426–427
PRINT method. *See* Particle replication in nonwetting templates (PRINT method)
Promastigote, 266
Prophylactic vaccines for leishmaniasis, 290–292
first-generation aspirant vaccines, 291
immunochemotherapy and therapeutic vaccines, 291–292
leishmanization, 290–291
second-generation vaccines, 291
Protein delivery
advances in MN technology in, 509–516, 510*f*
coated MNs technology, 511
dissolving microneedles technology, 513–514
hollow MNs technology, 511–513
hydrogel/swellable microneedles technology, 514–516
solid MNs technology, 510
MNPs applications in, 572
Protein(s), 165, 167, 170*f*, 193, 498, 532
adsorption, 128–129, 665
containing MNs in clinical trials and marketed MN products, 517–518
crystal engineering, 572
functionalization of CNTs with, 619–621
physicochemical instabilities of protein drugs, 508–509
protein-modified surface influence, 665–666
transdermal delivery of, 496–497
Proteoglycan synthesis, 419
Proteolytic enzymes, 165, 166*f*
PS. *See* Polysulfone (PS)
Pseudomonas aeruginosa, 99
PSF. *See* Polysulfone (PS)
PSS. *See* Poly(sodium 4-vinylbenzene sulfonate) (PSS)
Pterodon pubescens, 286
PTFE. *See* Poly(tetrafluoroethylene) (PTFE)
PTH. *See* Parathyroid hormone (PTH)
PtNPs. *See* Platinum nanoparticles (PtNPs)
PTX. *See* Paclitaxel (PTX)

PU. *See* Polyurethane (PU)
Pulmonary drug delivery, 99–100
Pulpectomy, 306
Pulsed laser physical vapor deposition, 74–75
Pure titanium, 349
Purification of CNT, 616–617
PVA. *See* Polyvinyl alcohol (PVA)
PVC. *See* Polyvinyl chloride (PVC)
PVP. *See* Polyvinylpyrrolidone (PVP)
Pyrene derivatives, 618
1-Pyrenemethylamine (PMA), 618
PZT. *See* Lead zirconate titanate (PZT)

Q

Quality by design (QbD), 2–3
Quantum dots, 251, 533, 539
Quaternary ammonium dimethacrylate (QADM), 316–317
Quercetin, 281, 327–328

R

Racemization, 70–71, 169
Radical emulsion polymerization, 475
Radiofrequency (RF), 376, 385–386
Radiolabeled HA, 421–422
Radiolytic coreduction method, 549
Radiotherapy, 28
Raman spectroscopy (RS), 560
Ranibizumab, 212
Rapid prototyping method, 353
Rayleigh scattering, 564–565
Reactive oxygen species (ROS), 47, 318, 420
Receptor blockade assay. *See* Competition assay
Receptor for HA-mediated motility (RHAMM), 416
Receptor-mediated transcytosis, 28
Recognition molecular systems, 117–119, 118*f*
Recombinant blood clotting factors, 176
Recombinant DNA technology, 154, 156–159, 157*f*
  host cells, 159
  vectors, 158–159
Recombinant hepatitis-B surface antigen, 477
Reconstituted HDL (rHDL), 283
Redox-responsive biomaterials, 114
Reduction of blood toxicity, 62
Regenerative medicine, 347
Regional-deep hyperthermia, 383
Regosterol, 271
Regulations governing cell therapies, 47, 48*f*
Regulatory requirements of pharmaceutical products, 12–13
Release specification of pharmaceutical products, 5
Remodeling, 339, 580–581
  of cell-mediated graft, 247–248
Replenish mini pump, 213
Reproductive toxicity, 360
RES. *See* Reticuloendothelial system (RES)
Reservoir system, 195, 217–218
Reservoir-based drug delivery system, 119–126. *See also* Intelligent drug delivery systems; Microneedle-mediated protein drug delivery
  hydrogels, 124–126
  microfabrication, 120
  nanobiomaterials, 120–124
Restriction enzymes, 157, 157*f*
Restriction sites, 157
Reticuloendothelial system (RES), 21, 275–276, 428, 571
Retisert, 218
RF. *See* Radiofrequency (RF)
RGD peptide, 129, 400, 623
RGD peptides. *See* Arginine/glycine/aspartic acid peptides (RGD peptides)
RGDC. *See* Arginine-glycine-aspartic acid-cystine (RGDC)
RHAMM. *See* Receptor for HA-mediated motility (RHAMM)
rhBMP-2 PLGA nanoparticles, 312*t*
rHDL. *See* Reconstituted HDL (rHDL)
RISC. *See* RNA-interfering silencing complex (RISC)
Risk analysis, 353
Ritger–Peppas model, 207
RNA interference (RNAi), 229, 424–434
  nanoparticles, 431–434
  problems in delivery of silencing RNA, 428–431
  silencing RNA technology and mechanism, 426–428
  structure of silencing RNA, 425–426
RNA interference therapy, 573
RNA-interfering silencing complex (RISC), 425
RNAi. *See* RNA interference (RNAi)
ROS. *See* Reactive oxygen species (ROS)
Rothstein's model, 209–210
Round window membrane (RWM), 98
RS. *See* Raman spectroscopy (RS)
Ruthenium nanoparticles (RuNPs), 548, 567*t*
  synthesis, 548–549
RWM. *See* Round window membrane (RWM)

S

Salinomycin (SAL), 30
Salvager for silencing RNA delivery, 431–434
SAMs. *See* Self-assembled monolayers (SAMs)
Satellite, 340
SBF. *See* Simulated body fluid (SBF)
SC. *See* Stratum corneum (SC)
SC injection. *See* Subcutaneous injection (SC injection)

Scaffolds, 347
  manufacturing techniques, 245
  strategies relating to of scaffold formation, 231–232
    bionanotubes/lipid tubules, 232
    ionic self-complementary peptide, 231
    miscellaneous, 232
    photolithography, 231
    templating, 231
Scanning electron microscopy (SEM), 309, 551–552, 557
Scanning tunneling microscopy (STM), 552, 565
SCT. *See* Subcutaneous (SCT)
SDF-1. *See* Stromal-derived-factor-1 (SDF-1)
SDS–PAGE. *See* Sodium dodecyl sulfate–polyacrylamide gel electrophoresis (SDS–PAGE)
SE mode. *See* Secondary electron mode (SE mode)
Second generation implant materials, 345–347
Second-generation vaccines for leishmaniasis, 291
Secondary electron mode (SE mode), 557
Segmented polyether urethane, 651
Selective targeting, 60–61
Selenium nanoparticles (Se NPs), 550, 567*t*, 579
  synthesis, 550–551
Self-assembled monolayers (SAMs), 69
Self-assembly
  HA nanoparticles, 423–424
  nanoparticulate nanodisks, 283
  process, 231
  structure/peptides, 108
Self-regulated glucose-responsive system, 114
Self-secreted cell sheets ECM technique, 232
SEM. *See* Scanning electron microscopy (SEM)
Sensitization, 358
Sericin, 541–542
Serine, 541
Serological diagnosis of leishmaniasis, 269
SERS. *See* Surface-enhanced Raman spectroscopy (SERS)
Shelf-life
  specification, 5
  and storage, 14–15
Short hairpin RNA (shRNA), 426
Silane copolymers, 362
Silencing RNA (siRNA), 416, 429*t*
  problems in delivery, 428–431, 430*f*
  technology and mechanism, 426–428
Silencing RNA structure, 425–426
Silica
  nanoparticles, 397
  silica-based tissue engineering scaffold, 237
  silica-coated AuNRs, 579
Silicon dioxide (SiO_2), 539
Silicone, 94, 106
  rubber, 196, 343
Silk
  fibroin, 69, 541
  proteins, 541–542
Silver (Ag), 315–316
  Ag^+ ions, 316
  silver-containing materials, 315
Silver nanoparticles (Ag NPs), 314–317, 528–529, 564, 566–568, 567*t*, 575
  aptamers, 581
  synthesis, 543–544
Simulated body fluid (SBF), 75–76
Single particle ICP-MS (SP-ICP-MS), 564
Single-walled carbon nanotubes (SWCNTs), 389–390, 477–478, 533, 615
  SWCNT-EGF, 625
Single–emulsion technique, 215
Sintering, 350
siPLK1, 629
siRNA. *See* Silencing RNA (siRNA); Small interference RNA (siRNA)
Sitamaquine, 273
Site-selective drug release through enteric coating, 64
Size exclusion chromatography, 161, 162*f*
Skin, 192–193, 193*f*
  aging process, 479
  barrier, 505–506, 505*f*
  properties and design of MNs, 500–505
  skin-based microneedle systems, 498–499
  tissue engineering, 485
SL. *See* Stereolithography (SL)
Small drug molecule, sustained and controlled delivery of, 134–135
Small interference RNA (siRNA), 425, 426*f*, 573
  functionalization of CNTs with, 619–621
Small molecules in hyperthermia, 398–399
Small organic NIR dyes, 398
Smart biomaterial challenges and toxicities, 131–132
Smart components, 108–116, 108*f*
Smart nano bombs, 109–110
Smart polymers, 64
SNPs. *See* Solid lipid NPs (SNPs)
4-SO_4GalNAc modified AmB-loaded liposomes, 276
Sodium (Na), 547
Sodium alginate, 488
Sodium borohydride ($NaBH_4$), 535–536
Sodium dodecyl sulfate–polyacrylamide gel electrophoresis (SDS–PAGE), 164
Sodium hydroxide treatment, 80–81
Sodium stibogluconate, 276–277, 283–285
Sol–gel methods, 78–79
Solid lipid NPs (SNPs), 533, 567*t*

Solid MNs, 509–510
  technology, 510
Solid phase peptide synthesis (SPPS), 69–70, 71*t*
Solvent evaporation method, 309, 473–474, 474*f*
Solvent extraction method, 216
Somatotropin. *See* Human growth hormone (hGH)
Sonophoresis, 506, 507*f*
SP-ICP-MS. *See* Single particle ICP-MS (SP-ICP-MS)
sp^3-hybridized deformations, 617
Specification, 3, 5*f*, 6*t*
  designing
    for drug substance/drug product, 5–9
    for packaging material, 10–11
  justification for, 5–6, 10
  pharmaceutical product, 3–5
Spectroscopy, 552
Spermicide IVR, 198
Spine
  drug delivery, 101–102
  implants, 366
SPIO. *See* Superparamagnetic iron oxide (SPIO)
SPIONs. *See* Superparamagnetic iron oxide NPs (SPIONs)
Spiral jet mills, 476
SPPS. *See* Solid phase peptide synthesis (SPPS)
Spray drying method, 215–216
Stabilizing/capping agent, 535–536, 544
Stainless steel, 77, 340, 342
  austenitic, 342
  coated with BSA, 665–666
  for MN fabrication, 500
  reactions due to orthopedic materials, 359*t*
  surface modification with bovine serum albumin, 666*f*
Stannum (Tin), 528–529
Staphylococcus aureus, 355
Stem cell
  engineering, 128
    nanotechnology for, 250
  stem cell–based multifunctional nanoplatforms, 46
  therapy, 182–183
Stents, coating polymer for, 483
Stereolithography (SL), 574
Sterilization protocols, 214–217
Stimuli-responsive biomaterials, 108–116
  biological stimuli-responsive, 114–115
  chemical stimuli-responsive, 113–114
  dual/multiple stimuli-responsive biomaterial systems, 115–116
  physical stimuli-responsive biomaterials, 109–113
STM. *See* Scanning tunneling microscopy (STM)
Stone–Walls defects, 617
Stratum corneum (SC), 193, 497
Streptococcus mutans, 315
Stromal-derived-factor-1 (SDF-1), 23
Structural biomaterials, 104
Styrene–maleic acid polymer-functionalized neocarzinostatin, 62–63
Subacute toxicity, 359
Subchronic toxicity, 359
Subcutaneous (SCT), 496
Subcutaneous injection (SC injection), 165
Substantial developments, 97
2-Substituted quinolines, 274
Succinimidyl ester group, 618
N-Succinimidyl ester pyrrole, 665–666
N-Succinimidyl-1-pyrenebutanoate, 618
Sugar molecules D-glucuronic, 416–417
Suicide bombing, nanotechnology-based tissue engineering for, 251–252
Sulfhydryl group-bearing agent, 469
Sulfur NPs, 551
Superficial epidermis, 505
Superficial hyperthermia. *See* Local hyperthermia
Superparamagnetic iron oxide (SPIO), 110
Superparamagnetic iron oxide NPs (SPIONs), 397, 575
Supramolecular biomaterials, 128
Surface energy, 348, 355
Surface functional group influence on cellular responses, 666–667
Surface heparinization, 68
Surface modification of biomaterials, 59–65, 59*f*, 60*f*, 65*f*
  approaches for, 646–657
  effect for biocompatibility, 665–668
  enhancement
    of bioadhesion, 63
    of drug loading, 60
    of drug stability, 62
    enhanced drug delivery to brain, 61
    enhanced transdermal delivery, 61–62
    enhanced uptake by cancer and inflamed tissues, 62–63
  increased blood plasma half-life, 63–64
  macrophage targeting, 61
  multiple drug release by layer-by-layer approach, 64–65
  reduction of blood toxicity, 62
  requirements for, 643–645
  selective targeting, 60–61
  site-selective drug release through enteric coating, 64
  stainless steel, 666*f*
  strategies employed in, 65–81
    biomimetic coatings, 80–81
    calcium phosphate deposition, 72
    electrochemical deposition, 77–78

Surface modification of biomaterials (*Continued*)
electrophoretic deposition, 77
heparinization to improving blood compatibility, 67–69
HIP, 79–80
ion beam assisted deposition, 74
magnetron sputtering deposition, 76
MAO, 75–76
peptide functionalization, 69–71
plasma polymerization, 65–67
pulsed laser physical vapor deposition, 74–75
sol–gel methods, 78–79
thermal spray deposition, 73–74
Surface NPs encapsulation of drug molecules, 569
Surface patterning as cellular behaviors, 129
Surface roughness, 348, 355
Surface tension, 348, 355
Surface-enhanced Raman spectroscopy (SERS), 543–544, 560–561
Sustained release systems, 90, 461
SWCNTs. *See* Single-walled carbon nanotubes (SWCNTs)
Swelling
controlled release, 199–200
degree, 463
SynchroMed, 201–202, 202*f*
Synovial fluid, 416, 422
Synthetic
antibodies, 117
dressings, 580–581
grafts approach, 246–247
materials, 342
polymers, 238, 533
Synthetic materials–based tissue engineering nanoscaffolds, 238–243. *See also* Natural materials–based tissue engineering nanoscaffold
dendrimer-based tissue engineering scaffold, 238–239, 239*f*
PEG–based tissue engineering scaffold, 242–243
PLA–based tissue engineering scaffold, 240–241
PLGA-based tissue engineering scaffold, 240
Systemic lupus erythematosus, 620
Systemic toxicity, 359

T

T helper cell type 1 (Th-1), 267
T lymphocytes, 25
t-butoxy carbonyl (Boc), 70
TAFs. *See* Tumor-associated fibroblasts (TAFs)
Tamoxifen, 35–36, 271–273
TAT peptide. *See* Trans-activator of transcription peptide (TAT peptide)
"Taylor cone", 122–123
TCP. *See* Tricalcium phosphate (TCP)
Teflon, 106
Telomerase reverse transcriptase (TERT), 626–627
TEM. *See* Transmission electron microscopy (TEM)
Temozolomide (TMZ), 37
Temperature glass transition (T_g), 109
Temperature melting range (T_m), 109
Template molecule, 117
Templating, 231
TERS. *See* Tip-enhanced Raman spectroscopy (TERS)
TERT. *See* Telomerase reverse transcriptase (TERT)
Tethadur, 219
Tetraethylene glycol dimethyl ether, 645
Tetraglyme, 645
Th-1. *See* T helper cell type 1 (Th-1)
Theophylline, 515
Theragnostic agents, 431
Theranostics, 569
appeal in cancer therapy, 570*f*
approach, 22
Theranostics, MNPs applications in, 579–580
Therapeutic siRNA loaded nanoparticles, 573*f*
Therapeutic vaccines, 291–292
Thermal evaporation method, 534–535
Thermal spray deposition method, 73–74
Thermoresponsive biomaterials, 109–110
Thermosensitive hydrogel
based on thiolated chitosan, 480–482
containing paclitaxel nanocrystals, 121
Thermosensitive liposome system (TSL system), 109
Thermotolerance, 379–380
Thioethyl amide, 471–472, 472*f*, 472*t*
Thioglycolic acid, 469, 470*f*
Thiolated-chitosan
chitosan as mucoadhesive polymer, 468
coating polymer for stents, 483
mucoadhesive polymers, 462–464
mucoadhesive thiolated chitosan, 468–480
polymers in drug delivery system, 461
theories of mucoadhesion, 464–467
thermosensitive hydrogel based on, 480–482
tissue engineering, 484–487
Thiolation
using 2-iminothiolane, 470, 470*f*
using 4 mercaptobenzoic acid, 470–471
using thioglycolic acid and cysteine, 469
thiolation using thioethyl amide, 471–472
Thiomers, 468
Thioredoxin-2 (Trx-2), 114

Third-generation biomaterials, 347
Three-dimension (3D)
  porous structures, 306
  structure of polymers, 60
  structures of biomolecules, 155
Ti−13Nb−13Zr alloy (TNZ alloy), 661
Ti−35Nb−7Zr−5Ta alloy (TNZT alloy), 661
"Tiny nanoneedle" mechanism, 615
TiO_2 nanotubes (TNT), 309
Tip-enhanced Raman spectroscopy (TERS), 552, 561
Tissue engineering, 226−227, 306, 347, 484−487, 484*f*
  applications, 243−252
    nanotechnology in cell tissue engineering, 244−250
  bone, 486−487
  cartilage, 487
  clinical trial status, 254−256
    to amalgamate tissue engineering and nanotechnology, 256*t*
    patents and, 255*t*
  matrix tablet for controlled drug delivery, 487−488
  MNPs applications in, 573−574
  nanotechnology in, 227−230
  natural materials−based tissue engineering nanoscaffold, 232−237
  patents, 252−254
    degradable polyurethane foams, 253−254
    differentiable human MSCs, 253
    magnetic pole matrices, 253
    multilayer polymer scaffolds, 254
  skin, 485
  strategies relating to formation of scaffolds, 231−232
  synthetic materials−based tissue engineering nanoscaffolds, 238−243
Tissue regeneration, 128
Tissue-based therapy, 46−47
Tissue-implant responses, 356−358
Titanium (Ti), 106, 320, 360−361
  and alloys, 77
Titanium dioxide (TiO_2), 320
  applied in dentistry, 323*t*
  TiO_2 NP, 320−323, 400
  TiO_2/dicalcium phosphate dehydrate coating, 78
TLRs. *See* Toll-like receptors (TLRs)
TMC. *See N,N,N*-Trimethyl chitosan (TMC)
TMZ. *See* Temozolomide (TMZ)
TNBC. *See* Triple negative breast cancer (TNBC)
TNF. *See* Tumor necrosis factor (TNF)
TNT. *See* TiO_2 nanotubes (TNT)
TNZ alloy. *See* Ti−13Nb−13Zr alloy (TNZ alloy)
TNZT alloy. *See* Ti−35Nb−7Zr−5Ta alloy (TNZT alloy)
Toll-like receptors (TLRs), 26−27
Tooth enamel, HA delivery in remineralization of, 307−308
Top-down approach, 530−531, 531*f*
Topiramate, 100−101
Torus chamber mills. *See* Oval chamber jet mills
TOS. *See* d-α-Tocopheryl succinate (TOS)
Total hip arthroplasty, 351
Toughness of implant materials, 348, 354
Toxicity
  blood toxicity reduction, 62
  consideration CNT, 630−631
  developmental, 360
  genotoxicity, 360
  reproductive, 360
  subacute, 359
  subchronic, 359
TPE. *See* Two-photon excitation (TPE)
TPP. *See* Tripolyphosphate (TPP)
TPPS. *See* Meso-tetrakis (4-sulfonatophenyl) porphyrin (TPPS)
TRAIL. *See* Tumor necrosis factor apoptosis-inducing ligand (TRAIL)
Trans-activator of transcription peptide (TAT peptide), 620
Transappendageal route, 193
Transcutol P, 327
Transdermal delivery enhancement, 61−62
Transdermal drug delivery, 100−101, 119−126, 503. *See also* Intelligent drug delivery systems; Microneedle-mediated protein drug delivery
  enhanced, 61−62
  of protein and peptides, 496−497
    skin-based microneedle systems, 498−499
Transdermal penetration, 61−62
Transepidermal route, 193
Transfersomes, 287−288
Transforming growth factor (TGF)
  TGF-1, 658
  TGF-β, 42
  TGFb1, 27
Transmission electron microscopy (TEM), 436, 551−552, 553*t*, 558
Trastuzumab, 178, 400−401
  emtansine, 21
Trauma in postwar or premodern era, 341
Traut's reagent, 470
Tricalcium phosphate (TCP), 94−95
Triclosan, 310, 312*t*, 649
Tridodecyl methyl ammonium chloride, 68
Trilaurin emulsomes, 286
N,N,N-Trimethyl chitosan (TMC), 486
Triple negative breast cancer (TNBC), 446

Tripolyphosphate (TPP), 473
Tristimuli/multiple responsive systems, 116
Trx-2. *See* Thioredoxin-2 (Trx-2)
TSL system. *See* Thermosensitive liposome system (TSL system)
TTPs. *See* Tumor-targeting peptides (TTPs)
Tumor
  angiogenesis, 24
  cell–secreted TGFb1 induces hypomethylation, 28
  disease management, 23
  enhancing target specificity in, 435–446
  immunotherapy, 181
  tumor-associated macrophage, 61
  tumor-associated MSCs, 27, 28*f*
  vasculature, 378
Tumor necrosis factor (TNF), 267–268
  gene, 404
  TNF-I synthesis inhibitor, 268
  TNF-α, 388–389
Tumor necrosis factor apoptosis-inducing ligand (TRAIL), 37, 43
Tumor-associated fibroblasts (TAFs), 27
Tumor-targeting peptides (TTPs), 622
Two-dimensional surface materials (2D surface materials), 69
Two-photon excitation (TPE), 111, 132

U
UCNPs. *See* Upconversion nanoparticles (UCNPs)
UCST. *See* Upper critical solution temperature (UCST)
Ultra-performance liquid chromatography, 7–9
Ultrasonic radiation, 550
Ultrasound (US), 109, 386–387
  ultrasound-responsive biomaterials, 112–113
Ultraviolet (UV), 318, 542
  visible spectroscopy, 552–555
UMR106 osteoblast cells, 303–304
United States Food and Drug Administration (FDA), 2, 72, 363, 398, 496
  FDA-friendly natural/synthetic biomaterials, 132
United States Pharmacopoeia (USP), 6
Upconversion nanoparticles (UCNPs), 111
Upper critical solution temperature (UCST), 109
UPRT. *See* Uracil phosphoribosyltransferase (UPRT)
Upstream process, 155–160. *See also* Downstream process
  DNA libraries, 159–160
  gene cloning, 156
  recombinant DNA technology, 156–159
Uracil phosphoribosyltransferase (UPRT), 36–37
Uronic acid, 416–417
US. *See* Ultrasound (US)
User-programmed Boolean logic-based algorithm, 115–116
USP. *See* United States Pharmacopoeia (USP)
USP and National Formulary (USP-NP), 6
UV. *See* Ultraviolet (UV)

V
Vaccines, 178–179
  cancer, 181
  Mayrink vaccine, 291–292
  therapeutic, 291–292
Vacuum plasma spraying (VPS), 73
van der Waals forces, 466, 562
Vapor method, 545
  exploding wire, 535
  gas evaporation, 535
  laser ablation, 535
Vapor phase preparation, 534–535
Vascular cells tissue engineering, nanotechnology in, 245–248
Vascularization process, 23
Vasculature diseases, 483
VCD. *See* Vibrational CD (VCD)
Vectors, 158–159
Vehicle-based drug delivery, 497
Vehicle-mediated sustained release systems, 497
Vibrational CD (VCD), 563
Vinyl acetate, 78
Viruses, NPs via, 539
Visceral leishmaniasis (VL), 264, 267
Viscoelastic flow, 93
Viscosity of mucoadhesive polymers, 463
Vitallium, 340
Vitamin H, 114–115
Vitamin K, 175
Vitrasert, 218
Vitronectin, 650
VL. *See* Visceral leishmaniasis (VL)
VPS. *See* Vacuum plasma spraying (VPS)

W
w/o/w emulsion. *See* Water-in-oil-in-water emulsion (w/o/w emulsion)
Water-borne resin formation, 475
Water-in-oil-in-water emulsion (w/o/w emulsion), 215
Water-soluble initiator, 475
Water-soluble SWCNT conjugate, 625–626
Wet-SEM, 557
Wettability, 66, 92
Wetting theory, 465–466, 466*f*
Whole-body hyperthermia, 383–384, 403
Wilm's tumor protein (WT1), 623–624
Wireless implantable system, 210, 211*f*

Wound(s)
drug delivery for wound closure, 106
hyperthermia in treatment of, 402
MNPs applications in wound dressings, 580–581
WT1. *See* Wilm's tumor protein (WT1)

X
X-ray crystallography (XRD), 552, 558–559
X-ray energy dispersive spectroscopy (XEDS), 557
X-ray photon correlation spectroscopy, 552
Xenotransplantation, 27

Y
Yeasts, NPs via, 539
Yield strength, 348, 354

Z
Zero-order model, 207
Zero-order release kinetics for nanoemulgel, 327–328, 328*f*
Zeta potential (ZP), 552, 561–562
Zinc (Zn), 528–529
Zinc 2,9,16,23-tetrakis(phenylthio)-*29H*,*31H*-phthalocyanine (ZnPc), 326
Zinc oxide (ZnO), 317
NPs, 317–320, 545–546, 567*t*
synthesis, 545–546
Zinc sulfide (ZnS), 539
Zirconia, 105–106, 342, 361
ceramic, 351

BIOMATERIALS AND BIONANOTECHNOLOGY

Advances in Pharmaceutical Product Development and Research Series

Rakesh K. Tekade, M.Pharm., Ph.D.
National Institute of Pharmaceutical Education and Research (NIPER) — Ahmedabad, Gandhinagar, India.

Biomaterials and Bionanotechnology examines the current state of the field within pharmaceutical sciences and concisely explains the history of biomaterials including key developments. Written by experts in the field, this volume within the Advances in Pharmaceutical Product Development and Research series deepens understanding of biomaterials and bionanotechnology within drug discovery and drug development. Each chapter delves into a particular aspect of this fast-moving field to cover the fundamental principles, advanced methodologies and technologies employed by pharmaceutical scientists, researchers and pharmaceutical industries to transform a drug candidate or new chemical entity into a final administrable dosage form, with particular focus on biomaterials and bionanomaterials. This book provides a comprehensive examination suitable for researchers working in the pharmaceutical, cosmetics, biotechnology, food and related industries as well as advanced students in these fields.

Key Features

- Examines the most recent developments in biomaterials and nanomaterials for pharmaceutical sciences.
- Covers important topics such as fundamentals of polymers science, transportation and bio interaction of properties in nanomaterials across biological systems, and nanotechnology in tissue engineering as they pertain specifically to pharmaceutical sciences.
- Contains extensive references for further discovery and learning of the role of biomaterials and nanomaterials in the drug discovery process.

Look for these other titles in the Advances in Pharmaceutical Product Development and Research series:

- Tekade, *Dosage Form Design Considerations, Volume I,* July 2018, 9780128144237
- Tekade, *Dosage Form Design Parameters, Volume II*, July 2018, 9780128144213
- Tekade, *Basic Fundamentals of Drug Delivery*, December 2018, 9780128179093
- Tekade, *Drug Delivery Systems*, Forthcoming, 9780128144879

ELSEVIER

ACADEMIC PRESS
An imprint of Elsevier
elsevier.com/books-and-journals

ISBN 978-0-12-814427-5